Scientific and Technical Aerospace Reports

STAR

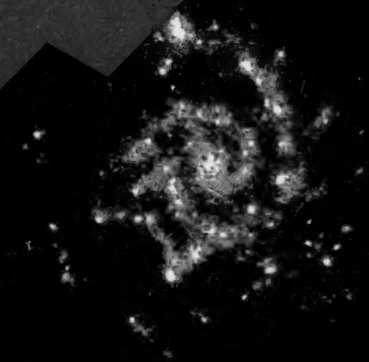

An Abstract Journal

Volume 30, Number 23
December 8, 1992
N92-32243 to N92-33247

Scientific and Technical Aerospace Reports

Scientific and Technical Aerospace Reports (STAR) is an abstract journal that provides comprehensive coverage of worldwide aerospace-related reports. It is a major product of the International Aerospace Database managed by the NASA Scientific and Technical Information (STI) Program. The coverage includes reports on aeronautics, space, and supporting disciplines. *STAR* lists current, publicly available reports entered into the NASA STI Database during the 2-week period preceding publication. A typical citation and abstract appear on page viii. They explain how to read the items that are announced in this journal.

NASA sponsors a companion journal, *International Aerospace Abstracts (IAA)* (*NOVA* for internal NASA use) that lists abstracts of the open literature on aerospace subjects available worldwide. *IAA* is available for sale through the AIAA.

Entries found in *STAR* and *IAA* are available through NASA's online service, RECON, as the International Aerospace Database and through DIALOG as the Aerospace Database.

Information on aerospace and related subjects is gathered by the NASA STI Program through national and international agreements and exchanges and is made available to the NASA community as well as to the public in many forms through various outlets. The section on NASA STI Program Products and Services contains additional information.

For further information please contact:
NASA Center for AeroSpace Information (CASI)
P.O. Box 8757
Baltimore, Maryland 21240-0757
(301) 621-0390

US ISSN 0036-8741

Volume 30 Number 23 / December 8, 1992

TABLE OF CONTENTS

AERONAUTICS For related information see also *Astronautics.*

01 AERONAUTICS (GENERAL) **3929**

02 AERODYNAMICS **3929**
Includes aerodynamics of bodies, combinations, wings, rotors, and control surfaces; and internal flow in ducts and turbomachinery. For related information see also *34 Fluid Mechanics and Heat Transfer.*

03 AIR TRANSPORTATION AND SAFETY **3932**
Includes passenger and cargo air transport operations; and aircraft accidents. For related information see also *16 Space Transportation* and *85 Urban Technology and Transportation.*

04 AIRCRAFT COMMUNICATIONS AND NAVIGATION **3933**
Includes digital and voice communication with aircraft; air navigation systems (satellite and ground based); and air traffic control. For related information see also *17 Space Communications, Spacecraft Communications, Command and Tracking* and *32 Communications and Radar.*

05 AIRCRAFT DESIGN, TESTING AND PERFORMANCE **3934**
Includes aircraft simulation technology. For related information see also *18 Spacecraft Design, Testing and Performance* and *39 Structural Mechanics.* For land transportation vehicles see *85 Urban Technology and Transportation.*

06 AIRCRAFT INSTRUMENTATION **3935**
Includes cockpit and cabin display devices; and flight instruments. For related information see also *19 Space craft Instrumentation* and *35 Instrumentation and Photography.*

07 AIRCRAFT PROPULSION AND POWER **3938**
Includes prime propulsion systems and systems components, e.g., gas turbine engines and compressors; and onboard auxiliary power plants for aircraft. For related information see also *20 Spacecraft Propulsion and Power, 28 Propellants and Fuels,* and *44 Energy Production and Conversion.*

08 AIRCRAFT STABILITY AND CONTROL **3938**
Includes aircraft handling qualities; piloting; flight controls; and autopilots. For related information see also *05 Aircraft Design, Testing and Performance.*

09 RESEARCH AND SUPPORT FACILITIES (AIR) **3940**
Includes airports, hangars and runways; aircraft repair and overhaul facilities; wind tunnels; shock tubes; and aircraft engine test stands. For related information see also *14 Ground Support Systems and Facilities (Space).*

ASTRONAUTICS For related information see also *Aeronautics.*

12 ASTRONAUTICS (GENERAL) **3941**
For extraterrestrial exploration see *91 Lunar and Planetary Exploration.*

13 ASTRODYNAMICS ..... **N.A.**
Includes powered and free-flight trajectories; and orbital and launching dynamics.

14 GROUND SUPPORT SYSTEMS AND FACILITIES (SPACE) ..... **N.A.**
Includes launch complexes, research and production facilities; ground support equipment, e.g., mobile transporters; and simulators. For related information see also *09 Research and Support Facilities (Air).*

15 LAUNCH VEHICLES AND SPACE VEHICLES **3941**
Includes boosters; operating problems of launch/space vehicle systems; and reusable vehicles. For related information see also *20 Spacecraft Propulsion and Power.*

16 SPACE TRANSPORTATION **3941**
Includes passenger and cargo space transportation, e.g., shuttle operations; and space rescue techniques. For related information see also *03 Air Transportation and Safety* and *18 Spacecraft Design, Testing and Performance.* For space suits see *54 Man/System Technology and Life Support.*

17 SPACE COMMUNICATIONS, SPACECRAFT COMMUNICATIONS, COMMAND AND TRACKING . **N.A.**
Includes telemetry; space communications networks; astronavigation and guidance; and radio blackout. For related information see also *04 Aircraft Communications and Navigation* and *32 Communications and Radar.*

N.A.—no abstracts were assigned to this category for this issue.

18 SPACECRAFT DESIGN, TESTING AND PERFORMANCE **3942**
Includes satellites; space platforms; space stations; spacecraft systems and components such as thermal and environmental controls; and attitude controls. For life support systems see *54 Man/System Technology and Life Support.* For related information see also *05 Aircraft Design, Testing and Performance, 39 Structural Mechanics,* and *16 Space Transportation.*

19 SPACECRAFT INSTRUMENTATION **3943**
For related information see also *06 Aircraft Instrumentation* and *35 Instrumentation and Photography.*

20 SPACECRAFT PROPULSION AND POWER **3944**
Includes main propulsion systems and components, e.g., rocket engines; and spacecraft auxiliary power sources. For related information see also *07 Aircraft Propulsion and Power, 28 Propellants and Fuels, 44 Energy Production and Conversion,* and *15 Launch Vehicles and Space Vehicles.*

CHEMISTRY AND MATERIALS

23 CHEMISTRY AND MATERIALS (GENERAL) **3945**

24 COMPOSITE MATERIALS **3946**
Includes physical, chemical, and mechanical properties of laminates and other composite materials. For ceramic materials see *27 Nonmetallic Materials.*

25 INORGANIC AND PHYSICAL CHEMISTRY **3960**
Includes chemical analysis, e.g., chromatography; combustion theory; electrochemistry; and photochemistry. For related information see also *77 Thermodynamics and Statistical Physics.*

26 METALLIC MATERIALS **3966**
Includes physical, chemical, and mechanical properties of metals, e.g., corrosion; and metallurgy.

27 NONMETALLIC MATERIALS **3970**
Includes physical, chemical, and mechanical properties of plastics, elastomers, lubricants, polymers, textiles, adhesives, and ceramic materials. For composite materials see *24 Composite Materials.*

28 PROPELLANTS AND FUELS **3974**
Includes rocket propellants, igniters and oxidizers; their storage and handling procedures; and aircraft fuels. For related information see also *07 Aircraft Propulsion and Power, 20 Spacecraft Propulsion and Power,* and *44 Energy Production and Conversion.*

29 MATERIALS PROCESSING ..... **N.A.**
Includes space-based development of products and processes for commercial application. For biological materials see *55 Space Biology.*

ENGINEERING For related information see also *Physics.*

31 ENGINEERING (GENERAL) **3977**
Includes vacuum technology; control engineering; display engineering; cryogenics; and fire prevention.

32 COMMUNICATIONS AND RADAR **3978**
Includes radar; land and global communications; communications theory; and optical communications. For related information see also *04 Aircraft Communications and Navigation* and *17 Space Communications, Spacecraft Communications, Command and Tracking.* For search and rescue see *03 Air Transportation and Safety,* and *16 Space Transportation.*

33 ELECTRONICS AND ELECTRICAL ENGINEERING **3988**
Includes test equipment and maintainability; components, e.g., tunnel diodes and transistors; microminiaturization; and integrated circuitry. For related information see also *60 Computer Operations and Hardware* and *76 Solid-State Physics.*

34 FLUID MECHANICS AND HEAT TRANSFER **3994**
Includes boundary layers; hydrodynamics; fluidics; mass transfer and ablation cooling. For related information see also *02 Aerodynamics* and *77 Thermodynamics and Statistical Physics.*

35 INSTRUMENTATION AND PHOTOGRAPHY **4013**
Includes remote sensors; measuring instruments and gauges; detectors; cameras and photographic supplies; and holography. For aerial photography see *43 Earth Resources and Remote Sensing.* For related information see also *06 Aircraft Instrumentation* and *19 Spacecraft Instrumentation.*

36 LASERS AND MASERS **4015**
Includes parametric amplifiers. For related information see also *76 Solid-State Physics.*

37 MECHANICAL ENGINEERING **4017**
Includes auxiliary systems (nonpower); machine elements and processes; and mechanical equipment.

38 QUALITY ASSURANCE AND RELIABILITY **4020**
Includes product sampling procedures and techniques; and quality control.

39 STRUCTURAL MECHANICS **4020**
Includes structural element design and weight analysis; fatigue; and thermal stress. For applications see *05 Aircraft Design, Testing and Performance* and *18 Spacecraft Design, Testing and Performance.*

GEOSCIENCES For related information see also *Space Sciences.*

42 GEOSCIENCES (GENERAL) ..... **N.A.**

43 EARTH RESOURCES AND REMOTE SENSING **4024**
Includes remote sensing of earth resources by aircraft and spacecraft; photogrammetry; and aerial photography. For instrumentation see *35 Instrumentation and Photography.*

44 ENERGY PRODUCTION AND CONVERSION **4024**
Includes specific energy conversion systems, e.g., fuel cells; global sources of energy; geophysical conversion; and windpower. For related information see also *07 Aircraft Propulsion and Power, 20 Spacecraft Propulsion and Power,* and *28 Propellants and Fuels.*

45 ENVIRONMENT POLLUTION **4027**
Includes atmospheric, noise, thermal, and water pollution.

46 GEOPHYSICS **4031**
Includes aeronomy; upper and lower atmosphere studies; ionospheric and magnetospheric physics; and geomagnetism. For space radiation see *93 Space Radiation.*

47 METEOROLOGY AND CLIMATOLOGY **4032**
Includes weather forecasting and modification.

48 OCEANOGRAPHY **4034**
Includes biological, dynamic, and physical oceanography; and marine resources. For related information see also *43 Earth Resources and Remote Sensing.*

LIFE SCIENCES

51 LIFE SCIENCES (GENERAL) **4035**

52 AEROSPACE MEDICINE **4036**
Includes physiological factors; biological effects of radiation; and effects of weightlessness on man and animals.

53 BEHAVIORAL SCIENCES **4038**
Includes psychological factors; individual and group behavior; crew training and evaluation; and psychiatric research.

54 MAN/SYSTEM TECHNOLOGY AND LIFE SUPPORT **4039**
Includes human engineering; biotechnology; and space suits and protective clothing. For related information see also *16 Space Transportation.*

55 SPACE BIOLOGY ..... **N.A.**
Includes exobiology; planetary biology; and extraterrestrial life.

MATHEMATICAL AND COMPUTER SCIENCES

59 MATHEMATICAL AND COMPUTER SCIENCES (GENERAL) **4040**

60 COMPUTER OPERATIONS AND HARDWARE **4040**
Includes hardware for computer graphics, firmware, and data processing. For components see *33 Electronics and Electrical Engineering.*

61 COMPUTER PROGRAMMING AND SOFTWARE **4041**
Includes computer programs, routines, algorithms, and specific applications, e.g., CAD/CAM.

62 COMPUTER SYSTEMS **4050**
Includes computer networks and special application computer systems.

63 CYBERNETICS **4053**
Includes feedback and control theory, artificial intelligence, robotics and expert systems. For related information see also *54 Man/System Technology and Life Support.*

64 NUMERICAL ANALYSIS **4055**
Includes iteration, difference equations, and numerical approximation.

65 STATISTICS AND PROBABILITY **4059**
Includes data sampling and smoothing; Monte Carlo method; and stochastic processes.

66 SYSTEMS ANALYSIS **4060**
Includes mathematical modeling; network analysis; and operations research.

67 THEORETICAL MATHEMATICS **4060**
Includes topology and number theory.

PHYSICS For related information see also *Engineering.*

70 PHYSICS (GENERAL) **4061**
For precision time and time interval (PTTI) see *35 Instrumentation and Photography;* for geophysics, astrophysics or solar physics see *46 Geophysics, 90 Astrophysics,* or *92 Solar Physics.*

71 ACOUSTICS **4061**
Includes sound generation, transmission, and attenuation. For noise pollution see *45 Environment Pollution.*

72 ATOMIC AND MOLECULAR PHYSICS **4064**
Includes atomic structure, electron properties, and molecular spectra.

73 NUCLEAR AND HIGH-ENERGY PHYSICS **4069**
Includes elementary and nuclear particles; and reactor theory. For space radiation see *93 Space Radiation.*

74 OPTICS **4073**
Includes light phenomena and optical devices. For lasers see *36 Lasers and Masers.*

75 PLASMA PHYSICS **4077**
Includes magnetohydrodynamics and plasma fusion. For ionospheric plasmas see *46 Geophysics.* For space plasmas see *90 Astrophysics.*

76 SOLID-STATE PHYSICS **4081**
Includes superconductivity. For related information see also *33 Electronics and Electrical Engineering* and *36 Lasers and Masers.*

77 THERMODYNAMICS AND STATISTICAL PHYSICS **4087**
Includes quantum mechanics; theoretical physics; and Bose and Fermi statistics. For related information see also *25 Inorganic and Physical Chemistry* and *34 Fluid Mechanics and Heat Transfer.*

SOCIAL SCIENCES

80 SOCIAL SCIENCES (GENERAL) ..... **N.A.**
Includes educational matters.

81 ADMINISTRATION AND MANAGEMENT **4088**
Includes management planning and research.

82 DOCUMENTATION AND INFORMATION SCIENCE **4089**
Includes information management; information storage and retrieval technology; technical writing; graphic arts; and micrography. For computer documentation see *61 Computer Programming and Software.*

83 ECONOMICS AND COST ANALYSIS ..... **N.A.**
Includes cost effectiveness studies.

84 LAW, POLITICAL SCIENCE AND SPACE POLICY **4091**
Includes NASA appropriation hearings; aviation law; space law and policy; international law; international cooperation; and patent policy.

85 URBAN TECHNOLOGY AND TRANSPORTATION ..... **N.A.**
Includes applications of space technology to urban problems; technology transfer; technology assessment; and surface and mass transportation. For related information see *03 Air Transportation and Safety, 16 Space Transportation,* and *44 Energy Production and Conversion.*

SPACE SCIENCES For related information see also *Geosciences.*

88 SPACE SCIENCES (GENERAL) ..... **N.A.**

89 ASTRONOMY **4092**
Includes radio, gamma-ray, and infrared astronomy; and astrometry.

90 ASTROPHYSICS **4093**
Includes cosmology; celestial mechanics; space plasmas; and interstellar and interplanetary gases and dust. For related information see also *75 Plasma Physics.*

91 LUNAR AND PLANETARY EXPLORATION **4093**
Includes planetology; and manned and unmanned flights. For spacecraft design or space stations see *18 Spacecraft Design, Testing and Performance.*

92 SOLAR PHYSICS **4103**
Includes solar activity, solar flares, solar radiation and sunspots. For related information see *93 Space Radiation.*

93 SPACE RADIATION ..... **N.A.**
Includes cosmic radiation; and inner and outer earth's radiation belts. For biological effects of radiation see *52 Aerospace Medicine.* For theory see *73 Nuclear and High-Energy Physics.*

GENERAL

Includes aeronautical, astronautical, and space science related histories, biographies, and pertinent reports too broad for categorization; histories or broad overviews of NASA programs.

99 GENERAL **4103**

SUBJECT INDEX **I-1**

PERSONAL AUTHOR INDEX **I-79**

CORPORATE SOURCE INDEX **I-87**

CONTRACT NUMBER INDEX **I-101**

REPORT NUMBER INDEX **I-105**

ACCESSION NUMBER INDEX **I-113**

APPENDIX **A-1**

TYPICAL CITATION AND ABSTRACT

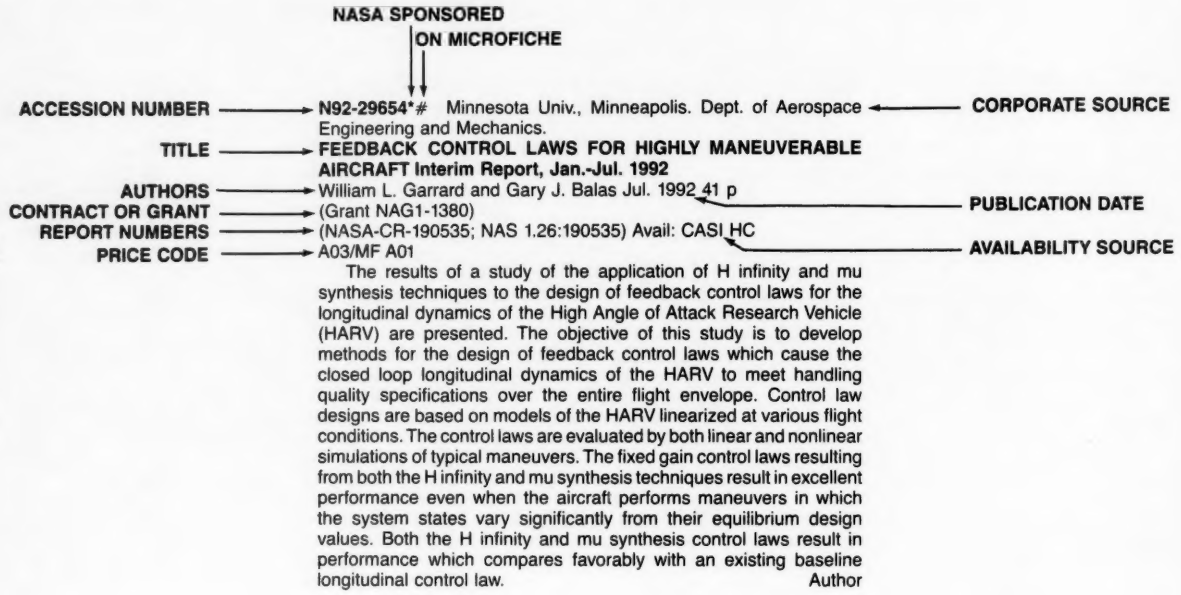
NASA SPONSORED
ON MICROFICHE
ACCESSION NUMBER
N92-29654*# Minnesota Univ., Minneapolis. Dept. of Aerospace Engineering and Mechanics.
CORPORATE SOURCE
TITLE
FEEDBACK CONTROL LAWS FOR HIGHLY MANEUVERABLE AIRCRAFT Interim Report, Jan.-Jul. 1992
AUTHORS
William L. Garrard and Gary J. Balas Jul. 1992 41 p
CONTRACT OR GRANT
(Grant NAG1-1380)
PUBLICATION DATE
REPORT NUMBERS
(NASA-CR-190535; NAS 1.26:190535) Avail: CASI HC
AVAILABILITY SOURCE
PRICE CODE
A03/MF A01
The results of a study of the application of H infinity and mu synthesis techniques to the design of feedback control laws for the longitudinal dynamics of the High Angle of Attack Research Vehicle (HARV) are presented. The objective of this study is to develop methods for the design of feedback control laws which cause the closed loop longitudinal dynamics of the HARV to meet handling quality specifications over the entire flight envelope. Control law designs are based on models of the HARV linearized at various flight conditions. The control laws are evaluated by both linear and nonlinear simulations of typical maneuvers. The fixed gain control laws resulting from both the H infinity and mu synthesis techniques result in excellent performance even when the aircraft performs maneuvers in which the system states vary significantly from their equilibrium design values. Both the H infinity and mu synthesis control laws result in performance which compares favorably with an existing baseline longitudinal control law.
Author

VOLUME 30 NUMBER 23 / DECEMBER 8, 1992

Scientific and Technical Aerospace Reports

A Semimonthly Publication of the National Aeronautics and Space Administration

01 AERONAUTICS (GENERAL)

N92-32691# Air Force Inst. of Tech., Wright-Patterson AFB, OH.
CHINA'S AEROSPACE INDUSTRY: TECHNOLOGY, FUNDING, AND MODERNIZATION M.S. Thesis
Bret D. Johnson 1992 55 p
(AD-A252618; AFIT/CI/CIA-92-028) Avail: CASI HC A04/MF A01

Modernization in China's military industry is a vast subject. This paper will seek to understand the method of modernization by looking at one portion of that industry, the aviation branch. The aviation industry has undergone some critical changes within the last decade which make it a critical element in China's overall modernization plans. The importation of technology has taken on many different forms and has been driven by different forces. The aviation industry's actions determine the direction and technological level of both the military and economic sectors in China. Aviation, as is the case in most other countries, is a booming business. The subject of technology transfers in and out of China cannot fully be understood unless one understands the methods in which China has acquired technology since the establishment of the PRC. The mechanisms include: indigenous R and D and production, co-production with the USSR, modifications to Chinese or foreign systems, reverse engineering, co-production with other countries, and captured systems. These mechanisms for obtaining military technology can be a guideline to understanding the different periods of Chinese technology transfer and the motives of the government with regards to technology transfer at those certain periods of time in history. GRA

N92-33176# Federal Aviation Administration, Washington, DC.
FEDERAL AVIATION REGULATIONS. PART 91: GENERAL OPERATING AND FLIGHT RULES
Feb. 1992 218 p
(PB92-197334) Avail: CASI HC A10/MF A03; SOD HC

Given here are general flight rules, visual flight rules, and instrument flight rules. Regulations are given covering special flight operations, aircraft maintenance, preventive maintenance, alterations, large and turbine-powered multiengine aircraft, additional equipment and operating requirements for large and transport category aircraft, foreign aircraft operations and operations of U.S. registered civil aircraft outside the United States, and operating noise limits and waivers. Author

02 AERODYNAMICS

Includes aerodynamics of bodies, combinations, wings, rotors, and control surfaces; and internal flow in ducts and turbomachinery.

For related information see also *34 Fluid Mechanics and Heat Transfer.*

N92-32422*# National Aeronautics and Space Administration. Ames Research Center, Moffett Field, CA.
POTENTIAL FLOW THEORY AND OPERATION GUIDE FOR THE PANEL CODE PMARC
Dale L. Ashby, Michael R. Dudley, Steve K. Iguchi (San Diego State Univ., CA.), Lindsey Browne (San Diego State Univ., CA.), and Joseph Katz (San Diego State Univ., CA.) Jan. 1991 86 p
(RTOP 505-61-71)
(NASA-TM-102851; A-90244; NAS 1.15:102851) Avail: CASI HC A05/MF A01

The theoretical basis for PMARC, a low-order potential-flow panel code for modeling complex three-dimensional geometries, is outlined. Several of the advanced features currently included in the code, such as internal flow modeling, a simple jet model, and a time-stepping wake model, are discussed in some detail. The code is written using adjustable size arrays so that it can be easily redimensioned for the size problem being solved and the computer hardware being used. An overview of the program input is presented, with a detailed description of the input available in the appendices. Finally, PMARC results for a generic wing/body configuration are compared with experimental data to demonstrate the accuracy of the code. The input file for this test case is given in the appendices. Author

N92-32479 ESDU International Ltd., London (England).
AERODYNAMIC CENTRE OF WING-BODY COMBINATIONS Abstract Only
Jul. 1992 17 p
(ESDU-92024; ISBN-0-85679-829-0) Avail: ESDU

ESDU 92024 applies to a parallel-sided axisymmetric body with a truncated rear-end and a straight-tapered mid-set wing in subsonic or supersonic flow at low angles of attack. The wing may have moderate trailing-edge sweep of up to 10 degrees. The calculation of the aerodynamic center requires the pitching-moment-curve slope for the body alone (for which ESDU 89008 or 90034 may be used), the wing-alone lift-curve slope (for which at subsonic speeds ESDU 70011 may be used or supersonically ESDU 70012), and the lift-curve of the configuration together with interference factors for the effect of body-lift on the wing and wing-lift on the body (for which ESDU 91007 may be used). The other quantity required is the aerodynamic center of the interference load, for which this document provides both graphically and as a complete set of equations the required data. For missile-type configurations the method is accurate to within 2 percent of body length. The use of the method is illustrated by means of a fully worked example. For configurations with smoothly tapered afterbodies, such as found on transport aircraft, ESDU 76015 provides a method for subcritical speeds. ESDU

N92-32480*# National Aeronautics and Space Administration. Langley Research Center, Hampton, VA.
A METHOD FOR DESIGNING BLENDED WING-BODY CONFIGURATIONS FOR LOW WAVE DRAG
Raymond L. Barger Sep. 1992 19 p
(RTOP 505-59-53-01)
(NASA-TP-3261; L-17095; NAS 1.60:3261) Avail: CASI HC A03/MF A01

A procedure for tailoring a blended wing-body configuration to reduce its computed wave drag is described. The method utilizes an iterative algorithm within the framework of first-order linear theory. Four computed examples are included. In each case, the zero-lift wave drag was reduced without an increase in the drag due to lift. Author

N92-32494*# Pennsylvania State Univ., University Park. Dept. of Mechanical Engineering.
SWEPT SHOCK/BOUNDARY LAYER INTERACTION EXPERIMENTS IN SUPPORT OF CFD CODE VALIDATION
Final Report, 15 Jan. 1989 - 14 Jan. 1992
G. S. Settles and Y. Lee Jul. 1992 21 p
(Grant NAG2-592)
(NASA-CR-190583; NAS 1.26:190583) Avail: CASI HC A03/MF A01

Research on the topic of shock wave/turbulent boundary-layer interaction was carried out during the past three years at the Penn State Gas Dynamics Laboratory. This report describes the experimental research program which provides basic knowledge and establishes new data on heat transfer in swept shock wave/boundary-layer interactions. An equilibrium turbulent boundary-layer on a flat plate is subjected to impingement by swept planar shock waves generated by a sharp fin. Five different interactions with fin angle ranging from 10 deg to 20 deg at freestream Mach numbers of 3.0 and 4.0 produce a variety of interaction strengths from weak to very strong. A foil heater generates a uniform heat flux over the flat plate surface, and miniature thin-film-resistance sensors mounted on it are used to measure the local surface temperature. The heat convection equation is then solved for the heat transfer distribution within an interaction, yielding a total uncertainty of about +/- 10 percent. These experimental data are compared with the results of numerical Navier-Stokes solutions which employ a k-epsilon turbulence model. Finally, a simplified form of the peak heat transfer correlation for fin interactions is suggested. Author

N92-32648*# Arizona Univ., Tucson. Dept. of Aerospace and Mechanical Engineering.
LEADING-EDGE RECEPTIVITY FOR BLUNT-NOSE BODIES
Semiannual Progress Report
P. W. Hammerton and E. J. Kerschen Jul. 1992 10 p
(Grant NAG1-1135)
(NASA-CR-190563; NAS 1.26:190563) Avail: CASI HC A02/MF A01

Boundary-layer receptivity in the leading edge region for bodies with blunt leading edges is investigated in this research program. Receptivity theory provides the link between the unsteady disturbance environment in the freestream and the initial amplitudes of instability waves in the boundary layer. This is a critical problem which must be addressed in order to develop more accurate prediction methods for boundary-layer transition. D.R.D.

N92-32651# Wright Lab., Wright-Patterson AFB, OH.
VORTEX FLOW VISUALIZATION USING COLORED AND FLUORESCENT DYES ON FLAT PLATE DELTA WING WITH LEADING EDGE EXTENSION
Scott P. LeMay May 1992 22 p
(AD-A251139; WL-TM-92-323) Avail: CASI HC A03/MF A01

A water tunnel study was conducted in the Wright Laboratory 2ft x 2ft water tunnel to examine the vortex flowfield about a 60 deg flat plate diamond delta wing with an 80 deg leading edge extension (LEX). Flood light illuminated colored dye and laser light sheet illuminated fluorescent dye were used to visualize light sheet illuminated fluorescent dye were used to visualize the wing and LEX vortex core trajectories and vortex breakdown locations. The fluorescent dye flow visualization technique proved to be an excellent tool for examining the structure of vortex breakdown in detail. Angle of attack was varied between 10 deg and 45 deg for sideslip angles of 0 deg, 5 deg, and 10 deg, and the freestream Reynolds number was approximately 31,000 based upon model length. At angles of attack above 10 deg and zero sideslip, interaction was observed between the LEX and wing vortices. At 30 deg angle of attack, asymmetric breakdown of the LEX vortices occurred. At sideslip angles of 5 deg and 10 deg, large asymmetries in the vortex flowfield were present. GRA

N92-32673# National Aerospace Lab., Amsterdam (Netherlands). Fluid Dynamics Div.
MODELING AND NUMERICAL SIMULATION OF VORTEX FLOW IN AERODYNAMICS
H. W. M. Hoeijmakers 15 Dec. 1990 53 p Presented at the AGARD Fluid Dynamics Panel Symposium on Vortex Flow Aerodynamics, Scheveningen, Netherlands, 1-4 Oct. 1990 Previously announced as N92-12997 Sponsored by Netherlands Agency for Aerospace Programs
(NLR-TP-91154-U; ETN-92-92000) Avail: CASI HC A04/MF A01

A review of mathematical models of different levels of approximation for and their application to the numerical simulation of vortical type of flows occurring in subsonic and transonic aircraft aerodynamics is presented. Computational methods for predicting the downstream development of vortex wakes as well as methods for simulating the detailed characteristics of configurations with leading edge or body vortices are covered with the emphasis on the latter. Developments of the methods used at present are discussed. The possibilities, limitations and prospects of improvement of the methods are indicated and results of different methods are discussed. Some more fundamental aspects of the numerical simulation such as separation at sharp and round leading edges, separation at a smooth part of the surface, the structure of the leading edge vortex and the merging of the vortices, are considered. ESA

N92-32730# National Aerospace Lab., Amsterdam (Netherlands). Informatics Div.
NEW CONCEPTS FOR MULTI-BLOCK GRID GENERATION FOR FLOW DOMAINS AROUND COMPLEX AERODYNAMIC CONFIGURATIONS
S. P. Spekreijse, J. W. Boerstoel, and P. L. Vitagilano (Alenia Spazio S.p.A., Naples, Italy) 15 Feb. 1991 17 p Presented at the 3rd International Conference on Numerical Grid Generation in Computational Fluid Mechanics and Related Fields, Barcelona, Spain, 3-7 Jun. 1991 Previously announced in IAA as A92-47079
(Contract NIVR-01604-N)
(NLR-TP-91046-U; ETN-92-91994) Avail: CASI HC A03/MF A01

A multiblock grid generation procedure that is suitable for the construction of multiblock grids for numerical simulations of flows around complex aerodynamic configurations is described. The major new concepts are topology and geometry of block decomposition specified first by an interactive domain model, the use of compound edges and faces, grid embedding, grid lines only C continuous over block faces, and the use of a biharmonic solver for grid generation in faces. ESA

N92-32732# National Aerospace Lab., Amsterdam (Netherlands). Fluid Dynamics Div.
AN EXPERIMENTAL STUDY OF THE FLOW OVER A SHARP-EDGED DELTA WING AT SUBSONIC AND TRANSONIC SPEEDS
A. Elsenaar and H. W. M. Hoeijmakers 28 Feb. 1991 25 p Presented at the AGARD Fluid Dynamics Panel Symposium on Vortex Flow Aerodynamics, Scheveningen, Netherlands, 1-4 Oct. 1990 Previously announced as N92-13011 Sponsored by Netherlands Agency for Aerospace Programs
(NLR-TP-91117-U; ETN-92-91997) Avail: CASI HC A03/MF A01

The flow about a sharp edged cropped delta wing is investigated experimentally. The experiment comprised detailed surface pressure measurements at low subsonic, transonic and low supersonic freestream Mach numbers for angles of attack up to 27 deg. The major part of the measurements were carried out at a Reynolds number of 9 million, but some data was also obtained at lower and at higher Reynolds numbers. The investigation included continuous schlieren flow field visualization as well as surface flow visualizations at a limited number of free stream conditions. The analysis of the measured data embraced flow field phenomena such as primary separation and the formation of the

leading edge vortex, secondary separation and the formation of the secondary vortex, shock waves and the onset of vortex breakdown. The influence of Mach number, incidence and Reynolds number on these flow features is considered. ESA

N92-32769# Institut de Mecanique de Grenoble (France).
NUMERICAL SIMULATION OF TURBULENCE AT THE BACK OF THE AIRPLANE Final Report [SIMULATION NUMERIQUE DE LA TURBULENCE DANS LES ARRIERE-CORPS. RAPPORT FINAL]
M. Lesieur 1991 39 p In FRENCH
(Contract DRET-89-204)
(ETN-92-91664) Avail: CASI HC A03/MF A01

Numerical experiments for a two dimensional flat jet and for a three dimensional circular jet were performed. The results revealed that the effect of compressibility, and of the density gradient on the initial flow profile produce, during the formation of the first vortices, the same effects as those observed in the case of the two dimensional mixture layer. It was also observed that the cold jet develops more rapidly than the hot jet, and that when the Mach number increases, the time required to form and to develop vortices increases. After the formation of the Karman vortex street, the description of the flat jet as a double mixture layer is not justified. The compression zones tend to disappear. Shocks were observed for M(sub r) = 2.5. In the circular jet experiment, a helical mode was observed. From M(sub r) = 0.6 to M(sub r) = 2, the time required to observe the first helical structures and the wavelength of the fundamental mode are two fold. Following the development structures, the flow becomes locally turbulent and an energy cascade at (K(sub x)exp -5/3) is established. A simulation study is carried out at high Reynolds number for the three dimensional circular jet at 0.6 Mach number. ESA

N92-32773# Office National d'Etudes et de Recherches Aerospatiales, Paris (France). Direction de l'Aerodynamique.
RESEARCH ON SOME CENTERED IMPLICIT METHODS FOR CALCULATING TRANSONIC FLOWS BY SOLVING NAVIER-STOKES EQUATIONS Final Summary Report [RECHERCHES SUR DES METHODES IMPLICITES CENTREES POUR LE CALCUL D'ECOULEMENTS TRANSSONIQUES A PARTIR DE LA RESOLUTION DES EQUATIONS DE NAVIER-STOKES. RAPPORT DE SYNTHESE FINAL]
Sylvie Plot-Locatelli Oct. 1991 59 p In FRENCH
(Contract DRET-89-34-001)
(ONERA-RSF-24/1408-AY-150A; ETN-92-91671) Avail: CASI HC A04/MF A01

The development and operation of a simplified implicit phase, occurring during the solution of two dimensional Navier-Stokes equations, are presented. The equations to be solved and the resolution method are described. The numerical calculation of the implicit phase is presented. Two cases involving turbulent transonic flows are studied. The improvement of the accuracy concerning the convergence towards a steady solution was tested. These results and those from the explicit code are compared, with and without multiple grid accelerators. The time required by the central processing unit to calculate the converging solution by using the implicit method is: equal to 3, when compared to the explicit method with multiple grid phases; and of about 1.4 when compared to the explicit method with multiple grid phase. ESA

N92-32782 ESDU International Ltd., London (England).
LIFT AND ROLLING MOMENT DUE TO SPOILERS ON WINGS WITH TRAILING-EDGE FLAPS DEFLECTED AT SUBSONIC SPEEDS
1 Jan. 1992 16 p Supplement to ESDU-90030
(ESDU-92002-Suppl; ESDU-90030; ISBN-0-85679-807-X) Avail: ESDU

ESDU 92002 provides an empirical method of estimating the lift and rolling moment due to upper-surface spoiler deflection on a wing with flaps deployed. The method is to determine the additional decrement over that obtained when the spoiler is deflected on the plain wing (calculated using ESDU 90030) and the corresponding change in rolling moment. The method applies to the same range of wing planform and spoiler parameters as the methods of 90030 for plain, single- or double-slotted flaps having flap/wing chord ratio of 0.2 to 0.4 and with flap deflections up to 60 degrees. It applies for practical Reynolds number and Mach number up to 0.25, although it will apply up to Mach numbers of 0.5 for flap deflections of 10 degrees or less. From a comparison with test data, the method predicts total lift coefficient decrement within 0.1 and total rolling moment coefficient within 0.01 with no venting from the lower to the upper wing surface. Some guidance is included on the effect of venting, which can increase spoiler effectiveness by 30 percent for large spoiler deflections. Two worked examples illustrated the use of the data. ESDU

N92-32800# Office National d'Etudes et de Recherches Aerospatiales, Paris (France). Direction de l'Aerodynamique.
EXPERIMENTAL STUDY OF THE VORTEX SYSTEM GENERATED BY A MISSILE FUSELAGE AT INCIDENCE. PART 3: THREE DIRECTIONAL LASER VELOCIMETRY MEASUREMENTS [ETUDE EXPERIMENTALE DU SYSTEME TOURBILLONAIRE ENGENDRE PAR UN FUSELAGE DE MISSILE EN INCIDENCE. TROISIEME PARTIE: MESURES PAR VELOCIMETRIE LASER TRI DIRECTIONNELLE]
P. Molton and D. Barberis Mar. 1991 35 p In FRENCH
(Contract DRET-89-34-001)
(ONERA-RT-47/1147-AY-146A-Pt-3; ETN-92-92082) Avail: CASI HC A03/MF A01

Results of experiments carried out in a supersonic wind tunnel to validate a three dimensional vortex flow calculation code are presented. The three velocity components and the Reynolds stress components for Mach(infinity) = 2 were determined. Flow distribution visualizations were achieved by laser tomoscopy in seven planes in order to determine the problems of laser velocimetry measurements. For comparison with the preceding tests, wall flow visualization and wall pressure measurements were carried out for an incidence angle of 20 deg. The results were compared with measurements with a five hole probe of the preceding tests. ESA

N92-32811# Bombardier, Inc., Montreal (Quebec). Canadair Div.
FURTHER DEVELOPMENT OF THE CANAERO COMPUTER CODE TO INCLUDE PROPULSOR MODELLING
John T. Conway Mar. 1990 130 p
(Contract DREA-W7707-8-1140-01-SC)
(DREA-CR-90-425; CTN-92-60357) Avail: CASI HC A07/MF A02

This report documents the development at Canadair of a propeller model for the CANAERO code. The CANAERO code is a low order panel method which uses a vortex sheets lifting model. CANAERO represents the geometry of a configuration by replacing the external surface with a large number of flat quadrilateral panels. This document reports on further development, implementation, and testing of the CANAERO computer code to include propulsor modelling. The formulation, implementation, and testing of the CANAERO actuator disk with swirl propulsor model is described, and the mathematical details of a theory of slipstream contraction used in the model are given. This now enables the code to calculate the propeller effects on overall aircraft or submarine performance without great increases in computer time compared to the non-propeller case. Results are given for the code for a submarine hull plus sail configuration with an aft-mounted propeller, a simple wing immersed in a propeller slipstream, and for an axisymmetrical shrouded propeller configuration. No convergence difficulties were encountered with any of these configurations. An updated user's guide and input data description are included in the report, together with sample datasets. Author (CISTI)

N92-32900# Army Cold Regions Research and Engineering Lab., Hanover, NH.
EFFECTS OF THE ABRASIVENESS OF TEST AND TRAINING SITE SOILS ON PARACHUTE LIFE

Austin W. Hogan May 1992 33 p
(AD-A252389; CRREL-SR-92-11) Avail: CASI HC A03/MF A01

The failure of individual parachutes, as a function of service life and exposure, has long been of interest. Examination of a sampling of parachutes used by the U.S. Army and the U.S. Forest Service 'Smokejumpers' indicates that suspension lines begin to degrade during the first 30 users. Laboratory tests confirmed that suspension line degradation is the most common way that parachutes fail, and that this degradation is primarily a result of the accumulation of grit within the suspension lines. It was concluded that inherent geological differences in soil properties would alter the service life of personnel parachutes deployed in varying geographic locales. This report describes the physical properties of surface soil samples collected in varying locales, at established drop zones, maneuver areas, test centers and from the test pit used by Rodier et al. (1989). Table 1 presents the soil specimens provided for analysis. Representative specimens were collected from the surface, sealed in plastic bags and transported to the laboratory. GRA

N92-33063*# Texas A&M Univ., College Station.
FURTHER WIND TUNNEL INVESTIGATION OF THE SM701 AIRFOIL WITH AILERON AND TURBULATORS Final Report
Gregory Steen, Oran Nicks, and Michael Heffner Aug. 1992 17 p
(Grant NAG1-1260; TEES Proj. 30540-AE)
(NASA-CR-190702; NAS 1.26:190702) Avail: CASI HC A03/MF A01

Wind tunnel tests were performed on a two-dimensional model of the SM701 airfoil designed for use on the World Class gliders. The test covered a range of Reynolds numbers from 500,000 to 1.7 million. Aerodynamic forces and moments were measured with an external balance. Momentum loss method measurements of the section drag coefficient were also made. Flow visualization techniques provided information on transition from laminar to turbulent flow. Lift, drag, and pitching moment were analyzed and comparisons were made with predicted and previously obtained experimental data. The effects of V-tape turbulators for use in turbulent drag reduction were studied. The performance of a 25 percent chord aileron deflected through plus or minus 20 degrees was researched. The model was designed, constructed, and tested by students at Texas A&M University. Author

03 AIR TRANSPORTATION AND SAFETY

Includes passenger and cargo air transport operations; and aircraft accidents.

For related information see also *16 Space Transportation* and *85 Urban Technology and Transportation.*

N92-32455# National Transportation Safety Board, Washington, DC.
AIRCRAFT ACCIDENT REPORT: L'EXPRESS AIRLINES, INC., FLIGHT 508, BEECH C99, N7217L WEATHER ENCOUNTER AND CRASH NEAR BIRMINGHAM, ALABAMA, JULY 10, 1991
3 Mar. 1992 143 p
(PB92-910401; NTSB/AAR-92/01) Avail: CASI HC A07/MF A02

This report explains the weather encounter and crash of L'Express Flight 508 while the airplane was conducting an instrument landing system approach on runway 5 at the Birmingham Airport, Birmingham, Alabama. The safety issues discussed in this report include pilot training in recognizing thunderstorm hazards and recovering from unusual attitudes, radar interpretation, and the relaying of complete weather information to pilots by air traffic controllers. Recommendations concerning these issues were made to the Federal Aviation Administration. Author

N92-32606*# Clemson Univ., SC. Radar Systems Lab.
REAL-TIME PROCESSING OF RADAR RETURN ON A PARALLEL COMPUTER Final Report
David D. Aalfs Aug. 1992 84 p
(Grant NGT-50414; RTOP 505-64-12-02)
(NASA-CR-4456; NAS 1.26:4456; CU-TR-14; DOT/FAA/RD-92/20) Avail: CASI HC A05/MF A01

NASA is working with the FAA to demonstrate the feasibility of pulse Doppler radar as a candidate airborne sensor to detect low altitude windshears. The need to provide the pilot with timely information about possible hazards has motivated a demand for real-time processing of a radar return. Investigated here is parallel processing as a means of accommodating the high data rates required. A PC based parallel computer, called the transputer, is used to investigate issues in real time concurrent processing of radar signals. A transputer network is made up of an array of single instruction stream processors that can be networked in a variety of ways. They are easily reconfigured and software development is largely independent of the particular network topology. The performance of the transputer is evaluated in light of the computational requirements. A number of algorithms have been implemented on the transputers in OCCAM, a language specially designed for parallel processing. These include signal processing algorithms such as the Fast Fourier Transform (FFT), pulse-pair, and autoregressive modelling, as well as routing software to support concurrency. The most computationally intensive task is estimating the spectrum. Two approaches have been taken on this problem, the first and most conventional of which is to use the FFT. By using table look-ups for the basis function and other optimizing techniques, an algorithm has been developed that is sufficient for real time. The other approach is to model the signal as an autoregressive process and estimate the spectrum based on the model coefficients. This technique is attractive because it does not suffer from the spectral leakage problem inherent in the FFT. Benchmark tests indicate that autoregressive modeling is feasible in real time. Author

N92-32941# Battelle Columbus Labs., OH.
A REVIEW AND DISCUSSION OF FLIGHT MANAGEMENT SYSTEM INCIDENTS REPORTED TO THE AVIATION SAFETY REPORTING SYSTEM Final Report, Oct. 1990 - Jul. 1991
Robert S. Dodd, Donald Eldredge, and Susan J. Mangold Feb. 1992 77 p Sponsored by FAA
(AD-A252438; DOT-VNTSC-FAA-92-2; DOT/FAA/RD-92/2)
Avail: CASI HC A05/MF A01

This report covers the activities related to the description, classification, and analysis of the types and kinds of flight crew errors, incidents, and actions, as reported to the Aviation Safety Reporting System (ASRS) database, that can occur as a result of using the Flight Management Systems (FMS's) to fly within the National Airspace System (NAS). The analysis of the ASRS FMS-related database reports was conducted for the purpose of determining the types and kinds of design-induced problems that flight crews are having with FMS's that can result in the occurrence of errors, incidents, and other operational problems. It was believed that review of these reports would provide a useful background and understanding of the FMS use domain (i.e., the flight environment) and offer a window into the cockpit setting, enabling the identification of categories of difficulties that flight crews appear to have with the FMS and its subsystems. Those elements of the FMS operational logic that are identified as potentially problematic will then be investigated in more detail in the Description and Characterization Study that is also ongoing. Together, these two documents will result in a clearer understanding of the design-related FMS contributors to pilot error. GRA

N92-33005# Federal Aviation Administration, Atlantic City, NJ.
BIRD INGESTION INTO LARGE TURBOFAN ENGINES Interim Report
Howard Banilower and Colin Goodall (Princeton Univ., NJ.) May 1992 77 p
(DOT/FAA/CT-91/17) Avail: CASI HC A05/MF A01

The Federal Aviation Administration (FAA) is conducting a study

of bird ingestion into certain modern, large high-bypass turbofan engines. The engines under consideration were certificated to current FAA standards and are installed in A300, A310, A320, B747, B757, B767, DC10, and MD11 aircraft in commercial service worldwide. Data were collected during 1989-1991 by the principle manufacturers of such engines. Analysis of the initial 381 aircraft ingestion events is given, with emphasis on the kinds and numbers of ingested birds and the adverse effects of bird ingestion on aircraft engines and flights. Author

N92-33080*# National Aeronautics and Space Administration. Ames Research Center, Moffett Field, CA.
CTAS: COMPUTER INTELLIGENCE FOR AIR TRAFFIC CONTROL IN THE TERMINAL AREA
Heinz Erzberger Jul. 1992 6 p
(RTOP 505-64-13)
(NASA-TM-103959; A-92156; NAS 1.15:103959) Avail: CASI HC A02/MF A01

A system for the automated management and control of arrival traffic, referred to as the Center-TRACON Automation System (CTAS), has been designed by the ATC research group at NASA Ames research center. In a cooperative program, NASA and the FAA have efforts underway to install and evaluate the system at the Denver and Dallas/Ft. Worth airports. CTAS consists of three types of integrated tools that provide computer-generated intelligence for both Center and TRACON controllers to guide them in managing and controlling arrival traffic efficiently. One tool, the Traffic Management Advisor (TMA), establishes optimized landing sequences and landing times for aircraft arriving in the center airspace several hundred miles from the airport. In TRACON, TMA frequencies missed approach aircraft and unanticipated arrivals. Another tool, the Descent Advisor (DA), generates clearances for the center controllers handling at crossing times provided by TMA. In the TRACON, the final approach spacing tool (FAST) provides heading and speed clearances that produce and accurately spaced flow of aircraft on the final approach course. A data base consisting of aircraft performance models, airline preferred operational procedures and real time wind measurements contribute to the effective operation of CTAS. Extensive simulator evaluations of CTAS have demonstrated controller acceptance, delay reductions, and fuel savings. Author

N92-33194*# National Aeronautics and Space Administration. Ames Research Center, Moffett Field, CA.
ANALYSIS OF DELAY REDUCING AND FUEL SAVING SEQUENCING AND SPACING ALGORITHMS FOR ARRIVAL TRAFFIC
Frank Neuman and Heinz Erzberger Oct. 1991 44 p Supersedes NASA-TM-102795
(RTOP 505-64-13)
(NASA-TM-103880; A-91203; NAS 1.15:103880) Avail: CASI HC A03/MF A01

The air traffic control subsystem that performs sequencing and spacing is discussed. The function of the sequencing and spacing algorithms is to automatically plan the most efficient landing order and to assign optimally spaced landing times to all arrivals. Several algorithms are described and their statistical performance is examined. Sequencing brings order to an arrival sequence for aircraft. First-come-first-served sequencing (FCFS) establishes a fair order, based on estimated times of arrival, and determines proper separations. Because of the randomness of the arriving traffic, gaps will remain in the sequence of aircraft. Delays are reduced by time-advancing the leading aircraft of each group while still preserving the FCFS order. Tightly spaced groups of aircraft remain with a mix of heavy and large aircraft. Spacing requirements differ for different types of aircraft trailing each other. Traffic is reordered slightly to take advantage of this spacing criterion, thus shortening the groups and reducing average delays. For heavy traffic, delays for different traffic samples vary widely, even when the same set of statistical parameters is used to produce each sample. This report supersedes NASA TM-102795 on the same subject. It includes a new method of time-advance as well as an efficient method of sequencing and spacing for two dependent runways. Author

04 AIRCRAFT COMMUNICATIONS AND NAVIGATION

Includes digital and voice communication with aircraft; air navigation systems (satellite and ground based); and air traffic control.

For related information see also *17 Space Communications, Spacecraft Communications, Command and Tracking* and *Communications and Radar.*

N92-32424*# National Aeronautics and Space Administration. Ames Research Center, Moffett Field, CA.
VISION-BASED RANGE ESTIMATION USING HELICOPTER FLIGHT DATA
Philip N. Smith, Banavar Sridhar, and Bassam Hussien Jun. 1992 20 p
(RTOP 505-64-36)
(NASA-TM-103930; A-92085; NAS 1.15:103930) Avail: CASI HC A03/MF A01

Pilot aiding during low-altitude flight depends on the ability to detect and locate obstacles near the helicopter's intended flightpath. Computer-vision-based methods provide one general approach for obstacle detection and range estimation. Several algorithms have been developed for this purpose, but have not been tested with actual flight data. This paper presents results obtained using helicopter flight data with a feature-based range estimation algorithm. A method for recursively estimating range using a Kalman filter with a monocular sequence of images and knowledge of the camera's motion is described. The helicopter flight experiment and four resulting datasets are discussed. Finally the performance of the range estimation algorithm is explored in detail based on comparison of the range estimates with true range measurements collected during the flight experiment. Author

N92-32537# Mitre Corp., McLean, VA.
SAFETY STUDY OF TCAS 2 FOR LOGIC VERSION 6.04
Michael P. McLaughlin and Andrew D. Zeitlin Jul. 1992 90 p
(Contract DTFA01-89-C-00001)
(DOT/FAA/RD-92/22) Avail: CASI HC A05/MF A01

A system safety study of Traffic Alert and Collision Avoidance System 2 (TCAS 2) was performed to compare the safety of logic version 6.04 with the present version 6.0. The study uses a considerable body of encounter data extracted from Automated Radar Terminal System (ARTS) ground-based radar data at eight US sites. Encounter geometries are modeled using the statistics of the observed data. The performance of TCAS logic is simulated using both complete logic versions. The perceived separation statistics are combined with altimetry error models to calculate risk for each encounter geometry. These results are combined in the proportions of encounter geometries found in the airspace at each site. Using a fault tree for the critical near midair collision event, the risk ratio is calculated for each logic version relative to the risk of not using TCAS. This result is discussed in the context of the improved compatibility of the newer logic with respect to the Air Traffic Control System, which would increase overall safety. Author

N92-32830# National Aerospace Lab., Amsterdam (Netherlands). Flight Div.
DEVELOPMENT OF NEW FLIGHT PROCEDURES FOR THE MICROWAVE LANDING SYSTEM (MLS)
L. J. J. Erkelens 23 Apr. 1991 44 p Presented at the Sipke Wynia Symposium 1991 on Environmental Issues and Pollution in Aviation, Haarlem, Netherlands, 11 Apr. 1991
(NLR-TP-91156-U; ETN-92-92001) Avail: CASI HC A03/MF A01

The shortcomings of the current Instrument Landing System (ILS), which have led to the development of the Microwave Landing System (MLS), are summarized. The basic principles of MLS are

outlined. The wide coverage volume of MLS, in both azimuth and elevation, enables new flight procedures to be defined, taking into account such patterns as noise abatement, obstacle clearance, and airspace restrictions. Research on developing approach, interception, and departure procedures for the MLS, which consists of both flight trials with laboratory aircraft and flight simulator investigations on the research flight simulator, is outlined. Focus is on a recently completed flight simulator investigation on operational curved approach feasibility for a wide body type of aircraft. The test objectives of the 1990 flight simulation program are discussed. ESA

N92-32845# Toronto Univ. (Ontario). Inst. for Aerospace Studies.
AN EVALUATION OF DECELERATING IFR APPROACHES UTILIZING A HELICOPTER FLIGHT SIMULATOR
L. D. Reid, S. Advani, and J. H. DeLeeuw Jul. 1990 218 p
(Contract W2207-7-AF69/01-SS)
(CTN-92-60348) Avail: CASI HC A10/MF A03

This project involved development of a helicopter flight simulator and its application to study instrumented flight rules (IFR) landing approaches. The helicopter simulator was implemented on the University of Toronto Institute for Aerospace Studies (UTIAS) Flight Research Simulator. It employed all the major subsystems of that facility including the motion systems, visual display system, sound system, and computer system. In addition, the flight controls and seat of a Bell 205 helicopter were installed and interfaced with the flight computer. An electronic flight instrumentation system (EFIS) was developed to act as the pilot helicopter interface. A side arm controller was also included in the simulation. The helicopter flight equations were based on an ARMCOP software package. The system was tuned with the help of an experienced Bell 205 test pilot. The simulated flight test project was directed towards establishing the ability of the simulator to duplicate handling qualities results achieved in actual flight. The task selected was that of decelerating IFR approaches using flight control systems and a three cue flight director. A group of 6 evaluation pilots repeated flying tasks previously completed in an actual Bell 205. Good agreement between the simulator and flight test data was achieved except for one configuration. This configuration was found to be easier to fly in the simulator. The cause of this was felt to be incorrect simulation of the corresponding flight control system.
Author (CISTI)

N92-32849# Institute for Aerospace Research, Ottawa (Ontario). Flight Research Lab.
A KALMAN FILTER INTEGRATED NAVIGATION DESIGN FOR THE IAR TWIN OTTER ATMOSPHERIC RESEARCH AIRCRAFT [METHODE DE NAVIGATION INTEGREE A FILTRE DE KALMAN DESTINEE AU TWIN OTTER DE L'IRA CHARGE DES RECHERCHES ATMOSPHERIQUES]
B. W. Leach Apr. 1991 113 p
(NRC-32148; IAR-AN-72; CTN-92-60369) Avail: CASI HC A06/MF A02

The Institute of Aerospace Research Twin Otter Atmospheric Research Aircraft requires accurate, inertially based navigation data for both track recovery and the calculation of wind gust components. The Kalman filter integrated navigation design described in this report is based on the optimal blending of data from an LTN-90-100 strapdown Inertial Reference System (IRS), a Decca Type 72 Doppler velocity sensing (DVS) system and an ARNAV R-40 airborne Loran-C receiver - sensors that are available on the Twin Otter. All three of these navigation sensors are interfaced to the onboard LSI-11/73 microcomputer system, and a complete set of navigation parameters is recorded. A major reason for the integrated navigation approach is the observation that significant velocity errors can occur in the LTN-90-100 IRS over the course of a flight, and the observed error levels can seriously degrade the accuracy of the wind calculations. The airborne Loran-C positional data has been demonstrated to be consistently more accurate than the IRS position information, in the long term. An integrated navigation system approach, using the principles of Kalman filtering, is shown to have the ability to use Loran C data (and, to a lesser extent, Doppler velocity data) to accurately track the dominant IRS errors and provide IRS error corrections at a rate appropriate for Twin Otter requirements.
Author (CISTI)

N92-32861# General Accounting Office, Washington, DC. Information Management and Technology Div.
AIR TRAFFIC CONTROL: FAA'S ADVANCED AUTOMATION SYSTEM CONTRACT
Mar. 1991 14 p
(GAO/IMTEC-91-25; B-242745) Avail: CASI HC A03/MF A01; GAO, PO Box 6015, Gaithersburg, MD 20877 HC

A report to the Chairman of the Senate Subcommittee on Transportation and Related Agencies is presented for the Federal Aviation Administration's (FAA) Advanced Automation System (AAS) contract. The AAS was awarded to IBM to complete the design and production of a new computerized air traffic control system intended to replace aging hardware, software, and air traffic controller workstations. The report addresses the development and implementation of a management control installed by IBM which provides detailed contract information and allows FAA to identify the cost and performance of AAS. I.I.C.

N92-33098# Mitre Corp., McLean, VA.
SIMULATION TEST AND EVALUATION OF TCAS 2 LOGIC VERSION 6.04
Suzanne Bradley Jul. 1992 108 p
(Contract DTFA01-89-C-00001)
(DOT/FAA/RD-92/23) Avail: CASI HC A06/MF A02

The objectives of the Traffic Alert and Collision Avoidance System 2 (TCAS 2) version 6.04 logic and the testing and evaluation of it are presented. The operational problems experienced with its predecessor, version 6.0, along with the modifications that address them are described. Performance of the two logic versions were compared using simulations of encounters derived from ground radar data from eleven U.S. locations. The two major goals in comparing the logic versions were the following: to obtain an assessment of the effectiveness of the changes of the collision avoidance capability, and to characterize the effect of changes on the air traffic control. Author

05 AIRCRAFT DESIGN, TESTING AND PERFORMANCE

Includes aircraft simulation technology.

For related information see also *18 Spacecraft Design, Testing and Performance* and *39 Structural Mechanics*.For land transportation vehicles see *85 Urban Technology and Transportation.*

N92-32308# Sandia National Labs., Albuquerque, NM.
B-52G/H NUCLEAR CERTIFICATION TASKS PERFORMED BY THE AIRCRAFT COMPATIBILITY DIVISION AT SANDIA NATIONAL LABORATORIES
L. E. Stevenson and J. R. Wifall Feb. 1992 41 p
(Contract DE-AC04-76DP-00789)
(DE92-013681; SAND-91-2664) Avail: CASI HC A03/MF A01

This report documents aircraft compatibility evaluations performed on the current versions of the B-52G/H aircraft and how those efforts led to the recommendation that the aircraft be added to the Aircraft Compatibility Control Drawing (ACCD) of an associated bomb or warhead system. The B-52 Aircraft Compatibility personnel, Division 5147, shall initially assemble this document and then update it on a yearly basis as defined in Reference 1. DOE

N92-32536*# National Aeronautics and Space Administration. Langley Research Center, Hampton, VA.
THE MULTIPLE-FUNCTION MULTI-INPUT/MULTI-OUTPUT DIGITAL CONTROLLER SYSTEM FOR THE AFW WIND-TUNNEL MODEL
Sherwood T. Hoadley and Sandra M. McGraw (Lockheed

Engineering and Sciences Co., Hampton, VA.) Jul. 1992 11 p Presented at the Active Flexible Wing I Session at the AIAA Dynamic Specialists' Conference, Dallas, TX, 16-17 Apr. 1992 Previously announced in IAA as A92-35655
(RTOP 505-63-50-15)
(NASA-TM-107600; NAS 1.15:107600) Avail: CASI HC A03/MF A01

A real time multiple-function digital controller system was developed for the Active Flexible Wing (AFW) Program. The digital controller system (DCS) allowed simultaneous execution of two control laws: flutter suppression and either roll trim or a rolling maneuver load control. The DCS operated within, but independently of, a slower host operating system environment, at regulated speeds up to 200 Hz. It also coordinated the acquisition, storage, and transfer of data for near real time controller performance evaluation and both open- and closed-loop plant estimation. It synchronized the operation of four different processing units, allowing flexibility in the number, form, functionality, and order of control laws, and variability in the selection of the sensors and actuators employed. Most importantly, the DCS allowed for the successful demonstration of active flutter suppression to conditions approximately 26 percent (in dynamic pressure) above the open-loop boundary in cases when the model was fixed in roll and up to 23 percent when it was free to roll. Aggressive roll maneuvers with load control were achieved above the flutter boundary. The purpose here is to present the development, validation, and wind tunnel testing of this multiple-function digital controller system. Author

N92-32612# Logicon, Inc., San Diego, CA. Tactical and Training Systems Div.
TACTICAL STATE AND PERFORMANCE ASSESSMENT DURING AIR COMBAT MANEUVERING Final Report, Sep. 1986 - Dec. 1991
William B. Raspotnik and Jeffrey L. Leeds Feb. 1992 70 p
(Contract F33615-86-C-0012)
(AD-A247426; AL-TP-1992-0001) Avail: CASI HC A04/MF A01

The purpose of this research was to investigate the feasibility of developing a diagnostic measure of tactical decision-making skill in the context of air combat maneuvering (ACM). Two experiments were conducted. Both employed a Tactical State Model (TSM) to characterize position and used a 7-point scale to rate tactical performance. Subjects were experienced F-15 and F-16 instructor pilots. In each experiment, they viewed two prerecorded ACM engagements and used the TSM to assign a tactical position or 'state' to the designed aircraft. Subjects then rated the performance of the designated aircraft. Results indicated that a tactical state model can be used reasonably well by experts to characterize position during an air-to-air engagement. Relationships were also established for one of the engagements in experiment two between these state assignments and an objective measure of positional advantage. The results failed to establish sufficient reliability for the tactical performance rating scale that was developed. Also, the results failed to establish a consistent relationship link between changes in position and quality of performance. It is concluded that development of a diagnostic measure of tactical decision making will require a different approach. GRA

N92-32887*# National Aeronautics and Space Administration. Ames Research Center, Moffett Field, CA.
SKI JUMP TAKEOFF PERFORMANCE PREDICTIONS FOR A MIXED-FLOW, REMOTE-LIFT STOVL AIRCRAFT
Lourdes G. Birckelbaw Feb. 1992 24 p
(RTOP 505-59-30)
(NASA-TM-103866; A-91156; NAS 1.15:103866) Avail: CASI HC A03/MF A01

A ski jump model was developed to predict ski jump takeoff performance for a short takeoff and vertical landing (STOVL) aircraft. The objective was to verify the model with results from a piloted simulation of a mixed flow, remote lift STOVL aircraft. The prediction model is discussed. The predicted results are compared with the piloted simulation results. The ski jump model can be utilized for basic research of other thrust vectoring STOVL aircraft performing a ski jump takeoff. Author

N92-33149*# National Aeronautics and Space Administration. Hugh L. Dryden Flight Research Facility, Edwards, CA.
RAPID DEVELOPMENT OF THE X-31 SIMULATION TO SUPPORT FLIGHT-TESTING
Dale Mackall, Kenneth Norlin, Dorothea Cohen, Gary Kellogg, Lawrence Schilling, and John Sheen (Rockwell International Corp., Downey, CA.) Sep. 1992 20 p Presented at the AIAA/AHS Flight Simulation Technologies Conference, Hilton Head, SC, 24-26 Aug. 1992
(RTOP 505-64-30)
(NASA-TM-104256; H-1857; NAS 1.15:104256; AIAA Paper 92-4176) Copyright Avail: CASI HC A03/MF A01

The X-31 Enhanced Fighter Maneuverability Program has been recognized to form the International Test Organization, with the NASA Dryden Flight Research Facility (NASA-Dryden) as the responsible test organization. The two X-31 research aircraft and engineering support personnel were colocated at NASA-Dryden, with flight test operations beginning in Apr. 1992. Therefore, rapid development of a hardware-in-the-loop simulation was needed to support the flight test operations at NASA-Dryden, and to perform verification and validation of flight control software. The X-31 simulation system requirements, distributed simulation system architecture, simulation components math models to the visual system, and the advanced capabilities the X-31 simulation provides. In addition, unique software tools and the methods used to rapidly develop this simulation system will be highlighted. Author

06 AIRCRAFT INSTRUMENTATION

Includes cockpit and cabin display devices; and flight instruments.

For related information see also *19 Spacecraft Instrumentation* and *35 Instrumentation and Photography.*

N92-32326# Aeronautical Research Labs., Melbourne (Australia).
BRIEFING NOTES ON A MANNED AIRCRAFT RESEARCH AND SUPPORT SIMULATION FACILITY
S. Steuart, N. L. Wing, J. Millar, and R. A. Feik Apr. 1992 24 p
(AD-A250373; ARL-GD-029; DODA-AR-007-052) Avail: CASI HC A03/MF A01

The proposal by Aircraft Systems Division to acquire a manned aircraft research and support simulation facility is outlined here in a background briefing document for use at a preliminary planning workshop being held in June 1992. It is envisaged that MARSSF will comprise a series of simulator stations with various degrees of fidelity networked together in a simulated tactical environment thus providing flexible, scenario-driven tools for future research, development and support to the ADF. GRA

N92-32437# Advisory Group for Aerospace Research and Development, Neuilly-Sur-Seine (France). Avionics Panel.
INTEGRATED TARGET ACQUISITION AND FIRE CONTROL SYSTEMS [SYSTEMES INTEGRES D'ACQUISITION D'OBJECTIFS ET DE CONDUITE DE TIR]
Feb. 1992 109 p In ENGLISH and FRENCH Symposium held in Ottawa, Canada, 7-10 Oct. 1991 Original contains color illustrations
(AGARD-CP-500; ISBN-92-835-0658-8) Copyright Avail: CASI HC A06/MF A02; 1 functional color page

The characterization of targets is of primary interest because it is needed for establishing the tactical situation, optimizing target acquisition, and optimizing armaments utilization. Due to the necessity of obtaining information on threats which have low signatures and are equipped with counter-measure systems, the operational specification of airborne systems have come to rely on the technologies providing multispectral analysis of targets.

Specific topics discussed include aircraft fire control, air to air missiles, air to ground missiles, aerial warfare, multispectral detectors, integrated systems architectures and algorithms, and data fusion. For individual titles, see N92-32438 through N92-32450.

N92-32438# National Defence Headquarters, Ottawa (Ontario).
OPERATIONAL NEEDS FOR AN UNMANNED AIR VEHICLE c66

L. R. Mader *In* AGARD, Integrated Target Acquisition and Fire Control Systems Feb. 1992 9 p (For primary document see N92-32437 23-06)
Copyright Avail: CASI HC A01/MF A02; 1 functional color page

In order for sound and timely decisions to be made, commanders and staffs require a continuous source of information about the tactical situation they are facing. Unmanned Air Vehicle (UAV) technology offers a potential solution to augment a commander's surveillance resources. UAV's offer the land force commander the possibility of conducting wide range surveillance and target acquisition in near real time. UAV's will extend the range of observed fire to the limits of available weapons. Maritime forces could employ UAV's from or in support of small ships to augment manned aircraft. Examined here are the requirements for UAV's to support both land and marine operations. The characteristics and concepts of employment which make UAV's desirable for military applications are discussed. Author

N92-32439# GEC Ferranti, Edinburgh (Scotland). Electro Optic Systems Group.
MULTISENSOR AIRBORNE TARGET ACQUISITION SYSTEMS AND THEIR INTEGRATION

J. W. Jack *In* AGARD, Integrated Target Acquisition and Fire Control Systems Feb. 1992 6 p Sponsored by Ministry of Defence (For primary document see N92-32437 23-06)
Copyright Avail: CASI HC A02/MF A02; 1 functional color page

Discussed here are the requirements for increased sensor performance. It is suggested that one solution may be to provide a dual sensor capability. The difficulties of conducting tests under realistic conditions are set out, and the alternative of providing calculated performance based on recorded weather and target data is suggested. Based on modeling for two locations in the Gulf region, it is shown that TV can offer major advantages in hot humid conditions. Equipment providing a dual sensor capability is described and the results of carrying out trials flying in the United Kingdom are presented. Author

N92-32440# Naval Weapons Center, China Lake, CA. Attack Weapons Dept.
GENERIC MODULAR IMAGING IR SIGNAL PROCESSOR c60

John Eric Auborn and William Harris *In* AGARD, Integrated Target Acquisition and Fire Control Systems Feb. 1992 6 p (For primary document see N92-32437 23-06)
Copyright Avail: CASI HC A02/MF A02; 1 functional color page

We have developed a modular signal processor architecture that is suitable for many applications to meet real time requirements and adaptable to multiple uses. This generic modular architecture was developed and demonstrated in real time hardware for representative filters and a target detection algorithm. Computer aided design tools were used throughout the hardware development. An application specific integrated circuit (ASIC) or other custom IC implementation can be used for actual production hardware. Author

N92-32441# Naval Weapons Center, China Lake, CA. Attack Weapons Dept.
IMAGE ENHANCEMENT OF INFRARED UNCOOLED FOCAL PLANE ARRAY IMAGERY c74

Howard McCauley and John Eric Auborn *In* AGARD, Integrated Target Acquisition and Fire Control Systems Feb. 1992 4 p (For primary document see N92-32437 23-06)
Copyright Avail: CASI HC A01/MF A02; 1 functional color page

Several simple, low-cost algorithms were explored for use in the enhancement of imagery produced by uncooled focal plane arrays (UFPA). These algorithms address the main problems that UFPA-produced imagery typically demonstrate. In addition to enhancing UFPA-produced imagery, all of the algorithms are simple and allow for inexpensive hardware implementation. Author

N92-32442# Naval Weapons Center, China Lake, CA. Attack Weapons Dept.
TARGET CUING: A HETEROGENEOUS NEURAL NETWORK APPROACH c63

Howard McCauley *In* AGARD, Integrated Target Acquisition and Fire Control Systems Feb. 1992 4 p (For primary document see N92-32437 23-06)
Copyright Avail: CASI HC A01/MF A02; 1 functional color page

Autonomous analysis of complex image data is a critical technology in today's world of expanding automation. The growth of this critical field is slowed by problems in traditional image analysis methods. Traditional methods lack the speed, generality, and robustness that many modern image analysis problems require. While neural networks promise to improve traditional techniques, homogeneous neural network systems have difficulty performing all the diverse analysis required of an autonomous system. Proposed here is a dual-staged, heterogeneous neural network approach to image analysis; specifically, a way to solve the cuing problem. Author

N92-32443# Naval Weapons Center, China Lake, CA. Attack Weapons Dept.
TARGET DETECTION USING CO-OCCURRENCE MATRIX SEGMENTATION AND ITS HARDWARE IMPLEMENTATION c61

John Eric Auborn and James M. Fuller *In* AGARD, Integrated Target Acquisition and Fire Control Systems Feb. 1992 4 p (For primary document see N92-32437 23-06)
Copyright Avail: CASI HC A01/MF A02; 1 functional color page

Our goal was to develop a method for detection of man-made targets in infrared (IR) scenes. The application required detection to be independent of the polarity of the image and independent of the rotation. The approach had to be realizable in real time hardware and compatible with size and weight restraints. We made a laboratory demonstration of the detection algorithm using a general purpose image processor. The resultant demonstration showed the capability of detecting targets. Real imagery was used and the results were promising. We made an architectural design to implement the algorithm in hardware, simulated the feasibility of the approach, and made a detailed hardware design. A prototype system was fabricated and tested. Author

N92-32444# Thomson-CSF, Cesson-Sevigne (France).
METHODS OF OPTO-ELECTRONIC FUSION OF INFRARED AND VISIBLE IMAGES [METHODES DE FUSION OPTRONIQUE D'IMAGES IR ET VISIBLE] c74

D. Thoreau and J. Quignon (Thomson-CSF, Bagneux, France) *In* AGARD, Integrated Target Acquisition and Fire Control Systems Feb. 1992 8 p In FRENCH Original contains color illustrations (For primary document see N92-32437 23-06)
Copyright Avail: CASI HC A02/MF A02; 1 functional color page

The interpretation of images could be greatly facilitated by simultaneously considering the images of the same scene produced by captors of different types. Thus, a global approach to the problem of opto-electronic fusion between two captors, infrared (IR) and visible, is arrived at here, with three levels of association of data. The fusion of data can be made at the decision making level (class of objects), at the intermediary level (elementary objects), and finally at the level that the signal is issued directly to the captors. At each step of fusion, the problem of the placement

in the correspondence of the IR and visible data is posed. This alignment must be as much or more precise as the level of data. The preliminary phase of treatment strongly affects the fusion step. The rules of fusion are developed in such a way as to improve the power of classification, augmenting the probability of detection, utilizing the eventual complementarity of the captors, and permitting a simultaneous visualization of pertinent IR and visible information to the operator. Author

N92-32445# Thomson-CSF, Bagneux (France). Div. Systemes Electroniques.
AUTOMATIC DETECTION, PURSUIT, AND CLASSIFICATION IN INFRARED IMAGERY [DETECTION, POURSUITE ET CLASSIFICATION AUTOMATIQUES EN IMAGERIE INFRA-ROUGE] **c74**
J. Quignon *In* AGARD, Integrated Target Acquisition and Fire Control Systems Feb. 1992 6 p In FRENCH (For primary document see N92-32437 23-06)
Copyright Avail: CASI HC A02/MF A02; 1 functional color page

Presented here are certain aspects of the treatment techniques of images and the reconnaissance of forms for automatic detection of targets in infrared imagery. The algorithms described here are put to work in real time for plane, helicopter, and missile targets in view of their integration into the solar defense system. Nevertheless, the algorithms are sufficiently general to be applied to optoelectronic equipment in air to ground and air to air systems. The treatments are of two categories. The first category includes those which are carried over the reduced zones of the entire field analyzed by the sensor (typically, 2 degrees by 3 degrees for a thermal camera from a short range arms system). These systems extract from the background potential targets (called alarms). The criteria of segmentation are based on the contrast and the movement of targets in relation to the background. The second category includes those which are carried over the reduced zones of an image (pursuit window) and which have as a goal the classification (recognition) of potential targets and their pursuit. Author

N92-32446# Wright Lab., Wright-Patterson AFB, OH.
INFRARED TARGETING SYSTEM (IRTS) DEMONSTRATION **c74**
Mark A. OHair, Shelly S. Eucker (Boeing Military Airplane Development, Wichita, KS.), Brad A. Eucker (Boeing Military Airplane Development, Wichita, KS.), and Tim Lewis *In* AGARD, Integrated Target Acquisition and Fire Control Systems Feb. 1992 6 p (For primary document see N92-32437 23-06)
Copyright Avail: CASI HC A02/MF A02; 1 functional color page

The objective of the Infrared Targeting System (IRTS) is to successfully demonstrate the mission performance that can be achieved in manned air-to-ground targeting applications utilizing a synergistic combination of state of the art active/passive infrared sensor and automatic target recognizer (ATR) technologies. The IRTS program is centered around a demonstration FLIR/Laser Radar/ATR (FLASHER). The FLASHER consists of a dual field of view (2 x 2 degree and 6 x 6 degree) second generation FLIR pixel mapped to a CO2 laser radar, with a FLIR ATR processor, a laser radar ATR processor, and a sensor fusion ATR processor. Following construction and laboratory testing of the IRTS, the system will be installed on a test aircraft and demonstrated in flight against realistic tactical, strategic, and special operations scenarios. Author

N92-32447# Zeiss (Carl), Oberkochen (Germany, F.R.).
AIRBORNE EXPERIMENTAL FLIR PROGRAM
Klaus F. Boecking *In* AGARD, Integrated Target Acquisition and Fire Control Systems Feb. 1992 12 p (For primary document see N92-32437 23-06)
Copyright Avail: CASI HC A03/MF A02; 1 functional color page

The German Air Force has decided to build a forward looking infrared (FLIR) system in order to derive and to consolidate the different technical requirements for their different technical tasks. This FLIR design was designed and built on the basis of available and proven technologies. The equipment is pod-mounted in order to avoid modification of existing Tornado aircraft. Two different modes of operation are comprised in one hardware. These are the navigation mode, used as a pilot aid for flying at night and in adverse weather, and the fire control mode, used for passive targeting and navigation-update. The mechanical and optical designs are presented as well as the electronics architecture. The performance of the sensor system is described. Author

N92-32448# Messerschmitt-Boelkow-Blohm G.m.b.H., Munich (Germany, F.R.). Helicopter Div.
THE GERMAN ANTI TANK HELICOPTER PAH 2: AN EXAMPLE OF A FUTURE SENSOR PLATFORM
Rudolf Schranner, K. Rueskamp, and Hans-Dieter VonBoehm *In* AGARD, Integrated Target Acquisition and Fire Control Systems Feb. 1992 4 p (For primary document see N92-32437 23-06)
Copyright Avail: CASI HC A01/MF A02; 1 functional color page

The German antitank helicopter PAH 2 is presently under full scale development, together with the French antitank helicopter HAP, in a cooperative effort between France and Germany. The PAH 2 represents the current state of the art in target acquisition and fire control systems for helicopters in Europe. The targeting system consists mainly of a mast mounted platform housing several sensors operating in different spectral ranges. It is used for the detection, recognition, and identification of targets at increased ranges as well as to aim and guide 2nd and 3rd generation antitank missiles. Further sensors and systems are available to support the crew target acquisition or detection of threats in the battlefield and to support coordination of several helicopters in a flight. Author

N92-32449# Canadair Ltd., Montreal (Quebec). Surveillance Systems Div.
NAVAL TARGET CLASSIFICATION AND DESIGNATION WITH THE CL-227 SEA SENTINEL
Henry J. Szot and Stephen P. Jones (Paramax Electronic, Inc., Montreal, Quebec) *In* AGARD, Integrated Target Acquisition and Fire Control Systems Feb. 1992 14 p (For primary document see N92-32437 23-06)
Copyright Avail: CASI HC A03/MF A02; 1 functional color page

The integration of the CL-227 Unmanned Air Vehicle (UAV) Sea Sentinel System with the Canadian Patrol Frigate (CPF) platform provides the naval target classification and designation capability that meets the mission requirements of this and the following decade. The developmental history and the operation of the system is described. Author

N92-32450# Wright Lab., Wright-Patterson AFB, OH.
AN INTEGRATED MULTIPLE-SENSOR FIRE CONTROL SYSTEM FOR AIR-TO-AIR COMBAT
Robert A. Manske and William E. Moore *In* AGARD, Integrated Target Acquisition and Fire Control Systems Feb. 1992 12 p (For primary document see N92-32437 23-06)
Copyright Avail: CASI HC A03/MF A02; 1 functional color page

Described here is a system that includes integrated fire control algorithms, software, and related control and display concepts for air to air combat in the multiple target environment of the 1990's. This system, now completing advanced development, fuses data from multiple sensors and presents integrated fire control information to the pilot in a simplified manner for improved situation awareness and decreased workload. The resulting algorithms, software, and display concepts are described. The system was demonstrated and evaluated in a flight simulator with Air Force pilots. The fire control software, which was developed in the Ada language, was implemented in a distributed data processing complex using MIL-STD-1750A processors. The sensors and data links, as well as the aircraft and its environment, were simulated by mathematical models. Author

N92-32850# National Aeronautical Establishment, Ottawa (Ontario).
THE USE OF KALMAN FILTERING TECHNIQUES TO IMPROVE THE ACCURACY OF FLIGHT TEST DATA
B. W. Leach and J. I. MacPherson 1990 16 p Presented at the CASI Flight Test Symposium, Toronto, Ontario, 6-7 Mar. 1990
(NRC-32139; CTN-92-60371) Avail: CASI HC A03/MF A01

Flight test programs for which high accuracy aircraft inertial data and air data are required can benefit from the advantages of a Kalman filter integrated systems approach. This paper describes one such approach that is being developed at the Flight Research Laboratory of the National Aeronautical Establishment (NAE) for improving the accuracy of inertial data from a medium accuracy inertial reference system (IRS). This particular IRS was integrated with a variety of other standard airborne navaids in order to improve the accuracy of the complete set of inertial parameters available from the IRS digital data bus (i.e., body accelerations, body rates, attitude components, inertial velocity components, and geographical position components). Using the computer algorithms that were developed, accurate calibration of the IRS can be accomplished either in real-time or off-line. Furthermore, the accurate determination of aircraft inertial velocity components results in a much more accurate calculation of the computed wind components, and can lead to improved calibration of the onboard air data system. Actual flight test data from the NAE Twin Otter Atmospheric Research Aircraft are used to demonstrate how the performance of a baro-damped Litton LTN-90-100 IRS can be improved when it is integrated with an airborne Loran-C receiver and a Doppler radar velocity sensor. Author (CISTI)

N92-32866*# National Aeronautics and Space Administration. Hugh L. Dryden Flight Research Facility, Edwards, CA.
THE DEVELOPMENT OF AN AIRBORNE INFORMATION MANAGEMENT SYSTEM FOR FLIGHT TEST
Glenn A. Bever Sep. 1992 13 p Presented at the 6th Biennial Flight Test Conference, Hilton Head, SC, 24-26 Aug. 1992; sponsored by AIAA
(RTOP 505-68-50)
(NASA-TM-104251; H-1839; NAS 1.15:104251; AIAA Paper 92-4113) Copyright Avail: CASI HC A03/MF A01

An airborne information management system is being developed at the NASA Dryden Flight Research Facility. This system will improve the state of the art in management data acquisition on-board research aircraft. The design centers around highly distributable, high-speed microprocessors that allow data compression, digital filtering, and real-time analysis. This paper describes the areas of applicability, approach to developing the system, potential for trouble areas, and reasons for this development activity. System architecture (including the salient points of what makes it unique), design philosophy, and tradeoff issues are also discussed. Author

07 AIRCRAFT PROPULSION AND POWER

Includes prime propulsion systems and systems components, e.g., gas turbine engines and compressors; and onboard auxilliary power plants for aircraft.

For related information see also *20 Spacecraft Propulsion and Power, 28 Propellants and Fuels,* and *44 Energy Production and Conversion.*

N92-32452*# National Aeronautics and Space Administration. Ames Research Center, Moffett Field, CA.
COMPUTATIONS OF UNSTEADY MULTISTAGE COMPRESSOR FLOWS IN A WORKSTATION ENVIRONMENT
Karen L. Gundy-Burlet Jun. 1992 14 p Previously announced in IAA as A92-15701
(RTOP 505-60-00)
(NASA-TM-103839; A-91074; NAS 1.15:103839) Avail: CASI HC A03/MF A01

High-end graphics workstations are becoming a necessary tool in the computational fluid dynamics environment. In addition to their graphic capabilities, workstations of the latest generation have powerful floating-point-operation capabilities. As workstations become common, they could provide valuable computing time for such applications as turbomachinery flow calculations. This report discusses the issues involved in implementing an unsteady, viscous multistage-turbomachinery code (STAGE-2) on workstations. It then describes work in which the workstation version of STAGE-2 was used to study the effects of axial-gap spacing on the time-averaged and unsteady flow within a 2 1/2-stage compressor. The results included time-averaged surface pressures, time-averaged pressure contours, standard deviation of pressure contours, pressure amplitudes, and force polar plots. Author

N92-33102# Toronto Univ. (Ontario). Inst. for Aerospace Studies.
IDEAL EFFICIENCY OF PROPELLERS BASED ON THEODORSEN'S THEORY: A REVIEW AND COMPUTER STUDY, WITH EXTENDED PLUS SIMPLIFIED CHARTS
Stephen P. Foster and H. S. Ribner Feb. 1991 145 p Sponsored by Natural Sciences and Engineering Research Council
(UTIAS-TN-271; CTN-92-60378) Copyright Avail: CASI HC A07/MF A02

Ideal propeller performance is explored in an examination of Theodorsen's theory of propellers. This work presents an overview of the theory with analysis and interpretation. Computational methods are used in place of Theodorsen's analog technique to calculate key parameters for most cases. In addition, relations between the fundamental quantities (thrust, power, advance, and efficiency) are presented in this format plus a more convenient one that avoids iteration. Theodorsen's methodology is further applied to calculate slipstream contraction. A slightly more general approach is taken with the removal of several light loading assumptions. A review of how the updated results may be applied to the design of single rotation propellers is also provided.
Author (CISTI)

N92-33105# Naval Air Propulsion Test Center, Trenton, NJ.
STATISTICS ON AIRCRAFT GAS TURBINE ENGINE ROTOR FAILURES THAT OCCURRED IN US COMMERCIAL AVIATION DURING 1988 Final Report
R. A. Delucia, E. R. Chapdelaine (Federal Aviation Administration, Atlantic City, NJ.), and B. C. Fenton (Federal Aviation Administration, Atlantic City, NJ.) Mar. 1992 27 p
(Contract DOD/FA7INA-AP)
(DOT/FAA/CT-91/28) Avail: CASI HC A03/MF A01

Statistical information relating to gas turbine engine rotor failures, which occurred during 1988 in U.S. commercial aviation service, is presented. Four hundred and thirteen failures occurred in 1988. Rotor fragments were generated in 175 of the failures, and of these 14 were uncontained. The predominant failure involved blade fragments, 95 percent of which were contained. Five disk failures occurred and all were uncontained. Forty-two percent of the 413 failures occurred during the takeoff and climb stages of flight. This service data analysis is prepared on a calendar year basis and published yearly. The data are useful in support of flight safety analyses, proposed regulatory actions, certification standards, and cost benefit analyses. Author

08 AIRCRAFT STABILITY AND CONTROL

Includes aircraft handling qualities; piloting; flight controls; and autopilots.

For related information see also *05 Aircraft Design, Testing and Performance.*

N92-32435# Air Force Inst. of Tech., Wright-Patterson AFB, OH.
A LEARNING ENHANCED FLIGHT CONTROL SYSTEM FOR HIGH PERFORMANCE AIRCRAFT M.S. Thesis

Noel F. Nistler 1992 100 p
(AD-A252520; AFIT/CI/CIA-92-039) Avail: CASI HC A05/MF A01

Numerous approaches to flight control system design have been proposed in an attempt to govern the complex behavior of high performance aircraft. Gain scheduled linear control and adaptive control have traditionally been the most widely used methodologies, but they are not without their limitations. Gain scheduling requires large amounts of a priori design information and costly manual tuning in conjunction with flight tests, while still lacking an ability to accommodate unmodeled dynamics and model uncertainty beyond a limited amount of robustness that can be incorporated into the design. Adaptive control is suitable for nonlinear systems with unmodeled dynamics, but has deficiencies in accounting for quasi-static state dependencies. Moreover, inherent time delays in adaptive control make it difficult to match the performance of a well-designed gain scheduled controller. An alternative approach that is able to compensate for the inadequacies experienced with traditional control techniques and to automate the tuning process is desired. Recent Teaming techniques have demonstrated an ability to synthesize multivariable mappings and are thus able to learn a functional approximation of the initially unknown state dependent dynamic behavior of the vehicle. By combining a learning component with an adaptive controller, a new hybrid control system that is able to adapt to unmodeled dynamics and novel situations, as well as to learn to anticipate quasi-static state dependencies is formed. GRA

N92-32487 ESDU International Ltd., London (England).
CONTRIBUTION OF TAILPLANE-MOUNTED TWIN FINS TO SIDEFORCE, YAWING MOMENT, AND ROLLING MOMENT DERIVATIVES DUE TO SIDESLIP
Mar. 1992 17 p Supersedes ESDU-Aero-C.01.01.02
(ESDU-92007; ESDU-Aero-C.01.01.02; ISBN-0-85679-812-6)
Avail: ESDU

ESDU 92007 gives a semi-empirical method applying to fins of small sweep (up to 20 deg) for small sideslip angles up to Mach 0.7. From an analysis of limited experimental data extracted from the literature, a fin effective aspect ratio was determined as a function of fin vertical height on the tailplane that allows for the end plate effect of the tailplane. The lift-curve slope for the effective aspect ratio is then corrected for the effect of fuselage sidewash by a factor that depends on fuselage height/width at the tail and the exposed tailplane span. To determine the moment derivatives, the sideforce is assumed to be divided according to the areas above and below the tailplane, and to act at a point 0.424 of the height of each portion from the tailplane (assuming half elliptical loading on each portion). For the rolling derivative an additional correction is made to allow for the asymmetric loading on the tailplane induced by the fins in sideslip. Sketches compare experimental and predicted results and show the sideforce, rolling, and yawing derivatives to be predicted to within 0.03, 0.005, and 0.012 respectively. The ranges of geometry considered are tabulated, and a worked example illustrates the use of the data. ESDU

N92-32750# National Aerospace Lab., Amsterdam (Netherlands). Fluid Dynamics Div.
NLR INVESTIGATIONS OF FLUTTER BEHAVIOUR OF FIGHTER AIRCRAFT WITH EXTERNAL STORES
J. J. Meijer 29 Apr. 1991 26 p Presented at the International Aerospace Congress, Melbourne, Australia, 12-16 May 1991
(NLR-TP-91134-U; ETN-92-91999) Avail: CASI HC A03/MF A01

The state of the art in flutter-stability prediction of fighter aircraft with external stores is discussed. Available computer software, measuring equipment and techniques, and other means and devices useful in flutter clearance activities are covered. Some past F-16 clearance activities are presented. Special attention is devoted to the flutter stability investigation of the transonic speed regime, which assists in the development and validation of new prediction methods. ESA

N92-32778*# Douglas Aircraft Co., Inc., Long Beach, CA.
FLY-BY-LIGHT TECHNOLOGY DEVELOPMENT PLAN Final Report
J. R. Todd, T. Williams, S. Goldthorpe, J. Hay, M. Brennan, B. Sherman, J. Chen, Larry J. Yount (Honeywell, Inc., Phoenix, AZ.), Richard F. Hess (Honeywell, Inc., Phoenix, AZ.), and J. Kravetz (Honeywell, Inc., Phoenix, AZ.) et al Aug. 1990 187 p
(Contract NAS1-18028; RTOP 506-46-21-05)
(NASA-CR-181954; NAS 1.26:181954) Avail: CASI HC A09/MF A02

The driving factors and developments which make a fly-by-light (FBL) viable are discussed. Documentation, analyses, and recommendations are provided on the major issues pertinent to facilitating the U.S. implementation of commercial FBL aircraft before the turn of the century. Areas of particular concern include ultra-reliable computing (hardware/software); electromagnetic environment (EME); verification and validation; optical techniques; life-cycle maintenance; and basis and procedures for certification. Author

N92-32780 ESDU International Ltd., London (England).
A BACKGROUND TO THE HANDLING QUALITIES OF AIRCRAFT
Mar. 1992 28 p
(ESDU-92006; ISBN-0-85679-811-8) Avail: ESDU

ESDU 92006 examines those factors that affect the ease and safety with which an aircraft may be flown. For consideration of aircraft handling, aircraft are divided by class or role indicating the primary purpose of the operation of the aircraft. Within each class, flight or sorties are subdivided by flight phase which describes the type of tasks to be completed. A discussion of piloting techniques and the development of pilot opinion ratings, including the Cooper-Harper ratings, precedes an examination according to the mode of motion (short period, phugoid, roll, spiral or Dutch roll) of the primary parameters that characterize the handling qualities criteria. Extracts from current UK Design and Airworthiness Requirements for services Aircraft then cover the required flying qualities according to aircraft class and flight phase that define the acceptable characteristics for the control feel in longitudinal maneuvering flight and for the response in the five modes of motion. ESDU

N92-32788*# National Aeronautics and Space Administration. Ames Research Center, Moffett Field, CA.
COLLABORATIVE RESEARCH ON V/STOL CONTROL SYSTEM/COCKPIT DISPLAY TRADEOFFS UNDER THE NASA/MOD JOINT AERONAUTICAL PROGRAM
J. A. Franklin and O. P. Nicholas (Royal Aircraft Establishment, Bedford, England) Jan. 1992 32 p
(RTOP 533-02-37)
(NASA-TM-103910; A-92039; NAS 1.15:103910) Avail: CASI HC A03/MF A01

Summarized here are activities that have taken place from 1979 to the present in a collaborative program between NASA Ames Research Center and the Royal Aerospace Establishment (now Defence Research Agency), Bedford on flight control system and cockpit display tradeoffs for low-speed and hover operations of future V/STOL aircraft. This program was created as Task 8A of the Joint Aeronautical Program between NASA in the United States and the Ministry of Defence (Procurement Executive) in the United Kingdom. The program was initiated based on a recognition by both parties of the strengths of the efforts of their counterparts and a desire to participate jointly in future simulation and flight experiments. In the ensuing years, teams of NASA and RAE engineers and pilots have participated in each other's simulation experiments to evaluate control and display concepts and define design requirements for research aircraft. Both organizations possess Harrier airframes that have undergone extensive modification to provide in-flight research capabilities in the subject areas. Both NASA and RAE have profited by exchanges of control/display concepts, design criteria, fabrication techniques, software development and validation, installation details, and ground and flight clearance techniques for their respective aircraft.

This collaboration has permitted the two organizations to achieve jointly substantially more during the period than if they had worked independently. The two organizations are now entering the phase of flight research for the collaborative program as currently defined. Author

N92-32864*# National Aeronautics and Space Administration. Hugh L. Dryden Flight Research Facility, Edwards, CA.
FLIGHT TESTING AND SIMULATION OF AN F-15 AIRPLANE USING THROTTLES FOR FLIGHT CONTROL
Frank W. Burcham, Jr., Trindel Maine, and Thomas Wolf Aug. 1992 21 p Presented at the AIAA Flight Test Conference, Hilton Head, SC, 24 Aug. 1992
(RTOP 533-02-36)
(NASA-TM-104255; H-1826; NAS 1.15:104255; AIAA Paper 92-4109) Avail: CASI HC A03/MF A01

Flight tests and simulation studies using the throttles of an F-15 airplane for emergency flight control have been conducted at the NASA Dryden Flight Research Facility. The airplane and the simulation are capable of extended up-and-away flight, using only throttles for flight path control. Initial simulation results showed that runway landings using manual throttles-only control were difficult, but possible with practice. Manual approaches flown in the airplane were much more difficult, indicating a significant discrepancy between flight and simulation. Analysis of flight data and development of improved simulation models that resolve the discrepancy are discussed. An augmented throttle-only control system that controls bank angle and flight path with appropriate feedback parameters has also been developed, evaluated in simulations, and is planned for flight in the F-15. Author

N92-32988# Naval Postgraduate School, Monterey, CA.
INVESTIGATION OF THE FLIGHT CONTROL REQUIREMENTS OF A HALF-SCALE DUCTED FAN UNMANNED AERIAL VEHICLE M.S. Thesis
Mark A. Brynestad 26 Mar. 1992 82 p
(AD-A252730) Avail: CASI HC A05/MF A01

The goal of this investigation was to study the requirements to fly a previously constructed, half-scale, ducted-fan Unmanned Aerial Vehicle (UAV) in horizontal and vertical flight as a proof of concept for a full-scale UAV of similar design. The following items were investigated: (1) methods to increase thrust from the ducted-fan propulsion system; (2) the determination of the effectiveness and necessary coupling of the four control vanes in controlling the vehicle in vertical flight (pitch, roll, yaw) and in countering the engine torque; and (3) the design, construction, and effectiveness of stator vanes. The following items were accomplished: (1) thrust was improved over the original vehicle through the design and construction of an effective bellmouth and nine-bladed fan; (2) control-vane effectiveness was determined, and stator vanes were designed and installed; (3) gyro stabilization was incorporated into the roll axis controls and the ducted fan flew in a controlled, tethered hover; and (4) gyroscopic cross-coupling was demonstrated. GRA

N92-33107*# Florida Atlantic Univ., Boca Raton. Dept. of Mechanical Engineering.
COMPUTATIONAL ASPECTS OF HELICOPTER TRIM ANALYSIS AND DAMPING LEVELS FROM FLOQUET THEORY Final Technical Report, 1 Aug. 1991 - 31 Jul. 1992
Gopal H. Gaonkar and N. S. Achar Sep. 1992 50 p
(Grant NAG2-727)
(NASA-CR-190736; NAS 1.26:190736) Avail: CASI HC A03/MF A01

Helicopter trim settings of periodic initial state and control inputs are investigated for convergence of Newton iteration in computing the settings sequentially and in parallel. The trim analysis uses a shooting method and a weak version of two temporal finite element methods with displacement formulation and with mixed formulation of displacements and momenta. These three methods broadly represent two main approaches of trim analysis: adaptation of initial-value and finite element boundary-value codes to periodic boundary conditions, particularly for unstable and marginally stable systems. In each method, both the sequential and in-parallel schemes are used and the resulting nonlinear algebraic equations are solved by damped Newton iteration with an optimally selected damping parameter. The impact of damped Newton iteration, including earlier-observed divergence problems in trim analysis, is demonstrated by the maximum condition number of the Jacobian matrices of the iterative scheme and by virtual elimination of divergence. The advantages of the in-parallel scheme over the conventional sequential scheme are also demonstrated. Author

N92-33161 Department of the Navy, Washington, DC.
METHOD OF GUIDING AN IN-FLIGHT VEHICLE TOWARD A TARGET Patent
Roger L. Gray, inventor (to Navy) 21 Jan. 1992 7 p Filed 3 Dec. 1990
(AD-D015308; US-Patent-5,082,200; US-Patent-Appl-SN-620671; US-Patent-Class-244-315) Avail: US Patent and Trademark Office

A method of guiding an in-flight vehicle toward a target exhibiting a known or predictable thrusting profile is provided. The vehicle undergoes an alternating series of vehicle coasts and diverts during the vehicle's terminal intercept phase of flight. Position and velocity information of the target with respect to the vehicle is used to select a course change during each vehicle coast. The course change is intentionally offset from a collision course with the target and is effected by the next divert in the series. The amount of offset is such that the final coast results in a target intercept. GRA

09 RESEARCH AND SUPPORT FACILITIES (AIR)

Includes airports, hangars and runways; aircraft repair and overhaul facilities; wind tunnels; shock tubes; and aircraft engine test stands.

For related information see also *14 Ground Support Systems and Facilities (Space).*

N92-32734# National Aerospace Lab., Amsterdam (Netherlands). Fluid Dynamics Div.
INTEGRATION OF WALL INTERFERENCE ASSESSMENT AND WALL ADAPTATION
J. Smith 25 Mar. 1991 13 p Presented at the International Conference on Adaptive Wall Wind Tunnel Research and Wall Interference Correction, Xian, China, 10-14 Jun. 1991 Previously announced in IAA as A91-52782
(NLR-TP-91119-U; ETN-92-91998) Avail: CASI HC A03/MF A01

The fact that the normal velocity distribution on the test section walls suffices to calculate the associated harmonic perturbation flow field inside it is fully exploited for adaptive wall applications. It is shown to provide a key to test section design. In addition, wall adaptation is applied to obtain correctable, instead of zero, interference. Wall interference assessment is applied to determine, in succession, initial and residual interference. A major advantage of accepting correctability is that deviations of the center of the test section exit from the nominal test section center line, which may give rise to unnecessarily high losses in the diffuser entry area, are avoided. ESA

N92-32903# Army Cold Regions Research and Engineering Lab., Hanover, NH. Experimental Engineering Div.
PERFORMANCE OF INSULATED PAVEMENTS AT NEWTON FIELDS, JACKMAN, MAINE Final Report
Maureen A. Kestler and Richard L. Berg May 1992 30 p
(Contract DTFA01-89-Z-02050)
(CRREL-92-9; DOT/FAA/RD-92/8) Avail: CASI HC A03/MF A01

In 1986, the runway at Newton Field, a small airport in Jackman, Maine, was reconstructed using a 2-inch thick layer of extruded polystyrene insulation as part of the pavement structure. At the same time, a nearby town road was reconstructed using a

conventional uninsulated pavement cross section for relatively heavy loads. Both pavements were monitored for frost penetration, frost heave, and seasonal changes in pavement strength. Since frost penetration beneath the insulation layer of the runway at Newton field exceeded empirical estimates during the winter of 1986-1987, four additional test sections with varying combinations of insulation and subbase thicknesses were constructed adjacent to the airport's parking apron during the summer of 1987. Although the thermal performance of the insulated pavement test sections was comparable to design expectations for the following three years, evidence of discontinuities in the insulation layer in the Newton field runway demonstrates the insulated pavements' susceptibility to variations in construction. Discussed here is pavement performance at each of the test sites over the observation periods 1986-1990 and 1987-1990. Author

N92-33002# National Inst. of Standards and Technology, Gaithersburg, MD.
NATIONAL VOLUNTARY LABORATORY ACCREDITATION PROGRAM 1992 DIRECTORY Final Report
Vanda R. White, ed, Apr. 1992 177 p Supersedes PB92-222646
(PB92-201094; NIST/SP-810-ED-1992) Avail: CASI HC A09/MF A02; SOD HC

The 1992 Directory provides a listing of laboratories accredited by the National Institute of Standards and Technology, National Voluntary Laboratory Accreditation Program (NVLAP). The names of approximately 800 laboratories in 19 fields of testing are included. A brief description of the NVAP program and a summary of laboratory participation are provided. As an aid to the user, indexes are cross-referenced by laboratory name, field of testing, geographic location (state or county) and NVLAP Lab Code. A listing of the test methods is provided for each laboratory. Author

12 ASTRONAUTICS (GENERAL)

For extraterrestrial exploration see *91 Lunar and Planetary Exploration.*

N92-33007*# National Aeronautics and Space Administration, Washington, DC.
TOWARD THE NEXT MILLENNIUM: A VISION FOR SPACESHIP EARTH
Daniel S. Goldin 1992 7 p Presented at the World Space Congress, 2 Sep. 1992
(NASA-TM-107986; NAS 1.15:107986) Avail: CASI HC A02/MF A01

The transcript of NASA Administrator Daniel S. Goldin's address to the World Space Congress is presented. The address discusses the current international flavor of space exploration, especially in the context of cooperative ventures with the former Soviet Union, and establishes the need for a return to the Moon. Goldin's speech emphasizes that returning to the moon is only the beginning of a program of exploration that will lead to human investigation of Mars, the rest of the solar system, and beyond. By following this program to its logical conclusion, human beings will eventually establish themselves as a multi-planetary species. D.R.D.

13 ASTRODYNAMICS

Includes powered and free-flight trajectories; and orbital and launching dynamics.

No abstracts in this category.

14 GROUND SUPPORT SYSTEMS AND FACILITIES (SPACE)

Includes launch complexes, research and production facilities; ground support equipment, e.g., mobile transporters; and simulators.

For related information see also *09 Research and Support Facilities (Air).*

No abstracts in this category.

15 LAUNCH VEHICLES AND SPACE VEHICLES

Includes boosters; operating problems of launch/space vehicle systems; and reusable vehicles.

For related information see also *20 Spacecraft Propulsion and Power.*

N92-32456*# National Aeronautics and Space Administration. Lewis Research Center, Cleveland, OH.
RELIABILITY TRAINING
Vincent R. Lalli, ed., Henry A. Malec, ed. (Siemens Stromberg-Carlson, Albuquerque, NM.), Richard B. Dillard (Martin Marietta Corp., Orlando, FL.), Kam L. Wong (Hughes Aircraft Co., El Segundo, CA.), Frank J. Barber, and Frank J. Barina Jun. 1992 225 p A reliability/probability device as supplement
(RTOP 572-10-00)
(NASA-RP-1253; E-5456; NAS 1.61:1253) Avail: CASI HC A10/MF A03

Discussed here is failure physics, the study of how products, hardware, software, and systems fail and what can be done about it. The intent is to impart useful information, to extend the limits of production capability, and to assist in achieving low cost reliable products. A review of reliability for the years 1940 to 2000 is given. Next, a review of mathematics is given as well as a description of what elements contribute to product failures. Basic reliability theory and the disciplines that allow us to control and eliminate failures are elucidated. Author

16 SPACE TRANSPORTATION

Includes passenger and cargo space transportation, e.g., shuttle operations; and space rescue techniques.

For related information see also *03 Air Transportation and Safety* and *18 Spacecraft Design, Testing and Performance.* For space suits see *54 Man/System Technology and Life Support.*

N92-32454*# National Aeronautics and Space Administration. John F. Kennedy Space Center, Cocoa Beach, FL.
DEBRIS/ICE/TPS ASSESSMENT AND INTEGRATED PHOTOGRAPHIC ANALYSIS FOR SHUTTLE MISSION STS-49
Gregory N. Katnik, Scott A. Higginbotham, and J. Bradley Davis Jul. 1992 186 p Original contains color illustrations
(NASA-TM-107547; NAS 1.15:107547) Avail: CASI HC A09/MF A02; 91 functional color pages

A debris/ice/Thermal Protection System (TPS) assessment and integrated photographic analysis was conducted for Shuttle Mission STS-49. Debris inspections of the flight elements and launch pad were performed before and after launch. Ice/frost conditions on the External Tank were assessed by the use of computer programs, nomographs, and infrared scanner data during cryogenic loading of the vehicle followed by on-pad visual inspection. High speed photography was analyzed after launch to identify ice/debris sources and evaluate potential vehicle damage and/or in-flight anomalies. Debris/ice/TPS conditions and integrated photographic

analysis of Shuttle Mission STS-49, and the resulting effect on the Space Shuttle Program are discussed. Author

N92-32610*# Rockwell Space Operations Co., Houston, TX.
SUPERHEAVYWEIGHT MISSIONS SI VERSUS DI: ASCENT FLIGHT DESIGN OPTIONS AND RECOMMENDATIONS
26 Oct. 1990 40 p Prepared in cooperation with Bendix Corp., Southfield, MI, Unisys Corp., Detroit, MI, Omniplan Corp., Houston, TX, and Systems Management American Corp., Houston, TX
(Contract NAS9-18000)
(NASA-CR-183208; NAS 1.26:183208; STSOC-RT-001283)
Avail: CASI HC A03/MF A01

AFD has completed the trade study on Standard Insertion (SI) vs Direct Insertion (DI) for STS-50. RSOC Range Safety has developed acceptable DI targets from 130 n.mi. to 150 n.mi. and the corresponding performance assessment for these targets using STS-50 data has been completed. This mission has sufficient performance capability to perform this mission as a DI to 160 n.mi. A reduced OMS load corresponding to a DI mission is required for this option. The increase in altitude over the AFP baseline (SI to 145 n.mi.) is highly desirable for this mission. The orientation on orbit for the orbiter/USML-1 payload is such that orbital decay is maximized (maximum frontal cross-sectional area with vehicle normal to velocity vector). Increasing the operational altitude reduces the amount of vernier thruster firings necessary to maintain a constant gravity gradient. The results of this trade study can also be applied to other superheavyweight missions (EDO flights) and will allow for use of the DI technique for lower orbital altitudes, thereby eliminating the SI option for due east, low altitude missions. STSOC transmittal form no. 330-330-130, which documents the technical issues and assumptions used for this trade study effort in detail, should be referenced for further information. The main reason that a DI is desired for STS-50 and other superheavyweight flights (low altitude) is that ESMC range safety has expressed reservations about SI missions in general. The concern is that the current SI design underspeed exposes Africa and Madagascar to potential ET debris impact. In the past range safety has waived the requirement that these areas be protected in the event of an engine failure. With the advent of the pre-MECO OMS dump, the viability of DI and the high casualty expectations from the ACTA press to MECO hazard study, range safety has become more reluctant to approve SI flights. It is felt that to perform an SI mission there would have to be a large decrease in design underspeed to protect these landmasses, which would result in possible gaps between a late TAL and PTA. The assumed limit on a DI has been to altitudes greater than 160 n.mi. It was assumed that for altitudes less than 160 n.mi. the nominal ET impact envelope would overlap the Gilbert Islands. Author

17 SPACE COMM., SPACECRAFT COMM., COMMAND & TRACKING

Includes telemetry; space communications networks; astronavigation and guidance; and radio blackout.

For related information see also *04 Aircraft Communications and Navigation* and *32 Communications and Radar.*

No abstracts in this category.

18 SPACECRAFT DESIGN, TESTING AND PERFORMANCE

Includes satellites; space platforms; space stations; spacecraft systems and components such as thermal and environmental controls; and attitude controls.

For life support systems see *54 Man/System Technology and Life Support.* For related information see also *05 Aircraft Design, Testing and Performance, 39 Structural Mechanics,* and *16 Space Transportation.*

N92-32244*# Research Inst. for Computing and Information Systems, Houston, TX.
ROBUST STABILIZATION OF THE SPACE STATION Final Report
Bong Wie (Arizona State Univ., Tempe.) 30 Sep. 1991 33 p
(Contract NCC9-16; RICIS Proj. MS-03)
(NASA-CR-190627; NAS 1.26:190627) Avail: CASI HC A03/MF A01

A robust H-infinity control design methodology and its application to a Space Station Freedom (SSF) attitude and momentum control problem are presented. This approach incorporates nonlinear multi-parameter variations in the state-space formulation of H-infinity control theory. An application of this robust H-infinity control synthesis technique to the SSF control problem yields remarkable results in stability robustness with respect to moments of inertia variation of about 73 percent in one of the structured uncertainty directions. The performance and stability of this robust H-infinity controller for the SSF are compared to those of other controllers designed using a standard linear-quadratic-regulator synthesis technique. Author

N92-32421*# National Aeronautics and Space Administration, Washington, DC.
SPACE STATION FREEDOM MEDIA HANDBOOK
May 1992 106 p
(NASA-TM-107981; NAS 1.15:107981) Avail: CASI HC A06/MF A02

Work underway at NASA to design and develop Space Station Freedom is described in this handbook. The roles, responsibilities, and tasks at NASA are discussed in order to provide information for the media. Ground facilities are described with a look towards future possibilities and requirements. Historical perspectives, international cooperation, and the responsibilities of specific NASA centers are also examined. H.A.

N92-32477*# Texas A&M Univ., College Station. Dept. of Mechanical Engineering.
VISIONLESS TRAC Final Report
Louis J. Everett 10 Sep. 1992 45 p
(Grant NAG9-549)
(NASA-CR-190732; NAS 1.26:190732) Avail: CASI HC A03/MF A01

This final report documents the activities during a sabbatical. Leo Monford was the principal NASA contact for this work. The work supported a flight experiment planned by the Space Research Consortium which investigated the potential of using a Targeting Reflective Alignment Concept (TRAC) sensor to automatically rendezvous satellites. Other work supported the Explorer flight experiment by providing TRAC reflectors for future rendezvous experiments. The third project initiated was a visionless TRAC sensing concept called the PSD concept. Author

N92-32538# Naval Postgraduate School, Monterey, CA.
SATELLITE ANOMALIES AND ELECTROSTATIC SURFACE DISCHARGES M.S. Thesis
Yan Chun Wong Sep. 1991 84 p
(AD-A246880) Avail: CASI HC A05/MF A01

Various aspects of the space environment can cause on-orbit satellite anomalies. Studies have shown that adverse interactions between the natural space environment and space systems can have deleterious consequences comparable to those caused by human or design errors. Electrostatic surface discharges (ESD),

electron caused electromagnetic pulse (ECEMP), and single event upset (SEU) are the three most common anomaly producing mechanisms in space systems. The plasma environment, such as in geosynchronous orbit, can cause differential charging of satellite components and lead to ESD's on satellite surfaces. By using the Spacecraft Anomaly Manager (SAM) software package, spacecraft anomaly data of operational satellite contained in the database of National Geophysical Data Center (NGDC) were analyzed. The analysis concluded that ESD is directly related to geomagnetic storm activity, and ESD related anomalies are local time and seasonal dependent. Proper engineering solutions should be integrated into satellite designs to prevent ESD from causing anomalies. This can be done effectively on multi-satellite programs such as GPS. Active charge control is recommended for DoD satellites which cannot tolerate functional anomalies due to ESD's, and on the first flight of new satellite designs. Passive engineering solutions should be integrated into satellite designs. GRA

N92-32704# Sandia National Labs., Albuquerque, NM.
A SIMPLE APPROACH FOR THE DESIGN AND OPTIMIZATION OF STAND-OFF HYPERVELOCITY PARTICLE SHIELDS
R. J. Lawrence 1992 22 p Presented at the AIAA Space Programs and Technologies Conference, Huntsville, AL, 24-27 Mar. 1992 Previously announced in IAA as A92-38586
(Contract DE-AC04-76DP-00789)
(DE92-011383; SAND-92-0662C; CONF-920373-4; AIAA Paper 92-1465) Avail: CASI HC A03/MF A01

A simple engineering model applicable to stand-off 'Whipple bumper' shields, which are used to protect space-based assets from impacts by orbital debris particles is described. The model provides a framework for analyzing: (1) the parameter limits governing the penetration and breakup or decomposition of the hypervelocity debris particle; (2) the behavior of the induced debris cloud, including its velocity and divergence; and (3) the design and optimization of the stand-off shield for a specific threat and level of protection required. The model is normalized to actual stand-off debris shield experiments and multi-dimensional numerical simulations at impact velocities of about 10 km/s. The subsequent analysis of a current space station shield design suggests that: (1) for acceptable levels of protection, stand-off shields can be significantly thinner than previously thought; and (2) with the proper balance between shield thickness and stand-off distance, the total shield mass can be reduced substantially. DOE

N92-32834# National Aerospace Lab., Amsterdam (Netherlands). Space Div.
INVESTIGATIONS PREPARATORY TO THE WET SATELLITE MODEL EXPERIMENT
J. P. B. Vreeburg 30 Jun. 1991 18 p Presented at the International Symposium on Hydromechanics and Heat/Mass Transfer in Microgravity, Perm-Moscow, USSR, 6-12 Jul. 1991
(NLR-TP-91219-U; ETN-92-92005) Avail: CASI HC A03/MF A01

The Wet Satellite Model (WSM) Experiment is to be executed with a small spacecraft that has a tank partially filled with liquid. The spacecraft is instrumented with a distributed arrangement of linear accelerometers in order to determine its angular and translational motions. From these data, the forces and moments exerted by the liquid on the rigid part of the spacecraft are to be calculated. Investigations on different subjects were conducted in preparation of the experiment. These concern the formulation of the dynamic behavior of the spacecraft, the stability of various spacecraft configurations, the arrangement of the accelerometers, and some practical difficulties. For numerical simulation of the dynamics of the spacecraft, use is made of a computer program having a routine that simulates the behavior of liquid in microgravity and under capillary forces. A breadboard model of the spacecraft was operated during aircraft parabolic flight. This environment is not suitable for investigations on a model with a partially filled tank but provides useful results with empty or completely filled tanks. The planned further development of the WSM Experiment is elaborated. ESA

N92-32934# Los Alamos National Lab., NM.
COLLABORATIVE, REMOTE, IN-DEPTH INSPECTION AND VERIFICATION OF SATELLITES WITH NEUTRAL PARTICLE BEAMS
G. H. Canavan and D. Holtkamp May 1992 50 p
(Contract W-7405-eng-36)
(DE92-014195; LA-11804-MS) Avail: CASI HC A03/MF A01

Neutral particle beams can probe satellites' interiors, which enable them to discriminate on mass and determine the satellite's function with confidence. That capability, now absent, is essential for enforcing existing space agreements, defining the verifiability of future agreements, and determining the capabilities of unknown space objects. It is complemented by their ability to image at close ranges and measure spectral information at intermediate ranges. The platforms would be of very low current and moderate energies, which would give them no significant antisatellite capability. DOE

N92-33013* National Aeronautics and Space Administration. Langley Research Center, Hampton, VA.
INTEGRATED LAUNCH AND EMERGENCY VEHICLE SYSTEM Patent
James A. Martin, inventor (to NASA) 1 Sep. 1992 9 p Filed 31 Aug. 1990 Supersedes N91-13481 (29 - 5, p 628)
(NASA-Case-LAR-13780-1; US-Patent-5,143,327;
US-Patent-Appl-SN-575737; US-Patent-Class-244-158R;
US-Patent-Class-244-160; US-Patent-Class-244-172;
Int-Patent-Class-B64G-1/40) Avail: US Patent and Trademark Office

A heavy launch vehicle is discussed. The launch vehicle is comprised of an expendable, multi-container, propellant tank that has a plurality of winged booster propulsion modules at one end and a payload supported by adapter structure at the other end. The preferred payload is an entry module that can be adapted for docking to the space station and used as a return vehicle for the space station crew. Additionally, the payload may include communication satellites, supplies, equipment, and/or structural elements for the space station. The winged propulsion modules are released from the expendable propellant tank, in pairs, and they return to Earth in a controlled glide. After a safe landing, at or near the launch site, the modules are prepared for reuse. The rocket engines for each propulsion module are dual-fuel, dual-mode engines and use methane-oxygen and hydrogen-oxygen from the multi-containers of the propellant tank. When the propulsion modules are released from the expendable propellant tank, the rocket engines are moved into the module cargo bay for the return glide flight.
Official Gazette of the U.S. Patent and Trademark Office

19 SPACECRAFT INSTRUMENTATION

For related information see also *06 Aircraft Instrumentation* and *35 Instrumentation and Photography.*

N92-32728 Institut d'Aeronomie Spatiale de Belgique, Brussels.
GRILL SPECTROMETRY ON THE SPACE SHUTTLE DURING THE ATLAS 1 MISSION [L'EXPERIENCE DE SPECTROMETRIE A GRILLE A BORD DE LA NAVETTE SPATIALE LORS DE LA MISSION ATLAS 1]
C. Camy-Peyret (Office National d'Etudes et de Recherches Aerospatiales, Paris, France), N. Papineau (Office National d'Etudes et de Recherches Aerospatiales, Paris, France), R. Armante (Office National d'Etudes et de Recherches Aerospatiales, Paris, France), V. Achard (Office National d'Etudes et de Recherches Aerospatiales, Paris, France), J. Besson (Office National d'Etudes et de Recherches Aerospatiales, Paris, France), C. Muller, M. DeMaziere, C. Lippens, J. Vercheval, and M. Ackerman et al 1992 32 p In FRENCH Submitted for publication
(Aeronautica-Acta-A-364-1992; ETN-92-91979) Avail: Institut d'Aeronomie Spatiale de Belgique, 3 Avenue Circulaire, B-1180 Brussels, Belgium

The scientific program prepared for the Atlas 1 grill spectrometer are described. In particular, spectral intervals are discussed for each molecule. The instrument characteristics are outlined. The observations made by the Atlas 1 instruments will give vertical profiles of trace species concentration in the Earth atmosphere.
ESA

N92-33112*# National Aeronautics and Space Administration. Langley Research Center, Hampton, VA.
IMPROVED HIRAP FLIGHT CALIBRATION TECHNIQUE
Christina D. Moats (Lockheed Engineering and Sciences Co., Hampton, VA.), Robert C. Blanchard, and Kevin T. Larman (Lockheed Engineering and Sciences Co., Hampton, VA.) Jul. 1992 28 p
(RTOP 506-48-11-04)
(NASA-TM-107656; NAS 1.15:107656) Avail: CASI HC A03/MF A01

A method of removing non-aerodynamic acceleration signals and calibrating the High Resolution Accelerometer Package (HiRAP) has been developed and improved. Twelve HiRAP mission data sets have been analyzed applying the improved in-flight calibration technique. The application of flight calibration factors to the data sets from these missions produced calibrated acceleration levels within +/- 5.7 micro-g of zero during a time in-flight when the acceleration level was known to be less than 1 g. To validate the current in-flight calibration technique, the atmospheric density results, specifically the normal-to-axial density ratios, have been compared with the analysis results obtained with the previous in-flight calibration technique. This comparison shows an improvement (up to 12.4 percent per flight) in the density ratio when the updated in-flight calibration technique is used.
Author

20 SPACECRAFT PROPULSION AND POWER

Includes main propulsion systems and components, e.g., rocket engines; and spacecraft auxilliary power sources.

For related information see also *07 Aircraft Propulsion and Power, 28 Propellants and Fuels, 44 Energy Production and Conversion,* and *15 Launch Vehicles and Space Vehicles.*

N92-32463*# National Aeronautics and Space Administration. Lewis Research Center, Cleveland, OH.
NASA'S NUCLEAR ELECTRIC PROPULSION TECHNOLOGY PROJECT
James R. Stone and James S. Sovey Jul. 1992 18 p Presented at the 28th Joint Propulsion Conference and Exhibit, Nashville, TN, 6-8 Jul. 1992; sponsored by AIAA, SAE, ASME, and ASEE
(RTOP 593-72-41)
(NASA-TM-105811; E-7242; NAS 1.15:105811) Copyright Avail: CASI HC A03/MF A01

The National Aeronautics and Space Administration (NASA) has initiated a program to establish the readiness of nuclear electric propulsion (NEP) technology for relatively near-term applications to outer planet robotic science missions with potential future evolution to system for piloted Mars vehicles. This program was initiated in 1991 with a very modest effort identified with nuclear thermal propulsion (NTP); however, NEP is also an integral part of this program and builds upon NASA's Base Research and Technology Program in power and electric propulsion as well as the SP-100 space nuclear power program. The NEP Program will establish the feasibility and practicality of electric propulsion for robotic and piloted solar system exploration. The performance objectives are high specific impulse (200 greater than I(sub sp) greater than 10000 s), high efficiency (over 0.50), and low specific mass. The planning for this program was initially focussed on piloted Mars missions, but has since been redirected to first focus on 100-kW class systems for relatively near-term robotic missions, with possible future evolution to megawatt- and multi-megawatt-class systems applicable to cargo vehicles supporting human missions as well as to the piloted vehicles. This paper reviews current plans and recent progress for the overall nuclear electric propulsion project and closely related activities.
Author

N92-33064*# National Aeronautics and Space Administration. Lewis Research Center, Cleveland, OH.
THE EVOLUTIONARY DEVELOPMENT OF HIGH SPECIFIC IMPULSE ELECTRIC THRUSTER TECHNOLOGY
James S. Sovey, John A. Hamley, Michael J. Patterson, Vincent K. Rawlin, and Roger M. Meyers (Sverdrup Technology, Inc., Brook Park, OH.) Mar. 1992 33 p Presented at the Space Programs and Technologies Conference; sponsored by AIAA
(RTOP 506-42-31)
(NASA-TM-105758; E-7170; NAS 1.15:105758) Avail: CASI HC A03/MF A01

Electric propulsion flight and technology demonstrations conducted primarily by Europe, Japan, Peoples Republic of China, USA, and USSR are reviewed. Evolutionary mission applications for high specific impulse electric thruster systems are discussed, and the status of arcjet, ion, and magnetoplasmadynamic thruster and associated power processor technologies are summarized.
Author

N92-33162 Department of the Navy, Washington, DC.
DEVICE AND PROCESS FOR ATTACHMENT OF PARTS TO ROCKET MOTORS Patent
Jon J. Yagla, inventor (to Navy), Robert W. Lowry, inventor (to Navy), and Otho L. Mears, inventor (to Navy) 21 Apr. 1992 5 p Filed 28 Feb. 1991
(AD-D015309; US-Patent-5,106,034; US-Patent-Appl-SN-664010; US-Patent-Class-244-324) Avail: US Patent and Trademark Office

An attachment platform positioned longitudinally on a rocket motor chamber and secured with laser welding techniques is described. Each attachment platform is continuously sealed longitudinally to the rocket motor chamber through the application of laser welding and optical seam tracking. Application of laser welding techniques allows for repair and installation of attachment platforms on rocket motors fully loaded with live propellant.
GRA

N92-33166# Sandia National Labs., Albuquerque, NM.
ROAR: A 3-D TETHERED ROCKET SIMULATION CODE
A. R. York, II and J. S. Ludwigsen Apr. 1992 50 p
(Contract DE-AC04-76DP-00789)
(DE92-017358; SAND-90-1439) Avail: CASI HC A03/MF A01

A high-velocity impact testing technique, utilizing a tethered rocket, is being developed at Sandia National Laboratories. The technique involves tethering a rocket assembly to a pivot location and flying it in a semicircular trajectory to deliver the rocket and payload to an impact target location. Integral to developing this testing technique is the parallel development of accurate simulation models. An operational computer code, called ROAR (Rocket-on-a-Rope), has been developed to simulate the three-dimensional transient dynamic behavior of the tether and motor/payload assembly. This report presents a discussion of the parameters modeled, the governing set of equations, the through-time integration scheme, and the input required to set up a model. Also included is a sample problem and a comparison with experimental results.
DOE

N92-32246*# Aerojet-General Corp., Sacramento, CA. Advanced Solid Rocket Motors Div.
CURRENT STATUS OF THE DEVELOPMENT OF AN IGNITION TRANSIENT MODEL FOR SOLID ROCKET MOTORS
Gary D. Luke and Harry A. Dwyer *In* NASA. Goddard Space Flight Center, Tenth Workshop for Computational Fluid Dynamic Applications in Rocket Propulsion, Part 2 Jul. 1992 p 725-761 Prepared in cooperation with California Univ., Davis (For primary document see N92-32245 23-34)
Avail: CASI HC A03/MF A05

N92-32248*# National Aeronautics and Space Administration. Marshall Space Flight Center, Huntsville, AL.
A COMPARATIVE STUDY OF THE EFFECTS OF INHIBITOR STUB LENGTH ON SOLID ROCKET MOTOR COMBUSTION CHAMBER PRESSURE OSCILLATIONS: RSRM AT T = 80 SECONDS, PRELIMINARY RESULTS
D. Chasman (Rockwell International Corp., Huntsville, AL.), D. Burnette (Rockwell International Corp., Huntsville, AL.), J. Holt (Rockwell International Corp., Huntsville, AL.), and R. Farr *In* NASA. Goddard Space Flight Center, Tenth Workshop for Computational Fluid Dynamic Applications in Rocket Propulsion, Part 2 Jul. 1992 p 787-790 (For primary document see N92-32245 23-34)
Avail: CASI HC A01/MF A05

N92-32259*# Rockwell International Corp., Canoga Park, CA. Rocketdyne Div.
MODELING OF SSME FUEL PREBURNER ASI
Pak-Yan Liang *In* NASA. Goddard Space Flight Center, Tenth Workshop for Computational Fluid Dynamic Applications in Rocket Propulsion, Part 2 Jul. 1992 p 1013-1031 (For primary document see N92-32245 23-34)
Avail: CASI HC A03/MF A05

N92-32262*# Aerojet-General Corp., Sacramento, CA. Propulsion Div.
STME HYDROGEN MIXER STUDY
Rob Blumenthal, Dongmoon Kim, and George Bache *In* NASA. Goddard Space Flight Center, Tenth Workshop for Computational Fluid Dynamic Applications in Rocket Propulsion, Part 2 Jul. 1992 p 1093-1116 (For primary document see N92-32245 23-34)
Avail: CASI HC A01/MF A05

N92-32272*# Aerotherm Corp., Huntsville, AL.
DEVELOPMENT OF THE KIVA-2 CFD CODE FOR ROCKET PROPULSION APPLICATIONS
Robert V. Shannon, Jr. and Alvin L. Murray *In* NASA. Goddard Space Flight Center, Tenth Workshop for Computational Fluid Dynamic Applications in Rocket Propulsion, Part 2 Jul. 1992 p 1349-1378 (For primary document see N92-32245 23-34)
Avail: CASI HC A03/MF A05

N92-32280*# National Aeronautics and Space Administration. Marshall Space Flight Center, Huntsville, AL.
ADVANCED SOLID ROCKET MOTOR PROJECT STATUS
Keith Coates *In* NASA. Goddard Space Flight Center, Tenth Workshop for Computational Fluid Dynamic Applications in Rocket Propulsion, Part 1 Jul. 1992 p 27-43 (For primary document see N92-32278 23-34)
Avail: CASI HC A03/MF A05

N92-32281*# National Aeronautics and Space Administration. Marshall Space Flight Center, Huntsville, AL.
SPACE TRANSPORTATION MAIN ENGINE
Jan C. Monk *In* NASA. Goddard Space Flight Center, Tenth Workshop for Computational Fluid Dynamic Applications in Rocket Propulsion, Part 1 Jul. 1992 p 45-82 (For primary document see N92-32278 23-34)
Avail: CASI HC A03/MF A05

N92-33245# Hercules, Inc., Rocket Center, WV. Ballistics Lab.
HAZARDS REDUCTION FOR TACTICAL MISSILES
K. O. Hartman *In* AGARD, Insensitive Munitions Jul. 1992 22 p (For primary document see N92-33240 23-28)
Copyright Avail: CASI HC A03/MF A03

23 CHEMISTRY AND MATERIALS (GENERAL)

N92-32484 ESDU International Ltd., London (England).
THERMAL CONDUCTIVITY OF LIQUID ALIPHATIC HYDROCARBONS. PART 1: ALKANES Abstract Only
Apr. 1992 178 p Supersedes ESDU-75003
(ESDU-92011-Pt-1; ESDU-75003; ISBN-0-85679-816-9) Avail: ESDU

ESDU 92011 gives data for 81 alkanes. Experimental results drawn from the literature for each compound were fitted with a four-term polynomial equation in reduced temperature. The coefficients were also paired with changing molecular structure to ensure the best correlation not only for the individual alkanes but also as members of their chemical series. The coefficient correlations also allowed values to be predicted for compounds for which no measure data exist. The equations were used to tabulate thermal conductivity values from the melting point to about 0.9 critical temperature in SI units at 10 K and 10 C intervals. The critical point, coefficients, and sources of the data are given for each compound. Conversion factors are provided for common British units, the effect of pressure is briefly considered, and the likely accuracy of the tabulated values is discussed. ESDU

N92-32485 ESDU International Ltd., London (England).
THERMAL CONDUCTIVITY OF GASEOUS HALOGENATED HYDROCARBONS: ETHYLENES AND BENZENES Abstract Only
Apr. 1992 27 p
(ESDU-92010; ISBN-0-85679-815-0) Avail: ESDU

ESDU 92010 uses a third order polynomial in reduced temperature to correlate experimental data extracted from the literature for seven chloro- and fluoroethylenes and for fluoro-, chloro-, bromo- and iodobenzene over the temperature range from the boiling point to at least 1.1 times the critical temperature, or from 200 to 650 K. The coefficients of the equation are given for each compound, and the equation is used to tabulate thermal conductivity in SI units at both 20 K and 20 C intervals. The sources of data used for each compound are listed, and values that involve extrapolation of the available data are indicated. The likely accuracy of the values quoted is discussed, and the effect of pressure on thermal conductivity is briefly considered. ESDU

N92-32486 ESDU International Ltd., London (England).
ORTHOBARIC DENSITIES AND MOLAR VOLUMES OF LIQUIDS: HALOGENATED ETHANES Abstract Only
Mar. 1992 92 p
(ESDU-92009; ISBN-0-85679-814-2) Avail: ESDU

ESDU 92009 tabulates density and molar volumes for 39 haloethanes and 7 azeotropic mixtures. The tables are in units of kg/cu m and cu cm/mol respectively from near the melting point to within a few degrees of the critical point. The temperature interval chosen is varied from 10 K to 1 K to keep the increments in density reasonably small. Although the Rackett equation does not represent the variation of density over the full temperature range so well as the equation used in ESDU 92009 (log reduced density as a polynomial function of reduced temperature), it was used to estimate the critical density. The log/polynomial equation was then fitted to the experimental data for density for each compound taken from a wide range of sources in the literature; values established for the coefficients in the equation for each compound are also tabulated. Estimates of the accuracy of the predictions are included, as is a list of the sources of data actually used for each compound. Values at the critical point are provided together with normal boiling and melting points. ESDU

24 COMPOSITE MATERIALS

Includes physical, chemical, and mechanical properties of laminates and other composite materials.
For ceramic materials see *27 Nonmetallic Materials.*

N92-32327# Lawrence Livermore National Lab., CA.
QUANTITATIVE NON-DESTRUCTIVE ENVIRONMENTAL CHARACTERIZATION OF ADVANCED MATERIALS
D. Dobie, J. Celeste, and G. Krauter 1991 5 p Presented at the American Society for Nondestructive Testing Spring Conference, Oakland, CA, 18-22 Mar. 1991
(Contract W-7405-eng-48)
(DE92-011462; UCRL-JC-105233; CONF-910399-7) Avail: CASI HC A01/MF A01

Polymethylpentene, polystyrene, agar, carbon, and composites are advanced materials that have unique engineering properties. Of particular interest to our engineering department is their response to temperature and humidity excursions. We built computer-controlled environmental test chambers to evaluate the materials and derive thermal and hygroscopic (water absorption) properties. DOE

N92-32339# Stanford Univ., CA. Dept. of Materials Science and Engineering.
HIGH TEMPERATURE DEFORMATION PROCESSES AND STRENGTHENING MECHANISMS IN INTERMETALLIC PARTICULATE COMPOSITES Final Technical Report, Dec. 1988 - Dec. 1991
William D. Nix, Keith R. Forbes, and D. D. Sternbergh 31 Mar. 1992 46 p
(Contract F49620-92-J-0009; AF-AFOSR-0201-89)
(AD-A250220; AFOSR-92-0356TR; AFOSR-92-1) Avail: CASI HC A03/MF A01

Research on the high temperature deformation processes and strengthening mechanisms in Intermetallic Particulate Composites is described. Work of the grant included high temperature compression tests of Ni3Al-Al2O3 composites; mechanical alloying of Ni3Al+Y2O3; transient deformation studies of the intermetallics Ni3Al, NiAl, and NiBe; and development of a model of dislocation structure control of plastic deformation. Work during the past year on the high temperature deformation of NiA1 single crystals is also described. GRA

N92-32459# Air Force Systems Command, Wright-Patterson AFB, OH.
HEATING FIXTURE AND INSTRUMENTATION DESIGN FOR ELEVATED TEMPERATURE TESTS OF A COMPOSITE REPAIR TECHNIQUE Technical Report, Jan. - Sep. 1989
Larry Bates and Donald Cook Dec. 1991 30 p
(WL-TM-90-326-FIBE) Avail: CASI HC A03/MF A01

Static tension tests were conducted for the Structural Concepts Branch (WL/FIBC) on composite bolted repair samples. The purpose of these tests was to compare experimental results with strains predicted by the Composite Bolted Repair Analysis program. This program was originally developed under contract by McDonnell Douglas to predict elevated temperature (0-250 F) strains, but these strains were not confirmed experimentally. Ten panels, 12 inches x 22 inches, were made from AS4/3501 graphite/epoxy. Five panels were laid up as (+ and - 45,0,90)(sub 3S) and five panels were laid up as ((+ and - 45,0,90)(sub 2)(+ and - 45,90,90)) symmetric. Each ply was approximately 0.005 inch thick for a total panel thickness of 0.120 inch. For more details about the panels and the entire test program, refer to the WL Technical Report being written by Mr. Forrest Sandow of Wright Laboratory Structural Concepts Branch (WL/FIBC). This TM addresses only the oven and instrumentation designs. The oven was designed to be integrated into FIBEC's 100 Kip Instron static test frame and meet the environmental requirements specified by FIBC. The instrumentation included five thermocouples to confirm the specimens were in the required environment, twenty-seven strain gauge channels to measure the strains, and one load cell channel ranging from five-thousand pounds to fifty-thousand pounds. Author

N92-32466*# National Aeronautics and Space Administration. Lewis Research Center, Cleveland, OH.
COMPUTATIONAL SIMULATION OF MATRIX MICRO-SLIP BANDS IN SiC/Ti-15 COMPOSITE
S. K. Mital (Toledo Univ., OH.), H.-J. Lee, P. L. N. Murthy, and C. C. Chamis 1992 9 p Proposed for presentation at the 1992 Winter Annual Meeting of ASME, Anaheim, CA, 8-13 Nov. 1992
(RTOP 505-63-5B)
(NASA-TM-105762; E-7179; NAS 1.15:105762) Avail: CASI HC A02/MF A01

Computational simulation procedures are used to identify the key deformation mechanisms for (0)(sub 8) and (90)(sub 8) SiC/Ti-15 metal matrix composites. The computational simulation procedures employed consist of a three-dimensional finite-element analysis and a micromechanics based computer code METCAN. The interphase properties used in the analysis have been calibrated using the METCAN computer code with the (90)(sub 8) experimental stress-strain curve. Results of simulation show that although shear stresses are sufficiently high to cause the formation of some slip bands in the matrix concentrated mostly near the fibers, the nonlinearity in the composite stress-strain curve in the case of (90)(sub 8) composite is dominated by interfacial damage, such as microcracks and debonding rather than microplasticity. The stress-strain curve for (0)(sub 8) composite is largely controlled by the fibers and shows only slight nonlinearity at higher strain levels that could be the result of matrix microplasticity. Author

N92-32491*# Virginia Polytechnic Inst. and State Univ., Blacksburg. Coll. of Engineering.
COMPRESSION OF THICK LAMINATED COMPOSITE BEAMS WITH INITIAL IMPACT-LIKE DAMAGE Interim Report No. 90, Jan. 1990 - Dec. 1991
N. L. Breivik, Z. Guerdal, and O. H. Griffin, Jr. Jun. 1992 169 p
(Grant NAG1-343)
(NASA-CR-190573; NAS 1.26:190573; VPI-E-92-15; CCMS-92-16) Avail: CASI HC A08/MF A02

While the study of compression after impact of laminated composites has been under consideration for many years, the complexity of the damage initiated by low velocity impact has not lent itself to simple predictive models for compression strength. The damage modes due to non-penetrating, low velocity impact by large diameter objects can be simulated using quasi-static three-point bending. The resulting damage modes are less coupled and more easily characterized than actual impact damage modes. This study includes the compression testing of specimens with well documented initial damage states obtained from three-point bend testing. Compression strengths and failure modes were obtained for quasi-isotropic stacking sequences from 0.24 to 1.1 inches thick with both grouped and interspersed ply stacking. Initial damage prior to compression testing was divided into four classifications based on the type, extent, and location of the damage. These classifications are multiple through-thickness delaminations, isolated delamination, damage near the surface, and matrix cracks. Specimens from each classification were compared to specimens tested without initial damage in order to determine the effects of the initial damage on the final compression strength and failure modes. A finite element analysis was used to aid in the understanding and explanation of the experimental results. Author

N92-32513*# National Aeronautics and Space Administration. Langley Research Center, Hampton, VA.
EIGHTH DOD/NASA/FAA CONFERENCE ON FIBROUS COMPOSITES IN STRUCTURAL DESIGN, PART 1
James H. Starnes, Jr., comp., Herman L. Bohon, comp. (Lockheed Engineering and Sciences Co., Hampton, VA.), and Sherry B. Garzon, comp. Sep. 1990 383 p Conference held in Norfolk, VA, 28-30 Nov. 1989
(RTOP 505-63-01-09)
(NASA-CP-3087-Pt-1; L-16832-Pt-1; NAS 1.55:3087-Pt-1) Avail: CASI HC A17/MF A03

The status, problems, and requirements in the technical

disciplines related to the design of composite structures are discussed. Papers are presented in the areas of applications in design; concepts in design; and methodology in design. For individual titles, see N92-32514 through N92-32532.

N92-32514*# Grumman Aerospace Corp., Bethpage, NY.
DESIGN, EVALUATION AND EXPERIMENTAL EFFORT TOWARD DEVELOPMENT OF A HIGH STRAIN COMPOSITE WING FOR NAVY AIRCRAFT
Joseph Bruno and Mark Libeskind (Naval Air Development Center, Warminster, PA.) *In* NASA. Langley Research Center, Eighth DOD/NASA/FAA Conference on Fibrous Composites in Structural Design, Part 1 Sep. 1990 p 3-27 (For primary document see N92-32513 23-24)
Avail: CASI HC A03/MF A03

This design development effort addressed significant technical issues concerning the use and benefits of high strain composite wing structures (Epsilon(sub ult) = 6000 micro-in/in) for future Navy aircraft. These issues were concerned primarily with the structural integrity and durability of the innovative design concepts and manufacturing techniques which permitted a 50 percent increase in design ultimate strain level (while maintaining the same fiber/resin system) as well as damage tolerance and survivability requirements. An extensive test effort consisting of a progressive series of coupon and major element tests was an integral part of this development effort, and culminated in the design, fabrication and test of a major full-scale wing box component. The successful completion of the tests demonstrated the structural integrity, durability and benefits of the design. Low energy impact testing followed by fatigue cycling verified the damage tolerance concepts incorporated within the structure. Finally, live fire ballistic testing confirmed the survivability of the design. The potential benefits of combining newer/emerging composite materials and new or previously developed high strain wing design to maximize structural efficiency and reduce fabrication costs was the subject of subsequent preliminary design and experimental evaluation effort.
Author

N92-32515*# Army Materials Technology Lab., Watertown, MA. Composites Development Branch.
COMPOSITE STRUCTURAL ARMOR FOR COMBAT VEHICLE APPLICATIONS
William E. Haskell, III, A. L. Alesi, and G. R. Parsons *In* NASA. Langley Research Center, Eighth DOD/NASA/FAA Conference on Fibrous Composites in Structural Design, Part 1 Sep. 1990 p 29-47 (For primary document see N92-32513 23-24)
Avail: CASI HC A03/MF A03

Several projects that have demonstrated the advantages of using thick composite armor technology for structural applications in armored combat vehicles are discussed. The first involved composite cargo doors for the Marine Corps LVTP-7 amphibious landing vehicle. Another was a demonstration composite turret that offered a weight reduction of 15.5 percent. The advantages of this composite armor compared to metallic armors used for combat vehicle hull and turret applications are reduced weight at equal ballistic protection; reduced back armor spall; excellent corrosion resistance; reduced production costs by parts consolidation; and inherent thermal and acoustic insulative properties. Based on the encouraging results of these past programs, the Demonstration Composite Hull Program was started in September 1986. To demonstrate this composite armor technology, the Army's newest infantry fighting vehicle, the Bradley Fighting Vehicle (BFV), was selected as a model. A composite infantry fighting vehicle, designated the CIFV for this program, has been designed and fabricated and is currently undergoing a 6000 mile field endurance test. The CIFV demonstration vehicle uses the BFV engine, transmission, suspension, track and other equipment.
Author

N92-32516*# Army Materials Technology Lab., Watertown, MA.
APPLICATIONS OF COMPOSITES TO ARMAMENTS
Don W. Oplinger *In* NASA. Langley Research Center, Eighth DOD/NASA/FAA Conference on Fibrous Composites in Structural Design, Part 1 Sep. 1990 p 49-101 (For primary document see N92-32513 23-24)
Avail: CASI HC A04/MF A03

The U.S. Army Materials Technology Laboratory (MTL) has been engaged in investigating the feasibility of applying composite materials to the lightening of artillery structural components since about 1982. In this period a number of efforts were carried out either in-house at MTL or by supporting organizations, including Benet Laboratory and the Oak Ridge National Laboratory, aimed at investigating applications to various components of towed artillery. Salient features of these efforts and some important conclusions that have come out of them are described. In addition to organic matrix composites, discontinuously reinforced metal matrix composites appear to have great potential for weight reduction in this type of application.
Author

N92-32517*# Simula, Inc., Phoenix, AZ.
THE WEIGHT OPTIMIZATION OF AN ARMORED CRASHWORTHY CREWSEAT THROUGH THE USE OF ADVANCED COMPOSITES AND DESIGN
Howard A. Lindsay, Stephen M. Motoyama, and Kent F. Smith (Army Aviation Applied Technology Directorate, Fort Eustis, VA.) *In* NASA. Langley Research Center, Eighth DOD/NASA/FAA Conference on Fibrous Composites in Structural Design, Part 1 Sep. 1990 p 103-117 (For primary document see N92-32513 23-24)
Avail: CASI HC A03/MF A03

The development of composite-related technology applicable to armored crashworthy helicopter crewseats is discussed. The main objective was to achieve a significant weight reduction relative to the first-generation seats exemplified by the UH-60A and the AH-64A designs. This weight reduction was achieved while maintaining full compliance with the most recent version of the military crashworthy crewseat specification, MIL-S-58095A. The technology developed during this effort is intended to apply to the next generation of Army helicopters, such as LHX.
Author

N92-32518*# Wright Research Development Center, Wright-Patterson AFB, OH.
DESIGN, ANALYSIS, AND TESTING OF A REUSABLE WINGBOX FOR BALLISTIC EVALUATION OF COMPOSITE STRUCTURES
W. G. Baron and J. D. Oetting *In* NASA. Langley Research Center, Eighth DOD/NASA/FAA Conference on Fibrous Composites in Structural Design, Part 1 Sep. 1990 p 119-129 (For primary document see N92-32513 23-24)
Avail: CASI HC A03/MF A03

Future fighter aircraft will continue to be subjected to severe mechanical loading and ballistic impact. In the past aircraft primary wing structure was constructed predominantly with aluminum, but with increasing aircraft performance the need for more structurally efficient materials is necessary. In an attempt to achieve structural efficiency requirements, aircraft designers have begun using an increasing amount of composite materials. Composite materials were indicated to have a low level of ballistic tolerance in some applications. Composite materials possess the characteristic of structural tailoring, which was utilized to demonstrate that survivability can be designed into a structure. The combat flight environment subjects fighter aircraft wing structures to the effects of combined loading during ballistic impact. These loads were previously demonstrated independently, i.e., the application of structural load, hydrodynamic ram damage, and the effects of airflow. The objective was to design a reusable test fixture for the ballistic evaluation of advanced composite structures under all the effects of combined loading. The fixture that was developed provides a test bed that can completely simulate the flight environment of a generic fighter aircraft wing, but can be used for an indefinite number and variety of tests. It is intended that this fixture will provide a standardized method of ballistically evaluating an advanced composite primary wing structure. This fixture will be used to accomplish the development of designs and/or advanced concepts that lead to a survivable composite wing structure.
Author

N92-32519*# McDonnell Aircraft Co., Saint Louis, MO.
DEVELOPMENT OF COMPOSITE WING CARRYTHROUGH BULKHEADS FOR FIGHTER AIRCRAFT
J. C. Goering, R. S. Behrens, and Mark Libeskind (Naval Air Development Center, Warminster, PA.) *In* NASA. Langley Research Center, Eighth DOD/NASA/FAA Conference on Fibrous Composites in Structural Design, Part 1 Sep. 1990 p 131-149 (For primary document see N92-32513 23-24)
Avail: CASI HC A03/MF A03

Potential weight savings due to the use of composite materials for highly loaded primary structures are being demonstrated through the design, fabrication, and test of an all composite wing carrythrough bulkhead for the F/A-18 fighter aircraft. A one piece composite design which results in a 24 percent weight savings, relative to the existing aluminum bulkhead, was developed. Critical details of this design were evaluated through element tests, and a full scale prototype component was fabricated. The structural integrity of this design will be demonstrated in a comprehensive full scale test program. Author

N92-32520*# Army Armament Research, Development and Engineering Center, Watervliet, NY. Close Combat Armament Center.
BRAIDED COMPOSITE BORE EVACUATOR CHAMBERS FOR TANK CANNONS
Philip C. Wheeler *In* NASA. Langley Research Center, Eighth DOD/NASA/FAA Conference on Fibrous Composites in Structural Design, Part 1 Sep. 1990 p 151-166 (For primary document see N92-32513 23-24)
Avail: CASI HC A03/MF A03

Typically, continuous filament composite components are fabricated using a filament winding technique. In this operation, fibers are introduced to a rotating mandrel while a guide holding the material traverses back and forth to place the material in a helical pattern over the surface of the mandrel. This procedure is continued until complete coverage is obtained. An alternative method for fabricating continuous filament composite components is braiding. In the braiding operation a mandrel is traversed through the center of the braider while 144 strands of material traverse around a carrier ring. As the fibers are applied to a mandrel surface, 72 carriers holding the fibers travel clockwise, while another 72 carriers travel counterclockwise to interlock fibers. An additional 72 carriers located on the back of the braider introduce longitudinal fibers to the composite giving the composite lateral strength. The goal of using the braider is to reduce production time by simultaneously applying 144 strands of material onto a mandrel as opposed to the four-strand wrapping most filament winding techniques offer. Benefits to braiding include the ability to (1) introduce longitudinal fibers to the composite structure; (2) fabricate non-symmetric components without using complex functions to produce full coverage; and (3) produce a component with a higher degree of damage tolerance due to the interlocking of fibers. The fabrication of bore evacuator chambers for a tank cannon system is investigated by utilizing a 144 carrier braiding machine, an industrial robot, and a resin applicator system. Author

N92-32521*# Virginia Polytechnic Inst. and State Univ., Blacksburg. Dept. of Engineering Science and Mechanics.
THE USE OF CURVILINEAR FIBER FORMAT TO IMPROVE BUCKLING RESISTANCE OF PLATES WITH CENTRAL CIRCULAR HOLES
H. H. Lee and M. W. Hyer *In* NASA. Langley Research Center, Eighth DOD/NASA/FAA Conference on Fibrous Composites in Structural Design, Part 1 Sep. 1990 p 167-178 (For primary document see N92-32513 23-24)
(Grant NAG1-665)
Avail: CASI HC A03/MF A03

The potential gain in buckling resistance is explored by using the curvilinear format with a plate containing a centrally located circular hole and subjected to a uniaxial compressive load. The buckling loads for a uniform stress loading and simple support boundary conditions were examined. The method of analysis is outlined for the buckling improvement study. Several designs that represent an improvement over a baseline quasi-isotropic design (a design that is quite good for buckling resistance) are discussed. The tensile load of these designs is examined. A recommended design is presented that not only shows an improved buckling capacity, but also shows improved tensile performance. Follow-on activities are also discussed. Author

N92-32522*# Boeing Military Airplane Development, Wichita, KS.
DEVELOPMENT OF THERMOPLASTIC COMPONENTS FOR STRUCTURAL VAL'DATION
John G. Avery and Gary G. Cassatt *In* NASA. Langley Research Center, Eighth DOD/NASA/FAA Conference on Fibrous Composites in Structural Design, Part 1 Sep. 1990 p 179-198 (For primary document see N92-32513 23-24)
Avail: CASI HC A03/MF A03

Recent activity directed toward advancing the development and validation of graphite reinforced thermoplastic primary and secondary structures is described. The efforts discussed include the design, manufacture and test of a highly-loaded multi-spar wing-box component, and the development of a flight-worthy article that is form, fit and functionally replaceable with the nose landing gear door of the V-22 Osprey. Author

N92-32523*# National Aeronautics and Space Administration. Langley Research Center, Hampton, VA.
A PROTECTION AND DETECTION SURFACE (PADS) FOR DAMAGE TOLERANCE
M. J. Shuart, C. B. Prasad (Analytical Services and Materials, Inc., Hampton, VA.), and S. B. Biggers (Lockheed Aeronautical Systems Co., Burbank, CA.) *In its* Eighth DOD/NASA/FAA Conference on Fibrous Composites in Structural Design, Part 1 Sep. 1990 p 199-219 (For primary document see N92-32513 23-24)
Avail: CASI HC A03/MF A03

A protection and detection surface (PADS) concept was studied for application to composite primary aircraft structures. A Kevlar-epoxy woven face sheet with a Rohacell foam core was found to be the most effective PADS configuration among the configurations evaluated. The weight of the PADS configuration was estimated to be approximately 17 percent of the structural weight. The PADS configuration was bonded to graphite-epoxy base laminates, and up to a 70 percent improvement in compression-after-impact failure strains was observed. Author

N92-32524*# Army Armament Research, Development and Engineering Center, Watervliet, NY. Close Combat Armaments Center.
INVESTIGATION INTO THE FABRICATION OF A COMPOSITE TOP ATTACK RECOILLESS RIFLE
Kevin R. Miner *In* NASA. Langley Research Center, Eighth DOD/NASA/FAA Conference on Fibrous Composites in Structural Design, Part 1 Sep. 1990 p 221-225 (For primary document see N92-32513 23-24)
Avail: CASI HC A01/MF A03

The fabrication of a lightweight, expendable recoilless rifle using composite materials was investigated. Filament winding and braiding were successfully employed in the construction of several of these shoulder-fired weapons. Author

N92-32525*# Northrop Corp., Hawthorne, CA.
STRUCTURAL ASSESSMENT OF ULTRALIGHTWEIGHT COMPOSITES
David M. Kane, M. A. Jankowski, and Robin S. Whitehead *In* NASA. Langley Research Center, Eighth DOD/NASA/FAA Conference on Fibrous Composites in Structural Design, Part 1 Sep. 1990 p 227-243 (For primary document see N92-32513 23-24)
(Contract F33615-88-C-5447)
Avail: CASI HC A03/MF A03

The potential weight savings of advanced ultralightweight (ULW) materials were investigated using the F/A-18 and 747 as baseline aircraft. Weight savings were calculated using a weight ratio methodology. Material properties used in the analysis were those

projected for 1993 ULW production materials. The study results indicated that these ULW materials could save 30 percent airframe weight for both baseline aircraft studied. Author

N92-32526*# National Aeronautics and Space Administration. Ames Research Center, Moffett Field, CA.
A CURVED BEAM TEST SPECIMEN FOR DETERMINING THE INTERLAMINAR TENSILE STRENGTH OF A LAMINATED COMPOSITE
Clement C. Hiel, Mark Sumich, and David P. Chappell *In* NASA. Langley Research Center, Eighth DOD/NASA/FAA Conference on Fibrous Composites in Structural Design, Part 1 Sep. 1990 p 247-261 (For primary document see N92-32513 23-24)
Avail: CASI HC A03/MF A03

A curved beam type of test specimen is evaluated for use in determining the through-the-thickness strength of laminated composites. Two variations of a curved beam specimen configuration (semi-circular and elliptical) were tested to failure using static and fatigue loads. The static failure load for the semi-circular specimens was found to be highly sensitive to flaw content, with the specimens falling into two distinct groups. This result supports the use of proof testing for structural validation. Static design allowables are derived based on the Weibull distribution. Fatigue data indicates no measured increase in specimen compliance prior to final fracture. All static and fatigue failures at room temperature dry conditions occurred catastrophically. The elliptical specimens demonstrated unusually high failure strengths indicating the presence of phenomena requiring further study. Results are also included for specimens exposed to a wet environment showing a matrix strength degradation due to moisture content. Further testing is under way to evaluate a fatigue methodology for matrix dominated failures based on residual static strength (wearout). Author

N92-32527*# McDonnell Aircraft Co., Saint Louis, MO.
OUT OF PLANE ANALYSIS FOR COMPOSITE STRUCTURES
P. C. Paul, C. R. Saff, Kenneth B. Sanger, M. A. Mahler (Northrop Corp., Hawthorne, CA.), Han Pin Kan (Northrop Corp., Hawthorne, CA.), and Edward F. Kautz (Naval Air Development Center, Warminster, PA.) *In* NASA. Langley Research Center, Eighth DOD/NASA/FAA Conference on Fibrous Composites in Structural Design, Part 1 Sep. 1990 p 263-279 (For primary document see N92-32513 23-24)
(Contract N62269-87-C-0226)
Avail: CASI HC A03/MF A03

Simple two dimensional analysis techniques were developed to aid in the design of strong joints for integrally stiffened/bonded composite structures subjected to out of plane loads. It was found that most out of plane failures were due to induced stresses arising from rapid changes in load path direction or geometry, induced stresses due to changes in geometry caused by buckling, or direct stresses produced by fuel pressure or bearing loads. While the analysis techniques were developed to address a great variety of out of plane loading conditions, they were primarily derived to address the conditions described above. The methods were developed and verified using existing element test data. The methods were demonstrated using the data from a test failure of a high strain wingbox that was designed, built, and tested under a previous program. Subsequently, a set of design guidelines were assembled to assist in the design of safe, strong integral composite structures using the analysis techniques developed. Author

N92-32528*# National Aeronautics and Space Administration. Langley Research Center, Hampton, VA.
GLOBAL/LOCAL METHODS RESEARCH USING THE CSM TESTBED
Norman F. Knight, Jr., Jonathan B. Ransom, O. Hayden Griffin, Jr. (Virginia Polytechnic Inst. and State Univ., Blacksburg.), and Danniella M. Thompson (Virginia Polytechnic Inst. and State Univ., Blacksburg.) *In its* Eighth DOD/NASA/FAA Conference on Fibrous Composites in Structural Design, Part 1 Sep. 1990 p 281-309 (For primary document see N92-32513 23-24)
Avail: CASI HC A03/MF A03

Research activities in global/local stress analysis are described including both two- and three-dimensional analysis methods. These methods are being developed within a common structural analysis framework. Representative structural analysis problems are presented to demonstrate the global/local methodologies being developed. Author

N92-32529*# Army Materials Technology Lab., Watertown, MA.
EFFICIENT FINITE ELEMENT MODELING OF LAMINATED COMPOSITE PLATES BASED ON HIGHER-ORDER THEORY
Alexander Tessler and Erik Saether *In* NASA. Langley Research Center, Eighth DOD/NASA/FAA Conference on Fibrous Composites in Structural Design, Part 1 Sep. 1990 p 311-323 (For primary document see N92-32513 23-24)
Avail: CASI HC A03/MF A03

A simple and efficient three-node plate bending element for the analysis of composite laminates is developed from a variational principle. The deformations due to transverse shear and transverse normal effects are accounted for, allowing accurate predictions in the range of thin to thick plates. The methodology incorporates C(exp 0) and C(exp 1) continuous displacement approximations and yields accurate ply-by-ply predictions of all displacement, strain, and stress variables. Author

N92-32530*# Naval Air Development Center, Warminster, PA.
A NEW APPROXIMATE FRACTURE MECHANICS ANALYSIS METHODOLOGY FOR COMPOSITES WITH A CRACK OR HOLE
H. C. Tsai and A. Arocho *In* NASA. Langley Research Center, Eighth DOD/NASA/FAA Conference on Fibrous Composites in Structural Design, Part 1 Sep. 1990 p 325-353 (For primary document see N92-32513 23-24)
Avail: CASI HC A03/MF A03

A new approximate theory which links the inherent flaw concept with the theory of crack tip stress singularities at a bi-material interface was developed. Three assumptions were made: (1) the existence of inherent flaw (i.e., damage zone) at the tip of the crack, (2) a fracture of the filamentary composites initiates at a crack lying in the matrix material at the interface of the matrix/filament, and (3) the laminate fails whenever the principal load-carrying laminae fails. This third assumption implies that for a laminate consisting of 0 degree plies, cracks into matrix perpendicular to the 0 degree filaments are the triggering mechanism for the final failure. Based on this theory, a parameter bar K sub Q which is similar to the stress intensity factor for isotropic materials but with a different dimension was defined. Utilizing existing test data, it was found that bar K sub Q can be treated as a material constant. Based on this finding a fracture mechanics analysis methodology was developed. The analytical results are correlated well with test results. This new approximate theory can apply to both brittle and metal matrix composite laminates with crack or hole. Author

N92-32531*# National Aeronautics and Space Administration. Lewis Research Center, Cleveland, OH.
COMPUTATIONAL SIMULATION OF STRUCTURAL FRACTURE IN FIBER COMPOSITES
C. C. Chamis and P. L. N. Murthy *In* NASA. Langley Research Center, Eighth DOD/NASA/FAA Conference on Fibrous Composites in Structural Design, Part 1 Sep. 1990 p 355-371 (For primary document see N92-32513 23-24)
Avail: CASI HC A03/MF A03

A methodology was developed for the computational simulation of structural fracture in fiber composites. This methodology consists of step-by-step procedures for mixed mode fracture in generic components and of an integrated computer code, Composite Durability Structural Analysis (CODSTRAN). The generic types of composite structural fracture include single and combined mode fracture in beams, laminate free-edge delamination fracture, and laminate center flaw progressive fracture. Structural fracture is assessed in one or all of the following: (1) the displacements increase very rapidly; (2) the frequencies decrease very rapidly; (3) the buckling loads decrease very rapidly; or (4) the strain

energy release rate increases very rapidly. These rapid changes are herein assumed to denote imminent structural fracture. Based on these rapid changes, parameters/guidelines are identified which can be used as criteria for structural fracture, inspection intervals, and retirement for cause. Author

N92-32532*# Virginia Polytechnic Inst. and State Univ., Blacksburg. Dept. of Engineering Science and Mechanics.
SCALING OF FIBER COMPOSITE STRUCTURES
Todd M. Wieland and John Morton *In* NASA. Langley Research Center, Eighth DOD/NASA/FAA Conference on Fibrous Composites in Structural Design, Part 1 Sep. 1990 p 373-390 (For primary document see N92-32513 23-24)
(Grant NAG1-343)
Avail: CASI HC A03/MF A03

Structural scaling is being investigated using graphite/epoxy Z-section stiffeners loaded in compression. Sections of various web, flange and web-to-flange corner radii dimensions are being considered. Initial local buckling loads and modes have been determined analytically, numerically and by experiment. A normalizing parameter has been developed for initial buckling data. Postbuckling behavior has been evaluated numerically and experimentally. The nature of the load redistribution following buckling is a key factor in relating the response of the various section sizes. Additional experiments and the development of scaling parameters for postbuckling and crippling are underway. Author

N92-32574*# National Aeronautics and Space Administration. Langley Research Center, Hampton, VA.
EIGHTH DOD/NASA/FAA CONFERENCE ON FIBROUS COMPOSITES IN STRUCTURAL DESIGN, PART 2
James H. Starnes, Jr., comp., Herman L. Bohon, comp. (Lockheed Engineering and Sciences Co., Hampton, VA.), and Sherry B. Garzon, comp. Sep. 1990 315 p Conference held in Norfolk, VA, 28-30 Nov. 1989
(RTOP 505-63-01-09)
(NASA-CP-3087-Pt-2; L-16832-Pt-2; NAS 1.55:3087-Pt-2) Avail: CASI HC A14/MF A03

Papers presented at the conference are compiled. The conference provided a forum for the scientific community to exchange composite structures design information and an opportunity to observe recent progress in composite structures design and technology. Part 2 contains papers related to the following subject areas: the application in design; methodology in design; and reliability in design. For individual titles, see N92-32575 through N92-32589.

N92-32575*# Army Aviation Systems Command, Hampton, VA. Aerostructures Directorate.
EVALUATION OF COMPOSITE COMPONENTS ON THE BELL 206L AND SIKORSKY S-76 HELICOPTERS
Donald J. Baker *In* NASA. Langley Research Center, Eighth DOD/NASA/FAA Conference on Fibrous Composites in Structural Design, Part 2 Sep. 1990 p 393-428 (For primary document see N92-32574 23-24)
Avail: CASI HC A03/MF A03

Progress on two programs to evaluate structural composite components in flight service on Bell 206L and Sikorsky S-76 commercial helicopters is described. Forty ship sets of composite components that include the litter door, baggage door, forward fairing, and vertical fin have been installed on Bell Model 206L helicopters that are operating in widely different climates. Component installation started in 1981 and selected components were removed and tested at prescribed intervals over a ten year evaluation. Four horizontal stabilizers and eleven tail rotor spars that are production components on the S-76 helicopter were tested after prescribed periods of service to determine the effects of the operating environment on their performance. Concurrent with the flight evaluation, materials used to fabricate the components were exposed in ground racks and tested at specified intervals to determine the effects of outdoor environments. Results achieved from 123,000 hours of accumulated service on the Bell 206L components and 53,000 hours on the Sikorsky S-76 components are reported. Seventy-eight Bell 206L components were removed and tested statically. Results of seven years of ground exposure of materials used to fabricate the Bell 206L components are presented. Results of tests on four Sikorsky S-76 horizontal stabilizers and eleven tail rotor spars are also presented. Panels of material used to fabricate the Sikorsky S-76 components that were exposed for six years were tested and results are presented. Author

N92-32576*# Northrop Corp., Hawthorne, CA. Aircraft Div.
SUPPORTABILITY EVALUATION OF THERMOPLASTIC AND THERMOSET COMPOSITES
G. R. Chanani, D. Boldi, S. G. Cramer, and M. W. Heimerdinger *In* NASA. Langley Research Center, Eighth DOD/NASA/FAA Conference on Fibrous Composites in Structural Design, Part 2 Sep. 1990 p 429-437 (For primary document see N92-32574 23-24)
Avail: CASI HC A02/MF A03

Nearly 300 advanced composite components manufactured by Northrop Corporation are flying on U.S. Air Force and U.S. Navy supersonic aircraft as part of a three-year Air Force/Navy/Northrop supportability evaluation. Both thermoplastic and high-temperature thermoset composites were evaluated for their in-service performance on 48 USAF and Navy F-5E fighter and USAFT-38 trainer aircraft in the first large-scale, long-term maintenance evaluation of these advanced materials. Northrop manufactured four types of doors for the project-avionics bay access, oil fill, inlet duct inspection, and a main landing gear door. The doors are made of PEEK (polyetheretherketone) thermoplastic, which is tougher and potentially less expensive to manufacture than conventional composites; and 5250-3 BMI (bismaleimide) thermoset, which is manufactured like a conventional epoxy composite but can withstand higher service temperatures. Results obtained so far indicate that both the BMI and PEEK are durable with PEEK being somewhat better than BMI. Author

N92-32577*# National Aeronautics and Space Administration. Langley Research Center, Hampton, VA.
RESIDUAL STRENGTH OF REPAIRED GRAPHITE/EPOXY LAMINATES AFTER 5 YEARS OF OUTDOOR EXPOSURE
Jerry W. Deaton *In its* Eighth DOD/NASA/FAA Conference on Fibrous Composites in Structural Design, Part 2 Sep. 1990 p 439-454 (For primary document see N92-32574 23-24)
Avail: CASI HC A03/MF A03

The NASA Langley Research Center has sponsored research to develop generic repair techniques and processes for advanced graphite/epoxy (Gr/Ep) composites applicable to secondary structures for commercial transport aircraft. The long-term durability of such repairs is being addressed in a 10-year outdoor exposure program at the Langley Research Center. Details of the program and results of residual strength tests after 5 years of outdoor exposure are presented. Four repair methods are being evaluated. These include: (1) externally bolted aluminum-plus adhesive; (2) precured, bonded external Gr/Ep; (3) cure-in-place external Gr/Ep; and (4) cure-in-place flush Gr/Ep. Repaired specimens as well as undamaged and damaged unrepaired controls are being exposed outdoors for 1, 3, 5, 7, and 10 years. The residual tensile strength of stressed, unstressed, and fatigue specimens from each group is reported and compared with the tensile strength of baseline specimens which received no outdoor exposure. Identification of the commercial products and companies is used to describe adequately the test materials. The identification of these commercial products does not constitute endorsement, expressed or implied, of such products by the National Aeronautics and Space Administration. Author

N92-32578*# Boeing Military Airplane Development, Wichita, KS.
SURVIVABILITY CHARACTERISTICS OF COMPOSITE COMPRESSION STRUCTURE
John G. Avery, M. R. Allen, D. Sawdy, and S. Avery (Wichita State Univ., KS.) *In* NASA. Langley Research Center, Eighth

DOD/NASA/FAA Conference on Fibrous Composites in Structural Design, Part 2 Sep. 1990 p 455-478 (For primary document see N92-32574 23-24)
(Contract F33615-83-C-3228)
Avail: CASI HC A03/MF A03

Test and evaluation was performed to determine the compression residual capability of graphite reinforced composite panels following perforation by high-velocity fragments representative of combat threats. Assessments were made of the size of the ballistic damage, the effect of applied compression load at impact, damage growth during cyclic loading and residual static strength. Several fiber/matrix systems were investigated including high-strain fibers, tough epoxies, and APC-2 thermoplastic. Additionally, several laminate configurations were evaluated including hard and soft laminates and the incorporation of buffer strips and stitching for improved damage resistance of tolerance. Both panels (12 x 20-inches) and full scale box-beam components were tested to assure scalability of results. The evaluation generally showed small differences in the responses of the material systems tested. The soft laminate configurations with concentrated reinforcement exhibited the highest residual strength. Ballistic damage did not grow or increase in severity as a result of cyclic loading, and the effects of applied load at impact were not significant under the conditions tested. Author

N92-32579*# Northrop Corp., Hawthorne, CA.
DAMAGE TOLERANCE CERTIFICATION METHODOLOGY FOR COMPOSITE STRUCTURES
Han Pin Kan, Robin S. Whitehead, and Edward F. Kautz (Naval Air Development Center, Warminster, PA.) *In* NASA. Langley Research Center, Eighth DOD/NASA/FAA Conference on Fibrous Composites in Structural Design, Part 2 Sep. 1990 p 479-498 (For primary document see N92-32574 23-24)
(Contract N62269-87-C-0259)
Avail: CASI HC A03/MF A03

An advanced certification methodology was developed for composite structures to include the effects of impact damage. The methodology has the capability to determine the reliability of impact damaged structure at any prescribed load level and impact threat, which may be specified in terms of impact energy or C-scan damage area. In addition, the methodology can also calculate the allowable impact threat level at a given applied load and specified reliability. The developed damage tolerance certification methodology was demonstrated on the F/A-18 inner wing. The results of the methodology demonstration showed that the F/A-18 inner wing has excellent damage tolerance capability. Author

N92-32580*# McDonnell Aircraft Co., Saint Louis, MO.
CERTIFICATION OF DAMAGE TOLERANT COMPOSITE STRUCTURE
Andrew J. Rapoff, Harold D. Dill, Kenneth B. Sanger, and Edward F. Kautz (Naval Air Development Center, Warminster, PA.) *In* NASA. Langley Research Center, Eighth DOD/NASA/FAA Conference on Fibrous Composites in Structural Design, Part 2 Sep. 1990 p 499-514 (For primary document see N92-32574 23-24)
(Contract N62269-87-C-0227)
Avail: CASI HC A03/MF A03

A reliability based certification testing methodology for impact damage tolerant composite structure was developed. Cocured, adhesively bonded, and impact damaged composite static strength and fatigue life data were statistically analyzed to determine the influence of test parameters on the data scatter. The impact damage resistance and damage tolerance of various structural configurations were characterized through the analysis of an industry wide database of impact test results. Realistic impact damage certification requirements were proposed based on actual fleet aircraft data. The capabilities of available impact damage analysis methods were determined through correlation with experimental data. Probabilistic methods were developed to estimate the reliability of impact damaged composite structures. Author

N92-32581*# Army Materials Technology Lab., Watertown, MA.
STATISTICALLY BASED MATERIAL PROPERTIES: A MILITARY HANDBOOK-17 PERSPECTIVE
Donald M. Neal and Mark G. Vangel *In* NASA. Langley Research Center, Eighth DOD/NASA/FAA Conference on Fibrous Composites in Structural Design, Part 2 Sep. 1990 p 515-535 (For primary document see N92-32574 23-24)
Avail: CASI HC A03/MF A03

The statistical procedures and their importance in obtaining composite material property values in designing structures for aircraft and military combat systems are described. The property value is such that the strength exceeds this value with a prescribed probability with 95 percent confidence in the assertion. The survival probabilities are the 99th percentile and 90th percentile for the A and B basis values respectively. The basis values for strain to failure measurements are defined in a similar manner. The B value is the primary concern. Author

N92-32582*# National Aeronautics and Space Administration. Langley Research Center, Hampton, VA.
COMPRESSION BEHAVIOR OF GRAPHITE-EPOXY AND GRAPHITE-THERMOPLASTIC PANELS WITH CIRCULAR HOLES OR IMPACT DAMAGE
Dawn C. Jegley *In its* Eighth DOD/NASA/FAA Conference on Fibrous Composites in Structural Design, Part 2 Sep. 1990 p 537-558 (For primary document see N92-32574 23-24)
Avail: CASI HC A03/MF A03

An experimental investigation of the compression behavior of laminated specimens made from graphite-epoxy tape (AS4-3502), graphite-thermoplastic tape (AS4-PEEK), and graphite-thermoplastic fabric (AS4-PEEK) was conducted. Specimens with five different stacking sequences were loaded to failure in uniaxial compression. Some of the specimens had central circular holes with diameters up to 65 percent of the specimen width. Other specimens were subjected to low speed impact with impact energy up to 30 J prior to compressive loading. This investigation indicates that graphite-thermoplastic specimens with holes have up to 15 percent lower failure stresses and strains than graphite-epoxy specimens with the same stacking sequence and hole size. However, graphite-thermoplastic specimens subjected to low speed impact have up to 15 percent higher failure stresses and strains than graphite-epoxy specimens with the same stacking sequence and impact energy. Compression tests of graphite-thermoplastic specimens constructed of unidirectional tape and of fabric indicate that the material form has little effect on failure strains in specimens with holes or low speed impact damage. Author

N92-32583*# Massachusetts Inst. of Tech., Cambridge. Technology Lab. for Advanced Composites.
IMPACT RESPONSE OF GRAPHITE/EPOXY FABRIC STRUCTURES
Paul A. Lagace and Michael J. Kraft *In* NASA. Langley Research Center, Eighth DOD/NASA/FAA Conference on Fibrous Composites in Structural Design, Part 2 Sep. 1990 p 559-571 (For primary document see N92-32574 23-24)
(Contract N00019-85-C-0090)
Avail: CASI HC A03/MF A03

The impact damage resistance and damage tolerance of graphite/epoxy fabric plate (coupon) and cylinder structures were investigated and compared in an analytical and experimental study. Hercules A370-5H/3501-6 five-harness satin weave cloth in a quasi-isotropic (0,45)(sub s) laminate configuration was utilized. Specimens were impacted with 12.7 mm diameter steel spheres at velocities ranging from 10 m/s to 100 m/s. Damage resistance of the specimens was determined through the use of dye penetrant enhanced x-radiography, sectioning, epoxy burnoff, and visual methods. Damage tolerance of the flat plate structures was assessed in a residual tensile test while damage tolerance of the cylinder structures was assessed via pressurization tests. Impacted fabric laminates exhibited matrix crushing, fiber breakage, delamination, and fiber bundle disbonds; the latter being a unique damage mode for fabric laminates. Plate delamination and bundle

disbonding was found to be more extensive around the central core area of fiber damage in the coupon specimens than in the cylinder specimens which showed a cleaner damage area due to impact. Damage resistance and damage tolerance were predicted by utilizing a five-step analysis approach previously utilized for coupon configurations. Two of the five steps were adapted to account for the effects of the structural configuration of the pressurized cylinder. The damage resistance analysis provided good correlation to the fiber damage region of both the coupon and cylinder specimens. There was little difference in the size of this region in the two specimen types. However, the analysis was not able to predict the distribution of damage through-the-thickness. This was important in assessing the damage tolerance of the cylinders. The damage tolerance analysis was able to predict the residual tensile strength of the coupons. A general methodology to predict the impact damage resistance and damage tolerance of composite structures utilizing coupon data is presented.

Author

N92-32584*# Northrop Corp., Hawthorne, CA. Aircraft Div.
POSTBUCKLING BEHAVIOR OF CURVED PANELS UNDER COMBINED COMPRESSION AND SHEAR LOADS
Ravi B. Deo, Han Pin Kan, and Narain M. Bhatia *In* NASA. Langley Research Center, Eighth DOD/NASA/FAA Conference on Fibrous Composites in Structural Design, Part 2 Sep. 1990 p 573-589 (For primary document see N92-32574 23-24)
(Contract F33615-84-C-3220)
Avail: CASI HC A03/MF A03

A validated semiempirical design procedure and fatigue data were developed for curved, stiffened composite panels operating in the postbuckled regime under the action of combined compression and shear loading. A previously developed design methodology for composite panels under pure shear or pure compression loading was used as the starting point for the program. Initially, the well established interaction rules for metal panels were adopted to predict buckling under combined loading. Test data were then developed to verify these rules and suggest modifications where necessary. Postbuckling failure envelopes were developed by accounting for the failure modes possible under shear loading only, and under pure compression loading. Static failure predictions under combined loading were based on test verified interaction criteria. Fatigue tests were conducted under combined loading to determine strength degradation and the possible failure modes.

Author

N92-32585*# Lockheed Aeronautical Systems Co., Marietta, GA.
POSTBUCKLING OF STIFFENED COMPOSITE PLATES UNDER COMBINED LOADING
Richard K. Kunz *In* NASA. Langley Research Center, Eighth DOD/NASA/FAA Conference on Fibrous Composites in Structural Design, Part 2 Sep. 1990 p 591-608 (For primary document see N92-32574 23-24)
(Contract NAS1-15949)
Avail: CASI HC A03/MF A03

An analysis methodology for the postbuckling behavior of laminated plates under combined in-plane normal and shear loading is presented. The plates are simply supported on their ends and elastically restrained against rotation along their longitudinal edges. Discrete thickness changes along the plate edges are included in the formulation to account for attached stiffener flanges and/or edge pad-ups. The resulting analytical approach is suitable for inclusion in a preliminary sizing procedure for longitudinally stiffened composite panels.

Author

N92-32586*# Virginia Polytechnic Inst. and State Univ., Blacksburg.
INITIAL POSTBUCKLING RESPONSE OF AN UNSYMMETRICALLY LAMINATED RECTANGULAR PLATE
Raphael T. Haftka and Eric R. Johnson *In* NASA. Langley Research Center, Eighth DOD/NASA/FAA Conference on Fibrous Composites in Structural Design, Part 2 Sep. 1990 p 609-623 (For primary document see N92-32574 23-24)
(Grants NAG1-168; NAG1-537)
Avail: CASI HC A03/MF A03

It was shown that anisotropic plates can have unstable postbuckling behavior resulting in potential imperfection sensitivity. The degree of instability for rectangular, simply-supported, cross-ply laminated plates is quantified. The analysis is based on asymptotic Koiter-type expansion of postbuckling response. The degree of postbuckling instability is quantified in terms of the reduction in load carrying capacity in the immediate postbuckling range. For graphite-epoxy plates it is found that this measure of instability is very small. Only a low aspect ratio plate with a high degree of anisotropy can have any significant reduction in its buckling load.

Author

N92-32587*# National Aeronautics and Space Administration. Langley Research Center, Hampton, VA.
BUCKLING AND POSTBUCKLING BEHAVIOR OF SQUARE COMPRESSION-LOADED GRAPHITE-EPOXY PLATES WITH CIRCULAR CUTOUTS
Michael P. Nemeth *In its* Eighth DOD/NASA/FAA Conference on Fibrous Composites in Structural Design, Part 2 Sep. 1990 p 625-661 (For primary document see N92-32574 23-24)
Avail: CASI HC A03/MF A03

Results are presented for unidirectional (0, 10)(sub s) and (90,10)(sub s) plates, ((0/90)(sub 5)(sub s)) plates, and for aluminum plates. Results are also presented for ((+/- theta)(sub 6)(sub s)) angle-ply plates for values of theta = 30, 45, and 60 degrees. The results indicate that the change in axial stiffness of a plate at buckling is strongly dependent upon cutout size and plate orthotropy. The presence of a cutout gives rise to an internal load distribution that changes, sometimes dramatically, as a function of cutout size coupled with the plate orthotropy. In the buckled state, the role of orthotropy becomes more significant since bending in addition to membrane orthotropy is present. Most of the plates with cutouts exhibited less postbuckling stiffness than the corresponding plate without a cutout, and the postbuckling stiffness decreased with increasing cutout size. However, some of the highly orthotropic plates with cutouts exhibited more postbuckling stiffness than the corresponding plate without a cutout. These results suggest the possibility of tailoring the cutout size and the stacking sequence of a composite plate to optimize postbuckling stiffness. It was found that plates with large radius cutouts do exhibit some postbuckling strength. The results also indicate that a cutout can influence modal interaction in a plate. Specifically, results are presented that show a plate with a relatively small cutout buckling at a higher load than the corresponding plate without a cutout, due to modal interaction. Other results are presented that indicate the presence of nonlinear prebuckling deformations, due to material nonlinearity, in the angle-ply plates with theta = 45 and 60 degrees. The nonlinear prebuckling deformations are more pronounced in the plates with theta = 45 degrees and become even more pronounced as the cutout size increases. Results are also presented that show how load-path eccentricity due to improper machining of the test specimens affects the buckling behavior. Some of the plates with cutouts and eccentricity exhibited a snap-through type of buckling behavior.

Author

N92-32588*# Douglas Aircraft Co., Inc., Saint Louis, MO.
A NEW APPROACH TO FIBROUS COMPOSITE LAMINATE STRENGTH PREDICTION
L. J. Hart-Smith *In* NASA. Langley Research Center, Eighth DOD/NASA/FAA Conference on Fibrous Composites in Structural Design, Part 2 Sep. 1990 p 663-693 (For primary document see N92-32574 23-24)
Avail: CASI HC A03/MF A03

A method of predicting the strength of cross-plied fibrous composite laminates is based on expressing the classical maximum-shear-stress failure criterion for ductile metals in terms of strains. Starting with such a formulation for classical isotropic materials, the derivation is extended to orthotropic materials having a longitudinal axis of symmetry, to represent the fibers in a

unidirectional composite lamina. The only modification needed to represent those same fibers with properties normalized to the lamina rather than fiber is a change in axial modulus. A mirror image is added to the strain-based lamina failure criterion for fiber-dominated failures to reflect the cutoffs due to the presence of orthogonal fibers. It is found that the combined failure envelope is now identical with the well-known maximum-strain failure model in the tension-tension and compression-compression quadrants but is truncated in the shear quadrants. The successive application of this simple failure model for fibers in the 0/90 degree and +/- 45 degree orientations, in turn, is shown to be the necessary and sufficient characterization of the fiber-dominated failures of laminates made from fibers having the same tensile and compressive strengths. When one such strength is greater than the other, the failure envelope is appropriately truncated for the lesser direct strain. The shear-failure cutoffs are now based on the higher axial strain to failure since they occur at lower strains than and are usually not affected by such mechanisms as microbuckling. Premature matrix failures can also be covered by appropriately truncating the fiber failure envelope. Matrix failures are excluded from consideration for conventional fiber/polymer composites but the additional features needed for a more rigorous analysis of exotic materials are covered. The new failure envelope is compared with published biaxial test data. The theory is developed for unnotched laminates but is easily shrunk to incorporate reductions to allow for bolt holes, cutouts, reduced compressive strength after impact, and the like. Author

N92-32589*# North Carolina State Univ., Raleigh.
SHEAR BUCKLING OF SPECIALLY ORTHOTROPIC PLATES WITH CENTRALLY LOCATED CUTOUTS
Vicki L. Owen and Eric C. Klang *In* NASA. Langley Research Center, Eighth DOD/NASA/FAA Conference on Fibrous Composites in Structural Design, Part 2 Sep. 1990 p 695-706
(For primary document see N92-32574 23-24)
(Grant NAG1-917)
Avail: CASI HC A03/MF A03

There is significant industry demand for a method of analyzing the shear buckling of composite plates with cutouts. This method should be able to easily accommodate frequent changes in model design; inflexibility is the major drawback to current finite element methods. The approach taken here is broken into two problems, prebuckling and buckling. To solve for the prebuckling stresses, complex variable equations are used in conjunction with boundary collocation. The least squares approach is utilized to improve the accuracy of the results. The buckling problem is solved using the Ritz method. A product of the Ritz method is a complicated integral equation which is solved using numerical integration. To date, the aforementioned method of determining the prebuckling stresses was verified against infinite plate theory and finite elements. Author

N92-32629# South Carolina Research Authority. Charleston.
PDES APPLICATION PROTOCOL SUITE FOR COMPOSITES (PAS-C). FUNCTIONAL NEEDS REPORT FOR THE PAS-C PROGRAM Final Report, Jul. - Aug. 1991
Mike Stowe, Ray Grella, Jon Judd, Keith Hunten, and Greg Paul Sep. 1991 123 p
(Contract F33615-91-C-5713)
(AD-A247886; PASC002-01-00; WL-TR-92-8017) Avail: CASI HC A06/MF A02

This document addresses the first portion of an informational needs analysis for composites parts. A sample part set of Aircraft Composite Structural Components is described with the supporting life-cycle functional activities node trees. An attempt was made to standardize a set of terminology and informational constructs so that a Framework/Building-Block (FW/BB) approach could be established which would organize and capture the information into a usable/reusable structure. The sample part set was then mapped to the FW/BB structure identifying what was in and out of scope for the PDES Application Protocol Suite for Composites (PAS-C) Project. There have been many attempts to analyze the needs of composites parts, in particular, the informational needs that support data exchange of composite data between life-cycle applications. The challenge has been to scope the needs gathering process into a structured, achievable task that provides usable/reusable knowledge. Most previous composite needs analyses have been focused on a narrow application view or particular part type which has limited the reusability of the information. What has been lacking is a methodology that allows for the informational needs of all aspects of composite parts to be captured. This methodology requires an approach that manages and utilizes existing needs-gathering methods to capture existing composite needs-analysis work. GRA

N92-32638# Argonne National Lab., IL.
THERMAL STRAINS IN TITANIUM ALUMINIDE AND NICKEL ALUMINIDE COMPOSITES
A. Saigal and D. S. Kupperman 1992 9 p Presented at the 7th World Conference and Exhibition on Titanium, San Diego, CA, 28 Jun. - 2 Jul. 1992
(Contract W-31-109-eng-38)
(DE92-015181; ANL/CP-75762; CONF-920604-3) Avail: CASI HC A02/MF A01

Neutron diffraction was used to measure residual thermal strains developed during postfabrication cooling in titanium aluminide and nickel aluminide intermetallic matrix composites. Silicon carbide/Ti14Al-21Nb, tungsten and sapphire/NiAl, and sapphire and SiC-coated sapphire/NiAl25Fe10 composites were investigated. The thermal expansion coefficient of the matrix is usually greater than that of the fibers. As such, during cooldown, compressive residual strains are generated in the fibers and tensile residual strains are generated in the matrix, parallel to the fibers. Liquid-nitrogen dipping and thermal cycling tend to reduce the fabrication-induced residual strains in silicon carbide fiber-reinforced titanium aluminide matrix composites. However, matrix cracking can occur as a result of these processes. The axial residual strains in the matrix were lower in the nickel aluminide matrix than in the titanium aluminide matrix. As the matrix undergoes plastic deformation, residual thermal strains are related to the yield stress of the matrix. DOE

N92-32674# Joint Inst. for Lab. Astrophysics, Boulder, CO.
APPLICATIONS OF THE PHOTOREFRACTIVE EFFECT AND DAMAGE INDUCED EFFECTS IN FIBERS Annual Report, 1 Nov. 1990 - 31 Oct. 1991
Dana Z. Anderson 26 Mar. 1992 17 p
(Grant AF-AFOSR-0198-90)
(AD-A250767; AFOSR-92-0313TR) Avail: CASI HC A03/MF A01

One aspect of this work concerns the processes of self-organized second-harmonic generation in fibers. We have experimentally investigated the nature of grating formation in the glass fibers and found it to be reversible. That is, a grating can be repetitively written, erased, and re-written. We have also shown that the grating erasure follows a power-law time dependence and explains the dependence as a consequence of the transverse mode structure of the fields in the fiber. Numerical work has focused on the microscopic aspect of ionization from a model defect potential. We have integrated Schrodinger's equation exactly in the one-dimensional case. Results so far indicate that a photovoltaic explanation of second-harmonic generation in fibers is robust against variation of the physical parameters of the model. The second aspect concerns the dynamics and self-organization of photorefractive optical circuits. We have produced circuits that self-organize according to the nature of their time dependent input. After self-organizing they process information in an adaptive and useful way. Our most highly developed circuit is a demultiplexer that separates signals from a multimode fiber. GRA

N92-32676# United Technologies Research Center, East Hartford, CT.
INTERFACIAL STUDIES OF REFRACTORY GLASS-CERAMIC MATRIX/ADVANCED SIC FIBER REINFORCED COMPOSITES Annual Report, 1 Feb. 1991 - 1 Feb. 1992
J. J. Brennan 30 Apr. 1992 76 p

(Contract F33615-89-C-5628)
(AD-A250784; UTRC/R92-918246-4) Avail: CASI HC A05/MF A01

The main objective of this program is to characterize the chemistry and structure of new advanced small diameter silicon-based fibers and how these factors influence the nature of the fiber/matrix interface in refractory glass-ceramic matrix composites. It is the nature of this interface that determines, to a great degree, the composite thermal, environmental, and mechanical properties. The fibers under investigation during the second year of this program included the new experimental polymer derived crystalline SiC fibers, the Si-N-C-O 'Black' fibers, as well as the new low oxygen radiation-cured Nicalon SiC type fibers. Since the availability of all of these fibers was extremely limited, emphasis was placed on the mechanical, chemical, and microstructural characterization of the fibers through tensile testing, SEM of fiber fracture characteristics, scanning Auger depth profiling of fiber surfaces, and TEM of fiber thin sections, as well as their fracture behavior, bonding characteristics, and interfacial compatibility with various glass-ceramic matrix materials. Results of these analyses are discussed. GRA

N92-32677# Universiteit Twente, Enschede (Netherlands).
SYNTHESIS, MICROSCTRUCTURE, AND MECHANICAL PROPERTIES OF ZIRCONIA-ALUMINA COMPOSITES Ph.D. Thesis
Petrus denExter 1991 188 p Sponsored by Ministry of Economic Affairs
(ISBN-90-9004656-9; ETN-92-92044) Avail: CASI HC A09/MF A02

The preparation and characterization of zirconia-alumina composites are described. An overview of sirconia-alumina composites in general, and of the toughening mechanisms in particular, is given. A subdivision is made in the following composition areas: zirconia toughened alumina, alumina dispersed in Y-TZP, and intermediate compositions. A concept proposed for the densification of sirconia toughened alumina is described. The preparation and characterization of zirconia-alumina ceramic composites for high temperature applications is presented. The preparation and characterization of alumina dispersed zirconia ceramics is presented with main focus on phase composition, phase distribution and densification behavior. Preliminary sinter forging experiments of zirconia alumina, focusing on the enhancement for densification during transition alumina sintering and transition to alpha-alumina transformation, are presented. Bending strength and fracture toughness data of zirconia toughened alumina and alumina dispersed zirconia ceramics are presented. ESA

N92-32740# Messerschmitt-Boelkow-Blohm G.m.b.H., Munich (Germany, F.R.). Central Labs.
THE USE OF PIEZOELECTRIC SENSORS TO DETECT DELAMINATION INITIATION IN CARBON FIBER REINFORCED COMPOSITES
Alexander Horoschenkoff and Erwin Wittmann 1991 11 p Submitted for publication
(MBB-Z-0391-91-PUB; ETN-92-92117) Avail: CASI HC A03/MF A01

The use of piezoelectric sensors to detect delamination initiation at the free edges of composite laminates subjected to tensile loads was investigated. Thin PVDF films applied to the specimens were used as sensors. All laminates investigated had a quasi-isotropic layup, but different stacking sequences and thicknesses. The material investigated was the carbon fiber reinforced prepreg system Narmco 5245/T800 (supplier: BASF AG). It was found that the use of piezoelectric films made it possible to detect delamination initiation and to document different failure mechanisms. The laminate stacking sequence had a great influence on the sensitivity to delamination initiation and the ultimate stress level. Laminates composed such that plies with the same angles are grouped together showed the highest sensitivity to delamination. However, no direct correlation between the stress level at which delaminations were initiated and the ultimate strength was found, due to very complex interactions between different failure modes. ESA

N92-32775# Office National d'Etudes et de Recherches Aerospatiales, Paris (France). Direction des Structures.
NONLINEAR TRANSIENT RESPONSES OF STRATIFIED COMPOSITE STRUCTURES [REPONSES TRANSITOIRES NON LINEAIRES DES STRUCTURES STRATIFIEES COMPOSITES]
R. Girard and D. Louis Oct. 1991 43 p In FRENCH
(Contract DRET-89-34-001)
(ONERA-RT-26/3542-RY-007-R; ETN-92-91674) Avail: CASI HC A03/MF A01

The development of a calculation code for the analysis of transient responses from stratified composite structures is presented. The mechanical behavior of the component materials is assumed to be linear and elastic, with large geometrical displacements. The calculation code is based on a finite element method with three dimensional isoparametric elements and can be applied to beam or shell models. The time integration and the resolution of nonlinear dynamical equations are performed using a Newmark step by step scheme and a Newton interactive method. The model was tested for several either homogeneous or composite plates and beams. ESA

N92-32791# Institute for Aerospace Research, Ottawa (Ontario). Structures and Materials Lab.
PROCESSING AND ENVIRONMENTAL EFFECTS ON MECHANICAL PROPERTIES OF COMPOSITE REPAIRS
F. Elaldi (Middle East Technical Univ., Ankara, Turkey), S. Lee, and R. F. Scott 22 May 1991 28 p Sponsored by National Research Council of Canada
(NRC-LTR-ST-1826; CTN-92-60370) Avail: CASI HC A03/MF A01

The scarf joint technique is one of the latest techniques used for repairing composite aircraft structures. This paper describes scarf joints comprised of vacuum and autoclave precured and co-cured fiber glass epoxy patches bonded to autoclave and vacuum precured parent fiber glass epoxy laminates. Autoclave and vacuum cured parent laminates and the scarf joints were prepared and exposed to the same temperature and moisture environment for comparison. All specimens were loaded in tension at three temperatures. Interlaminar shear strength (ILSS) tests were also carried out for the parent materials. As expected, the tensile strength and ILSS decrease when the material has been exposed to moisture and tested at elevated temperature. No significant difference was reported for either tensile strength or ILSS between autoclave and vacuum cured materials. The room temperature repair efficiencies are reported for single scarf repairs comprised of vacuum co-cured and precured patches. These repair efficiencies were found to be similar to the efficiency of the autoclave precured patch repair. This result supports the feasibility of scarf joint repairs in base level facilities. Author (CISTI)

N92-32792# Office National d'Etudes et de Recherches Aerospatiales, Paris (France). Direction des Structures.
FREE-EDGE DELAMINATION OF A STRATIFIED COMPOSITE: INTERACTION WITH THE TRANSVERSAL CRACK [DELAMINAGE DE BORD LIBRE DANS UN COMPOSITE STRATIFIE. INTERACTION AVEC FISSURATION TRANSVERSE]
A. Thionnet, P. M. Lesne, and J. Renard Aug. 1991 41 p In FRENCH
(Contract DRET-89-34-001)
(ONERA-RT-13/7256-RY-006-R; ETN-92-91672) Avail: CASI HC A03/MF A01

The symmetrical delamination of a flat plate is studied. The consequences of mechanical resistance to failure of the material are evaluated. A delamination law is obtained by means of thermodynamic equations. In the case of a flat plate, the model allows local and generalized degradation to be combined. The local degradation is due to cracks in each layer of the structure. The evolution and the continuous interaction of both damages

are observed. The two degradation models are implemented on a computer program in order to analyze more complex structures. A finite element method and a hypothesis stating that either there is no delamination or that the delamination occurs all over the material are applied. The results obtained from calculations performed on a flat plate with holes are in good agreement with the estimation. ESA

N92-32813# Sherbrooke Univ. (Quebec).
STUDY OF THE MECHANICAL BEHAVIOUR OF GRAPHITE/EPOXY LAMINATES SUBJECTED TO STATIC AND CYCLIC LOADING [ETUDE DU COMPORTEMENT MECANIQUE D'UN COMPOSITE STRATIFIE GRAPHITE/EPOXY SOUMIS A DES SOLLICITATIONS MONOTONES ET CYCLIQUES]
L. Dupont, C. Roy, and Jerzy P. Komorowski (National Research Council of Canada, Ottawa, Ontario) Aug. 1989 143 p In FRENCH
(Contract NAE-31946-7-0005/01-SS)
(NRC-30833; NAE-CR-2; CTN-92-60367) Avail: CASI HC A07/MF A02

The main objective of this work was to verify experimentally, existing analytical models that predict the effect of the stacking sequence in fiber reinforced plastic laminates on the growth of edge delaminations. Two computer programs, INTCAL and AEE were used for the analysis of seventeen different laminates. Three laminates with different susceptibility to edge delaminations were retained for mechanical testing. To test these laminates in tension-compression (static and fatigue modes), experimental accessories (grips and anti-buckling guides) and tabless specimen gripping techniques were developed. Static strengths measured were equal to or better than those predicted by lamination theory. The analytical models were used to calculate the values of three quantities at the interfaces: INTCAL - mismatch of Poisson ratio, coefficient of mutual influence, and reactive moments; AEE - three stresses at the edge. However, the models do not include a rigorous method for combining these different quantities for the purpose of ranking the stacking sequences and determining whether an edge delamination will grow before the load exceeds the strength of the specimen. Similar stacking sequence ranking was obtained from both analytical models. The relative size of delaminations observed under tensile loading correlated well with ranking obtained from analytical models. In compression, specimens failed before any delamination was observed. The results of the FALSTAFF spectrum loading fatigue tests were inconclusive. Author (CISTI)

N92-32828# California Univ., Berkeley. Dept. of Chemistry.
ULTRA-LOW DENSITY ORGANIC-INORGANIC COMPOSITE MATERIALS POSSESSING THERMALLY INSULATING AND ACOUSTIC DAMPING PROPERTIES
Bruce M. Novak 7 May 1992 13 p
(Contract N00014-91-J-1772)
(AD-A251182) Avail: CASI HC A03/MF A01

We, as well as others, have been interested in the sol-gel process for the synthesis of hybrid inorganic/organic composite materials. Since our first report on the application of tetraalkoxysilanes possessing polymerizable alkoxides for the production of nonshrinking sol-gel composites, we have extended our efforts towards increasing the glass content in these composite materials. The stoichiometry in the tetraalkoxysilanes limits the maximum glass content in the original non-shrinking composites to 10 to 18 percent. In order to increase the glass content to greater than 50 percent, we focused our efforts toward the use of silicic acid oligomers. Molecular weights of the poly(silicic acid) materials have been varied from Mn = 5,000 to 2,000,000 by controlling reaction conditions. In addition, branching ratios (i.e., linear vs. spherical particles) can be controlled by changing the catalysts used. The properties of the resulting composite can range from a transparent flexible material to a transparent hard material simply by changing the organic polymer in the composite. GRA

N92-32829# Toronto Univ. (Ontario). Inst. for Aerospace Studies.
A UNIQUE METHOD OF DETERMINING THE ELASTIC AND ENGINEERING CONSTANTS OF UNIDIRECTIONAL FIBRE-REINFORCED COMPOSITE PLATES USING ULTRASOUND
Li Che Ted Chen Mar. 1991 177 p
(UTIAS-TN-274; CTN-92-60377) Copyright Avail: CASI HC A09/MF A02

A unique method was developed to determine the elastic constants (fourth order stiffness tensor), and the engineering (Young's Modulus, Poisson's ratio, and the shear modulus) constants of unidirectional fiber reinforced composite plates from ultrasonic measurements. The ultrasonic measurements were performed on only one surface of any plate. This was to simulate real-life situations where often it is only possible to access a structure from one surface. The main parameter measured was the acoustic velocity of the ultrasonic wave. Equations relating the acoustic velocity to the elastic constants of a transversely isotropic material were developed. The composite materials investigated were APC2 (PEEK), IM7/8551-7, Kevlar/CE-321R, and AS4/3501-6. Using this method, the elastic constants and the engineering constants of the plates were within 5 percent of the accepted values. In developing this method, it was discovered that ultrasonic nondestructive evaluation of materials is extremely efficient in determining the quality of the material under test. Author (CISTI)

N92-32846# Defence Research Establishment Pacific, Victoria (British Columbia). Research and Development Branch.
DETECTION OF HONEYCOMB DAMAGE USING HEXAGONAL GRID DISCONTINUITIES
J. E. Boyd May 1989 37 p
(DREP-89-9; CTN-92-60350) Avail: CASI HC A03/MF A01

Inspection of an aircraft structure with film radiography can be time consuming and wasteful of human resources. Filmless real-time radiography provides one method of streamlining the inspection process. It also permits implementation of automated inspection systems. The report presents a method for automatically inspecting honeycomb sandwich panels for certain types of damage. The hexagonal grid discontinuity (HGD) inspection exploits the regularity of the grid of a honeycomb in order to locate irregularities and possible damage. Teflon inserts, which simulate disbonds, and entrapped water were successfully detected by the HGD method. Undamaged honeycomb did not produce false alarms in the detection system. The method is suitable for use with a real-time video x-ray inspection system. Author (CISTI)

N92-32852# Institute for Aerospace Research, Ottawa (Ontario). Structures and Materials Lab.
TENSILE FRACTURE OF NOTCHED COMPOSITE LAMINATES [RUPTURE PAR TRACTION DE MATERIAUX COMPOSITES STRATIFIES]
C. Poon Apr. 1991 51 p Sponsored by National Research Council of Canada
(NRC-32147; IAR-AN-71; CTN-92-60373) Avail: CASI HC A04/MF A01

This report describes the determination of empirical parameters for a fracture model which can be used to predict the uniaxial tensile strength of composite laminates containing notches of various sizes. The parameters required the characteristic dimension and the unnotched tensile strength of the subject laminate. A data base including notched and unnotched strengths of the subject laminates and elastic ply properties was generated for the determination of these parameters using a statistical procedure based on the two parameter Weibull distribution. Three second generation high toughness graphite fiber reinforced composites, and two first generation brittle graphite/epoxy composites, were used to fabricate the specimens containing either a through the thickness cylindrical hole or a countersunk hole. The two parameter fracture model assessed was found to be capable of predicting accurately the tensile notched strength of composite laminates. The characteristic dimension was found to be dependent on a

variety of intrinsic and extrinsic factors; therefore, it must be determined by experiment for each new composite material, laminate configuration, etc.. Results showed that a decrease in the characteristic dimension indicated an increase in notch sensitivity. Since the characteristic dimensions of the three second generation composites were found to be larger than those of the first generation composites, they were less notch sensitive. The notched strength of a countersunk hole was predicted by approximating the countersunk hole by a uniform hole with a diameter equal to the outer diameter of the countersunk hole.
Author (CISTI)

N92-32906# Laser Science, Inc., Ames, IA.
LASER COATING OF COMPOSITES FOR ENHANCED WEAR AND CORROSION RESISTANCE Final Report, 1 Jul. - 31 Dec. 1991
Madhav R. Govindaraju, Arul Molian, and P. Molian 28 Jan. 1992 53 p
(Contract DAAL03-91-C-0040)
(AD-A249231; ARO-29044.1-MS-SBI) Avail: CASI HC A04/MF A01

A new technique has been developed to produce glassy surface coatings on Metal Matrix Composites (MMC's) based on laser induced chemical reduction of metal salts. The substrate is first coated with a paste containing concentrated salts of the elements to be coated (ex. nickel formate, cobalt acetate, phosphorous, etc.) along with a thickening agent. The rise in the surface temperatures during laser irradiation will lead to the decomposition of salts to their native metals. The combination of these metal and metalloid elements in the reaction zone form an amorphous layer due to the specific chemical ratio and rapid cooling rate. The thickness of the coatings obtained were on the order of 50-100 microns, exhibited amorphous and microcrystalline structures, possessed hardness in the range of 300-1700 HV (substrate hardness 80-90 HV), and had superior sliding wear resistance and excellent corrosion resistance. The formation of glassy surface coatings depends on the specific ratio of the metal-metal or metal-metalloids in the surface layers. The advantages of this process include the formation of glassy coatings on MMC's by a simple, versatile, technique which does not require any vacuum or inert atmospheres. GRA

N92-32945# Oak Ridge National Lab., TN.
CHARACTERIZATION OF SINTERED REACTION-BONDED SILICON NITRIDE PROCESSED BY MICROWAVE HEATING
J. O. Kiggans, Jr. and T. N. Tiegs 1992 7 p Presented at the Material Research Society Spring Meeting, San Francisco, CA, 27 Apr. - 2 May 1992
(Contract DE-AC05-84OR-21400)
(DE92-014408; CONF-920402-12) Avail: CASI HC A02/MF A01

Sintered reaction-bonded silicon nitride (SRBSN) tiles were fabricated by using microwave and conventional heating. Materials from both processes were analyzed at various stages in their fabrication. Microwave processing resulted in a SRBSN material of higher density and strength than the conventionally processed material. DOE

N92-33033# Advisory Group for Aerospace Research and Development, Neuilly-Sur-Seine (France). Structures and Materials Panel.
THE UTILIZATION OF ADVANCED COMPOSITES IN MILITARY AIRCRAFT [L'EMPLOI DES MATERIAUX COMPOSITES DE POINTE POUR LES AVIONS MILITAIRES]
Apr. 1992 194 p In ENGLISH and FRENCH The 73rd meeting was held in San Diego, CA, 7-11 Oct. 1991
(AGARD-R-785; ISBN-92-835-0666-9) Copyright Avail: CASI HC A09/MF A03

The purpose of this workshop was to identify the current state-of-the-art in key issues related to compression loading and fluid effects in composite materials. In the area of compression loading, there was considerable concern over the different results obtained from various test methods. It was agreed that failure modes produced by the various test methods along with a better fundamental understanding of compression failure were key issues in the development of compression test methods. In the area of fluid effects, a lack of a comprehensive data base hampers identification of key mechanisms leading to fluid degradation. This is further complicated by the fact that interactions depend on the fluid and composite under consideration. For individual titles, see N92-33034 through N92-33054.

N92-33034# Dayton Univ., OH.
ISSUES IN COMPRESSION LOADING OF COMPOSITE STRUCTURES
James M. Whitney *In* AGARD, The Utilization of Advanced Composites in Military Aircraft Apr. 1992 5 p (For primary document see N92-33033 23-24)
Copyright Avail: CASI HC A01/MF A03

Compression loading causes difficulty in development of test methods and failure criteria. Compression testing has produced considerable controversy with a number of different experimental methods being considered. Each method, however, often produces different values of apparent compression strength. The failure mode is the key issue, as each test may produce a different failure mode. In addition, the failure modes often depend on fiber and matrix properties and on laminate geometry. When data is reported, the failure mode is often ignored. In analyzing failure modes, one must consider how relevant the test geometry and load introduction is to the actual application for which the data is being generated. Development of failure criteria also creates difficulty because of the various possible failure modes. Author

N92-33035# Dayton Univ. Research Inst., OH.
A NEW TEST METHOD TO DETERMINE THE COMPRESSIVE STRENGTH OF FIBER-REINFORCED COMPOSITES
A. S. Crasto, R. Y. Kim, and J. M. Whitney (Wright Lab., Wright-Patterson AFB, OH.) *In* AGARD, The Utilization of Advanced Composites in Military Aircraft Apr. 1992 12 p (For primary document see N92-33033 23-24)
Copyright Avail: CASI HC A03/MF A03

The measured compression strength of advanced composites is sensitive to specimen inhomogeneities, loading geometry, and test conditions. Consequently, the reported strength is not an intrinsic material property, but simply the failure stress under compression loading, and varies widely for a given composite system. To obtain a more accurate measure of the material property, premature failure must be avoided, and a specimen was specifically designed for this purpose. The specimen is a miniature sandwich beam with identical composite skins on either side of a neat resin core, and can be tested in axial compression as well as four-point flexure. The axial compressive properties of epoxy composites reinforced with carbon, glass, and boron filaments, and composites of carbon fibers in a polyetheretherketone (PEEK) matrix has been evaluated with this specimen in an IITRI test fixture. Failure occurred predominantly in the gage section for unidirectional composites at composite stresses and strains substantially higher than those observed with all-composite test coupons and with substantially less variation in the data. Multidirectional laminates also displayed higher strengths with the sandwich specimen. Author

N92-33036# British Aerospace Aircraft Group, Warton (England). Materials and Development Dept.
ASPECTS OF COMPRESSION IN AEROSPACE COMPOSITES: FUTURE REQUIREMENTS
Stuart Green *In* AGARD, The Utilization of Advanced Composites in Military Aircraft Apr. 1992 13 p (For primary document see N92-33033 23-24)
Copyright Avail: CASI HC A03/MF A03

To keep the overall mass of combat aircraft to a minimum level, and to optimize performance, designers have exploited the benefits offered by advanced polymer composite materials. The ability to resist load in compression is, however, particularly important in some aircraft structures such as wings. Advantages in terms of reduced mass and increased performance to be gained

with composite materials is highlighted in this paper. A general overview is given of the materials science aspects of compression and compression after impact. Recent developments aimed at improving the reliability of compression test data is reviewed.
Author

N92-33037# Nottingham Univ. (England). Dept. of Theoretical Mechanics.
THREE-DIMENSIONAL ELASTICITY ANALYSIS OF BUCKLING OF LAMINATED PLATES
A. J. M. Spencer *In* AGARD, The Utilization of Advanced Composites in Military Aircraft Apr. 1992 5 p (For primary document see N92-33033 23-24)
Copyright Avail: CASI HC A01/MF A03

The analysis of failure mechanisms for laminated composite materials depends on obtaining a three dimensional analysis of the elastic stress and deformation in the material, with particular regard to interlaminar stresses. A transfer matrix method is used which determines the stress and displacement at any point in the plate in terms of the stress and displacement at a reference surface. Standard two dimensional equations governing these surfaces may be solved by numerical methods. Elastic buckling of plates subject to pre-stress is investigated in this paper. Buckling is treated as a bifurcation from the initial stress state, giving rise to an eigenvalue problem.
Author

N92-33038# Royal Aerospace Establishment, Farnborough (England). Materials and Structures Dept.
A REVIEW OF RAE SPONSORED WORK ON THE COMPRESSIVE BEHAVIOUR OF COMPOSITE MATERIALS
P. T. Curtis *In* AGARD, The Utilization of Advanced Composites in Military Aircraft Apr. 1992 9 p (For primary document see N92-33033 23-24)
Copyright Avail: CASI HC A02/MF A03

The Non-metallic Materials Division at RAE has mounted a major program to study the compressive behavior of composite materials and seek improvements in compressive strength. This is being done by developing improved compressive test techniques, studying failure processes fractographically, investigating the effect of notches and impact damage, and modelling these behaviors mathematically to develop a predictive capability.
Author

N92-33039# Institute for Aerospace Research, Ottawa (Ontario).
INFLUENCE OF EDGE EFFECT ON COMPRESSION-TENSION FATIGUE OF TOUGHENED GRAPHITE/EPOXY LAMINATES
J. P. Komorowski, J. B. R. Heath, D. Lefebvre (Sherbrooke Univ., Quebec), C. Roy (Sherbrooke Univ., Quebec), and R. Masmoudi (Sherbrooke Univ., Quebec) *In* AGARD, The Utilization of Advanced Composites in Military Aircraft Apr. 1992 7 p (For primary document see N92-33033 23-24)
(Contract FE220788NRC21)
Copyright Avail: CASI HC A02/MF A03

Results are reported of fatigue tests on a toughened graphite/epoxy (IM6/5245C) using a specimen and grip design that allows a relatively large volume of material to be tested. The loading was compression dominated with specimens having a layup of (0/45/90)-(44.4 percent,44.4 percent,11.1 percent). Specimen stiffness and residual strength were measured. Results indicate that fatigue in composite specimens is dominated by the edge effects. The proper selection of stacking sequence is crucial in achieving long fatigue lives. Under compression dominated loading, fatigue is a local process, with damage always initiating at the edge and could be related to interlaminar shear stresses. The fatigue process consists of a relatively long period before initiation, followed by a period of rapid growth leading to compressive failure.
Author

N92-33040# Institute for Aerospace Research, Ottawa (Ontario).
DAMAGE PROGRESSION UNDER COMPRESSIVE LOADING IN COMPOSITE LAMINATES CONTAINING AN OPEN HOLE
C. Poon, N. C. Bellinger, R. W. Gould, and M. D. Raizenne *In* AGARD, The Utilization of Advanced Composites in Military Aircraft Apr. 1992 16 p (For primary document see N92-33033 23-24)
(Contract FE220788NRC21)
Copyright Avail: CASI HC A03/MF A03

An experimental investigation into damage progression in compressively loaded quasi-isotropic laminates with a circular hole and the prediction of damage initiation using 3-D finite element failure analysis is described. Notched laminated plates were fabricated from Narmco IM6/5245C with three different stacking sequences. The tests revealed that the notched strength decreased as the ply group thickness increased. Based on the numerical and experimental results, a mechanism for damage initiation and progression was proposed. However, considering the damage initiation occurred at 90 percent of the ultimate load, a damage progression model would not be practical for the material systems presently used in aircraft.
Author

N92-33041# Office National d'Etudes et de Recherches Aerospatiales, Paris (France).
PROPAGATION OF A DELAMINATION IN A COMPOSITE PANEL SUBJECTED TO A COMPRESSION LOAD [PROPAGATION D'UN DELAMINAGE DANS UN PANNEAU COMPOSITE SOUMIS A UN CHARGEMENT DE COMPRESSION]
R. Girard *In* AGARD, The Utilization of Advanced Composites in Military Aircraft Apr. 1992 9 p In FRENCH Previously announced in IAA as A92-16123 (For primary document see N92-33033 23-24)
Copyright Avail: CASI HC A02/MF A03

The DAM-STRAT finite element code is used to study the propagation of an artificial delamination between two layers of a laminate plate subjected to compression forces. The propagation is preceded by local buckling and a rupture of the layers along two sides of the rectangular delamination zone. The problem is analyzed in the framework of large displacements in the buckling and postbuckling regions. The results obtained demonstrate that DAM-STRAT is an effective tool for predicting various phenomena associated with the compression of composite panels with an initial delamination.
Author

N92-33042# National Aerospace Lab., Amsterdam (Netherlands).
GARTEUR COMPRESSION BEHAVIOUR OF ADVANCED CFRP
W. G. J. tHart, R. Aoki (Deutsche Forschungsanstalt fuer Luft- und Raumfahrt, Stuttgart, Germany, F.R.), H. Bookholt (Fokker B.V., Amsterdam, Netherlands), P. T. Curtis (Royal Aerospace Establishment, Farnborough, England), I. Kroeber (Deutsche Airbus G.m.b.H., Bremen, Germany, F.R.), N. Marks (Westland Helicopters Ltd., Yeovil, England), and P. Sigety (Office National d'Etudes et de Recherches Aerospatiales, Paris, France) *In* AGARD, The Utilization of Advanced Composites in Military Aircraft Apr. 1992 6 p (For primary document see N92-33033 23-24)
Copyright Avail: CASI HC A02/MF A03

The susceptibility of currently used carbon fiber reinforced plastics (CFRP) to impact damage has stimulated the development of improved composites. This new generation of composites shows increased toughness and damage tolerance as well as improved tensile performance. This is generally not matched by an improvement in compressive properties which then become the limiting factor. To improve the compressive strength, a better understanding of the compressive failure modes is needed. For experimental verification of failure models, special attention must be paid to compressive test procedures in order to achieve optimal strength values with minimum scatter.
Author

N92-33043# Dassault-Breguet Aviation, Saint Cloud (France).
INNOVATIVE CONSTITUENTS REQUIREMENTS TO IMPROVE COMPOSITES COMPRESSIVE STRENGTH
L. Anquez and P. Vautey *In* AGARD, The Utilization of Advanced Composites in Military Aircraft Apr. 1992 10 p (For primary document see N92-33033 23-24)
Copyright Avail: CASI HC A02/MF A03

While the recent development of intermediate modulus carbon fibers led to very high specific tensile strength over the first generation of high strength composites, the composite compressive properties did not improve at all. Because most aeronautical structures are subject to alternate tension and compression, it is not possible to take full advantage of carbon fiber composites, as the compressive loading becomes the design limitation. After a focus on the matrix dominating role in composite compression behavior, this paper will clear out which matrix characteristics, stiffness or strength, determines the unidirectional compressive failure. H.A.

N92-33044# Alenia, Foggia (Italy). Engineering Dept. for Advanced Composite Structures.
CFRP STIFFENED PANELS UNDER COMPRESSION
A. Bucci and U. Mercurio *In* AGARD, The Utilization of Advanced Composites in Military Aircraft Apr. 1992 14 p (For primary document see N92-33033 23-24)
Copyright Avail: CASI HC A03/MF A03

The purpose was to experimentally demonstrate the validity of the conceptual carbon fiber reinforced plastics (CFRP) stiffened panel suitable for application in the unpressurized aft fuselage of a middle size aircraft. Both theoretical and experimental behavior have been analyzed taking into account the effects of different materials, curvature, impact damage, and static and fatigue loads. Composite materials with stiff fibers of the last generation coupled with toughened thermosetting resin systems were used. Author

N92-33045# British Aerospace Aircraft Group, Warton (England). Materials and Development Dept.
AN OVERVIEW OF CONCERNS RELATING TO FLUID EFFECTS ON COMPOSITES
Geoffrey A. Wright *In* AGARD, The Utilization of Advanced Composites in Military Aircraft Apr. 1992 6 p (For primary document see N92-33033 23-24)
Copyright Avail: CASI HC A02/MF A03

The effect of the interaction of fluids on composite fiber/resin systems plays an important role in determining the suitability and design values used for these materials. A brief overview is provided of the questions posed by the designer and the materials engineer and looks at the test methodologies proposed to answer these questions. The advantages for standardization of these fluid/environment exposure regimes, together with agreement on the range and extent of the follow-up tests is examined. Author

N92-33046# Construcciones Aeronauticas S.A., Madrid (Spain). Research and Development, Technology and Materials Dept.
EFFECTS OF FUEL ON HERCULES AS-4/8552 COMPOSITE MATERIAL
A. T. Rodriguez, A. Lavia, I. Fernandez, and E. Redondo *In* AGARD, The Utilization of Advanced Composites in Military Aircraft Apr. 1992 6 p (For primary document see N92-33033 23-24)
Copyright Avail: CASI HC A02/MF A03

The behavior of an advanced toughened epoxy resin/carbon fiber composite material, Hercules AS-4/8552, in contact with fuel has been studied. Interlaminar shear strength and compression strength tests were performed on unidirectional specimens after being exposed at 70 C to several conditions, including a combined exposure of JP8 and water. A correlation between the fluid content and the drop of the mechanical properties was found. The exposure to fuel or additive mixtures of impacted samples was found not to produce any effect in the damage size or detectability. Fuel leakage tests were conducted on impacted panels subjected to pressure and results are presented. Finally, the growth of micro-organisms in fuel/water solutions seemed not to effect the material properties, as deduced from some mechanical and microscopy studies carried out on samples exposed to such mixtures. Author

N92-33047# Naval Air Development Center, Warminster, PA.
ENVIRONMENTAL DEGRADATION OF HIGH TEMPERATURE COMPOSITES
R. C. Cochran, T. M. Donnellan, R. E. Trabocco, and J. Thompson (Naval Air Systems Command, Washington, DC.) *In* AGARD, The Utilization of Advanced Composites in Military Aircraft Apr. 1992 12 p (For primary document see N92-33033 23-24)
Copyright Avail: CASI HC A03/MF A03

A study was performed to assess the effect of galvanic corrosion phenomena on the strength of graphite/bismaleimide (BMI) composites. The results indicate that degradation occurred in BMI composites galvanically coupled to aluminum alloys. The mechanism responsible for the degradation involves hydroxyl ion generation in the cathodic reaction. Optical and electron microscopy of the surface of coupled specimens showed a great deal of cracking and degradation of the resin. This phenomena is thought to be associated with stresses in the resin imposed by thermal or chemical processes. These cracks may be an indication that the mechanism of degradation is not simply the hydroxyl attack on the resin but a combination of chemical and mechanical attack. Composite-aluminum material couples were exposed to salt water/fuel solutions and to salt spray environments after which material properties were determined. Conventional protection schemes were evaluated. The results indicate that the performance retention was test specific and that the bearing tests were most sensitive to the galvanic reaction. In addition, a systematic study of the electrochemical conditions which were most important in control of the degradation rates was performed. Author

N92-33048# Centre d'Essais Aeronautique Toulouse (France).
EVALUATION OF THE EFFECTS OF THE ENVIRONMENT ON THE BEHAVIOR OF THE PRIMARY STRUCTURES OF COMPOSITE MATERIAL AIRCRAFT IN SERVICE: HISTORIC AND CURRENT SITUATION [PRISE EN COMPTE DES EFFETS DE L'ENVIRONNEMENT SUR LE COMPORTEMENT EN SERVICE DES STRUCTURES PRIMAIRES D'AVIONS EN MATERIAU COMPOSITE: HISTORIQUE ET SITUATION ACTUELLE]
Jean Rouchon *In* AGARD, The Utilization of Advanced Composites in Military Aircraft Apr. 1992 7 p In FRENCH (For primary document see N92-33033 23-24)
Copyright Avail: CASI HC A02/MF A03

When the first application of composite materials with an organic base in the working structures of aircraft were envisaged, the greatest preoccupation of the designers and service officials was their behavior while aging. Some fifteen years later, the experience acquired in service associated with the numerous results obtained from the laboratory has greatly dissipated those fears, at least for structures not calling for extensive usage of composite technology. This does not mean that the aging of composites does not occur, but rather that the consequences are now considered to have limited and predictable impact. In other words, they are susceptible to being accounted for at the level of conception, certification, and thereafter in use in the structures. The principal steps leading to the current situation are retraced, and then analyzed to account for the phenomena of aging, in particular the determination of the concentration of water absorbed by the composite during use.
Transl.

N92-33049# Wright Lab., Wright-Patterson AFB, OH.
FLUID EFFECTS: THERMOSET AND THERMOPLASTIC MATRIX COMPOSITES
D. B. Curliss *In* AGARD, The Utilization of Advanced Composites in Military Aircraft Apr. 1992 8 p (For primary document see N92-33033 23-24)
Copyright Avail: CASI HC A02/MF A03

The sensitivity of several advanced composites to military jet fuel, JP-4, was investigated. The materials were processed into laminates using the manufacturer's recommended process. The test specimens were immersed in JP-4 in a sealed pressure vessel at 180 F. After 1680 hours of exposure, the mechanical properties of the composites along with any weight gain were examined. Material property degradation and other physical effects from exposure to jet fuel are presented in this study. Author

N92-33050# Patras Univ. (Greece). Dept. of Mechanical Engineering.
JET FUEL ABSORPTION AND DYNAMIC MECHANICAL ANALYSIS OF CARBON FIBRE COMPOSITES
S. A. Paipetis and V. Kostopoulos *In* AGARD, The Utilization of Advanced Composites in Military Aircraft Apr. 1992 6 p (For primary document see N92-33033 23-24)
Copyright Avail: CASI HC A02/MF A03

Fluid absorption of carbon fiber composites, both thermosetting and thermoplastic, immersed in jet fuel under controlled conditions of time and temperature, was determined and, in the sequence, DMA studies were performed. Storage modulus, loss factor, and glass transition temperature were the parameters utilized for the evaluation of the dynamic behavior of these materials. Author

N92-33051# Institute for Aerospace Research, Ottawa (Ontario). Structures and Materials Lab.
FRACTURE SURFACE CHARACTERISTICS OF COMPRESSIVE FAILURES IN CARBON FIBRE REINFORCED EPOXY LAMINATE SUBJECTED TO HOT/WET CONDITIONING
S. Lee, P. C. Gaudert, and R. F. Scott *In* AGARD, The Utilization of Advanced Composites in Military Aircraft Apr. 1992 8 p Sponsored by Dept. of National Defence and National Research Council of Canada (For primary document see N92-33033 23-24)
Copyright Avail: CASI HC A02/MF A03

Results of an investigation are presented into the effects of environmental exposure on the compressive fracture surface characteristics of carbon/epoxy composite materials such as Hercules AS-4/3501-6. The effects of temperature and absorbed moisture on laminates are explored. Specimens were preconditioned in either ambient laboratory humidity or in water at 64 C for four to seven weeks. The fractures were produced at room temperature and 93 C. The observed fracture features, by scanning electron microscope, of the specimens with different preconditioning and test environments are presented. These results illustrated differences in the amount of fiber/matrix separation, fiber fracture, and resin fracture with increasing temperature and absorbed moisture. The reduction in compressive strength of laminates due to hygrothermal effects is also discussed. Author

N92-33052# Middle East Technical Univ., Ankara (Turkey).
THE EFFECT OF HEAT TREATMENT ON THE PROPERTIES OF PEEK AND APC-2
A. Ankara, G. Kalay, and M. J. Folkes (Brunel Univ., Uxbridge, England) *In* AGARD, The Utilization of Advanced Composites in Military Aircraft Apr. 1992 7 p Sponsored in part by NATO (For primary document see N92-33033 23-24)
Copyright Avail: CASI HC A02/MF A03

This paper examines the effects of certain heat treatments on the properties of PEEK and carbon fiber reinforced PEEK. Tests were performed to study the changes in the amount of crystallinity and observe the effect this crystallinity change had on the other properties. DSC thermograms showed that there is no considerable change in crystallinity melting point of the composite specimens dependent on the heat treatment applied. Higher glass transition temperatures were observed for specimens with a higher crystallinity percentage. The frequency effect on the dynamic mechanical spectrum was also determined, and showed that this quantity is decreased to lower temperatures and the loss tangent increases in value. Flexture testing showed that the flexture properties are independent of crystallinity. Author

N92-33053# Alenia, Foggia (Italy).
ENVIRONMENTAL RESISTANCE OF AMORPHOUS BONDED THERMOPLASTIC JOINTS
C. Voto and M. Iannone *In* AGARD, The Utilization of Advanced Composites in Military Aircraft Apr. 1992 5 p (For primary document see N92-33033 23-24)
Copyright Avail: CASI HC A01/MF A03

Amorphous bonding appears to be a promising method of joining thermoplastic matrix advanced composites. The temperature to bond, lower than for fusion bonding, and the limited dimension of the melted zone, allow significant cost reduction and guarantee good mechanical characteristics. On the other hand, a potential problem exists, due to lower resistance to aeronautical solvents and service fluids, because of the amorphous nature of the bonding layers. The basic resistance to environmental degradation of the resins used for bonding, and the chemical stability of their blends with the semicrystalline matrices of the adherends, have been investigated. Author

N92-33054*# National Aeronautics and Space Administration. Langley Research Center, Hampton, VA.
FLIGHT SERVICE ENVIRONMENTAL EFFECTS ON COMPOSITE MATERIALS AND STRUCTURES
H. Benson Dexter and Donald J. Baker (Army Aviation Research and Technology Activity, Hampton, VA.) *In* AGARD, The Utilization of Advanced Composites in Military Aircraft Apr. 1992 13 p (For primary document see N92-33033 23-24)
Copyright Avail: CASI HC A03/MF A03

NASA Langley and the U.S. Army have jointly sponsored programs to assess the effects of realistic flight environments and ground-based exposure on advanced composite materials and structures. Composite secondary structural components were initially installed on commercial transport aircraft in 1973; secondary and primary structural components were installed on commercial helicopters in 1979; and primary structural components were installed on commercial aircraft in the mid-to-late 1980's. Service performance, maintenance characteristics, and residual strength of numerous components are reported. In addition to data on flight components, 10 year ground exposure test results on material coupons are reported. Comparison between ground and flight environmental effects for several composite material systems are also presented. Test results indicate excellent in-service performance with the composite components during the 15 year period. Good correlation between ground-based material performance and operational structural performance has been achieved. Author

N92-33075*# Virginia Polytechnic Inst. and State Univ., Blacksburg. Dept. of Engineering Science and Mechanics.
A COMPARISON OF THREE POPULAR TEST METHODS FOR DETERMINING THE SHEAR MODULUS OF COMPOSITE MATERIALS
Henjen Ho, Ming-Yi Tsai, John Morton, and Gary L. Farley (National Aeronautics and Space Administration. Langley Research Center, Hampton, VA.) 1991 26 p
(Grant NAG1-1053)
(NASA-CR-190659; NAS 1.26:190659) Avail: CASI HC A03/MF A01

Three popular shear tests (the 10 degree off-axis, the plus or minus 45 degree tensile, and the losipescu specimen tested in the modified Wyoming fixture) for shear modulus measurement are evaluated for a graphite-epoxy composite material system. A comparison of the shear stress-strain response for each test method is made using conventional strain gage instrumentation and moire interferometry. The uniformity and purity of the strain fields in the test sections of the specimens are discussed, and the shear responses obtained from each test technique are presented and compared. For accurate measurement of shear modulus, the 90 degree losipescu specimen is recommended. Author

N92-33078# Institute for Aerospace Research, Ottawa (Ontario). Structures and Materials Lab.
PUBLICATIONS BY STRUCTURES AND MATERIALS LABORATORY ON COMPOSITE MATERIALS (JANUARY 1983 - JUNE 1991)
P. C. Gaudert, comp 28 Jun. 1991 17 p Sponsored by Dept. of National Defence
(NRC-LTR-ST-1833; CTN-92-60381) Avail: CASI HC A03/MF A01

In 1982 the Structures and Materials Laboratory of the Institute for Aerospace Research (IAR) (Canada) decided that composite structural technology should be promoted as a matter of priority.

The major goal was to develop expertise and facilities that would allow the laboratory to provide advice and assistance to universities, industry and other government agencies. This report contains a compilation of all reports, publications and patents on composite structures and materials by the laboratory between 1983 and 1991. Included are references to reports on work carried out in the following areas: development of new materials, characterization of composite materials, materials processing, design and analysis of composite structures and special applications, nondestructive testing and evaluation of composites, failure, fatigue, and creep in composite materials and structures, development of new test methods, composite joining and repair, and environmental testing of composites. Also listed are a number of literature reviews on relevant topics. CISTI

N92-33174 Department of the Navy, Washington, DC.
APPARATUS FOR PREPARING THERMOPLASTIC COMPOSITES Patent
Roland C. Cochran, inventor (to Navy) and Edwin L. Rosenzweig, inventor (to Navy) 26 May 1992 10 p Filed 28 Feb. 1991
(AD-D015326; US-Patent-5,116,216; US-Patent-Appl-SN-662678; US-Patent-Class-425-50A) Avail: US Patent and Trademark Office

An apparatus for processing thermo-composites is discussed. In this method, individual plies of a prepreg, to be used in forming a laminate, are processed under two, concentric vacuum chambers. Heat and consolidating pressure are applied under a first vacuum, and a second vacuum is drawn under an outer, rigid shell. GRA

N92-32275*# Rockwell International Corp., Canoga Park, CA. Rocketdyne Div.
A MULTI-DOMAIN METHOD FOR SUBSONIC VISCOUS FLOWS
Daniel C. Chan and Munir M. Sindir *In* NASA. Goddard Space Flight Center, Tenth Workshop for Computational Fluid Dynamic Applications in Rocket Propulsion, Part 2 Jul. 1992 p 1427-1451 (For primary document see N92-32245 23-34)
Avail: CASI HC A03/MF A05

25 INORGANIC AND PHYSICAL CHEMISTRY

Includes chemical analysis, e.g., chromatography; combustion theory; electrochemistry; and photochemistry.

For related information see also *77 Thermodynamics and Statistical Physics.*.

N92-32330# Battelle Memorial Inst., Research Triangle Park, NC.
ROTATIONAL BARRIERS IN MODEL COMPOUNDS OF POLY (VINYL CHLORIDE): 2-CHLOROBUTANE AND 1,3,5,7,9,11-HEXACHLORODODECANE Final Report, May - Aug. 1991
G. R. Famini, J. O. Jensen, P. N. Krishnan, and L. A. Burke Mar. 1992 18 p
(Contract DAAL03-86-D-0001; DA Proj. 1C1-62622-A-553)
(AD-A250855; CRDEC-CR-144) Avail: CASI HC A03/MF A01

Rotational barriers and conformational energy differences were calculated for 2-chlorobutane and 1,3,5,7,9,11-hexachlorododecane. These are considered as model compounds for syndiotactic poly vinyl chloride. The theoretical methods include high level ab initio SCF and configuration interaction methods. Accessability to gauche and gauche states in the polymer are in light of these model compounds. GRA

N92-32332# Colorado Univ., Boulder.
METHANE CONVERSION TO METHANOL
R. D. Noble and J. L. Falconer 1992 10 p Presented at the US Department of Energy Contractor Review Meeting on Natural Gas Research and Development, Morgantown, WV, 5-6 May 1992
(Contract DE-FG21-90MC-27115)
(DE92-014349; DOE/MC-27115/92/C0035; CONF-920584-7)
Avail: CASI HC A02/MF A01

The objective of this research study is to demonstrate the effectiveness of a catalytic membrane reactor for the partial oxidation of methane. The specific goals are to demonstrate that we can improve product yield, demonstrate the optimal conditions for membrane reactor operation, determine the transport properties of the membrane, and provide demonstration of the process at the pilot plant scale. The last goal will be performed by Unocal, Inc., our industrial partner, upon successful completion of this study. DOE

N92-32334# Lehigh Univ., Bethlehem, PA.
METHANE OXIDATION OVER DUAL REDOX CATALYSTS
K. Klier and R. G. Herman 1992 17 p Presented at the US Department of Energy Contractor Review Meeting on Natural Gas Research and Development, Morgantown, WV, 5-6 May 1992
(Contract DE-FG21-89MC-26039)
(DE92-014358; DOE/MC-26039/92/C0031; CONF-920584-10)
Avail: CASI HC A03/MF A01

The objectives of this research were to achieve and understand the partial oxidation of methane to oxygenates and C2 hydrocarbons over dual redox catalysts. The catalysts were based on oxidic materials that will exhibit structural and thermal stability for long reactor lifetimes. A continuous flow reactor system with oxygen or air as the oxidizing gas, rather than nitrous oxide, was utilized over a wide range of temperatures less than or equal to 1000 C, with variable gas hourly space velocity, in order to maximize the space time yields of the desired products. All of the investigated processes are catalytic and are aimed at minimizing gas phase reactions. DOE

N92-32347# Grambling State Univ., LA. Dept. of Physics.
NQR-NMR STUDIES OF HIGHER ALCOHOL SYNTHESIS Cu-Co CATALYSTS
A. N. Murty May 1992 9 p
(Contract DE-FG22-89PC-89762)
(DE92-016614; DOE/PC-89762/T14) Avail: CASI HC A02/MF A01

During this period, we focused our attention in analyzing the magnetic nature of the extensively used trimetallic catalyst system Cu-Co-Cr for the production of higher alcohols. We believe that there could be some correspondence between the catalytic and magnetic behaviors of the transition metal catalyst systems. Both the morphology and metallic charge distribution of the particles are known to govern the catalytic as well as the magnetic properties of the system. DOE

N92-32464# Aerospace Corp., Los Angeles, CA. Space and Environment Technology Center.
A SHOCK TUBE STUDY OF THE REACTIONS OF THE HYDROXYL RADICAL WITH COMBUSTION SPECIES
N. Cohen 21 May 1991 5 p
(Contract DE-FG03-87ER-13812)
(DE92-012573; DOE/ER-13812/T1) Avail: CASI HC A01/MF A01

The reactions of OH radicals with hydrocarbons have received a great deal of attention in recent years because these processes are principal steps in the oxidation of organic fuels, whether occurring in combustion/propulsion systems, in the atmosphere, or elsewhere. Of the various radicals capable of attacking hydrocarbons, OH radicals are generally the most reactive, and their reactions directly yield water molecules, one of the major final oxidation products. In the atmosphere, the combined effect of the OH radical's reactivity and concentration make it the single species that determines the atmospheric lifetime of an organic substance. The principal goals of the kineticist in the field of oxidation chemistry are: (1) to measure as many elementary reaction rate coefficients as are conveniently studied in the laboratory; and (2) to develop theoretical and/or semi-empirical tools for extrapolating from measured rate coefficients to unmeasured ones. The latter step is necessary because of the sheer number of reactions of possible interest. DOE

N92-32475# Atomic Energy of Canada Ltd., Pinawa (Manitoba). Nuclear Research Establishment.
A STATE OF THE ART REPORT ON FLAME ACCELERATION AND TRANSITION TO DETONATION IN HYDROGEN/AIR/DILUENT MIXTURES
C. K. Chan and K. N. Tennankore Dec. 1991 44 p
(DE92-626850; AECL-10459) Avail: CASI HC A03/MF A01

Accidental ignition in pockets of flammable hydrogen/air/diluent mixtures will lead to a deflagration wave (slow flame). Particular conditions can accelerate this flame and cause a transition from deflagration to a detonation wave (rapid flame), with its associated spatially non-uniform and very high pressures. In this report, the differences between deflagration and detonation are outlined, and the various flame acceleration mechanisms, along with the related research results, are reviewed. The current understanding of transition to detonation as a two-step process, a local explosion followed by an amplification of the resulting blast wave into a detonation wave, is described in detail. Occurrence of a local explosion in hot spots generated by the focussing of shock waves existing ahead of a fast flame, or in high-reactivity centers generated by turbulence-induced rapid mixing of flame and unburnt gas, and the resulting local quenching of the flame, are described and relevant publications are cited. The current models for flame acceleration are listed and their limitations are identified. Also, the available qualitative criteria for assessing the likelihood of transition to detonation under given conditions are briefly discussed. The feasibility of developing a quantitative methodology for assessing this likelihood is discussed, and further more work required to complete this development is outlined. The development of a quantitative methodology is recommended. DOE

N92-32508# California Univ., Davis.
EXPERIMENTAL INVESTIGATION OF THE AXIAL IMPREGNATION OF ORIENTED FIBER BUNDLES BY CAPILLARY FORCES Final Report, Feb. 1988 - Mar. 1990
Erdal Bayramli (Middle East Technical Univ., Ankara, Turkey) and Robert L. Powell May 1992 32 p
(DA Proj. 1L1-62618-AH-80)
(AD-A250758; BRL-CR-690) Avail: CASI HC A03/MF A01

Capillary impregnation of a viscous liquid into carbon fiber bundles is investigated experimentally. Axial impregnation is examined in which flow occurs primarily parallel to the fibers' axes. For silicone oils, as well as for a curing epoxy system, the kinetics of axial impregnation follow closely h alpha t(sub 112) where h is the average displacement of the advancing front and t is the time of impregnation. The impregnation rates are higher than those predicted by models based upon simple geometries. The rates are strongly influenced by the pore size distribution in the fiber bundles. At a given overall average porosity, higher rates of impregnation are observed for samples having a higher pore heterogeneity than those with a narrow distribution of pore sizes. An analysis of the experimental data is presented which allows the effective pore size distribution to be calculated. GRA

N92-32509# State Univ. of New York, Buffalo. Dept. of Chemistry.
NEW APPLICATIONS OF IONIZATION AND FLUORESCENCE TECHNIQUES FOR DETECTING AND CHARACTERIZATION OF OPEN-SHELL ORGANOMETALLICS IN THE GAS PHASE
William R. Peifer, Robert L. DeLeon, and James F. Garvey 1 Jun. 1992 32 p
(Contract N00014-88-K-0483)
(AD-A250923; TR-32) Avail: CASI HC A03/MF A01

Recent advances are discussed in the development of electronic spectroscopic probes for the study of excited-state structure and photodissociation dynamics of gas-phase organometallics. Because of the short time scale for intermolecular energy transfer within van der Waals clusters, the UV photodissociation dynamics of cluster-bound transition metal carbonyls differs considerably from the photodissociation dynamics of the naked species in the gas phase. It is therefore possible to employ multiphoton ionization to produce cluster-bound metal carbonyl photoions in high yield. Resonant photoionization (accomplished with tunable lasers) and mass-resolved detection allow one to probe the excited states of both closed-shell and open-shell neutral organometallics. Finally, a time-resolved two-laser technique employing fluorescent detection of atomic photoproducts is described. This technique allows one to study photodissociation dynamics of organometallics with a temporal resolution competitive with the fastest transient absorption techniques, and a level of sensitivity which is far superior. GRA

N92-32544# Lawrence Livermore National Lab., CA.
SHOCK TUBE IGNITION OF ETHANOL, ISOBUTENE AND MTBE: EXPERIMENTS AND MODELING
H. J. Curran, M. P. Dunphy, J. M. Simmie (University Coll., Galway, Ireland), C. K. Westbrook, and W. J. Pitz 22 Nov. 1991 25 p Presented at the 24th International Symposium on Combustion, Sydney (Australia), 5-10 Jul. 1992
(Contract W-7405-eng-48)
(DE92-008563; UCRL-JC-109055; CONF-920707-19) Avail: CASI HC A03/MF A01

The ignition of ethanol, isobutene, and methyl tert-butyl ether (MTBE) has been studied experimentally in a shock tube and computationally with a detailed chemical kinetic model. Experimental results, consisting of ignition delay measurements, were obtained for a range of fuel/oxygen mixtures diluted in Argon, with temperatures varying over a range of 1100-1900 K. The numerical model consisted of a detailed kinetic reaction mechanism with more than 400 elementary reactions, chosen to describe reactions of each fuel and the smaller hydrocarbon and other species produced during their oxidation. The overall agreement between experimental and computed results was excellent, particularly for mixtures with greater than 0.3 percent fuel. The greatest sensitivity in the computed results was found to falloff parameters in the dissociation reactions of isobutene, ethane, methane, and ethyl and vinyl radicals, to the C3H4 and C3H5 reaction submechanisms in the model, and to the reactions in the H2-O2-CO submechanism. DOE

N92-32553# Texas A&M Univ., College Station. Dept. of Chemistry.
MORPHOLOGY, 31P SPIN DIFFUSION, AND PHASE TRANSITIONS IN A REPRESENTATIVE SEMICRYSTALLINE POLYPHOSPHAZENE BY SOLID-STATE NMR Technical Report No. 5, 1 Jan. - 14 May 1992
Sharon A. Taylor, Jeffery L. White, Nick C. Elbaum, Richard C. Crosby, and Gordon C. Campbell 1992 10 p
(Contract N00014-91-J-1475)
(AD-A250883) Avail: CASI HC A02/MF A01

Solid-state NMR spectroscopy was used to investigate the morphology and molecular dynamics of polyBIS(3-methylphenoxy) phosphazenel-PB3MP, a representative semicrystalline polyphosphazene. Variable temperature 31P magic-angle spinning (MAS) NMR spectra revealed two well resolved isotropic resonances for the crystalline and mesomorphic phases. The ability to resolve resonances for the two phases makes this class of polymers well suited for studying morphology and phase transitions using NMR. 31P spin-lattice relaxation (T1) behavior for PB3MP at 23 deg C suggested that spin diffusion occurs between the two phases, which was confirmed by the observation of cross peaks in a two-dimensional exchange experiment. The measured 31P spin diffusion rate is intermediate between the well established limits of 1H and 13C spin diffusion, and it appears as an apparent anomaly in the 31P spin-lattice relaxation behavior. Employing a model diffusion equation, the spin diffusion rate constant was used to estimate a characteristic diffusion distance of 4.5 nm, implying a lamellar thickness of ca. 9 nm. The amplitude of side-group motion in the crystalline and mesomorphic phases was investigated by the analysis of sideband patterns in 13C MAS spectra obtained at slow spinning speeds. Negligible motion occurs in the crystalline phase, whereas large amplitude motion occurs in the mesomorphic phase. Variable temperature 31P and 1H rotating frame spin-lattice relaxation (T1P) studies revealed activation energies of ca. 10 kcal/mol for motion in the mesomorphic phase. GRA

N92-32557# Oak Ridge National Lab., TN.
HEAT AND MASS EXCHANGE DURING CONDENSATION OF A WATER-AMMONIA MIXTURE
V. M. Stefanovskii (Astrakhan Inst. of Fish Industry, USSR), N. V. Stefanovskaya (Astrakhan Inst. of Fish Industry, USSR), and V. N. Koshaevskii (Astrakhan Inst. of Fish Industry, USSR) 1991 8 p Transl. into ENGLISH from Kholodil'naya Teknika (USSR), v. 44, no. 4, 1967 p 25-27
(Contract DE-AC05-84OR-21400)
(DE92-014524; ORNL/tr-91/33) Avail: CASI HC A02/MF A01

Our goal was to study heat and mass exchange during the condensation of water-ammonia vapor on a horizontal tube in the 8-16 bar pressure range. The experimental apparatus included a closed circuit for circulation of the working substance and a cooling water circuit. The water-ammonia vapor from the generator with electrically controlled heating, went to the space between the tubes of the condenser. The length of the inner experimental tube (of 1Kh18N9T stainless steel) was 0.5 m and its diameter was 0.025 m. The inside diameter of the shell of the condenser was 0.081 m. Eight Chromel-Copel thermocouples were fitted into the outer surface of the wall of the tube in order to measure its temperature. The thermocouples were arranged along the tube every 90 degrees on a helical line, with the leads (60 mm) going through the isothermal surface. The temperature of the vapor in the intratube space of the condenser was also measured with thermocouples. The temperature of the vapor entering the condenser, the outgoing condensate and the boiling point of the latter were measured with mercury laboratory thermometers with scale divisions of 0.1 C. The specific thermal load of the cooling surface was determined with a wattmeter (0.2 class) connected to the heater of the generator. DOE

N92-32562# Ames Lab., IA.
ELECTROCATALYSIS OF ANODIC, OXYGEN-TRANSFER REACTIONS AT NOBLE METAL ELECTRODES Ph.D. Thesis
J. E. Vitt Jun. 1992 179 p
(Contract W-7405-eng-82)
(DE92-016308; IS-T-1569) Avail: CASI HC A09/MF A02

Voltammetry at rotated disk and rotated ring-disk electrodes was applied to the study of several aspects of anodic, oxygen-transfer reactions at noble electrodes. Anodic reactions which involve the transfer of oxygen from H2O to the oxidation products generally exhibit a voltammetric response characterized by severe kinetic limitations. Mechanistic studies were performed at noble electrodes in order to contrive strategies for improving the kinetics of these reactions. Competitive adsorption studies were used to devise an adsorption hierarchy for Au rotated disk electrodes. It was concluded that adsorption was a prerequisite for oxidations involving the transfer of oxygen present on the electrodes surface as adsorbed hydroxyl radicals. The electrogenerated chemiluminescence (ECL) of luminol was studied at Au, Pt, Pd, glassy carbon, PbO2, and Bi-doped PbO2 electrodes. The ECL intensity was determined to be inversely related to electrochemical activity for the oxidation of luminol. It was concluded that the oxygen-transfer oxidation of luminol to 3-aminophthalate (n = 4 eq mol(exp -1) corresponded to the dark reaction, whereas the electron-transfer oxidation of luminol with n = 1 eq mol(exp -1) initiated the chemiluminescent reaction in solution. DOE

N92-32563# Ames Lab., IA.
STUDIES OF n-BUTANE CONVERSION OVER SILICA-SUPPORTED PLATINUM, PLATINUM-SILVER AND PLATINUM-COPPER CATALYSTS Ph.D. Thesis
Junhua Gu Jun. 1992 68 p
(Contract W-7405-eng-82)
(DE92-016309; IS-T-1594) Avail: CASI HC A04/MF A01

The present work was undertaken to elucidate the effect of adding silver and copper to silica-supported platinum catalyst on the activity and selectivity in the n-butane reactions. At the conditions of this study, n-butane underwent both hydrogenolysis and structural isomerization. The catalytic activity and selectivities between hydrogenolysis and isomerization and within hydrogenolysis were measured at temperature varying from 330 to 370 C. For platinum-silver catalysts at the lower temperatures studied, the catalytic activity per surface platinum atom (turnover frequency) remained constant at lower silver content (between 0 and 30 at. percent) and decreased with further increased silver loading, suggesting that low- index planes could be dominant in the hydrogenolysis of n-butane. Moreover, increasing silver content resulted in an enhancement of the selectivity of isomerization products relative to hydrogenolysis products. At the higher temperature studied, no suppression in catalytic activity was observed. It is postulated that surface structure could change due to the mobility of surface silver atoms, leading to surface silver atoms forming islands or going to the bulk, and leaving large portions of basal planes exposed with active platinum atoms. It is also suggested that the presence of inert silver atoms results in weakening of the H-surface bond. This results in increased mobility of hydrogen atoms on the surface and hence, higher reactivity with other adsorbed species. For platinum copper catalysts, the mixed ensembles could play an active role in the hydrogenolysis of n-butane. DOE

N92-32591# Cincinnati Univ., OH. Dept. of Chemistry.
ELECTROCATALYST SURFACES Annual Report, Jan. - Dec. 1991
Arthur T. Hubbard Feb. 1992 53 p
(Contract GRI-5086-260-1404)
(PB92-190420; GRI-92/0137) Avail: CASI HC A04/MF A01

The nature of absorbed reaction-intermediates and other surface species at catalyst surfaces is important in development of new uses for hydrocarbons and for increasing the efficiency of existing processes. To that end, adsorbed hydrocarbon and derivative layers formed on platinum, silver, and ruthenium surfaces in aqueous media were investigated as a function of electrode potential, pH, temperature, electrolyte, nature of the hydrocarbon, concentration of the hydrocarbon, and electrode surface structure. Data obtained during the project have identified fertile areas for practical development and have contributed to the framework for future basic research in the area. Important aspects of electrocatalytic processes are being studied, including: the most active surface structures, adsorbed intermediates, additives, electrolytic species and impurities; the reaction pathways of typical adsorbed hydrocarbon intermediates; and the fundamental causes of the influence of pH, potential, concentration, temperature, and surface structure on electrocatalyst activity. Author

N92-32594# United Technologies Research Center, East Hartford, CT.
AXIAL VORTICES IN GASEOUS-FIRED BURNER FLOW FIELDS Final Report, 1 Apr. 1988 - 13 Sep. 1990
J. B. Kennedy, J. C. Simonich, and P. L. Lavrich 31 Mar. 1992 127 p
(Contract GRI-5087-234-1492)
(PB92-190370; UTRC/R92-957912-23; GRI-92/0084) Avail: CASI HC A07/MF A02

Investigations were conducted of a mixing concept which, if applied to heat exchangers, appears to offer the promise of significantly enhanced convective heat transfer rates, and if applied to gas-fueled burners, would promote rapid, low-pressure loss mixing of fuel and air, and maintenance of uniform combustion gas temperature profiles. The mixing concept employs a straight-leading-edge, convoluted-trailing-edge surface to generate an array of streamwise vorticities which pass downstream of the surface and promote a large-scale stirring process. The stirring process was observed to be a rapid and efficient (low-pressure-loss) mechanism for mixing and for momentum transfer. The program comprised two principle tasks. The first task involved an investigation of the use of these vortices in heat exchangers to scrub away the insulating thermal boundary layer that impedes the transfer of heat. The second task involved an investigation of the use of these vortices in the burner proper to achieve control of the flame shape and volumetric heat release. Author

N92-32607# California Univ., Berkeley. Dept. of Mechanical Engineering.
SOLID FUEL FLAME SPREAD AND MASS BURNING IN TURBULENT FLOW Ph.D. Thesis
L. Zhou Mar. 1992 233 p
(Grant NANB7D737)
(PB92-181049; NIST/GCR-92/602) Avail: CASI HC A11/MF A03

An experimental study was carried out to investigate the controlling mechanisms of solid fuel flame spread and mass burning in turbulent flows. The effects of flow velocity, turbulence intensity, and buoyancy on concurrent and opposed flame spread rate and surface regression rate were examined in both floor and ceiling configurations. It is found that for opposed flows, the flame spread rate of thermally thick PMMA sheet increases initially with the flow velocity, reaches a peak value and then decreases as the flow velocity increases further. The flow turbulence effect is to increase the flame spread rate initially and then decrease it at higher turbulence intensity. The flame spread rate of thermally thin paper sheet in an opposed flow decreases monotonically with the flow velocity and turbulence intensity. The flow turbulence also has a significant effect on the flame extinction conditions, resulting in a smaller extinction velocity for larger flow turbulence intensity. For concurrent flow flame spread, it is found that the flow turbulence decreases the flame spread rate for both floor and ceiling geometries, mainly as a result of the flame length shortening at high turbulence intensity. It is also found that flow velocity intensifies the spread of the flame. Author

N92-32645# United Technologies Research Center, East Hartford, CT.
CARS DIAGNOSTICS FOR SOLID PROPELLANT COMBUSTION INVESTIGATIONS Final Report, 1 Sep. 1987 - 29 Nov. 1991
J. H. Stufflebeam Jan. 1992 62 p
(Contract DAAL03-87-C-0005)
(AD-A248660; UTRC/R92-957787-F; ARO-24413.6-CH) Avail: CASI HC A04/MF A01

The specific technical achievements of this Army Research Office contract are as follows. Coherent anti-Stokes Raman Spectroscopy (CARS) was first successfully applied to solid propellant combustion at elevated pressure (up to 35 atm) under this project. The high pressure equilibrium chemistry (temperature and multiple species concentration) of nitramine combustion was verified with the CARS measurements. The use of a high pressure, motorized combustion vessel allowed control of the spatial location of the burning propellant surface and data acquisition from the thin (100 micron), near-surface reaction zone. Dual broadband CARS of HCN, H2CO, and CH4 was utilized to observe the competition between two major reaction mechanisms; they determine the speed of the overall reaction. Resolution of the temperature and species profiles in the reaction zone, required for further insight, was provided by a major advance, the implementation of Line CARS (a 1-D imaging geometry), that allows single shot (10 nsec) measurement of the large temperature and concentration gradients near the surface with a spatial resolution of 25 microns. These milestones have expanded the database of propellant combustion knowledge and provided valuable information for future formulations of energetic materials. GRA

N92-32666# California Univ., Berkeley. Lawrence Berkeley Lab.
AC MICROCALORIMETRY OF ADSORBATES ON EVAPORATED METAL FILMS: ORIENTATIONAL ORDERING OF H2 MULTILAYERS Ph.D. Thesis
R. B. Phelps Nov. 1991 110 p
(Contract DE-AC03-76SF-00098)
(DE92-008317; LBL-31576) Avail: CASI HC A06/MF A02

We have improved and extended a novel ac calorimetric technique for measuring the heat capacity of adsorbates on evaporated metal films. Metallic substrates are of particular interest in current studies of the thermodynamics of adsorbed molecules. The method described in the present work is a calorimetric technique which allows measurements of molecules on simple metallic surfaces. Among other improvements, we have achieved significant progress in the preparation and characterization of the evaporated metal film. We have applied this novel technique to a study of hydrogen multilayers on gold and sapphire substrates. We have shown that samples of normal-hydrogen with a nominal coverage, n, of approximately 25 monolayers (ML) undergo a bulk-like orientational ordering transition. The transition is suppressed as the coverage is decreased, and no sign of the transition remains above 1.6 K for n approximately = 1 ML. For n approximately less than 8 ML, the peak in the heat capacity exhibits signs of finite-size effects. At higher coverages, finite-size effects are not observed, and the shape of the peak depends strongly on the substrate. We conclude that the peak is inhomogeneously broadened for n approximately less than 8 ML. This work represents the first measurements of the heat capacity due to orientational ordering in adsorbed hydrogen. The results of an earlier experiment involving vibrational spectroscopy of adsorbed molecules are included in the appendix. In this work, we have used infrared emission spectroscopy to study the spectral region in the vicinity of the C=O stretch vibration of bridge-bonded CO on Pt(111). DOE

N92-32722# Ecole Centrale de Lyon (France). Dept. de Machines Thermiques.
THE POLYCHROMATIC PYROMETER IN DIESEL COMBUSTION Ph.D. Thesis [CONTRIBUTION AU DEVELOPPEMENT DE LA PYROMETRIE POLYCHROMATIQUE EN COMBUSTION DIESEL]
Hedi Mahjoubi 1991 165 p In FRENCH
(ECL-91-42; ETN-92-91957) Avail: CASI HC A08/MF A02

Soot particles and their formation in different types of combustion are treated. Their physical, chemical and optical properties are examined. A guide to the choice of a method to determine the complex refraction index of soot and to characterize its radiative properties is outlined. Thermal radiation of semi-transparent mediums and applications to temperature determination are considered. Theoretical bases of polychromatic pyrometry are presented and applied to a simple configuration - the laminar diffusion flame which enables validation of the measurement technique. This method is transposed to an experimental and then an industrial diesel engine. The influence of several engine operation parameters on temperature, concentration and diameters of soot particles is examined showing the role played by this method in the research of optimal combustion conditions. ESA

N92-32724# Ecole Centrale de Lyon (France). Lab. de Machines Thermiques.
LOCAL AND TEMPORAL STUDY OF THE COMBUSTION AND HEAT TRANSFER IN A DIRECT INJECTION DIESEL ENGINE Ph.D. Thesis [CONTRIBUTION A L'ETUDE LOCALE ET TEMPORELLE DE LA COMBUSTION ET DES TRANSFERIS THERMIQUES DANS UN MOTEUR DIESEL A INJECTION DIRECTE]
Hoan Xuan Quoc 1991 219 p In FRENCH
(ECL-91-43; ETN-92-91958) Avail: CASI HC A10/MF A03

Local and instantaneous combustion of heat transfer in a direct injection industrial diesel engine was studied. Local combustion was calculated by measuring diesel flame monochromatic radiation. A two colored optical method was used to obtain gas temperature and soot particle concentration which in turn were used to calculate local and instantaneous radiation transfer in the combustion chamber. Local and instantaneous heat transfer was evaluated using thermal flux sensors. By combining these results, local and instantaneous heat transfer accross the wall of the combustion chamber was calculated. ESA

N92-32755# Department of the Navy, Washington, DC.
ELECTRIFIED MICROHETEROGENEOUS CATALYSIS Patent Application
Debra Rolison, inventor (to Navy) 21 Jan. 1992 42 p

(AD-D015270; US-Patent-Appl-SN-822812; Navy-Case-73545)
Avail: CASI HC A03/MF A01

In a method for enhancing chemical reactions, a reactant is brought in contact with a stable, non-soluble, porous, electronically non-conductive solid (reaction enhancer) in a fluidic medium to form a reaction mixture of low ionic strength. The formed reaction mixture is then subjected to an electrifying force, thereby enhancing the chemical reaction. Reaction products are then collected. GRA

N92-32826# Purdue Univ., West Lafayette, IN. Dept. of Chemistry.
SOME ELECTRONIC AND DYNAMICAL FACTORS IN ELECTRON-TRANSFER CHEMISTRY: METAL COMPLEXES, CLUSTERS, AND SURFACES
M. J. Weaver May 1992 15 p
(Contract N00014-91-J-1409)
(AD-A251169; TR-128) Avail: CASI HC A03/MF A01

Some selected concepts involving electronic and dynamical factors in the electron-transfer chemistry of inorganic and organometallic systems are outlined and illustrated by recent results primarily from the author's laboratory, with some emphasis placed on the redox properties of electrochemical interfaces in comparison with molecular reagents. Three interrelated topics are considered. The first concerns the control of electron-transfer rates by an interplay between donor-acceptor electronic coupling and nuclear dynamics. The role of the solvating medium in limiting the barrier-crossing frequency (solvent friction effects) is described, and the diagnostic capabilities (and limitations) of this phenomenon for probing the degree of electronic coupling by tuning the reaction dynamics are noted. Secondly, the behavioral differences anticipated between the kinetic properties of molecular redox reagents and electrode surfaces are discussed. A formalism is described for this purpose which intercompares homogeneous-phase and heterogeneous rate data on a unified basis, and is utilized in some illustrative experimental comparisons. Thirdly, the infrared spectroelectrochemical properties of high-nuclearity platinum carbonyl clusters in nonaqueous solvents are outlined in comparison with the potential-dependent properties of monocrystalline platinum electrode analogs. GRA

N92-32925# Westinghouse Savannah River Co., Aiken, SC.
RF-GD/FTMS: AN FTMS SYSTEM WITH A LENSLESS EXTERNAL ION SOURCE FOR HIGH RESOLUTION ELEMENTAL MASS SPECTROMETRY
R. R. Weller, J. M. Pochkowski, D. C. Duckworth, R. K. Marcus, and M. V. Buchanan 1991 24 p Presented at the 40th ASMS Conference on Mass Spectrometry and Allied Topics, Washington, DC, 31 May - 2 Jun. 1992
(Contract DE-AC09-89SR-18035)
(DE92-015343; WSRC-MS-91-521; CONF-9205196-1) Avail: CASI HC A03/MF A01

Two of the major challenges which face the field of elemental mass spectrometry are the development of versatile atomization/ionization sources for direct solids analysis and methods for reducing the impact of isobaric interferences found on commonly employed quadrupole and sector based instruments. The combination of radio frequency glow discharge (RF-GD) sources with Fourier transform ion cyclotron resonance mass spectrometry (FT-ICR or FTMS) is one technique which addresses both problems. A demonstration project was conducted at ORNL where an external RF-GD ion source was coupled to a commercial FTMS instrument. The ion transfer system utilized the lensless method developed by Weller, et al for laser desorbed ions. The RF-GD source was contained in a 2.75 inch CF cross and separated from the main vacuum system by a skimmer cone. An intermediate differential pumping chamber was separated from the FTMS pumping system. The differential pumping chamber attached directly to the 'analyzer' flange. Large ion signals could easily be obtained without complex trapping schemes which produced mass spectra with excellent signal-to-noise ratios and resolving powers. Resolutions were limited by the pressure at the analyzer cell. The NIST 1103 Brass sample shows good ratios for the Cu and Zn components. Expected peaks are observed for the Ar(+) and ArH(+) species. Minor components down to around 1 percent are observable without any ion ejection techniques. The NIST 1263 Steel sample demonstrates the moderate resolution attainable even with the high pressures in the ICR analyzer cell. This document is an extended abstract with viewgraphs. DOE

N92-32929# Lawrence Livermore National Lab., CA.
LIGHT-ION SPECTROSCOPY WITH EXOTIC TARGETS
G. L. Struble and R. G. Lanier 30 Jun. 1992 28 p
(Contract W-7405-eng-48)
(DE92-017258; UCRL-JC-110489) Avail: CASI HC A03/MF A01

Understanding the rich and diverse aspects that underly the physics of nuclear structure requires a variety of experimental techniques. In our laboratory, we have concentrated on experimental techniques that use light-ion probes and isotopes that are technically difficult to fabricate into targets. In particular, our studies of p-, d-, and t-induced nuclear reactions on the radioactive targets of Eu-152,154 and Gd-148 have illuminated some very specific and very interesting features of nuclear structure near the N = 89 shape-transition region. DOE

N92-32931# Argonne National Lab., IL.
CHEMICAL TECHNOLOGY DIVISION Annual technical report, 1991
Mar. 1992 248 p
(Contract W-31-109-eng-38)
(DE92-014059; ANL-92/15) Avail: CASI HC A11/MF A03

Highlights of the Chemical Technology (CMT) Division's activities during 1991 are presented. In this period, CMT conducted research and development in the following areas: (1) electrochemical technology, including advanced batteries and fuel cells; (2) technology for fluidized-bed combustion and coal-fired magnetohydrodynamics; (3) methods for treatment of hazardous and mixed hazardous/radioactive waste; (4) the reaction of nuclear waste glass and spent fuel under conditions expected for an unsaturated repository; (5) processes for separating and recovering transuranic elements from nuclear waste streams; (6) recovery processes for discharged fuel and the uranium blanket in the Integral Fast Reactor (IFR); (7) processes for removal of actinides in spent fuel from commercial water-cooled nuclear reactors and burnup in IFRs; and (8) physical chemistry of selected materials in environments simulating those of fission and fusion energy systems. The Division also conducts basic research in catalytic chemistry associated with molecular energy resources; chemistry of superconducting oxides and other materials of interest with technological application; interfacial processes of importance to corrosion science, catalysis, and high-temperature superconductivity; and the geochemical processes involved in water-rock interactions occurring in active hydrothermal systems. In addition, the Analytical Chemistry Laboratory in CMT provides a broad range of analytical chemistry support services to the technical programs at Argonne National Laboratory (ANL). DOE

N92-32996# California Univ., Berkeley. Lawrence Berkeley Lab.
PREMIXED TURBULENT COMBUSTION TO OPPOSED STREAMS
L. W. Kostiuk and R. K. Cheng Mar. 1992 20 p Presented at the 1992 Spring Meeting of the Western States Section of the Combustion Institute, Corvallis, OR, 23-24 Mar. 1992
(Contract DE-AC03-76SF-00098)
(DE92-016996; LBL-32020; CONF-9203140-2) Avail: CASI HC A03/MF A01

Premixed turbulent combustion in opposed streams has been studied experimentally by the use of two component laser Doppler anemometry. This flow geometry is part of a class of stagnating flows used to study turbulent combustion in recent years. It does not involve any surface near the flames because of the flow symmetry, thus circumventing many of the effects of flame surface interaction. The mean non-reacting flow is found to be self-similar for all the conditions studied in this and the stagnation plate

configuration. A homogeneous region of plane straining is produced in the vicinity of the stagnation and there is a strong interaction between the turbulence in the flow and the mean straining which can increase the rms velocity as the flow stagnates. The reacting flow fields are found to be symmetric about the free stagnation point. The traverses of mean axial velocity in the stagnation streamlines for reaction flows are not dramatically different from the non-reaction flows. These results differ from turbulent combustion experiments where the flow is stagnated by a flat plate. The extinction limits was studied for propane:air mixtures. DOE

N92-33009* National Aeronautics and Space Administration. Lyndon B. Johnson Space Center, Houston, TX.
MICROPOROUS STRUCTURE WITH LAYERED INTERSTITIAL SURFACE TREATMENT, AND METHOD AND APPARATUS FOR PREPARATION THEREOF Patent
Steven L. Koontz, inventor (to NASA) 25 Aug. 1992 11 p Filed 31 Oct. 1989 Supersedes N90-16887 (28 - 9, p 1189)
(NASA-Case-MSC-21487-1; US-Patent-5,141,806; US-Patent-Appl-SN-429739; US-Patent-Class-428-315.5; US-Patent-Class-210-198.2; US-Patent-Class-210-502.1; US-Patent-Class-210-635; US-Patent-Class-428-315.7; US-Patent-Class-428-404; US-Patent-Class-530-413) Avail: US Patent and Trademark Office

A microporous structure with layered interstitial surface treatments, and the method and apparatus for its preparation are disclosed. The structure is prepared by sequentially subjecting a uniformly surface treated structure to atomic oxygen treatment to remove an outer layer of surface treatment to a generally uniform depth, and then surface treating the so exposed layer with another surface treating agent. The atomic oxygen/surface treatment steps may optionally be repeated, each successive time to a lesser depth, to produce a microporous structure having multilayered surface treatments. The apparatus employs at least one side arm from a main oxygen-containing chamber. The side arm has characteristic relaxation times such that a uniform atomic oxygen dose rate is delivered to a specimen positioned transversely in the side arm spaced from the main gas chamber.
Official Gazette of the U.S. Patent and Trademark Office

N92-33029* National Aeronautics and Space Administration. Lyndon B. Johnson Space Center, Houston, TX.
PURIFICATION SYSTEM Patent
David T. Flanagan, inventor (to NASA) and Randall E. Gibbons, inventor (to NASA) 25 Aug. 1992 6 p Filed 8 Jan. 1991 Supersedes N91-24362 (29 - 16, p 2592)
(NASA-Case-MSC-21584-1; US-Patent-5,141,636; US-Patent-Appl-SN-638600; US-Patent-Class-210-209; US-Patent-Class-210-266; US-Patent-Class-210-269; US-Patent-Class-210-287; US-Patent-Class-210-670; US-Patent-Class-210-748; US-Patent-Class-210-758) Avail: US Patent and Trademark Office

A system for prolonging the life of a granulated activated charcoal (GAC) water treatment device is disclosed in which an ultraviolet light transparent material is used to constrain water to flow over carbon surfaces. It is configured to receive maximum flux from a UV radiation source for the purpose of preventing microbial proliferation on the carbon surfaces; oxidizing organic contaminants adsorbed from the water onto the carbon surfaces and from biodegradation of adsorbed microbial forms; disinfecting water; and oxidizing organic contaminants in the water.
Official Gazette of the U.S. Patent and Trademark Office

N92-33121# Yale Univ., New Haven, CT. Dept. of Mechanical Engineering.
COMPUTATIONAL AND EXPERIMENTAL STUDY OF LAMINAR FLAMES
M. Smooke and M. Long 1991 3 p
(Contract DE-FG02-88ER-13966)
(DE92-017978; DOE/ER-13966/3) Avail: CASI HC A01/MF A01

During FY-91, we have made substantial progress in both the computational and experimental portions of our research. In particular, we have continued our study of non-premixed axisymmetric methane-air flames. Computer calculations of multidimensional elliptic flames with two carbon atom chemistry using a shared memory parallel computer are reported for the first time. Also, laser spectroscopy of flames utilizing a neodymium laser are also reported. DOE

N92-33126# Lawrence Livermore National Lab., CA.
A STUDY OF THE DISSOLUTION MECHANISM BY CHEMICAL AND ELECTROCHEMICAL OXIDATION-REDUCTION OF ACTINIDE DIOXIDES (UO2, NpO2, PuO2, AND AmO2) IN AN ACID AQUEOUS MEDIUM Ph.D. Thesis
P. Berger (Paris VI Univ., France) 10 Sep. 1991 237 p Transl. into ENGLISH of a French document (France)
(Contract W-7405-eng-48)
(DE92-014834; UCRL-TT-108428) Avail: CASI HC A11/MF A03

The plan followed to describe our study will have five parts. First, we will review the general properties of MO2 oxides (M = U, Np, Pu, and Am), as well as the dissolution methods known so far. We will emphasize, in particular, the great similarities in their structures, properties, and methods of dissolution, which justifies a parallel study of these oxides using an electrochemical method. The second part will concern the experimental study of the dissolution under electrolysis. We will, first of all, investigate its thermodynamic aspect, with the calculation of the free enthalpies of dissolution; and we will next show the phenomena of oxidizing dissolution and reducing dissolution using carbon paste electrodes. In a third part, we will present the test results on oxidizing dissolution in solutions that are highly enriched with oxygen-18. The isotopic analysis of the oxygen in the actinyl ions formed, deduced from the Raman spectra of the solutions, will make it possible to demonstrate the existence of a first oxidation step involving the participation of the solid. In the fourth part, we will summarize the experimental observations that might contribute to a better understanding of the mechanisms of oxidizing dissolution. A fifth and last part will be devoted to the presentation of a simple model of the dissolution of oxides in a carbon paste electrode under a constant current. DOE

N92-33185# Oak Ridge National Lab., TN.
CONTINUUM CONFIGURATIONAL BIAS MONTE-CARLO STUDIES OF ALKANES AND POLYETHYLENE
J. J. dePablo (Eidgenoessische Technische Hochschule, Zurich, Switzerland), M. Laso (Eidgenoessische Technische Hochschule, Zurich, Switzerland), U. W. Suter (Eidgenoessische Technische Hochschule, Zurich, Switzerland), and H. D. Cochran Jun. 1992 18 p Presented at the 6th International Conference on Fluid Properties and Phase Equilibria for Chemical Process Design, Cortina d'Ampezzo (Italy), 19-24 Jul. 1992
(Contract DE-AC05-84OR-21400)
(DE92-016545; CONF-9207105-1) Avail: CASI HC A03/MF A01

A class of Monte-Carlo-simulation methods has recently been developed for the study of dense polymeric systems. Such methods allow the calculation of chemical potential and solubilities in macromolecular systems. In this work, results are presented for PVT properties of polyethylene, for solubilities of long alkanes in polyethylene, and for dilute solutions of long alkanes in near-critical solvents. DOE

N92-33222# Cornell Univ., Ithaca, NY.
MASS RESOLVED RESONANCE IONIZATION SPECTROSCOPY OF COMBUSTION RADICALS
23 Jun. 1992 24 p
(Contract DE-FG02-86ER-13508)
(DE92-016833; DOE/ER-13508/4) Avail: CASI HC A03/MF A01

This report discusses the following topics: REMPI spectroscopy of HCO and DCO; Rempi spectroscopy of the ethynyl radical; REMPI spectroscopy of new electronic states of C2; and a flame sampling laser ionization mass spectrometer. DOE

N92-33246# Pittsburgh Univ., PA. Dept. of Chemical and Petroleum Engineering.
PROBE MOLECULE STUDIES: ACTIVE SPECIES IN ALCOHOL SYNTHESIS
D. G. Blackmond Apr. 1992 9 p
(Contract DE-FG22-90PC-90305)
(DE92-016682; DOE/PC-90305/T7) Avail: CASI HC A02/MF A01

The goal of this research is to develop a better understanding of the formation mechanisms of alcohols and other oxygenates from syngas over supported catalysts. Probe molecules will be added in situ during the reaction to help delineate reaction pathways and identify reaction intermediate species. The key of our study is to investigate how the species generated by these probe molecules interact with surface species present during oxygenate formation. DOE

N92-32297*# Alabama Univ., Huntsville.
COMBUSTION INSTABILITY ANALYSIS FOR LIQUID PROPELLANT ROCKET ENGINES
Y. M. Kim, C. P. Chen, and J. P. Ziebarth *In* NASA. Goddard Space Flight Center, Tenth Workshop for Computational Fluid Dynamic Applications in Rocket Propulsion, Part 1 Jul. 1992 p 441-465 (For primary document see N92-32278 23-34)
Avail: CASI HC A03/MF A05

N92-32307*# Scientific Research Associates, Inc., Glastonbury, CT.
A TWO-PHASE RESTRICTED EQUILIBRIUM MODEL FOR COMBUSTION OF METALIZED SOLID PROPELLANTS
J. S. Sabnis, F. J. deJong, and H. J. Gibeling *In* NASA. Goddard Space Flight Center, Tenth Workshop for Computational Fluid Dynamic Applications in Rocket Propulsion, Part 1 Jul. 1992 p 713-724 (For primary document see N92-32278 23-34)
(Contract F04611-86-C-0096)
Avail: CASI HC A03/MF A05

26 METALLIC MATERIALS

Includes physical, chemical, and mechanical properties of metals, e.g., corrosion; and metallurgy.

N92-32315# Massachusetts Inst. of Tech., Cambridge.
MECHANISMS OF THE OXIDATION OF METALS AND ALLOYS WITH EMPHASIS ON SUPERCONDUCTORS
1991 5 p
(Contract DE-FG02-85ER-45179)
(DE92-016840; DOE/ER-45179/9) Avail: CASI HC A01/MF A01

Research work performed at MIT under this contract has had two major thrusts. One thrust deals with the oxidation processing of, and phase transformations in, the Yb(n)Ba(2n)Cu(3n+n)O(x) (n = 1, 2, infinity) superconducting oxide system while the second thrust deals with the optimization of the properties of oxidation processed Bi2Sr2Ca2Cu3O(y)/Ag superconducting microcomposites. DOE

N92-32432# Oak Ridge National Lab., TN.
STUDIES OF NEAR-SURFACE PHENOMENA AND EROSION MECHANISMS IN METALLIC ALLOYS USING SINGLE- AND MULTI-PARTICLE IMPACTS
M. Rao and J. R. Keiser Mar. 1992 125 p
(Contract DE-AC05-84OR-21400)
(DE92-014921; ORNL/TM-11946) Avail: CASI HC A06/MF A02

An experimental study of the effects of material properties on erosion mechanisms was conducted by subjecting targets to single as well as multiple impacts of spherical particles at various velocities. A mechanical properties microprobe was used to monitor the hardening due to the impacts. Initial studies on several engineering alloys showed that work hardening was associated with single impacts, and the results suggested that the capacity to distribute the impact energy over large volumes improved a material's erosion resistance. Studies also showed that the alloys work hardened significantly under multiple-particle impacts. Single-particle impact studies were found to correlate well with results from low-velocity, multiple-particle erosion experiments. DOE

N92-32614# Oak Ridge Y-12 Plant, TN.
TRANSMISSION ELECTRON MICROSCOPE CHARACTERIZATION OF DEFORMATION AND RECOVERY IN 304L STAINLESS STEEL PART
J. C. Mabon, M. C. Fleenor, D. A. Carpenter, and W. H. Smith (Allied-Signal Aerospace Co., Kansas City, MO.) Dec. 1991 38 p
(Contract DE-AC05-84OS-21400)
(DE92-013237; Y/DW-1125) Avail: CASI HC A03/MF A01

Type 304L stainless steel sheet formed by a semi-piercing process has regions of localized plastic deformation and material flow estimated to correspond to approximately 40 percent cold work at maximum. The resulting microstructures in the bulk (undeformed) and deformed regions were characterized by transmission electron microscopy prior to and following annealing treatments. The deformed region prior to annealing was observed to have complex microstructure consisting of gamma phase and the strain induced martensitic phases, alpha(prime) bcc and epsilon hcp. Additionally, high densities of dislocations, stacking faults, and deformation twins were observed. Annealing at 450 C for 15 minutes resulted in little observed microstructural change. After 30 minutes at 750 C, considerable recrystallization and recovery was evident with substantial reversion of the martensitic phases. The residual banded microstructural features associated with the deformed structure were identified as twin related gamma fcc. Finally, annealing at 1050 C showed a completely recrystallized microstructure having large equiaxed grains, annealing twins, and a with very low dislocation density. DOE

N92-32626# Air Force Inst. of Tech., Wright-Patterson AFB, OH.
AN IN VITRO CORROSION STUDY OF TWO IMPLANT MATERIALS USING ELECTROCHEMICAL IMPEDANCE SPECTROSCOPY AND POTENTIODYNAMIC POLARIZATION M.S. Thesis
Martin W. Kerber 1992 160 p
(AD-A252575; AFIT/CI/CIA-92-023) Avail: CASI HC A08/MF A01

In vitro corrosion evaluations of commercially pure titanium (CP-Ti) and Ti-6Al-4V samples with different surface treatments were conducted using potentiodynamic polarization and electrochemical impedance spectroscopy (EIS). The different surface treatments tested were as-polished, nitric acid passivated (ASTM F86), and anodized. The test solution consisted of oxygenated 0.9 normal NaCl buffered to a pH of 7.3 at 37 deg C. The corrosion properties were shown to be similar for the two metals in the polished and passivated condition. The CP-Ti was found to be more corrosion resistant than the Ti-6Al-4V in the anodized condition. For both metals, the anodized condition was much more corrosion resistant than the passivated condition which was more corrosion resistant than the as-polished condition. The oxide layer on both metals in the as-polished and passivated conditions as well as on the CP-Ti in the anodized condition was composed of non-porous TiO2. The protection provided by this layer was found to be related to its thickness. The oxide on the anodized Ti-6Al-4V was composed of a porous layer of hydrated TiO3 on top of a nonporous layer of TiO2. Although this layer was thicker than that on the anodized CP-Ti, it did not provide as much protection against corrosion. GRA

N92-32646# Lawrence Livermore National Lab., CA.
MOLECULAR DYNAMICS MODELING OF THE MECHANICAL PROPERTIES OF METAL SURFACES AT THE NANOMETER SCALE
J. Belak and I. F. Stowers Mar. 1992 42 p Presented at the International Conference on Metallurgical Coatings and Thin Films,

San Diego, CA, 6-10 Apr. 1992
(Contract W-7405-eng-48)
(DE92-010705; UCRL-JC-109024; CONF-920439-5) Avail: CASI HC A03/MF A01

We present an overview of the molecular dynamics computer simulation method as employed in the study of the mechanical properties of surfaces at the nanometer scale. The embedded atom method is used to model a clean metal surface and the computer experiment consists of the indentation and scraping of a hard diamond-like tool into and across the surface. The metal surface consists of 36 layers of atoms initially arranged on an fcc lattice with a rigid lower boundary condition. Results are presented for the (111) surface of copper and silver. We explicitly demonstrate in our point indentation simulations that nanoscale plasticity takes place by nondislocation mechanisms: a result suggested by recent nano-indentation experiments. We also observe the surface to accommodate nearly the entire volume of the tip and the annealing out of plastic work as the tip is removed. In our orthogonal cutting simulation, we observe an interesting phenomenon: the system dynamically reorients the grain in front of the tool tip to minimize the work performed on the shear plane (i.e., the shear plane becomes an easy slip plane). DOE

N92-32699# Carnegie-Mellon Univ., Pittsburgh, PA. Dept. of Materials Science and Engineering.
GENERIC CONSEQUENCES OF FUNDAMENTAL STUDIES OF BETA PHASE DECOMPOSITION MODES IN TITANIUM AND RELATED ALLOY SYSTEMS Final Report, 30 Sep. 1989 - 31 Mar. 1992
H. I. Aaronson, Y. Mou, and M. G. Hall 31 Mar. 1992 50 p
(Grant AF-AFOSR-0550-89)
(AD-A250789; AFOSR-92-0386TR) Avail: CASI HC A03/MF A01

Throughout this final grant from AFOSR, the P.I. spent much of his time in the preparation of generic overviews of numerous major topics in diffusional phase transformations. These overviews dealt with homogeneous nucleation, interphase boundary structures in Ti-base alloys, effects of interphase boundary structure upon growth kinetics, shear vs. diffusional transformation mechanism (with emphasis upon linking macroscopic observations with processes proceeding at the atomic level), the mechanism (and definitions) of the bainite reaction and the influence of alloying elements upon the growth kinetics of grain boundary allotriomorphs of proeutectoid ferrite. A major overview of the ledge mechanism in vapor-crystal, liquid-crystal and crystal-crystal diffusional phase transformations, and a still broader overview of atomic mechanisms of diffusional nucleation and growth are nearing completion. Collaborative research with Dr. M. G. Hall of the University of Birmingham, U.K., on topics concerned with distinction between diffusional and shear mechanisms of transformation from the standpoints of crystallography and surface relief effects, has also made progress. GRA

N92-32721# Mound Lab., Miamisburg, OH.
DENSITY VARIATIONS AND ANOMALIES IN PALLADIUM COMPACTS
D. Back, T. Jones, M. Ransick, T. Walburg, and D. Werkmeister 14 May 1992 47 p
(Contract DE-AC04-88DP-43495)
(DE92-014382; MLM-3746) Avail: CASI HC A03/MF A01

Low-density compacts of palladium powder have relative densities of about 30 plus or minus 10 percent TD. The variations in density are of concern for operations such as chemical/hydrogen pump systems because heat, mass, and momentum transport properties can be affected. Variations in density result from the inherent nature and interacting forces of UASA compaction of powder in cylinders. In addition to these expected variations, discontinuous density anomalies, such as cracks or high density ridges, are also found. An anomaly of particular concern was found to resemble a 'steer's head'. It is a symmetrical region of low density located at or near the center of a compact. Typically, this region is surrounded by a band of high density, compacted palladium that sometimes exceeds the density of the surrounding compact matrix by a factor of three. This report examines these density variations and anomalies both theoretically and empirically. DOE

N92-32779 ESDU International Ltd., London (England).
GUIDE TO THE EFFECT OF SHOT PEENING ON FATIGUE STRENGTH
May 1992 41 p
(ESDU-92015; ISBN-0-85679-823-1) Avail: ESDU

ESDU 92015 introduces the process, indicating the parameters involved (shot material, size and velocity, and exposure time and component hardness) that affect the plastic deformation and residual comprehensive stresses. The use of the Almen strip to assess intensity is explained. The effects on surface condition are considered and the need to anticipate at the design stage the use of shot peening is explained. Data extracted from the literature are presented graphically. For aluminum alloys the majority are stress-endurance curves for constant amplitude loading showing the endurance of a test specimen (including welded joints) with and without shot peening. Also shown are the effects of various pre- and post- treatments such as polishing, heat treatment and stretching. Some data include the effects of fretting and salt water, and one graph plots endurance of 7075 alloy against Almen intensity. For steels all data are stress-endurance plots for test specimens or welded joints with and without peening and including the effect of post-stretching in one case. Data for Ti-6Al-4V include the effect of fretting and elevated temperature on endurance with and without shot peening. For each set of data details are given of material specification, specimen geometry and test conditions. ESDU

N92-32794# Toronto Univ. (Ontario). Inst. for Aerospace Studies.
HYDROGEN PERMEATION THROUGH BILAYER METALLIC MEMBRRANES Thesis
Philip L. Andrew Apr. 1991 164 p Sponsored by Natural Sciences and Engineering Research Council and Canadian Fusion Fuels and Technology Project
(UTIAS-TN-342; CTN-92-60376) Copyright Avail: CASI HC A08/MF A02

The rates of hydrogen atoms permeating through metal bulk were obtained by measuring the steady state permeation rate through polycrystalline metal membranes. The experimental investigation focussed on composite membranes made up of iron, palladium and copper layers. The measurements were made under ultrahigh vacuum conditions using either hydrogen molecules or neutral atoms as the incident species. The mathematical dependence of the steady state permeating flux on the incident flux was used to determine whether hydrogen transport at the vacuum/metal interfaces or within the metal bulk (diffusion) is rate-limiting. The chemical composition of the membrane surfaces, measured by Auger Electron Spectroscopy, was found to have a profound effect on surface-limited permeation. The removal of impurities on an iron surface by Ar ion sputtering was found to increase the magnitude and decrease the temperature dependence of the surface-limited permeation rate constant. Deposition of palladium or iron on sputter-cleaned iron surfaces resulted in a reduction of non-metal surface impurities and a further increase in the rate of surface processes. Application of copper on iron, however, had the opposite effect. This is thought to be due to the slow hydrogen adsorption rates peculiar to group IB metals. A thin copper layer on a palladium membrane had a similar effect: hydrogen transport across that surface was impeded. The results are discussed in terms of practical applications of membranes for pumping or detecting hydrogen. In these schemes it is desired that hydrogen, once dissolved in the metal, preferentially exits on the downstream surface. Author (CISTI)

N92-32819# Messerschmitt-Boelkow-Blohm G.m.b.H., Munich (Germany, F.R.).
ALUMINUM BASED PARTICULATE COMPOSITES FOR AEROSPACE APPLICATIONS PRODUCED BY DIFFERENT PROCESSES

Peter-Juergen Winkler, Rainer Rauh, and P. R. Sahm (Technische Hochschule, Aachen, Germany, F.R.) 1991 7 p Presented at the 12th International Symposium on Metallurgy and Materials Science Metal Matrix Processing, Microstructure and Properties, Roskilde, Denmark, 2-6 Sep. 1991 Submitted for publication
(MBB-Z-0408-91-PUB; ETN-92-92125) Avail: CASI HC A02/MF A01

Al-Cu-Mg-type alloys reinforced with SiC particulates, produced by casting, rheocasting, spray deposition, and powder metallurgy, were evaluated and compared. The microstructure and properties are markedly influenced by the process used, mainly due to the differences in precipitation behavior. For all production routes, the greatest improvement was in the Young's modulus, with an increase of about 50 percent. A typical application for the aerospoace industry is presented. ESA

N92-32855 Martin Marietta Energy Systems, Inc., Livermore, CA.
HIGH TEMPERATURE FABRICABLE NICKEL-IRON ALUMINIDES Patent
C. T. Liu, inventor 27 Nov. 1990 15 p
(CA-Patent-1-276-814; Int-Patent-Class-C22C-19/00; Int-Patent-Class-C22C-19/03; CTN-92-60389) Avail: Micromedia Ltd., Technical Information Centre, 165 Hotel de Ville, Place du Portage, Phase 2, Hull, Quebec J8X 3X2, Canada HC/MF

A high strength nickel-iron aluminide superalloy that exhibits desirable hot ductility and fabricability is discussed. This alloy is comprised of a Ni3Al base, a sufficient concentration of a group IVb elements (particularly hafnium, zirconium, and mixtures thereof) to increase high temperature strength, a sufficient concentration of iron and a rare earth element to increase hot fabricability, and a sufficient concentration of boron to increase ductility. Molybdenum in the amount of 0.0 to 0.4 weight percent has the effect of reducing oxidation. Carbon in the amount of 0.0 to 0.06 weight percent reduces cracking. Iron is present in a range of 14.5 to 17.5 weight percent; group IVb elements are present in an amount less than one percent. CISTI

N92-32894# Messerschmitt-Boelkow-Blohm G.m.b.H., Munich (Germany, F.R.). Central Labs.
ACCOMMODATION MECHANISMS AND DISPERSOID-FREE ZONE S IN Al 7475 AFTER SUPERPLASTIC FORMING
Ursula Koch, Wolfgang Bunk (Deutsche Forschungs- und Versuchsanstalt fuer Luft- und Raumfahrt, Bonn, Germany, F.R.), and Peter-Juergen Winkler 1991 7 p Presented at the International Conference on Superplasticity in Advanced Materials, Osaka, Japan, 3-6 Jun. 1991 Submitted for publication
(MBB-Z-0404-91-PUB; ETN-92-92121) Avail: CASI HC A02/MF A01

Investigations which supplement accommodation models additional to grain boundary sliding for the alloy Al 7475, which are necessary to maintain material compatibility, are described. The experiments carried out under superplastic deformation conditions were performed on uniaxial tensile specimens as well as on experimental parts with a biaxial stress mode. The microstructure, the cavitation behavior, the strain, and the strain rate conditions were investigated on these specimens. During the superplastic forming process on Al 7475, large dispersoid free zones are generated. The interdependence between dispersoid free zone, accommodation process, cavitation behavior, strain, and strain rate are discussed. If these zones are regarded as markers for accommodation processes, grain boundary migration is the main accommodation mechanism of this alloy. ESA

N92-32895# Messerschmitt-Boelkow-Blohm G.m.b.H., Munich (Germany, F.R.). Metals Lab.
NEW ACCELERATED CORROSION TEST METHODS
Ursula Koch and Theodor Hack 1991 5 p Presented at BRITE-EURAM Aeronautics Days, Brussels, Belgium, 16-17 Apr. 1991 Submitted for publication
(MBB-Z-0406-91-PUB; ETN-92-92123) Avail: CASI HC A01/MF A01

A project which established accelerated corrosion test methods for conventional Al and new AlLi alloys and surface protection schemes is described. New accelerated testing methods will allow the selection of material and protection schemes with increased resistance to corrosion. The aim is to improve the corrosion performance of modern European aircraft. The objectives are the following: detection of general corrosion and stress corrosion cracking at a very early stage by means of electrochemical monitoring; development of accelerated corrosion tests which can reliably simulate service conditions; assessment of the corrosive environment in an aircraft by installation of sensors and in situ corrosion monitoring; clarification of the role of hydrogen on stress corrosion mechanism of Al alloys; determination of the influence of microorganisms on corrosion failure; and simulation of microbiological induced corrosion for material qualification purposes. Achievements to date and potential applications of the results are discussed. ESA

N92-32896# Mound Lab., Miamisburg, OH.
RADIOGRAPHY TO MEASURE THE LONGITUDINAL DENSITY GRADIENTS OF Pd COMPACTS
D. D. Back 14 May 1992 20 p
(Contract DE-AC04-88DP-43495)
(DE92-014383; MLM-3747) Avail: CASI HC A03/MF A01

This study used radiography to detect and quantify density gradients in green compacts of Palladium powder. Ultrasonic velocity measurements had been tried previously, but they were affected by material properties, in addition to the density, so that an alternative was sought. The alternative technique used radiographic exposures of a series of standard compacts whose density is known and correlated with the radiographic film density. These correlations are used to predict the density in subsequent compacts. DOE

N92-32897# Messerschmitt-Boelkow-Blohm G.m.b.H., Munich (Germany, F.R.). Central Labs.
LOW COST MMC MADE BY SPRAY DEPOSITION
Peter-Juergen Winkler and Rainer Rauh 1991 5 p Presented at BRITE-EURAM Aeronautics Days, Brussels, Belgium, 16-17 Apr. 1991 Submitted for publication
(MBB-Z-0407-91-PUB; ETN-92-92124) Avail: CASI HC A01/MF A01

Research into and development of an MMC (Metal Matrix Composites) production route by spray deposition with relatively low price, distinct improvements of mechanical properties, and priorities of increased elastic modulus and high strength at RT up to elevated temperatures is described. Achievements to date and potential applications of the results are outlined. ESA

N92-32991# Oak Ridge National Lab., TN.
THE OXIDATION OF TYPE 310S STAINLESS STEEL IN MIXED GASES AT ELEVATED TEMPERATURES
J. S. Wolf (Clemson Univ., SC.), O. B. Cavin, and J. H. DeVan Apr. 1992 92 p
(Contract DE-AC05-84OR-21400)
(DE92-014941; ORNL/TM-11887) Avail: CASI HC A05/MF A01

Sheet specimens of Type 310S stainless steel were exposed to air as well as to 'lean' and 'rich' sulfidizing atmospheres at temperatures near 900 C to determine the relationships that exist between the scale structure, the rate of reaction, and the stresses generated during exposure. One goal of this experimental research program was to examine how these factors might be related to the breakdown of protective scales in sulfidizing atmospheres. It was found that the scales formed in air and the 'lean' atmosphere are protective and non-spalling, while those formed in the 'rich' atmosphere spall, initially react at rates 1000 times greater than counterparts in less aggressive atmospheres, and later exhibit a 'breakaway' type rapid reaction. Only those scales formed in air provide the cooperative, tractive interfacial forces required to produce uniform dilatation and deformation of the substrate. However, evidence exists for at least localized stresses in all of the scales examined. DOE

N92-33081*# Nichols Research Corp., Huntsville, AL.
A PROTOTYPE BACKSIDE PURGE CONTROL SYSTEM Final Report, 27 Nov. 1991 - 27 Sep. 1992
Timothy B. Morris 24 Sep. 1992 25 p
(Contract NAS8-39203)
(NASA-CR-190816; NAS 1.26:190816) Avail: CASI HC A03/MF A01

New light-weight aluminum-lithium alloys are considered for propellant tank and aerospace structural applications. These alloys require more precise control of the welding atmosphere. Atmospheric oxygen contamination must be eliminated by flooding both the front and back sides of the weldment with an inert gas. This gas must be maintained at a desired pressure and flow rate that does not effect the stability of the weld process. The objective of the prototype backside purge control system being developed by Nichols Research Corporation (NRC) is to monitor and regulate the backside purge process and to develop a purge chamber design that enhances process controllability. This project will be conducted in two phases. The objective of Phase 1 is to develop a purge technique concept based on an investigation into the backside purge process. Phase 2 is to evaluate the backside purge concept developed in Phase 1. Author

N92-33115# Oak Ridge National Lab., TN.
MODELING THE INFLUENCE OF IRRADIATION TEMPERATURE AND DISPLACEMENT RATE ON HARDENING DUE TO POINT DEFECT CLUSTERS IN FERRITIC STEELS
R. E. Stoller 1992 34 p Presented at the 16th Annual Symposium of American Society of Testing and Materials (ASTM), Denver, CO, 21-22 Jun. 1992
(Contract DE-AC05-84OR-21400)
(DE92-016897; CONF-920673-6) Avail: CASI HC A03/MF A01

The influence of irradiation temperature and displacement rate have been investigated using a detailed kinetic model that incorporates an explicit description of point defect clustering. These clusters are potentially responsible for the fraction of the radiation-induced hardening that is attributed to the so-called 'matrix defect.' The model considers both interstitial and vacancy clustering, with the former treated as Frank loops and the later treated as microvoids. The point defect clusters can be formed either directly in the displacement cascade or by diffusive encounters between free point defects. The results indicate that the assumption of steady state point defect concentrations is not valid for temperatures much below the light water reactor pressure vessel operating temperature of about 288 C. At lower temperatures, the time required for the point defect concentrations to reach steady state can exceed an operating reactor's lifetime. Even at 288 C, the length of the point defect transient could influence the interpretation of irradiation experiments conducted at accelerated damage rates. The hardening due to point defect clusters was calculated using a simple dislocation barrier model. The model predicts that both cluster types can give rise to significant hardening. The relative importance of each type is shown to be a function of irradiation temperature and displacement rate. DOE

N92-33116# Lawrence Livermore National Lab., CA.
COLLECTIVE RESONANCES OF VALENCE ELECTRONS IN FREE METAL CLUSTERS
V. V. Kresin and W. D. Knight (California Univ., Berkeley.) 24 Mar. 1992 5 p Presented at the 14th International Symposium on Molecular Beams, Pacific Grove, CA, 7-12 Jun. 1992
(Contract W-7405-eng-48)
(DE92-014783; UCRL-JC-110177; CONF-9206174-1) Avail: CASI HC A01/MF A01

Photodissociation experiments on simple metal clusters in molecular beams have established that they exhibit strong dipole resonances. These giant resonances are due to collective oscillations of the delocalized valence electron cloud. With modern cluster-beam and spectroscopic techniques, the evolution of the resonance spectra can be studied as a function of cluster size, ionization state, composition, etc. In the course of these studies, interesting regularities emerge, and deviations from behavior expected for classical metallic particles are observed. We will review the experimental picture of collective-resonance spectroscopy and describe some aspects of the theoretical understanding of the data. DOE

N92-33120# Los Alamos National Lab., NM.
SYNTHESIS OF MoSi2-BASED ALLOYS BY MECHANICAL ALLOYING
S. R. Srinivasan and R. B. Schwarz 1992 15 p Presented at the 1992 Powder Metallurgy World Congress, San Francisco, CA, 21-26 Jun. 1992
(Contract W-7405-eng-36)
(DE92-017528; LA-UR-92-1870; CONF-9206195-3) Avail: CASI HC A03/MF A01

We prepared single-phase MoSi2 powders by mechanical alloying starting from elemental powders. We used high-energy ball-milling to prepare two-phase MoSi2-yttria-partially stabilized zirconia and MoSi2-SiC alloy powder mixtures. We consolidated these powders by hot-pressing. We present here the characterization of these alloys by optical and electron microscopy. Further, we have measured the room-temperature and high-temperature mechanical properties of these alloys and compare the properties of single-phase MoSi2 to the two-phase alloys. DOE

N92-33129# Joint Publications Research Service, Arlington, VA.
JPRS REPORT: SCIENCE AND TECHNOLOGY. CENTRAL EURASIA: MATERIALS SCIENCE
28 Jul. 1992 64 p Transl. into ENGLISH from various Russian articles
(JPRS-UMS-92-011) Avail: CASI HC A04/MF A01

Given here is a bibliography of Central Eurasian research in materials science. Topics covered include analysis and testing, coatings, corrosion, ferrous and nonferrous metals, nonmetallic materials, metal working, welding, metallurgy, and mining. Author

N92-33132# Lawrence Livermore National Lab., CA.
ELECTROCHEMICAL POLARIZATION MEASUREMENTS ON PITTING CORROSION SUSCEPTIBILITY OF NICKEL-RICH ALLOY 825
R. D. McCright and D. L. Fleming Oct. 1991 15 p Presented at the Focus 1991: Nuclear Waste Packaging, Las Vegas, NV, 29 Sep. - 4 Oct. 1991
(Contract W-7405-eng-48)
(DE92-014885; UCRL-JC-107065; CONF-910945-12) Avail: CASI HC A03/MF A01

Alloy 825 contains approximately 40 percent Ni, 30 percent Fe, 20 percent Cr, 3.5 percent Mo, 2 percent Cu, and 1 percent Ti. Alloy 825 has a number of performance features that make it attractive as a candidate material for nuclear waste containers. However, under certain environmental conditions Alloy 825 is susceptible to localized forms of corrosion, and the focus of this paper is determination of those conditions. Electrochemical polarization was used to determine the critical potential for passive film breakdown, a process which leads to localized corrosion attack. Results indicated that quite high levels of chloride ion concentrations coupled with low pH are required to lower the critical potential to approach the corrosion potential. DOE

N92-33158# Oak Ridge National Lab., TN.
A COMBINED AEM/APFIM CHARACTERIZATION OF ALLOY X-750
M. G. Burke (Westinghouse Electric Corp., Pittsburgh, PA.) and M. K. Miller 1992 3 p Presented at the Annual Meeting of the Electron Microscopy Society (EMS) of America, Boston, MA, 16-21 Aug. 1992
(Contract DE-AC05-84OR-21400)
(DE92-011049; CONF-920819-7) Avail: CASI HC A01/MF A01

In the development of advanced alloys for power system applications, the primary emphasis is placed on attaining specific mechanical properties with resistance to environmental attack. An important part of alloy development is the detailed characterization of the microstructure, because it is the composition, size and

morphology of the microstructural features that define the mechanical properties of the material. The good mechanical properties of Ni-base superalloys are a result of the formation of fine coherent precipitates. Analytical electron microscopy (AEM) provides important information concerning the type and distribution of the phases in the alloys, but quantitative microchemical analysis for the ultra-fine precipitates is not readily obtainable with conventional AEM techniques. The high optical resolution of the atom probe field-ion microscope (APFIM) make this technique ideally suited to the analysis of the ultra-fine precipitates and surrounding matrix. In this paper, a combined AEM/APFIM study of precipitation in Alloy X-750 is presented. DOE

27 NONMETALLIC MATERIALS

Includes physical, chemical, and mechanical properties of plastics, elastomers, lubricants, polymers, textiles, adhesives, and ceramic materials.

For composite materials see *24 Composite Materials*.

N92-32317# Southern California Association of Governments, Los Angeles
MICROWAVE ABSORPTION BY LOSSY CERAMIC MATERIALS
I. E. Campisi, L. K. Summers, K. E. Finger, and A. M. Johnson Apr. 1992 8 p
(Contract DE-AC05-84ER-40150)
(DE92-016963; DOE/ER-40150/190; CEBAF-PR-92-015) Avail: CASI HC A02/MF A01

Microwave energy generated by the electron beam in the superconducting cavities of the Continuous Electron Beam Accelerator Facility (CEBAF) is absorbed by special loads fabricated with a novel lossy ceramic material (AlN-glassy carbon) developed especially for this application. Strict environmental constraints (ultra-high vacuum compatibility, operation at 2 K, brazeability, etc.) are imposed on the materials which can be used. Several other ceramics were sintered with AlN and various minority conductive powders to obtain the desired electrical properties according to the 'artificial dielectric' model. Dielectric permittivity data and results of low temperature measurements are reported. DOE

N92-32341# Lawrence Livermore National Lab., CA. Chemistry and Materials Science Dept.
PHYSICAL BASIS FOR A PRESSURE-DEPENDENT YIELD CRITERION FOR POLYMERS Final Report, Sep. 1987 - Jan. 1989
Richard E. Lyon May 1992 20 p
(Contract W-7405-eng-48)
(AD-A250763; BRL-CR-689) Avail: CASI HC A03/MF A01

A previously empirical pressure-dependent yield criterion for polymeric solids is derived from linear thermoelasticity and equilibrium thermodynamics. The assumption of a critical value of the mechanical component of the internal energy density at the onset of plastic deformation leads to an explicit expression for the yield condition in terms of the stress invariants and thermomechanical properties of the material. Order of magnitude agreement between the linear theory and published experimental data is obtained for a variety of polymers, suggesting a possible physical basis for pressure-dependent yielding. GRA

N92-32429# Pennsylvania Univ., Philadelphia. Dept. of Materials Science and Engineering.
STRUCTURE AND DYNAMICS IN LOW-DIMENSIONAL GUEST-HOST SYSTEMS
J. E. Fischer Apr. 1992 8 p
(Contract DE-FG02-86ER-45254)
(DE92-014841; DOE/ER-45254/7) Avail: CASI HC A02/MF A01

New synthetic materials continue to be discovered at a rapid rate. Many of these can be broadly described as guest-host systems, in the sense that a range of compositions is accessible by selectively inserting heteroatoms or molecules into the interstitial sites in an otherwise pure starting material. The premier examples are layer intercalates (graphite, transition metal di- and trichalocogenides, and silicate clays) and doped polymers (notably polyacetylene). With a somewhat broader definition of intercalation, one might include the high-(Tc) cuprate superconductors (variable oxygen and alkaline earth concentrations), ion-exchanged beta-alumina and related defect oxides, and alkali metal-doped buckminsterfullerene (C60). The interest in these material families for energy applications is directly attributable to the guest-in-a-host feature, either by exploiting guest ion mobility in electrochemical devices or by tuning/optimizing properties via control of guest concentration and sublattice structure. DOE

N92-32471# Oregon Univ., Eugene. Dept. of Physics.
PAC SPECTROSCOPY OF ELECTRONIC CERAMICS
J. A. Gardner, Ruiping Wang, R. Schwenker, W. E. Evenson (Brigham Young Univ., Provo, UT.), and R. L. Rasera (Maryland Univ. Baltimore County, Catonsville.) 1991 16 p
(Contract DE-FG06-85ER-45191)
(DE92-014328; DOE/ER-45191/19) Avail: CASI HC A03/MF A01

Dilute indium dopants in cerium oxides and YBa2 Cu3O(x) were studied by In/Cd (111) Perturbed Angular Correlation (PAC) spectroscopy. By controlling oxygen vacancy concentration in the cerium oxides through doping or high-temperature vacuum annealing, we have found that indium always forms a defect complex unless the sample is doped to reduce greatly the oxygen vacancy concentration. Three different vacancy-associated complexes are found with concentrations that depend on doping and oxygen stoichiometry. Another defect complex occurs in samples having negligible vacancy concentration. At low temperatures, evidence is found of interaction with an electronic hole trapped by Cd (111) after the radioactive decay of the In (111) parent. In YBa2Cu3O(x) the indium substitutes preferentially at the Y site but has measurable probability of substitution in at least one of the two copper sites. A symmetry change near 650 C is consistent with the well-documented orthorhombic/tetragonal transition for samples in air or oxygen. DOE

N92-32476*# National Aeronautics and Space Administration. Ames Research Center, Moffett Field, CA.
THERMAL DEGRADATION STUDY OF SILICON CARBIDE THREADS DEVELOPED FOR ADVANCED FLEXIBLE THERMAL PROTECTION SYSTEMS
Huy Kim Tran and Paul M. Sawko Aug. 1992 14 p
(RTOP 506-43-31)
(NASA-TM-103952; A-92146; NAS 1.15:103952) Avail: CASI HC A03/MF A01

Silicon carbide (SiC) fiber is a material that may be used in advanced thermal protection systems (TPS) for future aerospace vehicles. SiC fiber's mechanical properties depend greatly on the presence or absence of sizing and its microstructure. In this research, silicon dioxide is found to be present on the surface of the fiber. Electron Spectroscopy for Chemical Analysis (ESCA) and Scanning Electron Microscopy (SEM) show that a thin oxide layer (SiO2) exists on the as-received fibers, and the oxide thickness increases when the fibers are exposed to high temperature. ESCA also reveals no evidence of Si-C bonding on the fiber surface on both as-received and heat treated fibers. The silicon oxide layer is thought to signal the decomposition of SiC bonds and may be partially responsible for the degradation in the breaking strength observed at temperatures above 400 C. The variation in electrical resistivity of the fibers with increasing temperature indicates a transition to a higher band gap material at 350 to 600 C. This is consistent with a decomposition of SiC involving silicon oxide formation. Author

N92-32489# Materials Research Labs., Ascot Vale (Australia).
CALCULATION OF THE ENERGY OF ELASTIC DEFORMATION OF KEVLAR BACKING PLATES FOR CERAMIC ARMOURS
R. G. ODonnell Jan. 1992 17 p
(AD-A250129; MRL-TN-596; DODA-AR-006-839) Avail: CASI HC A03/MF A01

An equation is developed which enables the calculation of the

elastic deformation energy of a Kevlar plate, which is used as a backing for ceramic armor, following projectile impact. Knowledge of the plate profile at maximum deflection is required. Plate profiles were obtained by photographically recording ballistic impacts. The energy of deformation of the composite backing represents 30 to 60 percent of the projectile's initial kinetic energy as calculated for two light weight ceramic armors. GRA

N92-32490# Pennsylvania State Univ., University Park. Materials Research Lab.
THERMOCHEMICAL AND KINETIC CONSIDERATIONS IN DIAMOND GROWTH Interim Report
W. A. Yarbrough 21 Feb. 1992 27 p
(Contract N00014-92-J-1125)
(AD-A247866; TR-1) Avail: CASI HC A03/MF A01

Considerations important to the modeling of the diamond growth process include the question of what surface structures may exist during the growth process and how these structures may be determined by the composition of the gas phase adjacent to the surface. The simple truncated lattice structures of the three low index surfaces are reviewed and the steric problem inherent to the hydrogenated unreconstructed (100) surface is illustrated. It is proposed that the group of zone axis (100) is the highest growth rate direction as this is the dominant texture seen in many experiments and that a model for diamond growth along this axis should, therefore, be of great interest. The assumptions inherent in much modeling are illustrated through the calculation of the mole fraction product of surface reactive sites and the methyl radical. If a methyl radical mole fraction of 10 exp -3 to 10 exp -4 is assumed then the mole fraction of reactive sites at the diamond surface would have to be approximately 10 exp -4 to 10 exp -3. Included in these assumptions are that the rate limiting process is the addition of carbon at the growth surface, that the diamond surface can be treated in effect as a large hydrocarbon, and that the only reactions of importance are those that would also be observed for simple hydrocarbon species in the gas phase. GRA

N92-32547# Carnegie-Mellon Univ., Pittsburgh, PA. Dept. of Chemistry.
TOWARDS WELL-DEFINED POLYSILANES AND POLYPHOSPHAZENES
Krzysztof Matyjaszewski 25 May 1992 4 p
(Contract N00014-90-J-1186)
(AD-A251098; TR-29) Avail: CASI HC A01/MF A01

Polysilanes belong to a new class of polymers with strong electron delocalization in the main chain. Electronic properties are strongly related to conformation and regularity of the macromolecular structure. Some new synthetic methods which increase structural control in polysilanes will be presented: ring-opening polymerization, and polymer modications. Block and graft copolymers based on polysilanes will be discussed. Polyphosphazenes with narrow molecular weight distribution and with functional groups are prepared by the catalyzed polymerization of phosphoranimines. Mechanistic aspects of this reaction will be covered. GRA

N92-32550# Florida Univ., Gainesville. Dept. of Chemistry.
THE EFFECT OF SURFACE PRESSURE ON THE LANGMUIR-BLODGETT POLYMERIZATION OF 2-PENTADECYL ANILINE
H.-C. Zhou and R. S. Duran 19 May 1992 29 p
(Contract N00014-91-J-1655)
(AD-A251141; TR-4) Avail: CASI HC A03/MF A01

The application of the Langmuir-Blodgett (LB) technique to the polymerization of 2-pentadecyl aniline on the LB trough is discussed in this paper. The changes in the mean molecular area (MMA) during the polymerization is mainly due to the change of the alkyl sidechain conformation. The polymerization rate (PR) is deduced from the change of the Mma. The effect of the surface pressure on the polymerization is investigated. It is found that the effect of the surface pressure is mainly on the reaction rate constant, not on the surface concentration. GRA

N92-32631# North Carolina Univ., Chapel Hill.
EXCITED STATE PROCESSES IN TRANSITION METAL COMPLEXES: REDOX SPLITTING IN SOLUBLE POLYMERS
T. J. Meyer Mar. 1992 9 p
(Contract DE-FG05-86ER-13633)
(DE92-011808; DOE/ER-13633/11) Avail: CASI HC A02/MF A01

In our research there were two major themes. The first was the continued development of excited states as sensitizers. In one sequence of experiments, the synthetic aspects of this area were developed in further detail both by extending the chemistry of the polypyridyl-accepting ligands associated with the excited state and by developing a new procedure for the preparation of unsymmetrical tris-chelate complexes. The second important aspect of this work was the continued investigation of the molecular and electronic structure characteristics of this class of excited states and how those factors determine such properties as photostability and excited state decay. This effort was extended to complexes of Re(I) and an examination of their excited state characteristics, the role of hydride ligand in determining the properties of excited states, the calculation of relative nonradiative decay rate constants for a series of complexes of Ru(II), the participation of higher lying excited states in decay in complexes of Ru(II) and Os(II), and the application of the transient infrared technique to the elucidation of a photochemical intermediate following laser flash excitation. The second area of study involved excited states in soluble polymers to investigate photoinduced electron and energy transfer in multi-component assemblies. This work was based on chemically derivatized polystyrene polymers which contain combinations of chromophores and electron or energy transfer quenchers. DOE

N92-32640# Argonne National Lab., IL.
NONDESTRUCTIVE EVALUATION DEVELOPMENT FOR PROCESS CONTROL
W. A. Ellingson, D. L. Holloway, E. A. Sivers, J. Ling (Academia Sinica, Shanghai, China), J. P. Pollinger (Allied-Signal Aerospace Co., Torrance, CA.), and H. C. Yeh (Allied-Signal Aerospace Co., Torrance, CA.) 1991 12 p Presented at the Automotive Technology Development Contractors' Coordination Meeting, Dearborn, MI, 22-25 Oct. 1991
(Contract W-31-109-eng-38)
(DE92-015272; ANL/CP-76077; CONF-911050-11) Avail: CASI HC A03/MF A01

A joint project between Garrett Ceramic Components (GCC) of Allied Signal Aerospace Corporation and Argonne National Laboratory (ANL) is ongoing to evaluate nondestructive characterization (NDC) methods to detect and measure process-induced variations in ceramic materials. The current process methods focus on slip-casting and injection molding and the NDC methods being evaluated are microfocus x-ray computed tomography (XCT) and nuclear magnetic resonance computed tomography (MRCT). As part of this work, SiC whisker reinforced Si3N4 (GCC's GN-10 material) has been pressure slip-cast at two casting pressures, 15 and 40 psi; and at length/diameter ratios of 1.5, 2.5 and 3.0 with whisker contents of 20, 23, 27 and 30 wt percent. Three-dimensional microfocus XCT has been used to study density variations in billets produced by different process conditions. Destructive measurement of density variation has been compared to the XCT measurements and correlations established. XCT has been shown to be able to detect less than 5 percent variations in as-cast density and these were destructively verified. DOE

N92-32665# California Univ., Santa Barbara. Inst. for Polymers and Organic Solids.
PROGRAM FOR RESEARCH IN CONDUCTING POLYMERS
Alan J. Heeger, Fred Wudl, and Paul Smith 18 May 1992 17 p
(Contract N00014-91-J-1235)
(AD-A250965) Avail: CASI HC A03/MF A01

Principal accomplishments during the past year related to Light Emitting Diodes fabricated from conducting polymers and to the related fundamental scientific and materials issues. Progress has been made toward passivating the low work function

electron-injecting contact to the point where stable operation outside the dry box is routine. Transient electroluminescence from polymer LEDs has been reported; RC limited response with rise and fall times below 50 nanoseconds has been achieved. The absence in saturation in pulsed operation implies that such devices can be used in applications which require multiplexing (e.g., displays). Photoconductivity studies of the parent PPV material demonstrate that the absorption and emission arise directly from a Pi-Pi interband transition (rather than a bond exciton). Work during the next year will focus on synthesis of blue emitters as well as a variety of fundamental experiments (enabled by the passivation of the devices) designed to clarify the mechanism and to enhance the efficiencies. GRA

N92-32667# North Carolina Univ., Chapel Hill. Dept. of Chemistry.
NEW THIOPHENE-BASED MATERIALS
V. V. Sheares, R. Cai, S. Stompel, J. H. Promislow, and T. Dingemans 20 May 1992 4 p
(Contract N00014-92-J-1374)
(AD-A250977; TR-2) Avail: CASI HC A01/MF A01

Our research is focused on the general synthesis of a new class of high performance aromatic thermoplastic and thermosetting engineering polymers from thiophene-based monomers. We are interested in the introduction of changes in polymers by an explicit geometric perturbation of the primary structure of the polymer chain substituting various amounts of thiophene into several classes of phenylene-based polymers. The anticipated property enhancements stem from unique molecular geometry of the aromatic 2,5-thiophene moiety; its nonlinear structure with an exocyclic bond angle of 148 deg is intermediate between that of 1,4-phenylene (180 deg) and 1,3-phenylene (120 deg) commonly used to prepare high performance materials. Often, the former are difficult to process and the latter exhibit poor mechanical properties. By focusing on the intermediate geometry of the thiophene moiety, we anticipate larger thermal processing windows without losing the desirable crystalline (and liquid crystalline) properties associated with the 1,4-phenylene-based materials. In addition, the bilateral asymmetry of the heterocycle will certainly influence the melting points, rates of crystallization, glass transition temperatures, solubility, miscibility with other polymers, adhesion, etc. relative to conventional phenylene-based materials. Our investigations of several distinct classes of polymers, thiophene-based poly(ester)s, poly(aramid)s, poly(benzoxazole)s, poly(arylene ether ketone)s, and poly(imide)s via the combination of a new route along with established methodologies, will be presented. GRA

N92-32752# Philips Gloeilampenfabrieken N.V., Eindhoven (Netherlands).
ORIENTATION, STRESS, AND DENSITY DISTRIBUTIONS IN INJECTION-MOULDED AMORPHOUS POLYMERS DETERMINED BY OPTICAL TECHNIQUES Ph.D. Thesis - Technische Univ.
Reinhold Wimberger-Friedl 1991 240 p
(ETN-92-92052) Avail: CASI HC A11/MF A03

The quantification of the complete state of an injection moulded amorphous polymer by measuring molecular orientation, residual stresses, and density distributions by optical techniques, is addressed. For this purpose the contribution of molecular orientation and residual stresses to birefringence is distinguished quantitatively, and an optical technique for density measurements is introduced. A collection of papers is presented. In order to be able to quantify orientation, stress, and density, the attention is focussed on four different items: (1) the stress optical behavior of the polymers in the entire temperature range of interest; (2) the thermomechanical history of the samples in quenching and injection moulding; (3) the entropy elastic and energy elastic contribution to birefringence; and (4) different experimental techniques, including a new technique to determine refractive index distributions. ESA

N92-32762# Institut National des Sciences Appliquees de Lyon, Villeurbanne (France). Lab. des Materiaux Macromoleculaires.
SYNTHESIS, MORPHOLOGY AND PROPERTIES OF POLYESTER-URETHANE IN SOLUTION IN STYRENE: APPLICATION TO COMPOSITES DEVELOPMENT Ph.D. Thesis [SYNTHESE, MORPHOLOGIE ET PROPRIETES DE POLYESTER-URETHANE EN SOLUTION DANS LE STYRENE: APPLICATION A LA MISE EN OEUVRE DE COMPOSITES]
Jean-Philippe Lecointe 1992 221 p In FRENCH
(ISAL-92-0007; ETN-92-92085) Avail: CASI HC A10/MF A03

A study on the isocyanate maturing (thickening) of unsaturated polyester resins is presented. The reaction between a diisocyanate and the final hydroxyl functions of the unsaturated polyester prepolymer in solution in styrene is addressed. Different steps of maturing are summarized. The maturing was shown to cause a decrease of the intramolecular reaction number at radical copolymerization time and an increase of the mechanical properties (better stability as a function of temperature). ESA

N92-32863*# National Aeronautics and Space Administration. Lewis Research Center, Cleveland, OH.
LIQUID LUBRICANTS FOR ADVANCED AIRCRAFT ENGINES
William R. Loomis and Robert L. Fusaro Aug. 1992 28 p
(RTOP 505-63-5A)
(NASA-TM-104531; E-6407; NAS 1.15:104531) Avail: CASI HC A03/MF A01

An overview of liquid lubricants for use in current and projected high performance turbojet engines is discussed. Chemical and physical properties are reviewed with special emphasis placed on the oxidation and thermal stability requirements imposed upon the lubrication system. A brief history is given of the development of turbine engine lubricants which led to the present day synthetic oils with their inherent modification advantages. The status and state of development of some eleven candidate classes of fluids for use in advanced turbine engines are discussed. Published examples of fundamental studies to obtain a better understanding of the chemistry involved in fluid degradation are reviewed. Alternatives to high temperature fluid development are described. The importance of continuing work on improving current high temperature lubricant candidates and encouraging development of new and improved fluid base stocks are discussed. Author

N92-32913# Texas A&M Univ., College Station.
MACROCYCLIC POLYCATION COMPLEXES FOR SECONDARY ANION BINDING, MOLECULAR RECOGNITION, AND CATALYSIS Report, 1 Jun. 1991 - 31 May 1992
Arthur E. Martell 31 May 1992 9 p
(Contract N00014-88-K-0451)
(AD-A251069) Avail: CASI HC A02/MF A01

The objective of this research project is to synthesize binuclear cobalt(II) and copper (I) complexes of macrocyclic and macrobicyclic ligands, in which the metal ions are coordinated and held apart at distances such as to recognize and coordinate secondary bridging groups, thus, activating the bridging groups for redox reactions or increasing the nucleophilic character of the groups to catalyze the rates of substitution reactions. The strengths of binding of the secondary bridging anions or molecules depends on their ability to coordinate to the two metal centers simultaneously. In other words, the bridging groups should be the correct size and shape to coordinate the metal ions readily. The strength of binding of the secondary bridging groups is determined from the equilibrium constants involving the combination of these groups with the metal ions that are determined potentiometrically and spectrophotometrically. A specific purpose of this research project is to activate dioxygen by forming a binuclear (peroxo) complex in which the dioxygen is partially reduced and the metal ions are partly oxidized to the next higher valence state. The dioxygen is activated for reaction with a second reducing bridging group or an outside reductant which may be added to the system. GRA

N92-33008* National Aeronautics and Space Administration. Langley Research Center, Hampton, VA.
POLYIMIDES WITH CARBONYL AND ETHER CONNECTING GROUPS BETWEEN THE AROMATIC RINGS Patent
Paul M. Hergenrother, inventor (to NASA) and Stephen J. Havens, inventor (to NASA) 8 Sep. 1992 10 p Filed 9 Nov. 1989 Supersedes N90-15260 (28 - 7, p 910)
(NASA-Case-LAR-14001-1; US-Patent-5,145,937; US-Patent-Appl-SN-433812; US-Patent-Class-528-125; US-Patent-Class-528-128; US-Patent-Class-528-172; US-Patent-Class-528-185; US-Patent-Class-528-229; US-Patent-Class-528-352; US-Patent-Class-528-353) Avail: US Patent and Trademark Office

New polyimides have been prepared from the reaction of aromatic dianhydrides with novel aromatic diamines containing carbonyl and ether connecting groups between the aromatic rings. Several of these polyimides are shown to be semi-crystalline as evidenced by wide angle x ray diffraction and differential scanning calorimetry. Most of the polyimides form tough solvent resistant films with high tensile properties. Several of these materials can be thermally processed to form solvent and base resistant moldings.
Official Gazette of the U.S. Patent and Trademark Office

N92-33014* National Aeronautics and Space Administration. Langley Research Center, Hampton, VA.
POLYIMIDE MOLDING POWDER, COATING, ADHESIVE, AND MATRIX RESIN Patent
Terry L. St.Clair, inventor (to NASA) and Donald J. Progar, inventor (to NASA) 15 Sep. 1992 6 p Filed 31 Jul. 1990 Supersedes NN91-13559 (29 - 5, p 642)
(NASA-Case-LAR-14163-1; US-Patent-5,147,966; US-Patent-Appl-SN-560717; US-Patent-Class-528-188; US-Patent-Class-528-125; US-Patent-Class-528-126; US-Patent-Class-528-128; US-Patent-Class-528-173; US-Patent-Class-528-179; US-Patent-Class-528-182) Avail: US Patent and Trademark Office

The invention is a polyimide prepared from 3,4'-oxydianiline (3,4'-ODA) and 4,4'-oxydiphthalic anhydride (ODPA), in 2-methoxyethyl ether (diglyme). The polymer was prepared in ultra high molecular weight and in a controlled molecular weight form which has a 2.5 percent offset in stoichiometry (excess diamine) with a 5.0 percent level of phthalic anhydride as an endcap. This controlled molecular weight form allows for greatly improved processing of the polymer for moldings, adhesive bonding, and composite fabrication. The higher molecular weight version affords tougher films and coatings. The overall polymer structure groups in the dianhydride, the diamine, and a metal linkage in the diamine affords adequate flow properties for making this polymer useful as a molding powder, adhesive, and matrix resin.
Official Gazette of the U.S. Patent and Trademark Office

N92-33015* National Aeronautics and Space Administration. Langley Research Center, Hampton, VA.
METHYL SUBSTITUTED POLYIMIDES CONTAINING CARBONYL AND ETHER CONNECTING GROUPS Patent
Paul M. Hergenrother, inventor (to NASA) and Stephen J. Havens, inventor (to NASA) 8 Sep. 1992 8 p Filed 28 Sep. 1990 Supersedes N91-13561 (29 - 5, p 642)
(NASA-Case-LAR-14351-1; US-Patent-5,145,942; US-Patent-Appl-SN-589571; US-Patent-Class-528-353; US-Patent-Class-528-125; US-Patent-Class-528-128; US-Patent-Class-528-172; US-Patent-Class-528-185; US-Patent-Class-528-352; US-Patent-Class-564-315) Avail: US Patent and Trademark Office

Polyimides were prepared from the reaction of aromatic dianhydrides with novel aromatic diamines having carbonyl and ether groups connecting aromatic rings containing pendant methyl groups. The methyl substituent polyimides exhibit good solubility and form tough, strong films. Upon exposure to ultraviolet irradiation and/or heat, the methyl substituted polyimides crosslink to become insoluble.
Official Gazette of the U.S. Patent and Trademark Office

N92-33059# Helsinki Univ. of Technology, Espoo (Finland). Lab. of Machine Design.
INFLUENCE OF OIL LUBRICANT ADDITIVES ON TRIBOLOGICAL BEHAVIOR OF ENGINEERING CERAMICS
O. Boming (Guangzhou Machine Tool Research Inst., Huangpu, China), P. Salonen, and M. Kleimola 1 Nov. 1991 66 p Sponsored by the Finnish Ministry of Trade and Industry
(PB92-180710; ISBN-951-22-0900-4; C-238) Avail: CASI HC A04/MF A01

The literature search, the survey, and the outcome of a series of pin-on-disc tests of ceramics and steel in oil, with and without additives, are presented. The results discuss the friction and wear of ceramics sliding against themselves and steel lubricated by oil with sulfonate additive and the friction and wear of ceramics sliding against themselves and steel in oil lubrication with sulfurized olefin. Author

N92-33065# Technische Univ., Delft (Netherlands).
KINETICS AND CHARACTERIZATION OF CVD-GROWN BP Ph.D. Thesis
Erik Maria Kelder 1991 276 p
(ETN-92-92024) Avail: CASI HC A13/MF A03

A study to understand the product properties of polycrystalline cubic Boron Monosphosphide (BP) as a function of the CVD (Chemical Vapor Decomposition) parameters is presented. Solid state parameters not dependent on synthesis technique are discussed. The CVD of boron phosphides is reviewed. The growth of epitaxial BP on silicon, performed on a cold wall reactor, as well as discussion of several properties, are presented. Thermodynamical calculations are performed using the program Solgamix, adapted to a personal computer. The thermodynamic calculations are required in order to understand the nature of the reactive species. For several hypothetical gaseous species, thermochemical data are calculated using theoretical and empirical considerations. The CVD process is described using boron deposition as an example. The results of the boron deposition are used to show several different ways of approaching the mechanism of the CVD process, without claiming to describe the process accurately. The results of the deposition kinetics of cubic BP are given: thermodynamical calculations are used to support the experimental results and to describe an equilibrium adsorption process in order to understand the nature of the adspecies. Calculations of the surface concentrations are used to explain the kinetic role of the carrier gas hydrogen, present in all the CVD experiments. The characterization of the CVD deposits is performed by XRD and XPS. The electrical conductivity, electron spin resonance, Hall, and Seebeck measurements are discussed and are correlated to the experimental CVD parameters. Preliminary results on the wear resistance of the BP coatings, a relevant property to the wear resistance, are discussed. ESA

N92-33157 Department of the Navy, Washington, DC.
SILVER COATED SUPERCONDUCTING CERAMIC POWDER Patent
William A. Ferrando, inventor (to Navy) 21 Jan. 1992 10 p Filed 2 Aug. 1990
(AD-D015294; US-Patent-5,082,826; US-Patent-Appl-SN-561750; US-Patent-Class-505-1) Avail: US Patent and Trademark Office

A silver coated superconducting ceramic powder made by (1) coating the superconducting ceramic powder particles with AgNO3; (2) melting the AgNO3 SO that it wets and forms a uniform coating over the surfaces of the particles; and (3) decomposing the AgNO3 to form a thin, uniform coating of silver metal on the surfaces of the particles. The product is a loose powder of superconducting ceramic particles which are uniformly coated with a thin layer of silver metal. The powder can be cold worked (e.g., swaged, forged etc.) to form superconducting structures such as rods or wires.
GRA

N92-33170 Department of the Navy, Washington, DC.
METHOD OF GROWING DIAMOND FILM ON SUBSTRATES Patent
Arthur A. Morrish, inventor (to Navy), Paul M. Natishan, inventor

(to Navy), and William A. Carrington, inventor (to Navy) 24 Dec. 1991 12 p Filed 30 Apr. 1990
(AD-D015313; US-Patent-5,075,094; US-Patent-Appl-SN-516585; US-Patent-Class-423-446) Avail: US Patent and Trademark Office

The deposition of diamond on a substrate is enhanced by coating the substrate surface with a thin layer of carbon before deposition. Preferably, the substrate is scratched before being coated with diamond. The carbon layer may be formed by applying an oil coating to the substrate and then heating the substrate to carbonize the coating, or by the evaporative deposition of carbon. GRA

N92-33177 Department of the Navy, Washington, DC.
CORROSION-RESISTANT ALKYD COATINGS Patent
Charles R. Hegedus, inventor (to Navy), Donald J. Hirst, inventor (to Navy), William J. Green, inventor (to Navy), and Anthony T. Eng, inventor (to Navy) 18 Feb. 1992 5 p Filed 14 Dec. 1990
(AD-D015330; US-Patent-5,089,551; US-Patent-Appl-SN-627670; US-Patent-Class-524-396) Avail: US Patent and Trademark Office

A corrosion-resistant coating is discussed. The coating is capable of being applied to various substrates, particularly metal and plastic surfaces, as a single coat characterized as having high-gloss, good adhesion, and a high degree of flexibility is discussed. The corrosion inhibiting coating comprises an alkyd resin containing an effective amount of a corrosion-inhibiting pigment consisting essentially of critical amounts of at least one zinc phosphate, zinc molybdate, and at least one zinc salt of a benzoic acid. GRA

N92-33247# Argonne National Lab., IL.
COATINGS FOR IMPROVED CORROSION RESISTANCE
K. Natesan May 1992 15 p Presented at the 3rd International Conference on Advances in Coatings and Surface Engineering for Corrosion and Wear Resistance, New Castle, England, 11-15 May 1992
(Contract W-31-109-eng-38)
(DE92-016779; ANL/CP-76309; CONF-9205213-1) Avail: CASI HC A03/MF A01

Several coating approaches are being developed to resist attack in coal-fired environments and thereby minimize corrosion of underlying substrate alloys and extend the time for onset of breakaway corrosion. In general, coating systems can be classified as either diffusion or overlay type, which are distinguished principally by the method of deposition and the structure of the resultant coating-substrate bond. The coating techniques examined are pack cementation, electrospark deposition, physical and chemical vapor deposition, plasma spray, and ion implantation. In addition, ceramic coatings are used in some applications. DOE

28 PROPELLANTS AND FUELS

Includes rocket propellants, igniters, and oxidizers; their storage and handling procedures; and aircraft fuels.

For related information see also *07 Aircraft Propulsion and Power, 20 Spacecraft Propulsion and Power,* and *44 Energy Production and Conversion.*

N92-32483# Department of Energy/Contractors Micrographics and Information Management Association, Washington, DC. Assistant Secretary for Conservation and Renewable Energy.
SECOND INTERIM REPORT OF THE INTERAGENCY COMMISSION ON ALTERNATIVE MOTOR FUELS
Sep. 1991 86 p
(DE92-013169; DOE/CE-92013169) Avail: CASI HC A05/MF A01

This report describes progress the commission and government agencies have made in implementing the provisions of the Alternative Motor Fuels Act (AMFA) of 1988, assessing the role of alternative motor fuels in the US transportation sector, and developing policies to promote the use of alternative fuels. The alternative motor-fuels policies proposed in the National Energy Strategy (NES) are described and shows how they compose an effective long-term plan to encourage the widespread use of alternative motor fuels. The progress to date of the Department of Energy (DOE) and other agencies in implementing the programs required by the AMFA is reported. A detailed scenario of future alternative-fuel use that displaces 2.5 million barrels per day (MMBD) of petroleum and a feasible path of vehicle production and fuel supply leading to that goal is described. An analytical tool for exploring and quantifying the energy market impacts of alternative fuels, the Alternative Fuels Trade Model (AFTM), is described. The AFTM provides a means of investigating the impacts of alternative fuels in interrelated world energy markets for petroleum and natural gas. Several major initiatives have recently been enacted that have important ramifications for alternative-fuels policy. The Clean Air Act Amendments of 1990 contain provisions mandating the use of nonpetroleum oxygenates in reformulated gasoline. Other provisions for much more stringent emissions standards may affect the ability of manufacturers to make and sell conventional-fuel vehicles or, at the very least, affect their cost-effectiveness in comparison to cleaner alternative-fuel vehicles (AFV's). Finally, the key areas in which technological advances could substantially improve the competitiveness of AFV technologies in the marketplace are reviewed. DOE

N92-32637# Sandia National Labs., Albuquerque, NM.
USE OF THIN-FILM SAMPLES TO STUDY THERMAL DECOMPOSITION CHEMISTRY OF EXPLOSIVES
K. L. Erickson, W. M. Trott, and A. M. Renlund 1992 14 p Presented at the 18th International Pyrotechnics Seminar, Breckenridge, CO, 13-17 Jul. 1992
(Contract DE-AC04-76DP-00789)
(DE92-014616; SAND-92-0081C; CONF-920796-2) Avail: CASI HC A03/MF A01

Development of reliable models for design, performance, stability, and hazard analyses of energetic materials requires detailed understanding of three principal chemical reaction regimes: initial condensed-phase decomposition, subsequent interaction of decomposition products with the remaining condensed phase, and gas-phase reaction of decomposition products to form the ultimate combustion products. The initial condensed-phase decomposition has been particularly difficult to study, due to the inability to directly probe chemistry in the condensed phase under isothermal conditions and with the spatial and temporal resolution needed at high temperatures and reaction rates. Thin-film samples provide a means to study condensed-phase chemistry at isothermal conditions and with microsecond temporal resolution. This paper describes results from experiments in which thin-film samples, and multiple diagnostics are used to examine condensed-phase chemistry and monitor evolved gas species from explosives such as RDX, HMX, and TATB. Sample heating rates, reaction temperatures, and reaction times varied from about 10(exp 8) to less that 1 C/s, from ambient to about 500 C, and from about 10(exp -3) to greater that 10(exp 5) seconds, respectively. Conventional infrared spectroscopy and time-resolved infrared spectral photography were used to detect condensed-phase decomposition products. Mass spectrometry, using both time-of-flight and quadrupole mass spectrometers, was used to monitor evolved gas species. Results from these experiments have been encouraging. For example, conventional infrared spectra from totally confined samples of RDX that were thermally aged at 170 C, for 18 hours, indicated condensed-phase formation of H2O and HCN. DOE

N92-32664# Army Chemical Research and Development Center, Aberdeen Proving Ground, MD.
CONDENSED-PHASE PROCESSES DURING SOLID PROPELLANT COMBUSTION. PART 2: CHEMICAL AND MICROSCOPIC EXAMINATION OF CONDUCTIVELY QUENCHED SAMPLES OF RDX, XM39, JA2, M30, AND HMX-BINDER COMPOSITIONS Final Report, Nov. 1989 - Oct. 1990

Michael A. Schroeder, Robert A. Fifer, Martin S. Miller, Rose A. Pesce-Rodriguez, and Gurbax Singh May 1992 50 p
(DA Proj. 1L1-61102-AH-43)
(AD-A250799; BRL-TR-3337) Avail: CASI HC A03/MF A01

Burning propellant samples were quenched, and the burned surfaces were examined microscopically and by chemical analysis. Studies are in progress on a series of propellants including XM39, M30, JA2, RDX, and HMX-polyester compositions. The results to date are consistent with the idea that at least at low pressures (below 2.0 MPa), a liquid layer forms during combustion of most of the propellants, with the possible exception of JA2; scanning electron microscope examination shows the existence of a liquid layer but does not provide evidence of degradation below this layer. The effect of composition and pressure on this liquid layer is discussed. Further gas chromatography mass spectrometry analysis confirms our earlier result that at least in the case of XM39, the stabilizer is depleted considerably in the surface layers, presumably by reaction with nitrogen oxides formed by decomposition of RDX and NC. Further high performance liquid chromatography results confirm our earlier result that for XM39, HMX2, and RDX (which contain the cyclic nitramines HMX and RDX), there is a significant increase in concentration of the mechanistically significant nitrosamines MRDX and DRDX over the very small amounts possibly present as impurities in RDX and HMX. FTIR-PAS results provide evidence for condensed-phase reaction in M30 and JA2. GRA

N92-32914# New Energy Development Organization, Tokyo (Japan).
NEDO ALCOHOL/BIOMASS TECHNOLOGY SUBCOMMITTEE
Oct. 1991 82 p In JAPANESE Presented at the 11th New Energy Development Organization Meeting, Tokyo, Japan, Oct. 1991
(DE92-526270; ETDE/JP-MF-92526270) Avail: CASI HC A05/MF A01

To develop technologies to produce alcohol directly from such unutilized resources as agricultural and forestry wastes, using bacteria, the alcohol/biomass technology development department at NEDO is moving forward development works on fuel alcohol technologies. The department is developing a composite methane gas manufacturing equipment using high-performance separation membranes to recover energies from organic matters contained in industrial waste waters using the latest methane fermentation process, which combines the biotechnology with the membrane separation technology. To serve for the methanol utilizing power generation technique expected to substitute the petroleum energy from its characteristics, the department is carrying out demonstration tests including conversion of fossil oil thermal generation to a methanol generation system. This paper introduces the summary of these researches presented at the 11th NEDO Subcommittee Conference (October 1991). For instance, the fuel alcohol technology development resulted in obtaining successfully excellent bacteria, and conducted the conceptual design and the comprehensive evaluations. DOE

N92-33003# Sandia National Labs., Albuquerque, NM.
EXTENDING ESTIMATION OF C-J PRESSURE OF EXPLOSIVES TO THE VERY LOW DENSITY REGION
P. W. Cooper 1992 6 p Presented at the 18th International Pyrotechnics Seminar, Breckenridge, CO, 13-17 Jul. 1992
(Contract DE-AC04-76DP-00789)
(DE92-015035; SAND-92-1130C; CONF-920796-3) Avail: CASI HC A02/MF A01

A previous paper showed that, for condensed phase explosives, the C-J density of the detonation product gases correlates to the initial density of the unreacted explosive by a simple power function. This paper extends that correlation to the very low density region which includes detonation of suspended particles of explosives in air, as well as gas phase detonations. Extending this correlation of experimental data by an additional three orders of magnitude caused a slight change in the empirical constants of the correlation. DOE

N92-33108# Lehigh Univ., Bethlehem, PA.
HIGH OCTANE ETHERS FROM SYNTHESIS GAS-DERIVED ALCOHOLS
K. Klier and R. G. Herman Mar. 1992 6 p
(Contract DE-AC22-90PC-90044)
(DE92-013802; DOE/PC-90044/T1) Avail: CASI HC A02/MF A01

The specific goals to achieve an efficient synthesis of high octane ethers from alcohols are (1) to determine the thermodynamic and kinetic limitations, primarily by competitive side reactions, to forming unsymmetrical ethers from alcohols over Nafion H resin, where the alcohols would be produced entirely from synthesis gas over alkali-promoted Cu/ZnO/M2O3 (M = Al,Cr) catalysts, (2) to determine the feasibility of using thermally stable inorganic acid catalysts such as acid zeolites, and (3) to establish the stability of the catalysts by carrying out long term testing and to perform reactions engineering for scale-up of the most prospective catalysts for the alcohols-to-ethers process. DOE

N92-33123# Kentucky Univ., Lexington. Center for Applied Energy Research.
CLEAN GASOLINE REFORMING WITH SUPERACID CATALYSTS
B. H. Davis 1991 12 p
(Contract DE-AC22-90PC-90049)
(DE92-013833; DOE/PC-90049/T4) Avail: CASI HC A03/MF A01

Tasks reported for this term include heteroatom removal, optimization of chlorided Pt-alumina catalysts, testing of the optimum Pt/Cl alumina catalysts, and preparation and testing of zirconia superacid catalyst. Data are provided on naphtha samples received from Wilsonville, effects of temperature and Pt concentration on n-C5 conversions, effect of temperature and Pt concentrations on cyclopentane conversion, catalyst weight gain (H2O) in humidification experiments, conversion of methylcyclohexane, and conversions obtained using a propriatary Zr catalyst. DOE

N92-33141# Amoco Oil Co., Naperville, IL. Research and Development Dept.
DIRECT CONVERSION OF LIGHT HYDROCARBON GASES TO LIQUID FUEL
M. J. Foral 1991 13 p
(Contract DE-AC22-89PC-89866)
(DE92-015592; DOE/PC-89866/T5) Avail: CASI HC A03/MF A01

The objective of this program is to investigate the direct conversion of light gaseous hydrocarbons, such as those produced during Fischer-Tropsch synthesis or as a product of gasification, to liquid transportation fuels via a partial oxidation process. The process will be tested in an existing pilot plant to obtain credible mass balances. Specific objectives to be met include determination of optimal process conditions, investigation of various processing options (e.g. feed injection, product quench, and recycle systems), and evaluation of an enhanced yield thermal/catalytic system. Economic evaluation of the various options will be performed as experimental data become available. DOE

N92-33240# Advisory Group for Aerospace Research and Development, Neuilly-Sur-Seine (France). Propulsion and Energetics Panel.
INSENSITIVE MUNITIONS [LES MUNITIONS A RISQUE ATTENUE]
Jul. 1992 287 p In ENGLISH and FRENCH 78th Meeting held in Bonn, Fed. Republic of Germany, 21-23 Oct. 1991
(AGARD-CP-511; ISBN-92-835-0679-0) Copyright Avail: CASI HC A13/MF A03

The papers presented reflect significant progress that has been made in understanding and characterizing the response of energetic materials to external stimuli such as shock, fire, and bullet impact. Small scale testing results, statistical data, and approaches to numerical modeling are reported. The need for deeper investigation

of the mechanisms involved, for corroboration of the statistical results, and for better fidelity criteria of small scale testing becomes apparent. The NATO Insensitive Munitions Information Center (NIMIC), recently established in Brussels, is charged with providing more exchange of information and international cooperation. For individual titles, see N92-33241 through N92-33245.

N92-33241# Air Force Armament Lab., Eglin AFB, FL. Insensitive Munitions Directorate.
THE UNITED STATES AIR FORCE EXPLOSIVES HAZARDS REDUCTION PROGRAM
Joseph Jenus, Jr. *In* AGARD, Insensitive Munitions Jul. 1992 13 p (For primary document see N92-33240 23-28)
Copyright Avail: CASI HC A03/MF A03

The Air Force Insensitive Munitions/Explosives Hazard Reduction Program is discussed. Key initiatives are in the barriers and packaging area are covered. Barriers and packaging which can be designed to prevent the propagation of one munitions item to the next will reduce the Maximum Credible Event (MCE). Barriers can be placed inside or outside munitions containers or between bombs on parked aircraft. Simple changes to the way munitions are packaged, such as orienting missiles within a container so that warheads do not align, may also reduce the MCE. Effective barriers and packaging can limit the MCE to one munitions item in a magazine full of munitions or one bomb in a mission ready aircraft. This will also result in significant reductions in quantity-distances required and allow more munitions to be stored in closer proximity to airbases, flightlines, and hardened aircraft shelters, where they are needed. Author

N92-33242# Phillips Lab., Edwards AFB, CA. Propellant Development Section.
ESD TRAITS OF BULK PROPELLANT UNDER PRESSURE
Claude I. Merrill and Jo Anne Askins (New Mexico Inst. of Mining and Technology, Socorro.) *In* AGARD, Insensitive Munitions Jul. 1992 13 p (For primary document see N92-33240 23-28)
Copyright Avail: CASI HC A03/MF A03

Since the Pershing booster motor incident occurred in 1985, much has been learned about how to test for electrostatic discharge (ESD) characteristics and what factors influence ESD initiation sensitivity for solid propellants. Small propellant samples have shown enhanced ESD sensitivity when placed under pressure. Since changes in bulk solid propellant ESD traits under the influence of elevated pressures were not found in our literature surveys, equipment was fabricated so that pressure effects on ESD behavior of a hydroxy terminated polybutadiene (HTPB) propellant could be observed. In addition, a limited additive study was conducted to see if large ion salts could reduce the ESD initiation sensitivity of a sensitive HTPB propellant. Author

N92-33243# Defence Research Establishment Valcartier (Quebec).
DEVELOPMENT OF A MINIMUM SMOKE PROPELLANT BASED ON GLYCIDYL AZIDE POLYMER AND AMMONIUM NITRATE
P. Lessard, L. Druet, S. Villeneuve, S. Thiboutot, M. Benchabane (Bristol Aerospace Ltd., Winnipeg, Manitoba), and D. Alexander (Bristol Aerospace Ltd., Winnipeg, Manitoba) *In* AGARD, Insensitive Munitions Jul. 1992 6 p (For primary document see N92-33240 23-28)
Copyright Avail: CASI HC A02/MF A03

Composite rocket propellants traditionally developed and produced in Canada are based primarily on ammonium perchlorate (AP) dispersed in a polybutadiene (HTPB) binder. Depending on the atmospheric conditions, such propellants can produce a significant amount of secondary smoke which is undesirable for certain applications. To overcome this problem, the Defence Research Establishment, Valcartier (DREV), has initiated the development of a minimum smoke, low vulnerability propellant. The new propellant uses ammonium nitrate (AN) as the oxidizer and glycidyl azide polymer (GAP) as the energetic binder. The efforts made and the characteristics of a baseline minimum smoke formulation are described. This formulation meets minimum criteria for processing safety, chemical stability, and mechanical integrity. It falls short of the performance of an AP/HTPB propellant. Means of improving the performance are described. Author

N92-33244# Royal Ordnace PLC, Kidderminster (England). Rocket Motors Div.
THE DESIGN FEATURES OF ROCKET MOTORS RELATING TO INSENSITIVE MUNITION RESPONSE TO THERMO-MECHANICAL STIMULI
A. C. Mason *In* AGARD, Insensitive Munitions Jul. 1992 18 p (For primary document see N92-33240 23-28)
Copyright Avail: CASI HC A03/MF A03

Since the late 1970's, the Royal Ordnance Rocket Motors Division has conducted insensitive munitions trials on approximately 500 solid propellant rocket motors and data from over 400 of these have been included in a recently structured database. These trials preceded the current standards of MIL-STD-2105 and OB Proc 42657, and as a result, most of these trials were conducted on an individual bases in order to understand the basic responses to a wide range of threats. Although the trials were not undertaken as a balanced series of experiments, analysis of the data does permit some useful observation and comparisons to be made. In particular, the results of the 0.5 inch bullet impact trials and fuel fire (Fast Cook-off) tests were considered to be particularly relevant to the current UK, NATO, and USA requirements and these are discussed in detail. The general conclusions from these trials emphasize the importance of both the propellant type and body structure in the response to either mechanical or thermal attack. The database has enabled the capability of designing solid propellant rocket motors to meet bullet impact and fuel fire requirements. Author

N92-33245# Hercules, Inc., Rocket Center, WV. Ballistics Lab.
HAZARDS REDUCTION FOR TACTICAL MISSILES **c20**
K. O. Hartman *In* AGARD, Insensitive Munitions Jul. 1992 22 p (For primary document see N92-33240 23-28)
Copyright Avail: CASI HC A03/MF A03

Substantial progress has been made over the past four years in characterizing and understanding the response of energetic materials and rocket motors to the energetic stimuli specified in MIL-STD-2105A. Approaches to reducing the sensitivity based upon that work are reviewed. Minimum smoke propellants with an improved performance shock sensitivity balance were formulated. Partial or complete replacement of the nitramine with phase stabilized ammonium nitrate reduced the shock sensitivity significantly at a performance loss of 4 to 10 percent. A number of routes to more extinguishable composite propellants, both reduced smoke and high performance types, are discussed. Replacement of the polybutadiene with alternative polymeric backbones has yielded more extinguishable compositions. The use of metal perchlorates in place of the ammonium perchlorate greatly increases thermal stability. In the area of inert components, alternatives to monolithic metal cases, such as composite cases, substantially improve the response to fast cook-off and, for minimum smoke propellants, to bullet impact. Author

29 MATERIALS PROCESSING

Includes space-based development of products and processes for commercial applications.
For biological materials see *55 Space Biology*.

No abstracts in this category.

31 ENGINEERING (GENERAL)

Includes vacuum technology; control engineering; display engineering; cryogenics; and fire prevention.

N92-32461# Wright Lab., Wright-Patterson AFB, OH. MANTECH Technology Transfer Center.
MANTECH PROJECT BOOK
1991 145 p
(AD-A245283) Avail: CASI HC A07/MF A02

The effective integration of processes, systems, and procedures used in the production of aerospace systems using computer technology is managed by the Integration Technology Division (MTI). Under its auspices are the Information Management Branch, which is actively involved with information management, information sciences and integration, and the Implementation Branch, whose technology areas include computer integrated manufacturing, engineering design, operations research, and material handling and assembly. The Integration Technology Division combines design, manufacturing, and supportability functions within the same organization. The Processing and Fabrication Division manages programs to improve structural and nonstructural materials processing and fabrication. Within this division, the Metals Branch directs the manufacturing methods program for metals and metal matrix composites processing and fabrication. The Nonmetals Branch directs the manufacturing methods programs, which include all manufacturing processes for producing and utilizing propellants, plastics, resins, fibers, composites, fluid elastomers, ceramics, glasses, and coatings. The objective of the Industrial Base Analysis Division is to act as focal point for the USAF industrial base program for productivity, responsiveness, and preparedness planning. GRA

N92-32467# Virginia Polytechnic Inst. and State Univ., Blacksburg. Dept. of Mining and Minerals Engineering.
DEVELOPMENT OF THE CHEMICAL AND ELECTROCHEMICAL COAL CLEANING PROCESS
C. I. Basilio and Roe-Hoan Yoon 1991 18 p
(Contract DE-AC22-87PC-79892)
(DE92-013353; DOE/PC-79892/T19) Avail: CASI HC A03/MF A01

The continuous testing of the Chemical and Electrochemical Coal Cleaning (CECC) was completed successfully using Middle Wyodak and Elkhorn No. 3 coal samples. The CECC unit was run under the optimum conditions established for these coal samples. For the Middle Wyodak coal, the ash content was reduced from 6.96 percent to as low 1.61 percent, corresponding to an ash rejection (by weight) of about 83 percent. The ash and sulfur contents of the Elkhorn No. 3 coal were reduced to as low as 1.8 percent and 0.9 percent. The average ash and sulfur rejections were calculated to be around 84 percent and 47 percent. The CECC continuous unit was used to treat -325 mesh Elkhorn No. 3 coal samples and gave ash and sulfur rejection values of as high as 77 percent and 66 percent. In these test, the clean -325 mesh coal particles were separated from the liberated mineral matter through microbubble column flotation, instead of wet-screening. DOE

N92-32690# Messerschmitt-Boelkow-Blohm G.m.b.H., Munich (Germany, F.R.).
FUNDAMENTAL QUESTIONS CONCERNING THE APPLICATION OF SUPERPLASTIC FORMING AND SUPERPLASTIC FORMING/DIFFUSION BONDING
H. E. Friedrich and Peter-Juergen Winkler 1991 11 p Presented at the International Conference on Superplasticity in Advanced Materials, Osaka, Japan, 3-6 Jun. 1991 Submitted for publication
(MBB-Z-0402-91-PUB; ETN-92-92119) Avail: CASI HC A03/MF A01

An overview of fundamental problems which limit or prevent broader application of Superplastic Forming (SPF) and superplastic forming/Diffusion Bonding (DB) technology is presented. The potential for overcoming such limiting factors is shown. Successful developments are underway to extend the application range for SPF and SPF/DB such as new materials, developments to increase the strain rate, new die concepts and finite element techniques to simulate and optimize the operating conditions. But there are inherent limitations which in any case prevent mass production with this technique. ESA

N92-32723# Trane Co., LaCrosse, WI.
DEVELOPMENT AND PROOF-TESTING OF ADVANCED ABSORPTION REFRIGERATION CYCLE CONCEPTS
R. J. Modahl and F. C. Hayes Mar. 1992 94 p Prepared for Oak Ridge National Lab., TN
(Contract DE-AC05-84OR-21400)
(DE92-014933; ORNL/Sub-86-17498/1) Avail: CASI HC A05/MF A01

The overall objectives of this project are to evaluate, develop, and proof-test advanced absorption refrigeration cycles that are applicable to residential and commercial heat pumps for space conditioning. The heat pump system is to be direct-fired with natural gas and is to use absorption working fluids whose properties are known. Target coefficients of performance (COPs) are 1.6 at 47 F and 1.2 at 17 F in the heating mode, and 0.7 at 95 F in the cooling mode, including the effect of fluid losses. The project is divided into three phases. Phase I entailed the analytical evaluation of advanced cycles and included the selection of preferred concepts for further development. Phase II involves the development and testing of critical components and of a complete laboratory breadboard version of the selected system. Phase III calls for the development of a prototype unit and is contingent on the successful completion of Phase II. This report covers Phase I work on the project. In Phase 1, 24 advanced absorption cycle/fluid combinations were evaluated, and computer models were developed to predict system performance. COP, theoretical pump power, and internal heat exchange were calculated for each system, and these calculations were used as indicators of operating and installed costs in order to rank the relative promise of each system. The highest ranking systems involve the cycle concept of absorber/generator heat exchange, generator heat exchanger/absorber heat exchange, regeneration, and resorption/desorption, in combination with the NH3/H2O/LiBr ternary absorption fluid mixture or with the NH3/H2O binary solution. Based upon these conclusions, the recommendation was made to proceed to Phase II, the laboratory breadboard proof-of-concept. DOE

N92-32742# Messerschmitt-Boelkow-Blohm G.m.b.H., Ottobrunn (Germany, F.R.).
EXAMPLES OF ADVANCED NEAR-NET SHAPE MANUFACTURING TECHNIQUES FOR AEROSPACE
P.-J. Winkler and H.-E. Friedrich 1991 29 p Presented at the 1991 Advanced Aerospace Material/Processes Conference, Long Beach, CA, 20-24 May 1991 Submitted for publication
(MBB-Z-0399-91-PUB; ETN-92-92118) Avail: CASI HC A03/MF A01

Aerospace industry manufacturing technology is reviewed. The following are described: development principles for materials and construction methods; influence of valuable materials; present and future requirements for metallic structural components in aircraft building; near-net shape technologies and typical applications; design and manufacturing principles for superelastic forming and the combination with diffusion bonding; the incremental forcing process; further developments in investment casting. The need to rationalize manufacturing processes and the wish to obtain improved performance in aircraft will continue to provide the necessary impulse to develop innovative manufacturing methods. The development of suitable 'near-net shape' technologies will play an important part in the design of the aircraft of the future. ESA

N92-32825# Swedish Council for Building Research, Stockholm.
DEMAND CONTROLLED VENTILATING SYSTEMS: SENSOR MARKET SURVEY. ENERGY CONSERVATION IN BUILDINGS AND COMMUNITY SYSTEMS PROGRAMME, ANNEX 18, DECEMBER 1991

W. Raatschen and M. Sjoegren 1991 87 p
(PB92-180892; ISBN-91-540-5417-6) Avail: CASI HC A05/MF A01

The subject of indoor and outdoor air quality has generated a great deal of attention in many countries. Areas of concern include outgassing of building materials as well as occupant-generated pollutants such as carbon dioxide, moisture, and odors. Progress has also been made towards addressing issues relating to the air tightness of the building envelope. Indoor air quality studies indicate that better control of supply flow rates as well as the air distribution pattern within buildings are necessary. One method of maintaining good indoor air quality without extensive energy consumption is to control the ventilation rate according to the needs and demands of the occupants, or to preserve the building envelope. This is accomplished through the use of demand controlled ventilating (DCV) systems. The specific objective of Annex 18 is to develop guidelines for demand controlled ventilating systems based on state of the art analyses, case studies on ventilation effectiveness, and proposed ventilation rates for different users in domestic, office, and school buildings. Author

N92-32893# Messerschmitt-Boelkow-Blohm G.m.b.H., Munich (Germany, F.R.). Central Labs.
SUPERPLASTIC FORMING OF Ti6Al4V AT LOWER TEMPERATURE USING HYDROGEN
Gerhard Hirt and Peter-Juergen Winkler 1991 7 p Presented at the International Conference on Superplasticity in Advanced Materials, Osaka, Japan, 3-6 Jun. 1991 Submitted for publication
(MBB-Z-0403-91-PUB; ETN-92-92120) Avail: CASI HC A02/MF A01

Basic results concerning the superplastic forming behavior of Ti6Al4V with internal hydrogen as transient alloying element are presented. Hydrogeneration tests, step strain rate tests (m value), constant strain rate tests, tensile tests after superplastic forming, and superplastic forming trials of a typical sample part are used to determine process parameters which allow reduction of the forming temperature by approximately 100 C. ESA

N92-32927# Oak Ridge National Lab., TN.
AN ANALYTICAL SCREENING OF ALTERNATIVES FOR R-502 IN LOW-TEMPERATURE REFRIGERATING APPLICATIONS
S. K. Fischer 1992 16 p Presented at the 1992 American Society of Heating, Refrigerating, and Air-Conditioning Engineers (ASHRAE) Meeting, Baltimore, MD, 27 Jun. - 1 Jul. 1992
(Contract DE-AC05-84OR-21400)
(DE92-017162; CONF-9206112-2) Avail: CASI HC A03/MF A01

R-502 is used as the working fluid of low-temperature refrigerating systems with evaporating temperatures as low as -40 F (-40 C). It was selected as the refrigerant of choice for these applications because it is both nonflammable and nontoxic and has an acceptable compressor discharge temperature when used in a high-efficiency vapor-compression system. Replacement fluids are going to be needed for use in place of R-502, however, because of the provisions of the Montreal Protocol. R-502 is an azeotropic blend of R-22 and R-115, and R-115 is a chlorofluorocarbon (CFC). The provisions of the Montreal Protocol currently require a total phase-out of the production of all fully halogenated CFCs, including R-115, by the year 2000. Consequently, replacement fluids will be needed for new and existing equipment. This study was initiated to identify other possible fluids that can be used either in new or retrofit applications for low-temperature refrigerant. It includes an evaluation of predicted cycle efficiency, system capacity, pressure ratio, fluid flammability, and compressor discharge temperature. Eight different chemical compounds are considered for use as pure refrigerants as well as components in binary and ternary mixtures: R-134a, R-134, R-125, R-143a, R-152a, R-32, R-124, and R-22. An exhaustive study of the composition of blends was performed to determine the mass fractions of each component in the mixtures that are most promising on the basis of efficiency, flammability, low discharge temperature, and acceptable capacity and pressure ratio. Several blends are identified for further laboratory and analytical evaluation. DOE

N92-33020* National Aeronautics and Space Administration. Langley Research Center, Hampton, VA.
FLUSH MOUNTING OF THIN FILM SENSORS Patent
Thomas C. Moore, Sr., inventor (to NASA) 22 Sep. 1992 4 p Filed 6 May 1991 Supersedes N91-28454 (29 - 20, p 3332)
(NASA-Case-LAR-14446-1; US-Patent-5,149,387;
US-Patent-Appl-SN-699288; US-Patent-Appl-156-241;
US-Patent-Appl-29-856; US-Patent-Appl-156-285;
US-Patent-Appl-156-293; US-Patent-Appl-264-272.15;
Int-Patent-Class-B29C-65/48) Avail: US Patent and Trademark Office

Flush mounting of a sensor on a surface is provided by first forming a recessed area on the surface. Next, an adhesive bonding mixture is introduced into the recessed area. The adhesive bonding mixture is chosen to provide thermal expansion matching with the surface surrounding the recessed area. A strip of high performance polymeric tape is provided, with the sensor attached to the underside thereof, and the tape is positioned over the recessed area so that it acts as a carrier of the sensor. A shim having flexibility so that it will conform to the surface surrounding the recessed area is placed over the tape, and a vacuum pad is placed over the shim. The area above the surface is then evacuated while holding the sensor flush with the surface during curing of the adhesive bonding mixture. After such curing, the pad, shim, and tape are removed from the sensor, electrical connections for the sensor are provided, after which the remaining space in the recessed area is filled with a polymeric foam.
Official Gazette of the U.S. Patent and Trademark Office

32 COMMUNICATIONS AND RADAR

Includes radar; land and global communications; communications theory; and optical communications.

For related information see also *04 Aircraft Communications and Navigation* and *17 Space Communications, Spacecraft Communications, Command and Tracking.* For search and rescue see *03 Air Transportation and Safety,* and *16 Space Transportation.*

N92-32458# Massachusetts Inst. of Tech., Cambridge.
SATELLITE RADIO INTERFEROMETRY Final Technical Report, 29 Apr. 1986 - 30 Apr. 1991
Charles C. Counselman, III 31 Jul. 1991 31 p
(Contract F19628-86-K-0009; AF Proj. 2309)
(PL-TR-91-2200) Avail: CASI HC A03/MF A01

Satellite radio interferometry techniques of geodesy, whereby relative positions of earth surface points and orbits of earth satellites are determined from phase difference measurements of radio signals propagating from the satellites to the earth surface points (or vice versa), were investigated under this contract. The RMS scatter of relative position vector determinations was 2 millimeters for horizontal coordinates of earth surface points separated by about 150 kilometers in the vicinity of Houston, Texas, when the orbits of the NAVSTAR Global Positioning System satellites whose carrier signal phases were measured at these points and were determined simultaneously from seven hours of phase measurements at a network of stations spanning 320 kilometers, without atomic frequency standards. Related techniques for determining positions of earth surface radio transmitters observed via repeater satellites were also investigated. Author

N92-32535# Defence Research Establishment, Ottawa (Ontario).
INTERCEPTION OF LPI RADAR SIGNALS
Jim P. Lee Nov. 1991 55 p
(AD-A246315; DREO-91-23) Avail: CASI HC A04/MF A01

Most current radars are designed to transmit short duration pulses with relatively high peak power. These radars can be detected easily by the use of relatively modest EW intercept

receivers. Three radar functions (search, anti-ship missile (ASM) seeker, and navigation) are examined to evaluate the effectiveness of potential low probability of intercept (LPI) techniques, such as waveform coding, antenna profile control, and power management that a radar may employ against current Electronic Warfare (EW) receivers. The general conclusion is that it is possible to design a LPI radar which is effective against current intercept EW receivers. LPI operation is most easily achieved at close ranges and against a target with a large radar cross section. The general system sensitivity requirement for the detection of current and projected LPI radars is found to be on the order of -100 dBmi which cannot be met by current EW receivers. Finally, three potential LPI receiver architectures, using channelized, superhet, and acousto-optic receivers with narrow RF and video bandwidths are discussed. They have shown some potential in terms of providing the sensitivity and capability in an environment where both conventional and LPI signals are present. GRA

N92-32555# National Telecommunications and Information Administration, Boulder, CO. Inst. for Telecommunication Sciences.

NEW APPROACH TO HF CHANNEL MODELING AND SIMULATION. PART 3: TRANSFER FUNCTION

L. E. Vogler and J. A. Hoffmeyer Mar. 1992 40 p
(PB92-192848; NTIA-92-284) Avail: CASI HC A03/MF A01

A new and unique approach for modeling either narrowband or wideband high frequency (HF) channels is given. Although narrowband models of the HF channel have existed for many years, they are applicable to only a limited set of actual narrowband propagation conditions. The need for an HF channel model that is valid for both narrow and wide bandwidths over a more extensive range of propagation conditions motivated the research. An explicit expression for the channel transfer function incorporating a random time-varying generator is derived and its relation to the impulse response and scattering function is discussed. Comparisons with measured data indicate the process is best modeled as a sequence of random variables with an exponential autocorrelation function; this leads to a scattering function having a Lorentzian shape. A brief discussion of a Gaussian random variable generator is also included. Comparisons of scattering functions from the model and from measurements on a near-vertical incidence auroral path for a wide range of spread-F conditions are shown. Author

N92-32559*# Michigan Univ., Ann Arbor. Radiation Lab.

A FINITE ELEMENT-BOUNDARY INTEGRAL METHOD FOR CONFORMAL ANTENNA ARRAYS ON A CIRCULAR CYLINDER Final Report

Leo C. Kempel, John L. Volakis, Alex C. Woo, and C. Long Yu Jul. 1992 35 p
(Contract NCA2-543)
(NASA-CR-190610; NAS 1.26:190610; UMICH-027723-6-F)
Avail: CASI HC A03/MF A01

Conformal antenna arrays offer many cost and weight advantages over conventional antenna systems. In the past, antenna designers have had to resort to expensive measurements in order to develop a conformal array design. This is due to the lack of rigorous mathematical models for conformal antenna arrays, and as a result the design of conformal arrays is primarily based on planar antenna design concepts. Recently, we have found the finite element-boundary integral method to be very successful in modeling large planar arrays of arbitrary composition in a metallic plane. Herewith we shall extend this formulation for conformal arrays on large metallic cylinders. In this we develop the mathematical formulation. In particular we discuss the finite element equations, the shape elements, and the boundary integral evaluation, and it is shown how this formulation can be applied with minimal computation and memory requirements. The implementation shall be discussed in a later report. Author

N92-32570# Naval Research Lab., Washington, DC.

THE PROBLEMS OF ROUTING AND SCHEDULING IN MULTIHOP RADIO NETWORKS. A HOPFIELD NEURAL NETWORK APPROACH Interim Report, Oct. 1989 - Apr. 1991

Jeffrey E. Wieselthier, Craig M. Barnhart, and Anthony Ephremides (Locus, Inc., Alexandria, VA.) 31 Dec. 1991 93 p Prepared in cooperation with Maryland Univ., College Park
(AD-A247431; NRL/FR/5521-91-9366) Avail: CASI HC A05/MF A01

Although the issues of routing and scheduling in packet radio networks are highly interdependent, few studies have addressed their interactions. After reviewing the major issues associated with the joint study of these problems, we address both components individually. Each is formulated as a combinatorial-optimization problem, and Hopfield neural network (NN) models are developed for solving several versions of these problems. A key feature of our models is the use of the method of Lagrange multipliers, which permits the coefficients in the connection weights to vary dynamically with the evolution of the system state. Extensive software simulation results demonstrate the capability of our approach to determine good sets of routes and link activation schedules. These results also demonstrate that these problems are not separable, i.e., that a model that jointly optimizes routes and link-activation schedules is needed. Issues associated with the extension of this approach to the join routing/scheduling problem are discussed, and a preliminary description of such a model is provided. GRA

N92-32573# Stanford Univ., CA. Space Telecommunications and Radioscience Lab.

WAVELENGTH DIVISION MULTIPLEXED LOCAL AREA NETWORKS

L. G. Kazovsky, C. Barry, M. Hickey, C. Noronha, and P. Poggiolini 1991 44 p
(Contract N00014-91-J-1857)
(AD-A247613) Avail: CASI HC A03/MF A01

The advent of new services, such as multimedia communications, high-volume file transfer, high-definition image transmission, video/audio retrieval, and others, has created a need for high speed data networks. Future networks are expected to support, in an integrated fashion, services with highly diverse traffic requirements. Due to the high data rates involved, such networks will use optical fiber as the transmission medium. It has been recognized that current network topologies, employing single shared channels to provide connectivity between the nodes, are not adequate to provide these new services, thus, creating the need for multichannel networks. One way to realize multiple channels on the optical fiber is through the use of Wavelength-Division Multiplexing (WDM); this method has the additional advantage that, by employing tunable transmitters and/or receivers, the network topology can change dynamically in time. This paper focuses on WDM Networks. Following a discussion of the possible network topologies, we investigate the technological issues related to the implementation of such topologies, and describe some experimental implementations reported in the literature. GRA

N92-32633# Army Missile Command, Redstone Arsenal, AL.

OPTICAL MODULATION CHARACTERISTICS AND APPLICATIONS OF LIQUID CRYSTAL TELEVISIONS Final Report, Feb. 1990 - Nov. 1991

James C. Kirsch 18 May 1992 74 p
(AD-A252466; AD-E951843; AMSMI/TR-RD-WS-92-6) Avail: CASI HC A04/MF A01

One of the most critical components in optical information processing systems is the spatial light modulator (SLM), which typically limits both system speed and space-bandwidth. Cost has been a major drawback for commercial applications. This report covers the improving SPL, the liquid crystal television (LCTV). Two LCTV's were selected for test measurements, the SEIKO LVD202 pocket color LCTV and the Epson Crystal Image video projector. Phase and amplitude modulation were checked with the LVD202 achieving a visibility of 0.94 in an amplitude modulating mode (AMM) and modulated in excess of 360 degrees of phase. The Epson LCTV achieved a visibility of 0.96 in AMM and modulated 336 degrees of phase. Two phase-mostly joint transform optical correlator constructed with two Seiko LCTV's performed as well

as a similar amplitude modulating (AM) JTC, with a much higher light efficiency. The Epson LCTV served as a phase-only input to a Vandderlugt optical correlator with results similar to traditional amplitude input correlator. This correlator also proved to be more light efficient than AM architecture. The report discusses experiment results and possible future research directions. GRA

N92-32680# Massachusetts Inst. of Tech., Lexington.
BEAM AND FILTER STRADDLE LOSSES IN AN ESA SEARCH RADAR
R. J. Galejs and C. E. Muehe 31 Mar. 1992 50 p
(Contract F19628-90-C-0002)
(AD-A250878; UMICH-TR-947; ESD-TR-91-245) Avail: CASI HC A03/MF A01

The present study was undertaken to quantify several types of losses encountered when using an electronically-scanned array (ESA). The losses examined include beam straddle losses, eclipsing losses, and range-Doppler straddling losses. The losses were studied for volume search radars with square and hexagonal search patterns as well as horizon search radar. The radar search equations for an ESA radar for both volume and horizon search are first derived. The beam straddle loss is then found, including the effect of range eclipsing for a high pulse repetition frequency (PRF) radar. The hexagonal search pattern has about 0.5 to 1 dB less loss than the square search. This loss is a strong function of probability of detection and duty factor precluding the insertion of a constant loss term in the radar range equation for these effects. A derivation of range and Doppler straddling losses follows, showing that they vary only slightly with the probability of detection and thus can be represented by a constant depending only on range-gate and Doppler-filter spacings. All losses were found to be very insensitive to the probability of false alarm in the range of 10-4 to 10-8, with the higher false-alarm rates giving slightly lower losses. The summary gives an example of a radar design to illustrate the use of the present results. GRA

N92-32686# Massachusetts Inst. of Tech., Lexington. Lincoln Lab.
AIRPORT SURVEILLANCE RADAR (ASR-9) WIND SHEAR PROCESSOR: 1991 TEST AT ORLANDO, FLORIDA
M. E. Weber 1 Jun. 1992 44 p
(Contract DTFA01-89-Z-02030)
(AD-A252246; ATC-189; DOT/FAA/NR-92/7) Avail: CASI HC A03/MF A01

An operational test of a Wind Shear Processor (WSP) add-on to the Federal Aviation Administration's airport surveillance radar (ASR-9) took place at Orlando International Airport during July and August 1991. The test allowed for both quantitative assessment of the WSP's signal processing and wind shear detection algorithms and for feedback from air traffic controllers and their supervisors on the strengths and weaknesses of the system. Thunderstorm activity during the test period was intense; low-altitude wind shear impacted the runways or approach/departure corridors on 40 of the 53 test days. As in previous evaluations of the WSP in the southeastern United States, microburst detection performance was very reliable. Over 95 percent of the strong microbursts that affected the Orlando airport during the test period were detected by the system. Gust front detection during the test, while operationally useful, was not as reliable as it should have been, given the quality of gust front signatures in the base reflectivity and radial velocity data from the WSP. Subsequent development of a Machine Intelligent Gust Front Algorithm has resulted in significantly improved detection capability. Results from the operational test are being utilized in ongoing refinement of the WSP. GRA

N92-32696# Massachusetts Inst. of Tech., Lexington. Lincoln Lab.
MULTIFREQUENCY MEASUREMENTS OF RADAR GROUND CLUTTER AT 42 SITES. VOLUME 1: PRINCIPAL RESULTS
J. B. Billingsley and J. F. Larrabee 15 Nov. 1991 295 p
(Contract F19628-90-C-0002)
(AD-A246710; ESD-TR-91-061-Vol-1) Avail: CASI HC A13/MF A03

This report determines how ground clutter strength varies with RF frequency from VHF to X-band in ground-sited radar. These results indicate that the frequency dependence of ground clutter strength depends upon terrain type and can vary, for example, from a strongly decreasing function of frequency in forest to a strongly increasing function of frequency in farmland. Five major terrain categories are defined that encompass this dependence, namely, urban, mountains, forest, farmland, and desert. Within each terrain category, results are also shown to be dependent upon relief or roughness of the terrain and upon the depression angle at which the terrain is illuminated. The depression angle dependence is important, even for the very low angles (typically within a degree of grazing incidence) and small (typical fractional) variations in angle that occur in ground-sited radar. This report presents specific clutter strength results at each of five frequencies (VHF, UHF, L-, S-, and X-band) from each of the 42 sites at which measurements were conducted. The report then combines results from similar sites to obtain the general dependence of clutter strength versus frequency for each terrain category. Clutter strengths are described in terms of moments (including the mean) and percentile levels (including the median) in measured clutter amplitude distributions resulting from cell-by-cell spatial variation over a selected large kilometer-sized macroregion of terrain at each site. GRA

N92-32719# Hughes Research Labs., Malibu, CA.
ELECTROMAGNETIC-WAVE PROPAGATION IN UNMAGNETIZED PLASMAS Final Report, 1 May 1989 - 31 Jan. 1992
D. J. Gregoire, J. Santoru, and R. W. Schumacher Mar. 1992 65 p
(Contract F49620-89-C-0063)
(AD-A250710; HAC-REF-G8200; AFOSR-92-0294TR) Avail: CASI HC A04/MF A01

This final report describes an investigation of electromagnetic-wave propagation in unmagnetized plasmas and its application to the reduction of the radar cross section (RCS) of a plasma-filled enclosure. We have demonstrated RCS reduction of 20 to 25 dB with a prototype system at the radar range at Hughes Aircraft's Microwave Products Division in Torrance. The prototype consists of a sealed ceramic enclosure with a microwave reflector and a plasma generator inside it. When the plasma is present, the RCS is significantly reduced over a frequency range of 4 to 14 GHz. As part of the program, we also investigated the basic-plasma-physics issues relating to the absorption and refraction of electromagnetic (EM) waves in collisional plasmas. We demonstrated absorption as high as 63 dB in a section of plasma-loaded C-band rectangular waveguide. We also developed a theoretical model for the plasma cloaking process that includes scattering contributions from the plasma-vacuum interface, partial reflections from the plasma, and collisional absorption in the plasma. The theoretical model is found to be in reasonable agreement with the experimental results and can be used to confidently design future plasma cloaking systems. GRA

N92-32739# Ecole Nationale Superieure des Telecommunications, Paris (France). Dept. Communications
STUDY AND DEVELOPMENT OF A SIX PORT NETWORK ANALYZER IN THE 1-18 GHz FREQUENCY RANGE Ph.D. Thesis [ETUDE ET REALISATION D'UN ANALYSEUR DE RESEAUX SIX PORTES DANS LA BANDE DE FREQUENCE 1-18 GHZ]
Eric Bergeault 1991 307 p In FRENCH Sponsored by Association Nationale pour la Recherche Technique
(Telecom-91-E-005; ETN-92-92095) Avail: CASI HC A14/MF A03

A theoretical and experimental study for the realization of a six port analyzer to calibrate the components of the verification kit, used to evaluate the measurement accuracy of automated network analyzers, is presented. The detection is performed at the frequency of use, and the scattering parameters are determined

in magnitude and phase by means of power measurements. The six port accuracy, realized in the 1 to 18 GHz frequency range, is limited by uncertainties in the power measurements. The detection law of the Schottky diodes used as power detectors, that relates the incident power level and the diode output voltage, is performed in situ. The characterization requires only two reference unknown test loads without any power measurement. The procedure is shown to be rather stable with frequency, so that a midband characterization is generally sufficient to provide enough accuracy in the whole frequency range. The measurement uncertainties due to the variation of the detector reflection coefficients with power, are estimated by determining the variations of the six port parameters. The principle of the six port compared to that of the heteordyne network analyzers is simpler, and it makes modeling and correcting systematic errors easier. Good agreement is found between the measurement results obtained with the dual six port and the other operating systems. Generally, the amplitude measurements are within a few thousands, while the phase measurement errors are below or around one degree for the parameters being measured. ESA

N92-32744# Sandia National Labs., Albuquerque, NM.
NAASW MODULAR RADAR RESEARCH TESTBED STUDY RESULTS
Dec. 1991 294 p
(Contract DE-AC04-76DP-00789)
(DE92-011339; SAND-91-2495-Vol-1) Avail: CASI HC A13/MF A03

Sandia National Laboratories has defined conceptual design approaches, development costs, and development schedules for a synthetic-aperture radar testbed system for imaging of the ocean. The proposed system, referred to as the Modular Radar Research Testbed (MRRT), is capable of simultaneous operation at multiple frequencies. The design features a nearly autonomous radar operating at each frequency. The architecture minimizes the number of frequency-dependent modules in the system and supports a variety of real-time imaging modes, including side-looking strip map, squinted strip map, coherent spotlight, long-dwell squint (multiple images of the same scene from different squint angles), interferometry, and polarimetry. Salient system features and modules are identified, and system modes are described. Systems specifications and block diagrams are provided. Requirements for the study are presented. The various aspects of the system's architecture (generic data link, digital signal processor, image processing assembly, etc.) are described. Descriptions of system modes of operation (strip map, squinted strip map, interferometry, etc.) are provided. Descriptions of analyses relating to interferometry and the Displaced-Phase-Center Antenna are presented. DOE

N92-32749# Juszko Scientific Services, Victoria (British Columbia).
PARAMETERIZATION OF DIRECTIONAL SPECTRA, PART 2. VOLUME 2: USER'S MANUAL FOR THE PROGRAMS RMODEL, FITHM, AND FITDM
Barbara-Ann Juszko 31 Dec. 1989 35 p
(Contract DREA-W7707-9-0214-01-OCS)
(DREA-CR-89-445-Pt-2-Vol-2; CTN-92-60328) Avail: CASI HC A03/MF A01

The description of complex directional wave spectra using a limited number of parameters would reduce data storage requirements and facilitate the theoretical and practical use of spectral characteristics. A 10 parameter model was developed in the WAVEC study of the North Atlantic to represent hindcast directional wave spectra. Software was developed to perform a nonlinear least squares fit of the Ochi and Hubble six parameter heave model and the extended 10 parameter directional wave model to spectra produced by the ODGP hindcast numerical model. The necessary programs are documented here, including a description of the unit numbers addressed, subroutines used, with appropriate calling sequence, the arrays and variables assigned, and any necessary user interaction required. Author (CISTI)

N92-32787# Manitoba Univ., Winnipeg. Dept. of Electrical Engineering.
PHASED ARRAY IMPLEMENTATION USING ELEMENTS WITH SCAN CAPABILITY Final Report
H. A. Ragheb and L. Shafai Jun. 1989 150 p
(Contract DREO-055SS-W7714-8-5684)
(CTN-92-60335) Avail: CASI HC A07/MF A02

In phased arrays, antenna elements are normally simple radiators, and beam control is achieved by varying the relative phase of each element. To reduce the complexity of the array, the number of elements can be reduced but at the expense of grating lobes in the field of view. In this study, more complex array elements were used to steer a null on a grating lobe. These array elements operate with two azimuthal modes that are controlled in amplitude and phase. The method reduces the number of array elements by about 35 percent but adds additional phase shifters to the beam forming network to scan the element pattern. It is a useful method when the array is too large and the number of elements must be reduced. Its full potential may be achieved in arrays using monolithic microwave integrated circuit technology, where the beam forming network complexity can be overcome or when element phase shifters are too fine (4-bit or higher), and the reduction in their number lowers the cost and complexity of circuit implementation. A major advantage accrues to the method in arrays where an excessive scan angle is desired. In such cases a standard array suffers excessive gain loss. The dual mode elements provide enhanced gain away from broadside and consequently increase the array gain at large scan angles. Author (CISTI)

N92-32789# Telesat Canada, Ottawa (Ontario).
THE MSAT SPACECRAFT OF TELESAT MOBILE, INC.
E. Bertenyi 1990 10 p Presented at the CASI Sixth Conference on Aeronautics, Ottawa, Ontario, 19-21 Nov. 1990
(CTN-92-60346) Avail: CASI HC A02/MF A01

The Canadian MSAT system will offer a mobile telephone, radio, and data services. The last two will be offered via feederlink earth stations. The earth stations will use a 13 GHz Ku-band uplink and an L-band for downlink from the satellite to mobile earth terminals. User access will be controlled by a network control center. The basic service area of MSAT includes the part of Canada which is accessible from the geostationary orbit of 106.5 deg W as well as the continental USA. The satellite will have a minimum service life of ten years. The main elements of the communication subsystem are the antennas which include two large unfurlable L-band reflectors and their feed elements, the cross-polarized Ku-band antenna, the L-band and Ku-band receivers, the up-down converters each serving one antennal beam, and the Ku-band travelling wave tube amplifiers and L-band solid state power amplifiers. Voice and data services are expected to be available in 1994. CISTI

N92-32807# Ecole Nationale Superieure des Telecommunications, Paris (France).
ENHANCEMENTS TO SPEECH RECOGNITION ON VOICE RESPONSE SYSTEMS Ph.D. Thesis [CONTRIBUTIONS A LA RECONNAISSANCE DE LA POUR LES SERVEURS VOCAUX INTERACTIFS]
Luc Mathan 1991 140 p In FRENCH
(Telecom-91-E-018; ETN-92-92099) Avail: CASI HC A07/MF A02

A study on the reduction of recognitioon error rates for speech recognition systems is presented. A method for building a hierarchy of Hidden Markov Model (HMM) networks by clustering training speakers is introduced. In this hierarchy, a parent HMM network, trained with a parent set of speakers, generates 'specialized' HMM networks, each trained with a subset of the parent speaker set. A rejection procedure, which was verified beforehand by examining real data from several voice response systems with different types of dialogue, is introduced. The use of a simple threshold on the HMM recognition score is inefficient. The states of an HMM, however, hold crucial information about the likelihood of observing a given word. This information (duration in each state, mean frame

observed by each state, etc.) constitutes the trace of the HMM, and is of constant size, independently of the input uterence length. The trace is then classified into acceptance or rejection, by using multilayer perceptrons trained with examples taken from the voice response system in operation. This method yields better results than another rejection method, which uses a score threshold and three 'filler' HMMs, modeling extraneous speech. The most significant result is obtained by combining these two complementary methods. ESA

N92-32818# Defence Research Establishment, Ottawa (Ontario). Electronics Div.
COVERAGE STUDIES FOR SPACED-BASED RADAR
Suzanne Y. Maskell and Brian C. Eatock Aug. 1990 31 p
(DREO-90-18; CTN-92-60360) Avail: CASI HC A03/MF A01

The global air surveillance coverage available with constellations of space-based radar satellites was simulated. The number, altitude, the orbital phasing, and orbital inclination of the satellites were varied. Targets were placed at various latitudes to provide data on coverage as a function of latitude. Data is presented in terms of the length of time a target was visible to at least one satellite vs the length of time it could not be observed. Constellations of satellites having low altitudes of around 1000 km require high inclinations for effective coverage at high latitudes. A constellation of seven satellites at 1000 km altitude and 80 deg inclination gave nearly continuous coverage at the pole. At an altitude of 5000 km or more, continuous coverage of latitudes above 80 deg was achieved with a constellation of 4 satellites. Author (CISTI)

N92-32820# Technische Univ., Berlin (Germany, F.R.). Fachbereich Physik.
ON 5-DIMENSIONAL KALUZA-KLEIN THEORY Ph.D. Thesis [ZUR 5-DIMENSIONALEN KALUZA-KLEIN THEORY]
Jose A. Ferrari 1991 153 p Sponsored by German Academic Exchange Service
(ETN-92-92130) Avail: CASI HC A08/MF A02

The foundations of the Kaluza-Klein theory are reviewed. The aim is to formulate a realistic version of the theory, motivated by the belief that the five dimensional relativity provides the natural framework to search for a fifth force and to answer the question of unity of physics. Field equations are derived from a variation principle, and the equation of motion of a test particle in a combined gravitational and electromagnetic field is investigated. Continuous distribution of matter is considered and the five dimensional version of Raychaudhuri's equation is discussed. ESA

N92-32837# Technische Univ., Delft (Netherlands).
EFFECTS OF FADING AND INTERFERENCE IN NARROWBAND LAND-MOBILE NETWORKS Ph.D. Thesis [INVLOED VAN SIGNAALFLUCTUATIES EN INTERFERENTIE OP SMALBANDIGE LAND-MOBIELE NETWERKEN]
Johan Paul Marie Ger Linnartz 1991 433 p
(ISBN-90-9004491-4; ETN-92-92023) Copyright Avail: CASI HC A19/MF A04

The performance of mobile radio systems with narrowband radio channels is studied. Several results of previous research are included. In particular, the effects of multipath and shadow 'fading' and of mutual 'interference' between mobile users is investigated. To this end, initially the relevant propagation mechanisms are addressed, focusing on statistical channel models. For the planning of real systems, the suitability of some propagation models using terrain data is empirically evaluated. The statistical channel description is used to compute the performance of mobile radio links. Expressions are given for the outage probability and for the average duration of fades, taking account of mutual interference between users. A simplified model for the bit error rate in digital transmission is proposed. Numerical results are given for mobile telephone networks. ESA

N92-32891# Aerospace Corp., El Segundo, CA. Engineering and Technology Group.
PHASE-ONLY SYNTHESIS FOR MULTIPLE-BEAM PHASED ARRAYS WITH ELEMENT FAILURES
T. J. Peters 31 May 1992 40 p
(Contract F04701-88-C-0089)
(AD-A252250; TR-92(2930)-3; SSD-TR-92-09) Avail: CASI HC A03/MF A01

The problem of reducing beam overlap in a multiple-beam planar array is investigated. A planar array of point sources radiates three separate beams. By using only phase adjustments, the synthesis algorithm minimizes the sidelobe level of each beam in the vicinity of the other two main beams. The conjugate gradient method is used to solve the system of equations for the unknown phases on each radiator. GRA

N92-32899# Georgia Inst. of Tech., Atlanta. School of Electrical Engineering.
SIGNAL PROCESSING IN IMPULSIVE ELECTROMAGNETIC INTERFERENCE
Serena M. Zabin 30 Jun. 1992 6 p
(Contract N00014-91-J-1334)
(AD-A252385) Avail: CASI HC A02/MF A01

Statistical signal processing functions such as signal detection, estimation, and identification play a key role in the development of effective communications, radar, and sonar systems. For example, advanced statistical methods are emerging as being particularly important in digital communications systems operating in channels corrupted by interference from such phenomena as multiple-access noise, intentional jamming, and impulsive noise sources. Conventional demodulation methods, such as coherent matched filtering, often suffer serious performance degradation when subjected to interference of these types; however, this degradation can frequently be eliminated through the use of more sophisticated signal processing techniques. GRA

N92-32905# National Inst. for Fusion Science, Nagoya (Japan).
THE ROLE OF STOCHASTICITY IN SAWTOOTH OSCILLATION
A. J. Lichtenberg (California Univ., Berkeley.), Kimitaka Itoh, Sanae Itoh, and Atsushi Fukuyama Aug. 1991 80 p
(DE92-782004; NIFS-103) Avail: CASI HC A05/MF A01

We demonstrate that stochastization of field lines, resulting from the interaction of the fundamental m/n=1/1 helical mode with other periodicities, plays an important role in sawtooth oscillations. The time scale for the stochastic temperature diffusion was determined. It was shown to be sufficiently fast to account for the fast sawtooth crash, and is generally shorter than the time scales for the redistribution of current. The enhancement of the electron and ion viscosity, arising from the stochastic field lines, was calculated. The enhanced electron viscosity always leads to an initial increase in the growth rate of the mode; the enhanced ion viscosity can ultimately lead to mode stabilization before a complete temperature redistribution or flux reconnection has occurred. A dynamical model was introduced to calculate the path of the sawtooth oscillation through a parameter space of shear and of helical perturbation amplitude. The stochastic trigger to the enhanced growth rate and the stabilization by the ion viscosity are also included in the mode. A reasonable prescription for the flux reconnection at the end of the growth phase allows us to determine the initial q-value for the successive sawtooth ramps. DOE

N92-32965*# National Aeronautics and Space Administration. Lewis Research Center, Cleveland, OH.
SOLID STATE TECHNOLOGY BRANCH OF NASA LEWIS RESEARCH CENTER Fourth Annual Digest, Jun. 1991 - Jun. 1992
Aug. 1992 214 p
(RTOP 506-72-1B)
(NASA-TM-105752; E-7160; NAS 1.15:105752) Avail: CASI HC A10/MF A03

A collection of papers written by the members of the Solid State Technology Branch of NASA LeRC from Jun. 1991 - Jun. 1992 is presented. A range of topics relating to superconductivity, Monolithic Microwave Circuits (MMIC's), coplanar waveguides, and

material characterization is covered. For individual titles, see N92-32966 through N92-32984.

N92-32966*# National Aeronautics and Space Administration. Lewis Research Center, Cleveland, OH.
V-BAND PSEUDOMORPHIC HEMT MMIC PHASED ARRAY COMPONENTS FOR SPACE COMMUNICATIONS
G. L. Lan (Hughes Aircraft Co., Torrance, CA.), C. K. Pao (Hughes Aircraft Co., Torrance, CA.), C. S. Wu (Hughes Aircraft Co., Torrance, CA.), M. Hu (Hughes Aircraft Co., Torrance, CA.), and Alan N. Downey *In its* Solid State Technology Branch of NASA Lewis Research Center Aug. 1992 p 15-20 (For primary document see N92-32965 23-32)
(Contract NAS3-25088)
Avail: CASI HC A02/MF A03

Recent advances in pseudomorphic high-electron-mobility transistor (PMHEMT) monolithic microwave integrated circuit (MMIC) technology have made it the preferred candidate for high performance millimeter-wave components for phased array applications. The development of V-band PMHEMT/MMIC components including power amplifiers and phase shifters is described. For the single-stage MMIC power amplifier employing a 200 micron PMHEMT, we achieved 151.4 mW output power (757.0 mW/mm) with 1.8 dB associated gain and 26.4 percent power-added efficiency at 60 GHz. A two-stage MMIC amplifier utilizing the same devices demonstrated small-signal gain as high as 15 dB at 58 GHz. And, for the phase shifter, a four-bit phase shifter with less than 8 dB insertion loss from 61 to 63 GHz was measured. Author

N92-32967*# National Aeronautics and Space Administration. Lewis Research Center, Cleveland, OH.
PLANAR DIELECTRIC RESONATOR STABILIZED HEMT OSCILLATOR INTEGRATED WITH CPW/APERTURE COUPLED PATCH ANTENNA
Rainee N. Simons and Richard Q. Lee *In its* Solid State Technology Branch of NASA Lewis Research Center Aug. 1992 p 21-23 Previously announced as N92-18473 (For primary document see N92-32965 23-32)
Avail: CASI HC A01/MF A03

A design of an active antenna with a dielectric resonator stabilized high-electron-mobility transistor (HEMT) oscillator (DRO) and an aperture-coupled patch antenna is reported. The circuit is fabricated using coplanar waveguide (CPW) with the oscillator and the antenna on opposite sides of the substrate. The active antenna was demonstrated at 7.6 GHz; however, the design can be scaled to higher frequencies. Excellent oscillator characteristics and radiation patterns were obtained. Author

N92-32968*# National Aeronautics and Space Administration. Lewis Research Center, Cleveland, OH.
AN OPTICALLY CONTROLLED Ka-BAND PHASED ARRAY ANTENNA
R. R. Kunath, Richard Q. Lee, K. S. Martzaklis, K. A. Shalkhauser, Alan N. Downey, and Rainee N. Simons (Sverdrup Technology, Inc., Middleburg Heights, OH.) *In its* Solid State Technology Branch of NASA Lewis Research Center Aug. 1992 p 35-44 (For primary document see N92-32965 23-32)
Avail: CASI HC A02/MF A03

The design and development of a small, optically controlled phased array antenna suitable for communication satellite applications are discussed. A vertical integration architecture is used which minimizes the size of the array with its associated beamforming network (BFN). The antenna features a four-element linear microstrip array that uses aperture coupling of the antenna elements to the BFN; a modified Wilkinson power divider BFN; and 32 GHz, four-bit monolithic microwave integrated circuit (MMIC) phase shifters in customized quartz packages with corresponding optoelectronic interface circuits (OEIC's) for control signal reception. Author

N92-32969*# National Aeronautics and Space Administration. Lewis Research Center, Cleveland, OH.
Ka-BAND DUAL FREQUENCY ARRAY FEED FOR A LOW COST ACTS GROUND TERMINAL
Richard Q. Lee, Rainee N. Simons, and Ajit K. Sil *In its* Solid State Technology Branch of NASA Lewis Research Center Aug. 1992 p 55-60 Previously announced in IAA as A92-29833 (For primary document see N92-32965 23-32)
Avail: CASI HC A02/MF A03

Because of low cost and ease of fabrication, microstrip arrays are attractive as feeds for reflector antenna systems. The development of a 4 x 4 microstrip array which will be used as a feed for a low cost Advanced Communications Technology Satellite (ACTS) ground terminal is described. The array feed consisting of four 2 x 2 subarrays is fed with coplanar waveguide power dividing networks. The patch radiator is designed to excite two orthogonal, linearly polarized waves at Ka-band frequencies (around 20 and 30 GHz). Test results for the developed array are presented. Author

N92-32970*# National Aeronautics and Space Administration. Lewis Research Center, Cleveland, OH.
COPLANAR WAVEGUIDE FEEDS FOR PHASED ARRAY ANTENNAS
Rainee N. Simons (Sverdrup Technology, Inc., Brook Park, OH.) and Richard Q. Lee *In its* Solid State Technology Branch of NASA Lewis Research Center Aug. 1992 p 61-67 (For primary document see N92-32965 23-32)
Avail: CASI HC A02/MF A03

The design and performance of the following coplanar waveguide (CPW) microwave distribution networks for linear as well as circularly polarized microstrip patches and printed dipole arrays is presented: (1) CPW/microstrip line feed; (2) CPW/balanced stripline feed; (3) CPW/slotline feed; (4) grounded CPW (GCPW)/balanced coplanar stripline feed; and (5) CPW/slot coupled feed. Typical measured radiation patterns are presented, and their relative advantages and disadvantages are compared. Author

N92-32971*# National Aeronautics and Space Administration. Lewis Research Center, Cleveland, OH.
ANALYSIS OF SHIELDED CPW DISCONTINUITIES WITH AIR-BRIDGES
N. I. Dib (Michigan Univ., Ann Arbor.), P. B. Katehi (Michigan Univ., Ann Arbor.), and George E. Ponchak *In its* Solid State Technology Branch of NASA Lewis Research Center Aug. 1992 p 71-74 Repr. from MTT-S Digest (IEEE), Apr. 1991 p 469-472 (For primary document see N92-32965 23-32)
(Grant NSF ECS-86-57951)
Avail: CASI HC A01/MF A03

The effect of air-bridges on the performance of various coplanar waveguides (CPW) discontinuities is studied. Specifically, the coupled open-end CPW's and the short-end shunt CPW stub discontinuities are considered. The high frequency effect of the air-bridge is evaluated using a hybrid technique. At first, the frequency dependent equivalent circuit of the planar discontinuity without the air-bridge is derived using the Space Domain Integral Equation (SDIE) method. Then, the circuit is modified by incorporating the air-bridge's parasitic inductance and capacitance which are evaluated using a simple quasi-static model. The frequency response of each discontinuity with and without the air-bridge is studied and the scattering parameters are plotted in the frequency range 30-50 GHz for typical CPW dimensions. Author

N92-32972*# National Aeronautics and Space Administration. Lewis Research Center, Cleveland, OH.
A FLEXIBLE CPW PACKAGE FOR A 30 GHz MMIC AMPLIFIER
Rainee N. Simons and Susan R. Taub *In its* Solid State Technology Branch of NASA Lewis Research Center Aug. 1992 p 75-78 Previously announced as N92-23193 (For primary

document see N92-32965 23-32)
Avail: CASI HC A01/MF A03

A package, which consists of a carrier and housing, was developed for monolithic-millimeter wave integrated circuit amplifiers which operate at 30 GHz. The carrier has coplanar waveguide (CPW) interconnects and provides heat-sinking, tuning, and cascading capabilities. The housing provides electrical isolation, mechanical protection, and a feed-through for biasing. Author

N92-32973*# National Aeronautics and Space Administration. Lewis Research Center, Cleveland, OH.
A 1-W, 30-GHz, CPW AMPLIFIER FOR ACTS SMALL TERMINAL UPLINK
Susan R. Taub and Rainee N. Simons (Sverdrup Technology, Inc., Brook Park, OH.) *In its* Solid State Technology Branch of NASA Lewis Research Center Aug. 1992 p 79-82 Previously announced as N92-26096 (For primary document see N92-32965 23-32)
Avail: CASI HC A01/MF A03

The progress to date of the development of a 1-W, 30-GHz, coplanar waveguide (CPW) amplifier for the Advanced Communication Technology Satellite (ACTS) Small Terminal Uplink is described. The amplifier is based on Texas Instruments' monolithic microwave integrated circuit (MMIC) amplifiers; a three-stage, low-power amplifier and a single stage, high-power amplifier. The amplifiers have a power output of 190 mW and 0.710 W, gain of 23 and 4.2 dB, and efficiencies of 30.2 and 24 percent for the three-stage and one-stage amplifiers, respectively. The chips are to be combined via a CPW power divider/combiner circuit to yield the desired 1 W of output power. Author

N92-32974*# National Aeronautics and Space Administration. Lewis Research Center, Cleveland, OH.
COMPARATIVE EVALUATION OF OPTICAL WAVEGUIDES AS ALTERNATIVE INTERCONNECTIONS FOR HIGH PERFORMANCE PACKAGING
S. E. Schacham, Henri Merkelo, L.-T. Hwang, Bradley D. McCredie, Mark S. Veatch, and I. Turlik *In its* Solid State Technology Branch of NASA Lewis Research Center Aug. 1992 p 83-92 Repr. from Transactions on Components, Hybrids, and Manufacturing Technology (IEEE), v. 15, no. 1, Feb. 1992 p 63-72 (For primary document see N92-32965 23-32)
Avail: CASI HC A02/MF A03

A detailed comparison between optical and electrical interconnections is presented, with emphasis on advantages and drawbacks of optical link utilization. The impact of attenuation, dispersive degradation, and fan out on signal integrity is discussed. Reflections from discontinuities are taken into account in the section on fan out. According to our results, there is no obvious advantage of using optical interconnections for the distribution of digital signals containing significant frequency components in excess of 10 GHz, unless substantial distances are involved, for which low dispersion optical waveguides could provide a solution. The implementation of a polyimide optical waveguide in the MCNC package is discussed. Author

N92-32975*# National Aeronautics and Space Administration. Lewis Research Center, Cleveland, OH.
INTERMODULATION IN THE OSCILLATORY MAGNETORESISTANCE OF A TWO-DIMENSIONAL ELECTRON GAS **c33**
S. E. Schacham, E. J. Haugland, and S. A. Alterovitz *In its* Solid State Technology Branch of NASA Lewis Research Center Aug. 1992 p 105-110 Repr. from Physical Review B (American Physical Society), v. 45, no. 23, Jun. 1992 p 45-50 Sponsored in part by NAS-NRC (For primary document see N92-32965 23-32)
Avail: CASI HC A02/MF A03

The oscillatory magnetoresistance wave form of a 2-D electron gas shows multiple structures when two subbands are populated. In addition to high-field oscillations at a frequency equal to the sum of the two frequencies corresponding to the concentrations of the subbands, and to a superposition at intermediate fields, we observed oscillations at the difference frequency at low fields and higher temperatures. The field range at which the frequency difference is observed increases with increasing temperature. The crossover from superposition to frequency difference is accompanied by a beat. Similar beats, whose field location shows identical temperature dependence, can be observed in data obtained by other groups on different structures. The various components of the wave form can be attributed to different phase relations between the diagonal and off-diagonal elements of the conductivity tensor. It is shown how the intermodulation term, when inserted into the extended oscillatory equation, can give rise to all three structures. Author

N92-32976*# National Aeronautics and Space Administration. Lewis Research Center, Cleveland, OH.
REDUCED MOBILITY AND PPC IN In(.20)Ga(.80)As / Al(.23)Ga(.77)As HEMT STRUCTURE **c76**
S. E. Schacham (Technion - Israel Inst. of Tech., Haifa.), Rafael A. Mena, Edward J. Haugland, and Samuel A. Alterovitz *In its* Solid State Technology Branch of NASA Lewis Research Center Aug. 1992 p 111-116 Submitted for publication (For primary document see N92-32965 23-32)
Avail: CASI HC A02/MF A03

Transport properties of a pseudomorphic In(.20)Ga(.80)-As/Al(.23)Ga(.77)As High Electron Mobility Transistor (HEMT) structure were measured by Hall and SdH techniques. Two samples of identical structures but with different doping levels were compared. Low temperature mobility measurements as a function of concentration coincides with the onset of second subband occupancy, indicating that the decrease in mobility is due to intersubband scattering. In spite of the low Al content (23 percent), large persistent photoconductivity (PPC) was observed in the highly doped sample only, showing a direct correlation between the PPC and doping concentration of the barrier layer. Author

N92-32977*# National Aeronautics and Space Administration. Lewis Research Center, Cleveland, OH.
STUDY OF InGaAs-BASED MODULATION DOPED FIELD EFFECT TRANSISTOR STRUCTURES USING VARIABLE-ANGLE SPECTROSCOPIC ELLIPSOMETRY **c76**
Samuel A. Alterovitz, R. M. Sieg (Cleveland State Univ., OH.), H. D. Yao (Nebraska Univ., Lincoln.), P. G. Snyder (Nebraska Univ., Lincoln.), J. A. Woollam (Nebraska Univ., Lincoln.), J. Pamulapati (Michigan Univ., Ann Arbor.), P. K. Bhattacharya (Michigan Univ., Ann Arbor.), and P. A. Sekula-Moise (Spire Corp., Bedford, MA.) *In its* Solid State Technology Branch of NASA Lewis Research Center Aug. 1992 p 117-122 Repr. from Journal of Thin Solid Films (Lausanne, Switzerland, Elsevier Sequoia), no. 206, 1991 p 288-293 (For primary document see N92-32965 23-32)
Avail: CASI HC A02/MF A03

Variable-angle spectroscopic ellipsometry was used to estimate the thicknesses of all layers within the optical penetration depth of InGaAs-based modulation doped field effect transistor structures. Strained and unstrained InGaAs channels were made by molecular beam epitaxy (MBE) on InP substrates and by metal organic chemical vapor deposition on GaAs substrates. In most cases, ellipsometrically determined thicknesses were within 10 percent of the growth-calibration results. The MBE-made InGaAs strained layers showed large strain effects, indicating a probable shift in the critical point of their dielectric function toward the InP lattice-matched concentration. Author

N92-32978*# National Aeronautics and Space Administration. Lewis Research Center, Cleveland, OH.
MICROWAVE PROPERTIES OF PEELED HEMT DEVICES SAPPHIRE SUBSTRATES **c76**
Paul G. Young (Toledo Univ., OH.), Samuel A. Alterovitz, Rafael A. Mena, and Edwyn D. Smith (Toledo Univ., OH.) *In its* Solid State Technology Branch of NASA Lewis Research Center Aug. 1992 p 123-126 (For primary document see N92-32965

23-32)
Avail: CASI HC A01/MF A03

The focus of this research is to demonstrate the first full radio frequency characterization of high electron mobility transistor (HEMT) device parameters. The results of this research are used in the design of circuits with peeled HEMT devices, e.g. 10 GHz amplifiers. Devices were fabricated using two HEMT structures grown by molecular beam epitaxy methods. A 500 A AlAs release layer for 'peel off' was included under the active layers of the structure. The structures are a homogeneously doped Al(0.3)GA(0.7)As/GaAs and a delta doped square well Al(.23)Ga(.77)As/GaAs HEMT structure. Devices were fabricated using a mesa isolation process. Contacts were done by sequentially evaporating Au/Ge/Au/Ni/Au followed by rapid thermal anneal at 400 C for 15 seconds. Gates were wet etch recessed and 1 to 1.4 micron Ti/Au gate metal was deposited. Devices were peeled off the GaAs substrate using Apiezon wax to support the active layer and a HF:DI (1:10) solution to remove the AlAs separation layer. Devices were then attached to sapphire substrates using van der Waals bonding. Author

N92-32979*# Technion - Israel Inst. of Tech., Haifa. Dept. of Electrical Engineering.
A MODEL FOR THE TRAP-ASSISTED TUNNELING MECHANISM IN DIFFUSED n-p AND IMPLANTED n(+)-p HgCdTe PHOTODIODES c76
David Rosenfeld and Gad Bahir *In* NASA. Lewis Research Center, Solid State Technology Branch of NASA Lewis Research Center Aug. 1992 p 127-134 Repr. from Transactions on Electron Devices (IEEE), v. 39, no. 7, Jul. 1992 p 1638-1645 Previously announced in IAA as A92-46007 (For primary document see N92-32965 23-32)
Avail: CASI HC A02/MF A03

A theoretical model for the trap-assisted tunneling process in diffused n-on-p and implanted n(+)-on-p HgCdTe photodiodes is presented. The model describes the traps and the trap characteristics: concentration, energy level, and capture cross sections. We have observed that the above two types of diodes differ in the voltage dependence of the trap-assisted tunneling current and dynamic resistance. Our model takes this difference into account and offers an explanation of the phenomenon. The good fit between measured and calculated DC characteristics of the photodiodes (for medium and high reverse bias and for temperatures from 65 to 140 K) supports the validity of the model. Author

N92-32980*# National Aeronautics and Space Administration. Lewis Research Center, Cleveland, OH.
NASA SPACE APPLICATIONS OF HIGH-TEMPERATURE SUPERCONDUCTORS c76
Vernon O. Heinen, Martin M. Sokoloski (National Aeronautics and Space Administration, Washington, DC.), Paul R. Aron, and Kul B. Bhasin *In its* Solid State Technology Branch of NASA Lewis Research Center Aug. 1992 p 143-149 (For primary document see N92-32965 23-32)
Avail: CASI HC A02/MF A03

The application of superconducting technology in space has been limited by the requirement of cooling to near liquid helium temperatures. The only means of attaining these temperatures has been with cryogenic fluids which severely limits mission lifetime. The development of materials with superconducting transition temperatures (T sub c) above 77 K has made superconducting technology more attractive and feasible for employment in aerospace systems. Potential applications of high-temperature superconducting technology in cryocoolers and remote sensing, communications, and power systems are discussed. Author

N92-32981*# National Aeronautics and Space Administration. Lewis Research Center, Cleveland, OH.
MEASUREMENT TECHNIQUES FOR CRYOGENIC Ka-BAND MICROSTRIP ANTENNAS
M. A. Richard (Case Western Reserve Univ., Cleveland, OH.), Kul B. Bhasin, C. Gilbert (Ball Communication Systems Div., Broomfield, CO.), S. Metzler (Ball Communication Systems Div., Broomfield, CO.), and P. C. Claspy (Case Western Reserve Univ., Cleveland, OH.) *In its* Solid State Technology Branch of NASA Lewis Research Center Aug. 1992 p 151-157 Previously announced as N91-30426 (For primary document see N92-32965 23-32)
Avail: CASI HC A02/MF A03

The measurement of cryogenic antennas poses unique logistical problems since the antenna under test must be embedded in the cooling chamber. A method for measuring the performance of cryogenic microstrip antennas using a closed cycle gas-cooled refrigerator in a far field range is described. Antenna patterns showing the performance of gold and superconducting Ka-band microstrip antennas at various temperatures are presented.
Author

N92-32982*# National Aeronautics and Space Administration. Lewis Research Center, Cleveland, OH.
PERFORMANCE OF A Y-Ba-Cu-O SUPERCONDUCTING FILTER/GaAs LOW NOISE AMPLIFIER HYBRID CIRCUIT c33
Kul B. Bhasin, S. S. Toncich, C. M. Chorey (Sverdrup Technology, Inc., Brook Park, OH.), R. R. Bonetti (Communications Satellite Corp., Clarksburg, MD.), and A. E. Williams (Communications Satellite Corp., Clarksburg, MD.) *In its* Solid State Technology Branch of NASA Lewis Research Center Aug. 1992 p 163-165 Previously announced as N92-21370 (For primary document see N92-32965 23-32)
Avail: CASI HC A01/MF A03

A superconducting 7.3 GHz two-pole microstrip bandpass filter and a GaAs low noise amplifier (LNA) were combined into a hybrid circuit and characterized at liquid nitrogen temperatures. This superconducting/seismology circuit's performance was compared to a gold filter/GaAs LNA hybrid circuit. The superconducting filter/GaAs LNA hybrid circuit showed higher gain and lower noise figure than its gold counterpart. Author

N92-32983*# National Aeronautics and Space Administration. Lewis Research Center, Cleveland, OH.
MAGNETIC PENETRATION DEPTH OF YBa2Cu3O(7-DELTA) THIN FILMS DETERMINED BY THE POWER TRANSMISSION METHOD c76
Vernon O. Heinen, Felix A. Miranda, and Kul B. Bhasin *In its* Solid State Technology Branch of NASA Lewis Research Center Aug. 1992 p 201-204 (For primary document see N92-32965 23-32)
Avail: CASI HC A01/MF A03

A power transmission measurement technique was used to determine the magnetic penetration depth (lambda) of YBa2Cu3O(7-delta) superconducting thin films on LaAlO3 within the 26.5 to 40.0 GHz frequency range, and at temperatures from 20 to 300 K. Values of lambda ranging from 1100 to 2500 A were obtained at low temperatures. The anisotropy of lambda was determined from measurements of c-axis and a-axis oriented films. An estimate of the intrinsic value of lambda of 90 +/- 30 nm was obtained from the dependence of lambda on film thickness. The advantage of this technique is that it allows lambda to be determined nondestructively. Author

N92-32984*# National Aeronautics and Space Administration. Lewis Research Center, Cleveland, OH.
MAGNETIC FLUX RELAXATION IN YBa2Cu3O(7-x) THIN FILM: THERMAL OR ATHERMAL c76
Satish Vitta, M. A. Stan (Kent State Univ., OH.), Joseph D. Warner, and Samuel A. Alterovitz *In its* Solid State Technology Branch of NASA Lewis Research Center Aug. 1992 p 205-210 Repr. from Journal of Thin Solid Films (Lausanne, Switzerland, Elsevier Sequoia), no. 206, 1991 p 137-142 (For primary document see N92-32965 23-32)
(Grant NAG3-440751)
Avail: CASI HC A02/MF A03

The magnetic flux relaxation behavior of YBa2Cu3O(7-x) thin film on LaAlO3 for H parallel c was studied in the range of 4.2-40 k and 0.2-1.0 T. Both the normalized flux relaxation rate (S) and the net flux pinning energy (U) increase continuously from 1.3 x

10 exp -2 to 3.0 x 10 exp -2 and from 70-240 meV respectively, as the temperature (T) increases from 10 to 40 K. This behavior is consistent with the thermally activated flux motion model. At low temperatures, however, S is found to decrease much more slowly as compared with kT, in contradiction to the thermal activation model. This behavior is discussed in terms of the athermal quantum tunneling of flux lines. The magnetic field dependence of U, however, is not completely understood.

Author

N92-32987# Naval Postgraduate School, Monterey, CA.
SELECTING A SUBSET OF STIMULUS-RESPONSE PAIRS WITH MAXIMAL TRANSMITTED INFORMATION M.S. Thesis
Michael J. Sheehan Mar. 1992 135 p
(AD-A252728) Avail: CASI HC A07/MF A02

System designers are often faced with the task of assigning symbolic representations to user actions, e.g., icons to choices in graphical interfaces. When a confusion matrix--on discriminability of symbols--is available, it is used to guide the selection of the set of symbols to be implemented. While trial and error methods or clustering approaches have been used to analyze this problem, it was only recently that a true optimization approach was offered. Theise (1989) formulated the symbol selection problem as a zero-one integer programming problem whose objective function was linked to the minimization of within-subset confusion. Confusion is not the traditional metric used by human factors engineers to analyze confusion matrices. Rather, transmitted-information--a metric from information theory--has long been used to evaluate system performance. The purpose of this thesis is to formulate a model of subset selection in which transmitted information will be maximized. It is possible to specify a correct model, although current algorithms are incapable of solving it. This thesis reports on the performance of a GAMS-based approximation to the original model, as well as an exhaustive enumeration scheme. Solutions from both information-theoretic approaches are compared to solutions from the confusion/recognition model. GRA

N92-33143# Universiteit Twente, Enschede (Netherlands).
ANALOG CMOS FILTERS FOR VERY-HIGH FREQUENCIES Ph.D. Thesis
Bram Nauta 26 Sep. 1991 241 p Sponsored by Dutch Innovative Research Program
(ISBN-90-9004420-5; ETN-92-92037) Copyright Avail: CASI HC A11/MF A03

The design and fabrication of monolithically integrated, analog continuous time filters in metal oxide semiconductor (MOS) technology are addressed. The general design philisophy is to allow only the absolute minimum of signal carrying nodes throughout the whole filter. This strategy starts at the filter synthesis level and is extended to the level of electronic circuitry. The advantage of this technique is that high frequency parasitic effects are minimally present. The filters to be discussed have cutoff frequencies ranging from high frequencies (HF--low megahertz range) to very high frequencies (VHF--up to several hundreds of megahertz). Applications of these HF and VHF filters can be found in the field of communication and instrumentation systems, for example video frequency filters (0 to 6 MHz) or intermediate frequency filters (33 to 39 MHz) for television applications. ESA

N92-33152# Draper (Charles Stark) Lab., Inc., Cambridge, MA.
AN IMPLEMENTATION OF A FAULT-TOLERANT, MULTIDIRECTIONAL, DIGITAL INTERPOLATION BEAMFORMER M.S. Thesis - MIT
W. Brad Bogan Jun. 1992 120 p
(AD-A252494; CSDL-T-1131) Avail: CASI HC A06/MF A01

In recent years, methods of incorporating fault-tolerance in computer architectures have shifted from the exclusive focus on traditional modular redundancy techniques to include more efficient, analytical means of achieving the same result. Song and Musicus (1990) describe such a method of analytic fault-tolerance by using a statistical test and minimal redundancy to protect linear operations. Aliphas, Wei, and Musicus (1991) in turn developed a hardware prototype to test this method of statistical fault-tolerance. Using this hardware prototype, a multidirectional, digital interpolation sonar beamformer was implemented. Whereas the original prototype used multiple processors performing the same task on different input data, this implementation uses a different architecture whereby the same data is sent to multiple processors performing different tasks. The digital beamformer relaxes the sampling requirement typically required by sampling the incoming waveform at the Nyquist rate and upsampling to form the beam. Implementing the beamformer on the current architecture offered double fault detection and single fault correction capabilities across a range of look angles. In conjunction with previous results, the results of this thesis verify that the same fault detection and correction algorithm may be used for architectures both with processors performing different operations on the same data, and with processors performing the same operation on different data.

GRA

N92-33171 Department of the Navy, Washington, DC.
IMPULSE TRANSMITTER AND QUANTUM DETECTION RADAR SYSTEM Patent
Robert E. Jehle, inventor (to Navy) and David H. Hudson, inventor (to Navy) 10 Mar. 1992 7 p Filed 12 Apr. 1991
(AD-D015323; US-Patent-5,095,312; US-Patent-Appl-SN-687602; US-Patent-Class-342-21) Avail: US Patent and Trademark Office

Short duration pulses are radiated by an impulse radar transmitter. The time domain intervals are under control of a clock. The pulses are used to monitor a moving target. The target reflects echo pulses. The received echo pulses are measured by a quantum detector. The quantum detector determines the photon energy levels to supply signal data, which will be processed during the periods between the time domain intervals. GRA

N92-33172 Department of the Navy, Washington, DC.
TRANSMITTER LOCATION SYSTEM FOR FREQUENCIES BELOW HF Patent
Wallace D. Westfall, inventor (to Navy) 17 Dec. 1991 7 p Filed 26 Apr. 1972
(AD-D015325; US-Patent-5,073,784; US-Patent-Appl-SN-249443; US-Patent-Class-342-465) Avail: US Patent and Trademark Office

Differential phase measurement techniques and an apparatus for accurately locating unknown transmitters over great distances at radio frequencies below HF are presented. A network of separated, time- and phase-synchronized, pairs of receiving stations are discussed. The stations are comprised of vertical whip antennas that have a known base-line geometry. The antennas are used to accurately measure VLF phase differentials. The measured phase differences are compared against theoretical calculated values to provide highly accurate transmitter location information. GRA

N92-33191 Manitoba Univ., Winnipeg. Dept. of Electrical and Computer Engineering.
ELECTROMAGNETIC SCATTERING BY SYSTEMS OF ARBITRARILY ORIENTED SPHEROIDS Ph.D. Thesis
M. Francis R. Cooray May 1990 165 p
(ISBN-0-315-63332-8; CTN-92-60551) Copyright Micromedia Ltd., Technical Information Centre, 165 Hotel de Ville, Place du Portage, Phase 2, Hull, Quebec J8X 3X2, Canada HC/MF

An exact solution is obtained for the problem of scattering of electromagnetic waves by spheroids of arbitrary orientation. The solution is obtained in general by expanding the incident, scattered, and transmitted electromagnetic fields in terms of appropriate vector spheroidal eigenfunctions. The excitation is a monochromatic uniform plane electromagnetic wave of arbitrary polarization and angle of incidence. The boundary conditions at the surface of a given spheroid are imposed by using the rotational translational addition theorems for vector spheroidal wave functions which transfer the outgoing waves from all the other spheroids as incoming waves to the spheroid under consideration. Imposing the boundary conditions at the surfaces of each of n spheroids leads to a set of algebraic equations, the solution of which can be expressed in matrix form. It is possible to evaluate the unknown transmitted and scattered field expansion coefficients for a new

direction of incidence and for a different polarization without repeatedly solving a new set of equations. Numerical results are presented for the bistatic and backscattering cross sections for two prolate spheroids. An analytic solution to the problem of electromagnetic coupling between two spheroidal dipole antennas in an arbitrary configuration is also obtained. Author (CISTI)

N92-33192 Manitoba Univ., Winnipeg.
NUMERICAL ANALYSIS OF SCATTERING FROM CERTAIN CONDUCTING AND DIELECTRIC BODIES OF ARBITRARY SHAPE Ph.D. Thesis
Hamid Moheb 1990 163 p
(ISBN-0-315-63282-8; CTN-92-60552) Copyright Micromedia Ltd., Technical Information Centre, 165 Hotel de Ville, Place du Portage, Phase 2, Hull, Quebec J8X 3X2, Canada HC/MF

A numerical method is developed to study electromagnetic scattering from three dimensional geometries. Two orthogonal tangent vectors are defined on an object's surface. Along one, the surface currents are represented by discrete triangular basis functions, and along the other, the surface currents are represented by a finite set of entire domain basis functions. Two different techniques are adopted to enable the latter expansion: coordinate transformation and direct use of Fourier type basis functions. The developed methods are then extended to treat dielectric geometries of arbitrary shape. The surface integral equations are formulated in terms of the equivalent electric and magnetic currents over the object's surface. The surface currents are obtained from the tangential components of the fields and related to the integral operators of the conducting objects. The resulting integral equations are solved similarly. Finally, the developed techniques are also applied to antenna problems, in particular, they are applied to the radiation from rectangular waveguides. An x-directed dipole is used as a source of excitation and the radiation characteristics of the rectangular waveguides are determined. Author (CISTI)

N92-33206 Carleton Univ., Ottawa (Ontario). Dept. of Electronics.
A DIGITAL IMPLEMENTATION OF A RADAR COHERENT-ON-RECEIVE SYSTEM M.S. Thesis
M. C. Fernando Sep. 1989 178 p
(ISBN-0-315-59028-9; CTN-92-60545) Copyright Micromedia Ltd., Technical Information Centre, 165 Hotel de Ville, Place du Portage, Phase 2, Hull, Quebec J8X 3X2, Canada HC/MF

A digital coherent-on receive subsystem was designed, built, and tested in order to provide coherent-on receive operation for pulsed radar systems employing incoherent magnetron transmitters. The design used two finite impulse response filters, which extracted the coherent phase from the return signal by performing a matched filter operation between the transmit and receive signals. The phase locking characteristics of this subsystem were evaluated using a magnetron transmitter, and its performance was compared with that of a conventional coherent oscillator (COHO) which was tested in a similar fashion. Results indicate that in a nonchirped environment, the performance of the digital technique is comparable to that obtained with the COHO, while the possibility of it displaying superior performance in a highly chirped scenario exists. Author (CISTI)

N92-33207 Carleton Univ., Ottawa (Ontario). Dept. of Systems and Computer Engineering.
PERFORMANCE ANALYSIS OF SPACE-BASED RADAR TRACKING TECHNIQUES M.S. Thesis
Richard Jerome 6 Jul. 1990 179 p
(ISBN-0-315-60464-6; CTN-92-60546) Copyright Micromedia Ltd., Technical Information Centre, 165 Hotel de Ville, Place du Portage, Phase 2, Hull, Quebec J8X 3X2, Canada HC/MF

The performances of the nearest neighbor standard filter (NNSF) and of the probabilistic data association filter (PDAF) were analyzed in the context of a space-based radar (SBR) application. Computer simulation experiments where the SBR/target geometry and the clutter environment were allowed to vary were performed. The presence of false measurements in the early stages of tracking significantly affects the performance of the NNSF, whereas the PDAF achieves adequate performance. This is particularly relevant to the case where tracking is initiated at low grazing angles. Typical track position estimate root mean square errors are of the order of a kilometer due to the large target range values involved. Extrapolation of the track estimate over a long coverage gap time, as may be the case in the SBR application, significantly affects the tracking accuracy of both filters and may lead to loss of the track. Author (CISTI)

N92-33209 Carleton Univ., Ottawa (Ontario). Dept. of Electronics.
TECHNIQUES FOR THE SYNTHESIS OF WIDEBAND, SERIES-FED ARRAYS OF MICROSTRIP PATCH RADIATORS Ph.D. Thesis
Peter C. Strickland Aug. 1989 259 p
(ISBN-0-315-58991-4; CTN-92-60548) Copyright Micromedia Ltd., Technical Information Centre, 165 Hotel de Ville, Place du Portage, Phase 2, Hull, Quebec J8X 3X2, Canada HC/MF

Two principal aspects of the design of microstrip radiator arrays are investigated: new broadband pattern synthesis techniques, and individual radiators or subarrays having increased bandwidth. One new pattern synthesis technique allows the power pattern to be optimized in a least mean square error sense over the desired operating band of the array. Another synthesis approach is a numerical optimization whereby the sum of the pattern errors at several discrete frequencies is minimized. This allows different limits on pattern error to be imposed on different regions, thus optimally tailoring the pattern to a given application. Computer program listings for these synthesis and optimization methods are included. A technique for synthesis of broadband radiating elements is also presented. This approach requires that a radiating element or subarray be broken up into multiple electrically coupled resonators allowing the quality factor and resonant frequency of each to be specified for the desired bandpass characteristic. A second approach focuses on making the elements non-resonant by periodically loading the high-impedance sections such that their characteristic impedance matches that of the low-impedance sections. Alternatively, the substrate thickness may be varied along the array such that the characteristic impedance remains constant. Author (CISTI)

N92-33213 Queens Univ., Kingston (Ontario).
DEVELOPMENTS IN THE THEORY OF CANTOR-TYPE VARIABLES WITH APPLICATION TO COMMUNICATIONS OVER FADING CHANNELS Ph.D. Thesis
Wendy Sarah Smith Aug. 1990 222 p
(ISBN-0-315-61378-5; CTN-92-60567) Copyright Micromedia Ltd., Technical Information Centre, 165 Hotel de Ville, Place du Portage, Phase 2, Hull, Quebec J8X 3X2, Canada HC/MF

A mathematical theory of signal dependent interferences is presented and applied to problems of digital communications over fading, noisy channels. The weighted sum of an infinite sequence of independent binary random variables has a Cantor-type distribution, provided the weights asymptotically decay exponentially and sufficiently rapidly. For an arbitrary number of Cantor-type random variables, the joint probability distribution function is derived. The expected value with respect to such a distribution is evaluated for any continuous function with continuous first partial derivatives. The N-dimensional characteristic function is also obtained. In the context of communications, the binary variables represent digital data and the weighting factors correspond to samples of the system response function. As such, the theory is applicable to problems involving intersymbol, adjacent, and co-channel interferences. Exact expressions for performance measures, such as probability of error, can be obtained. Several systems suitable for satellite to mobile communication are studied. The probabilities of error for detection of frequency or phase shift keying with different kinds of filtering are evaluated. Offset quadrature phase shift keying is shown to have the best performance on the basis of power and bandwidth efficiency.
CISTI

N92-32964*# Applied Acoustic Research, State College, PA.
A LIGHTWEIGHT LOUDSPEAKER FOR AIRCRAFT COMMUNICATIONS AND ACTIVE NOISE CONTROL
Glenn E. Warnaka, Mark Kleinle (Oxford Speaker Co., Chicago, IL.), Parry Tsangaris (Oxford Speaker Co., Chicago, IL.), Michael J. Oslac (Oxford Speaker Co., Chicago, IL.), and Harry J. Moskow (Oxford Speaker Co., Chicago, IL.) *In* NASA. Langley Research Center, Fourth Aircraft Interior Noise Workshop Jul. 1992 p 316-327 (For primary document see N92-32948 23-71)
Avail: CASI HC A03/MF A03

33 ELECTRONICS AND ELECTRICAL ENGINEERING

Includes test equipment and maintainability; components, e.g., tunnel diodes and transistors; microminiaturization; and integrated circuitry.

For related information see also *60 Computer Operations and Hardware* and *76 Solid-State Physics*.

N92-32243*# National Aeronautics and Space Administration. Lewis Research Center, Cleveland, OH.
SOLAR RADIATION ON A CATENARY COLLECTOR
M. Crutchik (Tel-Aviv Univ., Israel) and J. Appelbaum Jul. 1992 32 p
(Grant NAGw-2022; RTOP 506-41-11)
(NASA-TM-105751; E-7156; NAS 1.15:105751) Avail: CASI HC A03/MF A01

A tent-shaped structure with a flexible photovoltaic blanket acting as a catenary collector is presented. The shadow cast by one side of the collector produces a shadow on the other side of the collector. This self-shading effect is analyzed. The direct beam, the diffuse, and the albedo radiation on the collector are determined. An example is given for the insolation on the collector operating on Viking Lander 1 (VL1). Author

N92-32325# Maryland Univ., College Park. Dept. of Electrical Engineering.
PULSE CODED BIOLOGICALLY MOTIVATED NEURAL-TYPE MOS CIRCUITS Final Report, 1 Nov. 1989 - 31 Mar. 1992
29 Apr. 1992 4 p
(Contract N00014-90-J-1114)
(AD-A250367) Avail: CASI HC A01/MF A01

VLSI designs of SYNETSIM Modules and their extensions VLSI Designs for the major pools of SYNETSIM were made and MOSIS fabrications carried out. From these, some new elements were designed and in most cases fabricated via MOSIS, the key ones being a neural type arithmetic unit, and adjustable MOSFET transistor convenient for weight setting, and considerable improvement in the neural type cell being used in many of our pulse coded networks. Because capacitors take a large amount of the VLSI chip area, a new capacitance multiplier was designed and fabricated. Using the pools a realization for ART1 memories was obtained. Means for realizing long term potentiation were investigated which are leading to a new concept of memory based upon the pools and their incorporation of second messenger effects. GRA

N92-32495# Westinghouse Savannah River Co., Aiken, SC.
SYSTEM RESPONSE TO RELAY CHATTER
G. A. Antaki and J. A. Radder 1992 5 p Presented at the ASME Pressure Vessel and Piping Conference, New Orleans, LA, 21-25 Jun. 1992
(Contract DE-AC09-89SR-18035)
(DE92-013076; WSRC-MS-92-124; CONF-920631-21) Avail: CASI HC A01/MF A01

An important aspect of the qualification of safety related systems is the assessment of the possibility and consequences of seismic or vibration induced relay chatter. The current rules, contained in ANSI/IEEE C37.98 and the SQUG GIP, consider as seismic induced 'failure' of a relay, a chatter contact in excess of 2 milliseconds. While this rule is clear in defining 'failure' of single relay, the definition of 'failure' becomes more problematic when we consider the alignment of an assembly of relays in series or parallel, and the effects of chatter on the function of the system in which the relays are mounted. In this paper, we report a method, based on system test and probabilities analysis, used to assess 'failure' by relay chatter in an assembly of relays which control an electric motor. DOE

N92-32635# Brookhaven National Lab., Upton, NY.
LIFE TESTING OF A LOW VOLTAGE AIR CIRCUIT BREAKER
M. Subudhi and S. Aggarwal (Nuclear Regulatory Commission, Washington, DC.) 1992 19 p Presented at the Aging Research Information Conference, Rockville, MD, 24-27 Mar. 1992
(Contract DE-AC02-76CH-00016)
(DE92-014173; BNL-NUREG-47471; CONF-920375-15) Avail: CASI HC A03/MF A01

A DS-416 low voltage air circuit breaker manufactured by Westinghouse was mechanically cycled to identify age-related degradation in the various breaker subcomponents, specifically the power-operated mechanism. This accelerated aging test was performed on one breaker unit for over 36,000 cycles. Three separate pole shafts, one with a 60-degree weld, one with a 120-degree weld, and one with a 180-degree weld in the third pole lever were used to characterize cracking in the welds. In addition, during the testing three different operating mechanisms and several other parts were replaced as they became inoperable. Among the seven welds on the pole shaft, number 1 and number 3 were found to be critical ones whose fracture can result in misalignment of the pole levers. This can lead to problems with the operating mechanism, including the burning of coils, excessive wear in certain parts, and overstressed linkages. Furthermore, the limiting service life of a number of subcomponents of the power-operated mechanism, including the operating mechanism itself, were assessed. Based on these findings, suggestions are provided to alleviate the age-related degradation that could occur as a result of normal closing and opening of the breaker contacts during its service life. Also, cause and effect analyses of various age-related degradation in various breaker parts are discussed. DOE

N92-32639# Argonne National Lab., Idaho Falls, ID.
DEVELOPMENT OF HIGH-PERFORMANCE Na/NiCl2 CELL
L. Redey, D. R. Vissers, K. M. Myles, and J. Prakash 1992 3 p Presented at the 35th International Power Sources Symposium, Cherry Hill, NJ, 22-25 Jun. 1992
(Contract W-31-109-eng-38)
(DE92-015270; ANL/CP-75875; CONF-920669-6) Avail: CASI HC A01/MF A01

The performance of the Ni/NiCl2 positive electrode for the Na/NiCl2 battery has been significantly improved by lowering the impedance and increasing the usable capacity through the use of chemical additives and a tailored electrode morphology. The improved electrode has excellent performance even below 200 C and can be recharged within one hour. The performance of this new electrode was measured by a conventional galvanostatic method and by a newly developed 'powerdynamic' method. These measurements were used to project the performance of 40 to 60-kWh batteries built with this new electrode combined with already highly developed sodium/beta-alumina negative electrode. These calculated results yielded a specific power of 150-400 W/kg and a specific energy of 110-200 Wh/kg for batteries with single-tube and bipolar cell designs. This high performance, along with the high cell voltage, mid-temperature operation, fast recharge capability, and short-circuited failure mode of the electrode couple, makes the Na/NiCl2 battery attractive for electric vehicle applications. DOE

N92-32659# State Univ. of New York, Buffalo.
WORKSHOP ON RESEARCH NEEDS AND OPPORTUNITIES IN HIGH TEMPERATURE SUPERCONDUCTIVITY Final Report, 1 Jun. 1991 - 30 Apr. 1992
David T. Shaw, H. Kroger, S. Jin, D. U. Gubser, and C. M. Falco Nov. 1991 38 p Workshop held in Copper Mountain, CO,

19-20 Aug. 1991
(Contract N00014-91-J-4036)
(AD-A252674) Avail: CASI HC A03/MF A01

This is the report of the Workshop on New Research Opportunities in Superconductivity held at Copper Mountain, Colorado on August 19-20, 1991. The workshop is a follow-up to two previous meetings to evaluate progress in superconductivity. The first, held at Copper Mountain, Colorado in 1983, focuses on low-temperature superconductors (LTS), while the second in 1988 examined the progress of low-temperature materials and the potential of the then recently-discovered high-temperature superconductors (HTS). This workshop was the first in this series to concentrate largely on high-temperature superconductors. Its objectives were to identify the barriers limiting progress in high-temperature materials and to assess research areas that are ripe for important advances. The workshop was organized in four sessions: fundamentals, materials, thin films and devices, and bulk materials and large-scale applications. GRA

N92-32669# Cornell Univ., Ithaca, NY. Lab. of Atomic and Solid State Physics.
HIGH TRANSLATIONAL ENERGY INDUCED REACTION IN SEMICONDUCTORS Final Report, 1 Aug. 1988 - 30 Nov. 1991
Wilson Ho 5 May 1992 8 p
(Grant AF-AFOSR-0335-88)
(AD-A250980; AFOSR-92-0445TR) Avail: CASI HC A02/MF A01

The main objectives of this project are to develop novel instrumentation and to understand bond breaking and formation on semiconductor surfaces. The approaches used in achieving these objectives are to determine the dependence of adsorption on the translational and vibrational energies of incident molecules and to investigate energy exchange at surfaces. The systems which have been investigated in detail are the dissociative adsorption of carbon dioxide and the nondissociative adsorption of ethane on silicon surface. For these experiments a unique differentially pumped, time-resolved spectrometer, a molecular beamline, and a ultrahigh vacuum chamber with surface instrumentation were designed and constructed. GRA

N92-32678# Massachusetts Inst. of Tech., Lexington.
MULTICHIP MODULE STUDY
V. J. Sferrino 20 Mar. 1992 61 p
(Contract F19628-90-C-0002)
(AD-A250877; UMICH-TR-945; ESD-TR-91-238) Avail: CASI HC A04/MF A01

Multichip module (MCM) technology addresses the large gap that exists between the speed and circuit densities achieved in monolithic integrated circuits versus those achieved at the board and subsystem level using conventional through-hole and surface mount package technology. Multichip modules promise not only to improve board-level circuit densities but also to support dramatic increases in clock rate and reductions in overall power dissipation. This new technology is driven by the realization that current printed circuit board technologies are inadequate to achieve the speed and system throughput capabilities inherent in the chips that are now becoming available. Multichip module technology centers on the high-density interconnection of bare die on a suitable substrate, resulting in a module with up to 95 percent of the substrate area devoted to active circuits. The technology features substrates that are generally made of silicon or ceramic with insulating layers of polyimide. Various other materials are employed by a host of vendors, and the technology, which is available now, is continuing to mature at a rapid rate. MCM technology is supplanting printed circuit board technology for most high-performance applications and will provide a vehicle for leading-edge digital systems in the 1990s. GRA

N92-32700# Ballistic Research Labs., Aberdeen Proving Ground, MD.
A TEST CIRCUIT FOR CAPACITOR BANK GROUNDING STICKS
C. R. Hummer, K. A. Mahan, and C. E. Hollandsworth Jun. 1992
21 p
(DA Proj. 1L1-61102-AH-43)
(AD-A251121; BRL-MR-3980) Avail: CASI HC A03/MF A01

After completion of a charge-discharge cycle, energy-storage capacitor banks must be shorted to ground and the short maintained before the bank can be safely approached by an operator. It is essential that the grounding stick used by the operator to drain any residual charge have a proper electrical resistance. A test unit has been constructed and tested which checks the grounding circuit for proper resistance and provides a visual indication of its status. This unit also includes an auxiliary circuit which sounds an audible warning when an excessive current passes through the grounding circuit. The enhanced measure of safety which such a circuit could provide is illustrated by discussion of a recent capacitor-bank accident at Aberdeen Proving Ground, MD. GRA

N92-32754# Hawaii Univ., Manoa. Natural Energy Inst.
UHM/HNEI EV TEST AND EVALUATION PROGRAM
Mar. 1992 25 p
(Contract DE-FC07-79NV-10031)
(DE92-011631; DOE/NV-10031/T1) Avail: CASI HC A03/MF A01

The electric vehicle (EV) program of the Hawaii Natural Energy Institute (HNEI) focuses primarily on the field testing of promising EV/traction batteries. The intent is to utilize typical driving cycles to develop information that verifies or refutes what is obtained in the laboratory. Three different types of batteries were assigned by the U.S. DOE for testing in this program: Sonnenschein Dryfit 6V-160, Exide GC-5, Trojan T-145. We added the following battery to the test program: ALCO2200. The following EVs were chosen in our program: Converted Ford Escort station wagon, Converted Ford Escort two-door sedan, Converted Ford Escort two-door sedan, Converted Dodge van. Based on capacity tests, corrective action such as battery replacement, additional charging, adjusting terminal connections, etc., may be taken to maintain good performance. About 15,500 miles and 600 cycles have been accumulated on the Sonnenschein Dryfit 6V-160 battery pack. Five of its 18 modules have been changed. Based on DOE's standard, the battery has reached the end of its useful life. Nevertheless, the battery pack is still operational and its operating range is still greater than 40 miles per charge. It is too early to evaluate the life expectancy of the other three batteries. No module has been replaced in these three packs. HNEI will keep the Trojan and Exide battery packs in operation. The Alco 2200 batteries will be transferred to another vehicle. DOE

N92-32777# Laboratoire d'Automatique et d'Analyse des Systemes, Toulouse (France).
A DISCRETE NONLINEAR MODEL APPROACH TO STUDY THE BEHAVIOR OF LARGE SIGNAL DC TO DC CONVERTERS Ph.D. Thesis - Toulouse Univ. [ETUDE DU COMPORTEMENT A FORT SIGNAL DES CONVERTISSEURS CONTINU-CONTINU APPROCHE PAR UN MODELE DISCRET NONLINEAIRE]
Jose Luis GarciadeVicuna (Universidad Politecnica de Cataiunya, Spain) 1992 132 p In FRENCH
(LAAS-90028; ETN-92-91676) Avail: CASI HC A07/MF A02

The study of large switching DC-DC converters behavior when in the presence of large amplitude perturbations, either in the load, in the input voltage, or in the reference, is addressed. In this case linear methods are insufficient to analyze regulators behavior, thus they are not able to lead to an accurate conception of the control loop. A nonlinear discrete model of the power stages is obtained starting from the system state variable partition in two subsets, one corresponding to the fast variation components and the other to the slow variation ones. This model is linearized to obtain transfer functions for the current-voltage converters. The results obtained are compared with those of the state space averaging method. A nonlinear approach was utilized for the representation of trajectories in the state space, in order to obtain global stability criteria in large signal operation. The conception criteria of a regulator and those of an associated loop control are thus stated to guarantee asymptotic stability. Bearing in mind all

these criteria, a simulation program was developed, comparing the results obtained from the simulation with the experimental results. As a conclusion, a nonlinear discrete model for DC-DC converters is proposed. Its use in different examples made possible the control loop design, an aim which cannot be achieved by means of linear models. ESA

N92-32793# Laboratoire d'Automatique et d'Analyse des Systemes, Toulouse (France).
A CONTINUOUS NONLINEAR MODEL APPROACH TO STUDY THE BEHAVIOR OF LARGE SIGNAL DC TO DC CONVERTERS Ph.D. Thesis - Toulouse Univ. [ETUDE DU COMPORTEMENT A FORT SIGNAL DES CONVERTISSEURS CONTINU-CONTINU APPROCHE PAR UN MODELE CONTINU NON LINEAIRE]
Francisco Guinjoan (Universidad Politecnica de Catalunya, Spain) 1992 131 p In FRENCH
(LAAS-90027; ETN-92-91677) Avail: CASI HC A07/MF A02

The study of signal switching DC-DC converters behavior is addressed. Given the fact that the linear methods cannot be used in this case, a nonlinear model was developed. The power stage nonlinear continuous model, which can be applied in both conduction modes (continuous and discontinuous), is obtained from the partition of the characteristic state vector variables in two subsets. This method is applied to the elementary switching cells (buck, boost, and buck-boost) and Cuk converter. It is oriented to the fast numerical simulation by means of general purpose simulation programs. Different results from numerical simulations, confirming the accuracy of the method used, either in an open loop or in a closed loop, are obtained, provided the validity of its domain is respected. The nonlinear model linearization made it possible to obtain equivalent transmittances for the DC-DC converters. Its application to a boost converter operating in the discontinuous condition mode at variable frequency rate enables the comparison of the obtained results with other existing methods and equivalence between the two of them to be easily established. The revision of the initial hypothesis leads to the establishment of a small signal model valid in the high frequency domain and to the results obtained being derived in a more systematic way. A model for switching DC-DC converters is given. Its validity is established, whatever its order and conduction modes, either in an open loop or a closed loop. ESA

N92-32810# Communications Research Centre, Ottawa (Ontario).
A 19.2 GHz COOLED HEMT LOW NOISE AMPLIFIER
B. Clarke and J. Bradley Jun. 1990 59 p
(CTN-92-60354) Avail: CASI HC A04/MF A01

The objective of this project was to develop a breadboard 20 GHz low noise amplifier (LNA) capable of remote operations. The resulting system was to have very low power consumption. The frequency was chosen to correspond to the EHF transponder package of the European Space Agency's Olympus satellite. A 19.2 GHz cooled low-noise amplifier was developed utilizing high electron mobility transistors (HEMTs) and quartz substrate in a conventional microstrip format. Cooling was provided with thermoelectric devices and a 1.98 dB noise figure with 15 dB associated gain were achieved at 19.2 GHz. The noise figure over the 18.85 to 19.55 frequency band was under 2.2 dB. Two approaches were implemented, one in which the entire LNA module was cooled and a second in which only the HEMT chips were cooled. Author (CISTI)

N92-32812# Department of National Defence, Ottawa (Ontario). Research and Development Branch.
LITHIUM SULPHUR DIOXIDE BATTERY FAILURE FOLLOWING HIGH FREQUENCY VIBRATION
George J. Donaldson and Walter J. Moroz Mar. 1990 36 p
(CRAD-1-90; CTN-92-60361) Avail: CASI HC A03/MF A01

Lithium/sulfur dioxide batteries have several properties which suit them for use as personal locator beacons, such as: high cell voltage, flat voltage-time profile on load, fast activation on load even at low temperatures, excellent performance at -40 C, high energy density, and long shelf life. Progress toward an Li/SO2 battery system for a search and rescue beacon was impeded when explosions took place during high frequency vibrations tests on a prototype unit. The severity of the vibrational environment caused internal cell damage which weakened or detached the lithium electrode where it had been cold welded to the can. During discharge, individual cells having this defect exhibit a loss of voltage followed by venting and subsequent explosion of the battery. Manufacturing improvements to the lithium to can weld, coupled with battery design features aimed at damping out vibrational effects were successful in preventing this type of hazard. CISTI

N92-32823# Stuttgart Univ. (Germany, F.R.). Inst. fuer Plasmaforschung.
DETECTORS FOR LIDAR TYPE THOMSON SCATTERING DIAGNOSTICS
Kurt Hirsch Apr. 1991 25 p Presented at the IAEA Technical Committee Meeting in Lidar Thomson Scattering, Abingdon, England, 8 -10 Apr. 1991
(IPF-91-5; ETN-92-92155) Avail: CASI HC A03/MF A01

A report on the capability of a type of Microchannel Plate Photomultiplier (MCP) is presented. Detailed investigation on time response, low noise amplification, shutter ratio, gating behavior, linear mode of operation, and saturation pulse recovery carried out during the design phase for LIDAR ruby laser system are presented. New investigation with respect to DC and gated operation showed no measurable changes in sensitivity of this MCP photomultiplier. By comparing this type of detector with other MCP photomultipliers and with streak cameras, some detection schemes for future LIDAR type diagnostic are proposed. ESA

N92-32827# North Carolina Univ., Chapel Hill. Dept. of Chemistry.
THE RESPONSE OF THE DOUBLE LAYER CAPACITANCE OF A HIGH TEMPERATURE SUPERCONDUCTOR/FLUID ELECTROLYTE INTERFACE TO THE ONSET OF SUPERCONDUCTIVITY
S. R. Peck, L. S. Curtin, J. T. McDevitt, R. W. Murray, and J. P. Collman Apr. 1992 23 p
(Contract N00014-90-J-1230)
(AD-A251172; TR-53) Avail: CASI HC A03/MF A01

Measurements of interfacial double layer capacitance and charge transfer resistance have been made as a function of temperature at fluid electrolyte interfaces with electrodes made from two different TI-based high temperature superconductor (HTSC) materials. Measurements spanning the 112 and 119 K superconducting transition temperatures, Tc, of the HTSC electrodes, reveal a smooth decrease in double layer capacitance with decreasing temperatures, except that an abrupt, ca. one degree wide change in the shape of the double layer capacidance vs. temperature curve occurs at the Tc of the electrode. These are the first data which show that the onset of superconductivity can be reflected in a chemical phenomenon at a molecular fluid/HTSC interface. Of the several contributors to interfacial capacitance, it is hypothesized that alteration in charge carrier distribution or polarizability over the outermost electrode lattice layer as electron pairs start to appear at Tc is the most likely origin of the Tc-correlated capacitance feature. Alterations in the charge transfer resistance for electrochemical solvent reduction appear over the same temperature interval as the capacitance feature, but not as consistently. GRA

N92-32847# Canadian Astronautics Ltd., Ottawa (Ontario).
CONTINUATION OF THE DEVELOPMENT OF A MILLIMETER WAVE WIDEBAND TUNABLE WAVEGUIDE VOLTAGE CONTROLLED OSCILLATOR Final Report
A. Mascioli May 1990 131 p
(Contract DSS-W7714-8-5705-01-ST)
(CAL-504-88P120; CTN-92-60355) Avail: CASI HC A07/MF A02

A waveguide voltage controlled oscillator (VCO) was designed for use in the 26 GHz to 40 GHz range. The VCO uses a novel approach involving a double radial line concept to provide tuning bandwidths in excess of 3 GHz at these frequencies. The system

was modelled via an equivalent circuit and the various parameters influencing performance, particularly the tuning range, were analyzed. Software simulation of the system was developed to predict the behavior of the circuit. The simulation package allows for verification of assumptions made during the development of the equivalent circuit. Results obtained from the simulation are in agreement with those obtained experimentally. The simulation also verified that the Gunn diode capacitance and resistance exist within a certain known range. Their exact values must be determined empirically. Author (CISTI)

N92-32867*# National Aeronautics and Space Administration. Lewis Research Center, Cleveland, OH.

OVERVIEW AND EVOLUTION OF THE LeRC PMAD DC TESTBED

James F. Soeder and Robert J. Frye Aug. 1992 10 p Presented at the 27th Intersociety Energy Conversion Engineering Conference, San Diego, CA, 3-7 Aug. 1992; sponsored by ANS, SAE, ACS, AIAA, ASME, and IEEE
(RTOP 474-42-10)
(NASA-TM-105842; E-7285; NAS 1.15:105842) Avail: CASI HC A02/MF A01

Since the beginning of the Space Station Freedom Program (SSFP), the Lewis Research Center (LeRC) has been developed electrical power system test beds to support the overall design effort. Through this time, the SSFP has changed the design baseline numerous times, however, the test bed effort has endeavored to track these changes. Beginning in August 1989 with the baseline and an all DC system, a test bed was developed to support the design baseline. The LeRC power measurement and distribution (PMAD) DC test bed and the changes in the restructure are described. The changes includeed the size reduction of primary power channel and various power processing elements. A substantial reduction was also made in the amount of flight software with the subsequent migration of these functions to ground control centers. The impact of these changes on the design of the power hardware, the controller algorithms, the control software, and a description of their current status is presented. An overview of the testing using the test bed is described, which includes investigation of stability and source impedance, primary and secondary fault protection, and performance of a rotary utility transfer device. Finally, information is presented on the evolution of the test bed to support the verification and operational phases of the SSFP in light of these restructure scrubs. Author

N92-33011* National Aeronautics and Space Administration. Pasadena Office, CA.

VLSI ARCHITECTURE FOR A REED-SOLOMON DECODER Patent

In-Shek Hsu, inventor (to NASA) (Jet Propulsion Lab., California Inst. of Tech., Pasadena.) and Trieu-Kie Truong, inventor (to NASA) (Jet Propulsion Lab., California Inst. of Tech., Pasadena.) 14 Jul. 1992 12 p Filed 15 Feb. 1990 Supersedes N90-27040 (28 - 21, p 2998)
(NASA-Case-NPO-17897-1-CU; US-Patent-5,130,990;
US-Patent-Appl-SN-480449; US-Patent-Class-371-37.1;
Int-Patent-Class-G06F-11/10) Avail: US Patent and Trademark Office

A basic single-chip building block for a Reed-Solomon (RS) decoder system is partitioned into a plurality of sections, the first of which consists of a plurality of syndrome subcells each of which contains identical standard-basis finite-field multipliers that are programmable between 10 and 8 bit operation. A desired number of basic building blocks may be assembled to provide a RS decoder of any syndrome subcell size that is programmable between 10 and 8 bit operation.

Official Gazette of the U.S. Patent and Trademark Office

N92-33021* National Aeronautics and Space Administration. Langley Research Center, Hampton, VA.

VACUUM-ISOLATION VESSEL AND METHOD FOR MEASUREMENT OF THERMAL NOISE IN MICROPHONES Patent

Allan J. Zuckerwar, inventor (to NASA) and Kim Chi T. Ngo, inventor (to NASA) 15 Sep. 1992 9 p Filed 7 Oct. 1991 Supersedes N92-12174 (30 - 3, p 384)
(NASA-Case-LAR-14567-1-CU; US-Patent-5,146,780;
US-Patent-Appl-SN-773376; US-Patent-Class-374-175;
US-Patent-Class-73-1H; US-Patent-Class-73-571;
Int-Patent-Class-G01K-7/30) Avail: US Patent and Trademark Office

The vacuum isolation vessel and method in accordance with the present invention are used to accurately measure thermal noise in microphones. The apparatus and method could be used in a microphone calibration facility or any facility used for testing microphones. Thermal noise is measured to determine the minimum detectable sound pressure by the microphone. Conventional isolation apparatus and methods have been unable to provide an acoustically quiet and substantially vibration free environment for accurately measuring thermal noise. In the present invention, an isolation vessel assembly comprises a vacuum sealed outer vessel, a vacuum sealed inner vessel, and an interior suspension assembly coupled between the outer and inner vessels for suspending the inner vessel within the outer vessel. A noise measurement system records thermal noise data from the isolation vessel assembly. A vacuum system creates a vacuum between an internal surface of the outer vessel and an external surface of the inner vessel. The present invention thus provides an acoustically quiet environment due to the vacuum created between the inner and outer vessels and a substantially vibration free environment due to the suspension assembly suspending the inner vessel within the outer vessel. The thermal noise in the microphone, effectively isolated according to the invention, can be accurately measured.

Official Gazette of the U.S. Patent and Trademark Office

N92-33030* National Aeronautics and Space Administration. Marshall Space Flight Center, Huntsville, AL.

ARC/GAS ELECTRODE Patent

Richard M. Poorman, inventor (to NASA) and Jack L. Weeks, inventor (to NASA) 22 Sep. 1992 5 p Filed 29 Mar. 1991 Supersedes N91-25335 (29 - 17, p 2771)
(NASA-Case-MFS-29766-1; US-Patent-5,149,932;
US-Patent-Appl-SN-677182; US-Patent-Class-219-75;
US-Patent-Class-219-72; Int-Patent-Class-B23K-9/24) Avail: US Patent and Trademark Office

A gas/arc electrode is disclosed for use under vacuum conditions where a first housing encloses a second housing, with an end of the second housing extending through an opening in the first housing and having an outlet orifice. Provisions are made for circulating a coolant through the first housing to surround and cool the second housing. An electrical current and a gas, such as argon, as passed through the second housing, with the current flowing through a narrow stream of the ionized gas flowing through the outlet orifice to a workpiece to be treated. The second housing forms a chamber which has a cross sectional area, in a plane perpendicular to the direction of gas flow, of at least ten times the cross sectional area of the outlet orifice such that a gas pressure can be maintained in the chamber to reduce erosion of the chamber walls.

Official Gazette of the U.S. Patent and Trademark Office

N92-33061# National Inst. of Standards and Technology, Boulder, CO. Electromagnetic Fields Div.

CALIBRATION SERVICE FOR LOW-LOSS, THREE-TERMINAL CAPACITANCE STANDARDS AT 100 kHz AND 1 MHz

George M. Free and Ray N. Jones Feb. 1992 34 p
(PB92-189554; NIST/TN-1348; B91-0099) Avail: CASI HC A03/MF A01; SOD HC

The three-terminal capacitance calibration service at 100 kHz and 1 MHz at the National Institute of Standards and Technology, Boulder Laboratories, is described. The document discusses the purpose of the service, contact points for initiating the service, what capacitors are appropriate for calibration, the measurement methods used, the instrumentation used for the measurement, and an analysis of the errors in the measurement. It also lists the calibration uncertainties for the stated frequencies and

capacitances. Finally, the document discusses the quality assurance programs used at NIST to insure the integrity of the calibration. Author

N92-33068# Los Alamos National Lab., NM.
PLASMA OPENING SWITCH FOR LONG-PULSE INTENSE ION BEAM
H. A. Davis, R. J. Mason, R. R. Bartsch, J. B. Greenly, and D. J. Rej 1992 7 p Presented at the 9th International Conference on High Power Particle Beams, Washington, DC, 25-29 May 1992 (Contract W-7405-eng-36)
(DE92-017523; LA-UR-92-1915; CONF-920515-26) Avail: CASI HC A02/MF A01

A Plasma Opening Switch (POS) is being developed at Los Alamos, as part of an intense ion beam experiment with special application to materials processing. The switch must conduct up to 100 kA for 600 ns, and open quickly to avoid premature gap closure in the ion beam diode load. Power multiplication is not a necessity, but prepulse suppression is. A positive central polarity is desirable, since with it an ion beam can be conveniently launched beyond the switch from the central anode toward a negatively charged target. Thus, otherwise by virtue of traditional scaling rules, a POS was designed with a 1.25 cm radius inner anode, and a 4.75 cm radius outer cathode. This has been constructed, and subjected to circuit, and simulational analysis. The computations are being performed with the 2D ANTHEM implicit code. Preliminary results show a marked difference in switching dynamics, when the central positive polarity is used in place of the more conventional opposite choice. Opening goes by the fast development of a central anode magnetic layer, rather than by the more conventional slow evolution of a cathode gap. With the central anode, higher fill densities are needed to achieve desired conduction times. This has suggested switch design improvements, which are discussed. DOE

N92-33128# Argonne National Lab., IL.
SUPERCONDUCTIVITY: PAST, PRESENT, AND FUTURE
K. L. Uherka 1992 11 p Presented at the 54th Annual American Power Conference, Chicago, IL, 13-15 Apr. 1992 (Contract W-31-109-eng-38)
(DE92-014862; ANL/CP-75802; CONF-920432-13) Avail: CASI HC A03/MF A01

This paper provides an overview of superconductor research and development activities, with emphasis on the potential of high-(T(sub c)) materials for future applications. Superconductor applications are grouped under the following categories: electronics/instrumentation, bulk material/castings, research devices, industrial/commercial, electric power, and transportation/propulsion. Near-term applications are typically based on thin film and cast forms of high-(T(sub c)) materials, while large-scale applications requiring long lengths of wire are considered intermediate to long term. As a major side benefit of high-(T(sub c)) superconductor research, renewed interest is being focused on the use of low-(T(sub c)) materials for large-scale applications. DOE

N92-33144# Universiteit Twente, Enschede (Netherlands).
HIGH-ENERGY ION IMPLANTATION FOR BIPOLAR TRANSISTOR FABRICATION Ph.D. Thesis
Frederik Willem Ragay 1991 186 p Sponsored by Netherlands Technology Foundation
(ISBN-90-9003883-3; ETN-92-92038) Copyright Avail: CASI HC A09/MF A02

The development of a complementary vertical bipolar process, referred to as UT-COVER, for a 500 kV ion implanter, a keystone in the fabrication of semiconductor devices, is described. Both npn and pnp transistors are made vertically and high energy ion implantation is applied to create the collector regions. The basic bipolar device operation is reviewed with special consideration given to the phenomena relevant to the transistors realized in the UT-COVER process, e.g., the polysilicon emitter effect. The general characteristics of the UT-COVER process are discussed. Special attention is paid to the formation of the collector and isolation regions, which are realized by deep ion implantation. The impact on the device parameters is discussed. To make the npn transistor suitable for circuits with a 3 V supply voltage, the use of a polysilicon emitter is indispensable. In order to attain a similar performance for both types of transistors, the pnp device is made vertically instead of laterally. The standard pnp transistor is equipped with an implanted emitter, but also pnp devices with a polysilicon emitter are considered in greater depth. The process sequence is discussed and several process steps are treated. The measurement results are discussed: DC characteristics and AC measurements of the realized transistors are presented; a yield analysis of the npn transistors is given; the pnp transistors with a polysilicon emitter are compared to their counterparts with an implanted emitter region; and measured doping profiles are presented. ESA

N92-33145# Universiteit Twente, Enschede (Netherlands).
ON THE RESISTIVE TRANSITION OF COMPOSITE SUPERCONDUCTORS Ph.D. Thesis
Johannes Boschman 1991 193 p
(ISBN-90-9003899-X; ETN-92-92039) Copyright Avail: CASI HC A09/MF A03

Several aspects of the resistive transition of composite NbTi and Nb3Sn superconductors, studied by means of V-I characteristics, are addressed. The shapes of these curves are determined by a large number of parameters. The most essential parameter is the critical current density of the filaments, which in turn is influenced by irregularities in the superconducting material which results from the fabrication process, temperature, magnetic field and stress. Once the critical current density in (parts of) the filaments is exceeded, the V-I curve is in its current-sharing region and the properties of the matrix material and geometric factors (twist length, filament distribution etc.) also become important with respect to its shape. The influence of several mechanisms on voltage-current characteristics is investigated by means of model calculations and measurements. ESA

N92-33169 Department of the Navy, Washington, DC.
ULTRA-LOW-LOSS STRIP-TYPE TRANSMISSION LINES, FORMED OF BONDED SUBSTRATE LAYERS Patent
Jeffrey M. Pond, inventor (to Navy), Irving Kaufman, inventor (to Navy), and Henry F. Gray, inventor (to Navy) 24 Dec. 1991 7 p Filed 1 Dec. 1989
(AD-D015312; US-Patent-5,075,655; US-Patent-Appl-SN-444253; US-Patent-Class-333-238) Avail: US Patent and Trademark Office

A method of constructing ultra-low-loss miniaturized microstrip type microwave transmission lines, circuits, and resonators and their resulting structures are disclosed. The method includes etching a groove of the appropriate width and depth into the surface of a first substrate as determined by a preselected characteristic impedance. Appropriate thin film superconductors are then deposited on the surfaces of the first substrate and a second substrate. The thin film superconductors are then patterned after which the two substrates are sealed together by field-assisted thermal bonding such that a novel two-conductor electromagnetic transmission line results. GRA

N92-33175 Department of the Navy, Washington, DC.
ADAPTIVE FILTER TECHNIQUE FOR SUPPRESSION OF WIDEBAND OR OFFSET NARROWBAND RADIO FREQUENCY INTERFERENCE Patent
Jeffry J. Miller, inventor (to Navy) 17 Mar. 1992 8 p Filed 21 Dec. 1990
(AD-D015329; US-Patent-5,097,221; US-Patent-Appl-SN-631582; US-Patent-Class-329-318) Avail: US Patent and Trademark Office

The adaptive filter for frequency modulation of the present invention utilizes an audio tone multiplexed into the baseband modulation spectrum as a pilot tone to control and determine the amount of adaptation of the effective and variable bandwidth of the filter for optimum selectivity and rejection of wideband interference or narrowband offset interference. The multiplexed tone is detected and the filter is adjusted according to the

signal-to-noise ratio of the detected tone. A continuous and adaptive decrease or increase in bandwidth is produced to accommodate the actual signal bandwidth to achieve rejection of interference with minimum distortion. Additionally, the filter compensates for transmitter drift of center frequency. This filter may be used at radio or intermediate frequencies. GRA

N92-33183# California Univ., Berkeley. Lawrence Berkeley Lab.
DEVELOPMENT OF ADVANCED SECONDARY ZINC CELLS FOR POWER-SOURCE APPLICATIONS
Jenn-Shing Chen, F. R. McLarnon, and E. J. Cairns Dec. 1991 52 p
(Contract DE-AC03-76SF-00098)
(DE92-016358; LBL-31931) Avail: CASI HC A04/MF A01

The general advantages of Zn/AgO batteries are high specific energy, high discharge rate capability, good charge acceptance, and low self-discharge rate. However, the principal disadvantages of high cost and short cycle life have limited the use of this battery to applications where high specific energy is the prime requisite, such as military and flight applications, portable electronic equipment, etc. The major objectives of this research project are to improve the Zn/AgO cell cycle life and increases its performance. The redistribution of Zn active material (shape change) and the growth of Zn dendrites (which leads to cell shorting) have been identified as primary factors that limit the cycle-life performance of Zn/AgO cells. These phenomena can be largely overcome by improvements in separator materials, and by additives to the electrode and electrolyte. Recent development work on Zn/AgO cells has been concentrated in the area of Zn electrode and separator improvements to extend the lifetimes of cells. DOE

N92-33193 Manitoba Univ., Winnipeg.
A SIMPLIFIED SYNTHESIS OF LOSSLESS TWO-PORT WAVE DIGITAL AND ANALOG FILTERS Ph.D. Thesis
Mark R. Jarmasz Feb. 1990 120 p
(ISBN-0-315-63272-0; CTN-92-60553) Copyright Micromedia Ltd., Technical Information Centre, 165 Hotel de Ville, Place du Portage, Phase 2, Hull, Quebec J8X 3X2, Canada HC/MF

A synthesis algorithm of lossless 2-port networks is based on a simplified characterization of elementary sections and on an extraction step that eliminates the need for carrying out basic polynomial operations. It is shown that a chain (cascade) decomposition of lossless and real 2-port networks characterized using scattering variables can be completed to within a constant section by applying the given procedure. The synthesis algorithm is applicable to both the discrete and continuous time domain. It is shown that all elementary sections of degree one and two can be derived systematically from a basic 4-port topology that has zero reflectance at each port. A computable wave digital circuit for the general 2nd-order sections is derived via factorization of the scattering hybrid matrix. It is shown that the underlying topology is still that of the matched 4-port with the two allpass terminations forming a coupling network. By terminating two other ports with allpass sections, canonic sections are derived that are structurally lossless and consist of a minimum number of 2-port adaptors. Examples are presented to demonstrate the numerical robustness and relative immunity to roundoff error accumulation of the algorithm, and to show the effect of interchanging the reflectance and transmittance, as well as using voltage versus power wave 2-port adaptors, on the sensitivity of the filter response to parameter quantizations. Author (CISTI)

N92-33195 Queens Univ., Kingston (Ontario).
DESIGN AND IMPLEMENTATION OF N-DIMENSIONAL DIGITAL FILTERS Ph.D. Thesis
Yongbing Wan 1989 167 p
(ISBN-0-315-60747-5; CTN-92-60554) Copyright Micromedia Ltd., Technical Information Centre, 165 Hotel de Ville, Place du Portage, Phase 2, Hull, Quebec J8X 3X2, Canada HC/MF

In N-dimensional signal processing, the use of symmetries existing in the desired frequency specifications largely reduces the independent parameters in the design and also reduces the computation time in the implementation. N-dimensional digital filter symmetries existing in the frequency domain are developed and are related to numerator and denominator polynomials. Constraints for identity magnitude symmetries, anti-identity phase symmetries, and conjugate complex frequency response symmetries are developed and used to derive special forms of discrete polynomials possessing these symmetries. These forms can be used in the design and implementation of digital filters, and enable significant savings in computation and simplified hardware architecture. A new computer aided design technique for N-dimensional infinite impulse response (IIR) filters is developed, as well as a new optimization algorithm for minimizing performance error caused by truncating the filter coefficients. Several examples of 2- and 3-dimensional filters designed by the new algorithm are presented. Several linear array processors are developed for 2-dimensional digital filtering. These processors reach a high enough speed for real-time image processing and computer vision, and have high regularity, simple data communication schemes, simple control, and pipeline and/or data-driven format. Author (CISTI)

N92-33208 Carleton Univ., Ottawa (Ontario). Dept. of Electronics.
THE ARCHITECTURE DEVELOPMENT AND DESIGN CONSIDERATIONS OF A HIGH-SPEED, SINGLE CHIP, CMOS CONVOLUTIONAL DECODER BASED ON A MODIFICATION OF THE VITERBI ALGORITHM M.S. Thesis
D. Peter Noel Sep. 1990 228 p
(ISBN-0-315-60456-5; CTN-92-60547) Copyright Micromedia Ltd., Technical Information Centre, 165 Hotel de Ville, Place du Portage, Phase 2, Hull, Quebec J8X 3X2, Canada HC/MF

The rapidly increasing requirements for high speed data communications in satellite and mobile applications are straining existing devices to near limits. A cost-effective means for removing the obscurity from a received signal is to provide forward error correction through the use of an optimal and decoding scheme capable of relatively high speed operation. A solution providing a high speed encoder decoder device for reliable data communication is outlined. The development, design, and simulation of a high speed single-chip complementary metal oxide semiconductor (CMOS) convolutional decoder based on a derivation of the Viterbi algorithm is detailed. A complementary rate = 1/2, constant length 5 convolutional encoder is incorporated into the design to provide a complete forward error correcting code. Several of the general concepts are as found in several classical Viterbi decoder implementations, but are modified to produce optimal performance while operating at frequencies higher than those currently utilized. Other simplifications to accommodate hardware constraints cause a deviation from the original Viterbi algorithm. To maintain minimum area requirements while achieving the desired operating speeds in excess of 100 MHz, the 1.2 micron CMOS processing technology is the targeted fabrication process. Author (CISTI)

N92-33211 Carleton Univ., Ottawa (Ontario). Dept. of Electronics.
A LOW-CURRENT AMPLIFIER FOR MOBILE RADIO AND MONOLITHIC MICROWAVE INTEGRATED CIRCUIT DESIGN TECHNIQUES IN THE UHF AND L BANDS M.S. Thesis
Langis Roy 20 Nov. 1989 142 p
(ISBN-0-315-59034-3; CTN-92-60555) Copyright Micromedia Ltd., Technical Information Centre, 165 Hotel de Ville, Place du Portage, Phase 2, Hull, Quebec J8X 3X2, Canada HC/MF

Analytical transfer functions are developed to represent all commonly used field effect transistor (FET) subcircuits found in low frequency GaAs monolithic microwave integrated circuit (MMIC) amplifier design. A method is provided to describe their noise behavior. Using these techniques, a 0.1-2.1 GHz low current MMIC amplifier suitable for mobile radio applications was designed, fabricated, and tested. A gain of 19 dB was achieved along with a power dissipation of 63 mW, which compares favorably with other reported amplifiers. This performance was achieved through the use of small FET's, active loads, FET's biased at 5 percent of the drain saturated current, capacitive coupling of stages, and

the drain current saving technique. A noise figure of 7.5 dB was obtained. Experimental and simulated results are found to be in good agreement. CISTI

N92-33234 Alberta Univ., Edmonton. Dept. of Electrical Engineering.
TECHNIQUES OF MICROWAVE NOISE MEASUREMENT ON COOLED TRANSISTORS Ph.D. Thesis
Eric C. Valk 1990 242 p
(ISBN-0-315-65025-7; CTN-92-60544) Copyright Micromedia Ltd., Technical Information Centre, 165 Hotel de Ville, Place du Portage, Phase 2, Hull, Quebec J8X 3X2, Canada HC/MF

Cooled low-noise microwave field effect transistor (FET) amplifiers are widely used in radio telescopes, satellite earth stations, and radar systems to minimize noise added to the signal by the receiver. In designing these amplifiers, the noise parameters of the FETs must be known. It is hard to obtain these parameters, especially at cryogenic temperatures. A load having an electronically controlled reflection coefficient (RC) and noise temperature was built and used to measure the noise parameters of a GaAs FET at 12 K at frequencies in the 1.2-1.6 GHz range. The electronic load simplified the measurement of noise parameters at cryogenic temperatures because its RC was adjusted from outside the cooling apparatus, and the RCs were repeatable. A number of novel techniques for measuring noise and for estimating the noise parameters of a noise measurement receiver and of the device under test were developed. Singular value decomposition was used to improve and analyze noise parameter estimation by least squares fitting. The measurement errors due to frequency errors and non-zero noise power measurement bandwidth were analyzed. A new notation was introduced to simplify the analysis of noisy linear circuits and was used to develop cascading and de-embedding equations for noisy linear two-ports, and was also used to develop some of the new measurement techniques.
Author (CISTI)

N92-32975*# National Aeronautics and Space Administration. Lewis Research Center, Cleveland, OH.
INTERMODULATION IN THE OSCILLATORY MAGNETORESISTANCE OF A TWO-DIMENSIONAL ELECTRON GAS
S. E. Schacham, E. J. Haugland, and S. A. Alterovitz *In its* Solid State Technology Branch of NASA Lewis Research Center Aug. 1992 p 105-110 Repr. from Physical Review B (American Physical Society), v. 45, no. 23, Jun. 1992 p 45-50 Sponsored in part by NAS-NRC (For primary document see N92-32965 23-32)
Avail: CASI HC A02/MF A03

N92-32982*# National Aeronautics and Space Administration. Lewis Research Center, Cleveland, OH.
PERFORMANCE OF A Y-Ba-Cu-O SUPERCONDUCTING FILTER/GaAs LOW NOISE AMPLIFIER HYBRID CIRCUIT
Kul B. Bhasin, S. S. Toncich, C. M. Chorey (Sverdrup Technology, Inc., Brook Park, OH.), R. R. Bonetti (Communications Satellite Corp., Clarksburg, MD.), and A. E. Williams (Communications Satellite Corp., Clarksburg, MD.) *In its* Solid State Technology Branch of NASA Lewis Research Center Aug. 1992 p 163-165 Previously announced as N92-21370 (For primary document see N92-32965 23-32)
Avail: CASI HC A01/MF A03

34 FLUID MECHANICS AND HEAT TRANSFER

Includes boundary layers; hydrodynamics; fluidics; mass transfer; and ablation cooling.

For related information see also *02 Aerodynamics* and *77 Thermodynamics and Statistical Physics.*

N92-32245*# National Aeronautics and Space Administration. Goddard Space Flight Center, Greenbelt, MD.
TENTH WORKSHOP FOR COMPUTATIONAL FLUID DYNAMIC APPLICATIONS IN ROCKET PROPULSION, PART 2
R. W. Williams, comp. Washington Jul. 1992 755 p Workshop held in Huntsville, AL, 28-30 Apr. 1992
(NASA-CP-3163-Pt-2; M-693-Pt-2; NAS 1.55:3163-Pt-2) Avail: CASI HC A99/MF A05

Presented here are 59 abstracts and presentations and three invited presentations given at the Tenth Workshop for Computational Fluid Dynamic Applications in Rocket Propulsion held at the George C. Marshall Space Flight Center, April 28-30, 1992. The purpose of the workshop is to discuss experimental and computational fluid dynamic activities in rocket propulsion. The workshop is an open meeting for government, industry, and academia. A broad number of topics are discussed, including a computational fluid dynamic methodology, liquid and solid rocket propulsion, turbomachinery, combustion, heat transfer, and grid generation. For individual titles, see N92-32246 through N92-32277.

N92-32246*# Aerojet-General Corp., Sacramento, CA. Advanced Solid Rocket Motors Div.
CURRENT STATUS OF THE DEVELOPMENT OF AN IGNITION TRANSIENT MODEL FOR SOLID ROCKET MOTORS c20
Gary D. Luke and Harry A. Dwyer *In* NASA. Goddard Space Flight Center, Tenth Workshop for Computational Fluid Dynamic Applications in Rocket Propulsion, Part 2 Jul. 1992 p 725-761 Prepared in cooperation with California Univ., Davis (For primary document see N92-32245 23-34)
Avail: CASI HC A03/MF A05

The primary objectives of the computational fluid dynamics (CFD) code are to calculate the pressure rise rate and the maximum chamber pressure which occurs during the first second of the Advanced Solid Rocket Motor (ASRM) action time. A specific objective is to determine the relative difference between the ignition transients produced during a single port igniter and that produced by a multiport igniter. Discussed here are the results obtained from the one dimensional code and the plans for the development of the three dimensional code. Much of the information is given in viewgraph form. Author

N92-32247*# Engineering Research and Consulting, Inc., Tullahoma, TN.
SRMAFTE FACILITY CHECKOUT MODEL FLOW FIELD ANALYSIS
Richard A. Dill and Harold R. Whitesides *In* NASA. Goddard Space Flight Center, Tenth Workshop for Computational Fluid Dynamic Applications in Rocket Propulsion, Part 2 Jul. 1992 p 763-786 (For primary document see N92-32245 23-34)
Avail: CASI HC A03/MF A05

The Solid Rocket Motor Air Flow Equipment (SRMAFTE) facility was constructed for the purpose of evaluating the internal propellant, insulation, and nozzle configurations of solid propellant rocket motor designs. This makes the characterization of the facility internal flow field very important in assuring that no facility induced flow field features exist which would corrupt the model related measurements. In order to verify the design and operation of the facility, a three-dimensional computational flow field analysis was performed on the facility checkout model setup. The checkout model measurement data, one-dimensional and three-dimensional estimates were compared, and the design and proper operation of the facility was verified. The proper operation of the metering nozzles, adapter chamber transition, model nozzle, and diffuser

were verified. The one-dimensional and three-dimensional flow field estimates along with the available measurement data are compared. Author

N92-32248*# National Aeronautics and Space Administration. Marshall Space Flight Center, Huntsville, AL.
A COMPARATIVE STUDY OF THE EFFECTS OF INHIBITOR STUB LENGTH ON SOLID ROCKET MOTOR COMBUSTION CHAMBER PRESSURE OSCILLATIONS: RSRM AT T = 80 SECONDS, PRELIMINARY RESULTS c20
D. Chasman (Rockwell International Corp., Huntsville, AL.), D. Burnette (Rockwell International Corp., Huntsville, AL.), J. Holt (Rockwell International Corp., Huntsville, AL.), and R. Farr *In* NASA. Goddard Space Flight Center, Tenth Workshop for Computational Fluid Dynamic Applications in Rocket Propulsion, Part 2 Jul. 1992 p 787-790 (For primary document see N92-32245 23-34)
Avail: CASI HC A01/MF A05

Results from a continuing, time-accurate computational study of the combustion gas flow inside the Space Shuttle Redesigned Solid Rocket Motor (RSRM) are presented. These computational fluid dynamic (CFD) analyses duplicate unsteady flow effects which interact in the RSRM to produce pressure oscillations, and resulting thrust oscillations, at nominally 15, 30, and 45 Hz. Results of the Navier-Stokes computations made at mean pressure and flow conditions corresponding to 80 seconds after motor ignition both with and without a protruding, rigid inhibitor at the forward joint cavity are presented here. Author

N92-32249*# Thiokol Corp., Brigham City, UT. Space Operations.
OVERVIEW OF THE RELEVANT CFD WORK AT THIOKOL CORPORATION
Pawel Chwalowski and Hai-Tien Loh *In* NASA. Goddard Space Flight Center, Tenth Workshop for Computational Fluid Dynamic Applications in Rocket Propulsion, Part 2 Jul. 1992 p 791-806 (For primary document see N92-32245 23-34)
Avail: CASI HC A03/MF A05

An in-house developed proprietary advanced computational fluid dynamics code called SHARP (Trademark) is a primary tool for many flow simulations and design analyses. The SHARP code is a time dependent, two dimensional (2-D) axisymmetric numerical solution technique for the compressible Navier-Stokes equations. The solution technique in SHARP uses a vectorizable implicit, second order accurate in time and space, finite volume scheme based on an upwind flux-difference splitting of a Roe-type approximated Riemann solver, Van Leer's flux vector splitting, and a fourth order artificial dissipation scheme with a preconditioning to accelerate the flow solution. Turbulence is simulated by an algebraic model, and ultimately the kappa-epsilon model. Some other capabilities of the code are 2-D two-phase Lagrangian particle tracking and cell blockages. Extensive development and testing has been conducted on the 3-D version of the code with flow, combustion, and turbulence interactions. The emphasis here is on the specific applications of SHARP in Solid Rocket Motor design. Information is given in viewgraph form. Author

N92-32250*# National Aeronautics and Space Administration. Marshall Space Flight Center, Huntsville, AL.
A STATUS OF THE ACTIVITIES OF THE NASA. MARSHALL SPACE FLIGHT CENTER COMBUSTION DEVICES TECHNOLOGY TEAM
Kevin Tucker *In* NASA. Goddard Space Flight Center, Tenth Workshop for Computational Fluid Dynamic Applications in Rocket Propulsion, Part 2 Jul. 1992 p 807-829 (For primary document see N92-32245 23-34)
Avail: CASI HC A03/MF A05

The Consortium for Computational Fluid Dynamics (CFD) Applications in Propulsion Technology was established to focus on computational fluid dynamics applications in propulsion. Specific areas of effort include developing the CFD technology required to address rocket propulsion issues, validating the technology, and applying the validated technology to design problems. The Combustion Devices Technology Team was formed to implement the above objectives in the broad area of combustion driven flows. In an effort to bring CFD to bear in the design environment, the team has focused its efforts on the Space Transportation Main Engine nozzle. The main emphasis has been on the film cooling scheme used to cool the nozzle wall. Benchmark problems have been chosen to validate CFD film cooling capabilities. CFD simulations of the subscale nozzle have been made. Also, CFD predictions of the base flow resulting from this type of nozzle have been made. The status of these calculations is presented along with future plans. Information is given in viewgraph form. Author

N92-32251*# National Aeronautics and Space Administration. Marshall Space Flight Center, Huntsville, AL.
CFD ANALYSIS OF THE STME NOZZLE FLOWFIELD
Anantha Krishnan (CFD Research Corp., Huntsville, AL.) and Kevin Tucker *In* NASA. Goddard Space Flight Center, Tenth Workshop for Computational Fluid Dynamic Applications in Rocket Propulsion, Part 2 Jul. 1992 p 831-847 (For primary document see N92-32245 23-34)
Avail: CASI HC A03/MF A05

The Space Transportation Main Engine (STME) uses a gas generator cycle to cool the nozzle wall by a film-dump of the turbine exhaust. The ability to cool the skirt is a key concern in the design of the STME. CFD calculations were undertaken to predict the film cooling effectiveness and performance sensitivities for various configurations, operating points, and inlet conditions. The results presented here were obtained for the subscale nozzle. The computations were performed using REFLEQS. The computational analysis showed that a chemical equilibrium model was necessary to obtain correct predictions of the specific impulse. The frozen composition model underpredicts the ISP by about 6 percent. It was also observed that the coolant film was successful in maintaining the nozzle wall well below the stagnation temperature of the core flow. The effect of the coolant flow on the performance of the engine was found to be negligible. The computed heat fluxes at the wall were in good agreement with the empirical data obtained by Pratt and Whitney. Further test data from Pratt and Whitney are forthcoming for the subscale nozzle. Calculations will be performed to determine cooling efficiencies and nozzle performance over a range of conditions, and model predictions will be compared with experimental data. Information is given in viewgraph form. Author

N92-32252*# Pratt and Whitney Aircraft, West Palm Beach, FL.
NLS NOZZLE BASE FLOW CHARACTERISTICS
John J. Erhart *In* NASA. Goddard Space Flight Center, Tenth Workshop for Computational Fluid Dynamic Applications in Rocket Propulsion, Part 2 Jul. 1992 p 849-862 (For primary document see N92-32245 23-34)
Avail: CASI HC A03/MF A05

The flow characteristics of the National Launch System (NLS) nozzle base area need to be determined in order for heat transfer rates to be estimated. The objective of this work is to calculate these flow characteristics using computational fluid dynamics (CFD). A full Navier-Stokes code in an axisymmetric mode, using a kappa-epsilon model with wall functions is applied. Calculations were completed at an altitude of 3,250 and 80,000 feet in the flight trajectory. The results show flow features which can affect vehicle design. Calibration of a 3-D case with data is underway. Information is given in viewgraph form. Author

N92-32253*# SECA, Inc., Huntsville, AL.
HEAT TRANSFER IN ROCKET ENGINE COMBUSTION CHAMBERS AND NOZZLES
P. G. Anderson, Y. S. Chen (Engineering-Science, Inc., Huntsville, AL.), and R. C. Farmer *In* NASA. Goddard Space Flight Center, Tenth Workshop for Computational Fluid Dynamic Applications in Rocket Propulsion, Part 2 Jul. 1992 p 863-896 (For primary document see N92-32245 23-34)
Avail: CASI HC A03/MF A05

The complexities of liquid rocket engine heat transfer which

involve the injector faceplate and regeneratively and film cooled walls are being investigated by computational analysis. A conjugate heat transfer analysis will be used to describe localized heating phenomena associated with particular injector configurations and coolant channels and film coolant dumps. These components are being analyzed, and the analysis verified with appropriate test data. Finally, the component analysis will be synthesized into an overall flowfield/heat transfer model. The FDNS code is being used to make the component analyses. Particular attention is being given to the representation of the thermodynamic properties of the fluid streams and to the method of combining the detailed models to represent overall heating. Unit flow models of specific coaxial injector elements have been developed and will be described. Film cooling simulations of film coolant flows typical of the subscale Space Transportation Main Engine (STME) being experimentally studied by Pratt and Whitney have been made, and these results will be presented. Other film coolant experiments have also been simulated to verify the CFD heat transfer model being developed. The status of the study and its relevance as a new design tool are covered. Information is given in viewgraph form. Author

N92-32254*# Pratt and Whitney Aircraft, West Palm Beach, FL. Government Engine and Space Propulsion.

APPLICATION OF COMPUTATIONAL FLUID DYNAMICS TO THE DESIGN OF THE FILM COOLED STME SUBSCALE NOZZLE FOR THE NATIONAL LAUNCH SYSTEM

Joseph L. Garrett *In* NASA. Goddard Space Flight Center, Tenth Workshop for Computational Fluid Dynamic Applications in Rocket Propulsion, Part 2 Jul. 1992 p 897-922 (For primary document see N92-32245 23-34)

Avail: CASI HC A03/MF A05

The status of computational fluid dynamics (CFD) calculations for the Space Transportation Main Engine (STME) film/dump cooled nozzle design is presented, with an emphasis on the timely impact of CFD on the design of the sub-scale nozzle coolant system. The following aspects of the sub-scale coolant delivery system were analyzed with CFD: 1) a design trade study of a mechanical flow splitting device for uniform distribution of the subsonic cavity flow, 2) a design trade study of the subsonic cavity lip to achieve film integrity, and 3) an analysis of the primary flow interaction with the core/secondary coolant streams. All design calculations were performed with the Generalized Aerodynamic Simulation Program (GASP), a 3-D, multi-block, generalized Navier-Stokes code capable of solving with frozen, finite-rate or equilibrium chemical kinetics. The initial design of the subsonic cavity flow used square posts to distribute the sonic orifice jets into a uniform flow. Calculations for this design indicated that an unacceptable mal-distribution of film occurred. Design modifications involving curved and slotted posts were computed in an effort to uniformly distribute the secondary coolant flow. Analysis of these configurations showed that although the flowfield improved in uniformity, it was still unacceptable, especially at higher feed pressures. Results from these studies were then incorporated into a design that resulted in the insertion of a porous metal ring into the subsonic cavity. Subsequent water flow model studies showed that this concept was successful in uniformly distributing flow exiting the cavity. In addition to the design of the subsonic cavity, CFD was also used to analyze the secondary coolant lip and the primary flow interaction with the core/secondary coolant streams. A series of calculations were first performed to modify the subsonic cavity lip contour. The flow over the modified lip was then computed simultaneously with the primary injectors to determine the impact of the subsonic coolant stream on the primary slot jets. Pressure, temperature, velocity, and coolant mass fraction contours are presented for these configurations. Information is given in viewgraph form. Author

N92-32255*# Rockwell International Corp., Huntsville, AL. Space System Div.

COMPUTATIONAL FLUID DYNAMICS ANALYSIS OF SPACE SHUTTLE MAIN ENGINE MULTIPLE PLUME FLOWS AT HIGH-ALTITUDE FLIGHT CONDITIONS

N. S. Dougherty, J. B. Holt, B. L. Liu, and S. L. Johnson *In* NASA. Goddard Space Flight Center, Tenth Workshop for Computational Fluid Dynamic Applications in Rocket Propulsion, Part 2 Jul. 1992 p 923-943 Sponsored in part by NASA. Johnson Space Flight Center (For primary document see N92-32245 23-34)

Avail: CASI HC A03/MF A05

Computational fluid dynamics (CFD) analysis is providing verification of Space Shuttle flight performance details and is being applied to Space Shuttle Main Engine Multiple plume interaction flow field definition. Advancements in real-gas CFD methodology that are described have allowed definition of exhaust plume flow details at Mach 3.5 and 107,000 ft. The specific objective includes the estimate of flow properties at oblique shocks between plumes and plume recirculation into the Space Shuttle Orbiter base so that base heating and base pressure can be modeled accurately. The approach utilizes the Rockwell USA Real Gas 3-D Navier-Stokes (USARG3D) Code for the analysis. The code has multi-zonal capability to detail the geometry of the plumes based region and utilizes finite-rate chemistry to compute the plume expansion angle and relevant flow properties at altitude correctly. Through an improved definition of the base recirculation flow properties, heating, and aerodynamic design environments of the Space Shuttle Vehicle can be further updated. Author

N92-32256*# Rockwell International Corp., Canoga Park, CA. Rocketdyne Div.

DIRECT NUMERICAL SIMULATION OF A COMBUSTING DROPLET WITH CONVECTION

Pak-Yan Liang *In* NASA. Goddard Space Flight Center, Tenth Workshop for Computational Fluid Dynamic Applications in Rocket Propulsion, Part 2 Jul. 1992 p 945-964 (For primary document see N92-32245 23-34)

Avail: CASI HC A03/MF A05

The evaporation and combustion of a single droplet under forced and natural convection was studied numerically from first principles using a numerical scheme that solves the time-dependent multiphase and multispecies Navier-Stokes equations and tracks the sharp gas-liquid interface cutting across an arbitrary Eulerian grid. The flow fields both inside and outside of the droplet are resolved in a unified fashion. Additional governing equations model the interphase mass, energy, and momentum exchange. Test cases involving iso-octane, n-hexane, and n-propanol droplets show reasonable comparison rate, and flame stand-off distance. The partially validated code is, thus, readied to be applied to more demanding droplet combustion situations where substantial drop deformation render classical models inadequate. Author

N92-32257*# National Aeronautics and Space Administration. Marshall Space Flight Center, Huntsville, AL.

A NUMERICAL MODEL FOR ATOMIZATION-SPRAY COUPLING IN LIQUID ROCKET THRUST CHAMBERS

M. G. Giridharan (CFD Research Corp., Huntsville, AL.), Anantha Krishnan (CFD Research Corp., Huntsville, AL.), J. J. Lee (CFD Research Corp., Huntsville, AL.), A. J. Przekwas (CFD Research Corp., Huntsville, AL.), and K. Gross *In* NASA. Goddard Space Flight Center, Tenth Workshop for Computational Fluid Dynamic Applications in Rocket Propulsion, Part 2 Jul. 1992 p 965-985 (For primary document see N92-32245 23-34)

Avail: CASI HC A03/MF A05

The physical process of atomization is an important consideration in the stable operation of liquid rocket engines. Many spray combustion computational fluid dynamics (CFD) codes do not include an atomization sub-model but assume arbitrary drop size distributions, drop initial locations, and velocities. A method of coupling an atomization model with the spray model in a REFLEQS CFD code is presented. This method is based on a jet-embedding technique in which the equations governing the liquid jet core are solved separately using the surrounding gas phase conditions. The droplet initial conditions are calculated using a stability analysis appropriate for the atomization regime of liquid jet break-up. Author

N92-32258*# National Aeronautics and Space Administration. Marshall Space Flight Center, Huntsville, AL.

NUMERICAL MODELING FOR DILUTE AND DENSE SPRAYS

C. P. Chen (Alabama Univ., Huntsville.), Y. M. Kim (Alabama Univ., Huntsville.), H. M. Shang (Alabama Univ., Huntsville.), J. P. Ziebarth (Alabama Univ., Huntsville.), and T. S. Wang *In* NASA. Goddard Space Flight Center, Tenth Workshop for Computational Fluid Dynamic Applications in Rocket Propulsion, Part 2 Jul. 1992 p 987-1012 (For primary document see N92-32245 23-34)

Avail: CASI HC A03/MF A05

We have successfully implemented a numerical model for spray-combustion calculations. In this model, the governing gas-phase equations in Eulerian coordinate are solved by a time-marching multiple pressure correction procedure based on the operator-splitting technique. The droplet-phase equations in Lagrangian coordinate are solved by a stochastic discrete particle technique. In order to simplify the calculation procedure for the circulating droplets, the effective conductivity model is utilized. The k-epsilon models are utilized to characterize the time and length scales of the gas phase in conjunction with turbulent modulation by droplets and droplet dispersion by turbulence. This method entails random sampling of instantaneous gas flow properties and the stochastic process requires a large number of computational parcels to produce the satisfactory dispersion distributions even for rather dilute sprays. Two major improvements in spray combustion modelings were made. Firstly, we have developed a probability density function approach in multidimensional space to represent a specific computational particle. Secondly, we incorporate the Taylor Analogy Breakup (TAB) model for handling the dense spray effects. This breakup model is based on the reasonable assumption that atomization and drop breakup are indistinguishable processes within a dense spray near the nozzle exit. Accordingly, atomization is prescribed by injecting drops which have a characteristic size equal to the nozzle exit diameter. Example problems include the nearly homogeneous and inhomogeneous turbulent particle dispersion, and the non-evaporating, evaporating, and burning dense sprays. Comparison with experimental data will be discussed in detail. Author

N92-32259*# Rockwell International Corp., Canoga Park, CA. Rocketdyne Div.

MODELING OF SSME FUEL PREBURNER ASI **c20**

Pak-Yan Liang *In* NASA. Goddard Space Flight Center, Tenth Workshop for Computational Fluid Dynamic Applications in Rocket Propulsion, Part 2 Jul. 1992 p 1013-1031 (For primary document see N92-32245 23-34)

Avail: CASI HC A03/MF A05

The Augmented Spark Ignitor (ASI) is a LOX/H2/electrical spark system that functions as an ignition source and sustainer for stable combustion. It is used in the Space Shuttle Main Engine (SSME) preburner combustor, the SMME main combustion chamber, the J-1 and J-2 engines, as well as proposed designs of the Space Transportation Main Engine (STME) main combustor and gas generators. An undertaking to characterize the flow of the ASI is documented. The code consists of a marriage of the Implicit-Continuous Eulerian/Arbitrary Lagrangian Code (ICE-ALE) Navier-Stokes solver with the Volume-of-Fluid (VOF) Methodology for tracking of two immiscible fluids with sharp discontinuities. Spray droplets are represented by discrete numerical parcels tracked in a Lagrangian fashion. Numerous physical sub-models are also incorporated to describe the processes of atomization, droplet collision, droplet breakup, evaporation, and droplet and gas phase turbulence. An equilibrium chemistry model accounting for 8 active gaseous species is also used. Taking advantage of this symmetry plane, half of the actual ASI is modeled with a 3-D grid that geometrically resolves the LOX ports, the spark plug locations, and the hydrogen injection slots. Author

N92-32260*# National Aeronautics and Space Administration. Marshall Space Flight Center, Huntsville, AL.

CFD MODELING OF TURBULENT FLOWS AROUND THE SSME MAIN INJECTOR ASSEMBLY USING POROSITY FORMULATION

Gary C. Cheng (SECA, Inc., Huntsville, AL.), Y. S. Chen (Engineering-Science, Inc., Huntsville, AL.), and Joseph H. Ruf *In* NASA. Goddard Space Flight Center, Tenth Workshop for Computational Fluid Dynamic Applications in Rocket Propulsion, Part 2 Jul. 1992 p 1033-1069 (For primary document see N92-32245 23-34)

(Contract NAS8-38871)

Avail: CASI HC A03/MF A05

Hot gas turbulent flow distribution around the main injector assembly of the Space Shuttle Main Engine (SSME) and liquid oxygen (LOX) flow distributions through the LOX posts have great effect on the combustion phenomenon inside the main combustion chamber. An advanced computational fluid dynamics (CFD) analysis will help to provide more accurate and efficient characterization of this type of flow field. In order to design a CFD model to be an effective engineering analysis tool with good computational turn-around time and still maintain good accuracy in describing the flow features, the concept of porosity is employed to describe the effects of blockage and drag force due to the presence of the LOX posts in the turbulent flow field around the main injector assembly of the SSME. A validated non-isotropic porosity model is developed and incorporated into an existing Navier-Stokes flow solver (FDNS). Volume and surface porosity parameters, which are based on the configurations of local LOX post clustering, are introduced into the governing equations. Author

N92-32261*# National Aeronautics and Space Administration. Marshall Space Flight Center, Huntsville, AL.

COMPUTATIONAL FLUID DYNAMICS ANALYSIS OF SSME PHASE 2 AND PHASE 2+ PREBURNER INJECTOR ELEMENT HYDROGEN FLOW PATHS

Joseph H. Ruf *In* NASA. Goddard Space Flight Center, Tenth Workshop for Computational Fluid Dynamic Applications in Rocket Propulsion, Part 2 Jul. 1992 p 1071-1092 (For primary document see N92-32245 23-34)

Avail: CASI HC A03/MF A05

Phase 2+ Space Shuttle Main Engine powerheads, E0209 and E0215 degraded their main combustion chamber (MCC) liners at a faster rate than is normal for phase 2 powerheads. One possible cause of the accelerated degradation was a reduction of coolant flow through the MCC. Hardware changes were made to the preburner fuel leg which may have reduced the resistance and, therefore, pulled some of the hydrogen from the MCC coolant leg. A computational fluid dynamics (CFD) analysis was performed to determine hydrogen flow path resistances of the phase 2+ fuel preburner injector elements relative to the phase 2 element. FDNS was implemented on axisymmetric grids with the hydrogen assumed to be incompressible. The analysis was performed in two steps: the first isolated the effect of the different inlet areas and the second modeled the entire injector element hydrogen flow path. Author

N92-32262*# Aerojet-General Corp., Sacramento, CA. Propulsion Div.

STME HYDROGEN MIXER STUDY **c20**

Rob Blumenthal, Dongmoon Kim, and George Bache *In* NASA. Goddard Space Flight Center, Tenth Workshop for Computational Fluid Dynamic Applications in Rocket Propulsion, Part 2 Jul. 1992 p 1093-1116 (For primary document see N92-32245 23-34)

Avail: CASI HC A01/MF A05

The hydrogen mixer for the Space Transportation Main Engine is used to mix cold hydrogen bypass flow with warm hydrogen coolant chamber gas, which is then fed to the injectors. It is very important to have a uniform fuel temperature at the injectors in order to minimize mixture ratio problems due to the fuel density variations. In addition, the fuel at the injector has certain total pressure requirements. In order to achieve these objectives, the

hydrogen mixer must provide a thoroughly mixed fluid with a minimum pressure loss. The AEROVISC computational fluid dynamics (CFD) code was used to analyze the STME hydrogen mixer, and proved to be an effective tool in optimizing the mixer design. AEROVISC, which solves the Reynolds Stress-Averaged Navier-Stokes equations in primitive variable form, was used to assess the effectiveness of different mixer designs. Through a parametric study of mixer design variables, an optimal design was selected which minimized mixed fuel temperature variation and fuel mixer pressure loss. The use of CFD in the design process of the STME hydrogen mixer was effective in achieving an optimal mixer design while reducing the amount of hardware testing.
Author

N92-32263*# National Aeronautics and Space Administration. Marshall Space Flight Center, Huntsville, AL.
AN EXPERIMENTAL STUDY OF THE FLUID MECHANICS ASSOCIATED WITH POROUS WALLS
N. Ramachandran (Universities Space Research Association, Huntsville, AL.), J. Heaman, and A. Smith *In* NASA. Goddard Space Flight Center, Tenth Workshop for Computational Fluid Dynamic Applications in Rocket Propulsion, Part 2 Jul. 1992 p 1117-1134 Previously announced in IAA as A92-28227 Previously announced in IAA as A92-28227 (For primary document see N92-32245 23-34)
(AIAA Paper 92-0769) Avail: CASI HC A03/MF A05

The fluid mechanics of air exiting from a porous material is investigated. The experiments are filter rating dependent, as porous walls with filter ratings differing by about three orders of magnitude are studied. The flow behavior is investigated for its spatial and temporal stability. The results from the investigation are related to jet behavior in at least one of the following categories: (1) jet coalescence effects with increasing flow rate; (2) jet field decay with increasing distance from the porous wall; (3) jet field temporal turbulence characteristics; and (4) single jet turbulence characteristics. The measurements show that coalescence effects cause jet development, and this development stage can be traced by measuring the pseudoturbulence (spatial velocity variations) at any flow rate. The pseudoturbulence variation with increasing mass flow reveals an initial increasing trend followed by a leveling trend, both of which are directly proportional to the filter rating. A critical velocity begins this leveling trend and represents the onset of fully developed jetting action in the flow field. A correlation is developed to predict the onset of fully developed jets in the flow emerging from a porous wall. The data further show that the fully developed jet dimensions are independent of the filter rating, thus providing a length scale for this type of flow field (1 mm). Individual jet characteristics provide another unifying trend with similar velocity decay behavior with distance; however, the respective turbulence magnitudes show vast differences between jets from the same sample. Measurements of the flow decay with distance from the porous wall show that the higher spatial frequency components of the jet field dissipate faster than the lower frequency components. Flow turbulence intensity measurements show an out of phase behavior with the velocity field and are generally found to increase as the distance from the wall is increased.
Author

N92-32264*# Pennsylvania State Univ., University Park. Propulsion Engineering Research Center.
EXPERIMENTAL STUDIES OF CHARACTERISTIC COMBUSTION-DRIVEN FLOWS FOR CFD VALIDATION
R. J. Santoro, M. Moser, W. Anderson, S. Pal, H. Ryan, and C. L. Merkle *In* NASA. Goddard Space Flight Center, Tenth Workshop for Computational Fluid Dynamic Applications in Rocket Propulsion, Part 2 Jul. 1992 p 1135-1161 (For primary document see N92-32245 23-34)
(Contract NAS8-38862; AF-AFOSR-0336-91)
Avail: CASI HC A03/MF A05

A series of rocket-related studies intended to develop a suitable data base for validation of Computational Fluid Dynamics (CFD) models of characteristic combustion-driven flows was undertaken at the Propulsion Engineering Research Center at Penn State. Included are studies of coaxial and impinging jet injectors as well as chamber wall heat transfer effects. The objective of these studies is to provide fundamental understanding and benchmark quality data for phenomena important to rocket combustion under well-characterized conditions. Diagnostic techniques utilized in these studies emphasize determinations of velocity, temperature, spray and droplet characteristics, and combustion zone distribution. Since laser diagnostic approaches are favored, the development of an optically accessible rocket chamber has been a high priority in the initial phase of the project. During the design phase for this chamber, the advice and input of the CFD modeling community were actively sought through presentations and written surveys. Based on this procedure, a suitable uni-element rocket chamber was fabricated and is presently under preliminary testing. Results of these tests, as well as the survey findings leading to the chamber design, were presented.
Author

N92-32265*# United Technologies Research Center, East Hartford, CT.
TURBINE DISK CAVITY AERODYNAMICS AND HEAT TRANSFER
B. V. Johnson and W. A. Daniels *In* NASA. Goddard Space Flight Center, Tenth Workshop for Computational Fluid Dynamic Applications in Rocket Propulsion, Part 2 Jul. 1992 p 1163-1179 (For primary document see N92-32245 23-34)
(Contract NAS8-37462)
Avail: CASI HC A03/MF A05

Experiments were conducted to define the nature of the aerodynamics and heat transfer for the flow within the disk cavities and blade attachments of a large-scale model, simulating the Space Shuttle Main Engine (SSME) turbopump drive turbines. These experiments of the aerodynamic driving mechanisms explored the following: (1) flow between the main gas path and the disk cavities; (2) coolant flow injected into the disk cavities; (3) coolant density; (4) leakage flows through the seal between blades; and (5) the role that each of these various flows has in determining the adiabatic recovery temperature at all of the critical locations within the cavities. The model and the test apparatus provide close geometrical and aerodynamic simulation of all the two-stage cavity flow regions for the SSME High Pressure Fuel Turbopump and the ability to simulate the sources and sinks for each cavity flow.
Author

N92-32266*# Rockwell International Corp., Canoga Park, CA. Rocketdyne Div.
A NUMERICAL STUDY OF TWO-DIMENSIONAL VORTEX SHEDDING FROM RECTANGULAR CYLINDERS
A. H. Hadid, Munir M. Sindir, and R. I. Issa (Imperial Coll. of Science and Technology, London, England) *In* NASA. Goddard Space Flight Center, Tenth Workshop for Computational Fluid Dynamic Applications in Rocket Propulsion, Part 2 Jul. 1992 p 1181-1204 (For primary document see N92-32245 23-34)
Avail: CASI HC A03/MF A05

An efficient time-marching, non-iterative calculation method is used to analyze time-dependent flows around rectangular cylinders. The turbulent flow in the wake region of a square section cylinder is analyzed using an anisotropic k-epsilon model. Initiation and subsequent development of the vortex shedding phenomenon is naturally captured once a perturbation is introduced in the flow. Transient calculations using standard eddy-viscosity and an anisotropic k-epsilon model averaged over an integral number of cycles to get the fluctuating energy (organized and turbulent) are compared with experimental data. It is shown that the anisotropic k-epsilon model resolves the anisotropy of the Reynolds stresses and gives mean energy distribution closer to the experiment than the standard k-epsilon model.
Author

N92-32267*# National Aeronautics and Space Administration. Marshall Space Flight Center, Huntsville, AL.
A STATUS OF THE TURBINE TECHNOLOGY TEAM ACTIVITIES
Lisa W. Griffin *In* NASA. Goddard Space Flight Center, Tenth Workshop for Computational Fluid Dynamic Applications in Rocket

Propulsion, Part 2 Jul. 1992 p 1205-1226 (For primary document see N92-32245 23-34)
Avail: CASI HC A03/MF A05

The recent activities of the Turbine Technology Team of the Consortium for Computational Fluid Dynamics (CFD) Application in Propulsion Technology is presented. The team consists of members from the government, industry, and universities. The goal of this team is to demonstrate the benefits to the turbine design process attainable through the application of CFD. This goal is to be achieved by enhancing and validating turbine design tools for improved loading and flowfield definition and loss prediction, and transferring the advanced technology to the turbine design process. In order to demonstrate the advantages of using CFD early in the design phase, the Space Transportation Main Engine (STME) turbines for the National Launch System (NLS) were chosen on which to focus the team's efforts. The Turbine Team activities run parallel to the STME design work. Author

N92-32268*# National Aeronautics and Space Administration. Lewis Research Center, Cleveland, OH.
A CRITICAL EVALUATION OF A THREE-DIMENSIONAL NAVIER-STOKES CFD AS A TOOL TO DESIGN SUPERSONIC TURBINE STAGES
C. Hah, O. Kwon, and M. Shoemaker *In* NASA. Goddard Space Flight Center, Tenth Workshop for Computational Fluid Dynamic Applications in Rocket Propulsion, Part 2 Jul. 1992 p 1227-1241 (For primary document see N92-32245 23-34)
Avail: CASI HC A03/MF A05

Three-dimensional flow phenomena in a supersonic turbine blade row were studied numerically to evaluate CFD as a tool to design supersonic turbine stages. The details of the three-dimensional flow structure inside the supersonic turbine blade row and the overall aerodynamic performance at design and off-design conditions are analyzed and the results are compared between the experimental data and the numerical results. Author

N92-32269*# Scientific Research Associates, Inc., Glastonbury, CT.
NAVIER-STOKES ANALYSIS OF AN OXIDIZER TURBINE BLADE WITH TIP CLEARANCE
Howard J. Gibeling and Jayant S. Sabnis *In* NASA. Goddard Space Flight Center, Tenth Workshop for Computational Fluid Dynamic Applications in Rocket Propulsion, Part 2 Jul. 1992 p 1243-1273 (For primary document see N92-32245 23-34)
(Contract NAS8-38865)
Avail: CASI HC A03/MF A05

The Gas Generator Oxidizer Turbine (GGOT) Blade is being analyzed by various investigators under the NASA MSFC sponsored Turbine Stage Technology Team design effort. The present work concentrates on the tip clearance region flow and associated losses; however, flow details for the passage region are also obtained in the simulations. The present calculations simulate the rotor blade row in a rotating reference frame with the appropriate coriolis and centrifugal acceleration terms included in the momentum equation. The upstream computational boundary is located about one axial chord from the blade leading edge. The boundary conditions at this location were determined by using a Euler analysis without the vanes to obtain approximately the same flow profiles at the rotor as were obtained with the Euler stage analysis including the vanes. Inflow boundary layer profiles are then constructed assuming the skin friction coefficient at both the hub and the casing. The downstream computational boundary is located about one axial chord from the blade trailing edge, and the circumferentially averaged static pressure at this location was also obtained from the Euler analysis. Results were obtained for the 3-D baseline GGOT geometry at the full scale design Reynolds number. Details of the clearance region flow behavior and blade pressure distributions were computed. The spanwise variation in blade loading distributions are shown, and circumferentially averaged spanwise distributions of total pressure, total temperature, Mach number, and flow angle are shown at several axial stations. The spanwise variation of relative total pressure loss shows a region of high loss in the region near the casing. Particle traces in the near tip region show vortical behavior of the fluid which passes through the clearance region and exits at the downstream edge of the gap. Author

N92-32270*# Pennsylvania State Univ., University Park.
NUMERICAL SIMULATION OF TURBOMACHINERY FLOWS WITH ADVANCED TURBULENCE MODELS
B. Lakshminarayana, R. Kunz, J. Luo, and S. Fan *In* NASA. Goddard Space Flight Center, Tenth Workshop for Computational Fluid Dynamic Applications in Rocket Propulsion, Part 2 Jul. 1992 p 1275-1306 (For primary document see N92-32245 23-34)
Avail: CASI HC A03/MF A05

A three dimensional full Navier-Stokes (FNS) code is used to simulate complex turbomachinery flows. The code incorporates an explicit multistep scheme and solves a conservative form of the density averaged continuity, momentum, and energy equations. A compressible low Reynolds number form of the k-epsilon turbulence model, and a q-omega model and an algebraic Reynolds stress model have been incorporated in a fully coupled manner to approximate Reynolds stresses. The code is used to predict the viscous flow field in a backswept transonic centrifugal compressor for which laser two focus data is available. The code is also used to simulate the tip clearance flow in a cascade. The code has been extended to include unsteady Euler solutions for predicting the unsteady flow through a cascade due to incoming wakes, simulating rotor-stator interactions. Author

N92-32271*# Sverdrup Technology, Inc., Huntsville, AL.
DEVELOPMENT OF A CFD CODE FOR INTERNAL FLOWS IN LIQUID FUELED ENGINES
Youssef Dakhoul *In* NASA. Goddard Space Flight Center, Tenth Workshop for Computational Fluid Dynamic Applications in Rocket Propulsion, Part 2 Jul. 1992 p 1307-1348 (For primary document see N92-32245 23-34)
Avail: CASI HC A03/MF A05

To support the design efforts of engines in which liquid propellants are used, one is often required to analyze incompressible, two-dimensional or axisymmetric flows within ducts and cavities with rotating walls and complicated geometries. The steady-state solution is of interest in most cases. This code is intended to provide a tool for efficient computational fluid dynamics (CFD) analysis of such flow problems, taking advantage of the artificial compressibility concept and the Beam-Warming numerical scheme modified for second order accurate, implicit boundary conditions. These concepts ensure a stable, robust, and accurate algorithm due to the reduced speed of sound and the accuracy of the boundary conditions. The code is dedicated only to two-dimensional or axisymmetric flows with or without swirl. Three-dimensional computation is excluded to increase efficiency and speed. This paper briefly presents the theory of the code, as well as several benchmark applications with comparison to well known analytical solutions. In all these test cases, the code produced accurate results. Author

N92-32272*# Aerotherm Corp., Huntsville, AL.
DEVELOPMENT OF THE KIVA-2 CFD CODE FOR ROCKET PROPULSION APPLICATIONS **c20**
Robert V. Shannon, Jr. and Alvin L. Murray *In* NASA. Goddard Space Flight Center, Tenth Workshop for Computational Fluid Dynamic Applications in Rocket Propulsion, Part 2 Jul. 1992 p 1349-1378 (For primary document see N92-32245 23-34)
Avail: CASI HC A03/MF A05

The KIVA-2 code, originally developed to solve computational fluid dynamics problems in internal combustion engines, has been developed to solve rocket propulsion type flows. The objective of the work was to develop a code such that both liquid and solid particle motion could be simulated for arbitrary geometry and high speed as well as low speed reacting flows. Modification to the original code include: incorporating independently specific supersonic and subsonic inflows and outflows; symmetric as well as periodic boundary conditions; and the capability to use

generalized single or multi-specie thermodynamic data and transport coefficients allowing the user to specify arbitrary wall temperature/heat flux distributions. This code has been shown to successfully solve rocket propulsion flows as well as flows with entrained particles for several different rocket nozzles. Author

N92-32273*# Rockwell International Corp., Canoga Park, CA. Rocketdyne Div.

A COMPUTATIONAL DESIGN SYSTEM FOR RAPID CFD ANALYSIS

E. P. Ascoli, S. L. Barson, M. E. DeCroix, and Munir M. Sindir *In* NASA. Goddard Space Flight Center, Tenth Workshop for Computational Fluid Dynamic Applications in Rocket Propulsion, Part 2 Jul. 1992 p 1379-1396 (For primary document see N92-32245 23-34)

Avail: CASI HC A03/MF A05

A computation design system (CDS) is described in which these tools are integrated in a modular fashion. This CDS ties together four key areas of computational analysis: description of geometry; grid generation; computational codes; and postprocessing. Integration of improved computational fluid dynamics (CFD) analysis tools through integration with the CDS has made a significant positive impact in the use of CFD for engineering design problems. Complex geometries are now analyzed on a frequent basis and with greater ease. Author

N92-32274*# Columbia Univ., New York, NY. Dept. of Mechanical Engineering.

OPTIMUM DESIGN OF NINETY DEGREE BENDS

Vijay Modi, Hayri Cabuk, Jian-Chun Huan, and Richard Quadracci *In* NASA. Goddard Space Flight Center, Tenth Workshop for Computational Fluid Dynamic Applications in Rocket Propulsion, Part 2 Jul. 1992 p 1397-1426 (For primary document see N92-32245 23-34)

Avail: CASI HC A03/MF A05

An algorithm for the optimum design of an internal flow component to obtain the maximum pressure rise is presented. Maximum pressure rise in a duct with simultaneous turning and diffusion is shown to be related to the control of flow separation on the passage walls. Such a flow is usually associated with downstream conditions that are desirable in turbomachinery and propulsion applications to ensure low loss and stable performance. The algorithm requires the solution of an 'adjoint' problem in addition to the 'direct' equations governing the flow in a body, which in the present analysis are assumed to be the laminar Navier-Stokes equations. The theoretical framework and computational algorithms presented in this study are for the steady Navier-Stokes equations. A procedure is developed for the numerical solution of the adjoint equations. This procedure is coupled with a direct solver in a design iteration loop, that provides a new shape with a higher pressure rise. This procedure is first validated for the design of optimum plane diffusers in two-dimensional flow. The direct Navier-Stokes and the 'adjoint' equations are solved using a finite volume formulation for spatial discretization in an artificial compressibility framework. A simplified version of the above approach is then utilized to design ninety degree diffusing bends. Calculations were carried out for a mean radius ratio at inlet of 2.5 and Reynolds numbers varying from 100 to 500. While at this stage laminar flows is assumed, it is shown that a similar approach can be conceived for turbulent flows. Author

N92-32275*# Rockwell International Corp., Canoga Park, CA. Rocketdyne Div.

A MULTI-DOMAIN METHOD FOR SUBSONIC VISCOUS FLOWS **c24**

Daniel C. Chan and Munir M. Sindir *In* NASA. Goddard Space Flight Center, Tenth Workshop for Computational Fluid Dynamic Applications in Rocket Propulsion, Part 2 Jul. 1992 p 1427-1451 (For primary document see N92-32245 23-34)

Avail: CASI HC A03/MF A05

We have developed a Schwarz type domain decomposition method for a pressure base, two- and three-dimensional Navier-Stokes solver. This technique allows one to partition a flow path, which can be characterized by complex geometry and/or complicated flow physics, into smaller sub-domains according to the local geometric simplicity or estimated flow scales. We can, then, sweep the sub-domains in some order and solve the Navier-Stokes equations using as boundary conditions, along the domain interfaces, the Dirichlet conditions which are taken from the most recent update of the solution in the adjacent neighboring domains. With this technique, one can minimize the adverse effects caused by grid skewness and the stiffness problem caused by disparate flow scales. Here, we report the results of a few fundamental flow cases to demonstrate that a judicious use of the multi-domain method can offer a significant convergence acceleration over the traditional one-domain method. This method can be extended to exploit the architecture of a parallel computer to further improve the speed. Author

N92-32276*# Illinois Univ., Urbana-Champaign. Aerothermal Simulations Lab.

LARGE EDDY SIMULATION OF COMPRESSIBLE TURBULENT CHANNEL FLOWS Ph.D. Thesis

Robert A. Beddini and Jeffrey P. Ridder *In* NASA. Goddard Space Flight Center, Tenth Workshop for Computational Fluid Dynamic Applications in Rocket Propulsion, Part 2 Jul. 1992 p 1453-1468 (For primary document see N92-32245 23-34)

(Grant NGT-50363)

Avail: CASI HC A03/MF A05

The development of turbulence within rocket propulsion chamber flows remains a difficult problem to predict. Within solid propellant rockets, the flow can exhibit multiple regions of transition to turbulence, and is susceptible to various modes of aero-acoustic interaction. The objective is to formulate, develop, and validate, a large eddy simulation (LES) method for compressible channel flows. The LES method separates the resolvable scale motions from the unresolvable scales by applying a spatial filter to the compressible Navier-Stokes equations. The equations are solved numerically using a modified four-step Runge-Kutta procedure in time and second or fourth order finite differences in space. The current simulations have validated the algorithm in the incompressible limit and have demonstrated the ability of the method to simulate high subsonic Mach number flows. H.A.

N92-32277*# Florida Univ., Gainesville. Dept. of Aerospace Engineering.

TREATING CONVECTION IN SEQUENTIAL SOLVERS

Wei Shyy and Siddharth Thakur *In* NASA. Goddard Space Flight Center, Tenth Workshop for Computational Fluid Dynamic Applications in Rocket Propulsion, Part 2 Jul. 1992 p 1469-1483 (For primary document see N92-32245 23-34)

Avail: CASI HC A03/MF A05

The treatment of the convection terms in the sequential solver, a standard procedure found in virtually all pressure based algorithms, to compute the flow problems with sharp gradients and source terms is investigated. Both scalar model problems and one-dimensional gas dynamics equations have been used to study the various issues involved. Different approaches including the use of nonlinear filtering techniques and adoption of TVD type schemes have been investigated. Special treatments of the source terms such as pressure gradients and heat release have also been devised, yielding insight and improved accuracy of the numerical procedure adopted. Author

N92-32278*# National Aeronautics and Space Administration. Goddard Space Flight Center, Greenbelt, MD.

TENTH WORKSHOP FOR COMPUTATIONAL FLUID DYNAMIC APPLICATIONS IN ROCKET PROPULSION, PART 1

R. W. Williams, comp. Washington Jul. 1992 721 p Workshop held in Huntsville, AL, 28-30 Apr. 1992

(NASA-CP-3163-Pt-1; M-693-Pt-1; NAS 1.55:3163-Pt-1) Avail: CASI HC A99/MF A05

Experimental and computational fluid dynamic activities in rocket propulsion were discussed. The workshop was an open meeting of government, industry, and academia. A broad number of topics

were discussed including computational fluid dynamic methodology, liquid and solid rocket propulsion, turbomachinery, combustion, heat transfer, and grid generation. For individual titles, see N92-32279 through N92-32307.

N92-32279*# National Aeronautics and Space Administration. Marshall Space Flight Center, Huntsville, AL.
TECHNOLOGY TEST BED REVIEW
H. V. McConnaughey *In* NASA. Goddard Space Flight Center, Tenth Workshop for Computational Fluid Dynamic Applications in Rocket Propulsion, Part 1 Jul. 1992 p 1-26 (For primary document see N92-32278 23-34)
Avail: CASI HC A03/MF A05

The topics are presented in viewgraph form and include the following: (1) Space Shuttle Main Engine (SSME) technology test bed (TTB) history; (2) TTB objectives; (3) TTB major accomplishments; (4) TTB contributions to SSME; (5) major impacts of 3001 testing; (6) some challenges to computational fluid dynamics (CFD); (7) the high pressure fuel turbopump (HPFTP); and (8) 3001 lessons learned in design and operations. Author

N92-32280*# National Aeronautics and Space Administration. Marshall Space Flight Center, Huntsville, AL.
ADVANCED SOLID ROCKET MOTOR PROJECT STATUS c20
Keith Coates *In* NASA. Goddard Space Flight Center, Tenth Workshop for Computational Fluid Dynamic Applications in Rocket Propulsion, Part 1 Jul. 1992 p 27-43 (For primary document see N92-32278 23-34)
Avail: CASI HC A03/MF A05

The objectives of the project are the following: (1) to improve system safety and reliability; (2) to improve Space Shuttle Payload performance - 12,000 lb; (3) to optimize program cost; and (4) to promote a competitive solid rocket motor industry. The topics are presented in viewgraph form and include the Advanced Solid Rocket Motor (ASRM) project team, ASRM design, design schedules, and technical issues. Author

N92-32281*# National Aeronautics and Space Administration. Marshall Space Flight Center, Huntsville, AL.
SPACE TRANSPORTATION MAIN ENGINE c20
Jan C. Monk *In* NASA. Goddard Space Flight Center, Tenth Workshop for Computational Fluid Dynamic Applications in Rocket Propulsion, Part 1 Jul. 1992 p 45-82 (For primary document see N92-32278 23-34)
Avail: CASI HC A03/MF A05

The topics are presented in viewgraph form and include the following: Space Transportation Main Engine (STME) definition, design philosophy, robust design, maximum design condition, casting vs. machined and welded forgings, operability considerations, high reliability design philosophy, engine reliability enhancement, low cost design philosophy, engine systems requirements, STME schematic, fuel turbopump, liquid oxygen turbopump, main injector, and gas generator. The major engine components of the STME and the Space Shuttle Main Engine are compared. Author

N92-32282*# Pennsylvania State Univ., University Park. Dept. of Mechanical Engineering.
THE IMPACT OF TIME STEP DEFINITION ON CODE CONVERGENCE AND ROBUSTNESS
S. Venkateswaran, J. M. Weiss, and C. L. Merkle *In* NASA. Goddard Space Flight Center, Tenth Workshop for Computational Fluid Dynamic Applications in Rocket Propulsion, Part 1 Jul. 1992 p 83-107 (For primary document see N92-32278 23-34)
Avail: CASI HC A03/MF A05

We have implemented preconditioning for multi-species reacting flows in two independent codes, an implicit (ADI) code developed in-house and the RPLUS code (developed at LeRC). The RPLUS code was modified to work on a four-stage Runge-Kutta scheme. The performance of both the codes was tested, and it was shown that preconditioning can improve convergence by a factor of two to a hundred depending on the problem. Our efforts are currently focused on evaluating the effect of chemical sources and on assessing how preconditioning may be applied to improve convergence and robustness in the calculation of reacting flows. Author

N92-32283*# Rockwell International Corp., Canoga Park, CA. Rocketdyne Div.
DEVELOPMENT OF CFD CODE EVALUATION CRITERIA AND A PROCEDURE FOR ASSESSING PREDICTIVE CAPABILITY AND PERFORMANCE
S. J. Lin, D. C. Chan, M. M. Sindir, and S. L. Barson *In* NASA. Goddard Space Flight Center, Tenth Workshop for Computational Fluid Dynamic Applications in Rocket Propulsion, Part 1 Jul. 1992 p 109-121 (For primary document see N92-32278 23-34)
Avail: CASI HC A03/MF A05

Careful validation of computational fluid dynamic (CFD) codes is essential if they are to be used as engineering design tools. Validation must be carried out in a systematic manner to ensure that all code aspects as they apply to the application of interest are understood and, to the greatest extent possible, quantified. A study is being conducted in which a general code validation procedure is defined and demonstrated. A four phase validation procedure is defined in which a series of validation test cases are computed and compared with available analytical solutions and test data. The procedure is demonstrated using the REACT CFD code to compute validation cases for each of the four phases. For phase four, the application of interest, the Space Shuttle Main Engine high pressure fuel turbopump impeller flow field, is computed. Author

N92-32284*# Pennsylvania State Univ., University Park. Dept. of Mechanical Engineering.
COMPARISON BETWEEN THE PISO ALGORITHM AND PRECONDITIONING METHODS FOR COMPRESSIBLE FLOW
Charles L. Merkle, Philip E. O. Buelow, and S. Venkateswaran *In* NASA. Goddard Space Flight Center, Tenth Workshop for Computational Fluid Dynamic Applications in Rocket Propulsion, Part 1 Jul. 1992 p 123-146 (For primary document see N92-32278 23-34)
Avail: CASI HC A03/MF A05

Two widely used family of algorithms, pressure-based and density-based methods, have been developed for computational fluid dynamics (CFD) problems over the years. Pressure-based methods (such as SIMPLE and PISO) use a Poisson-like equation for updating pressure instead of the continuity equation, while density-based methods use the continuity equation to update density (an equation of state is used to provide density in pressure based schemes and pressure in density based schemes). Pressure-based methods were developed originally for incompressible flows at low Reynolds numbers and were then extended to high Reynolds numbers and compressible applications. On the other hand, density based methods were originally developed for transonic flows and have been extended down to low Mach numbers through the use of preconditioning techniques. We compare these two very different approaches to solving the Navier-Stokes equations in order to gain an understanding of their similarities and differences. Specifically, we consider the PISO scheme as a representative pressure-based method and contrast it with a recently developed preconditioning scheme. We also compare the relative performance of the PISO algorithm with a Euler implicit algorithm that is employed to solve the preconditioned equations by means of a vector stability analysis. Author

N92-32285*# University of Southern California, Los Angeles. Dept. of Aerospace Engineering.
A COMPARISON OF ARTIFICIAL COMPRESSIBILITY AND FRACTIONAL STEP METHODS FOR INCOMPRESSIBLE FLOW COMPUTATIONS
Daniel C. Chan, Armen Darian (Rockwell International Corp., Canoga Park, CA.), and Munir Sindir (Rockwell International Corp., Canoga Park, CA.) *In* NASA. Goddard Space Flight Center, Tenth Workshop for Computational Fluid Dynamic Applications in

Rocket Propulsion, Part 1 Jul. 1992 p 147-171 (For primary document see N92-32278 23-34)
Avail: CASI HC A03/MF A05

We have applied and compared the efficiency and accuracy of two commonly used numerical methods for the solution of Navier-Stokes equations. The artificial compressibility method augments the continuity equation with a transient pressure term and allows one to solve the modified equations as a coupled system. Due to its implicit nature, one can have the luxury of taking a large temporal integration step at the expense of higher memory requirement and larger operation counts per step. Meanwhile, the fractional step method splits the Navier-Stokes equations into a sequence of differential operators and integrates them in multiple steps. The memory requirement and operation count per time step are low, however, the restriction on the size of time marching step is more severe. To explore the strengths and weaknesses of these two methods, we used them for the computation of a two-dimensional driven cavity flow with Reynolds number of 100 and 1000, respectively. Three grid sizes, 41 x 41, 81 x 81, and 161 x 161 were used. The computations were considered after the L2-norm of the change of the dependent variables in two consecutive time steps has fallen below 10(exp -5). Author

N92-32286*# National Aeronautics and Space Administration. Marshall Space Flight Center, Huntsville, AL.
A STATUS OF THE ACTIVITIES OF THE NASA/MSFC PUMP STAGE TECHNOLOGY TEAM
R. Garcia, R. Williams, and Y. Dakhoul *In* NASA. Goddard Space Flight Center, Tenth Workshop for Computational Fluid Dynamic Applications in Rocket Propulsion, Part 1 Jul. 1992 p 173-200 (For primary document see N92-32278 23-34)
Avail: CASI HC A03/MF A05

The Consortium for Computational Fluid Dynamics (CFD) Application in Propulsion Technology was established to aid the transfer of CFD related advancements among academia, government agencies, and industry. The specific goals of the Consortium are to develop CFD methodologies necessary to solve propulsion problems, to validate these methodologies, and to apply these methodologies in the design process. To accomplish these goals, a team of experts in various related fields was formed, a schedule of activities necessary to meet the goals was generated, and funding for the activities was obtained from NASA. During the past year (Mar. 1991 - Mar. 1992) the team's activities have focused on preliminary code validation and on the design of an advanced impeller. Six codes were used to calculate the flow in a Rocketdyne 0.3 flow coefficient inducer, and the results were compared to L2F data available for the inducer. This activity identified shortcomings in the experimental data sets and in the analytical solutions which must be surmounted in any future team activity. The design of the advanced impeller relied heavily on CFD results to obtain an optimized geometry. The optimized geometry was analyzed using four different codes, at design and off-design conditions. Activities for the next year include the optimization of a tandem blade impeller design, benchmark of CFD codes for diffuser and volute flows, the collection of L2F data for 'state-of-the-art' impeller and inducer, and the verification of the advanced pump team impeller design in a water rig.
Author

N92-32287*# National Aeronautics and Space Administration. Marshall Space Flight Center, Huntsville, AL.
CFD ANALYSIS OF PUMP CONSORTIUM IMPELLER
Gary C. Cheng (SECA, Inc., Huntsville, AL.), Y. S. Chen (Engineering-Science, Inc., Huntsville, AL.), and R. W. Williams *In* NASA. Goddard Space Flight Center, Tenth Workshop for Computational Fluid Dynamic Applications in Rocket Propulsion, Part 1 Jul. 1992 p 201-218 (For primary document see N92-32278 23-34)
Avail: CASI HC A03/MF A05

Current design of high performance turbopumps for rocket engines requires effective and robust analytical tools to provide design impact in a productive manner. The main goal of this study is to develop a robust and effective computational fluid dynamics (CFD) pump model for general turbopump design and analysis applications. A Navier-Stokes flow solver, FDNS, embedded with the extended k-epsilon turbulence model and with appropriate moving interface boundary conditions, is developed to analyze turbulent flows in the turbomachinery devices. The FDNS code was benchmarked with its numerical predictions of the pump consortium inducer, and provides satisfactory results. In the present study, a CFD analysis of the pump consortium impeller will be conducted with the application of the FDNS code. The pump consortium impeller, with partial blades, is the new design concept of the advanced rocket engine. Author

N92-32288*# National Aeronautics and Space Administration. Ames Research Center, Moffett Field, CA.
CFD APPLICATIONS IN PUMP FLOWS
Cetin Kiris (MCAT Inst., San Jose, CA.), Liang Chang (MCAT Inst., San Jose, CA.), and Dochan Kwak *In* NASA. Goddard Space Flight Center, Tenth Workshop for Computational Fluid Dynamic Applications in Rocket Propulsion, Part 1 Jul. 1992 p 219-243 (For primary document see N92-32278 23-34)
Avail: CASI HC A03/MF A05

The objective of the proposed paper is to develop a computational procedure that solves incompressible Navier-Stokes equations for pump flows. The solution method is based on the pseudo-compressibility approach and uses an implicit-upwind differencing scheme together with the Gauss-Seidel line relaxation method. The equations are solved in steadily rotating reference frames and the centrifugal force and the Coriolis force are added to the equation of motion. As a benchmark problem, the flow through the Rocketdyne inducer is numerically simulated. A coarse grid solution is obtained with a single zone by using an algebraic turbulence model. In multi-zone fine grid computation, a one-equation Baldwin-Barth turbulence model is utilized. Numerical results are compared with experimental measurements and a good agreement is found between the two. The resulting computer code is then applied to the flow analysis inside a two-stage fuel pump impeller operating at 80 percent, 100 percent, and 120 percent of design flow. Author

N92-32289*# Scientific Research Associates, Inc., Glastonbury, CT.
COMPUTATION OF THE FLOW FIELD IN A CENTRIFUGAL IMPELLER WITH SPLITTER BLADES
Frederik J. deJong, Sang-Keun Choi, T. R. Govindan, and Jayant S. Sabnis *In* NASA. Goddard Space Flight Center, Tenth Workshop for Computational Fluid Dynamic Applications in Rocket Propulsion, Part 1 Jul. 1992 p 245-258 (For primary document see N92-32278 23-34)
Avail: CASI HC A03/MF A05

To support the design effort of the Space Transportation Main Engine (STME) Fuel Pump Stage, viscous flow calculations were performed in a centrifugal impeller with splitter blades. These calculations were carried out with a Navier-Stokes solver (MINT), which employs a linearized block-implicit Alternating Direction Implicit (ADI) procedure to iteratively solve a finite difference form of the system of conservation equations of mass, momentum, and energy in body-fitted coordinates. A computational grid was generated algebraically for the 'channel' between two main blades of the impeller and extended both upstream of the impeller inlet and downstream of the impeller exit so that the appropriate boundary conditions could be applied. The results of the calculations show that although the overall level of flow distortion near the impeller exit is not very large, there is a noticeable difference between the flow patterns in the two 'passages' (one passage between the pressure side of the splitter blade and the suction side of the next full blade). Author

N92-32290*# Aerojet Solid Propulsion Co., Sacramento, CA.
IMPELLER TANDEM BLADE STUDY WITH GRID EMBEDDING FOR LOCAL GRID REFINEMENT
George Bache *In* NASA. Goddard Space Flight Center, Tenth Workshop for Computational Fluid Dynamic Applications in Rocket

Propulsion, Part 1 Jul. 1992 p 259-288 (For primary document see N92-32278 23-34)
Avail: CASI HC A03/MF A05

Flow non-uniformity at the discharge of high power density impellers can result in significant unsteady interactions between impeller blades and downstream diffuser vanes. These interactions result in degradation of both performance and pump reliability. The MSFC Pump Technology Team has recognized the importance of resolving this problem and has thus initiated the development and testing of a high head coefficient impeller. One of the primary goals of this program is to improve impeller performance and discharge flow uniformity. The objective of the present work is complimentary. Flow uniformity and performance gains were sought through the application of a tandem blade arrangement. The approach adopted was to numerically establish flow characteristics at the impeller discharge for the baseline MSFC impeller and then parametrically evaluate tandem blade configurations. A tandem design was sought that improves both impeller performance and discharge uniformity. The Navier-Stokes solver AEROVISC was used to conduct the study. Grid embedding is used to resolve local gradients while attempting to minimize model size. Initial results indicate that significant gains in flow uniformity can be achieved through the tandem blade concept and that blade clocking rather than slot location is the primary driver for flow uniformity.
Author

N92-32291*# National Aeronautics and Space Administration. Lewis Research Center, Cleveland, OH.
THREE-DIMENSIONAL FLOW FIELDS INSIDE A SHROUDED INDUCER AT DESIGN AND OFF-DESIGN CONDITIONS (CFD STUDY)
C. Hah, O. Kwon, D. A. Greenwald, and R. Garcia (National Aeronautics and Space Administration. Marshall Space Flight Center, Huntsville, AL.) *In* NASA. Goddard Space Flight Center, Tenth Workshop for Computational Fluid Dynamic Applications in Rocket Propulsion, Part 1 Jul. 1992 p 289-314 (For primary document see N92-32278 23-34)
Avail: CASI HC A03/MF A05

Three-dimensional flow phenomena in a shrouded inducer were studied with a three-dimensional Navier-Stokes method. The details of the three-dimensional flow structure inside the inducer at design and off-design conditions are analyzed and the results are compared with some flow visualization results obtained at the California Institute of Technology.
Author

N92-32292*# Virginia Polytechnic Inst. and State Univ., Blacksburg. Dept. of Mechanical Engineering.
EFFECTS OF CURVATURE AND ROTATION ON TURBULENCE IN THE NASA LOW-SPEED CENTRIFUGAL COMPRESSOR IMPELLER
Joan G. Moore and John Moore *In* NASA. Goddard Space Flight Center, Tenth Workshop for Computational Fluid Dynamic Applications in Rocket Propulsion, Part 1 Jul. 1992 p 315-338 (For primary document see N92-32278 23-34)
Avail: CASI HC A03/MF A05

The flow in the NASA Low-Speed Impeller is affected by both curvature and rotation. The flow curves due to the following: (1) geometric curvature, e.g. the curvature of the hub and shroud profiles in the meridional plane and the curvature of the backswept impeller blades; and (2) secondary flow vortices, e.g. the tip leakage vortex. Changes in the turbulence and effective turbulent viscosity in the impeller are investigated. The effects of these changes on three-dimensional flow development are discussed. Two predictions of the flow in the impeller, one with, and one without modification to the turbulent viscosity due to rotation and curvature, are compared. Some experimental and theoretical background for the modified mixing length model of turbulent viscosity will also be presented.
Author

N92-32293*# Rockwell International Corp., Canoga Park, CA. Rocketdyne Div.
COMPUTATIONAL FLUID DYNAMIC DESIGN OF ROCKET ENGINE PUMP COMPONENTS
Wei-Chung Chen, George H. Prueger, Daniel C. Chan, and Anthony H. Eastland *In* NASA. Goddard Space Flight Center, Tenth Workshop for Computational Fluid Dynamic Applications in Rocket Propulsion, Part 1 Jul. 1992 p 339-359 (For primary document see N92-32278 23-34)
Avail: CASI HC A03/MF A05

Integration of computational fluid dynamics (CFD) for design and analysis of turbomachinery components is needed as the requirements of pump performance and reliability become more stringent for the new generation of rocket engine. A fast grid generator, designed specially for centrifugal pump impeller, which allows a turbomachinery designer to use CFD to optimize the component design will be presented. The CFD grid is directly generated from the impeller blade G-H blade coordinates. The grid points are first generated on the meridional plane with the desired clustering near the end walls. This is followed by the marching of grid points from the pressure side of one blade to the suction side of a neighboring blade. This fast grid generator has been used to optimize the consortium pump impeller design. A grid dependency study has been conducted for the consortium pump impeller. Two different grid sizes, one with 10,000 grid points and one with 80,000 grid points were used for the grid dependency study. The effects of grid resolution on the turnaround time, including the grid generation and completion of the CFD analysis, is discussed. The impeller overall mass average performance is compared for different designs. Optimum design is achieved through systematic change of the design parameters. In conclusion, it is demonstrated that CFD can be effectively used not only for flow analysis but also for design and optimization of turbomachinery components.
Author

N92-32294*# Rockwell International Corp., Canoga Park, CA. Rocketdyne Div.
SSME HPOTP IMPELLER BACKCAVITY CFD ANALYSIS
W. W. Hsu and S. J. Lin *In* NASA. Goddard Space Flight Center, Tenth Workshop for Computational Fluid Dynamic Applications in Rocket Propulsion, Part 1 Jul. 1992 p 361-388 (For primary document see N92-32278 23-34)
Avail: CASI HC A03/MF A05

The ball bearings behind the Space Shuttle Main Engine (SSME) HPOTP preburner pump have a history of premature wear requiring their replacement. Extensive tests have been conducted in an attempt to identify the operating factors that contribute to the wear. It has been conjectured that the coolant inflow velocity swirl pattern can aid bearing operation by matching ball orbit speed and thus affect bearing life. However, control of the velocity distribution up to now could only be achieved by trial and error following hardware testing. Observation of hardware from recent flight and development operation led to the hypothesis that certain assemblies with more extensive grinding patterns on the backwall of the impeller for rotor balancing correlated with improved bearing wear. To analytically evaluate the effect of cavity configuration on the flowfield, 3-D computational fluid dynamics (CFD) analyses of various geometries was successfully executed using REACT3D. Height of the anti-vortex ribs on the stationary wall was varied, as was the configuration of the rotating wall, from smooth to simulations of various grindout patterns. The results obtained indicate the effects of the various geometries and provide valuable guidelines for cavity modification to optimize bearing cooling.
Author

N92-32295*# Rockwell International Corp., Canoga Park, CA. Rocketdyne Div.
NLS CLUTCHING BEARING CAVITY FLOW ANALYSIS
Ken Tran, Daniel C. Chan, and Armen Darian *In* NASA. Goddard Space Flight Center, Tenth Workshop for Computational Fluid Dynamic Applications in Rocket Propulsion, Part 1 Jul. 1992 p 389-418 (For primary document see N92-32278 23-34)
Avail: CASI HC A03/MF A05

A flow model of the NLS clutching bearing cavity was built for 2-D axisymmetric viscous analysis. From the computational fluid dynamics (CFD) approach, the tangential force exerted on the surfaces of the inner race was integrated to calculate the dividing

torque which, in conjunction with the resistance torque, was used to predict the operating speed of the inner race. In order to further reduce the inner race rotation, the swirling flow at the cavity inlet was partially redirected to generate an opposing torque. Thirty six slanted slots were incorporated into the anti-vortex rib to achieve this goal. A 3-D flow analysis performed on this configuration indicates a drastic reduction of the driving torque and inner race RPM. Author

N92-32296*# National Aeronautics and Space Administration. Marshall Space Flight Center, Huntsville, AL.

CFD ANALYSIS TO OPTIMIZE A DESIGN MODIFICATION OF BSMT

Mark Ratcliff (CFD Research Corp., Huntsville, AL.), Ram Avva (CFD Research Corp., Huntsville, AL.), and Robert Williams *In* NASA. Goddard Space Flight Center, Tenth Workshop for Computational Fluid Dynamic Applications in Rocket Propulsion, Part 1 Jul. 1992 p 419-440 (For primary document see N92-32278 23-34)

Avail: CASI HC A03/MF A05

The Bearings, Seals and Materials Tester (BSMT) is a test article being used at MSFC to evaluate the performance of conventional rolling contact bearings. Pressure differentials between the BSMT inlet and exit cavities are found to cause large parasitic axial loads on the bearing-carrier walls. These parasitic loads, besides being detrimental to the life of bearings, make the testing and evaluation of bearing performance very difficult, and need to be eliminated if at all possible. The objectives of this study are to estimate the hydrodynamic loads on the bearings and to recommend feasible design modifications for BSMT to eliminate the parasitic loads. Three-dimensional computational analyses of inlet and exit cavities in their baseline configuration were performed with REFLEQS which is an advanced finite-volume Navier-Stokes code. Computations were performed with and without a 1/4 inch diameter temperature probe included in each of the cavities. The results of the analyses indicate that the temperature probes substantially alter the flow field and reduce the pressure drop/rise in the cavities. The overall pressure drop across the tester compares quite well with the measurements. Author

N92-32297*# Alabama Univ., Huntsville.

COMBUSTION INSTABILITY ANALYSIS FOR LIQUID PROPELLANT ROCKET ENGINES **c25**

Y. M. Kim, C. P. Chen, and J. P. Ziebarth *In* NASA. Goddard Space Flight Center, Tenth Workshop for Computational Fluid Dynamic Applications in Rocket Propulsion, Part 1 Jul. 1992 p 441-465 (For primary document see N92-32278 23-34)

Avail: CASI HC A03/MF A05

The multi-dimensional numerical model has been developed to analyze the nonlinear combustion instabilities in liquid-fueled engines. The present pressure-based approach can handle the implicit pressure-velocity coupling in a non-iterative way. The additional scalar conservation equations for the chemical species, the energy, and the turbulent transport quantities can be handled by the same predictor-corrector sequences. This method is time-accurate and it can be applicable to the all-speed, transient, multi-phase, and reacting flows. Special emphasis is given to the acoustic/vaporization interaction which may act as the crucial rate-controlling mechanism in the liquid-fueled rocket engines. The subcritical vaporization is modeled to account for the effects of variable thermophysical properties, non-unitary Lewis number in the gas-film, the Stefan flow effect, and the effect of transient liquid heating. The test cases include the one-dimenisonal fast transient non-reacting and reacting flows, and the multi-dimensional combustion instabilities encountered in the liquid-fueled rocket thrust chamber. The present numerical model successfully demonstrated the capability to simulate the fast transient spray-combusting flows in terms of the limiting-cycle amplitude phenomena, correspondence between combustion and acoustics, and the steep-fronted wave and flame propagation. The investigated parameters include the spray initial conditions, air-fuel mixture ratios, and the engine geometry. Stable and unstable operating conditions are found for the liquid-fueled combustors. Under certain conditions, the limiting cycle behavior of the combusting flowfields is obtained. The numerical results indicate that the spray vaporization processes play an important role in releasing thermal energy and driving the combustion instability. Author

N92-32298*# Pennsylvania State Univ., University Park. Dept. of Aerospace Engineering.

INVERSE DESIGN OF A PROPER NUMBER, SHAPES, SIZES, AND LOCATIONS OF COOLANT FLOW PASSAGES

George S. Dulikravich *In* NASA. Goddard Space Flight Center, Tenth Workshop for Computational Fluid Dynamic Applications in Rocket Propulsion, Part 1 Jul. 1992 p 467-486 (For primary document see N92-32278 23-34)

Avail: CASI HC A03/MF A05

During the past several years we have developed an inverse method that allows a thermal cooling system designer to determine proper sizes, shapes, and locations of coolant passages (holes) in, say, an internally cooled turbine blade, a scram jet strut, a rocket chamber wall, etc. Using this method the designer can enforce a desired heat flux distribution on the hot outer surface of the object, while simultaneously enforcing desired temperature distributions on the same hot outer surface as well as on the cooled interior surfaces of each of the coolant passages. This constitutes an over-specified problem which is solved by allowing the number, sizes, locations and shapes of the holes to adjust iteratively until the final internally cooled configuration satisfies the over-specified surface thermal conditions and the governing equation for the steady temperature field. The problem is solved by minimizing an error function expressing the difference between the specified and the computed hot surface heat fluxes. The temperature field analysis was performed using our highly accurate boundary integral element code with linearly varying temperature along straight surface panels. Examples of the inverse design applied to internally cooled turbine blades and scram jet struts (coated and non-coated) having circular and non-circular coolant flow passages will be shown. Author

N92-32299*# National Aeronautics and Space Administration. Marshall Space Flight Center, Huntsville, AL.

NUMERICAL ANALYSIS OF THE HOT-GAS-SIDE AND COOLANT-SIDE HEAT TRANSFER IN LIQUID ROCKET ENGINE COMBUSTORS

T. S. Wang and V. Luong *In* NASA. Goddard Space Flight Center, Tenth Workshop for Computational Fluid Dynamic Applications in Rocket Propulsion, Part 1 Jul. 1992 p 487-502 (For primary document see N92-32278 23-34)

Avail: CASI HC A03/MF A05

The objectives of this paper are to develop computational methods to predict the hot-gas-side and coolant-side heat transfer, and to use these methods in parametric studies to recommend optimized design of the coolant channels for regeneratively cooled liquid rocket engine combustors. An integrated numerical model which incorporates computational fluid dynamics (CFD) for the hot-gas thermal environment, and thermal analysis for the coolant channels, was developed. The mode was validated by comparing predicted heat fluxes with those of hot-firing test and industrial design methods. Parametric studies were performed to find a strategy for optimized combustion chamber coolant channel design. Author

N92-32300*# Mississippi Univ. for Women, Columbus. NSF Engineering Research Center for Computational Field Simulation.

AN EFFICIENT AND ROBUST GRID OPTIMIZATION ALGORITHM **c61**

Bharat K. Soni and Shaochen Yang *In* NASA. Goddard Space Flight Center, Tenth Workshop for Computational Fluid Dynamic Applications in Rocket Propulsion, Part 1 Jul. 1992 p 503-541 (For primary document see N92-32278 23-34)

Avail: CASI HC A03/MF A05

The development of an efficient and robust grid optimization is presented. This algorithm is developed by combining the best characteristics of algebraic, elliptic, and hyperbolic grid generation

techniques. This development is based on the following observations and evaluations: (1) algebraic systems are fast and economical; (2) precise spacing control is always achieved; (3) grid generation by elliptic systems is always smooth; and (4) the hyperbolic system preserves the orthogonality at the solid boundary and the point distribution in the field. Computational examples representing practical internal flow configurations are presented to demonstrate the algorithm. Author

N92-32301*# MDA Engineering, Inc., Arlington, TX.
ENHANCEMENTS TO THE GRIDGEN STRUCTURED GRID GENERATION SYSTEM FOR INTERNAL AND EXTERNAL FLOW APPLICATIONS **c61**
John P. Steinbrenner and John R. Chawner *In* NASA. Goddard Space Flight Center, Tenth Workshop for Computational Fluid Dynamic Applications in Rocket Propulsion, Part 1 Jul. 1992 p 543-576 (For primary document see N92-32278 23-34)
Avail: CASI HC A03/MF A05

GRIDGEN is a government domain software package for interactive generation of multiple block grids around general configurations. Though it has been freely available since 1989, it has not been widely embraced by the internal flow community due to a misconception that it was designed for external flow use only. In reality GRIDGEN has always worked for internal flow applications, and GRIDGEN ongoing enhancements are increasing the quality of and efficiency with which grids for external and internal flow problems may be constructed. The software consists of four codes used to perform the four steps of the grid generation process. GRIDBLOCK is first used to decompose the flow domain into a collection of component blocks and then to establish interblock connections and flow solver boundary conditions. GRIDGEN2D is then used to generate surface grids on the outer shell of each component block. GRIDGEN3D generates grid points on the interior of each block, and finally GRIDVUE3D is used to inspect the resulting multiple block grid. Three of these codes (GRIDBLOCK, GRIDGEN2D, and GRIDVUE3D) are highly interactive and graphical in nature, and currently run on Silicon Graphics, Inc., and IBM RS/6000 workstations. The lone batch code (GRIDGEN3D) may be run on any of several Unix based platforms. Surface grid generation in GRIDGEN2D is being improved with the addition of higher order surface definitions (NURBS and parametric surfaces input in IGES format and bicubic surfaces input in PATRAN Neutral File format) and double precision mathematics. In addition, two types of automation have been added to GRIDGEN2D that reduce the learning curve slope for new users and eliminate work for experienced users. Volume grid generation using GRIDGEN3D has been improved via the addition of an advanced hybrid control function formulation that provides both orthogonality and clustering control at the block faces and clustering control on the block interior. Author

N92-32302*# Mississippi Univ. for Women, Columbus. NSF Engineering Research Center for Computational Field Simulation.
CAGI: COMPUTER AIDED GRID INTERFACE. A WORK IN PROGRESS **c61**
Bharat K. Soni, Tzu-Yi Yu, and David Vaughn *In* NASA. Goddard Space Flight Center, Tenth Workshop for Computational Fluid Dynamic Applications in Rocket Propulsion, Part 1 Jul. 1992 p 577-613 (For primary document see N92-32278 23-34)
Avail: CASI HC A03/MF A05

Progress realized in the development of a Computer Aided Grid Interface (CAGI) software system in integrating CAD/CAM geometric system output and/or Interactive Graphics Exchange Standard (IGES) files, geometry manipulations associated with grid generation, and robust grid generation methodologies is presented. CAGI is being developed in a modular fashion and will offer fast, efficient and economical response to geometry/grid preparation, allowing the ability to upgrade basic geometry in a step-by-step fashion interactively and under permanent visual control along with minimizing the differences between the actual hardware surface descriptions and corresponding numerical analog. The computer code GENIE is used as a basis. The Non-Uniform Rational B-Splines (NURBS) representation of sculptured surfaces is utilized for surface grid redistribution. The computer aided analysis system, PATRAN, is adapted as a CAD/CAM system. The progress realized in NURBS surface grid generation, the development of IGES transformer, and geometry adaption using PATRAN will be presented along with their applicability to grid generation associated with rocket propulsion applications. Author

N92-32303*# National Aeronautics and Space Administration. Marshall Space Flight Center, Huntsville, AL.
USING ADAPTIVE GRID IN MODELING ROCKET NOZZLE FLOW
Alan S. Chow and Kang-Ren Jin (Mississippi State Univ., Mississippi State.) *In* NASA. Goddard Space Flight Center, Tenth Workshop for Computational Fluid Dynamic Applications in Rocket Propulsion, Part 1 Jul. 1992 p 615-645 (For primary document see N92-32278 23-34)
Avail: CASI HC A03/MF A05

The mechanical behavior of a rocket motor internal flow field results in a system of nonlinear partial differential equations which cannot be solved analytically. However, this system of equations called the Navier-Stokes equations can be solved numerically. The accuracy and the convergence of the solution of the system of equations will depend largely on how precisely the sharp gradients in the domain of interest can be resolved. With the advances in computer technology, more sophisticated algorithms are available to improve the accuracy and convergence of the solutions. An adaptive grid generation is one of the schemes which can be incorporated into the algorithm to enhance the capability of numerical modeling. It is equivalent to putting intelligence into the algorithm to optimize the use of computer memory. With this scheme, the finite difference domain of the flow field called the grid does neither have to be very fine nor strategically placed at the location of sharp gradients. The grid is self adapting as the solution evolves. This scheme significantly improves the methodology of solving flow problems in rocket nozzles by taking the refinement part of grid generation out of the hands of computational fluid dynamics (CFD) specialists and place it into the computer algorithm itself. Author

N92-32304*# National Aeronautics and Space Administration. Marshall Space Flight Center, Huntsville, AL.
COMPLEX THREE-DIMENSIONAL INTERNAL FLOWS IN THE ASRM AND RSRM AFT END SEGMENTS
Edward J. Reske, Dana F. Billings, and Joni W. Cornelison *In* NASA. Goddard Space Flight Center, Tenth Workshop for Computational Fluid Dynamic Applications in Rocket Propulsion, Part 1 Jul. 1992 p 647-662 (For primary document see N92-32278 23-34)
Avail: CASI HC A03/MF A05

Results from computational fluid dynamic analyses for complex three dimensional flows in the Advanced Solid Rocket Motor (ASRM) and Redesigned Solid Rocket Motor (RSRM) are presented. In particular, a parametric study for the case of a gimballed nozzle in these motors at various burn times and gimbal angles is presented. The resultant pressure fields are used to determine the location of the center of pressure and hinge moments due to the internal flow of these geometries. Author

N92-32305*# Engineering Research and Consulting, Inc., Tullahoma, TN.
AN ANALYSIS OF THE FLOW FIELD IN THE REGION OF THE ASRM FIELD JOINTS
Richard A. Dill and Harold R. Whitesides *In* NASA. Goddard Space Flight Center, Tenth Workshop for Computational Fluid Dynamic Applications in Rocket Propulsion, Part 1 Jul. 1992 p 663-688 (For primary document see N92-32278 23-34)
Avail: CASI HC A03/MF A05

The flow field in the region of a solid rocket motor field joint is very important since fluid dynamic and mechanical propellant stresses can couple to cause a motor failure at a joint. Presented here is an examination of the flow field in the region of the Advanced Solid Rocket Motor (ASRM) field joints. The analyses were performed as a first step in assessing the design of the

ASRM forward and aft field joints in order to assure the proper operation of the motor prior to further development of test firing. The analyses presented here were performed by employing a two-dimensional axisymmetric assumption. Fluent/BFC, a three dimensional full Navier-Stokes flow field code, was used to make the numerical calculations. This code utilizes a staggered grid formulation along with the SIMPLER numerical algorithm. Wall functions are used to determine the character of the laminar sublayer, and a standard kappa-epsilon turbulence model is used to close the fluid dynamic equations. The analyses performed to this date verify that the ASRM field joint design operates properly. The fluid dynamic stresses at the field joints are small due to the inherent design of the field joints. A problem observed in some other solid rocket motors is that large fluid dynamic stresses are generated at the motor joint on the downstream propellant grain due to forward facing step geometries. The design of the ASRM field joints are such that this is not a problem as shown by the analyses. Also, the analyses of the inhibitor stub left protruding into the port flow from normal propellant burn back show that more information is necessary to complete these analyses. These analyses were performed as parametric analyses in relation to the height of the inhibitor stub left protruding into the motor port. A better estimate of the amount of the inhibitor stub remaining at later burn times must be determined since the height which the inhibitor stub protrudes into the port flow drastically affects the fluid dynamics induced stresses on the propellant grain at the field joints. Author

N92-32306*# Aerojet-General Corp., Iuka, MS.
EFFECT OF INCLUDING VARIABLE GAS PROPERTIES AND ENTRAINED PARTICLES IN THE FLOW ANALYSIS OF THE ASRM NOZZLE
Curtis D. Clayton *In* NASA. Goddard Space Flight Center, Tenth Workshop for Computational Fluid Dynamic Applications in Rocket Propulsion, Part 1 Jul. 1992 p 689-711 (For primary document see N92-32278 23-34)
Avail: CASI HC A03/MF A05

The objective of this study is to determine the effect of using constant gas properties for the analysis of the Advanced Solid Rocket Motor (ASRM) nozzle and to gain more understanding concerning those types of analysis which might require this additional complexity. Kinetics data for viscosity, thermal conductivity, specific heat, and specific heat ratio are extracted from the Solid Propellant Rocket Motor Performance Prediction Computer Program (SPP) and tabulated as a function of temperature. These tables are added to the Aerovisc computational fluid dynamics (CFD) code in place of the constant gas property values. The results of a CFD analysis of the ASRM 48 inch motor with constant gas properties will be compared with an analysis which uses variable gas properties. Mach number, surface pressure, and torque plots are presented. A full scale ASRM analysis using SPP with and without particle flow is presented. Author

N92-32307*# Scientific Research Associates, Inc., Glastonbury, CT.
A TWO-PHASE RESTRICTED EQUILIBRIUM MODEL FOR COMBUSTION OF METALIZED SOLID PROPELLANTS c25
J. S. Sabnis, F. J. deJong, and H. J. Gibeling *In* NASA. Goddard Space Flight Center, Tenth Workshop for Computational Fluid Dynamic Applications in Rocket Propulsion, Part 1 Jul. 1992 p 713-724 (For primary document see N92-32278 23-34)
(Contract F04611-86-C-0096)
Avail: CASI HC A03/MF A05

An Eulerian-Lagrangian two-phase approach was adopted to model the multi-phase reacting internal flow in a solid rocket with a metalized propellant. An Eulerian description was used to analyze the motion of the continuous phase which includes the gas as well as the small (micron-sized) particulates, while a Lagrangian description is used for the analysis of the discrete phase which consists of the larger particulates in the motor chamber. The particulates consist of Al and Al2O3 such that the particulate composition is 100 percent Al at injection from the propellant surface with Al2O3 fraction increasing due to combustion along the particle trajectory. An empirical model is used to compute the combustion rate for agglomerates while the continuous phase chemistry is treated using chemical equilibrium. The computer code was used to simulate the reacting flow in a solid rocket motor with an AP/HTPB/Al propellant. The computed results show the existence of an extended combustion zone in the chamber rather than a thin reaction region. The presence of the extended combustion zone results in the chamber flow field and chemical being far from isothermal (as would be predicted by a surface combustion assumption). The temperature in the chamber increases from about 2600 K at the propellant surface to about 3350 K in the core. Similarly the chemical composition and the density of the propellant gas also show spatially non-uniform distribution in the chamber. The analysis developed under the present effort provides a more sophisticated tool for solid rocket internal flow predictions than is presently available, and can be useful in studying apparent anomalies and improving the simple correlations currently in use. The code can be used in the analysis of combustion efficiency, thermal load in the internal insulation, plume radiation, etc. Author

N92-32322# Lawrence Livermore National Lab., CA.
A NUMERICAL STUDY OF NATURAL CONVECTION IN A NARROW ANNULUS
V. Sahai Dec. 1991 15 p
(Contract W-7405-eng-48)
(DE92-017138; UCRL-ID-109125) Avail: CASI HC A03/MF A01

Various numerical models were used to predict the natural convection of a solidifying liquid metal in a narrow annulus. Previous work in this area does not consider the temperature variation that exists in the fluid and the resulting heat conduction in the solid mold material. The finite element fluid dynamics code FIDAP was used to solve these models. The results indicate that the natural convective effects are small. DOE

N92-32324# Notre Dame Univ., IN. Dept. of Aerospace and Mechanical Engineering.
ANNUAL PROGRESS REPORT ON IMPOSED 3-D DISTURBANCES ON BLUFF-BODY NEAR WAKE FLOWS
Annual Progress Report
Albin A. Szewczyk 1991 5 p
(Contract N00014-90-J-4083)
(AD-A250366) Avail: CASI HC A01/MF A01

We wish to achieve a better understanding of the underlying physical mechanisms that make bluff body flows. These flows are typically characterized in two-dimensions, but exhibit three-dimensional effects. Further we hope to be able to associate these effects, which are characterized by vortex splitting and vortex looping, to various properties of the flow such as drag, base pressure, shedding frequency, wake formation length and if possible to the global instability of the flow. GRA

N92-32468# Oak Ridge National Lab., TN.
PHASE DISTRIBUTION MEASUREMENTS IN NARROW RECTANGULAR CHANNELS USING IMAGE-PROCESSING TECHNIQUES
C. L. Bentley and A. E. Ruggles Jun. 1992 21 p
(Contract DE-AC05-84OR-21400)
(DE92-014084; ORNL/TM-12011) Avail: CASI HC A03/MF A01

Phase distribution of air-water flow in a narrow rectangular channel is examined using image-processing techniques. Ink is added to the water, and clear channel walls were used to allow high-speed, still photographs and video tape to be taken of the air-water flow field. Flow field images are digitized and stored in a Macintosh IIci computer using a frame grabber board. Local grey levels are related to liquid thickness in the flow channel using a calibration fixture. Image-processing shareware is used to calculate the spatially averaged liquid thickness from the image of the flow field. Time-averaged spatial liquid distributions are calculated using image calculation algorithms. The spatially averaged liquid distribution is calculated from the time-averaged spatial liquid

distribution to formulate the combined temporally and spatially averaged liquid fraction values. The temporally and spatially averaged liquid fractions measured using this technique compare well to those predicted from pressure gradient measurements at zero superficial liquid velocity. DOE

N92-32472*# National Aeronautics and Space Administration. Lewis Research Center, Cleveland, OH.
BREAKDOWN OF THE KARMAN VORTEX STREET DUE TO FORCED CONVECTION AND FLOW COMPRESSIBILITY
Shu-Cheng Chen Jul. 1992 41 p
(RTOP 505-62-52)
(NASA-TM-105853; E-7212; NAS 1.15:105853) Avail: CASI HC A03/MF A01

Low speed compressible flow around a heated/cooled circular cylinder was investigated. The phenomenon of sudden disappearing of the Karman vortex street was numerically simulated and studied. The vortex street at Re(sub d) = 100 and M(sub infinity) = 0.3 is primarily an effect of forced convection. The contribution of natural convection to the current event is inconsequential. The reason for the breakdown of vortex street is believed to be due to a high temperature zone in the wake generated by a high level of wall heating. This produces an effectively lower Reynolds number flow in the near wall region when a compressible gaseous media is used. Vortex shedding stops for a reason similar when flow Reynolds number is reduced globally below its minimum value. Periodic vortex sheddings were observed when the wall heating ratio was less than 0.6. In that region, the coefficient of lift decreased sharply to zero, drag increased slowly, and the Strouhal number reduced monotonically with respect to the wall heating. When the heating ratio was greater than or equal to 0.6, vortex shedding stopped, and steady flows with symmetric twin trailing vortices were observed. In this region, both lift and Strouhal number remained zero, the drag increased sharply, and the Nusselt number maintained the same decreasing slope as the one obtained from the previous region. In this paper quantitative results such as Strouhal number, lift, drag, and Nusselt number, as well as qualitative results such as streamline, isothermal, and vorticity contours obtained at various flow conditions are presented and compared with the results of Noto et al. and Chang et al. Contrast between the two are discussed. Author

N92-32474*# National Aeronautics and Space Administration. Ames Research Center, Moffett Field, CA.
THERMAL CONDUCTANCE OF AUGMENTED PRESSED METALLIC CONTACTS AT LIQUID HELIUM TEMPERATURES
L. J. Salerno, P. Kittel, and A. L. Spivak (Trans-Bay Electronics, Richmond, CA.) Aug. 1992 26 p
(RTOP 590-31-41)
(NASA-TM-103917; A-92055; NAS 1.15:103917) Avail: CASI HC A03/MF A01

The thermal conductance of uncoated oxygen-free high conductivity (OFHC) copper, 6061-T6 aluminum, free-machining brass, and 304 stainless steel sample pairs which were augmented with a gold coated 6061-T6 aluminum washer inserted between the contact surfaces was measured over the temperature range of 1.6 to 6.0 K, with applied forces from 22 to 670 N. The contact surfaces of the sample pairs were prepared with a 0.8 micron lapped finish, while the finish of the aluminum washer was 0.2 micron lapped. The contribution to the overall thermal impedance by the bulk conductance of the aluminum washer was negligible. It was found that addition of the washer offered no significant conductance improvement over an uncoated single contact pair; any benefits from using the gold plated washer were counteracted by the addition of two more contact surfaces. Additionally, the thermal conductance of a 'combination' aluminum sample pair having one gold coated and one uncoated surface was measured and compared to the washer pair. The ratio of the conductance of the washer pair to half the conductance of the 'combination' pair was found to be constant and near unity over the temperature range of the data obtained, within experimental error. Author

N92-32560*# California Univ., Los Angeles.
A COMPUTATIONAL FLUID DYNAMICS ANALYSIS OF THE HYPERSONIC FLIGHTS OF PEGASUS
Darren Fricker, John Mendoza, and Ivan Catton Aug. 1992 32 p Sponsored in part by NASA. Dryden Flight Research Facility
(Contract NCC2-374; RTOP 505-59-40)
(NASA-CR-186023; H-1835; NAS 1.26:186023) Avail: CASI HC A03/MF A01

The performance of a fully viscous, three-dimensional Navier-Stokes solver, PARC3D, was tested. The criteria for judging the performance of the CFD code were based on flight data from the first two flights of the Pegasus. The flight data consisted of heat-transfer rates and sparse pressure coefficients primarily in the fillet region of the vehicle. The code performed remarkably well in all aspects of the tests. As expected, the best heat-transfer results were obtained for the low Mach number simulations. These results are attributed to lack of high ablation rates at the lower Mach numbers since the CFD simulations did not account for ablation at the vehicle surface. As the Mach number increased, the ablative effects became more apparent in the comparisons. This effect was evident at the highest Mach numbers, when PARC3D would be required over the entire fillet region, rather than at a few discrete locations. In this manner, CFD heat-flux profiles could be accurately evaluated. Although the pressure data were sparse, the trends suggest that the code predicts surface pressures with reasonable accuracy. Three of the four locations yield pressures that are consistent, but the CFD results yield pressures below the flight data by a factor of 2 at the fourth location. Author

N92-32598# Michigan Univ., Ann Arbor. Gas Dynamics Labs.
A BASIC RESEARCH MODEL OF NATURAL GAS COMBUSTION IN TURBULENT FLOW, PHASE 2 Annual Report, 1 Jun. 1988 - 31 Jul. 1990
Werner J. A. Dahm, Gretar Tryggvason, and Robert Krasny 17 Feb. 1992 101 p
(Contract GRI-5088-260-1692)
(PB92-190362; GRI-91/0391-Phase-2) Avail: CASI HC A06/MF A02

Progress made in extending a local integral method (LIM) model for approximately simulating vorticity transport and mixing, as well as molecular diffusion and reaction of chemical species, in natural gas combustion is described. The LIM model is fundamentally different from conventional approaches for numerically simulating combustion in turbulent flames, and is based on the experimental observation that the strain-diffusion balance which establishes the mixing and reaction scales in turbulent flames leads to a self-similar internal structure which does not need to be continually recomputed. Instead, these scales are represented by a family of self-similar profile shapes, whose moments are allowed to evolve freely to satisfy the governing equations. The resulting LIM computations, thus, need only to track the evolution of a material surface in the flow, and solve ordinary differential equations on the surface, rather than partial differential equations throughout the whole flame. The application of the LIM model for computing the evolution of conserved scalar fields and the resulting equilibrium reaction processes is described, and the results from sample calculations are presented. The application of the LIM approach to the vorticity field is also described. Author

N92-32630# Massachusetts Inst. of Tech., Cambridge. Lab. for Water Resources and Hydrodynamics.
SIMPLE MODELS FOR TURBULENT WAVE-CURRENT BOTTOM BOUNDARY LAYER FLOW Final Report
O. S. Madsen and Palitha N. Wikramanayake Dec. 1991 158 p
(AD-A247942; CERC/CR/DRP-91-1) Avail: CASI HC A08/MF A02

The application of simple eddy viscosity models to the interaction between the turbulent wave and current boundary layer is studied. A comparison of the results of some recent models from the literature with data from laboratory experiments and

numerical models shows that none of these models reproduced the data satisfactorily. An improved model, which did not involve any additional fitting parameters, was developed and found to fit the data well for the case of waves and current in the same direction. The inability of the improved model to represent some features of the results of higher order turbulence models for the case of waves at an angle to the current was found to be due to the assumption of a time-invariant eddy viscosity. Therefore, a model that allowed the eddy viscosity to vary with time was developed and solved for the case of a weak current. This time varying model was found to improve the agreement with the numerical model for the case of waves at an angle to the current. Simple, accurate, analytic approximations were developed that allow the solution of practical problems with this model using no more powerful a tool than a hand calculator. GRA

N92-32632# Wright Lab., Wright-Patterson AFB, OH.
AN EXAMINATION OF SEVERAL HIGH RESOLUTION SCHEMES APPLIED TO COMPLEX PROBLEMS IN HIGH SPEED FLOWS Final Report, Jun - Dec. 1991
Norbert Kroll, Michael Aftosmis, and Datta Gaitonde 2 Feb. 1992 63 p
(AF Proj. 2307)
(AD-A250814; WL-TR-91-3089) Avail: CASI HC A04/MF A01

A comparative study of five upwind schemes was performed to evaluate their ability to accurately model the convective fluxes of the Euler equations for problems containing complex shock structure. The schemes investigated used a variety of Reimann solvers and obtained higher order accuracy using either a MUSCL or non-MUSCL approach. The MUSCL-type schemes included the flux vector split formulations of Steiger-Warming and van Leer and the flux difference split approach of Roe. The Non-MUSCL schemes included the Symmetric and Upwind TVD methods of Yee, and Harten and Yee. Two central difference schemes provide a basis for the evaluation of these upwind methods. The comparison was performed using identical meshes and convergence criteria. In a supersonic blunt body flow, all the upwind schemes displayed comparably resolved bow shocks, independent of free stream Mach number. However, a complex type IV shock on cowl lip example pointed out significant differences in the accuracy and convergence behavior of the schemes. A comparison of the flow structure shown by the various algorithms on identical grids indicated that the discrete solutions obtained with Upwind TVD and Roe flux difference splitting were the least diffusive of the upwind methods considered. GRA

N92-32652# David Taylor Research Center, Bethesda, MD. Propulsion and Auxiliary Systems Dept.
THE APPLICATION OF UNSTEADY POTENTIAL FLOW VORTEX LOOP/DIPOLE THEORY TO THE WORK AND ACOUSTICS OF LOW-SPEED TURBOMACHINERY
Earl Quandt Feb. 1992 53 p
(AD-A251160; DTRC-PAS-91/55) Avail: CASI HC A04/MF A01

An ideal turbomachine transfers energy from a rotating shaft to a fluid through the creation of a flow field that is unsteady in the absolute frame. In order to understand and control the work and acoustics of this process, the basic building-block singularities of potential flow are developed in a unified manner such that both near- and far-field effects appear naturally in the formulation. It is shown how the total vector force applied to the fluid by a discrete rigid blade is related to the bound and shed vortex system and the acceleration of the displaced mass. Following Lighthill, the volume integral of the vector moment of vorticity is found to describe most fundamentally how the unsteady fluid motions in a turbomachine are related to surface forces that do work on the fluid. Because unsteady flow is required for energy transfer, the work input of a single blade creates simultaneously in the fluid an acoustic signal that propagates to the far-field. The strength of this signal is determined by the time derivative of the instantaneous blade force component in the direction of a stationary observer, i.e., with the pattern of a rotating dipole. The summation of these tonal signals from combinations of blades and vanes is computed for free-field and cylindrical duct boundary conditions. Bessel functions are found to characterize both cases, their order being determined by specific blade/vane number differences. Rules for tonal sound control by acoustic interference or mode decay, such as those of Tyler and Sofrin, are examined. Implications for broadband acoustics are discussed. GRA

N92-32671# Illinois Inst. of Tech., Chicago. Fluid Dynamics Research Center.
INTERACTIVE CONTROL IN TURBULENT SHEAR LAYERS Annual Report, Feb. 1991 - Jan. 1992
Candace E. Wark and Hassan M. Nagib 5 Feb. 1992 35 p
(Grant AF-AFOSR-0171-90)
(AD-A250711; AFOSR-92-0374TR) Avail: CASI HC A03/MF A01

Using Particle Image Velocimetry in a turbulent pipe flow, instantaneous large-scale structures were observed, which are not seen in low Reynolds number direct numerical simulations of bounded turbulent shear flow. A probable explanation for this discrepancy is the much larger experimental Reynolds number, as compared with the DNS results. Further support of this Reynolds number influence was found when quantifying the relative role of the outer-layer structures and wall-layer structures on the spanwise correlation coefficient between the wall-shear stress and streamwise velocity. The results suggest that the influence of the outer flow on the streamwise velocity fluctuations at $y+ = 10$, increases with increasing Reynolds number. This outer-layer effect was then further examined in terms of the boundary layer intermittency/wall-layer dynamics coupling. Although the outer layer is directly influencing the wall-layer region, it was found that the alternating passages of laminar and turbulent regions in the intermittent part of the boundary layer were not directly influencing the buffer layer statistics. The mechanisms of this influence are currently being investigated. GRA

N92-32675# National Aerospace Lab., Amsterdam (Netherlands). Space Div.
THERMAL GRAVITATIONAL MODELLING AND SCALING OF TWO-PHASE HEAT TRANSPORT SYSTEMS FOR SPACE: AN ASSESSMENT AND A COMPARISON OF PREDICTIONS AND EXPERIMENTAL RESULTS
A. A. M. Delil 18 Oct. 1991 12 p Presented at the 4th European Symposium on Space Environmental Control Systems, Florence, Italy, 21-24 Oct. 1991 Previously announced as N92-25833
(Contract NIVR-2404-N)
(NLR-TP-91401-U; ETN-92-92008) Avail: CASI HC A03/MF A01

Terrestrial scaling experiments, using the ammonia test rig, are foreseen to support the development of the ESA capillary pumped Two Phase ammonia Experiment (TPX) in Get Away Special G-357 and the development of the mechanically pumped ESA R114 Two Phase Heat Transport System (TPHTS). The assessment of the applicability (validity and restrictions) of the modeling and scaling approach, based on similarity considerations, is supported by a comparison of measured two phase flow pressure drops under low gravity conditions and thermal gravitational modeling and scaling outcomes. ESA

N92-32683# Ballistic Research Labs., Aberdeen Proving Ground, MD.
CHARACTERIZATION OF FLOW DISTRIBUTION IN AXISYMMETRIC SHOCK TUBES Final Report, Mar. 1990 - Apr. 1992
Stephen J. Schraml and Richard J. Pearson Jun. 1992 39 p
(AD-A251095; BRL-TR-3353) Avail: CASI HC A03/MF A01

Experiments were conducted to study the characteristics of unsteady flow in a small, axisymmetric shock tube. These experiments have been supplemented by numerical results obtained from the SHARC hydrodynamic computer code. Early SHARC results indicated that a substantial gradient in flow velocity and dynamic pressure may exist along the cross section of the shock tube. To further investigate this phenomenon, additional

experiments were performed in which dynamic pressure measurements were made at various radii in the expansion section of the shock tube. Additional calculations with the SHARC code were also performed in which turbulence modeling, artificial viscosity, and second order advection were employed. The second set of calculations agree very well with the experimental results. These results indicate that the dynamic pressure is nearly constant across the radius of the shock tube. This contradicts the early computational results which were performed with first order advection and without turbulence modeling. As a result of these findings, it was concluded that turbulence modeling was necessary to obtain accurate shock tube flow simulations. GRA

N92-32687# Direction Generale de l'Aviation Civile, Paris (France).
INFLUENCE OF AN INTENSE ACOUSTIC FIELD ON BOUNDARY LAYER SEPARATION Final Summary Report [INFLUENCE D'UN CHAMP ACOUSTIQUE INTENSE SUR LE DECOLLEMENT D'UNE COUCHE LIMITE TURBULENTE. RAPPORT FINAL DE SYNTHESE]
E. Brocher, A. Andrianantoandro, V. Pugliesi (Centre National de la Recherche Scientifique, Paris, France), and J. P. Ardissone (Centre National de la Recherche Scientifique, Paris, France) 1991 58 p In FRENCH
(Contract DRET-89-168)
(ETN-92-92081) Avail: CASI HC A04/MF A01

A study on the influence of an intense acoustic field on the position of the separation point of a turbulent boundary layer is presented. Acoustic pressure measurements were carried out using piezoresistive sensors to determine the amplitude, phase differencing, and phase velocity, of the acoustic waves. Velocity measurements were carried out by laser anemometry. With appropriate signal processing, the mean velocity, the periodic velocity component, and the level of turbulence, were determined. The boundary layer response to the acoustic field is characterized by change in mean velocity and periodic components amplitude within the boundary layer. The geometry configuration used did not allow for the study of the influence on the separation itself, but only on boundary layer reattachment. In the presence of a perturbation provoked separation, the influence of the acoustic field was to slightly displace the reattachment upstream: it diminished the extend of the separated region. ESA

N92-32725# Ecole Centrale de Lyon (France).
MODEL OF REYNOLDS STRESS ON NONORTHOGONAL GRID STRUCTURES: APPLICATION TO A STAGGERED TUBE BUNDLE Ph.D. Thesis [MODELE AUX TENSIONS DE REYNOLDS SUR MAILLAGES STRUCTURES NON-ORTHOGONAUX: APPLICATION A UN ECOULEMENT DENS UN FAISCEAU DE TUBES EN QUINCONCE]
Samuel Sebag 1991 185 p In FRENCH
(ETN-92-91959) Avail: CASI HC A09/MF A02

The state of the art of models are reviewed. Developments in second order closing models are traced, highlighting their constraints, and an insight into new models whose complexity does not yet enable the generalization of wall flow is given. The adaptation of a numerical method, used for cartesian grids, to nonorthogonal grid structures, with the Gibson-Launder Reynolds stress model, in the framework of ULYSSE-4 two dimensional finite volume code, is presented. K-epsilon and second order closing models are compared in the flow in a staggered bundle tube. The limits of the closure model, of the numerical approach, and of the limit conditions, are analyzed. ESA

N92-32727# Stockholm Univ. (Sweden). Dept. of Meteorology.
NUMERICAL METHODS: SOLVING THE ADVECTION EQUATION IN FLOWS WITH SHARP GRADIENTS USING BOTT'S FLUX SCHEME
Elias Holm and Gerhard Erbes 2 Dec. 1991 51 p
(DM-59; ETN-92-91976) Avail: CASI HC A04/MF A01

A mass conservative positive definite advection scheme, which is formulated on flux form, is tested for the advection of functions with sharp gradients. A comparison is made with a modified version of the leapfrog method. For a given resolution, the performance of Bott's flux scheme is superior. For a given Central Processing Unit (CPU) time, a low resolution Bott flux scheme still performs better than a high resolution modified leapfrog scheme. Bott's flux scheme performs relatively well in regions with sharp gradients. The main drawback of Bott's scheme is its lack of monotonicity, that is, spurious oscillations are allowed to develop. ESA

N92-32765# Ecole Nationale d'Ingenieurs de Constructions Aeronautiques, Toulouse (France). Dept. de Mecanique des Fluides Aerodynamiques.
MASSIVELY SEPARATED FLOW MODELING. EXPERIMENTAL STUDY OF THE FINE STRUCTURE OF BOUNDARY LAYERS. STUDY OF THE INFLUENCE OF EXTERNAL TURBULENCE LEVEL Final Summary Report [MODELISATION D'ECOULEMENTS MASSIVEMENT DECOLLES. ETUDE EXPERIMENTALE DE LA STRUCTURE FINE DES COUCHES LIMITES. ETUDE DE L'INFLUENCE DU NIVEAU DE TURBULENCE EXTERIEURE. RAPPORT DE SYNTHESE FINAL]
J. B. Cazalbou and P. Chassaing 1991 26 p In FRENCH
Sponsored by Direction des Recherches, Etudes et Techniques
(ETN-92-92088) Avail: CASI HC A03/MF A01

Wind tunnel tests to define methods and models for reliable prediction of separated flow around high incidence wing profiles, in turbulent boundary layer and incompressible flow conditions, are presented. The problem is examined in the context of first order modeling, with internal region processing based on the use of wall laws. The following are reported: the behavior of the first order model in the case of unfavorable pressure gradients; the validity of wall laws in separated regions; and the influence of external turbulence rates. ESA

N92-32767# Technische Univ., Munich (Germany, F.R.). Inst. fuer Mathematik.
NUMERICAL SIMULATION OF TWO-DIMENSIONAL FLOWS BY THE FREE-LAGRANGIAN METHOD
Mikhail Y. Shashkov and Andrey V. Solovjov 1991 51 p
Sponsored by German Research Society
(TUM-M9105; ETN-92-92102) Copyright Avail: CASI HC A04/MF A01

The development, realization, and verification of a purely Lagrangian, conservative free-Lagrangian method are described. The term 'purely Lagrangian' means that the mass of particles is not changed; no mass, momentum, and energy exchange appears between particles; no interpolation or smoothing procedures are used; and the cell connected with a particle contains only one material (there are non-'mixed' cells). In the method, the network structure is determined by the Dirichlet tesselations of the computational domain. It is shown by a computational experiment that the volume of a Dirichlet cell varies more smoothly than that of comparable approaches when the structure of the grid changes. The continuity of the volume determines, for Lagrangian methods, the density continuity of the given particle. Another important property of the Dirichlet volume is that its derivatives, with respect to particle coordinates, are likewise continuous. These derivatives appear in the difference equations, so that acceleration, velocity, internal energy, and pressure are continuous. The conservative difference scheme is obtained by using the method of support operators. The approximation property of the constructed difference scheme is investigated. Some approaches to the treatment of free boundaries are described. Results of computation are presented for some two dimensional problems. ESA

N92-32770# Metraflu, Ecully (France).
PRESSURE FIELD DEVELOPED BY THE RANDOM MOVEMENT OF THE VORTICES NEAR A WALL Final Report [CHAMP DE PRESSION ENGENDRE PAR LE MOUVEMENT CHAOTIQUE DE TOURBILLONS AU VOISINAGE D'UNE PAROI. RAPPORT FINAL]
Luc Collorec and Daniel Juve Oct. 1991 71 p In FRENCH
(Contract DRET-90-1177A)
(ETN-92-91665) Avail: CASI HC A04/MF A01

The behavior of a linear ensemble of vortices, in a two dimensional non rotating fluid near a wall is modeled. The experimental results are presented and discussed. The initial motion of the vortices are characterized by Fourier transformation, by phase analysis and by Poincare section, for different initial vortex configurations. The existence of periodical or random regimes and order-disorder transition are highlighted. The pressure field at the wall is calculated during the passage of vortices. The configuration of the pressure distribution and of the somewhat chaotic motion of vortices were compared. The results revealed that the pressure oscillation frequency increases as the chaos increases. The directivity of the far acoustic field is shown to be quadrupolar and its intensity increases as the chaos increases. ESA

N92-32776# Office National d'Etudes et de Recherches Aerospatiales, Paris (France). Direction des Structures.
STRONG COUPLING BETWEEN INVISCID FLUID AND BOUNDARY LAYER OF SHARP LEADING EDGES: TWO-DIMENSIONAL STATIONARY AND TURBULENT CASES FOR ISOLATED PROFILES AND GUARD VANES [DOUPLAGE FORT FLUIDE PARFAIT COUCHE LIMITE POUR DES PROFILES A BORD D'ATTAQUE AIGU. CAS 2D STATIONNAIRE ET INSTATIONNAIRE POUR DES PROFILS ISOLES ET POUR LES GRILLES D'AUBES]
C. Soize Dec. 1991 75 p In FRENCH
(Contract DRET-89-34-001)
(ONERA-RT-44/1621-RY-016-R; ETN-92-91675) Avail: CASI HC A04/MF A01

The theory and the numerical model concerning the strong coupling between the inviscid fluid and the upper boundary layer are presented. The calculations are performed for two dimensional turbulent and stationary conditions. The results were compared to those obtained from wind tunnel tests, and a good agreement between them is obtained. A quasi-stationary simplified method to approximately calculate, at low costs, the turbulent aerodynamic forces for guard vanes, is given. ESA

N92-32781 ESDU International Ltd., London (England).
FORCED CONVECTION HEAT TRANSFER IN STRAIGHT TUBES. PART 1: FULLY DEVELOPED TURBULENT FLOW
May 1992 33 p Supersedes ESDU-67016 and ESDU-68007
(ESDU-92003-Pt-1; ESDU-67016; ESDU-68007; ISBN-0-85679-808-8) Avail: ESDU

ESDU 92003 recommends the Petukov equation for the prediction of the heat transfer in single-phase Newtonian flow, following a comparison of it and five other correlations with a database of nearly 800 experimental results extracted from the literature. The quality of the fit of the data with the six correlations is tabulated in various flow regimes defined by specific ranges of Reynolds and Prandtl numbers. The correlations are also compared as graphs of Nusselt number against Reynolds number for values of Prandtl number of 0.7, 10 and 100. Two forms of the equation are given, one applying in the higher ranges of Reynolds and Prandtl numbers. Corrections for variable fluid properties are suggested for liquid as a function of bulk-to-wall dynamic viscosity ratio and for specific gases in terms of bulk-to-wall temperature ratio. Information on regimes for forced, free and mixed convection for both horizontal and vertical flow is included. The Petukov equation may be applied provided the thermal entrance length is exceeded and values for that are given based on local or mean Nusselt number. Worked examples illustrate the use of the correlation. ESDU

N92-32784*# Institute for Computer Applications in Science and Engineering, Hampton, VA.
SINGULARITIES IN THE CLASSICAL RAYLEIGH-TAYLOR FLOW: FORMATION AND SUBSEQUENT MOTION Final Report
S. Tanveer Aug. 1992 44 p Submitted for publication
(Contract NAS1-18605; NSF DMS-91-07608; RTOP 505-90-52-01)
(NASA-CR-189690; NAS 1.26:189690; ICASE-92-37) Avail: CASI HC A03/MF A01

The creation and subsequent motion of singularities of solution to classical Rayleigh-Taylor flow (two dimensional inviscid, incompressible fluid over a vacuum) are discussed. For a specific set of initial conditions, we give analytical evidence to suggest the instantaneous formation of one or more singularities at specific points in the unphysical plane, whose locations depend sensitively on small changes in initial conditions in the physical domain. One-half power singularities are created in accordance with an earlier conjecture; however, depending on initial conditions, other forms of singularities are also possible. For a specific initial condition, we follow a numerical procedure in the unphysical plane to compute the motion of a one-half singularity. This computation confirms our previous conjecture that the approach of a one-half singularity towards the physical domain corresponds to the development of a spike at the physical interface. Under some assumptions that appear to be consistent with numerical calculations, we present analytical evidence to suggest that a singularity of the one-half type cannot impinge the physical domain in finite time. Author

N92-32786# National Aerospace Lab., Amsterdam (Netherlands). Space Div.
TWO-PHASE HEAT TRANSPORT SYSTEMS FOR SPACE: THERMAL GRAVITATIONAL MODELLING AND SCALING PREDICTIONS VERSUS RESULTS OF EXPERIMENTS
A. A. M. Delil 29 Jan. 1991 12 p Presented at the 1st ASME/JSME Fluids Engineering Conference, Portland, OR, 23-27 Jun. 1991 and IUTAM Symposium in Microgravity Fluid Mechanics, Bremen, Fed. Republic of Germany, 2-6 Sep. 1991
(Contract NIVR-2404-N)
(NLR-TP-91051-U; ETN-92-91995) Avail: CASI HC A03/MF A01

Measured two phase flow pressure drops under low gravity conditions are compared with thermal gravitational modeling and scaling predictions. The scaling serves as a first step: to assess the applicability (validity and restrictions) of the modeling/scaling approach; to define useful terrestrial scaling experiments with the ammonia test rig to support the development of the ESA Two Phase (ammonia) Experiment (TPX) in Get Away Special G-557, and the development of the mechanically pumped ESA (R114) Two Phase Heat Transport System (TPHTS). ESA

N92-32824# Lawrence Livermore National Lab., CA.
ADVANCES IN COMPRESSIBLE TURBULENT MIXING
W. P. Dannevik, ed., A. C. Buckingham, ed., and C. E. Leith, ed. 1 Jan. 1992 634 p Presented at the Workshop on the Physics of Compressible Turbulent Mixing, Princeton, NJ, 24-27 Oct. 1988
(Contract W-7405-eng-48)
(DE92-014326; CONF-8810234) Avail: CASI HC A99/MF A06

This volume includes some recent additions to original material prepared for the Princeton International Workshop on the Physics of Compressible Turbulent Mixing, held in 1988. Workshop participants were asked to emphasize the physics of the compressible mixing process rather than measurement techniques or computational methods. Actual experimental results and their meaning were given precedence over discussions of new diagnostic developments. Theoretical interpretations and understanding were stressed rather than the exposition of new analytical model developments or advances in numerical procedures. By design, compressibility influences on turbulent mixing were discussed--almost exclusively--from the perspective of supersonic flow field studies. The papers are arranged in three topical categories: Foundations, Vortical Domination, and Strongly Coupled Compressibility. The Foundations category is a collection of seminal studies that connect current study in compressible turbulent mixing with compressible, high-speed turbulent flow research that almost vanished about two decades ago. A number of contributions are included on flow instability initiation, evolution, and transition between the states of unstable flow onset through those descriptive of fully developed turbulence. The Vortical Domination category includes theoretical and experimental studies of coherent structures, vortex pairing, and vortex-dynamics-influenced pressure focusing. In the Strongly Coupled Compressibility category the organizers included the high-speed turbulent flow investigations in which the interaction of shock waves could be considered an

important source for production of new turbulence or for the enhancement of pre-existing turbulence. Individual papers are processed separately. DOE

N92-32831# National Aerospace Lab., Amsterdam (Netherlands). Space Div.
FREE MOTION OF AN UNSUPPORTED TANK THAT IS PARTIALLY FILLED WITH LIQUID
J. P. B. Vreeburg 10 May 1991 23 p Presented at the IUTAM Symposium on Microgravity Fluid Mechanics, Bremen, Fed. Republic of Germany, 2-6 Sep. 1991
(NLR-TP-91185-U; ETN-92-92002) Avail: CASI HC A03/MF A01

The motion of a partially filled tank is studied for its relevance to the control of maneuvering space vehicles with liquid stores. For numerical simulations, a number of computer programs were developed. An experimental program with investigations on parabolic flight in suborbital and orbital trajectories was defined and is in preparation. The present immediate objective is the synthesis of the so called Wet Satellite Model (WSM) experiment which includes the development of a diagnostic instrument ('ballistometer') and the launch of a test article in a seven minute parabola by sounding rocket. A breadboard model was flown on parabolic flight. The tests of the breadboard have as their primary purpose the assessment of the performance of the instrumentation to determine the motion. This instrument will consist of nine linear microaccelerometers that are arranged about the body. The equations that govern the behavior of the unsupported tank are given and discussed. ESA

N92-32835# National Aerospace Lab., Amsterdam (Netherlands). Informatics Div.
CFD EFFORTS IN THE NETHERLANDS
W. Loeve 4 Jul. 1991 14 p Presented at the 4th International Symposium on CFD, Davis, CA, 9-12 Sep. 1991
(NLR-TP-91250-U; ETN-92-92006) Avail: CASI HC A03/MF A01

Research in the Netherlands on technical and organizational methods, techniques, and tools to structure and integrate the growing amount of CFD (Computational Fluid Dynamics) software and supporting utility programs, is reviewed. This has resulted in ISNaS, an open software system for development, production, and application of CFD. The system is implemented on a powerful local network connected to the national network. The approach is described for cooperative development of CFD software that can form part of an open system such as ISNaS. Reference is made to application of the approach for solvers for the Reynolds averaged Navier-Stokes equations concerning three cooperative development projects. ESA

N92-32856 British Petroleum Co. Ltd., London (England).
SPRAY NOZZLE FOR FIRE CONTROL Patent Application
Panayiotis G. Papavergos, inventor 14 Sep. 1990 15 p
(CA-Patent-Appl-SN-2-011-945; Int-Patent-Class-B05B-1/00; CTN-92-60391) Avail: Micromedia Ltd., Technical Information Centre, 165 Hotel de Ville, Place du Portage, Phase 2, Hull, Quebec J8X 3X2, Canada HC/MF

The design of a spray nozzle for fire control is described. It produces a spray of gas and liquid having an oval transverse cross section and it comprises a mixing chamber with an oval transverse cross section adapted to induce a toroidal mixing pattern in pressurized gas and liquid introduced to the mixing chamber through a plurality of inlets. In a preferred embodiment the mixing chamber is toroidal. The spray nozzle produces an oval spray pattern for more efficient wetting of narrow passages and is suitable for fire control systems in vehicles or other confined spaces. Vehicles to which this invention may be applied include trains, armoured vehicles, ships, hovercraft, submarines, oil rigs, and most preferably, aircraft. CISTI

N92-32857# Kernforschungszentrum G.m.b.H., Karlsruhe (Germany, F.R.). Inst. fuer Neutronenphysik und Reaktortechnik.
A THREE-FIELD MODEL OF TRANSIENT 3D MULTIPHASE, THREE-COMPONENT FLOW FOR THE COMPUTER CODE 4 A3. PAR1: THEORETICAL BASIS: CONSERVATION AND STATE EQUATIONS, NUMERICS
N. I. Kolev Dec. 1991 107 p
(KfK-4948-Pt-1; ETN-92-92156) Copyright Avail: CASI HC A06/MF A02

The physical and mathematical basis on which the IVA3 computer code relies are described. IVA3 was developed for numerical simulation of flows of air, steam, water, microscopic solid particles which can be carried only by water, and 'liquid metal' that is immiscible with water. The state of the art of the 3D (three dimensional) modeling for transient multiphase flows, the model assumptions, and the modeling technique used in IVA3 are described. Starting with the principles of conservation of mass, momentum, and energy, the nonaveraged conservation equations are derived for each of the velocity fields which consist of different isothermal components. Thereafter, averaging is applied and the working form of the system of 21 partial differential equations is derived. Special attention is paid to the strict consistence of the modeling technique used in IVA3 with the second principle of thermodynamics. The entropy concept used is derived starting with the unaveraged conservation equations and subsequent averaging. ESA

N92-32858# Kernforschungszentrum G.m.b.H., Karlsruhe (Germany, F.R.). Inst. fuer Neutronenphysik und Reaktortechnik.
A THREE-FIELD MODEL OF TRANSIENT 3D MULTIPHASE, THREE-COMPONENT FLOW FOR THE COMPUTER CODE 4 A3. PART 2: MODELS FOR THE INTERFACIAL TRANSPORT PHENOMENA. CODE VALIDATION
N. I. Kolev Dec. 1991 139 p
(KfK-4949-Pt-2; ETN-92-92157) Copyright Avail: CASI HC A07/MF A02

The second part of the IVA3 code description contains the constitutive models used for the interfacial transport phenomena and the code validation results. IVA3 was developed for numerical simulation of flows of air, water, microscopic solid particles which can be carried only by water, and 'liquid metal' that are immiscible with water. First, 20 flow patterns are defined and the transition criteria are discussed. The dynamic fragmentation and coalescence models used in IVA3 are documented. Models for predicting the flow patterns and flow structure sizes of the models for the interfacial mechanical interaction are described. The models for interfacial heat and mass transfer are given with emphasis on the time averaging of the heat and mass source terms. The code validation passes several stages from simple tests on well known benchmarks through simulation of one, two, and three phase flows in simple and complicated geometries. The gradial increase of the complexity and the successful comparison of the predictions with experimental data is the main characteristic of the verification procedure. Several examples show that IVA3 is a powerful tool for three fluid modeling of complicated three phase flows in complex geometry with strong thermal and mechanical interaction between the velocity fields. ESA

N92-32868*# National Aeronautics and Space Administration. Lewis Research Center, Cleveland, OH.
A NEW TIME SCALE BASED K-EPSILON MODEL FOR NEAR WALL TURBULENCE
Z. Yang and T. H. Shih Sep. 1992 23 p
(NASA Order C-99066-6; RTOP 505-62-21)
(NASA-TM-105768; ICOMP-92-11; CMOTT-92-07; E-7194; NAS 1.15:105768) Avail: CASI HC A03/MF A01

A k-epsilon model is proposed for wall bonded turbulent flows. In this model, the eddy viscosity is characterized by a turbulent velocity scale and a turbulent time scale. The time scale is bounded from below by the Kolmogorov time scale. The dissipation equation is reformulated using this time scale and no singularity exists at the wall. The damping function used in the eddy viscosity is chosen to be a function of R(sub y) = (k(sup 1/2)y)/v instead of y(+).

Hence, the model could be used for flows with separation. The model constants used are the same as in the high Reynolds number standard k-epsilon model. Thus, the proposed model will be also suitable for flows far from the wall. Turbulent channel flows at different Reynolds numbers and turbulent boundary layer flows with and without pressure gradient are calculated. Results show that the model predictions are in good agreement with direct numerical simulation and experimental data. Author

N92-32947# Lawrence Livermore National Lab., CA.
NUMERICAL SIMULATION OF INCLINED CHUTE FLOWS OF MONODISPERSE, INELASTIC, FRICTIONAL SPHERES
O. R. Walton 17 Jan. 1992 9 p Presented at the 2nd US-Japan Seminar on Micromechanics of Granular Materials, Syracuse, NY, 4-10 Aug. 1991
(Contract W-7405-eng-48)
(DE92-014775; UCRL-JC-108341; CONF-9108127-4) Avail: CASI HC A02/MF A01

Molecular-dynamics-like simulations are utilized to map regions of flow parameter space where steady flows occur for monodisperse assemblies of inelastic, frictional spheres, flowing down frictional, inclined planar surfaces. The trajectory-following technique utilizes nearly-rigid particles interacting via contact forces and gravity. Energy losses in the simulations occur only via displacement-dependent hysteretic loading/unloading paths and sliding friction. Initial scoping calculations are examining flows on an incline tilted 17 degrees from the horizontal, determining the boundaries of various flow regimes. Assemblies of inelastic spheres with interparticle friction coefficients less than the tangent of the inclination angle accelerate unboundedly. Those with friction coefficients somewhat greater than the tangent of the inclination angle develop steady velocity and density profiles for a variety of flow depths but result in arrested flow for coefficients of friction greatly exceeding the inclination angle tangent (e.g., by more than a factor of 2). Conversely, a significant range of inclination angles is expected to exist that will result in steady flows for a given set of assembly properties. DOE

N92-33066# Universiteit Twente, Enschede (Netherlands). Fluid Mechanics and Heat Transfer Group.
ON THE ORIGIN AND ACOUSTICAL BEHAVIOUR OF CLOUD CAVITATION Ph.D. Thesis
Jakob Buist 1991 139 p Sponsored by Maritime Research Inst., Netherlands
(Contract TTN77-1038)
(ISBN-90-9004317-9; ETN-92-92041) Copyright Avail: CASI HC A07/MF A02

Cavitation noise, produced by ship propellers, is addressed. Here, cavitation is defined as the occurrence and physical behavior of vapor filled voids in a fluid flow. These cavities, which arise in low pressure areas, are carried with the flow and implode in high pressure regions. The subsequent oscillations produce high noise levels both on-board the ship concerned and in the far field. In particular, an investigation into the problem of how to provide rules for the prediction of cavitation noise, based upon measurements on model scale, is made. On model scale, all similarity conditions cannot be satisfied simultaneously, and hence, scaling rules are needed. Up to now the scaling rules, which are given in the literature, are obtained by considering the behavior of individual bubbles. In practical situations, however, bubble clouds are observed, in which interactions between bubbles are of utmost importance. The issues addressed cover: the prediction of cloud cavitation noise; the relative importance of cluster formation in bubble mixtures; and the origin of bubble clouds. ESA

N92-33082# Lawrence Livermore National Lab., CA.
CONNECTIVITY STRUCTURES AND DIFFERENCING TECHNIQUES FOR STAGGERED-GRID FREE-LAGRANGE HYDRODYNAMICS
D. E. Burton Jun. 1992 9 p Presented at the 7th International Association of Mathematics and Computer Simulation (IMACS) International Conference on Computer Methods for Partial Differential Equations, New Brunswick, NJ, 22-24 Jun. 1992
(Contract W-7405-eng-48)
(DE92-017313; UCRL-JC-110555; CONF-9206185-7) Avail: CASI HC A02/MF A01

We consider a variation of the free-Lagrange (FL) method which is appropriate to staggered-grid differencing of the hydrodynamics equations (SGH) and will be termed the staggered free-Lagrange method or SFL. The SFL method discretizes space into general polygonal or polyhedral cells. The numerical differencing techniques and connectivity templates used for SFL differ markedly from those used by other unstructured grid methods, such as finite element (FE) and triangular/tetrahedral based free-Lagrange (TFL). The paper discusses the spatial discretization for both 2D and 3D geometry, differencing templates, object-oriented data management, and mesh optimization and refinement strategies. The suite of mesh optimization primitives is extended, giving rise to a powerful hybrid method called adaptive free-Lagrange (AFL) which is applied to a test problem. DOE

N92-33110*# Institute for Computer Applications in Science and Engineering, Hampton, VA.
A NUMERICAL RESOLUTION STUDY OF HIGH ORDER ESSENTIALLY NON-OSCILLATORY SCHEMES APPLIED TO INCOMPRESSIBLE FLOW Final Report
E. Weinan (Institute for Advanced Study, Princeton, NJ.) and Chi-Wang Shu (Brown Univ., Providence, RI.) Aug. 1992 18 p Submitted for publication
(Contracts NAS1-18605; NAS1-19480; DAAL03-91-G-0123; NAG1-1145; AF-AFOSR-0090-90; NSF DMS-91-00383; RTOP 505-90-52-01)
(NASA-CR-189692; NAS 1.26:189692; ICASE-92-39) Avail: CASI HC A03/MF A01

High order essentially non-oscillatory (ENO) schemes, originally designed for compressible flow and in general for hyperbolic conservation laws, are applied to incompressible Euler and Navier-Stokes equations with periodic boundary conditions. The projection to divergence-free velocity fields is achieved by fourth order central differences through Fast Fourier Transforms (FFT) and a mild high-order filtering. The objective of this work is to assess the resolution of ENO schemes for large scale features of the flow when a coarse grid is used and small scale features of the flow, such as shears and roll-ups, are not fully resolved. It is found that high-order ENO schemes remain stable under such situations and quantities related to large-scale features, such as the total circulation around the roll-up region, are adequately resolved. Author

N92-33113*# National Aeronautics and Space Administration. Ames Research Center, Moffett Field, CA.
COMPUTATION OF INCOMPRESSIBLE VISCOUS FLOWS THROUGH TURBOPUMP COMPONENTS
Cetin Kiris (MCAT Inst., Moffett Field, CA.), Dochan Kwak, and Stuart Rogers Mar. 1992 17 p Original contains color illustrations
(RTOP 505-59-00)
(NASA-TM-103911; A-92041; NAS 1.15:103911) Avail: CASI HC A03/MF A01; 1 functional color pag

A finite-difference, three-dimensional, incompressible Navier-Stokes formulation for calculating the flow through turbopump components is presented. The solution method is based on the pseudocompressibility approach and uses an implicit-upwind differencing scheme together with the Gauss-Seidel line-relaxation method. Both steady and unsteady flow calculations can be performed using the presented algorithm. In this paper, the equations are solved in steadily rotating reference frames by using the steady-state formulation in order to simulate the flow through a turbopump inducer. Eddy viscosity is computed by using the Baldwin-Lomax model. Numerical results are compared with experimental measurements and good agreement is found between the two. Time-accurate calculations will be reported in future publications. Author

N92-33124# Northwestern Univ., Evanston, IL.
THINNING AND RUPTURE OF A THIN LIQUID FILM ON A HEATED SURFACE
S. G. Bankoff and S. H. Davis May 1992 5 p
(Contract DE-FG02-86ER-13641)
(DE92-014813; DOE/ER-13641/3) Avail: CASI HC A01/MF A01

The objective of this work continues to be the study of dynamics, stability, and rupture (including contact line motions) of thin liquid films, especially with heat and/or mass transfer. Following the publication of a comprehensive paper on thin-film stability and rupture, taking into account evaporation (condensation), thermocapillarity, surface tension, vapor recoil, van der Waals forces, and mass loss (gain), two follow-up papers have appeared. The first examines the conditions for a non-uniformly-heated liquid film to rupture, owing to thermocapillarity, while the second reports experimental results in excellent agreement with the theory on non-isothermal free-surface problems. Another paper extends some previous results to the case where the viscosity of the liquid is a function of temperature. By proper rescaling, it is shown that the evolution equation can be transformed into the constant-viscosity case, so that previous results can be applied directly. Another paper considers the nonlinear growth, steepening, and wavebreaking of an isothermal thin liquid film draining down an inclined plate. The competition between mean flow and evaporation gives important morphological changes that control the heat-transfer process in the wavy regime. DOE

N92-33140# Michigan State Univ., East Lansing. Dept. of Mechanical Engineering.
STUDY OF FLOW PROPERTIES OF WET SOLIDS USING LASER INDUCED PHOTOCHEMICAL ANEMOMETRY
B. Falco 17 Apr. 1992 7 p
(Contract DE-AC22-88PC-88948)
(DE92-015452; DOE/PC-88948/T14) Avail: CASI HC A02/MF A01

A new diagnostic measurement technique is being developed that will enable the investigation of the dynamics of flowing wet solids. The technique involves the use of Laser Induced Photochemical Anemometry (LIPA), enhanced to enable two photochemical species to be excited. It uses laser induced photochromic and photo luminescent molecules to separately tag the two phases for times long enough for them to distort the tagging. Recording the distortions of the tagging caused by the movement of each phase enables us to obtain local characterization of flow properties of both phases of the wet solids at many positions simultaneously across a pipe. DOE

N92-33159# Los Alamos National Lab., NM.
TURBULENCE TRANSPORT EQUATIONS FOR VARIABLE-DENSITY TURBULENCE AND THEIR RELATIONSHIP TO TWO-FIELD MODELS
D. Besnard, F. H. Harlow, R. M. Rauenzahn, and C. Zemach Jun. 1992 39 p
(Contract W-7405-eng-36)
(DE92-017292; LA-12303-MS) Avail: CASI HC A03/MF A01

This study gives an updated account of our current ability to describe multimaterial compressible turbulent flows by means of a one-point transport model. Evolution equations are developed for a number of second-order correlations of turbulent data, and approximations of the gradient type are applied to additional correlations to close the system of equations. The principal fields of interest are the one-point Reynolds tensor for variable-density flow, the turbulent energy dissipation rate, and correlations for density-velocity and density-density fluctuations. This single-field description of turbulent flows is compared in some detail to two-field flow equations for nonturbulent, highly dispersed flow with separate variables for each field. This comparison suggests means for improved modeling of some correlations not subjected to evolution equations. DOE

N92-33226 Victoria Univ. (British Columbia). Dept. of Physics.
TIME-RESOLVED HOLOGRAPHY FOR THE STUDY OF SHOCK WAVES Ph.D. Thesis
Roberto Giacomo G. Racca 1990 118 p
(ISBN-0-315-62369-1; CTN-92-60521) Copyright Micromedia Ltd., Technical Information Centre, 165 Hotel de Ville, Place du Portage, Phase 2, Hull, Quebec J8X 3X2, Canada HC/MF

A time-resolved holographic interferometer specially suited for high-speed visualization of the gas flow in shock tube experiments has been developed. Holographic interferometry, based on the recording of two coincident holograms at different times so that one of them acts as a reference field, can accurately reveal the density distribution in a gas. Multiple hologram recording was implemented on an existing holographic interferometry system through the technique of spatial frequency multiplexing, in which the holograms are overlaid but the reference beam is angled differently for each exposure. Because the object beam is not involved in the multiplexing process, the imaging optics of the original system could be left unmodified. The upgrade only entailed the introduction of an angular sweeping system in the reference beam path. A mechanical beam sweeping system was first tried unsuccessfully. A solid-state multiplexing system was then devised in which the reference beam was split into several branches, each aimed at the film from a different direction and shuttered individually by a ferroelectric liquid crystal light valve. A prototype 3-image system was constructed and successfully tested by recording interferometric sequences of a shock wave reflecting off a model at framing intervals down to 100 microseconds. CISTI

35 INSTRUMENTATION AND PHOTOGRAPHY

Includes remote sensors; measuring instruments and gages; detectors; cameras and photographic supplies; and holography.

For aerial photography see *43 Earth Resources and Remote Sensing*. For related information see also *06 Aircraft Instrumentation*, and *19 Spacecraft Instrumentation*.

N92-32323# Accuwave Corp., Santa Monica, CA.
HOLOGRAPHIC CROSSTALK AND SIGNAL-TO-NOISE RATIO IN ORTHOGONAL DATA STORAGE Final Technical Report, 16 Sep. - 31 Dec. 1991
George A. Rakuljic 28 Feb. 1992 26 p
(Contract DAAL03-91-C-0050)
(AD-A250146; ARO-29211.1-PHS) Avail: CASI HC A03/MF A01

This final technical report summarizes research performed under contract number DAAL03-91-C-0050. The holographic crosstalk and signal-to-noise ratio in orthogonal data storage were investigated by storing both plane holograms and high resolution holograms in a photorefractive crystal. These results were then used to predict the storage capacities of various photorefractive crystals using the orthogonal data storage technique. GRA

N92-32343# Naval Surface Warfare Center, Crane, IN.
RADIOMETRIC AND SPECTRAL MEASUREMENT INSTRUMENTS Final Report
Bernard E. Douda and Henry A. Webster 18 Mar. 1992 40 p
(AD-A250771; NSWCCR/RDTN-92/0003) Avail: CASI HC A03/MF A01

This is a description of an assortment of radiometric and spectral instrumentation used for measurement of the radiative output of assorted devices. These instruments are installed and routinely operated at this center. The contents describe some of the instrument parameters and measurement capability. GRA

N92-32460# Westinghouse Savannah River Co., Aiken, SC.
WIND TUNNEL TEST OF TELEDYNE GEOTECH MODEL 1564B CUP ANEMOMETER
M. J. Parker and R. P. Addis Apr. 1991 15 p

(Contract DE-AC09-89SR-18035)
(DE92-009590; WSRC-RP-91-415) Avail: CASI HC A03/MF A01

The Department of Energy (DOE) Environment, Safety, and Health Compliance Assessment (Tiger Team) of the Savannah River Site (SRS) questioned the method by which wind speed sensors (cup anemometers) are calibrated by the Environmental Technology Section (ETS). The Tiger Team member was concerned that calibration data was generated by running the wind tunnel to only 26 miles per hour (mph) when speeds exceeding 50 mph are readily obtainable. A wind tunnel experiment was conducted and confirmed the validity of the practice. Wind speeds common to SRS (6 mph) were predicted more accurately by 0-25 mph regression equations than 0-50 mph regression equations. Higher wind speeds were slightly overpredicted by the 0-25 mph regression equations when compared to 0-50 mph regression equations. However, the greater benefit of more accurate lower wind speed predictions accuracy outweigh the benefit of slightly better high (extreme) wind speed predictions. Therefore, it is concluded that 0-25 mph regression equations should continue to be utilized by ETS at SRS. During the Department of Energy Tiger Team audit, concerns were raised about the calibration of SRS cup anemometers. Wind speed is measured by ETS with Teledyne Geotech model 1564B cup anemometers, which are calibrated in the ETS wind tunnel. Linear regression lines are fitted to data points of tunnel speed versus anemometer output voltages up to 25 mph. The regression coefficients are then implemented into the data acquisition computer software when an instrument is installed in the field. The concern raised was that since the wind tunnel at SRS is able to generate a maximum wind speed higher than 25 mph, errors may be introduced in not using the full range of the wind tunnel. DOE

N92-32601# Instituto de Pesquisas Espaciais, Sao Jose dos Campos (Brazil).
DESIGN AND CONSTRUCTION OF A MAGNETIC SECTOR MASS SPECTROMETER [PROJECTO E CONSTRUCAO DE UM ESPECTROMETRO DE MASSA DO TIPO SETOR MAGNETICO]
Renato Sergio Dallaqua, Gerson Otto Ludwig, and Antonio Montes Aug. 1991 58 p In PORTUGESE
(INPE-5405-RPQ/659) Avail: CASI HC A04/MF A01

We describe the design and construction of a sector magnetic mass spectrometer. The main parts of the instrument are the following: ion source, grids (extraction, energy analysis, and ion acceleration), electrostatic lens, magnetic sector, and detector. All of these components are kept inside of a vacuum chamber evacuated by a turbomolecular pump. Author

N92-32620# California Inst. of Tech., Pasadena.
STRESS-RELIEF DISPLACEMENTS INDUCED BY DRILLING: APPLICATIONS TO HOLOGRAPHIC MEASUREMENTS OF IN SITU STRESS
T. J. Ahrens and C. L. Smither 24 Apr. 1992 77 p
(Contract DE-FG03-85ER-13422)
(DE92-013711; DOE/ER-13422/T1) Avail: CASI HC A05/MF A01

The holographic stressmeter is an instrument which has been developed at Caltech to allow the determination of the complete stress tensor from in situ borehole measurements. The stressmeter uses double-exposure holographic interferometry to record the displacements induced by the drilling of a small sidehole into the borehole wall. The local stresses, which are the result of the far-field stresses concentrated at the borehole, cause deformation of the surface of the borehole wall in the vicinity of the sidehole. The first part of this study uses a thin infinite elastic plate subjected to plane stress at infinity to model the displacements at the borehole wall. However, the existence of some holograms which were difficult to model closely led us to examine the validity of this model. In order to investigate the problem further, we performed a two-dimensional finite element analysis for an elastic box with a terminated hole. We varied the dimensions of the hole to see what effect the radius and depth of the hole might have on the displacements. The plate model predicts that the depth of the hole should have no effect on the horizontal components of displacement, but the finite element results show that the magnitude of both components of the displacement depends on the depth of the sidehole. After considering these results, we developed a new model for the analysis of stress-relief displacements, following the work of Youngdahl and Sternberg (1965). For holes with a depth-to-diameter ratio greater than unity, the simple plane stress elastic plate solution breaks down and does not adequately model the displacements at the surface of the body and near the hole. Since these are the areas most critical to calculate accurately with the holographic technique, the revised model does a better job of fitting the observed data. DOE

N92-32999# Lawrence Livermore National Lab., CA.
THE LLNL MULTI-USER TANDEM LABORATORY PIXE MICROPROBE
D. W. Heikkinen, G. S. Bench, A. J. Antolak (Sandia National Labs., Albuquerque, NM.), D. H. Morse (Sandia National Labs., Albuquerque, NM.), and A. E. Pontau (Sandia National Labs., Albuquerque, NM.) 26 May 1992 11 p Presented at the 3rd International Conference on Nuclear Microprobe Technology and Applications, Uppsala (Sweden), 8-12 Jun. 1992
(Contracts W-7405-eng-48; DE-AC04-76DP-00789)
(DE92-017252; UCRL-JC-109750; CONF-9206201-2) Avail: CASI HC A03/MF A01

We have recently completed the construction of a new ion beamline primarily for particle-induced x-ray emission (PIXE) analysis. This will supplement our current ion microtomography (IMT) material characterization capabilities using accelerator microanalysis. In this paper we describe the PIXE beamline and give some results that characterize the system. We also report the results of some initial experiments. DOE

N92-33000# Lawrence Livermore National Lab., CA.
APPLICATIONS OF ENERGY LOSS CONTRAST STIM
G. Bench, A. Saint, G. J. F. Legge, and M. Cholewa 26 May 1992 23 p Presented at the 3rd International Conference on Nuclear Microprobe Technology and Applications, Uppsala (Sweden), 8-12 Jun. 1992
(Contract W-7405-eng-48)
(DE92-017254; UCRL-JC-110753; CONF-9206201-4) Avail: CASI HC A03/MF A01

Scanning Transmission Ion Microscopy (STIM) with energy loss contrast is a quantitative imaging technique. A focussed MeV ion microbeam is scanned over the sample, and measured energy losses of residual ions at each beam location are used to provide the contrast in the image. The technique is highly efficient, as almost every ion carries useful information from which quantitative data can be obtained. The high efficiency of data collection at present necessitates the use of small beam currents. Therefore, small apertures can be used, and fine spatial resolution can be achieved. High efficiency also makes it possible to collect large data sets for high definition imaging with a small radiation dose. Owing to the simple relationship between energy loss and areal density, STIM with energy loss contrast can provide a quantitative image that can be used to obtain areal density information on the sample. These areal density maps can be used not only to provide a high resolution image of the sample but also to normalize Particle Induced X-ray Emission (PIXE) data. The small radiation dose required to form these areal density maps also allows one to use STIM with energy loss contrast to quantitatively monitor ion beam induced specimen changes caused by higher doses and dose rates used in other microanalytical techniques. STIM with energy loss contrast also provides the possibility of stereo imaging and ion microtomography. STIM has also been used in conjunction with channeling to explore transmission channeling in thin crystals. This paper will discuss these applications of STIM with energy loss contrast and look at further developments from them. DOE

N92-33010* National Aeronautics and Space Administration. Marshall Space Flight Center, Huntsville, AL.
ROTATING-UNBALANCED-MASS DEVICES AND METHODS FOR SCANNING BALLOON-BORNE-EXPERIMENTS, FREE-FLYING SPACECRAFT, AND SPACE SHUTTLE/SPACE STATION ATTACHED EXPERIMENTS Patent
Michael E. Polites, inventor (to NASA) 14 Jul. 1992 14 p Filed 23 May 1990 Supersedes N90-26304 (28 - 20, p 2866)
(NASA-Case-MFS-28425-1; US-Patent-5,129,600;
US-Patent-Appl-SN-527462; US-Patent-Class-244-158R;
US-Patent-Class-74-61; US-Patent-Class-74-87;
US-Patent-Class-343-766; Int-Patent-Class-B64G-1/66) Avail: US Patent and Trademark Office

A method and apparatus for scanning balloon-borne experiments, free-flying spacecraft, or gimballed experiments mounted on a space shuttle or space station, makes use of one or more rotating unbalanced mass devices for selectively generating circular, line, or raster scan patterns for the experiment line of sight. An auxiliary control system may also be used in combination with the rotating unbalanced mass device, for target acquisition, keeping the scan centered on the target, or for producing complementary motion for raster scanning. The rotating unbalanced mass makes use of a mass associated with a drive shaft, such mass having a center of gravity which is displaced from the drive shaft rotation axis. The drive shaft is driven with a substantially constant angular velocity, thereby resulting in relatively low power requirements since no acceleration or deceleration of the mass is generally involved during steady state operations. The resulting centrifugal force of the rotating unbalanced mass is used to generate desired reaction forces on the experiment or spacecraft to create a desired scan pattern for the experiment line of sight.
Official Gazette of the U.S. Patent and Trademark Office

N92-33016* National Aeronautics and Space Administration. Langley Research Center, Hampton, VA.
PASSIVE FETAL MONITORING SENSOR Patent
Allan J. Zuckerwar, inventor (to NASA), Earl T. Hall, inventor (to NASA), Donald A. Baker, inventor (to NASA), and Timothy D. Bryant, inventor (to NASA) 25 Aug. 1992 8 p Filed 16 Jul. 1990 Supersedes N91-13686 (29 - 5, p 663)
(NASA-Case-LAR-14088-1-CU; US-Patent-5,140,992;
US-Patent-Appl-SN-552670; US-Patent-Class-128-715;
US-Patent-Class-128-775; Int-Patent-Class-A61B-5/02) Avail: US Patent and Trademark Office

An ambulatory, passive sensor for use in a fetal monitoring system is discussed. The invention is comprised of a piezoelectric polymer film, combined with a metallic mounting plate fastened to a belt, and electrically connected to a signal processing unit by means of a shielded cable. The purpose of the sensor is to receive pressure pulses emitted by a fetus inside an expectant mother. Additionally, the monitor will filter out pressure pulses arising from other sources, such as the maternal heart.
Official Gazette of the U.S. Patent and Trademark Office

N92-33188# Commonwealth Scientific and Industrial Research Organization, Mordialoc (Australia). Div. of Atmospheric Research.
A PRECISE NARROW-BEAM FILTER INFRARED RADIOMETER AND ITS USE WITH LIDAR IN THE ARM PROGRAM
C. M. R. Platt May 1992 7 p
(Contract DE-FG02-92ER-61373)
(DE92-016872; DOE/ER-61373/1) Avail: CASI HC A02/MF A01

The first six months of the grant (December 1991 to May 1992) have been taken up with the design and specification for the new narrow-beam radiometer. The radiometer will be built and tested at the Division of Atmospheric Research over the next three months. Improved algorithms for obtaining cloud extinction have also been developed. It is proposed during 1993 to use the radiometer in conjunction with a new CSIRO 3-wavelength lidar in the ARM PROBE experiment at Kavieng, New Guinea, which is a test mission under tropical conditions for the ARM CART Tropical West Pacific site, and is part of the TOGA COARE experiment. During the latter part of 1992, the radiometer will be tested thoroughly and tested at the Division of Atmospheric Research, Aspendale. DOE

N92-32392# Kent Univ., Canterbury (England). Space Sciences Unit.
LABORATORY DETERMINATION OF THE THERMAL CONDUCTIVITY OF LIQUID METHANE AND ETHANE
P. N. W. Birchley, P. M. Daniell, John C. Zarnecki, and D. J. Parker (Rutherford Appleton Lab., Chilton, England) *In* ESA, Symposium on Titan Apr. 1992 p 311-314 Sponsored by Science Research Council (For primary document see N92-32348 23-91)
Copyright Avail: CASI HC A01/MF A01; ESA, EPD, ESTEC, Noordwijk, Netherlands, HC

36 LASERS AND MASERS

Includes parametric amplifiers.
For related information see also *76 Solid-State Physics.*

N92-32329# Naval Command, Control and Ocean Surveillance Center, San Diego, CA. RDT/E Div.
FEASIBILITY OF A 486 nm FRAUNHOFER LASER SOURCE BASED ON A 4F(SUB 3/2) YIELDS 4I(SUB 9/2) NEODYMIUM LASER Final Report
F. E. Hanson, D. L. Katz, and P. Poirier Mar. 1992 25 p
(AD-A250851; NRAD-TR-1480) Avail: CASI HC A03/MF A01

The objective of this research was to investigate the potential of a laser source based on the neodymium (4)F(sub 3/2) (yields) (4)I(sub 9/2) transition for operation at 486.1 nm, the H(sub beta) Fraunhofer wavelength. We characterized this transition in Nd:YAG. Also, we identified stimulated rotational Raman conversion in H2, D2, and HD as a critical step in such a system. GRA

N92-32335# Sandia National Labs., Albuquerque, NM.
LASER MEASUREMENTS FOR EXPERIMENTS ON THE TROLL ACCELERATOR
S. Hogeland (Ktech Corp., Albuquerque, NM.) Jun. 1992 14 p
(Contract DE-AC04-76DP-00789)
(DE92-016578; SAND-92-7065) Avail: CASI HC A03/MF A01

Propagation of an electron beam over long distances can be accomplished by using a laser produced plasma channel. In experiments at the EPOCH Laboratory, a krypton/fluoride laser, lasing at 248 nm, is used to ionize trimethylamine gas to create a 91 m long channel. The laser radius was measured as 2.4 cm. Laser energy was measured and ranged from 0.5 to 6 J. DOE

N92-32511# Brookhaven National Lab., Upton, NY.
OPTICS OF BEAM TRANSPORT IN THE NSLS UV-FEL
X. Zhang, S. L. Kramer, and J. Wachtel 1992 4 p Presented at the 3rd European Particle Accelerator Conference, Berlin (Germany), 24-28 Mar. 1992
(Contract DE-AC02-76CH-00016)
(DE92-014166; BNL-47376; CONF-920315-37) Avail: CASI HC A01/MF A01

The NSLS-FEL is designed as a single pass FEL to generate radiation 1 mJ per pulse (10 psec) in 10(exp -4) bandwidth, with continuously tunable wavelength in the range 100-300 nm. A superconducting, recirculating linac provides electron beams of energy 20 MeV to 260 MeV at 4 pi mm mrad normalized rms emittance with less than 0.1 percent momentum spread and 2 mm rms bunch length. The optics in this machine is seriously restricted by the requirement to not degrade the electron beam quality. We present a lattice design for the transport lines to be used in beam injection, linac focussing and recirculations. These beam lines are tuned to be linearly achromatic and isochronous, to avoid beam breakup in the cavities, and to minimize second order distortions of the emittance. Special transport lines are designed that allow rapid switching of the electron beam to drive

two different FEL wigglers. This provides the capability for up to four simultaneous, high power, independently energy tuned laser beams. DOE

N92-32540# Midwest Bio-Laser Inst., Chicago, IL.
MIDWEST FREE-ELECTRON LASER PROGRAM Final Report, 1 Mar. 1988 - 31 Oct. 1991
L. J. Cerullo, M. Epstein, M. E. Marhic, W. Z. Rymer, and K. G. Spears 17 Dec. 1991 11 p
(Contract N00014-90-C-0028)
(AD-A247264) Avail: CASI HC A03/MF A01

It has been shown that pulsed Nd:YAG irradiation of nervous tissue in both mammalian and frog preparations produces selective damage to conduction and axoplasmic transport in small caliber sensory afferent fibers, which may be those responsible for pain sensation. In addition, the thermal affects on peripheral nerve appear to be primarily on sodium channels. This preferential sodium effect can be enhanced or developed further for clinical use to provide novel interventions in anesthesia and surgical treatment of painful conditions. A laser system was built to simulate the high energy pulses of a low repetition rate FEL in the infrared and was used to develop the necessary techniques for the study of transient pump-probe experiments with infrared probe wavelengths. It was employed as a transient IR probe of UV laser effects in the study of metal-ligand dissociation. A novel chrono-coherent imaging technique has been developed which uses time gating with coherent holographic recording. Utilizing short pulses, such as those from the FEL, this technique should provide a means of imaging inside the skin using optical wavelengths. A unique method of short-range electron transfer across a single bond to form a dissociated ion pair has been studied as a function of solvent. Also, the laser mediated release of dye from liposomes has been investigated. Several types of flexible waveguides, suitable for the delivery of output beams of infrared FEL's tunable within the 1 to 10 micron range, have been developed. GRA

N92-32596# Washington Univ., Seattle. Dept. of Applied Mathematics.
NONLINEAR RESONANCE Report, 1 Aug. 1989 - 30 Nov. 1991
J. Kevorkian 1991 9 p
(Contract DE-FG06-86ER-25019)
(DE92-014313; DOE/ER-25019/25) Avail: CASI HC A02/MF A01

This report discusses research in the area of slowly varying nonlinear oscillatory systems. Some of the topics discussed are as follows: adiabatic invariants and transient resonance in very slowly varying Hamiltonian systems; sustained resonance in very slowly varying Hamiltonian systems; free-electron lasers with very slow wiggler taper; and bursting oscillators. DOE

N92-32622# New Mexico Univ., Albuquerque. Center for High Technology Materials.
LASER MATERIAL INTERACTION Final Report, 15 May 1989 - 14 Mar. 1992
S. R. Brueck 20 Apr. 1992 35 p
(Grant AF-AFOSR-0337-89)
(AD-A250853; AFOSR-92-0367TR) Avail: CASI HC A03/MF A01

The Laser-Materials Interaction Laboratory at the Center for High Technology Materials of the University of New Mexico is devoted to the study of a broad range of laser spectroscopic probes of semiconductor and nonlinear materials, fabrication processes and optoelectronic devices. Much of this work is being carried out in conjunction with the Optoelectronics Research Center Program at CHTM, which is also partially funded by the Air Force Office of Scientific Research. Significant progress was made during this reporting period in a number of areas including: ultrafast operation of optically-pumped resonant periodic-gain GaAs surface-emitting lasers; grating coupling to surface-plasma waves; nonlinear optics of PLZT films and SiO2, and confocal microscopy for the direct measurement of semiconductor transport parameters. GRA

N92-32736# Los Alamos National Lab., NM.
THE DEPENDENCE OF THE ANISOPLANATIC STREHL OF A COMPENSATED BEAM ON THE BEACON DISTRIBUTION
P. Stroud Feb. 1992 26 p
(Contract W-7405-eng-36)
(DE92-011272; LA-UR-92-479) Avail: CASI HC A03/MF A01

There are several applications for lasers where the effect of atmospheric turbulence is strong enough to require wavefront compensation, and the compensation can be made by an adaptive optics (AO) system which processes light returned from the target itself. The distribution of the target return light produces limitations to the performance of the AO system. The primary intent of this documentation is to present the new results of an analysis of the anisoplanatic effects arising from target return beacon geometries. It will also lay out the assumptions and steps in the analysis, so that the results can be validated or extended. The intent is to provide a self-consistent notation, simple physical interpretations of the mathematical formulations, and enough detail to reduce the investment of time required to become acquainted or reacquainted with the physics of laser propagation through turbulence, at a level needed to analyze anisoplanatic effects. A general formulation has been developed to calculate the anisoplanatic Strehl of a compensated beam for any beacon distribution and turbulence profile. Numerical calculations are also shown for several beacon geometries and turbulence profiles. The key result is that the spread of the beacon distribution has a much less deleterious effect than does the offset of the beacon centroid from the aimpoint. DOE

N92-33060# National Inst. of Standards and Technology, Boulder, CO. Ion Storage Group.
TRAPPED IONS AND LASER COOLING 3
James C. Bergquist, ed., John J. Bollinger, ed., Wayne M. Itano, ed., and David J. Wineland, ed. Apr. 1992 203 p Sponsored by ONR and AFOSR
(PB92-189547; NIST/TN-1353) Avail: CASI HC A10/MF A03; SOD HC

This collection represents the work of the Ion Storage Group, Time and Frequency Division, National Institute of Standards and Technology from Oct. 1988 to Feb. 1992. It follows the collections of papers contained in NBS Technical Note 1086 'Trapped Ions and Laser Cooling' (Jun. 1985) and NIST Technical Note 1324 'Trapped Ions and Laser Cooling 2' (Sep. 1988). Although the primary goal of the work was the development of techniques necessary for achieving high resolution spectroscopy, the authors were also able to investigate related areas of research. GRA

N92-33089# Thermo Electron Technologies Corp., San Diego, CA.
TRANSVERSE DIODE PUMPING OF SOLID-STATE LASERS Final Report, 24 Sep. 1987 - 31 Mar. 1992
Eric Korevaar 29 May 1992 94 p
(Contract N00014-87-C-2412)
(AD-A252213; TTC-2459-R) Avail: CASI HC A05/MF A01

The transverse pumping of solid-state lasers in a cylindrical rod configuration has been explored both analytically and experimentally. The pumping configuration coupled diode laser arrays to the laser rod through slits in a geometrically reflecting chamber using simple lenses. Fifty W of diode lasers in the form of ten 5 W, 1 cm bars were used to pump 2 cm of a Nd:YAG rod. Output powers for 3 mm and 4 mm diameter rods were compared with and without the reflecting multi-pass pump cavity. An increase in output power of 35 percent was achieved by using the multi-pass cavity, approximately in agreement with expectation. Although threshold pump powers agreed with our analysis, slope efficiencies were much lower than expected, and output powers seemed to saturate at 2.5 W with 35 W incident on the rod. Detailed data on the beam profiles and wavelength distributions of the diode laser bars is also presented. GRA

N92-33114# Argonne National Lab., IL.
MOLECULAR SURFACE ANALYSIS BY LASER IONIZATION OF DESORBED MOLECULES

M. J. Pellin, K. R. Lykke, P. Wurz, and D. H. Parker 1992 7 p Presented at the 6th International Symposium on Resonance Ionization Spectroscopy and its Applications, Santa Fe, NM, 24-29 May 1992
(Contract W-31-109-eng-38)
(DE92-016320; ANL/CP-75942; CONF-920574-9) Avail: CASI HC A02/MF A01

While elemental analysis of surfaces has progressed dramatically over the past ten years, quantitative molecular surface analysis remains difficult. This is particularly true in the analysis of complex materials such as polymers and rubbers which contain a wide compliment of additives and pigments to enhance their material characteristics. For mass spectrometric analysis the difficulty is two fold. First, desorption of surface molecules must be accompanied with minimal fragmentation and collateral surface damage. Second, the desorbed molecules must be ionized for subsequent mass analysis with high efficiency and without significant cracking. This paper focuses on the second of these problems. DOE

N92-33155# California Univ., Berkeley. Lawrence Berkeley Lab.
ESTIMATES OF SASE POWER IN THE SHORT WAVELENGTH REGION
Kwang-Je Kim Mar. 1992 10 p Presented at the 4th Generation Light Sources Workshop, Stanford, CA, 24-27 Feb. 1992
(Contract DE-AC03-76SF-00098)
(DE92-014504; LBL-31969; CONF-9202111-1) Avail: CASI HC A02/MF A01

Given a sufficiently bright electron beam, the self-amplified-spontaneous emission (SASE) can provide gigawatts of short wavelength coherent radiation. The advantages of the SASE approach are that it requires neither optical cavity nor an input seed laser. In this note, we estimate the peak power performance of SASE for wavelengths shorter than 1000 A. At each wavelength, we calculate the saturated power from a uniform parameter undulator and the enhanced power from a tapered undulator. The method described here is an adaptation of that discussed by L H. Yu, who discussed the harmonic generation scheme with seeded laser, for the case of the SASE. DOE

N92-33165 Department of the Navy, Washington, DC.
RESONANTLY PUMPED, ERBIUM-DOPED, 2.8 MICRON SOLID STATE LASER WITH HIGH SLOPE EFFICIENCY Patent
Leon Esterowitz, inventor (to Navy) and Robert C. Stoneman, inventor (to Navy) 4 Feb. 1992 10 p Filed 23 May 1991
(AD-D015310; US-Patent-5,086,432; US-Patent-Appl-SN-705048)
Avail: US Patent and Trademark Office

A laser system and method for producing a laser emission at a wavelength of substantially 2.8 microns is disclosed. In a preferred embodiment of the invention, the laser system comprises a crystal having a host material doped with erbium; a laser cavity defined by first and second reflective elements at opposing ends of the crystal to form a reflective path therebetween; and resonant pumping means for directly pumping the 4I11/2 upper laser state of the erbium with a pump beam at a preselected wavelength to cause the erbium-doped crystal to produce a laser emission corresponding to the 4I 11/2 4I 13/2 laser transition having a wavelength of substantially 2.8 microns, a portion of the laser emission at substantially 2.8 microns being outputted from one of the first and second reflective elements. GRA

N92-33180# Michigan State Univ., East Lansing. Dept. of Mechanical Engineering.
STUDY OF FLOW PROPERTIES OF WET SOLIDS USING LASER INDUCED PHOTOCHEMICAL ANEMOMETRY
B. Falco 23 Feb. 1992 18 p
(Contract DE-AC22-88PC-88948)
(DE92-014031; DOE/PC-88948/T2) Avail: CASI HC A03/MF A01

Research continues on the flow properties of wet solids. During this period we have made progress in the analysis of the accuracy of the technique, progress in firming the foundations of LIPA for Solid-Liquid Mixtures, progress in the construction of better prototype skimmers, continued progress in chemically manufacturing both more red europium imbedded CaF2 and Green liquid Flowlite, and progress in understanding the coupling of LIPA chemicals and dynamic range and timing. DOE

37 MECHANICAL ENGINEERING

Includes auxiliary systems (nonpower); machine elements and processes; and mechanical equipment.

N92-32482 ESDU International Ltd., London (England).
REDUCING TORQUE FLUCTUATION IN LINKAGE DRIVE SHAFTS Abstract Only
Jun. 1992 16 p
(ESDU-92016; ISBN-0-85679-820-7) Avail: ESDU

ESDU 92016 describes a range of established techniques for reducing the torque fluctuation in shafts that drive, or are driven by, planar linkages. The fluctuations result from inertial and gravitational effects of the moving links or from variable external loads. The peak-to-peak torque fluctuation may be reduced by appropriate techniques, of which six are considered. The design considerations involved in selection are discussed, and the principle underlying each technique is explained. General design guidance is given for each technique together with a table of typical characteristics so that the designer can assess rapidly the potential of each method for a particular application. The techniques covered include mass reduction of the links, dyad addition, addition of springs and dampers, use of a torsional-vibration isolator, and use of the flywheel (which does not reduce peak-to-peak torque fluctuation). A considerable bibliography lists references giving further information on each method. ESDU

N92-32615# Argonne National Lab., IL.
PUBLICATIONS ON MAGLEV TECHNOLOGIES
J. L. He, H. T. Coffey, D. M. Rote, and Z. Wang Dec. 1991 86 p
(Contract W-31-109-eng-38)
(DE92-013296; ANL/ESD/TM-29) Avail: CASI HC A05/MF A01

Magnetically levitated passenger-transportation vehicles, using attractive and repulsive magnetic forces, are currently in the development or prototype-revenue stages in Japan and Germany. The basic principles of these technologies have been understood for several decades, but their practical applications awaited advances in high-power electronic devices, modern controls, superconducting magnets, and improvements in our transportation infrastructures. A considerable amount of work was devoted to magnetic-levitation (maglev) transportation system in the late 1960s and the 1970s. Detailed development was sustained primarily in Germany and Japan. This listing of publications was begun as the initial phase of a design study for a maglev development facility sponsored by the State of Illinois. The listing has been continually updated under programs sponsored by the Federal Railroad Administration and the US Army Corps of Engineers. In 1991, the National Maglev Initiative issued 27 contracts for the study of technical issues related to maglev and four contracts for the definition of maglev systems. In December 1991, the Intermodal Surface Transportation Efficiency Act was enacted, mandating the development of a US-designed maglev system in a six-year period. This listing is offered as an aid to those working on these projects, to help them locate technical papers on relevant technologies. The design and installation of a maglev transportation system will require the efforts of workers in many disciplines, from electronics to economics to safety. Accordingly, the references have been grouped in 14 different sections to expedite review of the listing. In many cases, the references are annotated to indicate the general content of the papers. Abstracts are not available. A list of information services from which the listed documents might be obtained and an author index are provided. DOE

N92-32692# Universiteit Twente, Enschede (Netherlands).
TOLERANCE OPTIMIZATION OF SERVOMECHANISMS Ph.D. Thesis
Harold Hendrikus Ber Roelofs 1991 146 p
(ISBN-90-9004476-0; ETN-92-92047) Copyright Avail: CASI HC A07/MF A02

Design tools to perform the transcription of servo performance specifications to optimum nominal values and tolerance of the servomechanism components are addressed. The tools to be developed must not be confined to those appropriate to linear servomechanisms, but must also be suitable for nonlinear servomechanisms with Coulomb damping. The strategy followed consists of a problem definition phase where the original problem is formulated as a semi-infinite optimization problem and a problem solving phase where the optimization problem is addressed by semi-infinite optimization algorithms. Two optimization algorithms, the feasible directions algorithm and the outer approximations algorithm, are used to solve the semi-infinite optimization problem. The optimization method described is realized in the computer program TSP (Tolerance Specicication Package). TSP is used for tolerance optimization of a linear and a nonlinear servomechanism. The outer approximations algorithm gives the best results for linear servomechanisms while the feasible directions algorithm performs well for nonlinear servomechanisms. ESA

N92-32694# Oak Ridge National Lab., TN.
USING MINIMAX APPROACHES TO PLAN OPTIMAL TASK COMMUTATION CONFIGURATIONS FOR COMBINED MOBILE PLATFORM-MANIPULATOR SYSTEMS
F. G. Pin, J. C. Culioli, and D. B. Reister 1992 21 p Presented at the IEEE International Conference on Robotics and Automation, Nice, France, 10-15 May 1992
(Contract DE-AC05-84OR-21400)
(DE91-018864; CONF-920540-2) Avail: CASI HC A03/MF A01

An important characteristic of mobile manipulators is their particular kinematic redundancy created by the addition of the degrees of freedom of the platform and those of the manipulator. This kinematic redundancy is very desirable since it allows mobile manipulators to operate under many modes of motion and to perform a wide variety of tasks. On the other hand, it also significantly complicates the problem of planning a series of sequential tasks, in particular for the critical times at which the system needs to 'switch' from one task to the other (task commutation), with changes in mode of motion, task requirement, and task constraints. This paper focuses on the problem of planning the positions and configurations in which the system needs to be at task commutation in order to assure that it can properly initiate the next task to be performed. An optimization approach has been proposed for this purpose and a variety of optimization criteria were investigated to optimize the task commutation configurations of the system when task requirements involve obstacle avoidance, reach, maneuverability, and optimization of strength. In this paper, we show that a 'minimax' approach is particularly adapted for most of these requirements. We develop the corresponding criteria and discuss solution algorithms to solve the 'minimax' optimization problems. An implementation of the algorithms for our HERMIES-3 mobile manipulator is then described and sample results are presented and discussed. DOE

N92-32701# Sandia National Labs., Albuquerque, NM.
ORBITAL DEBRIS CHARACTERIZATION WITH IMPACT FLASH SIGNATURES
J. A. Ang 1991 6 p Presented at the American Institute of Aeronautics and Astronautics (AIAA) Space Programs and Technologies Conference, Huntsville, AL, 24-27 Mar. 1991 Previously announced in IAA as A92-38708
(Contract DE-AC04-76DP-00789)
(DE92-010666; SAND-91-1704C; CONF-9103235-1) Avail: CASI HC A02/MF A01

Orbital debris is recognized as a serious and growing threat to man's utilization and exploration of space. While some information is available on the material composition of orbital debris, most measurements of orbital debris size and velocity distributions do not distinguish material type. The analysis and understanding of impact flash signatures can lead to an in-situ detector system with the ability to determine size and impact velocity distribution for orbital debris segregated by material type. This detector concept is based on an understanding of how material shock properties govern the flash signature arising from the impact of a piece of orbital debris (impactor) against a witness plate (target). Analytical results are presented that identify the most promising witness plate materials with respect to producing impact flash signatures that characterize the orbital debris material. DOE

N92-32726# Ecole Centrale de Lyon (France).
CONTRIBUTION TO THE THEORETICAL AND EXPERIMENTAL ANALYSIS OF CAMSHAFT ENGINE OPERATION Ph.D. Thesis [CONTRIBUTION A L'ANALYSE THEORIQUE ET EXPERIMENTALE DU FONCTIONNEMENT D'UN MOTEUR A CAMES]
Guy Sutter 1991 243 p In FRENCH Sponsored by Association Nationale pour la Recherche Technique
(ETN-92-91961) Avail: CASI HC A11/MF A03

A study concerning an alternative engine whose linkage is replaced by a piston-pad-cam assembly is presented. The transmission systems are described in order to study the volume generated by the piston movement at output shaft rotation. The cam power transmission study is presented as follows: global description; piston dynamics; cam shaft synchronization; profile analysis. A mathematical model of the real time operation of the engine related to a cam shaft engine prototype study shows the advantage of choosing a cam profile, particularly during combustion. A method for determining the principle characteristics of the main components of a cam shaft engine, whose desired performances are known, is defined. ESA

N92-32737# Ecole Centrale de Lyon (France). Lab. de Mecaniques des Solides.
DYNAMIC SYSTEMS STABILITY WITH DRY FRICTION: APPLICATION TO BRAKE DISC SQUEALING Ph.D. Thesis [STABILITE DES SYSTEMES DYNAMIQUES AVEC FROTTEMENT SEC: APPLICATION AU CRISSEMENT DES FREINS A DISQUE]
Pierre Chambrette 1991 212 p In FRENCH
(ECL-91-48; ETN-92-92092) Avail: CASI HC A10/MF A03

An analysis of the dynamic unstable behavior induced by dry friction to further understand high frequency brake squeal is presented. Two numerical methods are proposed, one based on the periodic coefficients differential equations Floquet theory, and the second using the 'method of small parameters' borrowed from nonlinear mechanics. A complex mode method, implying an expansion of both structures displacements on their free modes eigenfunctions, shows flutter unstable behavior for a few specific modes. To validate the sprag-slip theory in a real brake configuration, experimental tests on the primary brake structure of a 405 vehicle were conducted to record squeal instabilities. Full finite element models of the components without friction are elaborated. A comparison is drawn with experimental modal analysis results, and an estimation of frequencies optimization numerical cost, which represents the first step to a predictive design model of brake squeal, is given. ESA

N92-32757# Oxford Univ. (England). Robotics Research Group.
INFLUENCE OF COMPLIANCE ON PERFORMANCE OF ROBOTIC DRILLING
Guersel Alici (Gaziantep Univ., Turkey) and R. W. Daniel 1992 35 p
(OUEL-1917/92; ETN-92-92065) Avail: CASI HC A03/MF A01

Experiments forming part of an investigation into telerobotic drilling within a nuclear contaminated environment, which is reported to cause excessive drill wear and operator fatigue, are reported. The vibrations present during robotic drilling due to the many sources of compliance present in the system were investigated. The experimental method and equipment are described. Low cycle impact and increase in cutting time are

discussed. Strain rate curve for steel, brass, aluminum, and copper are presented and discussed. The effect of hung mass and symptoms of impact wear are discussed. The main conclusions are that compliant drilling can cause low cycle impact and hence can generate impact wear, and that the cutting time is significantly increased by the presence of compliance. ESA

N92-32801# Ecole Centrale de Lyon (France). Lab. de Technologie des Surfaces.
IMPLANTED ALUMINUM: TRIBOLOGICAL BEHAVIOR AND MECHANICAL PROPERTIES OF THE SUPERFICIAL LAYERS Ph.D. Thesis [ALUMINE IMPLANTEE: COMPORTEMENT TRIBOLOGIQUE ET PROPRIETES MECANIQUES DES COUCHES SUPERFICIELLES]
Mireille Bauer 1991 213 p In FRENCH
(ECL-91-28; ETN-92-92091) Avail: CASI HC A10/MF A03

The modification of alumina friction coefficient due to ionic implantation of niobium, titanium, iron, aluminum, and xenon ions, is addressed. Tests are performed on reciprocating and rotating pins on flat tribometers in ambient atmosphere and temperature; the conditions of the tests correspond to alumina mild wear. Results are summarized and an interpretation of the differences between the measured friction coefficient values is proposed. The normal load is shown to be divided into two parts, the convergent inlet of the contact and the central elastic area. The mechanical properties of the friction film dictate the load distribution. The shear plan localization and therefore the adherence properties of the two friction surfaces with wear debris impose the value of friction coefficient for the studied cases. ESA

N92-32885*# Catholic Univ. of America, Washington, DC. Dept. of Electrical Engineering.
AUTONOMOUS BERTHING/UNBERTHING OF A WORK ATTACHMENT MECHANISM/WORK ATTACHMENT FIXTURE (WAM/WAF) Semiannual Progress Report, 1 Mar. - 31 Jul.1992
Charles C. Nguyen and Sami S. Antrazi Aug. 1992 8 p
(Grant NAG5-1415)
(NASA-CR-190647; NAS 1.26:190647) Avail: CASI HC A02/MF A01

Discussed here is the autonomous berthing of a Work Attachment Mechanism/Work Attachment Fixture (WAM/WAF) developed by NASA for berthing and docking applications in space. The WAM/WAF system enables fast and reliable berthing (unberthing) of space hardware. A successful operation of the WAM/WAF requires that the WAM motor velocity be precisely controlled. The operating principle and the design of the WAM/WAF is described as well as the development of a control system used to regulate the WAM motor velocity. The results of an experiment in which the WAM/WAF is used to handle an orbital replacement unit are given. Author

N92-32890# Oak Ridge National Lab., TN.
PUMP AND VALVE RESEARCH AT THE OAK RIDGE NATIONAL LABORATORY
H. D. Haynes 1992 41 p Presented at the Symposium on Testing of Pumps and Valves in Nuclear Power Plants, Washington, DC, 21-23 Jul. 1992
(Contract DE-AC05-84OR-21400)
(DE92-014419; CONF-920732-2) Avail: CASI HC A03/MF A01

Over the last several years, the Oak Ridge National Laboratory (ORNL) has carried out several aging assessments on pumps and valves under the NRC's Nuclear Plant Aging Research (NPAR) Program. In addition, ORNL has established an Advanced Diagnostic Engineering Research and Development Center (ADEC) in order to play a key role in the field of diagnostic engineering. Initial ADEC research projects have addressed problems that were identified, at least in part, by the NPAR and other NRC-sponsored programs. This paper summarizes the pump and valve related research that has been done at ORNL and describes in more detail several diagnostic techniques developed at ORNL which are now commercially available. DOE

N92-33018* National Aeronautics and Space Administration. Lyndon B. Johnson Space Center, Houston, TX.
ELECTROMAGNETIC ATTACHMENT MECHANISM Patent
Leo G. Monford, Jr., inventor (to NASA) 8 Sep. 1992 22 p Filed 31 Dec. 1990 Supersedes N91-23490 (29 - 15, p 2435)
(NASA-Case-MSC-21463-1; US-Patent-5,145,227; US-Patent-Appl-SN-636531; US-Patent-Class-294-65.5; US-Patent-Class-244-161; US-Patent-Class-294-66.2; US-Patent-Class-294-86.4; US-Patent-Class-294-907; US-Patent-Class-414-737; US-Patent-Class-901-40) Avail: US Patent and Trademark Office

An electromagnetic attachment mechanism is disclosed for use as an end effector of a remote manipulator system. A pair of electromagnets, each with a U-shaped magnetic core with a pull-in coil and two holding coils, are mounted by a spring suspension system on a base plate of the mechanism housing with end pole pieces adapted to move through openings in the base plate when the attractive force of the electromagnets is exerted on a strike plate of a grapple fixture affixed to a target object. The pole pieces are spaced by an air gap from the strike plate when the mechanism first contacts the grapple fixture. An individual control circuit and power source is provided for the pull-in coil and one holding coil of each electromagnet. A back-up control circuit connected to the two power sources and a third power source is provided for the remaining holding coils. When energized, the pull-in coils overcome the suspension system and air gap and are automatically de-energized when the pole pieces move to grapple and impose a preload force across the grapple interface. A battery backup is a redundant power source for each electromagnet in each individual control circuit and is automatically connected upon failure of the primary source. A centerline mounted camera and video monitor are used in cooperation with a target pattern on the reflective surface of the strike plate to effect targeting and alignment.
Official Gazette of the U.S. Patent and Trademark Office

N92-33031* National Aeronautics and Space Administration. Langley Research Center, Hampton, VA.
NONCIRCULAR ROLLING JOINTS FOR VIBRATIONAL REDUCTION IN SLEWING MANEUVERS Patent
Meng-Sang Chew, inventor (to NASA), Jer-Nan Juang, inventor (to NASA), and Li-Farn Yang, inventor (to NASA) 15 Sep. 1992 13 p Filed 28 Mar. 1991 Supersedes N91-28580 (29 - 20, p 3354)
(NASA-Case-LAR-14515-1-CU; US-Patent-5,146,803; US-Patent-Appl-SN-678551; US-Patent-Class-74-437; US-Patent-Class-74-25; Int-Patent-Class-F16H-49/00; Int-Patent-Class-F16H-21/16) Avail: US Patent and Trademark Office

A rolling joint is provided for obtaining slewing maneuvers for various apparatus including space structures, space vehicles, robotic manipulators, and simulators. Two noncircular cylinders, namely a drive and a driven cylinder, are provided in driving contact with one another. This contact is maintained by two pairs of generally S-shaped bands, each pair forming a generally 8-shaped coupling tightly about the circumferential periphery of the noncircular drive and driven cylinders. A stationarily fixed arm extends between and is rotatably journalled with a drive axle and a spindle axle respectively extending through selected rotational points of the drive cylinder and of the driven cylinder. The noncircular cylinders are profiled to obtain the desired varying gear ratio. The novelty of the present invention resides in using specifically profiled noncircular cylinders to obtain a desired varying gear ratio.
Official Gazette of the U.S. Patent and Trademark Office

N92-33077# National Research Council of Canada, Boucherville (Quebec). Industrial Materials Inst.
A REVIEW OF RECENT DEVELOPMENTS IN JOINING HIGH-PERFORMANCE THERMOPLASTIC COMPOSITES
K. C. Cole 11 Jun. 1991 57 p
(CNRC-33030; IMI-91RT-31200-1155-G; CTN-92-60380) Avail: CASI HC A04/MF A01

There is currently a great deal of interest in the use of thermoplastic polymers as matrices in fiber reinforced composites for high performance applications, such as those encountered in the aerospace industry. These materials include polyether ether ketone (PEEK), polyphenylene sulphide (PPS), polyetherimide (PEI), polyamideimide (PAI), polyamides, polyimides, and polysulphones. A literature review is provided on the different ways of joining high performance thermoplastic composites by adhesive and fusion bonding. The discussion on adhesive bonding includes examination of the performance of specific adhesive/thermoplastic combinations and of techniques for the preparation of composite surfaces: abrasion, etching, flame, and plasma treatments. Thermoplastic composite welding techniques discussed in depth include the following: heated press welding, resistance welding, induction welding, and ultrasonic welding. Works which examine or compare applications for these bonding techniques are also reviewed. CISTI

N92-33085# Oak Ridge National Lab., TN.
WELDABILITY OF Fe3Al BASED IRON ALUMINIDE ALLOYS
T. Zacharia, P. J. Maziasz, S. A. David, and C. G. McKamey 1992 10 p Presented at the 6th Annual Fossil Energy Materials Conference, Oak Ridge, TN, 12-14 May 1992
(Contract DE-AC05-84OR-21400)
(DE92-017802; CONF-9205123-12) Avail: CASI HC A02/MF A01

An investigation was carried out to determine the weldability of Fe3Al type alloys. Sigmajig tests of a commercial heat of FA-129 alloy indicate that hot-cracking may not be a problem for this alloy. Additionally, several new Fe3Al based iron aluminides were evaluated for weldability. The preliminary results are encouraging and suggest that some of these alloys have comparable or better weldability than FA-129 based iron-aluminides. For the first time, successful welds, without hot or cold cracking, were made on 13 mm (0.5 in.) thick plates from a commercial heat of FA-129 using the proper choice of welding conditions and parameters. DOE

38 QUALITY ASSURANCE AND RELIABILITY

Includes product sampling procedures and techniques; and quality control.

N92-32425*# Alabama Univ., Huntsville. Materials Processing Lab.
STUDY OF EDDY CURRENT PROBES Final Report
Gary L. Workman and Morgan Wang 24 Aug. 1992 31 p
(Contract NAS8-36955)
(NASA-CR-190814; NAS 1.26:190814) Avail: CASI HC A03/MF A01

The recognition of materials properties still presents a number of problems for nondestructive testing in aerospace systems. This project attempts to utilize current capabilities in eddy current instrumentation, artificial intelligence, and robotics in order to provide insight into defining geometrical aspects of flaws in composite materials which are capable of being evaluated using eddy current inspection techniques. Author

N92-32436*# Cornell Univ., Ithaca, NY. Dept. of Computer Science.
FAULT-TOLERANT WAIT-FREE SHARED OBJECTS
Prasad Jayanti, Tushar Deepak Chandra, and Sam Toueg Aug. 1992 59 p Prepared for presentation at the 33rd Annual Symposium on Foundations of Computer Science, Ithaca, NY, Oct. 1992 Sponsored in part by IBM Endicott Programming Lab.; and by an IBM Graduate Fellowship
(Grants NAG2-593; NSF CCR-89-01780; NSF CCR-91-02231)
(NASA-CR-190679; NAS 1.26:190679; TR92-1298) Avail: CASI HC A04/MF A01

A concurrent system consists of processes and shared objects. Previous research focused on the problem of tolerating process failure. We study the complementary problem of tolerating failures. We divide object failures into two broad classes: responsive and non-responsive. With responsive failures, a faulty object responds to every invocation, but responses may be incorrect. With non-responsive failures, a faulty object may also 'hang' without responding. For each class, we consider crash, and arbitrary types of failures. For each type of failure, we are seeking a universal implementation for fault-tolerant wait-free shared objects. We present (deterministic) implementations for all types of responsive failures, including arbitrary failures. In contrast, we show that even the most benign type of non-responsive failures requires the use of randomization. Of special interest is the problem of implementing fault-tolerant objects using only objects of the same type. We present such fault-tolerant self-implementations for many common object types. Graceful degradation is a desirable property of fault-tolerant implementations: the implemented object never fails more severely than the base objects it is derived from, even if all the base objects fail. For several failure models, we show whether this property can be achieved, and, if so, how. In addition to the above possibility/impossibility results, we also consider the resources complexity of fault-tolerant implementations. In many cases, we present lower bounds and give matching algorithms. Author

N92-32564# Brown Univ., Providence, RI.
SURFACES AND THIN FILMS STUDIED BY PICOSECOND ULTRASONICS
J. H. Maris and J. Tauc May 1992 12 p
(Contract DE-FG02-86ER-45267)
(DE92-016313; DOE/ER-45267/6) Avail: CASI HC A03/MF A01

This research is the study of thin films and interfaces via the use of the picosecond ultrasonic technique. In these experiments ultrasonic waves are excited in a structure by means of a picosecond light pulse ('pump pulse'). The propagation of these waves is detected through the use of a probe light pulse that is time-delayed relative to the pump. This probe pulse measures the change delta(R(t)) in the optical reflectivity of the structure that occurs because the ultrasonic wave changes the optical properties of the structure. This technique makes possible the study of the attenuation and velocity of ultrasonic waves up to much higher frequencies than was previously possible (up to at least 500 GHz). In addition, the excellent time-resolution of the method makes it possible to study nanostructures of linear dimensions down to 100 A or less by ultrasonic pulse-echo techniques. DOE

N92-33151# California Univ., Berkeley. Dept. of Industrial Engineering and Operations Research.
STOCHASTIC MODELS IN RELIABILITY Final Report, 1 Oct. 1990 - 30 Sep. 1991
Sheldon M. Ross 30 Sep. 1991 15 p
(Grant AF-AFOSR-0019-91)
(AD-A250934; AFOSR-92-0428TR) Avail: CASI HC A03/MF A01

Two approaches for simulating the reliability function are considered - one using the total hazard estimator and the other using importance sampling. It is shown both for the Wheatstone Bridge system and also for a triangular system that the total hazard estimator has significantly smaller variance when compared both to the standard importance sampling estimator and also to an improved version of it. GRA

39 STRUCTURAL MECHANICS

Includes structural element design and weight analysis; fatigue; and thermal stress.

For applications see *05 Aircraft Design, Testing and Performance* and *18 Spacecraft Design, Testing and Performance.*

N92-32328# Lawrence Livermore National Lab., CA.
AN IMPLEMENTATION OF HILL'S THEORY OF NORMAL ANISOTROPIC PLASTICITY FOR EXPLICIT SHELL ANALYSIS

R. G. Whirley and B. E. Engelmann 20 Aug. 1991 17 p Presented at the 1991 DYNA3D User's Group Conference, Bournemouth (England), 27-28 Sep. 1991
(Contract W-7405-eng-48)
(DE92-011468; UCRL-JC-107883; CONF-9109364-1) Avail: CASI HC A03/MF A01

This paper summarizes the formulation and numerical implementation of a general anisotropic elastic-plastic material model for shell analysis. The 1948 Hill yield function is presented and specialized to conditions of plane stress. Next, an unconditionally stable and fully vectorized numerical algorithm for this constitutive model is presented. Finally, the model is specialized to conditions of normal anisotropy, and the implementation in DYNA3D is discussed. This development in material modeling should substantially extend the applicability of DYNA3D for many sheet metal forming applications. Several large-scale sheet metal forming examples are presented to illustrate these new analysis capabilities. DOE

N92-32423*# National Aeronautics and Space Administration. Langley Research Center, Hampton, VA.
ENVIRONMENTAL FATIGUE IN ALUMINUM-LITHIUM ALLOYS
Robert S. Piascik Jul. 1992 27 p Submitted for publication
(RTOP 538-02-10-01)
(NASA-TM-107640; NAS 1.15:107640) Avail: CASI HC A03/MF A01

Aluminum-lithium alloys exhibit similar environmental fatigue crack growth characteristics compared to conventional 2000 series alloys and are more resistant to environmental fatigue compared to 7000 series alloys. The superior fatigue crack growth behavior of Al-Li alloys 2090, 2091, 8090, and 8091 is due to crack closure caused by tortuous crack path morphology and crack surface corrosion products. At high R and reduced closure, chemical environment effects are pronounced resulting in accelerated near threshold da/dN. The beneficial effects of crack closure are minimized for small cracks resulting in rapid growth rates. Limited data suggest that the 'chemically small crack' effect, observed in other alloy system, is not pronounced in Al-Li alloys. Modeling of environmental fatigue in Al-Li-Cu alloys related accelerated fatigue crack growth in moist air and salt water to hydrogen embrittlement. Author

N92-32621# Dayton Univ., OH. Research Inst.
INVESTIGATION OF A RELATIONSHIP BETWEEN UNIAXIAL AND BIAXIAL CHEMICAL STRESS CRAZING OF CAST ACRYLIC Interim Report, Jan. - Dec. 1990
Daniel R. Bowman Jan. 1992 51 p
(Contract F33615-84-C-3404)
(AD-A250852; UDR-TR-90-127; WL-TR-91-3076) Avail: CASI HC A04/MF A01

Chemical crazing is directly responsible for many aircraft transparency removals. Laboratory chemical stress craze testing can be used to evaluate the effects of different chemicals on aircraft transparencies. Most craze testing to date has been uniaxial, while the stress state in an installed aircraft transparency is biaxial. The uniaxial craze test is easier to conduct and requires simplified fixturing as opposed to the biaxial craze test. It is desirable to be able to use uniaxial data to predict the effects of a biaxial stress field on crazing. An experimental program was conducted to develop a relationship between uniaxial and biaxial chemical stress crazing of aircraft grade cast acrylic with isopropyl alcohol. ASTM Standard Test Methods F484 and F1164 were used as guidelines for the uniaxial craze testing and biaxial craze testing, respectively. Time to craze as a function of stress level was determined and used to develop relationships between uniaxial and biaxial crazing in the form of craze initiation criterion, utilizing theoretical and empirical equations. GRA

N92-32657*# National Aeronautics and Space Administration. Langley Research Center, Hampton, VA.
FREQUENCY DOMAIN STATE-SPACE SYSTEM IDENTIFICATION
Chung-Wen Chen (North Carolina State Univ., Raleigh.), Jer-Nan Juang, and Gordon Lee (North Carolina State Univ., Raleigh.) Jul. 1992 20 p
(RTOP 590-14-61-01)
(NASA-TM-107659; NAS 1.15:107659) Avail: CASI HC A03/MF A01

An algorithm for identifying state-space models from frequency response data of linear systems is presented. A matrix-fraction description of the transfer function is employed to curve-fit the frequency response data, using the least-squares method. The parameters of the matrix-fraction representation are then used to construct the Markov parameters of the system. Finally, state-space models are obtained through the Eigensystem Realization Algorithm using Markov parameters. The main advantage of this approach is that the curve-fitting and the Markov parameter construction are linear problems which avoid the difficulties of nonlinear optimization of other approaches. Another advantage is that it avoids windowing distortions associated with other frequency domain methods. Author

N92-32681# Illinois Inst. of Tech., Chicago. Dept. of Civil Engineering.
FATIGUE, HYSTERESIS, AND ACOUSTIC EMISSION, PARTS 1 AND 2 Final Report
S. A. Guralnick and T. Erber 15 May 1992 176 p
(Grant AF-AFOSR-0136-91)
(AD-A251073; AFOSR-92-0453TR-Pt-1-2) Avail: CASI HC A09/MF A02

The basic objective of this research program is to characterize the development of material fatigue by means of stress-strain hysteresis and acoustic emission measurements. We have conjectured that the accumulation and organization of damage in material fatigue is similar to the progressive failure of structures under cyclic loading. And, specifically, that the endurance limit of a material in fatigue is the analogue of the incremental collapse load of a structure. Since the principal features of the service life and failure of structures can be completely described by hysteresis methods, it is plausible that similar means can be used to characterize the inception and organization of microplastic processes in materials. Experiments were conducted upon nearly 100 specimens made of Rimmed AISI 1018 Unannealed Steel. This material was selected because extensive data on its performance exists in the engineering literature and because its stress-strain curve is of the gradual yielding type, mirroring at least the monotonic stress-strain behavior of many of the kinds of metals used in the aircraft industry. GRA

N92-32698# Rensselaer Polytechnic Inst., Troy, NY. Mechanics of Materials Lab.
INELASTIC DEFORMATION AND DAMAGE AT HIGH TEMPERATURE
E. Krempl 1992 4 p
(Contract DE-FG02-86ER-13566)
(DE92-012241; DOE/ER-13566/5) Avail: CASI HC A01/MF A01

Combined experimental and theoretical investigations into the inelastic deformation and damage behavior of engineering alloys at elevated temperatures are being pursued. The analysis of previously performed strain rate change and relaxation tests on modified 9Cr-1Mo steel showed the need for inclusion of a recovery of state term in the growth laws for the state variables of the viscoplasticity theory based on overstress (VBO). Recovery of state terms were introduced and the experimental results were satisfactorily simulated. The finite deformation theory of VBO has been developed further to include a convected derivative rationale for the choice of the objective stress rate. The reversing direct current voltage drop measurements during low cycle fatigue at elevated temperature were improved. A passive filter bank and new positioning devices for the coils were installed. Tests at 650 C and lasting several days showed excessive, uncontrollable temperature changes. It was decided to drop the test temperature to 538 C which is close to the operating temperature of type 304 stainless steel. The temperature fluctuations in torsion tests were within +/- 3 C which was considered satisfactory. DOE

N92-32706# Lawrence Livermore National Lab., CA.
FREE VIBRATION OF THICK ISOTROPIC AND ORTHOTROPIC CYLINDRICAL SHELLS Ph.D. Thesis
S. E. Bumpas Aug. 1991 142 p
(Contract W-7405-eng-48)
(DE92-011653; UCRL-LR-109428) Avail: CASI HC A07/MF A02

The vibration of free, thick cylindrical shells that are composed of either isotropic materials or orthotropic materials like modern composite laminates are studied. The formulation starts with an approximate five-term displacement field that has been used previously. The subsequent approximate strains, stresses, and force and moment resultants are successively substituted into a variational form of Hamilton's principle to yield the governing vibration equations and boundary condition equations. The two sets of equations are solved simultaneously to obtain dimensionless frequencies. The constitutive law for the material is assumed to be orthogonal with respect to the mid-surface coordinate system. Explicit shear coefficients are assumed for all resultants that have a shear stress in their definition. The computer algorithm that solves the equations is explained along with the exception testing for any found frequency. Results mainly consist of contour plots of the first fundamental frequency for a particular circumferential wave number, n, and symmetric or antisymmetric form. Differences with an accurate series solution for the isotropic case are given. Through-thickness shear coefficients are found that would make this formulation agree with the isotropic series solution. A study of higher frequencies is presented and favorably compared to the series solution. Two typical sets of results are presented for orthotropic materials representative of composite laminates that are stiff in the longitudinal and tangential directions. A concluding summary and areas of future work are discussed. DOE

N92-32717# David Taylor Research Center, Bethesda, MD. Ship Materials Engineering Dept.
MIXED MODEL FATIGUE CRACK GROWTH BEHAVIOR IN A HIGH STRENGTH STEEL Final Report, Oct. 1989 - Sep. 1991
Richard E. Link Nov. 1991 26 p
(AD-A250667; DTRC-SME-91/74) Avail: CASI HC A03/MF A01

Most of the currently available methods for predicting fatigue crack growth in structures do not consider effects due to mixed-mode loading. This is partly due to the limited information available concerning the fatigue crack growth under mixed mode loading. Previous investigations of mixed mode effects on fatigue crack growth have shown that under combined opening and in-plane shear loading, the cracks turn abruptly so that the in-plane shear mode is eliminated. Very little data is generated before the crack curvature eliminates the mixed-mode loading. The changing orientation of the crack during the test makes analysis of the problem difficult and may cloud the intrinsic fatigue crack growth rate behavior under mixed-mode loading. Situations can exist in engineering structures in which cracks may grow in a self-similar manner, even under the influence of mixed-mode loading. Examples of such situations are radial cracks in bearing rates and transverse cracks in rotating shafts under shear and bending loads. The cracks may not change orientation because the in-plane shear component is fully reversed. It is necessary to understand the effects of mixed mode loading on fatigue crack growth in order to properly predict the behavior of these components. GRA

N92-32774# Office National d'Etudes et de Recherches Aerospatiales, Paris (France). Direction des Structures.
BUCKLING AND DAMAGE OF A COMPOSITE PLATE UNDER COMPRESSION [FLAMBAGE ET ENDOMMAGEMENT DE PANNEAUX COMPOSITES EN COMPRESSION]
R. Girard and D. Louis Sep. 1991 22 p In FRENCH
(Contract DRET-89-34-001)
(ONERA-RT-25/3542-RY-006-R; ETN-92-91673) Avail: CASI HC A03/MF A01

The mechanical resistance of a stratified composite plate with delamination is investigated under compressive stresses. The DAM-STRAT computer program was applied. For either simple or imbedded contact points, the results revealed a generalized deformation all over the plate, and failure occurs at the delamination boundary. Such localized failure can be evaluated from the model's instability criterion. The development of a model taking account of the transversal microcracks of composites as well as the degradation of fiber matrix bindings is discussed. ESA

N92-32783# Indian Inst. of Tech., Bombay. Dept. of Civil Engineering.
BUCKLING OF FIBRE REINFORCED COMPOSITE AND SANDWICH LAMINATES WITH HIGHER-ORDER SHEAR DEFORMATION THEORIES Final Report
Tarun Kant and H. S. Patil Mar. 1992 66 p
(Grant Aero/RD-134/100/10/88-89/518)
(IIT-B/CE/RR/92/2) Avail: CASI HC A04/MF A01

A higher-order shear deformation theory, employing C(sup 0) continuous finite elements, is used to determine the buckling loads of symmetric, crossply composite and multilayer sandwich plates. This theory accounts for the quadratic variation of the transverse shear strains, thus eliminating the use of shear correction coefficients. The discrete element is a nine-noded Lagrangian quadrilateral with nine degrees of freedom per node. Numerical examples are presented to demonstrate the behavior and accuracy of the proposed formulation. In all cases, the comparisons made with theory and/or published data show that the higher-order theory predicts accurate results for composite laminates and provides more realistic values or buckling loads for conventional/multilayer sandwich plates. Author

N92-32848# Institute for Aerospace Research, Ottawa (Ontario). Structures and Materials Lab.
A DESCRIPTION OF THE ANALYTICAL METHODOLOGY AND REPORTING PROCEDURES USED IN THE ANALYSIS AND PREPARATION OF CALIBRATION REPORTS FOR FORCE MEASURING INSTRUMENTS
C. W. MacKenzie 17 Apr. 1991 90 p
(NRC-LTR-ST-1817; CTN-92-60368) Avail: CASI HC A05/MF A01

The Technical Services Section of The Structures and Materials Laboratory offers a calibration service for force measuring instruments. The calibration range available is from 89 N in tension and compression, and from 445 KN to 2.67 MN in compression. Force transducers with capacities less than 445 KN are calibrated by direct loading with deadweight primary force standards. The uncertainty of the applied load is determined to be less than 0.002 percent. In spite of the low uncertainty in the prediction of the applied forces based on mass, acceleration due to gravity and air buoyancy, forced intercomparisons on an international scale, using the best available equipment and techniques show disagreements in the order of 0.005 percent between countries. This difference is attributed to interactions between a force machine and the force sensor. Calibrations in the range from 445 KN to 2.67 MN are performed using a hydraulic test machine as a loading device and three secondary standard load cells combined in parallel and loaded in series with the test force transducer. This results in uncertainties of 0.02 or 0.06 percent depending on the capacity of the force transducer. Many types of force transducers can be accommodated and calibrated. This report describes the procedures used to acquire, analyze, tabulate, plot and report the calibration results. Author (CISTI)

N92-32911# Denver Univ., CO. Dept. of Physics.
INVESTIGATION OF FRACTURE TOUGHNESS AND FRACTURE MECHANISMS USING ACOUSTIC EMISSION MEASUREMENTS
S. H. Carpenter 1991 11 p
(Contract DE-FG02-85ER-45182)
(DE92-011907; DOE/ER-45182/6) Avail: CASI HC A03/MF A01

The research program consisted of three separate but closely related investigations: (1) an investigation of the acoustic emission generated during the deformation and fracture of premium grade 4340 steel as a function of mechanical properties; (2) an

investigation of the acoustic emission generated during the deformation and fracture of Ti-641-4V alloys as a function of microstructure; (3) an investigation of the acoustic emission generated from second phase particles in aluminum-silicon alloys as a function of second phase particle size and density. A synopsis of each of the individual investigations is presented, including pertinent data and meaningful results. A listing of graduate student involvement, publications, and presentations is also provided.
DOE

N92-32918# Army Chemical Research and Development Center, Aberdeen Proving Ground, MD.
A REEXAMINATION OF THE PLASTIC FLOW CRITERION FOR COPPER Final Report, Jan. - Dec. 1991
Norris J. Huffington, Jr. Jul. 1992 21 p
(DA Proj. 1L1-61102-AH-43)
(AD-A252370; BRL-TR-3368) Avail: CASI HC A02/MF A01

It was found impossible to reconcile discrepancies between uniaxial and torsion test data for copper within the framework of the von Mises yield function. A more general function that employs both the second and third invariants of the stress deviator was studied. Certain limitations on the use of such functions are discussed.
GRA

N92-32936# Washington Univ., Seattle. Dept. of Mechanical Engineering.
AN EXPERIMENTAL STUDY ON THE TWO-PARAMETER CRACK TIP FIELD
Mahyar S. Dadkhah and A. S. Kobayashi May 1992 10 p
(Contract N00014-89-J-1276)
(AD-A251173; UWA/DME/TR-92/69) Avail: CASI HC A02/MF A01

J-integral values were determined directly from the measured orthogonal displacement fields surrounding a crack in 2024-0, 2024-T3, 2091-T3 and 5052-H32 aluminum alloy SEN and cruciform specimens of 0.8 mm thickness. These J-values were then used to compute the crack tip displacements associated with the HRR field. The second order displacement component in the two-parameter, J-T and the more general J-Q ductile fracture theories was obtained by subtracting the HRR displacement from the measured crack tip displacement. This second order displacement component in the direction parallel to the crack was an order larger than the corresponding component perpendicular to the crack as predicted by the J-Q theory but not by the J-T theory. The negative slope of the log-log plots of the two orthogonal, second order displacement components with respect to the radial distance, however, suggests a strain singularity higher than that of the HRR strain singularity. The basic postulate of the asymptotic expansion of crack tip pansion stress is violated and thus neither the J-T nor the J-Q theory can be a valid criterion in elastic-plastic fracture mechanics.
GRA

N92-33076# Institute for Aerospace Research, Ottawa (Ontario). Structures and Materials Lab.
A TRANSGRANULAR FATIGUE CRACK GROWTH MODEL BASED ON RESTRICTED SLIP REVERSIBILITY
X. J. Wu (Ottawa Univ., Ontario), A. S. Koul, and A. S. Krausz (Ottawa Univ., Ontario) 19 Jun. 1991 25 p Sponsored by National Research Council of Canada
(NRC-LTR-ST-1831; CTN-92-60379) Avail: CASI HC A03/MF A01

This paper presents a transgranular crack growth model based on a restricted slip reversal process where the transgranular crack growth rate is related to the cyclic plastic strain range ahead of the crack tip. Upon applying deformation and fracture kinetics theories, a physically based constitutive law for fatigue crack growth rate is derived. In the absence of any environmental contributions to crack growth, the model takes the form of the Paris equation with a power law exponent of 3 at positive R values. The model expresses the fatigue crack growth rate explicitly in terms of material properties such as yield strength or elastic modulus, work hardening coefficient, microstructural quantities such as activation energy, activation volume and work factor, as well as test constraints such as delta K and R (where R is the ratio of maximum and minimum strain, and delta K is the difference between maximum and minimum strain). The absence of a fatigue threshold is predicted for test conditions where environment does not influence the crack growth process and the material microstructure remains stable.
Author (CISTI)

N92-33104*# National Aeronautics and Space Administration. Langley Research Center, Hampton, VA.
COMPUTATIONAL METHODS FOR GLOBAL/LOCAL ANALYSIS
Jonathan B. Ransom, Susan L. McCleary (Lockheed Engineering and Sciences Co., Hampton, VA.), Mohammad A. Aminpour (Analytical Services and Materials, Inc., Hampton, VA.), and Norman F. Knight, Jr. (Clemson Univ., SC.) Aug. 1992 24 p
(RTOP 505-63-53-01)
(NASA-TM-107591; NAS 1.15:107591) Avail: CASI HC A03/MF A01

Computational methods for global/local analysis of structures which include both uncoupled and coupled methods are described. In addition, global/local analysis methodology for automatic refinement of incompatible global and local finite element models is developed. Representative structural analysis problems are presented to demonstrate the global/local analysis methods.
Author

N92-33139*# National Aerospace Lab., Amsterdam (Netherlands). Structures and Materials Div.
GLOBAL/LOCAL INTERLAMINAR STRESS ANALYSIS OF A GRID-STIFFENED COMPOSITE PANEL
J. F. M. Wiggenraad and N. R. Bauld, Jr. (Clemson Univ., SC.) 30 May 1991 21 p Presented at the 6th American Society for Composites Technical Conference, Albany, NY, 6-9 Oct. 1991
(Contract NAS1-17925)
(NASA-CR-190822; NAS 1.26:190822; NLR-TP-91052-U; ETN-92-91996) Avail: CASI HC A03/MF A01

A global/local procedure for the computation of the interlaminar stress components at the skin wrap, skin core, and wrap core interfaces for an advanced concept stiffened panel, is described. The procedure consists of a global model of two dimensional shell elements that is used to design a grid stiffened panel with blade type stiffeners, a local model of three dimensional solid elements that is used to compute interlaminar stress components, and a scheme devised to assign displacement boundary conditions for a local model that are based on displacement and rotation data of a few nodes of the global model. A global panel was designed according to strength, stiffness, and stability criteria associated with the design of traditional aircraft wing panels. Interlaminar normal and shearing stress components, computed via the local model, were found to be well below typical tensile normal and shearing strengths of a graphite epoxy material.
ESA

N92-33200 Waterloo Univ. (Ontario).
SOME NEW PERSPECTIVES IN PHOTOELASTICITY AND CURVED-RAY TOMOGRAPHY Ph.D. Thesis
Allan T. Dolovich 1990 153 p
(ISBN-0-315-57756-8; CTN-92-60523) Copyright Micromedia Ltd., Technical Information Centre, 165 Hotel de Ville, Place du Portage, Phase 2, Hull, Quebec J8X 3X2, Canada HC/MF

Transmission photoelasticity is a well established tool for experimental determination of stress fields in solid bodies. It has been shown, however, that the classical assumption used in photoelastic analyses, that light propagates rectilinearly through a loaded transparent body, is invalid for regions of high stress gradient. A critical review of standard methods in photoelasticity is presented, and an iterative approach for incorporating the effects due to ray bending is proposed. Closely related disciplines such as holographic interferometry and geophysical imaging are discussed to show that photoelasticity may be regarded as a special case within a more general set of problems which may be described as inverse problems in curved-ray tomography. Accordingly, relevant iterative schemes similar to that proposed for

photoelasticity are examined and compared. A unified approach to evaluation of existing iterative methods is developed and a means for quantifying the convergence of these nonlinear schemes is thus established. Practical algorithms for enlarging the domain of convergence are proposed. New approaches for qualifying and enhancing convergence are illustrated. The effects of instability due to ill-posed equations, and the application of well-known stabilization techniques, are discussed. Author (CISTI)

N92-33228 Waterloo Univ. (Ontario).
CLASSICAL DYNAMICS OF SYSTEMS WITH TIME-VARYING INERTIAL PROPERTIES WITH APPLICATION TO MULTI-RIGID-BODY SYSTEMS Ph.D. Thesis
John Joseph McPhee 1990 166 p
(ISBN-0-315-57834-3; CTN-92-60524) Copyright Micromedia Ltd., Technical Information Centre, 165 Hotel de Ville, Place du Portage, Phase 2, Hull, Quebec J8X 3X2, Canada HC/MF

A general and systematic procedure for formulating the equations of motion for systems with time-varying inertial properties is developed. The time-varying mass of interest is identified using a control volume that can translate, rotate, and deform with the system. A set of general motion equations is then applied to this control volume. Some of these control-volume equations can be found scattered throughout the literature, while some represent new results. These equations have now been organized into a unified and self-consistent dynamic theory. A vector-dyadic formulation of the equations of motion for a variable-mass multibody system is also presented. This system has been modelled as a constant number of rigid bodies plus a time-varying number of particle masses, all executing known motions relative to an unconstrained rigid base body. The governing equations reflect the time-varying nature of the system's inertial properties, and have been encoded into a computer program. The orientation of each rigid body is represented using a conformal rotation vector. Using a 4th order Runge-Kutta algorithm, the program can numerically integrate the nonlinear equations of motion for a particular multibody system. The application of this program to the dynamic analysis of several physical systems, including a rocket with swivelling engine and a satellite with solar panels, is demonstrated. Author (CISTI)

42 GEOSCIENCES (GENERAL)

No abstracts in this category.

43 EARTH RESOURCES AND REMOTE SENSING

Includes remote sensing of earth resources by aircraft and spacecraft; photogrammetry; and aerial photography.

For instrumentation see *35 Instrumentation and Photography.*

N92-32590*# National Aeronautics and Space Administration. Goddard Space Flight Center, Greenbelt, MD.
DEVELOPMENT OF A PROTOTYPE SPATIAL INFORMATION PROCESSING SYSTEM FOR HYDROLOGIC RESEARCH
Jayanta K. Sircar Nov. 1991 52 p
(Grant NAG5-1466)
(NASA-CR-190579; NAS 1.26:190579) Avail: CASI HC A04/MF A01

Significant advances have been made in the last decade in the areas of Geographic Information Systems (GIS) and spatial analysis technology, both in hardware and software. Science user requirements are so problem specific that currently no single system can satisfy all of the needs. The work presented here forms part of a conceptual framework for an all-encompassing science-user workstation system. While definition and development of the system as a whole will take several years, it is intended that small scale projects such as the current work will address some of the more short term needs. Such projects can provide a quick mechanism to integrate tools into the workstation environment forming a larger, more complete hydrologic analysis platform. Described here are two components that are very important to the practical use of remote sensing and digital map data in hydrology. Described here is a graph-theoretic technique to rasterize elevation contour maps. Also described is a system to manipulate synthetic aperture radar (SAR) data files and extract soil moisture data. Author

N92-33233 Waterloo Univ. (Ontario).
INTEGRATING EXPERT VISION SYSTEMS AND SPATIAL DATABASE BY UNIFYING KNOWLEDGE REPRESENTATION SCHEMES.DEVELOPMENT IN REMOTE SENSING IMAGE ANALYSIS EXPERT SYSTEMS AND GEOGRAPHICAL INFORMATION SYSTEMS Ph.D. Thesis
Fangfu Wang 1989 227 p
(ISBN-0-315-49130-2; CTN-92-60543) Copyright Micromedia Ltd., Technical Information Centre, 165 Hotel de Ville, Place du Portage, Phase 2, Hull, Quebec J8X 3X2, Canada HC/MF

A new path is explored for integration of remote sensing and geographical information system (GIS) technologies. The major barriers to such integration include problems with data format, data accuracy, and system communication. These problems, which at first may seem to be independent of each other, are considered as different aspects of a problem with knowledge representation and are tackled by unifying the systems to be integrated on a common knowledge representation framework. Three new techniques, the communication subschema, the relational linear quadtree, and the fuzzy representation method, have been developed to provide such a framework. A unified data model has been defined to implement the techniques. The three techniques have been successfully applied to the integration of GIS and remote sensing systems. Encouraging results have been achieved in the practice of designing, implementing, and integrating a GIS and two remote sensing image analysis systems.
Author (CISTI)

44 ENERGY PRODUCTION AND CONVERSION

Includes specific energy conversion systems, e.g., fuel cells; global sources of energy; geophysical conversion; and windpower.

For related information see also *07 Aircraft Propulsion and Power, 20 Spacecraft Propulsion and Power,* and *28 Propellants and Fuels.*

N92-32510# Midwest Research Inst., Golden, CO. National Renewable Energy Lab.
THIN FILM CADMIUM TELLURIDE, ZINC TELLURIDE, AND MERCURY ZINC TELLURIDE SOLAR CELLS
T. L. Chu (University of South Florida, Tampa.) Apr. 1992 97 p
(Contract DE-AC02-83CH-10093)
(DE92-001237; NREL/TP-413-4791) Avail: CASI HC A05/MF A02

This report describes research to demonstrate (1) thin film cadmium telluride solar cells with a quantum efficiency of 75 percent or higher at 0.44 microns and a photovoltaic efficiency of 11.5 percent or greater, and (2) thin film zinc telluride and mercury zinc telluride solar cells with a transparency to sub-band-gap radiation of 65 percent and a photovoltaic conversion efficiency of 5 percent and 8 percent, respectively. Work was directed at (1) depositing transparent conducting semiconductor films by solution growth and metal-organic chemical vapor deposition (MOCVD) technique, (2) depositing CdTe films by close-spaced sublimation (CSS) and MOCVD techniques, (3) preparing and evaluating thin film CdTe solar cells, and (4) preparing and

characterizing thin film ZnTe, CD(1-x)Zn(1-x)Te, and Hg(1-x)Zn(x)Te solar cells. The deposition of CdS films from aqueous solutions was investigated in detail, and their crystallographic, optical, and electrical properties were characterized. CdTe films were deposited from DMCd and DIPTe at 400 C using TEGa and AsH3 as dopants. CdTe films deposited by CSS had significantly better microstructures than those deposited by MOCVD. Deep energy states in CdTe films deposited by CSS and MOCVD were investigated. Thin films of ZnTe, Cd(1-x)Zn(x)Te, and Hg(1-x)Zn(x)Te were deposited by MOCVD, and their crystallographic, optical, and electrical properties were characterized. DOE

N92-32549# Sandia National Labs., Albuquerque, NM.
TESTING OF THE SINGLE-ELEMENT STRETCHED-MEMBRANE DISH
J. W. Grossman, R. M. Houser, and W. W. Erdman Feb. 1992 39 p
(Contract DE-AC04-76DP-00789)
(DE92-013680; SAND-91-2203) Avail: CASI HC A03/MF A01

The goal of the Stretched-Membrane Dish Program is the development of a dish solar concentrator fabricated with a single optical element capable of collecting 60 kWt. Solar Kinetics, Inc., has constructed a prototype 7-meter dish to demonstrate the manufacturability and optical performance of this innovative design. The reflective surface of the dish consists of a plastically deformed metal membrane with a separate reflective polymer membrane on top, both held in place by a low-level vacuum. Sandia conducted a test program to determine the on-sum performance of the dish. The vacuum setting was varied 8.9- to 17. 2-cm of water column and the vertex to target distance was varied over a range of 15.24 cm to evaluate beam quality. The optimal setting for the vacuum was 11.4 centimeters of water column with the best beam quality of 6.4 centimeters behind the theoretical focal point of the dish. Flux arrays based on slope error from the CIRCE2 computer code were compared to the measured flux array of the dish. The uniformly distributed slope error of 2.3 milliradians was determined as the value that would produce a modeled array with the minimum mean square difference to the measured array. Cold water calorimetry measured a power of 23.3 (plus minus) .3 kWt. Reflectivity changed from an initial value of 88.3 percent to 76.7 percent over a one year period. DOE

N92-32565# Sandia National Labs., Albuquerque, NM.
CONCENTRATOR SILICON CELL RESEARCH
M. A. Green (New South Wales Univ., Kensington, Australia), S. R. Wenham (New South Wales Univ., Kensington, Australia), F. Zhang (New South Wales Univ., Kensington, Australia), J. Zhao (New South Wales Univ., Kensington, Australia), and A. Wang (New South Wales Univ., Kensington, Australia) Apr. 1992 40 p
(Contract DE-AC04-76DP-00789)
(DE92-016576; SAND-91-7016) Avail: CASI HC A03/MF A01

This project continued the development of high-efficiency silicon concentrator solar cells with the goal of achieving a cell efficiency in the 26 to 27 percent range at a concentration level of 150 suns of greater. The target efficiency was achieved with the new PERL (passivated emitter, rear locally diffused) cell structure, but only at low concentration levels around 20 suns. The PERL structure combines oxide passivation of both top and rear surfaces of the cells with small area contact to heavily doped regions on the top and rear surfaces. Efficiency in the 22 to 23 percent range was also demonstrated for large-area concentrator cells fabricated with the buried contact solar cell processing sequence, either when combined with prismatic covers or with other innovative approaches to reduce top contact shadowing. DOE

N92-32605# Swedish Council for Building Research, Stockholm.
ENVIRONMENTAL CONSEQUENCES OF NEW ENERGY TECHNOLOGY. SOLAR HEATING, HEAT STORES, AND HEAT PUMPS
T. Svensson 1991 75 p Prepared in cooperation with Chalmers Univ. of Technology, Goeteborg, Sweden; and Royal Inst. of Technology, Stockholm, Sweden
(PB92-180843; D18:1991; ISBN-91-540-5369-2) Avail: CASI HC A04/MF A01

The report summarizes and assesses the environmental consequences associated with new energy technologies, with particular emphasis on their use for space heating supplies in the building environment. In the case of solar heating, it is primarily the processes associated with the production of the necessary materials and ground use requirements that can adversely affect the environment. There is also a certain risk associated with the leakage of heat transfer fluid. For heat stores, problem areas with heating of the ground, discharge of foreign substances in connection with water treatment, and conflicts of other users of groundwater. The main adverse effects of heat pumps are as follows: their emissions of CFCs - which damage the ozone layer; utilization of certain types of heat sources; and the need to provide primary energy for mechanical drive of the pumps. Author

N92-32608# Chalmers Univ. of Technology, Goeteborg (Sweden). Inst. foer Vattenbyggnad.
ENERGY TAKE-OUT FROM A WAVE ENERGY DEVICE. A THEORETICAL STUDY OF THE HYDRODYNAMICS OF A TWO-BODY PROBLEM CONSISTING OF A BUOY AND A SUBMERGED PLATE
L. Berggren 1992 85 p Sponsored in part by Statens Energiverk, Stockholm, Sweden
(PB92-178821; SER-A-23) Avail: CASI HC A05/MF A01

A method for calculating the energy take-out from a single wave energy converter is presented. The converter consists of a buoy connected via a hose pump to a submerged plate. The equations of motion of the buoy and plate are solved linearly in the frequency domain, which shows that frequency dependent hydrodynamic properties can be used. The emphasis in the report is placed on the calculation of the frequency dependent hydrodynamic properties, such as the wave excited forces and the hydrodynamic coefficients. The structure is considered to be large in comparison with the wave length and, therefore, the diffraction theory was used. A method of calculating the forces that act on the bodies is presented, as well as the interaction between the bodies. The two-body problem is solved analytically. The present solution is compared with a numerical one and an analytical one, the latter, however, treats simply a single buoy riding in the waves. The calculated energy take-out of the present model is compared with a time domain dependent model, and reasonable agreement was found. Author

N92-32695# Los Alamos National Lab., NM.
HDR OPPORTUNITIES AND CHALLENGES BEYOND THE LONG-TERM FLOW TEST ISCO, CA, 24-26 MAR. 1992
D. V. Duchane 1992 8 p Presented at the Geothermal Energy Program Review: Geothermal Energy and the Utility Market - the Opportunities and Challenges for Expanding Geothermal Energy in a Competitive Supply Market, San Francisco, CA. 24-26 Mar. 1992
(Contract W-7405-eng-36)
(DE92-011234; LA-UR-92-978; CONF-920378-1) Avail: CASI HC A02/MF A01

The long term flow test (LTFT) of the world's largest, deepest, and hottest hot dry rock (HDR) reservoir currently underway at Fenton Hill, NM is expected to demonstrate that thermal energy can be mined from hot rock within the earth on a sustainable basis with minimal water consumption. This test will simulate the operations of a commercial facility in some ways, but it will not show that energy from HDR can be produced at a variety of locations with different geological settings. Since the Fenton Hill system was designed as a research facility rather than strictly for production purposes, it will also not demonstrate economic viability, although it may well give indications of system modifications needed for economic HDR operations. A second production site must be constructed, ideally under the direction of the private geothermal community, to begin the process of proving that the vast HDR resources can be accessed on a worldwide scale. Finally, research and development work in areas such as reservoir interrogation

and system modeling must be accelerated to increase the competitiveness and geographical applications of HDR and the geothermal industry in general. This paper addresses the above issues in detail and outlines possible paths to future prosperity for the commercial geothermal industry. DOE

N92-32908# Midwest Research Inst., Golden, CO. National Renewable Energy Lab.
SOLAR PHOTO-THERMAL CATALYTIC REACTIONS TO PRODUCE HIGH VALUE CHEMICALS
H. W. Prengle, Jr. and W. E. Wentworth (Houston Univ., TX.) Apr. 1992 30 p
(Contract DE-AC02-83CH-10093)
(DE91-002140; NREL/TP-253-4275) Avail: CASI HC A03/MF A01

This report presents a summary of the research work accomplished to date on the utilization of solar photo-thermal energy to convert low cost chemical feedstocks into high dollar-value chemical products. The rationale is that the solar IR-VIS-UV spectrum is unique, supplying endothermic reaction energy as well as VIS-UV for photochemical activation. Chemical market analysis and product price distribution focused attention on speciality chemicals with prices greater than $1.00/lb, and a synthesis sequence of n-paraffins to aromatics to partial oxidized products. The experimental work has demonstrated that enhanced reaction effects result from VIS-UV irradiation of catalytically active V2O5/SiO2. Experiments of the past year have been on dehydrogenation and dehydrocyclization of n-paraffins to olefins and aromatics with preference for the latter. Recent results using n-hexane produced 95 percent conversion with 56 percent benzene; it is speculated that aromatic yield should reach approximately 70 percent by further optimization. Pilot- and commercial-scale reactor configurations have been examined; the odds-on-favorite being a shallow fluid-bed of catalyst with incident radiation from the top. Sequencing for maximum cost effectiveness would be day-time endothermic followed by night-time exothermic reactions to produce the products. DOE

N92-32909# Midwest Research Inst., Golden, CO. National Renewable Energy Lab.
THERMOCHEMICAL CYCLES FOR ENERGY STORAGE: THERMAL DECOMPOSITION OF ZnSO4 SYSTEMS
W. E. Wentworth (Houston Univ., TX.) Apr. 1992 115 p
(Contract DE-AC02-83CH-10093)
(DE91-002144; NREL/TP-253-4279) Avail: CASI HC A06/MF A02

The overall objective of our research has been to develop thermochemical cycles that can be used for energy storage. A specific cycle involving ammonium hydrogen sulfate (NH4HSO4) has been proposed. Each reaction in the proposed cycle has been examined experimentally. Emphasis has been placed on the basic chemistry of these reactions. In the concluding phase of this research, we have shown that when NH4HSO4 is mixed with ZnO and decomposed, the resulting products can be released stepwise (H2O (gaseous) at approximately 163 C, NH3 (gaseous) at 365-418 C, and a mixture of SO2 (gaseous) and SO3 (gaseous) at approximately 900 C) and separated by controlling the reaction temperature. Side reactions do not appear to be significant and the respective yields are high, as would be required for the successful use of this energy storage reaction in the proposed cycle. Thermodynamic, kinetic, and other reaction parameters have been measured for the various steps of the reaction. Finally, we have completed a detailed investigation of one particular reaction: the thermal decomposition of zinc sulfate (ZnSO4). We have demonstrated that this reaction can be accelerated and the temperature required reduced by the addition of excess ZnO, V2A5, and possibly other metal oxides. DOE

N92-32923# Sandia National Labs., Albuquerque, NM.
SOLAR THERMAL ENERGY: VIABLE ENERGY TECHNOLOGY FOR TODAY AND TOMORROW
D. Menicucci and P. Klimas 1992 12 p Presented at the Eco-World Exhibition and Conference on Ecology, Economics and Engineering, Washington, DC, 14-17 Jun. 1992
(Contract DE-AC04-76DP-00789)
(DE92-015039; SAND-91-2789C; CONF-920658-2) Avail: CASI HC A03/MF A01

Most modern solar energy systems can be cost effective when properly applied and, in some cases, are competitive with fossil-fuel energy systems (e.g., water heating and energy generation in remote areas). Systems being developed today have the potential to be used efficiently in large-scale applications. However, many barriers still exist that prevent the widespread use of these systems. This paper presents an overview of solar energy, including the rationale for solar thermal energy systems, a description of the systems that are commercially available, and an explanation of why these systems are not more common. The Department of Energy's direct technical assistance and educational efforts regarding solar energy are also discussed. DOE

N92-32924# Morgantown Technology Center, WV.
HIGH-TEMPERATURE SOLID OXIDE FUEL CELL (SOFC) GENERATOR DEVELOPMENT PROJECT: ENVIRONMENTAL ASSESSMENT
Aug. 1991 7 p
(DE92-014698; DOE/EA-0510) Avail: CASI HC A02/MF A01

The proposed project involves research, development, fabrication, and testing of solid oxide fuel cells/generators. All of the work, with the exception of various SOFC generator tests, would be conducted at two existing permitted Westinghouse facilities in the greater metropolitan Pittsburgh, Pennsylvania area. The DOE has prepared this Environmental Assessment (EA). This site-specific analysis addresses the two existing permitted Westinghouse facilities. The sources of information for this EA include the following: the technical proposal submitted as part of the assistance application by the Westinghouse Electric Corporation; discussions with the Westinghouse staff and information provided on the sites to be utilized; and site visits during work conducted under the prior Westinghouse effort with DOE. DOE

N92-32943# Department of the Navy, Washington, DC.
HOT WATER STORAGE TANK FOR SOLAR COLLECTORS Patent Application
James S. Roehl, inventor (to Navy) 26 Feb. 1992 14 p
(AD-D015301; US-Patent-Appl-SN-841699; Navy-Case-73767)
Avail: CASI HC A03/MF A01

A baffled hot storage tank for solar collector systems is provided. The tank includes a concentric of the baffle and another circulation part at the top of the baffle. This configuration restricts the mixing of water allowing both a vertical temperature gradient and a lateral gradient to be maintained. The maintaining of hot water at the desired supply temperature is restricted to only the upper section of the center core inside the baffle. This location reduces radiant heat loss. Additionally, inlet and outlet pipes are also positioned to take advantage of the tank temperature gradients. GRA

N92-32946# Sandia National Labs., Albuquerque, NM.
THE PHOTOVOLTICS PROGRAM AT SANDIA NATIONAL LABORATORIES
D. E. Hasti 1992 6 p Presented at the 11th Review Meeting of the National Renewable Energy Laboratories: Photovoltaic Advanced Research and Development, Lakewood, CO, 13-15 May 1992
(Contract DE-AC04-76DP-00789)
(DE92-014617; SAND-92-0680C; CONF-9205115-1) Avail: CASI HC A02/MF A01

The Photovoltaic (PV) Projects at Sandia National Laboratories support the Department of Energy (DOE) National Photovoltaics Program through silicon solar cell research and development, concentrator module research and development, evaluation of cells and modules for both one-sun and concentrator applications development and evaluation of hardware for PV applications, and domestic and international applications identification and verification. In all of these activities, close ties are maintained

with industry to assure that the US PV industry benefits from the Sandia/DOE effort. These industry ties include collaborative agreements between industrial partners and Sandia to improve fabrication processes, evaluating industry components and prototype products for performance and reliability, direct funding of industry for process and product development, and assuring that industry and users are brought together when systems are being developed for new applications. This paper offers an overview of the Sandia Photovoltaic Projects and their contributions to this effort. DOE

N92-33072# Kauppa-ja Teollisuusministerio, Helsinki (Finland). Energy Dept.
NEMO: ADVANCED ENERGY SYSTEMS AND TECHNOLOGIES
W. A. Beckman (Wisconsin Univ., Madison.), E. L. Petersen (Risoe National Lab., Roskilde, Denmark), and B. Sellberg (Swedish Council for Building Research, Stockholm.) 1992 25 p
(DE92-540920; KTM/E-B-105; ISBN-951-47-4472-1) Avail: CASI HC A03/MF A01

The NEMO program, one of ten Finnish energy research programs, has supported research and development in wind energy storage and solar energy systems since 1988. The focus is on problems of particular interest to Finland with emphasis on technologies that may be important within the next 10 years. The projects covered the range from product development in close collaboration with industrial partners to basic research. The committee was generally impressed with the level of competence of the research teams. It is clear that in some areas the Finnish research is on a par with the best in the world. In some areas the research may be described as being in a necessary 'catch-up' phase. Although the program is less than three years old, the results to date are encouraging and the committee recommends continuing NEMO or a similar program beyond 1992. Specific observations are included in the final section of this report. DOE

N92-33090# Japan Solar Energy Society, Tokyo.
THE 1991 JAPAN SOLAR ENERGY SOCIETY. JAPAN WIND ENERGY ASSOCIATION JOINT CONFERENCE
20 Sep. 1991 434 p Conference held in Hokkaido (Japan), 20-21 Sep. 1991
(DE92-530733; CONF-9109393) Avail: CASI HC A19/MF A04

Thie paper summarizes the lectures presented at the research presentation conference held by the Japan Solar Energy Society and the Japan Wind Energy Association. The contents include a lecture relating to photovoltaic cells intended for efficiency improvement; a lecture relating to a light power generation system including the field test reports, improvements on peripheral devices and output characteristics; a lecture relating to optical chemistry; a lecture relating to heat pumps utilizing solar heat and well water; a lecture relating air conditioning utilizing photovoltaic cells; a lecture relating to heat systems utilizing solar heat directly; a lecture relating to heat collection; a lecture relating to cold heat for cooling using earth tubes; a lecture relating to direct utilization of ground water heat and solar heat; a lecture relating to underground heat storage; a lecture relating to accumulation of cold heat and hot heat; a lecture relating to insolation on the amount of insolation and spectroscopy; a lecture relating to light collection intended of energy saving; a lecture relating to improving materials including light collecting plates and thin films; a lecture relating to development and characteristics of solar cars; and a lecture relating to wind energy. DOE

N92-33138# Midwest Research Inst., Golden, CO. National Renewable Energy Lab.
HIGH-FLUX SOLAR PHOTON PROCESSES
Donald C. Lorents (SRI International Corp., Menlo Park, CA.), Subhash Narang (SRI International Corp., Menlo Park, CA.), David C. Huestis (SRI International Corp., Menlo Park, CA.), Jack L. Mooney (SRI International Corp., Menlo Park, CA.), Theodore Mill (SRI International Corp., Menlo Park, CA.), Her-King Song (SRI International Corp., Menlo Park, CA.), and Susanna Ventura (SRI International Corp., Menlo Park, CA.) Jun. 1992 30 p
(Contract DE-AC02-83CH-10093)
(DE92-001247; NREL/TP-253-4471) Avail: CASI HC A03/MF A01

This study was commissioned by the National Renewable Energy Laboratory (NREL) for the purpose of identifying high-flux photoprocesses that would lead to beneficial national and commercial applications. The specific focus on high-flux photoprocesses is based on the recent development by NREL of solar concentrator technology capable of delivering record flux levels. We examined photolytic and photocatalytic chemical processes as well as photothermal processes in the search for processes where concentrated solar flux would offer a unique advantage. DOE

N92-33150# Sandia National Labs., Albuquerque, NM.
SUMMARY OF ENGINEERING-SCALE EXPERIMENTS FOR THE SOLAR DETOXIFICATION OF WATER PROJECT
J. E. Pacheco and L. Yellowhorse Mar. 1992 173 p
(Contract DE-AC04-76DP-00789)
(DE92-013776; SAND-92-0385) Avail: CASI HC A08/MF A02

This report contains a summary of large-scale experiments conducted at Sandia National Laboratories under the Solar Detoxification of Water project. The objectives of the work performed were to determine the potential of using solar radiation to destroy organic contaminants in water by photocatalysis and to develop the process and improve its performance. For these experiments, we used parabolic troughs to focus sunlight onto glass pipes mounted at the trough's focus. Water spiked with a contaminant and containing suspended titanium dioxide catalyst was pumped through the illuminated glass pipe, activating the catalyst with the ultraviolet portion of the solar spectrum. The activated catalyst creates oxidizers that attack and destroy the organics. Included in this report are a summary and discussion of the implications of experiments conducted to determine: the effect of process kinetics on the destruction of chlorinated solvents (such as trichloroethylene, perchloroethylene, trichloroethane, methylene chloride, chloroform and carbon tetrachloride), the enhancement due to added hydrogen peroxide, the optimal catalyst loading, the effect of light intensity, the inhibition due to bicarbonates, and catalyst issues. DOE

45 ENVIRONMENT POLLUTION

Includes atmospheric, noise, thermal, and water pollution.

N92-32415# Los Alamos National Lab., NM.
NATIONAL ENVIRONMENTAL COMPLIANCE STRATEGY
M. Gerety and K. Rea May 1992 25 p
(Contract W-7405-eng-36)
(DE92-013639; LA-12260-MS) Avail: CASI HC A03/MF A01

The authors produced this document as part of their mission in support of the Department of Energy's Albuquerque Field Office (DOE/AL) Environmental Restoration (ER) Program. The document was written as a road map to provide a practical and usable strategy for compliance with the National Environmental Policy Act (NEPA). The ER Program has components regulated by the Environmental Protection Agency (EPA), the individual states in which the installation is located, and DOE itself. The architecture for all these requirements is basically the same. The document illustrates how the Resource Conservation and Recovery Act (RCRA), the Comprehensive Environmental Response, Compensation, and Liability Act (CERCLA), and NEPA fit together conceptually. Many of the state-generated requirements also fit within this framework, but these must be handled on a case-by-case basis. The compliance strategy we present here portrays the process in the most general terms possible but provides enough specific information to ensure compliance. We have tried to show the specific steps that are required to achieve compliance. Because individual installations have different systems to deal with regulatory and environmental requirements, we made no attempt to place tight constraints on exactly how to accomplish compliance. DOE

N92-32543# Battelle Columbus Labs., OH.
PHASE DISTRIBUTIONS OF AIRBORNE POLYCYCLIC AROMATIC HYDROCARBONS IN TWO US CITIES Report, Jun. 1991 - Feb. 1992
R. G. Lewis, T. J. Kelly, J. C. Chuang, P. J. Callahan, and R. W. Coutant 28 Feb. 1992 14 p
(Contract EPA-68-D0-0007)
(PB92-164979) Avail: CASI HC A03/MF A01

Ambient air concentrations of 18 polycyclic aromatic hydrocarbons (PAHs) were monitored in Boston, Massachusetts and Houston, Texas. The PAHs were generated by fossil fuel and wood combustion, motor vehicle traffic, oil refineries, or other sources. Since PAHs may exist in air both as vapors and absorbed on particles, a denuder sampler that denudes tha air of vapors and collects only particles was operated next to a traditional sampler at each site from August 27, 1990 to August 27, 1991. Phase distributions were determined on a seasonal basis. A significant portion of each PAH was found to be in the vapor phase. The amount volatilized from the particles depended on vapor pressure, atmospheric concentration of the PAH, and ambient temperature. Author

N92-32554# National Center for Atmospheric Research, Boulder, CO. Climate and Global Dynamics Div.
ANNUAL VARIATION OF SURFACE TEMPERATURES OVER THE WORLD
Wilhelm May, Dennis J. Shea, and Roland A. Madden Mar. 1992 142 p
(PB92-193259; NCAR/TN-372+STR) Avail: CASI HC A07/MF A02

The authors present the annual variation of the daily minimum, maximum and mean surface temperatures determined from 4 to 11 years of daily observations from 3905 stations distributed over the world. This leads to a comprehensive presentation of the annual cycle of temperature on a global scale. The study is an extension of Shea (1984), who documented the annual variation of temperature over North America. These data are useful in many disciplines, including agricultural studies and climate research. In agricultural studies, the annual variation of the daily minimum and maximum temperatures are of major interest. Also, they can be used to check the ability of climate models to correctly simulate the diurnal cycle of temperature. Author

N92-32558# Sandia National Labs., Albuquerque, NM.
INTERNATIONAL TECHNOLOGY TRANSFER TO SUPPORT THE ENVIRONMENTAL RESTORATION NEEDS OF THE DOE COMPLEX
A. R. DuCharme, R. D. Jimenez (Applied Sciences Lab., Inc., Albuquerque, NM.), and W. J. Roberds (Golder Associates, Inc., Redmond, WA.) 1992 8 p Presented at the Spectrum 1992: Nuclear and Hazardous Waste Management International Topical Meeting, Boise, ID, 23-27 Aug. 1992
(Contract DE-AC04-76DP-00789)
(DE92-013663; SAND-92-0959C; CONF-920851-6) Avail: CASI HC A02/MF A01

One of the principal objectives of the International Technology Exchange Program (ITEP) is the exchange of waste management and environmental restoration (WM/ER) technologies between the US and other nations. The current emphasis of ITEP is the transfer of technologies to the US that could provide better, faster, cheaper, or safer solutions to the needs of the DOE complex. The 10 candidate technologies that have been identified thus far by ITEP are discussed. The highlights of preliminary evaluations of these technologies through a systems approach are also described. The technologies have been evaluated by a screening process to determine their applicability to the leading WM/ER needs of the DOE complex. The technologies have been qualitatively compared with the known or anticipated capabilities of domestic, base case technologies. DOE

N92-32609# Environmental Protection Agency, Research Triangle Park, NC. Air and Energy Engineering Research Lab.
US EPA'S GLOBAL CLIMATE CHANGE PROGRAM: LANDFILL EMISSIONS AND MITIGATION RESEARCH Report, Aug. 1990 - May 1991
S. A. Thorneloe 14 Oct. 1991 20 p Presented at the 3rd Sardinia 1991 International Landfill Symposium, Cagliari, Italy, 14 Oct. 1991
(PB92-180215; EPA/600/A-92/102) Avail: CASI HC A03/MF A01

The paper discusses the U.S. Environmental Protection Agency's (EPA) global climate change program, concentrating on global landfill methane (CH4) emissions and mitigation research. The EPA's Air and Energy Engineering Research Laboratory (AEERL) has begun research on developing more reliable emission estimates of the key greenhouse gas sources that are amenable to cost-effective control. Research was initiated on biomass and CH4 utilization, tropospheric ozone, and evaluation of potential mitigation opportunities for emissions contributing to global climate change. The emissions program has begun to identify and quantify emission sources of greenhouse gases for anthropogenic sources including landfills, coal mines, natural gas production/distribution, cookstoves, and biomass burning. Development of enhanced emission estimates will improve the understanding of atmospheric chemistry and feedback effects, target mitigation opportunities, and ensure cost-effective mitigation strategies. Author

N92-32616# Oak Ridge National Lab., TN.
SUGGESTIONS FOR IMPROVEMENT OF THE METHODOLOGY AND USE OF MEPAS, THE MULTIMEDIA ENVIRONMENTAL POLLUTANT ASSESSMENT SYSTEM
L. Shevenell and F. O. Hoffman Apr. 1992 31 p
(Contract DE-AC05-84OR-21400)
(DE92-013135; ORNL/ER-47) Avail: CASI HC A03/MF A01

The Multimedia Environmental Pollutant Assessment System (MEPAS) was evaluated for the purpose of determining if the current ranking of waste sites is realistic and reliable. There are two main reasons for the uncertainty of the rankings identified in this study: the use of the hazard potential index (HPI) and the user input. The HPI contributes to unreliable rankings because risks to human populations are summarized in a single numerical value. A final result from MEPAS should include risks to the maximally exposed individual, average individual, and the population (noting the population size) so that users can evaluate and weigh these risks. Examination of user input indicates that exposure pathways and exposed populations were sometimes arbitrarily selected. Users must be better informed about the characteristics of the waste site and its potential interaction with human populations for realistic input to the MEPAS model to be developed. Without realistic and consistent input to the MEPAS, or any model, reliable results cannot be expected and any prioritizations based on the results will be questionable. DOE

N92-32619# Maryland Univ., College Park.
EXPLOITATION OF PARALLELISM IN CLIMATE MODELS
F. Baer, J. J. Tribbia, and D. L. Williamson 1992 9 p
(Contract DE-FG05-91ER-61219)
(DE92-012595; DOE/ER-61219/1) Avail: CASI HC A02/MF A01

The US Department of Energy (DOE) through its CHAMMP initiative, hopes to develop the capability to make meaningful regional climate forecasts on time scales exceeding a decade. Such a capability is to be based on numerical prediction type models. We propose research to contribute to each of the specific items enumerated in the CHAMMP announcement (Notice 9103): to consider theoretical limits to prediction of climate and climate change on appropriate time scales; to develop new mathematical techniques to utilize massively parallel processors (MPP); to actually utilize MPP's as a research tool; and to develop improved representations of some processes essential to climate prediction. To explore these initiatives, we will exploit all available computing technology, and in particular MPP machines. We anticipate that significant improvements in modeling of climate on the decadal

and longer time scales for regional space scales will result from our efforts. This report summarizes the activities of our group during a part of the first year's effort to meet the objectives stated in our proposal. We will comment on three research foci, time compression studies, subgrid scale model studies, and distributed climate ensemble studies, and additional significant technical matters. DOE

N92-32650# Andrulis Research Corp., Salt Lake City, UT.
DEVELOPMENT OF METHODOLOGY AND TECHNOLOGY FOR IDENTIFYING AND QUANTIFYING EMISSION PRODUCTS FROM OPEN BURNING AND OPEN DETONATION THERMAL TREATMENT METHODS. BANGBOX TEST SERIES. VOLUME 3: QUALITY ASSURANCE AND QUALITY CONTROL Final Report, Dec. 1988 - Jan. 1992
MacDonald Johnson Jan. 1992 306 p
(Contract DAAD09-87-D-0008)
(AD-A251099) Avail: CASI HC A14/MF A03

The 1989 BangBox test validated technologies and methodologies proposed for identifying and quantifying emissions resulting from the open burning (OB) of propellants and open detonation (OD) of explosives. This test also provided the first credible data on combustion products resulting from OB/OD treatment procedures. The vigorous quality assurance/quality control (QA/QC) program established well before the first trial was continued through the reporting phase. Major elements of the OA/QC program were a quality assurance program plan (QAPP), letters of instruction (LOI) covering all technical aspects of the testing program, a sample identification and tracking system, test monitoring by the scientific support contractor, visits to the test site and assay laboratories by an independent QA contractor, assays by different laboratories using different instruments (gas chromatograph/mass spectrometer and supercritical fluid chromatograph/mass spectrometer), equipment audits by the U.S. Environmental Protection Agency's Atmospheric Research and Exposure Assessment Laboratory (AREAL), assay of samples spiked by the AREAL, and cooperative assistance from the U.S. Army Toxic and Hazardous Material Agency, and the U.S. Army Environmental Hygiene Agency. GRA

N92-32708# National Oceanic and Atmospheric Administration, Washington, DC. National Ocean Pollution Program Office.
FEDERAL PLAN FOR OCEAN POLLUTION RESEARCH, DEVELOPMENT, AND MONITORING, FISCAL YEARS 1992-1996
Sep. 1991 179 p
(PB92-185164) Avail: CASI HC A09/MF A02

The National Ocean Pollution Planning Act of 1978 calls for the establishment of a comprehensive, coordinated, and effective Federal Program for ocean pollution research, development, and monitoring. As required by the Act, the Department of Commerce's National Oceanic and Atmospheric Administration, in consultation with other agencies, prepares a 5-year Federal Plan for Ocean Pollution Research, Development, and Monitoring every 3 years. The document represents the fifth edition of the Plan and covers Fiscal Years 1992-1996. The Plan discusses six goals of the National Ocean Pollution Program, discusses the extent to which ongoing Federal programs are meeting these goals, and provides recommendations for improving the overall effort in marine pollution research and monitoring. Author

N92-32731# Office of the Deputy Secretary of Defense, Washington, DC.
DEFENSE ENVIRONMENTAL RESTORATION PROGRAM ANNUAL REPORT TO CONGRESS FOR FISCAL YEAR 1991
Thomas Baca Feb. 1992 282 p
(AD-A244196) Avail: CASI HC A13/MF A03

The Defense Environmental Restoration Program (DERP) was established in 1984 to promote and coordinate efforts for the evaluation and cleanup of contamination at Department of Defense (DoD) installations. The program currently includes: the Installation Restoration Program (IRP), where potential contamination at DoD installations and formerly owned or used properties are investigated and, as necessary, site cleanups are conducted; and other hazardous waste (OHW) operations, through which research, development, and demonstration programs aimed at improving remediation technology and reducing DoD waste generation rates are conducted. In addition, a small number of building demolition and debris removal (BDDR) projects were conducted under DERP in fiscal year (FY) 1991. These involved demolishing structures at DoD installations and formerly used properties. FY 1991 marked the first time any BDDR projects had been conducted under DERP since FY 1987. GRA

N92-32785# National Defence Research Establishment, Umea (Sweden). Dept. of NBC Defence.
A SIMULATION OF RADIOACTIVE FALLOUT USING THE MATHEW/ADPIC MODEL [SIMULERING AV RADIOAKTIVT NEDFALL MED HJAELP AV DATORMODELLEN MATHEW/ADPIC]
Lennart Thaning and Erik Naeslund Dec. 1991 25 p
(FOA-C-40292-4.3; ETN-92-91978) Avail: CASI HC A03/MF A01; National Defence Research Establishment, S-901 82 Umea, Sweden

Transport and deposition of radioactive particles emerging from a nuclear explosion in the middle part of Europe is simulated via the Eulerian computer model MATHEW/ADPIC. Comparisons are made between the calculated outcomes when varying parameters governing vertical wind and wet deposition. The resulting deposition patterns are compared to calculations performed earlier with a Lagrangian trajectory model. It is shown that the outcome of the simulations is very sensitive to the varied parameters (vertical wind and precipitation) and it is therefore of great importance that those parts of the model are correctly described. ESA

N92-32841# Kernforschungszentrum G.m.b.H., Karlsruhe (Germany, F.R.). Inst. fuer Radiochemie.
STUDY ON LIFETIME SPECIFIC, LASER-INDUCED ULTRAFAST FLUORESCENCE DETECTION IN THE TIME AND FREQUENCY DOMAIN FOR IN-SITU ENVIRONMENTAL ANALYSIS OF ORGANIC POLLUTANTS
G. Kannen Dec. 1991 79 p
(KfK-4975; ETN-92-92159) Copyright Avail: CASI HC A05/MF A01

The capability and applicability of time resolved fluorescence detection techniques is investigated. Directly time resolved and phase modulation measuring techniques are able to resolve excited molecular state lifetimes in the microsecond time scale by application of modern laser and detection systems. The temporal resolution and its precision is discussed for highly developed phase modulation instrumentation and the older, phase resolved fluorescence emission detection method. A comment on the application of lifetime techniques for in situ environmental analysis is given. ESA

N92-32860# Sparta, Inc., Lexington, MA.
STAMP, THE SWOE THERMAL ANALYSIS AND MEASUREMENT PROGRAM: SUMMARY OF THE 1990 FIELD TESTS Report No. 11
J. R. Hummel, N. L. Paul, J. R. Jones, and D. R. Longtin 30 Dec. 1991 48 p
(Contract F19628-88-C-0038)
(LTR-91-013; PL-TR-91-2242) Avail: CASI HC A03/MF A01

The Balanced Technology Initiative on Smart Weapons Operability (BTIO/SWOE) has a goal to develop a computer simulation capability of the radiant field from the natural environment. This simulation capability would then be used by designers and testers of smart weapons electro-optic sensor systems to study the performance of the systems under anticipated environmental conditions. Vegetation offers a particular challenge to the BTI/SWOE modeling community due to the wide variety in types, shapes, sizes, and distributions of vegetation. To aid in the development of energy budget models of surfaces containing vegetation, a measurement program was designed and conducted near Howland, Maine. The SWOE Thermal Analysis and Measurement Program (STAMP) was designed with the goal of

providing data to support models for a 3-D thermal model of an individual tree and an interim model of the thermal response at a forest edge. Author

N92-32933# Lawrence Livermore National Lab., CA.
SMALL PASSIVE CHEMICAL DETECTOR
K. C. Hong 26 Mar. 1992 13 p
(Contract W-7405-eng-48)
(DE92-014188; UCRL-ID-110176) Avail: CASI HC A03/MF A01

A novel technique has been developed for the detection of organic compounds in the environment. These detectors are 'passive' in the sense that they do not contain any electronic or mechanical instrumentation. A visual color change of the devices after exposure to the target compounds of interest allows a quick identification and quantitative determination of the targets. The detection mechanism is based on colorimetry and combines two molecular biology techniques, Enzyme Multiplied Immunoassay Technique (EMIT) and Ouchterlony Double Diffusion in Two Dimensions. Preliminary studies have shown that the presence of 2,4-dinitrophenol can be monitored by the formation of the blue colored complexes as a result of the reaction between an enzyme (alkaline phosphatase) and a substrate (5-bromo-4-chloro-3-indolyl phosphate). DOE

N92-32986# Pacific Northwest Lab., Richland, WA.
INTERNATIONAL RESEARCH INTO CHLOROFLUOROCARBON (CFC) ALTERNATIVES
T. J. Marseille, D. L. Shankle, and A. G. Thurman May 1992 58 p
(Contract DE-AC06-76RL-01830)
(DE92-014241; PNL-8086) Avail: CASI HC A04/MF A01

Selected researchers from 21 countries were queried through questionnaires about their current and planned research activities. The results of the survey show that the majority of research being conducted by the respondents is devoted to investigating the hydrogenated fluorocarbon HFC-134a as a replacement for CFC-12 in refrigeration applications. The main issue with this alternative is identifying compatible lubricants that do not reduce its effectiveness. DOE

N92-33062# Environmental Protection Agency, Washington, DC. Office of Toxic Substances.
EPCRA SECTION 313 ROADMAPS DATABASE: USER'S MANUAL, VERSION 2.2
Sep. 1991 86 p
(PB92-169523; EPA/DF/DK-92/040A) Avail: CASI HC A05/MF A01

The Environmental Protection Agency (EPA) has developed a database of sources of information on the chemicals listed in Section 313 of the Emergency Planning and Community Right-to-Know Act of 1986 (EPCRA), also known as Title 3 of the Superfund Amendments and Reauthorization Act of 1986 (SARA). The database is intended to assist users of the Section 313 Toxic Release Inventory (TRI) data to perform assessments of these chemicals. The Roadmaps system displays and/or prints out information for the EPCRA Section 313 chemicals on health and environmental effects, carcinogenicity and other properties, federal regulations, state air and water regulations, and monitoring data. It also includes lists of state contacts. The document describes the design of the EPCRA Section 313 Roadmaps Database microcomputer program and provides instructions for using the system. Author

N92-33087# Environmental Protection Agency, Washington, DC. Office of Policy, Planning and Evaluation.
GUIDE TO SELECTED NATIONAL ENVIRONMENTAL STATISTICS IN THE US GOVERNMENT
Apr. 1992 100 p Sponsored by Environmental Monitoring Systems Lab.
(PB92-201144; EPA/230/R-92/003) Avail: CASI HC A05/MF A02

The Guide is a reference to national-level, time-series environmental statistics that are compiled and distributed by the U.S. government on a regular basis. It is a guide to statistical programs and the primary and secondary summary statistics they generate, not a guide to raw data or databases. The Guide includes references to statistical programs that characterize and/or monitor the state of the natural environment, those that study underlying and proximate pressures on the environment, and those that assess societal impacts on the environment and environmentally-mediated impacts on society. These include statistical programs on environmental quality such as ambient air and water quality and on natural resources such as water resources and land use; statistical programs on environmental pressures such as energy, mining, agriculture, manufacturing, transportation, and other human activities that have direct impacts on the environment; and statistical programs on human and institutional responses to environmental problems such as activities and expenditures to prevent or control pollution, establish parks and protected areas, protect critical ecosystems, fight forest fires, and manage fisheries. Author

N92-33125# Massachusetts Inst. of Tech., Cambridge. Dept. of Chemical Engineering.
DIRECT CATALYTIC DECOMPOSITION OF NITRIC OXIDE
M. Flytzani-Stephanopoulos and A. F. Sarofim 2 Mar. 1992 3 p
(Contract DE-FG22-91PC-91293)
(DE92-013847; DOE/PC-91293/1) Avail: CASI HC A01/MF A01

This project will investigate a suitable catalyst system for the direct NO decomposition for post-combustion NO(x) control. The proposed process will not use a reductant such as ammonia in the case of Selective Catalytic Reduction (SCR) process for catalytic reduction of NO(x) to nitrogen. This is a simplified process basically involving passing the flue gas through a catalytic converter, thus avoiding problems generally associated with the commercial Selective Catalytic Reduction (SCR) process, namely high operating cost, ammonia slip, and potential N2O emissions. DOE

N92-33156# Pacific Northwest Lab., Richland, WA.
POTENTIAL ENVIRONMENTAL EFFECTS OF ENERGY CONSERVATION MEASURES IN NORTHWEST INDUSTRIES
M. C. Baechler, K. F. Gygi, and P. L. Hendrickson Jan. 1992 297 p
(Contract DE-AC06-76RL-01830)
(DE92-013993; PNL-8015) Avail: CASI HC A13/MF A03

The Bonneville Power Administration (Bonneville) has identified 101 plants in the Pacific Northwest that account for 80 percent of the region's industrial electricity consumption. These plants offer a precise target for a conservation program. PNL determined that most of these 101 plants were represented by 11 major industries. We then reviewed 36 major conservation technologies used in these 11 industrial settings to determine their potential environmental impacts. Energy efficiency technologies designed for industrial use may result in direct or indirect environmental impacts. Effects may result from the production of the conservation measure technology, changes in the working environment due to different energy and material requirements, or changes to waste streams. Industry type, work-place conditions, worker training, and environmental conditions inside and outside the plant are all key variables that may affect environmental outcomes. To address these issues this report has three objectives: to describe potential conservation measures that Bonneville may employ in industrial programs and discuss potential primary impacts; to characterize industrial systems and processes where the measure may be employed and describe general environmental issues associated with each industry type; and to review environmental permitting, licensing, and other regulatory actions required for industries and summarize the type of information available from these sources for further analysis. DOE

46 GEOPHYSICS

Includes aeronomy; upper and lower atmosphere studies; ionospheric and magnetospheric physics; and geomagnetism.

For space radiation see *93 Space Radiation.*

N92-32572# Colorado Univ., Boulder. Cooperative Inst. for Research in Environmental Science.

WAVE PROPAGATION IN LATERALLY VARYING MEDIA: A MODEL EXPANSION METHOD Final Report, 1 Aug. 1988 - 1 Feb. 1991

Charles B. Archambeau 1 May 1991 40 p

(Contract F19628-88-K-0033)

(AD-A247553; PL-TR-91-2113; AD-E200882) Avail: CASI HC A03/MF A01

A general approach, using modes defined on subregions of the medium, has been developed to model seismic wave propagation in media with vertically and horizontally acoustic waves in fluid media and electromagnetic wave propagation in laterally varying media. The restriction on the medium variability is that it can be represented by step function variations in its properties in both the vertical and horizontal directions. The basic method makes use of normal mode expansion of the wave field in each partitioned sub-region of the medium within which the medium is uniform in the lateral directions. Thus, the medium is partitioned into laterally uniform zones, and complete normal mode solutions are obtained for each horizontally layered zone. In the analytical development, the zonal eigenvalues and eigenfunctions are generated by treating each zone as a layered half space or radially layered sphere, as is appropriate for medium geometry. The resulting set of modes are then used as a basis for expansions of the wave fields in the layered subregions. The modes are then used as bases for expansions of the wave fields in each zone at the common boundaries between the zones where continuity of displacement and traction is required. This results in the definition of a lateral propagator of the wave field when applied to all the zones making up the entire medium and is, in application, very similar to the classical vertical propagator method. GRA

N92-32655*# National Aeronautics and Space Administration. Goddard Space Flight Center, Greenbelt, MD.

STEADY INDUCTION EFFECTS IN GEOMAGNETISM. PART 1A: STEADY MOTIONAL INDUCTION OF GEOMAGNETIC CHAOS

Coerte V. Voorhies Sep. 1992 31 p

(NASA-TP-3272-Pt-1A; NAS 1.60:3272-Pt-1A; Rept-92B00100) Avail: CASI HC A03/MF A01

Geomagnetic effects of magnetic induction by hypothetically steady fluid motion and steady magnetic flux diffusion near the top of Earth's core are investigated using electromagnetic theory, simple magnetic earth models, and numerical experiments with geomagnetic field models. The problem of estimating a steady fluid velocity field near the top of Earth's core which induces the secular variation indicated by broad-scale models of the observed geomagnetic field is examined and solved. In Part 1, the steady surficial core flow estimation problem is solved in the context of the source-free mantle/frozen-flux core model. In the first paper (IA), the theory underlying such estimates is reviewed and some consequences of various kinematic and dynamic flow hypotheses are derived. For a frozen-flux core, fluid downwelling is required to change the mean square normal magnetic flux density averaged over the core-mantle boundary. For surficially geostrophic flow, downwelling implies poleward flow. The solution of the forward steady motional induction problem at the surface of a frozen-flux core is derived and found to be a fine, easily visualized example of deterministic chaos. Geomagnetic effects of statistically steady core surface flow may well dominate secular variation over several decades. Indeed, effects of persistent, if not steady, surficially geostrophic core flow are described which may help explain certain features of the present broad-scale geomagnetic field and perhaps paleomagnetic secular variation. Author

N92-32889# Centre d'Etude Spatiale des Rayonnements, Toulouse (France).

POLAR UPPER ATMOSPHERE CHARACTERIZATION AND SUPERSONIC ION ESCAPE (POLAR WIND) Final Report [CARACTERISATION DE LA HAUTE ATMOSPHERE POLAIRE ET MODELISATION DE L'ECHAPPEMENT SUPERSONIQUE DE IONS (VENT POLAIRE). RAPPORT DE FIN D'ETUDE]

Pierre Louis Blelly, Vincent Foliot, Jean Fontanari, Michel Herse (Centre National de la Recherche Scientifique, Verrieres-Le Buisson, France), Wlodek Kofman (Centre National de la Recherche Scientifique, Grenoble, France), Charley Taieb (Centre de Recherches en Physique de l'Environnement, Issy-les-Moulineaux, France), and Gerard Thuillier (Centre National de la Recherche Scientifique, Verrieres-Le Buisson, France) Sep. 1991 42 p In FRENCH

(Contract DRET-89-174)

(GDR-0917; ETN-92-92083) Avail: CASI HC A03/MF A01

A study on auroral upper atmosphere characterization by incoherent scattering technique and another study on polar upper atmosphere modeling are reported. For the first study, observations with the MICADO Michelson interferometer instrument, and EISCAT (European Incoherent Scatter radar/MICADO coordinated) measurements are described. For the second study, EISCAT observations and digital simulations are described. Vertical ionic temperature profiles for different seasons, vertical collision frequencies, and simulation results of the O(+) and H(+) ions are given. ESA

N92-32902# Aerospace Corp., El Segundo, CA. Space Systems Div.

THE ENERGETIC RADIATION ENVIRONMENT IN A HIGHLY ELLIPTICAL (MOLNIYA) ORBIT

J. B. Blake 15 May 1992 9 p

(Contract F04701-88-C-0089)

(AD-A252394; TR-0091(6940-05)-2; SSD-TR-92-07) Avail: CASI HC A02/MF A01

Measurements have been made of the dose received by silicon components under 100 mils of aluminum aboard satellites in a Molniya orbit. Nearly continuous data are presented for the time period from August 1983 until March 1990. It is concluded that the observations are consonant with the predictions of the NASA AP-8 model but not with those of the AE-8 model. GRA

N92-33097*# National Aeronautics and Space Administration. Langley Research Center, Hampton, VA.

SAGE 1 DATA USER'S GUIDE

Leonard R. McMaster, William P. Chu, and Michael W. Rowland (ST Systems Corp., Hampton, VA.) Aug. 1992 26 p

(RTOP 665-45-30-21)

(NASA-RP-1275; L-16879; NAS 1.61:1275) Avail: CASI HC A03/MF A01

A guide for using the data products from the Stratospheric Aerosol and Gas Experiment 1 (SAGE 1) for scientific investigations of stratospheric chemistry related to aerosol, ozone, nitrogen dioxide, dynamics, and climate change is presented. A detailed description of the aerosol profile tape, the ozone profile tape, and the nitrogen dioxide profile tape is included. These tapes are the SAGE 1 data products containing aerosol extinction data and ozone and nitrogen dioxide concentration data for use in the different scientific investigations. Brief descriptions of the instrument operation, data collection, processing, and validation, and some of the scientific analyses that were conducted are also included. Author

N92-33153# Atmospheric and Environmental Research, Inc., Cambridge, MA.

A RESEARCH PROGRAM ON RADIATIVE TRANSFER MODEL DEVELOPMENT IN SUPPORT OF THE ARM PROGRAM

S. A. Clough 1 May 1992 10 p

(Contract DE-FG02-90ER-61064)

(DE92-014495; DOE/ER-61064/2) Avail: CASI HC A02/MF A01

Research continued on the development of a radiative transfer

model. This report discusses the revised continuum model. The water vapor continuum plays an important role in atmospheric radiative transfer providing increased opacity between spectral lines over the full spectral region from the microwave to the visible. The continuum has a significant influence on atmospheric fluxes and cooling rates. Additionally the continuum is important to the physical solution of the inverse problem, the remote sensing of atmospheric state to retrieve temperature, water vapor, surface properties and other state parameters. There are two components to the continuum: (1) the self-broadened continuum, dependent on the square of the partial pressure of water vapor; and (2) the foreign-broadened continuum, principally dependent on the product of the water vapor partial pressure and the total pressure. As a consequence the self broadened continuum tends to be more important in the lower atmosphere while the foreign broadened continuum tends to be more important in the mid to upper troposphere. To address this situation and to improve overall accuracy, we have embarked on the development of an improved water vapor continuum model. DOE

N92-33197 University of Western Ontario, London.
CHARACTERISTICS OF LARGE ASPECT ANGLE VHF RADAR ECHOES IN THE PRESENCE AND ABSENCE OF OPTICAL AURORA Ph.D. Thesis
Gregory E. Hall Aug. 1990 125 p
(ISBN-0-315-59091-2; CTN-92-60519) Copyright Micromedia Ltd., Technical Information Centre, 165 Hotel de Ville, Place du Portage, Phase 2, Hull, Quebec J8X 3X2, Canada HC/MF

Auroral echo data from the radars and optical instruments of the CANOPUS ground based system in central Canada have been examined. The two radars operate at 48.5 MHz and have large aspect angles. A statistical study of the spatial relationship between the radar echos and the optical aurora during 13 hours was performed, and data from the radar during daylight were examined for evidence of aspect sensitivity. The most noticeable observation from that study was that there was a strong tendency for the radar echoes to occur on the side of the optical aurora remote from the radar. This result is shown to be consistent with refraction reducing the apparently large aspect angles. For the daylight periods, a self-consistent study found an aspect sensitivity which varied from 8 dB per deg at an aspect angle of 4.5 deg down to about 4 dB per deg at an aspect angle of 6 deg. These aspect sensitivities are in agreement with experiments at small aspect angles and higher frequencies. Two strikingly different kinds of large aspect angle echoes were found. The strongest echoes occurred on the remote side of optical features and generally had strong echo powers and strong echo power dependence on flow angle. The other type were the actual large aspect angle echoes which had moderate to weak powers and weak or nonexistent flow angle dependence. CISTI

47 METEOROLOGY AND CLIMATOLOGY

Includes weather forecasting and modification.

N92-32331# California Univ., San Diego, La Jolla.
ARM TROPICAL PACIFIC EXPERIMENT (ATPEX): ROLE OF CLOUD, WATER VAPOR AND CONVECTION FEEDBACKS IN THE COUPLED OCEAN/ATMOSPHERE SYSTEM
V. Ramanathan and T. P. Barnett Mar. 1992 17 p
(Contract DE-FG03-91ER-61198)
(DE92-013772; DOE/ER-61198/T1) Avail: CASI HC A03/MF A01

We have initiated studies that include radiation model validation, improved treatment of the three-dimensional structure of cloud-radiation interactions, and sensitivity runs that will unravel the role of cloud-convection-radiation interactions in the Pacific Sear Surface Temperatures and the overlying Walker and Hadley circulation. The research program is divided into three phases: (1) radiation; (2) cloud parameterization issues; and (3) feedback and ocean-atmosphere interactions. DOE

N92-32427# Sandia National Labs., Albuquerque, NM.
THE 1991 ROCKET-TRIGGERED LIGHTNING TEST OF THE DoD SECURITY OPERATIONS TEST SITE (SOTS) MUNITIONS STORAGE BUNKER, FORT MCCLELLAN, ALABAMA
G. H. Schnetzer and R. J. Fisher Feb. 1992 135 p
(Contract DE-AC04-76DP-00789)
(DE92-012449; SAND-91-2343) Avail: CASI HC A07/MF A02

During June and July 1991, the Sandia Transportable Lightning Instrumentation Facility (SATTLIF) was fielded at the Department of Defense (DoD) Security Operations Test Site (SOTS) at Ft. McClellan, Alabama. Nine negative cloud-to-ground lightning flashes were artifically triggered to designated locations on Igloo 2, a weapons storage bunker specially prepared to allow instrumentation access to various of its structural and electrical system elements. Simultaneous measurements of the incident flash currents and responses at 24 test points within the igloo and its grounding counterpoise network were recorded under lightning attachments to the front and rear air terminals of the structure's lightning protection system. In Volume 1 the test is described in detail. The measured data are summarized and discussed. Appendix A contains the full set of recorded incident flash currents, while Appendix B presents the set of largest responses measured at each test point, for both front and rear attachments to the structure. As part of these tests, 0.050 in. thick stainless steel, 0.08 in. copper, and 0.08-in titanium samples were exposed to triggered flash currents. In this way, damage spots created by direct-strike triggered lightning have been obtained, along with the measurement of the return-stroke and continuing currents that produced them. These data points, along with similar ones on aluminum and ferrous steel obtained during 1990 will be used as benchmarks against which to quantify the fidelity of burnthrough testing achievable Sandia's advanced laboratory lightning simulator. DOE

N92-32431# Oak Ridge National Lab., TN. Carbon Dioxide Information Analysis Center.
US HISTORICAL CLIMATOLOGY NETWORK DAILY TEMPERATURE AND PRECIPITATION DATA
D. P. Kaiser, P. Y. Hughes (National Oceanic and Atmospheric Administration, Asheville, NC.), E. H. Mason (National Oceanic and Atmospheric Administration, Asheville, NC.), T. R. Karl (National Oceanic and Atmospheric Administration, Asheville, NC.), and W. A. Brower (National Oceanic and Atmospheric Administration, Asheville, NC.) Feb. 1992 138 p
(Contract DE-AC05-84OR-21400)
(DE92-014920; ORNL/CDIAC-50; NDP-042) Avail: CASI HC A07/MF A02

This document describes a data base containing daily observations of maximum and minimum temperature and precipitation amounts from 138 US stations. These stations are a specially chosen subset of the 1219-station US Historical Climatology Network (HCN), compiled by the National Climatic Data Center (Asheville, North Carolina). The daily data network (herein referred to as the HCN/D) consists of stations considered to be the best of those from the HCN, selected to provide reasonably homogeneous spatial coverage of the contiguous US after considering the temporal homogeneity of each station's observing times, instrument types/positions, and surroundings. The data for each station extend through 1987, and most station records are complete for at least 80 years. The daily resolution of these data lends maximum flexibility for studies attempting to detect and monitor long-term climatic changes on a regional scale. Studies using daily data may be able to detect changes in regional climate that would not be apparent from analysis of the more commonly used monthly temperature and precipitation data. Such studies may include analyses of trends in maximum/minimum temperatures, temperature extremes, daily temperature range, precipitation 'event size' frequency, and the magnitude and duration of wet and dry periods. Other applications of the data include planning and risk assessment in areas such as agriculture, natural resource exploration, and construction. This document describes how the stations in the HCN/D were selected, defines limitations

and restrictions of the data, describes the format and contents of the magnetic tape, and provides reprints of literature pertinent to the collection and application of daily climate data. DOE

N92-32502# National Severe Storms Forecast Center, Kansas City, MO.
VERIFICATION OF SEVERE LOCAL STORMS FORECASTS ISSUED BY THE NATIONAL SEVERE STORMS FORECAST CENTER, 1991
R. W. Anthony and P. W. Leftwich May 1992 18 p
(PB92-186063; NOAA-TM-NWS-NSSFC-34) Avail: CASI HC A03/MF A01

The SELS unit of the National Severe Storms Forecast Center routinely issues convective outlooks and severe local storm watches to delineate areas that are favorable for development of severe local storms. The report summarizes verification of those forecasts that were issued during 1991. During 1991, 100 percent of the tornado-related fatalities and 83 percent of the tornado-related injuries occurred within valid severe local storm watches. Author

N92-32503# National Hurricane Center, Coral Gables, FL.
DIAGNOSTIC REPORT OF THE NATIONAL HURRICANE CENTER, AUGUST AND SEPTEMBER 1991, VOLUME 4, NUMBER 2
1991 77 p
(PB92-179407) Avail: CASI HC A05/MF A01

Tropical cyclone activity in the Atlantic and Eastern Pacific Basins during Aug. and Sep. 1991 is described. Named tropical storms and hurricanes are discussed. Forecasting performance is assessed by discussing the forecast tracking errors. Author

N92-32534# Naval Postgraduate School, Monterey, CA.
TROPICAL CYCLONE MOTION DUE TO ENVIRONMENTAL INTERACTIONS REPRESENTED BY EMPIRICAL ORTHOGONAL FUNCTIONS OF THE VORTICITY FIELDS M.S. Thesis
Mark J. Gunzelman Jun. 1991 115 p
(AD-A246137) Avail: CASI HC A06/MF A02

Tropical cyclone motion influenced by adjacent synoptic features is examined with relative vorticity fields at 700, 400, and 250 mb computed from operationally-analyzed wind fields. When an empirical orthogonal function (EOF) method is used to map the vorticity onto spatial grids, a smoother but more dependable depiction of the vorticity dynamics is provided than by the original fields. The effect of five processes that contribute to motion relative to the steering flow during periods of interaction with adjacent circulations are evaluated for their contribution to binary rotation and to changing the separation distance between interacting circulations. This vorticity dynamics approach indicates that tropical cyclones interact with various features at different levels. The Fujiwhara effect is most evident with stronger interaction events. Only the convergence effect of one tropical cyclone circulation on another tropical cyclone can explain the cases with decreasing separations. By contrast, the advection by the tropical cyclone circulation of the vorticity gradient of the other cyclone could not explain the decreasing separations. The Beta effect depends on the orientation of two interacting systems of different sizes, but the environmental vorticity gradient is not due entirely to earth vorticity in these interacting cases. The effects of environmental shear strongly depend on the orientation of the ITCZ and geographical orientation of the two cyclones. GRA

N92-32545# National Severe Storms Forecast Center, Kansas City, MO.
SEVERE LOCAL STORM WARNING VERIFICATION: 1991
L. A. Grenier and J. T. Halmstad Apr. 1992 30 p
(PB92-185982; NOAA-TM-NWS-NSSFC-33) Avail: CASI HC A03/MF A01

Tornado and severe thunderstorm warnings are issued by local offices of the National Weather Service. Routine verification of these warnings is accomplished at the National Severe Storms Forecast Center. The report highlights verification procedures and summarizes national, regional, and local verification results for the year 1991. Stations in the Southern and Central regions have issued most of the warnings and experienced most of the severe local storm events. A record number of severe local storm events were again confirmed in 1991. Author

N92-32714# National Oceanic and Atmospheric Administration, Boulder, CO. Wave Propagation Lab.
BOUNDARY LAYER PROCESSES IN COASTAL METEOROLOGY: PROSPECTS FOR REMOTE SENSING APPLICATIONS
C. W. Fairall Mar. 1992 34 p
(PB92-177849; NOAA-TM-ERL-WPL-220) Avail: CASI HC A03/MF A01

Recent advances in observing systems and models have led to a renewed interest in the special problems of coastal meteorology. In the report the boundary layer aspects of the coastal regime are examined. The current state of understanding is assessed for homogeneous boundary layers, surface interactions, internal boundary layers, and various inhomogeneous conditions. The inhomogeneities can be due to topography, land-ocean contrast, land-surface horizontal variations, or clouds. Surface-based remote sensing systems are ideal for studying the boundary layer on coastal scales. Six recently developed systems are described and their prospects for coastal studies are discussed. Author

N92-32720# Lamont-Doherty Geological Observatory, Palisades, NY.
RECENT CHANGES OF WEATHER PATTERNS IN NORTH AMERICA
G. J. Kukla and J. E. Gavin Apr. 1992 5 p
(Contract DE-FG02-85ER-60372)
(DE92-014342; DOE/ER-60372/7) Avail: CASI HC A01/MF A01

The objectives of this report are (1) to analyze the time related changes and variability in the property and frequency of air masses and the weather extremes over North America; and (2) to determine to what degree the observed changes agree with the predictions based on climate models. Climate models predict a general increase of surface air temperature and drought over parts of the North American continent due to increased CO2 concentrations. Regional climate change results in part from the changed frequency of the atmospheric and oceanic circulation patterns and partly from the changed properties of the different air mass types. We plan to investigate the changing frequency and properties of the air mass types focusing on moisture dependent variables and comparing the findings with the results of numerical climate models. DOE

N92-32758# Stockholm Univ. (Sweden). Dept. of Meteorology.
SHORT RANGE FORECAST OF THE INITIATION OF CONVECTION
Ulla Hammarstrand Feb. 1992 34 p
(DM-60; ETN-92-91977) Avail: CASI HC A03/MF A01

A simple one dimensional model for the prediction of the initiation of convection is formulated. The model is used as a complement to a large scale forecast model with a coarse resolution. It is applied on a fine grid to a small part of the forecast area where convection is studied in more detail. An experiment is undertaken, and satellite data are used to verify the prediction. The results show that it is possible to use the model for interpretation of the output from a model with coarse resolution in terms of the predicted onset of convection with a high resolution. The results are also used to determine which parameters are important for the initiation of convection. In the present case, surface wetness and cover of low clouds turned out to be the most important parameters. ESA

N92-32859# Atmospheric and Environmental Research, Inc., Cambridge, MA.
A SIMPLE DOPPLER WIND LIDAR SENSOR: SIMULATED MEASUREMENTS AND IMPACTS IN A GLOBAL ASSIMILATION AND FORECAST SYSTEM Report No. 1
C. Grassotti, R. G. Isaacs, R. N. Hoffman, M. Mickelson, T. Nehrkorn, and J.-F. Louis 1 Oct. 1991 95 p
(Contract F19628-89-C-0137; AF Proj. 6670)
(PL-TR-91-2253) Avail: CASI HC A05/MF A01

The wind measurements which might be obtained from a low power Doppler wind lidar (DWL) sensor were simulated. Wind profiles obtained from such an instrument will not be as complete as those expected from planned higher energy sensors (e.g. LAWS), with measurements only from cirrus clouds, the tops of other clouds, and from marine boundary layer aerosols. The potential impact of such a scaled down DWL system has been assessed by inserting the simulated measurements into the Air Force Geophysics Laboratory (GL) Global Data Assimilation System (GDA). Results from the observing system simulation experiment (OSSE) indicate that significant improvement in the analysis and forecast of geopotential height, horizontal wind, and relative humidity may be expected in the southern hemisphere extratropics. Comparison of impacts with those obtained in a previously conducted OSSE which assumed a full blown DWL instrument (WINDSAT) indicate that the low energy lidar yields improvements which are 1/2 to 3/4 the magnitude of improvements with WINDSAT. Thus, if the development cost of a simple lidar is found to be substantially less than a LAWS-type sensor, such an instrument may warrant consideration in the planning of future spacebased observing systems. Author

N92-33073# World Meteorological Organization, Geneva (Switzerland). World Climate Data and Monitoring Programme.
CLIMATE SYSTEM MONITORING (CSM) MONTHLY BULLETIN, ISSUE NO. 1
Jan. 1992 42 p
Avail: CASI MF A01; print copy available at WMO, Geneva, Switzerland

Given here, as a routine feature, are global analyses of temperature and precipitation anomalies and statistics which indicate the persistence of hot/cold, wet/dry events; global analyses of sea surface temperature, outgoing long wave radiation, circulation anomalies, and drought monitoring indices. Specifically included are 1991 annual global temperature and precipitation anomalies. January 1992 significant temperature and precipitation anomalies, November 1991 to January 1992 precipitation anomalies, and unusual monthly climate distribution, satellite outgoing long wave radiation for January 1992. Special reports are given for the United States in January, the South-West Pacific Region January Climate Review, and tropical cyclones for January 1992. Author

N92-33163# National Weather Service, Salt Lake City, UT.
FORECASTING HEAVY SNOW EVENTS IN MISSOULA, MONTANA
Mike Richmond May 1992 24 p
(PB92-196104; NOAA-TM-NWS-WR-217) Avail: CASI HC A03/MF A01

The characteristics of all the heaviest snow events (defined as seven inches or more) that have occurred in Missoula, Montana, over the past 25 years are examined. The events were separated into four categories to aid in pattern recognition. One or more cases from each category are examined in some detail to gain an understanding of what factors may result in heavy snow in Missoula. It is hoped that studying these events will aid in the forecasting of similar ones in the future. GRA

N92-33173# Illinois State Water Survey, Champaign. Office of Applied Climatology.
APPLICATIONS OF STATISTICAL METHODS TO THE STUDY OF CLIMATE AND FLOODING FLUCTUATIONS IN THE CENTRAL US Final Report
K. E. Kunkel, S. A. Changnon, and R. T. Shealy Mar. 1992 182 p Sponsored by Geological Survey
(Grant USGS-14-08-0001-G1731)
(PB92-205137; USGS/G-1731) Avail: CASI HC A09/MF A02

Because of concern about the potential hydrologic impacts of potential future climate change, historical streamflow and precipitation data were analyzed to determine whether significant temporal fluctuations in flooding and heavy precipitation event frequencies have occurred in the 20th century. The study encompasses 80 streamgaging stations and 230 precipitation stations located in a 9-state region (IL, IN, IA, KY, MI, MN, MO, OH, and WI) in the central U.S. The time period for the study was 1921-1985. Partial duration series analysis of the daily data were used to identify extreme events using a threshold for a 1-year recurrence event. The warm season and cold season were analyzed separately. Statistical techniques, including the Kolmogorov-Smirnov test and robust regression with Huber-weighting of the residuals, were used to identify significant temporal fluctuations in event frequencies, magnitudes, and durations. Many stations did not exhibit significant fluctuations. However, upward trends in flood frequencies were found in MN, IA, and northern IL in the warm season, and IA, southwestern IL, and OH in the cold season. Trends were less noticeable in duration and magnitude. Analysis of the precipitation data indicated that the occurrence of heavy rainfall events is not well correlated with overall climate anomalies. Author

N92-33225 McGill Univ., Montreal (Quebec). Dept. of Meteorology.
DYNAMICS OF ROSSBY WAVES IN A PARABOLIC JET Ph.D Thesis [DYNAMIQUE DES ONDES DE ROSSBY DANS UN JET PARABOLIQUE]
Gilbert Brunet Jul. 1989 159 p In FRENCH
(ISBN-0-315-57159-4; CTN-92-60517) Copyright Micromedia Ltd., Technical Information Centre, 165 Hotel de Ville, Place du Portage, Phase 2, Hull, Quebec J8X 3X2, Canada HC/MF

A study of the initial-value problem for barotropic Rossby waves linearized around a parabolic zonal flow shows that the non-dimensional equation for the perturbation depends on only one essential parameter A. The associated Rayleigh-Kuo equation has a continuous spectrum of singular modes for all A's and an infinite number of discrete Rossby waves for A's under -0.25. In Fourier space, the problem has a formulation that allows a simple qualitative discussion concerning the nature of the interaction between the perturbation and the zonal flow. New conservation laws have been found that elucidate the jet dynamics. The results show a significant difference between dynamics of easterlies and westerlies. Using the theory of Lie groups, separations of variables have been obtained which allow the initial value problem to be solved completely and which also provide a number of exact solutions. For certain A's, these have a simple analytical form allowing comparison to previous results for a linear zonal wind. For an arbitrary initial condition of small order-E amplitude, the linearity hypothesis is shown to be invalidated when the parameter is much less than 1 after a time (order 1/E) in a critical layer of width (order of the square root of E) centered at the jet extremum. The governing equations for the nonlinear stage are strikingly similar to those for a forced Rossby wave on a linear wind profile.
Author (CISTI)

48 OCEANOGRAPHY

Includes biological, dynamic, and physical oceanography; and marine resources.

For related information see also *43 Earth Resources and Remote Sensing.*

N92-32333# Geological Survey, Reston, VA.
HYDRATE DETECTION
W. P. Dillon and T. S. Ahlbrandt 1992 15 p Presented at the US Department of Energy Contractor Review Meeting on Natural Gas Research and Development, Morgantown, WV, 5-6 May 1992

(Contract DE-AI21-83MC-20422)
(DE92-014350; DOE/MC-20422/92/C0030; CONF-920584-8)
Avail: CASI HC A03/MF A01

Project objectives were: (1) to create methods of analyzing gas hydrates in natural sea-floor sediments, using available data, (2) to make estimates of the amount of gas hydrates in marine sediments, (3) to map the distribution of hydrates, and (4) to relate concentrations of gas hydrates to natural processes and infer the factors that control hydrate concentration or that result in loss of hydrate from the sea floor. DOE

N92-32336# Princeton Univ., NJ.
SIMULATIONS OF THE CARBON CYCLE IN THE OCEANS
1992 7 p
(Contract DE-FG02-90ER-61052)
(DE92-016622; DOE/ER-61052/2) Avail: CASI HC A02/MF A01

This study includes models of oceanic CO2 uptake. This perturbation simulation of carbon dioxide uptake gives strong support to estimates of oceanic uptake of fossil CO2 on the order of 2 GtC/year over the last decade. Carbon and carbon-nitrogen models are considered. DOE

N92-32688# Naval Command, Control and Ocean Surveillance Center, San Diego, CA.
AN EVALUATION OF AN INFRARED/RESISTANCE TEMPERATURE DEVICE FOR AIR/SEA-SURFACE TEMPERATURE MEASUREMENTS Final Report, Jun. - Oct. 1991
W. L. Patterson Jun. 1992 53 p
(AD-A252279; MRAD-TD-2271) Avail: CASI HC A04/MF A01

An infrared/resistance temperature device (IR/RTD) and a hand-held psychrometer were used at sea for 12 days, onboard the USS Ranger (CV 61), to gather air and sea-surface temperatures. Although not supported by the evaporation duct height calculations of this test period, the clearly artificial trend in sea-surface temperature readings reported from the seawater intake makes the IR/RTD the preferred instrument to measure sea-surface temperatures. While tests reported in this document were primarily setup to see if the IR/RTD is practical for use in evaporation duct calculations, two other uses of the device were identified: (1) it was determined that sea-surface temperatures as an aid in forecasting the time fog will dissipate; and (2) it was used to sense the temperatures of sensitive electronic equipment, thus, permitting operators to safely turn off their equipment when the maximum operating temperature was reached. GRA

N92-33198 British Columbia Univ., Vancouver. Dept. of Oceanography.
A QUASI-GEOSTROPHIC CIRCULATION MODEL OF THE NORTHEAST PACIFIC OCEAN Ph.D. Thesis
Patrick F. Cummins 30 Aug. 1989 160 p
(ISBN-0-315-55106-2; CTN-92-60520) Copyright Micromedia Ltd., Technical Information Centre, 165 Hotel de Ville, Place du Portage, Phase 2, Hull, Quebec J8X 3X2, Canada HC/MF

A limited-area numerical model with mesoscale resolution is developed to study the circulation in the northeast Pacific out to 170 deg west and down to 45 deg north, incorporating the coastline geometry and bottom topography of the region. In a benchmark experiment, the circulation is driven with a steady, climatological wind stress curl field. Statistical properties of the solution are determined and compared with observations from the Gulf of Alaska. The cyclonic circulation of the model basin contains the analogue of a meandering Alaska Current. At the head of the Gulf, this current flows into an intense boundary current corresponding to the Alaskan Stream. Within the model Alaska Current, anticyclonic closed streamline features are occasionally generated which are representative of the Sitka Eddy. The model Alaskan Stream displays perturbations with similar characteristics to those recently verified in satellite imagery. The characteristics of the Alaskan Stream are shown to depend crucially on the presence of the Aleutian Trench. Experiments with a climatological seasonal cycle in the wind field show that bottom topography has an important influence in moderating the intensity of the seasonal response. Author (CISTI)

N92-33220# Naval Ocean Systems Center, San Diego, CA.
FEASIBILITY OF MEASURING TRANSVERSE ELECTRIC NOISE AT VLF AND LF ON AN ICE CAP Final Report
C. H. Shellman Dec. 1991 25 p
(NR Proj. RR0-3308)
(AD-A252280; NOSC/TR-1492) Avail: CASI HC A03/MF A01

There is an existing need for very low frequency (VLF) and low frequency (LF) transverse electric (TE) air-to-air communications. However, TE noise cannot be measured at ground level on highly conducting or even moderately conducting ground, and routine measurements from an aircraft would be prohibitively expensive. The amplitudes of TE waves at the surface of an ice cap are evidently strong enough to be measured at LF when the ice cap is about 1000 meters thick and at VLF when the ice cap is about 2000 meters thick. Amplitudes are stronger over colder ice. Measurements of temperature in a drill hole would be needed for extrapolating fields to higher heights. GRA

51 LIFE SCIENCES (GENERAL)

N92-32345# Maryland Univ., College Park.
MEASUREMENT OF THE MAGNETIC AND ELECTRICAL ACTIVITY OF INDIVIDUAL CELLS IN VITRO Report, 24 Sep. 1990 - 23 Sep. 1991
Christopher C. Davis 3 Dec. 1991 17 p
(Contract DAMD17-90-Z-0052; DA Proj. 3M1-61102-BS-15)
(AD-A250881) Avail: CASI HC A03/MF A01

This progress report has two parts. The first part reports progress to date on the development of a common-path, optical heterodyne fiber sensor for remote monitoring of the electrically induced birefringence of cells and tissue. The second part concerns the the development of a very small SQUID, NanoSQUID, which will allow monitoring of the magnetic fields from cells and tissues within about 2mm of tissue at physiological temperature. The SQUID is at (-)4K. GRA

N92-32571# Washington Univ., Seattle.
BACTERIAL RESPONSES TO EXTREME TEMPERATURES AND PRESSURES AND TO HEAVY ORGANIC LOADING Final Report
20 Feb. 1992 6 p
(Contract N00014-89-J-1048)
(AD-A247456) Avail: CASI HC A02/MF A01

The goals of this project centered around two areas of research: (1) the study of hyperthermophilic archaebacteria from submarine hydrothermnal vents on the East Pacific Rise; and (2) the study of physiologically diverse microbial populations associated with a whale carcass partially buried in sediments of the Santa Catalina Basin. Specific objectives included the following: (1) completion of analyses of all geochemical, biochemical, and microbiological measurements made on smoker fluid samples; (2) further characterization of DNA from smoker samples and selected isolates to assess phylogenetic origin; (3) determination of upper temperature and pressure limits for growth and survival of hyperthermophilic archaebacteria; and (4) tests for production of thermostable extra-cellular enzymes at extreme conditions. It was found that physiological types of bacterial-invertebrate symbioses in the deep sea directly reflect available energy sources, and that deep-sea conditions of low temperature and elevated pressure do not limit bacterial responses to intense organic loading. GRA

N92-32844# Laboratoire d'Automatique et d'Analyse des Systemes, Toulouse (France). Equipe Conduite Automatique de Procedes Biotechnologiques.
ON PHYSICAL SYSTEMS QUALITATIVE APPROACH: REAL TIME HELP FOR FERMENTATION PROCESS CONTROL Ph.D. Thesis - Toulouse Univ. [SUR UNE APPROCHE QUALITATIVE DES SYSTEMES PHYSIQUES: AIDE EN TEMPS REEL A LA CONDUITE DES PROCEDES FERMENTAIRES]
Jean-Philippe Steyer 1991 198 p In FRENCH Sponsored in part by SANOFI
(LAAS-91445; ETN-92-91678) Avail: CASI HC A09/MF A03

The main features and the advantages of qualitative physics are addressed and the following methodologies are proposed: modeling the influences among the process variables by means of a causal graph; seasoning about the standard state to retrace the causal path explaining the observed behavior according to the trends of the observable variables; in conflict situations (i.e., a single event having a multiple cause), the aforementioned reasoning technique needs to be supported by temporal notions and relations to filter out the behaviors. Those concepts, which can be generalized to most physical systems, were tailored to biotechnological processes, mainly to batch fermentation processes, with the aim of deriving the behavior of the process's inner variables (from microscopic standpoint) from the process's outer behavior (macroscopic variables). To process with the causal graph, ten operators were defined to express the main interactions among the process variables. Those operators were then implemented using KHEOPS, an extended propositional logic based system. Tests were made on different fermentation processes. Two online expert systems which deal with real world problems are developed. ESA

N92-33103*# National Aeronautics and Space Administration. Marshall Space Flight Center, Huntsville, AL.
DEVELOPMENT OF STATIC SYSTEM PROCEDURES TO STUDY AQUATIC BIOFILMS AND THEIR RESPONSES TO DISINFECTION AND INVADING SPECIES
G. A. Smithers Aug. 1992 17 p
(NASA-TM-103598; NAS 1.15:103598) Avail: CASI HC A03/MF A01

The microbial ecology facility in the Analytical and Physical Chemistry Branch at Marshall Space Flight Center is tasked with anticipation of potential microbial problems (and opportunities to exploit microorganisms) which may occur in partially closed systems such as space station/vehicles habitats and in water reclamation systems therein, with particular emphasis on the degradation of materials. Within this context, procedures for microbial biofilm research are being developed. Reported here is the development of static system procedures to study aquatic biofilms and their responses to disinfection and invading species. Preliminary investigations have been completed. As procedures are refined, it will be possible to focus more closely on the elucidation of biofilm phenomena. Author

N92-33181# California Univ., Davis.
NEUTRON SCATTER STUDIES OF CHROMATIN STRUCTURES RELATED TO FUNCTIONS
E. M. Bradbury 1992 7 p
(Contract DE-FG03-88ER-60673)
(DE92-014032; DOE/ER-60673/T4) Avail: CASI HC A02/MF A01

We have made considerable progress in chromatin reconstitution with very lysine rich histone H1/H5 and in understanding the dynamics of nucleosomes. A ferromagnetic fluid was developed to align biological molecules for structural studies using small-angle-neutron-scattering. We have also identified and characterized an intrinsically bent DNA region flaking the RNA polymerase I binding site of the ribosomal RNA gene in Physarum Polycephalum. Projects in progress are in the areas of studying the interactions of histone H4 amino-terminus peptide 1-23 and acetylated 1-23 peptide with DNA using thermal denaturation; studying the GGAAT repeats found in human centromeres using high resolution Nuclear Magnetic Resonance and nuclease sentivity assay; and studying the role of histones and other sperm specific proteins with sperm chromatin. DOE

52 AEROSPACE MEDICINE

Includes physiological factors; biological effects of radiation; and effects of weightlessness on man and animals.

N92-32344# Harvard Univ., Cambridge, MA. Dept. of Psychology.
PET STUDIES OF COMPONENTS OF HIGH-LEVEL VISION
William J. Hall 15 May 1992 3 p
(Contract N00014-91-J-1243)
(AD-A250873) Avail: CASI HC A01/MF A01

This document describes progress on the PET Studies of Components of High-Level Vision project. We have made progress primarily by testing more subjects in four PET experiments, developing new software for data analysis, and carrying out preliminary data analyses. It is premature to report the results in detail, but some intriguing trends are evident in the images, as noted in this report. GRA

N92-32434# Essex Corp., Orlando, FL.
CORRELATING VISUAL SCENE ELEMENTS WITH SIMULATOR SICKNESS INCIDENCE: HARDWARE AND SOFTWARE DEVELOPMENT Final Report, Apr. - Oct. 1991
R. S. Kennedy, K. S. Berbaum, and M. G. Smith 27 Oct. 1991 20 p
(Contract N00019-91-C-0149)
(AD-A252235) Avail: CASI HC A02/MF A01

Simulator sickness occurs in a large number of Army, Navy, and Marine Corps simulators, and is most prevalent in moving-base, rotary-wing devices which employ cathode ray tube (CRT) video displays as opposed to fixed-wing, dome-display trainers with no motion base. Based on data from a factor analysis of over 1000 Navy and Marine Corps pilot simulation exposures, a new scoring procedure was applied to two helicopter simulators with similar rates of simulator sickness incidence. Based on the factor analytic scoring key, the two simulators showed slightly different sickness profiles. Preliminary work was begun to record the visual scene by video frame-by-frame decomposition and automated scoring algorithms were developed. The findings are discussed from the standpoints of (1) recommendations for future design and use of simulators, and (2) the metric advantages and other merits of the field experiment methodology to address human factors problems with simulator sickness. GRA

N92-32492# Krug Life Sciences, Inc., San Antonio, TX.
COMPARATIVE EFFECTS OF ANTIHISTAMINES ON AIRCREW PERFORMANCE OF SIMPLE AND COMPLEX TASKS UNDER SUSTAINED OPERATIONS Interim Technical Report, Jul. 1989 - Jul. 1991
Thomas E. Nesthus, Samuel G. Schiflett, Douglas R. Eddy (NTI, Inc., Dayton, OH.), and Jeffrey N. Whitmore Dec. 1991 47 p
(Contract F33615-89-C-0603)
(AD-A248752; AL-TR-1991-0104) Avail: CASI HC A03/MF A01

Airborne Warning and Control System (AWACS) Weapons Director (WD) cognitive and psychomotor skills were evaluated with terfenadine (Seldane) and diphenhydramine (Benadryl) using a performance assessment battery (PAB). After nondrug Day 1 training, twelve 3 member teams were tested with Placebo on Day 2, then randomly assigned to Seldane (60 mg/12h TID), Benadryl (25 mg/4h QID), or Placebo groups on Days 3 and 4. An 8-test PAB was given at 1230 and 1330 each testing day. The Seldane and Placebo groups did not differ appreciably from each other on Days 3 or 4, but differed significantly from the Benadryl group. The group showed degraded performance for 7 variables on Day 3 and for 3 variables on Day 4 compared to the Seldane and/or Placebo groups. Subjective measures of fatigue and antihistamine symptoms supported the Day 3 Benadryl

impairment. Overall results were consistent with previous research demonstrating cognitive and psychomotor task impairment with Benadryl but not with Seldane. Support for awarding medical flying waivers to non-pilot aircrew who are taking Seldane under the supervision of flight surgeons is offered. GRA

N92-32504# Naval Air Station, Pensacola, FL.
DEVELOPMENT OF THE OMPAT NEUROPSYCHOLOGICAL/PSYCHOMOTOR PERFORMANCE EVALUATION AND OMPAT DATA AND TIMING SUPPORT Annual Report, 15 Nov. 1990 - 14 Nov. 1991
Kathryn P. Winter 5 Dec. 1991 11 p
(DA Proj. 3M2-63002-D-995)
(AD-A250793) Avail: CASI HC A03/MF A01

The objectives of this project have been (1) to create a millisecond accuracy software timer module that could be incorporated into OMPAT and other testing programs, (2) to construct a set of automated, i.e., computerized OMPAT Level I neuropsychological and psychomotor tests with documentation that provides a standardized, clinically relevant, and rapid method for assessment of nervous system integrity, and (3) to construct a version of UTCPAB that incorporates the software timer. GRA

N92-32539*# Pennsylvania State Univ., Hershey. Coll. of Medicine.
EFFECTS OF CSF HORMONES AND IONIC COMPOSITION ON SALT/WATER METABOLISM Final Technical Report, 1 Mar. 1981 - 31 Dec. 1992
Walter B. Severs and Lanny C. Keil 1992 32 p
(Contract NCC2-127)
(NASA-CR-190693; NAS 1.26:190693) Avail: CASI HC A03/MF A01

This collaborative agreement between Drs. Severs and Keil began in 1981, arising from a continuing interest in the issue of what, exactly, are the consequences of headward fluid shifts during manned spaceflight. Such shifts were recognized early by both U.S. and Soviet Scientists because of signs and symptoms referable to the head. Some of these include disturbed vision, puffiness in the face and periorbital areas, headache, vestibular dysfunction and distended jugular veins. We posited that the fluid shift had an immediate effect on the brain, and a long-term action requiring a neural interpretation of the flight environment. This would re-adjust both efferent neural as well as hormonal mechanisms to sustain cardiovascular and fluid/electrolyte balance consonent with survival in microgravity. Work along these lines is summarized. Author

N92-32663# Polish Academy of Sciences, Warsaw. Inst. Podstawowych Problemow Techniki.
BONE AS A LIQUID-FILLED DIPHASE POROUS MEDIUM [KOSC JAKO WYPELNIONY PLYNEM DWUFAZOWY OSRODEK POROWATY]
R. Uklejewski (Polish Academy of Sciences, Poznan.) 1992 66 p In POLISH
Avail: CASI HC A04/MF A01

The purpose of the present paper (which is the initial part of a more comprehensive work on the properties of electromechanical effects of compact and long bones) is to convince the readers (both technical and medical workers) that the basic, natural biomechanical model of both compact and spongy bones is the diphase liquid-filled porous medium, both the solid and liquid phases being, of course, multicomponent (we do not deny that the single-phase model may be useful in many detailed problems of bone biomechanics). Unlike porous technological materials, the bone is a biological porous solid which has, under in vivo conditions, an interesting property of adapting its inner structure and shape under the influence of mechanical loads. Author

N92-32816# Defence and Civil Inst. of Environmental Medicine, Downsview (Ontario).
DCIEM/CENTRAL MEDICAL BOARD AIRCREW ECG PROGRAM: RECOMMENDATIONS FOR RESTRUCTURING Annual Report, 1989
Gary W. Gray Aug. 1990 17 p
(DCIEM-90-47; CTN-92-60353) Avail: CASI HC A03/MF A01

This report summarizes the results of the Canadian Forces electrocardiogram (ECG) program in 1989. A total of 4810 ECGs were interpreted and coded at the Canadian Medical Board. Of 1767 ECGs on aircrew candidates, only 4 showed abnormalities incompatible with initial aircrew selection. Among 3043 ECGs on serving aircrew, only 14 showed abnormalities incompatible with flying duties, and 13 of these had been previously documented. There was one new myocardial infarction which had been already detected clinically. Recommendations were made for a restructuring of the ECG program which will result in an approximately 40 percent reduction in the number of routine aircrew ECGs. For experienced aircrew, it is recommended that the ECG become part of an expanded cardiovascular risk evaluation carried out every four years to the age of 40 then biannually. Aircrew candidates should continue to have an initial ECG, but this should be done only on academically successful candidates during screening at the Central Medical Board. Author (CISTI)

N92-32916# Human Engineering Labs., Aberdeen Proving Ground, MD.
MODELING THE EAR'S RESPONSE TO INTENSE IMPULSES AND THE DEVELOPMENT OF IMPROVED DAMAGE RISK CRITERIA Final Report
G. R. Price May 1992 8 p
(DA Proj. 1L1-61102-B-74-A)
(AD-A252365; HEL-TN-5-92) Avail: CASI HC A02/MF A01

Research indicates that traditional measures fail to distinguish hazardous from intense impulses accurately. This failure may be due to increased complexities in the ear's response at such high sound pressure levels. Therefore, to gain insight into the problem, we have been developing a mathematical model of the ear that reproduces the response of the ear from free field pressures to basilar membrane displacements and calculates the hazard (modeled as mechanical stress). This model is conformal with the structure of the ear and includes the spectral tuning of the external and middle ears, a non-linear stapes, and a changing susceptibility along the cochlear partition. The model can be used to calculate a hazard index for virtually any impulse and although work is still continuing on the development of the model, it is thus far able to explain the hearing loss data better than any other system. If the model were incorporated into an integrated circuit/meter, it would have the virtues of being complex enough to rate hazard accurately, be simple to use, and because it is theoretically based, be useful in suggesting design changes for impulse-producing sources as well as more effective designs for hearing protectors. GRA

N92-32942# Naval Health Research Center, San Diego, CA.
A CAUSAL ANALYSIS OF INTERRELATIONSHIPS AMONG EXERCISE, PHYSICAL FITNESS, AND WELL-BEING IN US NAVY PERSONNEL Interim Report
Rita S. Dytell, Linda K. Trent, and Terry L. Conway Aug. 1991 27 p
(NR Proj. MR0-095)
(AD-A252719; NHRC-91-27) Avail: CASI HC A03/MF A01

The relationships among physical fitness, physical exercise, and health outcomes were examined among 4,272 U.S. Navy personnel who completed the following: (1) a physical fitness test; (2) Wallston and Wallston's Multidimensional Health Locus of Control Scale (MHLOC); (3) eight items tapping health values; (4) five dimensions of health care behaviors; and (5) seven measures of mental and physical health outcomes. Regression analyses revealed that physical fitness was a better predictor than exercise of health outcomes among women. Fitness among both males and females was predicted first by the combination of Internal Health Locus of Control and high Health Values and second by exercise. It appears that certain health care behaviors (prevention activities, eating habits, substance use) are associated with exercise activities which, in turn, affect physical fitness. Fitness tends to mediate the relationship between exercise and well-being in females, while both exercise and fitness lead directly to positive health consequences in males. GRA

N92-33032* National Aeronautics and Space Administration. Goddard Space Flight Center, Greenbelt, MD.
DEVICE FOR REMOVING FOREIGN OBJECTS FROM ANATOMIC ORGANS Patent
Earl D. Angulo, inventor (to NASA) 28 Jul. 1992 10 p Filed 19 Mar. 1991 Supersedes N91-28727 (29 - 20, p 3380)
(NASA-Case-GSC-13306-1; US-Patent-5,133,721; US-Patent-Appl-SN-674828; US-Patent-Class-606-106; US-Patent-Class-148-402; US-Patent-Class-606-78; US-Patent-Class-606-127; Int-Patent-Class-A61M-1/00) Avail: US Patent and Trademark Office

A device is disclosed for removing foreign objects from anatomic organs such as the ear canal or throat. It has a housing shaped like a flashlight, an electrical power source such as a battery or AC power from a wall socket, and a tip extending from the housing. The tip has at least one wire loop made from a shape-memory-effect alloy, such as Nitinol, switchably connected to the electrical power source such that when electric current flows through the wire loop the wire loop heats up and returns to a previously programmed shape such as a curet or tweezers so as to facilitate removal of the foreign object.
Official Gazette of the U.S. Patent and Trademark Office

53 BEHAVIORAL SCIENCES

Includes psychological factors; individual and group behavior; crew training and evaluation; and psychiatric research.

N92-32569# Michigan Univ., Ann Arbor. Technical Communication Program.
HUMAN LEARNING OF SCHEMAS FROM EXPLANATIONS IN PRACTICAL ELECTRONICS Interim Report
David E. Kieras 4 Dec. 1991 48 p
(Contract N00014-88-K-0133)
(AD-A247429; TR-91/ONR-34) Avail: CASI HC A03/MF A01

Training materials in practical electronics appear to follow a building blocks approach in which common simple circuits are presented and then combined into more complex circuits. Each circuit is presented in the form of a circuit diagram and an explanation of how the circuit works in terms of a causal chain of events. Such materials suggest that teaming electronics consists of learning schemas for the building block circuits; complex circuits can then be understood as combinations of these simpler schematic circuits. The process of teaming appears to be based on extracting schemas from the explanations. This report presents human experimental results based on earlier artificial intelligence work. In this project, engineering students learned building block circuits and then learned complex circuits; the time required to understand the explanations and answer questions about the circuit behavior were compared to an AI system that learned from explanations and a model of question-answering. Generally, learning the schematic building block circuits facilitated performance, and the AI system and question-answering model could predict the amount of facilitation. However, the benefit of learning circuit schemas under these conditions was surprisingly mild. GRA

N92-32660# White House Military Office, Falls Church, VA. Office of Emergency Operations.
TOWARD ADVANCED HUMAN RELIABILITY PROGRAMS. STRUCTURAL DEVELOPMENT CONSIDERATIONS AND OPTIONS FOR EXTREME RISK ENVIRONMENTS Report, Oct. 1990 - Jun. 1991
Richard C. Nelson May 1992 107 p
(AD-A250786) Avail: CASI HC A06/MF A02

Operational populations exposed to extreme risk environments (EREs) might expect to sustain substantial losses, yet must be able to be relied upon to complete their mission or missions regardless. Existing human (personnel) reliability programs are inadequate to assure that personnel capable of meeting both the necessary security and operational requirements are available for response to such conditions. This study explores a number of issues to consider in building a robust human reliability program (HRP) structure capable of supporting single to multiple operational populations, scenarios, and missions, using any of several program structure formats. The HRP structure format may be used within a single agency or government-wide. GRA

N92-32817# Defence and Civil Inst. of Environmental Medicine, Downsview (Ontario).
INSTRUMENT SCANNING AND SUBJECTIVE WORKLOAD WITH THE PERIPHERAL VISION HORIZON DISPLAY Final report
Donald Hameluck and Paul Stager Jun. 1989 132 p
(Contract W7711-7-7004/01-SE)
(CTN-92-60359) Copyright Avail: CASI HC A07/MF A02

The Peripheral Vision Horizon Display (PVHD) is an expanded artificial horizon line which is produced by sweeping the beam of a red laser across the instrument panel in front of the pilot. The PVHD is intended to provide the pilot with visual orientation information through peripheral vision without the need to look directly at the attitude indicator (AI) display. The present study examined the effect of the PVHD on the instrument scanning behavior of pilots during two types of instrumented approaches. The effect of PVHD on subjective workload was also examined to test the hypothesis that the PVHD would reduce the experience of workload during the approaches. Two of the four pilots showed a change in their scanning behavior which could be interpreted as a decrease in the visual workload involved in scanning the AI. However, it appeared that the PVHD increased the subjective workload. It is argued that workload was increased because the PVHD reflected off certain instruments and that it distracted the pilots from their normal scanning pattern by attracting attention to small attitude changes. It is noted that the results obtained in this study might be partially due to pilot inexperience with the PVHD. It was concluded that the PVHD would be most useful when flight operations require the pilot to look outside the cockpit and stable orientation cues such as the earth's horizon are not visible.
Author (CISTI)

N92-32990# Allen Corp. of America, Alexandria, VA.
FEASIBILITY STUDY FOR PREDICTING HUMAN RELIABILITY GROWTH THROUGH TRAINING AND PRACTICE Final Report, Dec. 1989 - Dec. 1990
John C. Lowry, Virginia A. Rappold, and Michael M. Copenhaver May 1992 209 p
(AD-A252371; ARI-RN-92-39) Avail: CASI HC A10/MF A01

This report examines the feasibility of developing a stand alone, quantitative Human Reliability Growth Model (HRGM) that predicts the impact of training variables on a soldier's performance. Such a model would incorporate learning curve fitting techniques to predict the impact of training variables on performance and would be based on empirical data from behavioral and social science literature and available government data bases. This report describes the effort to collect empirical data on the effects of learning and practice on human performance. In addition, the report contains a review of the theoretical literature involving human learning and practice in which the nature and application of learning curves and curve fitting techniques are derived and summarized. The results of this effort reveal that, out of approximately 3,000 research titles and abstracts reviewed, only 27 articles meet minimal criteria for use in developing the HRGM. It was concluded that, although a theoretical basis for developing an HRGM exists, the data could not support its development. GRA

54 MAN/SYSTEM TECHNOLOGY AND LIFE SUPPORT

Includes human engineering; biotechnology; and space suits and protective clothing.

For related information see also *16 Space Transportation.*

N92-32433# Klein Associates, Yellow Springs, OH.
OBSERVING TEAM COORDINATION WITHIN ARMY ROTARY-WING AIRCRAFT CREWS Interim Report, Apr. - Oct. 1990
Marvin L. Thordsen, Gary A. Klein, and Steve Wolf May 1992 41 p
(Contract MDA903-87-C-0523; DA Proj. 2Q1-62785-A-791)
(AD-A252234; ARI-RN-92-40) Avail: CASI HC A03/MF A01

The purpose of this project was to demonstrate the feasibility of using team decision models to help train crew coordination in the tactical helicopter domain. Ten aircrews were studied as they performed a tactical mission in a UH-60 simulator facility at Fort Campbell, Kentucky. The results indicate that the methods can be adapted for observing team decision-making processes during some types of helicopter missions. Five opportunities for aircrew coordination training were identified: rehearsing mission functional profiles, analyzing commander's intent during preplanning sessions, focusing the time horizon, avoiding micromanagement, and getting cues for anticipation/confirmation during the actual mission. Recommendations were presented for training observers and instructors to use these categories. GRA

N92-32790# Defence and Civil Inst. of Environmental Medicine, Downsview (Ontario).
THERMAL ASSESSMENT OF MUSTANG INDUSTRIES, INC. NEOPRENE QUICK-DON ANTI-EXPOSURE IMMERSION SUITS AND STORAGE EVALUATION FOR THE CP140 AURORA AIRCRAFT
Donald W. Ferguson and Wayne R. Sturgeon Apr. 1990 24 p
(DCIEM-90-23; CTN-92-60351) Avail: CASI HC A03/MF A01

The Defence and Civil Institute of Environmental Medicine (Canada) (DCIEM) has undertaken a study to develop or identify a commercially available quick-don immersion suit to replace the suit in use on the CP121, CP140, CH135, and CH124A aircraft. Operational evaluation of a suit developed to DCIEM specifications and constructed of 3 mm closed cell neoprene has been carried out. It was concluded that the new suit was acceptable on the CH124A and CH135 but the bulk of the 3 mm suit precluded proper storage on the CP140 and CP121. A stowage assessment was made on 1 mm, 2 mm, and 3 mm immersion suits onboard a CP140. In addition, the three suits were evaluated for thermal insulation values while immersed in both still and turbulent water. It was found that all three suits provide considerably more thermal protection than the existing quick-don suit in use by Canadian forces. In addition, all three suits can be stored in the CP140 if appropriate modification or relocation of some storage positions is made. CISTI

N92-33056# Institut National des Sciences Appliquees de Lyon, Villeurbanne (France).
CONTRIBUTION TO ROBOT-TASK ADAPTATION, INTRODUCTION AND USE OF ROBOT ANISOTROPY AND TASK OBJECT FOR THE DESIGN OF THE WORKSTATION Ph.D. Thesis [CONTRIBUTION A L'ADAPTATION ROBOT TACHE, PRISE EN COMPTE ET EXPLOITATION DE L'ANISOTROPIE DU ROBOT ET DE L'OBJET DE LA TACHE EN VUE DE LA CONCEPTION DU POSTE DE TRAVAIL]
Guy M. Cloutier 1991 228 p In FRENCH
(ISAL-91-0095; ETN-92-92086) Avail: NTIS HC A11/MF A01

The grounds of a procedure for the design of robot workstations, based on an offline 'preadaptation' of the robot hinging on the satisfaction of intrinsic and extrinsic task constraints are discussed. Means to evaluate and achieve a better robot task adequacy are introduced. Hyper-ellipsoids, revealing the capabilities of the robot as to its probability of pose (compliance), are projected on (intersect with) the task subspace. The intrinsic constraints of the task are reduced to a sufficient ellipsoid. The simultaneous diagonalization of robot and task ellipsoids, specifies a new conformity index. It expresses the robot task adequacy for joint postures. However, the design of the coupling device linking the tool to the orbit, impacts the satisfaction of intrinsic task constraints. The 'agreement' between the robot and the task determines an adapted domain in jointspace. Its boundaries set fictitious joint limits not to surpass, in order to meet, the intrinsic constraints of the task. For a single task, the direct kinematics of the inverted structure maps it into the adapted Cartesian implementation domain of the base frame. Within a 'multitask' production context, the relative situations of the tasks impose intrinsic 'between task' constraints in the space of large solid body motions. Two solutions are proposed for the design of an adapted workstation layout, given an environment of rigidly predetermined tasks. Appropriate categories of workspaces are introduced to provide practical means to apply the standardized concept of a useful workspace. ESA

N92-33079# Defence and Civil Inst. of Environmental Medicine, Downsview (Ontario).
AN EVALUATION OF THE PERFORMANCE CHARACTERISTICS OF A TWO-MAN MOLECULAR SIEVE OXYGEN GENERATING SYSTEM
David G. Mohn Feb. 1991 23 p
(DCIEM-91-20; CTN-92-60386) Avail: CASI HC A03/MF A01

This report provides a detailed description of a two-man molecular sieve oxygen generating (MSOG) system and an evaluation of its performance characteristics at ground level and altitude. The system was designed to provide adequate oxygen enriched breathing gas for two crew members up to a cabin altitude of 25,000 feet. The study consisted of operating the MSOG system through a range of product gas flowrates at ground level and various aircraft cabin altitude combinations in order to determine if the system is as efficient as it was designed to be. The results indicated that up to a cabin altitude of 8,000 feet and an aircraft altitude of 23,000 feet, the system is capable of providing sufficient oxygen enriched breathing gas for two active crew members. The maximum oxygen generating capability of the system was 95 percent, the present limit for molecular sieve oxygen concentrators. Evaluation of outlet pressure indicated that the MSOG system requires a breathing regulator with a low pressure operating capability. It was recommended that a high altitude evaluation of the MSOG system be completed in order to further verify the systems effectiveness. Author (CISTI)

N92-33099 American Astronautical Society, San Diego, CA.
HUMANS AND MACHINES IN SPACE: THE PAYOFF
Paula Korn, ed. and James A. Abrahamson, ed. Univelt, Inc. 1992 126 p Symposium held in Washington, DC, 15 Mar. 1991 Sponsored in part by Hughes Aircraft Co. and Lockheed Engineering and Sciences Co. Its Science and Technology Series Original contains color illustrations
(ISBN-0-87703-343-9) Avail: Issuing Activity

This publication was prepared from a transcript of a panel discussion held on March 15, 1991, in Washington, DC. The panel was part of the 29th American Astronautical Society Goddard Memorial Symposium, whose theme was, 'Humans and Machines in Space: The Vision, The Challenge, The Payoff.' The speakers discussed the anticipated outcome of our efforts to put humans and machines in space. Specific topics included space science payoffs in an era of human-machine partnership, the economic impact of the space program, the impact of the space program on education, the space program's impact on society, and the payoff of humans and machines in space. Author

55 SPACE BIOLOGY

Includes exobiology; planetary biology; and extraterrestrial life.

No abstracts in this category.

59 MATHEMATICAL AND COMPUTER SCIENCES (GENERAL)

N92-32809*# National Aeronautics and Space Administration. Ames Research Center, Moffett Field, CA.
ADVANCING AUTOMATION AND ROBOTICS TECHNOLOGY FOR THE SPACE STATION FREEDOM AND FOR THE US ECONOMY Progress Report No. 14, 15 Aug. 1991 - 27 Feb. 1992
Henry Lum, Jr. May 1992 55 p
(RTOP 476-14-01)
(NASA-TM-103940; A-92110; NAS 1.15:103940) Avail: CASI HC A04/MF A01

Described here is the progress made by Levels 1, 2, and 3 of the Space Station Freedom in developing and applying advanced automation and robotics technology. Emphasis was placed on the Space Station Freedom program responses to specific recommendations made in the Advanced Technology Advisory Committee (ATAC) Progress Report 13, and issues of A&R implementation into the payload operations integration Center at Marshall Space Flight Center. Assessments are presented for these and other areas as they apply to the advancement of automation and robotics technology for Space Station Freedom. Author

60 COMPUTER OPERATIONS AND HARDWARE

Includes hardware for computer graphics, firmware, and data processing.

For components see *33 Electronics and Electrical Engineering.*

N92-32642# Fermi National Accelerator Lab., Batavia, IL.
BALANCE IN MACHINE ARCHITECTURE: BANDWIDTH ON BOARD AND OFFBOARD, INTEGER/CONTROL SPEED AND FLOPS VERSUS MEMORY
M. Fischler Apr. 1992 45 p Presented at the Terraflop Workshop, Tallahassee, FL, Jan. 1990
(Contract DE-AC02-76CH-03000)
(DE92-016006; FNAL/C-92/125; CONF-9001172-1) Avail: CASI HC A03/MF A01

The issues to be addressed here are those of 'balance' in machine architecture. By this, we mean how much emphasis must be placed on various aspects of the system to maximize its usefulness for physics. There are three components that contribute to the utility of a system: the ways the machine can be used, the size of the problem that can be attacked, and the effective capabilities (power) of the hardware. The effective power issue is a matter of evaluating the impact of design decisions trading off architectural features such as memory bandwidth and interprocessor communication capabilities. What is studied is the effect these machine parameters have on how quickly the system can solve desired problems. There is a reasonable method for studying this: one selects a few representative algorithms and computes the impact of changing memory bandwidths, and so forth. The only room for controversy here is in the selection of representative problems. The issue of how big a problem can be attacked boils down to a balance of memory size versus power. Although this is a balance issue it is very different than the effective power situation, because no firm answer can be given at this time. The power to memory ratio is highly problem dependent, and optimizing it requires several pieces of physics input, including: the size of the lattice needed for interesting results; the kind of algorithms to use; and the number of sweeps needed to get valid results. We seem to be at the threshold of learning things about these issues, but for now, the memory size issue is necessarily addressed in terms of best guesses, rules of thumb, and researcher opinions. DOE

N92-32766# Laboratoire d'Automatique et d'Analyse des Systemes, Toulouse (France).
FAULT TOLERANCE FOR SECURITY MANAGEMENT IN DISTRIBUTED SYSTEMS Ph.D. Thesis [LA TOLERANCE AUX FAUTES POUR LA GESTION DE LA SECURITE DANS LES SYSTEMES REPARTIS]
Laurent Blain 1992 159 p In FRENCH
(LAAS-92011; ETN-92-92089) Avail: CASI HC A08/MF A02

The application of a particular technique for tolerating both accidental and intentional faults, called fragmentation redundancy scattering, in conjunction with classical fault avoidance techniques, is proposed. The security server provides three functionalities: user authentication, authorization, and sensitive data management. These functionalities are made intrusion tolerant in spite of failures of a minority of the server sites due to accidental faults, or intrusions perpetrated by external intruders, users, or administrators. Server security is ensured by fragmentation of confidential data, replication of unconfidential data, and interprocess consensus. The study of functionalities required to control access to both centralized and intrusion tolerant servers led to the building of smartcard authentication mechanisms, a sensitive data manangement system based on threshold schemes, and a ticket based authorization protocol. ESA

N92-32851# National Research Council of Canada, Ottawa (Ontario). Flight Research Lab.
THE DESIGN AND DEVELOPMENT OF A PORTABLE, DSP MICRO-PROCESSOR BASED, HIGH-ACCURACY DATA ACQUISITION SYSTEM
Gary M. Beauchamp and K. K. Lum 1989 24 p Presented at the CASI Flight Test Symposium, Cold Lake, Alberta, Mar. 1989
(NRC-32146; CTN-92-60372) Avail: CASI HC A03/MF A01

A self contained strapdown data acquisition system which combines portability with accuracy and which is suitable for aircraft parameter estimation is described. This system was designed to be transferrable from one aircraft to another with minimal effort. This system involves the application of state of the art thermally modelled instrumentation, modern computer hardware, temperature compensation and carefully selected low temperature sensitivity, and minimum power consumption electronic components. Much of this technology was unavailable until the 1980s, including the Digital Signal Processing (DSP) microprocessor, FACT low power consumption devices, and portable large capacity hard disc drives. Thermally modelled instrumentation is a relatively recent advance which not only increases accuracy, but reduces system complexity, size, and weight, while increasing flexibility and portability. Combining these modern technologies has produced a very capable data acquisition system which is expected to encounter a wide range of uses over and above its intended parameter estimation applications. CISTI

N92-32910# Los Alamos National Lab., NM.
AUTOMATED DATA ACQUISITION AND ANALYSIS IN THE MECHANICAL TEST LAB
D. H. Carter and W. S. Gibbs 1992 15 p Presented at the Symposium on Automation of Mechanical Testing, Pittsburgh, PA, 20-21 May 1992
(Contract W-7405-eng-36)
(DE92-011231; LA-UR-92-958; CONF-9205139-1) Avail: CASI HC A03/MF A01

Computers and enhanced control technology have made it possible to perform more sophisticated mechanical tests than ever before, as well as to allow routine tests to be run and analyzed

with much greater efficiency. Automated data acquisition, storage, and analysis have become key ingredients in a mechanical test facility, especially in one which utilizes a wide variety of test equipment and techniques. This paper will discuss one such mechanical test facility where many different types of mechanical tests are performed utilizing automated data acquisition, centralized data storage, and a complex system of automated data analysis. Various systems of data acquisition are discussed, including those used on servohydraulic and screw-driven systems, as well as those used for higher-rate, formability and creep tests. Methods for networking equipment used in such a facility are described. Networking is an important criterion for establishing a centralized data base, and for eventually building a system of automated data analysis. DOE

N92-33057* National Aeronautics and Space Administration. Pasadena Office, CA.
AUTO AND HETERO-ASSOCIATIVE MEMORY USING A 2-D OPTICAL LOGIC GATE Patent
Tien-Hsin Chao, inventor (to NASA) (Jet Propulsion Lab., California Inst. of Tech., Pasadena.) 14 Jul. 1992 9 p Filed 16 Feb. 1990 Supersedes N91-13888 (29 - 5, p 698)
(NASA-Case-NPO-17997-1-CU; US-Patent-5,131,055; US-Patent-Appl-SN-481013; US-Patent-Class-382-32; US-Patent-Class-382-31; US-Patent-Class-365-49; US-Patent-Class-359-107; US-Patent-Class-359-108; US-Patent-Class-359-559; US-Patent-Class-359-561) Avail: US Patent and Trademark Office

An optical system for auto-associative and hetero-associative recall utilizing Hamming distance as the similarity measure between a binary input image vector V(sup k) and a binary image vector V(sup m) in a first memory array using an optical Exclusive-OR gate for multiplication of each of a plurality of different binary image vectors in memory by the input image vector. After integrating the light of each product V(sup k) x V(sup m), a shortest Hamming distance detection electronics module determines which product has the lowest light intensity and emits a signal that activates a light emitting diode to illuminate a corresponding image vector in a second memory array for display. That corresponding image vector is identical to the memory image vector V(sup m) in the first memory array for auto-associative recall or related to it, such as by name, for hetero-associative recall.
Official Gazette of the U.S. Patent and Trademark Office

N92-33205*# National Aeronautics and Space Administration. Langley Research Center, Hampton, VA.
IMAGE PROCESSING MINI MANUAL
Christine G. Matthews (Computer Sciences Corp., Hampton, VA.), Mary-Anne Posenau, Desiree M. Leonard (Computer Sciences Corp., Hampton, VA.), Elizabeth L. Avis (Computer Sciences Corp., Hampton, VA.), Kelly R. Debure (Computer Sciences Corp., Hampton, VA.), Kathryn Stacy, and Bill vonOfenheim Jun. 1992 80 p
(RTOP 505-90-53-02)
(NASA-TM-107680; NAS 1.15:107680; CSCC-A-9) Avail: CASI HC A05/MF A01

The intent is to provide an introduction to the image processing capabilities available at the Langley Research Center (LaRC) Central Scientific Computing Complex (CSCC). Various image processing software components are described. Information is given concerning the use of these components in the Data Visualization and Animation Laboratory at LaRC. Author

N92-32440# Naval Weapons Center, China Lake, CA. Attack Weapons Dept.
GENERIC MODULAR IMAGING IR SIGNAL PROCESSOR
John Eric Auborn and William Harris *In* AGARD, Integrated Target Acquisition and Fire Control Systems Feb. 1992 6 p
(For primary document see N92-32437 23-06)
Copyright Avail: CASI HC A02/MF A02; 1 functional color page

61 COMPUTER PROGRAMMING AND SOFTWARE

Includes computer programs, routines, alogorithms, and specific applications, e.g., CAD/CAM.

N92-32414# Los Alamos National Lab., NM.
AN ADAPTIVE ALGORITHM FOR MODIFYING HYPERELLIPSOIDAL DECISION SURFACES
P. M. Kelly, D. R. Hush, and J. M. White 1992 6 p Presented at the International Joint Conference on Neural Networks, Baltimore, MD, 7-11 Jun. 1992
(Contract W-7405-eng-36)
(DE92-013540; LA-UR-92-1261; CONF-9206102-5) Avail: CASI HC A02/MF A01

The LVQ algorithm is a common method which allows a set of reference vectors for a distance classifier to adapt to a given training set. We have developed a similar learning algorithm, LVQ-MM, which manipulates hyperellipsoidal cluster boundaries as opposed to reference vectors. Regions of the input feature space are first enclosed by ellipsoidal decision boundaries, and then these boundaries are iteratively modified to reduce classification error. Results obtained by classifying the Iris data set are provided. DOE

N92-32416# Lawrence Livermore National Lab., CA.
PROGRAM PLOTTAB: A CODE DESIGNED TO PLOT CONTINUOUS AND/OR DISCRETE PHYSICAL DATA
D. E. Cullen 20 Mar. 1992 111 p
(Contract W-7405-eng-48)
(DE92-013754; UCRL-ID-110240) Avail: CASI HC A06/MF A02

The code PLOTTAB is designed as a simple plotting code which can be used on virtually any computer and graphics device to plot continuous and/or discrete physical data. To date this code has been successfully interfaced and used on a wide variety of computers as simple IBM-PCs and as advanced as CRAY supercomputers. In order to use this code on any given computer all you have to be able to do is turn your plotting device on or off and draw a line from on (X,Y) position to another. That's all you have to be able to do to interface this code to any plotting device. Although the graphics interface used by this code is very simple, it can still take advantage of many features of individual plotting devices in order to produce either hardcopy or images on screens. This code can be used with plotting devices of any physical size, whose size is defined in any set of units. This code allows you to define the physical size of your plotting device in whatever dimensions you are used to using, e.g., inches, millimeters, centimeters; so that you can properly size the plots for use with any plotting device. DOE

N92-32451*# Research Inst. for Computing and Information Systems, Houston, TX.
GROUND SYSTEMS DEVELOPMENT ENVIRONMENT (GSDE) INTERFACE REQUIREMENTS AND PROTOTYPING PLAN
Victor E. Church (Computer Sciences Corp., Beltsville, MD.), John Philips (Computer Sciences Corp., Beltsville, MD.), Mitchell Bassman (Computer Sciences Corp., Beltsville, MD.), and C. Williams (Computer Sciences Corp., Beltsville, MD.) Sep. 1990 69 p
(Contract NCC9-16; RICIS Proj. SE-34)
(NASA-CR-190713; NAS 1.26:190713; CSC/TR-90/6155) Avail: CASI HC A04/MF A01

This report describes the data collection and requirements analysis effort of the Ground System Development Environment (GSDE) Interface Requirements study. It identifies potential problems in the interfaces among applications and processors in the heterogeneous systems that comprises the GSDE. It describes possible strategies for addressing those problems. It also identifies areas for further research and prototyping to demonstrate the capabilities and feasibility of those strategies and defines a plan for building the necessary software prototypes. Author

N92-32507*# National Aeronautics and Space Administration. Hugh L. Dryden Flight Research Facility, Edwards, CA.
USER'S MANUAL FOR AeroFcn: A FORTRAN PROGRAM TO COMPUTE AERODYNAMIC PARAMETERS
Joseph L. Conley May 1992 24 p
(RTOP 533-02-36)
(NASA-TM-104237; H-1675; NAS 1.15:104237) Avail: CASI HC A03/MF A01

The computer program AeroFcn is discussed. AeroFcn is a utility program that computes the following aerodynamic parameters: geopotential altitude, Mach number, true velocity, dynamic pressure, calibrated airspeed, equivalent airspeed, impact pressure, total pressure, total temperature, Reynolds number, speed of sound, static density, static pressure, static temperature, coefficient of dynamic viscosity, kinematic viscosity, geometric altitude, and specific energy for a standard- or a modified standard-day atmosphere using compressible flow and normal shock relations. Any two parameters that define a unique flight condition are selected, and their values are entered interactively. The remaining parameters are computed, and the solutions are stored in an output file. Multiple cases can be run, and the multiple case solutions can be stored in another output file for plotting. Parameter units, the output format, and primary constants in the atmospheric and aerodynamic equations can also be changed. Author

N92-32546# Cornell Univ., Ithaca, NY. Dept. of Computer Science.
SIMLAB: AUTOMATICALLY CREATING PHYSICAL SYSTEMS SIMULATORS
Richard S. Palmer and James F. Cremer Nov. 1991 53 p
(AD-A250970; TR-91-1246) Avail: CASI HC A04/MF A01

SIMLAB, a software environment for creating simulators directly from computer-readable physics models, is based on the following concept: creating physical systems simulators should be as simple as describing the underlying physics to a colleague. Rather than programming in a conventional programming language, a SIMLAB user expresses physics models (and thus simulators) directly in terms of the concepts, quantities, and equations familiar to a scientist or engineer. The benefits of the SIMLAB approach include: (1) reducing the time and effort required to create simulators, (2) providing more understandable and reliable simulators, and (3) support for more sophisticated simulators, e.g., for multiple domain problems, which have proven intractible in the past. GRA

N92-32617# Sandia National Labs., Albuquerque, NM.
TARGET CUEING AND TRACKING SYSTEM (TCATS): USER'S GUIDE
R. Horton, ed. and B. Naylor, ed. Mar. 1992 81 p
(DE92-015385; SAND-92-0397) Avail: CASI HC A05/MF A01

The Target Cueing And Tracking System (TCATS) is an advanced video image processing system that uses digital computing techniques for automatic target detection and tracking. This document provides both developers and users with sufficient information to properly set up and operate TCATS using a configuration computer as an interface. This document includes guidelines on how to operate the TCATS user interface, descriptions of the parameters which must be adjusted for proper operation of TCATS, and information on the configuration computer communications design. Brief descriptions of the TCATS algorithms, software, and custom hardware are also included. Additional documents are referenced to provide the reader with a complete source of information for TCATS. Department for more information. DOE

N92-32627# Knowledge Based Systems, Inc. College Station, TX.
INFORMATION INTEGRATION FOR CONCURRENT ENGINEERING (IICE) IDEF3 PROCESS DESCRIPTION CAPTURE METHOD REPORT Interim Report, Feb. 1991 - Apr. 1992
Richard J. Mayer, Thomas P. Cullinane, Paula S. DeWette, William B. Knappenberger, and Benjamin Perakath May 1992 155 p
(Contract F33615-90-C-0012)
(AD-A252633; KBSI-IICE-90-STR-01-0592-02; AL-TR-1992-0057)
Avail: CASI HC A08/MF A01

This document provides a method overview, practice and use description, and language reference for the IDEF3 Process Description Capture Method. The name IDEF originates from the Air Force program for Integrated Computer-Aided Manufacturing (ICAM) from which the first ICAM Definition, or IDEF, methods emerged. It was in recognition of this foundational work, and in support of an overall strategy to provide a family of mutually-supportive methods for enterprise integration, that continued development of IDEF technology was undertaken. More recently, with their expanded focus and widespread use as part of Concurrent Engineering, Total Quality Management (TQM), and business re-engineering initiatives, the IDEF acronym has been re-cast as the name referring to an integrated family of integration definition methods. IDEF3 was designed as a complementary addition to the IDEF family of methods serving the role of a knowledge acquisition and requirements definition tool that structures the user's understanding of how a given process, event, or system works around process flow and object state transition descriptions. A special-purpose graphical language accompanying the IDEF3 method serves to highlight temporal precedence and causality relationships relative to the process or event being described. GRA

N92-32656*# Research Inst. for Computing and Information Systems, Houston, TX.
GUARANTEEING SYNCHRONOUS MESSAGE DEADLINES WITH THE TIMED TOKEN MEDIUM ACCESS CONTROL PROTOCOL
Gopal Agrawal (Texas A&M Univ., College Station.), Baio Chen (Texas A&M Univ., College Station.), Wei Zhao (Texas A&M Univ., College Station.), and Sadegh Davari (Houston Univ., Clear Lake, TX.) 22 Mar. 1992 45 p
(Contract NCC9-16)
(NASA-CR-190710; NAS 1.26:190710) Avail: CASI HC A03/MF A01

We study the problem of guaranteeing synchronous message deadlines in token ring networks where the timed token medium access control protocol is employed. Synchronous capacity, defined as the maximum time for which a node can transmit its synchronous messages every time it receives the token, is a key parameter in the control of synchronous message transmission. To ensure the transmission of synchronous messages before their deadlines, synchronous capacities must be properly allocated to individual nodes. We address the issue of appropriate allocation of the synchronous capacities. Several synchronous capacity allocation schemes are analyzed in terms of their ability to satisfy deadline constraints of synchronous messages. We show that an inappropriate allocation of the synchronous capacities could cause message deadlines to be missed even if the synchronous traffic is extremely low. We propose a scheme called the normalized proportional allocation scheme which can guarantee the synchronous message deadlines for synchronous traffic of up to 33 percent of available utilization. To date, no other synchronous capacity allocation scheme has been reported to achieve such substantial performance. Another major contribution of this paper is an extension to the previous work on the bounded token rotation time. We prove that the time elapsed between any consecutive visits to a particular node is bounded by upsilon TTRT, where TTRT is the target token rotation time set up at system initialization time. The previous result by Johnson and Sevcik is a special case where upsilon = 2. We use this result in the analysis of various synchronous allocation schemes. It can also be applied in other similar studies. Author

N92-32658# Knowledge Based Systems, Inc. College Station, TX.
IDEF4 OBJECT-ORIENTED DESIGN METHOD MANUAL Interim Report, Feb. 1991 - Apr. 1992
Richard J. Mayer, Arthur A. Keen, and M. S. Wells May 1992 131 p

(Contract F33615-90-C-0012)
(AD-A252634; KBSI-IICE-90-STR-01-0592-01; AL-TR-1992-0056)
Avail: CASI HC A07/MF A01

This document provides a method overview, practice and use description, and language reference for the IDEF4 Object-Oriented Design Method. The name IDEF originates from the Air Force program for Integrated Computer-Aided Manufacturing (ICAM) from which the first ICAM Definition, or IDEF, methods emerged. It was in recognition of this foundational work, and in support of an overall strategy to provide a family of mutually-supportive methods for enterprise integration, that continued development of IDEF technology was undertaken. More recently, with their expanded focus and widespread use as part of Concurrent Engineering, Total Quality Management (TQM), and business re-engineering initiatives, the IDEF acronym has been re-cast as the name referring to an integrated family of Integration Definition methods. IDEF4 was developed as a design method to assist in the production of quality designs for object oriented implementations. This document is targeted at both object-oriented programmers looking for a design method and programmers learning an object-oriented programming language who want to know how to design good object-oriented programs. GRA

N92-32741# Lawrence Livermore National Lab., CA.
PANACEA USER'S MANUAL
S. A. Brown 16 Dec. 1991 56 p
(Contract W-7405-eng-48)
(DE92-011289; M-276-Rev-1) Avail: CASI HC A04/MF A01

A numerical simulation code is fundamentally a device to solve an initial value problem. Very often these programs are written starting with the routines that solve some system of equations. Unless care is taken to formulate these routines with regard to a host of issues, it can be very awkward to set up a problem or to look at the answers that the code returns. Furthermore, it can be nearly impossible to take advantage of some of the excellent work that various groups have done because the data flow and structuring issues have not been given sufficient attention in the program design stages. One way to avoid some of these difficulties is to write the data flow controls, the I/O mechanisms, and the database manager first. With these parts in place, there is a great deal of guidance for building the parts of a simulation code that deal with the specific set of equations to be solved. Thus, initial value data is fed in and the solution is written out clearly and conveniently. Furthermore, this approach provides a basis for defining some conventions to allow the sharing of simulation modules. It also helps isolate the machine dependencies of a code in a very few places, which greatly enhances the portability of the code. PANACEA is a library of routines built to address these issues. In essence, PANACEA attempts to embody all of the functionality of a numerical simulation code, which is generic to all simulation codes. It accomplishes this by implementing a model of the simulation as a system of services, which are bound together with the simulation specific routines provided by the code developer. One useful result of this approach is that it effectively imposes a discipline for the development of simulation codes that promote shareability, portability, and inter-operability. DOE

N92-32804# Ecole Nationale Superieure des Telecommunications, Paris (France).
THREE DIMENSIONAL OBJECT RECONSTRUCTION USING A VERY LIMITED NUMBER OF PROJECTIONS. APPLICATION TO INDUSTRIAL RADIOGRAPHY Ph.D. Thesis [RECONSTRUCTION TRIDIMENSIONNELLE D'OBJECTS A PARTIR D'UN NOMBRE TRES LIMITE DE PROJECTIONS. APPLICATION A LA RADIOGRAPHIE INDUSTRIELLE]
Catherine Klifa 1991 245 p In FRENCH
(Telecom-91-E-008; ETN-92-92096) Avail: CASI HC A11/MF A03

The study on three dimensional fault reconstruction, using a very limited number of X-rays taken at different incidences to give data on the fault orientation, is presented. The study is oriented towards a reconstruction of the general shape of the fault and not only on the fault itself, and towards a method which introduces a priori data on the fault. The method uses algebraic reconstruction techniques and a Markov model which takes into account, in the three dimensional region, the geometric and local characteristics of the fault. Implementation of the algorithm on real X-rays is described. ESA

N92-32832# National Aerospace Lab., Amsterdam (Netherlands). Informatics Div.
SOFTWARE DEVELOPMENT PRACTICE IN A SCIENTIFIC COMPUTING ENVIRONMENT
H. deJong and S. deJong 3 Jun. 1991 23 p Presented at the VDM 1991 Symposium, Noordwijkerhout, Netherlands, 21-25 Oct. 1991
(NLR-TP-91193-U; ETN-92-92003) Avail: CASI HC A03/MF A01

An approach to software development is described. Generally the software development process is divided into several phases, each phase having its specific reviews, documents, and products. The method applied to follow this phased approach and the tools and techniques needed for support are presented. ESA

N92-32833# National Aerospace Lab., Amsterdam (Netherlands). Informatics Div.
LIFE CYCLE ORIENTED METHOD FOR DEVELOPMENT AND PRODUCTION OF LARGE SCALE INDUSTRIAL MATHEMATICS SOFTWARE
W. Loeve 14 Oct. 1991 37 p Presented at the 2nd International Conference on Industrial and Applied Mathematics, Washington, DC, 8-12 Jul. 1991
(NLR-TP-91196-U; ETN-92-92004) Avail: CASI HC A03/MF A01

The development of mathematics software, which is of growing importance for computer simulation in industrial computer aided engineering, is addressed. Mathematics sofware has to fulfill functional requirements to be applicable in industry and performance requirements must be met. The performance requirements concern availability, continuity, integrity, accessibility, and timeliness. In general, mathematics software for simulation of aspects of for example fluid and solid mechanics is complex and mathematics software must cooperate with other software. The total software collection will be implemented in industry on a variety of interconnected computer systems. The mathematics software must be structured in such a way that functions and performance can be maintained easily. This means easy adaption to extensions and improvements in the complex combination of hardware and software in which mathematics software is integrated in the industrial environment. For application of the method, it is considered necessary that representatives of various specialisms contribute to the development and production of mathematics software. In view of this, the method is designed to enable efficient cooperation of groups of skilled specialists in development and production of mathematics software. ESA

N92-32865*# Research Inst. for Computing and Information Systems, Houston, TX.
ADVANCED SOFTWARE DEVELOPMENT WORKSTATION: EFFECTIVENESS OF CONSTRAINT-CHECKING Interim Report
Michel Izygon (Barrios Technology, Inc., Houston, TX.) 1 Jul. 1992 21 p
(Contract NCC9-16; RICIS Proj. SR-02)
(NASA-CR-190712; NAS 1.26:190712) Avail: CASI HC A03/MF A01

This report summarizes the findings and lessons learned from the development of an intelligent user interface for a space flight planning simulation program, in the specific area related to constraint-checking. The different functionalities of the Graphical User Interface part and of the rule-based part of the system have been identified. Their respective domain of applicability for error prevention and error checking have been specified. Author

N92-32869*# National Aeronautics and Space Administration. Goddard Space Flight Center, Greenbelt, MD.
PROCEEDINGS OF THE SIXTEENTH ANNUAL SOFTWARE ENGINEERING WORKSHOP
Dec. 1991 344 p Workshop held in Greenbelt, MD, 4-5 Dec. 1991
(NASA-TM-107964; SEL-91-006; NAS 1.15:107964) Avail: CASI HC A15/MF A03; NASA Goddard Space Flight Center, Code 552, Greenbelt, MD 20771 HC

Materials for each session of this conference include a summary of the live presentation and any viewgraphs, abstracts, or papers, submitted for inclusion. Materials for each panel include a summary of the presentation and transcripts of the subsequent discussion. The panel topics covered include: the software engineering laboratory; investigating error; process analysis; testing/verification; and life cycle issues. For individual titles, see N92-32870 through N92-32884.

N92-32870*# Maryland Univ., College Park. Inst. for Advanced Computer Studies.
METHODOLOGICAL AND ARCHITECTURAL ISSUES IN THE EXPERIENCE FACTORY
Victor R. Basili and Gianluigi Caldiera *In* NASA. Goddard Space Flight Center, Proceedings of the Sixteenth Annual Software Engineering Workshop Dec. 1991 p 17-46 (For primary document see N92-32869 23-61)
Avail: CASI HC A03/MF A03; NASA Goddard Space Flight Center, Code 552, Greenbelt, MD 20771 HC

The concept of the experience factory has been introduced in order to institutionalize the collective learning of the organization that is at the root of continuous improvement and competitive advantage. The real advantage will come from the ability of the software organization to deliver solutions that anticipate the needs of the system users. The experience factory can be a logical and/or physical organization, but it is important that activities are separated and made independent from the ones of the project organization. H.A.

N92-32871*# National Aeronautics and Space Administration. Goddard Space Flight Center, Greenbelt, MD.
CLEANROOM PROCESS EVOLUTION IN THE SEL
Scott E. Green and Rose Pajerski *In its* Proceedings of the Sixteenth Annual Software Engineering Workshop Dec. 1991 p 47-63 (For primary document see N92-32869 23-61)
Avail: CASI HC A03/MF A03; NASA Goddard Space Flight Center, Code 552, Greenbelt, MD 20771 HC

The cleanroom development methodology is a software life cycle approach which emphasizes as its primary goal defect prevention rather than defect removal, and focuses on incrementally producing error-free software through statistical quality control. Since all testing is performed by independent groups, the development team is forced to rely on a structured and verifiable design approach, complemented with a peer review process, as its central verification technique. The focus of the system testing is on intended operational scenarios, rather than a pure and evenly distributed functional testing of the system requirements. The testing approach also involves a statistical profile of all system inputs, selections and paths, ensuring that the testing activities mimic the projected end-user actions. Author

N92-32872*# National Aeronautics and Space Administration. Goddard Space Flight Center, Greenbelt, MD.
EXPERIMENTS IN SOFTWARE ENGINEERING TECHNOLOGY: RECENT STUDIES IN THE SEL (1990-1991)
Frank McGarry and Sharon R. Waligora (Computer Sciences Corp., Silver Spring, MD.) *In its* Proceedings of the Sixteenth Annual Software Engineering Workshop Dec. 1991 p 65-85 (For primary document see N92-32869 23-61)
Avail: CASI HC A03/MF A03; NASA Goddard Space Flight Center, Code 552, Greenbelt, MD 20771 HC

During the history of the Software Engineering Laboratory (SEL), nearly 100 specific experiments have been completed, each focusing on some particular software technology to be analyzed for potential applications to the standard development process within the production environment. This paper describes some results of SEL studies completed during the last several years, including computer aided software engineering (CASE), object oriented techniques (OOT), and Ada. Author

N92-32873*# Bell Telephone Labs., Inc., Murray Hill, NJ.
INVESTIGATING THE APPLICATION OF CAPTURE-RECAPTURE TECHNIQUES TO REQUIREMENT AND DESIGN REVIEWS
Lawrence G. Votta, Stephen G. Eick, Clive R. Loader, M. David Long, and Scott VanderWiel *In* NASA. Goddard Space Flight Center, Proceedings of the Sixteenth Annual Software Engineering Workshop Dec. 1991 p 89-102 (For primary document see N92-32869 23-61)
Avail: CASI HC A03/MF A03; NASA Goddard Space Flight Center, Code 552, Greenbelt, MD 20771 HC

An objective of all software projects is to minimize the number of faults in the delivered code. Standard software development processes consist of multiple steps, resulting in a delivered system. At each stage of the process a key objective is to minimize the number of faults passed onto the next stage. Reviews consist of engineers who in preparation identify parts of the document that may contain design faults. Described are techniques to estimate the number of residual faults at each stage in the software development process. Author

N92-32874*# Osaka Univ. (Japan). Faculty of Engineering Science.
BETTER PREDICTIONS EVEN IN REDUCED INPUT VARIABLE NUMBERS USING NEURAL NETWORKS IN SOFTWARE DEVELOPMENT
Yoshihiro Takada, Margaret C. Thompson, and Koji Torii *In* NASA. Goddard Space Flight Center, Proceedings of the Sixteenth Annual Software Engineering Workshop Dec. 1991 p 103-120 (For primary document see N92-32869 23-61)
Avail: CASI HC A03/MF A03; NASA Goddard Space Flight Center, Code 552, Greenbelt, MD 20771 HC

A quantitative approach in software engineering, in which various aspects of the software process and products are measured and used to guide the software engineering process, is becoming important. This paper presents a framework for developing prediction models using artificial neural networks. In this method, an initial model is generated on a neural network with an initial set of data with input for all variables for which data is available. The contribution measure for a variable is an estimation of the square increase in prediction error when that variable is removed from the set of inputs. Variables are eliminated as long as prediction remains sufficiently accurate. H.A.

N92-32875*# Maryland Univ., College Park. Dept. of Computer Science.
OPTIMIZED SET REDUCTION FOR EMPIRICALLY GUIDING SOFTWARE DEVELOPMENT
Adam A. Porter and Lionel C. Briand *In* NASA. Goddard Space Flight Center, Proceedings of the Sixteenth Annual Software Engineering Workshop Dec. 1991 p 121-128 (For primary document see N92-32869 23-61)
Avail: CASI HC A02/MF A03; NASA Goddard Space Flight Center, Code 552, Greenbelt, MD 20771 HC

Classification modeling is presented for software engineering errors. Errors are categorized into different groups and a code is developed to detect these faults and classify them accordingly. All information is presented in viewgraph format. H.A.

N92-32876*# Master Systems, Inc., McLean, VA.
MEASUREMENT IN PRACTICE
Stan Rifkin and Charles Cox (Naval Weapons Center, China Lake, CA.) *In* NASA. Goddard Space Flight Center, Proceedings of the Sixteenth Annual Software Engineering Workshop Dec. 1991 p 131-142 (For primary document see N92-32869 23-61)

Avail: CASI HC A03/MF A03; NASA Goddard Space Flight Center, Code 552, Grrenbelt, MD 20771 HC

Software researchers, such as the Software Engineering Institute (SEI) Software Process Program, encourage the use of measurement to aid the management of software development and maintenance. Measurement, for example, is critical to the software process maturity framework promulgated by the SEI. In an effort to validate the value of measurement, the background of organizations that have reputations for obtaining the greatest benefits and have the best operation of measurement programs was explored. The results of eleven divisions of eight organizations that have gained reputations for having excellent measurement practices are presented. Persistent patterns emerged from our discussions with measurement leaders, and we found numerous interrelationships among the patterns. There were two patterns that ran through all the organizations: errors have been decriminalized, and measurement is part of something larger. Author

N92-32877*# New South Wales Univ., Kensington (Australia). School of Information Systems.

A CONCEPTUAL MODEL OF COGNITIVE COMPLEXITY OF ELEMENTS OF THE PROGRAMMING PROCESS

S. Cant, D. Ross Jeffery, and B. Henderson-Sellers *In* NASA. Goddard Space Flight Center, Proceedings of the Sixteenth Annual Software Engineering Workshop Dec. 1991 p 143-156 (For primary document see N92-32869 23-61)

Avail: CASI HC A03/MF A03; NASA Goddard Space Flight Center, Code 552, Greenbelt, MD 20771 HC

Measures of software complexity are necessary to monitor code, manage the programming process, and to ensure quality of the process and product. The history of complexity measurement has been marked by too many metrics that are not always based on theory appropriate to the programming process and that have been difficult to empirically validate. The cognitive complexity of software is defined, in this paper, as those characteristics of the software that affect the level of resources used by a person performing a given task. The theoretical approaches used for complexity measurement in the past, such as information theory, graph theory, lattice theory, communication theory, and empirical techniques are compared with the cognitive theoretical approach used. It is concluded that it is necessary to first analyze the processes involved in programmer tasks and the parameters that govern the effort involved in those processes. From these symptoms of complexity, a comprehensive conceptual model of software complexity is developed. Author

N92-32878*# Naval Surface Warfare Center, Dahlgren, VA.

SOFTWARE PROCESS ASSESSMENT FOR SMALL SOFTWARE SHOPS

Joseph P. Rich and Augustus Cooper *In* NASA. Goddard Space Flight Center, Proceedings of the Sixteenth Annual Software Engineering Workshop Dec. 1991 p 157-172 (For primary document see N92-32869 23-61)

Avail: CASI HC A03/MF A03; NASA Goddard Space Flight Center, Code 552, Greenbelt, MD 20771 HC

Software process assessment is rapidly becoming an important technique for improving software development within organizations. The maturity framework is the basis for the Software Engineering Institute's (SEI) Software Process Assessment (SPA), which has become the standard assessment procedure. One of the main reasons that this has become a standard is that SEI SPA has a companion process, the SEI Software Capability Evaluations (SCE), the scores from which may be used by U.S. government agencies (such as the Department of Defense) for awarding contracts. Naturally, companies develping software for U.S. government agencies want to perform the SPA and SCE, with hopes of a high score. One aspect of the popularity of software process assessments is that they are often associated with very large software organizations. This may cause smaller software organizations to feel as if they will not benefit from, or are not large enough to perform, a process assessment. This is not true. We have performed a software process assessment at our small software shop of 17 programmers, our small software shop of 17 programmers, and we have already received benefits from it. In fact, small software shops have an advantage in that they can more easily implement change. This paper describes the software process assessment that we performed, the benefits that we received, and the continuing modifications that we plan to do. Author

N92-32879*# International Business Machines Corp., Poughkeepsie, NY.

A STUDY OF LARGE SCALE SOFTWARE TESTING

Mitsuru Ohba and Victor R. Basili (Maryland Univ., College Park.) *In* NASA. Goddard Space Flight Center, Proceedings of the Sixteenth Annual Software Engineering Workshop Dec. 1991 p 175-207 Prepared in cooperation with IBM Japan (For primary document see N92-32869 23-61)

Avail: CASI HC A03/MF A03; NASA Goddard Space Flight Center, Code 552, Greenbelt, Md 20771 HC

Summarized here are the results of a study done in the United States and a comparison with state-of-the-practice software testing in large scale system software development projects in Japan. The primary observations were that those who participate in these projects are as good as the people who participate in similar projects in Japan, that there is a difference in emphasis on testing, that there is a significant difference in the use of measurements for process improvements between the U.S. and Japan, and that there are differences in development and deployment of common techniques and standard tools. Author

N92-32880*# National Aeronautics and Space Administration. Langley Research Center, Hampton, VA.

ANALYSIS OF DATA FROM A DO-178A SOFTWARE DEVELOPMENT PROCESS

Kelly J. Hayhurst and George B. Finelli *In* NASA. Goddard Space Flight Center, Proceedings of the Sixteenth Annual Software Engineering Workshop Dec. 1991 p 209-226 (For primary document see N92-32869 23-61)

Avail: CASI HC A03/MF A03; NASA Goddard Space Flight Center, Code 552, Greenbelt, MD 20771 HC

A clear understanding of the software development process is essential to defining more accurate software reliability models and more effective software development procedures that will yield reliable software. The Guidance and Control Software Project (GCS) experiment establishes an environment for investigating the effectiveness of various development and verification methods for avionics software, such as those prescribed by the FAA. The data collected during the development cycle of the GCS implementations will be used to assess the effectiveness of the DO-178A guidelines. Since adequate models for dependable reliability estimation of mission critical, real time software do not currently exist, the data from the GCS experiment will also provide an indispensable basis for improving methods for assessing reliability and safety. Analysis of faults found during the development cycle of one GCS implementation has already yielded interesting results that will be useful in characterizing the software failure process. Author

N92-32881*# Florida Inst. of Tech., Melbourne.

A MARKOV MODEL OF SOFTWARE USAGE

Harlan D. Mills *In* NASA. Goddard Space Flight Center, Proceedings of the Sixteenth Annual Software Engineering Workshop Dec. 1991 p 227-242 Prepared in cooperation with Software Engineering Technology, Inc., Vero Beach, FL (For primary document see N92-32869 23-61)

Avail: CASI HC A03/MF A03; NASA Goddard Space Flight Center, Code 552, Greenbelt, MD 20771 HC

Discussed here is the use of a Markov model of software usage as it relates to the software certification process. Stratification, test case generation, creation of a Markov transition matrix, representation of Markov transition matrices, stratified sampling, and the purposes of testing are covered. Author

N92-32882*# George Mason Univ., Fairfax, VA. Center for Software Systems Engineering.
A PROTOTYPE SOFTWARE ENGINEERING ENVIRONMENT FOR DOMAIN MODELING AND REUSE
Hassan Gomaa, Larry Kerschberg, Christopher Bosch, Vijayan Sugumaran, and Iraj Tavakoli *In* NASA. Goddard Space Flight Center, Proceedings of the Sixteenth Annual Software Engineering Workshop Dec. 1991 p 245-263 Sponsored in part by Virginia Center of Innovative Technology (For primary document see N92-32869 23-61)
Avail: CASI HC A03/MF A03; NASA Goddard Space Flight Center, Code 552, Greenbelt, MD 20771 HC

The topics are presented in viewgraph form and include the following: the evolutionary domain life cycle; domain modeling; NASA payload operations control center domain modeling; prototype software engineering environment creating domain model; prototype software engineering environment target system specification; and the Knowledge Based Requirements Elicitation Tool (KBRET). Author

N92-32883*# Hewlett-Packard Co., Palo Alto, CA. Logic Systems Div.
THE SUCCESSFUL INTRODUCTION OF SOFTWARE REUSE ACROSS AN ENTITY
Jim Jost *In* NASA. Goddard Space Flight Center, Proceedings of the Sixteenth Annual Software Engineering Workshop Dec. 1991 p 265-282 (For primary document see N92-32869 23-61)
Avail: CASI HC A03/MF A03; NASA Goddard Space Flight Center, Code 552, Greenbelt, MD 20771 HC

The topics are presented in viewgraph form and include the following: software reuse results at Logic Systems Division; reuse history; classification of reuse, and key success factors. Author

N92-32884*# TRW, Inc., Cleveland, OH. Systems Integration Group.
DEVELOPING BETTER SOFTWARE: A FIVE YEAR HISTORY OF SOFTWARE ENGINEERING ADVANCEMENT
Herbert P. Woodward *In* NASA. Goddard Space Flight Center, Proceedings of the Sixteenth Annual Software Engineering Workshop Dec. 1991 p 283-301 (For primary document see N92-32869 23-61)
Avail: CASI HC A03/MF A03; NASA Goddard Space Flight Center, Code 552, Greenbelt, MD 20771 HC

The topics covered include the following: the spiral model requirement development approach; the spiral model of the software development process; the Ada total quality management factory; architecture and software layering; building on a layered architecture; achieving a software requirements baseline; designing and building a quality low cost system; and the Ada programming support environment. Author

N92-32907# Dayton Univ. Research Inst., OH.
TEMPORAL AND SPATIAL FACTORS AFFECTING THE PERCEPTION OF COMPUTER-GENERATED IMAGERY Final Report, Jan. 1988 - Dec. 1990
Julie M. Lindholm Mar. 1992 46 p
(AF Proj. 1123)
(AD-A249242; AL-TR-1991-0140) Avail: CASI HC A03/MF A01

When computer-generated imagery is presented on a raster display device, the spatiotemporal representation of a given dynamic scene varies with the update of the image generator and the refresh pattern of the display device. The effects of these variables on form perception were examined in 3 experiments. In experiment 1, observers were instructed to maintain a steady fixation during 267-ms motion sequences. Target shape, target velocity image update rate, and raster pattern were varied orthogonally. Identification responses indicated that the temporal interval between successive fields of an interlaced display tended to be perceived as a spatial interval. The probability and extent of this temporal-to-spatial conversion (TSC) declined as target velocity increased. In experiment 2, observers were instructed to track the target in 30 Hz, interlaced displays of 3 durations (133, 267, and 533 ms). Under these conditions, complete TSC was the predominant percept for all velocities (4.7 to 18.8 deg/s) at the longest sequence duration. In experiment 3, observers were instructed to track the target in noninterlaced displays. Sequence duration (267, 533, 800, and 1,067 ms), image update rate (15, 30, and 60 Hz), target velocity (4.7, 9.4, and 14.1 deg/s) and direction of target-surround contrast (dark on light, as in experiments 1 and 2, and light on dark) were varied. GRA

N92-32917# Texas Univ., Austin. Applied Research Lab.
ABF ALGORITHMS IMPLEMENTED AT ARL:UT, FDS SYSTEM ENGINEERING AND ACOUSTICS
Richard A. Gramann 12 May 1992 28 p
(Contract N00039-91-C-0082)
(AD-A252368; ARL-TR-92-7) Avail: CASI HC A03/MF A01

Two adaptive beamforming (ABF) algorithms were implemented in order to assess algorithm performance. Using data obtained with acoustic data acquisition systems, these algorithms are being used to assess performance of future surveillance systems. This report describes the two element-level ABF algorithms implemented to this point. They are the single point constraint ABF and the multiple linear constraint ABF. Both algorithms have a quadratic white noise gain constraint included in the implementation. This report also provides some details on how the algorithms were programmed on an Alliant mini-supercomputer. Examples of the ABF output are also included and briefly discussed. GRA

N92-33071# Pennsylvania State Univ., University Park. Dept. of Computer Science.
SPARSE MATRIX ALGORITHMS ON DISTRIBUTED MEMORY MULTIPROCESSORS
A. Pothen 1992 4 p
(Contract DE-FG02-91ER-25095)
(DE92-017870; DOE/ER-25095/1) Avail: CASI HC A01/MF A01

The past year has seen significant progress in algorithms and software for the solution of large-scale sparse systems of equations, least-squares problems, and optimization problems on advanced distributed-memory parallel machines. The progress made to date is described in this paper. DOE

N92-33091*# Washington Univ., Seattle. Dept. of Aeronautics and Astronautics.
MIXED H(2)/H(SUB INFINITY): CONTROL WITH OUTPUT FEEDBACK COMPENSATORS USING PARAMETER OPTIMIZATION Annual Interim Technical Report
Ewald Schoemig and Uy-Loi Ly Feb. 1992 60 p Proposed for presentation at the 1992 ACC Conference, Chicago, IL, 24-26 Jun. 1992
(Grant NAG2-629)
(NASA-CR-190070; NAS 1.26:190070) Avail: CASI HC A04/MF A01

Among the many possible norm-based optimization methods, the concept of H-infinity optimal control has gained enormous attention in the past few years. Here the H-infinity framework, based on the Small Gain Theorem and the Youla Parameterization, effectively treats system uncertainties in the control law synthesis. A design approach involving a mixed H(sub 2)/H-infinity norm strives to combine the advantages of both methods. This advantage motivates researchers toward finding solutions to the mixed H(sub 2)/H-infinity control problem. The approach developed in this research is based on a finite time cost functional that depicts an H-infinity bound control problem in a H(sub 2)-optimization setting. The goal is to define a time-domain cost function that optimizes the H(sub 2)-norm of a system with an H-infinity-constraint function. H.A.

N92-33092*# Nebraska Univ., Lincoln. Dept. of Electrical Engineering.
SEMIANNUAL STATUS REPORT
30 Mar. 1992 24 p

(Grant NAG5-1612)
(NASA-CR-190239; NAS 1.26:190239) Avail: CASI HC A03/MF A01

The work performed in the previous six months can be divided into three main cases: (1) transmission of images over local area networks (LAN's); (2) coding of color mapped (pseudo-color) images; and (3) low rate video coding. A brief overview of the work done in the first two areas is presented. The third item is reported in somewhat more detail. Author

N92-33093*# Research Inst. for Computing and Information Systems, Houston, TX.
FUZZY SET METHODS FOR OBJECT RECOGNITION IN SPACE APPLICATIONS Quarterly Report No. 3, 1 Jan. - 31 Mar. 1992
James M. Keller (Missouri Univ., Columbia.) 31 Mar. 1992 81 p
(Contract NCC9-16; RICIS Proj. SE-42)
(NASA-CR-190388; NAS 1.26:190388) Avail: CASI HC A05/MF A01

Progress on the following tasks is reported: feature calculation; membership calculation; clustering methods (including initial experiments on pose estimation); and acquisition of images (including camera calibration information for digitization of model). The report consists of 'stand alone' sections, describing the activities in each task. We would like to highlight the fact that during this quarter, we believe that we have made a major breakthrough in the area of fuzzy clustering. We have discovered a method to remove the probabilistic constraints that the sum of the memberships across all classes must add up to 1 (as in the fuzzy c-means). A paper, describing this approach, is included. Author

N92-33118# Argonne National Lab., IL. Mathematics and Computer Science Div.
SWEEPING ALGORITHMS FOR FIVE-POINT STENCILS AND BANDED MATRICES
Man Kam Kwong Jun. 1992 25 p
(Contract W-31-109-eng-38)
(DE92-017309; ANL/MCS-TM-165) Avail: CASI HC A03/MF A01

We record MATLAB experiments implementing the sweeping algorithms we proposed recently to solve five-point stencils arising from the discretization of partial differential equations, notably the Ginzburg-Landau equations from the theory of superconductivity. Algorithms tested include two-direction, multistage, and partial sweeping. DOE

N92-33131*# Old Dominion Univ., Norfolk, VA. Dept. of Mechanical Engineering and Mechanics.
CONVERGENCE ACCELERATION OF THE PROTEUS COMPUTER CODE WITH MULTIGRID METHODS Interim Progress Report No. 1, period ending 31 Jul. 1992
A. O. Demuren and S. O. Ibraheem Aug. 1992 213 p
(Grant NAG3-1329)
(NASA-CR-190607; NAS 1.26:190607) Avail: CASI HC A10/MF A03

Presented here is the first part of a study to implement convergence acceleration techniques based on the multigrid concept in the Proteus computer code. A review is given of previous studies on the implementation of multigrid methods in computer codes for compressible flow analysis. Also presented is a detailed stability analysis of upwind and central-difference based numerical schemes for solving the Euler and Navier-Stokes equations. Results are given of a convergence study of the Proteus code on computational grids of different sizes. The results presented here form the foundation for the implementation of multigrid methods in the Proteus code. Author

N92-33142# Universiteit Twente, Enschede (Netherlands).
FAULT TOLERANCE THROUGH PROGRAM TRANSFORMATION Ph.D. Thesis
Lambertus Johannes M Nieuwenhuis 12 Dec. 1991 286 p
(ISBN-90-72125-29-0; ETN-92-92036) Copyright Avail: CASI HC A13/MF A03

The hypothesis that any application program can be replicated and implemented in a general purpose processor network is addressed. A strategy to transform systems into replicated versions such that reliability is improved without severe performance losses is devised. The original system is a program consisting of parallel processes, which are allocated to a general purpose processor network. The replicated system is a program consisting of replicated processes, which are allocated to an enlarged general purpose processor network. The transformation must be carried out automatically and indeed provide 'fault tolerance through program transformation'. The concept of fault tolerance by program replication is presented. The reliability of replicated systems and the implementation of replicated programs on general purpose processors are discussed. The replicated program is based on the Byzantine Merge protocol. This algorithm and its validation are given. An extensive and formal correctness proof of the algorithm is given. The implementation of a prototype system with transputers and OCCAM is discussed. ESA

N92-33189 Carleton Univ., Ottawa (Ontario). Dept. of Systems and Computer Engineering.
MULTI-STAGE HYBRID CODING OF DIGITAL IMAGES Ph.D. Thesis
Yiyan Wu 23 Apr. 1990 210 p
(ISBN-0-315-58989-2; CTN-92-60550) Copyright Micromedia Ltd., Technical Information Centre, 165 Hotel de Ville, Place du Portage, Phase 2, Hull, Quebec J8X 3X2, Canada HC/MF

Image compression coding techniques and fidelity measurements are reviewed, and three hybrid coding techniques which achieve compromises between the criteria of fidelity, computational complexity, and compression ratio are presented. BTC-VQ-DCT coding combines the advantages of simple computation and edge preservation of block truncation coding (BTC), the high fidelity and high compression ratio of adaptive discrete cosine transform (DCT) coding, and the high compression ratio and good performance of vector quantization (VQ). Multi-level BTC can preserve the spatial details in composite imagery while providing compression ratios of up to 6:1. VQ and predictive coding are used to compress the coded data further. The coding algorithm demonstrates very high fidelity, with no perceived visual degradation, and very low computational complexity. Single bit-map BTC is a color image data compression algorithm. BTC is implemented first, generating a bit map which is then used to compress each of the red, green, and blue images separately. Another approach using a bit-wise majority rule on the bit-maps is also discussed. The algorithm preserves the spatial details in the image content and has low computational complexity. Adaptive DCT is used to compress the truncated data further; the total compression ratio is about 12:1. Author (CISTI)

N92-33196*# National Academy of Sciences - National Research Council, Washington, DC. Committee for Review of Oversight Mechanisms for Space Shuttle Flight Software Processes.
INDEPENDENT VERIFICATION AND VALIDATION FOR SPACE SHUTTLE FLIGHT SOFTWARE
Jul. 1992 19 p
(Contract NASw-4003)
(NASA-CR-190826; NAS 1.26:190826) Avail: CASI HC A03/MF A01

The Committee for Review of Oversight Mechanisms for Space Shuttle Software was asked by the National Aeronautics and Space Administration's (NASA) Office of Space Flight to determine the need to continue independent verification and validation (IV&V) for Space Shuttle flight software. The Committee found that the current IV&V process is necessary to maintain NASA's stringent safety and quality requirements for man-rated vehicles. Therefore, the Committee does not support NASA's plan to eliminate funding for the IV&V effort in fiscal year 1993. The Committee believes that the Space Shuttle software development process is not adequate without IV&V and that elimination of IV&V as currently

practiced will adversely affect the overall quality and safety of the software, both now and in the future. Furthermore, the Committee was told that no organization within NASA has the expertise or the manpower to replace the current IV&V function in a timely fashion, nor will building this expertise elsewhere necessarily reduce cost. Thus, the Committee does not recommend moving IV&V functions to other organizations within NASA unless the current IV&V is maintained for as long as it takes to build comparable expertise in the replacing organization. Author

N92-33201 Concordia Univ., Montreal (Quebec). Dept. of Computer Science.
PATTERN RECOGNITION BASED ON ENTROPY ANALYSIS AND SHAPE TRANSFORMATIONS Ph.D. Thesis
Yuan Yan Tang Feb. 1990 259 p
(ISBN-0-315-56074-6; CTN-92-60525) Copyright Micromedia Ltd., Technical Information Centre, 165 Hotel de Ville, Place du Portage, Phase 2, Hull, Quebec J8X 3X2, Canada HC/MF

Two new models are proposed to analyze systematically the changes in entropy which occur in the different phases of pattern recognition. These models also provide a systematic way to design a pattern recognition system. Image transformation is one of the most important entropy transformations, having two completely different characteristics which are frequently used in image processing and pattern recognition. Several new theorems on image transformation are presented and proved, and some new algorithms are proposed for performing simultaneous mapping and filling while preserving the connectivities of the original image. A series of experiments is conducted to verify the performance of the proposed algorithms. To solve the problem of variance in size and orientation in pattern recognition, a new method called transformation ring projection is proposed. This method employs image transformation to reduce the entropy produced by such variance, and requires only simple and regular operations. An approximation of some perspective projection distortions is presented using the shape transformation theory under certain conditions. In this way, bilinear, bi-quadratic and bi-cubic transformations are used to model the nonlinear shape distortion problems, and some useful algorithms are presented. Inverse shape transformations are used in nonlinear restorations.
Author (CISTI)

N92-33204 McGill Univ., Montreal (Quebec). Dept. of Electrical Engineering.
THE LOCAL STRUCTURE OF IMAGE INTENSITY DISCONTINUITIES Ph.D. Thesis
Yvan G. Leclerc May 1989 199 p
(ISBN-0-315-57231-0; CTN-92-60539) Copyright Micromedia Ltd., Technical Information Centre, 165 Hotel de Ville, Place du Portage, Phase 2, Hull, Quebec J8X 3X2, Canada HC/MF

Two solutions to a critical problem in computer vision are presented. The problem considered is that of describing an image as the sum of an underlying piecewise smooth image and spatially varying white noise. Both solutions employ the idea that simplicity and stability of description lead to important inferences about the processes that give rise to an image. The first solution uses a set of local operators, each hypothesizing a simplest description of the underlying image within its spatial domain by estimation theoretical means. Hypotheses from overlapping operators are then combined to produce the simplest overall description. The second and more powerful solution uses an objective function based on the information theoretic complexity of describing an image in a given language. This objective function is highly non-convex, so that standard optimization techniques cannot be used. Instead, a local, parallel, and iterative optimization algorithm is devised for finding near-optimal solutions. The algorithm is adaptive, requiring no change in parameters across a wide range of images, and has the added advantage of finding the most stable features of the simplest description first. Even though the language contains no models of three-dimensional shape, lighting, or texture, the simplest and most stable descriptions in this language are intuitively satisfying. Author (CISTI)

N92-33210 Waterloo Univ. (Ontario).
HYPOTHESIS REFINEMENT FOR 3-D SCENE INTERPRETATION Ph.D. Thesis
Kurt Dieter Rueb 1990 185 p
(ISBN-0-315-57864-5; CTN-92-60527) Copyright Micromedia Ltd., Technical Information Centre, 165 Hotel de Ville, Place du Portage, Phase 2, Hull, Quebec J8X 3X2, Canada HC/MF

A method is presented for identifying and precisely locating modeled objects through analysis of single or multiple perspective images. The method provides efficient and reliable scene interpretation by means of incremental refinement of interpretation hypotheses. The hypothesized position and orientation of an object, referred to as a configuration of the object model, is represented through use of a hypothesis field which expresses the likelihood of the continuous domain of model configurations. Hypotheses are refined on the basis of knowledge of the application environment, representation of the characteristic views or visual aspects of the object model, and the evidence of features detected in the image. The constraint provided by the evolving scene interpretation guides the selection of key features used to establish object position and provides improved position accuracy. Automated visual detection of camera viewpoints permits use of unconventional viewing conditions, such as multiple views per image due to reflective surfaces or mirrors, and removes the need for precise camera positioning. Application of the system to robotic tasks, scene interpretation for a robot vehicle, and visual inspection is demonstrated. Author (CISTI)

N92-33212 Concordia Univ., Montreal (Quebec). Dept. of Electrical Engineering.
PRIMAL ACCESS RECOGNITION OF VISUAL OBJECTS Ph.D. Thesis
Robert Bergevin Oct. 1989 211 p
(ISBN-0-315-63509-6; CTN-92-60556) Copyright Micromedia Ltd., Technical Information Centre, 165 Hotel de Ville, Place du Portage, Phase 2, Hull, Quebec J8X 3X2, Canada HC/MF

The PARVO computer vision system addresses the problem of fast and generic recognition of unexpected 3-dimensional objects from single 2-dimensional views. The PARVO system makes explicit the main assumptions of the RBC (recognition by components) human image understanding theory, which was originally proposed on the basis of some psychological results from studying the human visual system. The PARVO system is designed to handle partially occluded objects of different shape and dimension in various spatial locations and orientations in the image plane. Its part segmentation algorithm is able to deal with objects formed of both simple and complex part structures; it is a boundary-based approach independent of the particular shape of the parts making up an object. The part inference algorithm for labelling of even partially occluded parts is efficiently implemented as a simple discrimination tree traversed on the basis of the qualitative properties of a part's faces. The object matching algorithm includes an efficient pruning mechanism based on geon indexing of the database of models. A simple metric was defined that permits good discrimination between models and provides an intuitively satisfying measure of similarity. The system is shown to compute generic descriptions successfully and then to recognize many common man-made objects. Author (CISTI)

N92-33214 Calgary Univ. (Alberta). Dept. of Computer Science.
CSP: A DISTRIBUTED LOGIC PROGRAMMING LANGUAGE FOR DISCRETE EVENT SIMULATION Ph.D. Thesis
Xining Li Jun. 1989 156 p
(ISBN-0-315-54272-1; CTN-92-60529) Copyright Micromedia Ltd., Technical Information Centre, 165 Hotel de Ville, Place du Portage, Phase 2, Hull, Quebec J8X 3X2, Canada HC/MF

The development of a large computer simulation is a complex and difficult task. Research was conducted to reduce the costs of simulation in two ways: simplifying simulation development by providing a new programming language which can be used for both model specification and program implementation; and enabling the use of more cost-effective parallel computers to execute simulations. First, an abstract distributed logic programming model

is described. The model is based on first order logic theory with extensions for temporal, cooperative execution. Within this framework, the programmer is able to describe simulation models in a declarative way. Secondly, an implementation of the language framework is presented. Based on an optimistic synchronization mechanism, the time warp system developed by Jefferson (1985), the implementation not only provides a temporal coordinate system for measuring computational progress and defining synchronizations, but also provides a spatial coordinate system for supporting nondeterministic computations. Finally, a practical language proposal, Communicating Sequential Prolog, is introduced. Several programming examples of discrete event simulation reveal the simplicity, flexibility, understandability, and expressive power of this language. Author (CISTI)

N92-33215 Carleton Univ., Ottawa (Ontario). Dept. of Systems and Computer Engineering.
AN EVALUATION OF KNOWLEDGE-BASED DIAGNOSTIC TECHNIQUES FOR DEBUGGING CONCURRENT SOFTWARE Ph.D. Thesis
Gregory William Bond 17 Apr. 1989 140 p
(ISBN-0-315-51189-3; CTN-92-60530) Copyright Micromedia Ltd., Technical Information Centre, 165 Hotel de Ville, Place du Portage, Phase 2, Hull, Quebec J8X 3X2, Canada HC/MF

The possible application of knowledge based diagnosis for locating semantic errors encountered while implementing concurrent software applications is explored. Taxonomies of diagnostic processes and diagnostic models are proposed which provide bases for a critical examination of their effectiveness in diagnostic systems. The behavioral diagnostic process combined with deep causal models of expectations and the faulty program is found as being the most suitable for the diagnosis of concurrent software. A deep causal modelling formalism is presented, capable of representing many of the structural and behavioral characteristics of concurrent software. Comprehensive definitions of faults and errors are given in terms of this formalism. Alternative sources are identified for models of concurrent software in an implementation environment. Two behavioral diagnostic techniques are also assessed: one originally intended for hardware diagnosis; and the other intended for diagnosing sequential Prolog programs. It is determined that neither technique is especially well suited to diagnosing concurrent software, but those elements of both procedures which are applicable are isolated. Author (CISTI)

N92-33227 Concordia Univ., Montreal (Quebec). Dept. of Computer Science.
OPTIMIZATION OF LOGIC QUERIES IN KNOWLEDGE BASE SYSTEMS Ph.D. Thesis
Premchand Sukumaran Nair May 1989 143 p
(ISBN-0-315-51346-2; CTN-92-60536) Copyright Micromedia Ltd., Technical Information Centre, 165 Hotel de Ville, Place du Portage, Phase 2, Hull, Quebec J8X 3X2, Canada HC/MF

One way to implement a knowledge base system is to augment a traditional relational data base system with deductive capabilities. A major issue has been to find an efficient implementation supporting queries expressed in first-order logic. An efficient optimization strategy called the IMS (integrated magic set) method is introduced and shown to be superior to other known query optimization methods. Two parallel algorithms for efficient query evaluation of Datalog programs are developed which can be implemented in any distributed architecture. Performance comparisons between the parallel algorithms and a serial algorithm, using an analytical model, establish the superiority of the parallel algorithms over the semi-naive serial algorithm. Optimization techniques based on the concept of permutation dependency are presented. This achieves optimization at different levels: for storing a base predicate, for removing redundant rules, for rewriting a Datalog program, and for efficient computation of a derived predicate satisfying a permutation dependency. A classification of chain rule programs based on their computational complexity is provided. A non-regular chain rule program is shown to be computationally more complex than a chain rule program. An algorithm is presented for determining whether a given binary rule program has an equivalent chain rule program. Author (CISTI)

N92-33229 McGill Univ., Montreal (Quebec). School of Computer Science.
VISIBILITY PROPERTIES OF POLYGONS Ph.D. Thesis
Thomas C. Shermer Jun. 1989 127 p
(ISBN-0-315-57272-8; CTN-92-60540) Copyright Micromedia Ltd., Technical Information Centre, 165 Hotel de Ville, Place du Portage, Phase 2, Hull, Quebec J8X 3X2, Canada HC/MF

Link-visibility is an extended notion of visibility arising from robotics and motion planning problems. Hidden sets are sets of points in a polygon such that no two points of the set are visible, and guard sets are sets such that each point of the polygon is visible to some point in the guard set. Both maximum hidden set sizes and minimum guard set sizes can be used as polygon shape complexity measures. Tight bounds are established on the maximum size of maximum hidden sets, minimum guard sets, and minimum partitions and covers of polygons, using link-visibility. These results unify and generalize the guard set results of Chvatal and O'Rourke (1975, 1983). The method also provides tight bounds on the size of hidden sets, guard sets, covers, and partitions of polygon exteriors. In addition, it is proved that, using link-visibility, the optimization problems of finding maximum hidden sets, minimum guard sets, or minimum covers are NP-hard.
Author (CISTI)

N92-33230 Toronto Univ. (Ontario).
METHODOLOGIES FOR DESIGNING BLOCK CIPHERS AND CRYPTOGRAPHIC PROTOCOLS Ph.D. Thesis
Richard Erwin Alexan Cleve 12 Apr. 1989 98 p
(ISBN-0-315-50983-X; CTN-92-60541) Copyright Micromedia Ltd., Technical Information Centre, 165 Hotel de Ville, Place du Portage, Phase 2, Hull, Quebec J8X 3X2, Canada HC/MF

A model of computation called a reversible program is investigated, along with its relationship to the level of cryptographic security attainable by a type of algorithm for encrypting fixed length blocks of data called a simple product cipher. It is shown that, under a cryptographic assumption, a very strong form of security is attainable. The cryptographic assumption is that there exists a pseudorandom function generator that is feasibly computed in a model of computation called an iterated integer matrix product. As a byproduct of this investigation, it has been found that over an arbitrary ring, any polynomial size algebraic formula is computed by an algebraic straight-line program that uses only three registers. The cryptographic security attainable in two-party protocols that carry out collective coin flipping and secret bit exchanging transactions is then examined. Non-trivial lower bounds are determined for the insecurity inherent in any protocol for either of the transactions. Protocols are also constructed for both transactions that attain various levels of security under some widely believed number theoretic intractability assumptions.
Author (CISTI)

N92-33232 Concordia Univ., Montreal (Quebec). Dept. of Computer Science.
CONCURRENCY CONTROL SCHEME FOR DESIGN OBJECT BASES Ph.D. Thesis
T. Srinivasan Narayanan Aug. 1989 85 p
(ISBN-0-315-56113-0; CTN-92-60537) Copyright Micromedia Ltd., Technical Information Centre, 165 Hotel de Ville, Place du Portage, Phase 2, Hull, Quebec J8X 3X2, Canada HC/MF

Recent research has focused on the need to modify the concurrency control criterion to make it applicable to non-traditional applications like design activity. It is proposed that enforcement of constraints defined on application, domain, or database behavior should be the goal of concurrency control schemes. These constraints define the correctness criteria, and as long as these criteria are satisfied, it is immaterial whether the concurrent execution of transactions is serializable or not. Thus, concurrency can be allowed without compromising the correctness of the results. A design activity model is presented, where a design activity involves other design activities and/or transactions. A transaction

is a set of actions; it is also a unit of consistency and atomicity. Two types of constraints are associated with each design activity: validation constraints, which specify correctness criteria and the conditions under which a design activity is deemed complete; and visibility constraints, which specify the conditions under which sharing among design activities occurs. An optimistic validation scheme is also suggested for object oriented databases. In this scheme, validation constraints are verified at the time of the completion of a design activity. Author (CISTI)

N92-32300*# Mississippi Univ. for Women, Columbus. NSF Engineering Research Center for Computational Field Simulation.
AN EFFICIENT AND ROBUST GRID OPTIMIZATION ALGORITHM
Bharat K. Soni and Shaochen Yang *In* NASA. Goddard Space Flight Center, Tenth Workshop for Computational Fluid Dynamic Applications in Rocket Propulsion, Part 1 Jul. 1992 p 503-541 (For primary document see N92-32278 23-34)
Avail: CASI HC A03/MF A05

N92-32301*# MDA Engineering, Inc., Arlington, TX.
ENHANCEMENTS TO THE GRIDGEN STRUCTURED GRID GENERATION SYSTEM FOR INTERNAL AND EXTERNAL FLOW APPLICATIONS
John P. Steinbrenner and John R. Chawner *In* NASA. Goddard Space Flight Center, Tenth Workshop for Computational Fluid Dynamic Applications in Rocket Propulsion, Part 1 Jul. 1992 p 543-576 (For primary document see N92-32278 23-34)
Avail: CASI HC A03/MF A05

N92-32302*# Mississippi Univ. for Women, Columbus. NSF Engineering Research Center for Computational Field Simulation.
CAGI: COMPUTER AIDED GRID INTERFACE. A WORK IN PROGRESS
Bharat K. Soni, Tzu-Yi Yu, and David Vaughn *In* NASA. Goddard Space Flight Center, Tenth Workshop for Computational Fluid Dynamic Applications in Rocket Propulsion, Part 1 Jul. 1992 p 577-613 (For primary document see N92-32278 23-34)
Avail: CASI HC A03/MF A05

N92-32443# Naval Weapons Center, China Lake, CA. Attack Weapons Dept.
TARGET DETECTION USING CO-OCCURRENCE MATRIX SEGMENTATION AND ITS HARDWARE IMPLEMENTATION
John Eric Auborn and James M. Fuller *In* AGARD, Integrated Target Acquisition and Fire Control Systems Feb. 1992 4 p (For primary document see N92-32437 23-06)
Copyright Avail: CASI HC A01/MF A02; 1 functional color page

62 COMPUTER SYSTEMS

Includes computer networks and special application computer systems.

N92-32412# Lawrence Livermore National Lab., CA.
A SCALABLE, SWITCHED CIRCUIT LAN FOR Gb/S CHANNELS WITH OVER Tb/S TOTAL CAPACITY
W. J. Lennon and R. M. Bryant Jan. 1992 5 p Presented at the DOD Fiber Optics Conference, McLean, VA, 25 Mar. 1992
(Contract W-7405-eng-48)
(DE92-013444; UCRL-JC-109601; CONF-920367-8) Avail: CASI HC A01/MF A01

To keep abreast of increasing high performance computing requirements at Lawrence Livermore National Laboratory (LLNL), the High Performance Switching System (HPSS) Project is currently prototyping a circuit switched Local Area Network (LAN). This network will employ the set of protocols being defined by the ANSI Fiber Channel Standard (FCS). The effort to build LAN is a collaborative one with several industrial partners developing the enabling technologies. Through the HPSS Project, LLNL has taken the catalytic role for the development and integration of these technologies into a gigabit/sec LAN technology. Out of this collaborative development effort will come a gigabit/sec networking technology that will be readily available to the academic, industrial, and scientific communities. Once we have a successfully operating prototype and have investigated other gigabit/sec networking alternatives, we will go to an open bid to provide access for over 2,000 users of supercomputers and high performance workstations. The results of our prototype evaluation should aid us in building and maintaining the large scale gigabit/sec local area network necessary for high performance computing at LLNL. DOE

N92-32568# Rochester Univ., NY. Dept. of Computer Science.
THE ROCHESTER CHECKERS PLAYER: MULTI-MODEL PARALLEL PROGRAMMING FOR ANIMATE VISION
B. D. Marsh, C. M. Brown, T. J. LeBlanc, M. L. Scott, and T. G. Becker Jun. 1991 18 p
(Contract N00014-82-K-0193; NSF CDA-88-22724; NSF IRI-89-03582; NSF IRI-89-20771; NSF CCR-90-05633)
(AD-A247427) Avail: CASI HC A03/MF A01

Animate vision systems couple computer vision and robotics to achieve robust and accurate vision, as well as other complex behavior. These systems combine low-level sensory processing and effector output with high-level cognitive planning - all computationally intensive tasks that can benefit from parallel processing. No single model of parallel programming is likely to serve for all tasks, however. Early vision algorithms are intensely data parallel, often utilizing fine-grain parallel computations that share an image, while cognition algorithms decompose naturally by function, often consisting of loosely-coupled, coarse-grain parallel units. A typical animate vision application will likely consist of many tasks, each of which may require a different parallel programming model, and all of which must cooperate to achieve the desired behavior. These multi-model programs require an underlying software system that not only supports several different models of parallel computation simultaneously, but which also allows tasks implemented in different models to interact. GRA

N92-32628# Stanford Univ., CA. Dept. of Electrical Engineering.
STARNET: A MULTIGBIT/S OPTICAL LOCAL AREA NETWORK WITH BOTH PACKET AND CIRCUIT SWITCHING
Leonid Kazovsky and P. Poggiolini 1991 5 p
(Contract N00014-91-J-1857)
(AD-A247617) Avail: CASI HC A01/MF A01

The potential of passive star WDM networks is believed to be extremely high. STARNET is a new broadband optical LAN based on such physical structure. Every STARNET node supports both packet traffic and a high-speed WDM circuit interconnect, simultaneously and independently. As a result, STARNET carries diverse types of traffic (i.e., bursty and continuous, low-speed and broadband) in an efficient way. Each node requires only two lasers and its structure permits frequency stabilization of the whole network. An experimental 4-node, 12 Gbit/s (3 Gbit/s per node), FDDI-compatible (at the packet network level) STARNET is being built at Stanford University. Each node of the network is optically connected to a passive optical star. Each node is also equipped with a fixed frequency transmitter which is assigned a unique frequency, so that a comb of optical carriers is formed. Transmitters multiplex two independent data streams on the same optical carrier, the C ('circuit') stream and the P ('packet') stream, using non-interfering modulation formats, DPSK, and low-modulation-index ASK, respectively. GRA

N92-32689# Messerschmitt-Boelkow-Blohm G.m.b.H., Bremen (Germany, F.R.). Space System Group.
PARALLEL PROCESSING IN SPACE APPLICATIONS USING TRANSPUTER NETWORKS
Gerhard Urban (Erno Raumfahrttechnik G.m.b.H. Bremen, Germany, F.R.) 1990 5 p Presented at the International Symposium on Artificial Intelligence, Robotics and Automation in Space, Kobe, Japan, 18-20 Nov. 1990 Previously announced in IAA as A92-23684
(MBB-UO-0172-90-PUB; ETN-92-92111) Avail: CASI HC A01/MF A01

The use of transputer networks for space applications is discussed. GNC processors and complex data handling systems to use the advantage of the transputer architecture for embedded controller are discussed. The practical use of transputer networks is demonstrated for image processing for automation in orbit and three dimensional computer graphics for real time simulation. The transputer is now an off-the-shelf available microprocessor product with sufficient software tools and application support. It makes it easy for engineers to design and realize parallel processing applications with reduced price and risk. ESA

N92-32715# Grenoble-1 Univ. (France). Lab. de Modelisation et Calcul.

OPTIMAL COMMUNICATION SCHEMES ON AN SIMD DISTRIBUTED-MEMORY HYPERCUBE

Denis Delesalle, Denis Trystram, and Didier Wenzek Apr. 1991 22 p Sponsored by CNRS and Electricite de France
(IMAG-RR-848-M; ETN-92-92076) Avail: CASI HC A03/MF A01

Optimality results on the implementation of fundamental communication schemes in a distributed memory SIMD hypercube multiprocessor (namely, global exchange and personalized global exchange with accumulation) are addressed. The iterative computation of vector matrix products illustrates these results which are experimented on, on a connection machine. ESA

N92-32759# Oxford Univ. (England). Robotics Research Group.

PARALLEL IMPLEMENTATION OF DROID AND PERFORMANCE EVALUATION

Han Wang and Michael Brady 17 Apr. 1992 19 p
(OUEL-1926/92; ETN-92-92066) Avail: CASI HC A03/MF A01

The implementation of a 3D (three dimensional) vision algorithm, Droid, on the Oxford parallel vision architecture, PARADOX, and the results of experiments to gauge the algorithm's effectiveness providing navigation data for an autonomous guided vehicle, are described. The algorithm reconstructs 3D structure by analyzing image sequences obtained from a moving camera. The primary components of PARADOX are a Datacube pipelined image processor, a configurable network of 32 T800 transputers, a Sun-4 workstation and a special purpose interface connecting the Datacube to the transputer network. The Datacube handles the image digitization, storage and display; the transputer network performs the feature extraction (corner points) in parallel, and the Sun-4 computes the three dimensionalization. In this application, the architecture delivers a performance of greater than 1 frame per second--17 times the performance of a Sun-4 alone. Experiments suggest that this system is capable of maintaining an estimate of true camera position to within 5 percent over 600 image frames by using visual data alone. ESA

N92-32768# Institut National Polytechnique, Grenoble (France). Lab. de Genie Informatique.

STUDY OF A CELLULAR PROGRAMMABLE ARCHITECTURE: FUNCTIONAL DEFINITION AND PROGRAMMING METHOD Ph.D. Thesis [ETUDE D'UNE ARCHITECTURE CELLULAIRE PROGRAMMABLE: DEFINITION FONCTIONNELLE ET METHODOLOGIE DE PROGRAMMATION]

Eric Payan 1991 189 p In FRENCH
(ETN-92-91663) Avail: CASI HC A09/MF A02

The proposals of several parallel architectures to satisfy the increasing demand of computing power are discussed. In spite of the number of proposed solutions, one class of applications that cannot be executed in parallel on existing computers still remains. An architecture based on a two dimensional grid of asynchronous processing units, each including a processing part made of a small 8 bits microprocessor and its memory (data plus program), and a routing part which allow message transmission, is proposed. The design and development of a programming tool for this architecture is addressed. The solution chosen is to map a data flow graph, extracted from a LUSTRE program, onto the asynchronous cellular network. A first prototype of the compiler which can study such things as load balancing between cells or execution of several nodes mapped onto a single cell, is developed. ESA

N92-32771# Institut National Polytechnique, Grenoble (France). Lab. d'Informatique Fondamentale et d'Intelligence Artificielle.

FUNCTIONS AND GENERICITY IN A PARALLEL PROGRAMMING LANGUAGE Ph.D. Thesis [FONCTIONS ET GENERICITE DANS UN LANGAGE DE PROGRAMMATION PARALLELE]

Jean-Michel Hufflen 1989 246 p In FRENCH Sponsored by Institut National Polytechnique de Grenoble, and EEC
(ETN-92-91667) Avail: CASI HC A11/MF A03

The functional part of Functional Parallel Programming (FP2), a language combining both functional and parallel programming through the algebraic specification approach and term rewriting systems, is presented. Genericity (i.e., parameterization of a specification) is presented: principles are recalled; the semantics are studied; the compilation of generic operators in a functional framework is formalized; and the notational facilities provided to the users are analyzed. The exception mechanism is investigated and is operationally presented, while the definition of a presentation with exceptions as an order sorted presentation is shown. Thus, the existence of an initial algebra is ensured. This method permits treatment of exceptions with generic parameters. Methods for transforming recursive functional definitions into parallel programs are presented. The hypotheses on the functional definitions are specified by means of generic operators. An arbitrarily deep recursive stack is simulated by means of networks with a statistically fixed topology. ESA

N92-32795# Technische Univ., Berlin (Germany, F.R.). Fachbereich Informatik.

EXPLOITING TWO-DIMENSIONAL EXPLICIT PARALLELISM ON VECTOR ARCHITECTURES Ph.D. Thesis

Hua Bi 1991 136 p
(ETN-92-92136) Avail: CASI HC A07/MF A02

The necessity and the availability of exploiting two dimensional (2D) explicit parallelism in architecture design, in language expressiveness and in compiler construction, is examined. The forms of 1D and 2D explicit parallelism can be extracted from the elementary numerical algorithms and abstracted by subarray patterns. New sampling modes are introduced to access subarrays for both 1D and 2D explicit parallelisms. A programming language for 1D and 2D explicit parallelism called MODULA-S, an extension to MODULA-2, is designed. Subarrays for 1D and 2D explicit parallelism can be expressed systematically in MODULA-S. A compiler for 1D and 2D explicit parallelism can be efficiently implemented, in which subarray accessing and memory module allocation are discussed. The simulation results show that by exploiting 2D explicit parallelisms in vector architectures the sustained performance and the memory throughput can be improved significantly. ESA

N92-32821# Technische Univ., Berlin (Germany, F.R.). Fachbereich Informatik.

METHODS OF FINE-GRAIN OPTIMIZATION FOR PARALLEL COMPUTER ARCHITECTURES Ph.D. Thesis

Diantong Liu 1991 131 p
(ETN-92-92144) Avail: CASI HC A07/MF A02

Research concentrating on aspects of compiler optimization techniques for uniprocessor machines that exploit implicit fine grain parallelism at the machine instruction level is presented. The fine grain optimization aims at detecting parallelism between individual machine operations and translating it to the architectural parallelism provided by the hardware of the target machine by scheduling these operations at compile time (termed static scheduling). In this context, a program is considered to consist of a set of atomic machine operations, each of which is carried out by one or more functional units. The parallel architecture processor in the consideration consists of one or more pipelined functional units that cooperate in a parallel fashion. The common hardware feature found in modern parallel computers are found and accommodated in the abstract machine model defined for the purpose of

retargetability. This machine model serves as a framework within which new techniques of code parallelization are developed. Attempts are made to find new concepts and more powerful methods of program analysis in order to detect more parallelism; to find good scheduling heuristics; and to develop sophisticated techniques in order to generate efficient parallel code that can take advantage of the parallel resources. ESA

N92-32886*# National Aeronautics and Space Administration. Ames Research Center, Moffett Field, CA.
ANALYSIS OF A BENCHMARK SUITE TO EVALUATE MIXED NUMERIC AND SYMBOLIC PROCESSING
Bharathi Ragharan and David Galant Aug. 1992 36 p
(RTOP 506-59-31)
(NASA-TM-103907; A-92023; NAS 1.15:103907) Avail: CASI HC A03/MF A01

The suite of programs that formed the benchmark for a proposed advanced computer is described and analyzed. The features of the processor and its operating system that are tested by the benchmark are discussed. The computer codes and the supporting data for the analysis are given as appendices. Author

N92-32926# Oak Ridge National Lab., TN.
EXPERIMENTS WITH AN ORDINARY DIFFERENTIAL EQUATION SOLVER IN THE PARALLEL SOLUTION OF METHOD OF LINES PROBLEMS ON A SHARED MEMORY PARALLEL COMPUTER, PART 2
D. K. Kahaner, E. G. Ng, and W. E. Schiesser (Lehigh Univ., Bethlehem, PA.) 1992 8 p Presented at the 7th International Association of Mathematics and Computer Simulation (IMACS) International Conference on Computer Methods for Partial Differential Equations, New Brunswick, NJ, 22-24 Jun. 1992
(Contracts DE-AC05-84OR-21400; DE-AC35-89ER-40486)
(DE92-017159; CONF-9206185-6-Pt-2) Avail: CASI HC A02/MF A01

The authors previously considered the use of parallel direct dense matrix techniques for the solution of method of lines problems on a shared memory parallel computer. It was found that substantial speedups can be obtained for dense problems involving spatially discretized systems containing from a few to several hundred ordinary differential equations. This paper reports the results for similar experiments with parallel direct sparse matrix techniques for the solution of such problems. The methods are implemented in the context of a well-known stiff ordinary differential equation solver. Parallelism is exploited by forming the Jacobian matrix in parallel and by using parallel direct sparse linear algebra matrix techniques for the solution of the corrector equations. Timing results are given for several representative problems involving spatially discretized systems containing from several hundred to a few thousand ordinary differential equations. The experiments were performed on a Sequent Balance computer which is a parallel computer with 8 processors sharing a global memory. The results demonstrate that substantial speedups can be obtained in this manner for sparse method of lines problems. DOE

N92-32937# Mitre Corp., Bedford, MA.
ETHERNET BANDWIDTH UTILIZATION OF DATAFULL, DATALESS, AND DISKLESS NODE WORKSTATION AND X-TERMINALS Final Report
James E. Manley and Steven P. Trieber May 1992 110 p
(AD-A252374; MTR-11282; ESD-TR-92-051) Avail: CASI HC A06/MF A01

As users of open system technologies migrate towards use of the Network File System (NFS), the X-Window System, and workstations configured as datafull, dataless, and diskless nodes, as well as X-Terminals, many questions arise as to network capacity planning. This report examines the Ethernet bandwidth utilization of three applications, all X-Windows based, in four different workstation/terminal configurations. Information is provided to facilitate replication of the data collection techniques for individual sites and network/application configurations. Several conclusions and recommendations are drawn which may be of interest to system designers considering network capacity planning. GRA

N92-33100*# Draper (Charles Stark) Lab., Inc., Cambridge, MA.
ADVANCED INFORMATION PROCESSING SYSTEM: THE ARMY FAULT TOLERANT ARCHITECTURE CONCEPTUAL STUDY. VOLUME 1: ARMY FAULT TOLERANT ARCHITECTURE OVERVIEW
R. E. Harper, L. S. Alger, C. A. Babikyan, B. P. Butler, S. A. Friend, R. J. Ganska, J. H. Lala, T. K. Masotto, A. J. Meyer, and D. P. Morton et al Jul. 1992 140 p
(Contract NAS1-18565; RTOP 505-64-52-53)
(NASA-CR-189632-Vol-1; NAS 1.26:189632-Vol-1) Avail: CASI HC A07/MF A02

Digital computing systems needed for Army programs such as the Computer-Aided Low Altitude Helicopter Flight Program and the Armored Systems Modernization (ASM) vehicles may be characterized by high computational throughput and input/output bandwidth, hard real-time response, high reliability and availability, and maintainability, testability, and producibility requirements. In addition, such a system should be affordable to produce, procure, maintain, and upgrade. To address these needs, the Army Fault Tolerant Architecture (AFTA) is being designed and constructed under a three-year program comprised of a conceptual study, detailed design and fabrication, and demonstration and validation phases. Described here are the results of the conceptual study phase of the AFTA development. Given here is an introduction to the AFTA program, its objectives, and key elements of its technical approach. A format is designed for representing mission requirements in a manner suitable for first order AFTA sizing and analysis, followed by a discussion of the current state of mission requirements acquisition for the targeted Army missions. An overview is given of AFTA's architectural theory of operation. Author

N92-33101*# Draper (Charles Stark) Lab., Inc., Cambridge, MA.
ADVANCED INFORMATION PROCESSING SYSTEM: THE ARMY FAULT TOLERANT ARCHITECTURE CONCEPTUAL STUDY. VOLUME 2: ARMY FAULT TOLERANT ARCHITECTURE DESIGN AND ANALYSIS
R. E. Harper, L. S. Alger, C. A. Babikyan, B. P. Butler, S. A. Friend, R. J. Ganska, J. H. Lala, T. K. Masotto, A. J. Meyer, and D. P. Morton et al Jul. 1992 430 p
(Contract NAS1-18565; RTOP 505-64-52-53)
(NASA-CR-189632-Vol-2; NAS 1.26:189632-Vol-2) Avail: CASI HC A19/MF A04

Described here is the Army Fault Tolerant Architecture (AFTA) hardware architecture and components and the operating system. The architectural and operational theory of the AFTA Fault Tolerant Data Bus is discussed. The test and maintenance strategy developed for use in fielded AFTA installations is presented. An approach to be used in reducing the probability of AFTA failure due to common mode faults is described. Analytical models for AFTA performance, reliability, availability, life cycle cost, weight, power, and volume are developed. An approach is presented for using VHSIC Hardware Description Language (VHDL) to describe and design AFTA's developmental hardware. A plan is described for verifying and validating key AFTA concepts during the Dem/Val phase. Analytical models and partial mission requirements are used to generate AFTA configurations for the TF/TA/NOE and Ground Vehicle missions. Author

N92-33216 Carleton Univ., Ottawa (Ontario).
ANALYTIC PERFORMANCE OF SOFTWARE PIPELINES WITH RENDEZVOUS AND COMMUNICATION TASKS Ph.D. Thesis
Robert Halim Constantin 4 Aug. 1989 112 p
(ISBN-0-315-54414-7; CTN-92-60531) Copyright Micromedia Ltd., Technical Information Centre, 165 Hotel de Ville, Place du Portage, Phase 2, Hull, Quebec J8X 3X2, Canada HC/MF

Software systems that use the rendezvous for communications, including Ada and V, will suffer in performance due to waiting in the rendezvous. This may be alleviated by providing buffering in the form of mailbox tasks or transport tasks between the communicating tasks. Special approximate performance models were developed for the study of large systems of software pipelines that use the rendezvous for inter-process communication and are

supported with transport tasks or mailbox tasks between their stages. Three approximations for pipelines with transport tasks were derived, based on different analyses. One approximation was derived for pipelines with mailbox tasks and was extended to evaluate merging systems. Exact solutions based on Petri net models were used to evaluate the approximations and to examine the effect of buffering on pipeline systems. Author (CISTI)

N92-33217 Carleton Univ., Ottawa (Ontario). Dept. of Systems and Computer Engineering.
A FAST TASK ALLOCATOR FOR MULTIPROCESSING SYSTEMS Ph.D. Thesis
Gerald G. Monforton 28 Jul. 1989 118 p
(ISBN-0-315-54380-9; CTN-92-60532) Copyright Micromedia Ltd., Technical Information Centre, 165 Hotel de Ville, Place du Portage, Phase 2, Hull, Quebec J8X 3X2, Canada HC/MF

A static allocator which partitions software tasking networks onto multiprocessing systems is developed. The method proposes extensions to existing heuristic bin-packing and clustering techniques. A number of alternate options for the major steps in the algorithm are presented and their effectiveness is examined. A throughput bound calculation, which takes into account both the processor and communication link workloads, is the performance measure used to evaluate the allocations. The allocator does not achieve exact optimization, but is executable in polynomial time and is therefore suitable for large systems. Comparisons with optimal allocations of small systems found an average of 1 percent difference in performance, using a specified subset of the available options. The allocator also found solutions for a number of problems introduced by previous researchers, as well as a 119 task digital signal processing system. CISTI

N92-33224 Concordia Univ., Montreal (Quebec). Dept. of Electrical and Computer Engineering.
DIAGNOSABILITY AND DIAGNOSIS OF SPARSELY INTERCONNECTED MULTIPROCESSOR SYSTEMS Ph.D. Thesis
Anindya Das Oct. 1989 208 p
(ISBN-0-315-56107-6; CTN-92-60535) Copyright Micromedia Ltd., Technical Information Centre, 165 Hotel de Ville, Place du Portage, Phase 2, Hull, Quebec J8X 3X2, Canada HC/MF

Diagnosable multiprocessor systems are characterized, and it is shown how some reported characterizations can be easily modified to arrive at a characterization for the Barsi, Grandoni, and Maestrini model as well as characterizations for the sequentially diagnosable systems. Certain structural properties of general diagnosable systems are presented which lead to a new characterization. With the objective of determining an efficient test for a vertex to be in an allowable fault set of size at most t, several properties of allowable fault sets are established. An algorithm is then developed for diagnosis of a $t/t + 1$ diagnosable system. A $t/t + k$ diagnosis algorithm is also presented which runs in polynomial time for each fixed positive integer, k. It is shown how these algorithms can be modified to construct algorithms for sequential t-diagnosis. The comparison based approach is used to develop a theory wherein, instead of a single global constraint, local fault constraints on the number of faulty processors in the neighborhood of each processor in a multiprocessor system are considered. The local domain diagnosability of certain regular interconnected systems is studied, and diagnosis algorithms for these systems are included which can be executed in a distributed manner on the system itself. Author (CISTI)

N92-33235 McGill Univ., Montreal (Quebec). School of Computer Science.
MESSAGE DELAY MODELS OF PACKET-SWITCHING NETWORKS Ph.D. Thesis
Claude Evequoz Jun. 1989 250 p
(ISBN-0-315-57208-6; CTN-92-60538) Copyright Micromedia Ltd., Technical Information Centre, 165 Hotel de Ville, Place du Portage, Phase 2, Hull, Quebec J8X 3X2, Canada HC/MF

The prediction of mean end-to-end delay of multiple packet messages is studied. Two distinct models are developed that depend on the traffic load requested by network users. The first considers traffic conditions in which the traffic demand heavily loads the computer network. Mean end-to-end message delays are computed by assuming the existence of a product form solution of the obtained closed queueing network model. Heuristics are developed and validated via simulation to render the computation feasible and to extend the solution method to nonproduct form networks. Under light traffic conditions, clusters of packets resulting from message segmentation may enter the computer network. To this end, algorithms are developed to determine the network performance measures of closed queueing networks in which bulk transactions are possible. A second message delay model is then developed to take into account the clustered arrival of packets to the network. All models and heuristics are validated via simulation. Finally, the appropriate length of the packets into which a message should be segmented is addressed. The performance tradeoff between message delay and throughput is discussed. Boundaries delimiting the packet size to meet user requirements are established for delay and throughput. Author (CISTI)

63 CYBERNETICS

Includes feedback and control theory, artificial intelligence, robotics and expert systems.

For related information see also *54 Man/System Technology and Life Support.*

N92-32625# Cincinnati Univ., OH. Dept. of Electrical and Computer Engineering.
INTELLIGENT SIGNAL PROCESSING FOR ACTIVE CONTROL Final Report
P. A. Ramamoorthy 17 Jun. 1992 40 p
(Contract N00014-89-J-1633)
(AD-A252232) Avail: CASI HC A03/MF A01

This research is concerned with the use of neural architectures and fuzzy expert systems in nonlinear system identification and in the control of such systems. In particular, on-line identification/modeling is considered. The research has resulted in a technique where the network can evolve (in size) in time to provide an optimal model/controller. Also an adaptive algorithm, which is less sensitive to initial values of the weights and the learning rate, was developed. We have also established a common framework between neural networks and fuzzy expert systems and developed a neuro-fuzzy architecture that retains the best of the two areas. The architectures and the adaptation algorithm were demonstrated in a number of applications. GRA

N92-32748# Naval Postgraduate School, Monterey, CA. Dept. of Computer Science.
RATIONAL BEHAVIOR MODEL: A TRI-LEVEL MULTIPLE PARADIGM ARCHITECTURE FOR ROBOT VEHICLE CONTROL SOFTWARE
Se-Hung Kwak, R. B. McGhee, and T. E. Bihari Mar. 1992 35 p
(AD-A250370; NPSCS-92-003) Avail: CASI HC A03/MF A01

Computer control of robot vehicles of operation in unstructured environment typically involves both symbolic reasoning and numerical computation. Based on earlier experiences this paper proposes a three level architecture for control software for such vehicles. From the top down, the three levels are called the strategic level, the tactical level, and the execution level. This paper argues that a multiple paradigm multi-lingual approach facilitates the realization of such a scheme with logic programming, object-oriented/functional programming, and imperative programming respectively being used in the successive levels. Experiments are reported in which Prolog is used at the strategic level, Lisp or C++ at the tactical level, and Pascal or C at the execution level. Experience with control of a large six legged walking machine and an autonomous submarine has led the authors to the belief that the proposed software architecture greatly

facilitates the development and utilization of such vehicles through the isolation of a concise operational doctrine expressed horn clause form at the strategic level of control. GRA

N92-32854# Defence and Civil Inst. of Environmental Medicine, Downsview (Ontario).
SHAPE RECOGNITION BY COMPUTER IN SIMULATED AERIAL IMAGES M.S. Thesis - Queen's Univ., Kinston, Ontario
Tim R. H. Cutmore Jan. 1991 35 p
(DCIEM-91-05; CTN-92-60387) Avail: CASI HC A03/MF A01

Visual recognition of objects by a machine involves classifying an input using knowledge about the kinds of objects expected in the domain. Since a given object type may appear in a variety of forms and under a variety of viewing conditions, some efficient yet flexible means are required for guiding the recognition process to consider and then verify the object identity. The utility of low resolution shape information to constrain object recognition was investigated in the context of a system which is predicated upon a component description of objects. A computationally intensive prepass using a syntax for combining components yields a universe of constructions which are coded into a construction relation feature (CRF) map. Each construction is coded into the N-dimensional map according to a shape parameterization of its low resolution image (each dimension codes a shape feature). From a subset of these constructions, object models are specified in terms of their component structure. The CRF map, thus, links the low resolution shapes of an instance of an object as its object model. To recognize an unknown object, the input is first converted to low resolutions. Then, shape parameters are taken. The CFR map is examined in the region of these feature coordinates for possible matches with object models, first on the basis of a component match followed by a verification of the relations between components.
Author (CISTI)

N92-33019* National Aeronautics and Space Administration. Pasadena Office, CA.
OBSTACLE AVOIDANCE FOR REDUNDANT ROBOTS USING CONFIGURATION CONTROL Patent
Homayoun Seraji, inventor (to NASA) (Jet Propulsion Lab., California Inst. of Tech., Pasadena.), Richard D. Colbaugh, inventor (to NASA) (Jet Propulsion Lab., California Inst. of Tech., Pasadena.), and Kristin L. Glass, inventor (to NASA) (Jet Propulsion Lab., California Inst. of Tech., Pasadena.) et al 22 Sep. 1992 8 p Filed 19 Nov. 1990 Supersedes N91-23783 (29 - 15, p 2489)
(NASA-Case-NPO-17852-1-CU; US-Patent-5,150,026;
US-Patent-Appl-SN-615668; US-Patent-Class-318-568.11;
US-Patent-Class-318-567; US-Patent-Class-318-568.19;
US-Patent-Class-364-191; US-Patent-Class-901-47;
US-Patent-Class-395-90; Int-Patent-Class-G05B-19/42) Avail: US Patent and Trademark Office

A redundant robot control scheme is provided for avoiding obstacles in a workspace during the motion of an end effector along a preselected trajectory by stopping motion of the critical point on the robot closest to the obstacle when the distance between is reduced to a predetermined sphere of influence surrounding the obstacle. Algorithms are provided for conveniently determining the critical point and critical distance.
Official Gazette of the U.S. Patent and Trademark Office

N92-33184# Maryland Univ., College Park. Dept. of Mechanical Engineering.
JACOBIAN AND STIFFNESS ANALYSIS OF A NOVEL CLASS OF SIX-DOF PARALLEL MINIMANIPULATORS
F. Tashmasebi and Lung-Wen Tsai 1992 8 p Presented at the 22nd American Society of Mechanical Engineers (ASME) Biennial Mechanisms Conference, Scottsdale, AZ, Sep. 1992
(Contract DE-FG05-88ER-13977)
(DE92-016373; CONF-9209143-2) Avail: CASI HC A02/MF A01

The Jacobian and stiffness matrices of two types of novel, six-DOF parallel minimanipulators are derived. A minimanipulator consists of three inextensible limbs, each of which is driven by a two-DOF driver. Bilinear stepper motors are used as drivers in the first type minimanipulator, whereas, five-bar linkages are used as drivers in the second type minimanipulator. All of the minimanipulator actuators are base-mounted. Inextensible limbs (and five-bar linkage drivers in the second type minimanipulator) improve positional resolution and stiffness of the minimanipulators in certain directions. It is shown that, at the central configuration, the stiffness matrix of the first type minimanipulator can be diagonalized (decoupled). It is also shown that the first type minimanipulator can be designed to possess direct or torsional isotropic stiffness properties. Moreover, guidelines for designing the drivers of the second type minimanipulator are established.
DOE

N92-33203 Alberta Univ., Edmonton.
A HYBRID NUMERICAL/KNOWLEDGE BASED SYSTEM FOR LOCOMOTION CONTROL OF A MULTI-LEGGED ARTICULATED ROBOT Ph.D. Thesis
Ahmed S. Mohamed 1989 191 p
(ISBN-0-315-52925-3; CTN-92-60528) Copyright Micromedia Ltd., Technical Information Centre, 165 Hotel de Ville, Place du Portage, Phase 2, Hull, Quebec J8X 3X2, Canada HC/MF

A model is proposed for understanding, synthesizing, and learning coordinated movements within a cohesive framework which combines the mathematical rigor of approaches taken in robotics, biomechanics, and artificial intelligence literature with the behavioral relevance of psychological approaches. The model is demonstrated in a locomotion control system for a four-legged articulated robot. One of the primary objectives of this research is to examine the effectiveness of merging the concepts of computer numerical control with the concepts of motor learning. The expected result is that both methodologies can act together to provide an autonomous motion control system that is capable of synthesizing and learning coordinated locomotive movements and improving its performance as a result of practice and experience. The proposed locomotion system currently navigates a four-legged articulated robot through a simulated environment containing obstacles such as holes and rough terrain. The equations of motion of the robot are solved by a recursive method, implemented on an IRIS-2400 graphics workstation. The robot must show some prudence in choosing the most appropriate locomotive skill at any point during its navigation, such as to slow down while turning a corner, to prefer the paths it has travelled on before, and to reduce its total energy consumption in executing a mission.
Author (CISTI)

N92-33218 Carleton Univ., Ottawa (Ontario). School of Computer Science.
LEARNING SYSTEMS, ADAPTIVE DATA STRUCTURES, AND RANDOM ENVIRONMENTS Ph.D. Thesis
David Tung Him Ng 21 Apr. 1989 175 p
(ISBN-0-315-51158-3; CTN-92-60533) Copyright Micromedia Ltd., Technical Information Centre, 165 Hotel de Ville, Place du Portage, Phase 2, Hull, Quebec J8X 3X2, Canada HC/MF

Ideas from the theory of learning automata are applied to practical problems encountered in computer science. Various adaptive data structures including the linear list, the doubly linked list, and the binary search tree are described. For each of these data structures, new heuristics to restructure the data are presented. The aspect of studying absorbing automata is achieved using the relatively new concept of random races, in which a number of racers are progressing along a discrete track towards a goal and the probability of the racers arriving in a particular sequence is evaluated. Models for stochastic environments are studied in which new techniques for generating random permutations with non-uniform distributions are presented and analyzed. Also, in order to improve the asymptotic cost of retrieval in adaptive data structures, the novel idea of transparently modifying the user's query patterns was studied. The latter leads to methods which yield query patterns that are sharper and more informative from the point of view of the data reorganizing scheme. The decrease in the asymptotic cost of retrieval considerably improves

the data retrieval characteristics of these systems.
Author (CISTI)

N92-33219 Carleton Univ., Ottawa (Ontario). Dept. of Systems and Computer Engineering.
A STUDY OF ARTIFICIAL INTELLIGENCE PLANNING: A FRAMEWORK FOR A PLANNING DEVELOPMENT SYSTEM M.S. Thesis
Carl Roth Sep. 1989 173 p
(ISBN-0-315-54378-7; CTN-92-60534) Copyright Micromedia Ltd., Technical Information Centre, 165 Hotel de Ville, Place du Portage, Phase 2, Hull, Quebec J8X 3X2, Canada HC/MF
In a study of artificial intelligence planning, a framework for a planning development system is presented to be used as an aid to evaluating the vast array of planning approaches and techniques. An in-depth examination of planning as a field of artificial intelligence is presented. In particular, a comparative survey is made of planning systems that have been important to the field. A STRIPS style planner called the Puzzler is discussed, as it demonstrates some planning concepts and key techniques in solving a block puzzle problem. The framework for the planning development system presented is both modular and flexible. Its unifying concept of operators enables a variety of operator types to be invoked using a common control mechanism and global data structure. A separate constraint satisfaction mechanism allows sophisticated planning approaches to be modeled. The standardization and formalization of planning are also discussed.
Author (CISTI)

N92-33236 Carleton Univ., Ottawa (Ontario). Dept. of Systems and Computer Engineering.
INVESTIGATIONS OF ADAPTIVE CONTROL FOR A DIRECT DRIVE ROBOTIC MANIPULATOR M.S. Thesis
Gabriel D. Warshaw 19 Jan. 1990 150 p
(ISBN-0-315-59030-0; CTN-92-60549) Copyright Micromedia Ltd., Technical Information Centre, 165 Hotel de Ville, Place du Portage, Phase 2, Hull, Quebec J8X 3X2, Canada HC/MF
High speed robotic manipulators, such as direct drive manipulators, require effective controller designs. A number of adaptive control techniques have been proposed which offer stable and accurate performance. The direct and indirect methods of model-based adaptive control were selected for investigation. Simulation of a two degree of freedom direct drive manipulator is used to demonstrate how adaptive control laws can lead to inferior performance when the richness condition is not satisfied. A non-identifiable desired trajectory is chosen and a realistic level of Gaussian white noise is added to the velocity and acceleration measurements. Without persistent excitation, the control algorithms perform worse than a proportional derivative controller alone. Errors in parameter estimation, even after convergence, cause the manipulator to deviate from its desired path. Prior to convergence of the parameter estimates, adaptive control of the manipulator produces unacceptably large errors. The integration of a two degree of freedom, direct drive manipulator system is also described. Control algorithms for single joint motion were tested and simulation results were validated. Author (CISTI)

N92-32442# Naval Weapons Center, China Lake, CA. Attack Weapons Dept.
TARGET CUING: A HETEROGENEOUS NEURAL NETWORK APPROACH
Howard McCauley *In* AGARD, Integrated Target Acquisition and Fire Control Systems Feb. 1992 4 p (For primary document see N92-32437 23-06)
Copyright Avail: CASI HC A01/MF A02; 1 functional color page

64 NUMERICAL ANALYSIS

Includes iteration, difference equations, and numerical approximation.

N92-32428# Oak Ridge National Lab., TN.
A TIGHT AND EXPLICIT REPRESENTATION OF Q IN SPARSE QR FACTORIZATION
E. G. Ng and B. W. Peyton May 1992 33 p
(Contract DE-AC05-84OR-21400)
(DE92-014814; ORNL/TM-12059) Avail: CASI HC A03/MF A01
In QR factorization of a sparse m x n matrix A (m greater than or equal to n) the orthogonal factor Q is often stored implicitly as a lower trapezoidal matrix H known as the Householder matrix. This paper presents a simple characterization of the row structure of Q, which could be used as the basis for a sparse data structure that can store Q explicitly. The new characterization is a simple extension of a well known row-oriented characterization of the structure of H. Recently, a complete sparsity analysis of the QR factorization was provided. Let U be the matrix consisting of the first n columns of Q. We show that the data structures for H and U resulting from our characterizations are tight when A is a strong Hall matrix. We also show that H and the lower trapezoidal part of U have the same sparsity characterization when A is strong Hall. We then show that this characterization can be extended to any weak Hall matrix that has been permuted into block upper triangular form. Finally, we show that permuting to block triangular form never increases the fill incurred during the factorization.
DOE

N92-32602# Gosudarstvennyi Komitet po Ispolzovaniyu Atomnoi Energii, Serpukhov (USSR). Inst. Fiziki Vysokikh Ehnergij.
EQUIVALENCE BETWEEN LAGRANGIAN AND HAMILTONIAN BRST FORMALISMS
Kh. S. Nirov and A. V. Razumov 1991 29 p
(DE92-624556; IHEP-OTF-91-67) Avail: CASI HC A03/MF A01
Gauge invariant systems are mechanical systems for which it is possible to find a set of symmetry transformations parameterized by arbitrary functions of time. All gauge invariant systems are described by singular Lagrangians. This leads to the appearance of constraints in the Hamiltonian description. For a wide class of gauge invariant systems the equivalence between Lagrangian and Hamiltonian BRST formalisms is proven. DOE

N92-32661# Instituto de Pesquisas Espaciais, Sao Jose dos Campos (Brazil).
FINDING SOLUTIONS TO VALUE INDEPENDENT KNAPSACK PROBLEMS
Horacio Hideki Yanasse and Nei Yoshihiro Soma (Sheffield Univ., England) May 1992 31 p
(Grants SERC/GR/F/68942; CNPQ-201237/88.1)
(INPE-5390-TAE/011) Avail: CASI HC A03/MF A01
An enumeration scheme to find the k-best solutions to the value independent knapsack problem is presented. The scheme requires O(N(B-A(1))) of memory allocation where A(1), without loss of generality, is the smallest coefficient of the knapsack constraint. Memory requirements may be reduced to O(B-A(1)) with a slight deterioration in computational performance when retrieving the k-best solutions. Similar schemes are presented for the 0-1 case and when the variables have explicit upper bounds.
Author

N92-32670# Texas A&M Univ., College Station.
APPLICATION OF GAUGE THEORIES TO ENHANCE NUMERICAL SOLUTIONS TO MIXED POTENTIAL INTEGRAL EQUATIONS
R. D. Nevels 10 Apr. 1992 1 p
(Contract N00014-90-J-1334)
(AD-A248451) Avail: CASI HC A01/MF A01
The purpose of this research is to incorporate new advances in gauge techniques currently being researched in mathematical physics into numerical electromagnetic scattering routines with an

emphasis on improving computation speeds and the versatility of current methods. During this past year, we have developed a new scheme for solving two dimensional electromagnetic scattering problems in which the scatterer can be inhomogeneous. The Fourier Transform Path Integral Method (FTPI) is based on the Feynman path integral which is a Green's function for inhomogeneous regions. Although originally proposed in the late 1940', path integral applications have been restricted to a limited variety of problems in quantum physics. This has been the case primarily because it is not a closed form expression but rather a sequence of nested integrals with infinite limits, which can only be evaluated by making stringent approximations that in turn limit the geometries to which it is applicable. Our contribution has been that we were able to transform the original path integral into a form where the nested sequence becomes successive Fourier and inverse Fourier transforms. We can now take advantage of the well known fast Fourier transform (FFT) routines currently available to evaluate the path integral. Over the past year, we have worked on solving electromagnetic field problems in one and two dimensions and on the dual problem of determining the scattering coefficients for a particle in the presence of a potential barrier. GRA

N92-32679# Universiteit Twente, Enschede (Netherlands).
CONSISTENCY AND ROBUSTNESS OF KNOWLEDGE GRAPHS Ph.D. Thesis
Herman Jannes Smit 1991 191 p
(ISBN-90-9003729-2; ETN-92-92046) Copyright Avail: CASI HC A09/MF A02

A project for the construction and analysis of a knowledge graph that represents a scientific theory on the domain of medicine or social science is presented. The construction of a knowledge graph consists of procedures for the extraction of knowledge from several documents and of the procedures for the integration and structuring of the extracted knowledge. Complex relations that can be represented by a knowledge graph are used to create a hierarchy in the represented knowledge in order to inspect a knowledge graph at different levels of abstraction. The foundations of reasoning on knowledge graphs are based upon the properties of a path algebra structure. The project consistency and robustness of knowledge graphs is directed at the development of a consistency concept for knowledge graphs for the detection and handling of inconsistencies, and the development of measures for the robustness of the integrated knowledge structure. For the validation of the developed techniques, the progam KISS (Knowledge Integration and Structuring System) was developed. The developed methods and techniques were tested using different knowledge graphs in the domains of social dentistry and lung diseases. ESA

N92-32684# Grenoble-1 Univ. (France). Lab. de Modelisation et Calcul.
BANDWIDTH SELECTION FOR THE INTENSITY OF POINT PROCESSES: APPLICATION TO HAZARD RATE MODELS FOR CENSORED DATA
Gerard Gregoire Jul. 1991 32 p
(IMAG-RR-859-I/M; ETN-92-92079) Avail: CASI HC A03/MF A01

A procedure for choosing the bandwidth when the intensity of a counting process is estimated by a kernel method is presented. We assume that we are given an Aalen multiplicative model. The problem of choosing the bandwidth when smoothing the Aalen-Nelson estimator by the kernel method is addressed. The procedure is based on a leave-one-out method and provides an estimate of the ISE (Integrated Square Error) error. The precise form of the asymptotic expansion of the Mean USE (MISE) and some technical results are given. The estimate is proved to have a bias vanishing at a rate which is slightly smaller than n to the -1 power and that it is consistent. The particular case of censored survival data is considered and the performance of the procedure is checked via simulations. ESA

N92-32685# Grenoble-1 Univ. (France). Lab. de Modelisation et Calcul.
BOOTSTRAPPING THE CHANGE-POINT OF A HAZARD RATE
Tuan D. Pham and Hung T. Nguyen (New Mexico State Univ., Las Cruces.) Oct. 1991 15 p
(IMAG-RR-861-M; ETN-92-92080) Avail: CASI HC A03/MF A01

The asymptotic validity of the bootstrap method in a nonregular model is addressed. Specifically, the parametric bootstrap of the change point parameter in the change-point hazard rate model is shown to work. The model and bootstrap method for obtaining the distribution of the estimator are described. ESA

N92-32707# Technische Univ., Eindhoven (Netherlands).
STEADY STATE BEHAVIOR OF REDUCED DYNAMIC SYSTEMS WITH LOCAL NONLINEARITIES Ph.D. Thesis
Robertus Henricus Ba Fey 1992 130 p Sponsored by Inst. TNO voor Werktuigkundige Constructies
(ISBN-90-9004680-1; ETN-92-92050) Avail: CASI HC A07/MF A02

The long term behavior, also called steady state behavior, of complex dynamic systems with local nonlinearities, which are excited by periodic external loads, is addressed. The steady state behavior of a nonlinear dynamic system can have a periodic, quasiperiodic, or a chaotic character. Periodic solutions are calculated efficiently by solving a two point boundary value problem by applying a time discretization method (finite difference method). The local stability of a periodic solution is investigated using Floquet theory. The steady state behavior is investigated by means of standard numerical integration. In this case the character of the steady state behavior (periodic, quasiperiodic, or chaotic) is identified by calculation of the Lyapunov exponents and the Lyapunov dimension. The methods presented are applied to a harmonically excited beam system with different nonlinear supports, such as stiffening spring, a one sided stiffening spring, and a one sided linear spring. Superharmonic, subharmonic, and internal resonances are evaluated and bifurcations are met frequently. In systems with a one sided linear spring three transitions to chaos are observed: a transition via period doubling, intermittency, and a quasiperiodic locked chaotic transition. ESA

N92-32710# Grenoble-1 Univ. (France). Lab. ARTEMIS.
MINIMUM COST MULTIFLOWS IN UNDIRECTED NETWORKS
Alexander V. Karzanov (Institute for System Studies, Moscow, USSR) Apr. 1991 24 p
(IMAG-RR-849-M; ETN-92-92067) Avail: CASI HC A03/MF A01

A problem arising as a natural extension of the classical minimum-cost maximum-flow problem and the problem of finding a collection of flows (a multiflow) in an undirected network, such that a flow connecting any two terminals is allowed and the sum of values of these flows is maximum, is studied. It is known, due to Cherkasskji and Lovasz, that the latter problem has a half integral solution when the capacity function is integral. The problem of finding a multiflow (consisting of flows between any pairs of terminals) whose total cost is minimum provided that the sum of values of the partial flows is maximum is considered. It is proved to have a half integral optimal solution whenever the capacities are integral. A pseudopolynomial algorithm to solve this problem is described and the existence of a half integral optimal dual solution is shown. A strongly polynomial algorithm for finding half integral optimal primal and dual solutions is developed. ESA

N92-32711# Grenoble-1 Univ. (France). Lab. ARTEMIS.
A MIN-MAX RELATION FOR K3-COVERS IN GRAPHS NONCONTRACTIBLE TO K5/e
A. R. Mahjoub (King Saud Univ., Riyadh, Saudi Arabia) Apr. 1991 15 p
(IMAG-RR-850-I; ETN-92-92068) Avail: CASI HC A03/MF A01

The triangle free subgraph polytope of a graph noncontractible to K5/e, proved to be completely described by the trivial inequalities and the so called triangle and odd weel inequalities, is addressed. The system defined by those inequalities is shown to be totally

dual integral. As a consequence, the following min-max relation is obtained: if G is a graph noncontractible to K5/e, then the minimum number of edges covering all the triangles of G equal the maximum profit of a collection of mutually edge disjoint triangles and odd wheels in G. Here the profit of a triangle is 1 and the profit of a 2k + 1 wheel is equal to k + 1. ESA

N92-32713# Grenoble-1 Univ. (France). Lab. Structures Discretes et Didactiques.

CHARACTERIZATION OF LABORDE-MULDER GRAPHS AND THE HALFCUBE [CARACTERISATION DES GRAPHES DE LABORDE-MULDER ET DU DEMI-CUBE]

Rafai-Mourad Madani (Universite des Sciences et de la Technologie Houari Boumediene, Algiers, Algeria) Jul. 1991 10 p In FRENCH

(IMAG-RR-857-I; ETN-92-92070) Avail: CASI HC A02/MF A01

The Laborde-Mulder (LM) graphs (also called extended odd graphs) and the halfcube are addressed. Identification of antipodic vertices in the n dimensional cube (n greater than or equal to three) leads to a (0, 2) graph on 2(sup (n - 1)) power vertices, regular of degree n and of diameter closed interval (n/2); such graphs are called LM for n odd, and for n even the halfcubes are obtained. A proof that a (0, 2) graph on 2(sup (n - 1)) power vertices, regular of degree n, has a diameter at least closed interval (n/2), is given; further, the diameter is exactly closed interval (n/2) if an only if the graph is a LM or a halfcube graph. A proof that the identification of vertices joined by the edges of a given matching leads to a (0,2) graph on 2(sup (n - 2)) power vertices, regular of degree (n - 1) and of diameter closed interval ((n - 1)/2), is given. ESA

N92-32729# Aeronautical Research Inst. of Sweden, Stockholm. Aerodynamics Dept.

IMPROVED DISSIPATION MODELS FOR CENTRAL DIFFERENCE SCHEMES

Peter Eliasson 10 Jul. 1991 35 p

(FFA-TN-1991-41; ETN-92-91980) Avail: CASI HC A03/MF A01

Different numerical dissipation models for central difference schemes are tested. The standard Jameson type of dissipation is compared with numerical dissipation models constructed from flux limiters as in upwind methods. A scalar model equation is used to give conditions for the dissipation models to produce a Total Variation Diminishing (TVD) scheme. In all cases, central or upwind, the numerical flux can be written as a central flux plus additional dissipation terms. Several models are tested. Different types of limiters are used to limit the solution in order to ensure satisfaction of the TVD property. It is shown that the resolution and accuracy can be improved compared to the standard dissipation model when computing the one dimensional shock tube problem for the Euler equations. ESA

N92-32743# Lawrence Livermore National Lab., CA.

ADVANCED COMPUTATIONAL TRANSPORT METHODS FOR CURVILINEAR GEOMETRIES

W. R. Martin (Michigan Univ., Ann Arbor.), E. W. Larsen (Michigan Univ., Ann Arbor.), T. S. Palmer, and M. L. Adams 30 Oct. 1991 7 p

(Contract W-7405-eng-48)

(DE92-011290; UCRL-CR-109223) Avail: CASI HC A02/MF A01

During the last year, a considerable effort was mounted to devise accurate and efficient numerical methods for the solution of curvilinear transport problems in the optically thick, diffusive regime. Much work has already been completed on these methods in slab and x-y geometries. The principle tool in designing these methods is an asymptotic analysis that permits one to theoretically assess the accuracy of a transport numerical method for diffusive regions in which the spatial grid is optically thick. A transport numerical method is said to be accurate for thick, diffusive problems if an asymptotic analysis yields an accurate discretized diffusion equation and accurate boundary conditions. If a given transport discretization has this property, then it is possible to incorporate this 'asymptotic' diffusion equation into a diffusion synthetic acceleration (DSA) algorithm that will yield a very rapidly convergent iterative solution. The search for efficiently solvable DSA algorithms in one and two spatial dimensions has been going on for the past 20 years. Although many techniques are available now in one-dimensional geometries, in other geometries only the diamond differenced S(sub N) equations have been efficiently solved using conventional DSA. This is because this particular transport differencing yields a sufficiently simple low-order diffusion equation that lends itself to solution by multigrid methods. Conventional DSA when applied to most other transport discretizations leads to more complicated discrete diffusion equations that are not as efficiently solvable. The asymptotic analysis procedure outlined here is an attempt to overcome this obstacle. DOE

N92-32756# Technische Univ., Delft (Netherlands). Faculty of Technical Mathematics and Information.

POINT INTERACTIONS IN L(SUP p)

Wim Caspers and Philippe Clement 1991 22 p Submitted for publication

(Rept-91-97; ETN-92-91847) Copyright Avail: CASI HC A03/MF A01

An interpretation to point interactions of the form (-Delta + d) in L(sup p)(R(sup N)), where Delta is the Laplacian operator and d is a pseudopotential related to the 'Dirac measure at 0', depending on the dimension, is given. They are described as extensions of -Delta that are negative generators of analytic semigroups. This is done for N = 1,2 and p greater than 1 and less than infinity, and for N = 3 and p greater than 3/2 and less than 3. ESA

N92-32761# Grenoble-1 Univ. (France). Lab. de Modelisation et Calcul.

GEOMETRIC CONTINUITY AND FRENET CONTINUITY OF PARAMETRIC CURVES

Marie-Laurence Mazure Mar. 1991 26 p

(IMAG-RR-846-M; ETN-92-92075) Avail: CASI HC A03/MF A01

The notion of Frenet continuity of order p (F(sup p)) for parametric curves in the set of real numbers R(sup d) is defined in a new geometrical way and is compared to geometric continuity of order p (G(sup p)). ESA

N92-32772# Office National d'Etudes et de Recherches Aerospatiales, Paris (France). Direction de l'Aerodynamique.

RESOLUTION OF CONVECTION AND DIFFUSION BY THE BOOLEAN AUTOMATA METHOD Final Report [RESOLUTION D'EQUATIONS DE CONVECTION ET DE DIFFUSION PAR UNE METHODE D'AUTOMATES BOOLEENS. RAPPORT FINAL]

J. Ryan Nov. 1991 25 p In FRENCH

(Contract DRET-89-34-001)

(ONERA-RF-22/3419-AY-122A; ETN-92-91670) Avail: CASI HC A03/MF A01

An algorithm of the boolean automata parallelizable for the binary bits, was developed to solve the differential equations of convection and diffusion. The equations are discretized by the finite difference method and cartesian grids with variable steps are applied. The boolean elements represent the real variables and the logic operators represent the algebraic real operators. Accuracy was implemented and the cost analysis is presented. The algorithm was implemented on a Cray XMP 416 computer. The best system for this algorithm is a parallel computer with few bits, optimized for binary operations and allowing fast communication in regular grids. ESA

N92-32796# Universiteit Twente, Enschede (Netherlands). Faculty of Applied Mathematics.

HIERARCHICAL SETS IN MATHEMATICAL PROGRAMMING MODELING LANGUAGES

J. J. Bisschop and C. A. C. Kuip Aug. 1991 22 p

(MEMO-990; ETN-92-91747) Avail: CASI HC A03/MF A01

The mathematical notation commonly applied for the formulation of mathematical programming models is extended to include

hierarchical structures. The proposed notation is related to hierarchical set concepts in the languages UIMP, AMPL, and LPL. With the proposed notation it is possible to aggregate and disaggregate over hierarchical structures. In addition, views are introduced to permit the use of hierarchical substructures and to create new hierarchies out of existing ones. The proposed notation for hierarchical sets and views is illustrated by applying it to the representation and estimation of Social Accounting Matrices (SAMs). ESA

N92-32798# Universiteit Twente, Enschede (Netherlands).
ASPECTS OF SOLVING NON-LINEAR BOUNDARY VALUE PROBLEMS NUMERICALLY Ph.D. Thesis
Martina Elijda Kramer 1992 154 p
(ETN-92-92049) Avail: CASI HC A08/MF A02

The conditioning of both linear and nonlinear Boundary Value Problems (BVPs) and the relation between conditioning, dichotomy, and boundary conditions, are reviewed. Existing solution methods for BVPs are described and an estimate for the Lipschitz constant of the Jacobian of f(s) is derived. Preconditioned time stepping is addressed. Convergence and implementation of the mixed Euler integration method are described. The formulation and properties of the preconditioner are addressed and the generalization of multiple shooting is considered. ESA

N92-32799# Grenoble-1 Univ. (France). Lab. de Modelisation et Calcul.
DISSIMILARITIES, DENDOGRAMS, PREFILLERS, AND MULTIAPPLICATIONS OF LEVELS [DISSIMILARITES, DENDROGRAMMES, PREFILTRES ET MULTIAPPLICATIONS DES NIVEAUX]
Frank Critchley (Warwick Univ., Coventry, England) and Bernard VanCutsem (Warwick Univ., Coventry, England) Feb. 1991 20 p In FRENCH
(IMAG-RR-842-M; ETN-92-92074) Avail: CASI HC A03/MF A01

Improvements in the representation of an ultrametric on a finite set S by its dendogram are reviewed. The possibility of giving a general bijection between nonsymmetric dissimilarities defined on a set S with values in an ordered set L and some nondecreasing families of subsets of S(sup 2) indexed by L is demonstrated. The restrictions of these bijections to particular dissimilarities provide interesting representations. These results generalize those which were known for ultrametrics or dissimilarities on a finite set S. ESA

N92-32802# Ecole Nationale Superieure des Telecommunications, Paris (France). Groupe Image.
CONTINUOUS AND DISCRETE PROBLEMS IN IMAGE PROCESSING [PROBLEMES CONTINUS ET DISCRETS EN TRAITEMENT DES IMAGES]
Marc Sigelle Sep. 1991 10 p In FRENCH
(Telecom-91-D-007; ETN-92-92093) Avail: CASI HC A02/MF A01

A study to show the relation which exists between continuous variational formulation and discrete Markovian formulation of some image processing problems is presented. In particular, the problem of multiclass image restoration is shown to be able to be reduced to convolution filtering in some simple cases. Ising and Potts models for discrete formulation in image restoration are recalled. ESA

N92-32803# Ecole Nationale Superieure des Telecommunications, Paris (France). Groupe Image.
CONTRIBUTION TO THE DETERMINATION OF VANISHING POINTS USING HOUGH TRANSFORM
Evelyne Lutton, Henri Maitre, and Jaime Lopez-Krahe Sep. 1991 39 p Sponsored by Direction des Recherches, Etudes et Techniques and MATRA Espace
(Telecom-91-D-008; ETN-92-92094) Avail: CASI HC A03/MF A01

A method to locate three vanishing points on an image, corresponding to three orthogonal directions of the scene, based on two cascaded Hough transforms, is proposed. It is shown that even in the case of synthetic images of high quality, a naive approach may fail, essentially because of the errors due to the limitation of the image size. The errors, and errors due to detection inaccuracy of the image segments, are taken into account, and an efficient method, even in the case of real complex scenes, is provided. ESA

N92-32836# Technische Univ., Delft (Netherlands).
GENERALIZATIONS OF THE CLASSICAL LAGUERRE POLYNOMIALS AND SOME q-ANALOGUES Ph.D. Thesis
Roelof Koekoek 1990 111 p
(ISBN-90-9003765-9; ETN-92-92022) Copyright Avail: CASI HC A06/MF A02

The definition of the classical Laguerre polynomials and some of their properties are given with notations and terminology. The definition and some important properties of the new generalized Laguerre polynomials are given. Some properties of Koornwinder's generalized Laguerre polynomials are listed. A proof of the differential equation of infinite order is given. Another special case of the polynomials, the simplest case where the inner product cannot be derived from a weight function, is addressed. Some results concerning the zeros in this and some other special cases are given. A q-analog of the classical Laguerre polynomials is considered. This is not the only q-analogue of the Laguerre polynomials. Similar results can be found for other q-analogues. These particular q-Laguerre polynomials satisfy two different kinds of orthogonality relations. The definition and some properties of the generalizations of these q-Laguerre polynomials are given. These polynomials can be considered as q-analogues of the polynomials given earlier. A special case is considered and results concerning the zeros of these polynomials which contradict possible conjectures which may arise from the results earlier are given. ESA

N92-32838# Grenoble-1 Univ. (France). Lab. de Modelisation et Calcul.
POINCARE NORMAL FORM (SYSTEM OF ORDINARY DIFFERENTIAL EQUATIONS): AN ALGORITHMIC POINT OF VIEW
J. Della-Dora and L. Stolovitch Feb. 1991 18 p Sponsored by PRC Math-Info
(IMAG-RR-839-M; ETN-92-92071) Avail: CASI HC A03/MF A01

An algorithm for the computation of what can be called the Jordan canonical form of a nonlinear differential equation in the neighborhood of a singular point is provided. For this, the formal series is introduced on noncommutative indeterminates and a tensorial view point. ESA

N92-32840# Technische Univ., Berlin (Germany, F.R.). Fachbereich Mathematik.
SCHROEDINGER OPERATORS WITH SINGULAR POTENTIALS IN THE SEMICLASSICAL LIMIT Ph.D. Thesis
Klaus Chantelau 1991 45 p
(ETN-92-92145) Avail: CASI HC A03/MF A01

A study of the discrete spectrum of molecular Schroedinger operators is presented. The potentials under consideration have Coulomb type singularities. Since the problem of N electrons and n nuclei is highly complicated, approximations are made. More explicitly, the problem of one electron in the field of a finite number of fixed nuclei in two and three spatial dimensions is studied. To overcome difficulties due to the singularities, some kind of generalization of the Levi-Cavita transforms is used. After this regularization, the theory of smooth Schroedinger operators with nondegenerate minima of the potential can be applied to the full asymptotics for the eigenvalues in the semiclassical limit. ESA

N92-32888*# Ohio State Univ., Columbus. ElectroScience Lab.
NUMERICAL EVALUATION OF THE INCOMPLETE AIRY FUNCTIONS AND THEIR APPLICATION TO HIGH FREQUENCY SCATTERING AND DIFFRACTION Semiannual Report
E. D. Constantinides and R. J. Marhefka Sep. 1992 57 p

(Grant NsG-1492)
(NASA-CR-190745; NAS 1.26:190745; OSU-725311-1) Avail: CASI HC A04/MF A01

The incomplete Airy integrals serve as canonical functions for the uniform ray optical solutions to several high frequency scattering and diffraction problems that involve a class of integrals characterized by two stationary points that are arbitrarily close to one another or to an integration endpoint. Integrals of such analytical properties describe transition region phenomena associated with composite shadow boundaries. An efficient and accurate method for computing the incomplete Airy functions would make the solutions to such problems useful for engineering purposes. Here, a convergent series solution form for the incomplete Airy functions is derived. Asymptotic expansions involving several terms were also developed and serve as large argument approximations. The combination of the series solution form with the asymptotic formulae provides for an efficient and accurate computation of the incomplete Airy functions. Validation of accuracy is accomplished using direct numerical integration data. Author

N92-32989# Naval Underwater Systems Center, Newport, RI.
FEATURE DETECTION FOR MODEL ASSESSMENT IN STATE ESTIMATION
D. J. Ferkinhoff, J. G. Baylog, S. C. Nardone, and K. F. Gong 15 Oct. 1991 53 p
(AD-A252755; NUSC-TR-7064) Avail: CASI HC A04/MF A01

The presence of deterministic features in a residual sequence is oftentimes an indication of a modeling error in the state estimation process. Here, three methods of detecting and extracting the features of jump and/or drift in a predicted residual sequence are developed. Two of the methods are traditional ones. The first is a multiple hypothesis, generalized, likelihood ratio test that results in a chi-squared (XSQ) test statistic. The second is a similar, but computationally more efficient, intuitively derived test resembling a modified Neyman-Pearson (MNP) test. The third method is a nontraditional one; it uses a backpropagation artificial neural network (ANN) trained to emulate the MNP test. Monte Carlo experimental results show that the XSQ and MNP give essentially identical results, while the ANN--although apparently outperforming the XSQ in feature detection--does so at the expense of a higher feature misclassification probability, which is an undesirable effect. Overall, the ANN is judged as a feasible approach to feature detection, and improved performance is expected with better network training. GRA

N92-33006*# Institute for Computer Applications in Science and Engineering, Hampton, VA.
A BOUNDARY INTEGRAL METHOD FOR AN INVERSE PROBLEM IN THERMAL IMAGING Final Report
Kurt Bryan Aug. 1992 30 p Submitted for publication
(Contracts NAS1-18605; NAS1-19480; RTOP 505-90-52-01)
(NASA-CR-189693; NAS 1.26:189693; ICASE-92-38) Avail: CASI HC A03/MF A01

An inverse problem in thermal imaging involving the recovery of a void in a material from its surface temperature response to external heating is examined. Uniqueness and continuous dependence results for the inverse problem are demonstrated, and a numerical method for its solution is developed. This method is based on an optimization approach, coupled with a boundary integral equation formulation of the forward heat conduction problem. Some convergence results for the method are proved, and several examples are presented using computationally generated data. Author

N92-33058# Center for Mathematics and Computer Science, Amsterdam (Netherlands). Dept. of Operations Research, Statistics, and System Theory.
LIMIT THEOREMS FOR FUNCTIONALS OF CONVEX HULLS
A. J. Cabo and P. Groeneboom (Technische Hogeschool, Delft, Netherlands) Jun. 1991 23 p Submitted for publication
Sponsored by Netherlands Organization for Applied Scientific Research TNO
(CWI-BS-R9115; ETN-92-91641) Copyright Avail: CASI HC A03/MF A01

In a previous investigation a central limit theorem for the number of vertices of the convex hull of a uniform sample from the interior of a convex polygon was derived. This was done by approximating the process of vertices of the convex hull by the process of extreme points of a Poisson point process and by considering the latter process of extreme points as a Markov process. In this study, it is shown that this method can also be applied to derive limit theorems for the boundary length and for the area of the convex hull. This extends results of Renyi, Sulanke, and Buchta, and shows that the boundary length and the area have a strikingly different probabilistic behavior. The case of uniform samples from convex polygons are calculated, separately, since computations, involving second moments, are more complicated than for first moments. ESA

N92-33231 Toronto Univ. (Ontario).
COMPUTATIONS FOR ALGEBRAS AND GROUP REPRESENTATIONS Ph.D. Thesis
Wayne Eberly 1989 320 p
(ISBN-0-315-54684-0; CTN-92-60542) Copyright Micromedia Ltd., Technical Information Centre, 165 Hotel de Ville, Place du Portage, Phase 2, Hull, Quebec J8X 3X2, Canada HC/MF

Computational problems corresponding to the Wedderburn decomposition of matrix algebras over a field are studied. A simple and efficient probabilistic algorithm is presented for the computation of simple components of a semi-simple algebra. Probabilistic algorithms are also presented for the decomposition of simple algebras over C and R. If the inputs for these problems are algebraic numbers, and are represented as elements of a single number field, then the decompositions can be performed using exact computations, in polynomial time and with small probability of failure. It is well known that the problems of decomposing matrix algebras and of decomposing matrix representations of finitely generated groups are closely related. Formal reductions are stated between these compositional problems in order to obtain efficient algorithms for the problem of deciding whether a matrix representation is completely reducible, for the computation of isotypic components of a completely reducible matrix representation, and for computing a set of irreducible components of a completely reducible representation over C and over R. Efficient probabilistic algorithms for exact solutions of problems are obtained. The computation of character tables for various classes of groups is considered. Algorithms which have been observed to perform well in practice are analyzed.
Author (CISTI)

65 STATISTICS AND PROBABILITY

Includes data sampling and smoothing; Monte Carlo method; and stochastic processes.

N92-32481# Los Alamos National Lab., NM.
ANALYTIC SCORE COMPARISON OF GEOMETRY SPLITTING AND EXPONENTIAL TRANSFORM FOR A SIMPLE MONTE CARLO PROBLEM
T. E. Booth Mar. 1992 39 p
(Contract W-7405-eng-36)
(DE92-013108; LA-12258) Avail: CASI HC A03/MF A01

The interpretation of the statistical error estimates produced by Monte Carlo transport codes is still somewhat of an art. Empirically, there are variance reduction techniques whose error estimates are almost always reliable and there are variance reduction techniques whose error estimates are often unreliable. Unreliable error estimates usually result from inadequate large score sampling from the score distribution's tail. This paper provides the analytic score distribution for geometry splitting/Russian roulette applied to a simple Monte Carlo problem and the analytic score distribution for the exponential transform applied to the same Monte Carlo problem. It is shown that the large score tails of the

two distributions behave very differently. In particular, the exponential transform is shown to have an infinite variance for some parameter choices. DOE

N92-32709# Technische Univ., Eindhoven (Netherlands).
STATISTICAL SELECTION: MULTIPLE COMPARISON APPROACH Ph.D. Thesis
Stephanus Gerardus A Driessen 1992 173 p
(ETN-92-92051) Avail: CASI HC A08/MF A02

A study of statistical selection which is restricted to selection procedures for the normal distribution, probably the most important distribution from the viewpoint of applications, is presented. Only location parameters of univariate populations are considered, and focus is upon the selection of the treatment with the largest parameter value. The subject of Statistical Selection Procedures (SSPs) is introduced, and an attempt to place the contents of this thesis in the framework of ranking and selection theory is made. The origin of the SSPs, announced as better alternatives for the goal of selecting the best than the use of Multiple Comparison Procedures (MCPs), with or without the homogeneity test preceding, are addressed. Two SSPs are described and studied and the development SSPs, in a very specific direction, are sketched. MCB (Multiple Comparisons with the Best) intervals are proposed, and the subject of the specific selection constants that appear in the SSPs and the MCB intervals is addressed. ESA

N92-32716# Grenoble-1 Univ. (France). Lab. de Modelisation et Calcul.
A NEW FORM FOR THE CENTRAL LIMIT THEOREM [UNE NOUVELLE FORME POUR LE THEOREME DE LA LIMITE CENTRALE]
R. Blacher May 1991 21 p In FRENCH
(IMAG-RR-852-M; ETN-92-92077) Avail: CASI HC A03/MF A01

A form for the central limit theorem with hypothesis of asymptotical independence between the sequences of normalized sums is obtained. The assumption of uniformity of strong mixing sequences is suppressed. The same result is obtained for the hypothesis of stationarity. ESA

N92-32718# Grenoble-1 Univ. (France). Lab. de Modelisation et Calcul.
ON THE INCONSISTENCY OF BOOTSTRAP DISTRIBUTION ESTIMATORS
Peter Hall (Australian National Univ., Canberra.), Wolfgang Haerdle (Universite Catholique de Louvain, Belgium), and Leopold Simar (Brussels Univ., Belgium) Jul. 1991 12 p Sponsored in part by Universite Catholique de Louvain
(IMAG-RR-856-M; ETN-92-92078) Avail: CASI HC A03/MF A01

Bootstrap distribution estimators of a ranked parameter value are shown to be consistent if and only if there are no ties for the rank question. When inconsistency occurs, the bootstrap distribution estimator does not even converge in probability. This asymptotic result has important implications for small to moderate sample sizes, when poor distribution estimators can result when there are no ties but there are two or more closely spaced parameters values competing to the same rank. Several ways of alleviating the problem of inconsistency are suggested. ESA

N92-32839# Grenoble-1 Univ. (France). Lab. de Modelisation et Calcul.
APPROXIMATIONS AND DESIGNS FOR ESTIMATING REGRESSION COEFFICIENTS OF INDEPENDENT STOCHASTIC PROCESSES
Karim Benhenni Feb. 1991 21 p
(IMAG-RR-840-M; ETN-92-92072) Avail: CASI HC A03/MF A01

The problem of estimating the regression coefficients of a linear model for N independent stochastic processes Y(sub i), i = 1,...,N, is considered. The time integrated least square estimators depend on a random integral and, thus are hard to compute in practice. Optimal approximations of these estimators are given, which depend on the inverse of the covariance matrix generated by the observations of the process at a finite number of points of a regular sampling design and, thus are unstable and not robust. Simple nonparametric approximations based on an adjusted trapezoidal rule using regular sampling designs are derived. The estimators obtained from the two approximations are asymptotically unbiased, consistent, and asymptotically jointly normal. For processes Y(sub i), i = 1,...,N, having K quadratic mean derivatives, K = 0,1,2,..., exact rates of convergence of the performances in terms of variance are derived along with asymptotically optical designs. ESA

66 SYSTEMS ANALYSIS

Includes mathematical modeling; network analysis; and operations research.

N92-33055# Technische Univ., Delft (Netherlands).
AN INTELLIGENT GAMING ENVIRONMENT Ph.D. Thesis
Dirk Coppieters 12 Nov. 1990 179 p
(ISBN-90-6275-635-2; ETN-92-92035) Copyright Avail: CASI HC A09/MF A02

A modeling approach that supports the development of a gaming environment that has a good correspondence with that part of reality to be understood is presented. The necessary theoretical framework is discussed, and the feasibility of the approach through a case study is illustrated. Hence, an object-oriented simulation model that contains automata which can replace human players is shown. This provides the required flexibility and cost effectiveness to support decision makers in their process of learning to understand reality. ESA

N92-32438# National Defence Headquarters, Ottawa (Ontario).
OPERATIONAL NEEDS FOR AN UNMANNED AIR VEHICLE
L. R. Mader *In* AGARD, Integrated Target Acquisition and Fire Control Systems Feb. 1992 9 p (For primary document see N92-32437 23-06)
Copyright Avail: CASI HC A01/MF A02; 1 functional color page

67 THEORETICAL MATHEMATICS

Includes topology and number theory.

N92-32998# Superconducting Super Collider Lab., Dallas, TX.
MOL CALCULATION OF THE SOLITONS OF THE CUBIC SCHROEDINGER EQUATION
W. Schiesser Jun. 1992 7 p Presented at the 7th International Association of Mathematics and Computer Simulation (IMACS) International Conference on Computer Methods for Partial Differential Equations, New Brunswick, NJ, 22-24 Jun. 1992 Submitted for publication
(Contract DE-AC35-89ER-40486)
(DE92-017245; SSCL-Preprint-105; CONF-9206185-4) Avail: CASI HC A02/MF A01

The cubic Schroedinger equation (CSE) is a complex (in the mathematical sense) nonlinear partial differential equation (PDE) with a known analytical solution. Further, the solution consists of solitons (traveling waveforms that do not change shape with time or position) that are very sharp spatially. Thus, the CSE is a stringent test problem for any numerical procedure. We report here the results of a method of lines (MOL) solution using second-derivative, finite-difference approximations for spatial second derivatives that accommodate Dirichlet and Neumann boundary conditions without approximation of the boundary conditions. DOE

70 PHYSICS (GENERAL)

For precision time and time interval (PTTI) see *35 Instrumentation and Photography;* for geophysics, astrophysics or solar physics see *46 Geophysics, 90 Astrophysics,* or *92 Solar Physics.*

N92-32430# Rochester Univ., NY. Dept. of Physics and Astronomy.
THEORETICAL AND EXPERIMENTAL STUDIES OF ELEMENTARY PHYSICS
A. Bodek, T. Ferbel, A. C. Melissinos, S. Olsen, P. Slattery, P. Tipton, A. Das, C. R. Hagen, S. G. Rajeev, and S. Okubo 30 Apr. 1992 160 p
(Contract DE-FG02-91ER-40685)
(DE92-014877; DOE/ER-40685/712) Avail: CASI HC A08/MF A02

The experimental high energy physics program is directed toward the execution of experiments that probe the basic constituents of matter and the forces between them. These experiments are carried out at national and international accelerator facilities. At the current time, we are primarily concentrating on the following projects: (1) direct photon production in hadronic reactions (Fermilab E706); (2) production of hybrid mesons in the nuclear Coulomb field; (3) the D-Zero experiment at the Tevatron collider; (4) deep inelastic neutrino- and electron-nucleon scattering at FNAL and SLAC; (5) nonlinear QED at critical field strengths at SLAC; (6) the Experiments at KEK (AMY, 17keV neutrino); (7) the CDF experiment at the Tevatron collider; and (8) SSC-related detector R&D on scintillating tile- and diamond-based calorimetry and microstrip tracking detectors. DOE

71 ACOUSTICS

Includes sound generation, transmission and attenuation. For noise pollution see *45 Environmental Pollution.*

N92-32697# Federal Aviation Administration, Washington, DC. Office of Aviation Medicine.
EXPOSURES FROM HEADSET INTERFERENCE TONES Final Report
Noal D. May Jan. 1992 16 p
(AD-A247175; DOT/FAA/AM-92/4) Avail: CASI HC A03/MF A01

This study evaluated the acoustic characteristics of interference tones as experienced by FAA Air Traffic Control Specialists (ATCS's) and pilots who wear headsets with insert type ear pieces. The sound pressure levels (SPL's) of generated tones were measured through the headset at five randomly selected ATCS positions in each of seven Air Route Traffic Control Centers (ARTCC's). The SPL's were compared within and between four frequencies (.5, 1, 2, and 3 KHz) over ten discrete signal power levels. The comparisons demonstrated that SPL's of tones could not be predicted for ARTCC's or for positions within an ARTCC, and that the durations of exposure were brief, i.e., limited to the time needed to remove the headset earpiece from the ear canal. Potential amounts of temporary threshold shifts (TTS's) also were evaluated in a laboratory by checking hearing levels following exposures to tones played with ATCS/pilot communication through the same headset. Audiometric checks of 20 volunteer subjects indicated TTS could be detected following 1 KHz/114 dB/60 and 145 seconds, 2 KHz/108 dB/60 and 145 seconds, and 3 KHz/99 dB/145 seconds exposures, when hearing checks were made within the first 15 minutes. Such extended durations are highly unlikely for pilots and ATCS's and no TTS was detectable following exposures to shorter durations or to other frequencies with equivalent durations. GRA

N92-32842# Swedish Inst. of Space Physics, Umea. Lab. of Mechanical Waves.
BURNING OIL FIELDS AS A SOURCE OF INFRASONIC WAVES
Karina Waldemark and Ludwig Liszka Dec. 1991 14 p Submitted for publication
(IRF-Preprint-119; ETN-92-92160) Avail: CASI HC A03/MF A01

The consideration of burning oil fields in the Persian Gulf as an intense source of infrasonic waves is addressed. Propagation of these waves to high latitudes is discussed. Methods for sensitive detection of such a distant source are presented. Infrasonic data from two Swedish infrasonic stations, recording at 2 Hz (Lulea (65.7 north, 22.5 east) and Lycksele (64.6 north, 18.7 east) during the periods 6 Feb. - 14 Mar. and 7-13 Jun. 1991 are examined in order to demonstrate the reception of these long distance infrasonic waves. ESA

N92-32901# California Univ., La Jolla. Inst. for Nonlinear Science.
ACOUSTICAL EMISSION FROM BUBBLES Progress Report, 1 Mar. - 31 Dec. 1991
Michael S. Longuet-Higgins 31 Dec. 1991 4 p
(Contract N00014-91-J-1582)
(AD-A252390) Avail: CASI HC A02/MF A01

The scientific objectives of this report are to investigate the dynamics of bubbles formed from a free surface (particularly the upper surface of the ocean) by breaking waves, and the resulting emission of underwater sound. The chief natural source of underwater sound in the ocean at frequencies from 0.5 to 50 kHz is known to be the acoustical emission from newly-formed bubbles and bubble clouds, particularly those created by breaking waves and rain. Attention has been drawn to the occurrence of high-speed jets directed into the bubble just after bubble closure. They have been observed both in rain-drop impacts and in the release of bubbles from an underwater nozzle. Qualitatively they are similar to the inward jets seen in the collapse of a cavitation bubble. There is also a similarity to the highly-accelerated upward jets in standing water waves (accelerations greater than 20g) or in bubbles bursting at a free surface. We have adopted a theoretical approach based on the dynamics of incompressible fluids with a free surface. GRA

N92-32948*# National Aeronautics and Space Administration. Langley Research Center, Hampton, VA.
FOURTH AIRCRAFT INTERIOR NOISE WORKSHOP
David G. Stephens, comp. Jul. 1992 335 p Workshop held in Friedrichshafen, Fed. Republic of Germany, 19-20 May 1992; sponsored by NASA, Society of Automotive Engineers, and the German Aerospace Research Establishment
(RTOP 535-03-11-03)
(NASA-CP-10103; NAS 1.55:10103) Avail: CASI HC A15/MF A03

The fourth in a series of NASA/SAE Interior Noise Workshops was held on May 19 and 20, 1992. The theme of the workshop was new technology and applications for aircraft noise with emphasis on source noise prediction; cabin noise prediction; cabin noise control, including active and passive methods; and cabin interior noise procedures. This report is a compilation of the presentations made at the meeting which addressed the above issues. For individual titles, see N92-32949 through N92-32964.

N92-32949*# Lockheed Aeronautical Systems Co., Marietta, GA.
ACOUSTIC LOADS PREDICTION ON JET AIRCRAFT
N. N. Reddy *In* NASA. Langley Research Center, Fourth Aircraft Interior Noise Workshop Jul. 1992 p 1-12 (For primary document see N92-32948 23-71)
Avail: CASI HC A03/MF A03

A nearfield aircraft noise prediction computer program is presented for the F-22 aircraft. The dominant sources of noise are jet turbulent mixing noise, jet broadband shock noise, and fluctuating pressure under the turbulent boundary layer. All results from this investigation are presented in viewgraph format. H.A.

N92-32950*# Douglas Aircraft Co., Inc., Long Beach, CA.
MD-80 AFT CABIN NOISE CONTROL: A CASE HISTORY
M. A. Lang, D. R. Lorch, D. N. May, and M. A. Simpson *In*

NASA. Langley Research Center, Fourth Aircraft Interior Noise Workshop Jul. 1992 p 13-33 (For primary document see N92-32948 23-71)
Avail: CASI HC A03/MF A03

The interior noise technology program to improve the noise environment in the aft cabin of the MD-80 twin jet aircraft is discussed. Two potential noise control treatments were identified: vibration absorber devices for the airframe and for the engine. A series of ground and flight tests using in-service aircraft was then conducted. These tests showed that the vibration absorbers for the airframe and engine decreased aircraft noise significantly.
H.A.

N92-32951*# Dornier Luftfahrt G.m.b.H., Friedrichshafen (Germany, F.R.).
THE DORNIER 328 ACOUSTIC TEST CELL (ATC) FOR INTERIOR NOISE TESTS AND SELECTED TEST RESULTS
H. Josef Hackstein, Ingo U. Borchers, Klaus Renger, and Konrad Vogt *In* NASA. Langley Research Center, Fourth Aircraft Interior Noise Workshop Jul. 1992 p 34-43 (For primary document see N92-32948 23-71)
(AIAA Paper 92-2164) Avail: CASI HC A02/MF A03

To perform acoustic studies for achieving low noise levels for the Dornier 328, an acoustic test cell (ATC) of the Dornier 328 has been built. The ATC consists of a fuselage section, a realistic fuselage suspension system, and three exterior noise simulation rings. A complex digital 60 channel computer/amplifier noise generation system as well as multichannel digital data acquisition and evaluation system have been used. The noise control tests started with vibration measurements for supporting acoustic data interpretation. In addition, experiments have been carried out on dynamic vibration absorbers, the most important passive noise reduction measure for low frequency propeller noise. The design and arrangement of the current ATC are presented. Furthermore, exterior noise simulation as well as data acquisition are explained. The most promising results show noise reduction due to synchrophasing and dynamic vibration absorbers. Author

N92-32952*# Saab Aircraft Co., Linkoping (Sweden).
VIBRO-ACOUSTIC FE ANALYSES OF THE SAAB 2000 AIRCRAFT
Inge S. Green *In* NASA. Langley Research Center, Fourth Aircraft Interior Noise Workshop Jul. 1992 p 44-69 (For primary document see N92-32948 23-71)
Avail: CASI HC A03/MF A03

A finite element model of the Saab 2000 fuselage structure and interior cavity has been created in order to compute the noise level in the passenger cabin due to propeller noise. Areas covered in viewgraph format include the following: coupled acoustic/structural noise; data base creation; frequency response analysis; model validation; and planned analyses. H.A.

N92-32953*# National Research Council of Canada, Ottawa (Ontario). Inst. for Mechanical Engineering.
SOUND POWER DETERMINATION USING THE SOUND INTENSITY SCANNING TECHNIQUE
G. Krishnappa *In* NASA. Langley Research Center, Fourth Aircraft Interior Noise Workshop Jul. 1992 p 70-94 (For primary document see N92-32948 23-71)
Avail: CASI HC A03/MF A03

A technique is presented for determining sound power from sound intensity measurements. Sound power from sound pressure measurements needs approximations, a specific measurement environment, and costly facilities. Sound intensity measurements are the primary quantity required to determine sound power levels, require no costly facilities, and can be made in the presence of extraneous noise. All results are presented in viewgraph format.
H.A.

N92-32954*# Royal Aerospace Establishment, Farnborough (England).
RECENT ADVANCES IN STATISTICAL ENERGY ANALYSIS
K. H. Heron *In* NASA. Langley Research Center, Fourth Aircraft Interior Noise Workshop Jul. 1992 p 95-111 (For primary document see N92-32948 23-71)
Avail: CASI HC A03/MF A03

Statistical Energy Analysis (SEA) has traditionally been developed using modal summation and averaging approach, and has led to the need for many restrictive SEA assumptions. The assumption of 'weak coupling' is particularly unacceptable when attempts are made to apply SEA to structural coupling. It is now believed that this assumption is more a function of the modal formulation rather than a necessary formulation of SEA. The present analysis ignores this restriction and describes a wave approach to the calculation of plate-plate coupling loss factors. Predictions based on this method are compared with results obtained from experiments using point excitation on one side of an irregular six-sided box structure. Conclusions show that the use and calculation of infinite transmission coefficients is the way forward for the development of a purely predictive SEA code.
Author

N92-32955*# Cambridge Collaborative, Inc., MA.
USE OF SEA TO PREDICT STRUCTURE-BORNE NOISE IN AIRCRAFT
Jerome E. Manning *In* NASA. Langley Research Center, Fourth Aircraft Interior Noise Workshop Jul. 1992 p 112-128 (For primary document see N92-32948 23-71)
Avail: CASI HC A03/MF A03

A Statistical Energy Analysis is used to predict aircraft noise from the structural components. Structural-borne noise is vibration: (1) generated at one location; (2) transmitted by the structure to other locations; and (3) radiated into the cabin as noise. All results are presented in viewgraph format. H.A.

N92-32956*# Dornier Luftfahrt G.m.b.H., Friedrichshafen (Germany, F.R.).
ADVANCED STUDY FOR ACTIVE NOISE CONTROL IN AIRCRAFT (ASANCA)
Ingo U. Borchers, Urban Emborg (Saab Aircraft Co., Linkoping, Sweden), Antonio Sollo (Alenia Spazio S.p.A., Naples, Italy), Elly H. Waterman (Fokker B.V., Schipol-Oost, Netherlands), Jacques Paillard (MATRA Sep Imagerie et Informatique, Saint Quentin en Yvelines, France), Peter N. Larsen (Reson System A/S, Slangerup, Denmark), Gerard Venet (METRAVIB, Ecully, France), Peter Goeransson (Aeronautical Research Inst. of Sweden, Bromma.), and Vincent Martin (Centre National de la Recherche Scientifique, Marseilles, France) *In* NASA. Langley Research Center, Fourth Aircraft Interior Noise Workshop Jul. 1992 p 129-141 (For primary document see N92-32948 23-71)
(Contract EEC-Aero-0028-C)
(AIAA Paper 92-2092) Avail: CASI HC A03/MF A03

Aircraft interior noise and vibration measurements are included in this paper from ground and flight tests. In addition, related initial noise calculations with and without active noise control are conducted. The results obtained to date indicate that active noise control may be an effective means for reducing the critical low frequency aircraft noise. Author

N92-32957*# Southampton Univ. (England). Inst. of Sound and Vibration Research.
ACTIVE CONTROL OF SOUND TRANSMISSION THROUGH STIFF LIGHTWEIGHT COMPOSITE FUSELAGE CONSTRUCTIONS
D. R. Thomas, P. A. Nelson, R. J. Pinnington, and S. J. Elliott *In* NASA. Langley Research Center, Fourth Aircraft Interior Noise Workshop Jul. 1992 p 142-172 (For primary document see N92-32948 23-71)
Avail: CASI HC A03/MF A03

Work was performed on the active control of sound transmission in composite structures. First, a model was outlined of a vibrating plate with arbitrary boundary conditions. Second, the far field was minimized to radiate acoustic power using secondary force inputs. Third, a model of a simple case of freely mounted stiff lightweight panels was used. Fourth, experimental results for aluminum honeycomb composite panels is presented. Fifth, experimental

results are presented for the combination of a clamped steel plate and an aluminum honeycomb panel with secondary forces acting between the partitions. Finally, experimental results for the combination of a clamped steel plate with four secondary aluminum honeycomb panels is presented. All materials are shown in viewgraph format. H.A.

N92-32958*# National Aeronautics and Space Administration. Langley Research Center, Hampton, VA.
ACTIVE CONTROL OF INTERIOR NOISE IN A LARGE SCALE CYLINDER USING PIEZOELECTRIC ACTUATORS
H. C. Lester and R. J. Silcox *In its* Fourth Aircraft Interior Noise Workshop Jul. 1992 p 173-190 (For primary document see N92-32948 23-71)
Avail: CASI HC A03/MF A03

The noise reduction effectiveness of two types of control force actuator models has been analytically investigated: (1) a point actuator, and (2) an in-plane, piezoelectric actuator. The actuators were attached to the wall of a simply supported, elastic cylinder closed with rigid end caps. Control inputs to the actuators were determined such that the integrated square of the pressure over the interior of the vibrating cylinder was a minimum. Significant interior noise reductions were achieved for all actuator configurations, but especially for the structurally dominated response. Noise reduction of 9 dB to 26 dB were achieved using point force actuators, as well as localized and extended piezoelectric actuators. Control spillover was found to limit overall performance for all cases. However, the use of extended piezoelectric actuators was effective in reducing control spillover, without increasing the number of control degrees of freedom. Author

N92-32959*# Virginia Polytechnic Inst. and State Univ., Blacksburg. Vibration and Acoustics Lab.
SOUND TRANSMISSION REDUCTION WITH INTELLIGENT PANEL SYSTEMS
Chris R. Fuller and Robert L. Clark *In* NASA. Langley Research Center, Fourth Aircraft Interior Noise Workshop Jul. 1992 p 191-210 (For primary document see N92-32948 23-71)
Avail: CASI HC A03/MF A03

Experimental and theoretical investigations are performed of the use of intelligent panel systems to control the sound transmission and radiation. An intelligent structure is defined as a structural system with integrated actuators and sensors under the guidance of an adaptive, learning type controller. The system configuration is based on the Active Structural Acoustic Control (ASAC) concept where control inputs are applied directly to the structure to minimize an error quantity related to the radiated sound field. In this case multiple piezoelectric elements are employed as sensors. The importance of optimal shape and location is demonstrated to be of the same order of influence as increasing the number of channels of control. Author

N92-32960*# Deutsche Lufthansa A.G., Frankfurt am Main (Germany, F.R.).
PILOTS NOISE EXPOSURE DURING A BOEING 747-400 ROUND TRIP: AMBIENT NOISE AND ACOUSTIC-HEAD RECORDING AND ANALYSIS OF DATA
Knut Hoffman *In* NASA. Langley Research Center, Fourth Aircraft Interior Noise Workshop Jul. 1992 p 211-227 (For primary document see N92-32948 23-71)
Avail: CASI HC A03/MF A03

Pilot noise exposure is examined during the round trip flight of a Boeing 747-400 aircraft. Although the sound power origin is the aircraft, this paper examines the effects of this noise on the human occupants within the airplane. Data is acquired and analyzed to determine the noise exposure of pilots on long flights, in this case, a flight of 12 hours and 20 minutes. All results are presented in viewgraph format. H.A.

N92-32961*# Deutsche Insurance Germany (F.R.).
PILOT NOISE EXPOSURE DURING A BOEING 747-400 ROUND TRIP: JUDGEMENT OF NOISE AND ANALYSIS IN RESPECT TO HEARING IMPAIRMENT OF PILOTS
Hans Juergen Hooman *In* NASA. Langley Research Center, Fourth Aircraft Interior Noise Workshop Jul. 1992 p 228-251 (For primary document see N92-32948 23-71)
Avail: CASI HC A03/MF A03

Noise level measurements are made on Boeing 747 aircraft to determine the potential hazards to airline pilots. Measuring results have shown that most pilots work under conditions that where noise constitutes a health hazard. Long and short term effects of noise exposure in pilots is examined as well as the legal ramifications of this potential hazard. H.A.

N92-32962*# Alenia Aeronautica, Naples (Italy).
ACTIVE VIBRATIONS AND NOISE CONTROL FOR TURBOPROP APPLICATION RESEARCH PROGRAM ACTIVITIES
A. Paonessa, A. Concilio (Italian Aerospace Research Center, Naples.), and Leonardo V. Lecce (Istituto Progetto Velivoli, Naples, Italy) *In* NASA. Langley Research Center, Fourth Aircraft Interior Noise Workshop Jul. 1992 p 252-294 (For primary document see N92-32948 23-71)
Avail: CASI HC A03/MF A03

The objectives of this work include the following: (1) development of active noise control techniques to alleviate inefficiencies and drawbacks of passive noise control approach especially at low frequencies; (2) reduction of structurally radiated noise applying external forces to the vibrating structure by means of force actuators made of piezoelectric material; and (3) reduction of fuselage vibration levels in propeller driven aircraft by means of distributed piezoelectric actuators that are actively controlled. H.A.

N92-32963*# Fokker B.V., Schipol-Oost (Netherlands).
ACTIVE SYNCHROPHASING OF PROPELLER UNBALANCE
Dick Kaptein *In* NASA. Langley Research Center, Fourth Aircraft Interior Noise Workshop Jul. 1992 p 295-315 (For primary document see N92-32948 23-71)
Avail: CASI HC A03/MF A03

The results of a survey are presented to reduce the inflight propeller unbalance vibrations in the cabin of the Fokker 50 airplanes. Several approaches have been investigated. Active synchrophasing of the unbalance vibrations of both propellers appears to be successful. Author

N92-32964*# Applied Acoustic Research, State College, PA.
A LIGHTWEIGHT LOUDSPEAKER FOR AIRCRAFT COMMUNICATIONS AND ACTIVE NOISE CONTROL **c32**
Glenn E. Warnaka, Mark Kleinle (Oxford Speaker Co., Chicago, IL.), Parry Tsangaris (Oxford Speaker Co., Chicago, IL.), Michael J. Oslac (Oxford Speaker Co., Chicago, IL.), and Harry J. Moskow (Oxford Speaker Co., Chicago, IL.) *In* NASA. Langley Research Center, Fourth Aircraft Interior Noise Workshop Jul. 1992 p 316-327 (For primary document see N92-32948 23-71)
Avail: CASI HC A03/MF A03

A series of new, lightweight loudspeakers for use on commercial aircraft has been developed. The loudspeakers use NdFeB magnets and aluminum alloy frames to reduce the weight. The NdFeB magnet is virtually encapsulated by steel in the new speaker designs. Active noise reduction using internal loudspeakers was demonstrated to be effective in 1983. A weight, space, and cost efficient method for creating the active sound attenuating fields is to use the existing cabin loudspeakers for both communication and sound attenuation. This will require some additional loudspeaker design considerations. Author

N92-33160*# National Aeronautics and Space Administration. Langley Research Center, Hampton, VA.
BUILDING VIBRATIONS INDUCED BY NOISE FROM ROTORCRAFT AND PROPELLER AIRCRAFT FLYOVERS
Kevin P. Shepherd and Harvey H. Hubbard (Lockheed Engineering

and Sciences Co., Hampton, VA.) Jun. 1992 29 p
(RTOP 535-03-11-03)
(NASA-TM-104170; NAS 1.15:104170) Avail: CASI HC A03/MF A01

Noise and building vibrations were measured for a series of helicopter and propeller-driven aircraft flyovers at WFF during May 1978. The building response data are compared with similar data acquired earlier at sites near Dulles and Kennedy Airports for operation of commercial jet transports, including the Concorde supersonic transport. Results show that noise-induced vibration levels in windows and walls are directly proportional to sound pressure level and that for a given noise level, the acceleration levels induced by a helicopter or a propeller-driven aircraft flyover cannot be distinguished from the acceleration levels induced by a commercial jet transport flyover. Noise-induced building acceleration levels were found to be lower than those levels which might be expected to cause structural damage and were also lower than some acceleration levels induced by such common domestic events as closing windows and doors. Author

72 ATOMIC AND MOLECULAR PHYSICS

Includes atomic structure, electron properties, and molecular spectra.

N92-32310# Gosudarstvennyi Komitet po Ispolzovaniyu Atomnoi Energii, Serpukhov (USSR). Inst. Fiziki Vysokikh Ehnergij.
OBSERVATION OF (PI)(-)p YIELDS (OMEGA)(ETA)n REACTION AT 38 GeV/c MOMENTUM
V. D. Samojlenko 1991 7 p
(DE92-624690; IFVE-OEF-91-37) Avail: CASI HC A02/MF A01

The charge-exchange reaction in which the omega(eta)-system is produced was observed and studied for the first time. Measurements were performed at the 70-GeV IHEP accelerator using a GAMS-2000 hodoscope spectrometer. A narrow peak is observed in the invariant omega(eta) mass spectrum in the (t) greater than 0.25 (GeV/c)(exp 2) range corresponding to a possible omega(eta)-resonance with 1650 MeV mass and width Gamma less than 70 MeV. DOE

N92-32311# Gosudarstvennyi Komitet po Ispolzovaniyu Atomnoi Energii, Serpukhov (USSR). Inst. Fiziki Vysokikh Ehnergij.
COMPARISON OF SPIN ASYMMETRIES AND INVARIANT CROSS SECTIONS IN PRODUCTION OF (PI)(SUP 0) MESONS BY POLARIZED ANTIPROTONS AND PROTONS WITH 200 GeV ENERGY
D. L. Adams, N. Akchurin, and D. G. Underwood et al 1991 8 p
(DE92-624691; IFVE-OEF-91-51) Avail: CASI HC A02/MF A01

The single-spin asymmetry A(sub N)((bar-p)p) for inclusive (pi)(sup 0) production at 0.5 less than p(sub t) less than 2 GeV/c by 200-GeV transversely-polarized antiprotons on protons was measured at Fermilab over a wide range of x(sub F). It is observed that A(sub N)((bar-p)p) has the same sign, a similar x(sub F) dependence, and about half the magnitude as A(sub N)((bar-p)p) for (pi)(sup 0) production by protons. The ratio of the spin-averaged cross section for (pi)(sup 0) production by antiprotons and by protons is presented. DOE

N92-32312# California Univ., Berkeley. Lawrence Berkeley Lab.
HEAVY FLAVOR PHYSICS AT HADRON COLLIDERS
A. Barbaro-Galtieri Dec. 1991 14 p Presented at the 3rd Topical Seminar on Heavy Flavors, San Miniato (Italy), 3 Jun. 1991
(Contracts DE-AC03-76SF-00098; DE-AC02-76CH-03000)
(DE92-014482; LBL-31886; FNAL/C-92/45-E; CONF-9106289-6)
Avail: CASI HC A03/MF A01

The search for the top quark has dominated heavy flavor physics at hadron colliders. For Standard model decay of top, the present mass limit in m(sub t) is greater than 89 GeV (95 percent C.L.). Bottom production cross sections are quite large at hadron colliders, thus providing enough statistics for extensive studies. Results on cross sections, B(sup 0) - bar-B(sup 0) mixing, exclusive channels and rare B decays will be summarized. DOE

N92-32313# Florida Univ., Gainesville. Dept. of Physics.
QUARK-ANTIQUARK REGGE TRAJECTORIES IN LARGE N(SUB c) QCD
M. McGuigan and C. B. Thorn 1992 13 p
(Contract DE-FG05-86ER-40272)
(DE92-016462; DOE/ER-40272/160; UFIFT-HEP-92-12) Avail: CASI HC A03/MF A01

We apply methods developed by Lovelace, Lipatov, and Kirschner to evaluate the leading Regge trajectories alpha(t) with the quantum numbers of nonexotic quark-antiquark mesons at N(sub c) = infinity in the limit t yields negative infinity where renormalization group improved perturbation theory should be valid. We discuss the compatibility of nonlinear trajectories with narrow resonance approximations. DOE

N92-32316# Brookhaven National Lab., Upton, NY.
INVESTIGATION OF THE OXYGEN-VACANCY (A-CENTER) DEFECT COMPLEX PROFILE IN NEUTRON IRRADIATED HIGH RESISTIVITY SILICON JUNCTION PARTICLE DETECTORS
Zheng Li, H. W. Kraner, E. Verbitskaya, V. Eremin, A. Ivanov, M. Rattaggi, and P. G. Rancoita Feb. 1992 7 p Presented at the Nuclear and Space Radiation Effects Conference, New Orleans, LA, 13-17 Jul. 1992
(Contract DE-AC02-76CH-00016)
(DE92-016952; BNL-47550; CONF-920716-5) Avail: CASI HC A02/MF A01

Distributions of the A-center (oxygen-vacancy) in neutron silicon detectors have been studied using Deep Level Transient Spectroscopy. A-centers have been found to be nearly uniformly distributed in the silicon water depth for medium resistivity (0.1 - 0.2 k(omega)-cm) silicon detectors. A positive filling pulse was needed to detect the A-centers in high resistivity (greater than 4 k(omega)-cm) silicon detectors, and this effect was found to be dependent on the oxidation temperature. A discussion of this effect is presented. DOE

N92-32340# Flinders Univ., Adelaide (Australia). Electronic Structure of Materials Centre.
ELECTRON-ATOM SCATTERING
I. E. McCarthy Jul. 1991 10 p Presented at the 6th International Symposium on Correlations, Polarization in Electronica and Atomic Collisions and (e,2e) Reactions, Adelaide (Australia), 18-21 Jul. 1991
(DE92-625005; ESM-32; CONF-9107217) Avail: CASI HC A02/MF A01

The coupled-channels-optical method was implemented using two different approximations to the optical potential. The half-on-shell optical potential involves drastic approximations for numerical feasibility but still gives a good semi-quantitative description of the effect of uncoupled channels on electron scattering from hydrogen, helium, and sodium. The distorted-wave optical potential makes no approximations other than the weak coupling approximation for uncoupled channels. In applications to hydrogen and sodium it shows promise of describing scattering phenomena excellently at all energies. DOE

N92-32418# North Carolina Univ., Chapel Hill. Dept. of Chemistry.
LOCAL STRUCTURAL ORDER AND MOLECULAR ASSOCIATIONS IN WATER DMSO MIXTURES. MOLECULAR DYNAMICS STUDY Interim Technical Report, 1 Jul. 1991 - 30 Jun. 1992
I. Vaisman and M. Berkowitz May 1992 53 p
(Contract N00014-89-J-1169)
(AD-A250935; TR-9) Avail: CASI HC A04/MF A01

Pure dimethylsulfoxide (DMSO) and water-DMSO mixtures at three concentrations (XDMSO = 0.005, 0.04 and 0.2) are studied using molecular dynamics simulations. Structural properties of water in different regions of DMSO hydration are investigated using radial

distribution functions (RDF), hydrogen-bonded network parameters and statistical geometry approach. Reliability of RDF as indicators of structure changes at different concentrations is discussed. Enhancement of the water structure at the lowest DMSO concentration and its breakdown at XDMSO = 0.04 and XDMSO = 0.2 is observed. Structural effects in water-DMSO mixtures are attributed to the prevailing influence of the DMSO polar group on the water structure. It is found that the complex consisting of 1 DMSO and 2 water molecules hydrogen-bonded to the DMSO oxygen exists at all studied concentrations. Local order in pure DMSO is determined by dipolar forces as well as molecular association. Both components in water-DMSO mixture are tending to preserve their structural order upon dilution. AH simulation results are compared with numerous experimental data. A good agreement is found in most cases. GRA

N92-32426# Stanford Linear Accelerator Center, CA.
STUDIES OF HELIUM BASED DRIFT CHAMBER GASES FOR HIGH-LUMINOSITY LOW ENERGY MACHINES
A. Boyarski, D. Briggs, and P. R. Burchat (California Univ., Santa Cruz.) Feb. 1992 9 p Presented at the 6th International Wire Chamber Conference: Wire Chambers - Recent Trends and Alternative Techniques, Vienna (Austria), 17-21 Feb. 1992
(Contracts DE-AC03-76SF-00515; DE-AM03-76SF-00010)
(DE92-012415; SU-SLAC-PUB-5745; CONF-920219-1) Avail: CASI HC A02/MF A01

Future high luminosity low energy machines will need low mass tracking chambers in order to minimize multiple scattering of the relatively low momentum tracks produced at these facilities. A drift chamber using a helium based gas rather than a conventional argon based gas would greatly reduce the amount of multiple scattering. This paper summarizes measurements of the drift velocity and position resolution for gas mixtures of helium with CO2 and isobutane and helium with DME. Good spatial resolutions are obtained. A design of a drift chamber with only 0.12 percent of a radiation length (gas plus wire) over a 60 cm tracking distance is presented. DOE

N92-32473# Ames Lab., IA.
DESIGN AND CONSTRUCTION OF A SAMPLE PREPARATION CHAMBER FOR ATOMIC BEAM SCATTERING Ph.D. Thesis
C. Nielsen 18 May 1992 107 p
(Contract W-7405-eng-82)
(DE92-014509; IS-T-1578) Avail: CASI HC A06/MF A02

A new type of atomic beam scattering spectrometer was built to advance the usefulness of the atomic beam scattering technique as a surface dynamics probe. The facility was not only built to investigate the typical alkali halide samples such as NaCl, NaF, and LiF, but also to investigate metallic surfaces. Metal samples are more complicated to study, due to their reactive surfaces and the sample preparation process. A surface analysis chamber was constructed as an attachment to the scattering facility to treat samples under ultra high vacuum (UHV) and then transfer these samples into the scattering facility. This surface analysis chamber is referred to as the sample preparation chamber and is the basis for this thesis. DOE

N92-32497# Gosudarstvennyi Komitet po Ispolzovaniyu Atomnoi Energii, Serpukhov (USSR). Inst. Fiziki Vysokikh Ehnergij.
FIRST RESULTS OF MEASUREMENTS OF A(SUB LL) TWO-SPIN ASYMMETRY IN INCLUSIVE PRODUCTION OF (PI)(SUP 0) MESONS BY POLARIZED PROTONS AND ANTIPROTONS WITH 200 GeV ENERGY
D. L. Adams, N. Akchurin, and D. G. Underwood et al 1991 6 p
(DE92-624692; IFVE-OEF-91-52) Avail: CASI HC A02/MF A01

The two-spin parameter A(sub LL) in inclusive (pi)(sup 0)-production by longitudinally polarized protons and antiprotons on longitudinally polarized protons was measured at the 200-GeV Fermilab spin physics facility, at x(sub F) = 0 and for 1 less than P(sub t) less than 3 GeV/c. In this p(sub t) region, (A(sub LL)(PP)) is less than 10 percent and -20 percent is less than (A(sub LL)(P-bar(P)) is less than 10 percent, were measured at the 95 percent confidence level. The relevance of A(sub LL)(PP) for the gluon spin structure function is discussed. The data are in good agreement with 'conventional', small or zero, gluon polarization. DOE

N92-32498# Gosudarstvennyi Komitet po Ispolzovaniyu Atomnoi Energii, Serpukhov (USSR). Inst. Fiziki Vysokikh Ehnergij.
POSSIBLE EFFECTS OF ADDITIONAL VECTOR BOSONS IN e(SUP +)e(SUP -)(YIELDS)f(BAR-f) AT THE TRISTAN ENERGIES
A. A. Likhoded, O. P. Yushchenko, and A. A. Pankov (Gomel Polytechnic Inst., USSR) 1991 13 p
(DE92-624727; IHEP-OTF-91-116) Avail: CASI HC A03/MF A01

The phenomenological manifestation of the additional Y(Y(sub L)) boson arising in the models with the composite structure of electroweak interactions is studied for the process e(+)e(-) (yields) f(bar-f) at the TRISTAN energies (the square root of s = 55 - 70 GeV). It is shown that the experimentally observed deviation of R(sub mu) from the Standard Model predictions can be explained by the presence of the additional isoscalar Y-boson in the region of a small mixing parameter. The increase of statistics for the above processes at TRISTAN will permit an additional limitation to be set on the model parameters. DOE

N92-32499# Flinders Univ., Adelaide (Australia). Electronic Structure of Materials Centre.
SIMPLIFIED MODEL OF ELECTRON SCATTERING ON ATOMIC HYDROGEN
I. Bray and A. T. Stelbovics Nov. 1991 14 p
(DE92-625007; ESM-37) Avail: CASI HC A03/MF A01

The simplified model of electron-hydrogen atom scattering, which has all orbital angular momentum set to zero, is solved to convergence at a range of energies from 1 to 400 eV using a general coupled-channel approach. The results are in complete agreement with the solution of this problem by Poet using a method that is applicable to this model only. The corresponding T matrix elements for the transitions from the ground state to each one of 1s, 2s, and 3s are presented in tabular from. The 1s, 2s, 3s, ionization, and total cross sections are also presented at each energy. DOE

N92-32500# Gosudarstvennyi Komitet po Ispolzovaniyu Atomnoi Energii, Obninsk (USSR). Fiziko-Ehnergeticheskij Inst.
SCALING IN THE PROCESSES OF ION-ATOM EXCITATION
V. N. Klintsov and G. L. Yudin 1991 18 p
(DE92-625008; FEI-2189) Avail: CASI HC A03/MF A01

Atom excitation, in collisions with fully stripped ions, at intermediate and high energies is studied in the framework of the semiclassical sudden-Born approximation. Two different scaling rules are manifested for transitions in the target-atom with even and odd numbers of Delta(sub fi) = l(sub f) + m(sub f) - l(sub i) - m(sub i) where l(sub i) and m(sub i), and l(sub f) and m(sub f) are the orbital and magnetic quantum numbers of the initial and the final states respectively. DOE

N92-32501# Flinders Univ., Bedford Park (Australia). Inst. for Atomic Studies.
COUPLED-CHANNELS-OPTICAL CALCULATION OF ELECTRON-HELIUM SCATTERING
I. E. McCarthy, Y. Zhou, and K. Ratnavelu Jun. 1991 14 p
(DE92-625009; FIAS-R-215) Avail: CASI HC A03/MF A01

Cross sections for electron impact excitation of the singlet n = 1 and 2 states of the helium atom at various energies ranging from 30-200 eV are calculated using the coupled-channels optical method with the half-on-shell polarization potential. The electron impact coherence parameters for the excitation to the 2(sup 1)P state are also calculated. Semi-quantitative agreement with the experimental evidence is achieved. DOE

N92-32548# California Univ., Santa Barbara. Dept. of Chemistry.
SURFACE RECONSTRUCTION AND TEMPLATING FOR ZEOLITE THIN FILM SYNTHESIS OBSERVED BY ATOMIC FORCE MICROSCOPY Technical Report, 1 Jun. 1991 - 31 May 1992
A. L. Weisenhorn, J. E. MacDougall, P. K. Hansma, and G. D. Stucky 15 May 1992 12 p
(Contract N00014-90-J-1159)
(AD-A251140; TR-24) Avail: CASI HC A03/MF A01

Atomic force microscopy (AFM) allows one to nondestructively image insulating surfaces in air or under liquids with molecular resolution. When applied to zeolites, this technique allows observation of real time processes of crystal structure on the external surface of a single crystal under water, salt solutions or alcohols. It also offers the opportunity to directly observe surface reconstruction using solution cationic templates to generate new zeolitic thin film phases. In this study, AFM was used to monitor room temperature lattice reconstruction on the surface of a natural single crystal of stilbite using sodium ion templates to form a new periodic lattice. This is the first reported application of AFM for the investigation of reconstructive chemistry of a nonconducting surface. GRA

N92-32556# State Univ. of New York, Buffalo. Dept. of Chemistry.
NOVEL GAS PHASE ION MOLECULE REACTIONS OF C60(++) WITH O2 AND NH3
James Stry, M. T. Coolbaugh, Edward Turos, and James F. Garvey 1 Jun. 1992 14 p Submitted for publication
(Contract N00014-88-K-0483)
(AD-A250921; TR-31) Avail: CASI HC A03/MF A01

We have recently utilized a tandem triple quadrupole mass spectrometer to probe the gas phase ion-molecule chemistry of C60++ with a variety of target gases, at low collision energies. We have observed a high degree of reactivity of C60++ with oxygen to produce C60+, C6002+ and C600+. Likewise, we have also observed reactivity of C60++ with ammonia to produce C60NH2+, C60NH2(NH3)+, C60NH2(NH3)2+ and C60NH2(NH3)3+. We propose that the product ions result from an electron transfer reaction followed by covalent bond formation. All reactions were observed to be highly dependent on collision energy and target gas pressure. We believe that these processes are part of a larger family of charge exchange reactions for C60++, which occur for any molecule whose ionization potential lies below 12.25 eV, the first ionization potential of C60. GRA

N92-32597# Oregon Univ., Eugene.
THEORY OF ELEMENTARY PARTICLES STUDIES IN WEAK INTERACTION AND GRAND UNIFICATION AND STUDIES IN ACCELERATOR DESIGN
1991 50 p
(Contract DE-FG06-85ER-40224)
(DE92-014320; DOE/ER-40224/214) Avail: CASI HC A03/MF A01

This report discusses research on the following: the Stanford linear collider detector; Mark II; GEM; tau-charm factory; and SECC preradiator prototype and beam test. The progress of the Oregon group on all of these efforts has been substantial. DOE

N92-32600# Oregon Univ., Eugene. Inst. of Theoretical Science.
RELATIVISTIC HEAVY ION COLLISIONS
R. C. Hwa Feb. 1992 6 p
(Contract DE-FG06-91ER-40637)
(DE92-014415; DOE/ER-40637/1) Avail: CASI HC A02/MF A01

This report discusses the following topics: large transverse momentum hadrons in heavy ion collisions at LHC; ECCO - an event generator for soft production in pp collisions; proton-nucleus and nucleus-nucleus collisions; fractal behavior of multiplicity fluctuations; and quark-hadron phase transition. Additionally, ECCO is currently the only event generator of hadronic and nuclear collisions that survives the discriminating test of intermittency. DOE

N92-32682# North Carolina Univ., Chapel Hill. Dept. of Chemistry.
DYNAMICS OF ION SOLVATION IN A STOCKMAYER FLUID Interim Technical Report
L. Perera and Max L. Berkowitz May 1992 36 p
(Contract N00014-89-J-1169)
(AD-A251087; TR-7) Avail: CASI HC A03/MF A01

Molecular dynamics computer simulations were performed to study the dynamics of the ionic solvation in a Stockmayer fluid. The simulations show that the solvent relaxation proceeds in two time regimes. Most of the relaxation occurs in a short time period during which the relaxation process can be described by a Gaussian function. The long time regime can be described by an exponential relaxation. The decay exponent of the relaxation function in this regime is the same as the exponent describing the decay of the single dipole correlation function. In addition, the contribution of the rotational and translational modes of the solvent to the energy relaxation was investigated. It was found that when the rotational mode is the dominant mode of the solvent motion, the relaxation occurs from the outside-in, in accordance with the Onsager snowball picture. When the influence of the translational mode is increased, the Onsager picture breaks down. GRA

N92-32702# Pittsburgh Univ., PA. Dept. of Physics and Astronomy.
EXPERIMENTAL PARTICLE PHYSICS AT THE UNIVERSITY OF PITTSBURGH
E. Engels, Jr., U. Perera, P. F. Shepard, and J. A. Thompson Apr. 1992 87 p
(Contract DE-FG02-91ER-40646)
(DE92-014181; DOE/ER-40646/2) Avail: CASI HC A05/MF A01

During the past year, task A completed the HELIOS single and pair electron analyses and found no anomalous production or multiplicity dependence. The HELIOS electron-muon pair analysis continued in its search for lepton physics beyond the expected charm yields. Data taking began at the CMD2 detector at Novosibirsk. Measurements of the UV reflectivity and photomultiplier tests for the first Cerenkov counter to be used in the E865 experiment at BNL were carried out, along with the development of a general ray-tracing code. The design of the Cerenkov counter for E865 along with development of light mirror fabrication techniques were a major part of the task A program. The principal efforts of task B, the Fermilab program, have been the completion of the analysis of the 1987-1988 data with resulting publications, completion of the 1990-1991 data run, and the beginning of the analysis of the 1990-1991 data. In addition, the task B group is taking a leadership role in developing a proposal to Fermilab for the upgrade of the CDF silicon vertex detector in preparation for the 1995 data run. This proposal is to be presented to the laboratory management in time for the fall Fermilab Program Advisory Committee meeting. Task C has recently submitted results of its fractionally charged particle searches, placing new upper limits on the abundance of naturally-occurring fractionally-charged particles in various materials. This group has recently been approved by the Brookhaven management for an exposure of their p-i-n diodes in a high intensity proton beam. This measurement, along with its subsequent analysis, will complete the program. DOE

N92-32735# Laboratoire d'Automatique et d'Analyse des Systemes, Toulouse (France).
STUDY AND ACHIEVEMENT OF A PARALLEL SIMULATOR FOR DIFFUSION AT THE ATOMIC LEVEL: CREATION AND GROWTH OF DISLOCATION LOOPS UNDER ELECTRONIC RADIATION M.S. Thesis [ETUDE ET REALISATION D'UN SIMULATEUR PARALLELE DE LA DIFFUSION A L'ECHELLE ATOMIQUE: CREATION ET CROISSANCE DE BOUCLES DE

DISLOCATION SOUS IRRADIATION ELECTRONIQUE]
Hafida IdrissiAzami 1992 176 p In FRENCH
(LAAS-92118; ETN-92-92090) Avail: CASI HC A09/MF A02

The study and development of a tool for three dimensional simulation of the defect or impurity defection in a semiconductor, a phenomenon which allows production processes of electronic devices to be controlled, is addressed. Experimental results from two abnormal diffusions are recalled: Ga diffusion at the GaAs-CdTe interface during the heteroepitaxic growth of CdTe, and the diffusion of interstitials under a high energy electronic flow. A conventional model of diffusion is proposed, and the transcription of a physical model into a transputer network is presented. The formation of large defects and their spatial representations are described. A result of interest concerns the distribution of vacancies around the dislocation loops. Chaotic like behaviors are highlighted. ESA

N92-32753# Nationaal Inst. voor Kernfysica en Hoge Energiefysica, Amsterdam (Netherlands).
SUPERSYMMETRY SEARCHES AT ELECTRON-PROTON COLLIDERS Ph.D. Thesis
Michael Maria Johann Janssen 1992 114 p Sponsored by Netherlands Organization for the Advancement of Research
(ETN-92-92057) Avail: CASI HC A06/MF A02

The motivation for a Supersymmetric Standard Model (SSM) at the intermediate scale is given. The general ideas of supersymmetry are explained and a description of the Minimal (M) SSM is given. The importance of investigating whether nature is described by a supersymmetric theory, to see whether the supersymmetric particles can be produced in (future) high energy colliders, is addressed. The production of a squark pair in ep collisions is studied. The calculations for HERA, a possible upgrade of HERA, and the LEP/LHC collider are done within, the MSSM. The squark pair is produced and each squark is considered to decay very rapidly into a quark and a photino. Since the photinos of the MSSM escape the detector unobserved and are recognized by missing momentum, like the neutrino of the SM, all processes with neutrinos in the final state are studied for the HERA collider. These calculations give the possibility to do further research on W and Z bosons. The production and the signal coming from sleptons and squarks for several processes at the ep collider at LEP/LHC are studied. A demonstration of the extraction of the supersymmetric signal from the SM background processes is given. In particular the large backgrounds due to single W and Z production are considered. ESA

N92-32764# Stockholm Univ. (Sweden). Dept. of Physics.
RADIATIVE LIFETIME MEASUREMENTS OF THE AA pi 1/2 STATE IN CaH
M. Doverstaal and P. Weijnitz Oct. 1991 10 p
(USIP-91-03; ETN-92-91509) Avail: CASI HC A02/MF A01

An experimental setup for time resolved spectroscopy in CaH was developed. The CaH molecule was produced in a resistance furnace at a temperature around 1200 K where metallic calcium was exposed to hydrogen atmosphere. A series of lifetime measurements was performed in the pressure range of 2 to 10 Torr. At 1200 K the maximum of the Boltzmann distribution corresponds to a maximum population of rotational level J = 15.5 in the ground state. The molecule was excited by the P(sub 1)(14287.87/cm, J = 19.5) line of the (0,0) transition and the fluorescence from the corresponding R(sub 1)(14591.62/cm, J = 17.5) line was recorded with a PM tube. A small monochromator (f = 0.2 m Jobin/Yvon) was used as a bandpass filter in order to reduce the scattered light both from the furnace and the lasers. A Nd:YAG pumped Lumonics HD-500 dye laser, Pyradin 1 (660 to 730 nm), was used to excite the molecules. ESA

N92-32921# Yale Univ., New Haven, CT.
NUCLEAR THEORY Annual Report
F. Iachello, Y. Alhassid, and D. Kusnezov 1991 22 p
(Contract DE-FG02-91ER-40608)
(DE92-015012; DOE/ER-40608/1) Avail: CASI HC A03/MF A01

This report discusses topics on nuclear structure models; algebraic models of hadronic structure; nuclear reactions; hot rotating nuclei; chaos in nuclei; signatures of the quark-gluon plasma; hadronic spectroscopy; octupole collectivity in nuclei; finite-temperature methods for the many-body problem; and classical limit of algebraic hamiltonians. DOE

N92-32922# Iowa State Univ. of Science and Technology, Ames. Dept. of Physics and Astronomy.
RELATIVISTIC HEAVY ION PHYSICS
J. C. Hill and F. K. Wohn 1992 10 p
(Contract DE-FG02-92ER-40692)
(DE92-015025; DOE/ER-40692/1) Avail: CASI HC A02/MF A01

In 1992 a proposal by the Iowa State University experimental nuclear physics group entitled 'Relativistic Heavy Ion Physics' was funded by the US Department of Energy, Office of Energy Research, for a three-year period beginning November 15, 1991. This is a progress report for the first six months of that period but, in order to give a wider perspective, we report here on progress made since the beginning of calendar year 1991. In the first section, entitled 'Purpose and Trends,' we give some background on the recent trends in our research program and its evolution from an emphasis on nuclear structure physics to its present emphasis on relativistic heavy ion and RHIC physics. The next section, entitled, 'Physics Research Programs,' is divided into three parts. First, we discuss our participation in the program to develop a large detector named PHENIX for the RHIC accelerator. Second, we outline progress made in the study of electromagnetic dissociation (ED). A highlight of this endeavor is experiments carried out with the Au-197 beam from the AGS accelerator in April 1991. Third, we discuss progress in completion of our nuclear structure studies. In the final section, a list of publications, invited talks and contributed talks starting in 1991 is given. DOE

N92-32928# Oak Ridge National Lab., TN.
THE SHAPES AND COLLECTIVE BEHAVIOR OF RAPIDLY ROTATING NUCLEI
N. R. Johnson 1992 23 p Presented at the International Symposium on Spectroscopy and Structure of Molecules and Nuclei, Tallahassee, FL, 27 Mar. 1992
(Contract DE-AC05-84OR-21400)
(DE92-017192; CONF-9203162-2) Avail: CASI HC A03/MF A01

A review of our work on lifetime measurements of high-spin states in nuclei in the vicinity of neutron number 90 is presented. Recoil-distance experiments on Yb-159,160,161,162 show a loss of collectivity for states having rotational frequencies in the range of (Dirac h)omega is approximately 0.26 - 0.36 MeV. In similar measurements on nuclei whose Fermi surfaces lie nearer to the middle of the i(sub 13/2) neutron shell (W-170,171 and Os-172), we have found no evidence for such losses in this frequency range. These patterns of behavior are in qualitative agreement with current cranking theories which predict an evolving triaxiality with positive gamma values for the nuclei very close to N = 90. In recent Doppler-broadened line shape measurements on Yb-160 we found that in the frequency range of (Dirac h)omega is approximately 0.36 - 0.50 MeV there is a restoration of the collectivity to near that of the low-lying members of the ground band, a feature not predicted by cranking theories. Similar measurements on Yb-164 show that the collectivity in the yrast sequence is fairly constant up to (Dirac h)omega is approximately 0.42 MeV, with a loss showing up for states at somewhat higher frequencies. The trends of the transition quadrupole moments from available data on evenmass ytterbium nuclei with A = 160 - 168 are discussed and compared with theory. DOE

N92-32997# California Univ., Berkeley. Lawrence Berkeley Lab.
PHOTON EXCITATION FOR SATELLITE FREE X RAY SPECTROSCOPY: INSTRUMENTATION CHALLENGES
R. C. C. Perera Oct. 1991 18 p Presented at the 7th National Conference and Exhibition on Synchrotron Radiation

Instrumentation, Baton Rouge, LA, 28-31 Oct. 1991
(Contract DE-AC03-76SF-00098)
(DE92-016999; LBL-31741; CONF-9110146-22) Avail: CASI HC A03/MF A01

The first systematic study of satellites in the x-ray emission spectra was performed by Deslattes using quasi-monochromatic photon excitation from a group of L(alpha) x-ray sources lying close to the K edge of Cl. He observed significant alterations in the Cl K(beta) spectrum of KCl, depending on the character of the excitation radiation, and identified the initial state of these satellites as a double vacancy state. Recently, the valence electronic structure of the chlorofluoromethanes were analyzed by chlorine K x-ray emission under satellite-free conditions. These studies were based on the use of synchrotron radiation to eliminate the multivacancy effects that are inherent in conventional x-ray spectroscopy. In this report, satellite free x-ray emission spectra from chlorofluoromethanes will be presented to demonstrate that the simplified spectra can be obtained using selective photon excitation. Results from various research groups world wide, utilizing the tunable photon excitation form synchrotron sources to eliminate the obscuring features in x-ray emission spectra of rare-gas solids (RGS) and metals, will be discussed. Also, the technical challenges in utilizing the small phase-space attributes of high brightness from third generation SR sources producing x-ray and vacuum ultra-violet wavelengths to study weak features like satellites in x-ray emission spectra will be presented. DOE

N92-33001# Lawrence Livermore National Lab., CA.
ION MICROTOMOGRAPHY USING ION TIME-OF-FLIGHT
M. L. Roberts, D. W. Heikkinen, I. D. Proctor, A. E. Pontau (Sandia National Labs., Livermore, CA.), G. T. Olona (Sandia National Labs., Livermore, CA.), T. E. Felter (Sandia National Labs., Livermore, CA.), D. H. Morse (Sandia National Labs., Livermore, CA.), and B. V. Hess (Sandia National Labs., Livermore, CA.) Jun. 1992 10 p Presented at the 3rd International Conference on Nuclear Microprobe Technology and Applications, Uppsala (Sweden), 8-12 Jun. 1992
(Contract W-7405-eng-48)
(DE92-017257; UCRL-JC-110792; CONF-9206201-3) Avail: CASI HC A02/MF A01

We have developed and are in the process of testing an ion time-of-flight (TOF) detector system for use in our ion microtomography measurements. Using TOF, ion energy is determined by measurement of the ion's flight time over a certain path length. For ion microtomography, the principle advantage of TOF analysis is that ion count rates of several hundred thousand counts per second can be achieved as compared to a limit of about ten thousand ions per second when using a solid-state silicon surface barrier detector and associated electronics. This greater than 10 fold increase in count rate correspondingly shortens sample analysis time or increases the amount of data that can be collected on a given sample. Details of the system and progress to date are described. DOE

N92-33067# State Univ. of New York, Stony Brook. Dept. of Physics.
RESEARCH IN THEORETICAL NUCLEAR PHYSICS
Jun. 1992 105 p
(Contract DE-FG02-88ER-40388)
(DE92-016316; DOE/ER-40388/90) Avail: CASI HC A06/MF A02

This report discusses research in the following areas: strong interaction physics; relativistic heavy ion physics; nuclear structure and nuclear many-body theory; and nuclear astrophysics. DOE

N92-33083# North Carolina Univ., Chapel Hill. Dept. of Chemistry.
THE ENERGETICS AND DYNAMICS OF FREE RADICALS, IONS, AND CLUSTERS
T. Baer Mar. 1992 5 p
(Contract DE-FG05-88ER-13950)
(DE92-014124; DOE/ER-13950/T1) Avail: CASI HC A01/MF A01

The structure and energetics of free radicals, ions, and clusters have been investigated by photoelectron photoion coincidence (PEPICO) and analyzed with ab initio molecular orbital and statistical theory RRKM calculations. In these experiments, molecules are prepared in a molecular beam so that their internal as well as translational energies are cooled to near 0 K. The coincidence condition between energy analyzed electrons and their corresponding ions insures that the ions are energy selected. The primary experimental information includes ionization and fragment ion appearance energies, and the ion time of flight (TOF) distributions. The latter are obtained by using the energy selected electron as a start signal and the ion as the stop signal. These types of experiments allow us to measure the ion dissociation rates in the 10(exp 4) to 10(exp 7) sec (exp -1) range. Such ions are commonly referred to as metastable ions. In addition, the TOF peak widths are related to the release of translational energy in the ion dissociation process. Perhaps the most important advance during the past year has been in the study of cluster photoionization. We have developed an experimental method for differentiating similar mass cluster ions based on the kinetic energy of the ions measured by TOF. DOE

N92-33133# Rutherford Appleton Lab., Chilton (England).
SCALAR MESONS AND KAONS IN PHI RADIATIVE DECAY AND THEIR IMPLICATIONS FOR STUDIES OF CP VIOLATION AT DA(PHI)NE
Nick Brown and F. E. Close Dec. 1991 17 p
(RAL-91-085; ETN-92-91981) Avail: CASI HC A03/MF A01

A study which noticed inconsistencies in the scalar resonance contributions to the phi to a K x K(bar) gamma process is presented. Another study which questioned the intrinsic phi to S gamma rate to see if it can discriminate among models for the scalar mesons is summarized. It suggests that an accurate measurement of the absolute and relative branching ratios for phi to gamma f(sub 0) and gamma a(sub 0) may indeed provide such discrimination and reinforces the conclusions of the first study that overall phi to gamma K(sup 0)K(bar)(sup 0) will pose no significant background to CP violation studies of DA(phi)NE. ESA

N92-33135# Rutherford Appleton Lab., Chilton (England).
NEUTRINO MASSES IN THE FLIPPED SU(5) TENSOR PRODUCT U(1) AND THE SU(4) TENSOR PRODUCT O(4) GUT MODELS
Elena Papageorgiu and Stefano Ranfone Mar. 1992 16 p
(RAL-92-012; ETN-92-91982) Avail: CASI HC A03/MF A01

Different neutrino mass patterns arising in string inspired Grand Unified Theory (GUT) and supersymmetric GUT models based on the flipped SU(5) tensor product U(1) and the SU(4) tensor product O(4) gauge groups are classified. Phenomenologically interesting spectra are obtained through the interplay of the two seesaw mechanisms present, with typical neutrino masses approximately 0.001 eV in the supersymmetric GUT models and of order 0.1 to 10 KeV in the ordinary GUTs. ESA

N92-33137# Rutherford Appleton Lab., Chilton (England).
PARTONS AND THE EMC SPIN EFFECT
S. D. Bass (Adelaide Univ., Australia) Mar. 1992 24 p Submitted for publication Sponsored in part by Adelaide Univ.; British Council; and DOE
(RAL-92-015-Preprint; ETN-92-91983) Avail: CASI HC A03/MF A01

The parton model and the role of the axial anomaly in polarized deep inelastic scattering is considered. It is shown that the axial anomaly is relevant to each of the higher moments of the spin dependent structure function (g(sub 1)(x)) and not just the first moment. This result implies that the factorization of mass singularities is not sufficient to define the parton model on spin dependent quantum chromodynamics. (It is certainly a necessary condition.) The locality of the photon parton interaction needs to be considered. The anomaly is observed over all x in the EMC (g(sub 1)(x)) data. ESA

N92-33148# Stanford Linear Accelerator Center, CA.
THEORETICAL ASPECTS OF LEPTON-HADRON SCATTERING
S. D. Drell Jan. 1992 21 p Presented at the 19th SLAC Summer Inst. on Particle Physics, Stanford, CA, 5-16 Aug. 1991
(Contract DE-AC03-76SF-00515)
(DE92-013765; SLAC-PUB-5720; CONF-910836-5) Avail: CASI HC A03/MF A01

In this paper, I will emphasize two points on Theoretical Aspects of Lepton-Hadron Scattering. The first point concerns the crucial importance of testing the 'exact' sum rules as tests of the local current algebra. Discrepancies, if found, between experiment and theory cannot be 'interpreted away' in terms of more complex parton wave functions for the hadronic ground state. The three sum rules of interest are those of Adler, Bjorken, and Gross and Llewellyn-Smith. The second point involves an understanding of the corrections to scaling in QCD and what they teach us. DOE

N92-33164# Fermi National Accelerator Lab., Batavia, IL.
A STUDY OF FOUR JET EVENTS AND SEARCH FOR DOUBLE PARTON SCATTERING AT SQUARE ROOT s = 1.8 TeV
L. J. Keeble (Texas A&M Univ., College Station.) Jun. 1992 6 p Presented at the 27th Rencontres De Moriond, QCD and High Energy Hadronic Interactions, Les Arcs (France), 22-28 Mar. 1992
(Contract DE-AC02-76CH-03000)
(DE92-016351; FNAL/C-92/161-E; CONF-9203154-3) Avail: CASI HC A02/MF A01

Kinematic properties of four jet events taken during the 1988/89 run of the Tevatron at Fermilab are compared with the predictions of a leading order QCD calculation. Preliminary work on a search for double parton scattering is presented. DOE

N92-33186# Rochester Univ., NY.
THEORETICAL NUCLEAR PHYSICS
J. B. French and D. S. Koltun Jun. 1992 10 p
(Contract DE-FG02-88ER-40425)
(DE92-016837; DOE/ER-40425/256) Avail: CASI HC A02/MF A01

This report summarizes progress during the past year in the following areas of research: pion double charge exchange and the role of meson exchange currents, including vector mesons, deltas, and nuclear correlations; K(+)-nucleus scattering and the role of meson exchange currents in supplying 'missing cross section'; pion excess distributions in nuclei and the role of nuclear correlations; interactions of two hyperons and the possibility of an H dibaryon; shell model spectra and the NN tensor interaction; and statistical nuclear spectroscopy, including state densities and expectation values evaluated in terms of one-point and two-point (correlation) functions. DOE

N92-33187# Colorado Univ., Boulder. Dept. of Physics.
ELEMENTARY PARTICLE PHYSICS AND HIGH ENERGY PHENOMENA
A. R. Barker, J. P. Cumalat, S. P. deAlwis, T. A. DeGrand, W. T. Ford, K. T. Mahanthappa, U. Nauenberg, P. Rankin, and J. G. Smith Jun. 1992 103 p
(Contract DE-FG02-91ER-40672)
(DE92-016844; DOE/ER-40672/1; Colo-HEP-287) Avail: CASI HC A06/MF A02

This report discusses the following research in high energy physics: the properties of the z neutral boson with the SLD detector; the research and development program for the SDC muon detector; the fixed-target k-decay experiments; the Rocky Mountain Consortium for HEP; high energy photoproduction of states containing heavy quarks; and electron-positron physics with the CLEO II and Mark II detectors. DOE

73 NUCLEAR AND HIGH-ENERGY PHYSICS

Includes elementary and nuclear particles; and reactor theory.

For space radiation see *93 Space Radiation.*

N92-32314# Argonne National Lab., IL.
HIGH POWER TESTING OF THE PROTOTYPE ACCELERATING CAVITY (352 MHz) FOR THE ADVANCED PHOTON SOURCE (APS)
J. F. Bridges, Y. W. Kang, R. L. Kustom, and K. Primdahl 1992 4 p Presented at the 3rd European Particle Accelerator Conference, Berlin (Germany), 24-28 Mar. 1992
(Contract W-31-109-eng-38)
(DE92-016697; ANL/CP-75863; CONF-920315-40) Avail: CASI HC A01/MF A01

Measurement of the higher order of modes of a prototype single-cell 352 MHz cavity for the APS 7-Gev storage ring is presented and discussed. A cavity made from solid copper was built according to dimensions derived from URMEL program runs. The longitudinal and transverse impedances of the first several higher order modes have been measured using various-shaped metal beads. High power (greater than 60 kW) testing of the cavity is described along with design and operation of dampers for those modes with coupled-bunch instability threshold currents under 300 milliamperes, the maximum circulating positron current. Low power level rf circuitry for timing and synchronization of the various APS accelerators and storage ring are described. DOE

N92-32318# Southeastern Univ. Research Association, Newport News, VA.
ABSOLUTE MEASUREMENT OF BEAM ENERGY BY COMPTON SCATTERING
W. Barry, P. K. Kloeppel, and R. Rossmanith Apr. 1992 5 p
(Contract DE-AC05-84ER-40150)
(DE92-016964; DOE/ER-40150/191; CEBAF-PR-92-008) Avail: CASI HC A01/MF A01

We propose that the energy of a relativistic electron beam can be measured by observing the Compton radiation it scatters from a resonating cavity. The radiation is to be observed at the frequency at which the intensity does not depend upon the phase of the beam relative to the rf. The measurement will give delta E/E to within 10(exp 4) in about 10 seconds for a 1 mA beam. The number of photons can be significantly increased, and the measuring time decreased proportionately, by use of an rf wiggler in place of the cavity. DOE

N92-32319# Southern California Association of Governments, Los Angeles
HIGH ACCURACY BEAM ENERGY MEASUREMENT FOR LINEAR AND CIRCULAR ACCELERATORS
I. P. Karabekov and R. Rossmanith Mar. 1992 8 p
(Contract DE-AC05-84ER-40150)
(DE92-016966; DOE/ER-40150/193; CEBAF-PR-92-005) Avail: CASI HC A02/MF A01

A new method of measuring the absolute beam energy is presented. The method uses the nonlinear variation of the intensity of a narrow line, filtered from the synchrotron radiation (SR), as a function of beam energy. The resolution of the method is mainly limited by the absolute accuracy of the magnetic field measurement using NMR, the absolute knowledge of the wavelength of the photons, and the quantum fluctuations of the SR at low beam currents. In order to achieve an energy resolution of 2 x 10(exp -5) at a current of 10 micro-A the magnetic field has to be measured with an accuracy of 10(exp -5), and the wavelength, with 2.5 x 10(exp -5). The method is applicable both in linear and circular machines. DOE

N92-32337# Stanford Linear Accelerator Center, CA.
BEAMSTRAHLUNG SPECTRA IN NEXT GENERATION LINEAR COLLIDERS
T. Barklow, P. Chen, and W. Kozanecki (Commissariat a l'Energie

Atomique, Gif-sur-Yvette, France) Feb. 1992 10 p Presented at the ECFA Workshop on Physics with Linear Colliders, Hamburg, Germany, 2-4 Sep. 1991
(Contract DE-AC03-76SF-00515)
(DE92-010730; SLAC-PUB-5718; CONF-9109328-2) Avail: CASI HC A02/MF A01

For the next generation of linear colliders, the energy loss due to beamstrahlung during the collision of the e(+)e(-) beams is expected to substantially influence the effective center-of-mass energy distributions of the colliding particles. In this paper, we first derive analytical formulae for the electron and photon energy spectra under multiple beamstrahlung processes, and for the e(+)e(-) and gamma gamma differential luminosities. We then apply our formalism to various classes of 500 GeV e(+)e(-) linear collider designs currently under study. DOE

N92-32411# Brookhaven National Lab., Upton, NY.
BOOSTER APPLICATIONS FACILITY REPORT, PHASE 2
P. Thieberger, ed. Jun. 1991 334 p
(Contract DE-AC02-76CH-00016)
(DE92-013395; BNL-52291-Phase-2) Avail: CASI HC A15/MF A03

This report summarizes studies and planning performed by Brookhaven National Laboratory (BNL) personnel at the request of NASA for the design, construction and operation of experimental areas and facilities for utilization of ion beams from the BNL Booster synchrotron particle accelerator. These facilities would be primarily utilized to simulate space radiation for radiobiological research, shielding studies and detector calibrations. The feasibility of such a project has been established, preliminary designs and cost estimates have been developed and a formal proposal can be submitted pending DOE concurrence. The main body of this report consists of the material presented by BNL during the meeting with a NASA appointed Panel on December 10 and 11, 1990. The individual speakers have provided brief summaries of their talks and explanations of their figures. In addition there are two appendices. One, contains detailed discussion of the shared mode of operation and the corresponding beam compatibility tables. The second appendix contains cost estimate details. An executive summary on budgets and schedules has been added, containing possible phased construction and outfitting scenarios and the corresponding expense and commitment profiles as well as new operational cost estimates. Material contained in the executive summary reflects the correction of some errors and new studies performed in response to the NASA Panel suggestions. DOE

N92-32413# Lawrence Livermore National Lab., CA.
TRANSVERSE BEAM DYNAMICS IN RECIRCULATING ACCELERATORS FOR HEAVY-ION FUSION
W. M. Sharp, J. J. Barnard, and S. S. Yu 16 Apr. 1992 5 p Presented at the 3rd European Particle Accelerator Conference, Berlin (Germany), 24-28 Mar. 1992
(Contract W-7405-eng-48)
(DE92-013448; UCRL-JC-108512; CONF-920315-34) Avail: CASI HC A01/MF A01

A conceptual design for a circular induction accelerator has been proposed as a driver for heavy-ion fusion. In such an accelerator, errors in dipole strength and quadrupole alignment affect the transverse motion of the beam centroid. Analytic and numerical estimates are made of the beam-centroid displacement due to these errors, and a steering algorithm to correct the transverse mismatch from these errors is described and tested numerically. DOE

N92-32506# Fermi National Accelerator Lab., Batavia, IL.
TUTORIAL ON NEURAL NETWORK APPLICATIONS IN HIGH ENERGY PHYSICS: A 1992 PERSPECTIVE
B. Denby Apr. 1992 41 p Presented at the 2nd International Workshop on Software Engineering, Artificial Intelligence (AI), and Neural Nets for High Energy and Nuclear Physics, L'Agelonde (France), 13-18 Jan. 1992
(Contract DE-AC02-76CH-03000)
(DE92-016003; FNAL/C-92/121-E; CONF-920172-7) Avail: CASI HC A03/MF A01

Feed forward and recurrent neural networks are introduced and related to standard data analysis tools. Tips are given on applications of neural nets to various areas of high energy physics. A review of applications within high energy physics and a summary of neural net hardware status are given. DOE

N92-32567# Southeastern Univ. Research Association, Newport News, VA.
RF CAVITY VACUUM INTERLOCK SYSTEM
K. Jordan, K. Crawford, R. Bundy, H. F. Dylla, J. Heckman, J. Marshall, R. Nichols, S. OSullivan, J. Preble, and J. Robb et al Mar. 1992 5 p
(Contract DE-AC05-84ER-40150)
(DE92-016961; DOE/ER-40150/186; CEBAF-PR-92-012) Avail: CASI HC A01/MF A01

The Continuous Electron Beam Accelerator Facility (CEBAF), a continuous wave (CW) 4 GeV Electron Accelerator is undergoing construction in Newport News, Virginia. When completed in 1994, the accelerator will be the largest installation of radio-frequency superconductivity. Production of cryomodules, the fundamental building block of the machine, has started. A cryomodule consists of four sets of pairs of 1497 MHz, 5 cell niobium cavities contained in separate helium vessels and mounted in a cryostat with appropriate end caps for helium supply and return. Beam vacuum of the cavities, the connecting beam piping, the waveguides, and the cryostat insulating vacuum are crucial to the performance of the machine. The design and initial experience of the vacuum systems for the first 2 1/4 cryomodules that makeup the 45 MEV injector are discussed. DOE

N92-32647# Los Alamos National Lab., NM.
HIGH INTENSITY NEGATIVE PROTON BEAMS FROM A SNICS ION SOURCE
C. R. Evans and M. G. Hollander 1991 11 p Presented at the Symposium of Northeastern Accelerator Personnel, Albuquerque, NM, 15-19 Oct. 1991
(Contract W-7405-eng-36)
(DE92-011137; LA-UR-92-905; CONF-9110258-5) Avail: CASI HC A03/MF A01

For the past year we have been involved in a project to develop an intense (greater than 100 mu A) negative proton beam from a SNICS (Source of Negative Ions by Cesium Sputtering) ion source. This report will cover how we accomplished and exceeded this goal by more than 40 percent. Included in these observations will be the following: a description of an effective method for making titanium hydride cathodes; how to overcome the limitations of the titanium hydride cathode; the modification of the SNICS source to improve output, including the installation of the conical ionizer and the gas cathode; a discussion of problems, including poisoning the proton beam with oxygen, alternative gas cathode materials, the clogging of the gas inlet, long burn-in times, and limited cathode life times. Finally, how to optimize source performance when using a gas cathode; what is the mechanism by which a gas cathode operates; and facts, fantasies, or myth are discussed. DOE

N92-32746# National Inst. for Fusion Science, Nagoya (Japan).
STATUS OF LHD CONTROL SYSTEM DESIGN
K. Yamazaki, H. Kaneko, Y. Taniguchi, and O. Motojima et al Dec. 1991 17 p Presented at the International Conference on Accelerator and Large Experimental Physics Control Systems (ICALEP 1991), Tsukuba, Japan, 11-15 Nov. 1991
(NIFS-122) Avail: CASI HC A03/MF A01

The Large Helical Device (LHD) fusion system, using 1.6 GJ superconducting (SC) magnets, is now under construction, and its plasma experiments will be started in April 1997. For this purpose, a new national institute (National Institute for Fusion Science) was established in May 1989, and a new site (Toki city) was prepared for these experiments. The main objectives of the LHD project are as follows: (1) the study of the behavior of high temperature/high density plasmas using a helical torus device for comprehensive understanding of toroidal plasmas; and (2) the

investigation of the steady-state helical system reactor. The major plasma radius of the LHD is 3.9 m, and the magnetic field strength is 3 Tesla (4 Tesla in the second experimental phase). This makes the LHD the largest SC fusion machine now under construction. To maintain flexible and reliable operations of this SC machine, a new control concept is required. The present status of the control system design for the LHD system is presented. Author

N92-32751# Stanford Linear Accelerator Center, CA.
A HIGH-POWER SLED 2 PULSE COMPRESSION SYSTEM
N. M. Kroll (California Univ., La Jolla.), Z. D. Farkas, T. L. Lavine, A. Menegat, R. D. Ruth, P. B. Wilson, and C. Nantista Mar. 1992 3 p Presented at the Third European Particle Accelerator Conference, Berlin (Germany), 24-28 Mar. 1992
(Contracts DE-AC03-76SF-00515; DE-AS03-89ER-40527)
(DE92-011586; SLAC-PUB-5782; CONF-920315-13) Avail: CASI HC A01/MF A01

The enhancement of peak power by means of RF pulse compression has found important application for driving high energy electron linacs, the SLAC linac in particular. The SLAC Energy Doubler (SLED), however, yields a pulse shape in the form of a decaying exponential which limits the applicability of the method. Two methods of improving this situation have been suggested: binary pulse compression (BPC), in which the pulse is compressed by successive factors of two; and SLED 2 in which the pair of resonant cavities of SLED are replaced by long resonant delay lines (typically waveguides). Intermediate schemes in which the cavity pair is replaced by sequences of coupled cavities have also been considered. In this paper we describe our efforts towards the design and construction of high-power SLED 2 systems, which are intended to provide drivers for various advanced accelerator test facilities and potentially for the Next Linear Collider itself. The design path we have chosen requires the development of a number of microwave components in overmoded waveguide, and the bulk of this paper will be devoted to reporting our progress. DOE

N92-32763# Oesterreichisches Forschungszentrum Seibersdorf G.m.b.H., Vienna. Bereich Lebenswissenschaften.
EXECUTION OF MEASUREMENT SEQUENCES IN THE FRAMEWORK OF THE INSPECTION OF NEAR LIMIT REGIONS BY RADIOIODINE AND AEROSOL EMISSION MEASUREMENTS, AND GROUND EXAMINATIONS ON PLUTONIUM, STRONTIUM, AND GAMMA RAY RADIONUCLIDES [DURCHFUEHRUNG VON MESSFAHRTEN IM RAHMEN DER UEBERWACHUNG GRENZNAHER REGIONEN DURCH RADIOJOD- UND AEROSOL-IMMISSIONS-MESSUNGEN, SOWIE BODENUNTERSUCHUNGEN AUF PLUTONIUM, STRONTIUM UND GAMMASTRAHLENDE RADIONUKLIDE]
Ferdinand Steger, Ernst Lovranich, Ernst Urbanich, Sylvia Streit, and Josef Kozuh-Schneeberger Apr. 1991 21 p In GERMAN Sponsored by Bundeskanzleramt
(OEFZS-4579; ETN-92-91338) Copyright Avail: CASI HC A03/MF A01

Working methods and results of radioiodine measurements and arerosol measurements in an Austrian region are described and given. The plutonium concentration of ground specimens was in the same order of magnitude of that prior to the Chernobyl accident. The strontium 90 content doubled and is to be attributed to the Chernobyl effect. The cesium radionuclide content is to be attributed partly to Chernobyl, and partly to the nuclear weapon tests carried out in the sixties. ESA

N92-32808# Stuttgart Univ. (Germany, F.R.). Inst. fuer Plasmaforschung.
CONCEPTUAL DESIGN OF AN ELECTRON CYCLOTRON WAVE SYSTEM FOR NET/ITER Final Report
W. Kasparek, H. Kumric, G. A. Mueller, J. Pretterebner, P. G. Schueller, and D. Wagner Jul. 1991 136 p
(Contract FU-D-NET-419/90-4)
(IPF-91-6; ETN-92-92150) Avail: CASI HC A07/MF A02

A detailed study of the 120 GHz/20 MW ITER (International Thermonuclear Experimental Reactor) reference is presented. Scaling rules and additional antenna designs for higher frequency systems were developed. The design principle was to offer a high degree of flexibility for the wide range of envisaged uses of the Electron Cyclotron Waves (ECWs). The efficiency of the ECW system is estimated to be between 25 and 40 percent, depending mainly on the efficiency of the gyrotrons. An evaluation of the costs is given. The technical programs of the transmission components of the transmission line and antenna for the ITER 120 to 140 GHz ECW system are concluded to be solvable with today's technology. For other ECW heating and current drive applications, this system can be scaled in power and frequency. ESA

N92-32904# Lawrence Livermore National Lab., CA.
STUDY OF RECIRCULATING INDUCTION ACCELERATORS AS DRIVERS FOR HEAVY ION FUSION
J. J. Barnard, A. L. Brooks, J. P. Clay, F. E. Coffield, F. J. Deadrick, L. V. Griffith, A. R. Harvey, H. C. Kirbie, V. K. Neil, and M. A. Newton et al 21 Sep. 1991 279 p
(Contract W-7405-eng-48)
(DE92-016980; UCRL-LR-108095) Avail: CASI HC A13/MF A03

This report presents point designs for a recirculating induction accelerator that will function as the driver for an inertial confinement fusion reactor power plant that produces about 1 GW of electric power for a lifetime of about 30 years. The idea of a recirculator has been previously proposed, but no integrated driver system has ever been conceptually designed or evaluated. Our goal is to present design examples that meet the requirements set by target and reactor physics while minimizing the cost and maximizing efficiency. We wish to evaluate the feasibility of such an accelerator by performing a preliminary analysis of the major physics and engineering issues. A further goal is to compare the cost and efficiency of this point design with that of a linear accelerator, similarly designed, using the same costing algorithms. During the preparation of this report, new issues continually arose and appropriate solutions were devised. At times, different weights were given to the often conflicting goals of low cost, high efficiency, high confidence of achieving high beam quality at the target, and high confidence in technological achievability. We have therefore arrived at many point designs, three of which are the subject of this report. Today's Technology Design is the primary focus of the report, and it consists entirely of technology that could be built today or soon. The Low Cost/Advanced Technology Design uses more advanced or alternative technologies to implement the recirculator concept. In the Low Physics Risk Design, the driver system consists of several independent single-beam recirculators, rather than allowing several beams to share an induction core. DOE

N92-32912# Brookhaven National Lab., Upton, NY.
POLARIZED WIGGLER FOR NSLS X RAY RING DESIGN CONSIDERATIONS
A. Friedman, S. Krinsky, and E. Blum Mar. 1992 38 p
(Contract DE-AC02-76CH-00016)
(DE92-012212; BNL-47317) Avail: CASI HC A03/MF A01

We examine the properties of an elliptically polarized wiggler that will generate circularly polarized photons with energy spectrum of 3-12 KeV. The vertical wiggler magnetic field is produced by permanent magnets while the horizontal wiggler field is generated by electric coils capable of AC excitation. The radiation parameters of the wiggler are presented, including photon flux, circular and linear polarization, and spectrum. These parameters are compared to the synchrotron radiation from a bending magnet. Numerical values are calculated for radiation from the wiggler and bending magnet for the NSLS x-ray ring parameters. A conceptual design for such a wiggler is discussed, and several different alternatives are analyzed. We consider AC excitation of the wiggler to produce the time modulation of the elliptic polarization, and also to produce time modulated linearly polarized radiation. DOE

N92-32932# Argonne National Lab., IL. Advanced Photon Source Div.
PROCEEDINGS OF THE FOURTH USERS MEETING FOR THE ADVANCED PHOTON SOURCE
Feb. 1992 222 p Meeting held in Argonne, IL, 7-8 May 1991
(Contract W-31-109-eng-38)
(DE92-014061; ANL/APS-CP-4; CONF-9105180) Avail: CASI HC A10/MF A03

The Fourth Users Meeting for the Advanced Photon Source (APS) was held on May 7-8, 1991 at Argonne National Laboratory. Scientists and engineers from universities, industry, and national laboratories came to review the status of the facility and to look ahead to the types of forefront science that will be possible when the APS is completed. The presentations at the meeting included an overview of the project; critical issues for APS operation; advances in synchrotron radiation applications; users perspectives, and funding perspectives. The actions taken at the 1991 Business Meeting of the Advanced Photon Source Users Organization are also documented. DOE

N92-32994# Sandia National Labs., Albuquerque, NM.
SHIELDING ANALYSES FOR REPETITIVE HIGH ENERGY PULSED POWER ACCELERATORS
H. N. Jow and D. V. Rao (Science and Engineering Associates, Inc., Albuquerque, NM.) 1992 3 p Presented at the American Nuclear Society Annual Meeting, Boston, MA, 7-12 Jun. 1992
(Contract DE-AC04-76DP-00789)
(DE92-015004; SAND-92-0770C; CONF-920606-19) Avail: CASI HC A01/MF A01

Sandia National Laboratories (SNL) designs, tests and operates a variety of accelerators that generate large amounts of high energy Bremsstrahlung radiation over an extended time. Typically, groups of similar accelerators are housed in a large building that is inaccessible to the general public. To facilitate independent operation of each accelerator, test cells are constructed around each accelerator to shield it from the radiation workers occupying surrounding test cells and work-areas. These test cells, about 9 ft. high, are constructed of high density concrete block walls that provide direct radiation shielding. Above the target areas (radiation sources), lead or steel plates are used to minimize skyshine radiation. Space, accessibility and cost considerations impose certain restrictions on the design of these test cells. SNL Health Physics division is tasked to evaluate the adequacy of each test cell design and compare resultant dose rates with the design criteria stated in DOE Order 5480.11. In response, SNL Health Physics has undertaken an intensive effort to assess existing radiation shielding codes and compare their predictions against measured dose rates. This paper provides a summary of the effort and its results. DOE

N92-33070# Stanford Linear Accelerator Center, CA.
ACCELERATOR PHYSICS OF THE STANFORD LINEAR COLLIDER AND SLC ACCELERATOR EXPERIMENTS TOWARDS THE NEXT LINEAR COLLIDER
J. T. Seeman Jun. 1992 19 p
(Contract DE-AC03-76SF-00515)
(DE92-017552; SLAC-PUB-5748) Avail: CASI HC A03/MF A01

The Stanford Linear Collider (SLC) was built to collide single bunches of electrons and positrons head-on at a single interaction point with single beam energies up to 55 GeV. The small beam sizes and high currents required for high luminosity operation have significantly pushed traditional beam quality limits. The Polarized Electron Source produces about 8 x 10(exp 10) electrons in each of two bunches with up to 28 percent polarization. The damping rings provide coupled invariant emittances of 1.8 x 10(exp -5) r-m with 4.5 x 10(exp 10) particles per bunch. The 57 GeV Linac has successfully accelerated over 3 x 10(exp 10) particles with design invariant emittances of 3 x 10(exp -5) r-m. Both longitudinal and transverse wakefields strongly affect the trajectory and emittance corrections used for operations. The Arc systems routinely transport decoupled and betatron matched beams. In the Final Focus, the beams are chromatically corrected and demagnified producing spot sizes of 2 to 3 micrometers at the focal point. Spot sizes below 2 micrometers have been made during special tests. Instrumentation and feedback systems are well advanced, providing continuous beam monitoring and pulse-by-pulse control. A luminosity of 1.6 x 10(exp 29) cm(exp -2)sec(exp -1) has been produced. Several experimental tests for a Next Linear Collider (NLC) are being planned or constructed using the SLC accelerator as a test facility. The Final Focus Test Beam will demagnify a flat 50 GeV electron beam to dimensions near 60 nm vertically and 900 nm horizontally. A potential Emittance Dynamics Test Area has the capability to test the acceleration and transport of very low emittance beams, the compression of bunch lengths to 50 micrometers, the acceleration and control of multiple bunches, and the properties of wakefields in the very short bunch length regime. DOE

N92-33122# Lawrence Livermore National Lab., CA.
DEVELOPMENT OF ADVANCED MODULATORS FOR RECIRCULATING HEAVY ION ACCELERATORS
M. A. Newton, H. C. Kirbie, H. D. Shay, and S. S. Yu Mar. 1992 4 p Presented at the 3rd European Particle Accelerator Conference, Berlin (Germany), 24-28 Mar. 1992
(Contract W-7405-eng-48)
(DE92-014795; UCRL-JC-108513; CONF-920315-39) Avail: CASI HC A01/MF A01

Heavy-ion accelerators are considered to be one of the promising driver alternatives for inertial fusion. In a heavy-ion inertial-fusion driver, multiple beams of heavy ions are accelerated to the kinetic energies needed to ignite a fusion target. During acceleration, the beams of heavy ions are compressed from initial pulse durations of 10's to 100's of microseconds to a final pulse duration in the reactor of approximately 10 nanoseconds. The compressed beam of heavy ions is focused on the target in a reactor chamber where the energy released from the fusion reaction is converted to thermal energy and eventually to electricity. Several approaches for accelerating heavy-ions have been proposed including RF accelerators, conventional linear induction accelerators, multi-phase linear accelerators, and recirculating induction accelerators. A recirculator is an induction accelerator which accelerates the particles and bends them in a closed path with dipole magnetic fields. A single beam traverses the same accelerating cavities many times to acquire its final energy. The primary motivation to evaluate recirculators is the potential for significant cost reduction over conventional linear induction accelerators. The idea of recirculation is not new, but only recently has a thorough investigation of this concept been conducted. DOE

N92-33130# Argonne National Lab., IL.
THERMAL AND STRUCTURAL ANALYSIS OF HIGH PRECISION BEAMLINE POSITION MONITORS FOR SYNCHROTRON X RAY BEAMS
Z. Wang, D. Shu, A. M. Khounsary, and T. Kuzay 1992 7 p Presented at the American Society of Mechanical Engineers Pressure Vessel and Piping Conference, New Orleans, LA, 21-25 Jun. 1992
(Contract W-31-109-eng-38)
(DE92-014863; ANL/CP-74658; CONF-920631-36) Avail: CASI HC A02/MF A01

The photon beam position monitors (PBPM) on the front end of the 7-GeV Advanced Photon Source (APS) synchrotron facility, under construction at Argonne National Laboratory (ANL), are precision devices that measure spatial as well as angular positions of the x-ray beams. There exist two such devices on each APS front end, and they are set approximately 4 m apart. The required spatial resolution of these devices is on the order of a few microns; the required angular resolution is less than a micro-radian. These specifications make the material selection, design, and stability of the PBPM very challenging tasks. The PBPM blades, which generate the photo-electron signal from the x-ray beam, are indirectly cooled to prevent overheating by the x-ray beam. Even then, the blade is subject to severe thermal stresses. Prediction of the long-term material and position stability of the PBPM blade requires very careful heat transfer and stress analyses. In this

paper, thermal analyses under the prevailing high heat flux from the incident beam and the corresponding stress analyses for various blade configuration are presented. As a result of these analyses, several options in design were developed and compared, including material selection for the blade and its structural detail. DOE

N92-33134# Superconducting Super Collider Lab., Dallas, TX.
OVERVIEW OF SSC ACCELERATOR REQUIREMENTS
G. Dugan Mar. 1992 7 p Presented at the International Industrial Symposium on the Super Collider, New Orleans, LA, 4-6 Mar. 1992 Submitted for publication
(Contract DE-AC35-89ER-40486)
(DE92-014896; SSCL-Preprint-84; CONF-920331-47) Avail: CASI HC A02/MF A01

This paper will present a general overview of the requirements of the Superconducting Super Collider (SSC) accelerators. Each accelerator in the injector chain will be discussed separately, followed by a discussion of the collider itself. In conclusion, the top level requirements of the overall accelerator system will be presented. For each accelerator, the primary operating parameters will be presented in tabular form. A brief narrative discussion of the principal technical features of each machine will be given. Finally, the principal technical design challenges for the machine will be noted, together with the currently planned solution to these challenges. DOE

N92-33167 Department of the Navy, Washington, DC.
HIGH EFFICIENCY FAST NEUTRON THRESHOLD DEFLECTOR Patent
Robert A. August, Jr., inventor (to Navy) 7 Jan. 1992 7 p Filed 1 Aug. 1990
(AD-D015311; US-Patent-5,078,951; US-Patent-Appl-SN-560959; US-Patent-Class-376-154) Avail: US Patent and Trademark Office

A high-efficiency apparatus for detecting fast neutrons includes an assembly of disks of solid state charged particle detector material, or other appropriate charged particle detecting devices, disposed between adjacent thick (on the order of 1 mm) disks of fissionable material. The fissionable material must be an isotope that has a sharp increase in the neutron-induced fission cross section at a neutron energy of about 100 keV or greater, i.e., a fast neutron. An array of such assemblies housed in a thermal neutron shielding structure provides a threshold detector for fast neutrons resulting from neutron-induced fission of the fissionable material. GRA

N92-33179# Brookhaven National Lab., Upton, NY.
KINEMATICS OF COMPTON BACKSCATTERING X RAY SOURCE FOR ANGIOGRAPHY
L. N. Blumberg May 1992 31 p
(Contract DE-AC02-76CH-00016)
(DE92-014016; BNL-47503) Avail: CASI HC A03/MF A01

Calculations of X-Ray production rates, energy spread, and spectrum of Compton-backscattered photons from a Free Electron Laser on an electron beam in a low energy (136-MeV) compact (8.5-m circumference) storage ring indicate that an X-Ray intensity of 34.6 10(exp 7) X-Ray photons per 0.5-mm times 0.5-mm pixel for Coronary Angiography near the 33.169-keV iodine K-absorption edge can be achieved in a 4-msec pulse within a scattering cone of 1-mrad half angle. This intensity, at 10-m from the photon-electron interaction point to the patient, is about a factor of 10 larger than presently achieved from a 4.5-T superconducting wiggler source in the NSLS 2.5-GeV storage ring and over an area about 5 times larger. The 2.2-keV energy spread of the Compton-backscattered beam is, however, much larger than the 70-eV spread presently attained form the wiggler source and use of a monochromator. The beam spot at the 10-m interaction point-to-patient distance is 20-mm diameter; larger spots are attainable at larger distances, but with a corresponding reduction in X-Ray flux. Such a facility could be an inexpensive clinical alternative to present methods of non-invasive Digital Subtraction Angiography (DSA), small enough to be deployed in an urban medical center, and could have other medical, industrial and aerospace applications. Problems with the Compton backscattering source include laser beam heating of the mirror in the FEL oscillator optical cavity, achieving a large enough X-Ray beam spot at the patient, and obtaining radiation damping of the transverse oscillations and longitudinal emittance dilution of the storage ring electron beam resulting from photon-electron collisions without going to higher electron energy where the X-Ray energy spread becomes excessive for DSA. DOE

N92-33182# Purdue Univ., West Lafayette, IN. Dept. of Physics.
A THEORETICAL HIGH ENERGY PHYSICS PROGRAM: TASK F
E. Fischbach 1992 16 p
(Contract DE-AC02-76ER-01428)
(DE92-014054; DOE/ER-01428/T10) Avail: CASI HC A03/MF A01

This report briefly discusses research on new limits on light axionic fields; non-Newtonian gravity; the search for the fifth force; and a test of special relativity by a determination of the Lorentz limiting velocity. DOE

74 OPTICS

Includes light phenomena; and optical devices.
For lasers see *36 Lasers and Masers.*

N92-32321# California Univ., Berkeley. Lawrence Berkeley Lab.
DETERMINING SURFACE PROFILE FROM SEQUENTIAL INTERFERENCE PATTERNS FROM A LONG TRACE PROFILER
S. C. Irick Jul. 1991 10 p Presented at the 4th International Conference on Synchrotron Radiation Instrumentation, Chester (England), 15-19 Jul. 1991
(Contract DE-AC03-76SF-00098)
(DE92-017117; LBL-30464; CONF-910730-31) Avail: CASI HC A02/MF A01

The Long Trace Profiler (Takacs et al.) is a slope-measuring instrument which was introduced several years ago. Development of this instrument continues at Lawrence Berkeley Laboratory in improving both hardware design and software algorithms for turning the raw interference data (a sequence of intensity patterns) into properly interpreted representations of surface slope and height. This report presents a mathematical model of the interference pattern and methods of extracting the slope and height profile from such patterns. DOE

N92-32419# California Univ., Berkeley. Lawrence Berkeley Lab.
THERMAL EFFECTS AND MIRROR SURFACE FIGURE REQUIREMENTS FOR A DIAGNOSTIC BEAMLINE AT THE ADVANCED LIGHT SOURCE
T. Warwick and S. Sharma (Brookhaven National Lab., Upton, NY.) 28 Oct. 1991 9 p Presented at the 7th National Conference and Exhibition on Synchrotron Radiation Instrumentation, Baton Rouge, LA, 28-31 Oct. 1991
(Contract DE-AC03-76SF-00098)
(DE92-014483; LBL-31532; CONF-9110146-16) Avail: CASI HC A02/MF A01

An imaging beamline based on a Kirkpatrick-Baez mirror configuration was designed to image the electron beam in the ALS storage ring, to measure its size and shape. The electron beam emittance will be small ((epsilon)h = 3.4(10)(exp -9) m rad) and the quality of the image is extremely sensitive to surface figure distortion of the mirrors. Thermal distortions and surface temperatures were calculated for radiatively cooled mirrors of various materials in a search for a simple design which avoids water cooling. The choice of mirror material and the thermal and mechanical design is discussed. DOE

N92-32613# Naval Research Lab., Washington, DC.
CORRELATION OF SINGLE MODE FIBER FABRICATION FACTORS AND RADIATION RESPONSE Final Report
E. J. Friebele 28 Feb. 1992 149 p
(AD-A247301; NRL/MR/6505-92-6939; NCS-TIB-91-11) Avail: CASI HC A07/MF A02

Fiber optic transmission systems, because of their extraordinary channel capacity and decreasing cost, are the preferred terrestrial transmission media of the nation's long distance, inter-city telecommunications infrastructure. Since the commercial telephone network forms the foundation for emergency communication in the event of a national crisis or emergency, additional requirements are placed on the fibers and components of this system. The network must remain operational in the face of such threats as loss of commercial power, disruption by natural causes, violation of physical security, and exposure to the effects of nuclear weapons, including electromagnetic pulse (EMP) and ionizing radiation from the delayed gamma component and fallout. The most stressing environment for the fiber consists of fallout subsequent to a nuclear attack since the long lengths of fiber can be potentially exposed to high total doses. The susceptibility of some types of commercially available fiber optic cable to optical darkening (and hence increased signal loss and bit error rate) from exposure to ionizing radiation raises serious questions about the survivability of such systems in the reconstitution phase of a nuclear conflict. GRA

N92-32634# Department of the Navy, Washington, DC.
DEPOLARIZED LIGHT SOURCE FOR FIBER OPTIC SENSORS Patent Application
W. K. Burns, inventor (to Navy) and R. P. Moeller, inventor (to Navy) 13 Dec. 1991 22 p
(AD-D015289; US-Patent-Appl-SN-806384; Navy-Case-72926) Avail: CASI HC A03/MF A01

An apparatus comprised of a depolarized light source for fiber optic sensors is disclosed. In a preferred embodiment, the depolarized light source of the apparatus comprises: a first laser for generating a first beam at a first frequency with the first beam having a linear polarization state; a second laser for generating a second beam at a second frequency with the second beam having a linear polarization state; a means for rotating the polarization state of the second beam so that the first and second beams have orthogonal linear polarization states with respect to each other; and a means for combining the first beam with the polarization-rotated second beam to obtain a composite beam which is depolarized. In a system operation, the apparatus comprises a source of depolarized light; an integrated optic modulator means for receiving a modulator drive signal; a first low-birefringence fiber for conveying the depolarized light beam from the depolarized light source to the integrated optic modulator means (the integrated optic modulator mean modulating only one linear polarization state in the depolarized light beam as a function of the modulator drive signal to produce a modulated beam); a photodetector; and a second low-birefringence fiber for conveying the modulated light beam to the photodetector with the photodetector being responsive to the modulated light beam for developing an electrical signal proportional to the modulator drive signal. GRA

N92-32668# Stanford Univ., CA. Space Telecommunications and Radioscience Lab.
CAN THE SPEED OF LIGHT IN THE FIBER BE CONTROLLED?
Y. N. Taranenko and L. G. Kazovsky 1991 7 p
(Contract N00014-91-J-1857)
(AD-A247614) Avail: CASI HC A02/MF A01

Nonlinear effects in optical fibers lead to many interesting phenomena, including nonlinear wave coupling, optical pulse compression, stimulated Raman and Brillouin scattering, harmonic generation, optical solitons, etc. Solitons have been known to applied scientists for some 20 years. We predict that a nonlinear interaction between two copropagating modes and an acoustical wave in dual mode optical fibers can lead to a three-wave envelope soliton (TWES) and to controlling the speed of light in the fiber. To generate TWES, two light copropagating waves with slightly different frequencies have to be synchronously modulated and launched into the fiber; the acoustical wave is generated in the fiber by nonlinear coupling with intermodal beating. The same second order nonlinearity is responsible for this process; it is similar to the stimulated forward Brillouin scattering. TWES's are similar to conventional optical solitons in the sense that they are envelope solitons. However, unlike conventional optical solitons, the TWES is a nonlinear combination of three waves. GRA

N92-32672# Aerospace Corp., El Segundo, CA. Technology Operations.
A MOLECULE-SPECIFIC FILTER MODULATOR
J. T. Knudtson, T. M. Reese, and K. C. Herr 15 Sep. 1991 22 p
(Contract F04701-88-C-0089)
(AD-A250760; TR-0091(6940-09)-2; SSD-TR-92-05) Avail: CASI HC A03/MF A01

An optical Fabry-Perot filter was devised to aid in the detection of weak infrared emission from hot molecules. The comb-like transmission spectrum of the filter was matched to the comb-like infrared emission spectrum of CO. The filter can be made to perform rapid background subtraction by slightly detuning the filter spectrum from the molecular emission spectrum. This invention is called spectral dithering and can be performed at rates up to several kilohertz using a piezoelectrically driven Fabry-Perot filter. In cases where atmospheric fluctuations are a significant noise source, background subtraction at kilohertz rates can essentially freeze the fluctuations. This improves the effectiveness of the background subtraction. Estimates of the signal/background and signal/noise improvements for the filter are given. The spectral dithering capability was demonstrated in a laboratory experiment using CO emission from a flame. GRA

N92-32703# Universiteit Twente, Enschede (Netherlands).
LOCAL ASPECTS OF THE OPTICAL REFLECTION PROBLEM: THE DISCRETE DIPOLE APPROACH Ph.D. Thesis
Gert Pierre Maria Poppe 1991 165 p
(ISBN-90-9004118-4; ETN-92-92042) Avail: CASI HC A08/MF A02

The optical response of dielectric systems obeying parallel translational symmetry is described. Starting from the basic principles of the discrete dipole model, it is shown to be possible to derive in an exact way the expressions governing the reflection and transmission coefficients of a thin slab, a thick slab or a semi-infinite medium. The resulting optical parameters are very sensitive to the spatial arrangement of the individual atoms and molecules, especially at the surface. Therefore it is ideally suited to study the results of differential spectrometers. This is illustrated by applying the theory to the CO adsorption on NaCl(100) and the reflection anisotropy of GaP(110) and Si(110). ESA

N92-32705# Universiteit Twente, Enschede (Netherlands).
TOPOGRAPHICAL MEASURING BASED ON THE SHADOW AND PROJECTION MOIRE METHOD Ph.D. Thesis
Alfonsus Maria Frans Wegdam 1991 180 p
(ISBN-90-9004146-X; ETN-92-92043) Avail: CASI HC A09/MF A02

Considerations related to and the conditions to be made for the construction of a moire system for topographical measurement are addressed. Two different ways of generating moire patterns, which are of particular importance, were studied: projection and shadow moire. The effect of optical phenomena and of numerous system parameters are considered and analyzed. This includes contributions from diffraction, lens aberrations, system setup, system alignment, grating profile, and image acquisition system, to the overall performance of shadow and projection moire systems. A package of software was developed, based on the theoretical analyses presented. This software can be conveniently used to construct, and predict the performance, of the two different moire types. To verify the validity and acccuracy of the theoretical analysis presented, an experimental projection moire system was built, based on the guidelines and tools provided by the theory. As to

the shadow moire system, a more limited setup was built which only allowed measurement of some important properties. Experimental results compared favorably with theoretical predictions for both the projection and shadow moire system.
ESA

N92-32738# Los Alamos National Lab., NM.
THE EFFECT OF THE LIGHT ROUND-TRIP TIME ON THE PERFORMANCE OF AN ADAPTIVE OPTICS TURBULENCE COMPENSATION SYSTEM
P. Stroud 24 Feb. 1992 11 p
(Contract W-7405-eng-36)
(DE92-011273; LA-UR-92-693) Avail: CASI HC A03/MF A01

The propagation of a laser beam through atmospheric turbulence can, under many circumstances, be compensated to near diffraction limited levels, by use of an adaptive optics system. In the ideal case, a beacon light source is generated at the aimpoint. This light traverses through the turbulent path back to the aperture. The distribution of phase perturbations in the aperture plane is sensed, and the reverse of this phase is applied to the outgoing beam. When the turbulent path is long (i.e. a few hundred kilometers) and the effective wind speed is high (such as in the case when the laser is based on a plane with airspeeds around 200 m/s), the performance of the adaptive optics system can be significantly degraded due to the time delay from when the beacon samples the turbulence, until the beam propagates through the turbulence. This effect has not been treated in the past, because, for astronomical applications, the time delays due to the round trip of light are too short (tens of microseconds) to cause problems. This paper presents an analysis of the anisoplanatic effect of the round trip time of light. A formulation of the phase variance has been constructed for this effect. The time response of the adaptive optics system (i.e. servo bandwidth) is intimately related to the light round trip time effect, and is included in the analysis. Results are first obtained for the large aperture limit, and then the effects of finite aperture size are treated. A set of scaling relationships have been found that enable the formulation to be cast in a form that is insensitive to the turbulence strength profile along the propagation path.
DOE

N92-32805# Ecole Nationale Superieure des Telecommunications, Paris (France).
OPTO-ELECTRONIC SYSTEM FOR A FORMAL NEURAL NETWORK Ph.D. Thesis [UNE IMPLANTATION OPTO-ELECTRONIQUE D'UN RESEAU DE NEURONES FORMELS]
Keven Heggarty 1991 156 p In FRENCH
(Telecom-91-E-013; ETN-92-92097) Avail: CASI HC A08/MF A02

A study on the construction of an optoelectronic system which makes use of the capacities of holographic optics for performing interconnections is presented. In the chosen application (digit recognition) the system acts as an associative memory treating two dimensional data structures (images) in parallel. Starting from the Hopfield model, the synaptic matrix algorithm is modified to adapt the network to optical implementation and improve its discrimination of similar memory vectors. The approach leads to a correlation-reconstruction interpretation of pseudo-inverse techniques. The coding of the computed generated hologram used to perform the connections between two planes which form the outputs and the inputs of the neurons is addressed. This hologram is unusual in that it fulfills simultaneously the necessary correlation and reconstruction functions. The standard techniques of digital holography, usually optimized for one or the other of these functions, is therefore adapted to the specific needs of the connection hologram. In particular, the reduction of the dynamic range of the hologram, whilst retaining the correlation function and a useful degree of shift invariance, is demonstrated. The construction of the prototype system and the adaptation of a laser lithography facility to the fabrication of the holograms are described. The potential of the system is illustrated with experimental results demonstrating its capacity to recognize and discriminate to correlated images from noisy, translated input images. Generalization of the system for use as an interconnection stage in more complicated architectures is illustrated.
ESA

N92-32806# Ecole Nationale Superieure des Telecommunications, Paris (France).
USES OF STEREOVISION SURFACE MODELS Ph.D. Thesis [UTILISATIONS DES MODELES DE SURFACES EN STEREOVISION]
Wei Luo 1991 161 p In FRENCH
(Telecom-91-E-016; ETN-92-92098) Avail: CASI HC A08/MF A02

The development of an automatic three dimensional stereo reconstruction system is addressed. Three classical methods (correlation, zero crossing, and dynamic programming) are tested on a large number of real scenes to obtain a disparity map as dense as possible. The advantages and limitations of each method are discussed. Results show, for complex (such as urban) scenes, that surface discontinuities, hidden areas, and little textured surfaces exist, and many errors appear. A solution to solve these problems using surface models from integration of stereo and luminous data to help and improve stereo reconstruction and thereby correct disparity errors to reconstruct complete surfaces is proposed. This model oriented stereovision is quantitatively evaluated and its results are compared with a numerical terrain model from an analytical stereo reconstructor, showing that the quadratic mean distance error can be divided by two on complex scenes.
ESA

N92-32915# Cornell Univ., Ithaca, NY.
BETA-BARIUM BORATE OPTICAL PARAMETRIC OSCILLATOR Final Report, 16 Aug. 1990 - 15 Aug. 1991
C. L. Tang 15 Aug. 1991 6 p
(Contract N00014-90-C-2200)
(AD-A251177) Avail: CASI HC A02/MF A01

A Beta-Barium Borate Optical Parametric Oscillator (BBO OPO) has been constructed and shipped to the Army laboratory at White Sands. This OPO is a truly continuously tunable source with a very large spectral coverage. It is pumped at the third harmonic of Nd:YAG or 335 nm. The output is continuously tunable over the entire spectral range from 450 nm to 2.5 microns with relatively high efficiency. The tuning is completely computer controlled. The two-crystal configuration was needed to compensate for the walk-off in BBO. The intracavity pump beam steering mirrors are needed to reduce the change of UV damage of the resonator mirrors. The efficiency of the OPO is over 30 percent. The linewidth of the oscillator without using special line narrowing schemes is relatively large. However, there are special line narrowing schemes that can be employed to significantly reuse the linewidth with some sacrifice in the threshold for oscillation and efficiencies. An alternative is to use Type II phase-matching, by which a line width on the order of an Angstrom can be maintained throughout the tuning range without additional line narrowing elements in the oscillator cavity.
GRA

N92-32935# Naval Command, Control and Ocean Surveillance Center, San Diego, CA.
RECURSIVE ESTIMATION TECHNIQUES FOR DETECTION OF SMALL OBJECTS IN INFRARED IMAGE DATA
J. R. Zeidler, T. Soni, and W. H. Ku Apr. 1992 6 p
(AD-A250942) Avail: CASI HC A02/MF A01

This paper describes a recursive detection scheme for point targets in infrared (IR) images. Estimation of the background noise is done using a weighted autocorrelation matrix update method and the detection statistic is calculated using a recursive technique. A weighting factor allows the algorithm to have finite memory and deal with nonstationary noise characteristics. The detection statistic is created by using a matched filter for colored noise, using the estimated noise autocorrelation matrix. The relationship between the weighting factor, the nonstationarity of the noise and the probability of detection is described. Some results on one- and two-dimensional infrared images are presented.
GRA

N92-33004# EPITAXX, Inc., Princeton, NJ.
A SIMPLE HIGH-PERFORMANCE AVALANCHE PHOTODIODE FOR LONG-WAVELENGTH OPTICAL COMMUNICATIONS, PHASE 1
Gregory H. Olsen 17 Sep. 1987 32 p
(Grant NSF ISI-86-60941)
(PB92-188259; NSF/ISI-87031-Phase-1) Avail: CASI HC A03/MF A01

The feasibility of a highly-simplified indium gallium arsenide avalanche photodiode structure for optical communications at 1300 and 1550 nm was demonstrated. The simplicity of the device would eventually allow for a high-yield manufacturing process and remove one of the biggest obstacles to widespread use of long-wavelength fiber optics. Two-dimensional electric field modeling (via computer) was carried out to determine the optimum geometric parameters for the device. Based on the results, an actual device was constructed with vapor phase epitaxy, using the proprietary guard-ring structure. After full wafer processing, the devices were tested for optical performance. The effects of increasing breakdown voltage (by a factor of two) and reduction of edge fields, due to the structure, were clearly demonstrated. Leakage currents as low as 1 nA and capacitance values of 0.25 picofarads were measured at the half-breakdown voltage. Avalanche gains of three were also measured with the initial structure. Author

N92-33017* National Aeronautics and Space Administration. Langley Research Center, Hampton, VA.
HIGH TEMPERATURE FIBER OPTIC MICROPHONE HAVING A PRESSURE-SENSING REFLECTIVE MEMBRANE UNDER TENSILE STRESS Patent
Allan J. Zuckerwar, inventor (to NASA), Frank W. Cuomo, inventor (to NASA), William E. Robbins, inventor (to NASA), and Purnell Hopson, Jr., inventor (to NASA) 8 Sep. 1992 16 p Filed 21 Sep. 1990 Supersedes N91-15874 (29 - 7, p 1068)
(NASA-Case-LAR-14402-1-CU; US-Patent-5,146,083;
US-Patent-Appl-SN-586369; US-Patent-Class-250-227.21;
US-Patent-Class-250-231.19; US-Patent-Class-73-705;
US-Patent-Class-358-12; Int-Patent-Class-H01J-40/14) Avail: US Patent and Trademark Office

A fiber optic microphone is provided for measuring fluctuating pressures. An optical fiber probe having at least one transmitting fiber for transmitting light to a pressure-sensing membrane and at least one receiving fiber for receiving light reflected from a stretched membrane is provided. The pressure-sensing membrane may be stretched for high frequency response. Further, a reflecting surface of the pressure-sensing membrane may have dimensions which substantially correspond to dimensions of a cross section of the optical fiber probe. Further, the fiber optic microphone can be made of materials for use in high temperature environments, for example greater than 1000 F. A fiber optic probe is also provided with a backplate for damping membrane motion. The backplate further provides a means for on-line calibration of the microphone.
Official Gazette of the U.S. Patent and Trademark Office

N92-33022* National Aeronautics and Space Administration. Pasadena Office, CA.
REAL-TIME EDGE-ENHANCED OPTICAL CORRELATOR Patent
Tsuen-Hsi Liu, inventor (to NASA) (Jet Propulsion Lab., California Inst. of Tech., Pasadena.) and Li-Jen Cheng, inventor (to NASA) (Jet Propulsion Lab., California Inst. of Tech., Pasadena.) 22 Sep. 1992 9 p Filed 25 Nov. 1991 Supersedes N92-17675 (30 - 8, p 1367)
(NASA-Case-NPO-18379-1-CU; US-Patent-5,150,228;
US-Patent-Appl-SN-797569; US-Patent-Class-359-7;
US-Patent-Class-359-559; US-Patent-Class-359-561;
Int-Patent-Class-G03B-1/16; Int-Patent-Class-G02B-27/42) Avail: US Patent and Trademark Office

Edge enhancement of an input image by four-wave mixing a first write beam with a second write beam in a photorefractive crystal, GaAs, was achieved for VanderLugt optical correlation with an edge enhanced reference image by optimizing the power ratio of a second write beam to the first write beam (70:1) and optimizing the power ratio of a read beam, which carries the reference image to the first write beam (100:701). Liquid crystal TV panels are employed as spatial light modulators to change the input and reference images in real time.
Official Gazette of the U.S. Patent and Trademark Office

N92-33028* National Aeronautics and Space Administration. Pasadena Office, CA.
REAL TIME PRE-DETECTION DYNAMIC RANGE COMPRESSION Patent
Hua-Kuang Liu, inventor (to NASA) (Jet Propulsion Lab., California Inst. of Tech., Pasadena.) 14 Jul. 1992 5 p Filed 19 Dec. 1990 Supersedes N91-23890 (29 - 15, p 2507)
(NASA-Case-NPO-18098-1-CU; US-Patent-5,130,530;
US-Patent-Appl-SN-633746; US-Patent-Class-250-216;
US-Patent-Class-359-241; Int-Patent-Class-H01J-3/14) Avail: US Patent and Trademark Office

A real time, pre-detection optical dynamic range compression system uses a photorefractive crystal, such as BaTiO3 or LiNbO3, in which light induced scattering from crystal inhomogeneities of the optical input occurs as a nonlinear function of the input intensity. The greater the intensity, the faster random interference gratings are created to scatter the incident light. The unscattered portion of the optical signal is therefore reduced in dynamic range over time. The amount or range of dynamic range compression may be controlled by adjusting the time of application of the unscattered crystal output to the photodetector with regard to the time of application of the optical input to the crystal.
Official Gazette of the U.S. Patent and Trademark Office

N92-33074*# Rochester Photonics Corp., Fairport, NY.
DIFFRACTIVE OPTICS TECHNOLOGY AND THE NASA GEOSTATIONARY EARTH OBSERVATORY (GEO) Final Report
G. Michael Morris, Robert L. Michaels, and Dean Faklis 31 Jul. 1992 46 p
(NASA Order H-13026-D)
(NASA-CR-190611; NAS 1.26:190611; RPC-TR-1276-102-G-AR)
Avail: CASI HC A03/MF A01

Diffractive (or binary) optics offers unique capabilities for the development of large-aperture, high-performance, light-weight optical systems. The Geostationary Earth Observatory (GEO) will consist of a variety of instruments to monitor the environmental conditions of the earth and its atmosphere. The aim of this investigation is to analyze the design of the GEO instrument that is being proposed and to identify the areas in which diffractive (or binary) optics technology can make a significant impact in GEO sensor design. Several potential applications where diffractive optics may indeed serve as a key technology for improving the performance and reducing the weight and cost of the GEO sensors have been identified. Applications include the use of diffractive/refractive hybrid lenses for aft-optic imagers, diffractive telescopes for narrowband imaging, subwavelength structured surfaces for anti-reflection and polarization control, and aberration compensation for reflective imaging systems and grating spectrometers. Author

N92-33095# Department of the Navy, Washington, DC.
RADIATION SELECTIVE SYSTEM FOR TARGET RANGE AND IMAGING READOUT Patent Application
Bruce Maccabee, inventor (to Navy) 5 May 1992 13 p
(AD-D015285; US-Patent-Appl-SN-878597) Avail: CASI HC A02/MF A01

Optical radiation is propagated through an attenuating medium to a target from which it is reflected and picked up by an echo receiver system to provide ranging and imaging data during one mode of operation. The optical radiation is transformed into acoustical pulse energy alternatively radiated to and reflected from the target in another mode of operation. The operational mode is selected so as to optimize the data extracted from the echo receiver system under different conditions affecting receiver reception.
GRA

N92-33146# Universiteit Twente, Enschede (Netherlands).
SCANNING FORCE MICROSCOPY USING OPTICAL INTERFEROMETRY Ph.D. Thesis
Arie Jeffrey denBoef 1991 285 p
(ISBN-90-9003887-6; ETN-92-92040) Copyright Avail: CASI HC A13/MF A03

A dynamic and a static force microscope, which both use an interferometer to probe the deflection of the cantilever, are described. Both interferometers employ a commercially available laser diode as light source. The development in the investigation of the possibilities and limitations of force microscopy, is described. The theory of force microscopy is detailed and the interferometric detection of small displacements is addressed. The two force microscopes and test experiments are described. Some practical applications of force microscopy are presented. These examples were all taken from practical situations encountered at the laboratory and illustrate the possibilities of force microscopy. ESA

N92-33202 New Brunswick Univ., Fredericton. School of Computer Science.
AMBIENT LIGHT ARRAY VISION IN 3-D Ph.D. Thesis
Przemyslaw Pochec Apr. 1990 120 p
(ISBN-0-315-55748-6; CTN-92-60526) Copyright Micromedia Ltd., Technical Information Centre, 165 Hotel de Ville, Place du Portage, Phase 2, Hull, Quebec J8X 3X2, Canada HC/MF

Theoretical foundations of an advanced vision system capable of detecting the three dimensional orientation of a planar surface from a single view of a scene are presented. Data for a new vision system are represented in the form of an ambient light array (ALA). The surface reflectance characteristic is modeled upon the Lambertian reflectance function, while the illumination of a scene is modeled by a point light source located at the point of observation or at a known distance away from it. The first case simplifies the calculations for the orientation, while the latter case enables the distance as well as the orientation of the surface to be determined. Novel approaches to the detection of straight edge orientation in three dimensions are also presented. The relationship of the new ambient light based approach to conventional image processing is discussed. The results of extensive numerical simulation experiments which investigate the effects of noise on measurements of surface and edge orientation are described. In addition, experimental results verifying the ALA vision system concept using crude equipment are discussed. Author (CISTI)

N92-33239*# Lockheed Engineering and Sciences Co., Hampton, VA.
LASER TO SINGLE-MODE-FIBER COUPLING: A LABORATORY GUIDE Contractor Report, Jan. - Nov. 1991
I. Ladany Jul. 1992 15 p
(Contract NAS1-19000; RTOP 590-32-31)
(NASA-CR-4452; NAS 1.26:4452) Avail: CASI HC A03/MF A01

All the information necessary to achieve reasonably efficient coupling of semiconductor lasers to single mode fibers is collected from the literature, reworked when necessary, and presented in a mostly tabular form. Formulas for determining the laser waist radius and the fiber mode radius are given. Imaging relations connecting these values with the object and image distances are given for three types of lenses: ball, hemisphere, and Gradient Index (GRIN). Sources for these lenses are indicated, and a brief discussion is given about ways of reducing feedback effects. Author

N92-32441# Naval Weapons Center, China Lake, CA. Attack Weapons Dept.
IMAGE ENHANCEMENT OF INFRARED UNCOOLED FOCAL PLANE ARRAY IMAGERY
Howard McCauley and John Eric Auborn *In* AGARD, Integrated Target Acquisition and Fire Control Systems Feb. 1992 4 p (For primary document see N92-32437 23-06)
Copyright Avail: CASI HC A01/MF A02; 1 functional color page

N92-32444# Thomson-CSF, Cesson-Sevigne (France).
METHODS OF OPTO-ELECTRONIC FUSION OF INFRARED AND VISIBLE IMAGES [METHODES DE FUSION OPTRONIQUE D'IMAGES IR ET VISIBLE]
D. Thoreau and J. Quignon (Thomson-CSF, Bagneux, France) *In* AGARD, Integrated Target Acquisition and Fire Control Systems Feb. 1992 8 p In FRENCH Original contains color illustrations (For primary document see N92-32437 23-06)
Copyright Avail: CASI HC A02/MF A02; 1 functional color page

N92-32445# Thomson-CSF, Bagneux (France). Div. Systemes Electroniques.
AUTOMATIC DETECTION, PURSUIT, AND CLASSIFICATION IN INFRARED IMAGERY [DETECTION, POURSUITE ET CLASSIFICATION AUTOMATIQUES EN IMAGERIE INFRA-ROUGE]
J. Quignon *In* AGARD, Integrated Target Acquisition and Fire Control Systems Feb. 1992 6 p In FRENCH (For primary document see N92-32437 23-06)
Copyright Avail: CASI HC A02/MF A02; 1 functional color page

N92-32446# Wright Lab., Wright-Patterson AFB, OH.
INFRARED TARGETING SYSTEM (IRTS) DEMONSTRATION
Mark A. OHair, Shelly S. Eucker (Boeing Military Airplane Development, Wichita, KS.), Brad A. Eucker (Boeing Military Airplane Development, Wichita, KS.), and Tim Lewis *In* AGARD, Integrated Target Acquisition and Fire Control Systems Feb. 1992 6 p (For primary document see N92-32437 23-06)
Copyright Avail: CASI HC A02/MF A02; 1 functional color page

75 PLASMA PHYSICS

Includes magnetohydrodynamics and plasma fusion.

For ionospheric plasmas see *46 Geophysics*. For space plasmas see *90 Astrophysics*.

N92-32417# Oak Ridge Associated Universities, Inc., TN.
MAGNETOHYDRODYNAMIC STABILITY OF PLASMAS WITH RADIAL MOTION M.S. Thesis - Illinois Univ.
Elizabeth Ann Scholle (Illinois Univ., Urbana.) 1991 98 p
(Contract DE-AC05-76OR-00033; NSF ECS-88-18975)
(DE92-013917; DOE/OR-00033/T479) Avail: CASI HC A05/MF A02

The stability of a screw-pinch plasma with radial motion is explored. The linear theory of ideal magnetohydrodynamic (MHD) stability for stationary equilibrium has been generalized to include radial motion. This generalization results in the force operator, F, being non-self-adjoint and the widely used energy principle being no longer useful in this case. Because of this, a set of seven complex, first-order, simultaneous ordinary differential equations needs to be solved to determine the stability. The equations are solved subject to appropriate boundary conditions using the Runge-Kutta-Fehlberg. The eigenvalues for the set of equations are also complex, with the imaginary part of the eigenvalue corresponding to the exponential growth or decay of the instability. While the method derived can be used for any cylindrical equilibrium profiles, the results will be presented for imploding screw-pinch plasmas. DOE

N92-32533# California Univ., Davis.
INJECTION OF COMPACT TOROIDS FOR TOKAMAK FUELING AND CURRENT DRIVE
D. Q. Hwang, J. H. Rogers, J. C. Thomas, R. Evans, R. Foley, and T. Hillyer 1991 9 p
(Contract DE-FG03-90ER-54102)
(DE92-010031; DOE/ER-54102/T1) Avail: CASI HC A02/MF A01

The goals for the 1990-1991 period were the operation of the Davis Diverted Tokamak (DDT), the beat wave experiment, and

the construction of the compact toroid injection experiment (CTIX). The experiment results from these areas are summarized in the posters given in the APS meeting last November. The technical progress of the development of the diagnostic system for the beat wave experiment, and CT injection, especially in relation to the upcoming injection experiments into DDT tokamak, is described. The tokamak operation of DDT over the past year has been focused in two parameter ranges: the long pulse discharges (over 100 msec), and the low q short pulse discharges (about 10 msec). We found that the long pulse discharges required a position feedback that is more sophisticated than the simple passive program that we have. We are in the process of assembling this system. We also found an interesting low q(a) operating regime. Here an equilibrium can be established for a toroidal field between .5 and 1 kG. The typical plasma current is greater than 5kA. The density of the plasma is between 10(exp 12) and 10(exp 13)/cubic cm. The plasma condition in these discharges is sufficiently mild for the use of diagnostic probes to measure various plasma fluctuations. We believe that this will be the regime best suited to study the interaction between the tokamak plasma and the compact toroid. A sophisticated probe system of both electrostatic and electromagnetic types, similar to those used in the beat wave experiment, has been designed for the upcoming experiments. DOE

N92-32552# National Inst. for Fusion Science, Nagoya (Japan).
TWO- AND THREE-DIMENSIONAL SIMULATION CODE FOR RADIATION-HYDRODYNAMICS IN ICF
T. Yabe (Gunma Univ., Japan) and T. Ishikawa (Gunma Univ., Japan) Nov. 1991 29 p Submitted for publication
(NIFS-119) Avail: CASI HC A03/MF A01

A multi-dimensional radiation hydrodynamic code is developed and is applied to the interaction of an intense ion beam with plasmas. The hydrocode is based on a newly developed, highly-accurate scheme, Cubic-Interpolated Pseudoparticle (CIP). The radiation transport is solved with the Symmetrical Semi-Implicit (SSI) scheme, which is quite easily implemented and is 4-5 times faster than the incomplete Cholesky conjugate gradient algorithm (ICCG). The Thomas-Fermi equation of state (EOS) is used for the atomic data and the Tsakiris and Eidmann formula for the Rosseland mean-free path. This newly developed two-dimensional code is used to design an extraction method of the radiation from the high temperature region heated by ion beam. The ion beam of 3 TW/cm(exp 2) is converted into the soft X-ray of 40 TW/cm(exp 2) at the surface of the radiation emitter. Author

N92-32592# Maryland Univ., College Park. Lab. for Plasma Research.
NONLINEAR DYNAMICS AND PLASMA TRANSPORT
T. M. Antonsen, Jr., J. F. Drake, J. M. Finn, P. N. Guzdar, A. B. Hassam, and R. Z. Sagdeev 1992 9 p
(Contract DE-FG05-89ER-53301)
(DE92-014246; DOE/ER-53301/4) Avail: CASI HC A02/MF A01

This progress report details the work done on a program in nonlinear dynamical aspects of plasma turbulence and transport. Three different areas of research are discussed: (1) shear flow generation and reduced transport in fluids and plasma; (2) nonlinear dynamics and visualization of 3D flows; and (3) application of wavelet analysis to the study of fractal dimensions in experimental and numerical data. DOE

N92-32595# Washington Univ., Seattle.
FORMATION AND SUSTAINMENT OF A VERY LOW ASPECT RATIO TOKAMAK USING COAXIAL HELICITY INJECTION: HELICITY INJECTED TORUS (HIT) EXPERIMENT
T. R. Jarboe and B. A. Nelson 1992 52 p
(Contract DE-FG06-90ER-54095)
(DE92-014311; DOE/ER-54095/2; UWAERP-35) Avail: CASI HC A04/MF A01

In the paper, we will discuss the progress of the HIT experiment construction, including the following components: preliminary data and interpretation; diagnostic systems; vacuum vessel and pumping system; helicity source and power supplies; toroidal field coil and power supply; data acquisition system; and our collaboration with General Atomics. A brief summary of each topic will be given. DOE

N92-32599# Wisconsin Univ., Madison.
MHD COMPUTATION OF FEEDBACK OF RESISTIVE-SHELL INSTABILITIES IN THE REVERSED FIELD PINCH
E. J. Zita, S. C. Prager, Y. L. Ho, and D. D Schnack May 1992 30 p
(Contract DE-FG02-85ER-53212)
(DE92-014325; DOE/ER-53212/195) Avail: CASI HC A03/MF A01

MHD computation demonstrates that feedback can sustain reversal and reduce loop voltage in resistive-shell reversed field pinch (RFP) plasmas. Edge feedback on the (approximately 2R/a) tearing modes resonant near axis is found to restore plasma parameters to nearly their levels with a close-fitting conducting shell. When the original dynamo modes are stabilized, neighboring tearing modes grow to maintain the RFP dynamo more efficiently. This suggests that experimentally observed limits on RFP pulse lengths, on the order of the shell time, can be overcome by applying feedback to a few helical modes. DOE

N92-32623# General Atomic Co., San Diego, CA.
ALPHA PARTICLE DIAGNOSTICS USING IMPURITY PELLET INJECTION
R. K. Fisher, J. M. McChesney, A. W. Howald, P. B. Parks, J. A. Snipes (Massachusetts Inst. of Tech., Cambridge.), J. L. Terry (Massachusetts Inst. of Tech., Cambridge.), E. S. Marmar (Massachusetts Inst. of Tech., Cambridge.), S. J. Zweben (Princeton Univ., NJ.), and S. Medley (Princeton Univ., NJ.) May 1992 23 p Presented at the 9th Topical Conference on High-Temperature Plasma Diagnostics, Santa Fe, NM, 15-19 Mar. 1992
(Contracts DE-AC03-89ER-53277; DE-FG02-90ER-54084; DE-AC02-76CH-03073)
(DE92-013796; GA-A-20870; CONF-920362-31) Avail: CASI HC A03/MF A01

We have proposed using impurity injection to measure the energy distribution of the fast confined alpha particles in a reacting plasma. The ablation cloud surrounding the injected pellet is thick enough that an equilibrium fraction F(sub o)(sup (infinity))(E) of the incident alphas should be neutralized as they pass through the cloud. By observing neutrals created in the large spatial region of the cloud which is expected to be dominated by the helium-like ionization state, e.g., Li(+) ions, we can determine the incident alpha distribution dn(sub He)2+/dE from the measured energy distribution of neutral helium atoms. Initial experiments were performed on TEXT in which we compared pellet penetration with our impurity pellet ablation model, and measured the spatial distribution of various ionization states in carbon pellet clouds. Experiments have recently begun on TFTR with the goal of measuring the alpha particle energy distribution during D-T operation in 1993-94. A series of preliminary experiments are planned to test the diagnostic concept. The first experiments will observe neutrals from beam-injected deuterium ions and the high energy He-3 tail produced during ICH minority heating on TFTR interacting with the cloud. We will also monitor by line radiation the charge state distributions in lithium, boron, and carbon clouds. DOE

N92-32624# Wisconsin Univ., Madison.
ION HEATING AND MHD DYNAMO FLUCTUATIONS IN THE REVERSED FIELD PINCH Ph.D. Thesis
E. E. Scime May 1992 62 p
(Contract DE-FG02-85ER-53198)
(DE92-013902; DOE/ER-53198/194) Avail: CASI HC A04/MF A01

Ion temperature measurements, time resolved to 10 micro-s, have been made in the Madison Symmetric Torus (MST) reversed field pinch (RFP) with a five channel charge exchange analyzer. The characteristic anomalously high ion temperature of RFP

discharges has been observed in the MST. The evolution of the ion and electron temperature, as well as density and charge exchange power loss, were measured for a series of reproducible discharges. The ion heating expected from collisional processes with the electrons is calculated and shown too small to explain the measured ion temperatures. The charge exchange determined ion temperature is also compared to measurements of the thermally broadened CV 227.1 nano-m line. The ion temperature, T(sub i) approx. 250 eV for I = 360 kA, increases by more than 100 percent during discrete dynamo bursts in MST discharges. Magnetic field fluctuations in the range 0.5 to 5 MHz were also measured during the dynamo bursts. Structure in the fluctuation frequency spectrum at the ion cyclotron frequency appears as the bursts terminate, suggesting that the mechanism of ion heating involves the dissipation of dynamo fluctuations at ion cyclotron frequencies. Theoretical models for ion heating are reviewed and discussed in light of the experimental results. Similar electron heating mechanisms may be responsible for the discrepancy between measured and expected loop voltages in the RFP. The electrons, as well as the ions, may be heated by turbulent mechanisms, and a RFP energy budget including such phenomena is described. DOE

N92-32662# Instituto de Pesquisas Espaciais, Sao Jose dos Campos (Brazil).
PLASMA DIFFUSION THROUGH MULTIDIPOLE MAGNETIC FIELDS
Jose Leonardo Ferreira 1992 26 p
(INPE-5384-PRE/1750) Avail: CASI HC A03/MF A01

The diffusion of a cold plasma through multidipole fields of a magnetic picket fence is presented. The ion diffusion and trapping is determined by electric potentials inside the multidipole fields. The electron diffusion is regulated by an anomalous transport process driven by low frequency fluctuations inside the magnetic sheath. Particles drifting with velocities above the ion acoustic speed generates high amplitude waves responsible for an anomalous diffusion process. Author

N92-32733# Lawrence Livermore National Lab., CA.
THE NOVA UPGRADE FACILITY FOR ICF IGNITION AND GAIN
W. H. Lowdermilk, E. M. Campbell, J. T. Hunt, J. R. Murray, E. Storm, M. T. Tobin, and J. B. Trenholme 3 Jan. 1992 17 p
Presented at the 10th International Workshop on Laser Interaction and Related Plasma Phenomena, Monterey, CA, 11-15 Nov. 1991
(Contract W-7405-eng-48)
(DE92-010703; UCRL-JC-107386; CONF-911131-2) Avail: CASI HC A03/MF A01

Research on Inertial Confinement Fusion (ICF) is motivated by its potential defense and civilian applications, including ultimately the generation of electric power. The U.S. ICF Program was reviewed recently by the National Academy of Science (NAS) and the Fusion Policy Advisory Committee (FPAC). Both committees issued final reports in 1991 which recommended that first priority in the ICF program be placed on demonstrating fusion ignition and modest gain (G less than 10). The U.S. Department of Energy and Lawrence Livermore National Laboratory (LLNL) have proposed an upgrade of the existing Nova Laser Facility at LLNL to accomplish these goals. Both the NAS and FPAC have endorsed the upgrade of Nova as the optimal path to achieving ignition and gain. Results from Nova Upgrade Experiments will be used to define requirements for driver and target technology both for future high-yield military applications, such as the Laboratory Microfusion Facility (LMF) proposed by the Department of Energy, and for high-gain energy applications leading to an ICF engineering test facility. The central role and modifications which Nova Upgrade would play in the national ICF strategy are described. DOE

N92-32745# National Inst. for Fusion Science, Nagoya (Japan).
FAST ION LOSS AND RADIAL ELECTRIC FIELD IN WENDELSTEIN 7-A STELLARATOR
K. Itoh, H. Sanuki, and S. Itoh Oct. 1991 46 p
(DE92-782106; NIFS-117) Avail: CASI HC A03/MF A01

A theoretical model is developed to determine the radial electric field and the fast ion loss simultaneously in stellarators, and is applied to the Wendelstein 7-A stellarator. The predicted value of the radial electric field is more closer to experiments than the purely neoclassical calculation. The loss rate, which is determined simultaneously, is in the range of experimental observations. The partition of the injection energy by the bulk heating, direct orbit loss, and shine through is estimated by using the self consistent electric field profile. The orbit loss becomes noticeable as the injection energy increases. The influence of the neutral particles is also studied. Neutral particles enhances the negative radial electric field, and reduces the direct orbit loss by the expense of the charge exchange loss. The impact of the increased radial electric field on the neoclassical ion thermal energy loss is compared to the direct loss of fast ions. The reduction of the neoclassical loss is much smaller than the orbit loss. DOE

N92-32797# Stuttgart Univ. (Germany, F.R.). Inst. fuer Plasmaforschung.
[ACTIVITIES REPORT OF THE INSTITUTE OF PLASMA RESEARCH] Annual Report, 1990
1991 26 p
(ETN-92-92147) Avail: CASI HC A03/MF A01

Plasma research is reported. The following topics are reported: Electron Cyclotron Resonance Heating (ECRH); laser diagnostics; plasma edge diagnostics; plasma theory; plasma technology; and plasmas focus. A list of publications and conference reports, laboratory reports, invited talks, patents, and diploma theses is given. ESA

N92-32822# Stuttgart Univ. (Germany, F.R.). Inst. fuer Plasmaforschung.
DIAGNOSTICS AND MODELING OF ECRH MICROWAVE DISCHA RGES
K. Behringer Mar. 1991 28 p
(IPF-91-3; ETN-92-92153) Avail: CASI HC A03/MF A01

Stationary plasmas on various gases were generated at pressures of some 10 Pa in weak magnetic fields by electron cyclotron resonance frequency microwave heating (ECRH). Quantitative spectroscopy of atomic lines and molecular bands was applied for diagnostics of plasmas in hydrogen, nitrogen, methane, and argon helium mixtures. Simple model calculations were based on the well known balance equations of glow discharges including chemical reactions especially for methane. Some tests were performed in nitrogen glow discharges. Excitation, ionization, and dissociation rate coefficients for diagnostic or modeling purposes were taken from nuclear fusion research or calculated from experimental cross sections assuming a Maxwellian energy distribution. ESA

N92-32944# Wisconsin Univ., Madison.
EDGE GRADIENT AND SAFETY FACTOR EFFECTS ON ELECTROSTATIC TURBULENT TRANSPORT IN TOKAMAKS Ph.D. Thesis
Ing Hwie Tan May 1992 76 p
(Contract DE-FG02-85ER-53198)
(DE92-014323; DOE/ER-53198/193) Avail: CASI HC A05/MF A01

Electrostatic turbulence and transport measurements are performed on the Tokapole-II tokamak at the University of Wisconsin-Madison, as the safety-factor and the edge equilibrium gradients varied substantially. Tokapole-II is a poloidal divertor tokamak capable of operating at a wide range of safety factors due to its unique magnetic limiter configuration. It also has retractable material limiters in a large scrape-off region, which permits the study of edge boundary conditions like density and temperature gradients. The turbulence is independent of safety factor, but strongly sensitive to the local density gradient, which itself depends upon the limiter configuration. When a material limiter is inserted in a high qa discharge, the density gradient is increased locally together with a local increase of the turbulence. On the other hand, limiter insertion in low qa discharges did not increase the density gradient as much, and the turbulence properties are

unchanged with respect to the magnetic limiter case. It is concluded then, that electrostatic turbulence is caused by the density gradient. Although the electrostatic fluctuation driven transport is enhanced in the large density gradient case, it is in all cases too small to explain the observed energy confinement times. To explore instabilities with small wavelengths, a 0.5 mm diameter spherical Langmuir probe was constructed, and its power compared with the power measured by larger cylindrical probes. DOE

N92-32992# Sandia National Labs., Albuquerque, NM.
SPECTROSCOPIC CHARACTERIZATION OF LEVIS ACTIVE ION SOURCE ON PBFA 2
A. B. Filuk, J. E. Bailey, K. W. Bieg, A. L. Carlson, T. J. Renk, G. C. Tisone, and Y. Maron 1992 6 p Presented at the 9th International Conference on High Power Particle Beams, Washington, DC, 25-29 May 1992
(Contract DE-AC04-76DP-00789)
(DE92-014954; SAND-92-1230C; CONF-920515-2) Avail: CASI HC A02/MF A01

The laser-initiated LEVIS source is intended to provide an active source in the PBFA II ion diode by generation of a performed lithium anode plasma. Visible spectra recorded with a streaked spectrograph are used to help evaluate the source performance. The absence of Stark shifting of the Li I 2p-3d and 2s-2p light confirms that a plasma is created over the anode surface. At lower LEVIS laser intensities this plasma erodes back toward the anode as the ion beam current grows. Considerable improvements in anode is heated for several hours. The LEVIS source microdivergence estimated from the carbon ion transverse energy is less than 14 mrad, meeting the near term requirements for PBFA II target experiments. DOE

N92-32995# Sandia National Labs., Albuquerque, NM.
SCRAPE-OFF LAYER MODELING OF RADIATIVE DIVERTOR AND HIGH HEAT FLUX EXPERIMENTS ON D3-D
R. B. Campbell, T. W. Petrie (General Atomic Co., San Diego, CA.), and D. N. Hill (Lawrence Livermore National Lab., CA.) 1992 11 p Presented at the 10th International Conference on Plasma-Surface Interactions in Controlled Fusion Devices, Monterey, CA, 30 Mar. - 3 Apr. 1992
(Contract DE-AC04-76DP-00789)
(DE92-015007; SAND-91-2506C; CONF-920311-14) Avail: CASI HC A03/MF A01

We use a new multispecies 1-D fluid code, NEWT-1D, to model DIII-D scrape-off layer (SOL) behavior during radiative divertor and high heat flux experiments. The separatrix location and the width of the SOL are uncertain, and affect the comparison of the data in important ways. The model agrees with many of the experimental measurements for a particular prescription for the separatrix location. The model cannot explain the recent data on the separatrix T(sub i) with a conventional picture of ion and electron power flows across the separatrix. Radial transport of particles and heat in some form is required to explain the peak heat flux data before and after gas puffing. For argon puffing in the private flux region, entrainment is poor in the steady state. The calculations suggest that strike point argon puffing in a slot divertor geometry results in substantially better entrainment. Self-consistent, steady-state solutions with radiated powers up to 80 percent of the SOL power input are obtained in 1-D. We discuss significant radial effects which warrant the development of a code which can treat strongly radiating impurities in 2-D geometries. DOE

N92-33024# TRW Systems and Energy, Redondo Beach, CA. Applied Technology Div.
MHD INTEGRATED TOPPING CYCLE PROJECT
Jan. 1992 187 p
(Contract DE-AC22-87PC-90274)
(DE92-013904; DOE/PC-90274/T14; MHD-ITC-91-039) Avail: CASI HC A09/MF A02

The Magnetohydrodynamics (MHD) Integrated Topping Cycle (ITC) Projects represents the culmination of the proof-of-concept (POC) development stage in the U.S. Department of Energy (DOE) program to advance MHD technology to the early commercial development stage utility power applications. The project is a joint effort, combining the skills of three topping cycle component developers: TRW, Avco, and Westinghouse. TRW, the prime contractor and system integrator, is responsible for the 50 thermal megawatt slagging coal combustion subsystem. Avco is responsible for the MHD channel subsystem (nozzle, channel, diffuser, and power conditioning circuits). Westinghouse is responsible for the current consolidation subsystem. DOE

N92-33154# Wisconsin Univ., Madison. Dept. of Physics.
MEASUREMENT OF NONLINEAR MODE COUPLING OF TEARING FLUCTUATIONS
S. Assadi, S. C. Prager, and K. L. Sidikman Mar. 1992 14 p
(Contract DE-FG02-85ER-53198)
(DE92-013901; DOE/ER-53198/190) Avail: CASI HC A03/MF A01

Three-wave nonlinear coupling of spatial Fourier modes is measured in the MST reversed field pinch by applying bi-spectral analysis to magnetic fluctuations measured at the plasma edge at 64 toroidal locations and 16 poloidal locations, permitting observation of coupling over 8 polodial modes and 32 toroidal modes. Comparison to bi-spectra predicted by MHD computation indicates reasonably good agreement. However, during the crash phase of the sawtooth oscillation the nonlinear coupling is strongly enhanced, concomittant with a broadened (presumably nonlinearly generated) k-spectrum. DOE

N92-33168# Argonne National Lab., IL.
ANL ITER HIGH-HEAT-FLUX BLANKET-MODULE HEAT TRANSFER EXPERIMENTS
K. E. Kasza Feb. 1992 41 p
(Contract W-31-109-eng-38)
(DE92-017749; ANL/FPP/TM-262) Avail: CASI HC A03/MF A01

An Argonne National Laboratory facility for conducting tests on multilayered slab models of fusion blanket designs is being developed; some of its features are described. This facility will allow testing under prototypic high heat fluxes, high temperatures, thermal gradients, and variable mechanical loadings in a helium gas environment. Steady and transient heat flux tests are possible. Electrical heating by a two-sided, thin stainless steel (SS) plate electrical resistance heater and SS water-cooled cold panels placed symmetrically on both sides of the heater allow achievement of global one-dimensional heat transfer across blanket specimen layers sandwiched between the hot and cold plates. The heat transfer characteristics at interfaces, as well as macroscale and microscale thermomechanical interactions between layers, can be studied in support of the ITER engineering design effort. The engineering design of the test apparatus has shown that it is important to use multidimensional thermomechanical analysis of sandwich-type composites to adequately analyze heat transfer. This fact will also be true for the engineering design of ITER. DOE

N92-33223 York Univ. (Ontario).
THEORY AND NUMERICAL SIMULATION OF SOME WIDE-ANGLE WIDE-BANDPASS PLASMA PARTICLE ANALYZERS Ph.D. Thesis
Stephen Stewart Kerr May 1990 273 p
(ISBN-0-315-58015-1; CTN-92-60516) Copyright Micromedia Ltd., Technical Information Centre, 165 Hotel de Ville, Place du Portage, Phase 2, Hull, Quebec J8X 3X2, Canada HC/MF

Conventional electrostatic analyzers, employing restrictive apertures and electrically biased plates of many designs, are frequently used to measure plasma velocity distributions in space. In such devices, the ambient differential flux j of particles in a single channel of energy and solid angle is recovered by dividing a collection rate c in a single collector by the geometrical factor G of the device. Devices are proposed which possess a geometrical matrix G(mu,nu) and which deconvolute the ambient particle fluxes j(nu) from several particle collection rates c(mu) by inversion of the system c(mu) = Sigma(nu) G(mu,nu)j(nu). By relaxing the need to focus single energy-angle channels to single collectors, analyzers

of wider aperture and hence faster operating speed become possible, but likely at the expense of resolution in energy and angle. A method is presented for modelling analyzers employing cylindrically symmetric electromagnetic fields and intended for gyrotropic distributions. A theory is also given for calculating G(mu,nu) for such analyzers, and generalization of this theory to more arbitrary geometries is discussed. These techniques are employed to study several cylindrically symmetric electrostatic analyzer candidates. It is concluded that some show limited promise as analyzers. Author (CISTI)

76 SOLID-STATE PHYSICS

Includes superconductivity.

For related information, see also *33 Electronics and Electrical Engineering* and *36 Lasers and Masers.*

N92-32320# California Univ., Berkeley. Lawrence Berkeley Lab.

THE INFLUENCE OF ANHARMONIC PHONONS ON THE ISOTOPE EFFECT IN HIGH-(Tc) OXIDES

V. H. Crespi and M. L. Cohen Jan. 1992 6 p Presented at the Lattice Effects in High (Tc) Superconductors, Santa Fe, NM, 13-15 Jan. 1992

(Contract DE-AC03-76SF-00098)

(DE92-017083; LBL-31865; CONF-920141-8) Avail: CASI HC A02/MF A01

Anharmonic phonons are examined to study the unusual isotope effect exponents for the high-(Tc) oxides. Within a simple model of anharmonicity, the mass dependences of the electron-phonon coupling constant (lambda) and the phonon frequency determine the isotope effect exponent (alpha) as a function of coupling strength. A model in which the outer wells of a multiple-well potential deepen as the orthorhombic/low temperature tetragonal phase transition in La(2-x)M(x)CuO4 is approached is consistent with some experimentally observed variations in (Tc) and (alpha). DOE

N92-32346# Argonne National Lab., IL.

PROCESSING AND PROPERTIES OF SILVER-CLAD Tl-Ba-Ca-Cu-O WIRES AND TAPES

K. C. Goretta, C. T. Wu, M. T. Lanagan, M. A. Boling, D. Shi, D. J. Miller, Nan Chen, W. G. Hanewald, S. Sengupta, and Z. Wang et al Mar. 1992 6 p Presented at the Material Research Society Spring Meeting, San Francisco, CA, 27 Apr. - 2 May 1992

(Contract W-31-109-eng-38)

(DE92-015266; ANL/CP-74829; CONF-920402-30) Avail: CASI HC A02/MF A01

TlBa2Ca2Cu3O(sub x) and Tl2Ba2Ca2Cu3O(sub x) powders were synthesized, loaded into Ag tubes, and worked into wires and tapes by drawing and rolling. All processing outside of furnaces was in a dry-N2 glovebox. All heat treatments were performed in O2. The Ag-clad wires fabricated from these powders exhibited onset of superconductivity at approx. 18 K and critical current densities at 77 K of 2 x 10(exp 3) to 4 x 10(exp 3) A/sq cm. DOE

N92-32420# California Univ., Berkeley. Lawrence Berkeley Lab.

LOW-FREQUENCY NUCLEAR QUADRUPOLE RESONANCE WITH A dc SQUID Ph.D. Thesis

J. W. Chang Jul. 1991 149 p

(Contract DE-AC03-76SF-00098)

(DE92-014506; LBL-31124) Avail: CASI HC A07/MF A02

Conventional pure nuclear quadrupole resonance (NQR) is a technique well suited for the study of very large quadrupolar interactions. Numerous nuclear magnetic resonance (NMR) techniques have been developed for the study of smaller quadrupolar interactions. However, there are many nuclei which have quadrupolar interactions of intermediate strength. Quadrupolar interactions in this region are traditionally difficult or unfeasible to detect. This work describes the development and application of a SQUID NQR technique which is capable of measuring intermediate strength quadrupolar interactions, in the range of a few hundred kilohertz to several megahertz. In this technique, a dc SQUID (Superconducting QUantum Interference Device) is used to monitor the longitudinal sample magnetization, as opposed to the transverse magnetization, as a RF field is swept in frequency. This allows the detection of low-frequency nuclear quadrupole resonances over a very wide frequency range with high sensitivity. The theory of this NQR technique is discussed and a description of the dc SQUID system is given. In the following chapters, the spectrometer is discussed along with its application to the study of samples containing half-odd-integer spin quadrupolar nuclei, in particular boron-11 and aluminum-27. The feasibility of applying this NQR technique in the study of samples containing integer spin nuclei is discussed in the last chapter. DOE

N92-32462# California Univ., San Diego, La Jolla. Dept. of Physics.

PREPARATION AND CHARACTERIZATION OF SUPERLATTICES

I. K. Schuller 1992 13 p

(Contract DE-FG03-87ER-45332)

(DE92-012572; DOE/ER-45332/T1) Avail: CASI HC A03/MF A01

During this last year we were involved in a number of studies geared towards understanding the relationship between interfacial disorder and X-ray diffraction from superlattices. In addition, we have performed a number of physical properties studies in order to relate structure to physical properties. These studies include magnetism and superconducting studies in a variety of different thin film systems. A major development was the implementation of a structural refinement program capable of determining the important structural parameters in superlattices and thin films. This program is being supplied to many research groups for the study of related problems. We are currently devoted to detailed, comparative studies of magnetic samples prepared by Molecular Beam Epitaxy and sputtering. The unique facilities available to us not only allow preparing samples by the two different methods but also are capable of determining interfacial structure using in-situ characterization techniques such as Reflection High Energy Electron Diffraction (RHEED), Low Energy Electron Diffraction (LEED) and Auger Electron Spectroscopy (AES). We have developed a data acquisition system capable of acquiring electron diffraction in real time during growth. DOE

N92-32465# Ames Lab., IA.

FORMATION OF HIGH TEMPERATURE SUPERCONDUCTORS FROM THE SOLIDIFIED MELT Ph.D. Thesis

B. Merkle 3 Jan. 1992 97 p

(Contract W-7405-eng-82)

(DE92-012584; IS-T-1570) Avail: CASI HC A05/MF A02

The drop tube experiments with the YBa2Cu3O(7 - delta) (Y123) material have illustrated that the particle size, temperature and atmosphere during decomposition, melting and solidification is critical to the formation of the desired decomposition phases. Temperatures above 1450 C and small size, -75 +53 micro-m, particulate are necessary to produce complete decomposition of the Y123 and melting of all phases with the exception of Y2O3 (200). The importance of the atmosphere is demonstrated by the presence of the low P(sub O2) stable BaCu2O2 (012) phase in the solidified spheres produced in a nitrogen atmosphere and the cubic phase (phi) in the solidified spheres produced in an oxygen atmosphere. The as solidified microstructure of the spheres where the liquids temperature was not obtained, are relatively similar. The major features of the phase composition and microstructure are primarily attributed to what happens upon heating and depend relatively little upon the solidification rate. DOE

N92-32470# Brookhaven National Lab., Upton, NY.

LOCAL ENVIRONMENT AROUND THE OXYGEN ATOMS IN Y-Ba-Cu-O STUDIED X RAY ABSORPTION FINE STRUCTURE (XAFS) SPECTROSCOPY

A. Krol, Y. L. Soo, S. W. Huang, Z. H. Ming, Y. H. Kao, N. Nuecker,

G. Roth, and J. Fink Feb. 1992 8 p Presented at the 5th Annual Conference on Superconductivity and Applications, Buffalo, NY, 24-26 Sep. 1991
(Contract DE-AC02-76CH-00016)
(DE92-014165; BNL-47235; CONF-9109102-6) Avail: CASI HC A02/MF A01

The local environment about oxygen atoms in the CuO2 plane in YBa2Cu3O7 single crystals was investigated by orientation-dependent x-ray absorption fine structure (XAFS) spectroscopy at the O ls edge using bulk-sensitive fluorescence-yield-detection method. Within experimental accuracy (+/- 0.03 A) no structural change in local ordering about oxygen atoms in the CuO2 plane at 90 K was detected. DOE

N92-32493# California Univ., Berkeley. Lawrence Berkeley Lab.
SCINTILLATION PROPERTIES OF LEAD SULFATE
W. W. Moses, S. E. Derenzo, and P. J. Shlichta (Crystal Research, San Pedro, CA.) Nov. 1991 6 p Presented at the IEEE Nuclear Science Symposium, Santa Fe, NM, 5-9 Nov. 1991
(Contract DE-AC03-76SF-00098)
(DE92-010301; LBL-31456; CONF-911106-89) Avail: CASI HC A02/MF A01

We report on the scintillation properties of lead sulfate (PbSO4), a scintillator that show promise as a high energy photon detector. Its physical properties are well suited for gamma detection, as it has a density of 6.4 gm/cm(exp 3), a 1/e attenuation length for 511 keV photons of 1.2 cm, is not affected by air or moisture, and is cut and polished easily. In 99.998 percent pure PbSO4 crystals at room temperature excited by 511 keV annihilation photons, the fluorescence decay lifetime contains significant fast components having 1.8 ns (5 percent) and 19 ns (36 percent) decay times, but with longer components having 95 ns (36 percent) and 425 ns (23 percent) decays times. The peak emission wavelength is 335 nm, which is transmitted by borosilicate glass windowed photomultiplier tubes. The total scintillation light output increases with decreasing temperature from 3,200 photons/MeV at +45 C to 4,900 photons/MeV at room temperature (+25 C) and 68,500 photons/MeV at -145 C. In an imperfect, 3 mm cube of a naturally occurring mineral form of PbSO4 (anglesite) at room temperature, a 511 keV photopeak is seen with a total light output of 60 percent that BGO. There are significant sample to sample variations of the light output among anglesite samples, so the light output of lead sulfate may improve when large synthetic crystals become available. DOE

N92-32512# Naval Research Lab., Washington, DC.
PROBING THIN-FILM YBa2Cu3O(7-DELTA) SUPERCONDUCTORS BY SECOND HARMONIC GENERATION USING FEMTOSECOND LASER PULSES
Jane K. Rice, S. W. McCauley, A. P. Baronavski, J. S. Horwitz, and D. B. Chrisey 29 May 1992 36 p
(NR Proj. RR0-1310; NR Proj. RR0-1308)
(AD-A252350; NRL-TR-1) Avail: CASI HC A03/MF A01

High temperature superconducting thin films of YBa2Cu3O(7-delta) are examined by measuring the second-harmonic-generated (SHG) signal from an incident 60 fs laser pulse of 2.0 eV (620 nm) in air at room temperature. As oxygen stoichiometry is varied (0.00 less than delta less than 0.50), large changes in the SHG intensity are observed. The oxygen content of the films is independently determined by measuring the c-axis lattice parameter derived from x-ray diffraction and the stoichiometry of the films determined by elastic backscattering spectrometry. We report a negative correlation of the SHG intensity with the c-axis parameter, indicating that a known compression of the c-axis leads to a larger SHG signal. An additional experiment in which the SHG intensity is monitored as a function of temperature (300 K to 20 K) in vacuum is performed. A gradual increase of approximately 50 percent in the SHG intensity is observed as the temperature is lowered, which can also be correlated to a decrease in the length of the c-axis. Other experiments, including rotation anisotropy and polarization of the incident and analyzer beams, are also discussed. GRA

N92-32542# Argonne National Lab., IL.
HIGHER SUPERDEFORMED BAND MEMBERS IN Hg-190: EVIDENCE FOR A BAND INTERACTION?
I. G. Bearden (Purdue Univ., West Lafayette, IN.), P. J. Daly (Purdue Univ., West Lafayette, IN.), R. V. F. Janssens, M. P. Carpenter, I. Ahmad, T. L. Khoo, T. Lauritsen, Y. Liang, and M. W. Drigert (Edgerton, Germeshausen and Grier, Inc., Idaho Falls, ID.) 1992 5 p Presented at the Workshop on Large Gamma Ray Detector Arrays, Ottawa (Canada), 18-21 May 1992
(Contract W-31-109-eng-38)
(DE92-016778; ANL/CP-75691; CONF-920548-1) Avail: CASI HC A01/MF A01

The superdeformed band of Hg-190 has been traced up to a frequency Dirac(h), (Plancks constant divided by 2(pi)), greater than or equal to 0.4 MeV by combining data from several experiments. A distinct change in the slope of the dynamic moment of inertia J(sup 2) vs Dirac(h) is observed at Dirac(h) = 0.32 MeV. This result is interpreted as evidence for a band interaction at the highest frequencies. Possible interpretations are reviewed. DOE

N92-32561# Argonne National Lab., IL.
SINTERING OF BULK HIGH-(Tc) SUPERCONDUCTORS: Bi-Sr-Ca-Cu-O
K. C. Goretta, M. T. Lanagan, D. Y. Kaufman, A. C. Biondo, C. T. Wu, M. E. Loomans, M. R. Cheesman, R. B. Poeppel, and A. S. Nash May 1992 9 p Presented at the 1992 Powder Metallurgy World Congress, San Francisco, CA, 21-26 Jun. 1992
(Contract W-31-109-eng-38)
(DE92-016189; ANL/CP-74239; CONF-9206195-2) Avail: CASI HC A02/MF A01

Bi2Sr2CaCu2O(x) (2212) and (Bi,Pb)2Sr2Ca2Cu3O(x) (2223) superconductors have orthorhombic crystal structures. They form platelike grains that at high temperatures grow primarily in the a-b planes and not in the c direction. The diffusional properties of Bi-Sr-Ca-Cu-O superconductors are so anisotropic that 2212 and 2223 cannot, in general, be densified by solid-state sintering. Improved densification can be achieved by application of pressure or by use of transient liquid phases. Most useful bulk Bi-Sr-Ca-Cu-O superconductors are composites that contain Ag. The Ag lowers the melting points of the superconductors, which has significant effects on microstructural development. The results of disparate sintering studies are presented and discussed. DOE

N92-32636# Oak Ridge National Lab., TN.
ANISOTROPIC ELECTRICAL RESISTIVITY OF YBCO/PBCO SUPERLATTICE FILMS GROWN ON MISCUT SUBSTRATES
H. R. Kerchner, C. E. Klabunde, D. K. Christen, J. D. Budai, D. H. Lowndes, D. Norton, and J. O. Thomson Apr. 1992 7 p Presented at the Material Research Society Spring Meeting, San Francisco, CA, 27 Apr. - 2 May 1992
(Contract DE-AC05-84OR-21400)
(DE92-014409; CONF-920402-13) Avail: CASI HC A02/MF A01

Anisotropic electrical resistivity is studied in epitaxial superlattice films of YBa2Cu3O(7 epsilon) grown in situ by laser ablation on SrTiO3 surfaces aligned slightly away from the (100) direction. Layer thicknesses of each compound range from two to eight atomic cells. Electrical resistivity of these superlattice films always shows a peak at some cryogenic temperature that decreases with increasing PrBa2Cu3O(7 epsilon) layer thickness. Clear evidence is seen of vortex pinning or of supercurrent blocking by the step edges or by twin boundaries. The ratio of electrical resistivities for current directions parallel and perpendicular to these boundaries shows a large step-like change just above the superconductive critical temperature. The possibility is discussed that the Kosterlitz-Thouless explains this anisotropy change. DOE

N92-32641# Columbia Univ., New York, NY.
PHOTOGENERATED CARRIER-INDUCED REACTIONS ON UHV SEMICONDUCTOR SURFACES
R. M. Osgood, Jr. 28 May 1992 27 p

(Contract DE-FG02-90ER-14104)
(DE92-015355; DOE/ER-14104/3) Avail: CASI HC A03/MF A01

The objective for this experimental work was to examine the reaction mechanisms, half-collision dynamics, and other optically induced chemical effects, that are operable on a well characterized single-crystal semiconductor surface. Of particular interest were reactions induced by charge transfer from the semiconductor surface including hot carrier and thermalized carrier processes. The primary technique to measure the desorbed fragment translational energies was time-of-flight mass-spectroscopy, used in conjunction with a pulsed tunable laser source. The work was carried out in ultrahigh vacuum, thus, other surface spectroscopies such as temperature-programmed desorption (TPD), (LEED), etc. were used as needed. In the project, the photoreactions of several halogen-containing molecules on GaAs(110) surfaces have been investigated. The studies have made the first observations of several new photochemical processes on UHV prepared surfaces including intermolecular charge transfer; desorption by thermal-carrier-induced reactions (including the measurement of coverage-dependent changes in the translational energies of the desorbed products); interferometric oscillation of photoinduced reactions; and self-quenching of thermal carrier reactions on surfaces. DOE

N92-32653# Oak Ridge National Lab., TN.
T (SUB c)-DELTA RELATIONS IN YBa2Cu3O(7-DELTA) THIN FILMS: EFFECTS OF OXYGEN PRESSURE DURING GROWTH
R. Feenstra, D. P. Norton, J. D. Budai, D. K. Christen, D. H. Lowndes, V. C. Matijasevic (Stanford Univ., CA.), C. B. Eom (Stanford Univ., CA.), T. H. Geballe (Stanford Univ., CA.), E. S. Hellman (Bell Telephone Labs., Inc., Murray Hill, NJ.), and E. H. Hartford (Bell Telephone Labs., Inc., Murray Hill, NJ.) Apr. 1992 6 p Presented at the Material Research Society Spring Meeting, San Francisco, CA, 27 Apr. - 2 May 1992
(Contract DE-AC05-84OR-21400)
(DE92-014432; CONF-920402-9) Avail: CASI HC A02/MF A01

The (Tc) dependence on oxygen content was measured for YBa2Cu3O(7-delta) films grown with a variety of techniques (solid phase epitaxy, laser ablation, off-axis sputtering, co-evaporation) at oxygen pressures p(O2) ranging from 1.0 atm to 0.1 mTorr. Dissimilar dependences resulted for each film type, with (Tc) either increasing or decreasing for small increments in delta from maximum oxygen occupancy. Varying systematically with p(O2) during growth, the deviations are attributed to competing effects from hole-doping lattice defects (most likely on the Y-site) on the carrier density of the CuO2 planes and basal plane oxygen capacity, respectively, giving rise to overdoping or underdoping after low temperature oxidation in 1.0 atm of oxygen. DOE

N92-32693# California Univ., Berkeley. Lawrence Berkeley Lab.
INVESTIGATION ON THE LATTICE SITE LOCATION OF THE EXCESS ARSENIC ATOMS IN GaAs LAYERS GROWN BY LOW TEMPERATURE MOLECULAR BEAM EPITAXY
Kin Man Yu and Z. Liliental-Weber Nov. 1991 6 p Presented at the Annual Fall Meeting of the Materials Research Society, Boston, MA, 2-6 Dec. 1991
(Contract DE-AC03-76SF-00098)
(DE92-008253; LBL-30990; CONF-911202-60) Avail: CASI HC A02/MF A01

We have measured the excess As atoms present in GaAs layers grown by molecular beam epitaxy at low substrate temperatures using particle induced x-ray emission techniques. The amount of excess As atoms in layers grown by MBE at 200 C were found to be approximately = 4 x 10(exp 20)/sq. cm. Subsequent annealing of the layers under As overpressure at 600 C did not result in any substantial As loss. However, transmission electron microscopy revealed that As precipitates (2-5 nm in diameter) were present in the annealed layers. The lattice location of the excess As atoms in the As grown layers was investigated by ion channeling methods. Angular scans were performed in the group of zone axes (110) of the crystal. Our results strongly suggest that a large fraction of these excess As atoms are located in an interstitial position close to an As row. These As 'interstitials' are located at a site slightly displaced from the tetrahedral site in a diamond cubic lattice. No interstitial As signal is observed in the annealed layers. DOE

N92-32747# Florida Univ., Gainesville. Dept. of Electrical Engineering.
DEVELOPMENT OF ULTRA-LOW NOISE, HIGH SENSITIVITY PLANAR METAL GRATING COUPLED AlGaAs/GaAs MULTIQUANTUM WELL IR DETECTORS FOR FOCAL PLANE ARRAY STARING IR SENSOR SYSTEMS Quarterly Report No. 3, 1 Feb. - 30 Apr. 1992
Sheng S. Li 1 May 1992 27 p
(Contract N00014-91-J-1976)
(AD-A250368) Avail: CASI HC A03/MF A01

In this reporting period, we have continued to make significant progress towards the program goals. We have designed, fabricated and characterized several metal grating coupled bound-to-miniband (BTM) and step-bound-to-miniband (SBTM) transition QWIPs on the GaAs and InP substrates for 8-12 microns focal plane arrays staring infrared sensor applications. Specific tasks performed include: (1) the design and growth of several (BTM) GaAs- and (SBTM) GaAs-based QWIP structures as well as a new type-2 normal incident AlAs/AlGas QWIP structure by using molecular beam epitaxy (MBE) technique; (2) the design and fabrication of the 1-D (line-grating) and 2-D (cross-grating) metal grating couplers on the QWIP's with different grating periods (1.1, 3.2, 5, 7.2, and 10 microns); (3) the theoretical and experimental studies of the light coupling quantum efficiency versus grating period for the QWIP's; and (4) the theoretical and experimental studies of the dark current versus temperature and bias voltage for the BTM and SBTM QWIP's. GRA

N92-32760# Philips Gloeilampenfabrieken N.V., Eindhoven (Netherlands).
INVESTIGATION OF IMPURITY RELATED PHENOMENA, SIGNIFICANT FOR NOVEL SEMICONDUCTOR TECHNOLOGIES Ph.D. Thesis - Univ. Twente
Franciscus Petrus Widdershoven 1991 116 p
(ETN-92-92048) Avail: CASI HC A06/MF A02

The introduction of impurities into semiconductor materials during fabrication is addressed. Some phenomena related to the presence of such impurities are investigated. An investigation of the properties of erbium doped silicon is described, and the characterization, by several analysis techniques, of the interface between directly bonded n-type silicon wafers is reported. A theory describing the influence of correlation on electron mobility (between the positions of impurities within impurity clusters) is presented. The theory is applied to calculate the electron mobility of gallium arsenide in the presence of clusters of correlated impurities at a temperature of 77 K. This correlation is shown to have a significant influence on the mobility. ESA

N92-32892# Institut National des Sciences Appliquees, Lyon (France). Groupe d'Etude Metallurgie Physique et Physique des Materiaux.
CONTRIBUTION TO THE STUDY OF THE EFFECT OF THE HETEROGENEOUS DISTRIBUTION OF DISLOCATIONS ON THE CYCLIC PLASTICITY OF SINGLE CRYSTAL ALUMINUM Ph.D. Thesis [CONTRIBUTION A L'ETUDE DE L'EFFET DE LA REPARTITION HETEROGENE DES DISLOCATIONS SUR LA PLASTICITE CYCLIQUE DE L'ALUMINIUM PUR MONOCRISTALLIN]
Abdelilah Alhamany 1991 195 p In FRENCH
(ISAL-91-0099; ETN-92-92084) Avail: CASI HC A09/MF A03

A study carried out at ambient temperature on single crystals of aluminum, oriented for a single creep to deformation amplitudes between 0.0001 and 0.001, are reported. The aluminum does not present true mechanical saturation. A sequence of hardening, softening, and secondary hardening is present. The fatigued aluminum also shows a marked Bauschinger effect, with amplitude evolved along the stress cycle. The deformation is localized, from

the period of softening, in short segments of creep bands of the primary system that can be assimilated to persistent creep bands of aluminum. The microstructure is made up of elongated cells that are distributed in an equi-axial cell matrix. The distant constraints related to deformation incompatibilities, resulting from heterogeneous dislocation distribution, play a leading part in the cyclic plasticity and explain the presence of the Bauschinger effect. The effect of these compatibility constraints, related to the progressive establishment in the bands of a cellular structure, is at the origin of the observed secondary hardening. ESA

N92-32898# Harvard Univ., Cambridge, MA. Div. of Applied Sciences.
GEOMETRICAL EFFECTS IN TWO-DIMENSIONAL ARRAYS OF JOSEPHSON JUNCTIONS
Lydia L. Sohn May 1992 208 p
(Contract N00014-89-J-1023)
(AD-A252209; TR-33) Avail: CASI HC A10/MF A03

We present an extensive experimental and theoretical study of Josephson-junction arrays with both short- and long-range interaction. We first investigate the effects of current direction on the dynamical properties of RF and dc current-biased overdamped Josephson-junction arrays with short-range interaction in the presence of magnetic flux. We show that if the Lorentz force, produced by the transport current, acting on vortices is directed towards the island barrier, the array will behave like a set of coupled one-dimensional arrays and produce only integer giant Shapiro steps. If, however, the Lorentz force is directed towards any other direction, the array will produce both integer giant and fractional giant Shapiro steps. A moving vortex model and a pendulum model are used to describe our experimental and computational results. GRA

N92-32919# Oak Ridge National Lab., TN.
SUBSTRATE REACTIONS AND FLUX PINNING STRUCTURES IN MELT-PROCESSED YBa2Cu3O7 DEPOSITS ON Ag-Pd ALLOY SUBSTRATES
D. M. Kroeger, A. Goyal, Z. L. Wang, F. A. List, and K. B. Alexander 1992 8 p Presented at the High Tc SUH Workshop on High Temperature Superconductivity (HTS) Materials, Bulk Processing and Bulk Applications, Houston, TX, 27-28 Feb. 1992
(Contract DE-AC05-84OR-21400)
(DE92-014404; CONF-920240-5) Avail: CASI HC A02/MF A01

Results on melt-processing of thick deposits of highly homogeneous, submicron Y-123 powders prepared by aerosol pyrolysis on Ag-Pd alloy substrates are discussed. For long-term treatments at high temperatures, the extent of the substrate/deposit reaction increased with the Pd content of the substrate. At high Pd concentrations a Ba-Cu-Pd-O phase was formed, resulting in phase segregation of the deposit. For low Pd concentrations the only evidence of a reaction was the presence of a low density of copper oxide precipitates in the Ag-Pd substrate. TEM examination indicated that the substrate/deposit boundary was sharp, and no evidence of Pd contamination was found at 123/123 grain boundaries intersecting the substrate. The melt-processed deposits contain a very fine dispersion of 211 particles within the 123 phase. TEM examination has revealed the presence of a high density of stacking faults in the 123 near the 211/123 interfaces. Simple considerations suggest that these defects may be effective flux pinners for fields directed perpendicular to the basal plane. DOE

N92-32920# Sandia National Labs., Albuquerque, NM.
THICKNESS DEPENDENCE OF VORTEX PINNING IN EPITAXIAL Tl-Ca-Ba-Cu-O THIN FILMS
E. L. Venturini, B. Morosin, D. S. Ginley, and W. Y. Lee (IBM Research Lab., San Jose, CA.) 1992 6 p Presented at the Material Research Society Spring Meeting, San Francisco, CA, 27 Apr. - 2 May 1992
(Contract DE-AC04-76DP-00789)
(DE92-015011; SAND-92-0128C; CONF-920402-19) Avail: CASI HC A02/MF A01

The critical current density inferred from magnetization hysteresis for epitaxial Tl2Ca2Ba2Cu3O10 films on LaAlO3 exhibits a pronounced increase with film thickness in the high-field, high-current regime. This thickness dependence does not extend to comparatively 'thick' single crystals, however, suggesting that the grain boundaries play a major role in collective vortex pinning for Tl-based superconducting thin films. DOE

N92-32938# Naval Surface Warfare Center, Silver Spring, MD.
PSEUDOPOTENTIAL BAND CALCULATIONS ALONG A HIGH-SYMMETRY AXIS. PART 1: CENTRAL POTENTIAL AND THE (111) DIRECTION
D. Y. Agassi and J. B. Restorff 15 Jun. 1991 57 p
(AD-A252399; NAVSWC-TR-91-324) Avail: CASI HC A04/MF A01

A method for band structure calculations along a high-symmetry axis is introduced in this report. It entails a cylindrical coordinate multipole expansion of the wave function and an exact reduction of the three-dimensional Schroedinger equation into a set of one-dimensional wave equations for the multipoles. Group theoretic considerations and energy arguments imply good convergence, regardless of the unit-cell extension along the high-symmetry direction. Band calculations of a test case, PbSe along the 111 direction, demonstrate the good convergence. This method is expected to be particularly useful for structures highly anisotropic along a high-symmetry axis, e.g., superlattices. GRA

N92-32939# Army Lab. Command, Watertown, MA. Material Technology Lab.
SITE COMPETITION OF IMPURITIES AND GRAIN BOUNDARY STABILITY IN IRON Final Report
Genrich L. Krasko Jun. 1992 15 p
(AD-A252411; MTL-TR-92-38) Avail: CASI HC A02/MF A01

Impurities such as H, P, S, B, etc., have a very low solubility in iron and, therefore, prefer to segregate at the grain boundaries (GBs). In order to analyze the energetics of impurities on the iron GB, the Linear Muffin Tin Orbitals (LMTO) calculations were performed on a simple 8-atom supercell emulating a typical (capped trigonal prism) GB environment. The so-called environment-sensitive embedding energies (EE) were calculated for H, B, C, N, O, Al, Si, P, and S as a function of the electron charge density due to the host atoms at the impurity site. It was shown that, at the electron charge density typical of a GB, B and C have the lowest energy among the analyzed impurities and, thus, would compete with them for the site on the GB tending to push the other impurities off the GB. The above energies were then used in a modified Finnis-Sinclair embedded atom approach for calculating the equilibrium interplanar distances in the vicinity of a (111) 13 tilt GB plane, both for the clean GB and that with an impurity. These distances were found to be oscillating, returning to the equilibrium spacing between the (111) lanes in bulk BCC iron by the 10th to 12th lane off the GB lane. GRA

N92-32940# Texas A&M Univ., College Station. Dept. of Physics.
ANNUAL REPORT, 1 NOVEMBER 1990 - 31 OCTOBER 1991
Roland E. Allen 31 Oct. 1991 1 p
(Contract N00014-91-J-1126)
(AD-A252431) Avail: CASI HC A02/MF A01

A first-principles computer program was completed for calculations of surface properties of semiconductors, and of the interaction of a scanning-tunneling-microscopy tip with a semiconductor surface. We plan to use this program in studies of surface adsorption and diffusion, of the theoretical interpretation of STM, and of atomic manipulation with a STM tip. Since it involves state-of-the-art methods (norm-conserving pseudopotentials, conjugate-gradient techniques, etc.) and consists of 3340 lines of original code, writing it was a nontrivial task. By using a completely independent first-principles program for clusters, we generated first-principles-based models for molecular dynamics computer simulations that are more reliable than the models we used in the past. These new models consist of a third-neighbor tight-binding Hamiltonian and a three-body potential, with parameters fitted to the first-principles cluster calculations. GRA

N92-33023# Oak Ridge National Lab., TN.
SUPERCONDUCTING TRANSPORT PROPERTIES AND SURFACE MICROSTRUCTURE FOR YBa2Cu3O(7-DELTA) BASED SUPERLATTICES GROWN BY PULSED LASER DEPOSITION
D. P. Norton, D. H. Lowndes, X. Zheng, R. J. Warmack, S. J. Pennycook, and J. D. Budai May 1991 10 p Presented at the HASRD Workshop on Laser Ablation: Mechanisms and Application, Oak Ridge, 8-10 Apr. 1991
(Contract DE-AC05-84OR-21400)
(DE91-014224; CONF-9104192-11) Avail: CASI HC A02/MF A01

YBa2Cu3O(7 - delta)/PrBa2Cu3O(7 - delta), YB2Cu3O(7 - delta)/Pr(0.7)YBa2Cu3O(7 - delta), and YBa2Cu3O(7 - delta)/Pr(0.5)Ca(0.5)Ba2Cu3O(7 - delta) superlattice structures have been grown by pulsed laser deposition. The superconducting properties of these YBa2Cu3O(7 - delta) based superlattices are shown to depend on the electronic properties of the barrier layers. In particular, the superconducting transition width decreases as the hole carrier density in the barrier layers is increased, while (Tc)(onset) does not change with barrier layer carrier density. (Tc)(onset) is apparently determined by the YBa2Cu3O(7- delta) layer thickness, while the transition width, determined by the long-range phase coherence of the superconducting wave function, depends on the electronic properties of the isolating barrier layers. 3)O(sub 7-(delta)) thin films by grown by pulsed laser deposition, and find a highly terraced, granular morphology. This morphology suggests that multilayer thin film structures possess a high density of steps within the individual layers. These steps should be quite important in the transport properties of these superconducting structures. DOE

N92-33025# Purdue Univ., West Lafayette, IN.
GAMMA SCATTERING IN CONDENSED MATTER WITH HIGH INTENSITY MOESSBAUER RADIATION
1992 69 p
(Contract DE-FG02-85ER-45199)
(DE92-014811; DOE/ER-45199/2) Avail: CASI HC A04/MF A01

This report discusses quasielastic scattering studies on glycerol; gamma-ray scattering from alkali halides; lattice dynamics in metals; Moessbauer neutron scattering, x-ray diffraction, and macroscopic studies of high (Tc) superconductors containing tungsten; NiAl scattering studies; and atomic interference factors and nuclear Casimir effect. DOE

N92-33026# Los Alamos National Lab., NM.
SYNTHESIS, MICROSTRUCTURE, CRITICAL CURRENT DENSITY, MAGNETIZATION AND RELAXATION OF HOT-PRESSED YBa2Cu3O(6 + DELTA) THROUGH PARTIAL MELTING POST-OXYGENATION
P. J. Kung (Carnegie-Mellon Univ., Pittsburgh, PA.), M. P. Maley, and M. E. McHenry (Carnegie-Mellon Univ., Pittsburgh, PA.) 1992 7 p Presented at the Material Research Society Spring Meeting, San Francisco, CA, 27 Apr. - 2 May 1992
(Contract W-7405-eng-36)
(DE92-015205; LA-UR-92-1495; CONF-920402-26) Avail: CASI HC A02/MF A01

Hot-pressed YBa2Cu3O(6 + delta) (approx. 1000 C) followed by slow cooling in oxygen atmosphere has resulted in enhanced magnetization hysteresis loops which show weak dependence on magnetic field. The x-ray diffraction pattern exhibits the significant features associated with the reflection (003) and (006), and a higher compaction density in hot-pressed samples compared with cold-pressed samples was observed from the SEM micrographs. Morphology study and microstructural analysis by SEM and TEM, respectively, indicate that grains were well aligned during hot-pressing mostly with their c-axes parallel to the pressing axis, and many intersecting twins were actually formed during post-oxygenation. Local oxygen-deficient regions likely existing in these hot-pressed and oxygenated samples are believed to act as effective flux pinning centers at high temperatures (approx. 50 K and above). The measurement of magnetic relaxation was employed to interpret the observed pinning behavior. The critical magnetization current density (J(sub c)) calculated using the Bean model and the average grain dimension is in the order of 10(exp 4) Amp/sq cm at 75 K up to 1 T. Because of a shorter period of oxygenation and a weak field dependence of (J(sub c)) values, the process of hot-pressing combined with partial melting post-oxygenation is technologically practical in forming various shapes as desired from oxide superconductors. DOE

N92-33111# Ames Lab., IA.
USE OF A FOURIER DECONVOLUTION METHOD IN PARTICLE SIZE DETERMINATION AND USE OF MOLECULAR MECHANICS IN CRYSTAL STRUCTURE DETERMINATIONS Ph.D. Thesis
Yingzhong Su May 1992 147 p
(Contract W-7405-eng-82)
(DE92-014510; IS-T-1591) Avail: CASI HC A07/MF A02

A Fourier deconvolution method was employed to estimate the grain size from a recorded pattern. The usefulness of the method is shown to be very dependent on effects of noise and sampling discontinuities in the recorded patterns, and the treatment of data with a least squares spline smoothing method to ease their effects is discussed. The grain size results obtained by this program are compared with those obtained by Rietveld refinements and by transmission electron microscope investigations. X-ray structure determinations of single crystals of compounds I: benzo-(2,3) 4-methyl-thiophene, C9H10S-Ir-(C5(CH3))), and II: dibenzothiophene, C12H10S-Ir-(C5CH)5 were performed. It was expected that in the two compounds the Ir d-orbitals would be associated with the whole p-system of the complexing benzo-group, implying that all carbon atoms in this group would remain aromatic. The x-ray structure determinations and NMR H-1 results indicate that both I and II can be best described as complexes in which two carbon atoms of a benzo-group of the ligand have been converted from sp(sup 2) to sp(sup 3) character. The structural results of the x-ray determinations and those of molecular mechanics are also compared and discussed. An optical alignment procedure making use of ordinary optical telescopes was developed which provides an easy-to-use alignment operation for the first stage of diffractometer alignment. DOE

N92-33117# California Univ., Berkeley. Lawrence Berkeley Lab.
IMPLANTATION OF CARBON IN GaAs Ph.D. Thesis
A. J. Moll Mar. 1992 82 p
(Contract DE-AC03-76SF-00098)
(DE92-016921; LBL-32253) Avail: CASI HC A05/MF A01

Carbon implanted into GaAs and thermally annealed typically exhibits very low (less than 3 percent) electrical activity. It has been demonstrated that the electrical activity of C can be significantly enhanced by co-implantation with Ga. Improved activation may result from either additional damage of the crystal lattice or from stoichiometric changes, forcing the C atoms onto As sites. To determine the relative importance of each of these effects, I have undertaken a systematic study of carbon activation in GaAs. A range of co-implants have been used: group III (B, Ga), group V (N, P, As) and noble gases (Ar, Kr). The damage introduced to the substrate will depend on the mass of the ion implanted. The group III and group V co-implants will affect the crystal stoichiometry. The results indicate that both lattice damage and crystal stoichiometry are important for high electrical activity of C. Increasing the damage will increase the activation due to the increased number of As vacancies, but maximum activation can be obtained only by a co-implant which not only damages the lattice but also forces the C to occupy an As site. DOE

N92-33127# Oak Ridge National Lab., TN.
MODIFICATION OF THE OPTICAL PROPERTIES OF Al2O3 BY ION IMPLANTATION
C. W. White, D. K. Thomas, R. A. Zuhr, J. C. McCallum, A. Pogany, R. F. Haglund, and R. H. Magruder Apr. 1992 6 p Presented at the Material Research Society Spring Meeting, San Francisco,

CA, 27 Apr. - 2 May 1992
(Contract DE-AC05-84OR-21400)
(DE92-013861; CONF-920402-7) Avail: CASI HC A02/MF A01

The implantation of Au into Al2O3 followed by thermal annealing at 1100 C leads to dramatic changes in the optical properties. The linear and nonlinear optical properties are correlated to the presence of small Au precipitates which form during annealing. DOE

N92-33136# Brookhaven National Lab., Upton, NY.
STUDIES OF Y-Ba-Cu-O SINGLE CRYSTALS BY X RAY ABSORPTION SPECTROSCOPY
A. Krol (State Univ. of New York, Buffalo.), Z. H. Ming (State Univ. of New York, Buffalo.), Y. H. Kao (State Univ. of New York, Buffalo.), N. Nuecker (Kernforschungszentrum G.m.b.H., Karlsruhe, Germany, F.R.), G. Roth (Kernforschungszentrum G.m.b.H., Karlsruhe, Germany, F.R.), J. Fink (Kernforschungszentrum G.m.b.H., Karlsruhe, Germany, F.R.), and G. C. Smith Feb. 1992 9 p Presented at the 5th Annual Conference on Superconductivity and Applications, Buffalo, NY, 24-26 Sep. 1991
(Contract DE-AC02-76CH-00016)
(DE92-014687; BNL-47236; CONF-9109102-7) Avail: CASI HC A02/MF A01

The symmetry and density of unoccupied states of YBa2Cu3O7 YBa2Cu4O8 have been investigated by orientation dependent x-ray absorption spectroscopy on the O 1s edge using a bulk-sensitive fluorescence-yield-detection method. It has been found that the O 2p holes are distributed equally between the CuO2 planes and CuO chains and that the partial density of unoccupied O 2p states in the CuO2 planes are identical in both systems investigated. The upper Hubbard band has been observed in the planes but not in the chains in both systems. DOE

N92-33190 Tel-Aviv Univ. (Israel).
ELECTRIC AND MAGNETIC PROPERTIES OF RANDOM SUPERCONDUCTORS Ph.D. Thesis
Alexander Gerber Sep. 1989 147 p
(ITN-92-85165) Copyright Avail: Tel-Aviv Univ., Exact Sciences Library, Ramat Aviv, 69978, Israel

We studied the transport and superconducting properties of random discontinuous thin films above and below the percolation threshold. The conductivity of the samples below the percolation threshold is dominated by quasiparticle tunneling between the clusters. The conductivity in the normal state (N-I-N junction) is then larger than when the clusters are superconducting (S-I-S junction), owing to the opening of the superconducting energy gap. Reduction of this gap by the applied magnetic fields leads to the progressive reduction of the resistance to its normal value. The upper critical field of percolating lead films above and below the percolation threshold were measured by monitoring the samples' electrical resistance as a function of an applied magnetic field. We find that it remains constant across the threshold, as predicted by theory based on the fractal nature of the infinite cluster and of large finite clusters. The transport properties of disconnected lead films have been studied at zero and high magnetic field at which the superconductivity is suppressed in finite clusters. At low temperatures conductivity between separated clusters has been found to be dominated by voltage injection and not by thermal excitation of electrons. This gives rise to temperature independent resistance tails observed in both the superconducting and the normal phases at low temperatures. V-I characteristics were found to follow a power law. Author (ISA)

N92-33221# Argonne National Lab., IL.
DYNAMICS OF RADIATION-INDUCED AMORPHIZATION IN INTERMETALLIC COMPOUNDS
N. Q. Lam, P. R. Okamoto, R. Devanathan (Northwestern Univ., Evanston, IL.), and M. Meshii (Northwestern Univ., Evanston, IL.) Jun. 1992 11 p Presented at the NATO Advanced Study Institute on Statics and Dynamics of Alloy Phase Transformations, Rhodes (Greece), 21 Jun. - 3 Jul. 1992
(Contract W-31-109-eng-38)
(DE92-016774; ANL/CP-76482; CONF-9206202-1) Avail: CASI HC A03/MF A01

Recent progress in molecular-dynamics simulations of radiation-induced crystalline-to-amorphous transition in intermetallic compounds and the relationship between amorphization and melting are discussed. By focusing on the mean-square static displacement, which provides a generic measure of energy stored in the lattice in the forms of chemical and topological disorder, a unified description of solid-state amorphization as a disorder-induced, isothermal melting process can be developed within the framework of a generalized Lindemann criterion. DOE

N92-32976*# National Aeronautics and Space Administration. Lewis Research Center, Cleveland, OH.
REDUCED MOBILITY AND PPC IN In(.20)Ga(.80)As / Al(.23)Ga(.77)As HEMT STRUCTURE
S. E. Schacham (Technion - Israel Inst. of Tech., Haifa.), Rafael A. Mena, Edward J. Haugland, and Samuel A. Alterovitz *In its* Solid State Technology Branch of NASA Lewis Research Center Aug. 1992 p 111-116 Submitted for publication (For primary document see N92-32965 23-32)
Avail: CASI HC A02/MF A03

N92-32977*# National Aeronautics and Space Administration. Lewis Research Center, Cleveland, OH.
STUDY OF InGaAs-BASED MODULATION DOPED FIELD EFFECT TRANSISTOR STRUCTURES USING VARIABLE-ANGLE SPECTROSCOPIC ELLIPSOMETRY
Samuel A. Alterovitz, R. M. Sieg (Cleveland State Univ., OH.), H. D. Yao (Nebraska Univ., Lincoln.), P. G. Snyder (Nebraska Univ., Lincoln.), J. A. Woollam (Nebraska Univ., Lincoln.), J. Pamulapati (Michigan Univ., Ann Arbor.), P. K. Bhattacharya (Michigan Univ., Ann Arbor.), and P. A. Sekula-Moise (Spire Corp., Bedford, MA.) *In its* Solid State Technology Branch of NASA Lewis Research Center Aug. 1992 p 117-122 Repr. from Journal of Thin Solid Films (Lausanne, Switzerland, Elsevier Sequoia), no. 206, 1991 p 288-293 (For primary document see N92-32965 23-32)
Avail: CASI HC A02/MF A03

N92-32978*# National Aeronautics and Space Administration. Lewis Research Center, Cleveland, OH.
MICROWAVE PROPERTIES OF PEELED HEMT DEVICES SAPPHIRE SUBSTRATES
Paul G. Young (Toledo Univ., OH.), Samuel A. Alterovitz, Rafael A. Mena, and Edwyn D. Smith (Toledo Univ., OH.) *In its* Solid State Technology Branch of NASA Lewis Research Center Aug. 1992 p 123-126 (For primary document see N92-32965 23-32)
Avail: CASI HC A01/MF A03

N92-32979*# Technion - Israel Inst. of Tech., Haifa. Dept. of Electrical Engineering.
A MODEL FOR THE TRAP-ASSISTED TUNNELING MECHANISM IN DIFFUSED n-p AND IMPLANTED n(+)-p HgCdTe PHOTODIODES
David Rosenfeld and Gad Bahir *In* NASA. Lewis Research Center, Solid State Technology Branch of NASA Lewis Research Center Aug. 1992 p 127-134 Repr. from Transactions on Electron Devices (IEEE), v. 39, no. 7, Jul. 1992 p 1638-1645 Previously announced in IAA as A92-46007 (For primary document see N92-32965 23-32)
Avail: CASI HC A02/MF A03

N92-32980*# National Aeronautics and Space Administration. Lewis Research Center, Cleveland, OH.
NASA SPACE APPLICATIONS OF HIGH-TEMPERATURE SUPERCONDUCTORS
Vernon O. Heinen, Martin M. Sokoloski (National Aeronautics and Space Administration, Washington, DC.), Paul R. Aron, and Kul B. Bhasin *In its* Solid State Technology Branch of NASA Lewis Research Center Aug. 1992 p 143-149 (For primary document see N92-32965 23-32)
Avail: CASI HC A02/MF A03

N92-32983*# National Aeronautics and Space Administration. Lewis Research Center, Cleveland, OH.
MAGNETIC PENETRATION DEPTH OF YBa2Cu3O(7-DELTA) THIN FILMS DETERMINED BY THE POWER TRANSMISSION METHOD
Vernon O. Heinen, Felix A. Miranda, and Kul B. Bhasin *In its* Solid State Technology Branch of NASA Lewis Research Center Aug. 1992 p 201-204 (For primary document see N92-32965 23-32)
Avail: CASI HC A01/MF A03

N92-32984*# National Aeronautics and Space Administration. Lewis Research Center, Cleveland, OH.
MAGNETIC FLUX RELAXATION IN YBa2Cu3O(7-x) THIN FILM: THERMAL OR ATHERMAL
Satish Vitta, M. A. Stan (Kent State Univ., OH.), Joseph D. Warner, and Samuel A. Alterovitz *In its* Solid State Technology Branch of NASA Lewis Research Center Aug. 1992 p 205-210 Repr. from Journal of Thin Solid Films (Lausanne, Switzerland, Elsevier Sequoia), no. 206, 1991 p 137-142 (For primary document see N92-32965 23-32)
(Grant NAG3-440751)
Avail: CASI HC A02/MF A03

77 THERMODYNAMICS AND STATISTICAL PHYSICS

Includes quantum mechanics; theoretical physics; and Bose and Fermi statistics.

For related information see also *25 Inorganic and Physical Chemistry* and *34 Fluid Mechanics and Heat Transfer.*

N92-32309# Gosudarstvennyi Komitet po Ispolzovaniyu Atomnoi Energii, Serpukhov (USSR). Inst. Fiziki Vysokikh Ehnergij.
ON THE CHOICE OF MINIMIZATION FUNCTIONAL IN THE PARTIAL WAVE ANALYSIS
S. A. Sadovskij 1991 8 p
(DE92-624689; IFVE-OEF-91-15; IHEP-OEF-91-15) Avail: CASI HC A02/MF A01

After an example of the partial wave analysis of (pi)(sup -)p (yields) eta(pi)(sup 0)n reaction at 100 GeV/c (experiment NA12 at CERN), it is shown that the using of the approximate minimization functional outside of its valid range may result in the significant deterioration of the results. In the considered case, the sign inversion of the t(sub 40) spherical harmonics moment takes place in the region of the a(sub 2)(1320)-meson. This results in the opposite of the previous conclusion on a large D(sub 0)-wave contribution to a(sub 2)(1320) production cross section. DOE

N92-32496# Fermi National Accelerator Lab., Batavia, IL.
TWO PERSPECTIVES ON A DECOHERING SPIN
A. Albrecht 13 Feb. 1992 13 p Presented at the Workshop on Time Asymmetry, Mazagon (Spain), 30 Sep. - 4 Oct. 1991
(Contract DE-AC02-76CH-03000)
(DE92-013021; FNAL/C-92/41-A; CONF-9109371-1) Avail: CASI HC A03/MF A01

The quantum mechanics of a spin interacting with an environment are studied. Although the evolution of the whole system is unitary, the spin evolution is not. The system is chosen so that the spin exhibits loss of quantum coherence, or 'wavefunction collapse', of the sort usually associated with a quantum measurement. The system is analyzed from the point of view of the spin density matrix (or 'Schmidt path'), and also using the consistent histories (or decoherence functional) approach. DOE

N92-32566# Brown Univ., Providence, RI. Div. of Engineering.
TWO STUDIES OF NONLINEAR PROCESSES IN IRREVERSIBLE THERMODYNAMICS
J. Kestin 1992 9 p
(Contract DE-FG02-87ER-13667)
(DE92-016855; DOE/ER-13687/12) Avail: CASI HC A02/MF A01

The investigation dealt with two lines of research into two well-defined problems of engineering science: a study of two-phase flow and of nonelastic deformations in structural solids. Both topics fall into the broad field of nonlinear irreversible processes. The study of two-phase flow resulted in a complete topological analysis of the canonical mathematical model of one-dimensional flow of a mixture of two phases, now predominantly used in industry, especially the nuclear industry. The topological analysis is confronted with the practice of discretizing the analytic model for the purpose of formulating a numerical computer code. It is shown that in the presence of singular points in the phase space of the differential equations of the model there occur spurious numerical solutions. Such solutions may contain segments which are correct approximations to the exact trajectory, but always include branches which are totally false and misleading. The topological method allows the operator to formulate a subroutine which eliminates spurious solutions. The study of inelastic deformations, i.e., of irreversible processes in structural solids, provided a consistent presentation of the local-state approximation erroneously called the method of local equilibrium in the literature. The key concept which impedes the correct use of thermodynamics in this field is the definition of a measurable entropy of a nonequilibrium state. The local state approximation solves this problem by assigning to a nonequilibrium state n the entropy of the accompanying equilibrium state e. The two states, n and e, are linked by having the same values of a specified set of extensive properties. The same principle settles the comparison between the intensive properties of n and e, which are different. DOE

N92-32593# Texas Univ., Austin. Center for Studies in Statistical Mechanics.
THE BEHAVIOR OF MATTER UNDER NON-EQUILIBRIUM CONDITIONS: FUNDAMENTAL ASPECTS AND APPLICATIONS
I. Prigogine Apr. 1992 7 p
(Contract DE-FG05-88ER-13897)
(DE92-014247; DOE/ER-13897/13) Avail: CASI HC A02/MF A01

This report briefly discusses concepts of chaotic systems. The topics discussed are as follows: Bernoulli maps; mathematical aspects of the complex spectral representations; and large Poincare systems. DOE

N92-32603# Gosudarstvennyi Komitet po Ispolzovaniyu Atomnoi Energii, Serpukhov (USSR). Inst. Fiziki Vysokikh Ehnergij.
FRACTIONAL SPIN: MAJORANA-DIRAC FIELD
M. S. Plyushchaj 1991 10 p
(DE92-624558; IHEP-OTF-91-90) Avail: CASI HC A02/MF A01

A system of equations for a free relativistic field with fractional spin is proposed. The solutions realize the one-particle states as the unitary representations of the (2+1)-dimensional Poincare group. It contains a (2+1)-dimensional analog of the infinite-component Majorana equation and the Dirac equation. The classical action is constructed which leads to the proposed field equations. DOE

N92-32649# Flinders Univ., Adelaide (Australia). Electronic Structure of Materials Centre.
RANGE OF VALIDITY OF DISTORTED WAVE BORN AND IMPULSE APPROXIMATIONS FOR (e,2e)
I. E. McCarthy Aug. 1991 14 p
(DE92-624821; ESM-36) Avail: CASI HC A03/MF A01

The Distorted Wave Born Approximation (DWBA) is the separable approximation for the final state. This approximation was used in more-sophisticated calculations which amount to replacing the distorting potential U(sub 1) by a complex, nonlocal potential which includes the effect of exciting other channels. This potential includes all non-elastic channels which are coupled to the ground state but not to each other. Ionized channels are calculated by the DWBA. The overestimate of cross sections at lower energies is confirmed. The treatment of exchange in the

calculation is confirmed by the excellent agreement of the asymmetry with experiment. It is concluded that the Distorted Wave Impulse Approximation (DWIA), which is a simple, easily-computed model, gives a thoroughly-correct account of (e,2e) experiments at higher energy, under Bethe-ridge conditions, to the accuracy necessary for the determination of target-ion structure. It is invalid far off the Bethe ridge. Generally, the DWBA is more applicable, giving an excellent account of higher-energy experiments (greater than a few hundred eV). The DWBA becomes inaccurate as the long-range electron-electron repulsion becomes more important in the final state. The inclusion of the relative Coulomb factor to satisfy the final-state boundary condition seems to be a promising, but very difficult direction for investigation. DOE

N92-33069# Los Alamos National Lab., NM.
PHYSICS IN KNOTS
D. Holz (Princeton Univ., NJ.), J. A. Wheeler (Princeton Univ., NJ.), A. Kheyfets (North Carolina State Univ., Raleigh.), and W. A. Miller 1992 17 p Presented at the Workshop on Physical Origins of Time Asymmetry, Mazagon (Spain), Oct. 1991
(Contract W-7405-eng-36)
(DE92-017530; LA-UR-92-1853; CONF-9110397-1) Avail: CASI HC A03/MF A01

In this report the authors work out the relevant It-from-Bit means to measure spacetime curvature. Also described are the essential new features of the knot description of gravity and the one index loop variable and the Einstein tensor. DOE

N92-33109# Ames Lab., IA.
QUANTUM WAVE MODELING ON HIGHLY PARALLEL DISTRIBUTED MEMORY MACHINES Ph.D. Thesis
N. Nayar 18 May 1992 119 p
(Contract W-7405-eng-82)
(DE92-014507; IS-T-1599) Avail: CASI HC A06/MF A02

Parallel computers are finding major applications in almost all scientific and engineering disciplines. An interesting area that has received attention is quantum scattering. Algorithms for studying quantum scattering are computationally intensive and hence suitable for parallel machines. The state-of-the-art methods developed for uniprocessors require the computation of two Fast Fourier Transforms (FFTs) at each time step. However, the communication overhead in implementing FFTs make them an expensive operation on distributed memory parallel machines. The focus of this dissertation is the development of efficient parallel methods for studying the phenomenon of time-dependent quantum-wave scattering. The methods described belong to the class of integral equation methods, which involve the application of a repeated sequence of very short time step propagations. Free propagation of a wavepacket is most easily handled in the so-called momentum representation whereas the effect of the potential is most easily obtained in the coordinate representation. The two representations are Fourier Transforms of each other. The algorithm presented eliminates the computation of FFTs by performing the propagation totally within the coordinate representation. The communication required is only with the nearest neighbors and is load balanced, thus making the algorithm suitable for distributed memory parallel machines. Implementation results on the nCUBE hypercube and comparison with standard FFT methods are also presented. DOE

N92-33199 British Columbia Univ., Vancouver.
PERTUBATIVE FINITE TEMPERATURE FIELD THEORY IN MINKOWSKI SPACE Ph.D. Thesis
Werner H. Keil Jun. 1989 136 p
(ISBN-0-315-55158-5; CTN-92-60522) Copyright Micromedia Ltd., Technical Information Centre, 165 Hotel de Ville, Place du Portage, Phase 2, Hull, Quebec J8X 3X2, Canada HC/MF

A perturbative analysis is presented of decay and scattering rates in finite temperature and density environments, based on the Niemi-Semenoff real-time formulation of quantum field theory at finite temperature. Two systems are investigated: neutron beta decay and Higgs boson decay. For neutron beta decay, a fully relativistic analysis at tree level is given. An analytic formula for the free neutron decay rate is derived and generalized to a finite density environment. The decay rates are obtained from the imaginary part of the neutron self-energy (the two-point function of Green's function). This method includes all relevant decay and inverse decay modes in a nontrivial way. The decay of a Higgs boson into two fermions, with one-loop quantum electrodynamic corrections, is used to discuss the problem of renormalization at finite temperature. It is found that the finite temperature part of the self-energy corrections cannot be absorbed into temperature dependent mass and wave function renormalization counterterms due to the lack of Lorentz invariance. A general algorithm for the calculation of thermal self-energy corrections is derived and applied to the Higgs-fermion system. The result is explicitly shown to be free of infrared and mass singularities. Previous work is compared to this general approach, and possible applications in cosmology and astrophysics are discussed. Author (CISTI)

80 SOCIAL SCIENCES (GENERAL)

Includes educational matters.

No abstracts in this category.

81 ADMINISTRATION AND MANAGEMENT

Includes management planning and research.

N92-32551# George Mason Univ., Fairfax, VA. Center of Excellence in Command Control Communications/Intelligence.
COGNITIVE BIASES AND TIME STRESS IN TEAM DECISION MAKING Technical Report, Dec. 1991 - Mar. 1992
Paul E. Lehner, Mir-Masood Seyed-Solorforough, Bhashyam Nallappa, Michael OConnor, and Steve Sak Apr. 1992 12 p
(Contract N00014-90-J-1680)
(AD-A251153; GMU/C3I-220-R) Avail: CASI HC A03/MF A01

This experiment investigates the impact of time stress on the decision making performance of command and control teams. Two person teams were trained in a set of simple decision procedures. Some of these procedures required subjects to make judgments that were counter to normal heuristic decision processing. The principle hypothesis was that these decision procedures would be vulnerable-to-bias, and would therefore be more vulnerable to the effects of time stress than other decision procedures. The results support this hypothesis. In addition, the results suggest that the subjects adapted inappropriately to time stress. As time stress increased, they began to use a decision processing strategy that was less effective than the strategy they were trained to use. GRA

N92-32618# General Accounting Office, Washington, DC. National Security and International Affairs Div.
NASA PROCUREMENT: IMPROVING OVERSIGHT OF CONSTRUCTION PROJECTS AT THE LANGLEY RESEARCH CENTER. REPORT TO THE HONORABLE JOHN W. WARNER, US SENATE
9 Jul. 1992 9 p
(GAO/NSIAD-92-230; B-248821) Avail: CASI HC A02/MF A01; GAO, PO Box 6015, Gaithersburg, MD 20877 HC

This report responds to your request that we review construction contracting practices between the National Aeronautics and Space Administration's (NASA) Langley Research Center and EG&G Florida, Inc. Specifically, you requested that we review concerns expressed to you about EG&G's being authorized to perform under work orders noncompetitively, hiring unneeded additional employees, inspecting and approving its own construction work, doing poor work and taking longer than necessary to complete it, and performing all construction work at

Langley rather than subcontracting part of it to small businesses. Under the contract, EG&G has the right to do the work orders on a noncompetitive basis and may hire the employees it needs to do so. NASA officials told us that the agency's other field centers had similar arrangements with contractors. However, we identified weaknesses in how EG&G's performance was being monitored, evaluated, and documented. Specifically, we found the following. In certain circumstances, EG&G inspected its own construction work. Langley officials have recognized the potential conflict of interest in this and plan to transfer the inspection function to another contractor. They also plan to improve the contractor's procedures for documenting inspection results. Langley personnel were not following the Center's requirements for documenting their evaluations of EG&G's construction and inspection activities. Therefore, we were not able to determine whether (1) Langley accepted substandard work or (2) EG&G took longer than necessary to perform work. Langley officials have said they will implement procedures to ensure that this is done in the future. Langley had not implemented procedures to evaluate whether EG&G was meeting its goal of awarding 74 percent of subcontracts to small businesses, although Langley officials told us they would do so in the future. We could not verify EG&G's report that it met its subcontracting goals because the contractor did not have all the required supporting documentation. Correcting these problems will enable Langley to improve its contractor oversight and provide a better basis for supporting Langley's award fee determinations.
Author

82 DOCUMENTATION AND INFORMATION SCIENCE

Includes information management; information storage and retrieval technology; technical writing; graphic arts; and micrography.

For computer documentation see *61 Computer Programming and Software.*

N92-32342# Royal Radar Establishment, Malvern (England).
IMPROVING THE TRANSLATION FROM DATA FLOW DIAGRAMS INTO Z BY INCORPORATING THE DATA DICTIONARY
G. P. Randell Jan. 1992 34 p
(AD-A250769; RSRE-92004; BR309398) Avail: CASI HC A03/MF A01

Our earlier work developed formal translation rules for generating a specification in the formal language Z from a data flow diagram. The Z specification produced lacked detail, especially on the types of the data flowing around the system. This report describes how to use information from a data dictionary to improve the Z specification. Formal translation rules from a data dictionary to Z are presented. GRA

N92-32469# North Dakota Univ., Grand Forks. School of Engineering and Mines.
ERIP APPLICATION INSTRUCTIONS
D. M. Watt 2 Jan. 1992 20 p
(Contract DE-FG02-90CE-15991)
(DE92-014103; DOE/CE-15991/5) Avail: CASI HC A03/MF A01

This report provides background information and instructions to assist applicants in writing Energy-Related Inventions Program (ERIP) applications. Initial feedback from usage of the new instructions shows that the best instructions would not be read and followed by all applicants. Applications from more than thirty applicants who have received the new instructions indicated that few had read the instructions. Based on this feedback, the instructions were further revised to include a title page and table of contents. A warning was also added to advise applicants of the potential penalty of delayed review if these instructions are not followed. This revision was intended to address the possibility that some applicants did not see or bother to follow the instructions which followed the background information about ERIP. Included are two examples of ERIP applications which were prepared for handout at workshops or mailing to applicants. Writing of example applications was time consuming and more difficult than expected for several reasons: (1) full disclosures can be lengthy, very detailed, and technical (this contrasts with the desire to prepare examples which are comparatively short and easy for the non-technical person to read); (2) disclosures contain confidential information which should not be published; and (3) it is difficult to imagine that applicants will study examples when they do not bother to read the basic instructions. DOE

N92-32611# Software Productivity Solutions, Inc., Indialantic, FL.
AUTOMATIC ACCESS EXPERIMENT Final Report, Feb. 1989 - Nov. 1991
Dec. 1991 85 p
(Contract F30602-89-C-0003)
(AD-A252217; RL-TR-91-406) Avail: CASI HC A05/MF A01

AAE was a research and development program which attacked one of the most important problems experienced by large organizations in the 1990's; this was the problem of maintaining and using the many diverse data storage and retrieval systems on which organizations have come to rely on. There are three facets to this problem. One, data is stored in many different computer systems. Two, data is stored in many different management systems. Three, data is stored in many different formats. While retrieving data, a user must consider these varied ways data is stored and have knowledge of the information's location and the commands needed to retrieve the separately stored data. The AAE project conducted research to find methods which would provide transparent access to distributed, heterogeneous, multimedia data. Using principles uncovered by the research, a prototype program known as the Automated Transparent Object Management System (ATOMS) was developed which applies and demonstrates these principles. ATOMS is a prototype system, but one which can be scaled up to production performance requirements without deviating from the existing design. GRA

N92-32643# Office of Management and Budget, Washington, DC. Office of Information and Regulatory Affairs.
INFORMATION RESOURCES MANAGEMENT PLAN OF THE FEDERAL GOVERNMENT Annual Report
20 Nov. 1991 323 p Prepared in cooperation with General Services Administration, Washington, DC and Commerce Dept., Washington, DC
(PB92-147198; ISBN-0-16-036004-8) Avail: CASI HC A14/MF A03

A five-year plan for meeting the automatic data processing and telecommunications needs of the Federal Government is discussed. Additionally, the eleventh annual report of the Information Collection Budget (ICB) of the United States Government is presented. Also, a series of cross-cutting analyses covering agency computer security plans, disaster recovery for information technology operations, and devlopments in electronic commerce is included. Finally, strategic overviews that discuss how agencies intend to utilize information resources to meet programmatic goals are reported. These strategic overviews also discuss agency progress against previously announced plans.
Author

N92-32644# Illinois Univ., Urbana. Coordinated Science Lab.
ADAPTIVE INFORMATION PROCESSING AND GLOBAL OPTIMIZATION Final Report
P. R. Kumar 28 Nov. 1991 9 p
(Contract DAAL03-88-K-0046)
(AD-A248450) Avail: CASI HC A02/MF A01

In the area of global optimization, we have analyzed the necessary and sufficient condition for the simulated annealing algorithm to hit the global minimum with probability. This entailed the development of a new balance theory of recurrence orders for time-inhomogeneous Markov chains. In the area of adaptive control and filtering, we have developed the first convergence

theory for least-squares based adaptive control - the most popular scheme. We have also developed a theory of parallel model adaptation which resolves the question of convergence of the output error identification and adaptive IIR filtering algorithms, which has been an open problem for about a decade now. Also, we have proposed new algorithms for adaptive feedforward control and adaptive active noise cancelling, and developed their analysis. We have applied for a patent on the latter scheme. In the area of robustness, we have shown that the simple modification of projecting the parameter estimates to stay in a compact convex set gives robustness not only with respect to bounded disturbances but also to unmodeled dynamics. This resolves a question open for more than a decade. GRA

N92-32654*# Research Inst. for Computing and Information Systems, Houston, TX.
SUPPORTING MULTIPLE DOMAINS IN A SINGLE REUSE REPOSITORY
David Eichmann (West Virginia Univ., Morgantown.) 1 Jun. 1992 18 p
(Contract NCC9-16; RICIS Proj. SE-43)
(NASA-CR-190640; NAS 1.26:190640) Avail: CASI HC A03/MF A01

Domain analysis typically results in the construction of a domain-specific repository. Such a repository imposes artificial boundaries on the sharing of similar assets between related domains. A lattice-based approach to repository modeling can preserve a reuser's domain specific view of the repository, while avoiding replication of commonly used assets and supporting a more general perspective on domain interrelationships. Author

N92-32712# Department of Agriculture, Beltsville, MD. Current Research Information System.
PERMUTED KEYWORD BANK IN CRIS. TERMS FOR INDEXING AND RETRIEVING RESEARCH PROJECTS IN THE CURRENT RESEARCH INFORMATION SYSTEM Final Report
May 1991 298 p
(PB92-179456; USDA-CRIS-PKB-91-05) Avail: CASI HC A13/MF A03

A collection of terms that are used to index research projects in the Current Research Information System (CRIS) is presented. It is intended to serve as an authority file for project summaries entered in CRIS, as a source of keywords for retrieval purposes, and as a guide to the subject content and scope of the CRIS file. Containing over 19,000 terms, the list is based largely on the file of 32,000 research projects which reside in CRIS as of May 1991. Including permutations of multi-word terms, the list contains over 31,000 entries. The CRIS database consists of descriptions of research projects conducted or sponsored by the U.S. Department of Agriculture, the State agricultural experiment stations and land-grant institutions, State forestry schools, Tuskegee University, U.S. schools of veterinary medicine, and participants in the competitive research grants program of the Department. Projects on human nutrition research of other Federal agencies are also included in CRIS. These are maintained in the HNRIMS (Human Nutrition Research and Information Management System) subfile of the database. Author

N92-32843# Technical Research Centre of Finland, Espoo. Information Service.
HYPERTEXT AND HYPERMEDIA [HYPERTEKSTI JA HYPERMEDIA]
Anneli Heimbuerger, Riitta Alkula, and Taru Kuhanen Aug. 1990 304 p In ENGLISH and FINNISH
(VTT-RN-1154; ISBN-9651-38-3803-X; ETN-92-92161) Copyright Avail: CASI HC A14/MF A03; Government Printing Centre, P.O. Box 516, SF-00101 Helsinki, Finland, HC

A survey of basic features and functions of hypertext together with a short history and types of hypertext software available are given. Different methods for information retrieval from hypertext databases are discussed and a few of the most important application areas are introduced. Two hypermedia applications were programmed: a guide hypertext version of an article about hypertechnology and a SuperCard presentation of the Information Service. The applications are described together with the main features and limits of Guide, Hypercard, Supercard, and HyperPAD software. The future hypertext, i.e., an intelligent hypertext, is introduced. The apppendixes contain a hyperglossary, a list of hypertext and hypermedia applications at the Information Service of VTT, a list of hypertext software, and a list of information sources presently available. ESA

N92-32930# Federal Information Exchange, Inc., Gaithersburg, MD.
A MINORITY RESEARCH AND EDUCATION INFORMATION SERVICE: DESIGN, DEVELOP, PILOT TEST, AND IMPLEMENT ON-LINE ACCESS FOR HISTORICALLY BLACK COLLEGES AND UNIVERSITIES AND GOVERNMENT AGENCIES Annual Report, 1 Apr. 1991 - 31 Mar. 1992
J. A. Rodman 1992 49 p
(Contract DE-FG05-90ER-75602)
(DE92-013572; DOE/ER-75602/4) Avail: CASI HC A03/MF A01

This Annual Status Report describes the design, development and implementation of the Minority On-Line Information Service (MOLIS) project by Federal Information Exchange, Inc. for the period of April 1, 1991 to March 31, 1992. Summary information detailing developments prior to this reporting period will also be included to establish a comprehensive perspective of the project. The goal of the MOLIS project, was to develop, design, pilot test on-line access to current information on minority colleges and universities and federal minority opportunities. Federal Information Exchange, Inc. (FIE), a diversified information services company recognized by researchers and educators as a leader in the field of information delivery services, was awarded a 5 year small business research grant to develop and implement MOLIS. Since April 29, 1991, the inauguration of its on-line service, MOLIS has provided current information on 138 Black and Hispanic colleges and universities -- including faculty and student profiles, financial data, research centers and equipment information, pre-college and education programs, emerging capabilities, enrollment data, administrative personnel data, and current events, as well as minority opportunities from 8 participating federal agencies. DOE

N92-32985# Federal Information Exchange, Inc., Gaithersburg, MD.
FEDIX ON-LINE INFORMATION SERVICE: DESIGN, DEVELOP, TEST, AND IMPLEMENT, AN ON-LINE RESEARCH AND EDUCATION INFORMATION SERVICE Annual Status Report, 1 Mar. 1991 - 28 Feb. 1992
John A. Rodman 1992 53 p
(Contract DE-FG05-89ER-75527)
(DE92-013582; DOE/ER-75527/4) Avail: CASI HC A04/MF A01

The FEDIX Annual Status Report provides details regarding an on-line information project designed, developed and implemented by Federal Information Exchange, Inc., a diversified information services company. This document details the project design activities, summarizes the developmental phases of the project, and describes the implementation activities generated to fulfill the project's objectives. The information contained in this document illustrates FIE's continuing commitment to serve as the link that facilitates the dissemination of federal information to the education community. This report reviews the project accomplishments and describes intended service enhancements. DOE

N92-33084# Oak Ridge National Lab., TN.
OAK RIDGE ENVIRONMENTAL INFORMATION SYSTEM (OREIS). PHASE 1: SYSTEM DEFINITION DOCUMENT
Jun. 1992 62 p
(Contract DE-AC05-84OR-21400)
(DE92-017342; ES/ER/TM-34-Phase-1) Avail: CASI HC A04/MF A01

The Phase 1 - System Definition Document documents the basis for establishing a consolidated environmental data base and information system for the Department of Energy Oak Ridge Field

Office (OR) facilities operated by Martin Marietta Energy Systems, Inc. (Energy Systems). The Automated Data Processing System Development Methodology (ADPSDM), an Energy Systems procedure to assist in developing scientific and technical systems, was used to guide the preparation of the feasibility study and the system requirements definition, both of which are contained in this document. The Feasibility Study (Part 1) documents the existing system and data management practices and establishes and analyzes preliminary alternatives to be considered for the development of a consolidated system, i.e., the Oak Ridge Environmental Information System (OREIS). Alternatives were analyzed for technical and operational feasibility, benefits, and risks. Performance criteria used to rank alternatives included standardization, documentation, robustness, integration, reliability, and predictability. Of the three alternatives studied - request/referral, distributed, and centralized - the centralized system was selected to be most feasible because of its conformance to the performance criteria. DOE

N92-33088# Woods Hole Oceanographic Inst., MA.
ABSTRACTS OF MANUSCRIPTS SUBMITTED IN 1991 FOR PUBLICATION
Alora K. Paul, ed. May 1992 187 p
(PB92-204627; WHOI-92-19) Avail: CASI HC A09/MF A02

Given here are the abstracts of manuscripts submitted for publication during calendar year 1991 by the staff and students of the Woods Hole Oceanographic Institution. The authors identify the journal of those manuscripts which are in press or have been published. The volume is intended to be informative, but not a bibliography. The abstracts are listed by title in the Table of Contents and are grouped into one of the five departments, Marine Policy Center, Coastal Research Center, or the student category. An author index is presented in the back to facilitate locating specific papers. Author

N92-33096*# Research Inst. for Computing and Information Systems, Houston, TX.
OBJECT LINKS IN THE REPOSITORY Interim Report
Jon Beck (West Virginia Univ., Morgantown.) and David Eichmann (West Virginia Univ., Morgantown.) 27 Sep. 1991 17 p
(Contract NCC9-16; RICIS Proj. SE-43)
(NASA-CR-190644; NAS 1.26:190644) Avail: CASI HC A03/MF A01

Some of the architectural ramifications of extending the Eichmann/Atkins lattice-based classification scheme to encompass the assets of the full life-cycle of software development are explored. In particular, we wish to consider a model which provides explicit links between objects in addition to the edges connecting classification vertices in the standard lattice. The model we consider uses object-oriented terminology. Thus, the lattice is viewed as a data structure which contains class objects which exhibit inheritance. A description of the types of objects in the repository is presented, followed by a discussion of how they interrelate. We discuss features of the object-oriented model which support these objects and their links, and consider behavior which an implementation of the model should exhibit. Finally, we indicate some thoughts on implementing a prototype of this repository architecture. Author

N92-33178*# Research Inst. for Computing and Information Systems, Houston, TX.
OBJECT LINKING IN REPOSITORIES
David Eichmann, ed., Jon Beck, John Atkins, and Bill Bailey 1 Jun. 1992 52 p
(Contract NCC9-16; RICIS Proj. SE-43)
(NASA-CR-190629; NAS 1.26:190629) Avail: CASI HC A04/MF A01

This topic is covered in three sections. The first section explores some of the architectural ramifications of extending the Eichmann/Atkins lattice-based classification scheme to encompass the assets of the full life cycle of software development. A model is considered that provides explicit links between objects in addition to the edges connecting classification vertices in the standard lattice. The second section gives a description of the efforts to implement the repository architecture using a commercially available object-oriented database management system. Some of the features of this implementation are described, and some of the next steps to be taken to produce a working prototype of the repository are pointed out. In the final section, it is argued that design and instantiation of reusable components have competing criteria (design-for-reuse strives for generality, design-with-reuse strives for specificity) and that providing mechanisms for each can be complementary rather than antagonistic. In particular, it is demonstrated how program slicing techniques can be applied to customization of reusable components. Author

N92-33237*# National Aeronautics and Space Administration, Washington, DC.
AN INTERNATIONAL AEROSPACE INFORMATION SYSTEM: A COOPERATIVE OPPORTUNITY
Gladys A. Cotter and Walter R. Blados Oct. 1992 15 p Presented at the Second East-West Online Meeting, Moscow, USSR, 30 Sep. - 2 Oct. 1992
(NASA-TM-108171; NAS 1.15:108171) Avail: CASI HC A03/MF A01

Scientific and technical information (STI) is a valuable resource which represents the results of large investments in research and development (R&D), and the expertise of a nation. NASA and its predecessor organizations have developed and managed the preeminent aerospace information system. We see information and information systems changing and becoming more international in scope. In Europe, consistent with joint R&D programs and a view toward a united Europe, we have seen the emergence of a European Aerospace Database concept. In addition, the development of aeronautics and astronautics in individual nations have also lead to initiatives for national aerospace databases. Considering recent technological developments in information science and technology, as well as the reality of scarce resources in all nations, it is time to reconsider the mutually beneficial possibilities offered by cooperation and international resource sharing. The new possibilities offered through cooperation among the various aerospace database efforts toward an international aerospace database initiative which can optimize the cost/benefit equation for all participants are considered. Author

83 ECONOMICS AND COST ANALYSIS

Includes cost effectiveness studies.

No abstracts in this category.

84 LAW, POLITICAL SCIENCE AND SPACE POLICY

Includes NASA appropriation hearings; aviation law; space law and policy; international law; international cooperation; and patent policy.

N92-32505# Committee on Appropriations (U.S. House).
DEPARTMENTS OF VETERANS AFFAIRS AND HOUSING AND URBAN DEVELOPMENT, AND INDEPENDENT AGENCIES APPROPRIATIONS FOR 1993, PART 6
Bob Traxler Washington GPO 1992 211 p Hearings before a Subcommittee of the Committee on Appropriations, 102nd Congress, 2nd Session
(GAO-55-636-Pt-6; ISBN-0-16-038597-0) Avail: CASI HC A10/MF A03; Committee on Appropriations, House of Representatives, Washington, DC 20515 HC; SOD HC

Hearings before a subcommittee of the committee on Appropriations House of Representatives are presented for the National Aeronautics and Space Administration for the fiscal year

1993. All verbal testimony, procurement notices, and responses to written questions are included. The verbal testimony provides detailed outline of programs which include Space Station Freedom, science funding for Space Station, space science and applications, space transportation and operations, Advanced Solid Rocket Motor, National Aero-space Alane, aeronautics, space exploration, new launch system, research and program management, and construction of facilities. I.I.C.

N92-33147# Committee on Science, Space and Technology (U.S. House).
NASA AUTHORIZATION, 1993, VOLUME 1
Washington GPO 1992 201 p Hearing before the Committee on Science, Space, and Technology, 102nd Congress, 2nd Session, No. 128, 19 Feb. 1992
(GPO-55-260-Vol-1; ISBN-0-16-038832-5) Avail: CASI HC A10/MF A03; Subcommittee on Technology and Competitiveness, House of Representatives, Washington, DC 20515 HC

Discussed here is the NASA budget request for FY-93 for its Aeronautical Research and Technology Program. Additionally, the NASA Transatmospheric Research and Technology Program request is reviewed. Statements of witnesses from NASA and from outside the government are given. The testimony is related to a detailed study of the U.S. aviation industry's technical needs of the future. The testimony addresses whether or not NASA is on the path which is compatible with the recommendations of the study. Also given is testimony that represents a composite view of the manufacturers, their professional societies, and the industry's efforts to determine future needs for advanced technology. Author

85 URBAN TECHNOLOGY AND TRANSPORTATION

Includes applications of space technology to urban problems; technology transfer; technology assessment; and surface and mass transportation.

For related information see also *03 Air Transportation and Safety, 16 Space Transportation,* and *44 Energy Production and Conversion.*

No abstracts in this category.

88 SPACE SCIENCES (GENERAL)

No abstracts in this category.

89 ASTRONOMY

Includes radio, gamma-ray, and infrared astronomy, and astrometry.

N92-32478*# National Aeronautics and Space Administration. Marshall Space Flight Center, Huntsville, AL.
NASA MARSHALL SPACE FLIGHT CENTER SOLAR OBSERVATORY REPORT, JANUARY - JUNE 1992
James E. Smith Aug. 1992 108 p
(NASA-TM-103597; NAS 1.15:103597) Avail: CASI HC A06/MF A02

This report provides a description of the NASA Marshall Space Flight Center's Solar Vector Magnetograph Facility and gives a summary of its observations and data reduction during Jan. to Jun. 1992. The systems that make up the facility are a magnetograph telescope, and H-alpha telescope, a Questar telescope, and a computer code. Author

N92-33012*# National Aeronautics and Space Administration. Marshall Space Flight Center, Huntsville, AL.
MULTISPECTRAL VARIABLE MAGNIFICATION GLANCING INCIDENCE X RAY TELESCOPE Patent
Richard B. Hoover, inventor (to NASA) 8 Sep. 1992 13 p Filed 28 Jun. 1990 Supersedes N90-27595 (28 - 21, p 3096) Continuation-in-part of US-Patent-Appl-SN-765979, filed 15 Aug. 1989
(NASA-Case-MFS-28013-4; US-Patent-5,146,482; US-Patent-Appl-SN-545008; US-Patent-Appl-SN-765979; US-Patent-Class-378-43; US-Patent-Class-378-210; Int-Patent-Class-G21K-7/00) Avail: US Patent and Trademark Office

A multispectral, variable magnification, glancing incidence, x-ray telescope capable of broadband, high resolution imaging of solar and stellar x-ray and extreme ultraviolet radiation sources is discussed. The telescope includes a primary optical system which focuses the incoming radiation to a primary focus. Two or more rotatable mirror carriers, each providing a different magnification, are positioned behind the primary focus at an inclination to the optical axis. Each carrier has a series of ellipsoidal mirrors, and each mirror has a concave surface covered with a multilayer (layered synthetic microstructure) coating to reflect a different desired wavelength. The mirrors of both carriers are segments of ellipsoids having a common first focus coincident with the primary focus. A detector such as an x-ray sensitive photographic film is positioned at the second respective focus of each mirror so that each mirror may reflect the image at the first focus to the detector at the second focus. The carriers are selectively rotated to position a selected mirror for receiving radiation from the primary optical system, and at least the first carrier may be withdrawn from the path of the radiation to permit a selected mirror on the second carrier to receive the radiation. Official Gazette of the U.S. Patent and Trademark Office

N92-33094*# Radiation Science, Inc., Belmont, MA.
VOLUME 1. PRELIMINARY DESIGN STUDY: AXAF X RAY CALIBRATION SPECTROMETERS. VOLUME 2. REVISED PRELIMINARY DESIGN STUDY: AXAF X RAY CALIBRATION SPECTROMETERS Final Report
7 Apr. 1992 34 p Prepared for Smithsonian Astrophysical Observatory, Cambridge, MA
(Contracts NAS8-36123; S01-15526)
(NASA-CR-184340; NAS 1.26:184340; RS-30; SAO-AXAF-FR-92-004) Avail: CASI HC A03/MF A01

The objective of this work was to provide a preliminary design concept for a Flux Monitor Spectrometer (FMS) for use at the X Ray Astrophysics Facility (XRAF) during High Resolution Mirror Assembly (HRMA) testing that met the requirements of SAO-AXAF-88-025 dated July 31, 1991. The calibration test team determined that the spectral resolution of the FMS had to be greater than or equal to twice that of all the AXAF spectrometers throughout the 0.1 to 10 KeV range of x-ray energies. Since this effectively doubled the resolution required by SAO-AXAF-88-025, a change order was approved by the Marshall Space Flight Center and given to Radiation Sciences to revise their study. Author

90 ASTROPHYSICS

Includes cosmology; celestial mechanics; space plasmas; and interstellar and interplanetary gases and dust.
For related information see also *75 Plasma Physics.*

N92-32541*# Washington Univ., Saint Louis, MO. Center for the Space Sciences and Physics Dept.
ANALYSIS OF LDEF EXPERIMENT AO187-2: CHEMICALLY AND ISOTOPIC MEASUREMENTS OF MICROMETEOROIDS BY SECONDARY ION MASS SPECTROMETRY Progress Report, 15 Feb. - 14 Aug. 1992
14 Aug. 1992 17 p
(Grant NAG1-1174)
(NASA-CR-190697; NAS 1.26:190697) Avail: CASI HC A03/MF A01

Numerous 'extended impacts' found in both leading and trailing edge capture cells have been successfully analyzed for the chemical composition of projectile residues by secondary ion mass spectrometry (SIMS). Most data have been obtained from the trailing edge cells where 45 of 58 impacts have been classified as 'probably natural' and the remainder as 'possibly man-made debris.' This is in striking contrast to leading edge cells where 9 of 11 impacts so far measured are definitely classified as orbital debris. Although all the leading edge cells had lost their plastic entrance foils during flight, the rate of foil failure was similar to that of the trailing edge cells, 10 percent of which were recovered intact. Ultra-violet embrittlement is suspected as the major cause of failure on both leading and trailing edges. The major impediment to the accurate determination of projectile chemistry is the fractionation of volatile and refractory elements in the hypervelocity impact and redeposition processes. This effect had been noticed in simulation experiment but is more pronounced in the Long Duration Exposure Facility (LDEF) capture cells, probably due to the higher average velocities of the space impacts. Surface contamination of the pure Ge surfaces with a substance rich in Si but also containing Mg and Al provides an additional problem for the accurate determination of impactor chemistry. The effect is variable, being much larger on surfaces that were exposed to space than in those cells that remained intact. Future work will concentrate on the analyses of more leading edge impacts and the development of new SIMS techniques for the measurement of elemental abundances in extended impacts. Author

N92-32604# Instituto de Pesquisas Espaciais, Sao Jose dos Campos (Brazil).
IMPLEMENTATION OF A TREE-CODE FOR NUMERICAL SIMULATIONS OF STELLAR SYSTEMS M.S. Thesis [IMPLEMENTACAO DE UM CODIGO EM ARVORE PARA SIMULACOES NUMERICAS DE SISTEMAS ESTELARES]
Eraldo Pereira Marinho Oct. 1991 128 p In PORTUGESE
(INPE-5370-TDI/469) Avail: CASI HC A07/MF A02

An implementation of a tree code for the force calculation in gravitational N-body systems simulations is presented. The technique consists of virtualizing the entire system in a tree data-structure, which reduces the computational effort to theta(N log N) instead of the theta(N exp 2), typical of direct summation. The adopted time integrator is the simple leap-frog with second-order accuracy. A brief discussion about the truncation-error effects on the morphology of the system shows them to be essentially negligible. However, these errors do propagate in a Markovian way if a potential-adaptive time-step is used in order to maintain the expected truncation-error approximately constant in the entire system. The tests show that, even with totally arbitrary distributions, the total computation time obeys theta(N log N). As an application of the code, we evolved an initially cold and homogeneous sphere of point masses to simulate a primordial process of galaxy formation. The evolution of the global entropy of the system suggests that a quasi-equilibrium configuration is achieved after approximately 2 x 10 exp 9 years. It is shown that the final configuration displays a close resemblance to the well observed giant elliptical galaxies, in both kinematical and luminosity distribution properties. A discussion is given on the evolution of the important dynamic quantities characterizing the model. During all the computations, the energy is conserved to better than 0.1 percent. Author

N92-32993# State Univ. of New York, Stony Brook. Dept. of Earth and Space Sciences.
RESEARCH IN NUCLEAR ASTROPHYSICS: STELLAR COLLAPSE AND SUPERNOVAE Progress Report
J. M. Lattimer and A. Yahil 1992 7 p
(Contract DE-FG02-87ER-40317)
(DE92-014988; DOE/ER-40317/T2) Avail: CASI HC A02/MF A01

This progress report describes the nuclear astrophysics research activities in the Earth and Space Sciences Department at Stony Brook during the last year. Our research focused on three aspects of nuclear astrophysics: (1) the equation of state of hot, dense matter, (2) the origin of supernovae and neutron stars, and (3) the early cooling epoch of neutron stars. The following contains detailed reports which summarize each completed project. DOE

N92-32350# Rome Univ. (Italy). Reparto di Planetologia.
FORMATION OF THE SATELLITES
Angioletta Coradini, C. Federico (Perugia Univ., Italy), and G. Magni *In* ESA, Symposium on Titan Apr. 1992 p 9-17 (For primary document see N92-32348 23-91)
Copyright Avail: CASI HC A02/MF A01; ESA, EPD, ESTEC, Noordwijk, Netherlands, HC

91 LUNAR AND PLANETARY EXPLORATION

Includes planetology; and manned and unmanned flights.
For spacecraft design or space stations see *18 Spacecraft Design, Testing and Performance.*

N92-32348# European Space Agency, Paris (France).
SYMPOSIUM ON TITAN
Brigitte Kaldeich, comp. Apr. 1992 391 p Symposium held in Toulouse, France, 9-12 Sep. 1991; sponsored by JPL and CNES
(ESA-SP-338; ISBN-92-9092-194-3; ETN-92-91975) Copyright Avail: CASI HC A17/MF A04; ESA, EPD, ESTEC, Noordwijk, Netherlands, HC

Papers concerning the science underlying the Huygens mission are presented. Huygens is the probe that will descend through the atmosphere of Titan and is ESA's contribution to Cassini, a mission devoted to the exploration of the Saturnian system. Attention is focused on Titan, Saturn's largest satellite. Its structure, the composition and dynamics of its atmosphere, organic chemistry, clouds and aerosols, the solar wind and magnetosphere interaction, are discussed. Preparations for the Cassini mission are considered and previous measurements made are presented. For individual titles, see N92-32349 through N92-32410.

N92-32349*# Arizona Univ., Tucson. Lunar and Planetary Lab.
SOME ISSUES ASSOCIATED WITH THE FORMATION OF THE SATURNIAN SYSTEM
Jonathan I. Lunine *In* ESA, Symposium on Titan Apr. 1992 p 3-7 (For primary document see N92-32348 23-91)
(Grant NAGw-1039)
Copyright Avail: CASI HC A01/MF A01; ESA, EPD, ESTEC, Noordwijk, Netherlands, HC

Three of the current issues associated with the formation of the Saturn system which involve significant controversy and uncertainty and which bear on the formation of Titan itself are outlined: the notion that the formation of Jupiter and Saturn are well constrained is challenged by recent internal models, which suggest possible significant differences in the composition of planetesimals which formed the two bodies; the composition of volatile ices which was the source of the Saturnian satellites was likely a complex mix of relatively pristine solids from the collapsing interstellar cloud, gas and solid material processed in the solar

nebula and material chemically processed in a nebula around Saturn or in the primitive Saturn atmosphere itself; the deuterium enhancement in Titan's atmosphere, which initially appeared to be sufficiently large that it must be a signature of pristine interstellar material, could in fact be largely due to photochemical evolution of Titan's atmosphere. ESA

N92-32350# Rome Univ. (Italy). Reparto di Planetologia.
FORMATION OF THE SATELLITES **c90**
Angioletta Coradini, C. Federico (Perugia Univ., Italy), and G. Magni *In* ESA, Symposium on Titan Apr. 1992 p 9-17 (For primary document see N92-32348 23-91)
Copyright Avail: CASI HC A02/MF A01; ESA, EPD, ESTEC, Noordwijk, Netherlands, HC

The relation between the formation of the regular satellite system around giant planets, and the formation of the central planet is discussed. Some characteristics of regular satellites systems are quite similar, and suggest a common origin in an accretion disk present around the central body. The origin of this disk is described with attention being given to the so called 'disk phase', the disk phase links the formation of the primary body to that of satellites. The subsequent stages of the disk evolution can lead first to the formation of intermediate size bodies, and further, through the collisional evolution of these bodies, to the birth of satellite 'embryos' capable of gravitationally capturing smaller bodies. The predictivity of this scheme in explaining the characteristics of different satellite systems is reviewed. ESA

N92-32351*# National Aeronautics and Space Administration. Ames Research Center, Moffett Field, CA.
IMPACT ORIGIN OF TITAN'S ATMOSPHERE
Kevin Zahnle and L. Dones (Canadian Inst. for Theoretical Astrophysics, Toronto, Ontario) *In* ESA, Symposium on Titan Apr. 1992 p 19-25 (For primary document see N92-32348 23-91)
Copyright Avail: CASI HC A02/MF A01; ESA, EPD, ESTEC, Noordwijk, Netherlands, HC

The reason why Titan has a thick atmosphere while its Jovian clones Ganymede and Callisto have nothing is addressed. It is argued that this contrast is a predictable consequence of impact erosion, i.e., the escape of atmospheric gases as a consequence of hypervelocity impact, the average impact velocity of stray bodies on Titan being lower than on Ganymede and Callisto. A model to examine this hypothesis is presented. ESA

N92-32352*# California Inst. of Tech., Pasadena. Geological and Planetary Sciences Div.
INTERIOR OF TITAN
David J. Stevenson *In* ESA, Symposium on Titan Apr. 1992 p 29-33 (For primary document see N92-32348 23-91)
(Grant NAGw-185)
Copyright Avail: CASI HC A01/MF A01; ESA, EPD, ESTEC, Noordwijk, Netherlands, HC

General principles of Titan formation and evolution are addressed. Attention is focused on the volatile reservoir (defined as all constituents more volatile than water) of Titan's interior. Volatile poor models, in which Titan is like Granymede or Callisto with a thin (observed) volatile veneer are discussed and discarded. Volatile rich models in which the present Titan consists of a methane clathrate shell overlying a deep water ammonia ocean and solid ammonia hydrate are discussed. Titan has a central core of rock which is about one half of the total mass, and a superficial hydrocarbon 'ocean' stored in subsurface caverns and pore space. ESA

N92-32353# Arizona Univ., Tucson. Lunar and Planetary Lab.
THE THERMAL STRUCTURE OF THE ATMOSPHERE OF TITAN
Donald M. Hunten *In* ESA, Symposium on Titan Apr. 1992 p 37-40 (For primary document see N92-32348 23-91)
Copyright Avail: CASI HC A01/MF A01; ESA, EPD, ESTEC, Noordwijk, Netherlands, HC

Knowledge of Titan's atmosphere obtained from the beginning of the century up until 1988 and workshops held to discuss this are summarized. Voyager results and more recent studies based on Cassini studies are also summarized. A mild greenhouse is required to explain temperatures in the troposphere. ESA

N92-32354# Observatoire de Paris-Meudon (France). Dept. de Recherche Spatiale.
THE COMPOSITION OF THE TITAN ATMOSPHERE
Daniel Gautier *In* ESA, Symposium on Titan Apr. 1992 p 43-51 (For primary document see N92-32348 23-91)
Copyright Avail: CASI HC A02/MF A01; ESA, EPD, ESTEC, Noordwijk, Netherlands, HC

Information obtained since 1985 from ground based observations in the near infrared and in the millimeter range and the reanalysis of Voyager 1 Infrared Interferometer Spectrometer (IRIS) data are discussed. A substantial improvement of knowledge of the composition of the Titan's atmosphere was acquired. Progress is expected from ground based observations and Earth orbit observatories before the arrival of Cassini to the Saturn System. ESA

N92-32355# Observatoire de Paris-Meudon (France). Dept. de Recherche Spatiale.
TITAN'S ATMOSPHERE: LATITUDINAL VARIATIONS IN TEMPERATURE AND COMPOSITION
Athena Coustenis *In* ESA, Symposium on Titan Apr. 1992 p 53-58 (For primary document see N92-32348 23-91)
Copyright Avail: CASI HC A02/MF A01; ESA, EPD, ESTEC, Noordwijk, Netherlands, HC

Analyses of Voyager 1 infrared data which allowed the retrieval of temperature profiles and precise mean abundances of the minor constituents in Titan's atmosphere are discussed. Latitudinal variations in temperature were derived and variabilities in the composition of Titan's stratosphere as a function of latitude were discovered for all the trace constituents with the exception of the most abundant gases after CO: C2H2, C2H6 and C3H8. These variabilities are discussed. The enrichment of northern latitude in some molecules with respect to southern latitudes can account for the temperature field asymmetry observed in the situation of radiative atmospheric equilibrium. A tentative explanation for the enhancement of some nitriles based on seasonal effects is discussed, but no model exists to account for the other variations. ESA

N92-32356# Observatoire de Paris-Meudon (France). Dept. de Recherche Spatiale.
TITAN'S UV ALBEDO: OBSERVATIONS AND MODELING
Regis Courtin *In* ESA, Symposium on Titan Apr. 1992 p 59-67 (For primary document see N92-32348 23-91)
Copyright Avail: CASI HC A02/MF A01; ESA, EPD, ESTEC, Noordwijk, Netherlands, HC

The UV photometric measurements of Titan are reviewed. Previous models proposed for the interpretation of the UV albedo of Titan are reviewed and most recent attempts based on microphysical modeling of the haze thought to be the key factor in this part of the spectrum are presented. The possible links between albedo contrasts and compositional variation are addressed and an attempt is made to derive implications for the aspect of Titan in the UV. Modeling the Titan spectrum in the 160 to 300 nm range is addressed and the prospects for future compositional studies in this domain are examined. ESA

N92-32357*# Arizona Univ., Tucson. Lunar and Planetary Lab.
A REANALYSIS OF VOYAGER UVS OBSERVATIONS OF TITAN
D. T. Hall, D. E. Shemansky, and T. M. Tripp *In* ESA, Symposium on Titan Apr. 1992 p 67-74 (For primary document see N92-32348 23-91)
(Grant NAGw-649)
Copyright Avail: CASI HC A02/MF A01; ESA, EPD, ESTEC, Noordwijk, Netherlands, HC 90 Dutch guilders

Data from the Voyager 1 Ultraviolet Spectrometer (UVS) encounter at Titan were reanalyzed to reveal new spatial and

spectral information. The observations, data reduction and spectrum analysis are discussed. The following conclusions were drawn: Titan's airglow is driven by a combination of mechanisms including both EUV deposition and magnetospheric particle precipitation; the emissions are distributed throughout a range of altitudes in the atmosphere; enhanced nightside emissions of the Helium 58.4 nm line may be the result of a thermospheric diurnal temperature variation; the CD2 spectrum, with enhanced Ly(alpha) and N-2 64.5 and 67.0 nm emission, implies that some of the high altitude excitation is due to impact dissociative excitation of N2 by electrons with E greater than 150 eV; the CD2 spectrum is consistent with the existence of a high altitude bright spot in the dayside disk with dimensions from 400 to 900 km. ESA

N92-32358*# National Aeronautics and Space Administration. Ames Research Center, Moffett Field, CA.
THE ATMOSPHERIC TEMPERATURE STRUCTURE OF TITAN
Christopher P. McKay, J. B. Pollack, Regis Courtin (Observatoire de Paris-Meudon, France), and Jonathan I. Lunine (Arizona Univ., Tucson.) *In* ESA, Symposium on Titan Apr. 1992 p 77-80 (For primary document see N92-32348 23-91)
Copyright Avail: CASI HC A01/MF A01; ESA, EPD, ESTEC, Noordwijk, Netherlands, HC

The contribution of various factors to the thermal structure of Titan's past and present atmosphere are discussed. A one dimensional model of Titan's thermal structure is summarized. The greenhouse effect of Titan's atmosphere, caused primarily by pressure induced opacity of N2, CH4, and H2, is discussed together with the antigreenhouse effect dominated by the haze which absorbs incident sunlight. The implications for the atmosphere of the presence of an ocean on Titan are also discussed. ESA

N92-32359*# Jet Propulsion Lab., California Inst. of Tech., Pasadena.
GROUND-BASED OBSERVATIONS OF TITAN'S THERMAL SPECTRUM
Glenn Orton *In* ESA, Symposium on Titan Apr. 1992 p 81-85 Sponsored by NASA, Washnington (For primary document see N92-32348 23-91)
Copyright Avail: CASI HC A01/MF A01; ESA, EPD, ESTEC, Noordwijk, Netherlands, HC

Past, present and future observations of Titan's thermal spectrum are discussed. Ground based observations of Titan's mid-infrared thermal spectrum gave the first indications of the temperature regime and the role of hydrocarbons in the chemical composition. Significant progress exploring Titan using ground based observations may be achieved by increasing the spectral resolution, exploring new spectral regions, and by searching for seasonal or time dependent changes of the spectrum. ESA

N92-32360*# National Aeronautics and Space Administration. Goddard Space Flight Center, Greenbelt, MD.
THE METEOROLOGY OF TITAN
F. M. Flasar and Barney J. Conrath *In* ESA, Symposium on Titan Apr. 1992 p 89-99 (For primary document see N92-32348 23-91)
Copyright Avail: CASI HC A03/MF A01; ESA, EPD, ESTEC, Noordwijk, Netherlands, HC

Current knowledge of Titan's meteorology is reviewed, including diagnostic inferences of the large scale wind field and prognostic studies of thermal and momentum balances. Titan's winds were largely inferred from temperature maps whose spatial coverage is incomplete. The inferred winds are cyclostrophic, approximately 75 m/s in the upper stratosphere. The direction of the winds is ambiguous from the temperature data, but arguments based on the spin up of a planetary atmosphere from an initial state of rest strongly suggest that Titan's winds blow predominantly in the direction of the planetary rotation. Stratospheric temperatures exhibit a north-south asymmetry, suggesting that seasonal variations are controlled by a dynamical inertia associated with the need to transport angular momentum as well as heat. A consideration of the global angular momentum balance indicates that the zonally averaged winds near the surface are approximately 0.3 m/s. ESA

N92-32361*# National Aeronautics and Space Administration. Ames Research Center, Moffett Field, CA.
NUMERICAL SIMULATION OF THE CIRCULATION OF THE ATMOSPHERE OF TITAN
F. Hourdin (Ecole Normale Superieure, Paris, France), P. LeVan (Ecole Normale Superieure, Paris, France), O. Talagrand (Ecole Normale Superieure, Paris, France), Regis Courtin (Observatoire de Paris-Meudon, France), Daniel Gautier (Observatoire de Paris-Meudon, France), and Christopher P. McKay *In* ESA, Symposium on Titan Apr. 1992 p 101-106 (For primary document see N92-32348 23-91)
Copyright Avail: CASI HC A02/MF A01; ESA, EPD, ESTEC, Noordwijk, Netherlands, HC

A three dimensional General Circulation Model (GCM) of Titan's atmosphere is described. Initial results obtained with an economical two dimensional (2D) axisymmetric version of the model presented a strong superrotation in the upper stratosphere. Because of this result, a more general numerical study of superrotation was started with a somewhat different version of the GCM. It appears that for a slowly rotating planet which strongly absorbs solar radiation, circulation is dominated by global equator to pole Hadley circulation and strong superrotation. The theoretical study of this superrotation is discussed. It is also shown that 2D simulations systemically lead to instabilities which make 2D models poorly adapted to numerical simulation of Titan's (or Venus) atmosphere. ESA

N92-32362# Reading Univ. (England). Dept. of Meteorology.
SIMPLE DYNAMICAL MODELS OF TITAN'S ATMOSPHERIC CIRCULATION
Ian N. James *In* ESA, Symposium on Titan Apr. 1992 p 107-111 (For primary document see N92-32348 23-91)
Copyright Avail: CASI HC A01/MF A01; ESA, EPD, ESTEC, Noordwijk, Netherlands, HC

It is argued that Simple Global Circulation Models (SGCM) provide an efficient and effective tool for investigating the possible range of atmospheric circulations that might exist on Titan. Initial results of applying this SGCM to the Titan atmosphere show an overturning Hadley circulation which drives a jet in high winter latitudes. This jet is barotropically unstable. There is evidence that the unstable eddies are building up an equatorial superrotation. The implications for the steadiness of the Titan circulation are discussed. ESA

N92-32363*# National Aeronautics and Space Administration. Goddard Inst. for Space Studies, New York, NY.
A PRELIMINARY ASSESSMENT OF THE TITAN PLANETARY BOUNDARY LAYER
Michael Allison *In* ESA, Symposium on Titan Apr. 1992 p 113-118 Sponsored by Cassini Project Office (For primary document see N92-32348 23-91)
Copyright Avail: CASI HC A02/MF A01; ESA, EPD, ESTEC, Noordwijk, Netherlands, HC

Results of a preliminary assessment of the characteristic features of the Titan planetary boundary are addressed. These were derived from the combined application of a patched Ekman surface layer model and Rossby number similarity theory. Both these models together with Obukhov scaling, surface speed limits and saltation are discussed. A characteristic Akman depth of approximately 0.7 km is anticipated, with an eddy viscosity approximately equal to 1000 sq cm/s, an associated friction velocity approximately 0.01 m/s, and a surface wind typically smaller than 0.6 m/s. Actual values of these parameters probably vary by as much as a factor of two or three, in response to local temporal variations in surface roughness and stability. The saltation threshold for the windblown injection of approximately 50 micrometer particulates into the atmosphere is less than twice the nominal friction velocity, suggesting that dusty breezes might be an occassional feature of the Titan meteorology. ESA

N92-32364# European Space Agency. European Space Research and Technology Center, ESTEC, Noordwijk (Netherlands). Huygens Project Div.
GRAVITATIONAL TIDE IN THE ATMOSPHERE OF TITAN
Ralph D. Lorenz *In its* Symposium on Titan Apr. 1992 p 119-123 (For primary document see N92-32348 23-91)
Copyright Avail: CASI HC A01/MF A01; ESA, EPD, ESTEC, Noordwijk, Netherlands, HC

The idea of atmospheric tides is introduced and calculations are performed to calculate the atmospheric tide of Titan resulting from the Saturnian gavitational field. Engineering implications of this tide, for example in the arrival detection of the Huygens probe, are discussed. Other atmospheric tides on Titan are considered: the Saturn induced thermal tide, the solar driven thermal tide and the solar driven gravitational tidal forces. Prospects for experimental observation of the tide are reviewed. ESA

N92-32365# European Space Agency. European Space Research and Technology Center, ESTEC, Noordwijk (Netherlands). Space Science Dept.
THE SIGNIFICANCE OF METEORIC IONISATION FOR THE PROPAGATION OF LIGHTNING SPHERICS IN THE ATMOSPHERE OF TITAN
Rejean J. L. Grard *In its* Symposium on Titan Apr. 1992 p 125-128 (For primary document see N92-32348 23-91)
Copyright Avail: CASI HC A01/MF A01; ESA, EPD, ESTEC, Noordwijk, Netherlands, HC

The meteoric layer hypothesis which states that the precipitation of meteorites is the likely mechanics for the generation of an ionized layer at an altitude of 500 to 600 km above Titan is checked against constraints imposed by space observations. It was considered that the absence of electrophilic species in the atmosphere of Titan, an efficient charge exchange mechanism between ambient ions and metallic ions of meteoric origin and the low coefficient which characterizes the radiative recombination of atomic ions might be responsible for the existence of a dense plasma layer that would prevent the upward escape of electromagnetic waves with frequencies of up to several MHz. However, no ionization layers and no lightning spherics were detected when Voyager 1 approached Titan in Nov. 1980. ESA

N92-32366# Bordeaux 2 Univ. (France).
MODELING OF THE DIURNAL VARIATIONS OF THE ATMOSPHERE OF TITAN
D. Toublanc, J. P. Parisot, J. Brillet, and Daniel Gautier (Observatoire de Paris-Meudon, France) *In* ESA, Symposium on Titan Apr. 1992 p 131-136 (For primary document see N92-32348 23-91)
Copyright Avail: CASI HC A02/MF A01; ESA, EPD, ESTEC, Noordwijk, Netherlands, HC

Preliminary results of numerical modeling of the diurnal variations of Titan's atmosphere are presented. A one dimensional time dependent photochemical model was developed, including 169 updated chemical reactions, photochemical parameters (reaction rates, absorption cross sections, vapor pressures, etc.) and elaborated evaluation of the radiation field. Detailed Monte Carlo calculations, including Rayleigh and Mie scattering, were done. The vertical distribution of 56 species (hydrocarbons, nitriles, oxygen compounds, etc.) is computed between the surface and 1240 km (the duration of the day is assumed to be equal to 16 days at each level of the atmosphere). The results of these simulations are presented and compared to available observations. ESA

N92-32367# Granada Univ. (Spain). Inst. de Astrofisica de Andalucia.
NEUTRAL COMPOSITION OF TITAN'S ATMOSPHERE. A THEORETICAL MODEL
L. M. Lara, R. Rodrigo, Athena Coustenis (Observatoire de Paris-Meudon, France), J. J. Lopez-Moreno, and E. Chassefiere (Centre National de la Recherche Scientifique, Verrieres-Le Buisson, France) *In* ESA, Symposium on Titan Apr. 1992 p 137-146 (For primary document see N92-32348 23-91)
(Contracts CICYT-ESP88-0566; CICYT-ESP88-0567)
Copyright Avail: CASI HC A02/MF A01; ESA, EPD, ESTEC, Noordwijk, Netherlands, HC

Vertical profiles of hydrocarbon densities in the Titan's atmosphere were obtained by means of a theoretical model taking into account condensation, photochemical and dynamical processes and using a fixed aerosols distribution. The model is developed for noontime at the equatorial reqion, in equinox conditions with moderate solar activity and covers the 40 to 1400 km altitude region. A detailed study of the physical and chemical phenomena is performed and an analysis of their relative importance on the obtained concentrations is also carried out. ESA

N92-32368# Paris XII Univ., Creteil (France). Equipe Physico-Chimie Organique Spatiale.
ORGANIC CHEMISTRY ON TITAN VERSUS TERRESTRIAL PREBIOTIC CHEMISTRY: EXOBIOLOGICAL IMPLICATIONS
Francois Raulin, C. Frere, Leejo Do, M. Khlifi, P. Paillous, and E. deVanssay *In* ESA, Symposium on Titan Apr. 1992 p 149-160 (For primary document see N92-32348 23-91)
Copyright Avail: CASI HC A03/MF A01; ESA, EPD, ESTEC, Noordwijk, Netherlands, HC

Current thinking on the origins of life on Earth are reviewed and the plausible impact of the study of Titan chemistry on this field is discussed. On the primitive Earth, in the presence of liquid water, prebiotic organic chemistry starting from simple reactive molecules or their oligomers, allowed the emergence of life. On Titan, with very low temperature conditions, chemical evolution is still going on, but in the absence of liquid water. However, both environments and chemistries have close similarities and involve a subtle coupling between different parts of their 'geofluid', and two complementary classes of organics: simple volatile and reactive organics compounds and their nonvolatile solid oligomers. ESA

N92-32369*# Cornell Univ., Ithaca, NY. Planetary Studies Lab.
TITAN'S ORGANIC CHEMISTRY: RESULTS OF SIMULATION EXPERIMENTS
Carl Sagan, W. Reid Thompson, and Bishun N. Khare *In* ESA, Sympsosium on Titan Apr. 1992 p 161-165 Sponsored by NASA, Washington (For primary document see N92-32348 23-91)
Copyright Avail: CASI HC A01/MF A01; ESA, EPD, ESTEC, Noordwijk, Netherlands, HC

Recent low pressure continuous low plasma discharge simulations of the auroral electron driven organic chemistry in Titan's mesosphere are reviewed. These simulations yielded results in good accord with Voyager observations of gas phase organic species. Optical constants of the brownish solid tholins produced in similar experiments are in good accord with Voyager observations of the Titan haze. Titan tholins are rich in prebiotic organic constituents; the Huygens entry probe may shed light on some of the processes that led to the origin of life on Earth. ESA

N92-32370*# Cornell Univ., Ithaca, NY. Planetary Studies Lab.
ORGANIC CHEMISTRY ON TITAN: SURFACE INTERACTIONS
W. Reid Thompson and Carl Sagan *In* ESA, Symposium on Titan Apr. 1992 p 167-176 Sponsored by NASA, Washington (For primary document see N92-32348 23-91)
Copyright Avail: CASI HC A02/MF A01; ESA, EPD, ESTEC, Noordwijk, Netherlands, HC

The interaction of Titan's organic sediments with the surface (solubility in nonpolar fluids) is discussed. How Titan's sediments can be exposed to an aqueous medium for short, but perhaps significant, periods of time is also discussed. Interactions with hydrocarbons and with volcanic magmas are considered. The alteration of Titan's organic sediments over geologic time by the impacts of meteorites and comets is discussed. ESA

N92-32371# Rennes Univ. (France). Groupe de Physicochimie Structurale.
PHOTOCHEMISTRY OF UNSATURATED NITRILES ON TITAN
J. C. Guillemin and J. P. Ferris (Rensselaer Polytechnic Inst., Troy,

NY.) *In* ESA, Symposium on Titan Apr. 1992 p 177-181 (For primary document see N92-32348 23-91)
Copyright Avail: CASI HC A01/MF A01; ESA, EPD, ESTEC, Noordwijk, Netherlands, HC

The unsaturated nitrile cyanoacetylene and dicyanoacetylene were observed on Titan by the Voyager 1 mission. Studies in the laboratory of the photochemical reactions of these compounds alone or with another gas present on Titan (acetylene, ethene, hydrogen cyanide, and carbon monoxide) were performed. Trimeric and tetrameric compounds, (1 + 1), (1 + 2), or (2 + 2) adducts were observed depending on the ultraviolet radiation (185, 206, or 254 nm light) and the relative ratio of the two gases. Extrapolation to the atmosphere of Titan is discussed. ESA

N92-32372*# National Aeronautics and Space Administration. Ames Research Center, Moffett Field, CA.
TITAN'S ORGANIC HAZE
Christopher P. McKay and Owen B. Toon *In* ESA, Symposium on Titan Apr. 1992 p 185-190 (For primary document see N92-32348 23-91)
Copyright Avail: CASI HC A02/MF A01; ESA, EPD, ESTEC, Noordwijk, Netherlands, HC

The optical properties of the laboratory tholin is considered, and an attempt is made to critically evaluate the analog between laboratory tholin and Titan tholin. The processes that form the solid haze material from the gaseous atmosphere are considered. It is suggested that the N/C ratio may be a useful signature of the processes that determine the haze production rate. ESA

N92-32373*# National Aeronautics and Space Administration. Goddard Space Flight Center, Greenbelt, MD.
INFRARED PROPERTIES OF TITAN'S CLOUDS AND AEROSOLS
Robert E. Samuelson *In* ESA, Symposium on Titan Apr. 1992 p 191-195 (For primary document see N92-32348 23-91)
Copyright Avail: CASI HC A01/MF A01; ESA, EPD, ESTEC, Noordwijk, Netherlands, HC

Using Voyager 1 Infrared Interferometer Spectrometer (IRIS) data, the infrared properties of Titan's north polar hood continuum were deduced. Stratospheric opacities were found to increase monotonically with wavenumber between 250 and 600/cm. The increase becomes more extreme with decreasing altitude; this behavior is consistent with a photochemical aerosol overlying layers of condensated organics lower down. Stratospheric optical thicknesses of order 0.1 were found at 600/cm, which became smaller as the wavelength decreased. An aerosol mass mixing ratio approximately 6 x 10 exp -8 and a mass flux approximately 10 exp -14 g/sq cm/s was inferred at 160 km. The column abundance for condensed C4N2 was found to exceed that for the vapor by a factor of 30 or more. An upper limit of 4 x 10 exp -10 was inferred for the mole fraction of gaseous C4N2. ESA

N92-32374*# State Univ. of New York, Stony Brook. Dept. of Physics.
OBSERVING THE SURFACE OF TITAN THROUGH NEAR-INFRARED WINDOWS IN ITS ATMOSPHERE
Caitlin A. Griffith and Tobias Owen (Hawaii Univ., Honolulu.) *In* ESA, Symposium on Titan Apr. 1992 p 199-204 (For primary document see N92-32348 23-91)
(Grant NGR-33-015-141)
Copyright Avail: CASI HC A02/MF A01; ESA, EPD, ESTEC, Noordwijk, Netherlands, HC

Possibilities of observing the surface of Titan through near infrared windows in the atmosphere are explored. Studies of Titan's near infrared spectrum are discussed with particular attention being given to the opacity of Titan's atmosphere, infrared spectra of candidate materials of Titan's surface, and ground based studies of Titan's surface. Instruments on board Cassini which will have the capability to observe Titan in the near infrared are presented together with what they may observe. These instruments include the descent imager/spectral radiometer, the Huygens probe and the visible infrared mapping spectrometer, and the imaging science subsystem. ESA

N92-32375# European Space Agency. European Space Research and Technology Center, ESTEC, Noordwijk (Netherlands). Space Science Dept.
THE DETECTABILITY OF TITAN'S SURFACE IN THE NEAR-INFRARED
Piet Stammes *In its* Symposium on Titan Apr. 1992 p 205-210 (For primary document see N92-32348 23-91)
Copyright Avail: CASI HC A02/MF A01; ESA, EPD, ESTEC, Noordwijk, Netherlands, HC

The extent to which the surface of Titan, which is not visible in visual radiation, might be detectable in the near infrared was studied. Multiple scattering computations of the radiation reflected by Titan at 1.58 micrometers (in a methane window), and, as a comparison, at 0.635 micrometers were performed. A three layer optical model of Titan's atmosphere was used: an organic haze layer at the top, next a methane cloud layer, and a nitrogen gas layer at the bottom. Constrained by the geometric albedo and the haze scattering properties at both wavelengths, it was found that the atmosphere must be relatively thin at 1.58 micrometers (optical thickness approximately = 0.5). The presence of a backward peak in the scattering function of the cloud particles influenced the computed geometric albedo strongly. It was found that the surface must be brighter in the near IR than in the visual. Furthermore, it was found that surface features with strong contrast might be rather easily detectable at wavelengths equal to 1.58 micrometers. ESA

N92-32376*# Maryland Univ., College Park.
TITAN'S MID-IR ALBEDO: NEW OBSERVATIONS FROM 3 TO 5 MICRONS
K. S. Noll and R. F. Knacke (State Univ. of New York, Stony Brook.) *In* ESA, Symposium on Titan Apr. 1992 p 211-214 Sponsored by NAS-NRC (For primary document see N92-32348 23-91)
(Grant NAGw-2194)
Copyright Avail: CASI HC A01/MF A01; ESA, EPD, ESTEC, Noordwijk, Netherlands, HC

Photometric and spectrophotometric observations of Titan in the wavelength interval from 3 to 5 micrometers which were made in Jun. 1990 and Jun. 1991 are reported and analyzed. The broadband flux measured at 4.8 micrometers in both years and on two different telescopes is more than a factor of three lower than measurements made by two independent groups in 1971 and 1973. No other measurements were made in the 17 intervening years. It was concluded that either the original measurements were contaminated by long wavelength leaks or that Titan's albedo at 4.8 micrometers has decreased. The low resolution spectrum obtained near 4.8 micrometers is crudely consistent with the presence of CO at 60 ppm in the lower troposphere and a reflecting layer located between 100 mbar and the surface at 1500 mbar. The spectrum from 3.1 to 4.0 micrometers is relatively featureless at low spectral resolution but has some hints of structure that may yield information at higher resolution and signal to noise. ESA

N92-32377*# National Aeronautics and Space Administration. Ames Research Center, Moffett Field, CA.
VIMS/CASSINI MISSION AT TITAN: SCIENTIFIC OBJECTIVES AND OBSERVATIONAL SCENARIOS
Kevin H. Baines (Jet Propulsion Lab., California Inst. of Tech., Pasadena.), R. H. Brown (Jet Propulsion Lab., California Inst. of Tech., Pasadena.), Dennis L. Matson (Jet Propulsion Lab., California Inst. of Tech., Pasadena.), R. M. Nelson (Jet Propulsion Lab., California Inst. of Tech., Pasadena.), B. J. Buratti (Jet Propulsion Lab., California Inst. of Tech., Pasadena.), J. P. Bibring (Paris-Sud Univ., Orsay, France), Y. Langevin (Paris-Sud Univ., Orsay, France), C. Sotin (Paris-Sud Univ., Orsay, France), A. Carusi (Rome Univ., Italy), and Angioletta Coradini (Rome Univ., Italy) et al *In* ESA, Symposium on Titan Apr. 1992 p 215-219 (For primary document see N92-32348 23-91)
Copyright Avail: CASI HC A01/MF A01; ESA, EPD, ESTEC, Noordwijk, Netherlands, HC

The scientific objectives and observational scenarios of the

Cassini/Visual Infrared Mapping Spectrometer (VIMS) Mission at Titan are addressed. The VIMS represents a powerful and effective means to both investigate, in four dimensions (latitude, longitude, altitude, and time), Titan's atmospheric structure and to map the near infrared spectral character of Titan's surface. Its broad spectral coverage from 0.35 to 5.1 micrometers together with its significant spectral resolution allows it to determine minor constituent distributions and cloud optical/microphysical properties from the surface to several hundred km. A promising means of obtaining high vertical resolution stratospheric profiles of hydrocarbons, oxides, and hazes via stellar occultation observations is discussed. ESA

N92-32378*# National Aeronautics and Space Administration. Goddard Space Flight Center, Greenbelt, MD.
CASSINI/CIRS CAPABILITIES FOR AEROSOL, CLOUD, AND SURFACE MEASUREMENTS
Robert E. Samuelson *In* ESA, Symposium on Titan Apr. 1992 p 221-223 (For primary document see N92-32348 23-91)
Copyright Avail: CASI HC A01/MF A01; ESA, EPD, ESTEC, Noordwijk, Netherlands, HC

Information that should be revealed by the Cassini Composite Infrared Spectrometer (CIRS) about the aerosol, cloud, and surface properties of Titan are addressed. Limb sounding data will be used to determine aerosol abundances, scale heights, and gradients between 80 and 400 km for various latitudes. Stratospheric condensate cloud top altitudes and column abundances will be inferred as functions of latitude. A search for new species will be conducted. Thermal maps between 500 and 550/cm will be used to investigate tropospheric methane clouds and surface topography; time resolution provided by different orbits will be used to distinguish the two. ESA

N92-32379*# National Aeronautics and Space Administration. Goddard Space Flight Center, Greenbelt, MD.
HUYGENS/ACP: AN INSTRUMENT FOR AEROSOLS CHEMICAL COMPOSITION MEASUREMENTS
Guy Israel (Centre National de la Recherche Scientifique, Verrieres-Le Buisson, France), E. Chassefiere (Centre National de la Recherche Scientifique, Verrieres-Le Buisson, France), Hasso B. Niemann, Jaap J. Boon (FOM-Inst. voor Atoom- en Molecuulfysica, Amsterdam, Netherlands), Christian Mueller (Institut d'Aeronomie Spatiale de Belgique, Brussels.), Francois Raulin (Paris XII Univ., Creteil, France), M. Cabane (Paris VI Univ., France), and Claude Sable (Centre d'Etudes et de Recherches, Toulouse, France) *In* ESA, Symposium on Titan Apr. 1992 p 225-228 (For primary document see N92-32348 23-91)
Copyright Avail: CASI HC A01/MF A01; ESA, EPD, ESTEC, Noordwijk, Netherlands, HC

The Aerosol Collector Pyrolyzer (ACP) which will be used aboard the Huygens probe is introduced. The scientific objectives, scientific rationale, and a technical description of the ACP are given. The ACP will sample the aerosols of the Titan's atmosphere in two regions, 160 to 60 and 60 to 25 km, respectively. In the first region, it will collect aerosol particles absorbed by a complex core (organic polymers) coated with absorbed or condensed molecules. The second collect will sample larger aerosols and the N2-CH4 droplets. In each sampling, the particles are collected on a metallic filter through which the atmospheric gas is pumped. The filter is then inserted into an oven connected to the Gas Chromatograph Mass Spectrometer (GCMS) Experiment which analyzes the gases produced during the heating of the samples. For each sample it will be possible to bring information on the nature and abundance of the volatile components contained in the particles and/or the composition of the photochemical core. ESA

N92-32380*# National Aeronautics and Space Administration. Ames Research Center, Moffett Field, CA.
HUYGENS/ASI PLASMA WAVE ANALYZER CAPABILITIES FOR AEROSOL MEASUREMENT
William J. Borucki and Marcello Fulchignoni (Rome Univ., Italy) *In* ESA, Symposium on Titan Apr. 1992 p 229-230 (For primary document see N92-32348 23-91)
Copyright Avail: CASI HC A01/MF A01; ESA, EPD, ESTEC, Noordwijk, Netherlands, HC

The capabilities of the Huygens Atmospheric Structure Instrument (HASI) are described. These include measurement of atmospheric electrical conductivity by the plasma wave analyzer. How measurement of the atmospheric conductivity can lead to an estimate or the total surface area of the aerosols as a function of altitude is outlined. It is concluded that since the ASI is designed to measure the electrical conductivity as well as the pressure and temperature as a function of altitude, its results should provide a useful check on other instruments that are designed to measure the abundance of aerosols in a limited range of sizes. ESA

N92-32381*# Arizona Univ., Tucson. Lunar and Planetary Lab.
PLAUSIBLE SURFACE MODELS FOR TITAN
Jonathan I. Lunine *In* ESA, Symposium on Titan Apr. 1992 p 233-239 (For primary document see N92-32348 23-91)
(Grant NAGw-1039)
Copyright Avail: CASI HC A02/MF A01; ESA, EPD, ESTEC, Noordwijk, Netherlands, HC

Current understanding of the nature of Titan's surface and some new ideas for explaining the curious radar returns from Saturn's largest satellite are reviewed. Pre-Voyager models of the surface, based largely on cosmochemistry and the discovery of atmospheric methane, allowed for a range of possibilities, including pure methane oceans. The Voyager 1 flyby ruled out this last possibility, replacing it with compelling observational arguments in favor of a mixed light hydrocarbon and nitrogen ocean. Ground based radar observations indicated a surprisingly reflective surface which is inconsistent with a hydrocarbon ocean and more reminiscent of the Galilean Satellites. Nonetheless, passive radiometric measurements of the surface do not support the notion that Titan's surface is like that of the Galilean satellites. One of the arguments against hydrocarbon oceans reflecting radar energy is that most solid, complex hydrocarbon and nitriles will be denser than the liquid and sink. Nonetheless, many of the aerosol species will coagulate in highly nonspherical patterns, and some species probably polymerize in long chains. Such chains will have very low sedimendation velocities in the ocean and may remain near the surface through ocean mixing process. The prospect of an oceanic 'soup' of polar polymers acting as volume reflectors at radio wevelengths suggests that the interpretation of radar observations needs evaluation. ESA

N92-32382# Max-Planck-Inst. fuer Aeronomie, Katlenburg-Lindau (Germany, F.R.).
PLASMA INTERACTION OF TITAN WITH THE SATURNIAN MAGNETOSPHERE: A REVIEW OF CRITICAL ISSUES
Wing-H. Ip *In* ESA, Symposium on Titan Apr. 1992 p 243-253 (For primary document see N92-32348 23-91)
Copyright Avail: CASI HC A03/MF A01; ESA, EPD, ESTEC, Noordwijk, Netherlands, HC

The Cassini Mission to the Saturnian System and Titan will provide many far reaching results pertinent to the origin and evolution of Titan's atmosphere and the plasma interactions with the planetary magnetosphere and solar wind. Several critical issues related to the following are reviewed: the global magnetospheric signatures of Titan's ionosphere, the corresponding mass loading effect, the ionospheric magnetic field composition, and the formation of an atomic nitrogen torus in the Saturnian system. Observations required to resolve the major uncertainties are outlined. ESA

N92-32383*# Michigan Univ., Ann Arbor. Space Physics Research Lab.
MASS LOADING AT TITAN AND COMETS
Tamas I. Gombosi *In* ESA, Symposium on Titan Apr. 1992 p 255-261 (For primary document see N92-32348 23-91)
(Grants NAGw-2162; NAGw-1366)
Copyright Avail: CASI HC A02/MF A01; ESA, EPD, ESTEC, Noordwijk, Netherlands, HC

Present understanding of the cometary mass loading process (the addition of newborn ions to high speed magnetized plasma flows) is explored and the cometary lesson is applied to the environment of Titan. Mass loading is the dominant physical process controlling the interaction of the solar wind with comets, and it might play an important role in the interaction of Titan's neutral torus and exosphere with Saturn's magnetosphere. Freshly born ions follow cycloidal trajectories, resulting from the superposition of gyration and E/B drift. In the plasma frame, the resulting velocity space distribution is a ring beam distribution at comets and a ring distribution at Titan. This difference in free energy is expected to generate significantly different levels of low frequency broad band electromagnetic turbulence and, thus, result in important differences in the implanted ion distributions. It is predicted that mass loading creates a hot, equatorially trapped plasma population at Titan. ESA

N92-32384# Graz Univ. (Austria). Inst. for Meteorology and Geophysics.

ATMOSPHERIC ESCAPE FROM TITAN

Siegfried J. Bauer *In* ESA, Symposium on Titan Apr. 1992 p 263-265 Prepared in cooperation with Oesterreichische Akademie der Wissenschaften, Vienna (For primary document see N92-32348 23-91)

Copyright Avail: CASI HC A01/MF A01; ESA, EPD, ESTEC, Noordwijk, Netherlands, HC

The mass loss from Titan's atmosphere by different escape processes is reviewed with emphasis on its principal constituent, N2. The highly efficient escape of hydrogen is evidenced by the observed hydrogen torus on the Saturn system, having its origin in Titan's atmosphere. Atmospheric escape of atomic nitrogen is also considered. This happens as the result of impact ionization by magnetospheric electrons, dissociative recombination in Titan's ionosphere, and interactions with the magnetosphere/solar wind which now leads to estimates for the mass loss (over 4.5 B yrs) considerably below the originally assumed 10 percent of the present atmospheric mass; an upper limit for the mass loss of N now appears to be even less than 1 percent of the present atmospheric mass. ESA

N92-32385# Cologne Univ. (Germany, F.R.). Inst. fuer Geophysik und Meteorologie.

TITAN'S MAGNETOSPHERIC INTERACTION

F. M. Neubauer *In* ESA, Symposium on Titan Apr. 1992 p 267-272 Sponsored by BMFT (For primary document see N92-32348 23-91)

Copyright Avail: CASI HC A02/MF A01; ESA, EPD, ESTEC, Noordwijk, Netherlands, HC

Interaction between Titan and the surrounding magnetospheric plasma is considered, emphasizing the aspects of the global plasma dynamics of Titan's environment. The physical picture of the magnetospheric interaction is then developed from the theoretical point of view. Voyager 1 observations are presented to quantify the physical picture. An important aspect of Titan's induced magnetosphere, i.e., its tail with four lobes, is stressed and the Cassini Mission is briefly addressed. ESA

N92-32386*# Kansas Univ., Lawrence. Dept. of Physics and Astronomy.

THE IONOSPHERE OF TITAN AND ITS INTERACTION WITH SATURNIAN MAGNETOSPHERIC ELECTRONS

Thomas E. Cravens, C. N. Keller, and L. Gan *In* ESA, Symposium on Titan Apr. 1992 p 273-278 (For primary document see N92-32348 23-91)

(Grants NAGw-1588; NGT-50472; NSF ATM-89-96116)

Copyright Avail: CASI HC A02/MF A01; ESA, EPD, ESTEC, Noordwijk, Netherlands, HC

The interaction of superthermal electrons, including both magnetospheric electrons and photoelectrons, with the upper atmosphere and ionosphere of Titan, is studied using a two stream electron transport code. Ionization rates, electron heating rates, and airglow emission rates are calculated. Results of a one dimensional model of the ionosphere of Titan, which includes both photoionization and ionization by magnetospheric electrons, are presented. Preliminary calculations of ionospheric ion outflow down the wake (or tail) of Titan, for time periods when the wake region is illuminated by the Sun, are made. ESA

N92-32387*# Jet Propulsion Lab., California Inst. of Tech., Pasadena.

CASSINI: A MISSION TO SATURN AND TITAN

Dennis L. Matson *In* ESA, Symposium on Titan Apr. 1992 p 281-286 Sponsored by NASA, Washington (For primary document see N92-32348 23-91)

Copyright Avail: CASI HC A02/MF A01; ESA, EPD, ESTEC, Noordwijk, Netherlands, HC

The Cassini spacecraft that will carry out a detailed exploration of the Saturnian system is described. The spacecraft is composed of a Saturn orbiter and a Titan atmospheric probe called Huygens. The scientific objectives and investigations developed for the accommodation phase of the mission are discussed. The preferred trajectories available for transit to Saturn are discussed along with Titan specific features of the tour of the Saturnian system. ESA

N92-32388# European Space Agency. European Space Research and Technology Center, ESTEC, Noordwijk (Netherlands). Planetary and Space Science Div.

THE HUYGENS PROBE

Jean-Pierre Lebreton *In its* Symposium on Titan Apr. 1992 p 287-292 (For primary document see N92-32348 23-91)

Copyright Avail: CASI HC A02/MF A01; ESA, EPD, ESTEC, Noordwijk, Netherlands, HC

A description of the Huygens probe, its mission, and its scientifc payload is given. The Huygens Probe is an atmospheric probe designed to study the atmosphere and the surface of Titan. The objectives of Huygens are to make detailed in situ measurements of the structure, the composition, and the dynamics of the atmosphere of Titan and to characterize locally the surface near the impact site. Since it is anticipated that the probe may survive after the 6 to 8 m/s impact, provision is made in the payload and in the design of the probe to return data on the state and composition of the surface after impact. ESA

N92-32389*# National Aeronautics and Space Administration. Goddard Space Flight Center, Greenbelt, MD.

THE SYNTHETIC INFRARED SPECTRUM OF TITAN AT HIGH SPECTRAL RESOLUTION

Athena Coustenis (Observatoire de Paris-Meudon, France), T. Encrenaz (Observatoire de Paris-Meudon, France), Bruno Bezard (Observatoire de Paris-Meudon, France), G. Bjoraker, G. Graner (Paris-Sud Univ., Orsay, France), M. Dang-Nhu (Paris-Sud Univ., Orsay, France), and E. Arie (Paris-Sud Univ., Orsay, France) *In* ESA, Symposium on Titan Apr. 1992 p 293-299 (For primary document see N92-32348 23-91)

Copyright Avail: CASI HC A02/MF A01; ESA, EPD, ESTEC, Noordwijk, Netherlands, HC

A systematic study made of the observability of minor species in Titan's atmosphere is reported. This was done by modeling its thermal spectrum at 0.5/cm resolution under the conditions of the Infrared Space Observatory (ISO) and Composite Infrared Radiometer Spectrometer (CIRS), and by exploring the capabilities of the 0.03/cm resolution mode of ISO. ESA

N92-32390# Ecole Superieure de Physique et de Chimie Industrielles, Paris (France). Lab. de Spectroscopie en Lumiere Polarisee.

EXPERIMENTAL DETERMINATION OF THE REFRACTIVE INDEX OF LIQUEFIED GAS MIXTURES: APPLICATIONS TO HYPOTHESIZED TITAN OCEANS

J. Badoz, R. Nahoum, Guy Israel (Centre National de la Recherche Scientifique, Verrieres-Le Buisson, France), and Francois Raulin (Paris-Val de Marne Univ., Creteil, France) *In* ESA, Symposium on Titan Apr. 1992 p 303-305 (For primary document see N92-32348 23-91)

Copyright Avail: CASI HC A01/MF A01; ESA, EPD, ESTEC, Noordwijk, Netherlands, HC

A cryogenic refractometer, designed to measure refractive indices, is described. The device induces two main parts: a cryostat for liquefying and mixing constituents under known proportions, and an optical set up for measuring the refractive index of a liquid. Results of processes to determine the refractive indices of pure and mixed methane and ethane with and without dissolved nitrogen are given. ESA

N92-32391# Kent Univ., Canterbury (England). Space Sciences Unit.

LABORATORY DETERMINATION OF THE REFRACTIVE INDICES OF LIQUID METHANE AND ETHANE AT TEMPERATURES APPROPRIATE TO THE SURFACE OF TITAN

P. N. W. Birchley, M. J. Wright, John C. Zarnecki, P. R. Ratcliff, and C. S. Mill (Manchester Univ., England) *In* ESA, Symposium on Titan Apr. 1992 p 307-310 Sponsored by Science Research Council (For primary document see N92-32348 23-91)

Copyright Avail: CASI HC A01/MF A01; ESA, EPD, ESTEC, Noordwijk, Netherlands, HC

Preliminary results for refractive indices of liquid methane and ethane at cryogenic temperatures close to proposed temperatures for the surface of Titan are presented. The results for methane are compared to previously published results. The determinations were conducted using a prototype of the Huygens surface science package refractometer subsystem, based on a linear critical angle device. The principle of operation of the device and the experimental procedure are outlined. ESA

N92-32392# Kent Univ., Canterbury (England). Space Sciences Unit.

LABORATORY DETERMINATION OF THE THERMAL CONDUCTIVITY OF LIQUID METHANE AND ETHANE c35

P. N. W. Birchley, P. M. Daniell, John C. Zarnecki, and D. J. Parker (Rutherford Appleton Lab., Chilton, England) *In* ESA, Symposium on Titan Apr. 1992 p 311-314 Sponsored by Science Research Council (For primary document see N92-32348 23-91)

Copyright Avail: CASI HC A01/MF A01; ESA, EPD, ESTEC, Noordwijk, Netherlands, HC

Preliminary results of measurements of the thermal conductivities of liquid methane and ethane at temperatures close to the currently proposed surface temperature of Titan are reported. The measurements were taken using a prototype of the Huygens surface science package thermal properties subsystem, which will measure the temperature, thermal conductivity, and thermal diffusivity of Titan's putative ocean. ESA

N92-32393# Paris VI Univ. (France). Lab. de Meteorologie.

FORMATION AND GROWTH OF PHOTOCHEMICAL AEROSOLS IN TITAN'S ATMOSPHERE

M. Cabane, E. Chassefiere (Centre National de la Recherche Scientifique, Verrieres-Le Buisson, France), and Guy Israel (Centre National de la Recherche Scientifique, Verrieres-Le Buisson, France) *In* ESA, Symposium on Titan Apr. 1992 p 315-319 (For primary document see N92-32348 23-91)

Copyright Avail: NTIS HC A01/MF A01; ESA, EPD, ESTEC, Noordwijk, Netherlands, HC

Recent development in the understanding of the morphology of haze aerosols in Titan's atmosphere, aggregate particles, and their associated optical properties are considered in the flight of a microphysical model of aerosols. Two different phases of the formation process are identified: initial growth of aerosols near the formation altitude by accretion of very small elementary particles; and (2) settling during which particles of about the same size stock together, leading to the formation of aggregates which contain some tens to several hundred monomers. The first phase leads to the formation of nearly spherical 'monomers' (radius approximately equal to 0.05 micrometers). An eulerian microphysical model is used. It is shown that the monomer radius is extremely sensitive to the altitude where aerosols are created. The formation altitude of aerosols is found to lie in the range from 350 to 400 km. ESA

N92-32394# Chilworth Research Centre, Southampton (England). RSADU.

WAVES ON TITAN

Meric A. Srokosz, Peter G. Challenor, John C. Zarnecki (Kent Univ., Canterbury, England), and S. F. Green (Kent Univ., Canterbury, England) *In* ESA, Symposium on Titan Apr. 1992 p 321-323 (For primary document see N92-32348 23-91)

Copyright Avail: CASI HC A01/MF A01; ESA, EPD, ESTEC, Noordwijk, Netherlands, HC

A preliminary look at the possibility of surface waves existing on Titan, assuming it possesses an ethane/methane ocean, is taken. The properties of the waves are deduced using well understood theory and compared with the properties of waves on the Earth's oceans. Our calculations show that the lack of knowledge of surface wind speed on Titan produces the greatest uncertainty in the expected wave properties. ESA

N92-32395# Centre National de la Recherche Scientifique, Orsay (France). Lab. de Physique Moleculaire et Applications.

HCP AND HCN, MOLECULES OF PLANETARY INTEREST

M. Dang-Nhu and Francois Raulin (Paris-Val de Marne Univ., Creteil, France) *In* ESA, Symposium on Titan Apr. 1992 p 325-328 (For primary document see N92-32348 23-91)

Copyright Avail: CASI HC A01/MF A01; ESA, EPD, ESTEC, Noordwijk, Netherlands, HC

A systematic approach to obtain IR line frequencies and absorption line intensities of HCP and HCN molecules from the molar band integrated intensity is presented. A full compilation of the absorption line intensities of HCP fundamental IR bands is provided, ready to be used for further applications of planetary interest. Each transition is reported with its wavenumber and with its absolute intensity and other subsequent useful parameters. ESA

N92-32396# Bordeaux 2 Univ. (France). Obervatoire de Bordeaux.

PROPERTIES AND DISTRIBUTION OF THE AEROSOLS IN THE ATMOSPHERE OF TITAN

M. Dobrijevic, L. Goutoulli, D. Toublanc, J. P. Parisot, and J. Brillet *In* ESA, Symposium on Titan Apr. 1992 p 329-332 (For primary document see N92-32348 23-91)

Copyright Avail: CASI HC A01/MF A01; ESA, EPD, ESTEC, Noordwijk, Netherlands, HC

A description of a time dependent model which shows the distribution of size and density of the aerosols in the atmosphere of Titan is given. The distribution of size (0.1 to 10 micrometers) is computed including classical microphysical processes in clouds: sedimentation, diffusion, coagulation, and coalescence. The Titan's time required to reach equilibrium is on the order of 10(exp 8) s. At lower altitudes, condensation of hydrocarbons leads to a rapid increase of the aerosol size. In particular, as a structure of aerosols is stratified, a simple treatment with the theory of Mie is unworkable. More accurate treatment is presented where diffusion of light by stratified particles of hydrocarbons is computed. Comparison is given for spherical aerosol with two layers: a core of tholin and a mantel of C2H6. The calculation shows that the more important effect is due to the presence of the mantel creating a considerable reflection at the interface between the two layers. ESA

N92-32397# Paris-Val de Marne Univ., Creteil (France). Equipe Physico-Chimie Organique Spatiale.

GAS CHROMATOGRAPHY AND PYROLYSIS-GC WITH CAPILLARY COLUMNS: APPLICATION TO THE IN SITU ANALYSIS OF TITAN'S ATMOSPHERE

Leejo Do, E. deVanssay, P. Paillous, and Francois Raulin *In* ESA, Symposium on Titan Apr. 1992 p 333-337 (For primary document see N92-32348 23-91)

Copyright Avail: CASI HC A01/MF A01; ESA, EPD, ESTEC, Noordwijk, Netherlands, HC

Systematic studies on the chromatographic behavior of capillary columns which were developed for analyzing complex gas mixtures, the chemical composition of which is analogous to Titan atmosphere and aerosol pyrolyzates, are described. These include

permanent gases, C1-C6 hydrocarbons, C1-C4 nitriles, and CH(N) pyrolyzites. The tested columns are made of fused silica tubing (0.1 to 0.53 mm ID). They include 'PLOT' (Porous Layer Open Tubular) columns (internally covered by a porous layer of adsorbent material) and WCOT (Wall Coated Open Tubular) columns (internally covered by a liquid stationary phase which is chemically bonded to the wall of the fused silica tubing). For each tested column, Van Deemter Curves were determined. ESA

N92-32398# Padua Univ. (Italy). Dipartimento di Fisica.
TITAN'S ATMOSPHERE STRUCTURE FROM HUYGEN'S-ASI MEASUREMENTS
M. Fabris, F. Marzari, and V. Vanzani *In* ESA, Symposium on Titan Apr. 1992 p 339-342 (For primary document see N92-32348 23-91)
Copyright Avail: CASI HC A01/MF A01; ESA, EPD, ESTEC, Noordwijk, Netherlands, HC

A detailed procedure for reconstructing the trajectory, the velocity, and attitude temporal histories of the Huygens entry vehicle through Titan's atmosphere, and ultimately the structure of the atmosphere, is described starting from measurements of the aerodynamically induced accelerations experienced by the probe. This data will be obtained from the accelerometers for the Atmospheric Structure Instrument (ASI) carried aboard the Huygens probe. ESA

N92-32399# Manchester Univ. (England). Dept. of Pure and Applied Physics.
THE HUYGENS SSP REFRACTOMETER (REF)
J. E. Geake and C. S. Mill *In* ESA, Symposium on Titan Apr. 1992 p 343-346 (For primary document see N92-32348 23-91)
(Grant SERC-GR/H00581)
Copyright Avail: CASI HC A03/MF A01; ESA, EPD, ESTEC, Noordwijk, Netherlands, HC

The refractometer in the Huygens probe Surface Science Package (SSP) is a linear critical angle refractometer. Its optical principles, instrument construction, and details of its electronic system are described. This instrument covers the refractive index range 1.250 to 1.450 with a discrimination of 0.001; this gives a resolution of better than 1 percent in the relative abundance of methane and ethane in the expected mixture on the liquid surface of Titan. Light emitting diodes at 635 nm provide illumination; the ouput image shows a cutoff edge, whose position is a linear function of refractive index. The image intensity profile is sensed by a 512 element photodiode array and digitized; it is then differentiated numerically by the SSP's central computer, as this is found to enhance the discrimination and may give information about any suspended matter. ESA

N92-32400# Paris-Val de Marne Univ., Creteil (France). Equipe Physico-Chimie Organique Spatiale.
SOME PROBLEMS ABOUT IR BAND INTEGRATED INTENSITIES; 3 EXAMPLES FOR APPLICATION TO TITAN: C6H6, HC3N, AND C4H2
M. Khlifi, H. Djebloun, P. Paillous, Francois Raulin, and M. Dang-Nhu (Centre National de la Recherche Scientifique, Orsay, France) *In* ESA, Symposium on Titan Apr. 1992 p 347-351 (For primary document see N92-32348 23-91)
Copyright Avail: CASI HC A01/MF A01; ESA, EPD, ESTEC, Noordwijk, Netherlands, HC

A systematic study of the integrated intensity of the IR bands of butadiene (C4H2), developed to overcome the discrepancies between the published values of band intensities for diacetylene, is described. The obtained values, given with error bars, are reported and compared to the literature data. In addition, absolute IR band integrated intensities (from 2.5 to 45 micrometers) were measured in the laboratory for benzene, and cyanoacetylene from 220 up to 320 K. From this an idea of the intensity versus temperature was obtained. In particular for the nu(sub 4) band of benzene (14.8 micrometers) and for several fundamental bands of cyanoacetylene, an accurate empirical formula which provides the value of integrated band intensity and a function of temperature was deduced. ESA

N92-32401# Observatoire de Paris-Meudon (France).
THE SPECTRUM OF TITAN IN THE 1.06 AND 1.28 MICRON WINDOWS
Emmanuel Lellouch, Athena Coustenis, J.-P. Maillard (Institut d'Astrophysique, Paris, France), K. Strong (Oxford Univ., England), N. Deme, Caitlin Griffith (State Univ. of New York, Stony Brook.), and Bernard Schmitt (Centre National de la Recherche Scientifique, Grenoble, France) *In* ESA, Symposium on Titan Apr. 1992 p 353-358 (For primary document see N92-32348 23-91)
Copyright Avail: CASI HC A02/MF A01; ESA, EPD, ESTEC, Noordwijk, Netherlands, HC

Observations of Titan at 1.0 to 1.4 microns at resolutions of 8/cm and 1/cm are reported. The spectra include two methane windows centered at 1.28 and 1.07 microns. A preliminary analysis of the 9050 to 9200/cm region of Titan is presented, using new laboratory data of methane recorded under long paths (about 500 m-am). The data in this range seem to be more consistent with a methane profile governed by saturation in most of the troposhere than with a uniform methane mixing ratio of 1 to 2 throughout the atmosphere. ESA

N92-32402# European Space Agency. European Space Research and Technology Center, ESTEC, Noordwijk (Netherlands). Huygens Project Div.
HUYGENS PROBE: THE SURFACE MISSION
Ralph Lorenz *In its* Symposium on Titan Apr. 1992 p 359-364 (For primary document see N92-32348 23-91)
Copyright Avail: CASI HC A02/MF A01; ESA, EPD, ESTEC, Noordwijk, Netherlands, HC

The Huygens probe is designed for the in situ exploration of the atmosphere of Titan down to its surface and for low altitude remote observation of the surface. While not a design requirement, the probe may survive impact with the surface and return science data. The anticipated behavior of the probe at and after impact is described and a preliminary assessment is made of the range of duration of the surface mission. Interactions of the probe with the surface are considered and some of the possible mechanisms for termination of the mission are described. ESA

N92-32403# British Astronomical Association, West Barnham (England).
ON THE TITAN/28 SAGITTARII OCCULTATION OF 1989 JULY 3
R. Miles and A. J. Hollis *In* ESA, Symposium on Titan Apr. 1992 p 365-370 (For primary document see N92-32348 23-91)
Copyright Avail: CASI HC A02/MF A01; ESA, EPD, ESTEC, Noordwijk, Netherlands, HC

Preliminary results of photoelectric observations of this rare event depicting a central flash are discussed and the observational procedure is described. The occultation record represents the most northern path, projected at Titan, to be monitored photoelectrically. Two conspicuous minima observed at ingress and at egress are tentatively associated with the upper and lower detached haze layers detected by the Voyager spacecraft. The central flash lasted 0.7 s at half peak height, and at maximum reached 19 +/- 3 percent of the intensity of the unocculted star. Residual transmitted light during occultation fell to the unusually low value of 0.7 +/- 0.5 percent of its normal intensity indicative of absorption from atmospheric aerosols, possessing a tangential optical depth of 2 to 3 at an altitude of about 250 to 300 km. ESA

N92-32404# Rome Univ. (Italy). Ist. Astronomico.
TITAN IN A BOX
A. Rotundi and F. A. Farrelly *In* ESA, Symposium on Titan Apr. 1992 p 371-375 (For primary document see N92-32348 23-91)
Copyright Avail: CASI HC A01/MF A01; ESA, EPD, ESTEC, Noordwijk, Netherlands, HC

A planetary simulation system is described together with

preliminary results aimed at recreating Titan's atmospheric conditions specifically for the testing of the atmospheric structure instrument of the Huygens probe on the Cassini mission. The cylindrical test chamber has a usable space 80 cm long and 40 cm in diameter and is designed to work in the pressure range from about 0.1 microbar to 4 bar with temperatures ranging from 68 to 170 K. The pressure versus temperature profile of Titan's atmosphere is being simulated in a point by point fashion. Within the capabilities of the present set up are the condition present at altitudes higher than the inversion point in Titan's atmosphere at temperatures greater then 100 K with pressures of less then 40 mb. ESA

N92-32405*# National Aeronautics and Space Administration. Ames Research Center, Moffett Field, CA.

LABORATORY INVESTIGATIONS OF THE AEROSOLS IN THE STRATOSPHERE OF TITAN

Thomas W. Scattergood (State Univ. of New York, Stony Brook.), Bradley M. Stone (San Jose State Univ., CA.), and Edmond Y. Lau (San Jose State Univ., CA.) *In* ESA, Symposium on Titan Apr. 1992 p 377-381 Sponsored by California State Univ. and Stanford/ASEE Faculty Education Program (For primary document see N92-32348 23-91)

Copyright Avail: CASI HC A01/MF A01; ESA, EPD, ESTEC, Noordwijk, Netherlands, HC

Results of experiments in which particles were produced from UV photolysis of C2H2, C2H4, or HCN, separately or in mixtures, modeling Titan's upper atmosphere, are presented. The particles were collected on disks and examined by Scanning Electron Microscopy (SEM). Measurements of particle sizes and shapes and of aggregation were determined from the SEM photographs. ESA

N92-32406# Centre National de la Recherche Scientifique, Grenoble (France). Lab. de Glaciologie et Geophysique de l'Environnement.

NEAR INFRARED SPECTRA OF POTENTIAL SOLIDS AT THE SURFACE OF TITAN

Bernard Schmitt, Eric Quirico, and Emmanuel Lellouch (Observatoire de Paris-Meudon, France) *In* ESA, Symposium on Titan Apr. 1992 p 383-388 (For primary document see N92-32348 23-91)

(Grants ISU-80-3717; ISU-91-3720)

Copyright Avail: CASI HC A02/MF A01; ESA, EPD, ESTEC, Noordwijk, Netherlands, HC

The laboratory measurement of the optical properties in the near infrared (1 to 5 micrometers) of solid CH4, C2H6, and C2H4 and some of their mixtures is reported and results are given. With these data the spectra of three mixtures at a resolution comparable to the one of the near infrared spectrometer of the instrument of the Huygens probe were simulated. It was found that at the Descent Imager/Spectral Radiometer's (DISR's) resolution the best features to probe the composition of solid surface on Titan are near 6000, 7500, and 8600/cm for methane, near 7900, 7200, and 8400/cm for ethane and near 6100/cm for ethylene. In some cases concentrations lower than a few percent may be derived from the analysis of the complete infrared spectrum. ESA

N92-32407# European Space Agency. European Space Research and Technology Center, ESTEC, Noordwijk (Netherlands). Space Science Dept.

ON THE INTERPRETATION OF TITAN'S INTENSITY AND POLARIZATION PHASE CURVE

Piet Stammes *In its* Symposium on Titan Apr. 1992 p 389-395 (For primary document see N92-32348 23-91)

Copyright Avail: CASI HC A02/MF A01; ESA, EPD, ESTEC, Noordwijk, Netherlands, HC

Studies of the intensity and polarization curve of Titan which were carried out to find the properties of the Titan haze are discussed. For several types of model atmospheres the disk integrated intensity and polarization were computed, using the doubling/adding method and a nest method to integrate the reflected light over the visible disk. In these computations the scattering matrix aerosol particles was correctly taken into account. Comparison with the Pioneer 11 and Voyager 2 measurements of the intensity and polarization phase curve of Titan led to a three layer atmospheric model: (1) a top haze layer consisting of small (0.03 micrometers radius) tholin spheres with optical thickness 0.1 at wavelength 0.648 micrometers; (2) next, a main haze layer consisting of nonspherical tholin particles (prolate spheroids, axes ratio 4:1) with volume equivalent radius of 0.15 micrometers and optical thickness 1.0 at wavelength 0.648 micrometers; and (3) a nitrogen gas layer at the bottom. The fit to the Pioneer 11 data was good, but to the Voyager 2 data no fit could be found. ESA

N92-32408# Bordeaux 2 Univ. (France). Observatoire de Bordeaux.

STUDY OF TRANSMITTED LIGHT THROUGH THE ATMOSPHERE OF TITAN

D. Toublanc, J. P. Parisot, J. Brillet, and Daniel Gautier (Observatoire de Paris-Meudon, France) *In* ESA, Symposium on Titan Apr. 1992 p 397-399 (For primary document see N92-32348 23-91)

Copyright Avail: CASI HC A01/MF A01; ESA, EPD, ESTEC, Noordwijk, Netherlands, HC

A temperature pressure density model of Titan's atmosphere was used to describe the structure of the atmosphere and the major components identified. The optical depth was calculated for Rayleigh and Mie scattering and a Monte Carlo model developed. The history of one photon and the calculations performed on it are outlined. Results of computation with a ground albedo equal to 0.5 are presented together with calculated Boud and geometric albedos. ESA

N92-32409# Graz Univ. (Austria). Inst. fuer Meteorologie und Geophysik.

DIELECTRIC CONSTANT MEASUREMENTS IN SIMULATED TITAN OCEAN LIQUIDS

Stephan Ulamec, J. Badoz (Ecole Superieure de Physique et de Chimie Industrielles, Paris, France), and Jean-Pierre Lebreton (European Space Agency. European Space Research and Technology Center, ESTEC, Noordwijk, Netherlands) *In* ESA, Symposium on Titan Apr. 1992 p 401-405 Sponsored in part by ESA (For primary document see N92-32348 23-91)

Copyright Avail: CASI HC A01/MF A01; ESA, EPD, ESTEC, Noordwijk, Netherlands, HC

An experimental method used to characterize, in the laboratory, the dielectric properties of the liquid simulating the composition of the putative Titan ocean is described. The experimental setup is described and preliminary results are reported to illustrate the capabilities of the method. ESA

N92-32410# Kent Univ., Canterbury (England).

A SURFACE SCIENCE PACKAGE FOR THE HUYGENS TITAN PROBE

John C. Zarnecki, J. A. M. McDonnell, S. F. Green, T. J. Stevenson, P. N. W. Birchley, P. M. Daniell, D. H. Niblett, P. R. Ratcliff, H. A. Shaw, and M. J. Wright et al *In* ESA, Symposium on Titan Apr. 1992 p 407-409 Sponsored by Scienec Research Council and Italian Space Agency (For primary document see N92-32348 23-91)

Copyright Avail: CASI HC A01/MF A01; ESA, EPD, ESTEC, Noordwijk, Netherlands, HC

The outline design of the Surface Science Package (SSP) for the Huygens probe is described. The instrument is primarily intended to make measurements on the surface, particularly the determination of the physical and chemical composition of any Titan ocean, but several of the subsystems will also make useful atmospheric measurements to complement those of the atmospheric structure instrument and others. Independent determinations of the composition of any ocean may be inferred from measurements of its density, electrical permittivity, refractive index, thermal conductivity, and thermal diffusivity plus the measurement of the oceanic velocity of sound. Through accelerometry measurements, SSP will be able to provide some information on the general nature of the surface while time resolved

measurements of the probe's inclination to the vertical will provide wave profiles of interest both in constraining ocean properties and in providing a test for empirical models developed to describe terrestrial oceans. ESA

92 SOLAR PHYSICS

Includes solar activity, solar flares, solar radiation and sunspots.

For related information see *93 Space Radiation.*

N92-32488# Stanford Univ., CA. Center for Space Science and Astrophysics.
OBSERVATIONS OF HIGH FREQUENCY AND HIGH WAVENUMBER SOLAR OSCILLATIONS
D. N. Fernandes, P. H. Scherrer, T. D. Tarbell (Lockheed Missiles and Space Co., Palo Alto, CA.), and A. M. Title (Lockheed Missiles and Space Co., Palo Alto, CA.) 1992 11 p
(Contract N00014-89-J-1024; NSF ATM-90-22249)
(AD-A250099) Avail: CASI HC A03/MF A01

Doppler shift measurements of the Na D(sub 1) absorption line have revealed solar oscillations in a new regime of frequency and wavenumber. Oscillations of vertical velocities in the temperature minimum and low chromosphere of the Sun are observed with frequencies ranging up to 9.5 mHz. The fundamental modes appear with wavenumbers up to 5.33 M/m (equivalent spherical harmonic degree, 3710). We find no evidence for chromospheric modes of a 3-minute period. GRA

N92-33119# Brown Univ., Providence, RI. Dept. of Physics.
RESEARCH AND DEVELOPMENT OF A HELIUM-4 BASED SOLAR NEUTRINO DETECTOR
R. E. Lanou, H. J. Maris, and G. M. Seidel 30 Jun. 1992 15 p
(Contract DE-FG02-88ER-40452)
(DE92-017390; DOE/ER-40452/7) Avail: CASI HC A03/MF A01

In this report we describe results of experiments to detect low energy radiation in superfluid helium. The ultimate aim of this research is to establish the feasibility of this technique for use in detecting neutrinos from the p-p and Be-7 reactions in the sun. In these experiments we have seen the first detection of 5.5 MeV (alpha) particles via evaporation from a bath of superfluid helium. An (alpha) particle excites phonons and rotons in the liquid helium, and these excitations are sufficiently energetic to evaporate helium atoms when they reach the free surface of the liquid. The evaporated atoms are detected calorimetrically by a thin wafer suspended above the liquid. The approximate overall efficiency of this process has been determined and we compare the experimental results with expectations. We have also been able to detect evaporation induced by a flux of gamma rays from a Cs-137 source. Preparations made for new experiments are also discussed. DOE

93 SPACE RADIATION

Includes cosmic radiation; and inner and outer earth's radiation belts.

For biological effects of radiation see *52 Aerospace Medicine.* For theory see *73 Nuclear and High-Energy Physics.*

No abstracts in this category.

99 GENERAL

N92-32338# Research and Development Labs., Culver City, CA.
UNITED STATES AIR FORCE SUMMER RESEARCH PROGRAM 1991. VOLUME 1: PROGRAM MANAGEMENT REPORT Report, 30 Sep. 1990 - 30 Sep. 1991
Gary Moore 9 Jan. 1992 638 p
(Contract F49620-90-C-0076)
(AD-A248763; AFOSR-92-0167TR-Vol-1) Avail: CASI HC A99/MF A06

The Summer Faculty Research Program (SFRP), Graduate Student Research Program (GSRP), and the High School Apprenticeship Program (HSAP) are summarized. Statistics on each program from 1979 to the present are given. Included are efforts to recruit participants from Historically Black Colleges and Universities and Minority Institutions (HBCU/MI). Participating Air Force laboratories are listed and information is given on a number of applicants and participants at each laboratory. Finally, an abstract is provided for each of the reports written by the program participants. GRA

N92-32453# Federal Aviation Administration, Washington, DC.
THE 1991 FEDERAL AVIATION ADMINISTRATION PLAN FOR RESEARCH, ENGINEERING AND DEVELOPMENT
Aug. 1992 171 p Prepared for Congress of the United States, Washington, DC Original contains color illustrations
Avail: CASI HC A08/MF A02

The FAA's Research, Engineering and Development (R,E&D) Program is very forward looking, and concentrates on the known needs of the aviation system and it constituency. The FAA has published a vision of the future system which has been broadly accepted by the industry. The vision is rooted in the pursuit of a safe system that does not constrain flight. The system that results from this work will be more capable, efficient, and economical to operate. Increased automation will involve the controller, pilot, and maintenance technicians in different roles than today's system requires. Specific areas of this project which are discussed at length include the following: quality control; R,E&D goals; past lessons learned; planning for future aviation systems; R,E&D plan components; and system engineering. H.A.

N92-32457# Nagoya Univ. (Japan). Solar-Terrestrial Environment Lab.
STEL Annual Report, 1991 - 1992
1992 25 p
Avail: CASI HC A03/MF A01

An overview of the activities of the Solar-Terrestrial Environment Laboratory of Nagoya University is presented. Individual activity summaries are given for each of the four research divisions: (1) Atmospheric Environment - which studies the behavior of trace gases and particulate matter in the atmosphere, especially in relation to chemical and transport process; (2) Ionospheric and Magnetospheric Environment - which studies the physical processes of the magnetospheric/ionospheric environment particularly through ground-based observation from the global scale point of view; (3) Heliospheric Environment - which studies by means of ground-based observations and computer simulation; and (4) Coordinated Data Analysis. Programs of the Moshiri, Kagoshima, Sakushima, Fuji, and Sakashita observatories are also reported as well as collaborative research activities. I.I.C.

N92-32814# National Research Council of Canada, Boucherville (Quebec).
NATIONAL RESEARCH COUNCIL INDUSTRIAL MATERIALS INSTITUTE: FROM KNOWLEDGE TO KNOW-HOW Annual Report, 1989-1990 [CONSEIL NATIONAL DE RECHERCHES CANADA INSTITUT DES MATERIAUX INDUSTRIELS: DU SAVOIR AU SAVOIR-FAIRE, RAPPORT ANNUEL 1989-1990]
1990 24 p In FRENCH Original contains color illustrations
(CTN-92-60333) Avail: CASI HC A03/MF A01

This report describes the facilities for materials research and research activities at the Industrial Materials Research Institute

(IMRI), which is part of the National Research Council of Canada. The mandate of the institute is to carry out materials research and develop related technology in cooperation with Canadian industry. The institute has and will continue to concentrate on structural materials research with a special focus on materials processing. Projects carried out by IMRI scientists cover metals, ceramics, plastics, and composites. Specific research areas include: improved temperature control, detection of defects by remote techniques, development of techniques for the characterization of materials during processing, development of high temperature ceramic superconductors, high performance ceramic composite coatings technology, long fiber thermoplastic composites, closed loop control of polymer extrusion processes, morphology control of polymer blends, and strip casting of copper and steels. Software and expert systems have been developed for the computer integration of the materials design and manufacture processes, especially of injection molding, extrusion and blow molding of plastics, and die casting of zinc and aluminum and their alloys.
CISTI

N92-32815# National Research Council of Canada, Boucherville (Quebec). Industrial Materials Inst.
NATIONAL RESEARCH COUNCIL INDUSTRIAL MATERIALS INSTITUTE: FROM KNOWLEDGE TO KNOW-HOW Annual Report, 1989-1990
1990 24 p Original contains color illustrations
(CTN-92-60334) Avail: CASI HC A03/MF A01

This report describes the facilities for materials research and research activities at the Industrial Materials Research Institute (IMRI), which is part of the National Research Council of Canada. The mandate of the institute is to carry out materials research and develop related technology in cooperation with Canadian industry. The institute has and will continue to concentrate on structural materials research with a special focus on materials processing. Projects carried out by IMRI scientists cover metals, ceramics, plastics, and composites. Research areas include improved temperature control, detection of defects by remote techniques, development of techniques for the characterization of materials during processing, development of high temperature ceramic superconductors, high performance ceramic composite coatings technology, and long fiber thermoplastic composites, closed loop control of polymer extrusion processes, morphology control of polymer blends, strip casting of copper and steels. Software and expert systems have been developed for the computer integration of the materials design and manufacture process especially of injection molding, extrusion and blow molding of plastics, and die casting of zinc and aluminum and their alloys.
CISTI

N92-32853# Toronto Univ. (Ontario). Inst. for Aerospace Studies.
UNIVERSITY OF TORONTO INSTITUTE FOR AEROSPACE STUDIES Annual Progress Report, 1989-1990
1991 122 p
(CTN-92-60375) Avail: CASI HC A06/MF A02

This report includes descriptions of research facilities and progress reports on projects currently underway at the University of Toronto Institute for Aerospace Studies (UTIAS). Experimental facilities include the Aeroacoustics Laboratory, the Air Cushion Test Track, the Dusty Gas Shock Tube Facility, the Flexible Spacecraft Emulator, the Flight Simulator, the Fusion Plasma Simulator, the Heave Table Facility for research into suspension systems of earthbound or near-earth vehicles, the Implosion Dynamics Laboratory, the Space Robotics Laboratory, the Structure and Materials Laboratory, the Subsonic Wind Tunnel, the Turbulent Combustion Laboratory, and the Vacuum Sphere and Hot Flow Test Facility. The Applied Mass Spectroscopy Lab and the Physical and Analytical Characterization Lab provide analytical support for UTIAS activities. Brief summaries are provided on research related to aeroacoustics, aerodynamics, air cushion technology, combustion and propulsion, computational fluid dynamics, fiber optics smart structures, flight research, flight simulation, fusion energy, hypersonic aerodynamics, space processing of materials, production of materials under extreme conditions, non-stationary gas dynamics, shock waves, implosions and dusty gases, space robotics, spacecraft dynamics and control, and structural mechanics related to composites and other high performance materials.
CISTI

N92-32862# Los Alamos National Lab., NM.
FIFTY YEARS IN SCIENCE, THIRTY YEARS IN SPACE
Sep. 1992 43 p Original contains color illustrations
(Contract W-7405-eng-36)
(LALP-92-51) Avail: CASI HC A03/MF A01; 28 functional color pages

This brochure overviews the technologies developed at Los Alamos National Laboratory that have the potential to contribute to the space effort. In the area of power and propulsion, the technologies presented are: (1) nuclear fuel design and fabrication; (2) nuclear heart sources for space mission; (3) nuclear electric systems for space application; (4) safety analysis for nuclear reactor; (5) reactor core design and analysis; (6) advanced electric propulsion for 21st century space exploration; (7) nuclear thermal rocket development; (8) nuclear rocket testing; (9) laser space propulsion; and (10) innovative propulsion concepts. The technologies in the area of medical applications are: (1) multilaser system for space medicine; and (2) exposure to and protection from radiation during space mission. The technologies in the area of diagnostics and testing are: (1) computer codes for radiation transport; (2) laser diagnostics for space propulsion applications; (3) new facility for high-temperature flow testing; and (4) ensuring reliability of materials for space mission. In the area of instrumentation, technologies are: (1) analyzing the chemistry and mineralogy of planets with a single instrument; (2) the Vela satellite program; (3) the ALEXIS satellite project; (4) the shuttle-URA experiment; (5) studying surface composition with a new ion mass spectrometer; (7) gamma-ray and neutron spectrometer for lunar research; (8) mapping the lunar surface with the soft x-ray fluorescence imager; (9) the Army background experiment program; (10) laser-induced breakdown spectroscopy for space missions; and (11) a zero-gravity furnace for processing advanced materials. Partners in defense and partners in industrial competitiveness are also addressed.
I.I.C.

N92-33027# Department of Defense, Washington, DC. Defense Research and Engineering.
THE DOD SCIENCE AND TECHNOLOGY STRATEGY
Jul. 1992 106 p
(AD-A253691) Avail: CASI HC A06/MF A02

The new defense and acquisition strategies focus on the potentially dangerous regional challenges we face, while retaining the capacity to respond to any emerging global threats. The Director of Defense Research and Engineering (DDR&E) has formulated a new science and technology strategy. The core of this strategy is to provide for early, intensive, and continued involvement of warfighters, fuel and exploit the information technology explosion, and conduct extensive and realistic technology demonstrations. To provide the focus for the science and technology program, seven thrusts have been defined that represent the demands being placed on the science and technology program by the users' most pressing military and operational requirements. The seven thrusts are global surveillance and communications, precision strike, air superiority and defense, sea control and undersea superiority, advanced land combat, synthetic (battlefield) environments, and technology for affordability.
Author

N92-33086# Office of Science and Technology, Washington, DC.
SCIENCE AND TECHNOLOGY: A REPORT TO THE CONGRESS
17 Mar. 1992 133 p
(PB92-183219) Avail: CASI HC A07/MF A02

The Science and Technology Report and Outlook is submitted biennially to Congress by the Office of Science and Technology Policy in conformance with Public Law 97-375. The report highlights broad themes and priorities in national science and technology

efforts and seeks to convey a context for their consideration. Part 1 of the report focuses on science and technology's role in society and how science and technology are shaping and being shaped by current events. Part 2 examines the critical role of science and technology in enabling the Nation's future well-being and prosperity. The two areas of focus are the Nation's investment in basic research and the importance of educating our Nation's youth. Part 3 illuminates several priority areas essential for meeting national needs. Chapters focus on information technology, biotechnology, national security, foreign policy, international competitive advantage, and global environmental needs. Author

N92-33106*# National Aeronautics and Space Administration. Ames Research Center, Moffett Field, CA.
DIRECTOR'S DISCRETIONARY FUND REPORT FOR FY 1991
Jul. 1992 107 p
(RTOP 307-51-50)
(NASA-TM-103902; A-91218; NAS 1.15:103902) Avail: CASI HC A06/MF A02

The Director's Discretionary Fund (DDF) at the Ames Research Center was established to fund innovative, high-risk projects in basic research which would otherwise be difficult to initiate, but which are essential to our future programs. Here, summaries are given of individual projects within this program. Topics covered include scheduling electric power for the Ames Research Center, the feasibility of light emitting diode arrays as a lighting source for plant growth chambers in space, plasma spraying of nonoxide coatings using a constricted arcjet, and the characterization of vortex impingement footprint using non-intrusive measurement techniques. Author

N92-33238# Department of Defense, Washington, DC. Director of Defense Research and Engineering.
DOD KEY TECHNOLOGIES PLAN
Jul. 1992 228 p
(AD-A253692) Avail: CASI HC A11/MF A03

The primary objective of these development plans is to prove out and mature the technologies required to attain the goals of the science and technology (S&T) program of the Department of Defense (DoD). The activities delineated in the plan involve proof of concept experiments, laboratory demonstrations, and evaluations supported by models and simulations. The formulation of this Key Technology Plan is driven by the S&T Strategy. At the core of this strategy are the Seven Thrusts which focus the S&T program to address the users' most pressing military and operational requirements. These thrusts are global surveillance and communications, precision strike, air superiority and defense, sea control and undersea superiority, advanced land combat, synthetic environments, and technology for affordability. The key technology areas addressed in the plan are computers, software, sensors, communications networking, electronic devices, environmental effects, materials and processes, energy storage , propulsion and energy conversion, design automation, and human-system interfaces. The plan provides technology development roadmaps for the development and maturation of the technologies needed to achieve the stated goals of the thrusts. Author

SUBJECT INDEX

Typical Subject Index Listing

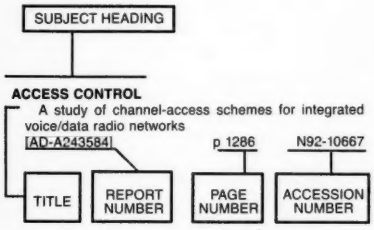

The subject heading is a key to the subject content of the document. Titles, report numbers, and accession numbers of pertinent documents are provided under each subject heading. When the title is insufficiently descriptive of the document content, a title extension has been added, separated from the title by three hyphens. The report number helps to indicate the type of document cited (e.g., NASA report, NASA translation, NASA contractor report). The accession number is the number by which the document abstracts are arranged in this journal and by which the document is sold or requested. The page number helps you locate the the citation in the abstract section. The titles, with title extensions if present, are arranged under each subject heading in ascending accession number order. The subject headings have been selected from the latest revision of the *NASA Thesaurus*.

A

ABERRATION
Diffractive optics technology and the NASA Geostationary Earth Observatory (GEO)
[NASA-CR-190611] p 4076 N92-33074

ABLATION
A computational fluid dynamics analysis of the hypersonic flights of Pegasus
[NASA-CR-186023] p 4007 N92-32560
Anisotropic electrical resistivity of YBCO/PBCO superlattice films grown on miscut substrates
[DE92-014409] p 4082 N92-32636

ABRASION
Effects of the abrasiveness of test and training site soils on parachute life
[AD-A252389] p 3931 N92-32900

ABSORBERS (MATERIALS)
Ultra-low density organic-inorganic composite materials possessing thermally insulating and acoustic damping properties
[AD-A251182] p 3955 N92-32828

ABSORPTION COOLING
Development and proof-testing of advanced absorption refrigeration cycle concepts
[DE92-014933] p 3977 N92-32723

ABSORPTION SPECTROSCOPY
Local environment around the oxygen atoms in Y-Ba-Cu-O studied X ray Absorption Fine Structure (XAFS) spectroscopy
[DE92-014165] p 4081 N92-32470
Small passive chemical detector
[DE92-014188] p 4030 N92-32933
Studies of Y-Ba-Cu-O single crystals by x ray absorption spectroscopy
[DE92-014687] p 4086 N92-33136

ABSTRACTS
Proceedings of the Sixteenth Annual Software Engineering Workshop
[NASA-TM-107964] p 4044 N92-32869
Abstracts of manuscripts submitted in 1991 for publication
[PB92-204627] p 4091 N92-33088

ACCELERATED LIFE TESTS
New accelerated corrosion test methods
[MBB-Z-0406-91-PUB] p 3968 N92-32895

ACCELEROMETERS
Improved HIRAP flight calibration technique
[NASA-TM-107656] p 3944 N92-33112

ACCESS CONTROL
Guaranteeing synchronous message deadlines with the timed token medium access control protocol
[NASA-CR-190710] p 4042 N92-32656
Fault tolerance for security management in distributed systems
[LAAS-92011] p 4040 N92-32766

ACCIDENTS
A test circuit for capacitor bank grounding sticks
[AD-A251121] p 3989 N92-32700
Execution of measurement sequences in the framework of the inspection of near limit regions by radioiodine and aerosol emission measurements, and ground examinations on plutonium, strontium, and gamma ray radionuclides
[OEFZS-4579] p 4071 N92-32763

ACCOMMODATION
Accommodation mechanisms and dispersoid-free zone s in Al 7475 after superplastic forming
[MBB-Z-0404-91-PUB] p 3968 N92-32894

ACCRETION DISKS
Formation of the satellites p 4093 N92-32350

ACETATES
Laser coating of composites for enhanced wear and corrosion resistance
[AD-A249231] p 3956 N92-32906

ACETYLENE
Laboratory investigations of the aerosols in the stratosphere of Titan p 4102 N92-32405

ACOUSTIC ATTENUATION
Ultra-low density organic-inorganic composite materials possessing thermally insulating and acoustic damping properties
[AD-A251182] p 3955 N92-32828
A lightweight loudspeaker for aircraft communications and active noise control p 3988 N92-32964

ACOUSTIC DUCTS
The application of unsteady potential flow vortex loop/dipole theory to the work and acoustics of low-speed turbomachinery
[AD-A251160] p 4008 N92-32652

ACOUSTIC EMISSION
Fatigue, hysteresis, and acoustic emission, parts 1 and 2
[AD-A251073] p 4021 N92-32681
Pump and valve research at the Oak Ridge National Laboratory
[DE92-014419] p 4019 N92-32890
Acoustical emission from bubbles
[AD-A252390] p 4061 N92-32901
Investigation of fracture toughness and fracture mechanisms using acoustic emission measurements
[DE92-011907] p 4022 N92-32911

ACOUSTIC MEASUREMENT
Pump and valve research at the Oak Ridge National Laboratory
[DE92-014419] p 4019 N92-32890
Investigation of fracture toughness and fracture mechanisms using acoustic emission measurements
[DE92-011907] p 4022 N92-32911
Sound power determination using the sound intensity scanning technique p 4062 N92-32953

ACOUSTIC PROPERTIES
Exposures from headset interference tones
[AD-A247175] p 4061 N92-32697

ACOUSTIC SIMULATION
The Dornier 328 Acoustic Test Cell (ATC) for interior noise tests and selected test results
[AIAA PAPER 92-2164] p 4062 N92-32951

ACOUSTICS
Hydrate detection
[DE92-014350] p 4034 N92-32333
The application of unsteady potential flow vortex loop/dipole theory to the work and acoustics of low-speed turbomachinery
[AD-A251160] p 4008 N92-32652
Ultra-low density organic-inorganic composite materials possessing thermally insulating and acoustic damping properties
[AD-A251182] p 3955 N92-32828

ACOUSTO-OPTICS
Can the speed of light in the fiber be controlled?
[AD-A247614] p 4074 N92-32668
Radiation selective system for target range and imaging readout
[AD-D015285] p 4076 N92-33095

ACRYLIC RESINS
Investigation of a relationship between uniaxial and biaxial chemical stress crazing of cast acrylic
[AD-A250852] p 4021 N92-32621

ACTIVATED CARBON
Purification system
[NASA-CASE-MSC-21584-1] p 3965 N92-33029

ACTIVE CONTROL
Intelligent signal processing for active control
[AD-A252232] p 4053 N92-32625
Active control of sound transmission through stiff lightweight composite fuselage constructions p 4062 N92-32957
Active control of interior noise in a large scale cylinder using piezoelectric actuators p 4063 N92-32958
Sound transmission reduction with intelligent panel systems p 4063 N92-32959
Active vibrations and noise control for turboprop application research program activities p 4063 N92-32962
Active synchrophasing of propeller unbalance p 4063 N92-32963
A lightweight loudspeaker for aircraft communications and active noise control p 3988 N92-32964

ACTS
Ka-band dual frequency array feed for a low cost ACTS ground terminal p 3983 N92-32969
A 1-W, 30-GHz, CPW amplifier for ACTS small terminal uplink p 3984 N92-32973

ACTUATORS
Active control of interior noise in a large scale cylinder using piezoelectric actuators p 4063 N92-32958
Active vibrations and noise control for turboprop application research program activities p 4063 N92-32962
Jacobian and stiffness analysis of a novel class of six-DOF parallel minimanipulators
[DE92-016373] p 4054 N92-33184

ADA (PROGRAMMING LANGUAGE)
Experiments in software engineering technology: Recent studies in the SEL (1990-1991) p 4044 N92-32872
Developing better software: A five year history of software engineering advancement p 4046 N92-32884

ADAPTATION
Contribution to robot-task adaptation, introduction and use of robot anisotropy and task object for the design of the workstation
[ISAL-91-0095] p 4039 N92-33056

ADAPTIVE CONTROL
A learning enhanced flight control system for high performance aircraft
[AD-A252520] p 3938 N92-32435
Adaptive information processing and global optimization
[AD-A248450] p 4089 N92-32644
Sound transmission reduction with intelligent panel systems p 4063 N92-32959

ADAPTIVE FILTERS
Adaptive filter technique for suppression of wideband or offset narrowband radio frequency interference
[AD-D015329] p 3992 N92-33175

ADAPTIVE OPTICS
The dependence of the anisoplanatic Strehl of a compensated beam on the beacon distribution
[DE92-011272] p 4016 N92-32736
The effect of the light round-trip time on the performance of an adaptive optics turbulence compensation system
[DE92-011273] p 4075 N92-32738
ADDITIVES
Reduced mobility and PPC in In(.20)Ga(.80)As / Al(.23)Ga(.77)As HEMT structure p 3984 N92-32976
Effects of fuel on Hercules AS-4/8552 composite material p 3958 N92-33046
ADHESION
Corrosion-resistant alkyd coatings
[AD-D015330] p 3974 N92-33177
ADHESIVE BONDING
Polyimide molding powder, coating, adhesive, and matrix resin
[NASA-CASE-LAR-14163-1] p 3973 N92-33014
Flush mounting of thin film sensors
[NASA-CASE-LAR-14446-1] p 3978 N92-33020
Environmental resistance of amorphous bonded thermoplastic joints p 3959 N92-33053
A review of recent developments in joining high-performance thermoplastic composites
[CNRC-33030] p 4019 N92-33077
ADIABATIC CONDITIONS
Nonlinear resonance
[DE92-014313] p 4016 N92-32596
ADIABATIC EQUATIONS
Nonlinear resonance
[DE92-014313] p 4016 N92-32596
ADSORPTION
Electrocatalyst surfaces
[PB92-190420] p 3962 N92-32591
AC microcalorimetry of adsorbates on evaporated metal films: Orientational ordering of H2 multilayers
[DE92-008317] p 3963 N92-32666
Purification system
[NASA-CASE-MSC-21584-1] p 3965 N92-33029
ADVANCED SOLID ROCKET MOTOR (STS)
Advanced solid rocket motor project status p 3945 N92-32280
ADVECTION
Numerical methods: Solving the advection equation in flows with sharp gradients using Bott's flux scheme
[DM-59] p 4009 N92-32727
AEROACOUSTICS
Fourth Aircraft Interior Noise Workshop
[NASA-CP-10103] p 4061 N92-32948
Acoustic loads prediction on jet aircraft p 4061 N92-32949
AERODYNAMIC BALANCE
Aerodynamic centre of wing-body combinations
[ESDU-92024] p 3929 N92-32479
Computational aspects of helicopter trim analysis and damping levels from Floquet theory
[NASA-CR-190736] p 3940 N92-33107
AERODYNAMIC CHARACTERISTICS
Turbine disk cavity aerodynamics and heat transfer p 3998 N92-32265
A critical evaluation of a three-dimensional Navier-Stokes CFD as a tool to design supersonic turbine stages p 3999 N92-32268
User's manual for AeroFcn: A FORTRAN program to compute aerodynamic parameters
[NASA-TM-104237] p 4042 N92-32507
An examination of several high resolution schemes applied to complex problems in high speed flows
[AD-A250814] p 4008 N92-32632
AERODYNAMIC COEFFICIENTS
Lift and rolling moment due to spoilers on wings with trailing-edge flaps deflected at subsonic speeds
[ESDU-92002-SUPPL] p 3931 N92-32782
Further wind tunnel investigation of the SM701 airfoil with aileron and turbulators
[NASA-CR-190702] p 3932 N92-33063
AERODYNAMIC CONFIGURATIONS
A method for designing blended wing-body configurations for low wave drag
[NASA-TP-3261] p 3929 N92-32480
New concepts for multi-block grid generation for flow domains around complex aerodynamic configurations
[NLR-TP-91046-U] p 3930 N92-32730
AERODYNAMIC DRAG
Further wind tunnel investigation of the SM701 airfoil with aileron and turbulators
[NASA-CR-190702] p 3932 N92-33063
AERODYNAMIC LOADS
Aerodynamic centre of wing-body combinations
[ESDU-92024] p 3929 N92-32479
AERODYNAMIC NOISE
Fourth Aircraft Interior Noise Workshop
[NASA-CP-10103] p 4061 N92-32948
Acoustic loads prediction on jet aircraft p 4061 N92-32949
AERODYNAMICS
ROAR: A 3-D tethered rocket simulation code
[DE92-017358] p 3944 N92-33166
AEROELASTICITY
Strong coupling between inviscid fluid and boundary layer of sharp leading edges: Two-dimensional stationary and turbulent cases for isolated profiles and guard vanes
[ONERA-RT-44/1621-RY-016-R] p 4010 N92-32776
AERONAUTICAL ENGINEERING
United States Air Force summer research program 1991. Volume 1: Program management report
[AD-A248763] p 4103 N92-32338
NASA authorization, 1993, volume 1
[GPO-55-260-VOL-1] p 4092 N92-33147
AERONAUTICS
An international aerospace information system: A cooperative opportunity
[NASA-TM-108171] p 4091 N92-33237
AEROSOLS
Infrared properties of Titan's clouds and aerosols p 4097 N92-32373
Cassini/CIRS capabilities for aerosol, cloud, and surface measurements p 4098 N92-32378
Huygens/ACP: An instrument for aerosols chemical composition measurements p 4098 N92-32379
Huygens/ASI plasma wave analyzer capabilities for aerosol measurement p 4098 N92-32380
Formation and growth of photochemical aerosols in Titan's atmosphere p 4100 N92-32393
Properties and distribution of the aerosols in the atmosphere of Titan p 4100 N92-32396
Laboratory investigations of the aerosols in the stratosphere of Titan p 4102 N92-32405
On the interpretation of Titan's intensity and polarization phase curve p 4102 N92-32407
Execution of measurement sequences in the framework of the inspection of near limit regions by radioiodine and aerosol emission measurements, and ground examinations on plutonium, strontium, and gamma ray radionuclides
[OEFZS-4579] p 4071 N92-32763
SAGE 1 data user's guide
[NASA-RP-1275] p 4031 N92-33097
AEROSPACE ENGINEERING
MANTECH project book
[AD-A245283] p 3977 N92-32461
University of Toronto Institute for Aerospace Studies
[CTN-92-60375] p 4104 N92-32853
Fifty years in science, thirty years in space
[LALP-92-51] p 4104 N92-32862
An international aerospace information system: A cooperative opportunity
[NASA-TM-108171] p 4091 N92-33237
AEROSPACE ENVIRONMENTS
Satellite anomalies and electrostatic surface discharges
[AD-A246880] p 3942 N92-32538
The energetic radiation environment in a highly elliptical (Molniya) orbit
[AD-A252394] p 4031 N92-32902
AEROSPACE INDUSTRY
China's aerospace industry: Technology, funding, and modernization
[AD-A252618] p 3929 N92-32691
AEROSPACE MEDICINE
DCIEM/Central Medical Board Aircrew ECG program: Recommendations for restructuring
[DCIEM-90-47] p 4037 N92-32816
Fifty years in science, thirty years in space
[LALP-92-51] p 4104 N92-32862
AEROSPACE SCIENCES
An international aerospace information system: A cooperative opportunity
[NASA-TM-108171] p 4091 N92-33237
AEROSPACE SYSTEMS
NASA space applications of high-temperature superconductors p 3985 N92-32980
Fuzzy set methods for object recognition in space applications
[NASA-CR-190388] p 4047 N92-33093
AEROSPACE TECHNOLOGY TRANSFER
An international aerospace information system: A cooperative opportunity
[NASA-TM-108171] p 4091 N92-33237
AEROSPACE VEHICLES
Thermal degradation study of silicon carbide threads developed for advanced flexible thermal protection systems
[NASA-TM-103952] p 3970 N92-32476
AFFERENT NERVOUS SYSTEMS
Midwest free-electron laser program
[AD-A247264] p 4016 N92-32540
AFTERBODIES
Aerodynamic centre of wing-body combinations
[ESDU-92024] p 3929 N92-32479
AGGLOMERATION
Study of flow properties of wet solids using laser induced photochemical anemometry
[DE92-015452] p 4013 N92-33140
AGGREGATES
Formation and growth of photochemical aerosols in Titan's atmosphere p 4100 N92-32393
Laboratory investigations of the aerosols in the stratosphere of Titan p 4102 N92-32405
AGING (MATERIALS)
Life testing of a low voltage air circuit breaker
[DE92-014173] p 3988 N92-32635
Pump and valve research at the Oak Ridge National Laboratory
[DE92-014419] p 4019 N92-32890
Evaluation of the effects of the environment on the behavior of the primary structures of composite material aircraft in service: Historic and current situation p 3958 N92-33048
AGRICULTURE
Permuted keyword bank in CRIS. Terms for indexing and retrieving research projects in the current research information system
[PB92-179456] p 4090 N92-32712
AILERONS
Further wind tunnel investigation of the SM701 airfoil with aileron and turbulators
[NASA-CR-190702] p 3932 N92-33063
AIR
Life testing of a low voltage air circuit breaker
[DE92-014173] p 3988 N92-32635
The oxidation of Type 310S stainless steel in mixed gases at elevated temperatures
[DE92-014941] p 3968 N92-32991
Computational and experimental study of laminar flames
[DE92-017978] p 3965 N92-33121
AIR DEFENSE
The DOD science and technology strategy
[AD-A253691] p 4104 N92-33027
DoD key technologies plan
[AD-A253692] p 4105 N92-33238
AIR FLOW
Phase distribution measurements in narrow rectangular channels using image-processing techniques
[DE92-014084] p 4006 N92-32468
Demand controlled ventilating systems: Sensor market survey. Energy conservation in buildings and community systems programme, annex 18, December 1991
[PB92-180892] p 3977 N92-32825
AIR NAVIGATION
The 1991 Federal Aviation Administration plan for research, engineering and development p 4103 N92-32453
CTAS: Computer intelligence for air traffic control in the terminal area
[NASA-TM-103959] p 3933 N92-33080
AIR POLLUTION
High-temperature Solid Oxide Fuel Cell (SOFC) generator development project: Environmental assessment
[DE92-014698] p 4026 N92-32924
International research into chlorofluorocarbon (CFC) alternatives
[DE92-014241] p 4030 N92-32986
Direct catalytic decomposition of nitric oxide
[DE92-013847] p 4030 N92-33125
AIR QUALITY
Demand controlled ventilating systems: Sensor market survey. Energy conservation in buildings and community systems programme, annex 18, December 1991
[PB92-180892] p 3977 N92-32825
High-temperature Solid Oxide Fuel Cell (SOFC) generator development project: Environmental assessment
[DE92-014698] p 4026 N92-32924
Guide to selected national environmental statistics in the US Government
[PB92-201144] p 4030 N92-33087
AIR SAMPLING
Phase distributions of airborne polycyclic aromatic hydrocarbons in two US cities
[PB92-164979] p 4028 N92-32543
AIR TRAFFIC
Analysis of delay reducing and fuel saving sequencing and spacing algorithms for arrival traffic
[NASA-TM-103880] p 3933 N92-33194
AIR TRAFFIC CONTROL
The 1991 Federal Aviation Administration plan for research, engineering and development p 4103 N92-32453
Safety study of TCAS 2 for logic version 6.04
[DOT/FAA/RD-92/22] p 3933 N92-32537
Airport Surveillance Radar (ASR-9) wind shear processor: 1991 test at Orlando, Florida
[AD-A252246] p 3980 N92-32686

Air traffic control: FAA's advanced automation system contract
[GAO/IMTEC-91-25] p 3934 N92-32861
CTAS: Computer intelligence for air traffic control in the terminal area
[NASA-TM-103959] p 3933 N92-33080
Simulation test and evaluation of TCAS 2 logic version 6.04
[DOT/FAA/RD-92/23] p 3934 N92-33098
Analysis of delay reducing and fuel saving sequencing and spacing algorithms for arrival traffic
[NASA-TM-103880] p 3933 N92-33194

AIR TRAFFIC CONTROLLERS (PERSONNEL)
Exposures from headset interference tones
[AD-A247175] p 4061 N92-32697

AIR WATER INTERACTIONS
ARM Tropical Pacific Experiment (ATPEX): Role of cloud, water vapor and convection feedbacks in the coupled ocean/atmosphere system
[DE92-013772] p 4032 N92-32331
Simulations of the carbon cycle in the oceans
[DE92-016622] p 4035 N92-32336

AIRBORNE EQUIPMENT
Multisensor airborne target acquisition systems and their integration p 3936 N92-32439

AIRCRAFT ACCIDENT INVESTIGATION
Aircraft accident report: L'Express Airlines, Inc., Flight 508, Beech C99, N7217L weather encounter and crash near Birmingham, Alabama, July 10, 1991
[PB92-910401] p 3932 N92-32455

AIRCRAFT ACCIDENTS
Aircraft accident report: L'Express Airlines, Inc., Flight 508, Beech C99, N7217L weather encounter and crash near Birmingham, Alabama, July 10, 1991
[PB92-910401] p 3932 N92-32455

AIRCRAFT APPROACH SPACING
Analysis of delay reducing and fuel saving sequencing and spacing algorithms for arrival traffic
[NASA-TM-103880] p 3933 N92-33194

AIRCRAFT COMMUNICATION
The 1991 Federal Aviation Administration plan for research, engineering and development
p 4103 N92-32453
A lightweight loudspeaker for aircraft communications and active noise control p 3988 N92-32964
Feasibility of measuring transverse electric noise at VLF and LF on an ice cap
[AD-A252280] p 4035 N92-33220

AIRCRAFT COMPARTMENTS
Vibro-acoustic FE analyses of the Saab 2000 aircraft
p 4062 N92-32952
Advanced Study for Active Noise Control in Aircraft (ASANCA)
[AIAA PAPER 92-2092] p 4062 N92-32956

AIRCRAFT CONSTRUCTION MATERIALS
Eighth DOD/NASA/FAA Conference on Fibrous Composites in Structural Design, part 2
[NASA-CP-3087-PT-2] p 3950 N92-32574
Residual strength of repaired graphite/epoxy laminates after 5 years of outdoor exposure p 3950 N92-32577
Damage tolerance certification methodology for composite structures p 3951 N92-32579
Investigation of a relationship between uniaxial and biaxial chemical stress crazing of cast acrylic
[AD-A250852] p 4021 N92-32621
Examples of advanced near-net shape manufacturing techniques for aerospace
[MBB-Z-0399-91-PUB] p 3977 N92-32742

AIRCRAFT CONTROL
A background to the handling qualities of aircraft
[ESDU-92006] p 3939 N92-32780

AIRCRAFT DESIGN
A method for designing blended wing-body configurations for low wave drag
[NASA-TP-3261] p 3929 N92-32480
Eighth DOD/NASA/FAA Conference on Fibrous Composites in Structural Design, part 1
[NASA-CP-3087-PT-1] p 3946 N92-32513
Design, evaluation and experimental effort toward development of a high strain composite wing for Navy aircraft p 3947 N92-32514
Development of thermoplastic components for structural validation p 3948 N92-32522
Global/local methods research using the CSM testbed
p 3949 N92-32528
Computational methods for global/local analysis
[NASA-TM-107591] p 4023 N92-33104

AIRCRAFT ENGINES
Liquid lubricants for advanced aircraft engines
[NASA-TM-104531] p 3972 N92-32863
Bird ingestion into large turbofan engines
[DOT/FAA/CT-91/17] p 3932 N92-33005
Statistics on aircraft gas turbine engine rotor failures that occurred in US commercial aviation during 1988
[DOT/FAA/CT-91/28] p 3938 N92-33105

AIRCRAFT EQUIPMENT
Airborne experimental FLIR program
p 3937 N92-32447
PDES application protocol suite for composites (PAS-C). Functional needs report for the PAS-C program
[AD-A247886] p 3953 N92-32629

AIRCRAFT GUIDANCE
Development of new flight procedures for the Microwave Landing System (MLS)
[NLR-TP-91156-U] p 3933 N92-32830
CTAS: Computer intelligence for air traffic control in the terminal area
[NASA-TM-103959] p 3933 N92-33080

AIRCRAFT INDUSTRY
Examples of advanced near-net shape manufacturing techniques for aerospace
[MBB-Z-0399-91-PUB] p 3977 N92-32742

AIRCRAFT INSTRUMENTS
Instrument scanning and subjective workload with the peripheral vision horizon display
[CTN-92-60359] p 4038 N92-32817

AIRCRAFT LANDING
Flight testing and simulation of an F-15 airplane using throttles for flight control
[NASA-TM-104255] p 3940 N92-32864
CTAS: Computer intelligence for air traffic control in the terminal area
[NASA-TM-103959] p 3933 N92-33080

AIRCRAFT MANEUVERS
Tactical state and performance assessment during air combat maneuvering
[AD-A247426] p 3935 N92-32612
Rapid development of the X-31 simulation to support flight-testing
[NASA-TM-104256] p 3935 N92-33149

AIRCRAFT NOISE
Fourth Aircraft Interior Noise Workshop
[NASA-CP-10103] p 4061 N92-32948
MD-80 aft cabin noise control: A case history
p 4061 N92-32950
The Dornier 328 Acoustic Test Cell (ATC) for interior noise tests and selected test results
[AIAA PAPER 92-2164] p 4062 N92-32951
Use of SEA to predict structure-borne noise in aircraft
p 4062 N92-32955
Advanced Study for Active Noise Control in Aircraft (ASANCA)
[AIAA PAPER 92-2092] p 4062 N92-32956
Active control of interior noise in a large scale cylinder using piezoelectric actuators p 4063 N92-32958
Active vibrations and noise control for turboprop application research program activities
p 4063 N92-32962
Active synchrophasing of propeller unbalance
p 4063 N92-32963
A lightweight loudspeaker for aircraft communications and active noise control p 3988 N92-32964
Building vibrations induced by noise from rotorcraft and propeller aircraft flyovers
[NASA-TM-104170] p 4063 N92-33160

AIRCRAFT PERFORMANCE
Tactical state and performance assessment during air combat maneuvering
[AD-A247426] p 3935 N92-32612
The design and development of a portable, DSP micro-processor based, high-accuracy data acquisition system
[NRC-32146] p 4040 N92-32851

AIRCRAFT PILOTS
Instrument scanning and subjective workload with the peripheral vision horizon display
[CTN-92-60359] p 4038 N92-32817

AIRCRAFT RELIABILITY
Tactical state and performance assessment during air combat maneuvering
[AD-A247426] p 3935 N92-32612
A background to the handling qualities of aircraft
[ESDU-92006] p 3939 N92-32780

AIRCRAFT SAFETY
The 1991 Federal Aviation Administration plan for research, engineering and development
p 4103 N92-32453
Aircraft accident report: L'Express Airlines, Inc., Flight 508, Beech C99, N7217L weather encounter and crash near Birmingham, Alabama, July 10, 1991
[PB92-910401] p 3932 N92-32455
A review and discussion of flight management system incidents reported to the aviation safety reporting system
[AD-A252438] p 3932 N92-32941

AIRCRAFT STRUCTURES
Design, analysis, and testing of a reusable wingbox for ballistic evaluation of composite structures
p 3947 N92-32518
A Protection And Detection Surface (PADS) for damage tolerance p 3948 N92-32523
Global/local methods research using the CSM testbed
p 3949 N92-32528
Evaluation of composite components on the Bell 206L and Sikorsky S-76 helicopters p 3950 N92-32575
Damage tolerance certification methodology for composite structures p 3951 N92-32579
Detection of honeycomb damage using hexagonal grid discontinuities
[DREP-89-9] p 3955 N92-32846
Aspects of compression in aerospace composites: Future requirements p 3956 N92-33036
Evaluation of the effects of the environment on the behavior of the primary structures of composite material aircraft in service: Historic and current situation
p 3958 N92-33048
Computational methods for global/local analysis
[NASA-TM-107591] p 4023 N92-33104

AIRFOILS
Further wind tunnel investigation of the SM701 airfoil with aileron and turbulators
[NASA-CR-190702] p 3932 N92-33063

AIRFRAME MATERIALS
Structural assessment of ultralightweight composites
p 3948 N92-32525
Out of plane analysis for composite structures
p 3949 N92-32527

AIRFRAMES
Structural assessment of ultralightweight composites
p 3948 N92-32525
PDES application protocol suite for composites (PAS-C). Functional needs report for the PAS-C program
[AD-A247886] p 3953 N92-32629

AIRLINE OPERATIONS
Aircraft accident report: L'Express Airlines, Inc., Flight 508, Beech C99, N7217L weather encounter and crash near Birmingham, Alabama, July 10, 1991
[PB92-910401] p 3932 N92-32455
Statistics on aircraft gas turbine engine rotor failures that occurred in US commercial aviation during 1988
[DOT/FAA/CT-91/28] p 3938 N92-33105

AIRPORTS
Airport Surveillance Radar (ASR-9) wind shear processor: 1991 test at Orlando, Florida
[AD-A252246] p 3980 N92-32686
Air traffic control: FAA's advanced automation system contract
[GAO/IMTEC-91-25] p 3934 N92-32861
Performance of insulated pavements at Newton Fields, Jackman, Maine
[CRREL-92-9] p 3940 N92-32903

AIRY FUNCTION
Numerical evaluation of the incomplete airy functions and their application to high frequency scattering and diffraction
[NASA-CR-190745] p 4058 N92-32888

ALBEDO
Titan's UV albedo: Observations and modeling
p 4094 N92-32356
Titan's mid-IR albedo: New observations from 3 to 5 microns p 4097 N92-32376

ALCOHOLS
NQR-NMR studies of higher alcohol synthesis Cu-Co catalysts
[DE92-016614] p 3960 N92-32347
High octane ethers from synthesis gas-derived alcohols
[DE92-013802] p 3975 N92-33108

ALGORITHMS
Optimum design of ninety degree bends
p 4000 N92-32274
Comparison between the PISO algorithm and preconditioning methods for compressible flow
p 4001 N92-32284
Transverse beam dynamics in recirculating accelerators for heavy-ion fusion
[DE92-013448] p 4070 N92-32413
An adaptive algorithm for modifying hyperellipsoidal decision surfaces
[DE92-013540] p 4041 N92-32414
Safety study of TCAS 2 for logic version 6.04
[DOT/FAA/RD-92/22] p 3933 N92-32537
Intelligent signal processing for active control
[AD-A252232] p 4053 N92-32625
An examination of several high resolution schemes applied to complex problems in high speed flows
[AD-A250814] p 4008 N92-32632
Balance in machine architecture: Bandwidth on board and offboard, integer/control speed and flops versus memory
[DE92-016006] p 4040 N92-32642
Adaptive information processing and global optimization
[AD-A248450] p 4089 N92-32644
Frequency domain state-space system identification
[NASA-TM-107659] p 4021 N92-32657

Finding solutions to value independent knapsack problems
[INPE-5390-TAE/011] p 4055 N92-32661
Consistency and robustness of knowledge graphs
[ISBN-90-9003729-2] p 4056 N92-32679
Airport Surveillance Radar (ASR-9) wind shear processor: 1991 test at Orlando, Florida
[AD-A252246] p 3980 N92-32686
Tolerance optimization of servomechanisms
[ISBN-90-9004476-0] p 4018 N92-32692
Minimum cost multiflows in undirected networks
[IMAG-RR-849-M] p 4056 N92-32710
Advanced computational transport methods for curvilinear geometries
[DE92-011290] p 4057 N92-32743
Parallel implementation of Droid and performance evaluation
[OUEL-1926/92] p 4051 N92-32759
Resolution of convection and diffusion by the boolean automata method
[ONERA-RF-22/3419-AY-122A] p 4057 N92-32772
Three dimensional object reconstruction using a very limited number of projections. Application to industrial radiography
[TELECOM-91-E-008] p 4043 N92-32804
Enhancements to speech recognition on voice response systems
[TELECOM-91-E-018] p 3981 N92-32807
Poincare normal form (system of ordinary differential equations): An algorithmic point of view
[IMAG-RR-839-M] p 4058 N92-32838
The use of Kalman filtering techniques to improve the accuracy of flight test data
[NRC-32139] p 3938 N92-32850
ABF algorithms implemented at ARL:UT, FDS system engineering and acoustics
[AD-A252368] p 4046 N92-32917
Experiments with an ordinary differential equation solver in the parallel solution of method of lines problems on a shared memory parallel computer, part 2
[DE92-017159] p 4052 N92-32926
Selecting a subset of stimulus-response pairs with maximal transmitted information
[AD-A252728] p 3986 N92-32987
Obstacle avoidance for redundant robots using configuration control
[NASA-CASE-NPO-17852-1-CU] p 4054 N92-33019
Sparse matrix algorithms on distributed memory multiprocessors
[DE92-017870] p 4046 N92-33071
Semiannual status report
[NASA-CR-190239] p 4046 N92-33092
Sweeping algorithms for five-point stencils and banded matrices
[DE92-017309] p 4047 N92-33118
A precise narrow-beam filter infrared radiometer and its use with lidar in the ARM Program
[DE92-016872] p 4015 N92-33188
Analysis of delay reducing and fuel saving sequencing and spacing algorithms for arrival traffic
[NASA-TM-103880] p 3933 N92-33194
CSP: A distributed logic programming language for discrete event simulation
[ISBN-0-315-54272-1] p 4048 N92-33214
A fast task allocator for multiprocessing systems
[ISBN-0-315-54380-9] p 4053 N92-33217

ALIGNMENT
Transverse beam dynamics in recirculating accelerators for heavy-ion fusion
[DE92-013448] p 4070 N92-32413

ALKANES
Thermal conductivity of liquid aliphatic hydrocarbons. Part 1: Alkanes
[ESDU-92011-PT-1] p 3945 N92-32484
Solar photo-thermal catalytic reactions to produce high value chemicals
[DE91-002140] p 4026 N92-32908
Continuum configurational bias Monte-Carlo studies of alkanes and polyethylene
[DE92-016545] p 3965 N92-33185

ALKENES
Mass resolved resonance ionization spectroscopy of combustion radicals
[DE92-016833] p 3965 N92-33222

ALKYD RESINS
Corrosion-resistant alkyd coatings
[AD-D015330] p 3974 N92-33177

ALKYL COMPOUNDS
The effect of surface pressure on the Langmuir-Blodgett polymerization of 2-pentadecyl aniline
[AD-A251141] p 3971 N92-32550

ALLOYING
Synthesis of MoSi2-based alloys by mechanical alloying
[DE92-017528] p 3969 N92-33120

ALLOYS
Mechanisms of the oxidation of metals and alloys with emphasis on superconductors
[DE92-016840] p 3966 N92-32315
Fundamental questions concerning the application of superplastic forming and superplastic forming/diffusion bonding
[MBB-Z-0402-91-PUB] p 3977 N92-32690
National Research Council Industrial Materials Institute: From knowledge to know-how
[CTN-92-60333] p 4103 N92-32814
National Research Council Industrial Materials Institute: From knowledge to know-how
[CTN-92-60334] p 4104 N92-32815

ALPHA PARTICLES
Alpha particle diagnostics using impurity pellet injection
[DE92-013796] p 4078 N92-32623

ALTERNATING CURRENT
AC microcalorimetry of adsorbates on evaporated metal films: Orientational ordering of H2 multilayers
[DE92-008317] p 3963 N92-32666

ALTERNATING DIRECTION IMPLICIT METHODS
Computation of the flow field in a centrifugal impeller with splitter blades p 4002 N92-32289

ALTERNATIVES
An analytical screening of alternatives for R-502 in low-temperature refrigerating applications
[DE92-017162] p 3978 N92-32927
International research into chlorofluorocarbon (CFC) alternatives
[DE92-014241] p 4030 N92-32986

ALTITUDE
User's manual for AeroFcn: A FORTRAN program to compute aerodynamic parameters
[NASA-TM-104237] p 4042 N92-32507

ALUMINIDES
High temperature fabricable nickel-iron aluminides
[CA-PATENT-1-276-814] p 3968 N92-32855
Weldability of Fe3Al based iron aluminide alloys
[DE92-017802] p 4020 N92-33085

ALUMINUM
Implanted aluminum: Tribological behavior and mechanical properties of the superficial layers
[ECL-91-28] p 4019 N92-32801
Contribution to the study of the effect of the heterogeneous distribution of dislocations on the cyclic plasticity of single crystal aluminum
[ISAL-91-0099] p 4083 N92-32892
The energetic radiation environment in a highly elliptical (Molniya) orbit
[AD-A252394] p 4031 N92-32902

ALUMINUM ALLOYS
An in vitro corrosion study of two implant materials using electrochemical impedance spectroscopy and potentiodynamic polarization
[AD-A252575] p 3966 N92-32626
Thermal strains in titanium aluminide and nickel aluminide composites
[DE92-015181] p 3953 N92-32638
Synthesis, microsctructure, and mechanical properties of zirconia-alumina composites
[ISBN-90-9004656-9] p 3954 N92-32677
Guide to the effect of shot peening on fatigue strength
[ESDU-92015] p 3967 N92-32779
Aluminum based particulate composites for aerospace applications produced by different processes
[MBB-Z-0408-91-PUB] p 3967 N92-32819
Superplastic forming of Ti6Al4V at lower temperature using hydrogen
[MBB-Z-0403-91-PUB] p 3978 N92-32893
Accommodation mechanisms and dispersoid-free zone s in Al 7475 after superplastic forming
[MBB-Z-0404-91-PUB] p 3968 N92-32894
New accelerated corrosion test methods
[MBB-Z-0406-91-PUB] p 3968 N92-32895
Investigation of fracture toughness and fracture mechanisms using acoustic emission measurements
[DE92-011907] p 4022 N92-32911
An experimental study on the two-parameter crack tip field
[AD-A251173] p 4023 N92-32936
Environmental degradation of high temperature composites p 3958 N92-33047

ALUMINUM COMPOUNDS
High temperature deformation processes and strengthening mechanisms in intermetallic particulate composites
[AD-A250220] p 3946 N92-32339

ALUMINUM GALLIUM ARSENIDES
Development of ultra-low noise, high sensitivity planar metal grating coupled AlGaAs/GaAs multiquantum well IR detectors for focal plane array staring IR sensor systems
[AD-A250368] p 4083 N92-32747
Intermodulation in the oscillatory magnetoresistance of a two-dimensional electron gas p 3984 N92-32975
Reduced mobility and PPC in In(.20)Ga(.80)As / Al(.23)Ga(.77)As HEMT structure p 3984 N92-32976

ALUMINUM NITRIDES
Microwave absorption by lossy ceramic materials
[DE92-016963] p 3970 N92-32317

ALUMINUM OXIDES
Thickness dependence of vortex pinning in epitaxial Tl-Ca-Ba-Cu-O thin films
[DE92-015011] p 4084 N92-32920
Clean gasoline reforming with superacid catalysts
[DE92-013833] p 3975 N92-33123
Modification of the optical properties of Al2O3 by ion implantation
[DE92-013861] p 4085 N92-33127

ALUMINUM-LITHIUM ALLOYS
Environmental fatigue in aluminum-lithium alloys
[NASA-TM-107640] p 4021 N92-32423
A prototype backside purge control system
[NASA-CR-190816] p 3969 N92-33081

AMMONIA
Novel gas phase ion molecule reactions of C60(++) with O2 and NH3
[AD-A250921] p 4066 N92-32556
Heat and mass exchange during condensation of a water-ammonia mixture
[DE92-014524] p 3962 N92-32557
Thermal gravitational modelling and scaling of two-phase heat transport systems for space: An assessment and a comparison of predictions and experimental results
[NLR-TP-91401-U] p 4008 N92-32675

AMMONIUM COMPOUNDS
Thermochemical cycles for energy storage: Thermal decomposition of ZnSO4 systems
[DE91-002144] p 4026 N92-32909

AMMONIUM NITRATES
Development of a minimum smoke propellant based on glycidyl azide polymer and ammonium nitrate p 3976 N92-33243
Hazards reduction for tactical missiles p 3945 N92-33245

AMMUNITION
Insensitive Munitions
[AGARD-CP-511] p 3975 N92-33240
The United States Air Force explosives hazards reduction program p 3976 N92-33241

AMORPHOUS MATERIALS
Surfaces and thin films studied by picosecond ultrasonics
[DE92-016313] p 4020 N92-32564
Orientation, stress, and density distributions in injection-moulded amorphous polymers determined by optical techniques
[ETN-92-92052] p 3972 N92-32752
Environmental resistance of amorphous bonded thermoplastic joints p 3959 N92-33053
Dynamics of radiation-induced amorphization in intermetallic compounds
[DE92-016774] p 4086 N92-33221

AMPHIBIOUS VEHICLES
Composite structural armor for combat vehicle applications p 3947 N92-32515

AMPLIFIERS
A flexible CPW package for a 30 GHz MMIC amplifier p 3983 N92-32972
Performance of a Y-Ba-Cu-O superconducting filter/GaAs low noise amplifier hybrid circuit p 3985 N92-32982

AMPLITUDES
Multifrequency measurements of radar ground clutter at 42 sites. Volume 1: Principal results
[AD-A246710] p 3980 N92-32696

ANALOG CIRCUITS
Analog CMOS filters for very-high frequencies
[ISBN-90-9004420-5] p 3986 N92-33143
A simplified synthesis of lossless two-port wave digital and analog filters
[ISBN-0-315-63272-0] p 3993 N92-33193

ANALOGIES
Auto and hetero-associative memory using a 2-D optical logic gate
[NASA-CASE-NPO-17997-1-CU] p 4041 N92-33057

ANALOGS
Generalizations of the classical Laguerre polynomials and some q-analogues
[ISBN-90-9003765-9] p 4058 N92-32836

ANALYSIS (MATHEMATICS)
Dissimilarities, dendograms, prefillers, and multiapplications of levels
[IMAG-RR-842-M] p 4058 N92-32799
A unique method of determining the elastic and engineering constants of unidirectional fibre-reinforced composite plates using ultrasound
[UTIAS-TN-274] p 3955 N92-32829

ANALYTIC GEOMETRY
Analytic score comparison of geometry splitting and exponential transform for a simple Monte Carlo problem
[DE92-013108] p 4059 N92-32481
Geometric continuity and Frenet continuity of parametric curves
[IMAG-RR-846-M] p 4057 N92-32761
ANALYZERS
Huygens/ASI plasma wave analyzer capabilities for aerosol measurement p 4098 N92-32380
Theory and numerical simulation of some wide-angle wide-bandpass plasma particle analyzers
[ISBN-0-315-58015-1] p 4080 N92-33223
ANEMOMETERS
Wind tunnel test of Teledyne Geotech model 1564B cup anemometer
[DE92-009590] p 4013 N92-32460
ANESTHESIA
Midwest free-electron laser program
[AD-A247264] p 4016 N92-32540
ANGIOGRAPHY
Kinematics of Compton backscattering x ray source for angiography
[DE92-014016] p 4073 N92-33179
ANGULAR CORRELATION
PAC spectroscopy of electronic ceramics
[DE92-014328] p 3970 N92-32471
ANGULAR DISTRIBUTION
On the choice of minimization functional in the partial wave analysis
[DE92-624689] p 4087 N92-32309
Neutron scatter studies of chromatin structures related to functions
[DE92-014032] p 4036 N92-33181
ANGULAR MOMENTUM
Robust stabilization of the Space Station
[NASA-CR-190627] p 3942 N92-32244
Simplified model of electron scattering on atomic hydrogen
[DE92-625007] p 4065 N92-32499
ANILINE
The effect of surface pressure on the Langmuir-Blodgett polymerization of 2-pentadecyl aniline
[AD-A251141] p 3971 N92-32550
ANISOTROPIC PLATES
Initial postbuckling response of an unsymmetrically laminated rectangular plate p 3952 N92-32586
ANISOTROPIC SHELLS
An implementation of Hill's theory of normal anisotropic plasticity for explicit shell analysis
[DE92-011468] p 4020 N92-32328
ANISOTROPY
Anisotropic electrical resistivity of YBCO/PBCO superlattice films grown on miscut substrates
[DE92-014409] p 4082 N92-32636
Contribution to robot-task adaptation, introduction and use of robot anisotropy and task object for the design of the workstation
[ISAL-91-0095] p 4039 N92-33056
ANNEALING
Formation of high temperature superconductors from the solidified melt
[DE92-012584] p 4081 N92-32465
Transmission electron microscope characterization of deformation and recovery in 304L stainless steel part
[DE92-013237] p 3966 N92-32614
Adaptive information processing and global optimization
[AD-A248450] p 4089 N92-32644
T (sub c)-delta relations in YBa2Cu3O(7-delta) thin films: Effects of oxygen pressure during growth
[DE92-014432] p 4083 N92-32653
Implantation of carbon in GaAs
[DE92-016921] p 4085 N92-33117
Modification of the optical properties of Al2O3 by ion implantation
[DE92-013861] p 4085 N92-33127
ANNUAL VARIATIONS
Annual variation of surface temperatures over the world
[PB92-193259] p 4028 N92-32554
ANODES
Electrocatalysis of anodic, oxygen-transfer reactions at noble metal electrodes
[DE92-016308] p 3962 N92-32562
ANOMALIES
Satellite anomalies and electrostatic surface discharges
[AD-A246880] p 3942 N92-32538
Density variations and anomalies in palladium compacts
[DE92-014382] p 3967 N92-32721
Climate System Monitoring (CSM) Monthly Bulletin, issue no. 1 p 4034 N92-33073
Partons and the EMC spin effect
[RAL-92-015-PREPRINT] p 4068 N92-33137
Applications of statistical methods to the study of climate and flooding fluctuations in the central US
[PB92-205137] p 4034 N92-33173
ANTENNA ARRAYS
A finite element-boundary integral method for conformal antenna arrays on a circular cylinder
[NASA-CR-190610] p 3979 N92-32559
Phased array implementation using elements with scan capability
[CTN-92-60335] p 3981 N92-32787
Phase-only synthesis for multiple-beam phased arrays with element failures
[AD-A252250] p 3982 N92-32891
V-band pseudomorphic HEMT MMIC phased array components for space communications p 3983 N92-32966
An optically controlled Ka-band phased array antenna p 3983 N92-32968
Ka-band dual frequency array feed for a low cost ACTS ground terminal p 3983 N92-32969
Coplanar waveguide feeds for phased array antennas p 3983 N92-32970
Techniques for the synthesis of wideband, series-fed arrays of microstrip patch radiators
[ISBN-0-315-58991-4] p 3987 N92-33209
ANTENNA DESIGN
A finite element-boundary integral method for conformal antenna arrays on a circular cylinder
[NASA-CR-190610] p 3979 N92-32559
Phased array implementation using elements with scan capability
[CTN-92-60335] p 3981 N92-32787
Ka-band dual frequency array feed for a low cost ACTS ground terminal p 3983 N92-32969
Techniques for the synthesis of wideband, series-fed arrays of microstrip patch radiators
[ISBN-0-315-58991-4] p 3987 N92-33209
ANTENNA FEEDS
Ka-band dual frequency array feed for a low cost ACTS ground terminal p 3983 N92-32969
Coplanar waveguide feeds for phased array antennas p 3983 N92-32970
ANTENNA RADIATION PATTERNS
Phased array implementation using elements with scan capability
[CTN-92-60335] p 3981 N92-32787
Planar dielectric resonator stabilized HEMT oscillator integrated with CPW/aperture coupled patch antenna p 3983 N92-32967
Measurement techniques for cryogenic Ka-band microstrip antennas p 3985 N92-32981
Numerical analysis of scattering from certain conducting and dielectric bodies of arbitrary shape
[ISBN-0-315-63282-8] p 3987 N92-33192
ANTIBODIES
Small passive chemical detector
[DE92-014188] p 4030 N92-32933
ANTIHISTAMINICS
Comparative effects of antihistamines on aircrew performance of simple and complex tasks under sustained operations
[AD-A248752] p 4036 N92-32492
ANTIMATTER
Quark-antiquark Regge trajectories in large N(sub c) QCD
[DE92-016462] p 4064 N92-32313
ANTIPROTONS
Comparison of spin asymmetries and invariant cross sections in production of (pi)(sup 0) mesons by polarized antiprotons and protons with 200 GeV energy
[DE92-624691] p 4064 N92-32311
Heavy flavor physics at hadron colliders
[DE92-014482] p 4064 N92-32312
A study of four jet events and search for double parton scattering at square root s = 1.8 TeV
[DE92-016351] p 4069 N92-33164
ANTISEPTICS
Development of static system procedures to study aquatic biofilms and their responses to disinfection and invading species
[NASA-TM-103598] p 4036 N92-33103
ANTISHIP MISSILES
Interception of LPI radar signals
[AD-A246315] p 3978 N92-32535
ANTITANK MISSILES
The German anti tank helicopter PAH 2: An example of a future sensor platform p 3937 N92-32448
APPLICATION SPECIFIC INTEGRATED CIRCUITS
Generic modular imaging IR signal processor p 3936 N92-32440
APPLICATIONS PROGRAMS (COMPUTERS)
Development of a CFD code for internal flows in liquid fueled engines p 3999 N92-32271
Development of the KIVA-2 CFD code for rocket propulsion applications p 3945 N92-32272
A multi-domain method for subsonic viscous flows p 3960 N92-32275
SSME HPOTP impeller backcavity CFD analysis p 4003 N92-32294
An efficient and robust grid optimization algorithm p 4004 N92-32300
Enhancements to the GRIDGEN structured grid generation system for internal and external flow applications p 4005 N92-32301
Potential flow theory and operation guide for the panel code PMARC
[NASA-TM-102851] p 3929 N92-32422
Computations of unsteady multistage compressor flows in a workstation environment
[NASA-TM-103839] p 3938 N92-32452
Computational simulation of matrix micro-slip bands in SiC/Ti-15 composite
[NASA-TM-105762] p 3946 N92-32466
User's manual for AeroFcn: A FORTRAN program to compute aerodynamic parameters
[NASA-TM-104237] p 4042 N92-32507
Safety study of TCAS 2 for logic version 6.04
[DOT/FAA/RD-92/22] p 3933 N92-32537
Relativistic heavy ion collisions
[DE92-014415] p 4066 N92-32600
Further development of the CANAERO computer code to include propulsor modelling
[DREA-CR-90-425] p 3931 N92-32811
Advanced software development workstation: Effectiveness of constraint-checking --- spaceflight simulation and planning
[NASA-CR-190712] p 4043 N92-32865
Independent verification and validation for Space Shuttle flight software
[NASA-CR-190826] p 4047 N92-33196
APPROACH CONTROL
Development of new flight procedures for the Microwave Landing System (MLS)
[NLR-TP-91156-U] p 3933 N92-32830
APPROPRIATIONS
Departments of Veterans Affairs and Housing and Urban Development, and independent agencies appropriations for 1993, part 6
[GAO-55-636-PT-6] p 4091 N92-32505
NASA authorization, 1993, volume 1
[GPO-55-260-VOL-1] p 4092 N92-33147
APPROXIMATION
A new approximate fracture mechanics analysis methodology for composites with a crack or hole p 3949 N92-32530
Numerical simulation of two-dimensional flows by the free-Lagrangian method
[TUM-M9105] p 4009 N92-32767
Approximations and designs for estimating regression coefficients of independent stochastic processes
[IMAG-RR-840-M] p 4060 N92-32839
ARC JET ENGINES
The evolutionary development of high specific impulse electric thruster technology
[NASA-TM-105758] p 3944 N92-33064
ARCHITECTURE (COMPUTERS)
A scalable, switched circuit LAN for Gb/S channels with over Tb/S total capacity
[DE92-013444] p 4050 N92-32412
Fault-tolerant wait-free shared objects
[NASA-CR-190679] p 4020 N92-32436
Tutorial on neural network applications in high energy physics: A 1992 perspective
[DE92-016003] p 4070 N92-32506
Target Cueing And Tracking System (TCATS): User's guide
[DE92-015385] p 4042 N92-32617
Balance in machine architecture: Bandwidth on board and offboard, integer/control speed and flops versus memory
[DE92-016006] p 4040 N92-32642
Parallel processing in space applications using transputer networks
[MBB-UO-0172-90-PUB] p 4050 N92-32689
Optimal communication schemes on an SIMD distributed-memory hypercube
[IMAG-RR-848-M] p 4051 N92-32715
Rational behavior model: A tri-level multiple paradigm architecture for robot vehicle control software
[AD-A250370] p 4053 N92-32748
Parallel implementation of Droid and performance evaluation
[OUEL-1926/92] p 4051 N92-32759
Study of a cellular programmable architecture: Functional definition and programming method
[ETN-92-91663] p 4051 N92-32768
Fly-by-light technology development plan
[NASA-CR-181954] p 3939 N92-32778
Exploiting two-dimensional explicit parallelism on vector architectures
[ETN-92-92136] p 4051 N92-32795

Methods of fine-grain optimization for parallel computer architectures
[ETN-92-92144] p 4051 N92-32821
The development of an airborne information management system for flight test
[NASA-TM-104251] p 3938 N92-32866
Methodological and architectural issues in the experience factory p 4044 N92-32870
Developing better software: A five year history of software engineering advancement p 4046 N92-32884
Object links in the repository
[NASA-CR-190644] p 4091 N92-33096
Advanced information processing system: The Army fault tolerant architecture conceptual study. Volume 1: Army fault tolerant architecture overview
[NASA-CR-189632-VOL-1] p 4052 N92-33100
Advanced information processing system: The Army fault tolerant architecture conceptual study. Volume 2: Army fault tolerant architecture design and analysis
[NASA-CR-189632-VOL-2] p 4052 N92-33101
An implementation of a fault-tolerant, multidirectional, digital interpolation beamformer
[AD-A252494] p 3986 N92-33152
Object linking in repositories
[NASA-CR-190629] p 4091 N92-33178

ARCTIC REGIONS
Coverage studies for spaced-based radar
[DREO-90-18] p 3982 N92-32818

ARGON
Studies of helium based drift chamber gases for high-luminosity low energy machines
[DE92-012415] p 4065 N92-32426

ARMED FORCES (FOREIGN)
China's aerospace industry: Technology, funding, and modernization
[AD-A252618] p 3929 N92-32691

ARMED FORCES (UNITED STATES)
United States Air Force summer research program 1991. Volume 1: Program management report
[AD-A248763] p 4103 N92-32338
The DOD science and technology strategy
[AD-A253691] p 4104 N92-33027

ARMOR
Calculation of the energy of elastic deformation of Kevlar backing plates for ceramic armours
[AD-A250129] p 3970 N92-32489
Composite structural armor for combat vehicle applications p 3947 N92-32515

AROMATIC COMPOUNDS
Solar photo-thermal catalytic reactions to produce high value chemicals
[DE91-002140] p 4026 N92-32908

ARRAYS
Geometrical effects in two-dimensional arrays of Josephson junctions
[AD-A252209] p 4084 N92-32898
Transverse diode pumping of solid-state lasers
[AD-A252213] p 4016 N92-33089

ARSENIC
Investigation on the lattice site location of the excess arsenic atoms in GaAs layers grown by low temperature molecular beam epitaxy
[DE92-008253] p 4083 N92-32693

ARTIFICIAL INTELLIGENCE
Human learning of schemas from explanations in practical electronics
[AD-A247429] p 4038 N92-32569
An intelligent gaming environment
[ISBN-90-6275-635-2] p 4060 N92-33055
CTAS: Computer intelligence for air traffic control in the terminal area
[NASA-TM-103959] p 3933 N92-33080
A study of artificial intelligence planning: A framework for a planning development system
[ISBN-0-315-54378-7] p 4055 N92-33219

ARTIFICIAL SATELLITES
Collaborative, remote, in-depth inspection and verification of satellites with neutral particle beams
[DE92-014195] p 3943 N92-32934

ARTILLERY
Applications of composites to armaments p 3947 N92-32516

ASCENT
Superheavyweight missions SI versus DI: Ascent flight design options and recommendations
[NASA-CR-183208] p 3942 N92-32610

ASHES
Development of the chemical and electrochemical coal cleaning process
[DE92-013353] p 3977 N92-32467

ASSESSMENTS
Suggestions for improvement of the methodology and use of MEPAS, the multimedia environmental pollutant assessment system
[DE92-013135] p 4028 N92-32616

ASTRONAUTICS
An international aerospace information system: A cooperative opportunity
[NASA-TM-108171] p 4091 N92-33237

ASTRONOMICAL MODELS
The synthetic infrared spectrum of Titan at high spectral resolution p 4099 N92-32389

ASTRONOMICAL PHOTOMETRY
Titan's mid-IR albedo: New observations from 3 to 5 microns p 4097 N92-32376

ASTRONOMICAL SPECTROSCOPY
Infrared properties of Titan's clouds and aerosols p 4097 N92-32373
Cassini/CIRS capabilities for aerosol, cloud, and surface measurements p 4098 N92-32378
Some problems about IR band integrated intensities; 3 examples for application to Titan: C6H6, HC3N, and C4H2 p 4101 N92-32400
The spectrum of Titan in the 1.06 and 1.28 micron windows p 4101 N92-32401

ASTRONOMY
United States Air Force summer research program 1991. Volume 1: Program management report
[AD-A248763] p 4103 N92-32338

ASTROPHYSICS
Research in nuclear astrophysics: Stellar collapse and supernovae
[DE92-014988] p 4093 N92-32993
Research in theoretical nuclear physics
[DE92-016316] p 4068 N92-33067

ASYMMETRY
Comparison of spin asymmetries and invariant cross sections in production of (pi)(sup 0) mesons by polarized antiprotons and protons with 200 GeV energy
[DE92-624691] p 4064 N92-32311
First results of measurements of A(sub LL) two-spin asymmetry in inclusive production of (pi)(sup 0) mesons by polarized protons and antiprotons with 200 GeV energy
[DE92-624692] p 4065 N92-32497

ASYMPTOTIC METHODS
Advanced computational transport methods for curvilinear geometries
[DE92-011290] p 4057 N92-32743

ASYMPTOTIC PROPERTIES
Bootstrapping the change-point of a hazard rate
[IMAG-RR-861-M] p 4056 N92-32685

ATMOSPHERIC BOUNDARY LAYER
Boundary layer processes in coastal meteorology: Prospects for remote sensing applications
[PB92-177849] p 4033 N92-32714

ATMOSPHERIC CHEMISTRY
Gas chromatography and pyrolysis-GC with capillary columns: Application to the in situ analysis of Titan's atmosphere p 4100 N92-32397
Some problems about IR band integrated intensities; 3 examples for application to Titan: C6H6, HC3N, and C4H2 p 4101 N92-32400
The spectrum of Titan in the 1.06 and 1.28 micron windows p 4101 N92-32401
US EPA's global climate change program: Landfill emissions and mitigation research
[PB92-180215] p 4028 N92-32609
SAGE 1 data user's guide
[NASA-RP-1275] p 4031 N92-33097

ATMOSPHERIC CIRCULATION
ARM Tropical Pacific Experiment (ATPEX): Role of cloud, water vapor and convection feedbacks in the coupled ocean/atmosphere system
[DE92-013772] p 4032 N92-32331
Numerical simulation of the circulation of the atmosphere of Titan p 4095 N92-32361
Simple dynamical models of Titan's atmospheric circulation p 4095 N92-32362
A preliminary assessment of the Titan planetary boundary layer p 4095 N92-32363
Tropical cyclone motion due to environmental interactions represented by empirical orthogonal functions of the vorticity fields
[AD-A246137] p 4033 N92-32534
Recent changes of weather patterns in North America
[DE92-014342] p 4033 N92-32720
Short range forecast of the initiation of convection
[DM-60] p 4033 N92-32758

ATMOSPHERIC COMPOSITION
Symposium on Titan
[ESA-SP-338] p 4093 N92-32348
The composition of the Titan atmosphere p 4094 N92-32354
Titan's atmosphere: Latitudinal variations in temperature and composition p 4094 N92-32355
Titan's UV albedo: Observations and modeling p 4094 N92-32356
A reanalysis of Voyager UVS observations of Titan p 4094 N92-32357
Ground-based observations of Titan's thermal spectrum p 4095 N92-32359
Neutral composition of Titan's atmosphere. A theoretical model p 4096 N92-32367
Titan's organic haze p 4097 N92-32372
The detectability of Titan's surface in the near-infrared p 4097 N92-32375
Huygens/ACP: An instrument for aerosols chemical composition measurements p 4098 N92-32379
Huygens/ASI plasma wave analyzer capabilities for aerosol measurement p 4098 N92-32380
Atmospheric escape from Titan p 4099 N92-32384
The synthetic infrared spectrum of Titan at high spectral resolution p 4099 N92-32389
Experimental determination of the refractive index of liquefied gas mixtures: Applications to hypothesized Titan oceans p 4099 N92-32390
Titan's atmosphere structure from Huygen's-ASI measurements p 4101 N92-32398
Study of transmitted light through the atmosphere of Titan p 4102 N92-32408
STEL p 4103 N92-32457
Phase distributions of airborne polycyclic aromatic hydrocarbons in two US cities
[PB92-164979] p 4028 N92-32543
Grill spectrometry on the Space Shuttle during the Atlas 1 mission
[AERONAUTICA-ACTA-A-364-199] p 3943 N92-32728
SAGE 1 data user's guide
[NASA-RP-1275] p 4031 N92-33097

ATMOSPHERIC GENERAL CIRCULATION MODELS
ARM Tropical Pacific Experiment (ATPEX): Role of cloud, water vapor and convection feedbacks in the coupled ocean/atmosphere system
[DE92-013772] p 4032 N92-32331
Numerical simulation of the circulation of the atmosphere of Titan p 4095 N92-32361
Simple dynamical models of Titan's atmospheric circulation p 4095 N92-32362

ATMOSPHERIC IONIZATION
The significance of meteoric ionisation for the propagation of lightning spherics in the atmosphere of Titan p 4096 N92-32365

ATMOSPHERIC MODELS
Modeling of the diurnal variations of the atmosphere of Titan p 4096 N92-32366
Neutral composition of Titan's atmosphere. A theoretical model p 4096 N92-32367
The detectability of Titan's surface in the near-infrared p 4097 N92-32375
The synthetic infrared spectrum of Titan at high spectral resolution p 4099 N92-32389
Laboratory investigations of the aerosols in the stratosphere of Titan p 4102 N92-32405
On the interpretation of Titan's intensity and polarization phase curve p 4102 N92-32407
Study of transmitted light through the atmosphere of Titan p 4102 N92-32408
Annual variation of surface temperatures over the world
[PB92-193259] p 4028 N92-32554
Exploitation of parallelism in climate models
[DE92-012595] p 4028 N92-32619
Recent changes of weather patterns in North America
[DE92-014342] p 4033 N92-32720
Grill spectrometry on the Space Shuttle during the Atlas 1 mission
[AERONAUTICA-ACTA-A-364-199] p 3943 N92-32728
Short range forecast of the initiation of convection
[DM-60] p 4033 N92-32758
A simulation of radioactive fallout using the MATHEW/ADPIC model
[FOA-C-40292-4.3] p 4029 N92-32785

ATMOSPHERIC OPTICS
The dependence of the anisoplanatic Strehl of a compensated beam on the beacon distribution
[DE92-011272] p 4016 N92-32736
The effect of the light round-trip time on the performance of an adaptive optics turbulence compensation system
[DE92-011273] p 4075 N92-32738

ATMOSPHERIC RADIATION
The synthetic infrared spectrum of Titan at high spectral resolution p 4099 N92-32389
A precise narrow-beam filter infrared radiometer and its use with lidar in the ARM Program
[DE92-016872] p 4015 N92-33188

ATMOSPHERIC SCATTERING
The detectability of Titan's surface in the near-infrared p 4097 N92-32375

ATMOSPHERIC SOUNDING
Huygens/ASI plasma wave analyzer capabilities for aerosol measurement p 4098 N92-32380

ATMOSPHERIC TEMPERATURE
The thermal structure of the atmosphere of Titan
p 4094 N92-32353
Titan's atmosphere: Latitudinal variations in temperature and composition p 4094 N92-32355
The atmospheric temperature structure of Titan
p 4095 N92-32358
Ground-based observations of Titan's thermal spectrum p 4095 N92-32359
The meteorology of Titan p 4095 N92-32360
US Historical Climatology Network daily temperature and precipitation data
[DE92-014920] p 4032 N92-32431
Annual variation of surface temperatures over the world
[PB92-193259] p 4028 N92-32554
An evaluation of an infrared/resistance temperature device for air/sea-surface temperature measurements
[AD-A252279] p 4035 N92-32688
Climate System Monitoring (CSM) Monthly Bulletin, issue no. 1 p 4034 N92-33073
A research program on radiative transfer model development in support of the ARM program
[DE92-014495] p 4031 N92-33153

ATMOSPHERIC TIDES
Gravitational tide in the atmosphere of Titan
p 4096 N92-32364

ATMOSPHERIC TURBULENCE
The dependence of the anisoplanatic Strehl of a compensated beam on the beacon distribution
[DE92-011272] p 4016 N92-32736
The effect of the light round-trip time on the performance of an adaptive optics turbulence compensation system
[DE92-011273] p 4075 N92-32738

ATOMIC BEAMS
Design and construction of a sample preparation chamber for atomic beam scattering
[DE92-014509] p 4065 N92-32473

ATOMIC CLOCKS
Satellite radio interferometry
[PL-TR-91-2200] p 3978 N92-32458

ATOMIC EXCITATIONS
Electron-atom scattering
[DE92-625005] p 4064 N92-32340
Scaling in the processes of ion-atom excitation
[DE92-625008] p 4065 N92-32500
Coupled-channels-optical calculation of electron-helium scattering
[DE92-625009] p 4065 N92-32501

ATOMIC STRUCTURE
New applications of ionization and fluorescence techniques for detecting and characterization of open-shell organometallics in the gas phase
[AD-A250923] p 3961 N92-32509

ATOMIZERS
A numerical model for atomization-spray coupling in liquid rocket thrust chambers p 3996 N92-32257

ATOMIZING
A numerical model for atomization-spray coupling in liquid rocket thrust chambers p 3996 N92-32257
Numerical modeling for dilute and dense sprays
p 3997 N92-32258
Modeling of SSME fuel preburner ASI
p 3945 N92-32259

ATOMS
Simplified model of electron scattering on atomic hydrogen
[DE92-625007] p 4065 N92-32499
Annual report, 1 November 1990 - 31 October 1991
[AD-A252431] p 4084 N92-32940

ATTITUDE CONTROL
Robust stabilization of the Space Station
[NASA-CR-190627] p 3942 N92-32244

ATTITUDE INDICATORS
Instrument scanning and subjective workload with the peripheral vision horizon display
[CTN-92-60359] p 4038 N92-32817

AUDIO FREQUENCIES
Exposures from headset interference tones
[AD-A247175] p 4061 N92-32697
Adaptive filter technique for suppression of wideband or offset narrowband radio frequency interference
[AD-D015329] p 3992 N92-33175

AUGER SPECTROSCOPY
Preparation and characterization of superlattices
[DE92-012572] p 4081 N92-32462

AUGMENTATION
Enhancements to the GRIDGEN structured grid generation system for internal and external flow applications p 4005 N92-32301

AURORAL ECHOES
Characteristics of large aspect angle VHF radar echoes in the presence and absence of optical aurora
[ISBN-0-315-59091-2] p 4032 N92-33197

AURORAL ZONES
Polar upper atmosphere characterization and supersonic ion escape (polar wind)
[GDR-0917] p 4031 N92-32889

AUTOCORRELATION
New approach to HF channel modeling and simulation. Part 3: Transfer function
[PB92-192848] p 3979 N92-32555
Recursive estimation techniques for detection of small objects in infrared image data
[AD-A250942] p 4075 N92-32935

AUTOMATA THEORY
Resolution of convection and diffusion by the boolean automata method
[ONERA-RF-22/3419-AY-122A] p 4057 N92-32772
An intelligent gaming environment
[ISBN-90-6275-635-2] p 4060 N92-33055
Learning systems, adaptive data structures, and random environments
[ISBN-0-315-51158-3] p 4054 N92-33218

AUTOMATED RADAR TERMINAL SYSTEM
Safety study of TCAS 2 for logic version 6.04
[DOT/FAA/RD-92/22] p 3933 N92-32537

AUTOMATIC CONTROL
Automatic detection, pursuit, and classification in infrared imagery p 3937 N92-32445
Air traffic control: FAA's advanced automation system contract
[GAO/IMTEC-91-25] p 3934 N92-32861
Automated data acquisition and analysis in the mechanical test lab
[DE92-011231] p 4040 N92-32910

AUTOMATIC LANDING CONTROL
CTAS: Computer intelligence for air traffic control in the terminal area
[NASA-TM-103959] p 3933 N92-33080

AUTOMATIC TEST EQUIPMENT
Study of eddy current probes
[NASA-CR-190814] p 4020 N92-32425

AUTOMOBILE FUELS
Second interim report of the Interagency Commission on Alternative Motor Fuels
[DE92-013169] p 3974 N92-32483

AUTOMORPHISMS
Poincare normal form (system of ordinary differential equations): An algorithmic point of view
[IMAG-RR-839-M] p 4058 N92-32838

AUTONOMOUS NAVIGATION
Rational behavior model: A tri-level multiple paradigm architecture for robot vehicle control software
[AD-A250370] p 4053 N92-32748
Parallel implementation of Droid and performance evaluation
[OUEL-1926/92] p 4051 N92-32759

AUTONOMY
Autonomous berthing/unberthing of a Work Attachment Mechanism/Work Attachment Fixture (WAM/WAF)
[NASA-CR-190647] p 4019 N92-32885

AUTOREGRESSIVE PROCESSES
Real-time processing of radar return on a parallel computer
[NASA-CR-4456] p 3932 N92-32606

AVALANCHE DIODES
A simple high-performance avalanche photodiode for long-wavelength optical communications, phase 1
[PB92-188259] p 4076 N92-33004

AVIONICS
Integrated Target Acquisition and Fire Control Systems
[AGARD-CP-500] p 3935 N92-32437
Analysis of data from a DO-178A software development process p 4045 N92-32880

AXIAL STRESS
Investigation of a relationship between uniaxial and biaxial chemical stress crazing of cast acrylic
[AD-A250852] p 4021 N92-32621

AXISYMMETRIC BODIES
Aerodynamic centre of wing-body combinations
[ESDU-92024] p 3929 N92-32479

AXISYMMETRIC FLOW
Development of a CFD code for internal flows in liquid fueled engines p 3999 N92-32271
Characterization of flow distribution in axisymmetric shock tubes
[AD-A251095] p 4008 N92-32683

B

B-52 AIRCRAFT
B-52G/H nuclear certification tasks performed by the Aircraft Compatibility Division at Sandia National Laboratories
[DE92-013681] p 3934 N92-32308

BACKSCATTERING
Certification of damage tolerant composite structure
p 3951 N92-32580
Kinematics of Compton backscattering x ray source for angiography
[DE92-014016] p 4073 N92-33179

BACKUPS
Electromagnetic attachment mechanism
[NASA-CASE-MSC-21463-1] p 4019 N92-33018

BACTERIA
Bacterial responses to extreme temperatures and pressures and to heavy organic loading
[AD-A247456] p 4035 N92-32571
NEDO Alcohol/Biomass Technology Subcommittee
[DE92-526270] p 3975 N92-32914

BACTERIOLOGY
Bacterial responses to extreme temperatures and pressures and to heavy organic loading
[AD-A247456] p 4035 N92-32571

BAFFLES
Wind tunnel test of Teledyne Geotech model 1564B cup anemometer
[DE92-009590] p 4013 N92-32460
Hot water storage tank for solar collectors
[AD-D015301] p 4026 N92-32943

BALANCING
Active synchrophasing of propeller unbalance
p 4063 N92-32963

BALL BEARINGS
SSME HPOTP impeller backcavity CFD analysis
p 4003 N92-32294

BALLISTICS
The design features of rocket motors relating to insensitive munition response to thermo-mechanical stimuli p 3976 N92-33244

BALLOON-BORNE INSTRUMENTS
Rotating-unbalanced-mass devices and methods for scanning balloon-borne-experiments, free-flying spacecraft, and space shuttle/space station attached experiments
[NASA-CASE-MFS-28425-1] p 4015 N92-33010

BAND STRUCTURE OF SOLIDS
Pseudopotential band calculations along a high-symmetry axis. Part 1: Central potential and the (111) direction
[AD-A252399] p 4084 N92-32938

BANDPASS FILTERS
Performance of a Y-Ba-Cu-O superconducting filter/GaAs low noise amplifier hybrid circuit
p 3985 N92-32982

BANDWIDTH
Balance in machine architecture: Bandwidth on board and offboard, integer/control speed and flops versus memory
[DE92-016006] p 4040 N92-32642
Bandwidth selection for the intensity of point processes: Application to hazard rate models for censored data
[IMAG-RR-859-I/M] p 4056 N92-32684
Continuation of the development of a millimeter wave wideband tunable waveguide voltage controlled oscillator
[CAL-504-88P120] p 3990 N92-32847
Ethernet bandwidth utilization of datafull, dataless, and diskless node workstation and x-terminals
[AD-A252374] p 4052 N92-32937
Adaptive filter technique for suppression of wideband or offset narrowband radio frequency interference
[AD-D015329] p 3992 N92-33175

BARIUM COMPOUNDS
Beta-barium borate optical parametric oscillator
[AD-A251177] p 4075 N92-32915

BARIUM OXIDES
T (sub c)-delta relations in YBa2Cu3O(7-delta) thin films: Effects of oxygen pressure during growth
[DE92-014432] p 4083 N92-32653
Substrate reactions and flux pinning structures in melt-processed YBa2Cu3O7 deposits on Ag-Pd alloy substrates
[DE92-014404] p 4084 N92-32919
Thickness dependence of vortex pinning in epitaxial Tl-Ca-Ba-Cu-O thin films
[DE92-015011] p 4084 N92-32920
Studies of Y-Ba-Cu-O single crystals by x ray absorption spectroscopy
[DE92-014687] p 4086 N92-33136

BAROTROPIC FLOW
Dynamics of Rossby waves in a parabolic jet
[ISBN-0-315-57159-4] p 4034 N92-33225

BARRIER LAYERS
Superconducting transport properties and surface microstructure for YBa2Cu3O(7-delta) based superlattices grown by pulsed laser deposition
[DE91-014224] p 4085 N92-33023

BARRIERS
Rotational barriers in model compounds of poly (vinyl chloride): 2-chlorobutane and 1,3,5,7,9,11-hexachlorododecane
[AD-A250855] p 3960 N92-32330
BARYONS
Theoretical nuclear physics
[DE92-016837] p 4069 N92-33186
BASE FLOW
NLS nozzle base flow characteristics
p 3995 N92-32252
BASE PRESSURE
Annual progress report on imposed 3-D disturbances on bluff-body near wake flows
[AD-A250366] p 4006 N92-32324
BATTERY CHARGERS
UHM/HNEI EV test and evaluation program
[DE92-011631] p 3989 N92-32754
BAUSCHINGER EFFECT
Contribution to the study of the effect of the heterogeneous distribution of dislocations on the cyclic plasticity of single crystal aluminum
[ISAL-91-0099] p 4083 N92-32892
BEACONS
The dependence of the anisoplanatic Strehl of a compensated beam on the beacon distribution
[DE92-011272] p 4016 N92-32736
The effect of the light round-trip time on the performance of an adaptive optics turbulence compensation system
[DE92-011273] p 4075 N92-32738
BEAM CURRENTS
High accuracy beam energy measurement for linear and circular accelerators
[DE92-016966] p 4069 N92-32319
BEAM INJECTION
Optics of beam transport in the NSLS UV-FEL
[DE92-014166] p 4015 N92-32511
Injection of compact toroids for tokamak fueling and current drive
[DE92-010031] p 4077 N92-32533
RF cavity vacuum interlock system
[DE92-016961] p 4070 N92-32567
Formation and sustainment of a very low aspect ratio tokamak using coaxial helicity injection: Helicity Injected Torus (HIT) experiment
[DE92-014311] p 4078 N92-32595
Study of recirculating induction accelerators as drivers for heavy ion fusion
[DE92-016980] p 4071 N92-32904
Scrape-off layer modeling of radiative divertor and high heat flux experiments on D3-D
[DE92-015007] p 4080 N92-32995
Overview of SSC accelerator requirements
[DE92-014896] p 4073 N92-33134
BEAM INTERACTIONS
Beamstrahlung spectra in next generation linear colliders
[DE92-010730] p 4069 N92-32337
Transverse beam dynamics in recirculating accelerators for heavy-ion fusion
[DE92-013448] p 4070 N92-32413
Phased array implementation using elements with scan capability
[CTN-92-60335] p 3981 N92-32787
Development of advanced modulators for recirculating heavy ion accelerators
[DE92-014795] p 4072 N92-33122
BEAMS (RADIATION)
High accuracy beam energy measurement for linear and circular accelerators
[DE92-016966] p 4069 N92-32319
Beamstrahlung spectra in next generation linear colliders
[DE92-010730] p 4069 N92-32337
Studies of helium based drift chamber gases for high-luminosity low energy machines
[DE92-012415] p 4065 N92-32426
First results of measurements of A(sub LL) two-spin asymmetry in inclusive production of (pi)(sup 0) mesons by polarized protons and antiprotons with 200 GeV energy
[DE92-624692] p 4065 N92-32497
Theory of elementary particles studies in weak interaction and grand unification and studies in accelerator design
[DE92-014320] p 4066 N92-32597
BEAMS (SUPPORTS)
Compression of thick laminated composite beams with initial impact-like damage
[NASA-CR-190573] p 3946 N92-32491
BEARINGS
NLS clutching bearing cavity flow analysis
p 4003 N92-32295
CFD analysis to optimize a design modification of BSMT p 4004 N92-32296
BELL AIRCRAFT
Evaluation of composite components on the Bell 206L and Sikorsky S-76 helicopters p 3950 N92-32575
BENDING
Compression of thick laminated composite beams with initial impact-like damage
[NASA-CR-190573] p 3946 N92-32491
BENZENE
Thermal conductivity of gaseous halogenated hydrocarbons: Ethylenes and benzenes
[ESDU-92010] p 3945 N92-32485
BERYLLIUM
High temperature deformation processes and strengthening mechanisms in intermetallic particulate composites
[AD-A250220] p 3946 N92-32339
BERYLLIUM 7
Research and development of a helium-4 based solar neutrino detector
[DE92-017390] p 4103 N92-33119
BIAS
Cognitive biases and time stress in team decision making
[AD-A251153] p 4088 N92-32551
BIBLIOGRAPHIES
Publications by Structures and Materials Laboratory on composite materials (January 1983 - June 1991)
[NRC-LTR-ST-1833] p 3959 N92-33078
BINARY MIXTURES
An analytical screening of alternatives for R-502 in low-temperature refrigerating applications
[DE92-017162] p 3978 N92-32927
BINDERS (MATERIALS)
Development of a minimum smoke propellant based on glycidyl azide polymer and ammonium nitrate
p 3976 N92-33243
BIOCONVERSION
NEDO Alcohol/Biomass Technology Subcommittee
[DE92-526270] p 3975 N92-32914
BIODYNAMICS
Bone as a liquid-filled diphase porous medium
p 4037 N92-32663
BIOLOGICAL EVOLUTION
Organic chemistry on Titan versus terrestrial prebiotic chemistry: Exobiological implications
p 4096 N92-32368
Titan's organic chemistry: Results of simulation experiments p 4096 N92-32369
BIOMASS ENERGY PRODUCTION
NEDO Alcohol/Biomass Technology Subcommittee
[DE92-526270] p 3975 N92-32914
BIOMEDICAL DATA
Kinematics of Compton backscattering x ray source for angiography
[DE92-014016] p 4073 N92-33179
BIOTECHNOLOGY
NEDO Alcohol/Biomass Technology Subcommittee
[DE92-526270] p 3975 N92-32914
Science and technology: A report to the Congress
[PB92-183219] p 4104 N92-33086
BIPOLAR TRANSISTORS
High-energy ion implantation for bipolar transistor fabrication
[ISBN-90-9003883-3] p 3992 N92-33144
BIRD-AIRCRAFT COLLISIONS
Bird ingestion into large turbofan engines
[DOT/FAA/CT-91/17] p 3932 N92-33005
BIRDS
Bird ingestion into large turbofan engines
[DOT/FAA/CT-91/17] p 3932 N92-33005
BIREFRINGENCE
Orientation, stress, and density distributions in injection-moulded amorphous polymers determined by optical techniques
[ETN-92-92052] p 3972 N92-32752
BISMALEIMIDE
Environmental degradation of high temperature composites p 3958 N92-33047
BISMUTH OXIDES
Sintering of bulk high-(Tc) superconductors: Bi-Sr-Ca-Cu-O
[DE92-016189] p 4082 N92-32561
BITUMENS
Development of the chemical and electrochemical coal cleaning process
[DE92-013353] p 3977 N92-32467
BLACK HOLES (ASTRONOMY)
Physics in knots
[DE92-017530] p 4088 N92-33069
BLANKETS (FUSION REACTORS)
ANL ITER high-heat-flux blanket-module heat transfer experiments
[DE92-017749] p 4080 N92-33168
BLASIUS FLOW
Leading-edge receptivity for blunt-nose bodies
[NASA-CR-190563] p 3930 N92-32648
BLUFF BODIES
Annual progress report on imposed 3-D disturbances on bluff-body near wake flows
[AD-A250366] p 4006 N92-32324
BLUNT BODIES
An examination of several high resolution schemes applied to complex problems in high speed flows
[AD-A250814] p 4008 N92-32632
BLUNT LEADING EDGES
Leading-edge receptivity for blunt-nose bodies
[NASA-CR-190563] p 3930 N92-32648
BODY-WING CONFIGURATIONS
Aerodynamic centre of wing-body combinations
[ESDU-92024] p 3929 N92-32479
A method for designing blended wing-body configurations for low wave drag
[NASA-TP-3261] p 3929 N92-32480
BOEING 747 AIRCRAFT
Structural assessment of ultralightweight composites
p 3948 N92-32525
BOLTZMANN DISTRIBUTION
Radiative lifetime measurements of the AA pi 1/2 state in CaH
[USIP-91-03] p 4067 N92-32764
BONES
Bone as a liquid-filled diphase porous medium
p 4037 N92-32663
BOOLEAN FUNCTIONS
Resolution of convection and diffusion by the boolean automata method
[ONERA-RF-22/3419-AY-122A] p 4057 N92-32772
BORATES
Beta-barium borate optical parametric oscillator
[AD-A251177] p 4075 N92-32915
BOREHOLES
Stress-relief displacements induced by drilling: Applications to holographic measurements of in situ stress
[DE92-013711] p 4014 N92-32620
BORN APPROXIMATION
Range of validity of distorted wave Born and impulse approximations for (e,2e)
[DE92-624821] p 4087 N92-32649
BORON PHOSPHIDES
Kinetics and characterization of CVD-grown BP
[ETN-92-92024] p 3973 N92-33065
BOSONS
Possible effects of additional vector bosons in e(sup +)e(sup -)(yields)f(bar-f) at the TRISTAN energies
[DE92-624727] p 4065 N92-32498
A Theoretical High Energy Physics Program: Task F
[DE92-014054] p 4073 N92-33182
Pertubative finite temperature field theory in Minkowski space
[ISBN-0-315-55158-5] p 4088 N92-33199
BOUNDARIES
Singularities in the classical Rayleigh-Taylor flow: Formation and subsequent motion
[NASA-CR-189690] p 4010 N92-32784
BOUNDARY CONDITIONS
Navier-Stokes analysis of an oxidizer turbine blade with tip clearance p 3999 N92-32269
Enhancements to the GRIDGEN structured grid generation system for internal and external flow applications p 4005 N92-32301
Aspects of solving non-linear boundary value problems numerically
[ETN-92-92049] p 4058 N92-32798
BOUNDARY INTEGRAL METHOD
A finite element-boundary integral method for conformal antenna arrays on a circular cylinder
[NASA-CR-190610] p 3979 N92-32559
A boundary integral method for an inverse problem in thermal imaging
[NASA-CR-189693] p 4059 N92-33006
BOUNDARY LAYER CONTROL
Annual progress report on imposed 3-D disturbances on bluff-body near wake flows
[AD-A250366] p 4006 N92-32324
BOUNDARY LAYER FLOW
Simple models for turbulent wave-current bottom boundary layer flow
[AD-A247942] p 4007 N92-32630
Massively separated flow modeling. Experimental study of the fine structure of boundary layers. Study of the influence of external turbulence level
[ETN-92-92088] p 4009 N92-32765
Strong coupling between inviscid fluid and boundary layer of sharp leading edges: Two-dimensional stationary and turbulent cases for isolated profiles and guard vanes
[ONERA-RT-44/1621-RY-016-R] p 4010 N92-32776
Experimental study of the vortex system generated by a missile fuselage at incidence. Part 3: Three directional laser velocimetry measurements
[ONERA-RT-47/1147-AY-146A-P] p 3931 N92-32800

BOUNDARY LAYER SEPARATION
Optimum design of ninety degree bends
p 4000 N92-32274
Influence of an intense acoustic field on boundary layer separation
[ETN-92-92081] p 4009 N92-32687
BOUNDARY LAYER TRANSITION
Leading-edge receptivity for blunt-nose bodies
[NASA-CR-190563] p 3930 N92-32648
BOUNDARY LAYERS
Swept shock/boundary layer interaction experiments in support of CFD code validation
[NASA-CR-190583] p 3930 N92-32494
Leading-edge receptivity for blunt-nose bodies
[NASA-CR-190563] p 3930 N92-32648
BOUNDARY VALUE PROBLEMS
Steady state behavior of reduced dynamic systems with local nonlinearities
[ISBN-90-9004680-1] p 4056 N92-32707
Integration of wall interference assessment and wall adaptation
[NLR-TP-91119-U] p 3940 N92-32734
Aspects of solving non-linear boundary value problems numerically
[ETN-92-92049] p 4058 N92-32798
Computational aspects of helicopter trim analysis and damping levels from Floquet theory
[NASA-CR-190736] p 3940 N92-33107
BRAIN
Effects of CSF hormones and ionic composition on salt/water metabolism
[NASA-CR-190693] p 4037 N92-32539
BRAKES (FOR ARRESTING MOTION)
Dynamic systems stability with dry friction: Application to brake disc squealing
[ECL-91-48] p 4018 N92-32737
BREATHING APPARATUS
An evaluation of the performance characteristics of a two-man molecular sieve oxygen generating system
[DCIEM-91-20] p 4039 N92-33079
BREMSSTRAHLUNG
Beamstrahlung spectra in next generation linear colliders
[DE92-010730] p 4069 N92-32337
Shielding analyses for repetitive high energy pulsed power accelerators
[DE92-015004] p 4072 N92-32994
BROADBAND
New approach to HF channel modeling and simulation. Part 3: Transfer function
[PB92-192848] p 3979 N92-32555
Multispectral variable magnification glancing incidence x ray telescope
[NASA-CASE-MFS-28013-4] p 4092 N92-33012
Adaptive filter technique for suppression of wideband or offset narrowband radio frequency interference
[AD-D015329] p 3992 N92-33175
BUBBLES
Acoustical emission from bubbles
[AD-A252390] p 4061 N92-32901
On the origin and acoustical behaviour of cloud cavitation
[ISBN-90-9004317-9] p 4012 N92-33066
BUCKLING
The use of curvilinear fiber format to improve buckling resistance of plates with central circular holes
p 3948 N92-32521
Scaling of fiber composite structures
p 3950 N92-32532
Postbuckling behavior of curved panels under combined compression and shear loads p 3952 N92-32584
Postbuckling of stiffened composite plates under combined loading p 3952 N92-32585
Initial postbuckling response of an unsymmetrically laminated rectangular plate p 3952 N92-32586
Buckling and postbuckling behavior of square compression-loaded graphite-epoxy plates with circular cutouts p 3952 N92-32587
Shear buckling of specially orthotropic plates with centrally located cutouts p 3953 N92-32589
Buckling and damage of a composite plate under compression
[ONERA-RT-25/3542-RY-006-R] p 4022 N92-32774
Buckling of fibre reinforced composite and sandwich laminates with higher-order shear deformation theories
[IIT-B/CE/RR/92/2] p 4022 N92-32783
Propagation of a delamination in a composite panel subjected to a compression load p 3957 N92-33041
BUFFER STORAGE
Analytic performance of software pipelines with rendezvous and communication tasks
[ISBN-0-315-54414-7] p 4052 N92-33216
BUILDINGS
Demand controlled ventilating systems: Sensor market survey. Energy conservation in buildings and community systems programme, annex 18, December 1991
[PB92-180892] p 3977 N92-32825
Building vibrations induced by noise from rotorcraft and propeller aircraft flyovers
[NASA-TM-104170] p 4063 N92-33160
BULKHEADS
Development of composite wing carrythrough bulkheads for fighter aircraft p 3948 N92-32519
BUMPERS
A simple approach for the design and optimization of stand-off hypervelocity particle shields
[DE92-011383] p 3943 N92-32704
BUNDLES
Experimental investigation of the axial impregnation of oriented fiber bundles by capillary forces
[AD-A250758] p 3961 N92-32508
BUOYS
Energy take-out from a wave energy device. A theoretical study of the hydrodynamics of a two-body problem consisting of a buoy and a submerged plate
[PB92-178821] p 4025 N92-32608
BURNERS
Axial vortices in gaseous-fired burner flow fields
[PB92-190370] p 3962 N92-32594
BUTANES
Studies of n-butane conversion over silica-supported platinum, platinum-silver and platinum-copper catalysts
[DE92-016309] p 3962 N92-32563
BUTENES
Shock tube ignition of ethanol, isobutene and MTBE: Experiments and modeling
[DE92-008563] p 3961 N92-32544

C

CADMIUM TELLURIDES
Thin film cadmium telluride, zinc telluride, and mercury zinc telluride solar cells
[DE92-001237] p 4024 N92-32510
Study and achievement of a parallel simulator for diffusion at the atomic level: Creation and growth of dislocation loops under electronic radiation
[LAAS-92118] p 4066 N92-32735
CALCIUM OXIDES
Sintering of bulk high-(Tc) superconductors: Bi-Sr-Ca-Cu-O
[DE92-016189] p 4082 N92-32561
Thickness dependence of vortex pinning in epitaxial Tl-Ca-Ba-Cu-O thin films
[DE92-015011] p 4084 N92-32920
CALIBRATING
Wind tunnel test of Teledyne Geotech model 1564B cup anemometer
[DE92-009590] p 4013 N92-32460
Study and development of a six port network analyzer in the 1-18 GHz frequency range
[TELECOM-91-E-005] p 3980 N92-32739
A description of the analytical methodology and reporting procedures used in the analysis and preparation of calibration reports for force measuring instruments
[NRC-LTR-ST-1817] p 4022 N92-32848
Calibration service for low-loss, three-terminal capacitance standards at 100 kHz and 1 MHz
[PB92-189554] p 3991 N92-33061
Volume 1. Preliminary design study: AXAF x ray calibration spectrometers. Volume 2. Revised preliminary design study: AXAF x ray calibration spectrometers
[NASA-CR-184340] p 4092 N92-33094
Improved HIRAP flight calibration technique
[NASA-TM-107656] p 3944 N92-33112
CALORIMETERS
AC microcalorimetry of adsorbates on evaporated metal films: Orientational ordering of H2 multilayers
[DE92-008317] p 3963 N92-32666
CAMS
Contribution to the theoretical and experimental analysis of camshaft engine operation
[ETN-92-91961] p 4018 N92-32726
CANADA
University of Toronto Institute for Aerospace Studies
[CTN-92-60375] p 4104 N92-32853
CANONICAL FORMS
Poincare normal form (system of ordinary differential equations): An algorithmic point of view
[IMAG-RR-839-M] p 4058 N92-32838
CAPACITANCE
The response of the double layer capacitance of a high temperature superconductor/fluid electrolyte interface to the onset of superconductivity
[AD-A251172] p 3990 N92-32827
Calibration service for low-loss, three-terminal capacitance standards at 100 kHz and 1 MHz
[PB92-189554] p 3991 N92-33061
CAPACITORS
A test circuit for capacitor bank grounding sticks
[AD-A251121] p 3989 N92-32700
Calibration service for low-loss, three-terminal capacitance standards at 100 kHz and 1 MHz
[PB92-189554] p 3991 N92-33061
CARBON
Thermochemical and kinetic considerations in diamond growth
[AD-A247866] p 3971 N92-32490
Novel gas phase ion molecule reactions of C60(++) with O2 and NH3
[AD-A250921] p 4066 N92-32556
Implantation of carbon in GaAs
[DE92-016921] p 4085 N92-33117
Method of growing diamond film on substrates
[AD-D015313] p 3973 N92-33170
CARBON CYCLE
Simulations of the carbon cycle in the oceans
[DE92-016622] p 4035 N92-32336
CARBON DIOXIDE
Simulations of the carbon cycle in the oceans
[DE92-016622] p 4035 N92-32336
Studies of helium based drift chamber gases for high-luminosity low energy machines
[DE92-012415] p 4065 N92-32426
CARBON FIBER REINFORCED PLASTICS
Survivability characteristics of composite compression structure p 3950 N92-32578
The use of piezoelectric sensors to detect delamination initiation in carbon fiber reinforced composites
[MBB-Z-0391-91-PUB] p 3954 N92-32740
Tensile fracture of notched composite laminates
[NRC-32147] p 3955 N92-32852
GARTEUR compression behaviour of advanced CFRP --- carbon fiber reinforced plastics p 3957 N92-33042
CFRP stiffened panels under compression
p 3958 N92-33044
CARBON FIBERS
Experimental investigation of the axial impregnation of oriented fiber bundles by capillary forces
[AD-A250758] p 3961 N92-32508
Innovative constituents requirements to improve composites compressive strength p 3957 N92-33043
Jet fuel absorption and dynamic mechanical analysis of carbon fibre composites p 3959 N92-33050
Fracture surface characteristics of compressive failures in carbon fibre reinforced epoxy laminate subjected to hot/wet conditioning p 3959 N92-33051
The effect of heat treatment on the properties of PEEK and APC-2 p 3959 N92-33052
CARBON TETRACHLORIDE
Photogenerated carrier-induced reactions on UHV semiconductor surfaces
[DE92-015355] p 4082 N92-32641
CARBONACEOUS MATERIALS
Experimental investigation of the axial impregnation of oriented fiber bundles by capillary forces
[AD-A250758] p 3961 N92-32508
CARBONIZATION
Method of growing diamond film on substrates
[AD-D015313] p 3973 N92-33170
CARBONYL COMPOUNDS
Polyimides with carbonyl and ether connecting groups between the aromatic rings
[NASA-CASE-LAR-14001-1] p 3973 N92-33008
Methyl substituted polyimides containing carbonyl and ether connecting groups
[NASA-CASE-LAR-14351-1] p 3973 N92-33015
CARDIOVASCULAR SYSTEM
Effects of CSF hormones and ionic composition on salt/water metabolism
[NASA-CR-190693] p 4037 N92-32539
CARRIER MOBILITY
Reduced mobility and PPC in In(.20)Ga(.80)As / Al(.23)Ga(.77)As HEMT structure p 3984 N92-32976
CASSINI MISSION
Symposium on Titan
[ESA-SP-338] p 4093 N92-32348
Observing the surface of Titan through near-infrared windows in its atmosphere p 4097 N92-32374
VIMS/Cassini mission at Titan: Scientific objectives and observational scenarios p 4097 N92-32377
Cassini/CIRS capabilities for aerosol, cloud, and surface measurements p 4098 N92-32378
Cassini: A mission to Saturn and Titan
p 4099 N92-32387
A surface science package for the Huygens Titan probe p 4102 N92-32410
CASTING
Polyimide molding powder, coating, adhesive, and matrix resin
[NASA-CASE-LAR-14163-1] p 3973 N92-33014

CATALYSIS
Methane conversion to methanol
[DE92-014349] p 3960 N92-32332
NQR-NMR studies of higher alcohol synthesis Cu-Co catalysts
[DE92-016614] p 3960 N92-32347
Electrocatalysis of anodic, oxygen-transfer reactions at noble metal electrodes
[DE92-016308] p 3962 N92-32562
Studies of n-butane conversion over silica-supported platinum, platinum-silver and platinum-copper catalysts
[DE92-016309] p 3962 N92-32563
Electrified microheterogeneous catalysis
[AD-D015270] p 3963 N92-32755
Solar photo-thermal catalytic reactions to produce high value chemicals
[DE91-002140] p 4026 N92-32908
Macrocyclic polycation complexes for secondary anion binding, molecular recognition, and catalysis
[AD-A251069] p 3972 N92-32913
High octane ethers from synthesis gas-derived alcohols
[DE92-013802] p 3975 N92-33108
Clean gasoline reforming with superacid catalysts
[DE92-013833] p 3975 N92-33123
Direct catalytic decomposition of nitric oxide
[DE92-013847] p 4030 N92-33125
Direct conversion of light hydrocarbon gases to liquid fuel
[DE92-015592] p 3975 N92-33141
Probe molecule studies: Active species in alcohol synthesis
[DE92-016682] p 3966 N92-33246

CATALYSTS
Methane oxidation over dual redox catalysts
[DE92-014358] p 3960 N92-32334
NQR-NMR studies of higher alcohol synthesis Cu-Co catalysts
[DE92-016614] p 3960 N92-32347
Studies of n-butane conversion over silica-supported platinum, platinum-silver and platinum-copper catalysts
[DE92-016309] p 3962 N92-32563
Clean gasoline reforming with superacid catalysts
[DE92-013833] p 3975 N92-33123
Probe molecule studies: Active species in alcohol synthesis
[DE92-016682] p 3966 N92-33246

CATALYTIC ACTIVITY
Direct catalytic decomposition of nitric oxide
[DE92-013847] p 4030 N92-33125

CATENARIES
Solar radiation on a catenary collector
[NASA-TM-105751] p 3988 N92-32243

CATHODE RAY TUBES
Correlating visual scene elements with simulator sickness incidence: Hardware and software development
[AD-A252235] p 4036 N92-32434

CATIONS
Polar upper atmosphere characterization and supersonic ion escape (polar wind)
[GDR-0917] p 4031 N92-32889

CAVITATION FLOW
Three-dimensional flow fields inside a shrouded inducer at design and off-design conditions (CFD study)
p 4003 N92-32291
On the origin and acoustical behaviour of cloud cavitation
[ISBN-90-9004317-9] p 4012 N92-33066

CAVITIES
Turbine disk cavity aerodynamics and heat transfer
p 3998 N92-32265
Transverse diode pumping of solid-state lasers
[AD-A252213] p 4016 N92-33089

CAVITY FLOW
Turbine disk cavity aerodynamics and heat transfer
p 3998 N92-32265
A comparison of artificial compressibility and fractional step methods for incompressible flow computations
p 4001 N92-32285
NLS clutching bearing cavity flow analysis
p 4003 N92-32295

CAVITY RESONATORS
High power testing of the prototype accelerating cavity (352 MHz) for the Advanced Photon Source (APS)
[DE92-016697] p 4069 N92-32314
Microwave absorption by lossy ceramic materials
[DE92-016963] p 3970 N92-32317
Absolute measurement of beam energy by Compton scattering
[DE92-016964] p 4069 N92-32318
RF cavity vacuum interlock system
[DE92-016961] p 4070 N92-32567
A high-power SLED 2 pulse compression system
[DE92-011586] p 4071 N92-32751

CELLS (BIOLOGY)
Measurement of the magnetic and electrical activity of individual cells in vitro
[AD-A250881] p 4035 N92-32345
Neutron scatter studies of chromatin structures related to functions
[DE92-014032] p 4036 N92-33181

CEMENTATION
Coatings for improved corrosion resistance
[DE92-016779] p 3974 N92-33247

CENSORED DATA (MATHEMATICS)
Bandwidth selection for the intensity of point processes: Application to hazard rate models for censored data
[IMAG-RR-859-I/M] p 4056 N92-32684

CENTRIFUGAL COMPRESSORS
Numerical simulation of turbomachinery flows with advanced turbulence models p 3999 N92-32270
Effects of curvature and rotation on turbulence in the NASA low-speed centrifugal compressor impeller
p 4003 N92-32292

CENTRIFUGAL FORCE
CFD applications in pump flows p 4002 N92-32288
Computation of the flow field in a centrifugal impeller with splitter blades p 4002 N92-32289
Rotating-unbalanced-mass devices and methods for scanning balloon-borne-experiments, free-flying spacecraft, and space shuttle/space station attached experiments
[NASA-CASE-MFS-28425-1] p 4015 N92-33010

CENTRIFUGAL PUMPS
A status of the activities of the NASA/MSFC pump stage technology team p 4002 N92-32286
CFD analysis of pump consortium impeller
p 4002 N92-32287
CFD applications in pump flows p 4002 N92-32288
Impeller tandem blade study with grid embedding for local grid refinement p 4002 N92-32290
Computational fluid dynamic design of rocket engine pump components p 4003 N92-32293

CERAMIC FIBERS
Interfacial studies of refractory glass-ceramic matrix/advanced SiC fiber reinforced composites
[AD-A250784] p 3953 N92-32676

CERAMIC MATRIX COMPOSITES
Interfacial studies of refractory glass-ceramic matrix/advanced SiC fiber reinforced composites
[AD-A250784] p 3953 N92-32676
Synthesis, microsctructure, and mechanical properties of zirconia-alumina composites
[ISBN-90-9004656-9] p 3954 N92-32677

CERAMICS
Microwave absorption by lossy ceramic materials
[DE92-016963] p 3970 N92-32317
PAC spectroscopy of electronic ceramics
[DE92-014328] p 3970 N92-32471
Calculation of the energy of elastic deformation of Kevlar backing plates for ceramic armours
[AD-A250129] p 3970 N92-32489
Nondestructive evaluation development for process control
[DE92-015272] p 3971 N92-32640
Electromagnetic-wave propagation in unmagnetized plasmas
[AD-A250710] p 3980 N92-32719
National Research Council Industrial Materials Institute: From knowledge to know-how
[CTN-92-60333] p 4103 N92-32814
National Research Council Industrial Materials Institute: From knowledge to know-how
[CTN-92-60334] p 4104 N92-32815
Influence of oil lubricant additives on tribological behavior of engineering ceramics
[PB92-180710] p 3973 N92-33059
Silver coated superconducting ceramic powder
[AD-D015294] p 3973 N92-33157

CERTIFICATION
B-52G/H nuclear certification tasks performed by the Aircraft Compatibility Division at Sandia National Laboratories
[DE92-013681] p 3934 N92-32308
A Markov model of software usage
p 4045 N92-32881

CHANNEL FLOW
Large eddy simulation of compressible turbulent channel flows p 4000 N92-32276
A new time scale based k-epsilon model for near wall turbulence
[NASA-TM-105768] p 4011 N92-32868

CHANNELS (DATA TRANSMISSION)
Wavelength division multiplexed local area networks
[AD-A247613] p 3979 N92-32573
Advanced information processing system: The Army fault tolerant architecture conceptual study. Volume 2: Army fault tolerant architecture design and analysis
[NASA-CR-189632-VOL-2] p 4052 N92-33101

CHAOS
The behavior of matter under non-equilibrium conditions: Fundamental aspects and applications
[DE92-014247] p 4087 N92-32593
Steady induction effects in geomagnetism. Part 1A: Steady motional induction of geomagnetic chaos
[NASA-TP-3272-PT-1A] p 4031 N92-32655
Steady state behavior of reduced dynamic systems with local nonlinearities
[ISBN-90-9004680-1] p 4056 N92-32707

CHARACTERIZATION
Preparation and characterization of superlattices
[DE92-012572] p 4081 N92-32462
Characterization of Laborde-Mulder graphs and the halfcube
[IMAG-RR-857-I] p 4057 N92-32713
Characterization of sintered reaction-bonded silicon nitride processed by microwave heating
[DE92-014408] p 3956 N92-32945
Kinetics and characterization of CVD-grown BP
[ETN-92-92024] p 3973 N92-33065

CHARGE EXCHANGE
Observation of (pi)(-)p yields (omega)(eta)n reaction at 38 GeV/c momentum
[DE92-624690] p 4064 N92-32310
Theoretical nuclear physics
[DE92-016837] p 4069 N92-33186

CHARGE TRANSFER
Observation of (pi)(-)p yields (omega)(eta)n reaction at 38 GeV/c momentum
[DE92-624690] p 4064 N92-32310

CHARGED PARTICLES
Scalar mesons and kaons in phi radiative decay and their implications for studies of CP violation at DA(phi)NE
[RAL-91-085] p 4068 N92-33133

CHECKOUT
SRMAFTE facility checkout model flow field analysis
p 3994 N92-32247
An evaluation of decelerating IFR approaches utilizing a helicopter flight simulator
[CTN-92-60348] p 3934 N92-32845
Diagnosability and diagnosis of sparsely interconnected multiprocessor systems
[ISBN-0-315-56107-6] p 4053 N92-33224

CHEMICAL BONDS
Local structural order and molecular associations in water DMSO mixtures. Molecular dynamics study
[AD-A250935] p 4064 N92-32418
High translational energy induced reaction in semiconductors
[AD-A250980] p 3989 N92-32669
Macrocyclic polycation complexes for secondary anion binding, molecular recognition, and catalysis
[AD-A251069] p 3972 N92-32913

CHEMICAL CLEANING
Development of the chemical and electrochemical coal cleaning process
[DE92-013353] p 3977 N92-32467

CHEMICAL COMPOSITION
Huygens/ACP: An instrument for aerosols chemical composition measurements p 4098 N92-32379
Local structural order and molecular associations in water DMSO mixtures. Molecular dynamics study
[AD-A250935] p 4064 N92-32418
Analysis of LDEF experiment AO187-2: Chemically and isotopic measurements of micrometeoroids by secondary ion mass spectrometry
[NASA-CR-190697] p 4093 N92-32541
Condensed-phase processes during solid propellant combustion. Part 2: Chemical and microscopic examination of conductively quenched samples of RDX, XM39, JA2, M30, and HMX-binder compositions
[AD-A250799] p 3974 N92-32664

CHEMICAL EFFECTS
Photogenerated carrier-induced reactions on UHV semiconductor surfaces
[DE92-015355] p 4082 N92-32641

CHEMICAL ENERGY
Novel gas phase ion molecule reactions of C60(++) with O2 and NH3
[AD-A250921] p 4066 N92-32556
Continuum configurational bias Monte-Carlo studies of alkanes and polyethylene
[DE92-016545] p 3965 N92-33185

CHEMICAL EVOLUTION
Organic chemistry on Titan versus terrestrial prebiotic chemistry: Exobiological implications
p 4096 N92-32368
Titan's organic chemistry: Results of simulation experiments p 4096 N92-32369
Organic chemistry on Titan: Surface interactions
p 4096 N92-32370

CHEMICAL EXPLOSIONS
Extending estimation of C-J pressure of explosives to the very low density region
[DE92-015035] p 3975 N92-33003
CHEMICAL PROPULSION
Development of the KIVA-2 CFD code for rocket propulsion applications p 3945 N92-32272
CHEMICAL REACTIONS
Shock tube ignition of ethanol, isobutene and MTBE: Experiments and modeling
[DE92-008563] p 3961 N92-32544
CARS diagnostics for solid propellant combustion investigations
[AD-A248660] p 3963 N92-32645
Electrified microheterogeneous catalysis
[AD-D015270] p 3963 N92-32755
Synthesis, morphology and properties of polyester-urethane in solution in styrene: Application to composites development
[ISAL-92-0007] p 3972 N92-32762
Diagnostics and modeling of ECRH microwave discha rges
[IPF-91-3] p 4079 N92-32822
Thermochemical cycles for energy storage: Thermal decomposition of ZnSO4 systems
[DE91-002144] p 4026 N92-32909
Environmental degradation of high temperature composites p 3958 N92-33047
Probe molecule studies: Active species in alcohol synthesis
[DE92-016682] p 3966 N92-33246
CHEMILUMINESCENCE
Electrocatalysis of anodic, oxygen-transfer reactions at noble metal electrodes
[DE92-016308] p 3962 N92-32562
CHINA
China's aerospace industry: Technology, funding, and modernization
[AD-A252618] p 3929 N92-32691
CHIPS
Pulse coded biologically motivated neural-type MOS circuits
[AD-A250367] p 3988 N92-32325
CHIPS (ELECTRONICS)
Multichip module study
[AD-A250877] p 3989 N92-32678
VLSI architecture for a Reed-Solomon decoder
[NASA-CASE-NPO-17897-1-CU] p 3991 N92-33011
CHLORIDES
Rotational barriers in model compounds of poly (vinyl chloride): 2-chlorobutane and 1,3,5,7,9,11-hexachlorododecane
[AD-A250855] p 3960 N92-32330
Development of high-performance Na/NiCl2 cell
[DE92-015270] p 3988 N92-32639
CHLOROCARBONS
International research into chlorofluorocarbon (CFC) alternatives
[DE92-014241] p 4030 N92-32986
CHLOROFLUOROCARBONS
An analytical screening of alternatives for R-502 in low-temperature refrigerating applications
[DE92-017162] p 3978 N92-32927
CHROMIUM STEELS
Inelastic deformation and damage at high temperature
[DE92-012241] p 4021 N92-32698
CHROMOSOMES
Neutron scatter studies of chromatin structures related to functions
[DE92-014032] p 4036 N92-33181
CHROMOSPHERE
Observations of high frequency and high wavenumber solar oscillations
[AD-A250099] p 4103 N92-32488
CHUTES
Numerical simulation of inclined chute flows of monodisperse, inelastic, frictional spheres
[DE92-014775] p 4012 N92-32947
CIRCUIT BOARDS
Multichip module study
[AD-A250877] p 3989 N92-32678
CIRCUIT BREAKERS
Life testing of a low voltage air circuit breaker
[DE92-014173] p 3988 N92-32635
CIRCUIT DIAGRAMS
Human learning of schemas from explanations in practical electronics
[AD-A247429] p 4038 N92-32569
CIRCUITS
Human learning of schemas from explanations in practical electronics
[AD-A247429] p 4038 N92-32569
A test circuit for capacitor bank grounding sticks
[AD-A251121] p 3989 N92-32700
Electromagnetic attachment mechanism
[NASA-CASE-MSC-21463-1] p 4019 N92-33018
Ultra-low-loss strip-type transmission lines, formed of bonded substrate layers
[AD-D015312] p 3992 N92-33169
CIRCULAR CYLINDERS
Breakdown of the Karman vortex street due to forced convection and flow compressibility
[NASA-TM-105853] p 4007 N92-32472
A finite element-boundary integral method for conformal antenna arrays on a circular cylinder
[NASA-CR-190610] p 3979 N92-32559
CIRCULATION
Study of recirculating induction accelerators as drivers for heavy ion fusion
[DE92-016980] p 4071 N92-32904
CITIES
Phase distributions of airborne polycyclic aromatic hydrocarbons in two US cities
[PB92-164979] p 4028 N92-32543
CIVIL AVIATION
Federal aviation regulations. Part 91: General operating and flight rules
[PB92-197334] p 3929 N92-33176
CLADDING
Processing and properties of silver-clad Tl-Ba-Ca-Cu-O wires and tapes
[DE92-015266] p 4081 N92-32346
CLASSIFICATIONS
An adaptive algorithm for modifying hyperellipsoidal decision surfaces
[DE92-013540] p 4041 N92-32414
Methods of opto-electronic fusion of infrared and visible images p 3936 N92-32444
Automatic detection, pursuit, and classification in infrared imagery p 3937 N92-32445
Naval target classification and designation with the CL-227 Sea Sentinel p 3937 N92-32449
Dissimilarities, dendograms, prefillers, and multiapplications of levels
[IMAG-RR-842-M] p 4058 N92-32799
Optimized set reduction for empirically guiding software development p 4044 N92-32875
Object links in the repository
[NASA-CR-190644] p 4091 N92-33096
Object linking in repositories
[NASA-CR-190629] p 4091 N92-33178
CLEAN ENERGY
Second interim report of the Interagency Commission on Alternative Motor Fuels
[DE92-013169] p 3974 N92-32483
CLEAN ROOMS
Cleanroom process evolution in the SEL p 4044 N92-32871
CLEARANCES
Navier-Stokes analysis of an oxidizer turbine blade with tip clearance p 3999 N92-32269
CLIMATE
Annual variation of surface temperatures over the world
[PB92-193259] p 4028 N92-32554
Exploitation of parallelism in climate models
[DE92-012595] p 4028 N92-32619
Recent changes of weather patterns in North America
[DE92-014342] p 4033 N92-32720
Climate System Monitoring (CSM) Monthly Bulletin, issue no. 1 p 4034 N92-33073
Applications of statistical methods to the study of climate and flooding fluctuations in the central US
[PB92-205137] p 4034 N92-33173
CLIMATE CHANGE
US Historical Climatology Network daily temperature and precipitation data
[DE92-014920] p 4032 N92-32431
US EPA's global climate change program: Landfill emissions and mitigation research
[PB92-180215] p 4028 N92-32609
Exploitation of parallelism in climate models
[DE92-012595] p 4028 N92-32619
SAGE 1 data user's guide
[NASA-RP-1275] p 4031 N92-33097
Applications of statistical methods to the study of climate and flooding fluctuations in the central US
[PB92-205137] p 4034 N92-33173
CLIMATOLOGY
US Historical Climatology Network daily temperature and precipitation data
[DE92-014920] p 4032 N92-32431
US EPA's global climate change program: Landfill emissions and mitigation research
[PB92-180215] p 4028 N92-32609
Exploitation of parallelism in climate models
[DE92-012595] p 4028 N92-32619
Climate System Monitoring (CSM) Monthly Bulletin, issue no. 1 p 4034 N92-33073
Forecasting heavy snow events in Missoula, Montana
[PB92-196104] p 4034 N92-33163
CLOUD COVER
Short range forecast of the initiation of convection
[DM-60] p 4033 N92-32758
CLOUD PHYSICS
Cassini/CIRS capabilities for aerosol, cloud, and surface measurements p 4098 N92-32378
CLOUDS (METEOROLOGY)
Infrared properties of Titan's clouds and aerosols p 4097 N92-32373
Boundary layer processes in coastal meteorology: Prospects for remote sensing applications
[PB92-177849] p 4033 N92-32714
CLUMPS
Some electronic and dynamical factors in electron-transfer chemistry: Metal complexes, clusters, and surfaces
[AD-A251169] p 3964 N92-32826
Selecting a subset of stimulus-response pairs with maximal transmitted information
[AD-A252728] p 3986 N92-32987
The energetics and dynamics of free radicals, ions, and clusters
[DE92-014124] p 4068 N92-33083
CLUSTER ANALYSIS
Fuzzy set methods for object recognition in space applications
[NASA-CR-190388] p 4047 N92-33093
CLUSTERS
Collective resonances of valence electrons in free metal clusters
[DE92-014783] p 3969 N92-33116
CLUTTER
Multifrequency measurements of radar ground clutter at 42 sites. Volume 1: Principal results
[AD-A246710] p 3980 N92-32696
CMOS
Analog CMOS filters for very-high frequencies
[ISBN-90-9004420-5] p 3986 N92-33143
The architecture development and design considerations of a high-speed, single chip, CMOS convolutional decoder based on a modification of the Viterbi algorithm
[ISBN-0-315-60456-5] p 3993 N92-33208
COAL
Development of the chemical and electrochemical coal cleaning process
[DE92-013353] p 3977 N92-32467
Coatings for improved corrosion resistance
[DE92-016779] p 3974 N92-33247
COASTS
Boundary layer processes in coastal meteorology: Prospects for remote sensing applications
[PB92-177849] p 4033 N92-32714
Abstracts of manuscripts submitted in 1991 for publication
[PB92-204627] p 4091 N92-33088
COATING
Laser coating of composites for enhanced wear and corrosion resistance
[AD-A249231] p 3956 N92-32906
Polyimide molding powder, coating, adhesive, and matrix resin
[NASA-CASE-LAR-14163-1] p 3973 N92-33014
Method of growing diamond film on substrates
[AD-D015313] p 3973 N92-33170
Coatings for improved corrosion resistance
[DE92-016779] p 3974 N92-33247
COATINGS
Testing of the single-element stretched-membrane dish
[DE92-013680] p 4025 N92-32549
Silver coated superconducting ceramic powder
[AD-D015294] p 3973 N92-33157
COBALT
NQR-NMR studies of higher alcohol synthesis Cu-Co catalysts
[DE92-016614] p 3960 N92-32347
Laser coating of composites for enhanced wear and corrosion resistance
[AD-A249231] p 3956 N92-32906
CODING
Pulse coded biologically motivated neural-type MOS circuits
[AD-A250367] p 3988 N92-32325
Semiannual status report
[NASA-CR-190239] p 4046 N92-33092
COEFFICIENT OF FRICTION
Implanted aluminum: Tribological behavior and mechanical properties of the superficial layers
[ECL-91-28] p 4019 N92-32801
COEFFICIENTS
Orthobaric densities and molar volumes of liquids: Halogenated ethanes
[ESDU-92009] p 3945 N92-32486

COGNITION
Cognitive biases and time stress in team decision making
[AD-A251153] p 4088 N92-32551
A conceptual model of cognitive complexity of elements of the programming process p 4045 N92-32877
COGNITIVE PSYCHOLOGY
A conceptual model of cognitive complexity of elements of the programming process p 4045 N92-32877
COHERENT RADAR
A digital implementation of a radar coherent-on-receive system
[ISBN-0-315-59028-9] p 3987 N92-33206
COHERENT RADIATION
Estimates of SASE power in the short wavelength region
[DE92-014504] p 4017 N92-33155
COLD PLASMAS
Plasma diffusion through multidipole magnetic fields
[INPE-5384-PRE/1750] p 4079 N92-32662
COLD WATER
Thermal assessment of Mustang Industries, Inc. neoprene quick-don anti-exposure immersion suits and storage evaluation for the CP140 Aurora aircraft
[DCIEM-90-23] p 4039 N92-32790
COLLIMATION
ABF algorithms implemented at ARL:UT, FDS system engineering and acoustics
[AD-A252368] p 4046 N92-32917
COLLISION AVOIDANCE
Safety study of TCAS 2 for logic version 6.04
[DOT/FAA/RD-92/22] p 3933 N92-32537
Simulation test and evaluation of TCAS 2 logic version 6.04
[DOT/FAA/RD-92/23] p 3934 N92-33098
COLLISION PARAMETERS
Electron-atom scattering
[DE92-625005] p 4064 N92-32340
Scaling in the processes of ion-atom excitation
[DE92-625008] p 4065 N92-32500
Coupled-channels-optical calculation of electron-helium scattering
[DE92-625009] p 4065 N92-32501
Relativistic heavy ion collisions
[DE92-014415] p 4066 N92-32600
COLLISIONAL PLASMAS
Electromagnetic-wave propagation in unmagnetized plasmas
[AD-A250710] p 3980 N92-32719
COLOR
Program for research in conducting polymers
[AD-A250965] p 3971 N92-32665
COLUMNS (PROCESS ENGINEERING)
Gas chromatography and pyrolysis-GC with capillary columns: Application to the in situ analysis of Titan's atmosphere p 4100 N92-32397
COMBAT
An integrated multiple-sensor fire control system for air-to-air combat p 3937 N92-32450
Design, analysis, and testing of a reusable wingbox for ballistic evaluation of composite structures p 3947 N92-32518
Tactical state and performance assessment during air combat maneuvering
[AD-A247426] p 3935 N92-32612
The DOD science and technology strategy
[AD-A253691] p 4104 N92-33027
DoD key technologies plan
[AD-A253692] p 4105 N92-33238
COMBUSTIBLE FLOW
Axial vortices in gaseous-fired burner flow fields
[PB92-190370] p 3962 N92-32594
A basic research model of natural gas combustion in turbulent flow, phase 2
[PB92-190362] p 4007 N92-32598
COMBUSTION
A comparative study of the effects of inhibitor stub length on solid rocket motor combustion chamber pressure oscillations: RSRM at T = 80 seconds, preliminary results p 3945 N92-32248
Overview of the relevant CFD work at Thiokol Corporation p 3995 N92-32249
A status of the activities of the NASA. Marshall Space Flight Center Combustion Devices Technology Team p 3995 N92-32250
A shock tube study of the reactions of the hydroxyl radical with combustion species
[DE92-012573] p 3960 N92-32464
Coatings for improved corrosion resistance
[DE92-016779] p 3974 N92-33247
COMBUSTION CHAMBERS
A comparative study of the effects of inhibitor stub length on solid rocket motor combustion chamber pressure oscillations: RSRM at T = 80 seconds, preliminary results p 3945 N92-32248
Heat transfer in rocket engine combustion chambers and nozzles p 3995 N92-32253
Computational fluid dynamics analysis of SSME phase 2 and phase 2+ preburner injector element hydrogen flow paths p 3997 N92-32261
Experimental studies of characteristic combustion-driven flows for CFD validation p 3998 N92-32264
Large eddy simulation of compressible turbulent channel flows p 4000 N92-32276
Numerical analysis of the hot-gas-side and coolant-side heat transfer in liquid rocket engine combustors p 4004 N92-32299
A two-phase restricted equilibrium model for combustion of metalized solid propellants p 3966 N92-32307
Local and temporal study of the combustion and heat transfer in a direct injection diesel engine
[ECL-91-43] p 3963 N92-32724
MHD Integrated Topping Cycle Project
[DE92-013904] p 4080 N92-33024
COMBUSTION CHEMISTRY
A two-phase restricted equilibrium model for combustion of metalized solid propellants p 3966 N92-32307
COMBUSTION EFFICIENCY
A two-phase restricted equilibrium model for combustion of metalized solid propellants p 3966 N92-32307
COMBUSTION PHYSICS
A state of the art report on flame acceleration and transition to detonation in hydrogen/air/diluent mixtures
[DE92-626850] p 3961 N92-32475
Solid fuel flame spread and mass burning in turbulent flow
[PB92-181049] p 3963 N92-32607
Premixed turbulent combustion to opposed streams
[DE92-016996] p 3964 N92-32996
COMBUSTION PRODUCTS
Development of methodology and technology for identifying and quantifying emission products from open burning and open detonation thermal treatment methods. BangBox test series. Volume 3: Quality assurance and quality control
[AD-A251099] p 4029 N92-32650
Mass resolved resonance ionization spectroscopy of combustion radicals
[DE92-016833] p 3965 N92-33222
COMBUSTION STABILITY
A numerical model for atomization-spray coupling in liquid rocket thrust chambers p 3996 N92-32257
Modeling of SSME fuel preburner ASI p 3945 N92-32259
Combustion instability analysis for liquid propellant rocket engines p 3966 N92-32297
COMETS
Mass loading at Titan and comets p 4098 N92-32383
COMMAND AND CONTROL
The DOD science and technology strategy
[AD-A253691] p 4104 N92-33027
COMMERCIAL AIRCRAFT
Aircraft accident report: L'Express Airlines, Inc., Flight 508, Beech C99, N7217L weather encounter and crash near Birmingham, Alabama, July 10, 1991
[PB92-910401] p 3932 N92-32455
Fly-by-light technology development plan
[NASA-CR-181954] p 3939 N92-32778
Flight service environmental effects on composite materials and structures p 3959 N92-33054
Statistics on aircraft gas turbine engine rotor failures that occurred in US commercial aviation during 1988
[DOT/FAA/CT-91/28] p 3938 N92-33105
COMMUNICATION
Balance in machine architecture: Bandwidth on board and offboard, integer/control speed and flops versus memory
[DE92-016006] p 4040 N92-32642
COMMUNICATION EQUIPMENT
The MSAT spacecraft of Telesat Mobile, Inc.
[CTN-92-60346] p 3981 N92-32789
DoD key technologies plan
[AD-A253692] p 4105 N92-33238
COMMUNICATION NETWORKS
Fault-tolerant wait-free shared objects
[NASA-CR-190679] p 4020 N92-32436
The problems of routing and scheduling in multihop radio networks. A Hopfield neural network approach
[AD-A247431] p 3979 N92-32570
Correlation of single mode fiber fabrication factors and radiation response
[AD-A247301] p 4074 N92-32613
Effects of fading and interference in narrowband land-mobile networks
[ISBN-90-9004491-4] p 3982 N92-32837
COMMUNICATION SATELLITES
The MSAT spacecraft of Telesat Mobile, Inc.
[CTN-92-60346] p 3981 N92-32789
COMMUTATION
Using minimax approaches to plan optimal task commutation configurations for combined mobile platform-manipulator systems
[DE91-018864] p 4018 N92-32694
COMPACTING
Density variations and anomalies in palladium compacts
[DE92-014382] p 3967 N92-32721
Radiography to measure the longitudinal density gradients of Pd compacts
[DE92-014383] p 3968 N92-32896
COMPATIBILITY
B-52G/H nuclear certification tasks performed by the Aircraft Compatibility Division at Sandia National Laboratories
[DE92-013681] p 3934 N92-32308
COMPENSATORS
Mixed H(2)/H(sub infinity): Control with output feedback compensators using parameter optimization
[NASA-CR-190070] p 4046 N92-33091
COMPILERS
Exploiting two-dimensional explicit parallelism on vector architectures
[ETN-92-92136] p 4051 N92-32795
Methods of fine-grain optimization for parallel computer architectures
[ETN-92-92144] p 4051 N92-32821
COMPLEX COMPOUNDS
Excited state processes in transition metal complexes: Redox splitting in soluble polymers
[DE92-011808] p 3971 N92-32631
Some electronic and dynamical factors in electron-transfer chemistry: Metal complexes, clusters, and surfaces
[AD-A251169] p 3964 N92-32826
COMPLEX SYSTEMS
The behavior of matter under non-equilibrium conditions: Fundamental aspects and applications
[DE92-014247] p 4087 N92-32593
COMPOSITE MATERIALS
Mechanisms of the oxidation of metals and alloys with emphasis on superconductors
[DE92-016840] p 3966 N92-32315
Quantitative non-destructive environmental characterization of advanced materials
[DE92-011462] p 3946 N92-32327
Study of eddy current probes
[NASA-CR-190814] p 4020 N92-32425
Composite structural armor for combat vehicle applications p 3947 N92-32515
The weight optimization of an armored crashworthy crewseat through the use of advanced composites and design p 3947 N92-32517
Braided composite bore evacuator chambers for tank cannons p 3948 N92-32520
Evaluation of composite components on the Bell 206L and Sikorsky S-76 helicopters p 3950 N92-32575
Supportability evaluation of thermoplastic and thermoset composites p 3950 N92-32576
Statistically based material properties: A military handbook-17 perspective p 3951 N92-32581
PDES application protocol suite for composites (PAS-C). Functional needs report for the PAS-C program
[AD-A247886] p 3953 N92-32629
Buckling and damage of a composite plate under compression
[ONERA-RT-25/3542-RY-006-R] p 4022 N92-32774
National Research Council Industrial Materials Institute: From knowledge to know-how
[CTN-92-60333] p 4103 N92-32814
National Research Council Industrial Materials Institute: From knowledge to know-how
[CTN-92-60334] p 4104 N92-32815
Ultra-low density organic-inorganic composite materials possessing thermally insulating and acoustic damping properties
[AD-A251182] p 3955 N92-32828
Active control of sound transmission through stiff lightweight composite fuselage constructions p 4062 N92-32957
The Utilization of Advanced Composites in Military Aircraft
[AGARD-R-785] p 3956 N92-33033
Aspects of compression in aerospace composites: Future requirements p 3956 N92-33036
A review of RAE sponsored work on the compressive behaviour of composite materials p 3957 N92-33038
An overview of concerns relating to fluid effects on composites p 3958 N92-33045
Evaluation of the effects of the environment on the behavior of the primary structures of composite material aircraft in service: Historic and current situation p 3958 N92-33048
Fluid effects: Thermoset and thermoplastic matrix composites p 3958 N92-33049

Flight service environmental effects on composite materials and structures p 3959 N92-33054
A comparison of three popular test methods for determining the shear modulus of composite materials [NASA-CR-190659] p 3959 N92-33075
Publications by Structures and Materials Laboratory on composite materials (January 1983 - June 1991) [NRC-LTR-ST-1833] p 3959 N92-33078

COMPOSITE PROPELLANTS
Development of a minimum smoke propellant based on glycidyl azide polymer and ammonium nitrate p 3976 N92-33243
Hazards reduction for tactical missiles p 3945 N92-33245

COMPOSITE STRUCTURES
Eighth DOD/NASA/FAA Conference on Fibrous Composites in Structural Design, part 1 [NASA-CP-3087-PT-1] p 3946 N92-32513
Design, evaluation and experimental effort toward development of a high strain composite wing for Navy aircraft p 3947 N92-32514
Applications of composites to armaments p 3947 N92-32516
The weight optimization of an armored crashworthy crewseat through the use of advanced composites and design p 3947 N92-32517
Design, analysis, and testing of a reusable wingbox for ballistic evaluation of composite structures p 3947 N92-32518
Development of composite wing carrythrough bulkheads for fighter aircraft p 3948 N92-32519
Braided composite bore evacuator chambers for tank cannons p 3948 N92-32520
Development of thermoplastic components for structural validation p 3948 N92-32522
Scaling of fiber composite structures p 3950 N92-32532
Eighth DOD/NASA/FAA Conference on Fibrous Composites in Structural Design, part 2 [NASA-CP-3087-PT-2] p 3950 N92-32574
Certification of damage tolerant composite structure p 3951 N92-32580
Statistically based material properties: A military handbook-17 perspective p 3951 N92-32581
Postbuckling behavior of curved panels under combined compression and shear loads p 3952 N92-32584
PDES application protocol suite for composites (PAS-C). Functional needs report for the PAS-C program [AD-A247886] p 3953 N92-32629
Active control of sound transmission through stiff lightweight composite fuselage constructions p 4062 N92-32957
The Utilization of Advanced Composites in Military Aircraft [AGARD-R-785] p 3956 N92-33033
Issues in compression loading of composite structures p 3956 N92-33034
A new test method to determine the compressive strength of fiber-reinforced composites p 3956 N92-33035
Aspects of compression in aerospace composites: Future requirements p 3956 N92-33036
CFRP stiffened panels under compression p 3958 N92-33044
Evaluation of the effects of the environment on the behavior of the primary structures of composite material aircraft in service: Historic and current situation p 3958 N92-33048
Fluid effects: Thermoset and thermoplastic matrix composites p 3958 N92-33049
Environmental resistance of amorphous bonded thermoplastic joints p 3959 N92-33053
Flight service environmental effects on composite materials and structures p 3959 N92-33054
Computational methods for global/local analysis [NASA-TM-107591] p 4023 N92-33104
Global/local interlaminar stress analysis of a grid-stiffened composite panel [NASA-CR-190822] p 4023 N92-33139

COMPRESSIBILITY
A comparison of artificial compressibility and fractional step methods for incompressible flow computations p 4001 N92-32285
Breakdown of the Karman vortex street due to forced convection and flow compressibility [NASA-TM-105853] p 4007 N92-32472
Advances in compressible turbulent mixing [DE92-014326] p 4010 N92-32824

COMPRESSIBILITY EFFECTS
Survivability characteristics of composite compression structure p 3950 N92-32578
Numerical simulation of turbulence at the back of the airplane [ETN-92-91664] p 3931 N92-32769

COMPRESSIBLE FLOW
Large eddy simulation of compressible turbulent channel flows p 4000 N92-32276
Comparison between the PISO algorithm and preconditioning methods for compressible flow p 4001 N92-32284
Breakdown of the Karman vortex street due to forced convection and flow compressibility [NASA-TM-105853] p 4007 N92-32472
User's manual for AeroFcn: A FORTRAN program to compute aerodynamic parameters [NASA-TM-104237] p 4042 N92-32507
Advances in compressible turbulent mixing [DE92-014326] p 4010 N92-32824
A numerical resolution study of high order essentially non-oscillatory schemes applied to incompressible flow [NASA-CR-189692] p 4012 N92-33110
Convergence acceleration of the Proteus computer code with multigrid methods [NASA-CR-190607] p 4047 N92-33131
Turbulence transport equations for variable-density turbulence and their relationship to two-field models [DE92-017292] p 4013 N92-33159

COMPRESSION LOADS
Compression of thick laminated composite beams with initial impact-like damage [NASA-CR-190573] p 3946 N92-32491
The use of curvilinear fiber format to improve buckling resistance of plates with central circular holes p 3948 N92-32521
Scaling of fiber composite structures p 3950 N92-32532
Postbuckling behavior of curved panels under combined compression and shear loads p 3952 N92-32584
Initial postbuckling response of an unsymmetrically laminated rectangular plate p 3952 N92-32586
Buckling and damage of a composite plate under compression [ONERA-RT-25/3542-RY-006-R] p 4022 N92-32774
A description of the analytical methodology and reporting procedures used in the analysis and preparation of calibration reports for force measuring instruments [NRC-LTR-ST-1817] p 4022 N92-32848
Issues in compression loading of composite structures p 3956 N92-33034
A new test method to determine the compressive strength of fiber-reinforced composites p 3956 N92-33035
Aspects of compression in aerospace composites: Future requirements p 3956 N92-33036
Damage progression under compressive loading in composite laminates containing an open hole p 3957 N92-33040
Propagation of a delamination in a composite panel subjected to a compression load p 3957 N92-33041
Innovative constituents requirements to improve composites compressive strength p 3957 N92-33043
CFRP stiffened panels under compression p 3958 N92-33044

COMPRESSION TESTS
The Utilization of Advanced Composites in Military Aircraft [AGARD-R-785] p 3956 N92-33033
Issues in compression loading of composite structures p 3956 N92-33034
A new test method to determine the compressive strength of fiber-reinforced composites p 3956 N92-33035
Aspects of compression in aerospace composites: Future requirements p 3956 N92-33036
A review of RAE sponsored work on the compressive behaviour of composite materials p 3957 N92-33038
Influence of edge effect on compression-tension fatigue of toughened graphite/epoxy laminates p 3957 N92-33039
Damage progression under compressive loading in composite laminates containing an open hole p 3957 N92-33040
Propagation of a delamination in a composite panel subjected to a compression load p 3957 N92-33041
GARTEUR compression behaviour of advanced CFRP --- carbon fiber reinforced plastics p 3957 N92-33042
Innovative constituents requirements to improve composites compressive strength p 3957 N92-33043
CFRP stiffened panels under compression p 3958 N92-33044
An overview of concerns relating to fluid effects on composites p 3958 N92-33045
Fracture surface characteristics of compressive failures in carbon fibre reinforced epoxy laminate subjected to hot/wet conditioning p 3959 N92-33051

COMPRESSIVE STRENGTH
The Utilization of Advanced Composites in Military Aircraft [AGARD-R-785] p 3956 N92-33033
Issues in compression loading of composite structures p 3956 N92-33034
A new test method to determine the compressive strength of fiber-reinforced composites p 3956 N92-33035
Aspects of compression in aerospace composites: Future requirements p 3956 N92-33036
A review of RAE sponsored work on the compressive behaviour of composite materials p 3957 N92-33038
Innovative constituents requirements to improve composites compressive strength p 3957 N92-33043
Fracture surface characteristics of compressive failures in carbon fibre reinforced epoxy laminate subjected to hot/wet conditioning p 3959 N92-33051

COMPTON EFFECT
Absolute measurement of beam energy by Compton scattering [DE92-016964] p 4069 N92-32318
Kinematics of Compton backscattering x ray source for angiography [DE92-014016] p 4073 N92-33179

COMPUTATION
A computational design system for rapid CFD analysis p 4000 N92-32273
Bandwidth selection for the intensity of point processes: Application to hazard rate models for censored data [IMAG-RR-859-I/M] p 4056 N92-32684
Computational methods for global/local analysis [NASA-TM-107591] p 4023 N92-33104
Computations for algebras and group representations [ISBN-0-315-54684-0] p 4059 N92-33231

COMPUTATIONAL CHEMISTRY
The energetics and dynamics of free radicals, ions, and clusters [DE92-014124] p 4068 N92-33083

COMPUTATIONAL FLUID DYNAMICS
Tenth Workshop for Computational Fluid Dynamic Applications in Rocket Propulsion, part 2 [NASA-CP-3163-PT-2] p 3994 N92-32245
Current status of the development of an ignition transient model for solid rocket motors p 3944 N92-32246
SRMAFTE facility checkout model flow field analysis p 3994 N92-32247
A comparative study of the effects of inhibitor stub length on solid rocket motor combustion chamber pressure oscillations: RSRM at T = 80 seconds, preliminary results p 3945 N92-32248
Overview of the relevant CFD work at Thiokol Corporation p 3995 N92-32249
A status of the activities of the NASA. Marshall Space Flight Center Combustion Devices Technology Team p 3995 N92-32250
CFD analysis of the STME nozzle flowfield p 3995 N92-32251
NLS nozzle base flow characteristics p 3995 N92-32252
Application of computational fluid dynamics to the design of the film cooled STME subscale nozzle for the National Launch System p 3996 N92-32254
Computational fluid dynamics analysis of Space Shuttle main engine multiple plume flows at high-altitude flight conditions p 3996 N92-32255
A numerical model for atomization-spray coupling in liquid rocket thrust chambers p 3996 N92-32257
CFD modeling of turbulent flows around the SSME main injector assembly using porosity formulation p 3997 N92-32260
Computational fluid dynamics analysis of SSME phase 2 and phase 2+ preburner injector element hydrogen flow paths p 3997 N92-32261
STME hydrogen mixer study p 3945 N92-32262
Experimental studies of characteristic combustion-driven flows for CFD validation p 3998 N92-32264
A status of the Turbine Technology Team activities p 3998 N92-32267
Numerical simulation of turbomachinery flows with advanced turbulence models p 3999 N92-32270
Development of a CFD code for internal flows in liquid fueled engines p 3999 N92-32271
Development of the KIVA-2 CFD code for rocket propulsion applications p 3945 N92-32272
A computational design system for rapid CFD analysis p 4000 N92-32273
A multi-domain method for subsonic viscous flows p 3960 N92-32275
Large eddy simulation of compressible turbulent channel flows p 4000 N92-32276
Treating convection in sequential solvers p 4000 N92-32277
Tenth Workshop for Computational Fluid Dynamic Applications in Rocket Propulsion, part 1 [NASA-CP-3163-PT-1] p 4000 N92-32278
Development of CFD code evaluation criteria and a procedure for assessing predictive capability and performance p 4001 N92-32283

Comparison between the PISO algorithm and preconditioning methods for compressible flow p 4001 N92-32284
A comparison of artificial compressibility and fractional step methods for incompressible flow computations p 4001 N92-32285
A status of the activities of the NASA/MSFC pump stage technology team p 4002 N92-32286
CFD analysis of pump consortium impeller p 4002 N92-32287
CFD applications in pump flows p 4002 N92-32288
Three-dimensional flow fields inside a shrouded inducer at design and off-design conditions (CFD study) p 4003 N92-32291
Computational fluid dynamic design of rocket engine pump components p 4003 N92-32293
SSME HPOTP impeller backcavity CFD analysis p 4003 N92-32294
NLS clutching bearing cavity flow analysis p 4003 N92-32295
CFD analysis to optimize a design modification of BSMT p 4004 N92-32296
Combustion instability analysis for liquid propellant rocket engines p 3966 N92-32297
Numerical analysis of the hot-gas-side and coolant-side heat transfer in liquid rocket engine combustors p 4004 N92-32299
An efficient and robust grid optimization algorithm p 4004 N92-32300
Complex three-dimensional internal flows in the ASRM and RSRM aft end segments p 4005 N92-32304
Effect of including variable gas properties and entrained particles in the flow analysis of the ASRM nozzle p 4006 N92-32306
Potential flow theory and operation guide for the panel code PMARC [NASA-TM-102851] p 3929 N92-32422
Computations of unsteady multistage compressor flows in a workstation environment [NASA-TM-103839] p 3938 N92-32452
Breakdown of the Karman vortex street due to forced convection and flow compressibility [NASA-TM-105853] p 4007 N92-32472
A computational fluid dynamics analysis of the hypersonic flights of Pegasus [NASA-CR-186023] p 4007 N92-32560
Modeling and numerical simulation of vortex flow in aerodynamics [NLR-TP-91154-U] p 3930 N92-32673
Model of Reynolds stress on nonorthogonal grid structures: Application to a staggered tube bundle [ETN-92-91959] p 4009 N92-32725
NLR investigations of flutter behaviour of fighter aircraft with external stores [NLR-TP-91134-U] p 3939 N92-32750
Numerical simulation of turbulence at the back of the airplane [ETN-92-91664] p 3931 N92-32769
Pressure field developed by the random movement of the vortices near a wall [ETN-92-91665] p 4009 N92-32770
Experimental study of the vortex system generated by a missile fuselage at incidence. Part 3: Three directional laser velocimetry measurements [ONERA-RT-47/1147-AY-146A-P] p 3931 N92-32800
Further development of the CANAERO computer code to include propulsor modelling [DREA-CR-90-425] p 3931 N92-32811
CFD efforts in the Netherlands [NLR-TP-91250-U] p 4011 N92-32835
A new time scale based k-epsilon model for near wall turbulence [NASA-TM-105768] p 4011 N92-32868
A numerical resolution study of high order essentially non-oscillatory schemes applied to incompressible flow [NASA-CR-189692] p 4012 N92-33110
Computation of incompressible viscous flows through turbopump components [NASA-TM-103911] p 4012 N92-33113

COMPUTATIONAL GRIDS
Impeller tandem blade study with grid embedding for local grid refinement p 4002 N92-32290
Computational fluid dynamic design of rocket engine pump components p 4003 N92-32293
NLS clutching bearing cavity flow analysis p 4003 N92-32295
An efficient and robust grid optimization algorithm p 4004 N92-32300
Enhancements to the GRIDGEN structured grid generation system for internal and external flow applications p 4005 N92-32301
Using adaptive grid in modeling rocket nozzle flow p 4005 N92-32303
A method for designing blended wing-body configurations for low wave drag [NASA-TP-3261] p 3929 N92-32480
New concepts for multi-block grid generation for flow domains around complex aerodynamic configurations [NLR-TP-91046-U] p 3930 N92-32730
Research on some centered implicit methods for calculating transonic flows by solving Navier-Stokes equations [ONERA-RSF-24/1408-AY-150A] p 3931 N92-32773
Connectivity structures and differencing techniques for staggered-grid free-Lagrange hydrodynamics [DE92-017313] p 4012 N92-33082
Convergence acceleration of the Proteus computer code with multigrid methods [NASA-CR-190607] p 4047 N92-33131

COMPUTER AIDED DESIGN
A computational design system for rapid CFD analysis p 4000 N92-32273
CAGI: Computer Aided Grid Interface. A work in progress p 4005 N92-32302
Generic modular imaging IR signal processor p 3936 N92-32440
SIMLAB: Automatically creating physical systems simulators [AD-A250970] p 4042 N92-32546
Experiments in software engineering technology: Recent studies in the SEL (1990-1991) p 4044 N92-32872

COMPUTER AIDED MANUFACTURING
CAGI: Computer Aided Grid Interface. A work in progress p 4005 N92-32302
MANTECH project book [AD-A245283] p 3977 N92-32461
Information Integration for Concurrent Engineering (IICE) IDEF3 process description capture method report [AD-A252633] p 4042 N92-32627
IDEF4 object-oriented design method manual [AD-A252634] p 4042 N92-32658

COMPUTER AIDED TOMOGRAPHY
PET studies of components of high-level vision [AD-A250873] p 4036 N92-32344
Nondestructive evaluation development for process control [DE92-015272] p 3971 N92-32640

COMPUTER ANIMATION
The Rochester Checkers Player: Multi-model parallel programming for animate vision [AD-A247427] p 4050 N92-32568

COMPUTER ASSISTED INSTRUCTION
Human learning of schemas from explanations in practical electronics [AD-A247429] p 4038 N92-32569

COMPUTER GRAPHICS
Program PLOTTAB: A code designed to plot continuous and/or discrete physical data [DE92-013754] p 4041 N92-32416

COMPUTER INFORMATION SECURITY
Fault tolerance for security management in distributed systems [LAAS-92011] p 4040 N92-32766
Methodologies for designing block ciphers and cryptographic protocols [ISBN-0-315-50983-X] p 4049 N92-33230

COMPUTER NETWORKS
Briefing notes on a manned aircraft research and support simulation facility [AD-A250373] p 3935 N92-32326
Fault-tolerant wait-free shared objects [NASA-CR-190679] p 4020 N92-32436
Automatic access experiment [AD-A252217] p 4089 N92-32611
Parallel processing in space applications using transputer networks [MBB-UO-0172-90-PUB] p 4050 N92-32689
Study of a cellular programmable architecture: Functional definition and programming method [ETN-92-91663] p 4051 N92-32768
Automated data acquisition and analysis in the mechanical test lab [DE92-011231] p 4040 N92-32910
Ethernet bandwidth utilization of datafull, dataless, and diskless node workstation and x-terminals [AD-A252374] p 4052 N92-32937
Message delay models of packet-switching networks [ISBN-0-315-57208-6] p 4053 N92-33235

COMPUTER PROGRAM INTEGRITY
Fault tolerance through program transformation [ISBN-90-72125-29-0] p 4047 N92-33142

COMPUTER PROGRAMMING
Improving the translation from data flow diagrams into Z by incorporating the data dictionary [AD-A250769] p 4089 N92-32342
Proceedings of the Sixteenth Annual Software Engineering Workshop [NASA-TM-107964] p 4044 N92-32869
Experiments in software engineering technology: Recent studies in the SEL (1990-1991) p 4044 N92-32872
Investigating the application of capture-recapture techniques to requirement and design reviews p 4044 N92-32873
Better predictions even in reduced input variable numbers using neural networks in software development p 4044 N92-32874
Optimized set reduction for empirically guiding software development p 4044 N92-32875
Measurement in practice p 4044 N92-32876
A conceptual model of cognitive complexity of elements of the programming process p 4045 N92-32877
Software process assessment for small software shops p 4045 N92-32878
A study of large scale software testing p 4045 N92-32879
Analysis of data from a DO-178A software development process p 4045 N92-32880
Developing better software: A five year history of software engineering advancement p 4046 N92-32884
Object links in the repository [NASA-CR-190644] p 4091 N92-33096
Fault tolerance through program transformation [ISBN-90-72125-29-0] p 4047 N92-33142
Independent verification and validation for Space Shuttle flight software [NASA-CR-190826] p 4047 N92-33196

COMPUTER PROGRAMS
Experimental studies of characteristic combustion-driven flows for CFD validation p 3998 N92-32264
A computational design system for rapid CFD analysis p 4000 N92-32273
The impact of time step definition on code convergence and robustness p 4001 N92-32282
Development of CFD code evaluation criteria and a procedure for assessing predictive capability and performance p 4001 N92-32283
Program PLOTTAB: A code designed to plot continuous and/or discrete physical data [DE92-013754] p 4041 N92-32416
NASA Marshall Space Flight Center Solar Observatory report, January - June 1992 [NASA-TM-103597] p 4092 N92-32478
Development of the OMPAT neuropsychological/psychomotor performance evaluation and OMPAT data and timing support [AD-A250793] p 4037 N92-32504
Implementation of a tree-code for numerical simulations of stellar systems [INPE-5370-TDI/469] p 4093 N92-32604
Suggestions for improvement of the methodology and use of MEPAS, the multimedia environmental pollutant assessment system [DE92-013135] p 4028 N92-32616
Finding solutions to value independent knapsack problems [INPE-5390-TAE/011] p 4055 N92-32661
Consistency and robustness of knowledge graphs [ISBN-90-9003729-2] p 4056 N92-32679
PANACEA User's Manual [DE92-011289] p 4043 N92-32741
Parameterization of directional spectra, part 2. Volume 2: User's manual for the programs RMODEL, FITHM, and FITDM [DREA-CR-89-445-PT-2-VOL-2] p 3981 N92-32749
Study of a cellular programmable architecture: Functional definition and programming method [ETN-92-91663] p 4051 N92-32768
CFD efforts in the Netherlands [NLR-TP-91250-U] p 4011 N92-32835
Hypertext and hypermedia [VTT-RN-1154] p 4090 N92-32843
A three-field model of transient 3D multiphase, three-component flow for the computer code 4 A3. Par1: Theoretical basis: Conservation and state equations, numerics [KFK-4948-PT-1] p 4011 N92-32857
A three-field model of transient 3D multiphase, three-component flow for the computer code 4 A3. Part 2: Models for the interfacial transport phenomena. Code validation [KFK-4949-PT-2] p 4011 N92-32858
Measurement in practice p 4044 N92-32876
Analysis of data from a DO-178A software development process p 4045 N92-32880
A Markov model of software usage p 4045 N92-32881
A prototype software engineering environment for domain modeling and reuse p 4046 N92-32882
Developing better software: A five year history of software engineering advancement p 4046 N92-32884
A reexamination of the plastic flow criterion for copper [AD-A252370] p 4023 N92-32918

Annual report, 1 November 1990 - 31 October 1991
[AD-A252431] p 4084 N92-32940
Oak Ridge Environmental Information System (OREIS). Phase 1: System definition document
[DE92-017342] p 4090 N92-33084
Object links in the repository
[NASA-CR-190644] p 4091 N92-33096
Simulation test and evaluation of TCAS 2 logic version 6.04
[DOT/FAA/RD-92/23] p 3934 N92-33098
Image processing mini manual
[NASA-TM-107680] p 4041 N92-33205
A study of artificial intelligence planning: A framework for a planning development system
[ISBN-0-315-54378-7] p 4055 N92-33219

COMPUTER STORAGE DEVICES
Balance in machine architecture: Bandwidth on board and offboard, integer/control speed and flops versus memory
[DE92-016006] p 4040 N92-32642

COMPUTER SYSTEMS DESIGN
A scalable, switched circuit LAN for Gb/S channels with over Tb/S total capacity
[DE92-013444] p 4050 N92-32412
Parallel implementation of Droid and performance evaluation
[OUEL-1926/92] p 4051 N92-32759
The design and development of a portable, DSP micro-processor based, high-accuracy data acquisition system
[NRC-32146] p 4040 N92-32851
The development of an airborne information management system for flight test
[NASA-TM-104251] p 3938 N92-32866
Ethernet bandwidth utilization of datafull, dataless, and diskless node workstation and x-terminals
[AD-A252374] p 4052 N92-32937

COMPUTER SYSTEMS PERFORMANCE
Analysis of a benchmark suite to evaluate mixed numeric and symbolic processing
[NASA-TM-103907] p 4052 N92-32886
Fault tolerance through program transformation
[ISBN-90-72125-29-0] p 4047 N92-33142

COMPUTER SYSTEMS PROGRAMS
CAGI: Computer Aided Grid Interface. A work in progress p 4005 N92-32302
Life cycle oriented method for development and production of large scale industrial mathematics software
[NLR-TP-91196-U] p 4043 N92-32833
A study of large scale software testing p 4045 N92-32879

COMPUTER TECHNIQUES
CAGI: Computer Aided Grid Interface. A work in progress p 4005 N92-32302
National Research Council Industrial Materials Institute: From knowledge to know-how
[CTN-92-60333] p 4103 N92-32814
Hypertext and hypermedia
[VTT-RN-1154] p 4090 N92-32843
Experiments in software engineering technology: Recent studies in the SEL (1990-1991) p 4044 N92-32872
Investigating the application of capture-recapture techniques to requirement and design reviews p 4044 N92-32873
A conceptual model of cognitive complexity of elements of the programming process p 4045 N92-32877
Advanced information processing system: The Army fault tolerant architecture conceptual study. Volume 1: Army fault tolerant architecture overview
[NASA-CR-189632-VOL-1] p 4052 N92-33100

COMPUTER VISION
Vision-based range estimation using helicopter flight data
[NASA-TM-103930] p 3933 N92-32424
Visionless TRAC
[NASA-CR-190732] p 3942 N92-32477
The Rochester Checkers Player: Multi-model parallel programming for animate vision
[AD-A247427] p 4050 N92-32568
Parallel implementation of Droid and performance evaluation
[OUEL-1926/92] p 4051 N92-32759
Shape recognition by computer in simulated aerial images
[DCIEM-91-05] p 4054 N92-32854
Ambient light array vision in 3-D
[ISBN-0-315-55748-6] p 4077 N92-33202
The local structure of image intensity discontinuities
[ISBN-0-315-57231-0] p 4048 N92-33204
Hypothesis refinement for 3-D scene interpretation
[ISBN-0-315-57864-5] p 4048 N92-33210
Primal access recognition of visual objects
[ISBN-0-315-63509-6] p 4048 N92-33212

COMPUTERIZED SIMULATION
Overview of the relevant CFD work at Thiokol Corporation p 3995 N92-32249
Large eddy simulation of compressible turbulent channel flows p 4000 N92-32276
SSME HPOTP impeller backcavity CFD analysis p 4003 N92-32294
A numerical study of natural convection in a narrow annulus
[DE92-017138] p 4006 N92-32322
Briefing notes on a manned aircraft research and support simulation facility
[AD-A250373] p 3935 N92-32326
STEL p 4103 N92-32457
Visionless TRAC
[NASA-CR-190732] p 3942 N92-32477
Analytic score comparison of geometry splitting and exponential transform for a simple Monte Carlo problem
[DE92-013108] p 4059 N92-32481
Tutorial on neural network applications in high energy physics: A 1992 perspective
[DE92-016003] p 4070 N92-32506
Computational simulation of structural fracture in fiber composites p 3949 N92-32531
SIMLAB: Automatically creating physical systems simulators
[AD-A250970] p 4042 N92-32546
Two- and three-dimensional simulation code for radiation-hydrodynamics in ICF
[NIFS-119] p 4078 N92-32552
Implementation of a tree-code for numerical simulations of stellar systems
[INPE-5370-TDI/469] p 4093 N92-32604
Adaptive information processing and global optimization
[AD-A248450] p 4089 N92-32644
Molecular dynamics modeling of the mechanical properties of metal surfaces at the nanometer scale
[DE92-010705] p 3966 N92-32646
Modeling and numerical simulation of vortex flow in aerodynamics
[NLR-TP-91154-U] p 3930 N92-32673
Dynamics of ion solvation in a Stockmayer fluid
[AD-A251087] p 4066 N92-32682
Study and achievement of a parallel simulator for diffusion at the atomic level: Creation and growth of dislocation loops under electronic radiation
[LAAS-92118] p 4066 N92-32735
PANACEA User's Manual
[DE92-011289] p 4043 N92-32741
NLR investigations of flutter behaviour of fighter aircraft with external stores
[NLR-TP-91134-U] p 3939 N92-32750
Numerical simulation of two-dimensional flows by the free-Lagrangian method
[TUM-M9105] p 4009 N92-32767
Numerical simulation of turbulence at the back of the airplane
[ETN-92-91664] p 3931 N92-32769
A simulation of radioactive fallout using the MATHEW/ADPIC model
[FOA-C-40292-4.3] p 4029 N92-32785
Life cycle oriented method for development and production of large scale industrial mathematics software
[NLR-TP-91196-U] p 4043 N92-32833
A simple Doppler wind lidar sensor: Simulated measurements and impacts in a global assimilation and forecast system
[PL-TR-91-2253] p 4034 N92-32859
STAMP, the SWOE Thermal Analysis and Measurement Program: Summary of the 1990 field tests
[LTR-91-013] p 4029 N92-32860
ABF algorithms implemented at ARL:UT, FDS system engineering and acoustics
[AD-A252368] p 4046 N92-32917
Annual report, 1 November 1990 - 31 October 1991
[AD-A252431] p 4084 N92-32940
Numerical simulation of inclined chute flows of monodisperse, inelastic, frictional spheres
[DE92-014775] p 4012 N92-32947
Scrape-off layer modeling of radiative divertor and high heat flux experiments on D3-D
[DE92-015007] p 4080 N92-32995
An intelligent gaming environment
[ISBN-90-6275-635-2] p 4060 N92-33055
Simulation test and evaluation of TCAS 2 logic version 6.04
[DOT/FAA/RD-92/23] p 3934 N92-33098
Ideal efficiency of propellers based on Theodorsen's theory: A review and computer study, with extended plus simplified charts
[UTIAS-TN-271] p 3938 N92-33102
Computational and experimental study of laminar flames
[DE92-017978] p 3965 N92-33121
ROAR: A 3-D tethered rocket simulation code
[DE92-017358] p 3944 N92-33166
Continuum configurational bias Monte-Carlo studies of alkanes and polyethylene
[DE92-016545] p 3965 N92-33185
CSP: A distributed logic programming language for discrete event simulation
[ISBN-0-315-54272-1] p 4048 N92-33214

COMPUTERS
An implementation of a fault-tolerant, multidirectional, digital interpolation beamformer
[AD-A252494] p 3986 N92-33152

CONCENTRATION (COMPOSITION)
T (sub c)-delta relations in YBa2Cu3O(7-delta) thin films: Effects of oxygen pressure during growth
[DE92-014432] p 4083 N92-32653

CONCENTRATORS
High-flux solar photon processes
[DE92-001247] p 4027 N92-33138

CONCURRENT PROCESSING
Real-time processing of radar return on a parallel computer
[NASA-CR-4456] p 3932 N92-32606
An evaluation of knowledge-based diagnostic techniques for debugging concurrent software
[ISBN-0-315-51189-3] p 4049 N92-33215
Concurrency control scheme for design object bases
[ISBN-0-315-56113-0] p 4049 N92-33232

CONDENSED MATTER PHYSICS
Gamma scattering in condensed matter with high intensity Moessbauer radiation
[DE92-014811] p 4085 N92-33025

CONDENSING
Heat and mass exchange during condensation of a water-ammonia mixture
[DE92-014524] p 3962 N92-32557

CONDUCTING POLYMERS
Program for research in conducting polymers
[AD-A250965] p 3971 N92-32665

CONDUCTIVE HEAT TRANSFER
A boundary integral method for an inverse problem in thermal imaging
[NASA-CR-189693] p 4059 N92-33006

CONFERENCES
Tenth Workshop for Computational Fluid Dynamic Applications in Rocket Propulsion, part 2
[NASA-CP-3163-PT-2] p 3994 N92-32245
Tenth Workshop for Computational Fluid Dynamic Applications in Rocket Propulsion, part 1
[NASA-CP-3163-PT-1] p 4000 N92-32278
Eighth DOD/NASA/FAA Conference on Fibrous Composites in Structural Design, part 1
[NASA-CP-3087-PT-1] p 3946 N92-32513
Eighth DOD/NASA/FAA Conference on Fibrous Composites in Structural Design, part 2
[NASA-CP-3087-PT-2] p 3950 N92-32574
Proceedings of the Sixteenth Annual Software Engineering Workshop
[NASA-TM-107964] p 4044 N92-32869
Proceedings of the fourth users meeting for the advanced photon source
[DE92-014061] p 4072 N92-32932
Fourth Aircraft Interior Noise Workshop
[NASA-CP-10103] p 4061 N92-32948
The 1991 Japan Solar Energy Society. Japan Wind Energy Association Joint Conference
[DE92-530733] p 4027 N92-33090
Humans and machines in space: The payoff
[ISBN-0-87703-343-9] p 4039 N92-33099
Insensitive Munitions
[AGARD-CP-511] p 3975 N92-33240

CONFIGURATION INTERACTION
Rotational barriers in model compounds of poly (vinyl chloride): 2-chlorobutane and 1,3,5,7,9,11-hexachlorododecane
[AD-A250855] p 3960 N92-32330

CONFIGURATION MANAGEMENT
Obstacle avoidance for redundant robots using configuration control
[NASA-CASE-NPO-17852-1-CU] p 4054 N92-33019

CONGRESSIONAL REPORTS
Departments of Veterans Affairs and Housing and Urban Development, and independent agencies appropriations for 1993, part 6
[GAO-55-636-PT-6] p 4091 N92-32505
NASA procurement: Improving oversight of construction projects at the Langley Research Center. Report to the Honorable John W. Warner, US Senate
[GAO/NSIAD-92-230] p 4086 N92-32618
Air traffic control: FAA's advanced automation system contract
[GAO/IMTEC-91-25] p 3934 N92-32861
Science and technology: A report to the Congress
[PB92-183219] p 4104 N92-33086
NASA authorization, 1993, volume 1
[GPO-55-260-VOL-1] p 4092 N92-33147

CONJUGATE GRADIENT METHOD
Phase-only synthesis for multiple-beam phased arrays with element failures
[AD-A252250] p 3982 N92-32891
CONSERVATION EQUATIONS
Computation of the flow field in a centrifugal impeller with splitter blades p 4002 N92-32289
Combustion instability analysis for liquid propellant rocket engines p 3966 N92-32297
Numerical methods: Solving the advection equation in flows with sharp gradients using Bott's flux scheme
[DM-59] p 4009 N92-32727
CONSERVATION LAWS
A numerical resolution study of high order essentially non-oscillatory schemes applied to incompressible flow
[NASA-CR-189692] p 4012 N92-33110
CONSISTENCY
Consistency and robustness of knowledge graphs
[ISBN-90-9003729-2] p 4056 N92-32679
Bandwidth selection for the intensity of point processes: Application to hazard rate models for censored data
[IMAG-RR-859-I/M] p 4056 N92-32684
Bootstrapping the change-point of a hazard rate
[IMAG-RR-861-M] p 4056 N92-32685
On the inconsistency of bootstrap distribution estimators
[IMAG-RR-856-M] p 4060 N92-32718
CONSTITUTIVE EQUATIONS
A three-field model of transient 3D multiphase, three-component flow for the computer code 4 A3. Part 2: Models for the interfacial transport phenomena. Code validation
[KFK-4949-PT-2] p 4011 N92-32858
CONSTRAINTS
Advanced software development workstation: Effectiveness of constraint-checking --- spaceflight simulation and planning
[NASA-CR-190712] p 4043 N92-32865
CONSTRUCTION
Design and construction of a sample preparation chamber for atomic beam scattering
[DE92-014509] p 4065 N92-32473
Investigation into the fabrication of a composite top attack recoilless rifle p 3948 N92-32524
Design and construction of a magnetic sector mass spectrometer
[INPE-5405-RPQ/659] p 4014 N92-32601
NASA procurement: Improving oversight of construction projects at the Langley Research Center. Report to the Honorable John W. Warner, US Senate
[GAO/NSIAD-92-230] p 4088 N92-32618
CONTAMINANTS
Suggestions for improvement of the methodology and use of MEPAS, the multimedia environmental pollutant assessment system
[DE92-013135] p 4028 N92-32616
Demand controlled ventilating systems: Sensor market survey. Energy conservation in buildings and community systems programme, annex 18, December 1991
[PB92-180892] p 3977 N92-32625
Study on lifetime specific, laser-induced ultrafast fluorescence detection in the time and frequency domain for in-situ environmental analysis of organic pollutants
[KFK-4975] p 4029 N92-32841
CONTAMINATION
Analysis of LDEF experiment AO187-2: Chemically and isotopic measurements of micrometeoroids by secondary ion mass spectrometry
[NASA-CR-190697] p 4093 N92-32541
Defense environmental restoration program annual report to Congress for fiscal year 1991
[AD-A244196] p 4029 N92-32731
CONTINUITY (MATHEMATICS)
Geometric continuity and Frenet continuity of parametric curves
[IMAG-RR-846-M] p 4057 N92-32761
CONTINUITY EQUATION
A comparison of artificial compressibility and fractional step methods for incompressible flow computations
p 4001 N92-32285
CONTINUUM MODELING
A research program on radiative transfer model development in support of the ARM program
[DE92-014495] p 4031 N92-33153
CONTRACTORS
NASA procurement: Improving oversight of construction projects at the Langley Research Center. Report to the Honorable John W. Warner, US Senate
[GAO/NSIAD-92-230] p 4088 N92-32618
CONTRACTS
Air traffic control: FAA's advanced automation system contract
[GAO/IMTEC-91-25] p 3934 N92-32861
CONTROL EQUIPMENT
The Rochester Checkers Player: Multi-model parallel programming for animate vision
[AD-A247427] p 4050 N92-32568
Publications on maglev technologies
[DE92-013296] p 4017 N92-32615
Study of recirculating induction accelerators as drivers for heavy ion fusion
[DE92-016980] p 4071 N92-32904
CONTROL STABILITY
Robust stabilization of the Space Station
[NASA-CR-190627] p 3942 N92-32244
CONTROL SYSTEMS DESIGN
Robust stabilization of the Space Station
[NASA-CR-190627] p 3942 N92-32244
A learning enhanced flight control system for high performance aircraft
[AD-A252520] p 3938 N92-32435
Status of LHD control system design
[NIFS-122] p 4070 N92-32746
Demand controlled ventilating systems: Sensor market survey. Energy conservation in buildings and community systems programme, annex 18, December 1991
[PB92-180892] p 3977 N92-32825
Automated data acquisition and analysis in the mechanical test lab
[DE92-011231] p 4040 N92-32910
An optically controlled Ka-band phased array antenna
p 3983 N92-32968
A prototype backside purge control system
[NASA-CR-190816] p 3969 N92-33081
Mixed H(2)/H(sub infinity): Control with output feedback compensators using parameter optimization
[NASA-CR-190070] p 4046 N92-33091
Analysis of delay reducing and fuel saving sequencing and spacing algorithms for arrival traffic
[NASA-TM-103880] p 3933 N92-33194
A study of artificial intelligence planning: A framework for a planning development system
[ISBN-0-315-54378-7] p 4055 N92-33219
CONTROL THEORY
The multiple-function multi-input/multi-output digital controller system for the AFW wind-tunnel model
[NASA-TM-107600] p 3934 N92-32536
Mixed H(2)/H(sub infinity): Control with output feedback compensators using parameter optimization
[NASA-CR-190070] p 4046 N92-33091
CONTROLLABILITY
A background to the handling qualities of aircraft
[ESDU-92006] p 3939 N92-32780
CONTROLLED FUSION
Fast ion loss and radial electric field in Wendelstein 7-A stellarator
[DE92-782106] p 4079 N92-32745
Status of LHD control system design
[NIFS-122] p 4070 N92-32746
CONTROLLERS
The multiple-function multi-input/multi-output digital controller system for the AFW wind-tunnel model
[NASA-TM-107600] p 3934 N92-32536
Autonomous berthing/unberthing of a Work Attachment Mechanism/Work Attachment Fixture (WAM/WAF)
[NASA-CR-190647] p 4019 N92-32885
CONVECTION
Treating convection in sequential solvers
p 4000 N92-32277
ARM Tropical Pacific Experiment (ATPEX): Role of cloud, water vapor and convection feedbacks in the coupled ocean/atmosphere system
[DE92-013772] p 4032 N92-32331
CONVECTION CLOUDS
Short range forecast of the initiation of convection
[DM-60] p 4033 N92-32758
CONVECTION CURRENTS
Short range forecast of the initiation of convection
[DM-60] p 4033 N92-32758
CONVECTION-DIFFUSION EQUATION
Resolution of convection and diffusion by the boolean automata method
[ONERA-RF-22/3419-AY-122A] p 4057 N92-32772
CONVECTIVE FLOW
A numerical study of natural convection in a narrow annulus
[DE92-017138] p 4006 N92-32322
Breakdown of the Karman vortex street due to forced convection and flow compressibility
[NASA-TM-105853] p 4007 N92-32472
CONVECTIVE HEAT TRANSFER
Swept shock/boundary layer interaction experiments in support of CFD code validation
[NASA-CR-190583] p 3930 N92-32494
Axial vortices in gaseous-fired burner flow fields
[PB92-190370] p 3962 N92-32594
Forced convection heat transfer in straight tubes. Part 1: Fully developed turbulent flow
[ESDU-92003-PT-1] p 4010 N92-32781
CONVERGENCE
The impact of time step definition on code convergence and robustness p 4001 N92-32282
Tropical cyclone motion due to environmental interactions represented by empirical orthogonal functions of the vorticity fields
[AD-A246137] p 4033 N92-32534
Convergence acceleration of the Proteus computer code with multigrid methods
[NASA-CR-190607] p 4047 N92-33131
CONVEXITY
Limit theorems for functionals of convex hulls
[CWI-BS-R9115] p 4059 N92-33058
COOLANTS
Application of computational fluid dynamics to the design of the film cooled STME subscale nozzle for the National Launch System p 3996 N92-32254
Inverse design of a proper number, shapes, sizes, and locations of coolant flow passages
p 4004 N92-32298
COOLERS
ANL ITER high-heat-flux blanket-module heat transfer experiments
[DE92-017749] p 4080 N92-33168
COOLING
Trapped ions and laser cooling 3
[PB92-189547] p 4016 N92-33060
COOLING SYSTEMS
Application of computational fluid dynamics to the design of the film cooled STME subscale nozzle for the National Launch System p 3996 N92-32254
STME hydrogen mixer study p 3945 N92-32262
Inverse design of a proper number, shapes, sizes, and locations of coolant flow passages
p 4004 N92-32298
COORDINATION
Observing team coordination within Army rotary-wing aircraft crews
[AD-A252234] p 4039 N92-32433
COPOLYMERS
Towards well-defined polysilanes and polyphosphazenes
[AD-A251098] p 3971 N92-32547
COPPER
High power testing of the prototype accelerating cavity (352 MHz) for the Advanced Photon Source (APS)
[DE92-016697] p 4069 N92-32314
NQR-NMR studies of higher alcohol synthesis Cu-Co catalysts
[DE92-016614] p 3960 N92-32347
Molecular dynamics modeling of the mechanical properties of metal surfaces at the nanometer scale
[DE92-010705] p 3966 N92-32646
Hydrogen permeation through bilayer metallic membrranes
[UTIAS-TN-342] p 3967 N92-32794
Macrocyclic polycation complexes for secondary anion binding, molecular recognition, and catalysis
[AD-A251069] p 3972 N92-32913
A reexamination of the plastic flow criterion for copper
[AD-A252370] p 4023 N92-32918
COPPER ALLOYS
Studies of n-butane conversion over silica-supported platinum, platinum-silver and platinum-copper catalysts
[DE92-016309] p 3962 N92-32563
Aluminum based particulate composites for aerospace applications produced by different processes
[MBB-Z-0408-91-PUB] p 3967 N92-32819
COPPER OXIDES
Sintering of bulk high-(Tc) superconductors: Bi-Sr-Ca-Cu-O
[DE92-016189] p 4082 N92-32561
T (sub c)-delta relations in YBa2Cu3O(7-delta) thin films: Effects of oxygen pressure during growth
[DE92-014432] p 4083 N92-32653
Substrate reactions and flux pinning structures in melt-processed YBa2Cu3O7 deposits on Ag-Pd alloy substrates
[DE92-014404] p 4084 N92-32919
Thickness dependence of vortex pinning in epitaxial Tl-Ca-Ba-Cu-O thin films
[DE92-015011] p 4084 N92-32920
Studies of Y-Ba-Cu-O single crystals by x ray absorption spectroscopy
[DE92-014687] p 4086 N92-33136
CORE FLOW
Steady induction effects in geomagnetism. Part 1A: Steady motional induction of geomagnetic chaos
[NASA-TP-3272-PT-1A] p 4031 N92-32655
CORRELATION
Correlating visual scene elements with simulator sickness incidence: Hardware and software development
[AD-A252235] p 4036 N92-32434
Applications of statistical methods to the study of climate and flooding fluctuations in the central US
[PB92-205137] p 4034 N92-33173

CORROSION
The oxidation of Type 310S stainless steel in mixed gases at elevated temperatures
[DE92-014941] p 3968 N92-32991
JPRS report: Science and technology. Central Eurasia: Materials science
[JPRS-UMS-92-011] p 3969 N92-33129
Corrosion-resistant alkyd coatings
[AD-D015330] p 3974 N92-33177
Coatings for improved corrosion resistance
[DE92-016779] p 3974 N92-33247

CORROSION RESISTANCE
An in vitro corrosion study of two implant materials using electrochemical impedance spectroscopy and potentiodynamic polarization
[AD-A252575] p 3966 N92-32626
Laser coating of composites for enhanced wear and corrosion resistance
[AD-A249231] p 3956 N92-32906
Electrochemical polarization measurements on pitting corrosion susceptibility of nickel-rich Alloy 825
[DE92-014885] p 3969 N92-33132
Corrosion-resistant alkyd coatings
[AD-D015330] p 3974 N92-33177
Coatings for improved corrosion resistance
[DE92-016779] p 3974 N92-33247

CORROSION TESTS
An in vitro corrosion study of two implant materials using electrochemical impedance spectroscopy and potentiodynamic polarization
[AD-A252575] p 3966 N92-32626
New accelerated corrosion test methods
[MBB-Z-0406-91-PUB] p 3968 N92-32895

COSMOCHEMISTRY
Plausible surface models for Titan
p 4098 N92-32381

COSMOLOGY
Two perspectives on a decohering spin
[DE92-013021] p 4087 N92-32496

COST ANALYSIS
NAASW modular radar research testbed study results
[DE92-011339] p 3981 N92-32744
Solar photo-thermal catalytic reactions to produce high value chemicals
[DE91-002140] p 4026 N92-32908
Solar thermal energy: Viable energy technology for today and tomorrow
[DE92-015039] p 4026 N92-32923

COST ESTIMATES
Booster Applications Facility report, phase 2
[DE92-013395] p 4070 N92-32411
Air traffic control: FAA's advanced automation system contract
[GAO/IMTEC-91-25] p 3934 N92-32861

COUPLED MODES
Can the speed of light in the fiber be controlled?
[AD-A247614] p 4074 N92-32668
Measurement of nonlinear mode coupling of tearing fluctuations
[DE92-013901] p 4080 N92-33154

COVALENT BONDS
Novel gas phase ion molecule reactions of C60(++) with O2 and NH3
[AD-A250921] p 4066 N92-32556

CRACK GEOMETRY
Environmental fatigue in aluminum-lithium alloys
[NASA-TM-107640] p 4021 N92-32423
A transgranular fatigue crack growth model based on restricted slip reversibility
[NRC-LTR-ST-1831] p 4023 N92-33076

CRACK PROPAGATION
Environmental fatigue in aluminum-lithium alloys
[NASA-TM-107640] p 4021 N92-32423
Mixed model fatigue crack growth behavior in a high strength steel
[AD-A250667] p 4022 N92-32717
An experimental study on the two-parameter crack tip field
[AD-A251173] p 4023 N92-32936
Propagation of a delamination in a composite panel subjected to a compression load p 3957 N92-33041
A transgranular fatigue crack growth model based on restricted slip reversibility
[NRC-LTR-ST-1831] p 4023 N92-33076

CRACK TIPS
A new approximate fracture mechanics analysis methodology for composites with a crack or hole
p 3949 N92-32530
Free-edge delamination of a stratified composite: Interaction with the transversal crack
[ONERA-RT-13/7256-RY-006-R] p 3954 N92-32792
An experimental study on the two-parameter crack tip field
[AD-A251173] p 4023 N92-32936
A transgranular fatigue crack growth model based on restricted slip reversibility
[NRC-LTR-ST-1831] p 4023 N92-33076

CRACKING (FRACTURING)
Free-edge delamination of a stratified composite: Interaction with the transversal crack
[ONERA-RT-13/7256-RY-006-R] p 3954 N92-32792

CRACKS
A new approximate fracture mechanics analysis methodology for composites with a crack or hole
p 3949 N92-32530
Weldability of Fe3Al based iron aluminide alloys
[DE92-017802] p 4020 N92-33085

CRASHWORTHINESS
The weight optimization of an armored crashworthy crewseat through the use of advanced composites and design p 3947 N92-32517

CRATERING
Impact origin of Titan's atmosphere
p 4094 N92-32351

CREEP PROPERTIES
High temperature deformation processes and strengthening mechanisms in intermetallic particulate composites
[AD-A250220] p 3946 N92-32339
Contribution to the study of the effect of the heterogeneous distribution of dislocations on the cyclic plasticity of single crystal aluminum
[ISAL-91-0099] p 4083 N92-32892

CREW PROCEDURES (INFLIGHT)
Observing team coordination within Army rotary-wing aircraft crews
[AD-A252234] p 4039 N92-32433

CRITERIA
A reexamination of the plastic flow criterion for copper
[AD-A252370] p 4023 N92-32918

CRITICAL FREQUENCIES
Advanced Study for Active Noise Control in Aircraft (ASANCA)
[AIAA PAPER 92-2092] p 4062 N92-32956

CRITICAL POINT
Thermal conductivity of liquid aliphatic hydrocarbons. Part 1: Alkanes
[ESDU-92011-PT-1] p 3945 N92-32484
Orthobaric densities and molar volumes of liquids: Halogenated ethanes
[ESDU-92009] p 3945 N92-32486

CRITICAL TEMPERATURE
Thermal conductivity of liquid aliphatic hydrocarbons. Part 1: Alkanes
[ESDU-92011-PT-1] p 3945 N92-32484

CRITICAL VELOCITY
An experimental study of the fluid mechanics associated with porous walls
[AIAA PAPER 92-0769] p 3998 N92-32263

CROSS SECTIONS
Scaling in the processes of ion-atom excitation
[DE92-625008] p 4065 N92-32500

CROSSLINKING
Methyl substituted polyimides containing carbonyl and ether connecting groups
[NASA-CASE-LAR-14351-1] p 3973 N92-33015

CROSSTALK
Holographic crosstalk and signal-to-noise ratio in orthogonal data storage
[AD-A250146] p 4013 N92-32323

CRYOGENIC COOLING
NASA space applications of high-temperature superconductors p 3985 N92-32980

CRYOGENIC EQUIPMENT
RF cavity vacuum interlock system
[DE92-016961] p 4070 N92-32567
NASA space applications of high-temperature superconductors p 3985 N92-32980
Measurement techniques for cryogenic Ka-band microstrip antennas p 3985 N92-32981

CRYOGENIC FLUIDS
NASA space applications of high-temperature superconductors p 3985 N92-32980

CRYOSTATS
Experimental determination of the refractive index of liquefied gas mixtures: Applications to hypothesized Titan oceans p 4099 N92-32390

CRYPTOGRAPHY
Methodologies for designing block ciphers and cryptographic protocols
[ISBN-0-315-50983-X] p 4049 N92-33230

CRYSTAL DEFECTS
Transmission electron microscope characterization of deformation and recovery in 304L stainless steel part
[DE92-013237] p 3966 N92-32614
Investigation on the lattice site location of the excess arsenic atoms in GaAs layers grown by low temperature molecular beam epitaxy
[DE92-008253] p 4083 N92-32693
Modeling the influence of irradiation temperature and displacement rate on hardening due to point defect clusters in ferritic steels
[DE92-016897] p 3969 N92-33115
Implantation of carbon in GaAs
[DE92-016921] p 4085 N92-33117

CRYSTAL DISLOCATIONS
High temperature deformation processes and strengthening mechanisms in intermetallic particulate composites
[AD-A250220] p 3946 N92-32339
Contribution to the study of the effect of the heterogeneous distribution of dislocations on the cyclic plasticity of single crystal aluminum
[ISAL-91-0099] p 4083 N92-32892

CRYSTAL GROWTH
Thermochemical and kinetic considerations in diamond growth
[AD-A247866] p 3971 N92-32490

CRYSTAL LATTICES
Structure and dynamics in low-dimensional guest-host systems
[DE92-014841] p 3970 N92-32429
Surface reconstruction and templating for zeolite thin film synthesis observed by atomic force microscopy
[AD-A251140] p 4066 N92-32548
Investigation on the lattice site location of the excess arsenic atoms in GaAs layers grown by low temperature molecular beam epitaxy
[DE92-008253] p 4083 N92-32693
Implantation of carbon in GaAs
[DE92-016921] p 4085 N92-33117

CRYSTAL OSCILLATORS
The influence of anharmonic phonons on the isotope effect in high-(Tc) oxides
[DE92-017083] p 4081 N92-32320

CRYSTAL STRUCTURE
The influence of anharmonic phonons on the isotope effect in high-(Tc) oxides
[DE92-017083] p 4081 N92-32320
Structure and dynamics in low-dimensional guest-host systems
[DE92-014841] p 3970 N92-32429
Surface reconstruction and templating for zeolite thin film synthesis observed by atomic force microscopy
[AD-A251140] p 4066 N92-32548
Photogenerated carrier-induced reactions on UHV semiconductor surfaces
[DE92-015355] p 4082 N92-32641
Investigation on the lattice site location of the excess arsenic atoms in GaAs layers grown by low temperature molecular beam epitaxy
[DE92-008253] p 4083 N92-32693
Contribution to the study of the effect of the heterogeneous distribution of dislocations on the cyclic plasticity of single crystal aluminum
[ISAL-91-0099] p 4083 N92-32892
Pseudopotential band calculations along a high-symmetry axis. Part 1: Central potential and the (111) direction
[AD-A252399] p 4084 N92-32938
Use of a Fourier deconvolution method in particle size determination and use of molecular mechanics in crystal structure determinations
[DE92-014510] p 4085 N92-33111

CRYSTAL SURFACES
Surface reconstruction and templating for zeolite thin film synthesis observed by atomic force microscopy
[AD-A251140] p 4066 N92-32548
Generic consequences of fundamental studies of beta phase decomposition modes in titanium and related alloy systems
[AD-A250789] p 3967 N92-32699

CRYSTALLINITY
The effect of heat treatment on the properties of PEEK and APC-2 p 3959 N92-33052

CRYSTALLIZATION
Dynamics of radiation-induced amorphization in intermetallic compounds
[DE92-016774] p 4086 N92-33221

CRYSTALLOGRAPHY
Generic consequences of fundamental studies of beta phase decomposition modes in titanium and related alloy systems
[AD-A250789] p 3967 N92-32699

CRYSTALS
Scintillation properties of lead sulfate
[DE92-010301] p 4082 N92-32493

CUBES (MATHEMATICS)
Characterization of Laborde-Mulder graphs and the halfcube
[IMAG-RR-857-I] p 4057 N92-32713

CUBIC EQUATIONS
MOL calculation of the solitons of the cubic Schroedinger equation
[DE92-017245] p 4060 N92-32998

CUES
Target cuing: A heterogeneous neural network approach p 3936 N92-32442
CURING
Experimental investigation of the axial impregnation of oriented fiber bundles by capillary forces
[AD-A250758] p 3961 N92-32508
Flush mounting of thin film sensors
[NASA-CASE-LAR-14446-1] p 3978 N92-33020
CURRENT ALGEBRA
Theoretical aspects of lepton-hadron scattering
[DE92-013765] p 4069 N92-33148
CURRENT DENSITY
Synthesis, microstructure, critical current density, magnetization and relaxation of hot-pressed YBa2Cu3O(6 + delta) through partial melting post-oxygenation
[DE92-015205] p 4085 N92-33026
CURVATURE
Effects of curvature and rotation on turbulence in the NASA low-speed centrifugal compressor impeller p 4003 N92-32292
CURVE FITTING
Frequency domain state-space system identification
[NASA-TM-107659] p 4021 N92-32657
Feasibility study for predicting human reliability growth through training and practice
[AD-A252371] p 4038 N92-32990
The local structure of image intensity discontinuities
[ISBN-0-315-57231-0] p 4048 N92-33204
CURVED BEAMS
A curved beam test specimen for determining the interlaminar tensile strength of a laminated composite p 3949 N92-32526
CURVED PANELS
Postbuckling behavior of curved panels under combined compression and shear loads p 3952 N92-32584
CURVES (GEOMETRY)
Geometric continuity and Frenet continuity of parametric curves
[IMAG-RR-846-M] p 4057 N92-32761
CYCLES
UHM/HNEI EV test and evaluation program
[DE92-011631] p 3989 N92-32754
CYCLIC HYDROCARBONS
Phase distributions of airborne polycyclic aromatic hydrocarbons in two US cities
[PB92-164979] p 4028 N92-32543
CYCLIC LOADS
Fatigue, hysteresis, and acoustic emission, parts 1 and 2
[AD-A251073] p 4021 N92-32681
CYCLOGENESIS
Tropical cyclone motion due to environmental interactions represented by empirical orthogonal functions of the vorticity fields
[AD-A246137] p 4033 N92-32534
CYCLONES
Diagnostic report of the National Hurricane Center, August and September 1991, volume 4, number 2
[PB92-179407] p 4033 N92-32503
Tropical cyclone motion due to environmental interactions represented by empirical orthogonal functions of the vorticity fields
[AD-A246137] p 4033 N92-32534
Climate System Monitoring (CSM) Monthly Bulletin, issue no. 1 p 4034 N92-33073
CYCLOTRON RESONANCE
RF-GD/FTMS: An FTMS system with a lensless external ion source for high resolution elemental mass spectrometry
[DE92-015343] p 3964 N92-32925
CYLINDRICAL BODIES
A numerical study of two-dimensional vortex shedding from rectangular cylinders p 3998 N92-32266
Magnetohydrodynamic stability of plasmas with radial motion
[DE92-013917] p 4077 N92-32417
Pseudopotential band calculations along a high-symmetry axis. Part 1: Central potential and the (111) direction
[AD-A252399] p 4084 N92-32938
CYLINDRICAL SHELLS
Free vibration of thick isotropic and orthotropic cylindrical shells
[DE92-011653] p 4022 N92-32706

D

DAMAGE
Computational simulation of matrix micro-slip bands in SiC/Ti-15 composite
[NASA-TM-105762] p 3946 N92-32466
A Protection And Detection Surface (PADS) for damage tolerance p 3948 N92-32523
Inelastic deformation and damage at high temperature
[DE92-012241] p 4021 N92-32698
Geometrical effects in two-dimensional arrays of Josephson junctions
[AD-A252209] p 4084 N92-32898
DAMAGE ASSESSMENT
Computational fluid dynamics analysis of SSME phase 2 and phase 2+ preburner injector element hydrogen flow paths p 3997 N92-32261
Debris/ice/TPS assessment and integrated photographic analysis for Shuttle Mission STS-49
[NASA-TM-107547] p 3941 N92-32454
Damage tolerance certification methodology for composite structures p 3951 N92-32579
Certification of damage tolerant composite structure p 3951 N92-32580
Fatigue, hysteresis, and acoustic emission, parts 1 and 2
[AD-A251073] p 4021 N92-32681
Effects of the abrasiveness of test and training site soils on parachute life
[AD-A252389] p 3931 N92-32900
Bird ingestion into large turbofan engines
[DOT/FAA/CT-91/17] p 3932 N92-33005
Damage progression under compressive loading in composite laminates containing an open hole p 3957 N92-33040
Propagation of a delamination in a composite panel subjected to a compression load p 3957 N92-33041
GARTEUR compression behaviour of advanced CFRP --- carbon fiber reinforced plastics p 3957 N92-33042
Effects of fuel on Hercules AS-4/8552 composite material p 3958 N92-33046
Building vibrations induced by noise from rotorcraft and propeller aircraft flyovers
[NASA-TM-104170] p 4063 N92-33160
DATA ACQUISITION
Ground Systems Development Environment (GSDE) interface requirements and prototyping plan
[NASA-CR-190713] p 4041 N92-32451
Injection of compact toroids for tokamak fueling and current drive
[DE92-010031] p 4077 N92-32533
The design and development of a portable, DSP micro-processor based, high-accuracy data acquisition system
[NRC-32146] p 4040 N92-32851
The development of an airborne information management system for flight test
[NASA-TM-104251] p 3938 N92-32866
Automated data acquisition and analysis in the mechanical test lab
[DE92-011231] p 4040 N92-32910
The Dornier 328 Acoustic Test Cell (ATC) for interior noise tests and selected test results
[AIAA PAPER 92-2164] p 4062 N92-32951
Pilots noise exposure during a Boeing 747-400 round trip: Ambient noise and acoustic-head recording and analysis of data p 4063 N92-32960
Applications of energy loss contrast STIM
[DE92-017254] p 4014 N92-33000
DATA BASE MANAGEMENT SYSTEMS
Automatic access experiment
[AD-A252217] p 4089 N92-32611
PANACEA User's Manual
[DE92-011289] p 4043 N92-32741
A minority research and education information service: Design, develop, pilot test, and implement on-line access for historically black colleges and universities and government agencies
[DE92-013572] p 4090 N92-32930
FEDIX on-line information service: Design, develop, test, and implement, an on-line research and education information service
[DE92-013582] p 4090 N92-32985
Oak Ridge Environmental Information System (OREIS). Phase 1: System definition document
[DE92-017342] p 4090 N92-33084
Concurrency control scheme for design object bases
[ISBN-0-315-56113-0] p 4049 N92-33232
DATA BASES
US Historical Climatology Network daily temperature and precipitation data
[DE92-014920] p 4032 N92-32431
Permuted keyword bank in CRIS. Terms for indexing and retrieving research projects in the current research information system
[PB92-179456] p 4090 N92-32712
EPCRA Section 313 Roadmaps Database: User's manual, version 2.2
[PB92-169523] p 4030 N92-33062
An international aerospace information system: A cooperative opportunity
[NASA-TM-108171] p 4091 N92-33237
DATA COMPRESSION
The development of an airborne information management system for flight test
[NASA-TM-104251] p 3938 N92-32866
Semiannual status report
[NASA-CR-190239] p 4046 N92-33092
Multi-stage hybrid coding of digital images
[ISBN-0-315-58989-2] p 4047 N92-33189
DATA CORRELATION
Extending estimation of C-J pressure of explosives to the very low density region
[DE92-015035] p 3975 N92-33003
DATA FLOW ANALYSIS
Improving the translation from data flow diagrams into Z by incorporating the data dictionary
[AD-A250769] p 4089 N92-32342
STARNET: A MultiGbit/s optical local area network with both packet and circuit switching
[AD-A247617] p 4050 N92-32628
DATA INTEGRATION
A Kalman filter integrated navigation design for the IAR Twin Otter Atmospheric Research Aircraft
[NRC-32148] p 3934 N92-32849
The use of Kalman filtering techniques to improve the accuracy of flight test data
[NRC-32139] p 3938 N92-32850
Integrating expert vision systems and spatial database by unifying knowledge representation schemes.Development in remote sensing image analysis expert systems and geographical information systems
[ISBN-0-315-49130-2] p 4024 N92-33233
DATA LINKS
An integrated multiple-sensor fire control system for air-to-air combat p 3937 N92-32450
DATA MANAGEMENT
SAGE 1 data user's guide
[NASA-RP-1275] p 4031 N92-33097
DATA PROCESSING
Program PLOTTAB: A code designed to plot continuous and/or discrete physical data
[DE92-013754] p 4041 N92-32416
Integrated Target Acquisition and Fire Control Systems
[AGARD-CP-500] p 3935 N92-32437
Tutorial on neural network applications in high energy physics: A 1992 perspective
[DE92-016003] p 4070 N92-32506
Development of a prototype spatial information processing system for hydrologic research
[NASA-CR-190579] p 4024 N92-32590
Target Cueing And Tracking System (TCATS): User's guide
[DE92-015385] p 4042 N92-32617
Information resources management plan of the Federal Government
[PB92-147198] p 4089 N92-32643
Adaptive information processing and global optimization
[AD-A248450] p 4089 N92-32644
Analysis of data from a DO-178A software development process p 4045 N92-32880
Automated data acquisition and analysis in the mechanical test lab
[DE92-011231] p 4040 N92-32910
Advanced information processing system: The Army fault tolerant architecture conceptual study. Volume 1: Army fault tolerant architecture overview
[NASA-CR-189632-VOL-1] p 4052 N92-33100
Advanced information processing system: The Army fault tolerant architecture conceptual study. Volume 2: Army fault tolerant architecture design and analysis
[NASA-CR-189632-VOL-2] p 4052 N92-33101
DATA REDUCTION
A reanalysis of Voyager UVS observations of Titan p 4094 N92-32357
NASA Marshall Space Flight Center Solar Observatory report, January - June 1992
[NASA-TM-103597] p 4092 N92-32478
DATA RETRIEVAL
Automatic access experiment
[AD-A252217] p 4089 N92-32611
Learning systems, adaptive data structures, and random environments
[ISBN-0-315-51158-3] p 4054 N92-33218
DATA SMOOTHING
Bandwidth selection for the intensity of point processes: Application to hazard rate models for censored data
[IMAG-RR-859-I/M] p 4056 N92-32684
DATA STORAGE
Holographic crosstalk and signal-to-noise ratio in orthogonal data storage
[AD-A250146] p 4013 N92-32323
Automatic access experiment
[AD-A252217] p 4089 N92-32611

DATA STRUCTURES
Improving the translation from data flow diagrams into Z by incorporating the data dictionary
[AD-A250769] p 4089 N92-32342
Fault-tolerant wait-free shared objects
[NASA-CR-190679] p 4020 N92-32436
Implementation of a tree-code for numerical simulations of stellar systems
[INPE-5370-TDI/469] p 4093 N92-32604
Object links in the repository
[NASA-CR-190644] p 4091 N92-33096
Object linking in repositories
[NASA-CR-190629] p 4091 N92-33178
Learning systems, adaptive data structures, and random environments
[ISBN-0-315-51158-3] p 4054 N92-33218
A study of artificial intelligence planning: A framework for a planning development system
[ISBN-0-315-54378-7] p 4055 N92-33219

DATA SYSTEMS
Frequency domain state-space system identification
[NASA-TM-107659] p 4021 N92-32657
CFD efforts in the Netherlands
[NLR-TP-91250-U] p 4011 N92-32835

DATA TRANSFER (COMPUTERS)
Analytic performance of software pipelines with rendezvous and communication tasks
[ISBN-0-315-54414-7] p 4052 N92-33216
A fast task allocator for multiprocessing systems
[ISBN-0-315-54380-9] p 4053 N92-33217

DATA TRANSMISSION
A scalable, switched circuit LAN for Gb/S channels with over Tb/S total capacity
[DE92-013444] p 4050 N92-32412
Target Cueing And Tracking System (TCATS): User's guide
[DE92-015385] p 4042 N92-32617
Semiannual status report
[NASA-CR-190239] p 4046 N92-33092

DC GENERATORS
Overview and evolution of the LeRC PMAD DC Testbed
[NASA-TM-105842] p 3991 N92-32867

DEATH
Toward advanced human reliability programs. Structural development considerations and options for extreme risk environments
[AD-A250786] p 4038 N92-32660

DEBONDING (MATERIALS)
Computational simulation of matrix micro-slip bands in SiC/Ti-15 composite
[NASA-TM-105762] p 3946 N92-32466

DEBRIS
Debris/ice/TPS assessment and integrated photographic analysis for Shuttle Mission STS-49
[NASA-TM-107547] p 3941 N92-32454
Superheavyweight missions SI versus DI: Ascent flight design options and recommendations
[NASA-CR-183208] p 3942 N92-32610

DECAY
Study on lifetime specific, laser-induced ultrafast fluorescence detection in the time and frequency domain for in-situ environmental analysis of organic pollutants
[KFK-4975] p 4029 N92-32841

DECISION MAKING
An adaptive algorithm for modifying hyperellipsoidal decision surfaces
[DE92-013540] p 4041 N92-32414
Observing team coordination within Army rotary-wing aircraft crews
[AD-A252234] p 4039 N92-32433
Cognitive biases and time stress in team decision making
[AD-A251153] p 4088 N92-32551
Tactical state and performance assessment during air combat maneuvering
[AD-A247426] p 3935 N92-32612

DECODERS
VLSI architecture for a Reed-Solomon decoder
[NASA-CASE-NPO-17897-1-CU] p 3991 N92-33011

DECODING
The architecture development and design considerations of a high-speed, single chip, CMOS convolutional decoder based on a modification of the Viterbi algorithm
[ISBN-0-315-60456-5] p 3993 N92-33208

DECOMPOSITION
Generic consequences of fundamental studies of beta phase decomposition modes in titanium and related alloy systems
[AD-A250789] p 3967 N92-32699
Thermochemical cycles for energy storage: Thermal decomposition of ZnSO4 systems
[DE91-002144] p 4026 N92-32909
Direct catalytic decomposition of nitric oxide
[DE92-013847] p 4030 N92-33125

DECONTAMINATION
International technology transfer to support the environmental restoration needs of the DOE complex
[DE92-013663] p 4028 N92-32558
Summary of engineering-scale experiments for the Solar Detoxification of Water project
[DE92-013776] p 4027 N92-33150

DEFECTS
PAC spectroscopy of electronic ceramics
[DE92-014328] p 3970 N92-32471
Cleanroom process evolution in the SEL
p 4044 N92-32871

DEFENSE PROGRAM
Defense environmental restoration program annual report to Congress for fiscal year 1991
[AD-A244196] p 4029 N92-32731
The DOD science and technology strategy
[AD-A253691] p 4104 N92-33027
DoD key technologies plan
[AD-A253692] p 4105 N92-33238

DEFLAGRATION
A state of the art report on flame acceleration and transition to detonation in hydrogen/air/diluent mixtures
[DE92-626850] p 3961 N92-32475

DEFLECTION
Lift and rolling moment due to spoilers on wings with trailing-edge flaps deflected at subsonic speeds
[ESDU-92002-SUPPL] p 3931 N92-32782
Further wind tunnel investigation of the SM701 airfoil with aileron and turbulators
[NASA-CR-190702] p 3932 N92-33063

DEFLECTORS
High efficiency fast neutron threshold deflector
[AD-D015311] p 4073 N92-33167

DEFORMATION
Efficient finite element modeling of laminated composite plates based on higher-order theory
p 3949 N92-32529
Buckling of fibre reinforced composite and sandwich laminates with higher-order shear deformation theories
[IIT-B/CE/RR/92/2] p 4022 N92-32783
Accommodation mechanisms and dispersoid-free zone s in Al 7475 after superplastic forming
[MBB-Z-0404-91-PUB] p 3968 N92-32894
A reexamination of the plastic flow criterion for copper
[AD-A252370] p 4023 N92-32918

DEGRADATION
Environmental degradation of high temperature composites p 3958 N92-33047
Jet fuel absorption and dynamic mechanical analysis of carbon fibre composites p 3959 N92-33050

DELAMINATING
Compression of thick laminated composite beams with initial impact-like damage
[NASA-CR-190573] p 3946 N92-32491
Computational simulation of structural fracture in fiber composites p 3949 N92-32531
The use of piezoelectric sensors to detect delamination initiation in carbon fiber reinforced composites
[MBB-Z-0391-91-PUB] p 3954 N92-32740
Free-edge delamination of a stratified composite: Interaction with the transversal crack
[ONERA-RT-13/7256-RY-006-R] p 3954 N92-32792
Study of the mechanical behaviour of graphite/epoxy laminates subjected to static and cyclic loading
[NRC-30833] p 3955 N92-32813
Propagation of a delamination in a composite panel subjected to a compression load p 3957 N92-33041

DELTA WINGS
Vortex flow visualization using colored and fluorescent dyes on flat plate delta wing with leading edge extension
[AD-A251139] p 3930 N92-32651
An experimental study of the flow over a sharp-edged delta wing at subsonic and transonic speeds
[NLR-TP-91117-U] p 3930 N92-32732

DELTAS
Theoretical nuclear physics
[DE92-016837] p 4069 N92-33186

DEMOGRAPHY
Toward advanced human reliability programs. Structural development considerations and options for extreme risk environments
[AD-A250786] p 4038 N92-32660

DENSITY (MASS/VOLUME)
Density variations and anomalies in palladium compacts
[DE92-014382] p 3967 N92-32721
Radiography to measure the longitudinal density gradients of Pd compacts
[DE92-014383] p 3968 N92-32896
Extending estimation of C-J pressure of explosives to the very low density region
[DE92-015035] p 3975 N92-33003

DENSITY DISTRIBUTION
Properties and distribution of the aerosols in the atmosphere of Titan p 4100 N92-32396

DEOXYRIBONUCLEIC ACID
Bacterial responses to extreme temperatures and pressures and to heavy organic loading
[AD-A247456] p 4035 N92-32571

DEPOLARIZATION
Depolarized light source for fiber optic sensors
[AD-D015289] p 4074 N92-32634

DEPOSITION
Low cost MMC made by spray deposition
[MBB-Z-0407-91-PUB] p 3968 N92-32897
Superconducting transport properties and surface microstructure for YBa2Cu3O(7-delta) based superlattices grown by pulsed laser deposition
[DE91-014224] p 4085 N92-33023
Method of growing diamond film on substrates
[AD-D015313] p 3973 N92-33170
Coatings for improved corrosion resistance
[DE92-016779] p 3974 N92-33247

DEPOSITS
Substrate reactions and flux pinning structures in melt-processed YBa2Cu3O7 deposits on Ag-Pd alloy substrates
[DE92-014404] p 4084 N92-32919

DEPTH
Magnetic penetration depth of YBa2Cu3O(7-delta) thin films determined by the power transmission method
p 3985 N92-32983

DESIGN ANALYSIS
SRMAFTE facility checkout model flow field analysis
p 3994 N92-32247
Overview of the relevant CFD work at Thiokol Corporation p 3995 N92-32249
A computational design system for rapid CFD analysis
p 4000 N92-32273
Optimum design of ninety degree bends
p 4000 N92-32274
Inverse design of a proper number, shapes, sizes, and locations of coolant flow passages
p 4004 N92-32298
Numerical analysis of the hot-gas-side and coolant-side heat transfer in liquid rocket engine combustors
p 4004 N92-32299
Design and construction of a sample preparation chamber for atomic beam scattering
[DE92-014509] p 4065 N92-32473
Design, analysis, and testing of a reusable wingbox for ballistic evaluation of composite structures
p 3947 N92-32518
Design and construction of a magnetic sector mass spectrometer
[INPE-5405-RPQ/659] p 4014 N92-32601
Superheavyweight missions SI versus DI: Ascent flight design options and recommendations
[NASA-CR-183208] p 3942 N92-32610
Lithium sulphur dioxide battery failure following high frequency vibration
[CRAD-1-90] p 3990 N92-32812
Polarized wiggler for NSLS x ray ring design considerations
[DE92-012212] p 4071 N92-32912
A flexible CPW package for a 30 GHz MMIC amplifier
p 3983 N92-32972
Volume 1. Preliminary design study: AXAF x ray calibration spectrometers. Volume 2. Revised preliminary design study: AXAF x ray calibration spectrometers
[NASA-CR-184340] p 4092 N92-33094
Global/local interlaminar stress analysis of a grid-stiffened composite panel
[NASA-CR-190822] p 4023 N92-33139

DESORPTION
Molecular surface analysis by laser ionization of desorbed molecules
[DE92-016320] p 4016 N92-33114

DESULFURIZING
Development of the chemical and electrochemical coal cleaning process
[DE92-013353] p 3977 N92-32467

DETECTION
Hydrate detection
[DE92-014350] p 4034 N92-32333
Target detection using co-occurrence matrix segmentation and its hardware implementation
p 3936 N92-32443
Automatic detection, pursuit, and classification in infrared imagery p 3937 N92-32445
The German anti tank helicopter PAH 2: An example of a future sensor platform p 3937 N92-32448
New applications of ionization and fluorescence techniques for detecting and characterization of open-shell organometallics in the gas phase
[AD-A250923] p 3961 N92-32509
Contribution to the determination of vanishing points using Hough transform
[TELECOM-91-D-008] p 4058 N92-32803

Collaborative, remote, in-depth inspection and verification of satellites with neutral particle beams
[DE92-014195] p 3943 N92-32934
Research and development of a helium-4 based solar neutrino detector
[DE92-017390] p 4103 N92-33119
High efficiency fast neutron threshold deflector
[AD-D015311] p 4073 N92-33167

DETECTORS
Small passive chemical detector
[DE92-014188] p 4030 N92-32933

DETONATION
A state of the art report on flame acceleration and transition to detonation in hydrogen/air/diluent mixtures
[DE92-626850] p 3961 N92-32475
Development of methodology and technology for identifying and quantifying emission products from open burning and open detonation thermal treatment methods. BangBox test series. Volume 3: Quality assurance and quality control
[AD-A251099] p 4029 N92-32650
Extending estimation of C-J pressure of explosives to the very low density region
[DE92-015035] p 3975 N92-33003

DETONATION WAVES
A state of the art report on flame acceleration and transition to detonation in hydrogen/air/diluent mixtures
[DE92-626850] p 3961 N92-32475

DIAMINES
Polyimides with carbonyl and ether connecting groups between the aromatic rings
[NASA-CASE-LAR-14001-1] p 3973 N92-33008

DIAMOND FILMS
Method of growing diamond film on substrates
[AD-D015313] p 3973 N92-33170

DIAMONDS
Thermochemical and kinetic considerations in diamond growth
[AD-A247866] p 3971 N92-32490
Method of growing diamond film on substrates
[AD-D015313] p 3973 N92-33170

DICTIONARIES
Improving the translation from data flow diagrams into Z by incorporating the data dictionary
[AD-A250769] p 4089 N92-32342

DIELECTRIC PROPERTIES
Microwave absorption by lossy ceramic materials
[DE92-016963] p 3970 N92-32317
Dielectric constant measurements in simulated Titan ocean liquids p 4102 N92-32409

DIELECTRICS
Local aspects of the optical reflection problem: The discrete dipole approach
[ISBN-90-9004118-4] p 4074 N92-32703
Planar dielectric resonator stabilized HEMT oscillator integrated with CPW/aperture coupled patch antenna p 3983 N92-32967
Numerical analysis of scattering from certain conducting and dielectric bodies of arbitrary shape
[ISBN-0-315-63282-8] p 3987 N92-33192

DIESEL ENGINES
The polychromatic pyrometer in diesel combustion
[ECL-91-42] p 3963 N92-32722
Local and temporal study of the combustion and heat transfer in a direct injection diesel engine
[ECL-91-43] p 3963 N92-32724

DIFFERENTIAL EQUATIONS
Two studies of nonlinear processes in irreversible thermodynamics
[DE92-016855] p 4087 N92-32566
Resolution of convection and diffusion by the boolean automata method
[ONERA-RF-22/3419-AY-122A] p 4057 N92-32772
Generalizations of the classical Laguerre polynomials and some q-analogues
[ISBN-90-9003765-9] p 4058 N92-32836
Poincare normal form (system of ordinary differential equations): An algorithmic point of view
[IMAG-RR-839-M] p 4058 N92-32838
Experiments with an ordinary differential equation solver in the parallel solution of method of lines problems on a shared memory parallel computer, part 2
[DE92-017159] p 4052 N92-32926

DIFFRACTION
Numerical evaluation of the incomplete airy functions and their application to high frequency scattering and diffraction
[NASA-CR-190745] p 4058 N92-32888
Diffractive optics technology and the NASA Geostationary Earth Observatory (GEO)
[NASA-CR-190611] p 4076 N92-33074

DIFFRACTION PATTERNS
Determining surface profile from sequential interference patterns from a long trace profiler
[DE92-017117] p 4073 N92-32321
Topographical measuring based on the shadow and projection Moire method
[ISBN-90-9004146-X] p 4074 N92-32705
Synthesis, microstructure, critical current density, magnetization and relaxation of hot-pressed YBa2Cu3O(6 + delta) through partial melting post-oxygenation
[DE92-015205] p 4085 N92-33026

DIFFUSION
Morphology, 31P spin diffusion, and phase transitions in a representative semicrystalline polyphosphazene by solid-state NMR
[AD-A250883] p 3961 N92-32553
Advanced computational transport methods for curvilinear geometries
[DE92-011290] p 4057 N92-32743
Hydrogen permeation through bilayer metallic membrranes
[UTIAS-TN-342] p 3967 N92-32794

DIFFUSION WELDING
Fundamental questions concerning the application of superplastic forming and superplastic forming/diffusion bonding
[MBB-Z-0402-91-PUB] p 3977 N92-32690

DIGITAL COMPUTERS
Advanced information processing system: The Army fault tolerant architecture conceptual study. Volume 1: Army fault tolerant architecture overview
[NASA-CR-189632-VOL-1] p 4052 N92-33100

DIGITAL DATA
Development of a prototype spatial information processing system for hydrologic research
[NASA-CR-190579] p 4024 N92-32590

DIGITAL FILTERS
The development of an airborne information management system for flight test
[NASA-TM-104251] p 3938 N92-32866
Analog CMOS filters for very-high frequencies
[ISBN-90-9004420-5] p 3986 N92-33143
A simplified synthesis of lossless two-port wave digital and analog filters
[ISBN-0-315-63272-0] p 3993 N92-33193
Design and implementation of N-dimensional digital filters
[ISBN-0-315-60747-5] p 3993 N92-33195

DIGITAL SYSTEMS
The multiple-function multi-input/multi-output digital controller system for the AFW wind-tunnel model
[NASA-TM-107600] p 3934 N92-32536
Comparative evaluation of optical waveguides as alternative interconnections for high performance packaging p 3984 N92-32974

DIGITAL TECHNIQUES
Target Cueing And Tracking System (TCATS): User's guide
[DE92-015385] p 4042 N92-32617
Fuzzy set methods for object recognition in space applications
[NASA-CR-190388] p 4047 N92-33093
An implementation of a fault-tolerant, multidirectional, digital interpolation beamformer
[AD-A252494] p 3986 N92-33152
Multi-stage hybrid coding of digital images
[ISBN-0-315-58989-2] p 4047 N92-33189

DILUTION
Local structural order and molecular associations in water DMSO mixtures. Molecular dynamics study
[AD-A250935] p 4064 N92-32418

DIMENSIONAL ANALYSIS
CFD analysis to optimize a design modification of BSMT p 4004 N92-32296
Out of plane analysis for composite structures p 3949 N92-32527
Thermal gravitational modelling and scaling of two-phase heat transport systems for space: An assessment and a comparison of predictions and experimental results
[NLR-TP-91401-U] p 4008 N92-32675
Advanced computational transport methods for curvilinear geometries
[DE92-011290] p 4057 N92-32743

DIODES
Program for research in conducting polymers
[AD-A250965] p 3971 N92-32665

DIOXIDES
A study of the dissolution mechanism by chemical and electrochemical oxidation-reduction of actinide dioxides (UO2, NpO2, PuO2, and AmO2) in an acid aqueous medium
[DE92-014834] p 3965 N92-33126

DIRAC EQUATION
Fractional spin: Majorana-Dirac field
[DE92-624558] p 4087 N92-32603

DIRECT CURRENT
Geometrical effects in two-dimensional arrays of Josephson junctions
[AD-A252209] p 4084 N92-32898

DIRECTORIES
National Voluntary Laboratory Accreditation Program 1992 Directory
[PB92-201094] p 3941 N92-33002

DIRICHLET PROBLEM
Sweeping algorithms for five-point stencils and banded matrices
[DE92-017309] p 4047 N92-33118

DISCONTINUITY
Analysis of shielded CPW discontinuities with air-bridges p 3983 N92-32971

DISCRETE FUNCTIONS
Analog CMOS filters for very-high frequencies
[ISBN-90-9004420-5] p 3986 N92-33143

DISLOCATIONS (MATERIALS)
Study and achievement of a parallel simulator for diffusion at the atomic level: Creation and growth of dislocation loops under electronic radiation
[LAAS-92118] p 4066 N92-32735

DISPLACEMENT
An experimental study on the two-parameter crack tip field
[AD-A251173] p 4023 N92-32936

DISPLAY DEVICES
Program PLOTTAB: A code designed to plot continuous and/or discrete physical data
[DE92-013754] p 4041 N92-32416
Correlating visual scene elements with simulator sickness incidence: Hardware and software development
[AD-A252235] p 4036 N92-32434
An integrated multiple-sensor fire control system for air-to-air combat p 3937 N92-32450
Optical modulation characteristics and applications of liquid crystal televisions
[AD-A252466] p 3979 N92-32633
Collaborative research on V/STOL control system/cockpit display tradeoffs under the NASA/MOD joint aeronautical program
[NASA-TM-103910] p 3939 N92-32788
Instrument scanning and subjective workload with the peripheral vision horizon display
[CTN-92-60359] p 4038 N92-32817
Temporal and spatial factors affecting the perception of computer-generated imagery
[AD-A249242] p 4046 N92-32907
EPCRA Section 313 Roadmaps Database: User's manual, version 2.2
[PB92-169523] p 4030 N92-33062

DISSIPATION
Improved dissipation models for central difference schemes
[FFA-TN-1991-41] p 4057 N92-32729
A new time scale based k-epsilon model for near wall turbulence
[NASA-TM-105768] p 4011 N92-32868

DISSOLVING
A study of the dissolution mechanism by chemical and electrochemical oxidation-reduction of actinide dioxides (UO2, NpO2, PuO2, and AmO2) in an acid aqueous medium
[DE92-014834] p 3965 N92-33126

DISTANCE
Auto and hetero-associative memory using a 2-D optical logic gate
[NASA-CASE-NPO-17997-1-CU] p 4041 N92-33057

DISTORTION
Range of validity of distorted wave Born and impulse approximations for (e,2e)
[DE92-624821] p 4087 N92-32649

DISTRIBUTED PROCESSING
A scalable, switched circuit LAN for Gb/S channels with over Tb/S total capacity
[DE92-013444] p 4050 N92-32412
An integrated multiple-sensor fire control system for air-to-air combat p 3937 N92-32450
Optimal communication schemes on an SIMD distributed-memory hypercube
[IMAG-RR-848-M] p 4051 N92-32715
Fault tolerance for security management in distributed systems
[LAAS-92011] p 4040 N92-32766
Quantum wave modeling on highly parallel distributed memory machines
[DE92-014507] p 4088 N92-33109
CSP: A distributed logic programming language for discrete event simulation
[ISBN-0-315-54272-1] p 4048 N92-33214

DISTRIBUTION (PROPERTY)
Phase distributions of airborne polycyclic aromatic hydrocarbons in two US cities
[PB92-164979] p 4028 N92-32543

DISTRIBUTION FUNCTIONS
On the resistive transition of composite superconductors
[ISBN-90-9003899-X] p 3992 N92-33145

DIURNAL VARIATIONS
Modeling of the diurnal variations of the atmosphere of Titan p 4096 N92-32366
US Historical Climatology Network daily temperature and precipitation data
[DE92-014920] p 4032 N92-32431
Annual variation of surface temperatures over the world
[PB92-193259] p 4028 N92-32554
DIVERTERS
Scrape-off layer modeling of radiative divertor and high heat flux experiments on D3-D
[DE92-015007] p 4080 N92-32995
DOCUMENTATION
Parameterization of directional spectra, part 2. Volume 2: User's manual for the programs RMODEL, FITHM, and FITDM
[DREA-CR-89-445-PT-2-VOL-2] p 3981 N92-32749
DOCUMENTS
Publications on maglev technologies
[DE92-013296] p 4017 N92-32615
Proceedings of the Sixteenth Annual Software Engineering Workshop
[NASA-TM-107964] p 4044 N92-32869
DOMAINS
Supporting multiple domains in a single reuse repository
[NASA-CR-190640] p 4090 N92-32654
A prototype software engineering environment for domain modeling and reuse p 4046 N92-32882
DOPED CRYSTALS
Structure and dynamics in low-dimensional guest-host systems
[DE92-014841] p 3970 N92-32429
PAC spectroscopy of electronic ceramics
[DE92-014328] p 3970 N92-32471
Investigation of impurity related phenomena, significant for novel semiconductor technologies
[ETN-92-92048] p 4083 N92-32760
Intermodulation in the oscillatory magnetoresistance of a two-dimensional electron gas p 3984 N92-32975
Reduced mobility and PPC in In(.20)Ga(.80)As / Al(.23)Ga(.77)As HEMT structure p 3984 N92-32976
Study of InGaAs-based modulation doped field effect transistor structures using variable-angle spectroscopic ellipsometry p 3984 N92-32977
Microwave properties of peeled HEMT devices sapphire substrates p 3984 N92-32978
DOPPLER EFFECT
Observations of high frequency and high wavenumber solar oscillations
[AD-A250099] p 4103 N92-32488
DOPPLER NAVIGATION
A Kalman filter integrated navigation design for the IAR Twin Otter Atmospheric Research Aircraft
[NRC-32148] p 3934 N92-32849
DOPPLER RADAR
A simple Doppler wind lidar sensor: Simulated measurements and impacts in a global assimilation and forecast system
[PL-TR-91-2253] p 4034 N92-32859
DOUBLE BASE PROPELLANTS
Development of methodology and technology for identifying and quantifying emission products from open burning and open detonation thermal treatment methods. BangBox test series. Volume 3: Quality assurance and quality control
[AD-A251099] p 4029 N92-32650
DRAG REDUCTION
A method for designing blended wing-body configurations for low wave drag
[NASA-TP-3261] p 3929 N92-32480
Further wind tunnel investigation of the SM701 airfoil with aileron and turbulators
[NASA-CR-190702] p 3932 N92-33063
DRIFT RATE
Studies of helium based drift chamber gases for high-luminosity low energy machines
[DE92-012415] p 4065 N92-32426
DRILLING
Stress-relief displacements induced by drilling: Applications to holographic measurements of in situ stress
[DE92-013711] p 4014 N92-32620
Influence of compliance on performance of robotic drilling
[OUEL-1917/92] p 4018 N92-32757
DROPS (LIQUIDS)
Direct numerical simulation of a combusting droplet with convection p 3996 N92-32256
Numerical modeling for dilute and dense sprays p 3997 N92-32258
Modeling of SSME fuel preburner ASI p 3945 N92-32259
DRY HEAT
HDR opportunities and challenges beyond the long-term flow test isco, CA, 24-26 Mar. 1992
[DE92-011234] p 4025 N92-32695
DUCTED FANS
Investigation of the flight control requirements of a half-scale ducted fan unmanned aerial vehicle
[AD-A252730] p 3940 N92-32988
DUCTED FLOW
The application of unsteady potential flow vortex loop/dipole theory to the work and acoustics of low-speed turbomachinery
[AD-A251160] p 4008 N92-32652
DUCTILITY
High temperature fabricable nickel-iron aluminides
[CA-PATENT-1-276-814] p 3968 N92-32855
DUCTS
Optimum design of ninety degree bends p 4000 N92-32274
DURABILITY
Supportability evaluation of thermoplastic and thermoset composites p 3950 N92-32576
Residual strength of repaired graphite/epoxy laminates after 5 years of outdoor exposure p 3950 N92-32577
DYNAMIC CHARACTERISTICS
Molecular dynamics modeling of the mechanical properties of metal surfaces at the nanometer scale
[DE92-010705] p 3966 N92-32646
Temporal and spatial factors affecting the perception of computer-generated imagery
[AD-A249242] p 4046 N92-32907
Dynamics of radiation-induced amorphization in intermetallic compounds
[DE92-016774] p 4086 N92-33221
DYNAMIC LOADS
An analysis of the flow field in the region of the ASRM field joints p 4005 N92-32305
Reducing torque fluctuation in linkage drive shafts
[ESDU-92016] p 4017 N92-32482
DYNAMIC MODELS
Molecular dynamics modeling of the mechanical properties of metal surfaces at the nanometer scale
[DE92-010705] p 3966 N92-32646
A discrete nonlinear model approach to study the behavior of large signal DC to DC converters
[LAAS-90028] p 3989 N92-32777
A continuous nonlinear model approach to study the behavior of large signal DC to DC converters
[LAAS-90027] p 3990 N92-32793
Classical dynamics of systems with time-varying inertial properties with application to multi-rigid-body systems
[ISBN-0-315-57834-3] p 4024 N92-33228
DYNAMIC PROGRAMMING
Finding solutions to value independent knapsack problems
[INPE-5390-TAE/011] p 4055 N92-32661
Enhancements to speech recognition on voice response systems
[TELECOM-91-E-018] p 3981 N92-32807
DYNAMIC STABILITY
Free motion of an unsupported tank that is partially filled with liquid
[NLR-TP-91185-U] p 4011 N92-32831
DYNAMIC STRUCTURAL ANALYSIS
Recent advances in statistical energy analysis p 4062 N92-32954
Use of SEA to predict structure-borne noise in aircraft p 4062 N92-32955
Active vibrations and noise control for turboprop application research program activities p 4063 N92-32962
Classical dynamics of systems with time-varying inertial properties with application to multi-rigid-body systems
[ISBN-0-315-57834-3] p 4024 N92-33228
DYNAMICAL SYSTEMS
The behavior of matter under non-equilibrium conditions: Fundamental aspects and applications
[DE92-014247] p 4087 N92-32593
Steady state behavior of reduced dynamic systems with local nonlinearities
[ISBN-90-9004680-1] p 4056 N92-32707

E

EAR
Exposures from headset interference tones
[AD-A247175] p 4061 N92-32697
Modeling the ear's response to intense impulses and the development of improved damage risk criteria
[AD-A252365] p 4037 N92-32916
EARPHONES
Exposures from headset interference tones
[AD-A247175] p 4061 N92-32697
EARTH (PLANET)
Organic chemistry on Titan versus terrestrial prebiotic chemistry: Exobiological implications p 4096 N92-32368
EARTH ATMOSPHERE
Grill spectrometry on the Space Shuttle during the Atlas 1 mission
[AERONAUTICA-ACTA-A-364-199] p 3943 N92-32728
EARTH ENVIRONMENT
STEL p 4103 N92-32457
Oak Ridge Environmental Information System (OREIS). Phase 1: System definition document
[DE92-017342] p 4090 N92-33084
EARTH IONOSPHERE
STEL p 4103 N92-32457
EARTH MAGNETOSPHERE
STEL p 4103 N92-32457
The energetic radiation environment in a highly elliptical (Molniya) orbit
[AD-A252394] p 4031 N92-32902
EARTH ORBITAL ENVIRONMENTS
Orbital debris characterization with impact flash signatures
[DE92-010666] p 4018 N92-32701
EARTH RESOURCES
Guide to selected national environmental statistics in the US Government
[PB92-201144] p 4030 N92-33087
EARTH SURFACE
Boundary layer processes in coastal meteorology: Prospects for remote sensing applications
[PB92-177849] p 4033 N92-32714
ECOLOGY
High-temperature Solid Oxide Fuel Cell (SOFC) generator development project: Environmental assessment
[DE92-014698] p 4026 N92-32924
ECOSYSTEMS
Simulations of the carbon cycle in the oceans
[DE92-016622] p 4035 N92-32336
Guide to selected national environmental statistics in the US Government
[PB92-201144] p 4030 N92-33087
EDDY CURRENTS
Study of eddy current probes
[NASA-CR-190814] p 4020 N92-32425
EDDY VISCOSITY
Simple models for turbulent wave-current bottom boundary layer flow
[AD-A247942] p 4007 N92-32630
A new time scale based k-epsilon model for near wall turbulence
[NASA-TM-105768] p 4011 N92-32868
EDGE DISLOCATIONS
Computational simulation of matrix micro-slip bands in SiC/Ti-15 composite
[NASA-TM-105762] p 3946 N92-32466
Influence of edge effect on compression-tension fatigue of toughened graphite/epoxy laminates p 3957 N92-33039
EDGES
Study of the mechanical behaviour of graphite/epoxy laminates subjected to static and cyclic loading
[NRC-30833] p 3955 N92-32813
EDUCATION
Human learning of schemas from explanations in practical electronics
[AD-A247429] p 4038 N92-32569
A minority research and education information service: Design, develop, pilot test, and implement on-line access for historically black colleges and universities and government agencies
[DE92-013572] p 4090 N92-32930
FEDIX on-line information service: Design, develop, test, and implement, an on-line research and education information service
[DE92-013582] p 4090 N92-32985
Feasibility study for predicting human reliability growth through training and practice
[AD-A252371] p 4038 N92-32990
EFFECTS
Effects of fuel on Hercules AS-4/8552 composite material p 3958 N92-33046
EIGENVALUES
Schroedinger operators with singular potentials in the semiclassical limit
[ETN-92-92145] p 4058 N92-32840
EKMAN LAYER
A preliminary assessment of the Titan planetary boundary layer p 4095 N92-32363
ELASTIC BUCKLING
Three-dimensional elasticity analysis of buckling of laminated plates p 3957 N92-33037

ELASTIC DEFORMATION
Calculation of the energy of elastic deformation of Kevlar backing plates for ceramic armours
[AD-A250129] p 3970 N92-32489
Three-dimensional elasticity analysis of buckling of laminated plates p 3957 N92-33037
ELASTIC PROPERTIES
Three-dimensional elasticity analysis of buckling of laminated plates p 3957 N92-33037
ELASTIC SCATTERING
Coupled-channels-optical calculation of electron-helium scattering
[DE92-625009] p 4065 N92-32501
ELECTRIC BATTERIES
Development of high-performance Na/NiCl2 cell
[DE92-015270] p 3988 N92-32639
UHM/HNEI EV test and evaluation program
[DE92-011631] p 3989 N92-32754
ELECTRIC CHARGE
Site competition of impurities and grain boundary stability in iron
[AD-A252411] p 4084 N92-32939
ELECTRIC CONNECTORS
Comparative evaluation of optical waveguides as alternative interconnections for high performance packaging p 3984 N92-32974
Flush mounting of thin film sensors
[NASA-CASE-LAR-14446-1] p 3978 N92-33020
ELECTRIC CONTACTS
Thermal conductance of augmented pressed metallic contacts at liquid helium temperatures
[NASA-TM-103917] p 4007 N92-32474
ELECTRIC CURRENT
Processing and properties of silver-clad Tl-Ba-Ca-Cu-O wires and tapes
[DE92-015266] p 4081 N92-32346
ELECTRIC DIPOLES
Local aspects of the optical reflection problem: The discrete dipole approach
[ISBN-90-9004118-4] p 4074 N92-32703
ELECTRIC DISCHARGES
Satellite anomalies and electrostatic surface discharges
[AD-A246880] p 3942 N92-32538
ESD traits of bulk propellant under pressure p 3976 N92-33242
ELECTRIC EQUIPMENT TESTS
The 1991 rocket-triggered lightning test of the DoD Security Operations Test Site (SOTS) munitions storage bunker, Fort McClellan, Alabama
[DE92-012449] p 4032 N92-32427
ELECTRIC FIELDS
Absolute measurement of beam energy by Compton scattering
[DE92-016964] p 4069 N92-32318
Measurement of the magnetic and electrical activity of individual cells in vitro
[AD-A250881] p 4035 N92-32345
Fast ion loss and radial electric field in Wendelstein 7-A stellarator
[DE92-782106] p 4079 N92-32745
Scanning force microscopy using optical interferometry
[ISBN-90-9003887-6] p 4077 N92-33146
ELECTRIC FILTERS
A simplified synthesis of lossless two-port wave digital and analog filters
[ISBN-0-315-63272-0] p 3993 N92-33193
ELECTRIC MOMENTS
The shapes and collective behavior of rapidly rotating nuclei
[DE92-017192] p 4067 N92-32928
ELECTRIC MOTOR VEHICLES
Second interim report of the Interagency Commission on Alternative Motor Fuels
[DE92-013169] p 3974 N92-32483
Development of high-performance Na/NiCl2 cell
[DE92-015270] p 3988 N92-32639
UHM/HNEI EV test and evaluation program
[DE92-011631] p 3989 N92-32754
ELECTRIC POTENTIAL
Plasma diffusion through multidipole magnetic fields
[INPE-5384-PRE/1750] p 4079 N92-32662
ELECTRIC POWER SUPPLIES
Solar radiation on a catenary collector
[NASA-TM-105751] p 3988 N92-32243
Plasma opening switch for long-pulse intense ion beam
[DE92-017523] p 3992 N92-33068
ELECTRIC PROPULSION
NASA's nuclear electric propulsion technology project
[NASA-TM-105811] p 3944 N92-32463
ELECTRIC RELAYS
System response to relay chatter
[DE92-013076] p 3988 N92-32495
ELECTRIC SWITCHES
Plasma opening switch for long-pulse intense ion beam
[DE92-017523] p 3992 N92-33068
ELECTRICAL GROUNDING
The 1991 rocket-triggered lightning test of the DoD Security Operations Test Site (SOTS) munitions storage bunker, Fort McClellan, Alabama
[DE92-012449] p 4032 N92-32427
A test circuit for capacitor bank grounding sticks
[AD-A251121] p 3989 N92-32700
ELECTRICAL IMPEDANCE
An in vitro corrosion study of two implant materials using electrochemical impedance spectroscopy and potentiodynamic polarization
[AD-A252575] p 3966 N92-32626
ELECTRICAL PROPERTIES
Mechanisms of the oxidation of metals and alloys with emphasis on superconductors
[DE92-016840] p 3966 N92-32315
ELECTRICAL RESISTANCE
A test circuit for capacitor bank grounding sticks
[AD-A251121] p 3989 N92-32700
ELECTRICAL RESISTIVITY
Investigation of the oxygen-vacancy (A-center) defect complex profile in neutron irradiated high resistivity silicon junction particle detectors
[DE92-016952] p 4064 N92-32316
Anisotropic electrical resistivity of YBCO/PBCO superlattice films grown on miscut substrates
[DE92-014409] p 4082 N92-32636
On the resistive transition of composite superconductors
[ISBN-90-9003899-X] p 3992 N92-33145
ELECTRO-OPTICS
Methods of opto-electronic fusion of infrared and visible images p 3936 N92-32444
STAMP, the SWOE Thermal Analysis and Measurement Program: Summary of the 1990 field tests
[LTR-91-013] p 4029 N92-32860
ELECTROCARDIOGRAPHY
DCIEM/Central Medical Board Aircrew ECG program: Recommendations for restructuring
[DCIEM-90-47] p 4037 N92-32816
ELECTROCATALYSTS
Electrocatalysis of anodic, oxygen-transfer reactions at noble metal electrodes
[DE92-016308] p 3962 N92-32562
Electrocatalyst surfaces
[PB92-190420] p 3962 N92-32591
Electrified microheterogeneous catalysis
[AD-D015270] p 3963 N92-32755
ELECTROCHEMICAL CORROSION
An in vitro corrosion study of two implant materials using electrochemical impedance spectroscopy and potentiodynamic polarization
[AD-A252575] p 3966 N92-32626
Environmental degradation of high temperature composites p 3958 N92-33047
Electrochemical polarization measurements on pitting corrosion susceptibility of nickel-rich Alloy 825
[DE92-014885] p 3969 N92-33132
ELECTROCHEMICAL OXIDATION
Electrocatalysis of anodic, oxygen-transfer reactions at noble metal electrodes
[DE92-016308] p 3962 N92-32562
ELECTROCHEMISTRY
Electrified microheterogeneous catalysis
[AD-D015270] p 3963 N92-32755
A study of the dissolution mechanism by chemical and electrochemical oxidation-reduction of actinide dioxides (UO2, NpO2, PuO2, and AmO2) in an acid aqueous medium
[DE92-014834] p 3965 N92-33126
ELECTRODES
Development of high-performance Na/NiCl2 cell
[DE92-015270] p 3988 N92-32639
Some electronic and dynamical factors in electron-transfer chemistry: Metal complexes, clusters, and surfaces
[AD-A251169] p 3964 N92-32826
Arc/gas electrode
[NASA-CASE-MFS-29766-1] p 3991 N92-33030
ELECTROLUMINESCENCE
Program for research in conducting polymers
[AD-A250965] p 3971 N92-32665
ELECTROLYSIS
A study of the dissolution mechanism by chemical and electrochemical oxidation-reduction of actinide dioxides (UO2, NpO2, PuO2, and AmO2) in an acid aqueous medium
[DE92-014834] p 3965 N92-33126
High-flux solar photon processes
[DE92-001247] p 4027 N92-33138
ELECTROLYTES
The response of the double layer capacitance of a high temperature superconductor/fluid electrolyte interface to the onset of superconductivity
[AD-A251172] p 3990 N92-32827
ELECTROMAGNETIC ABSORPTION
Program for research in conducting polymers
[AD-A250965] p 3971 N92-32665
ELECTROMAGNETIC FIELDS
Low-frequency nuclear quadrupole resonance with a dc SQUID
[DE92-014506] p 4081 N92-32420
On 5-dimensional Kaluza-Klein theory
[ETN-92-92130] p 3982 N92-32820
ELECTROMAGNETIC INTERACTIONS
The ionosphere of Titan and its interaction with Saturnian magnetospheric electrons p 4099 N92-32386
Possible effects of additional vector bosons in e(sup +)e(sup -)(yields)f(bar-f) at the TRISTAN energies
[DE92-624727] p 4065 N92-32498
ELECTROMAGNETIC INTERFERENCE
Determining surface profile from sequential interference patterns from a long trace profiler
[DE92-017117] p 4073 N92-32321
Fly-by-light technology development plan
[NASA-CR-181954] p 3939 N92-32778
Signal processing in impulsive electromagnetic interference
[AD-A252385] p 3982 N92-32899
ELECTROMAGNETIC NOISE
Feasibility of measuring transverse electric noise at VLF and LF on an ice cap
[AD-A252280] p 4035 N92-33220
Techniques of microwave noise measurement on cooled transistors
[ISBN-0-315-65025-7] p 3994 N92-33234
ELECTROMAGNETIC PULSES
Satellite anomalies and electrostatic surface discharges
[AD-A246880] p 3942 N92-32538
ELECTROMAGNETIC SCATTERING
Application of gauge theories to enhance numerical solutions to mixed potential integral equations
[AD-A248451] p 4055 N92-32670
Electromagnetic scattering by systems of arbitrarily oriented spheroids
[ISBN-0-315-63332-8] p 3986 N92-33191
Numerical analysis of scattering from certain conducting and dielectric bodies of arbitrary shape
[ISBN-0-315-63282-8] p 3987 N92-33192
ELECTROMAGNETIC SURFACE WAVES
The role of stochasticity in sawtooth oscillation
[DE92-782004] p 3982 N92-32905
ELECTROMAGNETIC WAVE FILTERS
A simplified synthesis of lossless two-port wave digital and analog filters
[ISBN-0-315-63272-0] p 3993 N92-33193
ELECTROMAGNETIC WAVE TRANSMISSION
Wave propagation in laterally varying media: A model expansion method
[AD-A247553] p 4031 N92-32572
Electromagnetic-wave propagation in unmagnetized plasmas
[AD-A250710] p 3980 N92-32719
ELECTROMAGNETS
Electromagnetic attachment mechanism
[NASA-CASE-MSC-21463-1] p 4019 N92-33018
ELECTRON ACCELERATORS
RF cavity vacuum interlock system
[DE92-016961] p 4070 N92-32567
ELECTRON BEAMS
Microwave absorption by lossy ceramic materials
[DE92-016963] p 3970 N92-32317
Laser measurements for experiments on the TROLL accelerator
[DE92-016578] p 4015 N92-32335
Thermal effects and mirror surface figure requirements for a diagnostic beamline at the advanced light source
[DE92-014483] p 4073 N92-32419
Optics of beam transport in the NSLS UV-FEL
[DE92-014166] p 4015 N92-32511
RF cavity vacuum interlock system
[DE92-016961] p 4070 N92-32567
Plasma opening switch for long-pulse intense ion beam
[DE92-017523] p 3992 N92-33068
Estimates of SASE power in the short wavelength region
[DE92-014504] p 4017 N92-33155
Kinematics of Compton backscattering x ray source for angiography
[DE92-014016] p 4073 N92-33179
ELECTRON CLOUDS
Collective resonances of valence electrons in free metal clusters
[DE92-014783] p 3969 N92-33116

ELECTRON CYCLOTRON HEATING
Activities report of the Institute of Plasma Research
[ETN-92-92147] p 4079 N92-32797
Conceptual design of an electron cyclotron wave system for NET/ITER
[IPF-91-6] p 4071 N92-32808
Diagnostics and modeling of ECRH microwave discharges
[IPF-91-3] p 4079 N92-32822
ELECTRON DENSITY (CONCENTRATION)
Site competition of impurities and grain boundary stability in iron
[AD-A252411] p 4084 N92-32939
ELECTRON DIFFRACTION
Preparation and characterization of superlattices
[DE92-012572] p 4081 N92-32462
ELECTRON DIFFUSION
Investigation of impurity related phenomena, significant for novel semiconductor technologies
[ETN-92-92048] p 4083 N92-32760
ELECTRON GAS
Intermodulation in the oscillatory magnetoresistance of a two-dimensional electron gas p 3984 N92-32975
ELECTRON IMPACT
Coupled-channels-optical calculation of electron-helium scattering
[DE92-625009] p 4065 N92-32501
ELECTRON MICROSCOPES
Use of a Fourier deconvolution method in particle size determination and use of molecular mechanics in crystal structure determinations
[DE92-014510] p 4085 N92-33111
ELECTRON MICROSCOPY
Transmission electron microscope characterization of deformation and recovery in 304L stainless steel part
[DE92-013237] p 3966 N92-32614
A combined AEM/APFIM characterization of Alloy X-750
[DE92-011049] p 3969 N92-33158
ELECTRON MOBILITY
Investigation of impurity related phenomena, significant for novel semiconductor technologies
[ETN-92-92048] p 4083 N92-32760
ELECTRON PUMPING
Transverse diode pumping of solid-state lasers
[AD-A252213] p 4016 N92-33089
ELECTRON RADIATION
Study and achievement of a parallel simulator for diffusion at the atomic level: Creation and growth of dislocation loops under electronic radiation
[LAAS-92118] p 4066 N92-32735
ELECTRON SCATTERING
Absolute measurement of beam energy by Compton scattering
[DE92-016964] p 4069 N92-32318
Electron-atom scattering
[DE92-625005] p 4064 N92-32340
Simplified model of electron scattering on atomic hydrogen
[DE92-625007] p 4065 N92-32499
Coupled-channels-optical calculation of electron-helium scattering
[DE92-625009] p 4065 N92-32501
Range of validity of distorted wave Born and impulse approximations for (e,2e)
[DE92-624821] p 4087 N92-32649
ELECTRON SOURCES
Accelerator physics of the Stanford Linear Collider and SLC accelerator experiments towards the next linear collider
[DE92-017552] p 4072 N92-33070
ELECTRON TRANSFER
Novel gas phase ion molecule reactions of C60(++) with O2 and NH3
[AD-A250921] p 4066 N92-32556
Electrocatalysis of anodic, oxygen-transfer reactions at noble metal electrodes
[DE92-016308] p 3962 N92-32562
Some electronic and dynamical factors in electron-transfer chemistry: Metal complexes, clusters, and surfaces
[AD-A251169] p 3964 N92-32826
ELECTRON-POSITRON PAIRS
Supersymmetry searches at electron-proton colliders
[ETN-92-92057] p 4067 N92-32753
ELECTRONIC COUNTERMEASURES
Signal processing in impulsive electromagnetic interference
[AD-A252385] p 3982 N92-32899
ELECTRONIC PACKAGING
Multichip module study
[AD-A250877] p 3989 N92-32678
ELECTRONIC WARFARE
Interception of LPI radar signals
[AD-A246315] p 3978 N92-32535
ELECTRONICS
Human learning of schemas from explanations in practical electronics
[AD-A247429] p 4038 N92-32569
ELECTRONS
The ionosphere of Titan and its interaction with Saturnian magnetospheric electrons p 4099 N92-32386
Some electronic and dynamical factors in electron-transfer chemistry: Metal complexes, clusters, and surfaces
[AD-A251169] p 3964 N92-32826
Collective resonances of valence electrons in free metal clusters
[DE92-014783] p 3969 N92-33116
ELECTROSTATIC PROBES
Edge gradient and safety factor effects on electrostatic turbulent transport in tokamaks
[DE92-014323] p 4079 N92-32944
ELECTROSTATICS
Satellite anomalies and electrostatic surface discharges
[AD-A246880] p 3942 N92-32538
Edge gradient and safety factor effects on electrostatic turbulent transport in tokamaks
[DE92-014323] p 4079 N92-32944
ESD traits of bulk propellant under pressure p 3976 N92-33242
ELEMENTARY EXCITATIONS
Higher superdeformed band members in Hg-190: Evidence for a band interaction?
[DE92-016778] p 4082 N92-32542
MOL calculation of the solitons of the cubic Schroedinger equation
[DE92-017245] p 4060 N92-32998
ELEMENTARY PARTICLE INTERACTIONS
Theoretical nuclear physics
[DE92-016837] p 4069 N92-33186
ELEMENTARY PARTICLES
Theory of elementary particles studies in weak interaction and grand unification and studies in accelerator design
[DE92-014320] p 4066 N92-32597
MOL calculation of the solitons of the cubic Schroedinger equation
[DE92-017245] p 4060 N92-32998
Elementary particle physics and high energy phenomena
[DE92-016844] p 4069 N92-33187
ELLIPSOIDS
Multispectral variable magnification glancing incidence x ray telescope
[NASA-CASE-MFS-28013-4] p 4092 N92-33012
ELLIPSOMETRY
Study of InGaAs-based modulation doped field effect transistor structures using variable-angle spectroscopic ellipsometry p 3984 N92-32977
ELLIPTICAL ORBITS
The energetic radiation environment in a highly elliptical (Molniya) orbit
[AD-A252394] p 4031 N92-32902
EMBRITTLEMENT
Modeling the influence of irradiation temperature and displacement rate on hardening due to point defect clusters in ferritic steels
[DE92-016897] p 3969 N92-33115
EMERGENCIES
Integrated launch and emergency vehicle system
[NASA-CASE-LAR-13780-1] p 3943 N92-33013
EPCRA Section 313 Roadmaps Database: User's manual, version 2.2
[PB92-169523] p 4030 N92-33062
EMISSION
The LLNL Multi-User Tandem Laboratory PIXE microprobe
[DE92-017252] p 4014 N92-32999
EMISSION SPECTRA
Scintillation properties of lead sulfate
[DE92-010301] p 4082 N92-32493
EMITTANCE
Accelerator physics of the Stanford Linear Collider and SLC accelerator experiments towards the next linear collider
[DE92-017552] p 4072 N92-33070
END EFFECTORS
Electromagnetic attachment mechanism
[NASA-CASE-MSC-21463-1] p 4019 N92-33018
Obstacle avoidance for redundant robots using configuration control
[NASA-CASE-NPO-17852-1-CU] p 4054 N92-33019
END PLATES
Contribution of tailplane-mounted twin fins to sideforce, yawing moment, and rolling moment derivatives due to sideslip
[ESDU-92007] p 3939 N92-32487
ENERGY ABSORPTION
Calculation of the energy of elastic deformation of Kevlar backing plates for ceramic armours
[AD-A250129] p 3970 N92-32489
ENERGY CONSERVATION
Potential environmental effects of energy conservation measures in northwest industries
[DE92-013993] p 4030 N92-33156
ENERGY CONSUMPTION
Potential environmental effects of energy conservation measures in northwest industries
[DE92-013993] p 4030 N92-33156
ENERGY CONVERSION
The 1991 Japan Solar Energy Society. Japan Wind Energy Association Joint Conference
[DE92-530733] p 4027 N92-33090
High octane ethers from synthesis gas-derived alcohols
[DE92-013802] p 3975 N92-33108
Direct conversion of light hydrocarbon gases to liquid fuel
[DE92-015592] p 3975 N92-33141
DoD key technologies plan
[AD-A253692] p 4105 N92-33238
ENERGY CONVERSION EFFICIENCY
Solar radiation on a catenary collector
[NASA-TM-105751] p 3988 N92-32243
Concentrator silicon cell research
[DE92-016576] p 4025 N92-32565
Development of high-performance Na/NiCl2 cell
[DE92-015270] p 3988 N92-32639
ENERGY DISSIPATION
Beamstrahlung spectra in next generation linear colliders
[DE92-010730] p 4069 N92-32337
Fast ion loss and radial electric field in Wendelstein 7-A stellarator
[DE92-782106] p 4079 N92-32745
Applications of energy loss contrast STIM
[DE92-017254] p 4014 N92-33000
ENERGY LEVELS
Impulse transmitter and quantum detection radar system
[AD-D015323] p 3986 N92-33171
ENERGY METHODS
Recent advances in statistical energy analysis p 4062 N92-32954
Use of SEA to predict structure-borne noise in aircraft p 4062 N92-32955
ENERGY POLICY
Second interim report of the Interagency Commission on Alternative Motor Fuels
[DE92-013169] p 3974 N92-32483
ENERGY STORAGE
Thermochemical cycles for energy storage: Thermal decomposition of ZnSO4 systems
[DE91-002144] p 4026 N92-32909
NEMO: Advanced energy systems and technologies
[DE92-540920] p 4027 N92-33072
DoD key technologies plan
[AD-A253692] p 4105 N92-33238
ENERGY TECHNOLOGY
Environmental consequences of new energy technology. Solar heating, heat stores, and heat pumps
[PB92-180843] p 4025 N92-32605
UHM/HNEI EV test and evaluation program
[DE92-011631] p 3989 N92-32754
NEDO Alcohol/Biomass Technology Subcommittee
[DE92-526270] p 3975 N92-32914
NEMO: Advanced energy systems and technologies
[DE92-540920] p 4027 N92-33072
ENERGY TRANSFER
New applications of ionization and fluorescence techniques for detecting and characterization of open-shell organometallics in the gas phase
[AD-A250923] p 3961 N92-32509
The application of unsteady potential flow vortex loop/dipole theory to the work and acoustics of low-speed turbomachinery
[AD-A251160] p 4008 N92-32652
High translational energy induced reaction in semiconductors
[AD-A250980] p 3989 N92-32669
ENGINE DESIGN
Development of a CFD code for internal flows in liquid fueled engines p 3999 N92-32271
Computational fluid dynamic design of rocket engine pump components p 4003 N92-32293
ENGINE FAILURE
Superheavyweight missions SI versus DI: Ascent flight design options and recommendations
[NASA-CR-183208] p 3942 N92-32610
Bird ingestion into large turbofan engines
[DOT/FAA/CT-91/17] p 3932 N92-33005

Statistics on aircraft gas turbine engine rotor failures that occurred in US commercial aviation during 1988
[DOT/FAA/CT-91/28] p 3938 N92-33105
ENGINE NOISE
MD-80 aft cabin noise control: A case history
p 4061 N92-32950
ENGINE PARTS
Contribution to the theoretical and experimental analysis of camshaft engine operation
[ETN-92-91961] p 4018 N92-32726
ENGINE TESTS
Technology test bed review p 4001 N92-32279
ENGINEERING MANAGEMENT
Information Integration for Concurrent Engineering (IICE) IDEF3 process description capture method report
[AD-A252633] p 4042 N92-32627
IDEF4 object-oriented design method manual
[AD-A252634] p 4042 N92-32658
Software process assessment for small software shops p 4045 N92-32878
ENTROPY
Two studies of nonlinear processes in irreversible thermodynamics
[DE92-016855] p 4087 N92-32566
A three-field model of transient 3D multiphase, three-component flow for the computer code 4 A3. Par1: Theoretical basis: Conservation and state equations, numerics
[KFK-4948-PT-1] p 4011 N92-32857
ENTROPY (STATISTICS)
Pattern recognition based on entropy analysis and shape transformations
[ISBN-0-315-56074-6] p 4048 N92-33201
ENUMERATION
Finding solutions to value independent knapsack problems
[INPE-5390-TAE/011] p 4055 N92-32661
Selecting a subset of stimulus-response pairs with maximal transmitted information
[AD-A252728] p 3986 N92-32987
ENVIRONMENT EFFECTS
Environmental fatigue in aluminum-lithium alloys
[NASA-TM-107640] p 4021 N92-32423
STEL p 4103 N92-32457
Second interim report of the Interagency Commission on Alternative Motor Fuels
[DE92-013169] p 3974 N92-32483
High-temperature Solid Oxide Fuel Cell (SOFC) generator development project: Environmental assessment
[DE92-014698] p 4026 N92-32924
Environmental degradation of high temperature composites p 3958 N92-33047
Fluid effects: Thermoset and thermoplastic matrix composites p 3958 N92-33049
Environmental resistance of amorphous bonded thermoplastic joints p 3959 N92-33053
Flight service environmental effects on composite materials and structures p 3959 N92-33054
EPCRA Section 313 Roadmaps Database: User's manual, version 2.2
[PB92-169523] p 4030 N92-33062
Potential environmental effects of energy conservation measures in northwest industries
[DE92-013993] p 4030 N92-33156
ENVIRONMENT MANAGEMENT
National environmental compliance strategy
[DE92-013639] p 4027 N92-32415
Defense environmental restoration program annual report to Congress for fiscal year 1991
[AD-A244196] p 4029 N92-32731
ENVIRONMENT MODELS
Plausible surface models for Titan
p 4098 N92-32381
A prototype software engineering environment for domain modeling and reuse p 4046 N92-32882
ENVIRONMENT POLLUTION
Defense environmental restoration program annual report to Congress for fiscal year 1991
[AD-A244196] p 4029 N92-32731
Study on lifetime specific, laser-induced ultrafast fluorescence detection in the time and frequency domain for in-situ environmental analysis of organic pollutants
[KFK-4975] p 4029 N92-32841
ENVIRONMENT PROTECTION
National environmental compliance strategy
[DE92-013639] p 4027 N92-32415
US EPA's global climate change program: Landfill emissions and mitigation research
[PB92-180215] p 4028 N92-32609
Development of methodology and technology for identifying and quantifying emission products from open burning and open detonation thermal treatment methods. BangBox test series. Volume 3: Quality assurance and quality control
[AD-A251099] p 4029 N92-32650
Defense environmental restoration program annual report to Congress for fiscal year 1991
[AD-A244196] p 4029 N92-32731
EPCRA Section 313 Roadmaps Database: User's manual, version 2.2
[PB92-169523] p 4030 N92-33062
ENVIRONMENT SIMULATION
Quantitative non-destructive environmental characterization of advanced materials
[DE92-011462] p 3946 N92-32327
ENVIRONMENTAL MONITORING
Oak Ridge Environmental Information System (OREIS). Phase 1: System definition document
[DE92-017342] p 4090 N92-33084
ENVIRONMENTAL QUALITY
Guide to selected national environmental statistics in the US Government
[PB92-201144] p 4030 N92-33087
ENVIRONMENTAL TESTS
Quantitative non-destructive environmental characterization of advanced materials
[DE92-011462] p 3946 N92-32327
Evaluation of composite components on the Bell 206L and Sikorsky S-76 helicopters p 3950 N92-32575
Residual strength of repaired graphite/epoxy laminates after 5 years of outdoor exposure p 3950 N92-32577
Evaluation of the effects of the environment on the behavior of the primary structures of composite material aircraft in service: Historic and current situation
p 3958 N92-33048
ENZYMES
Small passive chemical detector
[DE92-014188] p 4030 N92-32933
EPITAXY
Anisotropic electrical resistivity of YBCO/PBCO superlattice films grown on miscut substrates
[DE92-014409] p 4082 N92-32636
T (sub c)-delta relations in YBa2Cu3O(7-delta) thin films: Effects of oxygen pressure during growth
[DE92-014432] p 4083 N92-32653
Thickness dependence of vortex pinning in epitaxial Tl-Ca-Ba-Cu-O thin films
[DE92-015011] p 4084 N92-32920
Kinetics and characterization of CVD-grown BP
[ETN-92-92024] p 3973 N92-33065
EPOXY MATRIX COMPOSITES
A Protection And Detection Surface (PADS) for damage tolerance p 3948 N92-32523
Processing and environmental effects on mechanical properties of composite repairs
[NRC-LTR-ST-1826] p 3954 N92-32791
A new test method to determine the compressive strength of fiber-reinforced composites
p 3956 N92-33035
Fracture surface characteristics of compressive failures in carbon fibre reinforced epoxy laminate subjected to hot/wet conditioning p 3959 N92-33051
EQUATIONS OF MOTION
Energy take-out from a wave energy device. A theoretical study of the hydrodynamics of a two-body problem consisting of a buoy and a submerged plate
[PB92-178821] p 4025 N92-32608
Classical dynamics of systems with time-varying inertial properties with application to multi-rigid-body systems
[ISBN-0-315-57834-3] p 4024 N92-33228
EQUATIONS OF STATE
Orthobaric densities and molar volumes of liquids: Halogenated ethanes
[ESDU-92009] p 3945 N92-32486
Turbulence transport equations for variable-density turbulence and their relationship to two-field models
[DE92-017292] p 4013 N92-33159
EQUIVALENCE
Equivalence between Lagrangian and Hamiltonian BRST formalisms
[DE92-624556] p 4055 N92-32602
ERBIUM
Resonantly pumped, erbium-doped, 2.8 micron solid state laser with high slope efficiency
[AD-D015310] p 4017 N92-33165
EROSION
Studies of near-surface phenomena and erosion mechanisms in metallic alloys using single- and multi-particle impacts
[DE92-014921] p 3966 N92-32432
ERROR ANALYSIS
Fault-tolerant wait-free shared objects
[NASA-CR-190679] p 4020 N92-32436
Analytic score comparison of geometry splitting and exponential transform for a simple Monte Carlo problem
[DE92-013108] p 4059 N92-32481
Diagnostic report of the National Hurricane Center, August and September 1991, volume 4, number 2
[PB92-179407] p 4033 N92-32503
Implementation of a tree-code for numerical simulations of stellar systems
[INPE-5370-TDI/469] p 4093 N92-32604
A Kalman filter integrated navigation design for the IAR Twin Otter Atmospheric Research Aircraft
[NRC-32148] p 3934 N92-32849
A review and discussion of flight management system incidents reported to the aviation safety reporting system
[AD-A252438] p 3932 N92-32941
Feature detection for model assessment in state estimation
[AD-A252755] p 4059 N92-32989
Calibration service for low-loss, three-terminal capacitance standards at 100 kHz and 1 MHz
[PB92-189554] p 3991 N92-33061
ERROR CORRECTING CODES
VLSI architecture for a Reed-Solomon decoder
[NASA-CASE-NPO-17897-1-CU] p 3991 N92-33011
ERROR DETECTION CODES
Better predictions even in reduced input variable numbers using neural networks in software development
p 4044 N92-32874
Optimized set reduction for empirically guiding software development p 4044 N92-32875
ERRORS
Measurement in practice p 4044 N92-32876
ESSENTIALLY NON-OSCILLATORY SCHEMES
A numerical resolution study of high order essentially non-oscillatory schemes applied to incompressible flow
[NASA-CR-189692] p 4012 N92-33110
ESTIMATES
Bootstrapping the change-point of a hazard rate
[IMAG-RR-861-M] p 4056 N92-32685
On the inconsistency of bootstrap distribution estimators
[IMAG-RR-856-M] p 4060 N92-32718
Estimates of SASE power in the short wavelength region
[DE92-014504] p 4017 N92-33155
ESTIMATING
Approximations and designs for estimating regression coefficients of independent stochastic processes
[IMAG-RR-840-M] p 4060 N92-32839
ESTIMATORS
On the inconsistency of bootstrap distribution estimators
[IMAG-RR-856-M] p 4060 N92-32718
ETHANE
Laboratory determination of the refractive indices of liquid methane and ethane at temperatures appropriate to the surface of Titan p 4100 N92-32391
Laboratory determination of the thermal conductivity of liquid methane and ethane p 4015 N92-32392
Waves on Titan p 4100 N92-32394
Orthobaric densities and molar volumes of liquids: Halogenated ethanes
[ESDU-92009] p 3945 N92-32486
Direct conversion of light hydrocarbon gases to liquid fuel
[DE92-015592] p 3975 N92-33141
ETHERS
Shock tube ignition of ethanol, isobutene and MTBE: Experiments and modeling
[DE92-008563] p 3961 N92-32544
Polyimides with carbonyl and ether connecting groups between the aromatic rings
[NASA-CASE-LAR-14001-1] p 3973 N92-33008
Methyl substituted polyimides containing carbonyl and ether connecting groups
[NASA-CASE-LAR-14351-1] p 3973 N92-33015
High octane ethers from synthesis gas-derived alcohols
[DE92-013802] p 3975 N92-33108
ETHYL ALCOHOL
Shock tube ignition of ethanol, isobutene and MTBE: Experiments and modeling
[DE92-008563] p 3961 N92-32544
ETHYLENE
Thermal conductivity of gaseous halogenated hydrocarbons: Ethylenes and benzenes
[ESDU-92010] p 3945 N92-32485
EULER EQUATIONS OF MOTION
Improved dissipation models for central difference schemes
[FFA-TN-1991-41] p 4057 N92-32729
EULER-LAGRANGE EQUATION
Numerical simulation of two-dimensional flows by the free-Lagrangian method
[TUM-M9105] p 4009 N92-32767
EVALUATION
ERIP application instructions
[DE92-014103] p 4089 N92-32469
Thermal assessment of Mustang Industries, Inc. neoprene quick-don anti-exposure immersion suits and storage evaluation for the CP140 Aurora aircraft
[DCIEM-90-23] p 4039 N92-32790

An evaluation of the performance characteristics of a two-man molecular sieve oxygen generating system
[DCIEM-91-20] p 4039 N92-33079

EVAPORATION

AC microcalorimetry of adsorbates on evaporated metal films: Orientational ordering of H2 multilayers
[DE92-008317] p 3963 N92-32666
An analytical screening of alternatives for R-502 in low-temperature refrigerating applications
[DE92-017162] p 3978 N92-32927

EVOLUTION (DEVELOPMENT)

Impact origin of Titan's atmosphere
p 4094 N92-32351
Interior of Titan p 4094 N92-32352
Organic chemistry on Titan versus terrestrial prebiotic chemistry: Exobiological implications
p 4096 N92-32368

EXCITATION

Excited state processes in transition metal complexes: Redox splitting in soluble polymers
[DE92-011808] p 3971 N92-32631
Photon excitation for satellite free x ray spectroscopy: Instrumentation challenges
[DE92-016999] p 4067 N92-32997

EXHAUST GASES

Computational fluid dynamics analysis of Space Shuttle main engine multiple plume flows at high-altitude flight conditions p 3996 N92-32255

EXOBIOLOGY

Organic chemistry on Titan versus terrestrial prebiotic chemistry: Exobiological implications
p 4096 N92-32368
Organic chemistry on Titan: Surface interactions
p 4096 N92-32370

EXPERIENCE

Methodological and architectural issues in the experience factory p 4044 N92-32870

EXPERIMENT DESIGN

Two-phase heat transport systems for space: Thermal gravitational modelling and scaling predictions versus results of experiments
[NLR-TP-91051-U] p 4010 N92-32786

EXPERIMENTATION

Influence of compliance on performance of robotic drilling
[OUEL-1917/92] p 4018 N92-32757

EXPERT SYSTEMS

Study of eddy current probes
[NASA-CR-190814] p 4020 N92-32425
Information Integration for Concurrent Engineering (IICE) IDEF3 process description capture method report
[AD-A252633] p 4042 N92-32627
Advancing automation and robotics technology for the Space Station Freedom and for the US economy
[NASA-TM-103940] p 4040 N92-32809
On physical systems qualitative approach: Real time help for fermentation process control
[LAAS-91445] p 4036 N92-32844
Advanced software development workstation: Effectiveness of constraint-checking --- spaceflight simulation and planning
[NASA-CR-190712] p 4043 N92-32865
Integrating expert vision systems and spatial database by unifying knowledge representation schemes.Development in remote sensing image analysis expert systems and geographical information systems
[ISBN-0-315-49130-2] p 4024 N92-33233

EXPLOSIONS

Lithium sulphur dioxide battery failure following high frequency vibration
[CRAD-1-90] p 3990 N92-32812

EXPLOSIVES

Development of methodology and technology for identifying and quantifying emission products from open burning and open detonation thermal treatment methods. BangBox test series. Volume 3: Quality assurance and quality control
[AD-A251099] p 4029 N92-32650
Extending estimation of C-J pressure of explosives to the very low density region
[DE92-015035] p 3975 N92-33003
Insensitive Munitions
[AGARD-CP-511] p 3975 N92-33240
The United States Air Force explosives hazards reduction program p 3976 N92-33241

EXPOSURE

Residual strength of repaired graphite/epoxy laminates after 5 years of outdoor exposure p 3950 N92-32577
Suggestions for improvement of the methodology and use of MEPAS, the multimedia environmental pollutant assessment system
[DE92-013135] p 4028 N92-32616
An overview of concerns relating to fluid effects on composites p 3958 N92-33045
Effects of fuel on Hercules AS-4/8552 composite material p 3958 N92-33046
Fluid effects: Thermoset and thermoplastic matrix composites p 3958 N92-33049

EXTERNAL STORES

NLR investigations of flutter behaviour of fighter aircraft with external stores
[NLR-TP-91134-U] p 3939 N92-32750

EXTREMELY HIGH FREQUENCIES

V-band pseudomorphic HEMT MMIC phased array components for space communications
p 3983 N92-32966
An optically controlled Ka-band phased array antenna
p 3983 N92-32968
Ka-band dual frequency array feed for a low cost ACTS ground terminal p 3983 N92-32969

EYE MOVEMENTS

PET studies of components of high-level vision
[AD-A250873] p 4036 N92-32344
Instrument scanning and subjective workload with the peripheral vision horizon display
[CTN-92-60359] p 4038 N92-32817

F

F-15 AIRCRAFT

Tactical state and performance assessment during air combat maneuvering
[AD-A247426] p 3935 N92-32612
Flight testing and simulation of an F-15 airplane using throttles for flight control
[NASA-TM-104255] p 3940 N92-32864

F-16 AIRCRAFT

Tactical state and performance assessment during air combat maneuvering
[AD-A247426] p 3935 N92-32612

F-18 AIRCRAFT

Structural assessment of ultralightweight composites
p 3948 N92-32525

FABRICATION

Design, evaluation and experimental effort toward development of a high strain composite wing for Navy aircraft p 3947 N92-32514
Development of composite wing carrythrough bulkheads for fighter aircraft p 3948 N92-32519
Braided composite bore evacuator chambers for tank cannons p 3948 N92-32520
Investigation into the fabrication of a composite top attack recoilless rifle p 3948 N92-32524
Evaluation of composite components on the Bell 206L and Sikorsky S-76 helicopters p 3950 N92-32575
Correlation of single mode fiber fabrication factors and radiation response
[AD-A247301] p 4074 N92-32613
Investigation of impurity related phenomena, significant for novel semiconductor technologies
[ETN-92-92048] p 4083 N92-32760
Lithium sulphur dioxide battery failure following high frequency vibration
[CRAD-1-90] p 3990 N92-32812
High temperature fabricable nickel-iron aluminides
[CA-PATENT-1-276-814] p 3968 N92-32855
Polyimide molding powder, coating, adhesive, and matrix resin
[NASA-CASE-LAR-14163-1] p 3973 N92-33014
Superconductivity: Past, present, and future
[DE92-014862] p 3992 N92-33128
High-energy ion implantation for bipolar transistor fabrication
[ISBN-90-9003883-3] p 3992 N92-33144

FACTOR ANALYSIS

Correlating visual scene elements with simulator sickness incidence: Hardware and software development
[AD-A252235] p 4036 N92-32434

FACTORIZATION

A tight and explicit representation of Q in sparse QR factorization
[DE92-014814] p 4055 N92-32428
Sparse matrix algorithms on distributed memory multiprocessors
[DE92-017870] p 4046 N92-33071

FADING

Effects of fading and interference in narrowband land-mobile networks
[ISBN-90-9004491-4] p 3982 N92-32837

FAILURE

Reliability training
[NASA-RP-1253] p 3941 N92-32456
A curved beam test specimen for determining the interlaminar tensile strength of a laminated composite
p 3949 N92-32526
Out of plane analysis for composite structures
p 3949 N92-32527

FAILURE ANALYSIS

Reliability training
[NASA-RP-1253] p 3941 N92-32456
System response to relay chatter
[DE92-013076] p 3988 N92-32495
Statistically based material properties: A military handbook-17 perspective p 3951 N92-32581
A new approach to fibrous composite laminate strength prediction p 3952 N92-32588
Life testing of a low voltage air circuit breaker
[DE92-014173] p 3988 N92-32635
Electromagnetic attachment mechanism
[NASA-CASE-MSC-21463-1] p 4019 N92-33018
Issues in compression loading of composite structures
p 3956 N92-33034
Damage progression under compressive loading in composite laminates containing an open hole
p 3957 N92-33040
GARTEUR compression behaviour of advanced CFRP --- carbon fiber reinforced plastics p 3957 N92-33042
Publications by Structures and Materials Laboratory on composite materials (January 1983 - June 1991)
[NRC-LTR-ST-1833] p 3959 N92-33078

FAILURE MODES

Reliability training
[NASA-RP-1253] p 3941 N92-32456
System response to relay chatter
[DE92-013076] p 3988 N92-32495
Buckling and damage of a composite plate under compression
[ONERA-RT-25/3542-RY-006-R] p 4022 N92-32774
The Utilization of Advanced Composites in Military Aircraft
[AGARD-R-785] p 3956 N92-33033
Issues in compression loading of composite structures
p 3956 N92-33034
A new test method to determine the compressive strength of fiber-reinforced composites
p 3956 N92-33035
Three-dimensional elasticity analysis of buckling of laminated plates p 3957 N92-33037
A review of RAE sponsored work on the compressive behaviour of composite materials p 3957 N92-33038
Fracture surface characteristics of compressive failures in carbon fibre reinforced epoxy laminate subjected to hot/wet conditioning p 3959 N92-33051

FALLOUT

Execution of measurement sequences in the framework of the inspection of near limit regions by radioiodine and aerosol emission measurements, and ground examinations on plutonium, strontium, and gamma ray radionuclides
[OEFZS-4579] p 4071 N92-32763
A simulation of radioactive fallout using the MATHEW/ADPIC model
[FOA-C-40292-4.3] p 4029 N92-32785

FAST FOURIER TRANSFORMATIONS

Application of gauge theories to enhance numerical solutions to mixed potential integral equations
[AD-A248451] p 4055 N92-32670
Quantum wave modeling on highly parallel distributed memory machines
[DE92-014507] p 4088 N92-33109

FAST NEUTRONS

High efficiency fast neutron threshold deflector
[AD-D015311] p 4073 N92-33167

FATIGUE (MATERIALS)

A curved beam test specimen for determining the interlaminar tensile strength of a laminated composite
p 3949 N92-32526
Fatigue, hysteresis, and acoustic emission, parts 1 and 2
[AD-A251073] p 4021 N92-32681
Mixed model fatigue crack growth behavior in a high strength steel
[AD-A250667] p 4022 N92-32717
Study of the mechanical behaviour of graphite/epoxy laminates subjected to static and cyclic loading
[NRC-30833] p 3955 N92-32813
Contribution to the study of the effect of the heterogeneous distribution of dislocations on the cyclic plasticity of single crystal aluminum
[ISAL-91-0099] p 4083 N92-32892
A transgranular fatigue crack growth model based on restricted slip reversibility
[NRC-LTR-ST-1831] p 4023 N92-33076

FATIGUE LIFE

Certification of damage tolerant composite structure
p 3951 N92-32580

FATIGUE TESTS

Influence of edge effect on compression-tension fatigue of toughened graphite/epoxy laminates
p 3957 N92-33039

FAULT TOLERANCE

Fault-tolerant wait-free shared objects
[NASA-CR-190679] p 4020 N92-32436
Fault tolerance for security management in distributed systems
[LAAS-92011] p 4040 N92-32766

Investigating the application of capture-recapture techniques to requirement and design reviews p 4044 N92-32873
Better predictions even in reduced input variable numbers using neural networks in software development p 4044 N92-32874
Advanced information processing system: The Army fault tolerant architecture conceptual study. Volume 1: Army fault tolerant architecture overview [NASA-CR-189632-VOL-1] p 4052 N92-33100
Advanced information processing system: The Army fault tolerant architecture conceptual study. Volume 2: Army fault tolerant architecture design and analysis [NASA-CR-189632-VOL-2] p 4052 N92-33101
Fault tolerance through program transformation [ISBN-90-72125-29-0] p 4047 N92-33142
An implementation of a fault-tolerant, multidirectional, digital interpolation beamformer [AD-A252494] p 3986 N92-33152

FAULTS
Diagnosability and diagnosis of sparsely interconnected multiprocessor systems [ISBN-0-315-56107-6] p 4053 N92-33224

FEASIBILITY ANALYSIS
Electron-atom scattering [DE92-625005] p 4064 N92-32340
Booster Applications Facility report, phase 2 [DE92-013395] p 4070 N92-32411
Vision-based range estimation using helicopter flight data [NASA-TM-103930] p 3933 N92-32424
Ground Systems Development Environment (GSDE) interface requirements and prototyping plan [NASA-CR-190713] p 4041 N92-32451
Development of the chemical and electrochemical coal cleaning process [DE92-013353] p 3977 N92-32467
Feasibility study for predicting human reliability growth through training and practice [AD-A252371] p 4038 N92-32990

FEDERAL BUDGETS
Departments of Veterans Affairs and Housing and Urban Development, and independent agencies appropriations for 1993, part 6 [GAO-55-636-PT-6] p 4091 N92-32505

FEEDBACK
MHD computation of feedback of resistive-shell instabilities in the reversed field pinch [DE92-014325] p 4078 N92-32599

FEEDBACK CONTROL
The multiple-function multi-input/multi-output digital controller system for the AFW wind-tunnel model [NASA-TM-107600] p 3934 N92-32536
A discrete nonlinear model approach to study the behavior of large signal DC to DC converters [LAAS-90028] p 3989 N92-32777
Autonomous berthing/unberthing of a Work Attachment Mechanism/Work Attachment Fixture (WAM/WAF) [NASA-CR-190647] p 4019 N92-32885
Mixed H(2)/H(sub infinity): Control with output feedback compensators using parameter optimization [NASA-CR-190070] p 4046 N92-33091

FEEDFORWARD CONTROL
Tutorial on neural network applications in high energy physics: A 1992 perspective [DE92-016003] p 4070 N92-32506
Adaptive information processing and global optimization [AD-A248450] p 4089 N92-32644

FERMENTATION
On physical systems qualitative approach: Real time help for fermentation process control [LAAS-91445] p 4036 N92-32844
NEDO Alcohol/Biomass Technology Subcommittee [DE92-526270] p 3975 N92-32914

FERROUS METALS
JPRS report: Science and technology. Central Eurasia: Materials science [JPRS-UMS-92-011] p 3969 N92-33129

FETUSES
Passive fetal monitoring sensor [NASA-CASE-LAR-14088-1-CU] p 4015 N92-33016

FIBER COMPOSITES
Computational simulation of matrix micro-slip bands in SiC/Ti-15 composite [NASA-TM-105762] p 3946 N92-32466
Eighth DOD/NASA/FAA Conference on Fibrous Composites in Structural Design, part 1 [NASA-CP-3087-PT-1] p 3946 N92-32513
Design, evaluation and experimental effort toward development of a high strain composite wing for Navy aircraft p 3947 N92-32514
Composite structural armor for combat vehicle applications p 3947 N92-32515
Applications of composites to armaments p 3947 N92-32516
The use of curvilinear fiber format to improve buckling resistance of plates with central circular holes p 3948 N92-32521
Development of thermoplastic components for structural validation p 3948 N92-32522
A new approximate fracture mechanics analysis methodology for composites with a crack or hole p 3949 N92-32530
Computational simulation of structural fracture in fiber composites p 3949 N92-32531
Scaling of fiber composite structures p 3950 N92-32532
Eighth DOD/NASA/FAA Conference on Fibrous Composites in Structural Design, part 2 [NASA-CP-3087-PT-2] p 3950 N92-32574
Damage tolerance certification methodology for composite structures p 3951 N92-32579
Certification of damage tolerant composite structure p 3951 N92-32580
Compression behavior of graphite-epoxy and graphite-thermoplastic panels with circular holes or impact damage p 3951 N92-32582
Impact response of graphite/epoxy fabric structures p 3951 N92-32583
Postbuckling behavior of curved panels under combined compression and shear loads p 3952 N92-32584
Postbuckling of stiffened composite plates under combined loading p 3952 N92-32585
Initial postbuckling response of an unsymmetrically laminated rectangular plate p 3952 N92-32586
A new approach to fibrous composite laminate strength prediction p 3952 N92-32588
Thermal strains in titanium aluminide and nickel aluminide composites [DE92-015181] p 3953 N92-32638
Interfacial studies of refractory glass-ceramic matrix/advanced SiC fiber reinforced composites [AD-A250784] p 3953 N92-32676
Buckling of fibre reinforced composite and sandwich laminates with higher-order shear deformation theories [IIT-B/CE/RR/92/2] p 4022 N92-32783
A unique method of determining the elastic and engineering constants of unidirectional fibre-reinforced composite plates using ultrasound [UTIAS-TN-274] p 3955 N92-32829
A new test method to determine the compressive strength of fiber-reinforced composites p 3956 N92-33035
Innovative constituents requirements to improve composites compressive strength p 3957 N92-33043
Environmental degradation of high temperature composites p 3958 N92-33047
Jet fuel absorption and dynamic mechanical analysis of carbon fibre composites p 3959 N92-33050
Fracture surface characteristics of compressive failures in carbon fibre reinforced epoxy laminate subjected to hot/wet conditioning p 3959 N92-33051
The effect of heat treatment on the properties of PEEK and APC-2 p 3959 N92-33052
Apparatus for preparing thermoplastic composites [AD-D015326] p 3960 N92-33174

FIBER OPTICS
A scalable, switched circuit LAN for Gb/S channels with over Tb/S total capacity [DE92-013444] p 4050 N92-32412
Wavelength division multiplexed local area networks [AD-A247613] p 3979 N92-32573
Correlation of single mode fiber fabrication factors and radiation response [AD-A247301] p 4074 N92-32613
Depolarized light source for fiber optic sensors [AD-D015289] p 4074 N92-32634
Fly-by-light technology development plan [NASA-CR-181954] p 3939 N92-32778
A simple high-performance avalanche photodiode for long-wavelength optical communications, phase 1 [PB92-188259] p 4076 N92-33004
High temperature fiber optic microphone having a pressure-sensing reflective membrane under tensile stress [NASA-CASE-LAR-14402-1-CU] p 4076 N92-33017
Laser to single-mode-fiber coupling: A laboratory guide [NASA-CR-4452] p 4077 N92-33239

FIBER ORIENTATION
A new approach to fibrous composite laminate strength prediction p 3952 N92-32588

FIBERS
Thermal degradation study of silicon carbide threads developed for advanced flexible thermal protection systems [NASA-TM-103952] p 3970 N92-32476

FIELD EFFECT TRANSISTORS
Pulse coded biologically motivated neural-type MOS circuits [AD-A250367] p 3988 N92-32325
Microwave properties of peeled HEMT devices sapphire substrates p 3984 N92-32978
Techniques of microwave noise measurement on cooled transistors [ISBN-0-315-65025-7] p 3994 N92-33234

FIELD THEORY (PHYSICS)
Equivalence between Lagrangian and Hamiltonian BRST formalisms [DE92-624556] p 4055 N92-32602
Fractional spin: Majorana-Dirac field [DE92-624558] p 4087 N92-32603
Supersymmetry searches at electron-proton colliders [ETN-92-92057] p 4067 N92-32753
On 5-dimensional Kaluza-Klein theory [ETN-92-92130] p 3982 N92-32820
Pertubative finite temperature field theory in Minkowski space [ISBN-0-315-55158-5] p 4088 N92-33199

FIGHTER AIRCRAFT
A learning enhanced flight control system for high performance aircraft [AD-A252520] p 3938 N92-32435
An integrated multiple-sensor fire control system for air-to-air combat p 3937 N92-32450
NLR investigations of flutter behaviour of fighter aircraft with external stores [NLR-TP-91134-U] p 3939 N92-32750
Aspects of compression in aerospace composites: Future requirements p 3956 N92-33036
Rapid development of the X-31 simulation to support flight-testing [NASA-TM-104256] p 3935 N92-33149

FILAMENT WINDING
Braided composite bore evacuator chambers for tank cannons p 3948 N92-32520
Investigation into the fabrication of a composite top attack recoilless rifle p 3948 N92-32524

FILM COOLING
A status of the activities of the NASA. Marshall Space Flight Center Combustion Devices Technology Team p 3995 N92-32250
CFD analysis of the STME nozzle flowfield p 3995 N92-32251
Heat transfer in rocket engine combustion chambers and nozzles p 3995 N92-32253

FILM THICKNESS
Magnetic penetration depth of YBa2Cu3O(7-delta) thin films determined by the power transmission method p 3985 N92-32983

FINE STRUCTURE
Local environment around the oxygen atoms in Y-Ba-Cu-O studied X ray Absorption Fine Structure (XAFS) spectroscopy [DE92-014165] p 4081 N92-32470

FINITE DIFFERENCE THEORY
CFD applications in pump flows p 4002 N92-32288
Computation of the flow field in a centrifugal impeller with splitter blades p 4002 N92-32289
Using adaptive grid in modeling rocket nozzle flow p 4005 N92-32303
Improved dissipation models for central difference schemes [FFA-TN-1991-41] p 4057 N92-32729
Resolution of convection and diffusion by the boolean automata method [ONERA-RF-22/3419-AY-122A] p 4057 N92-32772
Connectivity structures and differencing techniques for staggered-grid free-Lagrange hydrodynamics [DE92-017313] p 4012 N92-33082
Computation of incompressible viscous flows through turbopump components [NASA-TM-103911] p 4012 N92-33113

FINITE ELEMENT METHOD
A numerical study of natural convection in a narrow annulus [DE92-017138] p 4006 N92-32322
An implementation of Hill's theory of normal anisotropic plasticity for explicit shell analysis [DE92-011468] p 4020 N92-32328
Computational simulation of matrix micro-slip bands in SiC/Ti-15 composite [NASA-TM-105762] p 3946 N92-32466
Eighth DOD/NASA/FAA Conference on Fibrous Composites in Structural Design, part 1 [NASA-CP-3087-PT-1] p 3946 N92-32513
The use of curvilinear fiber format to improve buckling resistance of plates with central circular holes p 3948 N92-32521
Efficient finite element modeling of laminated composite plates based on higher-order theory p 3949 N92-32529
A finite element-boundary integral method for conformal antenna arrays on a circular cylinder [NASA-CR-190610] p 3979 N92-32559

Stress-relief displacements induced by drilling: Applications to holographic measurements of in situ stress
[DE92-013711] p 4014 N92-32620
Dynamic systems stability with dry friction: Application to brake disc squealing
[ECL-91-48] p 4018 N92-32737
Nonlinear transient responses of stratified composite structures
[ONERA-RT-26/3542-RY-007-R] p 3954 N92-32775
Buckling of fibre reinforced composite and sandwich laminates with higher-order shear deformation theories
[IIT-B/CE/RR/92/2] p 4022 N92-32783
Vibro-acoustic FE analyses of the Saab 2000 aircraft p 4062 N92-32952
Propagation of a delamination in a composite panel subjected to a compression load p 3957 N92-33041
Connectivity structures and differencing techniques for staggered-grid free-Lagrange hydrodynamics
[DE92-017313] p 4012 N92-33082
Computational methods for global/local analysis
[NASA-TM-107591] p 4023 N92-33104
Computational aspects of helicopter trim analysis and damping levels from Floquet theory
[NASA-CR-190736] p 3940 N92-33107

FINS
Contribution of tailplane-mounted twin fins to sideforce, yawing moment, and rolling moment derivatives due to sideslip
[ESDU-92007] p 3939 N92-32487

FIR FILTERS
A digital implementation of a radar coherent-on-receive system
[ISBN-0-315-59028-9] p 3987 N92-33206

FIRE CONTROL
Integrated Target Acquisition and Fire Control Systems
[AGARD-CP-500] p 3935 N92-32437
Operational needs for an unmanned air vehicle p 3936 N92-32438
Airborne experimental FLIR program p 3937 N92-32447
The German anti tank helicopter PAH 2: An example of a future sensor platform p 3937 N92-32448
An integrated multiple-sensor fire control system for air-to-air combat p 3937 N92-32450

FIRE EXTINGUISHERS
Spray nozzle for fire control
[CA-PATENT-APPL-SN-2-011-94] p 4011 N92-32856

FIRE FIGHTING
Spray nozzle for fire control
[CA-PATENT-APPL-SN-2-011-94] p 4011 N92-32856

FIRES
Burning oil fields as a source of infrasonic waves
[IRF-PREPRINT-119] p 4061 N92-32842
The design features of rocket motors relating to insensitive munition response to thermo-mechanical stimuli p 3976 N92-33244

FIRING (IGNITING)
The design features of rocket motors relating to insensitive munition response to thermo-mechanical stimuli p 3976 N92-33244

FISSION
High efficiency fast neutron threshold deflector
[AD-D015311] p 4073 N92-33167

FIXTURES
Heating fixture and instrumentation design for elevated temperature tests of a composite repair technique
[WL-TM-90-326-FIBE] p 3946 N92-32459
Autonomous berthing/unberthing of a Work Attachment Mechanism/Work Attachment Fixture (WAM/WAF)
[NASA-CR-190647] p 4019 N92-32885

FLAME PROPAGATION
A state of the art report on flame acceleration and transition to detonation in hydrogen/air/diluent mixtures
[DE92-626850] p 3961 N92-32475
Solid fuel flame spread and mass burning in turbulent flow
[PB92-181049] p 3963 N92-32607
Premixed turbulent combustion to opposed streams
[DE92-016996] p 3964 N92-32996
Computational and experimental study of laminar flames
[DE92-017978] p 3965 N92-33121

FLAME TEMPERATURE
Shock tube ignition of ethanol, isobutene and MTBE: Experiments and modeling
[DE92-008563] p 3961 N92-32544

FLAMES
A state of the art report on flame acceleration and transition to detonation in hydrogen/air/diluent mixtures
[DE92-626850] p 3961 N92-32475
Solid fuel flame spread and mass burning in turbulent flow
[PB92-181049] p 3963 N92-32607
Premixed turbulent combustion to opposed streams
[DE92-016996] p 3964 N92-32996
Computational and experimental study of laminar flames
[DE92-017978] p 3965 N92-33121

FLAPS (CONTROL SURFACES)
Lift and rolling moment due to spoilers on wings with trailing-edge flaps deflected at subsonic speeds
[ESDU-92002-SUPPL] p 3931 N92-32782

FLASH POINT
Shock tube ignition of ethanol, isobutene and MTBE: Experiments and modeling
[DE92-008563] p 3961 N92-32544

FLAT PLATES
Swept shock/boundary layer interaction experiments in support of CFD code validation
[NASA-CR-190583] p 3930 N92-32494
Leading-edge receptivity for blunt-nose bodies
[NASA-CR-190563] p 3930 N92-32648
Vortex flow visualization using colored and fluorescent dyes on flat plate delta wing with leading edge extension
[AD-A251139] p 3930 N92-32651
A unique method of determining the elastic and engineering constants of unidirectional fibre-reinforced composite plates using ultrasound
[UTIAS-TN-274] p 3955 N92-32829

FLAVOR (PARTICLE PHYSICS)
Heavy flavor physics at hadron colliders
[DE92-014482] p 4064 N92-32312

FLEXIBILITY
Corrosion-resistant alkyd coatings
[AD-D015330] p 3974 N92-33177

FLEXIBLE WINGS
The multiple-function multi-input/multi-output digital controller system for the AFW wind-tunnel model
[NASA-TM-107600] p 3934 N92-32536

FLIGHT CHARACTERISTICS
Computational fluid dynamics analysis of Space Shuttle main engine multiple plume flows at high-altitude flight conditions p 3996 N92-32255
A background to the handling qualities of aircraft
[ESDU-92006] p 3939 N92-32780

FLIGHT CONDITIONS
Computational fluid dynamics analysis of Space Shuttle main engine multiple plume flows at high-altitude flight conditions p 3996 N92-32255
User's manual for AeroFcn: A FORTRAN program to compute aerodynamic parameters
[NASA-TM-104237] p 4042 N92-32507

FLIGHT CONTROL
A learning enhanced flight control system for high performance aircraft
[AD-A252520] p 3938 N92-32435
Fly-by-light technology development plan
[NASA-CR-181954] p 3939 N92-32778
Collaborative research on V/STOL control system/cockpit display tradeoffs under the NASA/MOD joint aeronautical program
[NASA-TM-103910] p 3939 N92-32788
An evaluation of decelerating IFR approaches utilizing a helicopter flight simulator
[CTN-92-60348] p 3934 N92-32845
Flight testing and simulation of an F-15 airplane using throttles for flight control
[NASA-TM-104255] p 3940 N92-32864
Investigation of the flight control requirements of a half-scale ducted fan unmanned aerial vehicle
[AD-A252730] p 3940 N92-32988
Rapid development of the X-31 simulation to support flight-testing
[NASA-TM-104256] p 3935 N92-33149
Independent verification and validation for Space Shuttle flight software
[NASA-CR-190826] p 4047 N92-33196

FLIGHT CREWS
Observing team coordination within Army rotary-wing aircraft crews
[AD-A252234] p 4039 N92-32433
Comparative effects of antihistamines on aircrew performance of simple and complex tasks under sustained operations
[AD-A248752] p 4036 N92-32492
DCIEM/Central Medical Board Aircrew ECG program: Recommendations for restructuring
[DCIEM-90-47] p 4037 N92-32816
A review and discussion of flight management system incidents reported to the aviation safety reporting system
[AD-A252438] p 3932 N92-32941

FLIGHT FITNESS
DCIEM/Central Medical Board Aircrew ECG program: Recommendations for restructuring
[DCIEM-90-47] p 4037 N92-32816

FLIGHT MANAGEMENT SYSTEMS
A review and discussion of flight management system incidents reported to the aviation safety reporting system
[AD-A252438] p 3932 N92-32941
CTAS: Computer intelligence for air traffic control in the terminal area
[NASA-TM-103959] p 3933 N92-33080

FLIGHT OPERATIONS
Development of new flight procedures for the Microwave Landing System (MLS)
[NLR-TP-91156-U] p 3933 N92-32830
Federal aviation regulations. Part 91: General operating and flight rules
[PB92-197334] p 3929 N92-33176

FLIGHT SAFETY
Safety study of TCAS 2 for logic version 6.04
[DOT/FAA/RD-92/22] p 3933 N92-32537
Statistics on aircraft gas turbine engine rotor failures that occurred in US commercial aviation during 1988
[DOT/FAA/CT-91/28] p 3938 N92-33105

FLIGHT SIMULATION
Collaborative research on V/STOL control system/cockpit display tradeoffs under the NASA/MOD joint aeronautical program
[NASA-TM-103910] p 3939 N92-32788
Development of new flight procedures for the Microwave Landing System (MLS)
[NLR-TP-91156-U] p 3933 N92-32830
Rapid development of the X-31 simulation to support flight-testing
[NASA-TM-104256] p 3935 N92-33149

FLIGHT SIMULATORS
Briefing notes on a manned aircraft research and support simulation facility
[AD-A250373] p 3935 N92-32326
Correlating visual scene elements with simulator sickness incidence: Hardware and software development
[AD-A252235] p 4036 N92-32434
An evaluation of decelerating IFR approaches utilizing a helicopter flight simulator
[CTN-92-60348] p 3934 N92-32845
Flight testing and simulation of an F-15 airplane using throttles for flight control
[NASA-TM-104255] p 3940 N92-32864
Advanced software development workstation: Effectiveness of constraint-checking --- spaceflight simulation and planning
[NASA-CR-190712] p 4043 N92-32865

FLIGHT TESTS
Vision-based range estimation using helicopter flight data
[NASA-TM-103930] p 3933 N92-32424
A learning enhanced flight control system for high performance aircraft
[AD-A252520] p 3938 N92-32435
Evaluation of composite components on the Bell 206L and Sikorsky S-76 helicopters p 3950 N92-32575
Fly-by-light technology development plan
[NASA-CR-181954] p 3939 N92-32778
An evaluation of decelerating IFR approaches utilizing a helicopter flight simulator
[CTN-92-60348] p 3934 N92-32845
The use of Kalman filtering techniques to improve the accuracy of flight test data
[NRC-32139] p 3938 N92-32850
The design and development of a portable, DSP micro-processor based, high-accuracy data acquisition system
[NRC-32146] p 4040 N92-32851
Flight testing and simulation of an F-15 airplane using throttles for flight control
[NASA-TM-104255] p 3940 N92-32864
The development of an airborne information management system for flight test
[NASA-TM-104251] p 3938 N92-32866
MD-80 aft cabin noise control: A case history p 4061 N92-32950
Advanced Study for Active Noise Control in Aircraft (ASANCA)
[AIAA PAPER 92-2092] p 4062 N92-32956
Pilots noise exposure during a Boeing 747-400 round trip: Ambient noise and acoustic-head recording and analysis of data p 4063 N92-32960
Flight service environmental effects on composite materials and structures p 3959 N92-33054
An evaluation of the performance characteristics of a two-man molecular sieve oxygen generating system
[DCIEM-91-20] p 4039 N92-33079
Improved HIRAP flight calibration technique
[NASA-TM-107656] p 3944 N92-33112
Rapid development of the X-31 simulation to support flight-testing
[NASA-TM-104256] p 3935 N92-33149

FLIR DETECTORS
Infrared Targeting System (IRTS) demonstration p 3937 N92-32446
Airborne experimental FLIR program p 3937 N92-32447

FLOODS
Applications of statistical methods to the study of climate and flooding fluctuations in the central US
[PB92-205137] p 4034 N92-33173

FLOQUET THEOREM
Computational aspects of helicopter trim analysis and damping levels from Floquet theory
[NASA-CR-190736] p 3940 N92-33107

FLOW CHARACTERISTICS
Overview of the relevant CFD work at Thiokol Corporation p 3995 N92-32249
NLS nozzle base flow characteristics p 3995 N92-32252
Numerical modeling for dilute and dense sprays p 3997 N92-32258
Impeller tandem blade study with grid embedding for local grid refinement p 4002 N92-32290
CFD analysis to optimize a design modification of BSMT p 4004 N92-32296
Study of flow properties of wet solids using laser induced photochemical anemometry
[DE92-015452] p 4013 N92-33140
Study of flow properties of wet solids using laser induced photochemical anemometry
[DE92-014031] p 4017 N92-33180

FLOW CHARTS
Improving the translation from data flow diagrams into Z by incorporating the data dictionary
[AD-A250769] p 4089 N92-32342

FLOW COEFFICIENTS
A status of the activities of the NASA/MSFC pump stage technology team p 4002 N92-32286
Three-dimensional flow fields inside a shrouded inducer at design and off-design conditions (CFD study) p 4003 N92-32291

FLOW DISTRIBUTION
SRMAFTE facility checkout model flow field analysis p 3994 N92-32247
CFD analysis of the STME nozzle flowfield p 3995 N92-32251
Application of computational fluid dynamics to the design of the film cooled STME subscale nozzle for the National Launch System p 3996 N92-32254
Computational fluid dynamics analysis of Space Shuttle main engine multiple plume flows at high-altitude flight conditions p 3996 N92-32255
Direct numerical simulation of a combusting droplet with convection p 3996 N92-32256
CFD modeling of turbulent flows around the SSME main injector assembly using porosity formulation p 3997 N92-32260
An experimental study of the fluid mechanics associated with porous walls
[AIAA PAPER 92-0769] p 3998 N92-32263
Development of CFD code evaluation criteria and a procedure for assessing predictive capability and performance p 4001 N92-32283
Computation of the flow field in a centrifugal impeller with splitter blades p 4002 N92-32289
CFD analysis to optimize a design modification of BSMT p 4004 N92-32296
Using adaptive grid in modeling rocket nozzle flow p 4005 N92-32303
An analysis of the flow field in the region of the ASRM field joints p 4005 N92-32305
A two-phase restricted equilibrium model for combustion of metalized solid propellants p 3966 N92-32307
Axial vortices in gaseous-fired burner flow fields
[PB92-190370] p 3962 N92-32594
An examination of several high resolution schemes applied to complex problems in high speed flows
[AD-A250814] p 4008 N92-32632
The application of unsteady potential flow vortex loop/dipole theory to the work and acoustics of low-speed turbomachinery
[AD-A251160] p 4008 N92-32652
Characterization of flow distribution in axisymmetric shock tubes
[AD-A251095] p 4008 N92-32683
Numerical methods: Solving the advection equation in flows with sharp gradients using Bott's flux scheme
[DM-59] p 4009 N92-32727
New concepts for multi-block grid generation for flow domains around complex aerodynamic configurations
[NLR-TP-91046-U] p 3930 N92-32730
An experimental study of the flow over a sharp-edged delta wing at subsonic and transonic speeds
[NLR-TP-91117-U] p 3930 N92-32732
Integration of wall interference assessment and wall adaptation
[NLR-TP-91119-U] p 3940 N92-32734

FLOW EQUATIONS
Treating convection in sequential solvers p 4000 N92-32277
Modeling and numerical simulation of vortex flow in aerodynamics
[NLR-TP-91154-U] p 3930 N92-32673
Numerical methods: Solving the advection equation in flows with sharp gradients using Bott's flux scheme
[DM-59] p 4009 N92-32727
Convergence acceleration of the Proteus computer code with multigrid methods
[NASA-CR-190607] p 4047 N92-33131

FLOW STABILITY
An experimental study of the fluid mechanics associated with porous walls
[AIAA PAPER 92-0769] p 3998 N92-32263
Advances in compressible turbulent mixing
[DE92-014326] p 4010 N92-32824

FLOW THEORY
The application of unsteady potential flow vortex loop/dipole theory to the work and acoustics of low-speed turbomachinery
[AD-A251160] p 4008 N92-32652

FLOW VELOCITY
An experimental study of the fluid mechanics associated with porous walls
[AIAA PAPER 92-0769] p 3998 N92-32263
Wind tunnel test of Teledyne Geotech model 1564B cup anemometer
[DE92-009590] p 4013 N92-32460
Demand controlled ventilating systems: Sensor market survey. Energy conservation in buildings and community systems programme, annex 18, December 1991
[PB92-180892] p 3977 N92-32825

FLOW VISUALIZATION
Experimental studies of characteristic combustion-driven flows for CFD validation p 3998 N92-32264
Three-dimensional flow fields inside a shrouded inducer at design and off-design conditions (CFD study) p 4003 N92-32291
Phase distribution measurements in narrow rectangular channels using image-processing techniques
[DE92-014084] p 4006 N92-32468
Vortex flow visualization using colored and fluorescent dyes on flat plate delta wing with leading edge extension
[AD-A251139] p 3930 N92-32651
An experimental study of the flow over a sharp-edged delta wing at subsonic and transonic speeds
[NLR-TP-91117-U] p 3930 N92-32732
Experimental study of the vortex system generated by a missile fuselage at incidence. Part 3: Three directional laser velocimetry measu.ements
[ONERA-RT-47/1147-AY-146A-P] p 3931 N92-32800
Study of flow properties of wet solids using laser induced photochemical anemometry
[DE92-014031] p 4017 N92-33180
Time-resolved holography for the study of shock waves
[ISBN-0-315-62369-1] p 4013 N92-33226

FLUE GASES
Direct catalytic decomposition of nitric oxide
[DE92-013847] p 4030 N92-33125

FLUID BOUNDARIES
The application of unsteady potential flow vortex loop/dipole theory to the work and acoustics of low-speed turbomachinery
[AD-A251160] p 4008 N92-32652
A three-field model of transient 3D multiphase, three-component flow for the computer code 4 A3. Part 2: Models for the interfacial transport phenomena. Code validation
[KFK-4949-PT-2] p 4011 N92-32858

FLUID DYNAMICS
An analysis of the flow field in the region of the ASRM field joints p 4005 N92-32305
Convergence acceleration of the Proteus computer code with multigrid methods
[NASA-CR-190607] p 4047 N92-33131

FLUID FILMS
Thinning and rupture of a thin liquid film on a heated surface
[DE92-014813] p 4013 N92-33124

FLUID FLOW
Heat transfer in rocket engine combustion chambers and nozzles p 3995 N92-32253
Model of Reynolds stress on nonorthogonal grid structures: Application to a staggered tube bundle
[ETN-92-91959] p 4009 N92-32725
Numerical methods: Solving the advection equation in flows with sharp gradients using Bott's flux scheme
[DM-59] p 4009 N92-32727

FLUID MECHANICS
An experimental study of the fluid mechanics associated with porous walls
[AIAA PAPER 92-0769] p 3998 N92-32263

FLUID-SOLID INTERACTIONS
The Utilization of Advanced Composites in Military Aircraft
[AGARD-R-785] p 3956 N92-33033
An overview of concerns relating to fluid effects on composites p 3958 N92-33045
Effects of fuel on Hercules AS-4/8552 composite material p 3958 N92-33046
Jet fuel absorption and dynamic mechanical analysis of carbon fibre composites p 3959 N92-33050

FLUORESCENCE
New applications of ionization and fluorescence techniques for detecting and characterization of open-shell organometallics in the gas phase
[AD-A250923] p 3961 N92-32509

FLUOROCARBONS
International research into chlorofluorocarbon (CFC) alternatives
[DE92-014241] p 4030 N92-32986

FLUTTER
The multiple-function multi-input/multi-output digital controller system for the AFW wind-tunnel model
[NASA-TM-107600] p 3934 N92-32536

FLUTTER ANALYSIS
NLR investigations of flutter behaviour of fighter aircraft with external stores
[NLR-TP-91134-U] p 3939 N92-32750

FLUX (RATE)
Numerical methods: Solving the advection equation in flows with sharp gradients using Bott's flux scheme
[DM-59] p 4009 N92-32727

FLUX PINNING
Substrate reactions and flux pinning structures in melt-processed YBa2Cu3O7 deposits on Ag-Pd alloy substrates
[DE92-014404] p 4084 N92-32919
Magnetic flux relaxation in YBa2Cu3O(7-x) thin film: Thermal or athermal p 3985 N92-32984
Synthesis, microstructure, critical current density, magnetization and relaxation of hot-pressed YBa2Cu3O(6 + delta) through partial melting post-oxygenation
[DE92-015205] p 4085 N92-33026

FLUX VECTOR SPLITTING
Overview of the relevant CFD work at Thiokol Corporation p 3995 N92-32249
An examination of several high resolution schemes applied to complex problems in high speed flows
[AD-A250814] p 4008 N92-32632

FOCAL PLANE DEVICES
Image enhancement of infrared uncooled focal plane array imagery p 3936 N92-32441
Development of ultra-low noise, high sensitivity planar metal grating coupled AlGaAs/GaAs multiquantum well IR detectors for focal plane array staring IR sensor systems
[AD-A250368] p 4083 N92-32747

FOILS (MATERIALS)
Analysis of LDEF experiment AO187-2: Chemically and isotopic measurements of micrometeoroids by secondary ion mass spectrometry
[NASA-CR-190697] p 4093 N92-32541

FOKKER AIRCRAFT
Active synchrophasing of propeller unbalance p 4063 N92-32963

FORCED CONVECTION
Direct numerical simulation of a combusting droplet with convection p 3996 N92-32256
Breakdown of the Karman vortex street due to forced convection and flow compressibility
[NASA-TM-105853] p 4007 N92-32472
Forced convection heat transfer in straight tubes. Part 1: Fully developed turbulent flow
[ESDU-92003-PT-1] p 4010 N92-32781

FOREIGN POLICY
Science and technology: A report to the Congress
[PB92-183219] p 4104 N92-33086

FOREST MANAGEMENT
Permuted keyword bank in CRIS. Terms for indexing and retrieving research projects in the current research information system
[PB92-179456] p 4090 N92-32712

FORMALDEHYDE
CARS diagnostics for solid propellant combustion investigations
[AD-A248660] p 3963 N92-32645

FORMALISM
Improving the translation from data flow diagrams into Z by incorporating the data dictionary
[AD-A250769] p 4089 N92-32342

FORMING TECHNIQUES
An implementation of Hill's theory of normal anisotropic plasticity for explicit shell analysis
[DE92-011468] p 4020 N92-32328

Fundamental questions concerning the application of superplastic forming and superplastic forming/diffusion bonding
[MBB-Z-0402-91-PUB] p 3977 N92-32690
Examples of advanced near-net shape manufacturing techniques for aerospace
[MBB-Z-0399-91-PUB] p 3977 N92-32742
Accommodation mechanisms and dispersoid-free zone s in Al 7475 after superplastic forming
[MBB-Z-0404-91-PUB] p 3968 N92-32894

FOURIER TRANSFORMATION
Application of gauge theories to enhance numerical solutions to mixed potential integral equations
[AD-A248451] p 4055 N92-32670
RF-GD/FTMS: An FTMS system with a lensless external ion source for high resolution elemental mass spectrometry
[DE92-015343] p 3964 N92-32925

FRACTALS
Nonlinear dynamics and plasma transport
[DE92-014246] p 4078 N92-32592

FRACTURE MECHANICS
A curved beam test specimen for determining the interlaminar tensile strength of a laminated composite
p 3949 N92-32526
A new approximate fracture mechanics analysis methodology for composites with a crack or hole
p 3949 N92-32530
Tensile fracture of notched composite laminates
[NRC-32147] p 3955 N92-32852
Investigation of fracture toughness and fracture mechanisms using acoustic emission measurements
[DE92-011907] p 4022 N92-32911
A comparison of three popular test methods for determining the shear modulus of composite materials
[NASA-CR-190659] p 3959 N92-33075

FRACTURE STRENGTH
A curved beam test specimen for determining the interlaminar tensile strength of a laminated composite
p 3949 N92-32526
Impact response of graphite/epoxy fabric structures
p 3951 N92-32583
Tensile fracture of notched composite laminates
[NRC-32147] p 3955 N92-32852
Investigation of fracture toughness and fracture mechanisms using acoustic emission measurements
[DE92-011907] p 4022 N92-32911

FRACTURES (MATERIALS)
A new approximate fracture mechanics analysis methodology for composites with a crack or hole
p 3949 N92-32530

FRACTURING
A curved beam test specimen for determining the interlaminar tensile strength of a laminated composite
p 3949 N92-32526
Computational simulation of structural fracture in fiber composites p 3949 N92-32531
Fracture surface characteristics of compressive failures in carbon fibre reinforced epoxy laminate subjected to hot/wet conditioning p 3959 N92-33051

FREE CONVECTION
Direct numerical simulation of a combusting droplet with convection p 3996 N92-32256
A numerical study of natural convection in a narrow annulus
[DE92-017138] p 4006 N92-32322
Forced convection heat transfer in straight tubes. Part 1: Fully developed turbulent flow
[ESDU-92003-PT-1] p 4010 N92-32781

FREE ELECTRON LASERS
Optics of beam transport in the NSLS UV-FEL
[DE92-014166] p 4015 N92-32511
Midwest free-electron laser program
[AD-A247264] p 4016 N92-32540
Estimates of SASE power in the short wavelength region
[DE92-014504] p 4017 N92-33155
Kinematics of Compton backscattering x ray source for angiography
[DE92-014016] p 4073 N92-33179

FREE FLOW
Swept shock/boundary layer interaction experiments in support of CFD code validation
[NASA-CR-190583] p 3930 N92-32494
An examination of several high resolution schemes applied to complex problems in high speed flows
[AD-A250814] p 4008 N92-32632
Leading-edge receptivity for blunt-nose bodies
[NASA-CR-190563] p 3930 N92-32648

FREE RADICALS
The energetics and dynamics of free radicals, ions, and clusters
[DE92-014124] p 4068 N92-33083

FREE VIBRATION
Free vibration of thick isotropic and orthotropic cylindrical shells
[DE92-011653] p 4022 N92-32706

FREEZING
Local structural order and molecular associations in water DMSO mixtures. Molecular dynamics study
[AD-A250935] p 4064 N92-32418

FREQUENCY DISTRIBUTION
Multifrequency measurements of radar ground clutter at 42 sites. Volume 1: Principal results
[AD-A246710] p 3980 N92-32696

FREQUENCY MEASUREMENT
Study and development of a six port network analyzer in the 1-18 GHz frequency range
[TELECOM-91-E-005] p 3980 N92-32739

FREQUENCY MODULATION
Adaptive filter technique for suppression of wideband or offset narrowband radio frequency interference
[AD-D015329] p 3992 N92-33175

FREQUENCY RESPONSE
Frequency domain state-space system identification
[NASA-TM-107659] p 4021 N92-32657

FREQUENCY STANDARDS
Trapped ions and laser cooling 3
[PB92-189547] p 4016 N92-33060

FRETTING
Guide to the effect of shot peening on fatigue strength
[ESDU-92015] p 3967 N92-32779

FRICTION FACTOR
Numerical simulation of inclined chute flows of monodisperse, inelastic, frictional spheres
[DE92-014775] p 4012 N92-32947

FROGS
Midwest free-electron laser program
[AD-A247264] p 4016 N92-32540

FROST
Performance of insulated pavements at Newton Fields, Jackman, Maine
[CRREL-92-9] p 3940 N92-32903

FUEL CELLS
High-temperature Solid Oxide Fuel Cell (SOFC) generator development project: Environmental assessment
[DE92-014698] p 4026 N92-32924
Chemical Technology Division
[DE92-014059] p 3964 N92-32931

FUEL COMBUSTION
Direct numerical simulation of a combusting droplet with convection p 3996 N92-32256
A numerical model for atomization-spray coupling in liquid rocket thrust chambers p 3996 N92-32257
Numerical modeling for dilute and dense sprays
p 3997 N92-32258
Modeling of SSME fuel preburner ASI
p 3945 N92-32259
Phase distributions of airborne polycyclic aromatic hydrocarbons in two US cities
[PB92-164979] p 4028 N92-32543
Axial vortices in gaseous-fired burner flow fields
[PB92-190370] p 3962 N92-32594
A basic research model of natural gas combustion in turbulent flow, phase 2
[PB92-190362] p 4007 N92-32598
The polychromatic pyrometer in diesel combustion
[ECL-91-42] p 3963 N92-32722
Local and temporal study of the combustion and heat transfer in a direct injection diesel engine
[ECL-91-43] p 3963 N92-32724

FUEL INJECTION
Modeling of SSME fuel preburner ASI
p 3945 N92-32259
CFD modeling of turbulent flows around the SSME main injector assembly using porosity formulation
p 3997 N92-32260
Computational fluid dynamics analysis of SSME phase 2 and phase 2+ preburner injector element hydrogen flow paths p 3997 N92-32261
STME hydrogen mixer study p 3945 N92-32262
Local and temporal study of the combustion and heat transfer in a direct injection diesel engine
[ECL-91-43] p 3963 N92-32724

FUEL PRODUCTION
NEDO Alcohol/Biomass Technology Subcommittee
[DE92-526270] p 3975 N92-32914

FUEL PUMPS
CFD applications in pump flows p 4002 N92-32288
Computation of the flow field in a centrifugal impeller with splitter blades p 4002 N92-32289

FUEL SPRAYS
Numerical modeling for dilute and dense sprays
p 3997 N92-32258

FUEL TESTS
Effects of fuel on Hercules AS-4/8552 composite material p 3958 N92-33046
The design features of rocket motors relating to insensitive munition response to thermo-mechanical stimuli p 3976 N92-33244

FULL SCALE TESTS
Development of composite wing carrythrough bulkheads for fighter aircraft p 3948 N92-32519

FUNCTIONAL DESIGN SPECIFICATIONS
Functions and genericity in a parallel programming language
[ETN-92-91667] p 4051 N92-32771
Software development practice in a scientific computing environment
[NLR-TP-91193-U] p 4043 N92-32832

FUSELAGES
The Dornier 328 Acoustic Test Cell (ATC) for interior noise tests and selected test results
[AIAA PAPER 92-2164] p 4062 N92-32951
Active control of sound transmission through stiff lightweight composite fuselage constructions
p 4062 N92-32957
CFRP stiffened panels under compression
p 3958 N92-33044

FUSION REACTORS
The Nova Upgrade Facility for ICF ignition and gain
[DE92-010703] p 4079 N92-32733

FUSION WELDING
A review of recent developments in joining high-performance thermoplastic composites
[CNRC-33030] p 4019 N92-33077

FUZZY SETS
Fuzzy set methods for object recognition in space applications
[NASA-CR-190388] p 4047 N92-33093

FUZZY SYSTEMS
Intelligent signal processing for active control
[AD-A252232] p 4053 N92-32625

G

GALACTIC EVOLUTION
Implementation of a tree-code for numerical simulations of stellar systems
[INPE-5370-TDI/469] p 4093 N92-32604

GALLIUM ARSENIDES
Laser material interaction
[AD-A250853] p 4016 N92-32622
Investigation on the lattice site location of the excess arsenic atoms in GaAs layers grown by low temperature molecular beam epitaxy
[DE92-008253] p 4083 N92-32693
Study and achievement of a parallel simulator for diffusion at the atomic level: Creation and growth of dislocation loops under electronic radiation
[LAAS-92118] p 4066 N92-32735
Intermodulation in the oscillatory magnetoresistance of a two-dimensional electron gas p 3984 N92-32975
Study of InGaAs-based modulation doped field effect transistor structures using variable-angle spectroscopic ellipsometry p 3984 N92-32977
Real-time edge-enhanced optical correlator
[NASA-CASE-NPO-18379-1-CU] p 4076 N92-33022
Implantation of carbon in GaAs
[DE92-016921] p 4085 N92-33117

GAME THEORY
An intelligent gaming environment
[ISBN-90-6275-635-2] p 4060 N92-33055

GAMMA RAYS
Gamma scattering in condensed matter with high intensity Moessbauer radiation
[DE92-014811] p 4085 N92-33025

GAS ANALYSIS
Effect of including variable gas properties and entrained particles in the flow analysis of the ASRM nozzle
p 4006 N92-32306

GAS CHROMATOGRAPHY
Huygens/ACP: An instrument for aerosols chemical composition measurements p 4098 N92-32379
Gas chromatography and pyrolysis-GC with capillary columns: Application to the in situ analysis of Titan's atmosphere p 4100 N92-32397

GAS DYNAMICS
Treating convection in sequential solvers
p 4000 N92-32277
Swept shock/boundary layer interaction experiments in support of CFD code validation
[NASA-CR-190583] p 3930 N92-32494
Numerical simulation of two-dimensional flows by the free-Lagrangian method
[TUM-M9105] p 4009 N92-32767

GAS FLOW
Numerical modeling for dilute and dense sprays
p 3997 N92-32258
CFD modeling of turbulent flows around the SSME main injector assembly using porosity formulation
p 3997 N92-32260

Computational fluid dynamics analysis of SSME phase 2 and phase 2+ preburner injector element hydrogen flow paths p 3997 N92-32261
A basic research model of natural gas combustion in turbulent flow, phase 2
[PB92-190362] p 4007 N92-32598
Numerical simulation of two-dimensional flows by the free-Lagrangian method
[TUM-M9105] p 4009 N92-32767
Arc/gas electrode
[NASA-CASE-MFS-29766-1] p 3991 N92-33030

GAS GENERATORS
CFD analysis of the STME nozzle flowfield p 3995 N92-32251
Navier-Stokes analysis of an oxidizer turbine blade with tip clearance p 3999 N92-32269
Space Transportation Main Engine p 3945 N92-32281

GAS GIANT PLANETS
Formation of the satellites p 4093 N92-32350

GAS IONIZATION
New applications of ionization and fluorescence techniques for detecting and characterization of open-shell organometallics in the gas phase
[AD-A250923] p 3961 N92-32509

GAS MIXTURES
Titan's organic haze p 4097 N92-32372
Experimental determination of the refractive index of liquefied gas mixtures: Applications to hypothesized Titan oceans p 4099 N92-32390
Gas chromatography and pyrolysis-GC with capillary columns: Application to the in situ analysis of Titan's atmosphere p 4100 N92-32397
Premixed turbulent combustion to opposed streams
[DE92-016996] p 3964 N92-32996

GAS PRESSURE
Arc/gas electrode
[NASA-CASE-MFS-29766-1] p 3991 N92-33030

GAS TURBINE ENGINES
Statistics on aircraft gas turbine engine rotor failures that occurred in US commercial aviation during 1988
[DOT/FAA/CT-91/26] p 3938 N92-33105

GAS-LIQUID INTERACTIONS
Direct numerical simulation of a combusting droplet with convection p 3996 N92-32256

GAS-METAL INTERACTIONS
Hydrogen permeation through bilayer metallic membrranes
[UTIAS-TN-342] p 3967 N92-32794

GASOLINE
Clean gasoline reforming with superacid catalysts
[DE92-013833] p 3975 N92-33123

GATES (CIRCUITS)
Auto and hetero-associative memory using a 2-D optical logic gate
[NASA-CASE-NPO-17997-1-CU] p 4041 N92-33057

GAUGE INVARIANCE
Equivalence between Lagrangian and Hamiltonian BRST formalisms
[DE92-624556] p 4055 N92-32602

GAUGE THEORY
Application of gauge theories to enhance numerical solutions to mixed potential integral equations
[AD-A248451] p 4055 N92-32670
Neutrino masses in the flipped SU(5) tensor product U(1) and the SU(4) tensor product O(4) GUT models
[RAL-92-012] p 4068 N92-33135

GELS
Ultra-low density organic-inorganic composite materials possessing thermally insulating and acoustic damping properties
[AD-A251182] p 3955 N92-32828

GEOCHEMISTRY
Chemical Technology Division
[DE92-014059] p 3964 N92-32931

GEODESY
Satellite radio interferometry
[PL-TR-91-2200] p 3978 N92-32458

GEOGRAPHIC INFORMATION SYSTEMS
Development of a prototype spatial information processing system for hydrologic research
[NASA-CR-190579] p 4024 N92-32590
Integrating expert vision systems and spatial database by unifying knowledge representation schemes.Development in remote sensing image analysis expert systems and geographical information systems
[ISBN-0-315-49130-2] p 4024 N92-33233

GEOMAGNETISM
Steady induction effects in geomagnetism. Part 1A: Steady motional induction of geomagnetic chaos
[NASA-TP-3272-PT-1A] p 4031 N92-32655

GEOMETRICAL OPTICS
Numerical evaluation of the incomplete airy functions and their application to high frequency scattering and diffraction
[NASA-CR-190745] p 4058 N92-32888

GEOPOTENTIAL
User's manual for AeroFcn: A FORTRAN program to compute aerodynamic parameters
[NASA-TM-104237] p 4042 N92-32507

GEOSYNCHRONOUS ORBITS
The MSAT spacecraft of Telesat Mobile, Inc.
[CTN-92-60346] p 3981 N92-32789

GEOTHERMAL ENERGY UTILIZATION
HDR opportunities and challenges beyond the long-term flow test isco, CA, 24-26 Mar. 1992
[DE92-011234] p 4025 N92-32695

GEOTHERMAL RESOURCES
HDR opportunities and challenges beyond the long-term flow test isco, CA, 24-26 Mar. 1992
[DE92-011234] p 4025 N92-32695

GLASS
Ultra-low density organic-inorganic composite materials possessing thermally insulating and acoustic damping properties
[AD-A251182] p 3955 N92-32828

GLASS FIBER REINFORCED PLASTICS
Processing and environmental effects on mechanical properties of composite repairs
[NRC-LTR-ST-1826] p 3954 N92-32791

GLASS FIBERS
Applications of the photorefractive effect and damage induced effects in fibers
[AD-A250767] p 3953 N92-32674

GLIDE LANDINGS
Integrated launch and emergency vehicle system
[NASA-CASE-LAR-13780-1] p 3943 N92-33013

GLIDERS
Further wind tunnel investigation of the SM701 airfoil with aileron and turbulators
[NASA-CR-190702] p 3932 N92-33063

GLOBAL POSITIONING SYSTEM
Satellite radio interferometry
[PL-TR-91-2200] p 3978 N92-32458

GLOBAL TRACKING NETWORK
Coverage studies for spaced-based radar
[DREO-90-18] p 3982 N92-32818

GLOW DISCHARGES
Diagnostics and modeling of ECRH microwave discharges
[IPF-91-3] p 4079 N92-32822
RF-GD/FTMS: An FTMS system with a lensless external ion source for high resolution elemental mass spectrometry
[DE92-015343] p 3964 N92-32925

GLUONS
First results of measurements of A(sub LL) two-spin asymmetry in inclusive production of (pi)(sup 0) mesons by polarized protons and antiprotons with 200 GeV energy
[DE92-624692] p 4065 N92-32497

GLYCIDYL AZIDE POLYMER
Development of a minimum smoke propellant based on glycidyl azide polymer and ammonium nitrate p 3976 N92-33243

GOLD
Electrocatalysis of anodic, oxygen-transfer reactions at noble metal electrodes
[DE92-016308] p 3962 N92-32562
Modification of the optical properties of Al2O3 by ion implantation
[DE92-013861] p 4085 N92-33127

GOVERNMENT PROCUREMENT
NASA procurement: Improving oversight of construction projects at the Langley Research Center. Report to the Honorable John W. Warner, US Senate
[GAO/NSIAD-92-230] p 4088 N92-32618
The DOD science and technology strategy
[AD-A253691] p 4104 N92-33027

GOVERNMENT/INDUSTRY RELATIONS
A status of the Turbine Technology Team activities p 3998 N92-32267

GOVERNMENTS
Information resources management plan of the Federal Government
[PB92-147198] p 4089 N92-32643

GRAIN BOUNDARIES
Generic consequences of fundamental studies of beta phase decomposition modes in titanium and related alloy systems
[AD-A250789] p 3967 N92-32699
Accommodation mechanisms and dispersoid-free zone s in Al 7475 after superplastic forming
[MBB-Z-0404-91-PUB] p 3968 N92-32894
Substrate reactions and flux pinning structures in melt-processed YBa2Cu3O7 deposits on Ag-Pd alloy substrates
[DE92-014404] p 4084 N92-32919
Site competition of impurities and grain boundary stability in iron
[AD-A252411] p 4084 N92-32939

GRAIN SIZE
Use of a Fourier deconvolution method in particle size determination and use of molecular mechanics in crystal structure determinations
[DE92-014510] p 4085 N92-33111

GRAND UNIFIED THEORY
Neutrino masses in the flipped SU(5) tensor product U(1) and the SU(4) tensor product O(4) GUT models
[RAL-92-012] p 4068 N92-33135

GRANTS
ERIP application instructions
[DE92-014103] p 4089 N92-32469

GRAPH THEORY
Development of a prototype spatial information processing system for hydrologic research
[NASA-CR-190579] p 4024 N92-32590

GRAPHITE-EPOXY COMPOSITES
Heating fixture and instrumentation design for elevated temperature tests of a composite repair technique
[WL-TM-90-326-FIBE] p 3946 N92-32459
A Protection And Detection Surface (PADS) for damage tolerance p 3948 N92-32523
Investigation into the fabrication of a composite top attack recoilless rifle p 3948 N92-32524
Global/local methods research using the CSM testbed p 3949 N92-32528
Scaling of fiber composite structures p 3950 N92-32532
Residual strength of repaired graphite/epoxy laminates after 5 years of outdoor exposure p 3950 N92-32577
Compression behavior of graphite-epoxy and graphite-thermoplastic panels with circular holes or impact damage p 3951 N92-32582
Impact response of graphite/epoxy fabric structures p 3951 N92-32583
Initial postbuckling response of an unsymmetrically laminated rectangular plate p 3952 N92-32586
Buckling and postbuckling behavior of square compression-loaded graphite-epoxy plates with circular cutouts p 3952 N92-32587
Study of the mechanical behaviour of graphite/epoxy laminates subjected to static and cyclic loading
[NRC-30833] p 3955 N92-32813
Tensile fracture of notched composite laminates
[NRC-32147] p 3955 N92-32852
Influence of edge effect on compression-tension fatigue of toughened graphite/epoxy laminates p 3957 N92-33039
Effects of fuel on Hercules AS-4/8552 composite material p 3958 N92-33046
A comparison of three popular test methods for determining the shear modulus of composite materials
[NASA-CR-190659] p 3959 N92-33075

GRAPHS (CHARTS)
Consistency and robustness of knowledge graphs
[ISBN-90-9003729-2] p 4056 N92-32679
Minimum cost multiflows in undirected networks
[IMAG-RR-849-M] p 4056 N92-32710
A min-max relation for K3-covers in graphs noncontractible to K5/e
[IMAG-RR-850-I] p 4056 N92-32711
Characterization of Laborde-Mulder graphs and the halfcube
[IMAG-RR-857-I] p 4057 N92-32713

GRATINGS (SPECTRA)
Determining surface profiie from sequential interference patterns from a long trace profiler
[DE92-017117] p 4073 N92-32321
Applications of the photorefractive effect and damage induced effects in fibers
[AD-A250767] p 3953 N92-32674

GRAVITATION
A Theoretical High Energy Physics Program: Task F
[DE92-014054] p 4073 N92-33182

GRAVITATION THEORY
On 5-dimensional Kaluza-Klein theory
[ETN-92-92130] p 3982 N92-32820

GRAVITATIONAL COLLAPSE
Research in nuclear astrophysics: Stellar collapse and supernovae
[DE92-014988] p 4093 N92-32993

GRAVITATIONAL FIELDS
On 5-dimensional Kaluza-Klein theory
[ETN-92-92130] p 3982 N92-32820

GRAVITY WAVES
Boundary layer processes in coastal meteorology: Prospects for remote sensing applications
[PB92-177849] p 4033 N92-32714
Acoustical emission from bubbles
[AD-A252390] p 4061 N92-32901

GREEN'S FUNCTIONS
Application of gauge theories to enhance numerical solutions to mixed potential integral equations
[AD-A248451] p 4055 N92-32670

GREENHOUSE EFFECT
ARM Tropical Pacific Experiment (ATPEX): Role of cloud, water vapor and convection feedbacks in the coupled ocean/atmosphere system
[DE92-013772] p 4032 N92-32331
The thermal structure of the atmosphere of Titan p 4094 N92-32353
US EPA's global climate change program: Landfill emissions and mitigation research
[PB92-180215] p 4028 N92-32609
International research into chlorofluorocarbon (CFC) alternatives
[DE92-014241] p 4030 N92-32986
GRID GENERATION (MATHEMATICS)
A computational design system for rapid CFD analysis p 4000 N92-32273
A multi-domain method for subsonic viscous flows p 3960 N92-32275
Tenth Workshop for Computational Fluid Dynamic Applications in Rocket Propulsion, part 1
[NASA-CP-3163-PT-1] p 4000 N92-32278
Impeller tandem blade study with grid embedding for local grid refinement p 4002 N92-32290
An efficient and robust grid optimization algorithm p 4004 N92-32300
Enhancements to the GRIDGEN structured grid generation system for internal and external flow applications p 4005 N92-32301
CAGI: Computer Aided Grid Interface. A work in progress p 4005 N92-32302
Using adaptive grid in modeling rocket nozzle flow p 4005 N92-32303
New concepts for multi-block grid generation for flow domains around complex aerodynamic configurations
[NLR-TP-91046-U] p 3930 N92-32730
GROUND EFFECT (COMMUNICATIONS)
Multifrequency measurements of radar ground clutter at 42 sites. Volume 1: Principal results
[AD-A246710] p 3980 N92-32696
GROUND STATE
Range of validity of distorted wave Born and impulse approximations for (e,2e)
[DE92-624821] p 4087 N92-32649
GROUND STATIONS
A 19.2 GHz cooled HEMT low noise amplifier
[CTN-92-60354] p 3990 N92-32810
GROUND SUPPORT EQUIPMENT
Ka-band dual frequency array feed for a low cost ACTS ground terminal p 3983 N92-32969
GROUND TESTS
Evaluation of composite components on the Bell 206L and Sikorsky S-76 helicopters p 3950 N92-32575
MD-80 aft cabin noise control: A case history p 4061 N92-32950
Advanced Study for Active Noise Control in Aircraft (ASANCA)
[AIAA PAPER 92-2092] p 4062 N92-32956
Flight service environmental effects on composite materials and structures p 3959 N92-33054
GROUND WATER
Environmental consequences of new energy technology. Solar heating, heat stores, and heat pumps
[PB92-180843] p 4025 N92-32605
Summary of engineering-scale experiments for the Solar Detoxification of Water project
[DE92-013776] p 4027 N92-33150
GROUP DYNAMICS
Observing team coordination within Army rotary-wing aircraft crews
[AD-A252234] p 4039 N92-32433
GROUP THEORY
Point interactions in L(sup p)
[REPT-91-97] p 4057 N92-32756
Computations for algebras and group representations
[ISBN-0-315-54684-0] p 4059 N92-33231
GUN PROPELLANTS
Condensed-phase processes during solid propellant combustion. Part 2: Chemical and microscopic examination of conductively quenched samples of RDX, XM39, JA2, M30, and HMX-binder compositions
[AD-A250799] p 3974 N92-32664
GUNS (ORDNANCE)
Braided composite bore evacuator chambers for tank cannons p 3948 N92-32520

H

HADRONS
Heavy flavor physics at hadron colliders
[DE92-014482] p 4064 N92-32312
Theoretical aspects of lepton-hadron scattering
[DE92-013765] p 4069 N92-33148
HALF LIFE
Radiative lifetime measurements of the AA pi 1/2 state in CaH
[USIP-91-03] p 4067 N92-32764
HALOGENATION
Thermal conductivity of gaseous halogenated hydrocarbons: Ethylenes and benzenes
[ESDU-92010] p 3945 N92-32485
HAMILTONIAN FUNCTIONS
Nonlinear resonance
[DE92-014313] p 4016 N92-32596
Equivalence between Lagrangian and Hamiltonian BRST formalisms
[DE92-624556] p 4055 N92-32602
HANDBOOKS
Space Station Freedom media handbook
[NASA-TM-107981] p 3942 N92-32421
HARDNESS
Guide to the effect of shot peening on fatigue strength
[ESDU-92015] p 3967 N92-32779
HARMONIC GENERATIONS
Probing thin-film YBa2Cu3O(7-delta) superconductors by second harmonic generation using femtosecond laser pulses
[AD-A252350] p 4082 N92-32512
Estimates of SASE power in the short wavelength region
[DE92-014504] p 4017 N92-33155
HARMONICS
Probing thin-film YBa2Cu3O(7-delta) superconductors by second harmonic generation using femtosecond laser pulses
[AD-A252350] p 4082 N92-32512
HARRIER AIRCRAFT
Collaborative research on V/STOL control system/cockpit display tradeoffs under the NASA/MOD joint aeronautical program
[NASA-TM-103910] p 3939 N92-32788
HAZARDS
Superheavyweight missions SI versus DI: Ascent flight design options and recommendations
[NASA-CR-183208] p 3942 N92-32610
Modeling the ear's response to intense impulses and the development of improved damage risk criteria
[AD-A252365] p 4037 N92-32916
Pilot noise exposure during a Boeing 747-400 round trip: Judgement of noise and analysis in respect to hearing impairment of pilots p 4063 N92-32961
Insensitive Munitions
[AGARD-CP-511] p 3975 N92-33240
The United States Air Force explosives hazards reduction program p 3976 N92-33241
Hazards reduction for tactical missiles p 3945 N92-33245
HAZE
Titan's organic haze p 4097 N92-32372
HEAD MOVEMENT
Effects of CSF hormones and ionic composition on salt/water metabolism
[NASA-CR-190693] p 4037 N92-32539
HEARING
Exposures from headset interference tones
[AD-A247175] p 4061 N92-32697
HEART FUNCTION
DCIEM/Central Medical Board Aircrew ECG program: Recommendations for restructuring
[DCIEM-90-47] p 4037 N92-32816
HEART RATE
Passive fetal monitoring sensor
[NASA-CASE-LAR-14088-1-CU] p 4015 N92-33016
HEAT BUDGET
STAMP, the SWOE Thermal Analysis and Measurement Program: Summary of the 1990 field tests
[LTR-91-013] p 4029 N92-32860
HEAT EXCHANGERS
STME hydrogen mixer study p 3945 N92-32262
Axial vortices in gaseous-fired burner flow fields
[PB92-190370] p 3962 N92-32594
HEAT FLUX
Inverse design of a proper number, shapes, sizes, and locations of coolant flow passages p 4004 N92-32298
A computational fluid dynamics analysis of the hypersonic flights of Pegasus
[NASA-CR-186023] p 4007 N92-32560
Scrape-off layer modeling of radiative divertor and high heat flux experiments on D3-D
[DE92-015007] p 4080 N92-32995
Turbulence transport equations for variable-density turbulence and their relationship to two-field models
[DE92-017292] p 4013 N92-33159
ANL ITER high-heat-flux blanket-module heat transfer experiments
[DE92-017749] p 4080 N92-33168
HEAT MEASUREMENT
Testing of the single-element stretched-membrane dish
[DE92-013680] p 4025 N92-32549
AC microcalorimetry of adsorbates on evaporated metal films: Orientational ordering of H2 multilayers
[DE92-008317] p 3963 N92-32666
HEAT PUMPS
Environmental consequences of new energy technology. Solar heating, heat stores, and heat pumps
[PB92-180843] p 4025 N92-32605
Development and proof-testing of advanced absorption refrigeration cycle concepts
[DE92-014933] p 3977 N92-32723
HEAT RESISTANT ALLOYS
High temperature deformation processes and strengthening mechanisms in intermetallic particulate composites
[AD-A250220] p 3946 N92-32339
High temperature fabricable nickel-iron aluminides
[CA-PATENT-1-276-814] p 3968 N92-32855
A combined AEM/APFIM characterization of Alloy X-750
[DE92-011049] p 3969 N92-33158
HEAT STORAGE
Thermochemical cycles for energy storage: Thermal decomposition of ZnSO4 systems
[DE91-002144] p 4026 N92-32909
HEAT TRANSFER
NLS nozzle base flow characteristics p 3995 N92-32252
Heat transfer in rocket engine combustion chambers and nozzles p 3995 N92-32253
Turbine disk cavity aerodynamics and heat transfer p 3998 N92-32265
Tenth Workshop for Computational Fluid Dynamic Applications in Rocket Propulsion, part 1
[NASA-CP-3163-PT-1] p 4000 N92-32278
Numerical analysis of the hot-gas-side and coolant-side heat transfer in liquid rocket engine combustors p 4004 N92-32299
Swept shock/boundary layer interaction experiments in support of CFD code validation
[NASA-CR-190583] p 3930 N92-32494
Heat and mass exchange during condensation of a water-ammonia mixture
[DE92-014524] p 3962 N92-32557
A computational fluid dynamics analysis of the hypersonic flights of Pegasus
[NASA-CR-186023] p 4007 N92-32560
Thermal gravitational modelling and scaling of two-phase heat transport systems for space: An assessment and a comparison of predictions and experimental results
[NLR-TP-91401-U] p 4008 N92-32675
Forced convection heat transfer in straight tubes. Part 1: Fully developed turbulent flow
[ESDU-92003-PT-1] p 4010 N92-32781
Two-phase heat transport systems for space: Thermal gravitational modelling and scaling predictions versus results of experiments
[NLR-TP-91051-U] p 4010 N92-32786
Thinning and rupture of a thin liquid film on a heated surface
[DE92-014813] p 4013 N92-33124
Turbulence transport equations for variable-density turbulence and their relationship to two-field models
[DE92-017292] p 4013 N92-33159
ANL ITER high-heat-flux blanket-module heat transfer experiments
[DE92-017749] p 4080 N92-33168
HEAT TRANSMISSION
Local and temporal study of the combustion and heat transfer in a direct injection diesel engine
[ECL-91-43] p 3963 N92-32724
HEAT TREATMENT
Processing and properties of silver-clad Tl-Ba-Ca-Cu-O wires and tapes
[DE92-015266] p 4081 N92-32346
Guide to the effect of shot peening on fatigue strength
[ESDU-92015] p 3967 N92-32779
The effect of heat treatment on the properties of PEEK and APC-2 p 3959 N92-33052
HEATERS
Hot water storage tank for solar collectors
[AD-D015301] p 4026 N92-32943
ANL ITER high-heat-flux blanket-module heat transfer experiments
[DE92-017749] p 4080 N92-33168
HEATING
Heating fixture and instrumentation design for elevated temperature tests of a composite repair technique
[WL-TM-90-326-FIBE] p 3946 N92-32459

HEAVING
Performance of insulated pavements at Newton Fields, Jackman, Maine
[CRREL-92-9] p 3940 N92-32903
HEAVY IONS
Transverse beam dynamics in recirculating accelerators for heavy-ion fusion
[DE92-013448] p 4070 N92-32413
Relativistic heavy ion collisions
[DE92-014415] p 4066 N92-32600
Study of recirculating induction accelerators as drivers for heavy ion fusion
[DE92-016980] p 4071 N92-32904
Relativistic heavy ion physics
[DE92-015025] p 4067 N92-32922
Development of advanced modulators for recirculating heavy ion accelerators
[DE92-014795] p 4072 N92-33122
HELICOPTER CONTROL
Computational aspects of helicopter trim analysis and damping levels from Floquet theory
[NASA-CR-190736] p 3940 N92-33107
HELICOPTER DESIGN
Evaluation of composite components on the Bell 206L and Sikorsky S-76 helicopters p 3950 N92-32575
HELICOPTERS
Vision-based range estimation using helicopter flight data
[NASA-TM-103930] p 3933 N92-32424
Observing team coordination within Army rotary-wing aircraft crews
[AD-A252234] p 4039 N92-32433
Correlating visual scene elements with simulator sickness incidence: Hardware and software development
[AD-A252235] p 4036 N92-32434
The German anti tank helicopter PAH 2: An example of a future sensor platform p 3937 N92-32448
Evaluation of composite components on the Bell 206L and Sikorsky S-76 helicopters p 3950 N92-32575
An evaluation of decelerating IFR approaches utilizing a helicopter flight simulator
[CTN-92-60348] p 3934 N92-32845
Flight service environmental effects on composite materials and structures p 3959 N92-33054
Building vibrations induced by noise from rotorcraft and propeller aircraft flyovers
[NASA-TM-104170] p 4063 N92-33160
HELIOSPHERE
STEL p 4103 N92-32457
HELIOTRONS
Status of LHD control system design
[NIFS-122] p 4070 N92-32746
HELIUM
Studies of helium based drift chamber gases for high-luminosity low energy machines
[DE92-012415] p 4065 N92-32426
HELIUM ATOMS
Coupled-channels-optical calculation of electron-helium scattering
[DE92-625009] p 4065 N92-32501
HELIUM ISOTOPES
Research and development of a helium-4 based solar neutrino detector
[DE92-017390] p 4103 N92-33119
HETEROCYCLIC COMPOUNDS
New thiophene-based materials
[AD-A250977] p 3972 N92-32667
HETEROGENEITY
Electrified microheterogeneous catalysis
[AD-D015270] p 3963 N92-32755
HETEROJUNCTIONS
Intermodulation in the oscillatory magnetoresistance of a two-dimensional electron gas p 3984 N92-32975
HEURISTIC METHODS
A fast task allocator for multiprocessing systems
[ISBN-0-315-54380-9] p 4053 N92-33217
Learning systems, adaptive data structures, and random environments
[ISBN-0-315-51158-3] p 4054 N92-33218
HIERARCHIES
Hierarchical sets in mathematical programming modeling languages
[MEMO-990] p 4057 N92-32796
Enhancements to speech recognition on voice response systems
[TELECOM-91-E-018] p 3981 N92-32807
HIGH ELECTRON MOBILITY TRANSISTORS
A 19.2 GHz cooled HEMT low noise amplifier
[CTN-92-60354] p 3990 N92-32810
V-band pseudomorphic HEMT MMIC phased array components for space communications p 3983 N92-32966
Planar dielectric resonator stabilized HEMT oscillator integrated with CPW/aperture coupled patch antenna p 3983 N92-32967
Reduced mobility and PPC in In(.20)Ga(.80)As / Al(.23)Ga(.77)As HEMT structure p 3984 N92-32976
Microwave properties of peeled HEMT devices sapphire substrates p 3984 N92-32978
HIGH ENERGY ELECTRONS
A high-power SLED 2 pulse compression system
[DE92-011586] p 4071 N92-32751
HIGH ENERGY INTERACTIONS
Theoretical and experimental studies of elementary physics
[DE92-014877] p 4061 N92-32430
Tutorial on neural network applications in high energy physics: A 1992 perspective
[DE92-016003] p 4070 N92-32506
Supersymmetry searches at electron-proton colliders
[ETN-92-92057] p 4067 N92-32753
A Theoretical High Energy Physics Program: Task F
[DE92-014054] p 4073 N92-33182
Elementary particle physics and high energy phenomena
[DE92-016844] p 4069 N92-33187
HIGH FREQUENCIES
Observations of high frequency and high wavenumber solar oscillations
[AD-A250099] p 4103 N92-32488
New approach to HF channel modeling and simulation. Part 3: Transfer function
[PB92-192848] p 3979 N92-32555
Numerical evaluation of the incomplete airy functions and their application to high frequency scattering and diffraction
[NASA-CR-190745] p 4058 N92-32888
HIGH IMPULSE
The evolutionary development of high specific impulse electric thruster technology
[NASA-TM-105758] p 3944 N92-33064
HIGH PRESSURE
CARS diagnostics for solid propellant combustion investigations
[AD-A248660] p 3963 N92-32645
Modeling the ear's response to intense impulses and the development of improved damage risk criteria
[AD-A252365] p 4037 N92-32916
HIGH RESOLUTION
The synthetic infrared spectrum of Titan at high spectral resolution p 4099 N92-32389
RF-GD/FTMS: An FTMS system with a lensless external ion source for high resolution elemental mass spectrometry
[DE92-015343] p 3964 N92-32925
Multispectral variable magnification glancing incidence x ray telescope
[NASA-CASE-MFS-28013-4] p 4092 N92-33012
Improved HIRAP flight calibration technique
[NASA-TM-107656] p 3944 N92-33112
HIGH SPEED
An examination of several high resolution schemes applied to complex problems in high speed flows
[AD-A250814] p 4008 N92-32632
HIGH STRENGTH
Innovative constituents requirements to improve composites compressive strength p 3957 N92-33043
HIGH STRENGTH STEELS
Mixed model fatigue crack growth behavior in a high strength steel
[AD-A250667] p 4022 N92-32717
HIGH TEMPERATURE
High temperature deformation processes and strengthening mechanisms in intermetallic particulate composites
[AD-A250220] p 3946 N92-32339
Inelastic deformation and damage at high temperature
[DE92-012241] p 4021 N92-32698
High temperature fabricable nickel-iron aluminides
[CA-PATENT-1-276-814] p 3968 N92-32855
The oxidation of Type 310S stainless steel in mixed gases at elevated temperatures
[DE92-014941] p 3968 N92-32991
HIGH TEMPERATURE LUBRICANTS
Liquid lubricants for advanced aircraft engines
[NASA-TM-104531] p 3972 N92-32863
HIGH TEMPERATURE SUPERCONDUCTORS
Mechanisms of the oxidation of metals and alloys with emphasis on superconductors
[DE92-016840] p 3966 N92-32315
The influence of anharmonic phonons on the isotope effect in high-(Tc) oxides
[DE92-017083] p 4081 N92-32320
Formation of high temperature superconductors from the solidified melt
[DE92-012584] p 4081 N92-32465
Local environment around the oxygen atoms in Y-Ba-Cu-O studied X ray Absorption Fine Structure (XAFS) spectroscopy
[DE92-014165] p 4081 N92-32470
Sintering of bulk high-(Tc) superconductors: Bi-Sr-Ca-Cu-O
[DE92-016189] p 4082 N92-32561
Workshop on research needs and opportunities in high temperature superconductivity
[AD-A252674] p 3988 N92-32659
The response of the double layer capacitance of a high temperature superconductor/fluid electrolyte interface to the onset of superconductivity
[AD-A251172] p 3990 N92-32827
NASA space applications of high-temperature superconductors p 3985 N92-32980
Magnetic penetration depth of YBa2Cu3O(7-delta) thin films determined by the power transmission method p 3985 N92-32983
Magnetic flux relaxation in YBa2Cu3O(7-x) thin film: Thermal or athermal p 3985 N92-32984
Superconductivity: Past, present, and future
[DE92-014862] p 3992 N92-33128
HIGH TEMPERATURE TESTS
Environmental degradation of high temperature composites p 3958 N92-33047
HISTORIES
Superconductivity: Past, present, and future
[DE92-014862] p 3992 N92-33128
HMX
Use of thin-film samples to study thermal decomposition chemistry of explosives
[DE92-014616] p 3974 N92-32637
Condensed-phase processes during solid propellant combustion. Part 2: Chemical and microscopic examination of conductively quenched samples of RDX, XM39, JA2, M30, and HMX-binder compositions
[AD-A250799] p 3974 N92-32664
HOLES (MECHANICS)
The use of curvilinear fiber format to improve buckling resistance of plates with central circular holes p 3948 N92-32521
A new approximate fracture mechanics analysis methodology for composites with a crack or hole p 3949 N92-32530
Compression behavior of graphite-epoxy and graphite-thermoplastic panels with circular holes or impact damage p 3951 N92-32582
Damage progression under compressive loading in composite laminates containing an open hole p 3957 N92-33040
HOLOGRAPHIC INTERFEROMETRY
Stress-relief displacements induced by drilling: Applications to holographic measurements of in situ stress
[DE92-013711] p 4014 N92-32620
Time-resolved holography for the study of shock waves
[ISBN-0-315-62369-1] p 4013 N92-33226
HOLOGRAPHY
Holographic crosstalk and signal-to-noise ratio in orthogonal data storage
[AD-A250146] p 4013 N92-32323
Midwest free-electron laser program
[AD-A247264] p 4016 N92-32540
Opto-electronic system for a formal neural network
[TELECOM-91-E-013] p 4075 N92-32805
HONEYCOMB STRUCTURES
Detection of honeycomb damage using hexagonal grid discontinuities
[DREP-89-9] p 3955 N92-32846
Active control of sound transmission through stiff lightweight composite fuselage constructions p 4062 N92-32957
HORIZON SCANNERS
Beam and filter straddle losses in an ESA search radar
[AD-A250878] p 3980 N92-32680
HORIZONTAL FLIGHT
Investigation of the flight control requirements of a half-scale ducted fan unmanned aerial vehicle
[AD-A252730] p 3940 N92-32988
HORIZONTAL TAIL SURFACES
Contribution of tailplane-mounted twin fins to sideforce, yawing moment, and rolling moment derivatives due to sideslip
[ESDU-92007] p 3939 N92-32487
HOT PRESSING
Synthesis, microstructure, critical current density, magnetization and relaxation of hot-pressed YBa2Cu3O(6 + delta) through partial melting post-oxygenation
[DE92-015205] p 4085 N92-33026
HOUSINGS
A flexible CPW package for a 30 GHz MMIC amplifier p 3983 N92-32972
Electromagnetic attachment mechanism
[NASA-CASE-MSC-21463-1] p 4019 N92-33018
Arc/gas electrode
[NASA-CASE-MFS-29766-1] p 3991 N92-33030

Device for removing foreign objects from anatomic organs
[NASA-CASE-GSC-13306-1] p 4038 N92-33032

HTPB PROPELLANTS
ESD traits of bulk propellant under pressure p 3976 N92-33242
Development of a minimum smoke propellant based on glycidyl azide polymer and ammonium nitrate p 3976 N92-33243

HUMAN BEHAVIOR
Feasibility study for predicting human reliability growth through training and practice
[AD-A252371] p 4038 N92-32990

HUMAN BEINGS
Development of the OMPAT neuropsychological/psychomotor performance evaluation and OMPAT data and timing support
[AD-A250793] p 4037 N92-32504
Toward advanced human reliability programs. Structural development considerations and options for extreme risk environments
[AD-A250786] p 4038 N92-32660
Toward the next millennium: A vision for spaceship Earth
[NASA-TM-107986] p 3941 N92-33007

HUMAN PERFORMANCE
Development of the OMPAT neuropsychological/psychomotor performance evaluation and OMPAT data and timing support
[AD-A250793] p 4037 N92-32504
Toward advanced human reliability programs. Structural development considerations and options for extreme risk environments
[AD-A250786] p 4038 N92-32660
A conceptual model of cognitive complexity of elements of the programming process p 4045 N92-32877
Feasibility study for predicting human reliability growth through training and practice
[AD-A252371] p 4038 N92-32990

HUMAN TOLERANCES
Exposures from headset interference tones
[AD-A247175] p 4061 N92-32697

HURRICANES
Diagnostic report of the National Hurricane Center, August and September 1991, volume 4, number 2
[PB92-179407] p 4033 N92-32503

HYBRID CIRCUITS
Performance of a Y-Ba-Cu-O superconducting filter/GaAs low noise amplifier hybrid circuit p 3985 N92-32982

HYDRATES
Hydrate detection
[DE92-014350] p 4034 N92-32333

HYDRATION
Local structural order and molecular associations in water DMSO mixtures. Molecular dynamics study
[AD-A250935] p 4064 N92-32418

HYDROCARBON FUELS
Direct conversion of light hydrocarbon gases to liquid fuel
[DE92-015592] p 3975 N92-33141

HYDROCARBONS
Neutral composition of Titan's atmosphere. A theoretical model p 4096 N92-32367
HCP and HCN, molecules of planetary interest p 4100 N92-32395
A shock tube study of the reactions of the hydroxyl radical with combustion species
[DE92-012573] p 3960 N92-32464
Thermal conductivity of gaseous halogenated hydrocarbons: Ethylenes and benzenes
[ESDU-92010] p 3945 N92-32485
Electrocatalyst surfaces
[PB92-190420] p 3962 N92-32591
Direct conversion of light hydrocarbon gases to liquid fuel
[DE92-015592] p 3975 N92-33141

HYDROCYANIC ACID
CARS diagnostics for solid propellant combustion investigations
[AD-A248660] p 3963 N92-32645

HYDRODYNAMIC COEFFICIENTS
Energy take-out from a wave energy device. A theoretical study of the hydrodynamics of a two-body problem consisting of a buoy and a submerged plate
[PB92-178821] p 4025 N92-32608

HYDRODYNAMICS
CFD analysis to optimize a design modification of BSMT p 4004 N92-32296
Two- and three-dimensional simulation code for radiation-hydrodynamics in ICF
[NIFS-119] p 4078 N92-32552
Energy take-out from a wave energy device. A theoretical study of the hydrodynamics of a two-body problem consisting of a buoy and a submerged plate
[PB92-178821] p 4025 N92-32608
Characterization of flow distribution in axisymmetric shock tubes
[AD-A251095] p 4008 N92-32683
PANACEA User's Manual
[DE92-011289] p 4043 N92-32741
On the origin and acoustical behaviour of cloud cavitation
[ISBN-90-9004317-9] p 4012 N92-33066
Connectivity structures and differencing techniques for staggered-grid free-Lagrange hydrodynamics
[DE92-017313] p 4012 N92-33082

HYDROGEN
Computational fluid dynamics analysis of SSME phase 2 and phase 2+ preburner injector element hydrogen flow paths p 3997 N92-32261
STME hydrogen mixer study p 3945 N92-32262
Simplified model of electron scattering on atomic hydrogen
[DE92-625007] p 4065 N92-32499
AC microcalorimetry of adsorbates on evaporated metal films: Orientational ordering of H2 multilayers
[DE92-008317] p 3963 N92-32666
Hydrogen permeation through bilayer metallic membrranes
[UTIAS-TN-342] p 3967 N92-32794

HYDROGEN EMBRITTLEMENT
Environmental fatigue in aluminum-lithium alloys
[NASA-TM-107640] p 4021 N92-32423

HYDROGEN IONS
Polar upper atmosphere characterization and supersonic ion escape (polar wind)
[GDR-0917] p 4031 N92-32889

HYDROGEN OXYGEN ENGINES
Tenth Workshop for Computational Fluid Dynamic Applications in Rocket Propulsion, part 2
[NASA-CP-3163-PT-2] p 3994 N92-32245
A status of the activities of the NASA. Marshall Space Flight Center Combustion Devices Technology Team p 3995 N92-32250
CFD analysis of the STME nozzle flowfield p 3995 N92-32251
NLS nozzle base flow characteristics p 3995 N92-32252
Heat transfer in rocket engine combustion chambers and nozzles p 3995 N92-32253
Application of computational fluid dynamics to the design of the film cooled STME subscale nozzle for the National Launch System p 3996 N92-32254
STME hydrogen mixer study p 3945 N92-32262
A status of the Turbine Technology Team activities p 3998 N92-32267
Space Transportation Main Engine p 3945 N92-32281

HYDROGENATION
Superplastic forming of Ti6Al4V at lower temperature using hydrogen
[MBB-Z-0403-91-PUB] p 3978 N92-32893

HYDROGENOLYSIS
Studies of n-butane conversion over silica-supported platinum, platinum-silver and platinum-copper catalysts
[DE92-016309] p 3962 N92-32563

HYDROLOGY
Development of a prototype spatial information processing system for hydrologic research
[NASA-CR-190579] p 4024 N92-32590

HYDROTHERMAL SYSTEMS
Chemical Technology Division
[DE92-014059] p 3964 N92-32931

HYDROXYL RADICALS
A shock tube study of the reactions of the hydroxyl radical with combustion species
[DE92-012573] p 3960 N92-32464

HYPERCUBE MULTIPROCESSORS
Optimal communication schemes on an SIMD distributed-memory hypercube
[IMAG-RR-848-M] p 4051 N92-32715

HYPERONS
Research in nuclear astrophysics: Stellar collapse and supernovae
[DE92-014988] p 4093 N92-32993
Theoretical nuclear physics
[DE92-016837] p 4069 N92-33186

HYPERSONICS
A computational fluid dynamics analysis of the hypersonic flights of Pegasus
[NASA-CR-186023] p 4007 N92-32560

HYPERVELOCITY IMPACT
Analysis of LDEF experiment AO187-2: Chemically and isotopic measurements of micrometeoroids by secondary ion mass spectrometry
[NASA-CR-190697] p 4093 N92-32541
Survivability characteristics of composite compression structure p 3950 N92-32578
A simple approach for the design and optimization of stand-off hypervelocity particle shields
[DE92-011383] p 3943 N92-32704

HYSTERESIS
Processing and properties of silver-clad Tl-Ba-Ca-Cu-O wires and tapes
[DE92-015266] p 4081 N92-32346
Fatigue, hysteresis, and acoustic emission, parts 1 and 2
[AD-A251073] p 4021 N92-32681

I

ICE
Feasibility of measuring transverse electric noise at VLF and LF on an ice cap
[AD-A252280] p 4035 N92-33220

ICE FORMATION
Debris/ice/TPS assessment and integrated photographic analysis for Shuttle Mission STS-49
[NASA-TM-107547] p 3941 N92-32454

IDENTIFYING
Naval target classification and designation with the CL-227 Sea Sentinel p 3937 N92-32449

IGNITERS
Current status of the development of an ignition transient model for solid rocket motors p 3944 N92-32246
Modeling of SSME fuel preburner ASI p 3945 N92-32259

IGNITION
Current status of the development of an ignition transient model for solid rocket motors p 3944 N92-32246
A state of the art report on flame acceleration and transition to detonation in hydrogen/air/diluent mixtures
[DE92-626850] p 3961 N92-32475
Shock tube ignition of ethanol, isobutene and MTBE: Experiments and modeling
[DE92-008563] p 3961 N92-32544
The Nova Upgrade Facility for ICF ignition and gain
[DE92-010703] p 4079 N92-32733

IMAGE ANALYSIS
Target cuing: A heterogeneous neural network approach p 3936 N92-32442
The local structure of image intensity discontinuities
[ISBN-0-315-57231-0] p 4048 N92-33204
Hypothesis refinement for 3-D scene interpretation
[ISBN-0-315-57864-5] p 4048 N92-33210
Primal access recognition of visual objects
[ISBN-0-315-63509-6] p 4048 N92-33212
Integrating expert vision systems and spatial database by unifying knowledge representation schemes.Development in remote sensing image analysis expert systems and geographical information systems
[ISBN-0-315-49130-2] p 4024 N92-33233

IMAGE CONTRAST
Temporal and spatial factors affecting the perception of computer-generated imagery
[AD-A249242] p 4046 N92-32907

IMAGE CORRELATORS
Opto-electronic system for a formal neural network
[TELECOM-91-E-013] p 4075 N92-32805

IMAGE ENHANCEMENT
Image enhancement of infrared uncooled focal plane array imagery p 3936 N92-32441
Real-time edge-enhanced optical correlator
[NASA-CASE-NPO-18379-1-CU] p 4076 N92-33022
Image processing mini manual
[NASA-TM-107680] p 4041 N92-33205

IMAGE FILTERS
Recursive estimation techniques for detection of small objects in infrared image data
[AD-A250942] p 4075 N92-32935

IMAGE PROCESSING
PET studies of components of high-level vision
[AD-A250873] p 4036 N92-32344
Target detection using co-occurrence matrix segmentation and its hardware implementation p 3936 N92-32443
Methods of opto-electronic fusion of infrared and visible images p 3936 N92-32444
Automatic detection, pursuit, and classification in infrared imagery p 3937 N92-32445
Phase distribution measurements in narrow rectangular channels using image-processing techniques
[DE92-014084] p 4006 N92-32468
Target Cueing And Tracking System (TCATS): User's guide
[DE92-015385] p 4042 N92-32617
Optical modulation characteristics and applications of liquid crystal televisions
[AD-A252466] p 3979 N92-32633
Continuous and discrete problems in image processing
[TELECOM-91-D-007] p 4058 N92-32802
Contribution to the determination of vanishing points using Hough transform
[TELECOM-91-D-008] p 4058 N92-32803

Uses of stereovision surface models
[TELECOM-91-E-016] p 4075 N92-32806
Detection of honeycomb damage using hexagonal grid discontinuities
[DREP-89-9] p 3955 N92-32846
Shape recognition by computer in simulated aerial images
[DCIEM-91-05] p 4054 N92-32854
Temporal and spatial factors affecting the perception of computer-generated imagery
[AD-A249242] p 4046 N92-32907
Recursive estimation techniques for detection of small objects in infrared image data
[AD-A250942] p 4075 N92-32935
Applications of energy loss contrast STIM
[DE92-017254] p 4014 N92-33000
Semiannual status report
[NASA-CR-190239] p 4046 N92-33092
Fuzzy set methods for object recognition in space applications
[NASA-CR-190388] p 4047 N92-33093
Multi-stage hybrid coding of digital images
[ISBN-0-315-58989-2] p 4047 N92-33189
Pattern recognition based on entropy analysis and shape transformations
[ISBN-0-315-56074-6] p 4048 N92-33201
Ambient light array vision in 3-D
[ISBN-0-315-55748-6] p 4077 N92-33202
Image processing mini manual
[NASA-TM-107680] p 4041 N92-33205

IMAGE RECONSTRUCTION
Continuous and discrete problems in image processing
[TELECOM-91-D-007] p 4058 N92-32802
Opto-electronic system for a formal neural network
[TELECOM-91-E-013] p 4075 N92-32805
Uses of stereovision surface models
[TELECOM-91-E-016] p 4075 N92-32806

IMAGE RESOLUTION
Surface reconstruction and templating for zeolite thin film synthesis observed by atomic force microscopy
[AD-A251140] p 4066 N92-32548

IMAGERY
Image enhancement of infrared uncooled focal plane array imagery p 3936 N92-32441
Target detection using co-occurrence matrix segmentation and its hardware implementation p 3936 N92-32443
Uses of stereovision surface models
[TELECOM-91-E-016] p 4075 N92-32806

IMAGING SPECTROMETERS
VIMS/Cassini mission at Titan: Scientific objectives and observational scenarios p 4097 N92-32377

IMAGING TECHNIQUES
Thermal effects and mirror surface figure requirements for a diagnostic beamline at the advanced light source
[DE92-014483] p 4073 N92-32419
Generic modular imaging IR signal processor p 3936 N92-32440
Midwest free-electron laser program
[AD-A247264] p 4016 N92-32540
Topographical measuring based on the shadow and projection Moire method
[ISBN-90-9004146-X] p 4074 N92-32705
NAASW modular radar research testbed study results
[DE92-011339] p 3981 N92-32744
Three dimensional object reconstruction using a very limited number of projections. Application to industrial radiography
[TELECOM-91-E-008] p 4043 N92-32804
Applications of energy loss contrast STIM
[DE92-017254] p 4014 N92-33000
A boundary integral method for an inverse problem in thermal imaging
[NASA-CR-189693] p 4059 N92-33006
Multispectral variable magnification glancing incidence x ray telescope
[NASA-CASE-MFS-28013-4] p 4092 N92-33012
Diffractive optics technology and the NASA Geostationary Earth Observatory (GEO)
[NASA-CR-190611] p 4076 N92-33074
Radiation selective system for target range and imaging readout
[AD-D015285] p 4076 N92-33095

IMMUNOASSAY
Small passive chemical detector
[DE92-014188] p 4030 N92-32933

IMPACT
Huygens probe: The surface mission p 4101 N92-32402

IMPACT DAMAGE
Organic chemistry on Titan: Surface interactions p 4096 N92-32370
Calculation of the energy of elastic deformation of Kevlar backing plates for ceramic armours
[AD-A250129] p 3970 N92-32489
Compression of thick laminated composite beams with initial impact-like damage
[NASA-CR-190573] p 3946 N92-32491
Survivability characteristics of composite compression structure p 3950 N92-32578
Damage tolerance certification methodology for composite structures p 3951 N92-32579
Certification of damage tolerant composite structure p 3951 N92-32580
Compression behavior of graphite-epoxy and graphite-thermoplastic panels with circular holes or impact damage p 3951 N92-32582
Impact response of graphite/epoxy fabric structures p 3951 N92-32583
GARTEUR compression behaviour of advanced CFRP --- carbon fiber reinforced plastics p 3957 N92-33042
CFRP stiffened panels under compression p 3958 N92-33044
Insensitive Munitions
[AGARD-CP-511] p 3975 N92-33240
The design features of rocket motors relating to insensitive munition response to thermo-mechanical stimuli p 3976 N92-33244

IMPACT TESTS
Design, evaluation and experimental effort toward development of a high strain composite wing for Navy aircraft p 3947 N92-32514
Survivability characteristics of composite compression structure p 3950 N92-32578
Certification of damage tolerant composite structure p 3951 N92-32580
Impact response of graphite/epoxy fabric structures p 3951 N92-32583
ROAR: A 3-D tethered rocket simulation code
[DE92-017358] p 3944 N92-33166

IMPELLERS
Development of CFD code evaluation criteria and a procedure for assessing predictive capability and performance p 4001 N92-32283
Impeller tandem blade study with grid embedding for local grid refinement p 4002 N92-32290
Effects of curvature and rotation on turbulence in the NASA low-speed centrifugal compressor impeller p 4003 N92-32292
SSME HPOTP impeller backcavity CFD analysis p 4003 N92-32294

IMPREGNATING
Experimental investigation of the axial impregnation of oriented fiber bundles by capillary forces
[AD-A250758] p 3961 N92-32508

IMPROVEMENT
A simple Doppler wind lidar sensor: Simulated measurements and impacts in a global assimilation and forecast system
[PL-TR-91-2253] p 4034 N92-32859

IMPULSES
Modeling the ear's response to intense impulses and the development of improved damage risk criteria
[AD-A252365] p 4037 N92-32916
Impulse transmitter and quantum detection radar system
[AD-D015323] p 3986 N92-33171

IMPURITIES
Alpha particle diagnostics using impurity pellet injection
[DE92-013796] p 4078 N92-32623
Investigation of impurity related phenomena, significant for novel semiconductor technologies
[ETN-92-92048] p 4083 N92-32760
Site competition of impurities and grain boundary stability in iron
[AD-A252411] p 4084 N92-32939

INCOHERENT SCATTERING
Polar upper atmosphere characterization and supersonic ion escape (polar wind)
[GDR-0917] p 4031 N92-32889

INCOMPRESSIBLE FLOW
Development of a CFD code for internal flows in liquid fueled engines p 3999 N92-32271
A comparison of artificial compressibility and fractional step methods for incompressible flow computations p 4001 N92-32285
CFD applications in pump flows p 4002 N92-32288
Massively separated flow modeling. Experimental study of the fine structure of boundary layers. Study of the influence of external turbulence level
[ETN-92-92088] p 4009 N92-32765
Singularities in the classical Rayleigh-Taylor flow: Formation and subsequent motion
[NASA-CR-189690] p 4010 N92-32784
A new time scale based k-epsilon model for near wall turbulence
[NASA-TM-105768] p 4011 N92-32868
A numerical resolution study of high order essentially non-oscillatory schemes applied to incompressible flow
[NASA-CR-189692] p 4012 N92-33110
Computation of incompressible viscous flows through turbopump components
[NASA-TM-103911] p 4012 N92-33113

INCONEL (TRADEMARK)
A combined AEM/APFIM characterization of Alloy X-750
[DE92-011049] p 3969 N92-33158

INDIUM GALLIUM ARSENIDES
Reduced mobility and PPC in In(.20)Ga(.80)As / Al(.23)Ga(.77)As HEMT structure p 3984 N92-32976
Study of InGaAs-based modulation doped field effect transistor structures using variable-angle spectroscopic ellipsometry p 3984 N92-32977
A simple high-performance avalanche photodiode for long-wavelength optical communications, phase 1
[PB92-188259] p 4076 N92-33004

INDOOR AIR POLLUTION
Demand controlled ventilating systems: Sensor market survey. Energy conservation in buildings and community systems programme, annex 18, December 1991
[PB92-180892] p 3977 N92-32825

INDUCTANCE
Calibration service for low-loss, three-terminal capacitance standards at 100 kHz and 1 MHz
[PB92-189554] p 3991 N92-33061

INDUSTRIAL ENERGY
Potential environmental effects of energy conservation measures in northwest industries
[DE92-013993] p 4030 N92-33156

INDUSTRIAL SAFETY
High-temperature Solid Oxide Fuel Cell (SOFC) generator development project: Environmental assessment
[DE92-014698] p 4026 N92-32924

INDUSTRIAL WASTES
Defense environmental restoration program annual report to Congress for fiscal year 1991
[AD-A244196] p 4029 N92-32731

INDUSTRIES
Potential environmental effects of energy conservation measures in northwest industries
[DE92-013993] p 4030 N92-33156

INELASTIC SCATTERING
On the choice of minimization functional in the partial wave analysis
[DE92-624689] p 4087 N92-32309
Theoretical and experimental studies of elementary physics
[DE92-014877] p 4061 N92-32430
Partons and the EMC spin effect
[RAL-92-015-PREPRINT] p 4068 N92-33137

INELASTIC STRESS
Inelastic deformation and damage at high temperature
[DE92-012241] p 4021 N92-32698

INERTIAL CONFINEMENT FUSION
Two- and three-dimensional simulation code for radiation-hydrodynamics in ICF
[NIFS-119] p 4078 N92-32552
The Nova Upgrade Facility for ICF ignition and gain
[DE92-010703] p 4079 N92-32733

INERTIAL NAVIGATION
A Kalman filter integrated navigation design for the IAR Twin Otter Atmospheric Research Aircraft
[NRC-32148] p 3934 N92-32849
The use of Kalman filtering techniques to improve the accuracy of flight test data
[NRC-32139] p 3938 N92-32850

INFORMATION DISSEMINATION
Space Station Freedom media handbook
[NASA-TM-107981] p 3942 N92-32421
A minority research and education information service: Design, develop, pilot test, and implement on-line access for historically black colleges and universities and government agencies
[DE92-013572] p 4090 N92-32930
FEDIX on-line information service: Design, develop, test, and implement, an on-line research and education information service
[DE92-013582] p 4090 N92-32985

INFORMATION MANAGEMENT
MANTECH project book
[AD-A245283] p 3977 N92-32461
Information resources management plan of the Federal Government
[PB92-147198] p 4089 N92-32643
Permuted keyword bank in CRIS. Terms for indexing and retrieving research projects in the current research information system
[PB92-179456] p 4090 N92-32712
Fault tolerance for security management in distributed systems
[LAAS-92011] p 4040 N92-32766
Hypertext and hypermedia
[VTT-RN-1154] p 4090 N92-32843

The development of an airborne information management system for flight test
[NASA-TM-104251] p 3938 N92-32866
An international aerospace information system: A cooperative opportunity
[NASA-TM-108171] p 4091 N92-33237

INFORMATION RETRIEVAL
Automatic access experiment
[AD-A252217] p 4089 N92-32611
Hypertext and hypermedia
[VTT-RN-1154] p 4090 N92-32843

INFORMATION SYSTEMS
MANTECH project book
[AD-A245283] p 3977 N92-32461
Information Integration for Concurrent Engineering (IICE) IDEF3 process description capture method report
[AD-A252633] p 4042 N92-32627
Permuted keyword bank in CRIS. Terms for indexing and retrieving research projects in the current research information system
[PB92-179456] p 4090 N92-32712
A minority research and education information service: Design, develop, pilot test, and implement on-line access for historically black colleges and universities and government agencies
[DE92-013572] p 4090 N92-32930
FEDIX on-line information service: Design, develop, test, and implement, an on-line research and education information service
[DE92-013582] p 4090 N92-32985
EPCRA Section 313 Roadmaps Database: User's manual, version 2.2
[PB92-169523] p 4030 N92-33062
Oak Ridge Environmental Information System (OREIS). Phase 1: System definition document
[DE92-017342] p 4090 N92-33084
Advanced information processing system: The Army fault tolerant architecture conceptual study. Volume 1: Army fault tolerant architecture overview
[NASA-CR-189632-VOL-1] p 4052 N92-33100
Advanced information processing system: The Army fault tolerant architecture conceptual study. Volume 2: Army fault tolerant architecture design and analysis
[NASA-CR-189632-VOL-2] p 4052 N92-33101
An international aerospace information system: A cooperative opportunity
[NASA-TM-108171] p 4091 N92-33237

INFORMATION THEORY
Selecting a subset of stimulus-response pairs with maximal transmitted information
[AD-A252728] p 3986 N92-32987

INFRARED ABSORPTION
HCP and HCN, molecules of planetary interest
p 4100 N92-32395

INFRARED ASTRONOMY
Infrared properties of Titan's clouds and aerosols
p 4097 N92-32373
Some problems about IR band integrated intensities; 3 examples for application to Titan: C6H6, HC3N, and C4H2 p 4101 N92-32400

INFRARED DETECTORS
Infrared Targeting System (IRTS) demonstration
p 3937 N92-32446
A molecule-specific filter modulator
[AD-A250760] p 4074 N92-32672
Development of ultra-low noise, high sensitivity planar metal grating coupled AlGaAs/GaAs multiquantum well IR detectors for focal plane array staring IR sensor systems
[AD-A250368] p 4083 N92-32747
Recursive estimation techniques for detection of small objects in infrared image data
[AD-A250942] p 4075 N92-32935

INFRARED IMAGERY
Methods of opto-electronic fusion of infrared and visible images p 3936 N92-32444
Automatic detection, pursuit, and classification in infrared imagery p 3937 N92-32445
Recursive estimation techniques for detection of small objects in infrared image data
[AD-A250942] p 4075 N92-32935

INFRARED INSTRUMENTS
Observing the surface of Titan through near-infrared windows in its atmosphere p 4097 N92-32374

INFRARED PHOTOMETRY
Titan's mid-IR albedo: New observations from 3 to 5 microns p 4097 N92-32376

INFRARED RADIATION
Image enhancement of infrared uncooled focal plane array imagery p 3936 N92-32441
Target detection using co-occurrence matrix segmentation and its hardware implementation
p 3936 N92-32443
A molecule-specific filter modulator
[AD-A250760] p 4074 N92-32672
An evaluation of an infrared/resistance temperature device for air/sea-surface temperature measurements
[AD-A252279] p 4035 N92-32688

INFRARED RADIOMETERS
Near infrared spectra of potential solids at the surface of Titan p 4102 N92-32406
A precise narrow-beam filter infrared radiometer and its use with lidar in the ARM Program
[DE92-016872] p 4015 N92-33188

INFRARED SPECTRA
Radiometric and spectral measurement instruments
[AD-A250771] p 4013 N92-32343
Ground-based observations of Titan's thermal spectrum p 4095 N92-32359
The synthetic infrared spectrum of Titan at high spectral resolution p 4099 N92-32389
Some problems about IR band integrated intensities; 3 examples for application to Titan: C6H6, HC3N, and C4H2 p 4101 N92-32400
Near infrared spectra of potential solids at the surface of Titan p 4102 N92-32406
A molecule-specific filter modulator
[AD-A250760] p 4074 N92-32672

INFRARED SPECTROMETERS
VIMS/Cassini mission at Titan: Scientific objectives and observational scenarios p 4097 N92-32377
Cassini/CIRS capabilities for aerosol, cloud, and surface measurements p 4098 N92-32378

INFRARED SPECTROSCOPY
Infrared properties of Titan's clouds and aerosols
p 4097 N92-32373
Titan's mid-IR albedo: New observations from 3 to 5 microns p 4097 N92-32376
Cassini/CIRS capabilities for aerosol, cloud, and surface measurements p 4098 N92-32378
The spectrum of Titan in the 1.06 and 1.28 micron windows p 4101 N92-32401
Near infrared spectra of potential solids at the surface of Titan p 4102 N92-32406

INFRARED WINDOWS
Observing the surface of Titan through near-infrared windows in its atmosphere p 4097 N92-32374

INFRASONIC FREQUENCIES
Burning oil fields as a source of infrasonic waves
[IRF-PREPRINT-119] p 4061 N92-32842

INGESTION (ENGINES)
Bird ingestion into large turbofan engines
[DOT/FAA/CT-91/17] p 3932 N92-33005

INHIBITORS
A comparative study of the effects of inhibitor stub length on solid rocket motor combustion chamber pressure oscillations: RSRM at T = 80 seconds, preliminary results p 3945 N92-32248

INJECTION MOLDING
Nondestructive evaluation development for process control
[DE92-015272] p 3971 N92-32640
Orientation, stress, and density distributions in injection-moulded amorphous polymers determined by optical techniques
[ETN-92-92052] p 3972 N92-32752

INJECTORS
Computational fluid dynamics analysis of SSME phase 2 and phase 2+ preburner injector element hydrogen flow paths p 3997 N92-32261
Space Transportation Main Engine
p 3945 N92-32281
Overview of SSC accelerator requirements
[DE92-014896] p 4073 N92-33134

INJURIES
Verification of severe local storms forecasts issued by the National Severe Storms Forecast Center, 1991
[PB92-186063] p 4033 N92-32502

INKS
Phase distribution measurements in narrow rectangular channels using image-processing techniques
[DE92-014084] p 4006 N92-32468

INSERTION LOSS
Beam and filter straddle losses in an ESA search radar
[AD-A250878] p 3980 N92-32680

INSPECTION
Debris/ice/TPS assessment and integrated photographic analysis for Shuttle Mission STS-49
[NASA-TM-107547] p 3941 N92-32454
Execution of measurement sequences in the framework of the inspection of near limit regions by radioiodine and aerosol emission measurements, and ground examinations on plutonium, strontium, and gamma ray radionuclides
[OEFZS-4579] p 4071 N92-32763
Collaborative, remote, in-depth inspection and verification of satellites with neutral particle beams
[DE92-014195] p 3943 N92-32934

INSTALLING
Device and process for attachment of parts to rocket motors
[AD-D015309] p 3944 N92-33162

INSTRUMENT ERRORS
A Kalman filter integrated navigation design for the IAR Twin Otter Atmospheric Research Aircraft
[NRC-32148] p 3934 N92-32849

INSTRUMENT FLIGHT RULES
An evaluation of decelerating IFR approaches utilizing a helicopter flight simulator
[CTN-92-60348] p 3934 N92-32845
Federal aviation regulations. Part 91: General operating and flight rules
[PB92-197334] p 3929 N92-33176

INSTRUMENT LANDING SYSTEMS
Aircraft accident report: L'Express Airlines, Inc., Flight 508, Beech C99, N7217L weather encounter and crash near Birmingham, Alabama, July 10, 1991
[PB92-910401] p 3932 N92-32455

INSTRUMENTS
Fifty years in science, thirty years in space
[LALP-92-51] p 4104 N92-32862

INSULATION
SRMAFTE facility checkout model flow field analysis
p 3994 N92-32247

INTEGRAL EQUATIONS
Application of gauge theories to enhance numerical solutions to mixed potential integral equations
[AD-A248451] p 4055 N92-32670
Analysis of shielded CPW discontinuities with air-bridges p 3983 N92-32971

INTEGRAL TRANSFORMATIONS
Application of gauge theories to enhance numerical solutions to mixed potential integral equations
[AD-A248451] p 4055 N92-32670
An experimental study on the two-parameter crack tip field
[AD-A251173] p 4023 N92-32936

INTEGRATED CIRCUITS
Pulse coded biologically motivated neural-type MOS circuits
[AD-A250367] p 3988 N92-32325
Multichip module study
[AD-A250877] p 3989 N92-32678
V-band pseudomorphic HEMT MMIC phased array components for space communications
p 3983 N92-32966
An optically controlled Ka-band phased array antenna
p 3983 N92-32968
A flexible CPW package for a 30 GHz MMIC amplifier
p 3983 N92-32972
A 1-W, 30-GHz, CPW amplifier for ACTS small terminal uplink p 3984 N92-32973
A low-current amplifier for mobile radio and monolithic microwave integrated circuit design techniques in the UHF and L bands
[ISBN-0-315-59034-3] p 3993 N92-33211

INTEGRATED OPTICS
Applications of the photorefractive effect and damage induced effects in fibers
[AD-A250767] p 3953 N92-32674

INTERACTIONAL AERODYNAMICS
Further development of the CANAERO computer code to include propulsor modelling
[DREA-CR-90-425] p 3931 N92-32811

INTERACTIVE CONTROL
Interactive control in turbulent shear layers
[AD-A250711] p 4008 N92-32671

INTERCEPTION
Interception of LPI radar signals
[AD-A246315] p 3978 N92-32535

INTERFACES
Program PLOTTAB: A code designed to plot continuous and/or discrete physical data
[DE92-013754] p 4041 N92-32416

INTERFACIAL TENSION
Thinning and rupture of a thin liquid film on a heated surface
[DE92-014813] p 4013 N92-33124

INTERFERENCE
Exposures from headset interference tones
[AD-A247175] p 4061 N92-32697

INTERFEROMETERS
Scanning force microscopy using optical interferometry
[ISBN-90-9003887-6] p 4077 N92-33146

INTERFEROMETRY
Satellite radio interferometry
[PL-TR-91-2200] p 3978 N92-32458
Scanning force microscopy using optical interferometry
[ISBN-90-9003887-6] p 4077 N92-33146

INTERLAMINAR STRESS
Three-dimensional elasticity analysis of buckling of laminated plates p 3957 N92-33037

Influence of edge effect on compression-tension fatigue of toughened graphite/epoxy laminates
p 3957 N92-33039

INTERMETALLICS
High temperature deformation processes and strengthening mechanisms in intermetallic particulate composites
[AD-A250220] p 3946 N92-32339
Dynamics of radiation-induced amorphization in intermetallic compounds
[DE92-016774] p 4086 N92-33221

INTERMITTENCY
Relativistic heavy ion collisions
[DE92-014415] p 4066 N92-32600

INTERMODULATION
Intermodulation in the oscillatory magnetoresistance of a two-dimensional electron gas p 3984 N92-32975

INTERNAL COMBUSTION ENGINES
Contribution to the theoretical and experimental analysis of camshaft engine operation
[ETN-92-91961] p 4018 N92-32726

INTERNAL ENERGY
Physical basis for a pressure-dependent yield criterion for polymers
[AD-A250763] p 3970 N92-32341

INTERNATIONAL COOPERATION
Toward the next millennium: A vision for spaceship Earth
[NASA-TM-107986] p 3941 N92-33007
An international aerospace information system: A cooperative opportunity
[NASA-TM-108171] p 4091 N92-33237

INTERPOLATION
Global/local methods research using the CSM testbed
p 3949 N92-32528
An implementation of a fault-tolerant, multidirectional, digital interpolation beamformer
[AD-A252494] p 3986 N92-33152

INTERPROCESSOR COMMUNICATION
Parallel processing in space applications using transputer networks
[MBB-UO-0172-90-PUB] p 4050 N92-32689
Optimal communication schemes on an SIMD distributed-memory hypercube
[IMAG-RR-848-M] p 4051 N92-32715
A fast task allocator for multiprocessing systems
[ISBN-0-315-54380-9] p 4053 N92-33217
Diagnosability and diagnosis of sparsely interconnected multiprocessor systems
[ISBN-0-315-56107-6] p 4053 N92-33224

INTERSTELLAR GAS
Some issues associated with the formation of the Saturnian system p 4093 N92-32349

INTERSTELLAR TRAVEL
Toward the next millennium: A vision for spaceship Earth
[NASA-TM-107986] p 3941 N92-33007

INTERSTITIALS
Structure and dynamics in low-dimensional guest-host systems
[DE92-014841] p 3970 N92-32429

INTERVALS
Statistical selection: Multiple comparison approach
[ETN-92-92051] p 4060 N92-32709

INVENTIONS
ERIP application instructions
[DE92-014103] p 4089 N92-32469
Noncircular rolling joints for vibrational reduction in slewing maneuvers
[NASA-CASE-LAR-14515-1-CU] p 4019 N92-33031
Corrosion-resistant alkyd coatings
[AD-D015330] p 3974 N92-33177

INVISCID FLOW
Singularities in the classical Rayleigh-Taylor flow: Formation and subsequent motion
[NASA-CR-189690] p 4010 N92-32784

ION ACCELERATORS
Development of advanced modulators for recirculating heavy ion accelerators
[DE92-014795] p 4072 N92-33122

ION ATOM INTERACTIONS
Scaling in the processes of ion-atom excitation
[DE92-625008] p 4065 N92-32500

ION BEAMS
Booster Applications Facility report, phase 2
[DE92-013395] p 4070 N92-32411
Two- and three-dimensional simulation code for radiation-hydrodynamics in ICF
[NIFS-119] p 4078 N92-32552
The LLNL Multi-User Tandem Laboratory PIXE microprobe
[DE92-017252] p 4014 N92-32999
Plasma opening switch for long-pulse intense ion beam
[DE92-017523] p 3992 N92-33068
Development of advanced modulators for recirculating heavy ion accelerators
[DE92-014795] p 4072 N92-33122
Overview of SSC accelerator requirements
[DE92-014896] p 4073 N92-33134

ION CYCLOTRON RADIATION
Ion heating and MHD dynamo fluctuations in the reversed field pinch
[DE92-013902] p 4078 N92-32624
RF-GD/FTMS: An FTMS system with a lensless external ion source for high resolution elemental mass spectrometry
[DE92-015343] p 3964 N92-32925

ION DISTRIBUTION
Local structural order and molecular associations in water DMSO mixtures. Molecular dynamics study
[AD-A250935] p 4064 N92-32418

ION IMPLANTATION
Implanted aluminum: Tribological behavior and mechanical properties of the superficial layers
[ECL-91-28] p 4019 N92-32801
Implantation of carbon in GaAs
[DE92-016921] p 4085 N92-33117
Modification of the optical properties of Al2O3 by ion implantation
[DE92-013861] p 4085 N92-33127
High-energy ion implantation for bipolar transistor fabrication
[ISBN-90-9003883-3] p 3992 N92-33144
Coatings for improved corrosion resistance
[DE92-016779] p 3974 N92-33247

ION MICROSCOPES
Applications of energy loss contrast STIM
[DE92-017254] p 4014 N92-33000
Ion microtomography using ion time-of-flight
[DE92-017257] p 4068 N92-33001

ION MOTION
Dynamics of ion solvation in a Stockmayer fluid
[AD-A251087] p 4066 N92-32682

ION PROBES
Light-ion spectroscopy with exotic targets
[DE92-017258] p 3964 N92-32929

ION PROPULSION
The evolutionary development of high specific impulse electric thruster technology
[NASA-TM-105758] p 3944 N92-33064

ION SOURCES
High intensity negative proton beams from a SNICS ion source
[DE92-011137] p 4070 N92-32647
RF-GD/FTMS: An FTMS system with a lensless external ion source for high resolution elemental mass spectrometry
[DE92-015343] p 3964 N92-32925
Spectroscopic characterization of LEVIS active ion source on PBFA 2
[DE92-014954] p 4080 N92-32992

ION STORAGE
Trapped ions and laser cooling 3
[PB92-189547] p 4016 N92-33060

ION TEMPERATURE
Ion heating and MHD dynamo fluctuations in the reversed field pinch
[DE92-013902] p 4078 N92-32624
Polar upper atmosphere characterization and supersonic ion escape (polar wind)
[GDR-0917] p 4031 N92-32889

ION TRAPS (INSTRUMENTATION)
Trapped ions and laser cooling 3
[PB92-189547] p 4016 N92-33060

IONIC COLLISIONS
Relativistic heavy ion collisions
[DE92-014415] p 4066 N92-32600

IONIC REACTIONS
A shock tube study of the reactions of the hydroxyl radical with combustion species
[DE92-012573] p 3960 N92-32464

IONIZATION
New applications of ionization and fluorescence techniques for detecting and characterization of open-shell organometallics in the gas phase
[AD-A250923] p 3961 N92-32509
Novel gas phase ion molecule reactions of C60(++) with O2 and NH3
[AD-A250921] p 4066 N92-32556
Mass resolved resonance ionization spectroscopy of combustion radicals
[DE92-016833] p 3965 N92-33222

IONIZATION CROSS SECTIONS
Simplified model of electron scattering on atomic hydrogen
[DE92-625007] p 4065 N92-32499

IONIZATION POTENTIALS
Novel gas phase ion molecule reactions of C60(++) with O2 and NH3
[AD-A250921] p 4066 N92-32556

IONIZED GASES
Arc/gas electrode
[NASA-CASE-MFS-29766-1] p 3991 N92-33030

IONOSPHERIC PROPAGATION
Characteristics of large aspect angle VHF radar echoes in the presence and absence of optical aurora
[ISBN-0-315-59091-2] p 4032 N92-33197

IONOSPHERIC TEMPERATURE
Polar upper atmosphere characterization and supersonic ion escape (polar wind)
[GDR-0917] p 4031 N92-32889

IONS
High intensity negative proton beams from a SNICS ion source
[DE92-011137] p 4070 N92-32647
Dynamics of ion solvation in a Stockmayer fluid
[AD-A251087] p 4066 N92-32682
Fast ion loss and radial electric field in Wendelstein 7-A stellarator
[DE92-782106] p 4079 N92-32745
The energetics and dynamics of free radicals, ions, and clusters
[DE92-014124] p 4068 N92-33083

IRON
Hydrogen permeation through bilayer metallic membranes
[UTIAS-TN-342] p 3967 N92-32794

IRRADIATION
Midwest free-electron laser program
[AD-A247264] p 4016 N92-32540
Methyl substituted polyimides containing carbonyl and ether connecting groups
[NASA-CASE-LAR-14351-1] p 3973 N92-33015
Modeling the influence of irradiation temperature and displacement rate on hardening due to point defect clusters in ferritic steels
[DE92-016897] p 3969 N92-33115

IRREVERSIBLE PROCESSES
Two studies of nonlinear processes in irreversible thermodynamics
[DE92-016855] p 4087 N92-32566

ISOCYANATES
Synthesis, morphology and properties of polyester-urethane in solution in styrene: Application to composites development
[ISAL-92-0007] p 3972 N92-32762

ISOMERIZATION
Studies of n-butane conversion over silica-supported platinum, platinum-silver and platinum-copper catalysts
[DE92-016309] p 3962 N92-32563

ISOTOPE EFFECT
The influence of anharmonic phonons on the isotope effect in high-(Tc) oxides
[DE92-017083] p 4081 N92-32320

ISOTOPIC ENRICHMENT
A study of the dissolution mechanism by chemical and electrochemical oxidation-reduction of actinide dioxides (UO2, NpO2, PuO2, and AmO2) in an acid aqueous medium
[DE92-014834] p 3965 N92-33126

ISOTROPY
Free vibration of thick isotropic and orthotropic cylindrical shells
[DE92-011653] p 4022 N92-32706

ITERATION
On the inconsistency of bootstrap distribution estimators
[IMAG-RR-856-M] p 4060 N92-32718

ITERATIVE SOLUTION
Experiments with an ordinary differential equation solver in the parallel solution of method of lines problems on a shared memory parallel computer, part 2
[DE92-017159] p 4052 N92-32926

J

J INTEGRAL
An experimental study on the two-parameter crack tip field
[AD-A251173] p 4023 N92-32936

JACOBI MATRIX METHOD
Aspects of solving non-linear boundary value problems numerically
[ETN-92-92049] p 4058 N92-32798
Jacobian and stiffness analysis of a novel class of six-DOF parallel minimanipulators
[DE92-016373] p 4054 N92-33184

JET AIRCRAFT NOISE
Acoustic loads prediction on jet aircraft
p 4061 N92-32949
MD-80 aft cabin noise control: A case history
p 4061 N92-32950
Pilots noise exposure during a Boeing 747-400 round trip: Ambient noise and acoustic-head recording and analysis of data p 4063 N92-32960

Pilot noise exposure during a Boeing 747-400 round trip: Judgement of noise and analysis in respect to hearing impairment of pilots p 4063 N92-32961

JET ENGINE FUELS

Jet fuel absorption and dynamic mechanical analysis of carbon fibre composites p 3959 N92-33050

JET FLOW

Numerical simulation of turbulence at the back of the airplane

[ETN-92-91664] p 3931 N92-32769

JET IMPINGEMENT

Experimental studies of characteristic combustion-driven flows for CFD validation p 3998 N92-32264

JET MIXING FLOW

Acoustic loads prediction on jet aircraft p 4061 N92-32949

JOINTS (JUNCTIONS)

Out of plane analysis for composite str. ..ures p 3949 N92-32527

Noncircular rolling joints for vibrational reduction in slewing maneuvers

[NASA-CASE-LAR-14515-1-CU] p 4019 N92-33031

Environmental resistance of amorphous bonded thermoplastic joints p 3959 N92-33053

JORDAN FORM

Poincare normal form (system of ordinary differential equations): An algorithmic point of view

[IMAG-RR-839-M] p 4058 N92-32838

JOSEPHSON JUNCTIONS

Geometrical effects in two-dimensional arrays of Josephson junctions

[AD-A252209] p 4084 N92-32898

JP-4 JET FUEL

Fluid effects: Thermoset and thermoplastic matrix composites p 3958 N92-33049

K

K-EPSILON TURBULENCE MODEL

Numerical modeling for dilute and dense sprays p 3997 N92-32258

A numerical study of two-dimensional vortex shedding from rectangular cylinders p 3998 N92-32266

Numerical simulation of turbomachinery flows with advanced turbulence models p 3999 N92-32270

CFD analysis of pump consortium impeller p 4002 N92-32287

A new time scale based k-epsilon model for near wall turbulence

[NASA-TM-105768] p 4011 N92-32868

KALMAN FILTERS

Vision-based range estimation using helicopter flight data

[NASA-TM-103930] p 3933 N92-32424

The use of Kalman filtering techniques to improve the accuracy of flight test data

[NRC-32139] p 3938 N92-32850

KALMAN-SCHMIDT FILTERING

A Kalman filter integrated navigation design for the IAR Twin Otter Atmospheric Research Aircraft

[NRC-32148] p 3934 N92-32849

The use of Kalman filtering techniques to improve the accuracy of flight test data

[NRC-32139] p 3938 N92-32850

KAONS

Scalar mesons and kaons in phi radiative decay and their implications for studies of CP violation at DA(phi)NE

[RAL-91-085] p 4068 N92-33133

KARMAN VORTEX STREET

Breakdown of the Karman vortex street due to forced convection and flow compressibility

[NASA-TM-105853] p 4007 N92-32472

KELVIN-HELMHOLTZ INSTABILITY

Boundary layer processes in coastal meteorology: Prospects for remote sensing applications

[PB92-177849] p 4033 N92-32714

KERNEL FUNCTIONS

Bandwidth selection for the intensity of point processes: Application to hazard rate models for censored data

[IMAG-RR-859-I/M] p 4056 N92-32684

KEVLAR (TRADEMARK)

Calculation of the energy of elastic deformation of Kevlar backing plates for ceramic armours

[AD-A250129] p 3970 N92-32489

A Protection And Detection Surface (PADS) for damage tolerance p 3948 N92-32523

KINEMATICS

Steady induction effects in geomagnetism. Part 1A: Steady motional induction of geomagnetic chaos

[NASA-TP-3272-PT-1A] p 4031 N92-32655

Singularities in the classical Rayleigh-Taylor flow: Formation and subsequent motion

[NASA-CR-189690] p 4010 N92-32784

KINETICS

Effect of including variable gas properties and entrained particles in the flow analysis of the ASRM nozzle p 4006 N92-32306

Experimental investigation of the axial impregnation of oriented fiber bundles by capillary forces

[AD-A250758] p 3961 N92-32508

Generic consequences of fundamental studies of beta phase decomposition modes in titanium and related alloy systems

[AD-A250789] p 3967 N92-32699

Some electronic and dynamical factors in electron-transfer chemistry: Metal complexes, clusters, and surfaces

[AD-A251169] p 3964 N92-32826

Kinematics of Compton backscattering x ray source for angiography

[DE92-014016] p 4073 N92-33179

KNOWLEDGE

Consistency and robustness of knowledge graphs

[ISBN-90-9003729-2] p 4056 N92-32679

KNOWLEDGE BASES (ARTIFICIAL INTELLIGENCE)

Optimization of logic queries in knowledge base systems

[ISBN-0-315-51346-2] p 4049 N92-33227

KNOWLEDGE REPRESENTATION

Shape recognition by computer in simulated aerial images

[DCIEM-91-05] p 4054 N92-32854

Optimization of logic queries in knowledge base systems

[ISBN-0-315-51346-2] p 4049 N92-33227

Integrating expert vision systems and spatial database by unifying knowledge representation schemes.Development in remote sensing image analysis expert systems and geographical information systems

[ISBN-0-315-49130-2] p 4024 N92-33233

KOLMOGOROFF-SMIRNOFF TEST

Applications of statistical methods to the study of climate and flooding fluctuations in the central US

[PB92-205137] p 4034 N92-33173

KRYPTON FLUORIDE LASERS

Laser measurements for experiments on the TROLL accelerator

[DE92-016578] p 4015 N92-32335

L

LABORATORIES

National Voluntary Laboratory Accreditation Program 1992 Directory

[PB92-201094] p 3941 N92-33002

LAGUERRE FUNCTIONS

Generalizations of the classical Laguerre polynomials and some q-analogues

[ISBN-90-9003765-9] p 4058 N92-32836

LAMINAR FLOW

Further wind tunnel investigation of the SM701 airfoil with aileron and turbulators

[NASA-CR-190702] p 3932 N92-33063

Computational and experimental study of laminar flames

[DE92-017978] p 3965 N92-33121

LAMINATES

Heating fixture and instrumentation design for elevated temperature tests of a composite repair technique

[WL-TM-90-326-FIBE] p 3946 N92-32459

Calculation of the energy of elastic deformation of Kevlar backing plates for ceramic armours

[AD-A250129] p 3970 N92-32489

Compression of thick laminated composite beams with initial impact-like damage

[NASA-CR-190573] p 3946 N92-32491

A Protection And Detection Surface (PADS) for damage tolerance p 3948 N92-32523

A curved beam test specimen for determining the interlaminar tensile strength of a laminated composite p 3949 N92-32526

Out of plane analysis for composite structures p 3949 N92-32527

Global/local methods research using the CSM testbed p 3949 N92-32528

Efficient finite element modeling of laminated composite plates based on higher-order theory p 3949 N92-32529

A new approximate fracture mechanics analysis methodology for composites with a crack or hole p 3949 N92-32530

Computational simulation of structural fracture in fiber composites p 3949 N92-32531

Residual strength of repaired graphite/epoxy laminates after 5 years of outdoor exposure p 3950 N92-32577

Survivability characteristics of composite compression structure p 3950 N92-32578

Damage tolerance certification methodology for composite structures p 3951 N92-32579

Compression behavior of graphite-epoxy and graphite-thermoplastic panels with circular holes or impact damage p 3951 N92-32582

Impact response of graphite/epoxy fabric structures p 3951 N92-32583

Postbuckling of stiffened composite plates under combined loading p 3952 N92-32585

Initial postbuckling response of an unsymmetrically laminated rectangular plate p 3952 N92-32586

Buckling and postbuckling behavior of square compression-loaded graphite-epoxy plates with circular cutouts p 3952 N92-32587

A new approach to fibrous composite laminate strength prediction p 3952 N92-32588

Shear buckling of specially orthotropic plates with centrally located cutouts p 3953 N92-32589

Free vibration of thick isotropic and orthotropic cylindrical shells

[DE92-011653] p 4022 N92-32706

The use of piezoelectric sensors to detect delamination initiation in carbon fiber reinforced composites

[MBB-Z-0391-91-PUB] p 3954 N92-32740

Buckling and damage of a composite plate under compression

[ONERA-RT-25/3542-RY-006-R] p 4022 N92-32774

Nonlinear transient responses of stratified composite structures

[ONERA-RT-26/3542-RY-007-R] p 3954 N92-32775

Buckling of fibre reinforced composite and sandwich laminates with higher-order shear deformation theories

[IIT-B/CE/RR/92/2] p 4022 N92-32783

Free-edge delamination of a stratified composite: Interaction with the transversal crack

[ONERA-RT-13/7256-RY-006-R] p 3954 N92-32792

Study of the mechanical behaviour of graphite/epoxy laminates subjected to static and cyclic loading

[NRC-30833] p 3955 N92-32813

Tensile fracture of notched composite laminates

[NRC-32147] p 3955 N92-32852

Issues in compression loading of composite structures p 3956 N92-33034

A new test method to determine the compressive strength of fiber-reinforced composites p 3956 N92-33035

Three-dimensional elasticity analysis of buckling of laminated plates p 3957 N92-33037

Influence of edge effect on compression-tension fatigue of toughened graphite/epoxy laminates p 3957 N92-33039

Damage progression under compressive loading in composite laminates containing an open hole p 3957 N92-33040

Propagation of a delamination in a composite panel subjected to a compression load p 3957 N92-33041

CFRP stiffened panels under compression p 3958 N92-33044

Fracture surface characteristics of compressive failures in carbon fibre reinforced epoxy laminate subjected to hot/wet conditioning p 3959 N92-33051

Global/local interlaminar stress analysis of a grid-stiffened composite panel

[NASA-CR-190822] p 4023 N92-33139

Silver coated superconducting ceramic powder

[AD-D015294] p 3973 N92-33157

Apparatus for preparing thermoplastic composites

[AD-D015326] p 3960 N92-33174

LAND MOBILE SATELLITE SERVICE

A 19.2 GHz cooled HEMT low noise amplifier

[CTN-92-60354] p 3990 N92-32810

LANDFILLS

US EPA's global climate change program: Landfill emissions and mitigation research

[PB92-180215] p 4028 N92-32609

LANTHANUM OXIDES

Thickness dependence of vortex pinning in epitaxial Tl-Ca-Ba-Cu-O thin films

[DE92-015011] p 4084 N92-32920

LAPLACE TRANSFORMATION

Point interactions in L(sup p)

[REPT-91-97] p 4057 N92-32756

LASER ANEMOMETERS

Study of flow properties of wet solids using laser induced photochemical anemometry

[DE92-015452] p 4013 N92-33140

Study of flow properties of wet solids using laser induced photochemical anemometry

[DE92-014031] p 4017 N92-33180

LASER APPLICATIONS

Laser measurements for experiments on the TROLL accelerator

[DE92-016578] p 4015 N92-32335

Depolarized light source for fiber optic sensors

[AD-D015289] p 4074 N92-32634

The dependence of the anisoplanatic Strehl of a compensated beam on the beacon distribution
[DE92-011272] p 4016 N92-32736
The effect of the light round-trip time on the performance of an adaptive optics turbulence compensation system
[DE92-011273] p 4075 N92-32738
Detectors for lidar type Thomson scattering diagnostics
[IPF-91-5] p 3990 N92-32823
Laser coating of composites for enhanced wear and corrosion resistance
[AD-A249231] p 3956 N92-32906
Trapped ions and laser cooling 3
[PB92-189547] p 4016 N92-33060
Estimates of SASE power in the short wavelength region
[DE92-014504] p 4017 N92-33155

LASER BEAMS
Laser measurements for experiments on the TROLL accelerator
[DE92-016578] p 4015 N92-32335
The dependence of the anisoplanatic Strehl of a compensated beam on the beacon distribution
[DE92-011272] p 4016 N92-32736
The effect of the light round-trip time on the performance of an adaptive optics turbulence compensation system
[DE92-011273] p 4075 N92-32738
Laser to single-mode-fiber coupling: A laboratory guide
[NASA-CR-4452] p 4077 N92-33239

LASER CAVITIES
Resonantly pumped, erbium-doped, 2.8 micron solid state laser with high slope efficiency
[AD-D015310] p 4017 N92-33165

LASER DAMAGE
Midwest free-electron laser program
[AD-A247264] p 4016 N92-32540

LASER FUSION
The Nova Upgrade Facility for ICF ignition and gain
[DE92-010703] p 4079 N92-32733

LASER INDUCED FLUORESCENCE
Study on lifetime specific, laser-induced ultrafast fluorescence detection in the time and frequency domain for in-situ environmental analysis of organic pollutants
[KFK-4975] p 4029 N92-32841

LASER MATERIALS
Laser material interaction
[AD-A250853] p 4016 N92-32622

LASER OUTPUTS
Feasibility of a 486 nm Fraunhofer laser source based on a 4F(sub 3/2) yields 4I(sub 9/2) neodymium laser
[AD-A250851] p 4015 N92-32329
Transverse diode pumping of solid-state lasers
[AD-A252213] p 4016 N92-33089
Resonantly pumped, erbium-doped, 2.8 micron solid state laser with high slope efficiency
[AD-D015310] p 4017 N92-33165

LASER PLASMAS
Laser measurements for experiments on the TROLL accelerator
[DE92-016578] p 4015 N92-32335
Activities report of the Institute of Plasma Research
[ETN-92-92147] p 4079 N92-32797

LASER RANGE FINDERS
A simple high-performance avalanche photodiode for long-wavelength optical communications, phase 1
[PB92-188259] p 4076 N92-33004

LASER SPECTROSCOPY
New applications of ionization and fluorescence techniques for detecting and characterization of open-shell organometallics in the gas phase
[AD-A250923] p 3961 N92-32509
Laser material interaction
[AD-A250853] p 4016 N92-32622
Computational and experimental study of laminar flames
[DE92-017978] p 3965 N92-33121
Mass resolved resonance ionization spectroscopy of combustion radicals
[DE92-016833] p 3965 N92-33222

LASER WELDING
Device and process for attachment of parts to rocket motors
[AD-D015309] p 3944 N92-33162

LASERS
Molecular surface analysis by laser ionization of desorbed molecules
[DE92-016320] p 4016 N92-33114

LATITUDE
Titan's atmosphere: Latitudinal variations in temperature and composition p 4094 N92-32355
Coverage studies for spaced-based radar
[DREO-90-18] p 3982 N92-32818

LATTICE PARAMETERS
The influence of anharmonic phonons on the isotope effect in high-(Tc) oxides
[DE92-017083] p 4081 N92-32320

LATTICES (MATHEMATICS)
Object links in the repository
[NASA-CR-190644] p 4091 N92-33096

LAUNCH VEHICLES
Integrated launch and emergency vehicle system
[NASA-CASE-LAR-13780-1] p 3943 N92-33013

LAWS
National environmental compliance strategy
[DE92-013639] p 4027 N92-32415

LEAD COMPOUNDS
Scintillation properties of lead sulfate
[DE92-010301] p 4082 N92-32493

LEADING EDGES
Vortex flow visualization using colored and fluorescent dyes on flat plate delta wing with leading edge extension
[AD-A251139] p 3930 N92-32651

LEARNING CURVES
Feasibility study for predicting human reliability growth through training and practice
[AD-A252371] p 4038 N92-32990

LEAST SQUARES METHOD
Adaptive information processing and global optimization
[AD-A248450] p 4089 N92-32644
Frequency domain state-space system identification
[NASA-TM-107659] p 4021 N92-32657

LENSES
Diffractive optics technology and the NASA Geostationary Earth Observatory (GEO)
[NASA-CR-190611] p 4076 N92-33074
Laser to single-mode-fiber coupling: A laboratory guide
[NASA-CR-4452] p 4077 N92-33239

LEPTONS
Experimental particle physics at the University of Pittsburgh
[DE92-014181] p 4066 N92-32702
Theoretical aspects of lepton-hadron scattering
[DE92-013765] p 4069 N92-33148

LICENSING
National Voluntary Laboratory Accreditation Program 1992 Directory
[PB92-201094] p 3941 N92-33002

LIE GROUPS
Fractional spin: Majorana-Dirac field
[DE92-624558] p 4087 N92-32603

LIFT
Lift and rolling moment due to spoilers on wings with trailing-edge flaps deflected at subsonic speeds
[ESDU-92002-SUPPL] p 3931 N92-32782

LIFTING BODIES
Aerodynamic centre of wing-body combinations
[ESDU-92024] p 3929 N92-32479

LIGANDS
Excited state processes in transition metal complexes: Redox splitting in soluble polymers
[DE92-011808] p 3971 N92-32631
Macrocyclic polycation complexes for secondary anion binding, molecular recognition, and catalysis
[AD-A251069] p 3972 N92-32913
Use of a Fourier deconvolution method in particle size determination and use of molecular mechanics in crystal structure determinations
[DE92-014510] p 4085 N92-33111

LIGHT (VISIBLE RADIATION)
Methods of opto-electronic fusion of infrared and visible images p 3936 N92-32444

LIGHT BEAMS
Determining surface profile from sequential interference patterns from a long trace profiler
[DE92-017117] p 4073 N92-32321
Optics of beam transport in the NSLS UV-FEL
[DE92-014166] p 4015 N92-32511

LIGHT EMITTING DIODES
Program for research in conducting polymers
[AD-A250965] p 3971 N92-32665
Director's discretionary fund report for FY 1991
[NASA-TM-103902] p 4105 N92-33106

LIGHT HELICOPTERS
The weight optimization of an armored crashworthy crewseat through the use of advanced composites and design p 3947 N92-32517

LIGHT IONS
Light-ion spectroscopy with exotic targets
[DE92-017258] p 3964 N92-32929

LIGHT MODULATION
Optical modulation characteristics and applications of liquid crystal televisions
[AD-A252466] p 3979 N92-32633
Depolarized light source for fiber optic sensors
[AD-D015289] p 4074 N92-32634
Real-time edge-enhanced optical correlator
[NASA-CASE-NPO-18379-1-CU] p 4076 N92-33022

LIGHT SCATTERING
On the interpretation of Titan's intensity and polarization phase curve p 4102 N92-32407
Can the speed of light in the fiber be controlled?
[AD-A247614] p 4074 N92-32668
Real time pre-detection dynamic range compression
[NASA-CASE-NPO-18098-1-CU] p 4076 N92-33028
Quantum wave modeling on highly parallel distributed memory machines
[DE92-014507] p 4088 N92-33109

LIGHT SOURCES
Depolarized light source for fiber optic sensors
[AD-D015289] p 4074 N92-32634

LIGHT SPEED
Can the speed of light in the fiber be controlled?
[AD-A247614] p 4074 N92-32668

LIGHT TRANSMISSION
Study of transmitted light through the atmosphere of Titan p 4102 N92-32408
The dependence of the anisoplanatic Strehl of a compensated beam on the beacon distribution
[DE92-011272] p 4016 N92-32736
The effect of the light round-trip time on the performance of an adaptive optics turbulence compensation system
[DE92-011273] p 4075 N92-32738

LIGHTING EQUIPMENT
Device for removing foreign objects from anatomic organs
[NASA-CASE-GSC-13306-1] p 4038 N92-33032

LIGHTNING
The significance of meteoric ionisation for the propagation of lightning spherics in the atmosphere of Titan p 4096 N92-32365
The 1991 rocket-triggered lightning test of the DoD Security Operations Test Site (SOTS) munitions storage bunker, Fort McClellan, Alabama
[DE92-012449] p 4032 N92-32427

LIGHTNING SUPPRESSION
The 1991 rocket-triggered lightning test of the DoD Security Operations Test Site (SOTS) munitions storage bunker, Fort McClellan, Alabama
[DE92-012449] p 4032 N92-32427

LIKELIHOOD RATIO
Bootstrapping the change-point of a hazard rate
[IMAG-RR-861-M] p 4056 N92-32685
Feature detection for model assessment in state estimation
[AD-A252755] p 4059 N92-32989

LIMITERS (FUSION REACTORS)
Edge gradient and safety factor effects on electrostatic turbulent transport in tokamaks
[DE92-014323] p 4079 N92-32944

LIMITS (MATHEMATICS)
A new form for the central limit theorem
[IMAG-RR-852-M] p 4060 N92-32716
Schroedinger operators with singular potentials in the semiclassical limit
[ETN-92-92145] p 4058 N92-32840
Limit theorems for functionals of convex hulls
[CWI-BS-R9115] p 4059 N92-33058

LINE SHAPE
The shapes and collective behavior of rapidly rotating nuclei
[DE92-017192] p 4067 N92-32928

LINE SPECTRA
HCP and HCN, molecules of planetary interest p 4100 N92-32395
Radiative lifetime measurements of the AA pi 1/2 state in CaH
[USIP-91-03] p 4067 N92-32764
A research program on radiative transfer model development in support of the ARM program
[DE92-014495] p 4031 N92-33153

LINEAR ACCELERATORS
High accuracy beam energy measurement for linear and circular accelerators
[DE92-016966] p 4069 N92-32319
Laser measurements for experiments on the TROLL accelerator
[DE92-016578] p 4015 N92-32335
Beamstrahlung spectra in next generation linear colliders
[DE92-010730] p 4069 N92-32337
Theory of elementary particles studies in weak interaction and grand unification and studies in accelerator design
[DE92-014320] p 4066 N92-32597
A high-power SLED 2 pulse compression system
[DE92-011586] p 4071 N92-32751
Study of recirculating induction accelerators as drivers for heavy ion fusion
[DE92-016980] p 4071 N92-32904
Accelerator physics of the Stanford Linear Collider and SLC accelerator experiments towards the next linear collider
[DE92-017552] p 4072 N92-33070
Development of advanced modulators for recirculating heavy ion accelerators
[DE92-014795] p 4072 N92-33122

LINEAR EQUATIONS
Aspects of solving non-linear boundary value problems numerically
[ETN-92-92049] p 4058 N92-32798
LINEAR SYSTEMS
Frequency domain state-space system identification
[NASA-TM-107659] p 4021 N92-32657
LINEARIZATION
A continuous nonlinear model approach to study the behavior of large signal DC to DC converters
[LAAS-90027] p 3990 N92-32793
LINKAGES
Reducing torque fluctuation in linkage drive shafts
[ESDU-92016] p 4017 N92-32482
LIPSCHITZ CONDITION
Aspects of solving non-linear boundary value problems numerically
[ETN-92-92049] p 4058 N92-32798
LIQUEFIED GASES
Experimental determination of the refractive index of liquefied gas mixtures: Applications to hypothesized Titan oceans p 4099 N92-32390
Laboratory determination of the refractive indices of liquid methane and ethane at temperatures appropriate to the surface of Titan p 4100 N92-32391
Laboratory determination of the thermal conductivity of liquid methane and ethane p 4015 N92-32392
LIQUID ALLOYS
Generic consequences of fundamental studies of beta phase decomposition modes in titanium and related alloy systems
[AD-A250789] p 3967 N92-32699
LIQUID CRYSTALS
Optical modulation characteristics and applications of liquid crystal televisions
[AD-A252466] p 3979 N92-32633
New thiophene-based materials
[AD-A250977] p 3972 N92-32667
Generic consequences of fundamental studies of beta phase decomposition modes in titanium and related alloy systems
[AD-A250789] p 3967 N92-32699
Real-time edge-enhanced optical correlator
[NASA-CASE-NPO-18379-1-CU] p 4076 N92-33022
LIQUID FILLED SHELLS
Free motion of an unsupported tank that is partially filled with liquid
[NLR-TP-91185-U] p 4011 N92-32831
LIQUID FLOW
Phase distribution measurements in narrow rectangular channels using image-processing techniques
[DE92-014084] p 4006 N92-32468
Experimental investigation of the axial impregnation of oriented fiber bundles by capillary forces
[AD-A250758] p 3961 N92-32508
Study of flow properties of wet solids using laser induced photochemical anemometry
[DE92-014031] p 4017 N92-33180
LIQUID FUELS
Second interim report of the Interagency Commission on Alternative Motor Fuels
[DE92-013169] p 3974 N92-32483
Direct conversion of light hydrocarbon gases to liquid fuel
[DE92-015592] p 3975 N92-33141
LIQUID HELIUM
Thermal conductance of augmented pressed metallic contacts at liquid helium temperatures
[NASA-TM-103917] p 4007 N92-32474
LIQUID METALS
A numerical study of natural convection in a narrow annulus
[DE92-017138] p 4006 N92-32322
LIQUID OXYGEN
CFD modeling of turbulent flows around the SSME main injector assembly using porosity formulation p 3997 N92-32260
LIQUID PHASES
Bone as a liquid-filled diphase porous medium p 4037 N92-32663
LIQUID PROPELLANT ROCKET ENGINES
Tenth Workshop for Computational Fluid Dynamic Applications in Rocket Propulsion, part 2
[NASA-CP-3163-PT-2] p 3994 N92-32245
Heat transfer in rocket engine combustion chambers and nozzles p 3995 N92-32253
A numerical model for atomization-spray coupling in liquid rocket thrust chambers p 3996 N92-32257
Experimental studies of characteristic combustion-driven flows for CFD validation p 3998 N92-32264
Tenth Workshop for Computational Fluid Dynamic Applications in Rocket Propulsion, part 1
[NASA-CP-3163-PT-1] p 4000 N92-32278
Combustion instability analysis for liquid propellant rocket engines p 3966 N92-32297
Numerical analysis of the hot-gas-side and coolant-side heat transfer in liquid rocket engine combustors p 4004 N92-32299
Integrated launch and emergency vehicle system
[NASA-CASE-LAR-13780-1] p 3943 N92-33013
LIQUID ROCKET PROPELLANTS
Development of a CFD code for internal flows in liquid fueled engines p 3999 N92-32271
LIQUID SLOSHING
Free motion of an unsupported tank that is partially filled with liquid
[NLR-TP-91185-U] p 4011 N92-32831
Investigations preparatory to the Wet Satellite Model Experiment
[NLR-TP-91219-U] p 3943 N92-32834
LIQUID SURFACES
Surface reconstruction and templating for zeolite thin film synthesis observed by atomic force microscopy
[AD-A251140] p 4066 N92-32548
Generic consequences of fundamental studies of beta phase decomposition modes in titanium and related alloy systems
[AD-A250789] p 3967 N92-32699
LIQUID-VAPOR INTERFACES
Direct numerical simulation of a combusting droplet with convection p 3996 N92-32256
Generic consequences of fundamental studies of beta phase decomposition modes in titanium and related alloy systems
[AD-A250789] p 3967 N92-32699
LIQUIDS
Orthobaric densities and molar volumes of liquids: Halogenated ethanes
[ESDU-92009] p 3945 N92-32486
LISP (PROGRAMMING LANGUAGE)
Analysis of a benchmark suite to evaluate mixed numeric and symbolic processing
[NASA-TM-103907] p 4052 N92-32886
LITHIUM ALLOYS
New accelerated corrosion test methods
[MBB-Z-0406-91-PUB] p 3968 N92-32895
LITHIUM SULFUR BATTERIES
Lithium sulphur dioxide battery failure following high frequency vibration
[CRAD-1-90] p 3990 N92-32812
LOAD DISTRIBUTION (FORCES)
Design, analysis, and testing of a reusable wingbox for ballistic evaluation of composite structures p 3947 N92-32518
Implanted aluminum: Tribological behavior and mechanical properties of the superficial layers
[ECL-91-28] p 4019 N92-32801
LOAD TESTS
Postbuckling behavior of curved panels under combined compression and shear loads p 3952 N92-32584
Postbuckling of stiffened composite plates under combined loading p 3952 N92-32585
Buckling and postbuckling behavior of square compression-loaded graphite-epoxy plates with circular cutouts p 3952 N92-32587
Automated data acquisition and analysis in the mechanical test lab
[DE92-011231] p 4040 N92-32910
LOADS (FORCES)
Energy take-out from a wave energy device. A theoretical study of the hydrodynamics of a two-body problem consisting of a buoy and a submerged plate
[PB92-178821] p 4025 N92-32608
Mixed model fatigue crack growth behavior in a high strength steel
[AD-A250667] p 4022 N92-32717
LOCAL AREA NETWORKS
A scalable, switched circuit LAN for Gb/S channels with over Tb/S total capacity
[DE92-013444] p 4050 N92-32412
Wavelength division multiplexed local area networks
[AD-A247613] p 3979 N92-32573
STARNET: A MultiGbit/s optical local area network with both packet and circuit switching
[AD-A247617] p 4050 N92-32628
Semiannual status report
[NASA-CR-190239] p 4046 N92-33092
LOCOMOTION
A hybrid numerical/knowledge based system for locomotion control of a multi-legged articulated robot
[ISBN-0-315-52925-3] p 4054 N92-33203
LOGIC CIRCUITS
Auto and hetero-associative memory using a 2-D optical logic gate
[NASA-CASE-NPO-17997-1-CU] p 4041 N92-33057
LOGIC DESIGN
Safety study of TCAS 2 for logic version 6.04
[DOT/FAA/RD-92/22] p 3933 N92-32537
LOGIC PROGRAMMING
CSP: A distributed logic programming language for discrete event simulation
[ISBN-0-315-54272-1] p 4048 N92-33214
Optimization of logic queries in knowledge base systems
[ISBN-0-315-51346-2] p 4049 N92-33227
LONG DURATION EXPOSURE FACILITY
Analysis of LDEF experiment AO187-2: Chemically and isotopic measurements of micrometeoroids by secondary ion mass spectrometry
[NASA-CR-190697] p 4093 N92-32541
LONG WAVE RADIATION
Climate System Monitoring (CSM) Monthly Bulletin, issue no. 1 p 4034 N92-33073
LORAN
A Kalman filter integrated navigation design for the IAR Twin Otter Atmospheric Research Aircraft
[NRC-32148] p 3934 N92-32849
LORENTZ FORCE
Geometrical effects in two-dimensional arrays of Josephson junctions
[AD-A252209] p 4084 N92-32898
LOSSY MEDIA
Microwave absorption by lossy ceramic materials
[DE92-016963] p 3970 N92-32317
LOUDSPEAKERS
A lightweight loudspeaker for aircraft communications and active noise control p 3988 N92-32964
LOW ALTITUDE
Advanced information processing system: The Army fault tolerant architecture conceptual study. Volume 1: Army fault tolerant architecture overview
[NASA-CR-189632-VOL-1] p 4052 N92-33100
LOW ASPECT RATIO
Formation and sustainment of a very low aspect ratio tokamak using coaxial helicity injection: Helicity Injected Torus (HIT) experiment
[DE92-014311] p 4078 N92-32595
LOW COST
Low cost MMC made by spray deposition
[MBB-Z-0407-91-PUB] p 3968 N92-32897
LOW FREQUENCIES
Low-frequency nuclear quadrupole resonance with a dc SQUID
[DE92-014506] p 4081 N92-32420
Feasibility of measuring transverse electric noise at VLF and LF on an ice cap
[AD-A252280] p 4035 N92-33220
LOW NOISE
Development of ultra-low noise, high sensitivity planar metal grating coupled AlGaAs/GaAs multiquantum well IR detectors for focal plane array staring IR sensor systems
[AD-A250368] p 4083 N92-32747
LOW REYNOLDS NUMBER
Numerical simulation of turbomachinery flows with advanced turbulence models p 3999 N92-32270
LOW SPEED
Effects of curvature and rotation on turbulence in the NASA low-speed centrifugal compressor impeller p 4003 N92-32292
LOW TEMPERATURE
Thermal conductance of augmented pressed metallic contacts at liquid helium temperatures
[NASA-TM-103917] p 4007 N92-32474
An analytical screening of alternatives for R-502 in low-temperature refrigerating applications
[DE92-017162] p 3978 N92-32927
Magnetic penetration depth of YBa2Cu3O(7-delta) thin films determined by the power transmission method p 3985 N92-32983
LOW TEMPERATURE TESTS
Superplastic forming of Ti6Al4V at lower temperature using hydrogen
[MBB-Z-0403-91-PUB] p 3978 N92-32893
Measurement techniques for cryogenic Ka-band microstrip antennas p 3985 N92-32981
LUBRICANT TESTS
Liquid lubricants for advanced aircraft engines
[NASA-TM-104531] p 3972 N92-32863
LUBRICANTS
Influence of oil lubricant additives on tribological behavior of engineering ceramics
[PB92-180710] p 3973 N92-33059
LUBRICATING OILS
Liquid lubricants for advanced aircraft engines
[NASA-TM-104531] p 3972 N92-32863
Influence of oil lubricant additives on tribological behavior of engineering ceramics
[PB92-180710] p 3973 N92-33059
LUBRICATION SYSTEMS
Liquid lubricants for advanced aircraft engines
[NASA-TM-104531] p 3972 N92-32863

LUMINOSITY
Absolute measurement of beam energy by Compton scattering
[DE92-016964] p 4069 N92-32318
High accuracy beam energy measurement for linear and circular accelerators
[DE92-016966] p 4069 N92-32319
Studies of helium based drift chamber gases for high-luminosity low energy machines
[DE92-012415] p 4065 N92-32426
Accelerator physics of the Stanford Linear Collider and SLC accelerator experiments towards the next linear collider
[DE92-017552] p 4072 N92-33070
LUMINOUS INTENSITY
Uses of stereovision surface models
[TELECOM-91-E-016] p 4075 N92-32806
LUNAR BASES
Toward the next millennium: A vision for spaceship Earth
[NASA-TM-107986] p 3941 N92-33007
LUNAR EXPLORATION
Director's discretionary fund report for FY 1991
[NASA-TM-103902] p 4105 N92-33106
LUNAR ROVING VEHICLES
Director's discretionary fund report for FY 1991
[NASA-TM-103902] p 4105 N92-33106

M

MACH NUMBER
Numerical simulation of turbulence at the back of the airplane
[ETN-92-91664] p 3931 N92-32769
MACHINE LEARNING
A learning enhanced flight control system for high performance aircraft
[AD-A252520] p 3938 N92-32435
Human learning of schemas from explanations in practical electronics
[AD-A247429] p 4038 N92-32569
A hybrid numerical/knowledge based system for locomotion control of a multi-legged articulated robot
[ISBN-0-315-52925-3] p 4054 N92-33203
Learning systems, adaptive data structures, and random environments
[ISBN-0-315-51158-3] p 4054 N92-33218
MAGNESIUM ALLOYS
Aluminum based particulate composites for aerospace applications produced by different processes
[MBB-Z-0408-91-PUB] p 3967 N92-32819
MAGNETIC CORES
Electromagnetic attachment mechanism
[NASA-CASE-MSC-21463-1] p 4019 N92-33018
MAGNETIC EFFECTS
Steady induction effects in geomagnetism. Part 1A: Steady motional induction of geomagnetic chaos
[NASA-TP-3272-PT-1A] p 4031 N92-32655
Magnetic flux relaxation in YBa2Cu3O(7-x) thin film: Thermal or athermal p 3985 N92-32984
MAGNETIC FIELD CONFIGURATIONS
The role of stochasticity in sawtooth oscillation
[DE92-782004] p 3982 N92-32905
MAGNETIC FIELD RECONNECTION
The role of stochasticity in sawtooth oscillation
[DE92-782004] p 3982 N92-32905
MAGNETIC FIELDS
Measurement of the magnetic and electrical activity of individual cells in vitro
[AD-A250881] p 4035 N92-32345
Plasma diffusion through multidipole magnetic fields
[INPE-5384-PRE/1750] p 4079 N92-32662
Polarized wiggler for NSLS x ray ring design considerations
[DE92-012212] p 4071 N92-32912
Scanning force microscopy using optical interferometry
[ISBN-90-9003887-6] p 4077 N92-33146
Electric and magnetic properties of random superconductors
[ITN-92-85165] p 4086 N92-33190
MAGNETIC FLUX
Steady induction effects in geomagnetism. Part 1A: Steady motional induction of geomagnetic chaos
[NASA-TP-3272-PT-1A] p 4031 N92-32655
Magnetic flux relaxation in YBa2Cu3O(7-x) thin film: Thermal or athermal p 3985 N92-32984
MAGNETIC INDUCTION
Steady induction effects in geomagnetism. Part 1A: Steady motional induction of geomagnetic chaos
[NASA-TP-3272-PT-1A] p 4031 N92-32655
MAGNETIC LEVITATION VEHICLES
Publications on maglev technologies
[DE92-013296] p 4017 N92-32615
MAGNETIC MEASUREMENT
Measurement of the magnetic and electrical activity of individual cells in vitro
[AD-A250881] p 4035 N92-32345
Synthesis, microstructure, critical current density, magnetization and relaxation of hot-pressed YBa2Cu3O(6 + delta) through partial melting post-oxygenation
[DE92-015205] p 4085 N92-33026
MAGNETIC PROPERTIES
Preparation and characterization of superlattices
[DE92-012572] p 4081 N92-32462
MAGNETIC SPECTROSCOPY
Design and construction of a magnetic sector mass spectrometer
[INPE-5405-RPQ/659] p 4014 N92-32601
MAGNETIZATION
Synthesis, microstructure, critical current density, magnetization and relaxation of hot-pressed YBa2Cu3O(6 + delta) through partial melting post-oxygenation
[DE92-015205] p 4085 N92-33026
MAGNETOHYDRODYNAMIC FLOW
Mass loading at Titan and comets p 4098 N92-32383
Titan's magnetospheric interaction p 4099 N92-32385
Polar upper atmosphere characterization and supersonic ion escape (polar wind)
[GDR-0917] p 4031 N92-32889
MAGNETOHYDRODYNAMIC GENERATORS
MHD Integrated Topping Cycle Project
[DE92-013904] p 4080 N92-33024
MAGNETOHYDRODYNAMIC STABILITY
Magnetohydrodynamic stability of plasmas with radial motion
[DE92-013917] p 4077 N92-32417
MHD computation of feedback of resistive-shell instabilities in the reversed field pinch
[DE92-014325] p 4078 N92-32599
Ion heating and MHD dynamo fluctuations in the reversed field pinch
[DE92-013902] p 4078 N92-32624
Measurement of nonlinear mode coupling of tearing fluctuations
[DE92-013901] p 4080 N92-33154
MAGNETOHYDRODYNAMICS
Plasma interaction of Titan with the Saturnian magnetosphere: A review of critical issues p 4098 N92-32382
MHD computation of feedback of resistive-shell instabilities in the reversed field pinch
[DE92-014325] p 4078 N92-32599
Ion heating and MHD dynamo fluctuations in the reversed field pinch
[DE92-013902] p 4078 N92-32624
Chemical Technology Division
[DE92-014059] p 3964 N92-32931
MHD Integrated Topping Cycle Project
[DE92-013904] p 4080 N92-33024
MAGNETOMETERS
NASA Marshall Space Flight Center Solar Observatory report, January - June 1992
[NASA-TM-103597] p 4092 N92-32478
MAGNETORESISTIVITY
Intermodulation in the oscillatory magnetoresistance of a two-dimensional electron gas p 3984 N92-32975
MAINTENANCE
Reliability training
[NASA-RP-1253] p 3941 N92-32456
Heating fixture and instrumentation design for elevated temperature tests of a composite repair technique
[WL-TM-90-326-FIBE] p 3946 N92-32459
Processing and environmental effects on mechanical properties of composite repairs
[NRC-LTR-ST-1826] p 3954 N92-32791
Device and process for attachment of parts to rocket motors
[AD-D015309] p 3944 N92-33162
MAMMALS
Midwest free-electron laser program
[AD-A247264] p 4016 N92-32540
MAN MACHINE SYSTEMS
Selecting a subset of stimulus-response pairs with maximal transmitted information
[AD-A252728] p 3986 N92-32987
Humans and machines in space: The payoff
[ISBN-0-87703-343-9] p 4039 N92-33099
MAN-COMPUTER INTERFACE
Advanced software development workstation: Effectiveness of constraint-checking --- spaceflight simulation and planning
[NASA-CR-190712] p 4043 N92-32865
MANAGEMENT INFORMATION SYSTEMS
Automatic access experiment
[AD-A252217] p 4089 N92-32611
Hypertext and hypermedia
[VTT-RN-1154] p 4090 N92-32843
The development of an airborne information management system for flight test
[NASA-TM-104251] p 3938 N92-32866
MANAGEMENT PLANNING
Information resources management plan of the Federal Government
[PB92-147198] p 4089 N92-32643
DoD key technologies plan
[AD-A253692] p 4105 N92-33238
MANAGEMENT SYSTEMS
Permuted keyword bank in CRIS. Terms for indexing and retrieving research projects in the current research information system
[PB92-179456] p 4090 N92-32712
Fault tolerance for security management in distributed systems
[LAAS-92011] p 4040 N92-32766
MANEUVERABILITY
Rapid development of the X-31 simulation to support flight-testing
[NASA-TM-104256] p 3935 N92-33149
MANIPULATORS
Using minimax approaches to plan optimal task commutation configurations for combined mobile platform-manipulator systems
[DE91-018864] p 4018 N92-32694
Jacobian and stiffness analysis of a novel class of six-DOF parallel minimanipulators
[DE92-016373] p 4054 N92-33184
Investigations of adaptive control for a direct drive robotic manipulator
[ISBN-0-315-59030-0] p 4055 N92-33236
MANNED MARS MISSIONS
Toward the next millennium: A vision for spaceship Earth
[NASA-TM-107986] p 3941 N92-33007
MANUAL CONTROL
Flight testing and simulation of an F-15 airplane using throttles for flight control
[NASA-TM-104255] p 3940 N92-32864
MANUALS
IDEF4 object-oriented design method manual
[AD-A252634] p 4042 N92-32658
MANUFACTURING
National Research Council Industrial Materials Institute: From knowledge to know-how
[CTN-92-60333] p 4103 N92-32814
National Research Council Industrial Materials Institute: From knowledge to know-how
[CTN-92-60334] p 4104 N92-32815
Aluminum based particulate composites for aerospace applications produced by different processes
[MBB-Z-0408-91-PUB] p 3967 N92-32819
Low cost MMC made by spray deposition
[MBB-Z-0407-91-PUB] p 3968 N92-32897
MANY BODY PROBLEM
Implementation of a tree-code for numerical simulations of stellar systems
[INPE-5370-TDI/469] p 4093 N92-32604
Research in theoretical nuclear physics
[DE92-016316] p 4068 N92-33067
MARINE BIOLOGY
Simulations of the carbon cycle in the oceans
[DE92-016622] p 4035 N92-32336
Bacterial responses to extreme temperatures and pressures and to heavy organic loading
[AD-A247456] p 4035 N92-32571
MARINE ENVIRONMENTS
Federal plan for ocean pollution research, development, and monitoring, fiscal years 1992-1996
[PB92-185164] p 4029 N92-32708
MARKET RESEARCH
Second interim report of the Interagency Commission on Alternative Motor Fuels
[DE92-013169] p 3974 N92-32483
MARKOV CHAINS
Adaptive information processing and global optimization
[AD-A248450] p 4089 N92-32644
MARKOV PROCESSES
Implementation of a tree-code for numerical simulations of stellar systems
[INPE-5370-TDI/469] p 4093 N92-32604
Frequency domain state-space system identification
[NASA-TM-107659] p 4021 N92-32657
Continuous and discrete problems in image processing
[TELECOM-91-D-007] p 4058 N92-32802
Three dimensional object reconstruction using a very limited number of projections. Application to industrial radiography
[TELECOM-91-E-008] p 4043 N92-32804
Enhancements to speech recognition on voice response systems
[TELECOM-91-E-018] p 3981 N92-32807

Limit theorems for functionals of convex hulls
[CWI-BS-R9115] p 4059 N92-33058

MARTINGALES
Limit theorems for functionals of convex hulls
[CWI-BS-R9115] p 4059 N92-33058

MASS FLOW
An experimental study of the fluid mechanics associated with porous walls
[AIAA PAPER 92-0769] p 3998 N92-32263
Solid fuel flame spread and mass burning in turbulent flow
[PB92-181049] p 3963 N92-32607

MASS SPECTRA
Observation of (pi)(-)p yields (omega)(eta)n reaction at 38 GeV/c momentum
[DE92-624690] p 4064 N92-32310

MASS SPECTROMETERS
Huygens/ACP: An instrument for aerosols chemical composition measurements p 4098 N92-32379
Design and construction of a magnetic sector mass spectrometer
[INPE-5405-RPQ/659] p 4014 N92-32601
RF-GD/FTMS: An FTMS system with a lensless external ion source for high resolution elemental mass spectrometry
[DE92-015343] p 3964 N92-32925
Molecular surface analysis by laser ionization of desorbed molecules
[DE92-016320] p 4016 N92-33114

MASS SPECTROSCOPY
Photogenerated carrier-induced reactions on UHV semiconductor surfaces
[DE92-015355] p 4082 N92-32641
RF-GD/FTMS: An FTMS system with a lensless external ion source for high resolution elemental mass spectrometry
[DE92-015343] p 3964 N92-32925
The LLNL Multi-User Tandem Laboratory PIXE microprobe
[DE92-017252] p 4014 N92-32999
Mass resolved resonance ionization spectroscopy of combustion radicals
[DE92-016833] p 3965 N92-33222

MASS TRANSFER
Heat and mass exchange during condensation of a water-ammonia mixture
[DE92-014524] p 3962 N92-32557
Thinning and rupture of a thin liquid film on a heated surface
[DE92-014813] p 4013 N92-33124

MATCHED FILTERS
Recursive estimation techniques for detection of small objects in infrared image data
[AD-A250942] p 4075 N92-32935

MATERIALS TESTS
Study of eddy current probes
[NASA-CR-190814] p 4020 N92-32425
The 1991 rocket-triggered lightning test of the DoD Security Operations Test Site (SOTS) munitions storage bunker, Fort McClellan, Alabama
[DE92-012449] p 4032 N92-32427
Transmission electron microscope characterization of deformation and recovery in 304L stainless steel part
[DE92-013237] p 3966 N92-32614
An overview of concerns relating to fluid effects on composites p 3958 N92-33045
Effects of fuel on Hercules AS-4/8552 composite material p 3958 N92-33046
Environmental degradation of high temperature composites p 3958 N92-33047
Evaluation of the effects of the environment on the behavior of the primary structures of composite material aircraft in service: Historic and current situation p 3958 N92-33048
Fluid effects: Thermoset and thermoplastic matrix composites p 3958 N92-33049
Jet fuel absorption and dynamic mechanical analysis of carbon fibre composites p 3959 N92-33050
The effect of heat treatment on the properties of PEEK and APC-2 p 3959 N92-33052
Environmental resistance of amorphous bonded thermoplastic joints p 3959 N92-33053
Flight service environmental effects on composite materials and structures p 3959 N92-33054
Publications by Structures and Materials Laboratory on composite materials (January 1983 - June 1991)
[NRC-LTR-ST-1833] p 3959 N92-33078

MATHEMATICAL MODELS
A numerical model for atomization-spray coupling in liquid rocket thrust chambers p 3996 N92-32257
Numerical modeling for dilute and dense sprays p 3997 N92-32258
Modeling of SSME fuel preburner ASI p 3945 N92-32259
NLS clutching bearing cavity flow analysis p 4003 N92-32295
Combustion instability analysis for liquid propellant rocket engines p 3966 N92-32297
An efficient and robust grid optimization algorithm p 4004 N92-32300
Determining surface profile from sequential interference patterns from a long trace profiler
[DE92-017117] p 4073 N92-32321
A numerical study of natural convection in a narrow annulus
[DE92-017138] p 4006 N92-32322
An implementation of Hill's theory of normal anisotropic plasticity for explicit shell analysis
[DE92-011468] p 4020 N92-32328
Impact origin of Titan's atmosphere p 4094 N92-32351
An adaptive algorithm for modifying hyperellipsoidal decision surfaces
[DE92-013540] p 4041 N92-32414
Magnetohydrodynamic stability of plasmas with radial motion
[DE92-013917] p 4077 N92-32417
Fault-tolerant wait-free shared objects
[NASA-CR-190679] p 4020 N92-32436
Analytic score comparison of geometry splitting and exponential transform for a simple Monte Carlo problem
[DE92-013108] p 4059 N92-32481
Calculation of the energy of elastic deformation of Kevlar backing plates for ceramic armours
[AD-A250129] p 3970 N92-32489
Tutorial on neural network applications in high energy physics: A 1992 perspective
[DE92-016003] p 4070 N92-32506
Eighth DOD/NASA/FAA Conference on Fibrous Composites in Structural Design, part 1
[NASA-CP-3087-PT-1] p 3946 N92-32513
Shock tube ignition of ethanol, isobutene and MTBE: Experiments and modeling
[DE92-008563] p 3961 N92-32544
Two studies of nonlinear processes in irreversible thermodynamics
[DE92-016855] p 4087 N92-32566
Wave propagation in laterally varying media: A model expansion method
[AD-A247553] p 4031 N92-32572
A basic research model of natural gas combustion in turbulent flow, phase 2
[PB92-190362] p 4007 N92-32598
Exploitation of parallelism in climate models
[DE92-012595] p 4028 N92-32619
Stress-relief displacements induced by drilling: Applications to holographic measurements of in situ stress
[DE92-013711] p 4014 N92-32620
Ion heating and MHD dynamo fluctuations in the reversed field pinch
[DE92-013902] p 4078 N92-32624
Adaptive information processing and global optimization
[AD-A248450] p 4089 N92-32644
Molecular dynamics modeling of the mechanical properties of metal surfaces at the nanometer scale
[DE92-010705] p 3966 N92-32646
Modeling and numerical simulation of vortex flow in aerodynamics
[NLR-TP-91154-U] p 3930 N92-32673
Thermal gravitational modelling and scaling of two-phase heat transport systems for space: An assessment and a comparison of predictions and experimental results
[NLR-TP-91401-U] p 4008 N92-32675
Bandwidth selection for the intensity of point processes: Application to hazard rate models for censored data
[IMAG-RR-859-I/M] p 4056 N92-32684
Bootstrapping the change-point of a hazard rate
[IMAG-RR-861-M] p 4056 N92-32685
Free vibration of thick isotropic and orthotropic cylindrical shells
[DE92-011653] p 4022 N92-32706
Statistical selection: Multiple comparison approach
[ETN-92-92051] p 4060 N92-32709
Mixed model fatigue crack growth behavior in a high strength steel
[AD-A250667] p 4022 N92-32717
Electromagnetic-wave propagation in unmagnetized plasmas
[AD-A250710] p 3980 N92-32719
Model of Reynolds stress on nonorthogonal grid structures: Application to a staggered tube bundle
[ETN-92-91959] p 4009 N92-32725
Improved dissipation models for central difference schemes
[FFA-TN-1991-41] p 4057 N92-32729
The dependence of the anisoplanatic Strehl of a compensated beam on the beacon distribution
[DE92-011272] p 4016 N92-32736
Dynamic systems stability with dry friction: Application to brake disc squealing
[ECL-91-48] p 4018 N92-32737
Fast ion loss and radial electric field in Wendelstein 7-A stellarator
[DE92-782106] p 4079 N92-32745
Parameterization of directional spectra, part 2. Volume 2: User's manual for the programs RMODEL, FITHM, and FITDM
[DREA-CR-89-445-PT-2-VOL-2] p 3981 N92-32749
Supersymmetry searches at electron-proton colliders
[ETN-92-92057] p 4067 N92-32753
Numerical simulation of two-dimensional flows by the free-Lagrangian method
[TUM-M9105] p 4009 N92-32767
Two-phase heat transport systems for space: Thermal gravitational modelling and scaling predictions versus results of experiments
[NLR-TP-91051-U] p 4010 N92-32786
Hierarchical sets in mathematical programming modeling languages
[MEMO-990] p 4057 N92-32796
Study of the mechanical behaviour of graphite/epoxy laminates subjected to static and cyclic loading
[NRC-30833] p 3955 N92-32813
Diagnostics and modeling of ECRH microwave discharges
[IPF-91-3] p 4079 N92-32822
CFD efforts in the Netherlands
[NLR-TP-91250-U] p 4011 N92-32835
A three-field model of transient 3D multiphase, three-component flow for the computer code 4 A3. Part1: Theoretical basis: Conservation and state equations, numerics
[KFK-4948-PT-1] p 4011 N92-32857
A three-field model of transient 3D multiphase, three-component flow for the computer code 4 A3. Part 2: Models for the interfacial transport phenomena. Code validation
[KFK-4949-PT-2] p 4011 N92-32858
Better predictions even in reduced input variable numbers using neural networks in software development p 4044 N92-32874
Optimized set reduction for empirically guiding software development p 4044 N92-32875
Modeling the ear's response to intense impulses and the development of improved damage risk criteria
[AD-A252365] p 4037 N92-32916
A reexamination of the plastic flow criterion for copper
[AD-A252370] p 4023 N92-32918
Vibro-acoustic FE analyses of the Saab 2000 aircraft p 4062 N92-32952
Active control of sound transmission through stiff lightweight composite fuselage constructions p 4062 N92-32957
Extending estimation of C-J pressure of explosives to the very low density region
[DE92-015035] p 3975 N92-33003
A review of RAE sponsored work on the compressive behaviour of composite materials p 3957 N92-33038
Damage progression under compressive loading in composite laminates containing an open hole p 3957 N92-33040
GARTEUR compression behaviour of advanced CFRP --- carbon fiber reinforced plastics p 3957 N92-33042
An intelligent gaming environment
[ISBN-90-6275-635-2] p 4060 N92-33055
On the origin and acoustical behaviour of cloud cavitation
[ISBN-90-9004317-9] p 4012 N92-33066
A transgranular fatigue crack growth model based on restricted slip reversibility
[NRC-LTR-ST-1831] p 4023 N92-33076
Mixed H(2)/H(sub infinity): Control with output feedback compensators using parameter optimization
[NASA-CR-190070] p 4046 N92-33091
Object links in the repository
[NASA-CR-190644] p 4091 N92-33096
Ideal efficiency of propellers based on Theodorsen's theory: A review and computer study, with extended plus simplified charts
[UTIAS-TN-271] p 3938 N92-33102
Neutrino masses in the flipped SU(5) tensor product U(1) and the SU(4) tensor product O(4) GUT models
[RAL-92-012] p 4068 N92-33135
Jacobian and stiffness analysis of a novel class of six-DOF parallel minimanipulators
[DE92-016373] p 4054 N92-33184

MATHEMATICAL PROGRAMMING
Hierarchical sets in mathematical programming modeling languages
[MEMO-990] p 4057 N92-32796
Life cycle oriented method for development and production of large scale industrial mathematics software
[NLR-TP-91196-U] p 4043 N92-32833

Selecting a subset of stimulus-response pairs with maximal transmitted information
[AD-A252728] p 3986 N92-32987

MATRICES (MATHEMATICS)
A tight and explicit representation of Q in sparse QR factorization
[DE92-014814] p 4055 N92-32428
Experiments with an ordinary differential equation solver in the parallel solution of method of lines problems on a shared memory parallel computer, part 2
[DE92-017159] p 4052 N92-32926
Sweeping algorithms for five-point stencils and banded matrices
[DE92-017309] p 4047 N92-33118
Computations for algebras and group representations
[ISBN-0-315-54684-0] p 4059 N92-33231

MATRIX MATERIALS
A curved beam test specimen for determining the interlaminar tensile strength of a laminated composite p 3949 N92-32526
A new approximate fracture mechanics analysis methodology for composites with a crack or hole p 3949 N92-32530
Polyimide molding powder, coating, adhesive, and matrix resin
[NASA-CASE-LAR-14163-1] p 3973 N92-33014
A review of recent developments in joining high-performance thermoplastic composites
[CNRC-33030] p 4019 N92-33077

MATTER (PHYSICS)
Research in nuclear astrophysics: Stellar collapse and supernovae
[DE92-014988] p 4093 N92-32993

MAXIMA
On the inconsistency of bootstrap distribution estimators
[IMAG-RR-856-M] p 4060 N92-32718

MAXIMUM LIKELIHOOD ESTIMATES
Bootstrapping the change-point of a hazard rate
[IMAG-RR-861-M] p 4056 N92-32685

MEAN SQUARE VALUES
Bandwidth selection for the intensity of point processes: Application to hazard rate models for censored data
[IMAG-RR-859-I/M] p 4056 N92-32684

MEASURING INSTRUMENTS
Determining surface profile from sequential interference patterns from a long trace profiler
[DE92-017117] p 4073 N92-32321
Symposium on Titan
[ESA-SP-338] p 4093 N92-32348
Huygens/ACP: An instrument for aerosols chemical composition measurements p 4098 N92-32379
Huygens/ASI plasma wave analyzer capabilities for aerosol measurement p 4098 N92-32380
Orbital debris characterization with impact flash signatures
[DE92-010666] p 4018 N92-32701
A description of the analytical methodology and reporting procedures used in the analysis and preparation of calibration reports for force measuring instruments
[NRC-LTR-ST-1817] p 4022 N92-32848
Probe molecule studies: Active species in alcohol synthesis
[DE92-016682] p 3966 N92-33246

MECHANICAL ENGINEERING
United States Air Force summer research program 1991. Volume 1: Program management report
[AD-A248763] p 4103 N92-32338

MECHANICAL PROPERTIES
Studies of near-surface phenomena and erosion mechanisms in metallic alloys using single- and multi-particle impacts
[DE92-014921] p 3966 N92-32432
Thermal degradation study of silicon carbide threads developed for advanced flexible thermal protection systems
[NASA-TM-103952] p 3970 N92-32476
Eighth DOD/NASA/FAA Conference on Fibrous Composites in Structural Design, part 1
[NASA-CP-3087-PT-1] p 3946 N92-32513
Molecular dynamics modeling of the mechanical properties of metal surfaces at the nanometer scale
[DE92-010705] p 3966 N92-32646
Synthesis, microstructure, and mechanical properties of zirconia-alumina composites
[ISBN-90-9004656-9] p 3954 N92-32677
Implanted aluminum: Tribological behavior and mechanical properties of the superficial layers
[ECL-91-28] p 4019 N92-32801
Investigation of fracture toughness and fracture mechanisms using acoustic emission measurements
[DE92-011907] p 4022 N92-32911
Effects of fuel on Hercules AS-4/8552 composite material p 3958 N92-33046
Fluid effects: Thermoset and thermoplastic matrix composites p 3958 N92-33049
Jet fuel absorption and dynamic mechanical analysis of carbon fibre composites p 3959 N92-33050
Environmental resistance of amorphous bonded thermoplastic joints p 3959 N92-33053
Synthesis of MoSi2-based alloys by mechanical alloying
[DE92-017528] p 3969 N92-33120
A combined AEM/APFIM characterization of Alloy X-750
[DE92-011049] p 3969 N92-33158

MECHANICAL SHOCK
Insensitive Munitions
[AGARD-CP-511] p 3975 N92-33240
The design features of rocket motors relating to insensitive munition response to thermo-mechanical stimuli p 3976 N92-33244

MELTING
Formation of high temperature superconductors from the solidified melt
[DE92-012584] p 4081 N92-32465
New thiophene-based materials
[AD-A250977] p 3972 N92-32667

MELTING POINTS
Thermal conductivity of liquid aliphatic hydrocarbons. Part 1: Alkanes
[ESDU-92011-PT-1] p 3945 N92-32484
Orthobaric densities and molar volumes of liquids: Halogenated ethanes
[ESDU-92009] p 3945 N92-32486

MEMBRANE STRUCTURES
NEDO Alcohol/Biomass Technology Subcommittee
[DE92-526270] p 3975 N92-32914
High temperature fiber optic microphone having a pressure-sensing reflective membrane under tensile stress
[NASA-CASE-LAR-14402-1-CU] p 4076 N92-33017

MEMBRANES
Testing of the single-element stretched-membrane dish
[DE92-013680] p 4025 N92-32549
Hydrogen permeation through bilayer metallic membranes
[UTIAS-TN-342] p 3967 N92-32794

MEMORY
A conceptual model of cognitive complexity of elements of the programming process p 4045 N92-32877

MEMORY (COMPUTERS)
Balance in machine architecture: Bandwidth on board and offboard, integer/control speed and flops versus memory
[DE92-016006] p 4040 N92-32642
Optimal communication schemes on an SIMD distributed-memory hypercube
[IMAG-RR-848-M] p 4051 N92-32715
Sparse matrix algorithms on distributed memory multiprocessors
[DE92-017870] p 4046 N92-33071
Quantum wave modeling on highly parallel distributed memory machines
[DE92-014507] p 4088 N92-33109

MENTAL HEALTH
A causal analysis of interrelationships among exercise, physical fitness, and well-being in US Navy personnel
[AD-A252719] p 4037 N92-32942

MENTAL PERFORMANCE
PET studies of components of high-level vision
[AD-A250873] p 4036 N92-32344
Cognitive biases and time stress in team decision making
[AD-A251153] p 4088 N92-32551

MERCURY CADMIUM TELLURIDES
A model for the trap-assisted tunneling mechanism in diffused n-p and implanted n(+)-p HgCdTe photodiodes p 3985 N92-32979

MERCURY ISOTOPES
Higher superdeformed band members in Hg-190: Evidence for a band interaction?
[DE92-016778] p 4082 N92-32542

MERCURY TELLURIDES
Thin film cadmium telluride, zinc telluride, and mercury zinc telluride solar cells
[DE92-001237] p 4024 N92-32510

MERGING ROUTINES
Analytic performance of software pipelines with rendezvous and communication tasks
[ISBN-0-315-54414-7] p 4052 N92-33216

MESONS
Theoretical and experimental studies of elementary physics
[DE92-014877] p 4061 N92-32430
Scalar mesons and kaons in phi radiative decay and their implications for studies of CP violation at DA(phi)NE
[RAL-91-085] p 4068 N92-33133

MESOSCALE PHENOMENA
Short range forecast of the initiation of convection
[DM-60] p 4033 N92-32758

MESSAGE PROCESSING
Message delay models of packet-switching networks
[ISBN-0-315-57208-6] p 4053 N92-33235

MESSAGES
Guaranteeing synchronous message deadlines with the timed token medium access control protocol
[NASA-CR-190710] p 4042 N92-32656

METAL BONDING
Macrocyclic polycation complexes for secondary anion binding, molecular recognition, and catalysis
[AD-A251069] p 3972 N92-32913

METAL FATIGUE
Environmental fatigue in aluminum-lithium alloys
[NASA-TM-107640] p 4021 N92-32423
Guide to the effect of shot peening on fatigue strength
[ESDU-92015] p 3967 N92-32779

METAL FILMS
AC microcalorimetry of adsorbates on evaporated metal films: Orientational ordering of H2 multilayers
[DE92-008317] p 3963 N92-32666

METAL HALIDES
Development of high-performance Na/NiCl2 cell
[DE92-015270] p 3988 N92-32639

METAL IONS
Macrocyclic polycation complexes for secondary anion binding, molecular recognition, and catalysis
[AD-A251069] p 3972 N92-32913

METAL MATRIX COMPOSITES
Computational simulation of matrix micro-slip bands in SiC/Ti-15 composite
[NASA-TM-105762] p 3946 N92-32466
Applications of composites to armaments p 3947 N92-32516
A new approximate fracture mechanics analysis methodology for composites with a crack or hole p 3949 N92-32530
A new approach to fibrous composite laminate strength prediction p 3952 N92-32588
Thermal strains in titanium aluminide and nickel aluminide composites
[DE92-015181] p 3953 N92-32638
Aluminum based particulate composites for aerospace applications produced by different processes
[MBB-Z-0408-91-PUB] p 3967 N92-32819
Low cost MMC made by spray deposition
[MBB-Z-0407-91-PUB] p 3968 N92-32897
Laser coating of composites for enhanced wear and corrosion resistance
[AD-A249231] p 3956 N92-32906

METAL OXIDES
Mechanisms of the oxidation of metals and alloys with emphasis on superconductors
[DE92-016840] p 3966 N92-32315
Processing and properties of silver-clad Tl-Ba-Ca-Cu-O wires and tapes
[DE92-015266] p 4081 N92-32346

METAL PARTICLES
Silver coated superconducting ceramic powder
[AD-D015294] p 3973 N92-33157

METAL PLATES
Buckling and postbuckling behavior of square compression-loaded graphite-epoxy plates with circular cutouts p 3952 N92-32587

METAL POWDER
Synthesis of MoSi2-based alloys by mechanical alloying
[DE92-017528] p 3969 N92-33120

METAL PROPELLANTS
A two-phase restricted equilibrium model for combustion of metalized solid propellants p 3966 N92-32307

METAL SHEETS
An implementation of Hill's theory of normal anisotropic plasticity for explicit shell analysis
[DE92-011468] p 4020 N92-32328

METAL SPRAYING
Low cost MMC made by spray deposition
[MBB-Z-0407-91-PUB] p 3968 N92-32897

METAL SURFACES
Design and construction of a sample preparation chamber for atomic beam scattering
[DE92-014509] p 4065 N92-32473
Thermal conductance of augmented pressed metallic contacts at liquid helium temperatures
[NASA-TM-103917] p 4007 N92-32474
Electrocatalyst surfaces
[PB92-190420] p 3962 N92-32591
Molecular dynamics modeling of the mechanical properties of metal surfaces at the nanometer scale
[DE92-010705] p 3966 N92-32646

METAL WORKING
An implementation of Hill's theory of normal anisotropic plasticity for explicit shell analysis
[DE92-011468] p 4020 N92-32328

JPRS report: Science and technology. Central Eurasia: Materials science
[JPRS-UMS-92-011] p 3969 N92-33129

METALS
Mechanisms of the oxidation of metals and alloys with emphasis on superconductors
[DE92-016840] p 3966 N92-32315

METEORITE CRATERS
Organic chemistry on Titan: Surface interactions
p 4096 N92-32370

METEOROID HAZARDS
A simple approach for the design and optimization of stand-off hypervelocity particle shields
[DE92-011383] p 3943 N92-32704

METEOROLOGICAL CHARTS
Diagnostic report of the National Hurricane Center, August and September 1991, volume 4, number 2
[PB92-179407] p 4033 N92-32503

METEOROLOGICAL PARAMETERS
Verification of severe local storms forecasts issued by the National Severe Storms Forecast Center, 1991
[PB92-186063] p 4033 N92-32502
STAMP, the SWOE Thermal Analysis and Measurement Program: Summary of the 1990 field tests
[LTR-91-013] p 4029 N92-32860
Forecasting heavy snow events in Missoula, Montana
[PB92-196104] p 4034 N92-33163

METEOROLOGICAL RADAR
Airport Surveillance Radar (ASR-9) wind shear processor: 1991 test at Orlando, Florida
[AD-A252246] p 3980 N92-32686

METEOROLOGY
Titan in a box p 4101 N92-32404
US Historical Climatology Network daily temperature and precipitation data
[DE92-014920] p 4032 N92-32431
Boundary layer processes in coastal meteorology: Prospects for remote sensing applications
[PB92-177849] p 4033 N92-32714
Recent changes of weather patterns in North America
[DE92-014342] p 4033 N92-32720

METHANE
Methane conversion to methanol
[DE92-014349] p 3960 N92-32332
Methane oxidation over dual redox catalysts
[DE92-014358] p 3960 N92-32334
Laboratory determination of the refractive indices of liquid methane and ethane at temperatures appropriate to the surface of Titan p 4100 N92-32391
Laboratory determination of the thermal conductivity of liquid methane and ethane p 4015 N92-32392
Waves on Titan p 4100 N92-32394
The spectrum of Titan in the 1.06 and 1.28 micron windows p 4101 N92-32401
US EPA's global climate change program: Landfill emissions and mitigation research
[PB92-180215] p 4028 N92-32609
CARS diagnostics for solid propellant combustion investigations
[AD-A248660] p 3963 N92-32645
NEDO Alcohol/Biomass Technology Subcommittee
[DE92-526270] p 3975 N92-32914
Computational and experimental study of laminar flames
[DE92-017978] p 3965 N92-33121

METHODOLOGY
Methodological and architectural issues in the experience factory p 4044 N92-32870
Better predictions even in reduced input variable numbers using neural networks in software development p 4044 N92-32874

METHYL ALCOHOL
Methane conversion to methanol
[DE92-014349] p 3960 N92-32332
NEDO Alcohol/Biomass Technology Subcommittee
[DE92-526270] p 3975 N92-32914

METHYL COMPOUNDS
Shock tube ignition of ethanol, isobutene and MTBE: Experiments and modeling
[DE92-008563] p 3961 N92-32544
Orientation, stress, and density distributions in injection-moulded amorphous polymers determined by optical techniques
[ETN-92-92052] p 3972 N92-32752
Methyl substituted polyimides containing carbonyl and ether connecting groups
[NASA-CASE-LAR-14351-1] p 3973 N92-33015

METRIC SPACE
Dissimilarities, dendograms, prefillers, and multiapplications of levels
[IMAG-RR-842-M] p 4058 N92-32799

MICROANALYSIS
Studies of near-surface phenomena and erosion mechanisms in metallic alloys using single- and multi-particle impacts
[DE92-014921] p 3966 N92-32432
The LLNL Multi-User Tandem Laboratory PIXE microprobe
[DE92-017252] p 4014 N92-32999

MICROBIOLOGY
Development of static system procedures to study aquatic biofilms and their responses to disinfection and invading species
[NASA-TM-103598] p 4036 N92-33103

MICROCHANNEL PLATES
Detectors for lidar type Thomson scattering diagnostics
[IPF-91-5] p 3990 N92-32823

MICROCOMPUTERS
EPCRA Section 313 Roadmaps Database: User's manual, version 2.2
[PB92-169523] p 4030 N92-33062

MICROCRACKS
Computational simulation of matrix micro-slip bands in SiC/Ti-15 composite
[NASA-TM-105762] p 3946 N92-32466
Investigation of a relationship between uniaxial and biaxial chemical stress crazing of cast acrylic
[AD-A250852] p 4021 N92-32621

MICROMECHANICS
Computational simulation of matrix micro-slip bands in SiC/Ti-15 composite
[NASA-TM-105762] p 3946 N92-32466

MICROMETEOROIDS
Analysis of LDEF experiment AO187-2: Chemically and isotopic measurements of micrometeoroids by secondary ion mass spectrometry
[NASA-CR-190697] p 4093 N92-32541

MICROORGANISMS
Development of static system procedures to study aquatic biofilms and their responses to disinfection and invading species
[NASA-TM-103598] p 4036 N92-33103

MICROPHONES
High temperature fiber optic microphone having a pressure-sensing reflective membrane under tensile stress
[NASA-CASE-LAR-14402-1-CU] p 4076 N92-33017
Vacuum-isolation vessel and method for measurement of thermal noise in microphones
[NASA-CASE-LAR-14567-1-CU] p 3991 N92-33021

MICROPOROSITY
Microporous structure with layered interstitial surface treatment, and method and apparatus for preparation thereof
[NASA-CASE-MSC-21487-1] p 3965 N92-33009

MICROPROCESSORS
The design and development of a portable, DSP micro-processor based, high-accuracy data acquisition system
[NRC-32146] p 4040 N92-32851
The development of an airborne information management system for flight test
[NASA-TM-104251] p 3938 N92-32866
Analysis of a benchmark suite to evaluate mixed numeric and symbolic processing
[NASA-TM-103907] p 4052 N92-32886

MICROSCOPY
Surface reconstruction and templating for zeolite thin film synthesis observed by atomic force microscopy
[AD-A251140] p 4066 N92-32548
Condensed-phase processes during solid propellant combustion. Part 2: Chemical and microscopic examination of conductively quenched samples of RDX, XM39, JA2, M30, and HMX-binder compositions
[AD-A250799] p 3974 N92-32664
Scanning force microscopy using optical interferometry
[ISBN-90-9003887-6] p 4077 N92-33146

MICROSTRIP ANTENNAS
An optically controlled Ka-band phased array antenna p 3983 N92-32968
Ka-band dual frequency array feed for a low cost ACTS ground terminal p 3983 N92-32969
Measurement techniques for cryogenic Ka-band microstrip antennas p 3985 N92-32981
Techniques for the synthesis of wideband, series-fed arrays of microstrip patch radiators
[ISBN-0-315-58991-4] p 3987 N92-33209

MICROSTRIP DEVICES
A 19.2 GHz cooled HEMT low noise amplifier
[CTN-92-60354] p 3990 N92-32810

MICROSTRIP TRANSMISSION LINES
Coplanar waveguide feeds for phased array antennas p 3983 N92-32970
Ultra-low-loss strip-type transmission lines, formed of bonded substrate layers
[AD-D015312] p 3992 N92-33169

MICROSTRUCTURE
Preparation and characterization of superlattices
[DE92-012572] p 4081 N92-32462
Formation of high temperature superconductors from the solidified melt
[DE92-012584] p 4081 N92-32465
Thermal degradation study of silicon carbide threads developed for advanced flexible thermal protection systems
[NASA-TM-103952] p 3970 N92-32476
Transmission electron microscope characterization of deformation and recovery in 304L stainless steel part
[DE92-013237] p 3966 N92-32614
Interfacial studies of refractory glass-ceramic matrix/advanced SiC fiber reinforced composites
[AD-A250784] p 3953 N92-32676
Synthesis, microsctructure, and mechanical properties of zirconia-alumina composites
[ISBN-90-9004656-9] p 3954 N92-32677
Electrified microheterogeneous catalysis
[AD-D015270] p 3963 N92-32755
Aluminum based particulate composites for aerospace applications produced by different processes
[MBB-Z-0408-91-PUB] p 3967 N92-32819
Contribution to the study of the effect of the heterogeneous distribution of dislocations on the cyclic plasticity of single crystal aluminum
[ISAL-91-0099] p 4083 N92-32892
Synthesis, microstructure, critical current density, magnetization and relaxation of hot-pressed YBa2Cu3O(6 + delta) through partial melting post-oxygenation
[DE92-015205] p 4085 N92-33026
A combined AEM/APFIM characterization of Alloy X-750
[DE92-011049] p 3969 N92-33158

MICROWAVE ABSORPTION
Microwave absorption by lossy ceramic materials
[DE92-016963] p 3970 N92-32317

MICROWAVE AMPLIFIERS
A 19.2 GHz cooled HEMT low noise amplifier
[CTN-92-60354] p 3990 N92-32810
A low-current amplifier for mobile radio and monolithic microwave integrated circuit design techniques in the UHF and L bands
[ISBN-0-315-59034-3] p 3993 N92-33211

MICROWAVE ANTENNAS
V-band pseudomorphic HEMT MMIC phased array components for space communications p 3983 N92-32966
Planar dielectric resonator stabilized HEMT oscillator integrated with CPW/aperture coupled patch antenna p 3983 N92-32967
An optically controlled Ka-band phased array antenna p 3983 N92-32968
Ka-band dual frequency array feed for a low cost ACTS ground terminal p 3983 N92-32969
Coplanar waveguide feeds for phased array antennas p 3983 N92-32970
Analysis of shielded CPW discontinuities with air-bridges p 3983 N92-32971

MICROWAVE CIRCUITS
V-band pseudomorphic HEMT MMIC phased array components for space communications p 3983 N92-32966
Planar dielectric resonator stabilized HEMT oscillator integrated with CPW/aperture coupled patch antenna p 3983 N92-32967
An optically controlled Ka-band phased array antenna p 3983 N92-32968
Coplanar waveguide feeds for phased array antennas p 3983 N92-32970
Analysis of shielded CPW discontinuities with air-bridges p 3983 N92-32971
A flexible CPW package for a 30 GHz MMIC amplifier p 3983 N92-32972
A 1-W, 30-GHz, CPW amplifier for ACTS small terminal uplink p 3984 N92-32973
Microwave properties of peeled HEMT devices sapphire substrates p 3984 N92-32978
A low-current amplifier for mobile radio and monolithic microwave integrated circuit design techniques in the UHF and L bands
[ISBN-0-315-59034-3] p 3993 N92-33211

MICROWAVE EQUIPMENT
Electromagnetic-wave propagation in unmagnetized plasmas
[AD-A250710] p 3980 N92-32719
A high-power SLED 2 pulse compression system
[DE92-011586] p 4071 N92-32751

MICROWAVE FREQUENCIES
Study and development of a six port network analyzer in the 1-18 GHz frequency range
[TELECOM-91-E-005] p 3980 N92-32739
Magnetic penetration depth of YBa2Cu3O(7-delta) thin films determined by the power transmission method p 3985 N92-32983

MICROWAVE LANDING SYSTEMS
Development of new flight procedures for the Microwave Landing System (MLS)
[NLR-TP-91156-U] p 3933 N92-32830
MICROWAVE OSCILLATORS
Continuation of the development of a millimeter wave wideband tunable waveguide voltage controlled oscillator
[CAL-504-88P120] p 3990 N92-32847
Planar dielectric resonator stabilized HEMT oscillator integrated with CPW/aperture coupled patch antenna
p 3983 N92-32967
MICROWAVE TRANSMISSION
Ultra-low-loss strip-type transmission lines, formed of bonded substrate layers
[AD-D015312] p 3992 N92-33169
MICROWAVES
Microwave absorption by lossy ceramic materials
[DE92-016963] p 3970 N92-32317
Diagnostics and modeling of ECRH microwave discharges
[IPF-91-3] p 4079 N92-32822
Characterization of sintered reaction-bonded silicon nitride processed by microwave heating
[DE92-014408] p 3956 N92-32945
Microwave properties of peeled HEMT devices sapphire substrates p 3984 N92-32978
MIDAIR COLLISIONS
Safety study of TCAS 2 for logic version 6.04
[DOT/FAA/RD-92/22] p 3933 N92-32537
MIDCOURSE GUIDANCE
Method of guiding an in-flight vehicle toward a target
[AD-D015308] p 3940 N92-33161
MILITARY AIRCRAFT
The Utilization of Advanced Composites in Military Aircraft
[AGARD-R-785] p 3956 N92-33033
MILITARY HELICOPTERS
Advanced information processing system: The Army fault tolerant architecture conceptual study. Volume 1: Army fault tolerant architecture overview
[NASA-CR-189632-VOL-1] p 4052 N92-33100
Advanced information processing system: The Army fault tolerant architecture conceptual study. Volume 2: Army fault tolerant architecture design and analysis
[NASA-CR-189632-VOL-2] p 4052 N92-33101
MILITARY TECHNOLOGY
Applications of composites to armaments
p 3947 N92-32516
China's aerospace industry: Technology, funding, and modernization
[AD-A252618] p 3929 N92-32691
The DOD science and technology strategy
[AD-A253691] p 4104 N92-33027
MILLIMETER WAVES
V-band pseudomorphic HEMT MMIC phased array components for space communications
p 3983 N92-32966
A flexible CPW package for a 30 GHz MMIC amplifier
p 3983 N92-32972
MINIMAX TECHNIQUE
Using minimax approaches to plan optimal task commutation configurations for combined mobile platform-manipulator systems
[DE91-018864] p 4018 N92-32694
MINING
JPRS report: Science and technology. Central Eurasia: Materials science
[JPRS-UMS-92-011] p 3969 N92-33129
MINORITIES
A minority research and education information service: Design, develop, pilot test, and implement on-line access for historically black colleges and universities and government agencies
[DE92-013572] p 4090 N92-32930
MIRRORS
Thermal effects and mirror surface figure requirements for a diagnostic beamline at the advanced light source
[DE92-014483] p 4073 N92-32419
Multispectral variable magnification glancing incidence x ray telescope
[NASA-CASE-MFS-28013-4] p 4092 N92-33012
MISSILE CONTROL
The German anti tank helicopter PAH 2: An example of a future sensor platform p 3937 N92-32448
MISSILES
Method of guiding an in-flight vehicle toward a target
[AD-D015308] p 3940 N92-33161
The United States Air Force explosives hazards reduction program p 3976 N92-33241
Hazards reduction for tactical missiles
p 3945 N92-33245
MISSING MASS (ASTROPHYSICS)
Atmospheric escape from Titan p 4099 N92-32384
MISSION PLANNING
Cassini: A mission to Saturn and Titan
p 4099 N92-32387
The Huygens probe p 4099 N92-32388
Advanced software development workstation: Effectiveness of constraint-checking --- spaceflight simulation and planning
[NASA-CR-190712] p 4043 N92-32865
MIXED OXIDES
Sintering of bulk high-(Tc) superconductors: Bi-Sr-Ca-Cu-O
[DE92-016189] p 4082 N92-32561
MIXING LENGTH FLOW THEORY
Effects of curvature and rotation on turbulence in the NASA low-speed centrifugal compressor impeller
p 4003 N92-32292
MIXTURES
Computational and experimental study of laminar flames
[DE92-017978] p 3965 N92-33121
MOBILE COMMUNICATION SYSTEMS
Effects of fading and interference in narrowband land-mobile networks
[ISBN-90-9004491-4] p 3982 N92-32837
A low-current amplifier for mobile radio and monolithic microwave integrated circuit design techniques in the UHF and L bands
[ISBN-0-315-59034-3] p 3993 N92-33211
MODAL RESPONSE
Recent advances in statistical energy analysis
p 4062 N92-32954
MODEL REFERENCE ADAPTIVE CONTROL
Investigations of adaptive control for a direct drive robotic manipulator
[ISBN-0-315-59030-0] p 4055 N92-33236
MODELS
Titan's UV albedo: Observations and modeling
p 4094 N92-32356
Stochastic models in reliability
[AD-A250934] p 4020 N92-33151
MODFETS
Intermodulation in the oscillatory magnetoresistance of a two-dimensional electron gas p 3984 N92-32975
Study of InGaAs-based modulation doped field effect transistor structures using variable-angle spectroscopic ellipsometry p 3984 N92-32977
MODULATION DOPING
High-energy ion implantation for bipolar transistor fabrication
[ISBN-90-9003883-3] p 3992 N92-33144
MODULATORS
A molecule-specific filter modulator
[AD-A250760] p 4074 N92-32672
Development of advanced modulators for recirculating heavy ion accelerators
[DE92-014795] p 4072 N92-33122
MODULES
Multichip module study
[AD-A250877] p 3989 N92-32678
MODULUS OF ELASTICITY
Influence of compliance on performance of robotic drilling
[OUEL-1917/92] p 4018 N92-32757
A unique method of determining the elastic and engineering constants of unidirectional fibre-reinforced composite plates using ultrasound
[UTIAS-TN-274] p 3955 N92-32829
MOIRE EFFECTS
Topographical measuring based on the shadow and projection Moire method
[ISBN-90-9004146-X] p 4074 N92-32705
MOIRE INTERFEROMETRY
Topographical measuring based on the shadow and projection Moire method
[ISBN-90-9004146-X] p 4074 N92-32705
MOLECULAR BEAM EPITAXY
Preparation and characterization of superlattices
[DE92-012572] p 4081 N92-32462
Investigation on the lattice site location of the excess arsenic atoms in GaAs layers grown by low temperature molecular beam epitaxy
[DE92-008253] p 4083 N92-32693
Development of ultra-low noise, high sensitivity planar metal grating coupled AlGaAs/GaAs multiquantum well IR detectors for focal plane array staring IR sensor systems
[AD-A250368] p 4083 N92-32747
Study of InGaAs-based modulation doped field effect transistor structures using variable-angle spectroscopic ellipsometry p 3984 N92-32977
MOLECULAR BEAMS
High translational energy induced reaction in semiconductors
[AD-A250980] p 3989 N92-32669
The energetics and dynamics of free radicals, ions, and clusters
[DE92-014124] p 4068 N92-33083
Collective resonances of valence electrons in free metal clusters
[DE92-014783] p 3969 N92-33116
MOLECULAR COLLISIONS
Novel gas phase ion molecule reactions of C60(++) with O2 and NH3
[AD-A250921] p 4066 N92-32556
MOLECULAR DIFFUSION
A basic research model of natural gas combustion in turbulent flow, phase 2
[PB92-190362] p 4007 N92-32598
Study and achievement of a parallel simulator for diffusion at the atomic level: Creation and growth of dislocation loops under electronic radiation
[LAAS-92118] p 4066 N92-32735
MOLECULAR ENERGY LEVELS
Mass resolved resonance ionization spectroscopy of combustion radicals
[DE92-016833] p 3965 N92-33222
MOLECULAR EXCITATION
Study on lifetime specific, laser-induced ultrafast fluorescence detection in the time and frequency domain for in-situ environmental analysis of organic pollutants
[KFK-4975] p 4029 N92-32841
MOLECULAR ORBITALS
The energetics and dynamics of free radicals, ions, and clusters
[DE92-014124] p 4068 N92-33083
MOLECULAR PHYSICS
Molecular dynamics modeling of the mechanical properties of metal surfaces at the nanometer scale
[DE92-010705] p 3966 N92-32646
Dynamics of radiation-induced amorphization in intermetallic compounds
[DE92-016774] p 4086 N92-33221
MOLECULAR SPECTRA
A molecule-specific filter modulator
[AD-A250760] p 4074 N92-32672
Grill spectrometry on the Space Shuttle during the Atlas 1 mission
[AERONAUTICA-ACTA-A-364-199] p 3943 N92-32728
Radiative lifetime measurements of the AA pi 1/2 state in CaH
[USIP-91-03] p 4067 N92-32764
MOLECULAR SPECTROSCOPY
A molecule-specific filter modulator
[AD-A250760] p 4074 N92-32672
MOLECULAR STRUCTURE
Thermal conductivity of liquid aliphatic hydrocarbons. Part 1: Alkanes
[ESDU-92011-PT-1] p 3945 N92-32484
Orientation, stress, and density distributions in injection-moulded amorphous polymers determined by optical techniques
[ETN-92-92052] p 3972 N92-32752
Use of a Fourier deconvolution method in particle size determination and use of molecular mechanics in crystal structure determinations
[DE92-014510] p 4085 N92-33111
MOLECULAR WEIGHT
Polyimide molding powder, coating, adhesive, and matrix resin
[NASA-CASE-LAR-14163-1] p 3973 N92-33014
MOLECULES
Local structural order and molecular associations in water DMSO mixtures. Molecular dynamics study
[AD-A250935] p 4064 N92-32418
Structure and dynamics in low-dimensional guest-host systems
[DE92-014841] p 3970 N92-32429
A molecule-specific filter modulator
[AD-A250760] p 4074 N92-32672
Molecular surface analysis by laser ionization of desorbed molecules
[DE92-016320] p 4016 N92-33114
MOLNIYA SATELLITES
The energetic radiation environment in a highly elliptical (Molniya) orbit
[AD-A252394] p 4031 N92-32902
MOLYBDENUM ALLOYS
Inelastic deformation and damage at high temperature
[DE92-012241] p 4021 N92-32698
MOLYBDENUM COMPOUNDS
Synthesis of MoSi2-based alloys by mechanical alloying
[DE92-017528] p 3969 N92-33120
MOMENTS OF INERTIA
Higher superdeformed band members in Hg-190: Evidence for a band interaction?
[DE92-016778] p 4082 N92-32542

MOMENTUM
Observation of (pi)(-)p yields (omega)(eta)n reaction at 38 GeV/c momentum
[DE92-624690] p 4064 N92-32310
MONITORS
Passive fetal monitoring sensor
[NASA-CASE-LAR-14088-1-CU] p 4015 N92-33016
Volume 1. Preliminary design study: AXAF x ray calibration spectrometers. Volume 2. Revised preliminary design study: AXAF x ray calibration spectrometers
[NASA-CR-184340] p 4092 N92-33094
Thermal and structural analysis of high precision beamline position monitors for synchrotron x ray beams
[DE92-014863] p 4072 N92-33130
MONOMERS
New thiophene-based materials
[AD-A250977] p 3972 N92-32667
MONTANA
Forecasting heavy snow events in Missoula, Montana
[PB92-196104] p 4034 N92-33163
MONTE CARLO METHOD
Analytic score comparison of geometry splitting and exponential transform for a simple Monte Carlo problem
[DE92-013108] p 4059 N92-32481
Feature detection for model assessment in state estimation
[AD-A252755] p 4059 N92-32989
Continuum configurational bias Monte-Carlo studies of alkanes and polyethylene
[DE92-016545] p 3965 N92-33185
MORPHOLOGY
Morphology, 31P spin diffusion, and phase transitions in a representative semicrystalline polyphosphazene by solid-state NMR
[AD-A250883] p 3961 N92-32553
MOSSBAUER EFFECT
Gamma scattering in condensed matter with high intensity Moessbauer radiation
[DE92-014811] p 4085 N92-33025
MOTION PERCEPTION
Correlating visual scene elements with simulator sickness incidence: Hardware and software development
[AD-A252235] p 4036 N92-32434
Temporal and spatial factors affecting the perception of computer-generated imagery
[AD-A249242] p 4046 N92-32907
MOTION SICKNESS
Correlating visual scene elements with simulator sickness incidence: Hardware and software development
[AD-A252235] p 4036 N92-32434
MOTION SIMULATION
Dynamics of ion solvation in a Stockmayer fluid
[AD-A251087] p 4066 N92-32682
MOTOR VEHICLES
Phase distributions of airborne polycyclic aromatic hydrocarbons in two US cities
[PB92-164979] p 4028 N92-32543
MOUNTING
Flush mounting of thin film sensors
[NASA-CASE-LAR-14446-1] p 3978 N92-33020
MOVING TARGET INDICATORS
Impulse transmitter and quantum detection radar system
[AD-D015323] p 3986 N92-33171
MRCA AIRCRAFT
Airborne experimental FLIR program
p 3937 N92-32447
MSAT
The MSAT spacecraft of Telesat Mobile, Inc.
[CTN-92-60346] p 3981 N92-32789
MULTIBEAM ANTENNAS
Phase-only synthesis for multiple-beam phased arrays with element failures
[AD-A252250] p 3982 N92-32891
MULTIGRID METHODS
New concepts for multi-block grid generation for flow domains around complex aerodynamic configurations
[NLR-TP-91046-U] p 3930 N92-32730
Advanced computational transport methods for curvilinear geometries
[DE92-011290] p 4057 N92-32743
Convergence acceleration of the Proteus computer code with multigrid methods
[NASA-CR-190607] p 4047 N92-33131
MULTIPHASE FLOW
A three-field model of transient 3D multiphase, three-component flow for the computer code 4 A3. Par1: Theoretical basis: Conservation and state equations, numerics
[KFK-4948-PT-1] p 4011 N92-32857
A three-field model of transient 3D multiphase, three-component flow for the computer code 4 A3. Part 2: Models for the interfacial transport phenomena. Code validation
[KFK-4949-PT-2] p 4011 N92-32858
Study of flow properties of wet solids using laser induced photochemical anemometry
[DE92-015452] p 4013 N92-33140
MULTIPHOTON ABSORPTION
Beamstrahlung spectra in next generation linear colliders
[DE92-010730] p 4069 N92-32337
MULTIPLE ACCESS
The problems of routing and scheduling in multihop radio networks. A Hopfield neural network approach
[AD-A247431] p 3979 N92-32570
MULTIPLEXING
Applications of the photorefractive effect and damage induced effects in fibers
[AD-A250767] p 3953 N92-32674
Adaptive filter technique for suppression of wideband or offset narrowband radio frequency interference
[AD-D015329] p 3992 N92-33175
MULTIPLIERS
VLSI architecture for a Reed-Solomon decoder
[NASA-CASE-NPO-17897-1-CU] p 3991 N92-33011
MULTIPOLES
Pseudopotential band calculations along a high-symmetry axis. Part 1: Central potential and the (111) direction
[AD-A252399] p 4084 N92-32938
MULTIPROCESSING (COMPUTERS)
The Rochester Checkers Player: Multi-model parallel programming for animate vision
[AD-A247427] p 4050 N92-32568
Study of a cellular programmable architecture: Functional definition and programming method
[ETN-92-91663] p 4051 N92-32768
Sparse matrix algorithms on distributed memory multiprocessors
[DE92-017870] p 4046 N92-33071
A fast task allocator for multiprocessing systems
[ISBN-0-315-54380-9] p 4053 N92-33217
Diagnosability and diagnosis of sparsely interconnected multiprocessor systems
[ISBN-0-315-56107-6] p 4053 N92-33224

N

N-P-N JUNCTIONS
High-energy ion implantation for bipolar transistor fabrication
[ISBN-90-9003883-3] p 3992 N92-33144
N-TYPE SEMICONDUCTORS
Investigation of impurity related phenomena, significant for novel semiconductor technologies
[ETN-92-92048] p 4083 N92-32760
NARROWBAND
New approach to HF channel modeling and simulation. Part 3: Transfer function
[PB92-192848] p 3979 N92-32555
Effects of fading and interference in narrowband land-mobile networks
[ISBN-90-9004491-4] p 3982 N92-32837
Adaptive filter technique for suppression of wideband or offset narrowband radio frequency interference
[AD-D015329] p 3992 N92-33175
NASA PROGRAMS
NASA's nuclear electric propulsion technology project
[NASA-TM-105811] p 3944 N92-32463
Departments of Veterans Affairs and Housing and Urban Development, and independent agencies appropriations for 1993, part 6
[GAO-55-636-PT-6] p 4091 N92-32505
NASA procurement: Improving oversight of construction projects at the Langley Research Center. Report to the Honorable John W. Warner, US Senate
[GAO/NSIAD-92-230] p 4088 N92-32618
Solid State Technology Branch of NASA Lewis Research Center
[NASA-TM-105752] p 3982 N92-32965
NASA authorization, 1993, volume 1
[GPO-55-260-VOL-1] p 4092 N92-33147
NASA SPACE PROGRAMS
Space Station Freedom media handbook
[NASA-TM-107981] p 3942 N92-32421
Toward the next millennium: A vision for spaceship Earth
[NASA-TM-107986] p 3941 N92-33007
NATIONAL AIRSPACE SYSTEM
A review and discussion of flight management system incidents reported to the aviation safety reporting system
[AD-A252438] p 3932 N92-32941
NATURAL GAS
A basic research model of natural gas combustion in turbulent flow, phase 2
[PB92-190362] p 4007 N92-32598
NATURAL SATELLITES
Formation of the satellites p 4093 N92-32350
NAVIER-STOKES EQUATION
Computational fluid dynamics analysis of Space Shuttle main engine multiple plume flows at high-altitude flight conditions p 3996 N92-32255
Direct numerical simulation of a combusting droplet with convection p 3996 N92-32256
Modeling of SSME fuel preburner ASI
p 3945 N92-32259
CFD modeling of turbulent flows around the SSME main injector assembly using porosity formulation
p 3997 N92-32260
STME hydrogen mixer study p 3945 N92-32262
A critical evaluation of a three-dimensional Navier-Stokes CFD as a tool to design supersonic turbine stages p 3999 N92-32268
Navier-Stokes analysis of an oxidizer turbine blade with tip clearance p 3999 N92-32269
Numerical simulation of turbomachinery flows with advanced turbulence models p 3999 N92-32270
Development of the KIVA-2 CFD code for rocket propulsion applications p 3945 N92-32272
Optimum design of ninety degree bends
p 4000 N92-32274
A multi-domain method for subsonic viscous flows
p 3960 N92-32275
Large eddy simulation of compressible turbulent channel flows p 4000 N92-32276
Comparison between the PISO algorithm and preconditioning methods for compressible flow
p 4001 N92-32284
Three-dimensional flow fields inside a shrouded inducer at design and off-design conditions (CFD study)
p 4003 N92-32291
CFD analysis to optimize a design modification of BSMT p 4004 N92-32296
Research on some centered implicit methods for calculating transonic flows by solving Navier-Stokes equations
[ONERA-RSF-24/1408-AY-150A] p 3931 N92-32773
CFD efforts in the Netherlands
[NLR-TP-91250-U] p 4011 N92-32835
A numerical resolution study of high order essentially non-oscillatory schemes applied to incompressible flow
[NASA-CR-189692] p 4012 N92-33110
Computation of incompressible viscous flows through turbopump components
[NASA-TM-103911] p 4012 N92-33113
NAVIGATION
Airborne experimental FLIR program
p 3937 N92-32447
Using minimax approaches to plan optimal task commutation configurations for combined mobile platform-manipulator systems
[DE91-018864] p 4018 N92-32694
NAVSTAR SATELLITES
Satellite radio interferometry
[PL-TR-91-2200] p 3978 N92-32458
NAVY
A causal analysis of interrelationships among exercise, physical fitness, and well-being in US Navy personnel
[AD-A252719] p 4037 N92-32942
NEAR INFRARED RADIATION
Observing the surface of Titan through near-infrared windows in its atmosphere p 4097 N92-32374
The detectability of Titan's surface in the near-infrared
p 4097 N92-32375
NEAR WAKES
Annual progress report on imposed 3-D disturbances on bluff-body near wake flows
[AD-A250366] p 4006 N92-32324
NEODYMIUM LASERS
Feasibility of a 486 nm Fraunhofer laser source based on a 4F(sub 3/2) yields 4I(sub 9/2) neodymium laser
[AD-A250851] p 4015 N92-32329
NERVOUS SYSTEM
Development of the OMPAT neuropsychological/psychomotor performance evaluation and OMPAT data and timing support
[AD-A250793] p 4037 N92-32504
NETS
Minimum cost multiflows in undirected networks
[IMAG-RR-849-M] p 4056 N92-32710
NETWORK ANALYSIS
A scalable, switched circuit LAN for Gb/S channels with over Tb/S total capacity
[DE92-013444] p 4050 N92-32412
Target cuing: A heterogeneous neural network approach p 3936 N92-32442
The problems of routing and scheduling in multihop radio networks. A Hopfield neural network approach
[AD-A247431] p 3979 N92-32570
Study and development of a six port network analyzer in the 1-18 GHz frequency range
[TELECOM-91-E-005] p 3980 N92-32739

Ethernet bandwidth utilization of datafull, dataless, and diskless node workstation and x-terminals
[AD-A252374] p 4052 N92-32937
NETWORK SYNTHESIS
A simplified synthesis of lossless two-port wave digital and analog filters
[ISBN-0-315-63272-0] p 3993 N92-33193
NEURAL NETS
Target cuing: A heterogeneous neural network approach p 3936 N92-32442
Tutorial on neural network applications in high energy physics: A 1992 perspective
[DE92-016003] p 4070 N92-32506
The problems of routing and scheduling in multihop radio networks. A Hopfield neural network approach
[AD-A247431] p 3979 N92-32570
Intelligent signal processing for active control
[AD-A252232] p 4053 N92-32625
Opto-electronic system for a formal neural network
[TELECOM-91-E-013] p 4075 N92-32805
Better predictions even in reduced input variable numbers using neural networks in software development p 4044 N92-32874
Feature detection for model assessment in state estimation
[AD-A252755] p 4059 N92-32989
NEUROPHYSIOLOGY
PET studies of components of high-level vision
[AD-A250873] p 4036 N92-32344
NEUTRAL BEAMS
Formation and sustainment of a very low aspect ratio tokamak using coaxial helicity injection: Helicity Injected Torus (HIT) experiment
[DE92-014311] p 4078 N92-32595
Scrape-off layer modeling of radiative divertor and high heat flux experiments on D3-D
[DE92-015007] p 4080 N92-32995
NEUTRAL PARTICLES
Collaborative, remote, in-depth inspection and verification of satellites with neutral particle beams
[DE92-014195] p 3943 N92-32934
NEUTRINOS
Theoretical and experimental studies of elementary physics
[DE92-014877] p 4061 N92-32430
Neutrino masses in the flipped SU(5) tensor product U(1) and the SU(4) tensor product O(4) GUT models
[RAL-92-012] p 4068 N92-33135
NEUTRON COUNTERS
Investigation of the oxygen-vacancy (A-center) defect complex profile in neutron irradiated high resistivity silicon junction particle detectors
[DE92-016952] p 4064 N92-32316
High efficiency fast neutron threshold deflector
[AD-D015311] p 4073 N92-33167
NEUTRON DECAY
Pertubative finite temperature field theory in Minkowski space
[ISBN-0-315-55158-5] p 4088 N92-33199
NEUTRON DIFFRACTION
Gamma scattering in condensed matter with high intensity Moessbauer radiation
[DE92-014811] p 4085 N92-33025
Neutron scatter studies of chromatin structures related to functions
[DE92-014032] p 4036 N92-33181
NEUTRON IRRADIATION
Investigation of the oxygen-vacancy (A-center) defect complex profile in neutron irradiated high resistivity silicon junction particle detectors
[DE92-016952] p 4064 N92-32316
NEUTRON STARS
Research in nuclear astrophysics: Stellar collapse and supernovae
[DE92-014988] p 4093 N92-32993
NEUTRONS
The shapes and collective behavior of rapidly rotating nuclei
[DE92-017192] p 4067 N92-32928
Neutron scatter studies of chromatin structures related to functions
[DE92-014032] p 4036 N92-33181
NICKEL ALLOYS
High temperature deformation processes and strengthening mechanisms in intermetallic particulate composites
[AD-A250220] p 3946 N92-32339
Thermal strains in titanium aluminide and nickel aluminide composites
[DE92-015181] p 3953 N92-32638
High temperature fabricable nickel-iron aluminides
[CA-PATENT-1-276-814] p 3968 N92-32855
NICKEL COATINGS
Laser coating of composites for enhanced wear and corrosion resistance
[AD-A249231] p 3956 N92-32906
NICKEL COMPOUNDS
Development of high-performance Na/NiCl2 cell
[DE92-015270] p 3988 N92-32639
NICKEL STEELS
High temperature fabricable nickel-iron aluminides
[CA-PATENT-1-276-814] p 3968 N92-32855
NIOBIUM
RF cavity vacuum interlock system
[DE92-016961] p 4070 N92-32567
NIOBIUM ALLOYS
Thermal strains in titanium aluminide and nickel aluminide composites
[DE92-015181] p 3953 N92-32638
NITINOL ALLOYS
Device for removing foreign objects from anatomic organs
[NASA-CASE-GSC-13306-1] p 4038 N92-33032
NITRAMINE PROPELLANTS
Condensed-phase processes during solid propellant combustion. Part 2: Chemical and microscopic examination of conductively quenched samples of RDX, XM39, JA2, M30, and HMX-binder compositions
[AD-A250799] p 3974 N92-32664
NITRILES
Photochemistry of unsaturated nitriles on Titan p 4096 N92-32371
NITROGEN
Atmospheric escape from Titan p 4099 N92-32384
NITROGEN DIOXIDE
SAGE 1 data user's guide
[NASA-RP-1275] p 4031 N92-33097
NOBLE METALS
Electrocatalysis of anodic, oxygen-transfer reactions at noble metal electrodes
[DE92-016308] p 3962 N92-32562
NOISE (SOUND)
Acoustical emission from bubbles
[AD-A252390] p 4061 N92-32901
Modeling the ear's response to intense impulses and the development of improved damage risk criteria
[AD-A252365] p 4037 N92-32916
NOISE INTENSITY
Pilot noise exposure during a Boeing 747-400 round trip: Judgement of noise and analysis in respect to hearing impairment of pilots p 4063 N92-32961
Building vibrations induced by noise from rotorcraft and propeller aircraft flyovers
[NASA-TM-104170] p 4063 N92-33160
NOISE MEASUREMENT
Fourth Aircraft Interior Noise Workshop
[NASA-CP-10103] p 4061 N92-32948
Sound power determination using the sound intensity scanning technique p 4062 N92-32953
Use of SEA to predict structure-borne noise in aircraft p 4062 N92-32955
Advanced Study for Active Noise Control in Aircraft (ASANCA)
[AIAA PAPER 92-2092] p 4062 N92-32956
Pilots noise exposure during a Boeing 747-400 round trip: Ambient noise and acoustic-head recording and analysis of data p 4063 N92-32960
Pilot noise exposure during a Boeing 747-400 round trip: Judgement of noise and analysis in respect to hearing impairment of pilots p 4063 N92-32961
Vacuum-isolation vessel and method for measurement of thermal noise in microphones
[NASA-CASE-LAR-14567-1-CU] p 3991 N92-33021
Feasibility of measuring transverse electric noise at VLF and LF on an ice cap
[AD-A252280] p 4035 N92-33220
Techniques of microwave noise measurement on cooled transistors
[ISBN-0-315-65025-7] p 3994 N92-33234
NOISE PREDICTION
Fourth Aircraft Interior Noise Workshop
[NASA-CP-10103] p 4061 N92-32948
NOISE PREDICTION (AIRCRAFT)
Acoustic loads prediction on jet aircraft p 4061 N92-32949
MD-80 aft cabin noise control: A case history p 4061 N92-32950
Vibro-acoustic FE analyses of the Saab 2000 aircraft p 4062 N92-32952
Use of SEA to predict structure-borne noise in aircraft p 4062 N92-32955
Advanced Study for Active Noise Control in Aircraft (ASANCA)
[AIAA PAPER 92-2092] p 4062 N92-32956
NOISE PROPAGATION
Use of SEA to predict structure-borne noise in aircraft p 4062 N92-32955
NOISE REDUCTION
A 19.2 GHz cooled HEMT low noise amplifier
[CTN-92-60354] p 3990 N92-32810
Fourth Aircraft Interior Noise Workshop
[NASA-CP-10103] p 4061 N92-32948
MD-80 aft cabin noise control: A case history p 4061 N92-32950
The Dornier 328 Acoustic Test Cell (ATC) for interior noise tests and selected test results
[AIAA PAPER 92-2164] p 4062 N92-32951
Vibro-acoustic FE analyses of the Saab 2000 aircraft p 4062 N92-32952
Sound power determination using the sound intensity scanning technique p 4062 N92-32953
Advanced Study for Active Noise Control in Aircraft (ASANCA)
[AIAA PAPER 92-2092] p 4062 N92-32956
Active control of interior noise in a large scale cylinder using piezoelectric actuators p 4063 N92-32958
Sound transmission reduction with intelligent panel systems p 4063 N92-32959
Pilots noise exposure during a Boeing 747-400 round trip: Ambient noise and acoustic-head recording and analysis of data p 4063 N92-32960
Pilot noise exposure during a Boeing 747-400 round trip: Judgement of noise and analysis in respect to hearing impairment of pilots p 4063 N92-32961
Active vibrations and noise control for turboprop application research program activities p 4063 N92-32962
Active synchrophasing of propeller unbalance p 4063 N92-32963
A lightweight loudspeaker for aircraft communications and active noise control p 3988 N92-32964
Performance of a Y-Ba-Cu-O superconducting filter/GaAs low noise amplifier hybrid circuit p 3985 N92-32982
NOISE SPECTRA
Modeling the ear's response to intense impulses and the development of improved damage risk criteria
[AD-A252365] p 4037 N92-32916
NONDESTRUCTIVE TESTS
Quantitative non-destructive environmental characterization of advanced materials
[DE92-011462] p 3946 N92-32327
Study of eddy current probes
[NASA-CR-190814] p 4020 N92-32425
Nondestructive evaluation development for process control
[DE92-015272] p 3971 N92-32640
Pump and valve research at the Oak Ridge National Laboratory
[DE92-014419] p 4019 N92-32890
A boundary integral method for an inverse problem in thermal imaging
[NASA-CR-189693] p 4059 N92-33006
NONEQUILIBRIUM THERMODYNAMICS
Two studies of nonlinear processes in irreversible thermodynamics
[DE92-016855] p 4087 N92-32566
NONFERROUS METALS
JPRS report: Science and technology. Central Eurasia: Materials science
[JPRS-UMS-92-011] p 3969 N92-33129
NONLINEAR EQUATIONS
User's manual for AeroFcn: A FORTRAN program to compute aerodynamic parameters
[NASA-TM-104237] p 4042 N92-32507
Aspects of solving non-linear boundary value problems numerically
[ETN-92-92049] p 4058 N92-32798
NONLINEAR OPTICS
Feasibility of a 486 nm Fraunhofer laser source based on a 4F(sub 3/2) yields 4I(sub 9/2) neodymium laser
[AD-A250851] p 4015 N92-32329
Laser material interaction
[AD-A250853] p 4016 N92-32622
Applications of the photorefractive effect and damage induced effects in fibers
[AD-A250767] p 3953 N92-32674
NONLINEAR SYSTEMS
Robust stabilization of the Space Station
[NASA-CR-190627] p 3942 N92-32244
Nonlinear dynamics and plasma transport
[DE92-014246] p 4078 N92-32592
The behavior of matter under non-equilibrium conditions: Fundamental aspects and applications
[DE92-014247] p 4087 N92-32593
Nonlinear resonance
[DE92-014313] p 4016 N92-32596
Intelligent signal processing for active control
[AD-A252232] p 4053 N92-32625
Steady state behavior of reduced dynamic systems with local nonlinearities
[ISBN-90-9004680-1] p 4056 N92-32707
Nonlinear transient responses of stratified composite structures
[ONERA-RT-26/3542-RY-007-R] p 3954 N92-32775
A discrete nonlinear model approach to study the behavior of large signal DC to DC converters
[LAAS-90028] p 3989 N92-32777

A continuous nonlinear model approach to study the behavior of large signal DC to DC converters
[LAAS-90027] p 3990 N92-32793
Measurement of nonlinear mode coupling of tearing fluctuations
[DE92-013901] p 4080 N92-33154
NONLINEARITY
Combustion instability analysis for liquid propellant rocket engines p 3966 N92-32297
Nonlinear resonance
[DE92-014313] p 4016 N92-32596
Can the speed of light in the fiber be controlled?
[AD-A247614] p 4074 N92-32668
NORTH AMERICA
Recent changes of weather patterns in North America
[DE92-014342] p 4033 N92-32720
NOTCH STRENGTH
Tensile fracture of notched composite laminates
[NRC-32147] p 3955 N92-32852
NOZZLE DESIGN
A status of the activities of the NASA. Marshall Space Flight Center Combustion Devices Technology Team p 3995 N92-32250
Application of computational fluid dynamics to the design of the film cooled STME subscale nozzle for the National Launch System p 3996 N92-32254
NOZZLE FLOW
NLS nozzle base flow characteristics p 3995 N92-32252
Using adaptive grid in modeling rocket nozzle flow p 4005 N92-32303
NOZZLE WALLS
A status of the activities of the NASA. Marshall Space Flight Center Combustion Devices Technology Team p 3995 N92-32250
CFD analysis of the STME nozzle flowfield p 3995 N92-32251
NLS nozzle base flow characteristics p 3995 N92-32252
NUCLEAR ASTROPHYSICS
Research in nuclear astrophysics: Stellar collapse and supernovae
[DE92-014988] p 4093 N92-32993
NUCLEAR DEFORMATION
Higher superdeformed band members in Hg-190: Evidence for a band interaction?
[DE92-016778] p 4082 N92-32542
Nuclear theory
[DE92-015012] p 4067 N92-32921
The shapes and collective behavior of rapidly rotating nuclei
[DE92-017192] p 4067 N92-32928
NUCLEAR ELECTRIC PROPULSION
NASA's nuclear electric propulsion technology project
[NASA-TM-105811] p 3944 N92-32463
NUCLEAR FUEL REPROCESSING
Chemical Technology Division
[DE92-014059] p 3964 N92-32931
NUCLEAR FUELS
Injection of compact toroids for tokamak fueling and current drive
[DE92-010031] p 4077 N92-32533
Alpha particle diagnostics using impurity pellet injection
[DE92-013796] p 4078 N92-32623
NUCLEAR INTERACTIONS
Relativistic heavy ion collisions
[DE92-014415] p 4066 N92-32600
NUCLEAR MAGNETIC RESONANCE
High accuracy beam energy measurement for linear and circular accelerators
[DE92-016966] p 4069 N92-32319
NQR-NMR studies of higher alcohol synthesis Cu-Co catalysts
[DE92-016614] p 3960 N92-32347
Low-frequency nuclear quadrupole resonance with a dc SQUID
[DE92-014506] p 4081 N92-32420
Morphology, 31P spin diffusion, and phase transitions in a representative semicrystalline polyphosphazene by solid-state NMR
[AD-A250883] p 3961 N92-32553
Nondestructive evaluation development for process control
[DE92-015272] p 3971 N92-32640
NUCLEAR MODELS
Nuclear theory
[DE92-015012] p 4067 N92-32921
NUCLEAR PHYSICS
Nuclear theory
[DE92-015012] p 4067 N92-32921
Relativistic heavy ion physics
[DE92-015025] p 4067 N92-32922
Research in theoretical nuclear physics
[DE92-016316] p 4068 N92-33067
Physics in knots
[DE92-017530] p 4088 N92-33069
Theoretical nuclear physics
[DE92-016837] p 4069 N92-33186
NUCLEAR POWER PLANTS
Oak Ridge Environmental Information System (OREIS). Phase 1: System definition document
[DE92-017342] p 4090 N92-33084
NUCLEAR QUADRUPOLE RESONANCE
NQR-NMR studies of higher alcohol synthesis Cu-Co catalysts
[DE92-016614] p 3960 N92-32347
Low-frequency nuclear quadrupole resonance with a dc SQUID
[DE92-014506] p 4081 N92-32420
NUCLEAR RADIATION
Correlation of single mode fiber fabrication factors and radiation response
[AD-A247301] p 4074 N92-32613
NUCLEAR REACTIONS
Electrocatalysis of anodic, oxygen-transfer reactions at noble metal electrodes
[DE92-016308] p 3962 N92-32562
Range of validity of distorted wave Born and impulse approximations for (e,2e)
[DE92-624821] p 4087 N92-32649
Nuclear theory
[DE92-015012] p 4067 N92-32921
Light-ion spectroscopy with exotic targets
[DE92-017258] p 3964 N92-32929
NUCLEAR REACTORS
Study of recirculating induction accelerators as drivers for heavy ion fusion
[DE92-016980] p 4071 N92-32904
Chemical Technology Division
[DE92-014059] p 3964 N92-32931
NUCLEAR SCATTERING
Theoretical nuclear physics
[DE92-016837] p 4069 N92-33186
NUCLEAR STRUCTURE
Higher superdeformed band members in Hg-190: Evidence for a band interaction?
[DE92-016778] p 4082 N92-32542
Nuclear theory
[DE92-015012] p 4067 N92-32921
Relativistic heavy ion physics
[DE92-015025] p 4067 N92-32922
The shapes and collective behavior of rapidly rotating nuclei
[DE92-017192] p 4067 N92-32928
Light-ion spectroscopy with exotic targets
[DE92-017258] p 3964 N92-32929
Research in theoretical nuclear physics
[DE92-016316] p 4068 N92-33067
NUCLEAR WEAPONS
B-52G/H nuclear certification tasks performed by the Aircraft Compatibility Division at Sandia National Laboratories
[DE92-013681] p 3934 N92-32308
NUCLEATION
Generic consequences of fundamental studies of beta phase decomposition modes in titanium and related alloy systems
[AD-A250789] p 3967 N92-32699
NUCLEI (NUCLEAR PHYSICS)
The shapes and collective behavior of rapidly rotating nuclei
[DE92-017192] p 4067 N92-32928
NUCLEONS
Research in nuclear astrophysics: Stellar collapse and supernovae
[DE92-014988] p 4093 N92-32993
NUMERICAL ANALYSIS
Numerical analysis of the hot-gas-side and coolant-side heat transfer in liquid rocket engine combustors p 4004 N92-32299
A tight and explicit representation of Q in sparse QR factorization
[DE92-014814] p 4055 N92-32428
Ideal efficiency of propellers based on Theodorsen's theory: A review and computer study, with extended plus simplified charts
[UTIAS-TN-271] p 3938 N92-33102
Computational aspects of helicopter trim analysis and damping levels from Floquet theory
[NASA-CR-190736] p 3940 N92-33107
NUMERICAL CONTROL
Quantitative non-destructive environmental characterization of advanced materials
[DE92-011462] p 3946 N92-32327
Rational behavior model: A tri-level multiple paradigm architecture for robot vehicle control software
[AD-A250370] p 4053 N92-32748
Air traffic control: FAA's advanced automation system contract
[GAO/IMTEC-91-25] p 3934 N92-32861
Automated data acquisition and analysis in the mechanical test lab
[DE92-011231] p 4040 N92-32910
NUMERICAL FLOW VISUALIZATION
Pressure field developed by the random movement of the vortices near a wall
[ETN-92-91665] p 4009 N92-32770
A numerical resolution study of high order essentially non-oscillatory schemes applied to incompressible flow
[NASA-CR-189692] p 4012 N92-33110
NUMERICAL INTEGRATION
Numerical evaluation of the incomplete airy functions and their application to high frequency scattering and diffraction
[NASA-CR-190745] p 4058 N92-32888
NUMERICAL WEATHER FORECASTING
Verification of severe local storms forecasts issued by the National Severe Storms Forecast Center, 1991
[PB92-186063] p 4033 N92-32502
Short range forecast of the initiation of convection
[DM-60] p 4033 N92-32758

O

OBJECT-ORIENTED PROGRAMMING
IDEF4 object-oriented design method manual
[AD-A252634] p 4042 N92-32658
Experiments in software engineering technology: Recent studies in the SEL (1990-1991) p 4044 N92-32872
Object links in the repository
[NASA-CR-190644] p 4091 N92-33096
Object linking in repositories
[NASA-CR-190629] p 4091 N92-33178
OBSERVATION
On the Titan/28 Sagittarii occultation of 1989 July 3 p 4101 N92-32403
OBSERVATORIES
Diffractive optics technology and the NASA Geostationary Earth Observatory (GEO)
[NASA-CR-190611] p 4076 N92-33074
OBSTACLE AVOIDANCE
Obstacle avoidance for redundant robots using configuration control
[NASA-CASE-NPO-17852-1-CU] p 4054 N92-33019
OCEAN BOTTOM
Hydrate detection
[DE92-014350] p 4034 N92-32333
Bacterial responses to extreme temperatures and pressures and to heavy organic loading
[AD-A247456] p 4035 N92-32571
OCEAN CURRENTS
A quasi-geostrophic circulation model of the northeast Pacific Ocean
[ISBN-0-315-55106-2] p 4035 N92-33198
OCEAN DATA ACQUISITIONS SYSTEMS
NAASW modular radar research testbed study results
[DE92-011339] p 3981 N92-32744
OCEAN DYNAMICS
Parameterization of directional spectra, part 2. Volume 2: User's manual for the programs RMODEL, FITHM, and FITDM
[DREA-CR-89-445-PT-2-VOL-2] p 3981 N92-32749
OCEAN MODELS
Parameterization of directional spectra, part 2. Volume 2: User's manual for the programs RMODEL, FITHM, and FITDM
[DREA-CR-89-445-PT-2-VOL-2] p 3981 N92-32749
A quasi-geostrophic circulation model of the northeast Pacific Ocean
[ISBN-0-315-55106-2] p 4035 N92-33198
OCEAN SURFACE
Waves on Titan p 4100 N92-32394
Energy take-out from a wave energy device. A theoretical study of the hydrodynamics of a two-body problem consisting of a buoy and a submerged plate
[PB92-178821] p 4025 N92-32608
Acoustical emission from bubbles
[AD-A252390] p 4061 N92-32901
OCEANOGRAPHY
Abstracts of manuscripts submitted in 1991 for publication
[PB92-204627] p 4091 N92-33088
OCEANS
Simulations of the carbon cycle in the oceans
[DE92-016622] p 4035 N92-32336
Plausible surface models for Titan p 4098 N92-32381
Experimental determination of the refractive index of liquefied gas mixtures: Applications to hypothesized Titan oceans p 4099 N92-32390
Dielectric constant measurements in simulated Titan ocean liquids p 4102 N92-32409
Federal plan for ocean pollution research, development, and monitoring, fiscal years 1992-1996
[PB92-185164] p 4029 N92-32708

OCTANES
High octane ethers from synthesis gas-derived alcohols
[DE92-013802] p 3975 N92-33108
OIL ADDITIVES
Influence of oil lubricant additives on tribological behavior of engineering ceramics
[PB92-180710] p 3973 N92-33059
OIL FIELDS
Burning oil fields as a source of infrasonic waves
[IRF-PREPRINT-119] p 4061 N92-32842
ON-LINE SYSTEMS
FEDIX on-line information service: Design, develop, test, and implement, an on-line research and education information service
[DE92-013582] p 4090 N92-32985
OPERATING SYSTEMS (COMPUTERS)
The Rochester Checkers Player: Multi-model parallel programming for animate vision
[AD-A247427] p 4050 N92-32568
Analysis of a benchmark suite to evaluate mixed numeric and symbolic processing
[NASA-TM-103907] p 4052 N92-32886
OPERATIONAL PROBLEMS
Simulation test and evaluation of TCAS 2 logic version 6.04
[DOT/FAA/RD-92/23] p 3934 N92-33098
OPERATORS (MATHEMATICS)
Schroedinger operators with singular potentials in the semiclassical limit
[ETN-92-92145] p 4058 N92-32840
OPTICAL COMMUNICATION
Feasibility of a 486 nm Fraunhofer laser source based on a 4F(sub 3/2) yields 4I(sub 9/2) neodymium laser
[AD-A250851] p 4015 N92-32329
Wavelength division multiplexed local area networks
[AD-A247613] p 3979 N92-32573
Correlation of single mode fiber fabrication factors and radiation response
[AD-A247301] p 4074 N92-32613
STARNET: A MultiGbit/s optical local area network with both packet and circuit switching
[AD-A247617] p 4050 N92-32628
Applications of the photorefractive effect and damage induced effects in fibers
[AD-A250767] p 3953 N92-32674
A simple high-performance avalanche photodiode for long-wavelength optical communications, phase 1
[PB92-188259] p 4076 N92-33004
OPTICAL CORRECTION PROCEDURE
The dependence of the anisoplanatic Strehl of a compensated beam on the beacon distribution
[DE92-011272] p 4016 N92-32736
The effect of the light round-trip time on the performance of an adaptive optics turbulence compensation system
[DE92-011273] p 4075 N92-32738
OPTICAL CORRELATORS
Real-time edge-enhanced optical correlator
[NASA-CASE-NPO-18379-1-CU] p 4076 N92-33022
OPTICAL COUPLING
Laser to single-mode-fiber coupling: A laboratory guide
[NASA-CR-4452] p 4077 N92-33239
OPTICAL EQUIPMENT
Beta-barium borate optical parametric oscillator
[AD-A251177] p 4075 N92-32915
An optically controlled Ka-band phased array antenna
p 3983 N92-32968
OPTICAL FIBERS
Correlation of single mode fiber fabrication factors and radiation response
[AD-A247301] p 4074 N92-32613
Can the speed of light in the fiber be controlled?
[AD-A247614] p 4074 N92-32668
High temperature fiber optic microphone having a pressure-sensing reflective membrane under tensile stress
[NASA-CASE-LAR-14402-1-CU] p 4076 N92-33017
Laser to single-mode-fiber coupling: A laboratory guide
[NASA-CR-4452] p 4077 N92-33239
OPTICAL FILTERS
A molecule-specific filter modulator
[AD-A250760] p 4074 N92-32672
A precise narrow-beam filter infrared radiometer and its use with lidar in the ARM Program
[DE92-016872] p 4015 N92-33188
OPTICAL MEASUREMENT
Orbital debris characterization with impact flash signatures
[DE92-010666] p 4018 N92-32701
OPTICAL MEASURING INSTRUMENTS
Depolarized light source for fiber optic sensors
[AD-D015289] p 4074 N92-32634
Scanning force microscopy using optical interferometry
[ISBN-90-9003887-6] p 4077 N92-33146
A precise narrow-beam filter infrared radiometer and its use with lidar in the ARM Program
[DE92-016872] p 4015 N92-33188
OPTICAL MEMORY (DATA STORAGE)
Holographic crosstalk and signal-to-noise ratio in orthogonal data storage
[AD-A250146] p 4013 N92-32323
Auto and hetero-associative memory using a 2-D optical logic gate
[NASA-CASE-NPO-17997-1-CU] p 4041 N92-33057
OPTICAL PROPERTIES
Titan's organic haze p 4097 N92-32372
Formation and growth of photochemical aerosols in Titan's atmosphere p 4100 N92-32393
The Huygens SSP Refractometer (REF)
p 4101 N92-32399
Thin film cadmium telluride, zinc telluride, and mercury zinc telluride solar cells
[DE92-001237] p 4024 N92-32510
Local aspects of the optical reflection problem: The discrete dipole approach
[ISBN-90-9004118-4] p 4074 N92-32703
Orientation, stress, and density distributions in injection-moulded amorphous polymers determined by optical techniques
[ETN-92-92052] p 3972 N92-32752
Real time pre-detection dynamic range compression
[NASA-CASE-NPO-18098-1-CU] p 4076 N92-33028
Modification of the optical properties of Al2O3 by ion implantation
[DE92-013861] p 4085 N92-33127
OPTICAL RADAR
Infrared Targeting System (IRTS) demonstration
p 3937 N92-32446
Detectors for lidar type Thomson scattering diagnostics
[IPF-91-5] p 3990 N92-32823
A simple Doppler wind lidar sensor: Simulated measurements and impacts in a global assimilation and forecast system
[PL-TR-91-2253] p 4034 N92-32859
A precise narrow-beam filter infrared radiometer and its use with lidar in the ARM Program
[DE92-016872] p 4015 N92-33188
OPTICAL SCANNERS
Time-resolved holography for the study of shock waves
[ISBN-0-315-62369-1] p 4013 N92-33226
OPTICAL WAVEGUIDES
Comparative evaluation of optical waveguides as alternative interconnections for high performance packaging p 3984 N92-32974
OPTICS
Diffractive optics technology and the NASA Geostationary Earth Observatory (GEO)
[NASA-CR-190611] p 4076 N92-33074
OPTIMAL CONTROL
Robust stabilization of the Space Station
[NASA-CR-190627] p 3942 N92-32244
Tolerance optimization of servomechanisms
[ISBN-90-9004476-0] p 4018 N92-32692
Using minimax approaches to plan optimal task commutation configurations for combined mobile platform-manipulator systems
[DE91-018864] p 4018 N92-32694
Mixed H(2)/H(sub infinity): Control with output feedback compensators using parameter optimization
[NASA-CR-190070] p 4046 N92-33091
OPTIMIZATION
The weight optimization of an armored crashworthy crewseat through the use of advanced composites and design p 3947 N92-32517
Adaptive information processing and global optimization
[AD-A248450] p 4089 N92-32644
Frequency domain state-space system identification
[NASA-TM-107659] p 4021 N92-32657
Tolerance optimization of servomechanisms
[ISBN-90-9004476-0] p 4018 N92-32692
Minimum cost multiflows in undirected networks
[IMAG-RR-849-M] p 4056 N92-32710
The polychromatic pyrometer in diesel combustion
[ECL-91-42] p 3963 N92-32722
Methods of fine-grain optimization for parallel computer architectures
[ETN-92-92144] p 4051 N92-32821
Approximations and designs for estimating regression coefficients of independent stochastic processes
[IMAG-RR-840-M] p 4060 N92-32839
OPTOELECTRONIC DEVICES
Laser material interaction
[AD-A250853] p 4016 N92-32622
Opto-electronic system for a formal neural network
[TELECOM-91-E-013] p 4075 N92-32805
ORBITALS
Site competition of impurities and grain boundary stability in iron
[AD-A252411] p 4084 N92-32939
ORDNANCE
The design features of rocket motors relating to insensitive munition response to thermo-mechanical stimuli p 3976 N92-33244
ORGANIC CHEMISTRY
Titan's organic chemistry: Results of simulation experiments p 4096 N92-32369
Organic chemistry on Titan: Surface interactions
p 4096 N92-32370
Photochemistry of unsaturated nitriles on Titan
p 4096 N92-32371
Titan's organic haze p 4097 N92-32372
ORGANIC COMPOUNDS
Some problems about IR band integrated intensities; 3 examples for application to Titan: C6H6, HC3N, and C4H2 p 4101 N92-32400
Small passive chemical detector
[DE92-014188] p 4030 N92-32933
ORGANIC MATERIALS
Study on lifetime specific, laser-induced ultrafast fluorescence detection in the time and frequency domain for in-situ environmental analysis of organic pollutants
[KFK-4975] p 4029 N92-32841
ORGANIC WASTES (FUEL CONVERSION)
NEDO Alcohol/Biomass Technology Subcommittee
[DE92-526270] p 3975 N92-32914
ORGANIZATIONS
Automatic access experiment
[AD-A252217] p 4089 N92-32611
ORGANOMETALLIC COMPOUNDS
New applications of ionization and fluorescence techniques for detecting and characterization of open-shell organometallics in the gas phase
[AD-A250923] p 3961 N92-32509
ORGANS
Device for removing foreign objects from anatomic organs
[NASA-CASE-GSC-13306-1] p 4038 N92-33032
ORIFICES
Arc/gas electrode
[NASA-CASE-MFS-29766-1] p 3991 N92-33030
ORTHOGONAL FUNCTIONS
Tropical cyclone motion due to environmental interactions represented by empirical orthogonal functions of the vorticity fields
[AD-A246137] p 4033 N92-32534
Generalizations of the classical Laguerre polynomials and some q-analogues
[ISBN-90-9003765-9] p 4058 N92-32836
ORTHOGONALITY
An efficient and robust grid optimization algorithm
p 4004 N92-32300
Holographic crosstalk and signal-to-noise ratio in orthogonal data storage
[AD-A250146] p 4013 N92-32323
Contribution to the determination of vanishing points using Hough transform
[TELECOM-91-D-008] p 4058 N92-32803
ORTHOTROPIC PLATES
Buckling and postbuckling behavior of square compression-loaded graphite-epoxy plates with circular cutouts p 3952 N92-32587
Shear buckling of specially orthotropic plates with centrally located cutouts p 3953 N92-32589
ORTHOTROPIC SHELLS
Free vibration of thick isotropic and orthotropic cylindrical shells
[DE92-011653] p 4022 N92-32706
OSCILLATIONS
A comparative study of the effects of inhibitor stub length on solid rocket motor combustion chamber pressure oscillations: RSRM at T = 80 seconds, preliminary results p 3945 N92-32248
The role of stochasticity in sawtooth oscillation
[DE92-782004] p 3982 N92-32905
Site competition of impurities and grain boundary stability in iron
[AD-A252411] p 4084 N92-32939
Intermodulation in the oscillatory magnetoresistance of a two-dimensional electron gas p 3984 N92-32975
Measurement of nonlinear mode coupling of tearing fluctuations
[DE92-013901] p 4080 N92-33154
OSCILLATORS
Beta-barium borate optical parametric oscillator
[AD-A251177] p 4075 N92-32915
OSMIUM COMPOUNDS
Excited state processes in transition metal complexes: Redox splitting in soluble polymers
[DE92-011808] p 3971 N92-32631

OUTGASSING
Demand controlled ventilating systems: Sensor market survey. Energy conservation in buildings and community systems programme, annex 18, December 1991
[PB92-180892] p 3977 N92-32825
OXIDATION
Mechanisms of the oxidation of metals and alloys with emphasis on superconductors
[DE92-016840] p 3966 N92-32315
Methane conversion to methanol
[DE92-014349] p 3960 N92-32332
Methane oxidation over dual redox catalysts
[DE92-014358] p 3960 N92-32334
A shock tube study of the reactions of the hydroxyl radical with combustion species
[DE92-012573] p 3960 N92-32464
T (sub c)-delta relations in YBa2Cu3O(7-delta) thin films: Effects of oxygen pressure during growth
[DE92-014432] p 4083 N92-32653
The oxidation of Type 310S stainless steel in mixed gases at elevated temperatures
[DE92-014941] p 3968 N92-32991
A study of the dissolution mechanism by chemical and electrochemical oxidation-reduction of actinide dioxides (UO2, NpO2, PuO2, and AmO2) in an acid aqueous medium
[DE92-014834] p 3965 N92-33126
OXIDATION RESISTANCE
Liquid lubricants for advanced aircraft engines
[NASA-TM-104531] p 3972 N92-32863
OXIDATION-REDUCTION REACTIONS
Methane oxidation over dual redox catalysts
[DE92-014358] p 3960 N92-32334
Excited state processes in transition metal complexes: Redox splitting in soluble polymers
[DE92-011808] p 3971 N92-32631
Macrocyclic polycation complexes for secondary anion binding, molecular recognition, and catalysis
[AD-A251069] p 3972 N92-32913
OXIDES
High-temperature Solid Oxide Fuel Cell (SOFC) generator development project: Environmental assessment
[DE92-014698] p 4026 N92-32924
OXIDIZERS
Navier-Stokes analysis of an oxidizer turbine blade with tip clearance p 3999 N92-32269
OXYGEN
Novel gas phase ion molecule reactions of C60(++) with O2 and NH3
[AD-A250921] p 4066 N92-32556
T (sub c)-delta relations in YBa2Cu3O(7-delta) thin films: Effects of oxygen pressure during growth
[DE92-014432] p 4083 N92-32653
OXYGEN ATOMS
Local environment around the oxygen atoms in Y-Ba-Cu-O studied X ray Absorption Fine Structure (XAFS) spectroscopy
[DE92-014165] p 4081 N92-32470
OXYGEN IONS
Novel gas phase ion molecule reactions of C60(++) with O2 and NH3
[AD-A250921] p 4066 N92-32556
Polar upper atmosphere characterization and supersonic ion escape (polar wind)
[GDR-0917] p 4031 N92-32889
OXYGEN PRODUCTION
An evaluation of the performance characteristics of a two-man molecular sieve oxygen generating system
[DCIEM-91-20] p 4039 N92-33079
OXYGEN SUPPLY EQUIPMENT
An evaluation of the performance characteristics of a two-man molecular sieve oxygen generating system
[DCIEM-91-20] p 4039 N92-33079
OZONE
SAGE 1 data user's guide
[NASA-RP-1275] p 4031 N92-33097
OZONOSPHERE
Environmental consequences of new energy technology. Solar heating, heat stores, and heat pumps
[PB92-180843] p 4025 N92-32605

P

P-N JUNCTIONS
A model for the trap-assisted tunneling mechanism in diffused n-p and implanted n(+)-p HgCdTe photodiodes p 3985 N92-32979
P-N-P JUNCTIONS
High-energy ion implantation for bipolar transistor fabrication
[ISBN-90-9003883-3] p 3992 N92-33144
PACIFIC OCEAN
ARM Tropical Pacific Experiment (ATPEX): Role of cloud, water vapor and convection feedbacks in the coupled ocean/atmosphere system
[DE92-013772] p 4032 N92-32331
A quasi-geostrophic circulation model of the northeast Pacific Ocean
[ISBN-0-315-55106-2] p 4035 N92-33198
PACKAGES
Comparative evaluation of optical waveguides as alternative interconnections for high performance packaging p 3984 N92-32974
PACKAGING
Comparative evaluation of optical waveguides as alternative interconnections for high performance packaging p 3984 N92-32974
Insensitive Munitions
[AGARD-CP-511] p 3975 N92-33240
The United States Air Force explosives hazards reduction program p 3976 N92-33241
PACKET SWITCHING
STARNET: A MultiGbit/s optical local area network with both packet and circuit switching
[AD-A247617] p 4050 N92-32628
Message delay models of packet-switching networks
[ISBN-0-315-57208-6] p 4053 N92-33235
PACKET TRANSMISSION
STARNET: A MultiGbit/s optical local area network with both packet and circuit switching
[AD-A247617] p 4050 N92-32628
PAIN
Midwest free-electron laser program
[AD-A247264] p 4016 N92-32540
PAINTS
Corrosion-resistant alkyd coatings
[AD-D015330] p 3974 N92-33177
PAIR PRODUCTION
Experimental particle physics at the University of Pittsburgh
[DE92-014181] p 4066 N92-32702
PALEOMAGNETISM
Steady induction effects in geomagnetism. Part 1A: Steady motional induction of geomagnetic chaos
[NASA-TP-3272-PT-1A] p 4031 N92-32655
PALLADIUM
Density variations and anomalies in palladium compacts
[DE92-014382] p 3967 N92-32721
Hydrogen permeation through bilayer metallic membranes
[UTIAS-TN-342] p 3967 N92-32794
Radiography to measure the longitudinal density gradients of Pd compacts
[DE92-014383] p 3968 N92-32896
PALLADIUM ALLOYS
Substrate reactions and flux pinning structures in melt-processed YBa2Cu3O7 deposits on Ag-Pd alloy substrates
[DE92-014404] p 4084 N92-32919
PANEL METHOD (FLUID DYNAMICS)
Potential flow theory and operation guide for the panel code PMARC
[NASA-TM-102851] p 3929 N92-32422
Further development of the CANAERO computer code to include propulsor modelling
[DREA-CR-90-425] p 3931 N92-32811
PANELS
Global/local methods research using the CSM testbed p 3949 N92-32528
Survivability characteristics of composite compression structure p 3950 N92-32578
Real-time edge-enhanced optical correlator
[NASA-CASE-NPO-18379-1-CU] p 4076 N92-33022
PARABOLIC FLIGHT
Free motion of an unsupported tank that is partially filled with liquid
[NLR-TP-91185-U] p 4011 N92-32831
PARABOLIC REFLECTORS
Testing of the single-element stretched-membrane dish
[DE92-013680] p 4025 N92-32549
Solar thermal energy: Viable energy technology for today and tomorrow
[DE92-015039] p 4026 N92-32923
Summary of engineering-scale experiments for the Solar Detoxification of Water project
[DE92-013776] p 4027 N92-33150
PARACHUTES
Effects of the abrasiveness of test and training site soils on parachute life
[AD-A252389] p 3931 N92-32900
PARAFFINS
Solar photo-thermal catalytic reactions to produce high value chemicals
[DE91-002140] p 4026 N92-32908
PARALLEL COMPUTERS
Methods of fine-grain optimization for parallel computer architectures
[ETN-92-92144] p 4051 N92-32821
Experiments with an ordinary differential equation solver in the parallel solution of method of lines problems on a shared memory parallel computer, part 2
[DE92-017159] p 4052 N92-32926
Quantum wave modeling on highly parallel distributed memory machines
[DE92-014507] p 4088 N92-33109
CSP: A distributed logic programming language for discrete event simulation
[ISBN-0-315-54272-1] p 4048 N92-33214
PARALLEL PROCESSING (COMPUTERS)
The Rochester Checkers Player: Multi-model parallel programming for animate vision
[AD-A247427] p 4050 N92-32568
Real-time processing of radar return on a parallel computer
[NASA-CR-4456] p 3932 N92-32606
Parallel processing in space applications using transputer networks
[MBB-UO-0172-90-PUB] p 4050 N92-32689
Study and achievement of a parallel simulator for diffusion at the atomic level: Creation and growth of dislocation loops under electronic radiation
[LAAS-92118] p 4066 N92-32735
Parallel implementation of Droid and performance evaluation
[OUEL-1926/92] p 4051 N92-32759
Study of a cellular programmable architecture: Functional definition and programming method
[ETN-92-91663] p 4051 N92-32768
Functions and genericity in a parallel programming language
[ETN-92-91667] p 4051 N92-32771
Methods of fine-grain optimization for parallel computer architectures
[ETN-92-92144] p 4051 N92-32821
Experiments with an ordinary differential equation solver in the parallel solution of method of lines problems on a shared memory parallel computer, part 2
[DE92-017159] p 4052 N92-32926
Sparse matrix algorithms on distributed memory multiprocessors
[DE92-017870] p 4046 N92-33071
CSP: A distributed logic programming language for discrete event simulation
[ISBN-0-315-54272-1] p 4048 N92-33214
PARALLEL PROGRAMMING
The Rochester Checkers Player: Multi-model parallel programming for animate vision
[AD-A247427] p 4050 N92-32568
Parallel implementation of Droid and performance evaluation
[OUEL-1926/92] p 4051 N92-32759
Study of a cellular programmable architecture: Functional definition and programming method
[ETN-92-91663] p 4051 N92-32768
Functions and genericity in a parallel programming language
[ETN-92-91667] p 4051 N92-32771
Exploiting two-dimensional explicit parallelism on vector architectures
[ETN-92-92136] p 4051 N92-32795
Methods of fine-grain optimization for parallel computer architectures
[ETN-92-92144] p 4051 N92-32821
PARAMETER IDENTIFICATION
The design and development of a portable, DSP micro-processor based, high-accuracy data acquisition system
[NRC-32146] p 4040 N92-32851
PARAMETERIZATION
Numerical analysis of the hot-gas-side and coolant-side heat transfer in liquid rocket engine combustors p 4004 N92-32299
Geometric continuity and Frenet continuity of parametric curves
[IMAG-RR-846-M] p 4057 N92-32761
Functions and genericity in a parallel programming language
[ETN-92-91667] p 4051 N92-32771
Shape recognition by computer in simulated aerial images
[DCIEM-91-05] p 4054 N92-32854
Mixed H(2)/H(sub infinity): Control with output feedback compensators using parameter optimization
[NASA-CR-190070] p 4046 N92-33091
PARAMETRIC AMPLIFIERS
Beta-barium borate optical parametric oscillator
[AD-A251177] p 4075 N92-32915

PARTIAL DIFFERENTIAL EQUATIONS
PDES application protocol suite for composites (PAS-C). Functional needs report for the PAS-C program
[AD-A247886] p 3953 N92-32629
PARTIAL PRESSURE
A research program on radiative transfer model development in support of the ARM program
[DE92-014495] p 4031 N92-33153
PARTICLE ACCELERATOR TARGETS
Light-ion spectroscopy with exotic targets
[DE92-017258] p 3964 N92-32929
PARTICLE ACCELERATORS
Heavy flavor physics at hadron colliders
[DE92-014482] p 4064 N92-32312
High accuracy beam energy measurement for linear and circular accelerators
[DE92-016966] p 4069 N92-32319
Booster Applications Facility report, phase 2
[DE92-013395] p 4070 N92-32411
Spectroscopic characterization of LEVIS active ion source on PBFA 2
[DE92-014954] p 4080 N92-32992
Shielding analyses for repetitive high energy pulsed power accelerators
[DE92-015004] p 4072 N92-32994
PARTICLE BEAMS
Collaborative, remote, in-depth inspection and verification of satellites with neutral particle beams
[DE92-014195] p 3943 N92-32934
Spectroscopic characterization of LEVIS active ion source on PBFA 2
[DE92-014954] p 4080 N92-32992
PARTICLE COLLISIONS
Supersymmetry searches at electron-proton colliders
[ETN-92-92057] p 4067 N92-32753
PARTICLE INTERACTIONS
On the choice of minimization functional in the partial wave analysis
[DE92-624689] p 4087 N92-32309
Observation of (pi)(-)p yields (omega)(eta)n reaction at 38 GeV/c momentum
[DE92-624690] p 4064 N92-32310
Comparison of spin asymmetries and invariant cross sections in production of (pi)(sup 0) mesons by polarized antiprotons and protons with 200 GeV energy
[DE92-624691] p 4064 N92-32311
Heavy flavor physics at hadron colliders
[DE92-014482] p 4064 N92-32312
Beamstrahlung spectra in next generation linear colliders
[DE92-010730] p 4069 N92-32337
First results of measurements of A(sub LL) two-spin asymmetry in inclusive production of (pi)(sup 0) mesons by polarized protons and antiprotons with 200 GeV energy
[DE92-624692] p 4065 N92-32497
Implantation of carbon in GaAs
[DE92-016921] p 4085 N92-33117
Research and development of a helium-4 based solar neutrino detector
[DE92-017390] p 4103 N92-33119
Partons and the EMC spin effect
[RAL-92-015-PREPRINT] p 4068 N92-33137
A study of four jet events and search for double parton scattering at square root s = 1.8 TeV
[DE92-016351] p 4069 N92-33164
PARTICLE MASS
Neutrino masses in the flipped SU(5) tensor product U(1) and the SU(4) tensor product O(4) GUT models
[RAL-92-012] p 4068 N92-33135
PARTICLE MOTION
Development of the KIVA-2 CFD code for rocket propulsion applications p 3945 N92-32272
The energetics and dynamics of free radicals, ions, and clusters
[DE92-014124] p 4068 N92-33083
PARTICLE PRODUCTION
On the choice of minimization functional in the partial wave analysis
[DE92-624689] p 4087 N92-32309
Observation of (pi)(-)p yields (omega)(eta)n reaction at 38 GeV/c momentum
[DE92-624690] p 4064 N92-32310
Comparison of spin asymmetries and invariant cross sections in production of (pi)(sup 0) mesons by polarized antiprotons and protons with 200 GeV energy
[DE92-624691] p 4064 N92-32311
First results of measurements of A(sub LL) two-spin asymmetry in inclusive production of (pi)(sup 0) mesons by polarized protons and antiprotons with 200 GeV energy
[DE92-624692] p 4065 N92-32497
PARTICLE SIZE DISTRIBUTION
Formation of high temperature superconductors from the solidified melt
[DE92-012584] p 4081 N92-32465
Orbital debris characterization with impact flash signatures
[DE92-010666] p 4018 N92-32701
PARTICLE SPIN
Partons and the EMC spin effect
[RAL-92-015-PREPRINT] p 4068 N92-33137
PARTICLE THEORY
First results of measurements of A(sub LL) two-spin asymmetry in inclusive production of (pi)(sup 0) mesons by polarized protons and antiprotons with 200 GeV energy
[DE92-624692] p 4065 N92-32497
Possible effects of additional vector bosons in e(sup +)e(sup -)(yields)f(bar-f) at the TRISTAN energies
[DE92-624727] p 4065 N92-32498
PARTICULATES
Aluminum based particulate composites for aerospace applications produced by different processes
[MBB-Z-0408-91-PUB] p 3967 N92-32819
PARTONS
Partons and the EMC spin effect
[RAL-92-015-PREPRINT] p 4068 N92-33137
A study of four jet events and search for double parton scattering at square root s = 1.8 TeV
[DE92-016351] p 4069 N92-33164
PATTERN RECOGNITION
An adaptive algorithm for modifying hyperellipsoidal decision surfaces
[DE92-013540] p 4041 N92-32414
Shape recognition by computer in simulated aerial images
[DCIEM-91-05] p 4054 N92-32854
Fuzzy set methods for object recognition in space applications
[NASA-CR-190388] p 4047 N92-33093
Pattern recognition based on entropy analysis and shape transformations
[ISBN-0-315-56074-6] p 4046 N92-33201
Primal access recognition of visual objects
[ISBN-0-315-63509-6] p 4048 N92-33212
PAVEMENTS
Performance of insulated pavements at Newton Fields, Jackman, Maine
[CRREL-92-9] p 3940 N92-32903
PAYLOAD CONTROL
A prototype software engineering environment for domain modeling and reuse p 4046 N92-32882
PAYLOAD INTEGRATION
Advancing automation and robotics technology for the Space Station Freedom and for the US economy
[NASA-TM-103940] p 4040 N92-32809
PAYLOADS
The Huygens probe p 4099 N92-32388
A surface science package for the Huygens Titan probe p 4102 N92-32410
Rotating-unbalanced-mass devices and methods for scanning balloon-borne-experiments, free-flying spacecraft, and space shuttle/space station attached experiments
[NASA-CASE-MFS-28425-1] p 4015 N92-33010
Integrated launch and emergency vehicle system
[NASA-CASE-LAR-13780-1] p 3943 N92-33013
PEEK
Compression behavior of graphite-epoxy and graphite-thermoplastic panels with circular holes or impact damage p 3951 N92-32582
A new test method to determine the compressive strength of fiber-reinforced composites p 3956 N92-33035
The effect of heat treatment on the properties of PEEK and APC-2 p 3959 N92-33052
PEGASUS AIR-LAUNCHED BOOSTER
A computational fluid dynamics analysis of the hypersonic flights of Pegasus
[NASA-CR-186023] p 4007 N92-32560
PELLETS
Alpha particle diagnostics using impurity pellet injection
[DE92-013796] p 4078 N92-32623
PENDULUMS
Geometrical effects in two-dimensional arrays of Josephson junctions
[AD-A252209] p 4084 N92-32898
PENETRATION
Magnetic penetration depth of YBa2Cu3O(7-delta) thin films determined by the power transmission method p 3985 N92-32983
ROAR: A 3-D tethered rocket simulation code
[DE92-017358] p 3944 N92-33166
PEPTIDES
Neutron scatter studies of chromatin structures related to functions
[DE92-014032] p 4036 N92-33181
PERCEPTION
Temporal and spatial factors affecting the perception of computer-generated imagery
[AD-A249242] p 4046 N92-32907
PERCOLATION
Electric and magnetic properties of random superconductors
[ITN-92-85165] p 4086 N92-33190
PERFORMANCE PREDICTION
Development of CFD code evaluation criteria and a procedure for assessing predictive capability and performance p 4001 N92-32283
Effect of including variable gas properties and entrained particles in the flow analysis of the ASRM nozzle p 4006 N92-32306
Compression of thick laminated composite beams with initial impact-like damage
[NASA-CR-190573] p 3946 N92-32491
Development and proof-testing of advanced absorption refrigeration cycle concepts
[DE92-014933] p 3977 N92-32723
Study of the mechanical behaviour of graphite/epoxy laminates subjected to static and cyclic loading
[NRC-30833] p 3955 N92-32813
Proceedings of the Sixteenth Annual Software Engineering Workshop
[NASA-TM-107964] p 4044 N92-32869
Optimized set reduction for empirically guiding software development p 4044 N92-32875
Ski jump takeoff performance predictions for a mixed-flow, remote-lift STOVL aircraft
[NASA-TM-103866] p 3935 N92-32887
Recent advances in statistical energy analysis p 4062 N92-32954
Feasibility study for predicting human reliability growth through training and practice
[AD-A252371] p 4038 N92-32990
PERFORMANCE TESTS
Technology test bed review p 4001 N92-32279
CFD analysis to optimize a design modification of BSMT p 4004 N92-32296
Supportability evaluation of thermoplastic and thermoset composites p 3950 N92-32576
Residual strength of repaired graphite/epoxy laminates after 5 years of outdoor exposure p 3950 N92-32577
A test circuit for capacitor bank grounding sticks
[AD-A251121] p 3989 N92-32700
UHM/HNEI EV test and evaluation program
[DE92-011631] p 3989 N92-32754
Study of the mechanical behaviour of graphite/epoxy laminates subjected to static and cyclic loading
[NRC-30833] p 3955 N92-32813
Overview and evolution of the LeRC PMAD DC Testbed
[NASA-TM-105842] p 3991 N92-32867
An evaluation of the performance characteristics of a two-man molecular sieve oxygen generating system
[DCIEM-91-20] p 4039 N92-33079
Simulation test and evaluation of TCAS 2 logic version 6.04
[DOT/FAA/RD-92/23] p 3934 N92-33098
Rapid development of the X-31 simulation to support flight-testing
[NASA-TM-104256] p 3935 N92-33149
PERIODIC FUNCTIONS
Steady state behavior of reduced dynamic systems with local nonlinearities
[ISBN-90-9004680-1] p 4056 N92-32707
PERIPHERAL EQUIPMENT (COMPUTERS)
Program PLOTTAB: A code designed to plot continuous and/or discrete physical data
[DE92-013754] p 4041 N92-32416
PERIPHERAL VISION
Instrument scanning and subjective workload with the peripheral vision horizon display
[CTN-92-60359] p 4038 N92-32817
PERMEATING
Hydrogen permeation through bilayer metallic membrranes
[UTIAS-TN-342] p 3967 N92-32794
PERMITTIVITY
Dielectric constant measurements in simulated Titan ocean liquids p 4102 N92-32409
PERSONNEL
Toward advanced human reliability programs. Structural development considerations and options for extreme risk environments
[AD-A250786] p 4038 N92-32660
A causal analysis of interrelationships among exercise, physical fitness, and well-being in US Navy personnel
[AD-A252719] p 4037 N92-32942
PERTURBATION THEORY
Quark-antiquark Regge trajectories in large N(sub c) QCD
[DE92-016462] p 4064 N92-32313

Point interactions in L(sup p)
[REPT-91-97] p 4057 N92-32756
PETN
Extending estimation of C-J pressure of explosives to the very low density region
[DE92-015035] p 3975 N92-33003
PETRI NETS
Analytic performance of software pipelines with rendezvous and communication tasks
[ISBN-0-315-54414-7] p 4052 N92-33216
PHASE DETECTORS
Study and development of a six port network analyzer in the 1-18 GHz frequency range
[TELECOM-91-E-005] p 3980 N92-32739
PHASE DIAGRAMS
Formation of high temperature superconductors from the solidified melt
[DE92-012584] p 4081 N92-32465
PHASE MODULATION
Study on lifetime specific, laser-induced ultrafast fluorescence detection in the time and frequency domain for in-situ environmental analysis of organic pollutants
[KFK-4975] p 4029 N92-32841
PHASE SEPARATION (MATERIALS)
Synthesis, morphology and properties of polyester-urethane in solution in styrene: Application to composites development
[ISAL-92-0007] p 3972 N92-32762
PHASE SHIFT CIRCUITS
V-band pseudomorphic HEMT MMIC phased array components for space communications
p 3983 N92-32966
An optically controlled Ka-band phased array antenna
p 3983 N92-32968
PHASE TRANSFORMATIONS
Mechanisms of the oxidation of metals and alloys with emphasis on superconductors
[DE92-016840] p 3966 N92-32315
Morphology, 31P spin diffusion, and phase transitions in a representative semicrystalline polyphosphazene by solid-state NMR
[AD-A250883] p 3961 N92-32553
Generic consequences of fundamental studies of beta phase decomposition modes in titanium and related alloy systems
[AD-A250789] p 3967 N92-32699
Continuum configurational bias Monte-Carlo studies of alkanes and polyethylene
[DE92-016545] p 3965 N92-33185
PHASE VELOCITY
Morphology, 31P spin diffusion, and phase transitions in a representative semicrystalline polyphosphazene by solid-state NMR
[AD-A250883] p 3961 N92-32553
PHASED ARRAYS
Phased array implementation using elements with scan capability
[CTN-92-60335] p 3981 N92-32787
Phase-only synthesis for multiple-beam phased arrays with element failures
[AD-A252250] p 3982 N92-32891
V-band pseudomorphic HEMT MMIC phased array components for space communications
p 3983 N92-32966
An optically controlled Ka-band phased array antenna
p 3983 N92-32968
Coplanar waveguide feeds for phased array antennas
p 3983 N92-32970
PHONONS
The influence of anharmonic phonons on the isotope effect in high-(Tc) oxides
[DE92-017083] p 4081 N92-32320
PHOSPHAZENE
Morphology, 31P spin diffusion, and phase transitions in a representative semicrystalline polyphosphazene by solid-state NMR
[AD-A250883] p 3961 N92-32553
PHOSPHORUS POLYMERS
Towards well-defined polysilanes and polyphosphazenes
[AD-A251098] p 3971 N92-32547
PHOTOCHEMICAL REACTIONS
Modeling of the diurnal variations of the atmosphere of Titan p 4096 N92-32366
Photochemistry of unsaturated nitriles on Titan
p 4096 N92-32371
Huygens/ACP: An instrument for aerosols chemical composition measurements p 4098 N92-32379
Formation and growth of photochemical aerosols in Titan's atmosphere p 4100 N92-32393
Study of transmitted light through the atmosphere of Titan p 4102 N92-32408
Excited state processes in transition metal complexes: Redox splitting in soluble polymers
[DE92-011808] p 3971 N92-32631
Photogenerated carrier-induced reactions on UHV semiconductor surfaces
[DE92-015355] p 4082 N92-32641
Solar photo-thermal catalytic reactions to produce high value chemicals
[DE91-002140] p 4026 N92-32908
High-flux solar photon processes
[DE92-001247] p 4027 N92-33138
Study of flow properties of wet solids using laser induced photochemical anemometry
[DE92-014031] p 4017 N92-33180
PHOTOCONDUCTIVITY
Program for research in conducting polymers
[AD-A250965] p 3971 N92-32665
Reduced mobility and PPC in In(.20)Ga(.80)As / Al(.23)Ga(.77)As HEMT structure p 3984 N92-32976
PHOTODIODES
A model for the trap-assisted tunneling mechanism in diffused n-p and implanted n(+)-p HgCdTe photodiodes
p 3985 N92-32979
A simple high-performance avalanche photodiode for long-wavelength optical communications, phase 1
[PB92-188259] p 4076 N92-33004
PHOTODISSOCIATION
Modeling of the diurnal variations of the atmosphere of Titan p 4096 N92-32366
New applications of ionization and fluorescence techniques for detecting and characterization of open-shell organometallics in the gas phase
[AD-A250923] p 3961 N92-32509
Collective resonances of valence electrons in free metal clusters
[DE92-014783] p 3969 N92-33116
PHOTOELASTIC ANALYSIS
Some new perspectives in photoelasticity and curved-ray tomography
[ISBN-0-315-57756-8] p 4023 N92-33200
PHOTOELASTICITY
Some new perspectives in photoelasticity and curved-ray tomography
[ISBN-0-315-57756-8] p 4023 N92-33200
PHOTOELECTRICITY
On the Titan/28 Sagittarii occultation of 1989 July 3
p 4101 N92-32403
PHOTOELECTROCHEMISTRY
High-flux solar photon processes
[DE92-001247] p 4027 N92-33138
PHOTOELECTRONS
The energetics and dynamics of free radicals, ions, and clusters
[DE92-014124] p 4068 N92-33083
PHOTOGRAPHIC MEASUREMENT
Debris/ice/TPS assessment and integrated photographic analysis for Shuttle Mission STS-49
[NASA-TM-107547] p 3941 N92-32454
PHOTOIONIZATION
The energetics and dynamics of free radicals, ions, and clusters
[DE92-014124] p 4068 N92-33083
Molecular surface analysis by laser ionization of desorbed molecules
[DE92-016320] p 4016 N92-33114
Mass resolved resonance ionization spectroscopy of combustion radicals
[DE92-016833] p 3965 N92-33222
PHOTOLYSIS
Laboratory investigations of the aerosols in the stratosphere of Titan p 4102 N92-32405
Summary of engineering-scale experiments for the Solar Detoxification of Water project
[DE92-013776] p 4027 N92-33150
PHOTOMETRY
Radiometric and spectral measurement instruments
[AD-A250771] p 4013 N92-32343
PHOTOMULTIPLIER TUBES
Detectors for lidar type Thomson scattering diagnostics
[IPF-91-5] p 3990 N92-32823
PHOTON BEAMS
Thermal and structural analysis of high precision beamline position monitors for synchrotron x ray beams
[DE92-014863] p 4072 N92-33130
PHOTONS
High power testing of the prototype accelerating cavity (352 MHz) for the Advanced Photon Source (APS)
[DE92-016697] p 4069 N92-32314
Theoretical and experimental studies of elementary physics
[DE92-014877] p 4061 N92-32430
Proceedings of the fourth users meeting for the advanced photon source
[DE92-014061] p 4072 N92-32932
Photon excitation for satellite free x ray spectroscopy: Instrumentation challenges
[DE92-016999] p 4067 N92-32997
High-flux solar photon processes
[DE92-001247] p 4027 N92-33138
PHOTOPRODUCTION
Elementary particle physics and high energy phenomena
[DE92-016844] p 4069 N92-33187
PHOTOSYNTHESIS
Simulations of the carbon cycle in the oceans
[DE92-016622] p 4035 N92-32336
High-flux solar photon processes
[DE92-001247] p 4027 N92-33138
PHOTOVOLTAIC CELLS
Solar radiation on a catenary collector
[NASA-TM-105751] p 3988 N92-32243
PHOTOVOLTAIC CONVERSION
Thin film cadmium telluride, zinc telluride, and mercury zinc telluride solar cells
[DE92-001237] p 4024 N92-32510
The photovoltics program at Sandia National Laboratories
[DE92-014617] p 4026 N92-32946
PHYSICAL EXERCISE
A causal analysis of interrelationships among exercise, physical fitness, and well-being in US Navy personnel
[AD-A252719] p 4037 N92-32942
PHYSICAL FITNESS
A causal analysis of interrelationships among exercise, physical fitness, and well-being in US Navy personnel
[AD-A252719] p 4037 N92-32942
PHYSICAL OPTICS
Determining surface profile from sequential interference patterns from a long trace profiler
[DE92-017117] p 4073 N92-32321
Optics of beam transport in the NSLS UV-FEL
[DE92-014166] p 4015 N92-32511
PHYSICAL PROPERTIES
Transmission electron microscope characterization of deformation and recovery in 304L stainless steel part
[DE92-013237] p 3966 N92-32614
PHYSIOLOGICAL EFFECTS
Comparative effects of antihistamines on aircrew performance of simple and complex tasks under sustained operations
[AD-A248752] p 4036 N92-32492
Bacterial responses to extreme temperatures and pressures and to heavy organic loading
[AD-A247456] p 4035 N92-32571
PHYSIOLOGICAL TESTS
Development of the OMPAT neuropsychological/psychomotor performance evaluation and OMPAT data and timing support
[AD-A250793] p 4037 N92-32504
DCIEM/Central Medical Board Aircrew ECG program: Recommendations for restructuring
[DCIEM-90-47] p 4037 N92-32816
PHYSIOLOGY
Measurement of the magnetic and electrical activity of individual cells in vitro
[AD-A250881] p 4035 N92-32345
PHYTOTRONS
Director's discretionary fund report for FY 1991
[NASA-TM-103902] p 4105 N92-33106
PICOSECOND PULSES
Surfaces and thin films studied by picosecond ultrasonics
[DE92-016313] p 4020 N92-32564
PIEZOELECTRIC GAGES
The use of piezoelectric sensors to detect delamination initiation in carbon fiber reinforced composites
[MBB-Z-0391-91-PUB] p 3954 N92-32740
PIEZOELECTRICITY
Active control of interior noise in a large scale cylinder using piezoelectric actuators p 4063 N92-32958
Passive fetal monitoring sensor
[NASA-CASE-LAR-14088-1-CU] p 4015 N92-33016
PIGMENTS
Corrosion-resistant alkyd coatings
[AD-D015330] p 3974 N92-33177
PILOT ERROR
A review and discussion of flight management system incidents reported to the aviation safety reporting system
[AD-A252438] p 3932 N92-32941
PILOT PERFORMANCE
Instrument scanning and subjective workload with the peripheral vision horizon display
[CTN-92-60359] p 4038 N92-32817
PILOT TRAINING
Briefing notes on a manned aircraft research and support simulation facility
[AD-A250373] p 3935 N92-32326
PILOTLESS AIRCRAFT
Operational needs for an unmanned air vehicle
p 3936 N92-32438
Naval target classification and designation with the CL-227 Sea Sentinel p 3937 N92-32449

PILOTS (PERSONNEL)
Pilots noise exposure during a Boeing 747-400 round trip: Ambient noise and acoustic-head recording and analysis of data p 4063 N92-32960
Pilot noise exposure during a Boeing 747-400 round trip: Judgement of noise and analysis in respect to hearing impairment of pilots p 4063 N92-32961

PINNING
Thickness dependence of vortex pinning in epitaxial Tl-Ca-Ba-Cu-O thin films
[DE92-015011] p 4084 N92-32920

PIONS
On the choice of minimization functional in the partial wave analysis
[DE92-624689] p 4087 N92-32309
Observation of (pi)(-)p yields (omega)(eta)n reaction at 38 GeV/c momentum
[DE92-624690] p 4064 N92-32310
Comparison of spin asymmetries and invariant cross sections in production of (pi)(sup 0) mesons by polarized antiprotons and protons with 200 GeV energy
[DE92-624691] p 4064 N92-32311
First results of measurements of A(sub LL) two-spin asymmetry in inclusive production of (pi)(sup 0) mesons by polarized protons and antiprotons with 200 GeV energy
[DE92-624692] p 4065 N92-32497
Theoretical nuclear physics
[DE92-016837] p 4069 N92-33186

PIPE FLOW
A numerical study of natural convection in a narrow annulus
[DE92-017138] p 4006 N92-32322
Interactive control in turbulent shear layers
[AD-A250711] p 4008 N92-32671

PIPELINING (COMPUTERS)
Methods of fine-grain optimization for parallel computer architectures
[ETN-92-92144] p 4051 N92-32821
Analytic performance of software pipelines with rendezvous and communication tasks
[ISBN-0-315-54414-7] p 4052 N92-33216

PISTONS
Contribution to the theoretical and experimental analysis of camshaft engine operation
[ETN-92-91961] p 4018 N92-32726

PITCH
Exposures from headset interference tones
[AD-A247175] p 4061 N92-32697

PITTING
Electrochemical polarization measurements on pitting corrosion susceptibility of nickel-rich Alloy 825
[DE92-014885] p 3969 N92-33132

PLANAR STRUCTURES
Reducing torque fluctuation in linkage drive shafts
[ESDU-92016] p 4017 N92-32482
Analysis of shielded CPW discontinuities with air-bridges p 3983 N92-32971

PLANCKS CONSTANT
Higher superdeformed band members in Hg-190: Evidence for a band interaction?
[DE92-016778] p 4082 N92-32542

PLANETARY ATMOSPHERES
Titan's organic chemistry: Results of simulation experiments p 4096 N92-32369
Gas chromatography and pyrolysis-GC with capillary columns: Application to the in situ analysis of Titan's atmosphere p 4100 N92-32397
On the Titan/28 Sagittarii occultation of 1989 July 3 p 4101 N92-32403

PLANETARY BOUNDARY LAYER
A preliminary assessment of the Titan planetary boundary layer p 4095 N92-32363

PLANETARY COMPOSITION
Interior of Titan p 4094 N92-32352

PLANETARY ENVIRONMENTS
Plausible surface models for Titan p 4098 N92-32381

PLANETARY EVOLUTION
Some issues associated with the formation of the Saturnian system p 4093 N92-32349
Formation of the satellites p 4093 N92-32350

PLANETARY GRAVITATION
Gravitational tide in the atmosphere of Titan p 4096 N92-32364

PLANETARY IONOSPHERES
Plasma interaction of Titan with the Saturnian magnetosphere: A review of critical issues p 4098 N92-32382
Atmospheric escape from Titan p 4099 N92-32384
The ionosphere of Titan and its interaction with Saturnian magnetospheric electrons p 4099 N92-32386

PLANETARY MAGNETOSPHERES
Plasma interaction of Titan with the Saturnian magnetosphere: A review of critical issues p 4098 N92-32382
Mass loading at Titan and comets p 4098 N92-32383
Titan's magnetospheric interaction p 4099 N92-32385
The ionosphere of Titan and its interaction with Saturnian magnetospheric electrons p 4099 N92-32386

PLANETARY MAGNETOTAILS
Titan's magnetospheric interaction p 4099 N92-32385

PLANETARY MAPPING
Observing the surface of Titan through near-infrared windows in its atmosphere p 4097 N92-32374

PLANETARY MASS
Atmospheric escape from Titan p 4099 N92-32384

PLANETARY NEBULAE
Some issues associated with the formation of the Saturnian system p 4093 N92-32349

PLANETARY SURFACES
Observing the surface of Titan through near-infrared windows in its atmosphere p 4097 N92-32374
The detectability of Titan's surface in the near-infrared p 4097 N92-32375
VIMS/Cassini mission at Titan: Scientific objectives and observational scenarios p 4097 N92-32377
Plausible surface models for Titan p 4098 N92-32381
Huygens probe: The surface mission p 4101 N92-32402

PLANETARY WAVES
Dynamics of Rossby waves in a parabolic jet
[ISBN-0-315-57159-4] p 4034 N92-33225

PLANETOLOGY
Formation of the satellites p 4093 N92-32350

PLANNING
Ethernet bandwidth utilization of datafull, dataless, and diskless node workstation and x-terminals
[AD-A252374] p 4052 N92-32937
A study of artificial intelligence planning: A framework for a planning development system
[ISBN-0-315-54378-7] p 4055 N92-33219

PLASMA ARC WELDING
A prototype backside purge control system
[NASA-CR-190816] p 3969 N92-33081

PLASMA COMPOSITION
Scrape-off layer modeling of radiative divertor and high heat flux experiments on D3-D
[DE92-015007] p 4080 N92-32995

PLASMA CONTROL
Transverse beam dynamics in recirculating accelerators for heavy-ion fusion
[DE92-013448] p 4070 N92-32413
Magnetohydrodynamic stability of plasmas with radial motion
[DE92-013917] p 4077 N92-32417
Formation and sustainment of a very low aspect ratio tokamak using coaxial helicity injection: Helicity Injected Torus (HIT) experiment
[DE92-014311] p 4078 N92-32595
Alpha particle diagnostics using impurity pellet injection
[DE92-013796] p 4078 N92-32623
Fast ion loss and radial electric field in Wendelstein 7-A stellarator
[DE92-782106] p 4079 N92-32745
Status of LHD control system design
[NIFS-122] p 4070 N92-32746
Study of recirculating induction accelerators as drivers for heavy ion fusion
[DE92-016980] p 4071 N92-32904
Spectroscopic characterization of LEVIS active ion source on PBFA 2
[DE92-014954] p 4080 N92-32992
Turbulence transport equations for variable-density turbulence and their relationship to two-field models
[DE92-017292] p 4013 N92-33159

PLASMA DENSITY
Theory and numerical simulation of some wide-angle wide-bandpass plasma particle analyzers
[ISBN-0-315-58015-1] p 4080 N92-33223

PLASMA DIAGNOSTICS
Laser measurements for experiments on the TROLL accelerator
[DE92-016578] p 4015 N92-32335
Injection of compact toroids for tokamak fueling and current drive
[DE92-010031] p 4077 N92-32533
Formation and sustainment of a very low aspect ratio tokamak using coaxial helicity injection: Helicity Injected Torus (HIT) experiment
[DE92-014311] p 4078 N92-32595
Alpha particle diagnostics using impurity pellet injection
[DE92-013796] p 4078 N92-32623
Activities report of the Institute of Plasma Research
[ETN-92-92147] p 4079 N92-32797
Diagnostics and modeling of ECRH microwave discharges
[IPF-91-3] p 4079 N92-32822
Edge gradient and safety factor effects on electrostatic turbulent transport in tokamaks
[DE92-014323] p 4079 N92-32944

PLASMA DIFFUSION
Plasma diffusion through multidipole magnetic fields
[INPE-5384-PRE/1750] p 4079 N92-32662

PLASMA DRIFT
Mass loading at Titan and comets p 4098 N92-32383

PLASMA DYNAMICS
Nonlinear dynamics and plasma transport
[DE92-014246] p 4078 N92-32592

PLASMA EQUILIBRIUM
Magnetohydrodynamic stability of plasmas with radial motion
[DE92-013917] p 4077 N92-32417
MHD computation of feedback of resistive-shell instabilities in the reversed field pinch
[DE92-014325] p 4078 N92-32599
Ion heating and MHD dynamo fluctuations in the reversed field pinch
[DE92-013902] p 4078 N92-32624
Measurement of nonlinear mode coupling of tearing fluctuations
[DE92-013901] p 4080 N92-33154

PLASMA FLUX MEASUREMENT
Theory and numerical simulation of some wide-angle wide-bandpass plasma particle analyzers
[ISBN-0-315-58015-1] p 4080 N92-33223

PLASMA GENERATORS
Electromagnetic-wave propagation in unmagnetized plasmas
[AD-A250710] p 3980 N92-32719

PLASMA HEATING
Ion heating and MHD dynamo fluctuations in the reversed field pinch
[DE92-013902] p 4078 N92-32624

PLASMA INTERACTIONS
Plasma interaction of Titan with the Saturnian magnetosphere: A review of critical issues p 4098 N92-32382
Mass loading at Titan and comets p 4098 N92-32383
Satellite anomalies and electrostatic surface discharges
[AD-A246880] p 3942 N92-32538

PLASMA PHYSICS
Status of LHD control system design
[NIFS-122] p 4070 N92-32746
Activities report of the Institute of Plasma Research
[ETN-92-92147] p 4079 N92-32797

PLASMA PROPULSION
The evolutionary development of high specific impulse electric thruster technology
[NASA-TM-105758] p 3944 N92-33064

PLASMA RADIATION
Diagnostics and modeling of ECRH microwave discharges
[IPF-91-3] p 4079 N92-32822

PLASMA SPRAYING
Director's discretionary fund report for FY 1991
[NASA-TM-103902] p 4105 N92-33106
Coatings for improved corrosion resistance
[DE92-016779] p 3974 N92-33247

PLASMA TURBULENCE
Nonlinear dynamics and plasma transport
[DE92-014246] p 4078 N92-32592

PLASMA WAVES
Huygens/ASI plasma wave analyzer capabilities for aerosol measurement p 4098 N92-32380

PLASMA-ELECTROMAGNETIC INTERACTION
Titan's magnetospheric interaction p 4099 N92-32385

PLASMAS (PHYSICS)
Transverse beam dynamics in recirculating accelerators for heavy-ion fusion
[DE92-013448] p 4070 N92-32413
Two- and three-dimensional simulation code for radiation-hydrodynamics in ICF
[NIFS-119] p 4078 N92-32552
Nonlinear dynamics and plasma transport
[DE92-014246] p 4078 N92-32592
MHD computation of feedback of resistive-shell instabilities in the reversed field pinch
[DE92-014325] p 4078 N92-32599
Alpha particle diagnostics using impurity pellet injection
[DE92-013796] p 4078 N92-32623
Study of recirculating induction accelerators as drivers for heavy ion fusion
[DE92-016980] p 4071 N92-32904

Spectroscopic characterization of LEVIS active ion source on PBFA 2
[DE92-014954] p 4080 N92-32992
Turbulence transport equations for variable-density turbulence and their relationship to two-field models
[DE92-017292] p 4013 N92-33159

PLASTIC DEFORMATION
High temperature deformation processes and strengthening mechanisms in intermetallic particulate composites
[AD-A250220] p 3946 N92-32339
Physical basis for a pressure-dependent yield criterion for polymers
[AD-A250763] p 3970 N92-32341
Computational simulation of matrix micro-slip bands in SiC/Ti-15 composite
[NASA-TM-105762] p 3946 N92-32466
Inelastic deformation and damage at high temperature
[DE92-012241] p 4021 N92-32698
Guide to the effect of shot peening on fatigue strength
[ESDU-92015] p 3967 N92-32779
Contribution to the study of the effect of the heterogeneous distribution of dislocations on the cyclic plasticity of single crystal aluminum
[ISAL-91-0099] p 4083 N92-32892
A transgranular fatigue crack growth model based on restricted slip reversibility
[NRC-LTR-ST-1831] p 4023 N92-33076

PLASTIC FLOW
A reexamination of the plastic flow criterion for copper
[AD-A252370] p 4023 N92-32918

PLASTIC PROPERTIES
Computational simulation of matrix micro-slip bands in SiC/Ti-15 composite
[NASA-TM-105762] p 3946 N92-32466

PLASTICS
National Research Council Industrial Materials Institute: From knowledge to know-how
[CTN-92-60333] p 4103 N92-32814
National Research Council Industrial Materials Institute: From knowledge to know-how
[CTN-92-60334] p 4104 N92-32815
An experimental study on the two-parameter crack tip field
[AD-A251173] p 4023 N92-32936

PLATE THEORY
Shear buckling of specially orthotropic plates with centrally located cutouts p 3953 N92-32589

PLATES (STRUCTURAL MEMBERS)
Calculation of the energy of elastic deformation of Kevlar backing plates for ceramic armours
[AD-A250129] p 3970 N92-32489
The use of curvilinear fiber format to improve buckling resistance of plates with central circular holes
p 3948 N92-32521
Efficient finite element modeling of laminated composite plates based on higher-order theory
p 3949 N92-32529
Postbuckling of stiffened composite plates under combined loading p 3952 N92-32585
Buckling and postbuckling behavior of square compression-loaded graphite-epoxy plates with circular cutouts p 3952 N92-32587

PLATINUM
Electrocatalysis of anodic, oxygen-transfer reactions at noble metal electrodes
[DE92-016308] p 3962 N92-32562
Studies of n-butane conversion over silica-supported platinum, platinum-silver and platinum-copper catalysts
[DE92-016309] p 3962 N92-32563
Electrocatalyst surfaces
[PB92-190420] p 3962 N92-32591
Some electronic and dynamical factors in electron-transfer chemistry: Metal complexes, clusters, and surfaces
[AD-A251169] p 3964 N92-32826
Clean gasoline reforming with superacid catalysts
[DE92-013833] p 3975 N92-33123

PLATINUM ALLOYS
Studies of n-butane conversion over silica-supported platinum, platinum-silver and platinum-copper catalysts
[DE92-016309] p 3962 N92-32563

PLOTTING
Program PLOTTAB: A code designed to plot continuous and/or discrete physical data
[DE92-013754] p 4041 N92-32416

PLUMES
Computational fluid dynamics analysis of Space Shuttle main engine multiple plume flows at high-altitude flight conditions p 3996 N92-32255

PLUTONIUM
Execution of measurement sequences in the framework of the inspection of near limit regions by radioiodine and aerosol emission measurements, and ground examinations on plutonium, strontium, and gamma ray radionuclides
[OEFZS-4579] p 4071 N92-32763
Chemical Technology Division
[DE92-014059] p 3964 N92-32931

PLY ORIENTATION
Compression behavior of graphite-epoxy and graphite-thermoplastic panels with circular holes or impact damage p 3951 N92-32582
Buckling and postbuckling behavior of square compression-loaded graphite-epoxy plates with circular cutouts p 3952 N92-32587

POINCARE PROBLEM
The behavior of matter under non-equilibrium conditions: Fundamental aspects and applications
[DE92-014247] p 4087 N92-32593
Poincare normal form (system of ordinary differential equations): An algorithmic point of view
[IMAG-RR-839-M] p 4058 N92-32838

POINT DEFECTS
Modeling the influence of irradiation temperature and displacement rate on hardening due to point defect clusters in ferritic steels
[DE92-016897] p 3969 N92-33115

POINTS (MATHEMATICS)
Bandwidth selection for the intensity of point processes: Application to hazard rate models for censored data
[IMAG-RR-859-I/M] p 4056 N92-32684

POISSON DENSITY FUNCTIONS
Limit theorems for functionals of convex hulls
[CWI-BS-R9115] p 4059 N92-33058

POISSON RATIO
A unique method of determining the elastic and engineering constants of unidirectional fibre-reinforced composite plates using ultrasound
[UTIAS-TN-274] p 3955 N92-32829

POLAR REGIONS
Polar upper atmosphere characterization and supersonic ion escape (polar wind)
[GDR-0917] p 4031 N92-32889

POLARIZATION CHARACTERISTICS
Electrochemical polarization measurements on pitting corrosion susceptibility of nickel-rich Alloy 825
[DE92-014885] p 3969 N92-33132

POLARIZED LIGHT
Depolarized light source for fiber optic sensors
[AD-D015289] p 4074 N92-32634

POLARIZED RADIATION
On the interpretation of Titan's intensity and polarization phase curve p 4102 N92-32407
First results of measurements of A(sub LL) two-spin asymmetry in inclusive production of (pi)(sup 0) mesons by polarized protons and antiprotons with 200 GeV energy
[DE92-624692] p 4065 N92-32497
Polarized wiggler for NSLS x ray ring design considerations
[DE92-012212] p 4071 N92-32912

POLLUTION CONTROL
Development of the chemical and electrochemical coal cleaning process
[DE92-013353] p 3977 N92-32467
Defense environmental restoration program annual report to Congress for fiscal year 1991
[AD-A244196] p 4029 N92-32731
International research into chlorofluorocarbon (CFC) alternatives
[DE92-014241] p 4030 N92-32986
Direct catalytic decomposition of nitric oxide
[DE92-013847] p 4030 N92-33125

POLLUTION MONITORING
Suggestions for improvement of the methodology and use of MEPAS, the multimedia environmental pollutant assessment system
[DE92-013135] p 4028 N92-32616
Federal plan for ocean pollution research, development, and monitoring, fiscal years 1992-1996
[PB92-185164] p 4029 N92-32708
Study on lifetime specific, laser-induced ultrafast fluorescence detection in the time and frequency domain for in-situ environmental analysis of organic pollutants
[KFK-4975] p 4029 N92-32841

POLLUTION TRANSPORT
Suggestions for improvement of the methodology and use of MEPAS, the multimedia environmental pollutant assessment system
[DE92-013135] p 4028 N92-32616

POLYATOMIC MOLECULES
HCP and HCN, molecules of planetary interest
p 4100 N92-32395

POLYBUTADIENE
ESD traits of bulk propellant under pressure
p 3976 N92-33242

POLYCARBONATES
Orientation, stress, and density distributions in injection-moulded amorphous polymers determined by optical techniques
[ETN-92-92052] p 3972 N92-32752

POLYESTERS
Synthesis, morphology and properties of polyester-urethane in solution in styrene: Application to composites development
[ISAL-92-0007] p 3972 N92-32762

POLYETHYLENES
Continuum configurational bias Monte-Carlo studies of alkanes and polyethylene
[DE92-016545] p 3965 N92-33185

POLYGONS
Limit theorems for functionals of convex hulls
[CWI-BS-R9115] p 4059 N92-33058
Visibility properties of polygons
[ISBN-0-315-57272-8] p 4049 N92-33229

POLYIMIDES
Polyimides with carbonyl and ether connecting groups between the aromatic rings
[NASA-CASE-LAR-14001-1] p 3973 N92-33008
Polyimide molding powder, coating, adhesive, and matrix resin
[NASA-CASE-LAR-14163-1] p 3973 N92-33014
Methyl substituted polyimides containing carbonyl and ether connecting groups
[NASA-CASE-LAR-14351-1] p 3973 N92-33015

POLYMER CHEMISTRY
Towards well-defined polysilanes and polyphosphazenes
[AD-A251098] p 3971 N92-32547

POLYMER MATRIX COMPOSITES
Physical basis for a pressure-dependent yield criterion for polymers
[AD-A250763] p 3970 N92-32341
A review of recent developments in joining high-performance thermoplastic composites
[CNRC-33030] p 4019 N92-33077

POLYMERIZATION
Towards well-defined polysilanes and polyphosphazenes
[AD-A251098] p 3971 N92-32547
The effect of surface pressure on the Langmuir-Blodgett polymerization of 2-pentadecyl aniline
[AD-A251141] p 3971 N92-32550

POLYMERS
Excited state processes in transition metal complexes: Redox splitting in soluble polymers
[DE92-011808] p 3971 N92-32631

POLYNOMIALS
Thermal conductivity of gaseous halogenated hydrocarbons: Ethylenes and benzenes
[ESDU-92010] p 3945 N92-32485
Generalizations of the classical Laguerre polynomials and some q-analogues
[ISBN-90-9003765-9] p 4058 N92-32836

POLYSILANES
Towards well-defined polysilanes and polyphosphazenes
[AD-A251098] p 3971 N92-32547

POLYSTYRENE
Performance of insulated pavements at Newton Fields, Jackman, Maine
[CRREL-92-9] p 3940 N92-32903

POLYTOPES
A min-max relation for K3-covers in graphs noncontractible to K5/e
[IMAG-RR-850-I] p 4056 N92-32711

POPULATIONS
Suggestions for improvement of the methodology and use of MEPAS, the multimedia environmental pollutant assessment system
[DE92-013135] p 4028 N92-32616

POROSITY
CFD modeling of turbulent flows around the SSME main injector assembly using porosity formulation
p 3997 N92-32260
Experimental investigation of the axial impregnation of oriented fiber bundles by capillary forces
[AD-A250758] p 3961 N92-32508
Bone as a liquid-filled diphase porous medium
p 4037 N92-32663

POROUS MATERIALS
Experimental investigation of the axial impregnation of oriented fiber bundles by capillary forces
[AD-A250758] p 3961 N92-32508
Bone as a liquid-filled diphase porous medium
p 4037 N92-32663

POROUS WALLS
An experimental study of the fluid mechanics associated with porous walls
[AIAA PAPER 92-0769] p 3998 N92-32263

POSITION (LOCATION)
Transmitter location system for frequencies below HF
[AD-D015325] p 3986 N92-33172

POSITION ERRORS
Transverse beam dynamics in recirculating accelerators for heavy-ion fusion
[DE92-013448] p 4070 N92-32413

A Kalman filter integrated navigation design for the IAR Twin Otter Atmospheric Research Aircraft
[NRC-32148] p 3934 N92-32849
POSITION INDICATORS
Thermal and structural analysis of high precision beamline position monitors for synchrotron x ray beams
[DE92-014863] p 4072 N92-33130
POSITION SENSING
Ambient light array vision in 3-D
[ISBN-0-315-55748-6] p 4077 N92-33202
POSITRONS
PET studies of components of high-level vision
[AD-A250873] p 4036 N92-32344
POSTFLIGHT ANALYSIS
Debris/ice/TPS assessment and integrated photographic analysis for Shuttle Mission STS-49
[NASA-TM-107547] p 3941 N92-32454
POTENTIAL ENERGY
Continuum configurational bias Monte-Carlo studies of alkanes and polyethylene
[DE92-016545] p 3965 N92-33185
POTENTIAL FLOW
Potential flow theory and operation guide for the panel code PMARC
[NASA-TM-102851] p 3929 N92-32422
The application of unsteady potential flow vortex loop/dipole theory to the work and acoustics of low-speed turbomachinery
[AD-A251160] p 4008 N92-32652
POTENTIAL THEORY
Schroedinger operators with singular potentials in the semiclassical limit
[ETN-92-92145] p 4058 N92-32840
POTENTIOMETRIC ANALYSIS
An in vitro corrosion study of two implant materials using electrochemical impedance spectroscopy and potentiodynamic polarization
[AD-A252575] p 3966 N92-32626
POWDER (PARTICLES)
Density variations and anomalies in palladium compacts
[DE92-014382] p 3967 N92-32721
Radiography to measure the longitudinal density gradients of Pd compacts
[DE92-014383] p 3968 N92-32896
Polyimide molding powder, coating, adhesive, and matrix resin
[NASA-CASE-LAR-14163-1] p 3973 N92-33014
Silver coated superconducting ceramic powder
[AD-D015294] p 3973 N92-33157
POWER AMPLIFIERS
A 1-W, 30-GHz, CPW amplifier for ACTS small terminal uplink p 3984 N92-32973
POWER CONDITIONING
Interception of LPI radar signals
[AD-A246315] p 3978 N92-32535
POWER TRANSMISSION
Magnetic penetration depth of YBa2Cu3O(7-delta) thin films determined by the power transmission method p 3985 N92-32983
PREBURNERS
Modeling of SSME fuel preburner ASI p 3945 N92-32259
Computational fluid dynamics analysis of SSME phase 2 and phase 2+ preburner injector element hydrogen flow paths p 3997 N92-32261
PRECIPITATION (CHEMISTRY)
Contribution to the study of the effect of the heterogeneous distribution of dislocations on the cyclic plasticity of single crystal aluminum
[ISAL-91-0099] p 4083 N92-32892
A combined AEM/APFIM characterization of Alloy X-750
[DE92-011049] p 3969 N92-33158
PRECIPITATION (METEOROLOGY)
US Historical Climatology Network daily temperature and precipitation data
[DE92-014920] p 4032 N92-32431
Recent changes of weather patterns in North America
[DE92-014342] p 4033 N92-32720
Climate System Monitoring (CSM) Monthly Bulletin, issue no. 1 p 4034 N92-33073
PRECONDITIONING
The impact of time step definition on code convergence and robustness p 4001 N92-32282
Comparison between the PISO algorithm and preconditioning methods for compressible flow p 4001 N92-32284
PREDICTION ANALYSIS TECHNIQUES
Effect of including variable gas properties and entrained particles in the flow analysis of the ASRM nozzle p 4006 N92-32306
A new approach to fibrous composite laminate strength prediction p 3952 N92-32588
Exploitation of parallelism in climate models
[DE92-012595] p 4028 N92-32619
Leading-edge receptivity for blunt-nose bodies
[NASA-CR-190563] p 3930 N92-32648
Mixed model fatigue crack growth behavior in a high strength steel
[AD-A250667] p 4022 N92-32717
Integration of wall interference assessment and wall adaptation
[NLR-TP-91119-U] p 3940 N92-32734
NLR investigations of flutter behaviour of fighter aircraft with external stores
[NLR-TP-91134-U] p 3939 N92-32750
Better predictions even in reduced input variable numbers using neural networks in software development p 4044 N92-32874
A review of RAE sponsored work on the compressive behaviour of composite materials p 3957 N92-33038
PREFLIGHT ANALYSIS
Debris/ice/TPS assessment and integrated photographic analysis for Shuttle Mission STS-49
[NASA-TM-107547] p 3941 N92-32454
PREMIXING
Premixed turbulent combustion to opposed streams
[DE92-016996] p 3964 N92-32996
PREPREGS
Apparatus for preparing thermoplastic composites
[AD-D015326] p 3960 N92-33174
PRESSURE
The effect of surface pressure on the Langmuir-Blodgett polymerization of 2-pentadecyl aniline
[AD-A251141] p 3971 N92-32550
A computational fluid dynamics analysis of the hypersonic flights of Pegasus
[NASA-CR-186023] p 4007 N92-32560
PRESSURE DEPENDENCE
Physical basis for a pressure-dependent yield criterion for polymers
[AD-A250763] p 3970 N92-32341
User's manual for AeroFcn: A FORTRAN program to compute aerodynamic parameters
[NASA-TM-104237] p 4042 N92-32507
PRESSURE DISTRIBUTION
Navier-Stokes analysis of an oxidizer turbine blade with tip clearance p 3999 N92-32269
Complex three-dimensional internal flows in the ASRM and RSRM aft end segments p 4005 N92-32304
Computations of unsteady multistage compressor flows in a workstation environment
[NASA-TM-103839] p 3938 N92-32452
Pressure field developed by the random movement of the vortices near a wall
[ETN-92-91665] p 4009 N92-32770
PRESSURE EFFECTS
The effect of surface pressure on the Langmuir-Blodgett polymerization of 2-pentadecyl aniline
[AD-A251141] p 3971 N92-32550
Bacterial responses to extreme temperatures and pressures and to heavy organic loading
[AD-A247456] p 4035 N92-32571
Building vibrations induced by noise from rotorcraft and propeller aircraft flyovers
[NASA-TM-104170] p 4063 N92-33160
PRESSURE GRADIENTS
Phase distribution measurements in narrow rectangular channels using image-processing techniques
[DE92-014084] p 4006 N92-32468
A new time scale based k-epsilon model for near wall turbulence
[NASA-TM-105768] p 4011 N92-32868
PRESSURE MEASUREMENT
High temperature fiber optic microphone having a pressure-sensing reflective membrane under tensile stress
[NASA-CASE-LAR-14402-1-CU] p 4076 N92-33017
PRESSURE OSCILLATIONS
A comparative study of the effects of inhibitor stub length on solid rocket motor combustion chamber pressure oscillations: RSRM at T = 80 seconds, preliminary results p 3945 N92-32248
PRESSURE PULSES
Passive fetal monitoring sensor
[NASA-CASE-LAR-14088-1-CU] p 4015 N92-33016
PRESSURE RATIO
A computational fluid dynamics analysis of the hypersonic flights of Pegasus
[NASA-CR-186023] p 4007 N92-32560
PRESSURE SENSORS
High temperature fiber optic microphone having a pressure-sensing reflective membrane under tensile stress
[NASA-CASE-LAR-14402-1-CU] p 4076 N92-33017
PRESSURE VESSELS
Modeling the influence of irradiation temperature and displacement rate on hardening due to point defect clusters in ferritic steels
[DE92-016897] p 3969 N92-33115
PRESSURIZED WATER REACTORS
Life testing of a low voltage air circuit breaker
[DE92-014173] p 3988 N92-32635
PRESTRESSING
Electromagnetic attachment mechanism
[NASA-CASE-MSC-21463-1] p 4019 N92-33018
PREVENTION
Cleanroom process evolution in the SEL p 4044 N92-32871
PRINTED CIRCUITS
Multichip module study
[AD-A250877] p 3989 N92-32678
PROBABILITY THEORY
Methods of opto-electronic fusion of infrared and visible images p 3936 N92-32444
Two perspectives on a decohering spin
[DE92-013021] p 4087 N92-32496
Interception of LPI radar signals
[AD-A246315] p 3978 N92-32535
Adaptive information processing and global optimization
[AD-A248450] p 4089 N92-32644
Statistical selection: Multiple comparison approach
[ETN-92-92051] p 4060 N92-32709
A new form for the central limit theorem
[IMAG-RR-852-M] p 4060 N92-32716
A Markov model of software usage p 4045 N92-32881
Recursive estimation techniques for detection of small objects in infrared image data
[AD-A250942] p 4075 N92-32935
Feature detection for model assessment in state estimation
[AD-A252755] p 4059 N92-32989
PROBLEM SOLVING
Aspects of solving non-linear boundary value problems numerically
[ETN-92-92049] p 4058 N92-32798
A study of artificial intelligence planning: A framework for a planning development system
[ISBN-0-315-54378-7] p 4055 N92-33219
PROCESS CONTROL (INDUSTRY)
Nondestructive evaluation development for process control
[DE92-015272] p 3971 N92-32640
On physical systems qualitative approach: Real time help for fermentation process control
[LAAS-91445] p 4036 N92-32844
A prototype backside purge control system
[NASA-CR-190816] p 3969 N92-33081
PROCESSING
Formation of high temperature superconductors from the solidified melt
[DE92-012584] p 4081 N92-32465
PRODUCT DEVELOPMENT
The 1991 Federal Aviation Administration plan for research, engineering and development p 4103 N92-32453
NAASW modular radar research testbed study results
[DE92-011339] p 3981 N92-32744
Software development practice in a scientific computing environment
[NLR-TP-91193-U] p 4043 N92-32832
Life cycle oriented method for development and production of large scale industrial mathematics software
[NLR-TP-91196-U] p 4043 N92-32833
Proceedings of the Sixteenth Annual Software Engineering Workshop
[NASA-TM-107964] p 4044 N92-32869
Investigating the application of capture-recapture techniques to requirement and design reviews p 4044 N92-32873
Optimized set reduction for empirically guiding software development p 4044 N92-32875
Software process assessment for small software shops p 4045 N92-32878
PRODUCTION COSTS
Low cost MMC made by spray deposition
[MBB-Z-0407-91-PUB] p 3968 N92-32897
PRODUCTION ENGINEERING
MANTECH project book
[AD-A245283] p 3977 N92-32461
China's aerospace industry: Technology, funding, and modernization
[AD-A252618] p 3929 N92-32691
PROGRAM VERIFICATION (COMPUTERS)
Development of CFD code evaluation criteria and a procedure for assessing predictive capability and performance p 4001 N92-32283
Measurement in practice p 4044 N92-32876
A study of large scale software testing p 4045 N92-32879
Simulation test and evaluation of TCAS 2 logic version 6.04
[DOT/FAA/RD-92/23] p 3934 N92-33098

An evaluation of knowledge-based diagnostic techniques for debugging concurrent software
[ISBN-0-315-51189-3] p 4049 N92-33215
Concurrency control scheme for design object bases
[ISBN-0-315-56113-0] p 4049 N92-33232

PROGRAMMING LANGUAGES
SIMLAB: Automatically creating physical systems simulators
[AD-A250970] p 4042 N92-32546
Functions and genericity in a parallel programming language
[ETN-92-91667] p 4051 N92-32771
Exploiting two-dimensional explicit parallelism on vector architectures
[ETN-92-92136] p 4051 N92-32795
Hierarchical sets in mathematical programming modeling languages
[MEMO-990] p 4057 N92-32796

PROJECT MANAGEMENT
United States Air Force summer research program 1991. Volume 1: Program management report
[AD-A248763] p 4103 N92-32338
NASA procurement: Improving oversight of construction projects at the Langley Research Center. Report to the Honorable John W. Warner, US Senate
[GAO/NSIAD-92-230] p 4088 N92-32618
DoD key technologies plan
[AD-A253692] p 4105 N92-33238

PROJECT PLANNING
NAASW modular radar research testbed study results
[DE92-011339] p 3981 N92-32744

PROJECTILES
ROAR: A 3-D tethered rocket simulation code
[DE92-017358] p 3944 N92-33166

PROLATE SPHEROIDS
Electromagnetic scattering by systems of arbitrarily oriented spheroids
[ISBN-0-315-63332-8] p 3986 N92-33191

PROLOG (PROGRAMMING LANGUAGE)
CSP: A distributed logic programming language for discrete event simulation
[ISBN-0-315-54272-1] p 4048 N92-33214
An evaluation of knowledge-based diagnostic techniques for debugging concurrent software
[ISBN-0-315-51189-3] p 4049 N92-33215

PROPAGATION MODES
Laser to single-mode-fiber coupling: A laboratory guide
[NASA-CR-4452] p 4077 N92-33239

PROPELLANT ADDITIVES
A two-phase restricted equilibrium model for combustion of metalized solid propellants p 3966 N92-32307

PROPELLANT BINDERS
Condensed-phase processes during solid propellant combustion. Part 2: Chemical and microscopic examination of conductively quenched samples of RDX, XM39, JA2, M30, and HMX-binder compositions
[AD-A250799] p 3974 N92-32664

PROPELLANT CHEMISTRY
Use of thin-film samples to study thermal decomposition chemistry of explosives
[DE92-014616] p 3974 N92-32637

PROPELLANT COMBUSTION
Tenth Workshop for Computational Fluid Dynamic Applications in Rocket Propulsion, part 1
[NASA-CP-3163-PT-1] p 4000 N92-32278
Development of methodology and technology for identifying and quantifying emission products from open burning and open detonation thermal treatment methods. BangBox test series. Volume 3: Quality assurance and quality control
[AD-A251099] p 4029 N92-32650
Condensed-phase processes during solid propellant combustion. Part 2: Chemical and microscopic examination of conductively quenched samples of RDX, XM39, JA2, M30, and HMX-binder compositions
[AD-A250799] p 3974 N92-32664

PROPELLANT DECOMPOSITION
Use of thin-film samples to study thermal decomposition chemistry of explosives
[DE92-014616] p 3974 N92-32637
Condensed-phase processes during solid propellant combustion. Part 2: Chemical and microscopic examination of conductively quenched samples of RDX, XM39, JA2, M30, and HMX-binder compositions
[AD-A250799] p 3974 N92-32664

PROPELLANT GRAINS
An analysis of the flow field in the region of the ASRM field joints p 4005 N92-32305

PROPELLANT SENSITIVITY
Insensitive Munitions
[AGARD-CP-511] p 3975 N92-33240
ESD traits of bulk propellant under pressure p 3976 N92-33242
Hazards reduction for tactical missiles p 3945 N92-33245

PROPELLANT TANKS
A prototype backside purge control system
[NASA-CR-190816] p 3969 N92-33081

PROPELLANTS
Condensed-phase processes during solid propellant combustion. Part 2: Chemical and microscopic examination of conductively quenched samples of RDX, XM39, JA2, M30, and HMX-binder compositions
[AD-A250799] p 3974 N92-32664
Insensitive Munitions
[AGARD-CP-511] p 3975 N92-33240
Development of a minimum smoke propellant based on glycidyl azide polymer and ammonium nitrate p 3976 N92-33243

PROPELLER BLADES
Active synchrophasing of propeller unbalance p 4063 N92-32963

PROPELLER DRIVE
Ideal efficiency of propellers based on Theodorsen's theory: A review and computer study, with extended plus simplified charts
[UTIAS-TN-271] p 3938 N92-33102

PROPELLER EFFICIENCY
Ideal efficiency of propellers based on Theodorsen's theory: A review and computer study, with extended plus simplified charts
[UTIAS-TN-271] p 3938 N92-33102

PROPELLER NOISE
Vibro-acoustic FE analyses of the Saab 2000 aircraft p 4062 N92-32952
Building vibrations induced by noise from rotorcraft and propeller aircraft flyovers
[NASA-TM-104170] p 4063 N92-33160

PROPELLER SLIPSTREAMS
Further development of the CANAERO computer code to include propulsor modelling
[DREA-CR-90-425] p 3931 N92-32811

PROPELLERS
Further development of the CANAERO computer code to include propulsor modelling
[DREA-CR-90-425] p 3931 N92-32811
On the origin and acoustical behaviour of cloud cavitation
[ISBN-90-9004317-9] p 4012 N92-33066

PROPULSION
CAGI: Computer Aided Grid Interface. A work in progress p 4005 N92-32302
DoD key technologies plan
[AD-A253692] p 4105 N92-33238

PROPULSION SYSTEM CONFIGURATIONS
Tenth Workshop for Computational Fluid Dynamic Applications in Rocket Propulsion, part 2
[NASA-CP-3163-PT-2] p 3994 N92-32245
Space Transportation Main Engine p 3945 N92-32281

PROPULSION SYSTEM PERFORMANCE
Computational fluid dynamics analysis of Space Shuttle main engine multiple plume flows at high-altitude flight conditions p 3996 N92-32255
Technology test bed review p 4001 N92-32279

PROTECTION
Local structural order and molecular associations in water DMSO mixtures. Molecular dynamics study
[AD-A250935] p 4064 N92-32418
A Protection And Detection Surface (PADS) for damage tolerance p 3948 N92-32523

PROTECTIVE CLOTHING
Thermal assessment of Mustang Industries, Inc. neoprene quick-don anti-exposure immersion suits and storage evaluation for the CP140 Aurora aircraft
[DCIEM-90-23] p 4039 N92-32790

PROTECTIVE COATINGS
Corrosion-resistant alkyd coatings
[AD-D015330] p 3974 N92-33177
Coatings for improved corrosion resistance
[DE92-016779] p 3974 N92-33247

PROTEINS
Neutron scatter studies of chromatin structures related to functions
[DE92-014032] p 4036 N92-33181

PROTOCOL (COMPUTERS)
Guaranteeing synchronous message deadlines with the timed token medium access control protocol
[NASA-CR-190710] p 4042 N92-32656
Fault tolerance for security management in distributed systems
[LAAS-92011] p 4040 N92-32766
Ethernet bandwidth utilization of datafull, dataless, and diskless node workstation and x-terminals
[AD-A252374] p 4052 N92-32937
Methodologies for designing block ciphers and cryptographic protocols
[ISBN-0-315-50983-X] p 4049 N92-33230

PROTON BEAMS
High intensity negative proton beams from a SNICS ion source
[DE92-011137] p 4070 N92-32647

PROTONS
Comparison of spin asymmetries and invariant cross sections in production of (pi)(sup 0) mesons by polarized antiprotons and protons with 200 GeV energy
[DE92-624691] p 4064 N92-32311
Heavy flavor physics at hadron colliders
[DE92-014482] p 4064 N92-32312

PROTOTYPES
High power testing of the prototype accelerating cavity (352 MHz) for the Advanced Photon Source (APS)
[DE92-016697] p 4069 N92-32314
Ground Systems Development Environment (GSDE) interface requirements and prototyping plan
[NASA-CR-190713] p 4041 N92-32451
A prototype software engineering environment for domain modeling and reuse p 4046 N92-32882
A prototype backside purge control system
[NASA-CR-190816] p 3969 N92-33081

PSEUDOPOTENTIALS
Pseudopotential band calculations along a high-symmetry axis. Part 1: Central potential and the (111) direction
[AD-A252399] p 4084 N92-32938

PSYCHOMOTOR PERFORMANCE
Comparative effects of antihistamines on aircrew performance of simple and complex tasks under sustained operations
[AD-A248752] p 4036 N92-32492
Development of the OMPAT neuropsychological/psychomotor performance evaluation and OMPAT data and timing support
[AD-A250793] p 4037 N92-32504

PSYCHROMETERS
An evaluation of an infrared/resistance temperature device for air/sea-surface temperature measurements
[AD-A252279] p 4035 N92-32688

PUBLIC HEALTH
Development of methodology and technology for identifying and quantifying emission products from open burning and open detonation thermal treatment methods. BangBox test series. Volume 3: Quality assurance and quality control
[AD-A251099] p 4029 N92-32650

PULSE COMMUNICATION
Signal processing in impulsive electromagnetic interference
[AD-A252385] p 3982 N92-32899
Developments in the theory of Cantor-type variables with application to communications over fading channels
[ISBN-0-315-61378-5] p 3987 N92-33213

PULSE COMPRESSION
A high-power SLED 2 pulse compression system
[DE92-011586] p 4071 N92-32751

PULSE DOPPLER RADAR
Real-time processing of radar return on a parallel computer
[NASA-CR-4456] p 3932 N92-32606

PULSE GENERATORS
Impulse transmitter and quantum detection radar system
[AD-D015323] p 3986 N92-33171

PULSE RADAR
Interception of LPI radar signals
[AD-A246315] p 3978 N92-32535
A digital implementation of a radar coherent-on-receive system
[ISBN-0-315-59028-9] p 3987 N92-33206

PULSED LASERS
Probing thin-film YBa2Cu3O(7-delta) superconductors by second harmonic generation using femtosecond laser pulses
[AD-A252350] p 4082 N92-32512

PULSED RADIATION
Radiation selective system for target range and imaging readout
[AD-D015285] p 4076 N92-33095

PUMP IMPELLERS
A status of the activities of the NASA/MSFC pump stage technology team p 4002 N92-32286
CFD analysis of pump consortium impeller p 4002 N92-32287
CFD applications in pump flows p 4002 N92-32288
Computation of the flow field in a centrifugal impeller with splitter blades p 4002 N92-32289
Computational fluid dynamic design of rocket engine pump components p 4003 N92-32293

PUMPS
Pump and valve research at the Oak Ridge National Laboratory
[DE92-014419] p 4019 N92-32890

PURGING
A prototype backside purge control system
[NASA-CR-190816] p 3969 N92-33081
PURIFICATION
Purification system
[NASA-CASE-MSC-21584-1] p 3965 N92-33029
Clean gasoline reforming with superacid catalysts
[DE92-013833] p 3975 N92-33123
PYROLYSIS
Huygens/ACP: An instrument for aerosols chemical composition measurements p 4098 N92-32379
Gas chromatography and pyrolysis-GC with capillary columns: Application to the in situ analysis of Titan's atmosphere p 4100 N92-32397
PYROMETERS
The polychromatic pyrometer in diesel combustion
[ECL-91-42] p 3963 N92-32722
PYROTECHNICS
Radiometric and spectral measurement instruments
[AD-A250771] p 4013 N92-32343

Q

QUADRUPOLES
The shapes and collective behavior of rapidly rotating nuclei
[DE92-017192] p 4067 N92-32928
QUALITATIVE ANALYSIS
On physical systems qualitative approach: Real time help for fermentation process control
[LAAS-91445] p 4036 N92-32844
QUALITY CONTROL
The 1991 Federal Aviation Administration plan for research, engineering and development p 4103 N92-32453
Cleanroom process evolution in the SEL p 4044 N92-32871
Investigating the application of capture-recapture techniques to requirement and design reviews p 4044 N92-32873
Measurement in practice p 4044 N92-32876
Software process assessment for small software shops p 4045 N92-32878
QUANTITATIVE ANALYSIS
Small passive chemical detector
[DE92-014188] p 4030 N92-32933
QUANTUM CHROMODYNAMICS
Quark-antiquark Regge trajectories in large N(sub c) QCD
[DE92-016462] p 4064 N92-32313
Research in theoretical nuclear physics
[DE92-016316] p 4068 N92-33067
Theoretical aspects of lepton-hadron scattering
[DE92-013765] p 4069 N92-33148
A study of four jet events and search for double parton scattering at square root s = 1.8 TeV
[DE92-016351] p 4069 N92-33164
QUANTUM EFFICIENCY
Thin film cadmium telluride, zinc telluride, and mercury zinc telluride solar cells
[DE92-001237] p 4024 N92-32510
QUANTUM ELECTRODYNAMICS
Theoretical and experimental studies of elementary physics
[DE92-014877] p 4061 N92-32430
QUANTUM ELECTRONICS
Development of ultra-low noise, high sensitivity planar metal grating coupled AlGaAs/GaAs multiquantum well IR detectors for focal plane array staring IR sensor systems
[AD-A250368] p 4083 N92-32747
QUANTUM MECHANICS
Two perspectives on a decohering spin
[DE92-013021] p 4087 N92-32496
Scaling in the processes of ion-atom excitation
[DE92-625008] p 4065 N92-32500
Application of gauge theories to enhance numerical solutions to mixed potential integral equations
[AD-A248451] p 4055 N92-32670
QUANTUM NUMBERS
Scaling in the processes of ion-atom excitation
[DE92-625008] p 4065 N92-32500
QUANTUM THEORY
Quantum wave modeling on highly parallel distributed memory machines
[DE92-014507] p 4088 N92-33109
Impulse transmitter and quantum detection radar system
[AD-D015323] p 3986 N92-33171
QUARK PARTON MODEL
Partons and the EMC spin effect
[RAL-92-015-PREPRINT] p 4068 N92-33137
QUARKS
Quark-antiquark Regge trajectories in large N(sub c) QCD
[DE92-016462] p 4064 N92-32313
Nuclear theory
[DE92-015012] p 4067 N92-32921
Relativistic heavy ion physics
[DE92-015025] p 4067 N92-32922
QUERY LANGUAGES
Optimization of logic queries in knowledge base systems
[ISBN-0-315-51346-2] p 4049 N92-33227

R

RADAR ANTENNAS
Interception of LPI radar signals
[AD-A246315] p 3978 N92-32535
RADAR ATTENUATION
Radiation selective system for target range and imaging readout
[AD-D015285] p 4076 N92-33095
RADAR CROSS SECTIONS
Electromagnetic-wave propagation in unmagnetized plasmas
[AD-A250710] p 3980 N92-32719
RADAR DATA
Development of a prototype spatial information processing system for hydrologic research
[NASA-CR-190579] p 4024 N92-32590
RADAR DETECTION
Interception of LPI radar signals
[AD-A246315] p 3978 N92-32535
Beam and filter straddle losses in an ESA search radar
[AD-A250878] p 3980 N92-32680
Impulse transmitter and quantum detection radar system
[AD-D015323] p 3986 N92-33171
RADAR ECHOES
Characteristics of large aspect angle VHF radar echoes in the presence and absence of optical aurora
[ISBN-0-315-59091-2] p 4032 N92-33197
RADAR EQUIPMENT
Airport Surveillance Radar (ASR-9) wind shear processor: 1991 test at Orlando, Florida
[AD-A252246] p 3980 N92-32686
RADAR IMAGERY
NAASW modular radar research testbed study results
[DE92-011339] p 3981 N92-32744
RADAR MEASUREMENT
Multifrequency measurements of radar ground clutter at 42 sites. Volume 1: Principal results
[AD-A246710] p 3980 N92-32696
A simple Doppler wind lidar sensor: Simulated measurements and impacts in a global assimilation and forecast system
[PL-TR-91-2253] p 4034 N92-32859
RADAR NAVIGATION
Interception of LPI radar signals
[AD-A246315] p 3978 N92-32535
RADAR NETWORKS
Coverage studies for spaced-based radar
[DREO-90-18] p 3982 N92-32818
RADAR RANGE
Beam and filter straddle losses in an ESA search radar
[AD-A250878] p 3980 N92-32680
RADAR RECEIVERS
Interception of LPI radar signals
[AD-A246315] p 3978 N92-32535
A digital implementation of a radar coherent-on-receive system
[ISBN-0-315-59028-9] p 3987 N92-33206
RADAR SCANNING
Beam and filter straddle losses in an ESA search radar
[AD-A250878] p 3980 N92-32680
RADAR TARGETS
Impulse transmitter and quantum detection radar system
[AD-D015323] p 3986 N92-33171
RADAR TRACKING
Performance analysis of space-based radar tracking techniques
[ISBN-0-315-60464-6] p 3987 N92-33207
RADAR TRANSMITTERS
Impulse transmitter and quantum detection radar system
[AD-D015323] p 3986 N92-33171
RADIAL DISTRIBUTION
Fast ion loss and radial electric field in Wendelstein 7-A stellarator
[DE92-782106] p 4079 N92-32745
RADIANT HEATING
Characterization of sintered reaction-bonded silicon nitride processed by microwave heating
[DE92-014408] p 3956 N92-32945
RADIATION COUNTERS
Experimental particle physics at the University of Pittsburgh
[DE92-014181] p 4066 N92-32702
High efficiency fast neutron threshold deflector
[AD-D015311] p 4073 N92-33167
RADIATION DAMAGE
Investigation of the oxygen-vacancy (A-center) defect complex profile in neutron irradiated high resistivity silicon junction particle detectors
[DE92-016952] p 4064 N92-32316
The energetic radiation environment in a highly elliptical (Molniya) orbit
[AD-A252394] p 4031 N92-32902
RADIATION DETECTORS
Investigation of the oxygen-vacancy (A-center) defect complex profile in neutron irradiated high resistivity silicon junction particle detectors
[DE92-016952] p 4064 N92-32316
Radiometric and spectral measurement instruments
[AD-A250771] p 4013 N92-32343
The detectability of Titan's surface in the near-infrared p 4097 N92-32375
Studies of helium based drift chamber gases for high-luminosity low energy machines
[DE92-012415] p 4065 N92-32426
Research and development of a helium-4 based solar neutrino detector
[DE92-017390] p 4103 N92-33119
Elementary particle physics and high energy phenomena
[DE92-016844] p 4069 N92-33187
RADIATION DISTRIBUTION
Alpha particle diagnostics using impurity pellet injection
[DE92-013796] p 4078 N92-32623
RADIATION DOSAGE
Shielding analyses for repetitive high energy pulsed power accelerators
[DE92-015004] p 4072 N92-32994
Applications of energy loss contrast STIM
[DE92-017254] p 4014 N92-33000
RADIATION EFFECTS
Correlation of single mode fiber fabrication factors and radiation response
[AD-A247301] p 4074 N92-32613
Photogenerated carrier-induced reactions on UHV semiconductor surfaces
[DE92-015355] p 4082 N92-32641
Chemical Technology Division
[DE92-014059] p 3964 N92-32931
Modeling the influence of irradiation temperature and displacement rate on hardening due to point defect clusters in ferritic steels
[DE92-016897] p 3969 N92-33115
Dynamics of radiation-induced amorphization in intermetallic compounds
[DE92-016774] p 4086 N92-33221
RADIATION HAZARDS
Execution of measurement sequences in the framework of the inspection of near limit regions by radioiodine and aerosol emission measurements, and ground examinations on plutonium, strontium, and gamma ray radionuclides
[OEFZS-4579] p 4071 N92-32763
RADIATION MEASUREMENT
Absolute measurement of beam energy by Compton scattering
[DE92-016964] p 4069 N92-32318
Execution of measurement sequences in the framework of the inspection of near limit regions by radioiodine and aerosol emission measurements, and ground examinations on plutonium, strontium, and gamma ray radionuclides
[OEFZS-4579] p 4071 N92-32763
The energetic radiation environment in a highly elliptical (Molniya) orbit
[AD-A252394] p 4031 N92-32902
Research and development of a helium-4 based solar neutrino detector
[DE92-017390] p 4103 N92-33119
A precise narrow-beam filter infrared radiometer and its use with lidar in the ARM Program
[DE92-016872] p 4015 N92-33188
RADIATION PROTECTION
Correlation of single mode fiber fabrication factors and radiation response
[AD-A247301] p 4074 N92-32613
RADIATION SHIELDING
Booster Applications Facility report, phase 2
[DE92-013395] p 4070 N92-32411
Shielding analyses for repetitive high energy pulsed power accelerators
[DE92-015004] p 4072 N92-32994

High efficiency fast neutron threshold deflector
[AD-D015311] p 4073 N92-33167

RADIATION SOURCES
Proceedings of the fourth users meeting for the advanced photon source
[DE92-014061] p 4072 N92-32932
Photon excitation for satellite free x ray spectroscopy: Instrumentation challenges
[DE92-016999] p 4067 N92-32997
Multispectral variable magnification glancing incidence x ray telescope
[NASA-CASE-MFS-28013-4] p 4092 N92-33012
Purification system
[NASA-CASE-MSC-21584-1] p 3965 N92-33029

RADIATION TOLERANCE
An evaluation of an infrared/resistance temperature device for air/sea-surface temperature measurements
[AD-A252279] p 4035 N92-32688

RADIATION TRANSPORT
Analytic score comparison of geometry splitting and exponential transform for a simple Monte Carlo problem
[DE92-013108] p 4059 N92-32481
Two- and three-dimensional simulation code for radiation-hydrodynamics in ICF
[NIFS-119] p 4078 N92-32552

RADIATIVE LIFETIME
Radiative lifetime measurements of the AA pi 1/2 state in CaH
[USIP-91-03] p 4067 N92-32764

RADIATIVE TRANSFER
A research program on radiative transfer model development in support of the ARM program
[DE92-014495] p 4031 N92-33153

RADICALS
Mass resolved resonance ionization spectroscopy of combustion radicals
[DE92-016833] p 3965 N92-33222

RADIO COMMUNICATION
The problems of routing and scheduling in multihop radio networks. A Hopfield neural network approach
[AD-A247431] p 3979 N92-32570
The MSAT spacecraft of Telesat Mobile, Inc.
[CTN-92-60346] p 3981 N92-32789
Effects of fading and interference in narrowband land-mobile networks
[ISBN-90-9004491-4] p 3982 N92-32837

RADIO DIRECTION FINDERS
Transmitter location system for frequencies below HF
[AD-D015325] p 3986 N92-33172

RADIO FREQUENCIES
RF cavity vacuum interlock system
[DE92-016961] p 4070 N92-32567
Multifrequency measurements of radar ground clutter at 42 sites. Volume 1: Principal results
[AD-A246710] p 3980 N92-32696
Geometrical effects in two-dimensional arrays of Josephson junctions
[AD-A252209] p 4084 N92-32898

RADIO FREQUENCY INTERFERENCE
Effects of fading and interference in narrowband land-mobile networks
[ISBN-90-9004491-4] p 3982 N92-32837
Adaptive filter technique for suppression of wideband or offset narrowband radio frequency interference
[AD-D015329] p 3992 N92-33175

RADIO INTERFEROMETERS
Satellite radio interferometry
[PL-TR-91-2200] p 3978 N92-32458

RADIO SIGNALS
Satellite radio interferometry
[PL-TR-91-2200] p 3978 N92-32458

RADIO TRANSMITTERS
Transmitter location system for frequencies below HF
[AD-D015325] p 3986 N92-33172

RADIOACTIVE CONTAMINANTS
Execution of measurement sequences in the framework of the inspection of near limit regions by radioiodine and aerosol emission measurements, and ground examinations on plutonium, strontium, and gamma ray radionuclides
[OEFZS-4579] p 4071 N92-32763
A simulation of radioactive fallout using the MATHEW/ADPIC model
[FOA-C-40292-4.3] p 4029 N92-32785

RADIOACTIVE DECAY
Heavy flavor physics at hadron colliders
[DE92-014482] p 4064 N92-32312
Radiative lifetime measurements of the AA pi 1/2 state in CaH
[USIP-91-03] p 4067 N92-32764
Scalar mesons and kaons in phi radiative decay and their implications for studies of CP violation at DA(phi)NE
[RAL-91-085] p 4068 N92-33133
Elementary particle physics and high energy phenomena
[DE92-016844] p 4069 N92-33187

RADIOACTIVE ISOTOPES
Execution of measurement sequences in the framework of the inspection of near limit regions by radioiodine and aerosol emission measurements, and ground examinations on plutonium, strontium, and gamma ray radionuclides
[OEFZS-4579] p 4071 N92-32763

RADIOACTIVE WASTES
International technology transfer to support the environmental restoration needs of the DOE complex
[DE92-013663] p 4028 N92-32558
Electrochemical polarization measurements on pitting corrosion susceptibility of nickel-rich Alloy 825
[DE92-014885] p 3969 N92-33132

RADIOGRAPHY
Three dimensional object reconstruction using a very limited number of projections. Application to industrial radiography
[TELECOM-91-E-008] p 4043 N92-32804
Detection of honeycomb damage using hexagonal grid discontinuities
[DREP-89-9] p 3955 N92-32846
Radiography to measure the longitudinal density gradients of Pd compacts
[DE92-014383] p 3968 N92-32896
Kinematics of Compton backscattering x ray source for angiography
[DE92-014016] p 4073 N92-33179

RAIL TRANSPORTATION
Publications on maglev technologies
[DE92-013296] p 4017 N92-32615

RAIN
Applications of statistical methods to the study of climate and flooding fluctuations in the central US
[PB92-205137] p 4034 N92-33173

RAMAN SPECTROSCOPY
CARS diagnostics for solid propellant combustion investigations
[AD-A248660] p 3963 N92-32645

RANDOM PROCESSES
The behavior of matter under non-equilibrium conditions: Fundamental aspects and applications
[DE92-014247] p 4087 N92-32593
Pressure field developed by the random movement of the vortices near a wall
[ETN-92-91665] p 4009 N92-32770

RANDOM VARIABLES
New approach to HF channel modeling and simulation. Part 3: Transfer function
[PB92-192848] p 3979 N92-32555

RANGE SAFETY
Superheavyweight missions SI versus DI: Ascent flight design options and recommendations
[NASA-CR-183208] p 3942 N92-32610

RANGEFINDING
Vision-based range estimation using helicopter flight data
[NASA-TM-103930] p 3933 N92-32424

RANK TESTS
On the inconsistency of bootstrap distribution estimators
[IMAG-RR-856-M] p 4060 N92-32718

RASTER SCANNING
Temporal and spatial factors affecting the perception of computer-generated imagery
[AD-A249242] p 4046 N92-32907
Rotating-unbalanced-mass devices and methods for scanning balloon-borne-experiments, free-flying spacecraft, and space shuttle/space station attached experiments
[NASA-CASE-MFS-28425-1] p 4015 N92-33010

RDX
Use of thin-film samples to study thermal decomposition chemistry of explosives
[DE92-014616] p 3974 N92-32637
Condensed-phase processes during solid propellant combustion. Part 2: Chemical and microscopic examination of conductively quenched samples of RDX, XM39, JA2, M30, and HMX-binder compositions
[AD-A250799] p 3974 N92-32664

REACTING FLOW
Development of the KIVA-2 CFD code for rocket propulsion applications p 3945 N92-32272
The impact of time step definition on code convergence and robustness p 4001 N92-32282
Combustion instability analysis for liquid propellant rocket engines p 3966 N92-32297

REACTION KINETICS
A two-phase restricted equilibrium model for combustion of metalized solid propellants p 3966 N92-32307
Mechanisms of the oxidation of metals and alloys with emphasis on superconductors
[DE92-016840] p 3966 N92-32315
Methane oxidation over dual redox catalysts
[DE92-014358] p 3960 N92-32334
A shock tube study of the reactions of the hydroxyl radical with combustion species
[DE92-012573] p 3960 N92-32464
Thermochemical and kinetic considerations in diamond growth
[AD-A247866] p 3971 N92-32490
Shock tube ignition of ethanol, isobutene and MTBE: Experiments and modeling
[DE92-008563] p 3961 N92-32544
The effect of surface pressure on the Langmuir-Blodgett polymerization of 2-pentadecyl aniline
[AD-A251141] p 3971 N92-32550
Study and achievement of a parallel simulator for diffusion at the atomic level: Creation and growth of dislocation loops under electronic radiation
[LAAS-92118] p 4066 N92-32735
Thermochemical cycles for energy storage: Thermal decomposition of ZnSO4 systems
[DE91-002144] p 4026 N92-32909
Macrocyclic polycation complexes for secondary anion binding, molecular recognition, and catalysis
[AD-A251069] p 3972 N92-32913
Kinetics and characterization of CVD-grown BP
[ETN-92-92024] p 3973 N92-33065
High octane ethers from synthesis gas-derived alcohols
[DE92-013802] p 3975 N92-33108
Summary of engineering-scale experiments for the Solar Detoxification of Water project
[DE92-013776] p 4027 N92-33150
Probe molecule studies: Active species in alcohol synthesis
[DE92-016682] p 3966 N92-33246

REACTIVITY
Thermochemical and kinetic considerations in diamond growth
[AD-A247866] p 3971 N92-32490
Novel gas phase ion molecule reactions of C60(++) with O2 and NH3
[AD-A250921] p 4066 N92-32556

REACTOR MATERIALS
Modeling the influence of irradiation temperature and displacement rate on hardening due to point defect clusters in ferritic steels
[DE92-016897] p 3969 N92-33115

REACTOR SAFETY
System response to relay chatter
[DE92-013076] p 3988 N92-32495
International technology transfer to support the environmental restoration needs of the DOE complex
[DE92-013663] p 4028 N92-32558

REACTOR STARTUP TESTS
The Nova Upgrade Facility for ICF ignition and gain
[DE92-010703] p 4079 N92-32733

REACTOR TECHNOLOGY
Chemical Technology Division
[DE92-014059] p 3964 N92-32931

READOUT
Radiation selective system for target range and imaging readout
[AD-D015285] p 4076 N92-33095

REAL TIME OPERATION
Generic modular imaging IR signal processor
p 3936 N92-32440
Preparation and characterization of superlattices
[DE92-012572] p 4081 N92-32462
The multiple-function multi-input/multi-output digital controller system for the AFW wind-tunnel model
[NASA-TM-107600] p 3934 N92-32536
Real-time processing of radar return on a parallel computer
[NASA-CR-4456] p 3932 N92-32606
On physical systems qualitative approach: Real time help for fermentation process control
[LAAS-91445] p 4036 N92-32844
The development of an airborne information management system for flight test
[NASA-TM-104251] p 3938 N92-32866
Real-time edge-enhanced optical correlator
[NASA-CASE-NPO-18379-1-CU] p 4076 N92-33022
Real time pre-detection dynamic range compression
[NASA-CASE-NPO-18098-1-CU] p 4076 N92-33028
Advanced information processing system: The Army fault tolerant architecture conceptual study. Volume 1: Army fault tolerant architecture overview
[NASA-CR-189632-VOL-1] p 4052 N92-33100
Rapid development of the X-31 simulation to support flight-testing
[NASA-TM-104256] p 3935 N92-33149

REATTACHED FLOW
Influence of an intense acoustic field on boundary layer separation
[ETN-92-92081] p 4009 N92-32687

RECONNAISSANCE
Automatic detection, pursuit, and classification in infrared imagery p 3937 N92-32445

RECTANGLES
A numerical study of two-dimensional vortex shedding from rectangular cylinders p 3998 N92-32266
RECTANGULAR PLANFORMS
Phase distribution measurements in narrow rectangular channels using image-processing techniques
[DE92-014084] p 4006 N92-32468
RECTANGULAR PLATES
Initial postbuckling response of an unsymmetrically laminated rectangular plate p 3952 N92-32586
RECTANGULAR WAVEGUIDES
Numerical analysis of scattering from certain conducting and dielectric bodies of arbitrary shape
[ISBN-0-315-63282-8] p 3987 N92-33192
RECURSIVE FUNCTIONS
Functions and genericity in a parallel programming language
[ETN-92-91667] p 4051 N92-32771
REDUCED GRAVITY
Effects of CSF hormones and ionic composition on salt/water metabolism
[NASA-CR-190693] p 4037 N92-32539
Thermal gravitational modelling and scaling of two-phase heat transport systems for space: An assessment and a comparison of predictions and experimental results
[NLR-TP-91401-U] p 4008 N92-32675
Two-phase heat transport systems for space: Thermal gravitational modelling and scaling predictions versus results of experiments
[NLR-TP-91051-U] p 4010 N92-32786
Free motion of an unsupported tank that is partially filled with liquid
[NLR-TP-91185-U] p 4011 N92-32831
Investigations preparatory to the Wet Satellite Model Experiment
[NLR-TP-91219-U] p 3943 N92-32834
Improved HIRAP flight calibration technique
[NASA-TM-107656] p 3944 N92-33112
REDUCTION (CHEMISTRY)
Direct catalytic decomposition of nitric oxide
[DE92-013847] p 4030 N92-33125
REDUNDANCY
An implementation of a fault-tolerant, multidirectional, digital interpolation beamformer
[AD-A252494] p 3986 N92-33152
REDUNDANCY ENCODING
Fault tolerance for security management in distributed systems
[LAAS-92011] p 4040 N92-32766
REENTRY VEHICLES
Improved HIRAP flight calibration technique
[NASA-TM-107656] p 3944 N92-33112
REFLECTANCE
Concentrator silicon cell research
[DE92-016576] p 4025 N92-32565
Local aspects of the optical reflection problem: The discrete dipole approach
[ISBN-90-9004118-4] p 4074 N92-32703
REFLECTION
Testing of the single-element stretched-membrane dish
[DE92-013680] p 4025 N92-32549
REFLECTOR ANTENNAS
Ka-band dual frequency array feed for a low cost ACTS ground terminal p 3983 N92-32969
REFLECTORS
Visionless TRAC
[NASA-CR-190732] p 3942 N92-32477
Electromagnetic-wave propagation in unmagnetized plasmas
[AD-A250710] p 3980 N92-32719
REFRACTIVITY
Laboratory determination of the refractive indices of liquid methane and ethane at temperatures appropriate to the surface of Titan p 4100 N92-32391
REFRACTOMETERS
Experimental determination of the refractive index of liquefied gas mixtures: Applications to hypothesized Titan oceans p 4099 N92-32390
Laboratory determination of the refractive indices of liquid methane and ethane at temperatures appropriate to the surface of Titan p 4100 N92-32391
The Huygens SSP Refractometer (REF) p 4101 N92-32399
REFRACTORY MATERIALS
Interfacial studies of refractory glass-ceramic matrix/advanced SiC fiber reinforced composites
[AD-A250784] p 3953 N92-32676
REFRIGERANTS
An analytical screening of alternatives for R-502 in low-temperature refrigerating applications
[DE92-017162] p 3978 N92-32927
International research into chlorofluorocarbon (CFC) alternatives
[DE92-014241] p 4030 N92-32986
REFRIGERATING
Development and proof-testing of advanced absorption refrigeration cycle concepts
[DE92-014933] p 3977 N92-32723
An analytical screening of alternatives for R-502 in low-temperature refrigerating applications
[DE92-017162] p 3978 N92-32927
REFUELING
Injection of compact toroids for tokamak fueling and current drive
[DE92-010031] p 4077 N92-32533
REGGE POLES
Quark-antiquark Regge trajectories in large N(sub c) QCD
[DE92-016462] p 4064 N92-32313
REGRESSION ANALYSIS
Wind tunnel test of Teledyne Geotech model 1564B cup anemometer
[DE92-009590] p 4013 N92-32460
Approximations and designs for estimating regression coefficients of independent stochastic processes
[IMAG-RR-840-M] p 4060 N92-32839
A causal analysis of interrelationships among exercise, physical fitness, and well-being in US Navy personnel
[AD-A252719] p 4037 N92-32942
REGRESSION COEFFICIENTS
Approximations and designs for estimating regression coefficients of independent stochastic processes
[IMAG-RR-840-M] p 4060 N92-32839
REGULATIONS
National environmental compliance strategy
[DE92-013639] p 4027 N92-32415
Federal aviation regulations. Part 91: General operating and flight rules
[PB92-197334] p 3929 N92-33176
REINFORCING FIBERS
A unique method of determining the elastic and engineering constants of unidirectional fibre-reinforced composite plates using ultrasound
[UTIAS-TN-274] p 3955 N92-32829
REJECTION
Enhancements to speech recognition on voice response systems
[TELECOM-91-E-018] p 3981 N92-32807
RELATIVISTIC ELECTRON BEAMS
Absolute measurement of beam energy by Compton scattering
[DE92-016964] p 4069 N92-32318
RELATIVISTIC VELOCITY
Relativistic heavy ion collisions
[DE92-014415] p 4066 N92-32600
Relativistic heavy ion physics
[DE92-015025] p 4067 N92-32922
RELATIVITY
Physics in knots
[DE92-017530] p 4088 N92-33069
RELAXATION (MECHANICS)
Magnetic flux relaxation in YBa2Cu3O(7-x) thin film: Thermal or athermal p 3985 N92-32984
RELIABILITY
Reliability training
[NASA-RP-1253] p 3941 N92-32456
Toward advanced human reliability programs. Structural development considerations and options for extreme risk environments
[AD-A250786] p 4038 N92-32660
Stochastic models in reliability
[AD-A250934] p 4020 N92-33151
RELIABILITY ANALYSIS
Damage tolerance certification methodology for composite structures p 3951 N92-32579
Statistically based material properties: A military handbook-17 perspective p 3951 N92-32581
Tactical state and performance assessment during air combat maneuvering
[AD-A247426] p 3935 N92-32612
Analysis of data from a DO-178A software development process p 4045 N92-32880
A Markov model of software usage p 4045 N92-32881
RELIABILITY ENGINEERING
Fault tolerance through program transformation
[ISBN-90-72125-29-0] p 4047 N92-33142
RELIEF MAPS
Development of a prototype spatial information processing system for hydrologic research
[NASA-CR-190579] p 4024 N92-32590
REMOTE CONTROL
Influence of compliance on performance of robotic drilling
[OUEL-1917/92] p 4018 N92-32757
REMOTE SENSING
Development of a prototype spatial information processing system for hydrologic research
[NASA-CR-190579] p 4024 N92-32590
Boundary layer processes in coastal meteorology: Prospects for remote sensing applications
[PB92-177849] p 4033 N92-32714
Collaborative, remote, in-depth inspection and verification of satellites with neutral particle beams
[DE92-014195] p 3943 N92-32934
Integrating expert vision systems and spatial database by unifying knowledge representation schemes.Development in remote sensing image analysis expert systems and geographical information systems
[ISBN-0-315-49130-2] p 4024 N92-33233
REMOVAL
Device for removing foreign objects from anatomic organs
[NASA-CASE-GSC-13306-1] p 4038 N92-33032
REPLICAS
Fault tolerance through program transformation
[ISBN-90-72125-29-0] p 4047 N92-33142
REQUIREMENTS
Fly-by-light technology development plan
[NASA-CR-181954] p 3939 N92-32778
RESEARCH
United States Air Force summer research program 1991. Volume 1: Program management report
[AD-A248763] p 4103 N92-32338
RESEARCH AIRCRAFT
Collaborative research on V/STOL control system/cockpit display tradeoffs under the NASA/MOD joint aeronautical program
[NASA-TM-103910] p 3939 N92-32788
Rapid development of the X-31 simulation to support flight-testing
[NASA-TM-104256] p 3935 N92-33149
RESEARCH AND DEVELOPMENT
Departments of Veterans Affairs and Housing and Urban Development, and independent agencies appropriations for 1993, part 6
[GAO-55-636-PT-6] p 4091 N92-32505
University of Toronto Institute for Aerospace Studies
[CTN-92-60375] p 4104 N92-32853
Publications by Structures and Materials Laboratory on composite materials (January 1983 - June 1991)
[NRC-LTR-ST-1833] p 3959 N92-33078
Science and technology: A report to the Congress
[PB92-183219] p 4104 N92-33086
RESEARCH FACILITIES
Briefing notes on a manned aircraft research and support simulation facility
[AD-A250373] p 3935 N92-32326
Booster Applications Facility report, phase 2
[DE92-013395] p 4070 N92-32411
Space Station Freedom media handbook
[NASA-TM-107981] p 3942 N92-32421
The 1991 rocket-triggered lightning test of the DoD Security Operations Test Site (SOTS) munitions storage bunker, Fort McClellan, Alabama
[DE92-012449] p 4032 N92-32427
NASA Marshall Space Flight Center Solar Observatory report, January - June 1992
[NASA-TM-103597] p 4092 N92-32478
NASA procurement: Improving oversight of construction projects at the Langley Research Center. Report to the Honorable John W. Warner, US Senate
[GAO/NSIAD-92-230] p 4088 N92-32618
The Nova Upgrade Facility for ICF ignition and gain
[DE92-010703] p 4079 N92-32733
Status of LHD control system design
[NIFS-122] p 4070 N92-32746
National Research Council Industrial Materials Institute: From knowledge to know-how
[CTN-92-60334] p 4104 N92-32815
University of Toronto Institute for Aerospace Studies
[CTN-92-60375] p 4104 N92-32853
Chemical Technology Division
[DE92-014059] p 3964 N92-32931
Shielding analyses for repetitive high energy pulsed power accelerators
[DE92-015004] p 4072 N92-32994
Publications by Structures and Materials Laboratory on composite materials (January 1983 - June 1991)
[NRC-LTR-ST-1833] p 3959 N92-33078
Director's discretionary fund report for FY 1991
[NASA-TM-103902] p 4105 N92-33106
Image processing mini manual
[NASA-TM-107680] p 4041 N92-33205
RESEARCH MANAGEMENT
Space Station Freedom media handbook
[NASA-TM-107981] p 3942 N92-32421
A minority research and education information service: Design, develop, pilot test, and implement on-line access for historically black colleges and universities and government agencies
[DE92-013572] p 4090 N92-32930
DoD key technologies plan
[AD-A253692] p 4105 N92-33238

RESIDUAL STRENGTH
A curved beam test specimen for determining the interlaminar tensile strength of a laminated composite p 3949 N92-32526
Residual strength of repaired graphite/epoxy laminates after 5 years of outdoor exposure p 3950 N92-32577
Influence of edge effect on compression-tension fatigue of toughened graphite/epoxy laminates p 3957 N92-33039
RESIDUAL STRESS
Orientation, stress, and density distributions in injection-moulded amorphous polymers determined by optical techniques
[ETN-92-92052] p 3972 N92-32752
Guide to the effect of shot peening on fatigue strength
[ESDU-92015] p 3967 N92-32779
RESIDUES
Analysis of LDEF experiment AO187-2: Chemically and isotopic measurements of micrometeoroids by secondary ion mass spectrometry
[NASA-CR-190697] p 4093 N92-32541
Development of methodology and technology for identifying and quantifying emission products from open burning and open detonation thermal treatment methods. BangBox test series. Volume 3: Quality assurance and quality control
[AD-A251099] p 4029 N92-32650
RESIN BONDING
A review of recent developments in joining high-performance thermoplastic composites
[CNRC-33030] p 4019 N92-33077
RESIN MATRIX COMPOSITES
Compression behavior of graphite-epoxy and graphite-thermoplastic panels with circular holes or impact damage p 3951 N92-32582
Environmental degradation of high temperature composites p 3958 N92-33047
RESINS
Polyimide molding powder, coating, adhesive, and matrix resin
[NASA-CASE-LAR-14163-1] p 3973 N92-33014
RESONANCE
Nonlinear resonance
[DE92-014313] p 4016 N92-32596
Collective resonances of valence electrons in free metal clusters
[DE92-014783] p 3969 N92-33116
Mass resolved resonance ionization spectroscopy of combustion radicals
[DE92-016833] p 3965 N92-33222
RESONATORS
Planar dielectric resonator stabilized HEMT oscillator integrated with CPW/aperture coupled patch antenna p 3983 N92-32967
RESOURCES MANAGEMENT
National environmental compliance strategy
[DE92-013639] p 4027 N92-32415
Information resources management plan of the Federal Government
[PB92-147198] p 4089 N92-32643
HDR opportunities and challenges beyond the long-term flow test isco, CA, 24-26 Mar. 1992
[DE92-011234] p 4025 N92-32695
RESTORATION
National environmental compliance strategy
[DE92-013639] p 4027 N92-32415
International technology transfer to support the environmental restoration needs of the DOE complex
[DE92-013663] p 4028 N92-32558
RETROFITTING
MHD Integrated Topping Cycle Project
[DE92-013904] p 4080 N92-33024
REVERSE FIELD PINCH
MHD computation of feedback of resistive-shell instabilities in the reversed field pinch
[DE92-014325] p 4078 N92-32599
Ion heating and MHD dynamo fluctuations in the reversed field pinch
[DE92-013902] p 4078 N92-32624
Measurement of nonlinear mode coupling of tearing fluctuations
[DE92-013901] p 4080 N92-33154
REYNOLDS NUMBER
Breakdown of the Karman vortex street due to forced convection and flow compressibility
[NASA-TM-105853] p 4007 N92-32472
A new time scale based k-epsilon model for near wall turbulence
[NASA-TM-105768] p 4011 N92-32868
REYNOLDS STRESS
Numerical simulation of turbomachinery flows with advanced turbulence models p 3999 N92-32270
Model of Reynolds stress on nonorthogonal grid structures: Application to a staggered tube bundle
[ETN-92-91959] p 4009 N92-32725
RHENIUM COMPOUNDS
Excited state processes in transition metal complexes: Redox splitting in soluble polymers
[DE92-011808] p 3971 N92-32631
RIFLES
Investigation into the fabrication of a composite top attack recoilless rifle p 3948 N92-32524
RIGID STRUCTURES
Classical dynamics of systems with time-varying inertial properties with application to multi-rigid-body systems
[ISBN-0-315-57834-3] p 4024 N92-33228
RING STRUCTURES
Polarized wiggler for NSLS x ray ring design considerations
[DE92-012212] p 4071 N92-32912
RISK
Suggestions for improvement of the methodology and use of MEPAS, the multimedia environmental pollutant assessment system
[DE92-013135] p 4028 N92-32616
Toward advanced human reliability programs. Structural development considerations and options for extreme risk environments
[AD-A250786] p 4038 N92-32660
ROBOT CONTROL
The Rochester Checkers Player: Multi-model parallel programming for animate vision
[AD-A247427] p 4050 N92-32568
Using minimax approaches to plan optimal task commutation configurations for combined mobile platform-manipulator systems
[DE91-018864] p 4018 N92-32694
Rational behavior model: A tri-level multiple paradigm architecture for robot vehicle control software
[AD-A250370] p 4053 N92-32748
Obstacle avoidance for redundant robots using configuration control
[NASA-CASE-NPO-17852-1-CU] p 4054 N92-33019
Jacobian and stiffness analysis of a novel class of six-DOF parallel minimanipulators
[DE92-016373] p 4054 N92-33184
Investigations of adaptive control for a direct drive robotic manipulator
[ISBN-0-315-59030-0] p 4055 N92-33236
ROBOT DYNAMICS
Using minimax approaches to plan optimal task commutation configurations for combined mobile platform-manipulator systems
[DE91-018864] p 4018 N92-32694
ROBOTICS
Study of eddy current probes
[NASA-CR-190814] p 4020 N92-32425
The Rochester Checkers Player: Multi-model parallel programming for animate vision
[AD-A247427] p 4050 N92-32568
Influence of compliance on performance of robotic drilling
[OUEL-1917/92] p 4018 N92-32757
Advancing automation and robotics technology for the Space Station Freedom and for the US economy
[NASA-TM-103940] p 4040 N92-32809
Contribution to robot-task adaptation, introduction and use of robot anisotropy and task object for the design of the workstation
[ISAL-91-0095] p 4039 N92-33056
Jacobian and stiffness analysis of a novel class of six-DOF parallel minimanipulators
[DE92-016373] p 4054 N92-33184
A hybrid numerical/knowledge based system for locomotion control of a multi-legged articulated robot
[ISBN-0-315-52925-3] p 4054 N92-33203
Hypothesis refinement for 3-D scene interpretation
[ISBN-0-315-57864-5] p 4048 N92-33210
Investigations of adaptive control for a direct drive robotic manipulator
[ISBN-0-315-59030-0] p 4055 N92-33236
ROBOTS
Rational behavior model: A tri-level multiple paradigm architecture for robot vehicle control software
[AD-A250370] p 4053 N92-32748
Advancing automation and robotics technology for the Space Station Freedom and for the US economy
[NASA-TM-103940] p 4040 N92-32809
Autonomous berthing/unberthing of a Work Attachment Mechanism/Work Attachment Fixture (WAM/WAF)
[NASA-CR-190647] p 4019 N92-32885
Obstacle avoidance for redundant robots using configuration control
[NASA-CASE-NPO-17852-1-CU] p 4054 N92-33019
Contribution to robot-task adaptation, introduction and use of robot anisotropy and task object for the design of the workstation
[ISAL-91-0095] p 4039 N92-33056
A hybrid numerical/knowledge based system for locomotion control of a multi-legged articulated robot
[ISBN-0-315-52925-3] p 4054 N92-33203
ROBUSTNESS (MATHEMATICS)
Robust stabilization of the Space Station
[NASA-CR-190627] p 3942 N92-32244
The impact of time step definition on code convergence and robustness p 4001 N92-32282
A learning enhanced flight control system for high performance aircraft
[AD-A252520] p 3938 N92-32435
Consistency and robustness of knowledge graphs
[ISBN-90-9003729-2] p 4056 N92-32679
ROCKET ENGINE DESIGN
Tenth Workshop for Computational Fluid Dynamic Applications in Rocket Propulsion, part 2
[NASA-CP-3163-PT-2] p 3994 N92-32245
SRMAFTE facility checkout model flow field analysis p 3994 N92-32247
CFD analysis of the STME nozzle flowfield p 3995 N92-32251
A status of the Turbine Technology Team activities p 3998 N92-32267
Technology test bed review p 4001 N92-32279
Advanced solid rocket motor project status p 3945 N92-32280
Space Transportation Main Engine p 3945 N92-32281
CFD analysis of pump consortium impeller p 4002 N92-32287
Complex three-dimensional internal flows in the ASRM and RSRM aft end segments p 4005 N92-32304
ROCKET ENGINES
Computational fluid dynamic design of rocket engine pump components p 4003 N92-32293
CAGI: Computer Aided Grid Interface. A work in progress p 4005 N92-32302
Using adaptive grid in modeling rocket nozzle flow p 4005 N92-32303
Device and process for attachment of parts to rocket motors
[AD-D015309] p 3944 N92-33162
ROCKET LININGS
Computational fluid dynamics analysis of SSME phase 2 and phase 2+ preburner injector element hydrogen flow paths p 3997 N92-32261
ROCKET NOZZLES
SRMAFTE facility checkout model flow field analysis p 3994 N92-32247
A status of the activities of the NASA. Marshall Space Flight Center Combustion Devices Technology Team p 3995 N92-32250
CFD analysis of the STME nozzle flowfield p 3995 N92-32251
Application of computational fluid dynamics to the design of the film cooled STME subscale nozzle for the National Launch System p 3996 N92-32254
Development of the KIVA-2 CFD code for rocket propulsion applications p 3945 N92-32272
Using adaptive grid in modeling rocket nozzle flow p 4005 N92-32303
ROCKET PROPELLANTS
Development of a minimum smoke propellant based on glycidyl azide polymer and ammonium nitrate p 3976 N92-33243
ROCKET TEST FACILITIES
Advanced solid rocket motor project status p 3945 N92-32280
ROCKET THRUST
A numerical model for atomization-spray coupling in liquid rocket thrust chambers p 3996 N92-32257
Combustion instability analysis for liquid propellant rocket engines p 3966 N92-32297
ROCKET VEHICLES
ROAR: A 3-D tethered rocket simulation code
[DE92-017358] p 3944 N92-33166
ROCKS
HDR opportunities and challenges beyond the long-term flow test isco, CA, 24-26 Mar. 1992
[DE92-011234] p 4025 N92-32695
RODS
Transverse diode pumping of solid-state lasers
[AD-A252213] p 4016 N92-33089
Silver coated superconducting ceramic powder
[AD-D015294] p 3973 N92-33157
ROLL
A background to the handling qualities of aircraft
[ESDU-92006] p 3939 N92-32780
ROLLING
Noncircular rolling joints for vibrational reduction in slewing maneuvers
[NASA-CASE-LAR-14515-1-CU] p 4019 N92-33031
ROLLING MOMENTS
Contribution of tailplane-mounted twin fins to sideforce, yawing moment, and rolling moment derivatives due to sideslip
[ESDU-92007] p 3939 N92-32487

Lift and rolling moment due to spoilers on wings with trailing-edge flaps deflected at subsonic speeds
[ESDU-92002-SUPPL] p 3931 N92-32782

ROSSBY REGIMES
Dynamics of Rossby waves in a parabolic jet
[ISBN-0-315-57159-4] p 4034 N92-33225

ROTARY WING AIRCRAFT
Building vibrations induced by noise from rotorcraft and propeller aircraft flyovers
[NASA-TM-104170] p 4063 N92-33160

ROTATING SHAFTS
Mixed model fatigue crack growth behavior in a high strength steel
[AD-A250667] p 4022 N92-32717
Contribution to the theoretical and experimental analysis of camshaft engine operation
[ETN-92-91961] p 4018 N92-32726

ROTATION
Effects of curvature and rotation on turbulence in the NASA low-speed centrifugal compressor impeller p 4003 N92-32292
Rotational barriers in model compounds of poly (vinyl chloride): 2-chlorobutane and 1,3,5,7,9,11-hexachlorododecane
[AD-A250855] p 3960 N92-32330
The shapes and collective behavior of rapidly rotating nuclei
[DE92-017192] p 4067 N92-32928
Rotating-unbalanced-mass devices and methods for scanning balloon-borne-experiments, free-flying spacecraft, and space shuttle/space station attached experiments
[NASA-CASE-MFS-28425-1] p 4015 N92-33010

ROTOR BLADES (TURBOMACHINERY)
A status of the activities of the NASA/MSFC pump stage technology team p 4002 N92-32286
Impeller tandem blade study with grid embedding for local grid refinement p 4002 N92-32290
Statistics on aircraft gas turbine engine rotor failures that occurred in US commercial aviation during 1988
[DOT/FAA/CT-91/28] p 3938 N92-33105

ROUTES
The problems of routing and scheduling in multihop radio networks. A Hopfield neural network approach
[AD-A247431] p 3979 N92-32570

RUN TIME (COMPUTERS)
Computations of unsteady multistage compressor flows in a workstation environment
[NASA-TM-103839] p 3938 N92-32452

RUNGE-KUTTA METHOD
The impact of time step definition on code convergence and robustness p 4001 N92-32282

RUNWAYS
Performance of insulated pavements at Newton Fields, Jackman, Maine
[CRREL-92-9] p 3940 N92-32903

RUTHENIUM
Electrocatalyst surfaces
[PB92-190420] p 3962 N92-32591

RUTHENIUM COMPOUNDS
Excited state processes in transition metal complexes: Redox splitting in soluble polymers
[DE92-011808] p 3971 N92-32631

S

SAAB AIRCRAFT
Vibro-acoustic FE analyses of the Saab 2000 aircraft p 4062 N92-32952

SAFETY
Insensitive Munitions
[AGARD-CP-511] p 3975 N92-33240
The United States Air Force explosives hazards reduction program p 3976 N92-33241

SAFETY FACTORS
Safety study of TCAS 2 for logic version 6.04
[DOT/FAA/RD-92/22] p 3933 N92-32537
Lithium sulphur dioxide battery failure following high frequency vibration
[CRAD-1-90] p 3990 N92-32812
Edge gradient and safety factor effects on electrostatic turbulent transport in tokamaks
[DE92-014323] p 4079 N92-32944

SAGE SATELLITE
SAGE 1 data user's guide
[NASA-RP-1275] p 4031 N92-33097

SAMPLERS
Phase distributions of airborne polycyclic aromatic hydrocarbons in two US cities
[PB92-164979] p 4028 N92-32543

SAMPLING
A Markov model of software usage p 4045 N92-32881
Stochastic models in reliability
[AD-A250934] p 4020 N92-33151

SANDWICH STRUCTURES
A Protection And Detection Surface (PADS) for damage tolerance p 3948 N92-32523
Buckling of fibre reinforced composite and sandwich laminates with higher-order shear deformation theories
[IIT-B/CE/RR/92/2] p 4022 N92-32783

SAPPHIRE
Thermal strains in titanium aluminide and nickel aluminide composites
[DE92-015181] p 3953 N92-32638
Microwave properties of peeled HEMT devices sapphire substrates p 3984 N92-32978

SATELLITE ATMOSPHERES
Symposium on Titan
[ESA-SP-338] p 4093 N92-32348
Some issues associated with the formation of the Saturnian system p 4093 N92-32349
Impact origin of Titan's atmosphere p 4094 N92-32351
The thermal structure of the atmosphere of Titan p 4094 N92-32353
The composition of the Titan atmosphere p 4094 N92-32354
Titan's atmosphere: Latitudinal variations in temperature and composition p 4094 N92-32355
A reanalysis of Voyager UVS observations of Titan p 4094 N92-32357
The atmospheric temperature structure of Titan p 4095 N92-32358
The meteorology of Titan p 4095 N92-32360
Numerical simulation of the circulation of the atmosphere of Titan p 4095 N92-32361
Simple dynamical models of Titan's atmospheric circulation p 4095 N92-32362
A preliminary assessment of the Titan planetary boundary layer p 4095 N92-32363
Gravitational tide in the atmosphere of Titan p 4096 N92-32364
The significance of meteoric ionisation for the propagation of lightning spherics in the atmosphere of Titan p 4096 N92-32365
Modeling of the diurnal variations of the atmosphere of Titan p 4096 N92-32366
Neutral composition of Titan's atmosphere. A theoretical model p 4096 N92-32367
Titan's organic chemistry: Results of simulation experiments p 4096 N92-32369
Titan's organic haze p 4097 N92-32372
Infrared properties of Titan's clouds and aerosols p 4097 N92-32373
Observing the surface of Titan through near-infrared windows in its atmosphere p 4097 N92-32374
The detectability of Titan's surface in the near-infrared p 4097 N92-32375
Titan's mid-IR albedo: New observations from 3 to 5 microns p 4097 N92-32376
VIMS/Cassini mission at Titan: Scientific objectives and observational scenarios p 4097 N92-32377
Cassini/CIRS capabilities for aerosol, cloud, and surface measurements p 4098 N92-32378
Huygens/ACP: An instrument for aerosols chemical composition measurements p 4098 N92-32379
Huygens/ASI plasma wave analyzer capabilities for aerosol measurement p 4098 N92-32380
Plausible surface models for Titan p 4098 N92-32381
Plasma interaction of Titan with the Saturnian magnetosphere: A review of critical issues p 4098 N92-32382
Atmospheric escape from Titan p 4099 N92-32384
Titan's magnetospheric interaction p 4099 N92-32385
The ionosphere of Titan and its interaction with Saturnian magnetospheric electrons p 4099 N92-32386
The Huygens probe p 4099 N92-32388
Experimental determination of the refractive index of liquefied gas mixtures: Applications to hypothesized Titan oceans p 4099 N92-32390
Formation and growth of photochemical aerosols in Titan's atmosphere p 4100 N92-32393
Properties and distribution of the aerosols in the atmosphere of Titan p 4100 N92-32396
Titan's atmosphere structure from Huygen's-ASI measurements p 4101 N92-32398
The Huygens SSP Refractometer (REF) p 4101 N92-32399
Some problems about IR band integrated intensities; 3 examples for application to Titan: C6H6, HC3N, and C4H2 p 4101 N92-32400
The spectrum of Titan in the 1.06 and 1.28 micron windows p 4101 N92-32401
Titan in a box p 4101 N92-32404
Study of transmitted light through the atmosphere of Titan p 4102 N92-32408
Dielectric constant measurements in simulated Titan ocean liquids p 4102 N92-32409
A surface science package for the Huygens Titan probe p 4102 N92-32410

SATELLITE COMMUNICATION
An optically controlled Ka-band phased array antenna p 3983 N92-32968
Developments in the theory of Cantor-type variables with application to communications over fading channels
[ISBN-0-315-61378-5] p 3987 N92-33213

SATELLITE INSTRUMENTS
Collaborative, remote, in-depth inspection and verification of satellites with neutral particle beams
[DE92-014195] p 3943 N92-32934
SAGE 1 data user's guide
[NASA-RP-1275] p 4031 N92-33097

SATELLITE NETWORKS
Coverage studies for spaced-based radar
[DREO-90-18] p 3982 N92-32818

SATELLITE SURFACES
A surface science package for the Huygens Titan probe p 4102 N92-32410
Satellite anomalies and electrostatic surface discharges
[AD-A246880] p 3942 N92-32538

SATELLITE-BORNE INSTRUMENTS
Grill spectrometry on the Space Shuttle during the Atlas 1 mission
[AERONAUTICA-ACTA-A-364-199] p 3943 N92-32728
Investigations preparatory to the Wet Satellite Model Experiment
[NLR-TP-91219-U] p 3943 N92-32834

SATELLITE-BORNE RADAR
Coverage studies for spaced-based radar
[DREO-90-18] p 3982 N92-32818

SATURN (PLANET)
Some issues associated with the formation of the Saturnian system p 4093 N92-32349
Plasma interaction of Titan with the Saturnian magnetosphere: A review of critical issues p 4098 N92-32382
The ionosphere of Titan and its interaction with Saturnian magnetospheric electrons p 4099 N92-32386
Cassini: A mission to Saturn and Titan p 4099 N92-32387

SATURN ATMOSPHERE
Some issues associated with the formation of the Saturnian system p 4093 N92-32349
Plasma interaction of Titan with the Saturnian magnetosphere: A review of critical issues p 4098 N92-32382
Mass loading at Titan and comets p 4098 N92-32383
The ionosphere of Titan and its interaction with Saturnian magnetospheric electrons p 4099 N92-32386

SAWTOOTH WAVEFORMS
The role of stochasticity in sawtooth oscillation
[DE92-782004] p 3982 N92-32905
Measurement of nonlinear mode coupling of tearing fluctuations
[DE92-013901] p 4080 N92-33154

SCALARS
Scalar mesons and kaons in phi radiative decay and their implications for studies of CP violation at DA(phi)NE
[RAL-91-085] p 4068 N92-33133

SCALING LAWS
Thermal gravitational modelling and scaling of two-phase heat transport systems for space: An assessment and a comparison of predictions and experimental results
[NLR-TP-91401-U] p 4008 N92-32675
Two-phase heat transport systems for space: Thermal gravitational modelling and scaling predictions versus results of experiments
[NLR-TP-91051-U] p 4010 N92-32786

SCANNING
Instrument scanning and subjective workload with the peripheral vision horizon display
[CTN-92-60359] p 4038 N92-32617

SCANNING TUNNELING MICROSCOPY
Annual report, 1 November 1990 - 31 October 1991
[AD-A252431] p 4084 N92-32940

SCARFING
Processing and environmental effects on mechanical properties of composite repairs
[NRC-LTR-ST-1826] p 3954 N92-32791

SCATTERING
Design and construction of a sample preparation chamber for atomic beam scattering
[DE92-014509] p 4065 N92-32473
Numerical evaluation of the incomplete airy functions and their application to high frequency scattering and diffraction
[NASA-CR-190745] p 4058 N92-32888

Gamma scattering in condensed matter with high intensity Moessbauer radiation
[DE92-014811] p 4085 N92-33025
Theoretical aspects of lepton-hadron scattering
[DE92-013765] p 4069 N92-33148
A study of four jet events and search for double parton scattering at square root s = 1.8 TeV
[DE92-016351] p 4069 N92-33164
Neutron scatter studies of chromatin structures related to functions
[DE92-014032] p 4036 N92-33181

SCATTERING AMPLITUDE
Study and development of a six port network analyzer in the 1-18 GHz frequency range
[TELECOM-91-E-005] p 3980 N92-32739

SCATTERING CROSS SECTIONS
On the choice of minimization functional in the partial wave analysis
[DE92-624689] p 4087 N92-32309
Comparison of spin asymmetries and invariant cross sections in production of (pi)(sup 0) mesons by polarized antiprotons and protons with 200 GeV energy
[DE92-624691] p 4064 N92-32311
Electron-atom scattering
[DE92-625005] p 4064 N92-32340
Range of validity of distorted wave Born and impulse approximations for (e,2e)
[DE92-624821] p 4087 N92-32649

SCATTERING FUNCTIONS
New approach to HF channel modeling and simulation. Part 3: Transfer function
[PB92-192848] p 3979 N92-32555

SCENE ANALYSIS
Hypothesis refinement for 3-D scene interpretation
[ISBN-0-315-57864-5] p 4048 N92-33210

SCHEDULES
The problems of routing and scheduling in multihop radio networks. A Hopfield neural network approach
[AD-A247431] p 3979 N92-32570
NAASW modular radar research testbed study results
[DE92-011339] p 3981 N92-32744

SCHEDULING
The problems of routing and scheduling in multihop radio networks. A Hopfield neural network approach
[AD-A247431] p 3979 N92-32570
Analysis of delay reducing and fuel saving sequencing and spacing algorithms for arrival traffic
[NASA-TM-103880] p 3933 N92-33194

SCHLIEREN PHOTOGRAPHY
An experimental study of the flow over a sharp-edged delta wing at subsonic and transonic speeds
[NLR-TP-91117-U] p 3930 N92-32732

SCHOOLS
A minority research and education information service: Design, develop, pilot test, and implement on-line access for historically black colleges and universities and government agencies
[DE92-013572] p 4090 N92-32930

SCHROEDINGER EQUATION
Two perspectives on a decohering spin
[DE92-013021] p 4087 N92-32496
Schroedinger operators with singular potentials in the semiclassical limit
[ETN-92-92145] p 4058 N92-32840
Pseudopotential band calculations along a high-symmetry axis. Part 1: Central potential and the (111) direction
[AD-A252399] p 4084 N92-32938
MOL calculation of the solitons of the cubic Schroedinger equation
[DE92-017245] p 4060 N92-32998

SCINTILLATION
Scintillation properties of lead sulfate
[DE92-010301] p 4082 N92-32493

SCREW PINCH
Magnetohydrodynamic stability of plasmas with radial motion
[DE92-013917] p 4077 N92-32417

SEA STATES
Parameterization of directional spectra, part 2. Volume 2: User's manual for the programs RMODEL, FITHM, and FITDM
[DREA-CR-89-445-PT-2-VOL-2] p 3981 N92-32749

SEA SURFACE TEMPERATURE
An evaluation of an infrared/resistance temperature device for air/sea-surface temperature measurements
[AD-A252279] p 4035 N92-32688
Climate System Monitoring (CSM) Monthly Bulletin, issue no. 1 p 4034 N92-33073

SEA WATER
Simulations of the carbon cycle in the oceans
[DE92-016622] p 4035 N92-32336

SEAMS (JOINTS)
Device and process for attachment of parts to rocket motors
[AD-D015309] p 3944 N92-33162

SEARCH RADAR
Beam and filter straddle losses in an ESA search radar
[AD-A250878] p 3980 N92-32680

SEATS
The weight optimization of an armored crashworthy crewseat through the use of advanced composites and design p 3947 N92-32517

SECONDARY ION MASS SPECTROMETRY
Analysis of LDEF experiment AO187-2: Chemically and isotopic measurements of micrometeoroids by secondary ion mass spectrometry
[NASA-CR-190697] p 4093 N92-32541

SECURITY
Correlation of single mode fiber fabrication factors and radiation response
[AD-A247301] p 4074 N92-32613
Toward advanced human reliability programs. Structural development considerations and options for extreme risk environments
[AD-A250786] p 4038 N92-32660
Science and technology: A report to the Congress
[PB92-183219] p 4104 N92-33086

SEDIMENTS
Hydrate detection
[DE92-014350] p 4034 N92-32333

SEGMENTS
Target detection using co-occurrence matrix segmentation and its hardware implementation p 3936 N92-32443

SEISMIC WAVES
Wave propagation in laterally varying media: A model expansion method
[AD-A247553] p 4031 N92-32572

SEISMOLOGY
System response to relay chatter
[DE92-013076] p 3988 N92-32495

SELECTION
Statistical selection: Multiple comparison approach
[ETN-92-92051] p 4060 N92-32709

SELF CONSISTENT FIELDS
Rotational barriers in model compounds of poly (vinyl chloride): 2-chlorobutane and 1,3,5,7,9,11-hexachlorododecane
[AD-A250855] p 3960 N92-32330

SELF ORGANIZING SYSTEMS
Enhancements to speech recognition on voice response systems
[TELECOM-91-E-018] p 3981 N92-32807

SEMICONDUCTOR DEVICES
Theory of elementary particles studies in weak interaction and grand unification and studies in accelerator design
[DE92-014320] p 4066 N92-32597
Investigation of impurity related phenomena, significant for novel semiconductor technologies
[ETN-92-92048] p 4083 N92-32760
The energetic radiation environment in a highly elliptical (Molniya) orbit
[AD-A252394] p 4031 N92-32902

SEMICONDUCTOR LASERS
Transverse diode pumping of solid-state lasers
[AD-A252213] p 4016 N92-33089
Laser to single-mode-fiber coupling: A laboratory guide
[NASA-CR-4452] p 4077 N92-33239

SEMICONDUCTORS (MATERIALS)
Pulse coded biologically motivated neural-type MOS circuits
[AD-A250367] p 3988 N92-32325
Laser material interaction
[AD-A250853] p 4016 N92-32622
Photogenerated carrier-induced reactions on UHV semiconductor surfaces
[DE92-015355] p 4082 N92-32641
High translational energy induced reaction in semiconductors
[AD-A250980] p 3989 N92-32669
Development of ultra-low noise, high sensitivity planar metal grating coupled AlGaAs/GaAs multiquantum well IR detectors for focal plane array staring IR sensor systems
[AD-A250368] p 4083 N92-32747
Annual report, 1 November 1990 - 31 October 1991
[AD-A252431] p 4084 N92-32940

SENSITIVITY
Development of ultra-low noise, high sensitivity planar metal grating coupled AlGaAs/GaAs multiquantum well IR detectors for focal plane array staring IR sensor systems
[AD-A250368] p 4083 N92-32747

SENSORS
Depolarized light source for fiber optic sensors
[AD-D015289] p 4074 N92-32634

SEPARATED FLOW
A critical evaluation of a three-dimensional Navier-Stokes CFD as a tool to design supersonic turbine stages p 3999 N92-32268
Massively separated flow modeling. Experimental study of the fine structure of boundary layers. Study of the influence of external turbulence level
[ETN-92-92088] p 4009 N92-32765

SEPARATORS
NEDO Alcohol/Biomass Technology Subcommittee
[DE92-526270] p 3975 N92-32914

SEQUENCING
Study of the mechanical behaviour of graphite/epoxy laminates subjected to static and cyclic loading
[NRC-30833] p 3955 N92-32813

SERVICE LIFE
Reliability training
[NASA-RP-1253] p 3941 N92-32456
Supportability evaluation of thermoplastic and thermoset composites p 3950 N92-32576
Residual strength of repaired graphite/epoxy laminates after 5 years of outdoor exposure p 3950 N92-32577
PDES application protocol suite for composites (PAS-C). Functional needs report for the PAS-C program
[AD-A247886] p 3953 N92-32629
Life testing of a low voltage air circuit breaker
[DE92-014173] p 3988 N92-32635
Fatigue, hysteresis, and acoustic emission, parts 1 and 2
[AD-A251073] p 4021 N92-32681
UHM/HNEI EV test and evaluation program
[DE92-011631] p 3989 N92-32754
Life cycle oriented method for development and production of large scale industrial mathematics software
[NLR-TP-91196-U] p 4043 N92-32833
A prototype software engineering environment for domain modeling and reuse p 4046 N92-32882
Effects of the abrasiveness of test and training site soils on parachute life
[AD-A252389] p 3931 N92-32900

SERVOMECHANISMS
Tolerance optimization of servomechanisms
[ISBN-90-9004476-0] p 4018 N92-32692

SET THEORY
Geometric continuity and Frenet continuity of parametric curves
[IMAG-RR-846-M] p 4057 N92-32761
Dissimilarities, dendograms, prefillers, and multiapplications of levels
[IMAG-RR-842-M] p 4058 N92-32799
Visibility properties of polygons
[ISBN-0-315-57272-8] p 4049 N92-33229

SHADOWGRAPH PHOTOGRAPHY
Topographical measuring based on the shadow and projection Moire method
[ISBN-90-9004146-X] p 4074 N92-32705

SHAFTS (MACHINE ELEMENTS)
Reducing torque fluctuation in linkage drive shafts
[ESDU-92016] p 4017 N92-32482
Life testing of a low voltage air circuit breaker
[DE92-014173] p 3988 N92-32635
Noncircular rolling joints for vibrational reduction in slewing maneuvers
[NASA-CASE-LAR-14515-1-CU] p 4019 N92-33031

SHAPE MEMORY ALLOYS
Device for removing foreign objects from anatomic organs
[NASA-CASE-GSC-13306-1] p 4038 N92-33032

SHAPES
Examples of advanced near-net shape manufacturing techniques for aerospace
[MBB-Z-0399-91-PUB] p 3977 N92-32742
Shape recognition by computer in simulated aerial images
[DCIEM-91-05] p 4054 N92-32854
The shapes and collective behavior of rapidly rotating nuclei
[DE92-017192] p 4067 N92-32928
Pattern recognition based on entropy analysis and shape transformations
[ISBN-0-315-56074-6] p 4048 N92-33201

SHARP LEADING EDGES
An experimental study of the flow over a sharp-edged delta wing at subsonic and transonic speeds
[NLR-TP-91117-U] p 3930 N92-32732
Strong coupling between inviscid fluid and boundary layer of sharp leading edges: Two-dimensional stationary and turbulent cases for isolated profiles and guard vanes
[ONERA-RT-44/1621-RY-016-R] p 4010 N92-32776

SHEAR FLOW
Interactive control in turbulent shear layers
[AD-A250711] p 4008 N92-32671

SHEAR LAYERS
Interactive control in turbulent shear layers
[AD-A250711] p 4008 N92-32671
SHEAR PROPERTIES
Buckling of fibre reinforced composite and sandwich laminates with higher-order shear deformation theories
[IIT-B/CE/RR/92/2] p 4022 N92-32783
A unique method of determining the elastic and engineering constants of unidirectional fibre-reinforced composite plates using ultrasound
[UTIAS-TN-274] p 3955 N92-32829
A comparison of three popular test methods for determining the shear modulus of composite materials
[NASA-CR-190659] p 3959 N92-33075
SHEAR STRAIN
Buckling of fibre reinforced composite and sandwich laminates with higher-order shear deformation theories
[IIT-B/CE/RR/92/2] p 4022 N92-32783
SHEAR STRENGTH
Processing and environmental effects on mechanical properties of composite repairs
[NRC-LTR-ST-1826] p 3954 N92-32791
SHEAR STRESS
Postbuckling behavior of curved panels under combined compression and shear loads p 3952 N92-32584
Shear buckling of specially orthotropic plates with centrally located cutouts p 3953 N92-32589
Free vibration of thick isotropic and orthotropic cylindrical shells
[DE92-011653] p 4022 N92-32706
SHIELDING
ANL ITER high-heat-flux blanket-module heat transfer experiments
[DE92-017749] p 4080 N92-33168
SHIPS
Naval target classification and designation with the CL-227 Sea Sentinel p 3937 N92-32449
Bacterial responses to extreme temperatures and pressures and to heavy organic loading
[AD-A247456] p 4035 N92-32571
SHOCK TUBES
Treating convection in sequential solvers
p 4000 N92-32277
A shock tube study of the reactions of the hydroxyl radical with combustion species
[DE92-012573] p 3960 N92-32464
Characterization of flow distribution in axisymmetric shock tubes
[AD-A251095] p 4008 N92-32683
SHOCK WAVES
A state of the art report on flame acceleration and transition to detonation in hydrogen/air/diluent mixtures
[DE92-626850] p 3961 N92-32475
Swept shock/boundary layer interaction experiments in support of CFD code validation
[NASA-CR-190583] p 3930 N92-32494
An examination of several high resolution schemes applied to complex problems in high speed flows
[AD-A250814] p 4008 N92-32632
Characterization of flow distribution in axisymmetric shock tubes
[AD-A251095] p 4008 N92-32683
Time-resolved holography for the study of shock waves
[ISBN-0-315-62369-1] p 4013 N92-33226
SHOPS
Software process assessment for small software shops p 4045 N92-32878
SHOT PEENING
Guide to the effect of shot peening on fatigue strength
[ESDU-92015] p 3967 N92-32779
SHROUDS
Effects of curvature and rotation on turbulence in the NASA low-speed centrifugal compressor impeller
p 4003 N92-32292
SIDELOBES
Phase-only synthesis for multiple-beam phased arrays with element failures
[AD-A252250] p 3982 N92-32891
SIDESLIP
Contribution of tailplane-mounted twin fins to sideforce, yawing moment, and rolling moment derivatives due to sideslip
[ESDU-92007] p 3939 N92-32487
SIEVES
An evaluation of the performance characteristics of a two-man molecular sieve oxygen generating system
[DCIEM-91-20] p 4039 N92-33079
SIGNAL ANALYZERS
Generic modular imaging IR signal processor
p 3936 N92-32440
Study and development of a six port network analyzer in the 1-18 GHz frequency range
[TELECOM-91-E-005] p 3980 N92-32739
SIGNAL DETECTION
Interception of LPI radar signals
[AD-A246315] p 3978 N92-32535
Recursive estimation techniques for detection of small objects in infrared image data
[AD-A250942] p 4075 N92-32935
Real time pre-detection dynamic range compression
[NASA-CASE-NPO-18098-1-CU] p 4076 N92-33028
SIGNAL ENCODING
Multi-stage hybrid coding of digital images
[ISBN-0-315-58989-2] p 4047 N92-33189
SIGNAL FADING
Developments in the theory of Cantor-type variables with application to communications over fading channels
[ISBN-0-315-61378-5] p 3987 N92-33213
SIGNAL PROCESSING
Generic modular imaging IR signal processor
p 3936 N92-32440
Real-time processing of radar return on a parallel computer
[NASA-CR-4456] p 3932 N92-32606
Intelligent signal processing for active control
[AD-A252232] p 4053 N92-32625
Optical modulation characteristics and applications of liquid crystal televisions
[AD-A252466] p 3979 N92-32633
Airport Surveillance Radar (ASR-9) wind shear processor: 1991 test at Orlando, Florida
[AD-A252246] p 3980 N92-32686
The design and development of a portable, DSP micro-processor based, high-accuracy data acquisition system
[NRC-32146] p 4040 N92-32851
Phase-only synthesis for multiple-beam phased arrays with element failures
[AD-A252250] p 3982 N92-32891
Signal processing in impulsive electromagnetic interference
[AD-A252385] p 3982 N92-32899
ABF algorithms implemented at ARL:UT, FDS system engineering and acoustics
[AD-A252368] p 4046 N92-32917
Passive fetal monitoring sensor
[NASA-CASE-LAR-14088-1-CU] p 4015 N92-33016
Real time pre-detection dynamic range compression
[NASA-CASE-NPO-18098-1-CU] p 4076 N92-33028
Auto and hetero-associative memory using a 2-D optical logic gate
[NASA-CASE-NPO-17997-1-CU] p 4041 N92-33057
An implementation of a fault-tolerant, multidirectional, digital interpolation beamformer
[AD-A252494] p 3986 N92-33152
Design and implementation of N-dimensional digital filters
[ISBN-0-315-60747-5] p 3993 N92-33195
SIGNAL TO NOISE RATIOS
Holographic crosstalk and signal-to-noise ratio in orthogonal data storage
[AD-A250146] p 4013 N92-32323
SIGNS AND SYMPTOMS
Effects of CSF hormones and ionic composition on salt/water metabolism
[NASA-CR-190693] p 4037 N92-32539
SIKORSKY AIRCRAFT
Evaluation of composite components on the Bell 206L and Sikorsky S-76 helicopters p 3950 N92-32575
SILICIDES
Ultra-low density organic-inorganic composite materials possessing thermally insulating and acoustic damping properties
[AD-A251182] p 3955 N92-32828
Synthesis of MoSi2-based alloys by mechanical alloying
[DE92-017528] p 3969 N92-33120
SILICON
Concentrator silicon cell research
[DE92-016576] p 4025 N92-32565
High translational energy induced reaction in semiconductors
[AD-A250980] p 3989 N92-32669
The energetic radiation environment in a highly elliptical (Molniya) orbit
[AD-A252394] p 4031 N92-32902
Intermodulation in the oscillatory magnetoresistance of a two-dimensional electron gas p 3984 N92-32975
SILICON CARBIDES
Computational simulation of matrix micro-slip bands in SiC/Ti-15 composite
[NASA-TM-105762] p 3946 N92-32466
Thermal degradation study of silicon carbide threads developed for advanced flexible thermal protection systems
[NASA-TM-103952] p 3970 N92-32476
Thermal strains in titanium aluminide and nickel aluminide composites
[DE92-015181] p 3953 N92-32638
Interfacial studies of refractory glass-ceramic matrix/advanced SiC fiber reinforced composites
[AD-A250784] p 3953 N92-32676
Aluminum based particulate composites for aerospace applications produced by different processes
[MBB-Z-0408-91-PUB] p 3967 N92-32819
SILICON JUNCTIONS
Investigation of the oxygen-vacancy (A-center) defect complex profile in neutron irradiated high resistivity silicon junction particle detectors
[DE92-016952] p 4064 N92-32316
SILICON NITRIDES
Characterization of sintered reaction-bonded silicon nitride processed by microwave heating
[DE92-014408] p 3956 N92-32945
SILICON OXIDES
Investigation of the oxygen-vacancy (A-center) defect complex profile in neutron irradiated high resistivity silicon junction particle detectors
[DE92-016952] p 4064 N92-32316
Studies of n-butane conversion over silica-supported platinum, platinum-silver and platinum-copper catalysts
[DE92-016309] p 3962 N92-32563
SILICON RADIATION DETECTORS
Theory of elementary particles studies in weak interaction and grand unification and studies in accelerator design
[DE92-014320] p 4066 N92-32597
SILICONES
Experimental investigation of the axial impregnation of oriented fiber bundles by capillary forces
[AD-A250758] p 3961 N92-32508
SILVER
Processing and properties of silver-clad Tl-Ba-Ca-Cu-O wires and tapes
[DE92-015266] p 4081 N92-32346
Electrocatalyst surfaces
[PB92-190420] p 3962 N92-32591
Molecular dynamics modeling of the mechanical properties of metal surfaces at the nanometer scale
[DE92-010705] p 3966 N92-32646
Silver coated superconducting ceramic powder
[AD-D015294] p 3973 N92-33157
SILVER ALLOYS
Studies of n-butane conversion over silica-supported platinum, platinum-silver and platinum-copper catalysts
[DE92-016309] p 3962 N92-32563
Substrate reactions and flux pinning structures in melt-processed YBa2Cu3O7 deposits on Ag-Pd alloy substrates
[DE92-014404] p 4084 N92-32919
SILVER OXIDES
Development of advanced secondary zinc cells for power-source applications
[DE92-016358] p 3993 N92-33183
SILVER ZINC BATTERIES
Development of advanced secondary zinc cells for power-source applications
[DE92-016358] p 3993 N92-33183
SIMD (COMPUTERS)
Optimal communication schemes on an SIMD distributed-memory hypercube
[IMAG-RR-848-M] p 4051 N92-32715
SIMULATION
Titan's organic chemistry: Results of simulation experiments p 4096 N92-32369
Titan in a box p 4101 N92-32404
Dielectric constant measurements in simulated Titan ocean liquids p 4102 N92-32409
Ski jump takeoff performance predictions for a mixed-flow, remote-lift STOVL aircraft
[NASA-TM-103866] p 3935 N92-32887
SIMULATORS
SIMLAB: Automatically creating physical systems simulators
[AD-A250970] p 4042 N92-32546
SINGLE CRYSTALS
Surface reconstruction and templating for zeolite thin film synthesis observed by atomic force microscopy
[AD-A251140] p 4066 N92-32548
Contribution to the study of the effect of the heterogeneous distribution of dislocations on the cyclic plasticity of single crystal aluminum
[ISAL-91-0099] p 4083 N92-32892
Use of a Fourier deconvolution method in particle size determination and use of molecular mechanics in crystal structure determinations
[DE92-014510] p 4085 N92-33111
Studies of Y-Ba-Cu-O single crystals by x ray absorption spectroscopy
[DE92-014687] p 4086 N92-33136
SINGLE EVENT UPSETS
Satellite anomalies and electrostatic surface discharges
[AD-A246880] p 3942 N92-32538

SINGLE-PHASE FLOW
Forced convection heat transfer in straight tubes. Part 1: Fully developed turbulent flow
[ESDU-92003-PT-1] p 4010 N92-32781
SINGULARITY (MATHEMATICS)
Singularities in the classical Rayleigh-Taylor flow: Formation and subsequent motion
[NASA-CR-189690] p 4010 N92-32784
Schroedinger operators with singular potentials in the semiclassical limit
[ETN-92-92145] p 4058 N92-32840
SINTERING
Sintering of bulk high-(Tc) superconductors: Bi-Sr-Ca-Cu-O
[DE92-016189] p 4082 N92-32561
Characterization of sintered reaction-bonded silicon nitride processed by microwave heating
[DE92-014408] p 3956 N92-32945
SIZE DETERMINATION
Use of a Fourier deconvolution method in particle size determination and use of molecular mechanics in crystal structure determinations
[DE92-014510] p 4085 N92-33111
SIZE DISTRIBUTION
Properties and distribution of the aerosols in the atmosphere of Titan p 4100 N92-32396
Laboratory investigations of the aerosols in the stratosphere of Titan p 4102 N92-32405
SKIRTS
CFD analysis of the STME nozzle flowfield p 3995 N92-32251
SLEWING
Noncircular rolling joints for vibrational reduction in slewing maneuvers
[NASA-CASE-LAR-14515-1-CU] p 4019 N92-33031
SLIDING FRICTION
Dynamic systems stability with dry friction: Application to brake disc squealing
[ECL-91-48] p 4018 N92-32737
Influence of oil lubricant additives on tribological behavior of engineering ceramics
[PB92-180710] p 3973 N92-33059
SLIP CASTING
Nondestructive evaluation development for process control
[DE92-015272] p 3971 N92-32640
SLOTS
Impeller tandem blade study with grid embedding for local grid refinement p 4002 N92-32290
SLURRIES
Study of flow properties of wet solids using laser induced photochemical anemometry
[DE92-015452] p 4013 N92-33140
SMART STRUCTURES
Sound transmission reduction with intelligent panel systems p 4063 N92-32959
Active vibrations and noise control for turboprop application research program activities p 4063 N92-32962
SMOKE
Development of a minimum smoke propellant based on glycidyl azide polymer and ammonium nitrate p 3976 N92-33243
SMOKE ABATEMENT
Development of a minimum smoke propellant based on glycidyl azide polymer and ammonium nitrate p 3976 N92-33243
SNOW
Forecasting heavy snow events in Missoula, Montana
[PB92-196104] p 4034 N92-33163
SOBOLEV SPACE
Point interactions in L(sup p)
[REPT-91-97] p 4057 N92-32756
SOCIAL FACTORS
Humans and machines in space: The payoff
[ISBN-0-87703-343-9] p 4039 N92-33099
SODIUM
Development of high-performance Na/NiCl2 cell
[DE92-015270] p 3988 N92-32639
SOFTWARE ENGINEERING
Ground Systems Development Environment (GSDE) interface requirements and prototyping plan
[NASA-CR-190713] p 4041 N92-32451
Supporting multiple domains in a single reuse repository
[NASA-CR-190640] p 4090 N92-32654
Software development practice in a scientific computing environment
[NLR-TP-91193-U] p 4043 N92-32832
Life cycle oriented method for development and production of large scale industrial mathematics software
[NLR-TP-91196-U] p 4043 N92-32833
Cleanroom process evolution in the SEL p 4044 N92-32871
Measurement in practice p 4044 N92-32876
Software process assessment for small software shops p 4045 N92-32878
A study of large scale software testing p 4045 N92-32879
Analysis of data from a DO-178A software development process p 4045 N92-32880
A Markov model of software usage p 4045 N92-32881
A prototype software engineering environment for domain modeling and reuse p 4046 N92-32882
The successful introduction of software reuse across an entity p 4046 N92-32883
Developing better software: A five year history of software engineering advancement p 4046 N92-32884
Object linking in repositories
[NASA-CR-190629] p 4091 N92-33178
Independent verification and validation for Space Shuttle flight software
[NASA-CR-190826] p 4047 N92-33196
SOFTWARE REUSE
Ground Systems Development Environment (GSDE) interface requirements and prototyping plan
[NASA-CR-190713] p 4041 N92-32451
Supporting multiple domains in a single reuse repository
[NASA-CR-190640] p 4090 N92-32654
A prototype software engineering environment for domain modeling and reuse p 4046 N92-32882
The successful introduction of software reuse across an entity p 4046 N92-32883
SOFTWARE TOOLS
A computational design system for rapid CFD analysis p 4000 N92-32273
Software development practice in a scientific computing environment
[NLR-TP-91193-U] p 4043 N92-32832
Life cycle oriented method for development and production of large scale industrial mathematics software
[NLR-TP-91196-U] p 4043 N92-32833
CFD efforts in the Netherlands
[NLR-TP-91250-U] p 4011 N92-32835
Rapid development of the X-31 simulation to support flight-testing
[NASA-TM-104256] p 3935 N92-33149
Image processing mini manual
[NASA-TM-107680] p 4041 N92-33205
An evaluation of knowledge-based diagnostic techniques for debugging concurrent software
[ISBN-0-315-51189-3] p 4049 N92-33215
SOIL MOISTURE
Development of a prototype spatial information processing system for hydrologic research
[NASA-CR-190579] p 4024 N92-32590
SOILS
Effects of the abrasiveness of test and training site soils on parachute life
[AD-A252389] p 3931 N92-32900
SOL-GEL PROCESSES
Ultra-low density organic-inorganic composite materials possessing thermally insulating and acoustic damping properties
[AD-A251182] p 3955 N92-32828
SOLAR ACTIVITY
Observations of high frequency and high wavenumber solar oscillations
[AD-A250099] p 4103 N92-32488
SOLAR ATMOSPHERE
Observations of high frequency and high wavenumber solar oscillations
[AD-A250099] p 4103 N92-32488
SOLAR BLANKETS
Solar radiation on a catenary collector
[NASA-TM-105751] p 3988 N92-32243
SOLAR CELLS
Thin film cadmium telluride, zinc telluride, and mercury zinc telluride solar cells
[DE92-001237] p 4024 N92-32510
Concentrator silicon cell research
[DE92-016576] p 4025 N92-32565
The photovoltics program at Sandia National Laboratories
[DE92-014617] p 4026 N92-32946
The 1991 Japan Solar Energy Society. Japan Wind Energy Association Joint Conference
[DE92-530733] p 4027 N92-33090
SOLAR COLLECTORS
Solar radiation on a catenary collector
[NASA-TM-105751] p 3988 N92-32243
Testing of the single-element stretched-membrane dish
[DE92-013680] p 4025 N92-32549
Solar thermal energy: Viable energy technology for today and tomorrow
[DE92-015039] p 4026 N92-32923
Hot water storage tank for solar collectors
[AD-D015301] p 4026 N92-32943
The photovoltics program at Sandia National Laboratories
[DE92-014617] p 4026 N92-32946
The 1991 Japan Solar Energy Society. Japan Wind Energy Association Joint Conference
[DE92-530733] p 4027 N92-33090
High-flux solar photon processes
[DE92-001247] p 4027 N92-33138
Summary of engineering-scale experiments for the Solar Detoxification of Water project
[DE92-013776] p 4027 N92-33150
SOLAR ENERGY
Solar thermal energy: Viable energy technology for today and tomorrow
[DE92-015039] p 4026 N92-32923
The photovoltics program at Sandia National Laboratories
[DE92-014617] p 4026 N92-32946
NEMO: Advanced energy systems and technologies
[DE92-540920] p 4027 N92-33072
The 1991 Japan Solar Energy Society. Japan Wind Energy Association Joint Conference
[DE92-530733] p 4027 N92-33090
High-flux solar photon processes
[DE92-001247] p 4027 N92-33138
SOLAR ENERGY CONVERSION
Solar radiation on a catenary collector
[NASA-TM-105751] p 3988 N92-32243
Solar photo-thermal catalytic reactions to produce high value chemicals
[DE91-002140] p 4026 N92-32908
Solar thermal energy: Viable energy technology for today and tomorrow
[DE92-015039] p 4026 N92-32923
The 1991 Japan Solar Energy Society. Japan Wind Energy Association Joint Conference
[DE92-530733] p 4027 N92-33090
Summary of engineering-scale experiments for the Solar Detoxification of Water project
[DE92-013776] p 4027 N92-33150
SOLAR FLUX
High-flux solar photon processes
[DE92-001247] p 4027 N92-33138
SOLAR GENERATORS
Solar thermal energy: Viable energy technology for today and tomorrow
[DE92-015039] p 4026 N92-32923
The 1991 Japan Solar Energy Society. Japan Wind Energy Association Joint Conference
[DE92-530733] p 4027 N92-33090
SOLAR HEATING
Environmental consequences of new energy technology. Solar heating, heat stores, and heat pumps
[PB92-180843] p 4025 N92-32605
Solar thermal energy: Viable energy technology for today and tomorrow
[DE92-015039] p 4026 N92-32923
Hot water storage tank for solar collectors
[AD-D015301] p 4026 N92-32943
The 1991 Japan Solar Energy Society. Japan Wind Energy Association Joint Conference
[DE92-530733] p 4027 N92-33090
SOLAR INSTRUMENTS
NASA Marshall Space Flight Center Solar Observatory report, January - June 1992
[NASA-TM-103597] p 4092 N92-32478
SOLAR NEUTRINOS
Research and development of a helium-4 based solar neutrino detector
[DE92-017390] p 4103 N92-33119
SOLAR OBSERVATORIES
NASA Marshall Space Flight Center Solar Observatory report, January - June 1992
[NASA-TM-103597] p 4092 N92-32478
SOLAR OSCILLATIONS
Observations of high frequency and high wavenumber solar oscillations
[AD-A250099] p 4103 N92-32488
SOLAR RADIATION
Solar radiation on a catenary collector
[NASA-TM-105751] p 3988 N92-32243
SOLAR SYSTEM
Formation of the satellites p 4093 N92-32350
SOLAR TEMPERATURE
Observations of high frequency and high wavenumber solar oscillations
[AD-A250099] p 4103 N92-32488
SOLAR TERRESTRIAL INTERACTIONS
STEL p 4103 N92-32457
SOLAR WIND
Mass loading at Titan and comets p 4098 N92-32383

SOLID ELECTROLYTES
High-temperature Solid Oxide Fuel Cell (SOFC) generator development project: Environmental assessment
[DE92-014698] p 4026 N92-32924
SOLID PHASES
Bone as a liquid-filled diphase porous medium
p 4037 N92-32663
SOLID PROPELLANT COMBUSTION
A two-phase restricted equilibrium model for combustion of metalized solid propellants p 3966 N92-32307
CARS diagnostics for solid propellant combustion investigations
[AD-A248660] p 3963 N92-32645
Condensed-phase processes during solid propellant combustion. Part 2: Chemical and microscopic examination of conductively quenched samples of RDX, XM39, JA2, M30, and HMX-binder compositions
[AD-A250799] p 3974 N92-32664
SOLID PROPELLANT ROCKET ENGINES
Tenth Workshop for Computational Fluid Dynamic Applications in Rocket Propulsion, part 2
[NASA-CP-3163-PT-2] p 3994 N92-32245
Current status of the development of an ignition transient model for solid rocket motors p 3944 N92-32246
SRMAFTE facility checkout model flow field analysis
p 3994 N92-32247
A comparative study of the effects of inhibitor stub length on solid rocket motor combustion chamber pressure oscillations: RSRM at T = 80 seconds, preliminary results p 3945 N92-32248
Overview of the relevant CFD work at Thiokol Corporation p 3995 N92-32249
Tenth Workshop for Computational Fluid Dynamic Applications in Rocket Propulsion, part 1
[NASA-CP-3163-PT-1] p 4000 N92-32278
Complex three-dimensional internal flows in the ASRM and RSRM aft end segments p 4005 N92-32304
An analysis of the flow field in the region of the ASRM field joints p 4005 N92-32305
Effect of including variable gas properties and entrained particles in the flow analysis of the ASRM nozzle
p 4006 N92-32306
A two-phase restricted equilibrium model for combustion of metalized solid propellants p 3966 N92-32307
The design features of rocket motors relating to insensitive munition response to thermo-mechanical stimuli p 3976 N92-33244
SOLID PROPELLANTS
SRMAFTE facility checkout model flow field analysis
p 3994 N92-32247
CARS diagnostics for solid propellant combustion investigations
[AD-A248660] p 3963 N92-32645
Condensed-phase processes during solid propellant combustion. Part 2: Chemical and microscopic examination of conductively quenched samples of RDX, XM39, JA2, M30, and HMX-binder compositions
[AD-A250799] p 3974 N92-32664
SOLID ROCKET PROPELLANTS
Current status of the development of an ignition transient model for solid rocket motors p 3944 N92-32246
SOLID STATE
Solid State Technology Branch of NASA Lewis Research Center
[NASA-TM-105752] p 3982 N92-32965
SOLID STATE DEVICES
Solid State Technology Branch of NASA Lewis Research Center
[NASA-TM-105752] p 3982 N92-32965
High efficiency fast neutron threshold deflector
[AD-D015311] p 4073 N92-33167
SOLID STATE LASERS
Transverse diode pumping of solid-state lasers
[AD-A252213] p 4016 N92-33089
Resonantly pumped, erbium-doped, 2.8 micron solid state laser with high slope efficiency
[AD-D015310] p 4017 N92-33165
SOLID-SOLID INTERFACES
Thermal conductance of augmented pressed metallic contacts at liquid helium temperatures
[NASA-TM-103917] p 4007 N92-32474
SOLIDIFICATION
Formation of high temperature superconductors from the solidified melt
[DE92-012584] p 4081 N92-32465
SOLIDS
Titan's organic haze p 4097 N92-32372
Near infrared spectra of potential solids at the surface of Titan p 4102 N92-32406
Study of flow properties of wet solids using laser induced photochemical anemometry
[DE92-015452] p 4013 N92-33140
Study of flow properties of wet solids using laser induced photochemical anemometry
[DE92-014031] p 4017 N92-33180
SOLIDS FLOW
Numerical simulation of inclined chute flows of monodisperse, inelastic, frictional spheres
[DE92-014775] p 4012 N92-32947
Study of flow properties of wet solids using laser induced photochemical anemometry
[DE92-014031] p 4017 N92-33180
SOLITARY WAVES
Can the speed of light in the fiber be controlled?
[AD-A247614] p 4074 N92-32668
MOL calculation of the solitons of the cubic Schroedinger equation
[DE92-017245] p 4060 N92-32998
SOLUBILITY
Excited state processes in transition metal complexes: Redox splitting in soluble polymers
[DE92-011808] p 3971 N92-32631
Synthesis, morphology and properties of polyester-urethane in solution in styrene: Application to composites development
[ISAL-92-0007] p 3972 N92-32762
Continuum configurational bias Monte-Carlo studies of alkanes and polyethylene
[DE92-016545] p 3965 N92-33185
SOLUTIONS
Continuum configurational bias Monte-Carlo studies of alkanes and polyethylene
[DE92-016545] p 3965 N92-33185
SOLVATION
Dynamics of ion solvation in a Stockmayer fluid
[AD-A251087] p 4066 N92-32682
SOLVENTS
Dynamics of ion solvation in a Stockmayer fluid
[AD-A251087] p 4066 N92-32682
Some electronic and dynamical factors in electron-transfer chemistry: Metal complexes, clusters, and surfaces
[AD-A251169] p 3964 N92-32826
Continuum configurational bias Monte-Carlo studies of alkanes and polyethylene
[DE92-016545] p 3965 N92-33185
SONAR
ABF algorithms implemented at ARL:UT, FDS system engineering and acoustics
[AD-A252368] p 4046 N92-32917
SOOT
The polychromatic pyrometer in diesel combustion
[ECL-91-42] p 3963 N92-32722
SOUND FIELDS
Influence of an intense acoustic field on boundary layer separation
[ETN-92-92081] p 4009 N92-32687
A lightweight loudspeaker for aircraft communications and active noise control p 3988 N92-32964
SOUND INTENSITY
Sound power determination using the sound intensity scanning technique p 4062 N92-32953
SOUND PRESSURE
Exposures from headset interference tones
[AD-A247175] p 4061 N92-32697
Modeling the ear's response to intense impulses and the development of improved damage risk criteria
[AD-A252365] p 4037 N92-32916
Sound power determination using the sound intensity scanning technique p 4062 N92-32953
Vacuum-isolation vessel and method for measurement of thermal noise in microphones
[NASA-CASE-LAR-14567-1-CU] p 3991 N92-33021
Building vibrations induced by noise from rotorcraft and propeller aircraft flyovers
[NASA-TM-104170] p 4063 N92-33160
SOUND PROPAGATION
Burning oil fields as a source of infrasonic waves
[IRF-PREPRINT-119] p 4061 N92-32842
SOUND TRANSMISSION
Sound power determination using the sound intensity scanning technique p 4062 N92-32953
Active control of sound transmission through stiff lightweight composite fuselage constructions
p 4062 N92-32957
Sound transmission reduction with intelligent panel systems p 4063 N92-32959
Pilot noise exposure during a Boeing 747-400 round trip: Judgement of noise and analysis in respect to hearing impairment of pilots p 4063 N92-32961
SOUND WAVES
Wave propagation in laterally varying media: A model expansion method
[AD-A247553] p 4031 N92-32572
Can the speed of light in the fiber be controlled?
[AD-A247614] p 4074 N92-32668
Exposures from headset interference tones
[AD-A247175] p 4061 N92-32697
Dynamic systems stability with dry friction: Application to brake disc squealing
[ECL-91-48] p 4018 N92-32737
SOUTHERN HEMISPHERE
A simple Doppler wind lidar sensor: Simulated measurements and impacts in a global assimilation and forecast system
[PL-TR-91-2253] p 4034 N92-32859
SPACE BASED RADAR
Performance analysis of space-based radar tracking techniques
[ISBN-0-315-60464-6] p 3987 N92-33207
SPACE COMMUNICATION
V-band pseudomorphic HEMT MMIC phased array components for space communications
p 3983 N92-32966
SPACE DEBRIS
Analysis of LDEF experiment AO187-2: Chemically and isotopic measurements of micrometeoroids by secondary ion mass spectrometry
[NASA-CR-190697] p 4093 N92-32541
Orbital debris characterization with impact flash signatures
[DE92-010666] p 4018 N92-32701
A simple approach for the design and optimization of stand-off hypervelocity particle shields
[DE92-011383] p 3943 N92-32704
SPACE EXPLORATION
Cassini: A mission to Saturn and Titan
p 4099 N92-32387
The Huygens probe p 4099 N92-32388
Fifty years in science, thirty years in space
[LALP-92-51] p 4104 N92-32862
Toward the next millennium: A vision for spaceship Earth
[NASA-TM-107986] p 3941 N92-33007
Humans and machines in space: The payoff
[ISBN-0-87703-343-9] p 4039 N92-33099
SPACE FLIGHT
Effects of CSF hormones and ionic composition on salt/water metabolism
[NASA-CR-190693] p 4037 N92-32539
SPACE HABITATS
Development of static system procedures to study aquatic biofilms and their responses to disinfection and invading species
[NASA-TM-103598] p 4036 N92-33103
SPACE OBSERVATIONS (FROM EARTH)
Ground-based observations of Titan's thermal spectrum p 4095 N92-32359
SPACE PLASMAS
Satellite anomalies and electrostatic surface discharges
[AD-A246880] p 3942 N92-32538
Director's discretionary fund report for FY 1991
[NASA-TM-103902] p 4105 N92-33106
SPACE POWER REACTORS
NASA's nuclear electric propulsion technology project
[NASA-TM-105811] p 3944 N92-32463
SPACE PROBES
Symposium on Titan
[ESA-SP-338] p 4093 N92-32348
The Huygens probe p 4099 N92-32388
Titan's atmosphere structure from Huygen's-ASI measurements p 4101 N92-32398
The Huygens SSP Refractometer (REF)
p 4101 N92-32399
Huygens probe: The surface mission
p 4101 N92-32402
A surface science package for the Huygens Titan probe p 4102 N92-32410
SPACE PROGRAMS
Humans and machines in space: The payoff
[ISBN-0-87703-343-9] p 4039 N92-33099
SPACE SHUTTLE MAIN ENGINE
Tenth Workshop for Computational Fluid Dynamic Applications in Rocket Propulsion, part 2
[NASA-CP-3163-PT-2] p 3994 N92-32245
Computational fluid dynamics analysis of Space Shuttle main engine multiple plume flows at high-altitude flight conditions p 3996 N92-32255
Modeling of SSME fuel preburner ASI
p 3945 N92-32259
CFD modeling of turbulent flows around the SSME main injector assembly using porosity formulation
p 3997 N92-32260
Computational fluid dynamics analysis of SSME phase 2 and phase 2+ preburner injector element hydrogen flow paths p 3997 N92-32261
Technology test bed review p 4001 N92-32279
Development of CFD code evaluation criteria and a procedure for assessing predictive capability and performance p 4001 N92-32283
SSME HPOTP impeller backcavity CFD analysis
p 4003 N92-32294
SPACE SHUTTLE MISSIONS
Debris/ice/TPS assessment and integrated photographic analysis for Shuttle Mission STS-49
[NASA-TM-107547] p 3941 N92-32454

Superheavyweight missions SI versus DI: Ascent flight design options and recommendations
[NASA-CR-183208] p 3942 N92-32610

SPACE SHUTTLE ORBITERS
Computational fluid dynamics analysis of Space Shuttle main engine multiple plume flows at high-altitude flight conditions p 3996 N92-32255

SPACE SHUTTLE PAYLOADS
Advanced solid rocket motor project status p 3945 N92-32280

SPACE SHUTTLES
A comparative study of the effects of inhibitor stub length on solid rocket motor combustion chamber pressure oscillations: RSRM at T = 80 seconds, preliminary results p 3945 N92-32248
Technology test bed review p 4001 N92-32279
Independent verification and validation for Space Shuttle flight software
[NASA-CR-190826] p 4047 N92-33196

SPACE STATION FREEDOM
Robust stabilization of the Space Station
[NASA-CR-190627] p 3942 N92-32244
Space Station Freedom media handbook
[NASA-TM-107981] p 3942 N92-32421
Ground Systems Development Environment (GSDE) interface requirements and prototyping plan
[NASA-CR-190713] p 4041 N92-32451
Advancing automation and robotics technology for the Space Station Freedom and for the US economy
[NASA-TM-103940] p 4040 N92-32809
Overview and evolution of the LeRC PMAD DC Testbed
[NASA-TM-105842] p 3991 N92-32867

SPACE STATION POWER SUPPLIES
Overview and evolution of the LeRC PMAD DC Testbed
[NASA-TM-105842] p 3991 N92-32867

SPACE STATIONS
Rotating-unbalanced-mass devices and methods for scanning balloon-borne-experiments, free-flying spacecraft, and space shuttle/space station attached experiments
[NASA-CASE-MFS-28425-1] p 4015 N92-33010

SPACE TECHNOLOGY EXPERIMENTS
Fifty years in science, thirty years in space
[LALP-92-51] p 4104 N92-32862

SPACE TRANSPORTATION
Heat transfer in rocket engine combustion chambers and nozzles p 3995 N92-32253

SPACE TRANSPORTATION SYSTEM
A status of the activities of the NASA. Marshall Space Flight Center Combustion Devices Technology Team p 3995 N92-32250
CFD analysis of the STME nozzle flowfield p 3995 N92-32251
NLS nozzle base flow characteristics p 3995 N92-32252
Heat transfer in rocket engine combustion chambers and nozzles p 3995 N92-32253
Application of computational fluid dynamics to the design of the film cooled STME subscale nozzle for the National Launch System p 3996 N92-32254
STME hydrogen mixer study p 3945 N92-32262
Space Transportation Main Engine p 3945 N92-32281

SPACE TRANSPORTATION SYSTEM FLIGHTS
Debris/ice/TPS assessment and integrated photographic analysis for Shuttle Mission STS-49
[NASA-TM-107547] p 3941 N92-32454
Independent verification and validation for Space Shuttle flight software
[NASA-CR-190826] p 4047 N92-33196

SPACE-TIME FUNCTIONS
Physics in knots
[DE92-017530] p 4088 N92-33069

SPACEBORNE EXPERIMENTS
Investigations preparatory to the Wet Satellite Model Experiment
[NLR-TP-91219-U] p 3943 N92-32834

SPACECRAFT CHARGING
Satellite anomalies and electrostatic surface discharges
[AD-A246880] p 3942 N92-32538

SPACECRAFT CONFIGURATIONS
Cassini: A mission to Saturn and Titan p 4099 N92-32387

SPACECRAFT CONSTRUCTION MATERIALS
Thermal degradation study of silicon carbide threads developed for advanced flexible thermal protection systems
[NASA-TM-103952] p 3970 N92-32476

SPACECRAFT CONTROL
Robust stabilization of the Space Station
[NASA-CR-190627] p 3942 N92-32244

SPACECRAFT DESIGN
Technology test bed review p 4001 N92-32279
A simple approach for the design and optimization of stand-off hypervelocity particle shields
[DE92-011383] p 3943 N92-32704

SPACECRAFT DOCKING
Autonomous berthing/unberthing of a Work Attachment Mechanism/Work Attachment Fixture (WAM/WAF)
[NASA-CR-190647] p 4019 N92-32885

SPACECRAFT LANDING
Huygens probe: The surface mission p 4101 N92-32402

SPACECRAFT MODELS
Investigations preparatory to the Wet Satellite Model Experiment
[NLR-TP-91219-U] p 3943 N92-32834

SPACECRAFT POWER SUPPLIES
Fifty years in science, thirty years in space
[LALP-92-51] p 4104 N92-32862
Overview and evolution of the LeRC PMAD DC Testbed
[NASA-TM-105842] p 3991 N92-32867

SPACECRAFT PROPULSION
Tenth Workshop for Computational Fluid Dynamic Applications in Rocket Propulsion, part 2
[NASA-CP-3163-PT-2] p 3994 N92-32245
A status of the activities of the NASA. Marshall Space Flight Center Combustion Devices Technology Team p 3995 N92-32250
Tenth Workshop for Computational Fluid Dynamic Applications in Rocket Propulsion, part 1
[NASA-CP-3163-PT-1] p 4000 N92-32278
Fifty years in science, thirty years in space
[LALP-92-51] p 4104 N92-32862

SPACECRAFT SHIELDING
A simple approach for the design and optimization of stand-off hypervelocity particle shields
[DE92-011383] p 3943 N92-32704

SPACECRAFT TRAJECTORIES
Titan's atmosphere structure from Huygen's-ASI measurements p 4101 N92-32398

SPACECREWS
Integrated launch and emergency vehicle system
[NASA-CASE-LAR-13780-1] p 3943 N92-33013

SPACING
An efficient and robust grid optimization algorithm p 4004 N92-32300

SPARK IGNITION
Modeling of SSME fuel preburner ASI p 3945 N92-32259

SPATIAL DISTRIBUTION
Alpha particle diagnostics using impurity pellet injection
[DE92-013796] p 4078 N92-32623
Temporal and spatial factors affecting the perception of computer-generated imagery
[AD-A249242] p 4046 N92-32907

SPECIFIC IMPULSE
NASA's nuclear electric propulsion technology project
[NASA-TM-105811] p 3944 N92-32463
The evolutionary development of high specific impulse electric thruster technology
[NASA-TM-105758] p 3944 N92-33064

SPECIFICATIONS
Overview of SSC accelerator requirements
[DE92-014896] p 4073 N92-33134

SPECIMEN GEOMETRY
A new test method to determine the compressive strength of fiber-reinforced composites p 3956 N92-33035

SPECTRAL BANDS
A research program on radiative transfer model development in support of the ARM program
[DE92-014495] p 4031 N92-33153

SPECTRAL REFLECTANCE
The detectability of Titan's surface in the near-infrared p 4097 N92-32375
Uses of stereovision surface models
[TELECOM-91-E-016] p 4075 N92-32806

SPECTRAL RESOLUTION
The synthetic infrared spectrum of Titan at high spectral resolution p 4099 N92-32389

SPECTROMETERS
Low-frequency nuclear quadrupole resonance with a dc SQUID
[DE92-014506] p 4081 N92-32420
Design and construction of a sample preparation chamber for atomic beam scattering
[DE92-014509] p 4065 N92-32473
Grill spectrometry on the Space Shuttle during the Atlas 1 mission
[AERONAUTICA-ACTA-A-364-199] p 3943 N92-32728
Diffractive optics technology and the NASA Geostationary Earth Observatory (GEO)
[NASA-CR-190611] p 4076 N92-33074
Volume 1. Preliminary design study: AXAF x ray calibration spectrometers. Volume 2. Revised preliminary design study: AXAF x ray calibration spectrometers
[NASA-CR-184340] p 4092 N92-33094

SPECTROPHOTOMETRY
Titan's UV albedo: Observations and modeling p 4094 N92-32356
Titan's mid-IR albedo: New observations from 3 to 5 microns p 4097 N92-32376

SPECTRORADIOMETERS
Radiometric and spectral measurement instruments
[AD-A250771] p 4013 N92-32343

SPECTROSCOPIC ANALYSIS
An in vitro corrosion study of two implant materials using electrochemical impedance spectroscopy and potentiodynamic polarization
[AD-A252575] p 3966 N92-32626
Photogenerated carrier-induced reactions on UHV semiconductor surfaces
[DE92-015355] p 4082 N92-32641
Radiative lifetime measurements of the AA pi 1/2 state in CaH
[USIP-91-03] p 4067 N92-32764
Study of InGaAs-based modulation doped field effect transistor structures using variable-angle spectroscopic ellipsometry p 3984 N92-32977
Mass resolved resonance ionization spectroscopy of combustion radicals
[DE92-016833] p 3965 N92-33222

SPECTROSCOPY
PAC spectroscopy of electronic ceramics
[DE92-014328] p 3970 N92-32471
Morphology, 31P spin diffusion, and phase transitions in a representative semicrystalline polyphosphazene by solid-state NMR
[AD-A250883] p 3961 N92-32553
Light-ion spectroscopy with exotic targets
[DE92-017258] p 3964 N92-32929

SPECTRUM ANALYSIS
A reanalysis of Voyager UVS observations of Titan p 4094 N92-32357
Ground-based observations of Titan's thermal spectrum p 4095 N92-32359
Near infrared spectra of potential solids at the surface of Titan p 4102 N92-32406
Grill spectrometry on the Space Shuttle during the Atlas 1 mission
[AERONAUTICA-ACTA-A-364-199] p 3943 N92-32728

SPEECH RECOGNITION
Enhancements to speech recognition on voice response systems
[TELECOM-91-E-018] p 3981 N92-32807

SPHERES
Numerical simulation of inclined chute flows of monodisperse, inelastic, frictional spheres
[DE92-014775] p 4012 N92-32947

SPHERICAL COORDINATES
Advanced computational transport methods for curvilinear geometries
[DE92-011290] p 4057 N92-32743

SPHERICAL HARMONICS
On the choice of minimization functional in the partial wave analysis
[DE92-624689] p 4087 N92-32309

SPIN DYNAMICS
Morphology, 31P spin diffusion, and phase transitions in a representative semicrystalline polyphosphazene by solid-state NMR
[AD-A250883] p 3961 N92-32553
Fractional spin: Majorana-Dirac field
[DE92-624558] p 4087 N92-32603

SPIN-ORBIT INTERACTIONS
Higher superdeformed band members in Hg-190: Evidence for a band interaction?
[DE92-016778] p 4082 N92-32542

SPINDLES
Noncircular rolling joints for vibrational reduction in slewing maneuvers
[NASA-CASE-LAR-14515-1-CU] p 4019 N92-33031

SPOILERS
Lift and rolling moment due to spoilers on wings with trailing-edge flaps deflected at subsonic speeds
[ESDU-92002-SUPPL] p 3931 N92-32782

SPRAY CHARACTERISTICS
Spray nozzle for fire control
[CA-PATENT-APPL-SN-2-011-94] p 4011 N92-32856

SPRAY NOZZLES
Numerical modeling for dilute and dense sprays p 3997 N92-32258
Spray nozzle for fire control
[CA-PATENT-APPL-SN-2-011-94] p 4011 N92-32856

SPRAYERS
A numerical model for atomization-spray coupling in liquid rocket thrust chambers p 3996 N92-32257

Numerical modeling for dilute and dense sprays p 3997 N92-32258
Modeling of SSME fuel preburner ASI p 3945 N92-32259

SQUID (DETECTORS)
Measurement of the magnetic and electrical activity of individual cells in vitro
[AD-A250881] p 4035 N92-32345
Low-frequency nuclear quadrupole resonance with a dc SQUID
[DE92-014506] p 4081 N92-32420

STABILITY
Dynamic systems stability with dry friction: Application to brake disc squealing
[ECL-91-48] p 4018 N92-32737

STABILITY TESTS
Comparison between the PISO algorithm and preconditioning methods for compressible flow p 4001 N92-32284
Overview and evolution of the LeRC PMAD DC Testbed
[NASA-TM-105842] p 3991 N92-32867

STAGNATION FLOW
Premixed turbulent combustion to opposed streams
[DE92-016996] p 3964 N92-32996

STAGNATION TEMPERATURE
Turbine disk cavity aerodynamics and heat transfer p 3998 N92-32265

STAINLESS STEELS
Transmission electron microscope characterization of deformation and recovery in 304L stainless steel part
[DE92-013237] p 3966 N92-32614
Inelastic deformation and damage at high temperature
[DE92-012241] p 4021 N92-32698
The oxidation of Type 310S stainless steel in mixed gases at elevated temperatures
[DE92-014941] p 3968 N92-32991
Electrochemical polarization measurements on pitting corrosion susceptibility of nickel-rich Alloy 825
[DE92-014885] p 3969 N92-33132

STANDARDIZATION
PDES application protocol suite for composites (PAS-C). Functional needs report for the PAS-C program
[AD-A247886] p 3953 N92-32629
An overview of concerns relating to fluid effects on composites p 3958 N92-33045

STATE ESTIMATION
Feature detection for model assessment in state estimation
[AD-A252755] p 4059 N92-32989

STATE VECTORS
Robust stabilization of the Space Station
[NASA-CR-190627] p 3942 N92-32244
Frequency domain state-space system identification
[NASA-TM-107659] p 4021 N92-32657

STATIC TESTS
Heating fixture and instrumentation design for elevated temperature tests of a composite repair technique
[WL-TM-90-326-FIBE] p 3946 N92-32459
Certification of damage tolerant composite structure p 3951 N92-32580

STATISTICAL ANALYSIS
Statistically based material properties: A military handbook-17 perspective p 3951 N92-32581
Statistical selection: Multiple comparison approach
[ETN-92-92051] p 4060 N92-32709
Continuous and discrete problems in image processing
[TELECOM-91-D-007] p 4058 N92-32802
A Markov model of software usage p 4045 N92-32881
Signal processing in impulsive electromagnetic interference
[AD-A252385] p 3982 N92-32899
Recent advances in statistical energy analysis p 4062 N92-32954
Use of SEA to predict structure-borne noise in aircraft p 4062 N92-32955
The energetics and dynamics of free radicals, ions, and clusters
[DE92-014124] p 4068 N92-33083
Guide to selected national environmental statistics in the US Government
[PB92-201144] p 4030 N92-33087

STATISTICAL CORRELATION
Correlation of single mode fiber fabrication factors and radiation response
[AD-A247301] p 4074 N92-32613

STATISTICAL DISTRIBUTIONS
Wind tunnel test of Teledyne Geotech model 1564B cup anemometer
[DE92-009590] p 4013 N92-32460
On the inconsistency of bootstrap distribution estimators
[IMAG-RR-856-M] p 4060 N92-32718
On the resistive transition of composite superconductors
[ISBN-90-9003899-X] p 3992 N92-33145

STATISTICAL TESTS
An implementation of a fault-tolerant, multidirectional, digital interpolation beamformer
[AD-A252494] p 3986 N92-33152

STATORS
Investigation of the flight control requirements of a half-scale ducted fan unmanned aerial vehicle
[AD-A252730] p 3940 N92-32988

STEADY FLOW
Numerical simulation of inclined chute flows of monodisperse, inelastic, frictional spheres
[DE92-014775] p 4012 N92-32947

STEADY STATE
Steady state behavior of reduced dynamic systems with local nonlinearities
[ISBN-90-9004680-1] p 4056 N92-32707

STEELS
Fatigue, hysteresis, and acoustic emission, parts 1 and 2
[AD-A251073] p 4021 N92-32681
Guide to the effect of shot peening on fatigue strength
[ESDU-92015] p 3967 N92-32779
Investigation of fracture toughness and fracture mechanisms using acoustic emission measurements
[DE92-011907] p 4022 N92-32911
Modeling the influence of irradiation temperature and displacement rate on hardening due to point defect clusters in ferritic steels
[DE92-016897] p 3969 N92-33115

STELLAR MODELS
Implementation of a tree-code for numerical simulations of stellar systems
[INPE-5370-TDI/469] p 4093 N92-32604

STELLAR OCCULTATION
On the Titan/28 Sagittarii occultation of 1989 July 3 p 4101 N92-32403

STELLAR SYSTEMS
Implementation of a tree-code for numerical simulations of stellar systems
[INPE-5370-TDI/469] p 4093 N92-32604

STELLARATORS
Fast ion loss and radial electric field in Wendelstein 7-A stellarator
[DE92-782106] p 4079 N92-32745

STIFFENING
Postbuckling of stiffened composite plates under combined loading p 3952 N92-32585

STIFFNESS MATRIX
A unique method of determining the elastic and engineering constants of unidirectional fibre-reinforced composite plates using ultrasound
[UTIAS-TN-274] p 3955 N92-32829
Jacobian and stiffness analysis of a novel class of six-DOF parallel minimanipulators
[DE92-016373] p 4054 N92-33184

STOCHASTIC PROCESSES
Approximations and designs for estimating regression coefficients of independent stochastic processes
[IMAG-RR-840-M] p 4060 N92-32839
The role of stochasticity in sawtooth oscillation
[DE92-782004] p 3982 N92-32905
Stochastic models in reliability
[AD-A250934] p 4020 N92-33151

STOICHIOMETRY
Probing thin-film YBa2Cu3O(7-delta) superconductors by second harmonic generation using femtosecond laser pulses
[AD-A252350] p 4082 N92-32512
Polyimide molding powder, coating, adhesive, and matrix resin
[NASA-CASE-LAR-14163-1] p 3973 N92-33014

STOPPING
Obstacle avoidance for redundant robots using configuration control
[NASA-CASE-NPO-17852-1-CU] p 4054 N92-33019

STORAGE BATTERIES
Development of advanced secondary zinc cells for power-source applications
[DE92-016358] p 3993 N92-33183

STORAGE RINGS (PARTICLE ACCELERATORS)
High power testing of the prototype accelerating cavity (352 MHz) for the Advanced Photon Source (APS)
[DE92-016697] p 4069 N92-32314
Proceedings of the fourth users meeting for the advanced photon source
[DE92-014061] p 4072 N92-32932

STORAGE TANKS
Hot water storage tank for solar collectors
[AD-D015301] p 4026 N92-32943

STORMS (METEOROLOGY)
Forecasting heavy snow events in Missoula, Montana
[PB92-196104] p 4034 N92-33163

STOVL AIRCRAFT
Ski jump takeoff performance predictions for a mixed-flow, remote-lift STOVL aircraft
[NASA-TM-103866] p 3935 N92-32887

STRAIN RATE
The use of piezoelectric sensors to detect delamination initiation in carbon fiber reinforced composites
[MBB-Z-0391-91-PUB] p 3954 N92-32740

STRANDS
Braided composite bore evacuator chambers for tank cannons p 3948 N92-32520

STRATOSPHERE
SAGE 1 data user's guide
[NASA-RP-1275] p 4031 N92-33097

STREAK PHOTOGRAPHY
Phase distribution measurements in narrow rectangular channels using image-processing techniques
[DE92-014084] p 4006 N92-32468

STRESS (PSYCHOLOGY)
Cognitive biases and time stress in team decision making
[AD-A251153] p 4088 N92-32551

STRESS ANALYSIS
An analysis of the flow field in the region of the ASRM field joints p 4005 N92-32305
An implementation of Hill's theory of normal anisotropic plasticity for explicit shell analysis
[DE92-011468] p 4020 N92-32328
Physical basis for a pressure-dependent yield criterion for polymers
[AD-A250763] p 3970 N92-32341
Global/local methods research using the CSM testbed p 3949 N92-32528
A new approximate fracture mechanics analysis methodology for composites with a crack or hole p 3949 N92-32530
Stress-relief displacements induced by drilling: Applications to holographic measurements of in situ stress
[DE92-013711] p 4014 N92-32620
Free vibration of thick isotropic and orthotropic cylindrical shells
[DE92-011653] p 4022 N92-32706
Accommodation mechanisms and dispersoid-free zone s in Al 7475 after superplastic forming
[MBB-Z-0404-91-PUB] p 3968 N92-32894
Computational methods for global/local analysis
[NASA-TM-107591] p 4023 N92-33104
Thermal and structural analysis of high precision beamline position monitors for synchrotron x ray beams
[DE92-014863] p 4072 N92-33130
Global/local interlaminar stress analysis of a grid-stiffened composite panel
[NASA-CR-190822] p 4023 N92-33139

STRESS CORROSION
New accelerated corrosion test methods
[MBB-Z-0406-91-PUB] p 3968 N92-32895

STRESS DISTRIBUTION
Investigation of a relationship between uniaxial and biaxial chemical stress crazing of cast acrylic
[AD-A250852] p 4021 N92-32621

STRESS INTENSITY FACTORS
A transgranular fatigue crack growth model based on restricted slip reversibility
[NRC-LTR-ST-1631] p 4023 N92-33076

STRESS RELAXATION
Stress-relief displacements induced by drilling: Applications to holographic measurements of in situ stress
[DE92-013711] p 4014 N92-32620

STRESS-STRAIN RELATIONSHIPS
Computational simulation of matrix micro-slip bands in SiC/Ti-15 composite
[NASA-TM-105762] p 3946 N92-32466
Thermal strains in titanium aluminide and nickel aluminide composites
[DE92-015181] p 3953 N92-32638
Fatigue, hysteresis, and acoustic emission, parts 1 and 2
[AD-A251073] p 4021 N92-32681
A comparison of three popular test methods for determining the shear modulus of composite materials
[NASA-CR-190659] p 3959 N92-33075

STRESS-STRAIN-TIME RELATIONS
Investigation of a relationship between uniaxial and biaxial chemical stress crazing of cast acrylic
[AD-A250852] p 4021 N92-32621

STRING THEORY
Neutrino masses in the flipped SU(5) tensor product U(1) and the SU(4) tensor product O(4) GUT models
[RAL-92-012] p 4068 N92-33135

STRONTIUM
Execution of measurement sequences in the framework of the inspection of near limit regions by radioiodine and aerosol emission measurements, and ground examinations on plutonium, strontium, and gamma ray radionuclides
[OEFZS-4579] p 4071 N92-32763
STRONTIUM COMPOUNDS
Sintering of bulk high-(Tc) superconductors: Bi-Sr-Ca-Cu-O
[DE92-016189] p 4082 N92-32561
STRUCTURAL ANALYSIS
Structural assessment of ultralightweight composites p 3948 N92-32525
Global/local methods research using the CSM testbed p 3949 N92-32528
Computational simulation of structural fracture in fiber composites p 3949 N92-32531
Eighth DOD/NASA/FAA Conference on Fibrous Composites in Structural Design, part 2
[NASA-CP-3087-PT-2] p 3950 N92-32574
Initial postbuckling response of an unsymmetrically laminated rectangular plate p 3952 N92-32586
Fatigue, hysteresis, and acoustic emission, parts 1 and 2
[AD-A251073] p 4021 N92-32681
Computational methods for global/local analysis
[NASA-TM-107591] p 4023 N92-33104
Thermal and structural analysis of high precision beamline position monitors for synchrotron x ray beams
[DE92-014863] p 4072 N92-33130
STRUCTURAL DESIGN
Eighth DOD/NASA/FAA Conference on Fibrous Composites in Structural Design, part 1
[NASA-CP-3087-PT-1] p 3946 N92-32513
Composite structural armor for combat vehicle applications p 3947 N92-32515
Applications of composites to armaments p 3947 N92-32516
Eighth DOD/NASA/FAA Conference on Fibrous Composites in Structural Design, part 2
[NASA-CP-3087-PT-2] p 3950 N92-32574
Evaluation of composite components on the Bell 206L and Sikorsky S-76 helicopters p 3950 N92-32575
Polarized wiggler for NSLS x ray ring design considerations
[DE92-012212] p 4071 N92-32912
STRUCTURAL DESIGN CRITERIA
Global/local interlaminar stress analysis of a grid-stiffened composite panel
[NASA-CR-190822] p 4023 N92-33139
STRUCTURAL FAILURE
Design, evaluation and experimental effort toward development of a high strain composite wing for Navy aircraft p 3947 N92-32514
Development of composite wing carrythrough bulkheads for fighter aircraft p 3948 N92-32519
Buckling and damage of a composite plate under compression
[ONERA-RT-25/3542-RY-006-R] p 4022 N92-32774
Free-edge delamination of a stratified composite: Interaction with the transversal crack
[ONERA-RT-13/7256-RY-006-R] p 3954 N92-32792
STRUCTURAL STABILITY
Sound transmission reduction with intelligent panel systems p 4063 N92-32959
STRUCTURAL VIBRATION
Recent advances in statistical energy analysis p 4062 N92-32954
Sound transmission reduction with intelligent panel systems p 4063 N92-32959
Building vibrations induced by noise from rotorcraft and propeller aircraft flyovers
[NASA-TM-104170] p 4063 N92-33160
STUDENTS
United States Air Force summer research program 1991. Volume 1: Program management report
[AD-A248763] p 4103 N92-32338
STYRENES
Synthesis, morphology and properties of polyester-urethane in solution in styrene: Application to composites development
[ISAL-92-0007] p 3972 N92-32762
SUBCONTRACTS
NASA procurement: Improving oversight of construction projects at the Langley Research Center. Report to the Honorable John W. Warner, US Senate
[GAO/NSIAD-92-230] p 4088 N92-32618
SUBSONIC FLOW
Development of the KIVA-2 CFD code for rocket propulsion applications p 3945 N92-32272
A multi-domain method for subsonic viscous flows p 3960 N92-32275
Large eddy simulation of compressible turbulent channel flows p 4000 N92-32276
An experimental study of the flow over a sharp-edged delta wing at subsonic and transonic speeds
[NLR-TP-91117-U] p 3930 N92-32732
SUBSTRATES
Multichip module study
[AD-A250877] p 3989 N92-32678
Substrate reactions and flux pinning structures in melt-processed YBa2Cu3O7 deposits on Ag-Pd alloy substrates
[DE92-014404] p 4084 N92-32919
Thickness dependence of vortex pinning in epitaxial Tl-Ca-Ba-Cu-O thin films
[DE92-015011] p 4084 N92-32920
Microwave properties of peeled HEMT devices sapphire substrates p 3984 N92-32978
Ultra-low-loss strip-type transmission lines, formed of bonded substrate layers
[AD-D015312] p 3992 N92-33169
Method of growing diamond film on substrates
[AD-D015313] p 3973 N92-33170
Corrosion-resistant alkyd coatings
[AD-D015330] p 3974 N92-33177
SULFATES
Scintillation properties of lead sulfate
[DE92-010301] p 4082 N92-32493
Thermochemical cycles for energy storage: Thermal decomposition of ZnSO4 systems
[DE91-002144] p 4026 N92-32909
SULFURIC ACID
Clean gasoline reforming with superacid catalysts
[DE92-013833] p 3975 N92-33123
SUM RULES
Theoretical aspects of lepton-hadron scattering
[DE92-013765] p 4069 N92-33148
SUPERCONDUCTING FILMS
Probing thin-film YBa2Cu3O(7-delta) superconductors by second harmonic generation using femtosecond laser pulses
[AD-A252350] p 4082 N92-32512
Anisotropic electrical resistivity of YBCO/PBCO superlattice films grown on miscut substrates
[DE92-014409] p 4082 N92-32636
T (sub c)-delta relations in YBa2Cu3O(7-delta) thin films: Effects of oxygen pressure during growth
[DE92-014432] p 4083 N92-32653
Workshop on research needs and opportunities in high temperature superconductivity
[AD-A252674] p 3988 N92-32659
Thickness dependence of vortex pinning in epitaxial Tl-Ca-Ba-Cu-O thin films
[DE92-015011] p 4084 N92-32920
Magnetic penetration depth of YBa2Cu3O(7-delta) thin films determined by the power transmission method p 3985 N92-32983
Superconducting transport properties and surface microstructure for YBa2Cu3O(7-delta) based superlattices grown by pulsed laser deposition
[DE91-014224] p 4085 N92-33023
Superconductivity: Past, present, and future
[DE92-014862] p 3992 N92-33128
Ultra-low-loss strip-type transmission lines, formed of bonded substrate layers
[AD-D015312] p 3992 N92-33169
Electric and magnetic properties of random superconductors
[ITN-92-85165] p 4086 N92-33190
SUPERCONDUCTING MAGNETS
Optics of beam transport in the NSLS UV-FEL
[DE92-014166] p 4015 N92-32511
Status of LHD control system design
[NIFS-122] p 4070 N92-32746
SUPERCONDUCTING SUPER COLLIDER
Overview of SSC accelerator requirements
[DE92-014896] p 4073 N92-33134
SUPERCONDUCTIVITY
Preparation and characterization of superlattices
[DE92-012572] p 4081 N92-32462
Workshop on research needs and opportunities in high temperature superconductivity
[AD-A252674] p 3988 N92-32659
The response of the double layer capacitance of a high temperature superconductor/fluid electrolyte interface to the onset of superconductivity
[AD-A251172] p 3990 N92-32827
NASA space applications of high-temperature superconductors p 3985 N92-32980
Performance of a Y-Ba-Cu-O superconducting filter/GaAs low noise amplifier hybrid circuit p 3985 N92-32982
Superconducting transport properties and surface microstructure for YBa2Cu3O(7-delta) based superlattices grown by pulsed laser deposition
[DE91-014224] p 4085 N92-33023
Sweeping algorithms for five-point stencils and banded matrices
[DE92-017309] p 4047 N92-33118
Superconductivity: Past, present, and future
[DE92-014862] p 3992 N92-33128
Silver coated superconducting ceramic powder
[AD-D015294] p 3973 N92-33157
Electric and magnetic properties of random superconductors
[ITN-92-85165] p 4086 N92-33190
SUPERCONDUCTORS
Microwave absorption by lossy ceramic materials
[DE92-016963] p 3970 N92-32317
Processing and properties of silver-clad Tl-Ba-Ca-Cu-O wires and tapes
[DE92-015266] p 4081 N92-32346
Probing thin-film YBa2Cu3O(7-delta) superconductors by second harmonic generation using femtosecond laser pulses
[AD-A252350] p 4082 N92-32512
Thickness dependence of vortex pinning in epitaxial Tl-Ca-Ba-Cu-O thin films
[DE92-015011] p 4084 N92-32920
Performance of a Y-Ba-Cu-O superconducting filter/GaAs low noise amplifier hybrid circuit p 3985 N92-32982
Studies of Y-Ba-Cu-O single crystals by x ray absorption spectroscopy
[DE92-014687] p 4086 N92-33136
On the resistive transition of composite superconductors
[ISBN-90-9003899-X] p 3992 N92-33145
Electric and magnetic properties of random superconductors
[ITN-92-85165] p 4086 N92-33190
SUPERFLUIDITY
Thermal conductance of augmented pressed metallic contacts at liquid helium temperatures
[NASA-TM-103917] p 4007 N92-32474
Research and development of a helium-4 based solar neutrino detector
[DE92-017390] p 4103 N92-33119
SUPERHIGH FREQUENCIES
Multifrequency measurements of radar ground clutter at 42 sites. Volume 1: Principal results
[AD-A246710] p 3980 N92-32696
Study and development of a six port network analyzer in the 1-18 GHz frequency range
[TELECOM-91-E-005] p 3980 N92-32739
SUPERLATTICES
Preparation and characterization of superlattices
[DE92-012572] p 4081 N92-32462
Anisotropic electrical resistivity of YBCO/PBCO superlattice films grown on miscut substrates
[DE92-014409] p 4082 N92-32636
Superconducting transport properties and surface microstructure for YBa2Cu3O(7-delta) based superlattices grown by pulsed laser deposition
[DE91-014224] p 4085 N92-33023
SUPERNOVAE
Research in nuclear astrophysics: Stellar collapse and supernovae
[DE92-014988] p 4093 N92-32993
SUPERPLASTICITY
Fundamental questions concerning the application of superplastic forming and superplastic forming/diffusion bonding
[MBB-Z-0402-91-PUB] p 3977 N92-32690
Superplastic forming of Ti6Al4V at lower temperature using hydrogen
[MBB-Z-0403-91-PUB] p 3978 N92-32893
Accommodation mechanisms and dispersoid-free zone s in Al 7475 after superplastic forming
[MBB-Z-0404-91-PUB] p 3968 N92-32894
SUPERROTATION
Numerical simulation of the circulation of the atmosphere of Titan p 4095 N92-32361
SUPERSONIC AIRCRAFT
A method for designing blended wing-body configurations for low wave drag
[NASA-TP-3261] p 3929 N92-32480
Supportability evaluation of thermoplastic and thermoset composites p 3950 N92-32576
SUPERSONIC FLOW
A status of the Turbine Technology Team activities p 3998 N92-32267
Development of the KIVA-2 CFD code for rocket propulsion applications p 3945 N92-32272
Experimental study of the vortex system generated by a missile fuselage at incidence. Part 3: Three directional laser velocimetry measurements
[ONERA-RT-47/1147-AY-146A-P] p 3931 N92-32800
Advances in compressible turbulent mixing
[DE92-014326] p 4010 N92-32824
Polar upper atmosphere characterization and supersonic ion escape (polar wind)
[GDR-0917] p 4031 N92-32889

SUPERSONIC TURBINES
A status of the Turbine Technology Team activities p 3998 N92-32267
A critical evaluation of a three-dimensional Navier-Stokes CFD as a tool to design supersonic turbine stages p 3999 N92-32268
SUPERSYMMETRY
Supersymmetry searches at electron-proton colliders [ETN-92-92057] p 4067 N92-32753
SUPPLYING
Integrated launch and emergency vehicle system [NASA-CASE-LAR-13780-1] p 3943 N92-33013
SURFACE CRACKS
Investigation of a relationship between uniaxial and biaxial chemical stress crazing of cast acrylic [AD-A250852] p 4021 N92-32621
SURFACE DIFFUSION
Generic consequences of fundamental studies of beta phase decomposition modes in titanium and related alloy systems [AD-A250789] p 3967 N92-32699
SURFACE DISTORTION
Thermal effects and mirror surface figure requirements for a diagnostic beamline at the advanced light source [DE92-014483] p 4073 N92-32419
SURFACE EMITTING LASERS
Laser material interaction [AD-A250853] p 4016 N92-32622
SURFACE FINISHING
Microporous structure with layered interstitial surface treatment, and method and apparatus for preparation thereof [NASA-CASE-MSC-21487-1] p 3965 N92-33009
SURFACE IONIZATION
Molecular surface analysis by laser ionization of desorbed molecules [DE92-016320] p 4016 N92-33114
SURFACE PROPERTIES
Determining surface profile from sequential interference patterns from a long trace profiler [DE92-017117] p 4073 N92-32321
Symposium on Titan [ESA-SP-338] p 4093 N92-32348
Observing the surface of Titan through near-infrared windows in its atmosphere p 4097 N92-32374
The detectability of Titan's surface in the near-infrared p 4097 N92-32375
VIMS/Cassini mission at Titan: Scientific objectives and observational scenarios p 4097 N92-32377
Cassini/CIRS capabilities for aerosol, cloud, and surface measurements p 4098 N92-32378
Plausible surface models for Titan p 4098 N92-32381
Near infrared spectra of potential solids at the surface of Titan p 4102 N92-32406
A surface science package for the Huygens Titan probe p 4102 N92-32410
Surfaces and thin films studied by picosecond ultrasonics [DE92-016313] p 4020 N92-32564
Photogenerated carrier-induced reactions on UHV semiconductor surfaces [DE92-015355] p 4082 N92-32641
Annual report, 1 November 1990 - 31 October 1991 [AD-A252431] p 4084 N92-32940
Molecular surface analysis by laser ionization of desorbed molecules [DE92-016320] p 4016 N92-33114
Probe molecule studies: Active species in alcohol synthesis [DE92-016682] p 3966 N92-33246
SURFACE REACTIONS
Organic chemistry on Titan: Surface interactions p 4096 N92-32370
Electrocatalyst surfaces [PB92-190420] p 3962 N92-32591
Photogenerated carrier-induced reactions on UHV semiconductor surfaces [DE92-015355] p 4082 N92-32641
High translational energy induced reaction in semiconductors [AD-A250980] p 3989 N92-32669
SURFACE TEMPERATURE
Thermal effects and mirror surface figure requirements for a diagnostic beamline at the advanced light source [DE92-014483] p 4073 N92-32419
Swept shock/boundary layer interaction experiments in support of CFD code validation [NASA-CR-190583] p 3930 N92-32494
Annual variation of surface temperatures over the world [PB92-193259] p 4028 N92-32554
A boundary integral method for an inverse problem in thermal imaging [NASA-CR-189693] p 4059 N92-33006
SURFACE VEHICLES
Publications on maglev technologies [DE92-013296] p 4017 N92-32615
SURFACE WAVES
Waves on Titan p 4100 N92-32394
SURFACTANTS
Electrocatalyst surfaces [PB92-190420] p 3962 N92-32591
SURGERY
Midwest free-electron laser program [AD-A247264] p 4016 N92-32540
SURGICAL INSTRUMENTS
Device for removing foreign objects from anatomic organs [NASA-CASE-GSC-13306-1] p 4038 N92-33032
SURVEILLANCE
Operational needs for an unmanned air vehicle p 3936 N92-32438
Naval target classification and designation with the CL-227 Sea Sentinel p 3937 N92-32449
DoD key technologies plan [AD-A253692] p 4105 N92-33238
SURVEILLANCE RADAR
Airport Surveillance Radar (ASR-9) wind shear processor: 1991 test at Orlando, Florida [AD-A252246] p 3980 N92-32686
Coverage studies for spaced-based radar [DREO-90-18] p 3982 N92-32818
SWITCHES
Plasma opening switch for long-pulse intense ion beam [DE92-017523] p 3992 N92-33068
SWITCHING CIRCUITS
A scalable, switched circuit LAN for Gb/S channels with over Tb/S total capacity [DE92-013444] p 4050 N92-32412
STARNET: A MultiGbit/s optical local area network with both packet and circuit switching [AD-A247617] p 4050 N92-32628
A discrete nonlinear model approach to study the behavior of large signal DC to DC converters [LAAS-90028] p 3989 N92-32777
A continuous nonlinear model approach to study the behavior of large signal DC to DC converters [LAAS-90027] p 3990 N92-32793
SYMBOLIC PROGRAMMING
Analysis of a benchmark suite to evaluate mixed numeric and symbolic processing [NASA-TM-103907] p 4052 N92-32886
SYMBOLS
Selecting a subset of stimulus-response pairs with maximal transmitted information [AD-A252728] p 3986 N92-32987
SYNCHRONISM
Guaranteeing synchronous message deadlines with the timed token medium access control protocol [NASA-CR-190710] p 4042 N92-32656
SYNCHROPHASING
The Dornier 328 Acoustic Test Cell (ATC) for interior noise tests and selected test results [AIAA PAPER 92-2164] p 4062 N92-32951
Active synchrophasing of propeller unbalance p 4063 N92-32963
SYNCHROTRON RADIATION
High accuracy beam energy measurement for linear and circular accelerators [DE92-016966] p 4069 N92-32319
Polarized wiggler for NSLS x ray ring design considerations [DE92-012212] p 4071 N92-32912
Proceedings of the fourth users meeting for the advanced photon source [DE92-014061] p 4072 N92-32932
Photon excitation for satellite free x ray spectroscopy: Instrumentation challenges [DE92-016999] p 4067 N92-32997
SYNCHROTRONS
Booster Applications Facility report, phase 2 [DE92-013395] p 4070 N92-32411
Theoretical and experimental studies of elementary physics [DE92-014877] p 4061 N92-32430
Optics of beam transport in the NSLS UV-FEL [DE92-014166] p 4015 N92-32511
Polarized wiggler for NSLS x ray ring design considerations [DE92-012212] p 4071 N92-32912
Photon excitation for satellite free x ray spectroscopy: Instrumentation challenges [DE92-016999] p 4067 N92-32997
Thermal and structural analysis of high precision beamline position monitors for synchrotron x ray beams [DE92-014863] p 4072 N92-33130
SYNTHESIS (CHEMISTRY)
NQR-NMR studies of higher alcohol synthesis Cu-Co catalysts [DE92-016614] p 3960 N92-32347
Solar photo-thermal catalytic reactions to produce high value chemicals [DE91-002140] p 4026 N92-32908
Polyimides with carbonyl and ether connecting groups between the aromatic rings [NASA-CASE-LAR-14001-1] p 3973 N92-33008
Microporous structure with layered interstitial surface treatment, and method and apparatus for preparation thereof [NASA-CASE-MSC-21487-1] p 3965 N92-33009
High octane ethers from synthesis gas-derived alcohols [DE92-013802] p 3975 N92-33108
Synthesis of MoSi2-based alloys by mechanical alloying [DE92-017528] p 3969 N92-33120
Direct conversion of light hydrocarbon gases to liquid fuel [DE92-015592] p 3975 N92-33141
Probe molecule studies: Active species in alcohol synthesis [DE92-016682] p 3966 N92-33246
SYNTHETIC APERTURE RADAR
Development of a prototype spatial information processing system for hydrologic research [NASA-CR-190579] p 4024 N92-32590
NAASW modular radar research testbed study results [DE92-011339] p 3981 N92-32744
SYNTHETIC FUELS
Probe molecule studies: Active species in alcohol synthesis [DE92-016682] p 3966 N92-33246
SYSTEM FAILURES
Phase-only synthesis for multiple-beam phased arrays with element failures [AD-A252250] p 3982 N92-32891
Diagnosability and diagnosis of sparsely interconnected multiprocessor systems [ISBN-0-315-56107-6] p 4053 N92-33224
SYSTEM IDENTIFICATION
Intelligent signal processing for active control [AD-A252232] p 4053 N92-32625
Frequency domain state-space system identification [NASA-TM-107659] p 4021 N92-32657
SYSTEMS ANALYSIS
Software development practice in a scientific computing environment [NLR-TP-91193-U] p 4043 N92-32832
Continuation of the development of a millimeter wave wideband tunable waveguide voltage controlled oscillator [CAL-504-88P120] p 3990 N92-32847
SYSTEMS ENGINEERING
An integrated multiple-sensor fire control system for air-to-air combat p 3937 N92-32450
Ground Systems Development Environment (GSDE) interface requirements and prototyping plan [NASA-CR-190713] p 4041 N92-32451
The 1991 Federal Aviation Administration plan for research, engineering and development p 4103 N92-32453
Publications on maglev technologies [DE92-013296] p 4017 N92-32615
Target Cueing And Tracking System (TCATS): User's guide [DE92-015385] p 4042 N92-32617
Tolerance optimization of servomechanisms [ISBN-90-9004476-0] p 4018 N92-32692
Conceptual design of an electron cyclotron wave system for NET/ITER [IPF-91-6] p 4071 N92-32808
Detectors for lidar type Thomson scattering diagnostics [IPF-91-5] p 3990 N92-32823
A study of large scale software testing p 4045 N92-32879
ABF algorithms implemented at ARL:UT, FDS system engineering and acoustics [AD-A252368] p 4046 N92-32917
Contribution to robot-task adaptation, introduction and use of robot anisotropy and task object for the design of the workstation [ISAL-91-0095] p 4039 N92-33056
SYSTEMS INTEGRATION
Integrated Target Acquisition and Fire Control Systems [AGARD-CP-500] p 3935 N92-32437
Multisensor airborne target acquisition systems and their integration p 3936 N92-32439
Naval target classification and designation with the CL-227 Sea Sentinel p 3937 N92-32449

Information Integration for Concurrent Engineering (IICE) IDEF3 process description capture method report
[AD-A252633] p 4042 N92-32627
IDEF4 object-oriented design method manual
[AD-A252634] p 4042 N92-32658
Conceptual design of an electron cyclotron wave system for NET/ITER
[IPF-91-6] p 4071 N92-32808

T

TABLES (DATA)
Diagnostic report of the National Hurricane Center, August and September 1991, volume 4, number 2
[PB92-179407] p 4033 N92-32503
SAGE 1 data user's guide
[NASA-RP-1275] p 4031 N92-33097
TACTICS
Tactical state and performance assessment during air combat maneuvering
[AD-A247426] p 3935 N92-32612
TAKEOFF
Ski jump takeoff performance predictions for a mixed-flow, remote-lift STOVL aircraft
[NASA-TM-103866] p 3935 N92-32887
TANKS (COMBAT VEHICLES)
Composite structural armor for combat vehicle applications p 3947 N92-32515
TANKS (CONTAINERS)
Free motion of an unsupported tank that is partially filled with liquid
[NLR-TP-91185-U] p 4011 N92-32831
Investigations preparatory to the Wet Satellite Model Experiment
[NLR-TP-91219-U] p 3943 N92-32834
TARGET ACQUISITION
Integrated Target Acquisition and Fire Control Systems
[AGARD-CP-500] p 3935 N92-32437
Operational needs for an unmanned air vehicle p 3936 N92-32438
Multisensor airborne target acquisition systems and their integration p 3936 N92-32439
Generic modular imaging IR signal processor p 3936 N92-32440
Target cuing: A heterogeneous neural network approach p 3936 N92-32442
Target detection using co-occurrence matrix segmentation and its hardware implementation p 3936 N92-32443
Automatic detection, pursuit, and classification in infrared imagery p 3937 N92-32445
The German anti tank helicopter PAH 2: An example of a future sensor platform p 3937 N92-32448
Visionless TRAC
[NASA-CR-190732] p 3942 N92-32477
Target Cueing And Tracking System (TCATS): User's guide
[DE92-015385] p 4042 N92-32617
TARGET RECOGNITION
Infrared Targeting System (IRTS) demonstration p 3937 N92-32446
Naval target classification and designation with the CL-227 Sea Sentinel p 3937 N92-32449
Temporal and spatial factors affecting the perception of computer-generated imagery
[AD-A249242] p 4046 N92-32907
Recursive estimation techniques for detection of small objects in infrared image data
[AD-A250942] p 4075 N92-32935
TARGETS
Target cuing: A heterogeneous neural network approach p 3936 N92-32442
Target detection using co-occurrence matrix segmentation and its hardware implementation p 3936 N92-32443
Automatic detection, pursuit, and classification in infrared imagery p 3937 N92-32445
Infrared Targeting System (IRTS) demonstration p 3937 N92-32446
The German anti tank helicopter PAH 2: An example of a future sensor platform p 3937 N92-32448
Naval target classification and designation with the CL-227 Sea Sentinel p 3937 N92-32449
An integrated multiple-sensor fire control system for air-to-air combat p 3937 N92-32450
Recursive estimation techniques for detection of small objects in infrared image data
[AD-A250942] p 4075 N92-32935
Radiation selective system for target range and imaging readout
[AD-D015285] p 4076 N92-33095
Method of guiding an in-flight vehicle toward a target
[AD-D015308] p 3940 N92-33161
TASK COMPLEXITY
A conceptual model of cognitive complexity of elements of the programming process p 4045 N92-32877
TASK PLANNING (ROBOTICS)
Using minimax approaches to plan optimal task commutation configurations for combined mobile platform-manipulator systems
[DE91-018864] p 4018 N92-32694
Contribution to robot-task adaptation, introduction and use of robot anisotropy and task object for the design of the workstation
[ISAL-91-0095] p 4039 N92-33056
TATB
Use of thin-film samples to study thermal decomposition chemistry of explosives
[DE92-014616] p 3974 N92-32637
TAYLOR INSTABILITY
Turbulence transport equations for variable-density turbulence and their relationship to two-field models
[DE92-017292] p 4013 N92-33159
TEARING
Measurement of nonlinear mode coupling of tearing fluctuations
[DE92-013901] p 4080 N92-33154
TECHNOLOGIES
Science and technology: A report to the Congress
[PB92-183219] p 4104 N92-33086
DoD key technologies plan
[AD-A253692] p 4105 N92-33238
TECHNOLOGY ASSESSMENT
The 1991 Federal Aviation Administration plan for research, engineering and development p 4103 N92-32453
International technology transfer to support the environmental restoration needs of the DOE complex
[DE92-013663] p 4028 N92-32558
Publications on maglev technologies
[DE92-013296] p 4017 N92-32615
Fundamental questions concerning the application of superplastic forming and superplastic forming/diffusion bonding
[MBB-Z-0402-91-PUB] p 3977 N92-32690
Examples of advanced near-net shape manufacturing techniques for aerospace
[MBB-Z-0399-91-PUB] p 3977 N92-32742
Fly-by-light technology development plan
[NASA-CR-181954] p 3939 N92-32778
Detectors for lidar type Thomson scattering diagnostics
[IPF-91-5] p 3990 N92-32823
Experiments in software engineering technology: Recent studies in the SEL (1990-1991) p 4044 N92-32872
Solar thermal energy: Viable energy technology for today and tomorrow
[DE92-015039] p 4026 N92-32923
A review of recent developments in joining high-performance thermoplastic composites
[CNRC-33030] p 4019 N92-33077
TECHNOLOGY TRANSFER
A status of the activities of the NASA/MSFC pump stage technology team p 4002 N92-32286
International technology transfer to support the environmental restoration needs of the DOE complex
[DE92-013663] p 4028 N92-32558
A minority research and education information service: Design, develop, pilot test, and implement on-line access for historically black colleges and universities and government agencies
[DE92-013572] p 4090 N92-32930
Humans and machines in space: The payoff
[ISBN-0-87703-343-9] p 4039 N92-33099
An international aerospace information system: A cooperative opportunity
[NASA-TM-108171] p 4091 N92-33237
TECHNOLOGY UTILIZATION
Publications on maglev technologies
[DE92-013296] p 4017 N92-32615
Fifty years in science, thirty years in space
[LALP-92-51] p 4104 N92-32862
Solid State Technology Branch of NASA Lewis Research Center
[NASA-TM-105752] p 3982 N92-32965
NASA space applications of high-temperature superconductors p 3985 N92-32980
Fuzzy set methods for object recognition in space applications
[NASA-CR-190388] p 4047 N92-33093
TELECOMMUNICATION
Information resources management plan of the Federal Government
[PB92-147198] p 4089 N92-32643
TELEPHONES
Correlation of single mode fiber fabrication factors and radiation response
[AD-A247301] p 4074 N92-32613
TELESCOPES
Diffractive optics technology and the NASA Geostationary Earth Observatory (GEO)
[NASA-CR-190611] p 4076 N92-33074
TELEVISION EQUIPMENT
Optical modulation characteristics and applications of liquid crystal televisions
[AD-A252466] p 3979 N92-32633
TELEVISION SYSTEMS
Optical modulation characteristics and applications of liquid crystal televisions
[AD-A252466] p 3979 N92-32633
Real-time edge-enhanced optical correlator
[NASA-CASE-NPO-18379-1-CU] p 4076 N92-33022
TEMPERATURE DEPENDENCE
T (sub c)-delta relations in YBa2Cu3O(7-delta) thin films: Effects of oxygen pressure during growth
[DE92-014432] p 4083 N92-32653
Superconducting transport properties and surface microstructure for YBa2Cu3O(7-delta) based superlattices grown by pulsed laser deposition
[DE91-014224] p 4085 N92-33023
TEMPERATURE DISTRIBUTION
Inverse design of a proper number, shapes, sizes, and locations of coolant flow passages p 4004 N92-32298
TEMPERATURE EFFECTS
High temperature deformation processes and strengthening mechanisms in intermetallic particulate composites
[AD-A250220] p 3946 N92-32339
Thermal effects and mirror surface figure requirements for a diagnostic beamline at the advanced light source
[DE92-014483] p 4073 N92-32419
Bacterial responses to extreme temperatures and pressures and to heavy organic loading
[AD-A247456] p 4035 N92-32571
Inelastic deformation and damage at high temperature
[DE92-012241] p 4021 N92-32698
Performance of insulated pavements at Newton Fields, Jackman, Maine
[CRREL-92-9] p 3940 N92-32903
Measurement techniques for cryogenic Ka-band microstrip antennas p 3985 N92-32981
Fracture surface characteristics of compressive failures in carbon fibre reinforced epoxy laminate subjected to hot/wet conditioning p 3959 N92-33051
The effect of heat treatment on the properties of PEEK and APC-2 p 3959 N92-33052
Modeling the influence of irradiation temperature and displacement rate on hardening due to point defect clusters in ferritic steels
[DE92-016897] p 3969 N92-33115
The design features of rocket motors relating to insensitive munition response to thermo-mechanical stimuli p 3976 N92-33244
TEMPERATURE GRADIENTS
Hot water storage tank for solar collectors
[AD-D015301] p 4026 N92-32943
TEMPERATURE MEASUREMENT
Heat and mass exchange during condensation of a water-ammonia mixture
[DE92-014524] p 3962 N92-32557
AC microcalorimetry of adsorbates on evaporated metal films: Orientational ordering of H2 multilayers
[DE92-008317] p 3963 N92-32666
An evaluation of an infrared/resistance temperature device for air/sea-surface temperature measurements
[AD-A252279] p 4035 N92-32688
STAMP, the SWOE Thermal Analysis and Measurement Program: Summary of the 1990 field tests
[LTR-91-013] p 4029 N92-32860
Reduced mobility and PPC in In(.20)Ga(.80)As / Al(.23)Ga(.77)As HEMT structure p 3984 N92-32976
Feasibility of measuring transverse electric noise at VLF and LF on an ice cap
[AD-A252280] p 4035 N92-33220
TEMPERATURE PROFILES
Titan's atmosphere: Latitudinal variations in temperature and composition p 4094 N92-32355
TEMPLATES
Surface reconstruction and templating for zeolite thin film synthesis observed by atomic force microscopy
[AD-A251140] p 4066 N92-32548
TEMPORAL DISTRIBUTION
Temporal and spatial factors affecting the perception of computer-generated imagery
[AD-A249242] p 4046 N92-32907
TENSILE STRENGTH
A curved beam test specimen for determining the interlaminar tensile strength of a laminated composite p 3949 N92-32526
Interfacial studies of refractory glass-ceramic matrix/advanced SiC fiber reinforced composites
[AD-A250784] p 3953 N92-32676

Processing and environmental effects on mechanical properties of composite repairs
[NRC-LTR-ST-1826] p 3954 N92-32791

TENSILE STRESS
The use of piezoelectric sensors to detect delamination initiation in carbon fiber reinforced composites
[MBB-Z-0391-91-PUB] p 3954 N92-32740
A description of the analytical methodology and reporting procedures used in the analysis and preparation of calibration reports for force measuring instruments
[NRC-LTR-ST-1817] p 4022 N92-32848
High temperature fiber optic microphone having a pressure-sensing reflective membrane under tensile stress
[NASA-CASE-LAR-14402-1-CU] p 4076 N92-33017

TENSILE TESTS
Heating fixture and instrumentation design for elevated temperature tests of a composite repair technique
[WL-TM-90-326-FIBE] p 3946 N92-32459
Influence of edge effect on compression-tension fatigue of toughened graphite/epoxy laminates p 3957 N92-33039

TENSORS
Poincare normal form (system of ordinary differential equations): An algorithmic point of view
[IMAG-RR-839-M] p 4058 N92-32838
Physics in knots
[DE92-017530] p 4088 N92-33069

TERMINAL BALLISTICS
Calculation of the energy of elastic deformation of Kevlar backing plates for ceramic armours
[AD-A250129] p 3970 N92-32489
Design, analysis, and testing of a reusable wingbox for ballistic evaluation of composite structures p 3947 N92-32518

TERMINAL GUIDANCE
CTAS: Computer intelligence for air traffic control in the terminal area
[NASA-TM-103959] p 3933 N92-33080
Method of guiding an in-flight vehicle toward a target
[AD-D015308] p 3940 N92-33161

TERMINOLOGY
PDES application protocol suite for composites (PAS-C). Functional needs report for the PAS-C program
[AD-A247886] p 3953 N92-32629

TERRAIN
Multifrequency measurements of radar ground clutter at 42 sites. Volume 1: Principal results
[AD-A246710] p 3980 N92-32696

TEST CHAMBERS
Titan in a box p 4101 N92-32404
A comparison of three popular test methods for determining the shear modulus of composite materials
[NASA-CR-190659] p 3959 N92-33075

TEST EQUIPMENT
Heating fixture and instrumentation design for elevated temperature tests of a composite repair technique
[WL-TM-90-326-FIBE] p 3946 N92-32459

TEST FACILITIES
The Nova Upgrade Facility for ICF ignition and gain
[DE92-010703] p 4079 N92-32733
A description of the analytical methodology and reporting procedures used in the analysis and preparation of calibration reports for force measuring instruments
[NRC-LTR-ST-1817] p 4022 N92-32848
Automated data acquisition and analysis in the mechanical test lab
[DE92-011231] p 4040 N92-32910

TEST FIRING
An analysis of the flow field in the region of the ASRM field joints p 4005 N92-32305

TEST STANDS
Technology test bed review p 4001 N92-32279
NAASW modular radar research testbed study results
[DE92-011339] p 3981 N92-32744
Overview and evolution of the LeRC PMAD DC Testbed
[NASA-TM-105842] p 3991 N92-32867

TESTS
Proceedings of the Sixteenth Annual Software Engineering Workshop
[NASA-TM-107964] p 4044 N92-32869

THEODORSEN TRANSFORMATION
Ideal efficiency of propellers based on Theodorsen's theory: A review and computer study, with extended plus simplified charts
[UTIAS-TN-271] p 3938 N92-33102

THEOREMS
Fault-tolerant wait-free shared objects
[NASA-CR-190679] p 4020 N92-32436
Bootstrapping the change-point of a hazard rate
[IMAG-RR-861-M] p 4056 N92-32685
Minimum cost multiflows in undirected networks
[IMAG-RR-849-M] p 4056 N92-32710
A min-max relation for K3-covers in graphs noncontractible to K5/e
[IMAG-RR-850-I] p 4056 N92-32711
Characterization of Laborde-Mulder graphs and the halfcube
[IMAG-RR-857-I] p 4057 N92-32713
A new form for the central limit theorem
[IMAG-RR-852-M] p 4060 N92-32716
Dissimilarities, dendograms, prefillers, and multiapplications of levels
[IMAG-RR-842-M] p 4058 N92-32799

THEORETICAL PHYSICS
Possible effects of additional vector bosons in e(sup +)e(sup -)(yields)f(bar-f) at the TRISTAN energies
[DE92-624727] p 4065 N92-32498
Application of gauge theories to enhance numerical solutions to mixed potential integral equations
[AD-A248451] p 4055 N92-32670
Experimental particle physics at the University of Pittsburgh
[DE92-014181] p 4066 N92-32702
Research in theoretical nuclear physics
[DE92-016316] p 4068 N92-33067
A Theoretical High Energy Physics Program: Task F
[DE92-014054] p 4073 N92-33182
Theoretical nuclear physics
[DE92-016837] p 4069 N92-33186

THERMAL ABSORPTION
Quantitative non-destructive environmental characterization of advanced materials
[DE92-011462] p 3946 N92-32327

THERMAL ANALYSIS
CFD analysis to optimize a design modification of BSMT p 4004 N92-32296
Numerical analysis of the hot-gas-side and coolant-side heat transfer in liquid rocket engine combustors p 4004 N92-32299
STAMP, the SWOE Thermal Analysis and Measurement Program: Summary of the 1990 field tests
[LTR-91-013] p 4029 N92-32860
Thermal and structural analysis of high precision beamline position monitors for synchrotron x ray beams
[DE92-014863] p 4072 N92-33130

THERMAL CONDUCTIVITY
Laboratory determination of the thermal conductivity of liquid methane and ethane p 4015 N92-32392
Thermal conductance of augmented pressed metallic contacts at liquid helium temperatures
[NASA-TM-103917] p 4007 N92-32474
Thermal conductivity of liquid aliphatic hydrocarbons. Part 1: Alkanes
[ESDU-92011-PT-1] p 3945 N92-32484
Thermal conductivity of gaseous halogenated hydrocarbons: Ethylenes and benzenes
[ESDU-92010] p 3945 N92-32485

THERMAL DECOMPOSITION
Use of thin-film samples to study thermal decomposition chemistry of explosives
[DE92-014616] p 3974 N92-32637

THERMAL DEGRADATION
Thermal degradation study of silicon carbide threads developed for advanced flexible thermal protection systems
[NASA-TM-103952] p 3970 N92-32476

THERMAL ENERGY
Solar thermal energy: Viable energy technology for today and tomorrow
[DE92-015039] p 4026 N92-32923
Development of advanced modulators for recirculating heavy ion accelerators
[DE92-014795] p 4072 N92-33122

THERMAL EXPANSION
Flush mounting of thin film sensors
[NASA-CASE-LAR-14446-1] p 3978 N92-33020

THERMAL INSULATION
Ultra-low density organic-inorganic composite materials possessing thermally insulating and acoustic damping properties
[AD-A251182] p 3955 N92-32828
Performance of insulated pavements at Newton Fields, Jackman, Maine
[CRREL-92-9] p 3940 N92-32903

THERMAL MAPPING
A boundary integral method for an inverse problem in thermal imaging
[NASA-CR-189693] p 4059 N92-33006

THERMAL NOISE
Vacuum-isolation vessel and method for measurement of thermal noise in microphones
[NASA-CASE-LAR-14567-1-CU] p 3991 N92-33021

THERMAL PROTECTION
Thermal degradation study of silicon carbide threads developed for advanced flexible thermal protection systems
[NASA-TM-103952] p 3970 N92-32476
Thermal assessment of Mustang Industries, Inc. neoprene quick-don anti-exposure immersion suits and storage evaluation for the CP140 Aurora aircraft
[DCIEM-90-23] p 4039 N92-32790

THERMAL REACTORS
Conceptual design of an electron cyclotron wave system for NET/ITER
[IPF-91-6] p 4071 N92-32808

THERMAL STABILITY
Liquid lubricants for advanced aircraft engines
[NASA-TM-104531] p 3972 N92-32863
Hazards reduction for tactical missiles p 3945 N92-33245

THERMAL STRESSES
Thermal strains in titanium aluminide and nickel aluminide composites
[DE92-015181] p 3953 N92-32638

THERMOCHEMICAL PROPERTIES
Thermochemical cycles for energy storage: Thermal decomposition of ZnSO4 systems
[DE91-002144] p 4026 N92-32909

THERMOCHEMISTRY
Thermochemical and kinetic considerations in diamond growth
[AD-A247866] p 3971 N92-32490
Thermochemical cycles for energy storage: Thermal decomposition of ZnSO4 systems
[DE91-002144] p 4026 N92-32909
Direct conversion of light hydrocarbon gases to liquid fuel
[DE92-015592] p 3975 N92-33141

THERMODYNAMIC CYCLES
Development and proof-testing of advanced absorption refrigeration cycle concepts
[DE92-014933] p 3977 N92-32723
Thermochemical cycles for energy storage: Thermal decomposition of ZnSO4 systems
[DE91-002144] p 4026 N92-32909
MHD Integrated Topping Cycle Project
[DE92-013904] p 4080 N92-33024

THERMODYNAMIC PROPERTIES
Quantitative non-destructive environmental characterization of advanced materials
[DE92-011462] p 3946 N92-32327
Composite structural armor for combat vehicle applications p 3947 N92-32515

THERMOELASTICITY
Physical basis for a pressure-dependent yield criterion for polymers
[AD-A250763] p 3970 N92-32341

THERMOELECTRIC COOLING
A 19.2 GHz cooled HEMT low noise amplifier
[CTN-92-60354] p 3990 N92-32810

THERMOGRAPHY
A boundary integral method for an inverse problem in thermal imaging
[NASA-CR-189693] p 4059 N92-33006

THERMOHYDRAULICS
Two-phase heat transport systems for space: Thermal gravitational modelling and scaling predictions versus results of experiments
[NLR-TP-91051-U] p 4010 N92-32786

THERMOMETERS
An evaluation of an infrared/resistance temperature device for air/sea-surface temperature measurements
[AD-A252279] p 4035 N92-32688

THERMONUCLEAR REACTIONS
Study of recirculating induction accelerators as drivers for heavy ion fusion
[DE92-016980] p 4071 N92-32904

THERMOPHYSICAL PROPERTIES
Combustion instability analysis for liquid propellant rocket engines p 3966 N92-32297

THERMOPLASTIC RESINS
Supportability evaluation of thermoplastic and thermoset composites p 3950 N92-32576
New thiophene-based materials
[AD-A250977] p 3972 N92-32667
Fluid effects: Thermoset and thermoplastic matrix composites p 3958 N92-33049
Jet fuel absorption and dynamic mechanical analysis of carbon fibre composites p 3959 N92-33050
Environmental resistance of amorphous bonded thermoplastic joints p 3959 N92-33053
A review of recent developments in joining high-performance thermoplastic composites
[CNRC-33030] p 4019 N92-33077
Apparatus for preparing thermoplastic composites
[AD-D015326] p 3960 N92-33174

THERMOPLASTICITY
Development of thermoplastic components for structural validation p 3948 N92-32522
Apparatus for preparing thermoplastic composites
[AD-D015326] p 3960 N92-33174

THERMOSETTING RESINS
Supportability evaluation of thermoplastic and thermoset composites p 3950 N92-32576
New thiophene-based materials [AD-A250977] p 3972 N92-32667
CFRP stiffened panels under compression p 3958 N92-33044

THICK PLATES
Efficient finite element modeling of laminated composite plates based on higher-order theory p 3949 N92-32529

THICKNESS
Thickness dependence of vortex pinning in epitaxial Tl-Ca-Ba-Cu-O thin films [DE92-015011] p 4084 N92-32920

THIN FILMS
Thin film cadmium telluride, zinc telluride, and mercury zinc telluride solar cells [DE92-001237] p 4024 N92-32510
Probing thin-film YBa2Cu3O(7-delta) superconductors by second harmonic generation using femtosecond laser pulses [AD-A252350] p 4082 N92-32512
Surface reconstruction and templating for zeolite thin film synthesis observed by atomic force microscopy [AD-A251140] p 4066 N92-32548
Surfaces and thin films studied by picosecond ultrasonics [DE92-016313] p 4020 N92-32564
Use of thin-film samples to study thermal decomposition chemistry of explosives [DE92-014616] p 3974 N92-32637
T (sub c)-delta relations in YBa2Cu3O(7-delta) thin films: Effects of oxygen pressure during growth [DE92-014432] p 4083 N92-32653
Workshop on research needs and opportunities in high temperature superconductivity [AD-A252674] p 3988 N92-32659
Investigation on the lattice site location of the excess arsenic atoms in GaAs layers grown by low temperature molecular beam epitaxy [DE92-008253] p 4083 N92-32693
Thickness dependence of vortex pinning in epitaxial Tl-Ca-Ba-Cu-O thin films [DE92-015011] p 4084 N92-32920
Magnetic penetration depth of YBa2Cu3O(7-delta) thin films determined by the power transmission method p 3985 N92-32983
Magnetic flux relaxation in YBa2Cu3O(7-x) thin film: Thermal or athermal p 3985 N92-32984
Flush mounting of thin film sensors [NASA-CASE-LAR-14446-1] p 3978 N92-33020
Superconducting transport properties and surface microstructure for YBa2Cu3O(7-delta) based superlattices grown by pulsed laser deposition [DE91-014224] p 4085 N92-33023
Thinning and rupture of a thin liquid film on a heated surface [DE92-014813] p 4013 N92-33124
Superconductivity: Past, present, and future [DE92-014862] p 3992 N92-33128
Ultra-low-loss strip-type transmission lines, formed of bonded substrate layers [AD-D015312] p 3992 N92-33169
Method of growing diamond film on substrates [AD-D015313] p 3973 N92-33170
Electric and magnetic properties of random superconductors [ITN-92-85165] p 4086 N92-33190

THOMSON SCATTERING
Detectors for lidar type Thomson scattering diagnostics [IPF-91-5] p 3990 N92-32823

THREE DIMENSIONAL FLOW
SRMAFTE facility checkout model flow field analysis p 3994 N92-32247
A critical evaluation of a three-dimensional Navier-Stokes CFD as a tool to design supersonic turbine stages p 3999 N92-32268
A multi-domain method for subsonic viscous flows p 3960 N92-32275
Three-dimensional flow fields inside a shrouded inducer at design and off-design conditions (CFD study) p 4003 N92-32291
NLS clutching bearing cavity flow analysis p 4003 N92-32295
Complex three-dimensional internal flows in the ASRM and RSRM aft end segments p 4005 N92-32304
Annual progress report on imposed 3-D disturbances on bluff-body near wake flows [AD-A250366] p 4006 N92-32324
Numerical simulation of turbulence at the back of the airplane [ETN-92-91664] p 3931 N92-32769
Experimental study of the vortex system generated by a missile fuselage at incidence. Part 3: Three directional laser velocimetry measurements [ONERA-RT-47/1147-AY-146A-P] p 3931 N92-32800
A three-field model of transient 3D multiphase, three-component flow for the computer code 4 A3. Part 2: Models for the interfacial transport phenomena. Code validation [KFK-4949-PT-2] p 4011 N92-32858

THREE DIMENSIONAL MODELS
An efficient and robust grid optimization algorithm p 4004 N92-32300
Potential flow theory and operation guide for the panel code PMARC [NASA-TM-102851] p 3929 N92-32422
Two- and three-dimensional simulation code for radiation-hydrodynamics in ICF [NIFS-119] p 4078 N92-32552
Study and achievement of a parallel simulator for diffusion at the atomic level: Creation and growth of dislocation loops under electronic radiation [LAAS-92118] p 4066 N92-32735
Three dimensional object reconstruction using a very limited number of projections. Application to industrial radiography [TELECOM-91-E-008] p 4043 N92-32804
Uses of stereovision surface models [TELECOM-91-E-016] p 4075 N92-32806
A three-field model of transient 3D multiphase, three-component flow for the computer code 4 A3. Part1: Theoretical basis: Conservation and state equations, numerics [KFK-4948-PT-1] p 4011 N92-32857
STAMP, the SWOE Thermal Analysis and Measurement Program: Summary of the 1990 field tests [LTR-91-013] p 4029 N92-32860
Three-dimensional elasticity analysis of buckling of laminated plates p 3957 N92-33037

THROTTLING
Flight testing and simulation of an F-15 airplane using throttles for flight control [NASA-TM-104255] p 3940 N92-32864

THRUST
Investigation of the flight control requirements of a half-scale ducted fan unmanned aerial vehicle [AD-A252730] p 3940 N92-32988
Ideal efficiency of propellers based on Theodorsen's theory: A review and computer study, with extended plus simplified charts [UTIAS-TN-271] p 3938 N92-33102

THRUST CHAMBERS
A numerical model for atomization-spray coupling in liquid rocket thrust chambers p 3996 N92-32257
Experimental studies of characteristic combustion-driven flows for CFD validation p 3998 N92-32264
Inverse design of a proper number, shapes, sizes, and locations of coolant flow passages p 4004 N92-32298

THRUST VECTOR CONTROL
Ski jump takeoff performance predictions for a mixed-flow, remote-lift STOVL aircraft [NASA-TM-103866] p 3935 N92-32887

THUNDERSTORMS
Verification of severe local storms forecasts issued by the National Severe Storms Forecast Center, 1991 [PB92-186063] p 4033 N92-32502
Severe local storm warning verification: 1991 [PB92-185982] p 4033 N92-32545
Airport Surveillance Radar (ASR-9) wind shear processor: 1991 test at Orlando, Florida [AD-A252246] p 3980 N92-32686

TIME
Cognitive biases and time stress in team decision making [AD-A251153] p 4088 N92-32551

TIME DEPENDENCE
Applications of the photorefractive effect and damage induced effects in fibers [AD-A250767] p 3953 N92-32674

TIME MARCHING
A numerical study of two-dimensional vortex shedding from rectangular cylinders p 3998 N92-32266
The impact of time step definition on code convergence and robustness p 4001 N92-32282
A comparison of artificial compressibility and fractional step methods for incompressible flow computations p 4001 N92-32285

TIME OF FLIGHT SPECTROMETERS
Ion microtomography using ion time-of-flight [DE92-017257] p 4068 N92-33001

TITAN
Symposium on Titan [ESA-SP-338] p 4093 N92-32348
Some issues associated with the formation of the Saturnian system p 4093 N92-32349
Impact origin of Titan's atmosphere p 4094 N92-32351
Interior of Titan p 4094 N92-32352
The thermal structure of the atmosphere of Titan p 4094 N92-32353
The composition of the Titan atmosphere p 4094 N92-32354
Titan's atmosphere: Latitudinal variations in temperature and composition p 4094 N92-32355
Titan's UV albedo: Observations and modeling p 4094 N92-32356
A reanalysis of Voyager UVS observations of Titan p 4094 N92-32357
The atmospheric temperature structure of Titan p 4095 N92-32358
Ground-based observations of Titan's thermal spectrum p 4095 N92-32359
The meteorology of Titan p 4095 N92-32360
Numerical simulation of the circulation of the atmosphere of Titan p 4095 N92-32361
Simple dynamical models of Titan's atmospheric circulation p 4095 N92-32362
A preliminary assessment of the Titan planetary boundary layer p 4095 N92-32363
Gravitational tide in the atmosphere of Titan p 4096 N92-32364
The significance of meteoric ionisation for the propagation of lightning spherics in the atmosphere of Titan p 4096 N92-32365
Modeling of the diurnal variations of the atmosphere of Titan p 4096 N92-32366
Neutral composition of Titan's atmosphere. A theoretical model p 4096 N92-32367
Organic chemistry on Titan versus terrestrial prebiotic chemistry: Exobiological implications p 4096 N92-32368
Titan's organic chemistry: Results of simulation experiments p 4096 N92-32369
Organic chemistry on Titan: Surface interactions p 4096 N92-32370
Photochemistry of unsaturated nitriles on Titan p 4096 N92-32371
Titan's organic haze p 4097 N92-32372
Infrared properties of Titan's clouds and aerosols p 4097 N92-32373
Observing the surface of Titan through near-infrared windows in its atmosphere p 4097 N92-32374
The detectability of Titan's surface in the near-infrared p 4097 N92-32375
Titan's mid-IR albedo: New observations from 3 to 5 microns p 4097 N92-32376
VIMS/Cassini mission at Titan: Scientific objectives and observational scenarios p 4097 N92-32377
Cassini/CIRS capabilities for aerosol, cloud, and surface measurements p 4098 N92-32378
Huygens/ACP: An instrument for aerosols chemical composition measurements p 4098 N92-32379
Huygens/ASI plasma wave analyzer capabilities for aerosol measurement p 4098 N92-32380
Plausible surface models for Titan p 4098 N92-32381
Plasma interaction of Titan with the Saturnian magnetosphere: A review of critical issues p 4098 N92-32382
Mass loading at Titan and comets p 4098 N92-32383
Atmospheric escape from Titan p 4099 N92-32384
Titan's magnetospheric interaction p 4099 N92-32385
The ionosphere of Titan and its interaction with Saturnian magnetospheric electrons p 4099 N92-32386
Cassini: A mission to Saturn and Titan p 4099 N92-32387
The Huygens probe p 4099 N92-32388
The synthetic infrared spectrum of Titan at high spectral resolution p 4099 N92-32389
Experimental determination of the refractive index of liquefied gas mixtures: Applications to hypothesized Titan oceans p 4099 N92-32390
Formation and growth of photochemical aerosols in Titan's atmosphere p 4100 N92-32393
Waves on Titan p 4100 N92-32394
Properties and distribution of the aerosols in the atmosphere of Titan p 4100 N92-32396
Titan's atmosphere structure from Huygen's-ASI measurements p 4101 N92-32398
The Huygens SSP Refractometer (REF) p 4101 N92-32399
Some problems about IR band integrated intensities; 3 examples for application to Titan: C6H6, HC3N, and C4H2 p 4101 N92-32400
The spectrum of Titan in the 1.06 and 1.28 micron windows p 4101 N92-32401
Huygens probe: The surface mission p 4101 N92-32402

On the Titan/28 Sagittarii occultation of 1989 July 3 p 4101 N92-32403
Titan in a box p 4101 N92-32404
Laboratory investigations of the aerosols in the stratosphere of Titan p 4102 N92-32405
Near infrared spectra of potential solids at the surface of Titan p 4102 N92-32406
On the interpretation of Titan's intensity and polarization phase curve p 4102 N92-32407
Study of transmitted light through the atmosphere of Titan p 4102 N92-32408
Dielectric constant measurements in simulated Titan ocean liquids p 4102 N92-32409
A surface science package for the Huygens Titan probe p 4102 N92-32410

TITANIUM ALLOYS
Computational simulation of matrix micro-slip bands in SiC/Ti-15 composite
[NASA-TM-105762] p 3946 N92-32466
An in vitro corrosion study of two implant materials using electrochemical impedance spectroscopy and potentiodynamic polarization
[AD-A252575] p 3966 N92-32626
Thermal strains in titanium aluminide and nickel aluminide composites
[DE92-015181] p 3953 N92-32638
Generic consequences of fundamental studies of beta phase decomposition modes in titanium and related alloy systems
[AD-A250789] p 3967 N92-32699
Superplastic forming of Ti6Al4V at lower temperature using hydrogen
[MBB-Z-0403-91-PUB] p 3978 N92-32893
Investigation of fracture toughness and fracture mechanisms using acoustic emission measurements
[DE92-011907] p 4022 N92-32911

TOKAMAK DEVICES
Injection of compact toroids for tokamak fueling and current drive
[DE92-010031] p 4077 N92-32533
Nonlinear dynamics and plasma transport
[DE92-014246] p 4078 N92-32592
Formation and sustainment of a very low aspect ratio tokamak using coaxial helicity injection: Helicity Injected Torus (HIT) experiment
[DE92-014311] p 4078 N92-32595
The role of stochasticity in sawtooth oscillation
[DE92-782004] p 3982 N92-32905
Edge gradient and safety factor effects on electrostatic turbulent transport in tokamaks
[DE92-014323] p 4079 N92-32944
Scrape-off layer modeling of radiative divertor and high heat flux experiments on D3-D
[DE92-015007] p 4080 N92-32995
ANL ITER high-heat-flux blanket-module heat transfer experiments
[DE92-017749] p 4080 N92-33168

TOLERANCES (MECHANICS)
A Protection And Detection Surface (PADS) for damage tolerance p 3948 N92-32523
Damage tolerance certification methodology for composite structures p 3951 N92-32579
Certification of damage tolerant composite structure p 3951 N92-32580
Statistically based material properties: A military handbook-17 perspective p 3951 N92-32581
Tolerance optimization of servomechanisms
[ISBN-90-9004476-0] p 4018 N92-32692

TOMOGRAPHY
The LLNL Multi-User Tandem Laboratory PIXE microprobe
[DE92-017252] p 4014 N92-32999
Applications of energy loss contrast STIM
[DE92-017254] p 4014 N92-33000
Ion microtomography using ion time-of-flight
[DE92-017257] p 4068 N92-33001
Some new perspectives in photoelasticity and curved-ray tomography
[ISBN-0-315-57756-8] p 4023 N92-33200

TOPOGRAPHY
Topographical measuring based on the shadow and projection Moire method
[ISBN-90-9004146-X] p 4074 N92-32705

TOPOLOGY
Wavelength division multiplexed local area networks
[AD-A247613] p 3979 N92-32573

TORNADOES
Verification of severe local storms forecasts issued by the National Severe Storms Forecast Center, 1991
[PB92-186063] p 4033 N92-32502

TOROIDAL PLASMAS
Magnetohydrodynamic stability of plasmas with radial motion
[DE92-013917] p 4077 N92-32417
Injection of compact toroids for tokamak fueling and current drive
[DE92-010031] p 4077 N92-32533
Formation and sustainment of a very low aspect ratio tokamak using coaxial helicity injection: Helicity Injected Torus (HIT) experiment
[DE92-014311] p 4078 N92-32595
Status of LHD control system design
[NIFS-122] p 4070 N92-32746

TOROIDS
Injection of compact toroids for tokamak fueling and current drive
[DE92-010031] p 4077 N92-32533
Spray nozzle for fire control
[CA-PATENT-APPL-SN-2-011-94] p 4011 N92-32856

TORQUE
NLS clutching bearing cavity flow analysis p 4003 N92-32295
Reducing torque fluctuation in linkage drive shafts
[ESDU-92016] p 4017 N92-32482

TORSION
A reexamination of the plastic flow criterion for copper
[AD-A252370] p 4023 N92-32918

TORSIONAL VIBRATION
Reducing torque fluctuation in linkage drive shafts
[ESDU-92016] p 4017 N92-32482

TORUSES
Formation and sustainment of a very low aspect ratio tokamak using coaxial helicity injection: Helicity Injected Torus (HIT) experiment
[DE92-014311] p 4078 N92-32595

TOTAL QUALITY MANAGEMENT
Methodological and architectural issues in the experience factory p 4044 N92-32870
Cleanroom process evolution in the SEL p 4044 N92-32871
Investigating the application of capture-recapture techniques to requirement and design reviews p 4044 N92-32873

TOUGHNESS
GARTEUR compression behaviour of advanced CFRP --- carbon fiber reinforced plastics p 3957 N92-33042

TOXIC HAZARDS
Suggestions for improvement of the methodology and use of MEPAS, the multimedia environmental pollutant assessment system
[DE92-013135] p 4028 N92-32616

TOXINS AND ANTITOXINS
Summary of engineering-scale experiments for the Solar Detoxification of Water project
[DE92-013776] p 4027 N92-33150

TRACKING (POSITION)
Visionless TRAC
[NASA-CR-190732] p 3942 N92-32477
Target Cueing And Tracking System (TCATS): User's guide
[DE92-015385] p 4042 N92-32617
Development of new flight procedures for the Microwave Landing System (MLS)
[NLR-TP-91156-U] p 3933 N92-32830

TRACKING FILTERS
Performance analysis of space-based radar tracking techniques
[ISBN-0-315-60464-6] p 3987 N92-33207

TRACKING RADAR
Coverage studies for spaced-based radar
[DREO-90-18] p 3982 N92-32818

TRAILING EDGE FLAPS
Lift and rolling moment due to spoilers on wings with trailing-edge flaps deflected at subsonic speeds
[ESDU-92002-SUPPL] p 3931 N92-32782

TRAINING DEVICES
Briefing notes on a manned aircraft research and support simulation facility
[AD-A250373] p 3935 N92-32326
Human learning of schemas from explanations in practical electronics
[AD-A247429] p 4038 N92-32569

TRAJECTORIES
Quark-antiquark Regge trajectories in large N(sub c) QCD
[DE92-016462] p 4064 N92-32313
ROAR: A 3-D tethered rocket simulation code
[DE92-017358] p 3944 N92-33166

TRAJECTORY PLANNING
Titan's atmosphere structure from Huygen's-ASI measurements p 4101 N92-32398

TRANSDUCERS
The 1991 rocket-triggered lightning test of the DoD Security Operations Test Site (SOTS) munitions storage bunker, Fort McClellan, Alabama
[DE92-012449] p 4032 N92-32427

TRANSFER FUNCTIONS
New approach to HF channel modeling and simulation. Part 3: Transfer function
[PB92-192848] p 3979 N92-32555
Frequency domain state-space system identification
[NASA-TM-107659] p 4021 N92-32657
A discrete nonlinear model approach to study the behavior of large signal DC to DC converters
[LAAS-90028] p 3989 N92-32777
Analog CMOS filters for very-high frequencies
[ISBN-90-9004420-5] p 3986 N92-33143

TRANSFORMATIONS (MATHEMATICS)
Contribution to the determination of vanishing points using Hough transform
[TELECOM-91-D-008] p 4058 N92-32803

TRANSIENT PRESSURES
A comparison of artificial compressibility and fractional step methods for incompressible flow computations p 4001 N92-32285

TRANSIENT RESPONSE
Nonlinear transient responses of stratified composite structures
[ONERA-RT-26/3542-RY-007-R] p 3954 N92-32775

TRANSITION METALS
Structure and dynamics in low-dimensional guest-host systems
[DE92-014841] p 3970 N92-32429
Excited state processes in transition metal complexes: Redox splitting in soluble polymers
[DE92-011808] p 3971 N92-32631

TRANSITION TEMPERATURE
On the resistive transition of composite superconductors
[ISBN-90-9003899-X] p 3992 N92-33145

TRANSLATING
Improving the translation from data flow diagrams into Z by incorporating the data dictionary
[AD-A250769] p 4089 N92-32342

TRANSMISSION LINES
Wavelength division multiplexed local area networks
[AD-A247613] p 3979 N92-32573

TRANSMISSION LOSS
Beam and filter straddle losses in an ESA search radar
[AD-A250878] p 3980 N92-32680

TRANSMISSIVITY
Local aspects of the optical reflection problem: The discrete dipole approach
[ISBN-90-9004118-4] p 4074 N92-32703

TRANSONIC COMPRESSORS
Numerical simulation of turbomachinery flows with advanced turbulence models p 3999 N92-32270

TRANSONIC FLIGHT
An experimental study of the flow over a sharp-edged delta wing at subsonic and transonic speeds
[NLR-TP-91117-U] p 3930 N92-32732
NLR investigations of flutter behaviour of fighter aircraft with external stores
[NLR-TP-91134-U] p 3939 N92-32750

TRANSONIC FLOW
Comparison between the PISO algorithm and preconditioning methods for compressible flow p 4001 N92-32284
An examination of several high resolution schemes applied to complex problems in high speed flows
[AD-A250814] p 4008 N92-32632
Research on some centered implicit methods for calculating transonic flows by solving Navier-Stokes equations
[ONERA-RSF-24/1408-AY-150A] p 3931 N92-32773

TRANSPARENCE
Purification system
[NASA-CASE-MSC-21584-1] p 3965 N92-33029

TRANSPORT PROPERTIES
Nonlinear dynamics and plasma transport
[DE92-014246] p 4078 N92-32592
Advanced computational transport methods for curvilinear geometries
[DE92-011290] p 4057 N92-32743
A three-field model of transient 3D multiphase, three-component flow for the computer code 4 A3. Part 2: Models for the interfacial transport phenomena. Code validation
[KFK-4949-PT-2] p 4011 N92-32858
Reduced mobility and PPC in In(.20)Ga(.80)As / Al(.23)Ga(.77)As HEMT structure p 3984 N92-32976
Superconducting transport properties and surface microstructure for YBa2Cu3O(7-delta) based superlattices grown by pulsed laser deposition
[DE91-014224] p 4085 N92-33023
Electric and magnetic properties of random superconductors
[ITN-92-85165] p 4086 N92-33190

TRANSPORT THEORY
Analytic score comparison of geometry splitting and exponential transform for a simple Monte Carlo problem
[DE92-013108] p 4059 N92-32481
Advanced computational transport methods for curvilinear geometries
[DE92-011290] p 4057 N92-32743

Turbulence transport equations for variable-density turbulence and their relationship to two-field models
[DE92-017292] p 4013 N92-33159

TRANSPORTATION
Second interim report of the Interagency Commission on Alternative Motor Fuels
[DE92-013169] p 3974 N92-32483
Air traffic control: FAA's advanced automation system contract
[GAO/IMTEC-91-25] p 3934 N92-32861

TRANSPUTERS
Real-time processing of radar return on a parallel computer
[NASA-CR-4456] p 3932 N92-32606
Parallel processing in space applications using transputer networks
[MBB-UO-0172-90-PUB] p 4050 N92-32689

TRAPPED PARTICLES
Trapped ions and laser cooling 3
[PB92-189547] p 4016 N92-33060

TRAPPING
Plasma diffusion through multidipole magnetic fields
[INPE-5384-PRE/1750] p 4079 N92-32662

TREES (MATHEMATICS)
Implementation of a tree-code for numerical simulations of stellar systems
[INPE-5370-TDI/469] p 4093 N92-32604
Finding solutions to value independent knapsack problems
[INPE-5390-TAE/011] p 4055 N92-32661
Consistency and robustness of knowledge graphs
[ISBN-90-9003729-2] p 4056 N92-32679

TRENDS
Applications of statistical methods to the study of climate and flooding fluctuations in the central US
[PB92-205137] p 4034 N92-33173

TRIBOLOGY
Implanted aluminum: Tribological behavior and mechanical properties of the superficial layers
[ECL-91-28] p 4019 N92-32801
Influence of oil lubricant additives on tribological behavior of engineering ceramics
[PB92-180710] p 3973 N92-33059

TRINITROTOLUENE
Development of methodology and technology for identifying and quantifying emission products from open burning and open detonation thermal treatment methods. BangBox test series. Volume 3: Quality assurance and quality control
[AD-A251099] p 4029 N92-32650

TROPICAL REGIONS
ARM Tropical Pacific Experiment (ATPEX): Role of cloud, water vapor and convection feedbacks in the coupled ocean/atmosphere system
[DE92-013772] p 4032 N92-32331

TROPICAL STORMS
Tropical cyclone motion due to environmental interactions represented by empirical orthogonal functions of the vorticity fields
[AD-A246137] p 4033 N92-32534

TUNGSTEN
Thermal strains in titanium aluminide and nickel aluminide composites
[DE92-015181] p 3953 N92-32638

TUNING
Continuation of the development of a millimeter wave wideband tunable waveguide voltage controlled oscillator
[CAL-504-88P120] p 3990 N92-32847

TUNNEL DIODES
A model for the trap-assisted tunneling mechanism in diffused n-p and implanted n(+)-p HgCdTe photodiodes
p 3985 N92-32979

TURBINE BLADES
A critical evaluation of a three-dimensional Navier-Stokes CFD as a tool to design supersonic turbine stages p 3999 N92-32268
Navier-Stokes analysis of an oxidizer turbine blade with tip clearance p 3999 N92-32269
Inverse design of a proper number, shapes, sizes, and locations of coolant flow passages
p 4004 N92-32298

TURBINE PUMPS
Turbine disk cavity aerodynamics and heat transfer
p 3998 N92-32265
Technology test bed review p 4001 N92-32279
Space Transportation Main Engine
p 3945 N92-32281
Development of CFD code evaluation criteria and a procedure for assessing predictive capability and performance p 4001 N92-32283
A status of the activities of the NASA/MSFC pump stage technology team p 4002 N92-32286
CFD analysis of pump consortium impeller
p 4002 N92-32287
NLS clutching bearing cavity flow analysis
p 4003 N92-32295
Computation of incompressible viscous flows through turbopump components
[NASA-TM-103911] p 4012 N92-33113

TURBINE WHEELS
Turbine disk cavity aerodynamics and heat transfer
p 3998 N92-32265

TURBOCOMPRESSORS
Computations of unsteady multistage compressor flows in a workstation environment
[NASA-TM-103839] p 3938 N92-32452

TURBOFAN ENGINES
Bird ingestion into large turbofan engines
[DOT/FAA/CT-91/17] p 3932 N92-33005

TURBOJET ENGINES
Liquid lubricants for advanced aircraft engines
[NASA-TM-104531] p 3972 N92-32863

TURBOMACHINE BLADES
The application of unsteady potential flow vortex loop/dipole theory to the work and acoustics of low-speed turbomachinery
[AD-A251160] p 4008 N92-32652

TURBOMACHINERY
Optimum design of ninety degree bends
p 4000 N92-32274
Tenth Workshop for Computational Fluid Dynamic Applications in Rocket Propulsion, part 1
[NASA-CP-3163-PT-1] p 4000 N92-32278
Computational fluid dynamic design of rocket engine pump components p 4003 N92-32293
The application of unsteady potential flow vortex loop/dipole theory to the work and acoustics of low-speed turbomachinery
[AD-A251160] p 4008 N92-32652

TURBOPROP AIRCRAFT
Active vibrations and noise control for turboprop application research program activities
p 4063 N92-32962

TURBULENCE
Effects of curvature and rotation on turbulence in the NASA low-speed centrifugal compressor impeller
p 4003 N92-32292
Swept shock/boundary layer interaction experiments in support of CFD code validation
[NASA-CR-190583] p 3930 N92-32494
Simple models for turbulent wave-current bottom boundary layer flow
[AD-A247942] p 4007 N92-32630
Interactive control in turbulent shear layers
[AD-A250711] p 4008 N92-32671
Model of Reynolds stress on nonorthogonal grid structures: Application to a staggered tube bundle
[ETN-92-91959] p 4009 N92-32725
Massively separated flow modeling. Experimental study of the fine structure of boundary layers. Study of the influence of external turbulence level
[ETN-92-92088] p 4009 N92-32765
Advances in compressible turbulent mixing
[DE92-014326] p 4010 N92-32824
A new time scale based k-epsilon model for near wall turbulence
[NASA-TM-105768] p 4011 N92-32868
Edge gradient and safety factor effects on electrostatic turbulent transport in tokamaks
[DE92-014323] p 4079 N92-32944
Premixed turbulent combustion to opposed streams
[DE92-016996] p 3964 N92-32996

TURBULENCE EFFECTS
Solid fuel flame spread and mass burning in turbulent flow
[PB92-181049] p 3963 N92-32607
The dependence of the anisoplanatic Strehl of a compensated beam on the beacon distribution
[DE92-011272] p 4016 N92-32736
The effect of the light round-trip time on the performance of an adaptive optics turbulence compensation system
[DE92-011273] p 4075 N92-32738

TURBULENCE MODELS
CFD modeling of turbulent flows around the SSME main injector assembly using porosity formulation
p 3997 N92-32260
CFD applications in pump flows p 4002 N92-32288
An analysis of the flow field in the region of the ASRM field joints p 4005 N92-32305
Simple models for turbulent wave-current bottom boundary layer flow
[AD-A247942] p 4007 N92-32630
Turbulence transport equations for variable-density turbulence and their relationship to two-field models
[DE92-017292] p 4013 N92-33159

TURBULENT BOUNDARY LAYER
Simple models for turbulent wave-current bottom boundary layer flow
[AD-A247942] p 4007 N92-32630
Interactive control in turbulent shear layers
[AD-A250711] p 4008 N92-32671
Massively separated flow modeling. Experimental study of the fine structure of boundary layers. Study of the influence of external turbulence level
[ETN-92-92088] p 4009 N92-32765
A new time scale based k-epsilon model for near wall turbulence
[NASA-TM-105768] p 4011 N92-32868
Acoustic loads prediction on jet aircraft
p 4061 N92-32949

TURBULENT COMBUSTION
Premixed turbulent combustion to opposed streams
[DE92-016996] p 3964 N92-32996

TURBULENT FLOW
CFD modeling of turbulent flows around the SSME main injector assembly using porosity formulation
p 3997 N92-32260
An experimental study of the fluid mechanics associated with porous walls
[AIAA PAPER 92-0769] p 3998 N92-32263
A numerical study of two-dimensional vortex shedding from rectangular cylinders p 3998 N92-32266
Optimum design of ninety degree bends
p 4000 N92-32274
Large eddy simulation of compressible turbulent channel flows p 4000 N92-32276
CFD analysis of pump consortium impeller
p 4002 N92-32287
A basic research model of natural gas combustion in turbulent flow, phase 2
[PB92-190362] p 4007 N92-32598
Solid fuel flame spread and mass burning in turbulent flow
[PB92-181049] p 3963 N92-32607
Numerical simulation of turbulence at the back of the airplane
[ETN-92-91664] p 3931 N92-32769
Forced convection heat transfer in straight tubes. Part 1: Fully developed turbulent flow
[ESDU-92003-PT-1] p 4010 N92-32781
Advances in compressible turbulent mixing
[DE92-014326] p 4010 N92-32824
A new time scale based k-epsilon model for near wall turbulence
[NASA-TM-105768] p 4011 N92-32868
Further wind tunnel investigation of the SM701 airfoil with aileron and turbulators
[NASA-CR-190702] p 3932 N92-33063

TURBULENT MIXING
Advances in compressible turbulent mixing
[DE92-014326] p 4010 N92-32824

TURBULENT WAKES
Annual progress report on imposed 3-D disturbances on bluff-body near wake flows
[AD-A250366] p 4006 N92-32324

TVD SCHEMES
Treating convection in sequential solvers
p 4000 N92-32277
Improved dissipation models for central difference schemes
[FFA-TN-1991-41] p 4057 N92-32729

TWO BODY PROBLEM
Energy take-out from a wave energy device. A theoretical study of the hydrodynamics of a two-body problem consisting of a buoy and a submerged plate
[PB92-178821] p 4025 N92-32608

TWO DIMENSIONAL FLOW
Development of a CFD code for internal flows in liquid fueled engines p 3999 N92-32271
Optimum design of ninety degree bends
p 4000 N92-32274
A comparison of artificial compressibility and fractional step methods for incompressible flow computations
p 4001 N92-32285
NLS clutching bearing cavity flow analysis
p 4003 N92-32295
Numerical simulation of two-dimensional flows by the free-Lagrangian method
[TUM-M9105] p 4009 N92-32767

TWO DIMENSIONAL JETS
Numerical simulation of turbulence at the back of the airplane
[ETN-92-91664] p 3931 N92-32769

TWO DIMENSIONAL MODELS
Two- and three-dimensional simulation code for radiation-hydrodynamics in ICF
[NIFS-119] p 4078 N92-32552
Research on some centered implicit methods for calculating transonic flows by solving Navier-Stokes equations
[ONERA-RSF-24/1408-AY-150A] p 3931 N92-32773

TWO PHASE FLOW
Phase distribution measurements in narrow rectangular channels using image-processing techniques
[DE92-014084] p 4006 N92-32468

Two studies of nonlinear processes in irreversible thermodynamics
[DE92-016855] p 4087 N92-32566
Thermal gravitational modelling and scaling of two-phase heat transport systems for space: An assessment and a comparison of predictions and experimental results
[NLR-TP-91401-U] p 4008 N92-32675
Two-phase heat transport systems for space: Thermal gravitational modelling and scaling predictions versus results of experiments
[NLR-TP-91051-U] p 4010 N92-32786

U

ULTRAHIGH FREQUENCIES
Multifrequency measurements of radar ground clutter at 42 sites. Volume 1: Principal results
[AD-A246710] p 3980 N92-32696
ULTRAHIGH VACUUM
Photogenerated carrier-induced reactions on UHV semiconductor surfaces
[DE92-015355] p 4082 N92-32641
ULTRASONIC RADIATION
Surfaces and thin films studied by picosecond ultrasonics
[DE92-016313] p 4020 N92-32564
ULTRASONIC TESTS
Study of eddy current probes
[NASA-CR-190814] p 4020 N92-32425
Surfaces and thin films studied by picosecond ultrasonics
[DE92-016313] p 4020 N92-32564
A unique method of determining the elastic and engineering constants of unidirectional fibre-reinforced composite plates using ultrasound
[UTIAS-TN-274] p 3955 N92-32829
Pump and valve research at the Oak Ridge National Laboratory
[DE92-014419] p 4019 N92-32890
Radiography to measure the longitudinal density gradients of Pd compacts
[DE92-014383] p 3968 N92-32896
ULTRASONICS
Surfaces and thin films studied by picosecond ultrasonics
[DE92-016313] p 4020 N92-32564
ULTRAVIOLET RADIATION
Titan's UV albedo: Observations and modeling
p 4094 N92-32356
Purification system
[NASA-CASE-MSC-21584-1] p 3965 N92-33029
ULTRAVIOLET SPECTROMETERS
A reanalysis of Voyager UVS observations of Titan
p 4094 N92-32357
UNDERWATER ACOUSTICS
Acoustical emission from bubbles
[AD-A252390] p 4061 N92-32901
ABF algorithms implemented at ARL:UT, FDS system engineering and acoustics
[AD-A252368] p 4046 N92-32917
On the origin and acoustical behaviour of cloud cavitation
[ISBN-90-9004317-9] p 4012 N92-33066
UNDERWATER COMMUNICATION
Feasibility of a 486 nm Fraunhofer laser source based on a 4F(sub 3/2) yields 4I(sub 9/2) neodymium laser
[AD-A250851] p 4015 N92-32329
UNIFIED FIELD THEORY
Theory of elementary particles studies in weak interaction and grand unification and studies in accelerator design
[DE92-014320] p 4066 N92-32597
UNITED STATES
Information resources management plan of the Federal Government
[PB92-147198] p 4089 N92-32643
Climate System Monitoring (CSM) Monthly Bulletin, issue no. 1 p 4034 N92-33073
Science and technology: A report to the Congress
[PB92-183219] p 4104 N92-33086
UNIVERSITIES
A status of the Turbine Technology Team activities
p 3998 N92-32267
United States Air Force summer research program 1991. Volume 1: Program management report
[AD-A248763] p 4103 N92-32338
University of Toronto Institute for Aerospace Studies
[CTN-92-60375] p 4104 N92-32853
UNIVERSITY PROGRAM
Experimental particle physics at the University of Pittsburgh
[DE92-014181] p 4066 N92-32702
UNIX (OPERATING SYSTEM)
Enhancements to the GRIDGEN structured grid generation system for internal and external flow applications p 4005 N92-32301
UNSTEADY AERODYNAMICS
Potential flow theory and operation guide for the panel code PMARC
[NASA-TM-102851] p 3929 N92-32422
NLR investigations of flutter behaviour of fighter aircraft with external stores
[NLR-TP-91134-U] p 3939 N92-32750
Strong coupling between inviscid fluid and boundary layer of sharp leading edges: Two-dimensional stationary and turbulent cases for isolated profiles and guard vanes
[ONERA-RT-44/1621-RY-016-R] p 4010 N92-32776
UNSTEADY FLOW
Computations of unsteady multistage compressor flows in a workstation environment
[NASA-TM-103839] p 3938 N92-32452
The application of unsteady potential flow vortex loop/dipole theory to the work and acoustics of low-speed turbomachinery
[AD-A251160] p 4008 N92-32652
Characterization of flow distribution in axisymmetric shock tubes
[AD-A251095] p 4008 N92-32683
UPLINKING
A 1-W, 30-GHz, CPW amplifier for ACTS small terminal uplink p 3984 N92-32973
UPPER ATMOSPHERE
Polar upper atmosphere characterization and supersonic ion escape (polar wind)
[GDR-0917] p 4031 N92-32889
UPWIND SCHEMES (MATHEMATICS)
Treating convection in sequential solvers
p 4000 N92-32277
Computation of incompressible viscous flows through turbopump components
[NASA-TM-103911] p 4012 N92-33113
URETHANES
Synthesis, morphology and properties of polyester-urethane in solution in styrene: Application to composites development
[ISAL-92-0007] p 3972 N92-32762
USER MANUALS (COMPUTER PROGRAMS)
User's manual for AeroFcn: A FORTRAN program to compute aerodynamic parameters
[NASA-TM-104237] p 4042 N92-32507
PANACEA User's Manual
[DE92-011289] p 4043 N92-32741
EPCRA Section 313 Roadmaps Database: User's manual, version 2.2
[PB92-169523] p 4030 N92-33062
USER REQUIREMENTS
Visionless TRAC
[NASA-CR-190732] p 3942 N92-32477
Life cycle oriented method for development and production of large scale industrial mathematics software
[NLR-TP-91196-U] p 4043 N92-32833

V

V-22 AIRCRAFT
Development of thermoplastic components for structural validation p 3948 N92-32522
V/STOL AIRCRAFT
Collaborative research on V/STOL control system/cockpit display tradeoffs under the NASA/MOD joint aeronautical program
[NASA-TM-103910] p 3939 N92-32788
VACANCIES (CRYSTAL DEFECTS)
Investigation of the oxygen-vacancy (A-center) defect complex profile in neutron irradiated high resistivity silicon junction particle detectors
[DE92-016952] p 4064 N92-32316
PAC spectroscopy of electronic ceramics
[DE92-014328] p 3970 N92-32471
VACUUM
Singularities in the classical Rayleigh-Taylor flow: Formation and subsequent motion
[NASA-CR-189690] p 4010 N92-32784
VACUUM APPARATUS
Vacuum-isolation vessel and method for measurement of thermal noise in microphones
[NASA-CASE-LAR-14567-1-CU] p 3991 N92-33021
VACUUM SYSTEMS
RF cavity vacuum interlock system
[DE92-016961] p 4070 N92-32567
Study of recirculating induction accelerators as drivers for heavy ion fusion
[DE92-016980] p 4071 N92-32904
VALENCE
Collective resonances of valence electrons in free metal clusters
[DE92-014783] p 3969 N92-33116
VALIDITY
Range of validity of distorted wave Born and impulse approximations for (e,2e)
[DE92-624821] p 4087 N92-32649
VALVES
Pump and valve research at the Oak Ridge National Laboratory
[DE92-014419] p 4019 N92-32890
VAN DE GRAAFF ACCELERATORS
The LLNL Multi-User Tandem Laboratory PIXE microprobe
[DE92-017252] p 4014 N92-32999
VAN DER WAALS FORCES
Thinning and rupture of a thin liquid film on a heated surface
[DE92-014813] p 4013 N92-33124
Scanning force microscopy using optical interferometry
[ISBN-90-9003887-6] p 4077 N92-33146
VANADIUM ALLOYS
An in vitro corrosion study of two implant materials using electrochemical impedance spectroscopy and potentiodynamic polarization
[AD-A252575] p 3966 N92-32626
Superplastic forming of Ti6Al4V at lower temperature using hydrogen
[MBB-Z-0403-91-PUB] p 3978 N92-32893
Investigation of fracture toughness and fracture mechanisms using acoustic emission measurements
[DE92-011907] p 4022 N92-32911
VANES
Strong coupling between inviscid fluid and boundary layer of sharp leading edges: Two-dimensional stationary and turbulent cases for isolated profiles and guard vanes
[ONERA-RT-44/1621-RY-016-R] p 4010 N92-32776
Investigation of the flight control requirements of a half-scale ducted fan unmanned aerial vehicle
[AD-A252730] p 3940 N92-32988
VAPOR DEPOSITION
Thin film cadmium telluride, zinc telluride, and mercury zinc telluride solar cells
[DE92-001237] p 4024 N92-32510
Kinetics and characterization of CVD-grown BP
[ETN-92-92024] p 3973 N92-33065
Method of growing diamond film on substrates
[AD-D015313] p 3973 N92-33170
Coatings for improved corrosion resistance
[DE92-016779] p 3974 N92-33247
VAPOR PHASES
New applications of ionization and fluorescence techniques for detecting and characterization of open-shell organometallics in the gas phase
[AD-A250923] p 3961 N92-32509
Phase distributions of airborne polycyclic aromatic hydrocarbons in two US cities
[PB92-164979] p 4028 N92-32543
Novel gas phase ion molecule reactions of C60(++) with O2 and NH3
[AD-A250921] p 4066 N92-32556
VAPOR PRESSURE
Orthobaric densities and molar volumes of liquids: Halogenated ethanes
[ESDU-92009] p 3945 N92-32486
A research program on radiative transfer model development in support of the ARM program
[DE92-014495] p 4031 N92-33153
VARIATIONAL PRINCIPLES
Efficient finite element modeling of laminated composite plates based on higher-order theory
p 3949 N92-32529
VARIATIONS
Density variations and anomalies in palladium compacts
[DE92-014382] p 3967 N92-32721
VECTOR ANALYSIS
Comparison between the PISO algorithm and preconditioning methods for compressible flow
p 4001 N92-32284
VECTOR MESONS
Theoretical nuclear physics
[DE92-016837] p 4069 N92-33186
VEGETATION
STAMP, the SWOE Thermal Analysis and Measurement Program: Summary of the 1990 field tests
[LTR-91-013] p 4029 N92-32860
VELOCITY DISTRIBUTION
Influence of an intense acoustic field on boundary layer separation
[ETN-92-92081] p 4009 N92-32687

Orbital debris characterization with impact flash signatures
[DE92-010666] p 4018 N92-32701

VELOCITY ERRORS
A Kalman filter integrated navigation design for the IAR Twin Otter Atmospheric Research Aircraft
[NRC-32148] p 3934 N92-32849

VELOCITY MEASUREMENT
Interactive control in turbulent shear layers
[AD-A250711] p 4008 N92-32671
Influence of an intense acoustic field on boundary layer separation
[ETN-92-92081] p 4009 N92-32687

VENTILATION
Demand controlled ventilating systems: Sensor market survey. Energy conservation in buildings and community systems programme, annex 18, December 1991
[PB92-180892] p 3977 N92-32825

VENTING
Lift and rolling moment due to spoilers on wings with trailing-edge flaps deflected at subsonic speeds
[ESDU-92002-SUPPL] p 3931 N92-32782

VERTICAL FLIGHT
Investigation of the flight control requirements of a half-scale ducted fan unmanned aerial vehicle
[AD-A252730] p 3940 N92-32988

VERY HIGH FREQUENCIES
Multifrequency measurements of radar ground clutter at 42 sites. Volume 1: Principal results
[AD-A246710] p 3980 N92-32696
Analog CMOS filters for very-high frequencies
[ISBN-90-9004420-5] p 3986 N92-33143
Characteristics of large aspect angle VHF radar echoes in the presence and absence of optical aurora
[ISBN-0-315-59091-2] p 4032 N92-33197

VERY LARGE SCALE INTEGRATION
Pulse coded biologically motivated neural-type MOS circuits
[AD-A250367] p 3988 N92-32325
VLSI architecture for a Reed-Solomon decoder
[NASA-CASE-NPO-17897-1-CU] p 3991 N92-33011

VERY LOW FREQUENCIES
Transmitter location system for frequencies below HF
[AD-D015325] p 3986 N92-33172
Feasibility of measuring transverse electric noise at VLF and LF on an ice cap
[AD-A252280] p 4035 N92-33220

VHSIC (CIRCUITS)
Analysis of a benchmark suite to evaluate mixed numeric and symbolic processing
[NASA-TM-103907] p 4052 N92-32886
Advanced information processing system: The Army fault tolerant architecture conceptual study. Volume 2: Army fault tolerant architecture design and analysis
[NASA-CR-189632-VOL-2] p 4052 N92-33101

VIBRATION
System response to relay chatter
[DE92-013076] p 3988 N92-32495
Influence of compliance on performance of robotic drilling
[OUEL-1917/92] p 4018 N92-32757

VIBRATION DAMPING
The multiple-function multi-input/multi-output digital controller system for the AFW wind-tunnel model
[NASA-TM-107600] p 3934 N92-32536
Noncircular rolling joints for vibrational reduction in slewing maneuvers
[NASA-CASE-LAR-14515-1-CU] p 4019 N92-33031
Computational aspects of helicopter trim analysis and damping levels from Floquet theory
[NASA-CR-190736] p 3940 N92-33107

VIBRATION ISOLATORS
MD-80 aft cabin noise control: A case history
p 4061 N92-32950
The Dornier 328 Acoustic Test Cell (ATC) for interior noise tests and selected test results
[AIAA PAPER 92-2164] p 4062 N92-32951
Active control of interior noise in a large scale cylinder using piezoelectric actuators p 4063 N92-32958
Sound transmission reduction with intelligent panel systems p 4063 N92-32959
Active vibrations and noise control for turboprop application research program activities
p 4063 N92-32962
Vacuum-isolation vessel and method for measurement of thermal noise in microphones
[NASA-CASE-LAR-14567-1-CU] p 3991 N92-33021

VIBRATION MEASUREMENT
The Dornier 328 Acoustic Test Cell (ATC) for interior noise tests and selected test results
[AIAA PAPER 92-2164] p 4062 N92-32951
Vibro-acoustic FE analyses of the Saab 2000 aircraft
p 4062 N92-32952
Advanced Study for Active Noise Control in Aircraft (ASANCA)
[AIAA PAPER 92-2092] p 4062 N92-32956
Active control of sound transmission through stiff lightweight composite fuselage constructions
p 4062 N92-32957

VIBRATION TESTS
Lithium sulphur dioxide battery failure following high frequency vibration
[CRAD-1-90] p 3990 N92-32812

VIDEO DATA
Target detection using co-occurrence matrix segmentation and its hardware implementation
p 3936 N92-32443
Target Cueing And Tracking System (TCATS): User's guide
[DE92-015385] p 4042 N92-32617
Semiannual status report
[NASA-CR-190239] p 4046 N92-33092
Fuzzy set methods for object recognition in space applications
[NASA-CR-190388] p 4047 N92-33093

VIDEO EQUIPMENT
Visionless TRAC
[NASA-CR-190732] p 3942 N92-32477

VIDEO SIGNALS
Optical modulation characteristics and applications of liquid crystal televisions
[AD-A252466] p 3979 N92-32633

VINYL POLYMERS
Rotational barriers in model compounds of poly (vinyl chloride): 2-chlorobutane and 1,3,5,7,9,11-hexachlorododecane
[AD-A250855] p 3960 N92-32330

VINYL RADICAL
Rotational barriers in model compounds of poly (vinyl chloride): 2-chlorobutane and 1,3,5,7,9,11-hexachlorododecane
[AD-A250855] p 3960 N92-32330
Shock tube ignition of ethanol, isobutene and MTBE: Experiments and modeling
[DE92-008563] p 3961 N92-32544

VISCOSITY
Effect of including variable gas properties and entrained particles in the flow analysis of the ASRM nozzle
p 4006 N92-32306
Forced convection heat transfer in straight tubes. Part 1: Fully developed turbulent flow
[ESDU-92003-PT-1] p 4010 N92-32781

VISCOUS FLOW
Numerical simulation of turbomachinery flows with advanced turbulence models p 3999 N92-32270
A multi-domain method for subsonic viscous flows
p 3960 N92-32275
Computation of the flow field in a centrifugal impeller with splitter blades p 4002 N92-32289
Computation of incompressible viscous flows through turbopump components
[NASA-TM-103911] p 4012 N92-33113

VISIBILITY
Visibility properties of polygons
[ISBN-0-315-57272-8] p 4049 N92-33229

VISUAL FLIGHT RULES
Federal aviation regulations. Part 91: General operating and flight rules
[PB92-197334] p 3929 N92-33176

VISUAL OBSERVATION
Vision-based range estimation using helicopter flight data
[NASA-TM-103930] p 3933 N92-32424

VITERBI DECODERS
The architecture development and design considerations of a high-speed, single chip, CMOS convolutional decoder based on a modification of the Viterbi algorithm
[ISBN-0-315-60456-5] p 3993 N92-33208

VOICE COMMUNICATION
The MSAT spacecraft of Telesat Mobile, Inc.
[CTN-92-60346] p 3981 N92-32789

VOIDS
A boundary integral method for an inverse problem in thermal imaging
[NASA-CR-189693] p 4059 N92-33006
On the origin and acoustical behaviour of cloud cavitation
[ISBN-90-9004317-9] p 4012 N92-33066

VOLT-AMPERE CHARACTERISTICS
A simple high-performance avalanche photodiode for long-wavelength optical communications, phase 1
[PB92-188259] p 4076 N92-33004
On the resistive transition of composite superconductors
[ISBN-90-9003899-X] p 3992 N92-33145

VOLTAGE CONTROLLED OSCILLATORS
Continuation of the development of a millimeter wave wideband tunable waveguide voltage controlled oscillator
[CAL-504-88P120] p 3990 N92-32847

VOLTAGE CONVERTERS (DC TO DC)
A discrete nonlinear model approach to study the behavior of large signal DC to DC converters
[LAAS-90028] p 3989 N92-32777
A continuous nonlinear model approach to study the behavior of large signal DC to DC converters
[LAAS-90027] p 3990 N92-32793

VORTEX BREAKDOWN
Breakdown of the Karman vortex street due to forced convection and flow compressibility
[NASA-TM-105853] p 4007 N92-32472
Modeling and numerical simulation of vortex flow in aerodynamics
[NLR-TP-91154-U] p 3930 N92-32673

VORTEX GENERATORS
Experimental study of the vortex system generated by a missile fuselage at incidence. Part 3: Three directional laser velocimetry measurements
[ONERA-RT-47/1147-AY-146A-P] p 3931 N92-32800

VORTEX SHEDDING
A numerical study of two-dimensional vortex shedding from rectangular cylinders p 3998 N92-32266
Annual progress report on imposed 3-D disturbances on bluff-body near wake flows
[AD-A250366] p 4006 N92-32324
Breakdown of the Karman vortex street due to forced convection and flow compressibility
[NASA-TM-105853] p 4007 N92-32472

VORTEX SHEETS
Vortex flow visualization using colored and fluorescent dyes on flat plate delta wing with leading edge extension
[AD-A251139] p 3930 N92-32651
Further development of the CANAERO computer code to include propulsor modelling
[DREA-CR-90-425] p 3931 N92-32811

VORTICES
Large eddy simulation of compressible turbulent channel flows p 4000 N92-32276
Breakdown of the Karman vortex street due to forced convection and flow compressibility
[NASA-TM-105853] p 4007 N92-32472
Axial vortices in gaseous-fired burner flow fields
[PB92-190370] p 3962 N92-32594
Vortex flow visualization using colored and fluorescent dyes on flat plate delta wing with leading edge extension
[AD-A251139] p 3930 N92-32651
The application of unsteady potential flow vortex loop/dipole theory to the work and acoustics of low-speed turbomachinery
[AD-A251160] p 4008 N92-32652
Modeling and numerical simulation of vortex flow in aerodynamics
[NLR-TP-91154-U] p 3930 N92-32673
Pressure field developed by the random movement of the vortices near a wall
[ETN-92-91665] p 4009 N92-32770
Geometrical effects in two-dimensional arrays of Josephson junctions
[AD-A252209] p 4084 N92-32898
Thickness dependence of vortex pinning in epitaxial Tl-Ca-Ba-Cu-O thin films
[DE92-015011] p 4084 N92-32920

VORTICITY
A basic research model of natural gas combustion in turbulent flow, phase 2
[PB92-190362] p 4007 N92-32598

VOYAGER PROJECT
A reanalysis of Voyager UVS observations of Titan
p 4094 N92-32357

W

WALKING MACHINES
Rational behavior model: A tri-level multiple paradigm architecture for robot vehicle control software
[AD-A250370] p 4053 N92-32748

WALL FLOW
Integration of wall interference assessment and wall adaptation
[NLR-TP-91119-U] p 3940 N92-32734
Pressure field developed by the random movement of the vortices near a wall
[ETN-92-91665] p 4009 N92-32770
Experimental study of the vortex system generated by a missile fuselage at incidence. Part 3: Three directional laser velocimetry measurements
[ONERA-RT-47/1147-AY-146A-P] p 3931 N92-32800
A new time scale based k-epsilon model for near wall turbulence
[NASA-TM-105768] p 4011 N92-32868

WALL TEMPERATURE
Breakdown of the Karman vortex street due to forced convection and flow compressibility
[NASA-TM-105853] p 4007 N92-32472

WAR GAMES
An intelligent gaming environment
[ISBN-90-6275-635-2] p 4060 N92-33055
WARFARE
Briefing notes on a manned aircraft research and support simulation facility
[AD-A250373] p 3935 N92-32326
WARHEADS
The United States Air Force explosives hazards reduction program p 3976 N92-33241
WARNING SYSTEMS
Automatic detection, pursuit, and classification in infrared imagery p 3937 N92-32445
Safety study of TCAS 2 for logic version 6.04
[DOT/FAA/RD-92/22] p 3933 N92-32537
Simulation test and evaluation of TCAS 2 logic version 6.04
[DOT/FAA/RD-92/23] p 3934 N92-33098
WASTE DISPOSAL
Electrochemical polarization measurements on pitting corrosion susceptibility of nickel-rich Alloy 825
[DE92-014885] p 3969 N92-33132
WASTE TREATMENT
International technology transfer to support the environmental restoration needs of the DOE complex
[DE92-013663] p 4028 N92-32558
WATER
Heat and mass exchange during condensation of a water-ammonia mixture
[DE92-014524] p 3962 N92-32557
Hot water storage tank for solar collectors
[AD-D015301] p 4026 N92-32943
Purification system
[NASA-CASE-MSC-21584-1] p 3965 N92-33029
A study of the dissolution mechanism by chemical and electrochemical oxidation-reduction of actinide dioxides (UO2, NpO2, PuO2, and AmO2) in an acid aqueous medium
[DE92-014834] p 3965 N92-33126
WATER CURRENTS
Simple models for turbulent wave-current bottom boundary layer flow
[AD-A247942] p 4007 N92-32630
WATER FLOW
Phase distribution measurements in narrow rectangular channels using image-processing techniques
[DE92-014084] p 4006 N92-32468
WATER MODERATED REACTORS
Life testing of a low voltage air circuit breaker
[DE92-014173] p 3988 N92-32635
WATER POLLUTION
Federal plan for ocean pollution research, development, and monitoring, fiscal years 1992-1996
[PB92-185164] p 4029 N92-32708
WATER QUALITY
High-temperature Solid Oxide Fuel Cell (SOFC) generator development project: Environmental assessment
[DE92-014698] p 4026 N92-32924
Guide to selected national environmental statistics in the US Government
[PB92-201144] p 4030 N92-33087
WATER RECLAMATION
Development of static system procedures to study aquatic biofilms and their responses to disinfection and invading species
[NASA-TM-103598] p 4036 N92-33103
WATER RESOURCES
Guide to selected national environmental statistics in the US Government
[PB92-201144] p 4030 N92-33087
WATER TREATMENT
Purification system
[NASA-CASE-MSC-21584-1] p 3965 N92-33029
Summary of engineering-scale experiments for the Solar Detoxification of Water project
[DE92-013776] p 4027 N92-33150
WATER TUNNEL TESTS
Vortex flow visualization using colored and fluorescent dyes on flat plate delta wing with leading edge extension
[AD-A251139] p 3930 N92-32651
WATER VAPOR
ARM Tropical Pacific Experiment (ATPEX): Role of cloud, water vapor and convection feedbacks in the coupled ocean/atmosphere system
[DE92-013772] p 4032 N92-32331
Environmental fatigue in aluminum-lithium alloys
[NASA-TM-107640] p 4021 N92-32423
A research program on radiative transfer model development in support of the ARM program
[DE92-014495] p 4031 N92-33153
WATER WAVES
Energy take-out from a wave energy device. A theoretical study of the hydrodynamics of a two-body problem consisting of a buoy and a submerged plate
[PB92-178821] p 4025 N92-32608
Parameterization of directional spectra, part 2. Volume 2: User's manual for the programs RMODEL, FITHM, and FITDM
[DREA-CR-89-445-PT-2-VOL-2] p 3981 N92-32749
Acoustical emission from bubbles
[AD-A252390] p 4061 N92-32901
WAVE DRAG
A method for designing blended wing-body configurations for low wave drag
[NASA-TP-3261] p 3929 N92-32480
WAVE FUNCTIONS
Two perspectives on a decohering spin
[DE92-013021] p 4087 N92-32496
Pseudopotential band calculations along a high-symmetry axis. Part 1: Central potential and the (111) direction
[AD-A252399] p 4084 N92-32938
WAVE GENERATION
Waves on Titan p 4100 N92-32394
WAVE INTERACTION
Simple models for turbulent wave-current bottom boundary layer flow
[AD-A247942] p 4007 N92-32630
Can the speed of light in the fiber be controlled?
[AD-A247614] p 4074 N92-32668
WAVE PACKETS
Quantum wave modeling on highly parallel distributed memory machines
[DE92-014507] p 4088 N92-33109
WAVE PROPAGATION
The significance of meteoric ionisation for the propagation of lightning spherics in the atmosphere of Titan p 4096 N92-32365
Wave propagation in laterally varying media: A model expansion method
[AD-A247553] p 4031 N92-32572
The dependence of the anisoplanatic Strehl of a compensated beam on the beacon distribution
[DE92-011272] p 4016 N92-32736
The effect of the light round-trip time on the performance of an adaptive optics turbulence compensation system
[DE92-011273] p 4075 N92-32738
Conceptual design of an electron cyclotron wave system for NET/ITER
[IPF-91-6] p 4071 N92-32808
Burning oil fields as a source of infrasonic waves
[IRF-PREPRINT-119] p 4061 N92-32842
WAVEFORMS
An implementation of a fault-tolerant, multidirectional, digital interpolation beamformer
[AD-A252494] p 3986 N92-33152
WAVEGUIDE ANTENNAS
Analysis of shielded CPW discontinuities with air-bridges p 3983 N92-32971
Numerical analysis of scattering from certain conducting and dielectric bodies of arbitrary shape
[ISBN-0-315-63282-8] p 3987 N92-33192
WAVEGUIDES
A high-power SLED 2 pulse compression system
[DE92-011586] p 4071 N92-32751
Coplanar waveguide feeds for phased array antennas p 3983 N92-32970
Analysis of shielded CPW discontinuities with air-bridges p 3983 N92-32971
A flexible CPW package for a 30 GHz MMIC amplifier p 3983 N92-32972
A 1-W, 30-GHz, CPW amplifier for ACTS small terminal uplink p 3984 N92-32973
WAVELENGTH DIVISION MULTIPLEXING
Wavelength division multiplexed local area networks
[AD-A247613] p 3979 N92-32573
WEAK INTERACTIONS (FIELD THEORY)
Possible effects of additional vector bosons in e(sup +)e(sup -)(yields)f(bar-f) at the TRISTAN energies
[DE92-624727] p 4065 N92-32498
Theory of elementary particles studies in weak interaction and grand unification and studies in accelerator design
[DE92-014320] p 4066 N92-32597
WEAPON SYSTEMS
Operational needs for an unmanned air vehicle p 3936 N92-32438
Multisensor airborne target acquisition systems and their integration p 3936 N92-32439
WEAPONS
China's aerospace industry: Technology, funding, and modernization
[AD-A252618] p 3929 N92-32691
WEAPONS DEVELOPMENT
STAMP, the SWOE Thermal Analysis and Measurement Program: Summary of the 1990 field tests
[LTR-91-013] p 4029 N92-32860
WEAR
Influence of compliance on performance of robotic drilling
[OUEL-1917/92] p 4018 N92-32757
Implanted aluminum: Tribological behavior and mechanical properties of the superficial layers
[ECL-91-28] p 4019 N92-32801
WEAR RESISTANCE
Laser coating of composites for enhanced wear and corrosion resistance
[AD-A249231] p 3956 N92-32906
WEAR TESTS
SSME HPOTP impeller backcavity CFD analysis p 4003 N92-32294
Influence of oil lubricant additives on tribological behavior of engineering ceramics
[PB92-180710] p 3973 N92-33059
WEATHER
Recent changes of weather patterns in North America
[DE92-014342] p 4033 N92-32720
WEATHER FORECASTING
Diagnostic report of the National Hurricane Center, August and September 1991, volume 4, number 2
[PB92-179407] p 4033 N92-32503
Severe local storm warning verification: 1991
[PB92-185982] p 4033 N92-32545
Exploitation of parallelism in climate models
[DE92-012595] p 4028 N92-32619
A simple Doppler wind lidar sensor: Simulated measurements and impacts in a global assimilation and forecast system
[PL-TR-91-2253] p 4034 N92-32859
Forecasting heavy snow events in Missoula, Montana
[PB92-196104] p 4034 N92-33163
WEIGHT REDUCTION
Applications of composites to armaments p 3947 N92-32516
The weight optimization of an armored crashworthy crewseat through the use of advanced composites and design p 3947 N92-32517
Structural assessment of ultralightweight composites p 3948 N92-32525
Aspects of compression in aerospace composites: Future requirements p 3956 N92-33036
Diffractive optics technology and the NASA Geostationary Earth Observatory (GEO)
[NASA-CR-190611] p 4076 N92-33074
WELDABILITY
Weldability of Fe3Al based iron aluminide alloys
[DE92-017802] p 4020 N92-33085
WELDED JOINTS
Life testing of a low voltage air circuit breaker
[DE92-014173] p 3988 N92-32635
Guide to the effect of shot peening on fatigue strength
[ESDU-92015] p 3967 N92-32779
WELDING
JPRS report: Science and technology. Central Eurasia: Materials science
[JPRS-UMS-92-011] p 3969 N92-33129
WHEATSTONE BRIDGES
Stochastic models in reliability
[AD-A250934] p 4020 N92-33151
WHIP ANTENNAS
Transmitter location system for frequencies below HF
[AD-D015325] p 3986 N92-33172
WHITE NOISE
The local structure of image intensity discontinuities
[ISBN-0-315-57231-0] p 4048 N92-33204
WIGGLER MAGNETS
Optics of beam transport in the NSLS UV-FEL
[DE92-014166] p 4015 N92-32511
Polarized wiggler for NSLS x ray ring design considerations
[DE92-012212] p 4071 N92-32912
WIND (METEOROLOGY)
The meteorology of Titan p 4095 N92-32360
A preliminary assessment of the Titan planetary boundary layer p 4095 N92-32363
Wind tunnel test of Teledyne Geotech model 1564B cup anemometer
[DE92-009590] p 4013 N92-32460
WIND MEASUREMENT
A simple Doppler wind lidar sensor: Simulated measurements and impacts in a global assimilation and forecast system
[PL-TR-91-2253] p 4034 N92-32859
WIND SHEAR
Airport Surveillance Radar (ASR-9) wind shear processor: 1991 test at Orlando, Florida
[AD-A252246] p 3980 N92-32686
WIND TUNNEL MODELS
The multiple-function multi-input/multi-output digital controller system for the AFW wind-tunnel model
[NASA-TM-107600] p 3934 N92-32536
WIND TUNNEL TESTS
Wind tunnel test of Teledyne Geotech model 1564B cup anemometer
[DE92-009590] p 4013 N92-32460

The multiple-function multi-input/multi-output digital controller system for the AFW wind-tunnel model
[NASA-TM-107600] p 3934 N92-32536

Integration of wall interference assessment and wall adaptation
[NLR-TP-91119-U] p 3940 N92-32734

Massively separated flow modeling. Experimental study of the fine structure of boundary layers. Study of the influence of external turbulence level
[ETN-92-92088] p 4009 N92-32765

Experimental study of the vortex system generated by a missile fuselage at incidence. Part 3: Three directional laser velocimetry measurements
[ONERA-RT-47/1147-AY-146A-P] p 3931 N92-32800

Further wind tunnel investigation of the SM701 airfoil with aileron and turbulators
[NASA-CR-190702] p 3932 N92-33063

WIND TUNNELS
Further wind tunnel investigation of the SM701 airfoil with aileron and turbulators
[NASA-CR-190702] p 3932 N92-33063

WIND VELOCITY
Waves on Titan p 4100 N92-32394

WINDPOWER UTILIZATION
NEMO: Advanced energy systems and technologies
[DE92-540920] p 4027 N92-33072

The 1991 Japan Solar Energy Society. Japan Wind Energy Association Joint Conference
[DE92-530733] p 4027 N92-33090

WING PANELS
Global/local interlaminar stress analysis of a grid-stiffened composite panel
[NASA-CR-190822] p 4023 N92-33139

WING PLANFORMS
Lift and rolling moment due to spoilers on wings with trailing-edge flaps deflected at subsonic speeds
[ESDU-92002-SUPPL] p 3931 N92-32782

WINGS
Aerodynamic centre of wing-body combinations
[ESDU-92024] p 3929 N92-32479

Design, evaluation and experimental effort toward development of a high strain composite wing for Navy aircraft p 3947 N92-32514

Development of composite wing carrythrough bulkheads for fighter aircraft p 3948 N92-32519

Out of plane analysis for composite structures p 3949 N92-32527

Damage tolerance certification methodology for composite structures p 3951 N92-32579

Lift and rolling moment due to spoilers on wings with trailing-edge flaps deflected at subsonic speeds
[ESDU-92002-SUPPL] p 3931 N92-32782

WIRE
Processing and properties of silver-clad Tl-Ba-Ca-Cu-O wires and tapes
[DE92-015266] p 4081 N92-32346

Device for removing foreign objects from anatomic organs
[NASA-CASE-GSC-13306-1] p 4038 N92-33032

Silver coated superconducting ceramic powder
[AD-D015294] p 3973 N92-33157

WORK HARDENING
Studies of near-surface phenomena and erosion mechanisms in metallic alloys using single- and multi-particle impacts
[DE92-014921] p 3966 N92-32432

WORKING FLUIDS
Environmental consequences of new energy technology. Solar heating, heat stores, and heat pumps
[PB92-180843] p 4025 N92-32605

An analytical screening of alternatives for R-502 in low-temperature refrigerating applications
[DE92-017162] p 3978 N92-32927

WORKLOADS (PSYCHOPHYSIOLOGY)
Instrument scanning and subjective workload with the peripheral vision horizon display
[CTN-92-60359] p 4038 N92-32817

WORKSTATIONS
Computations of unsteady multistage compressor flows in a workstation environment
[NASA-TM-103839] p 3938 N92-32452

Ethernet bandwidth utilization of datafull, dataless, and diskless node workstation and x-terminals
[AD-A252374] p 4052 N92-32937

Contribution to robot-task adaptation, introduction and use of robot anisotropy and task object for the design of the workstation
[ISAL-91-0095] p 4039 N92-33056

X

X RAY ABSORPTION
Local environment around the oxygen atoms in Y-Ba-Cu-O studied X ray Absorption Fine Structure (XAFS) spectroscopy
[DE92-014165] p 4081 N92-32470

X RAY ANALYSIS
The LLNL Multi-User Tandem Laboratory PIXE microprobe
[DE92-017252] p 4014 N92-32999

X RAY ASTROPHYSICS FACILITY
Volume 1. Preliminary design study: AXAF x ray calibration spectrometers. Volume 2. Revised preliminary design study: AXAF x ray calibration spectrometers
[NASA-CR-184340] p 4092 N92-33094

X RAY DIFFRACTION
Preparation and characterization of superlattices
[DE92-012572] p 4081 N92-32462

Formation of high temperature superconductors from the solidified melt
[DE92-012584] p 4081 N92-32465

Probing thin-film YBa2Cu3O(7-delta) superconductors by second harmonic generation using femtosecond laser pulses
[AD-A252350] p 4082 N92-32512

Proceedings of the fourth users meeting for the advanced photon source
[DE92-014061] p 4072 N92-32932

Characterization of sintered reaction-bonded silicon nitride processed by microwave heating
[DE92-014408] p 3956 N92-32945

Gamma scattering in condensed matter with high intensity Moessbauer radiation
[DE92-014811] p 4085 N92-33025

X RAY INSPECTION
Detection of honeycomb damage using hexagonal grid discontinuities
[DREP-89-9] p 3955 N92-32846

X RAY LASERS
Probing thin-film YBa2Cu3O(7-delta) superconductors by second harmonic generation using femtosecond laser pulses
[AD-A252350] p 4082 N92-32512

X RAY SOURCES
Polarized wiggler for NSLS x ray ring design considerations
[DE92-012212] p 4071 N92-32912

Kinematics of Compton backscattering x ray source for angiography
[DE92-014016] p 4073 N92-33179

X RAY SPECTRA
Photon excitation for satellite free x ray spectroscopy: Instrumentation challenges
[DE92-016999] p 4067 N92-32997

X RAY SPECTROSCOPY
Probing thin-film YBa2Cu3O(7-delta) superconductors by second harmonic generation using femtosecond laser pulses
[AD-A252350] p 4082 N92-32512

Photon excitation for satellite free x ray spectroscopy: Instrumentation challenges
[DE92-016999] p 4067 N92-32997

Studies of Y-Ba-Cu-O single crystals by x ray absorption spectroscopy
[DE92-014687] p 4086 N92-33136

X RAY TELESCOPES
Multispectral variable magnification glancing incidence x ray telescope
[NASA-CASE-MFS-28013-4] p 4092 N92-33012

X RAYS
Thermal and structural analysis of high precision beamline position monitors for synchrotron x ray beams
[DE92-014863] p 4072 N92-33130

Y

YAW
Contribution of tailplane-mounted twin fins to sideforce, yawing moment, and rolling moment derivatives due to sideslip
[ESDU-92007] p 3939 N92-32487

YAWING MOMENTS
Contribution of tailplane-mounted twin fins to sideforce, yawing moment, and rolling moment derivatives due to sideslip
[ESDU-92007] p 3939 N92-32487

YTTRIUM ALLOYS
Synthesis of MoSi2-based alloys by mechanical alloying
[DE92-017528] p 3969 N92-33120

YTTRIUM OXIDES
Formation of high temperature superconductors from the solidified melt
[DE92-012584] p 4081 N92-32465

T (sub c)-delta relations in YBa2Cu3O(7-delta) thin films: Effects of oxygen pressure during growth
[DE92-014432] p 4083 N92-32653

Substrate reactions and flux pinning structures in melt-processed YBa2Cu3O7 deposits on Ag-Pd alloy substrates
[DE92-014404] p 4084 N92-32919

Studies of Y-Ba-Cu-O single crystals by x ray absorption spectroscopy
[DE92-014687] p 4086 N92-33136

Z

ZEOLITES
Surface reconstruction and templating for zeolite thin film synthesis observed by atomic force microscopy
[AD-A251140] p 4066 N92-32548

ZINC COMPOUNDS
Thermochemical cycles for energy storage: Thermal decomposition of ZnSO4 systems
[DE91-002144] p 4026 N92-32909

ZINC TELLURIDES
Thin film cadmium telluride, zinc telluride, and mercury zinc telluride solar cells
[DE92-001237] p 4024 N92-32510

ZIRCONIUM
Synthesis of MoSi2-based alloys by mechanical alloying
[DE92-017528] p 3969 N92-33120

ZIRCONIUM ALLOYS
Synthesis, microstructure, and mechanical properties of zirconia-alumina composites
[ISBN-90-9004656-9] p 3954 N92-32677

ZIRCONIUM OXIDES
Clean gasoline reforming with superacid catalysts
[DE92-013833] p 3975 N92-33123

PERSONAL AUTHOR INDEX

Typical Personal Author Index Listing

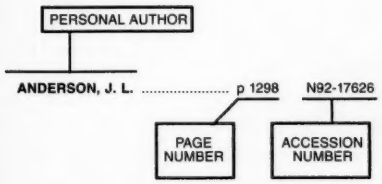

Listings in this index are arranged alphabetically by personal author. The page number helps you locate the citation in the abstract section. The accession number denotes the number by which the citation is identified.

A

AALFS, DAVID D. ..... p 3932 N92-32606
AARONSON, H. I. ..... p 3967 N92-32699
ABRAHAMSON, JAMES A. ..... p 4039 N92-33099
ACHAR, N. S. ..... p 3940 N92-33107
ACHARD, V. ..... p 3943 N92-32728
ACKERMAN, M. ..... p 3943 N92-32728
ADAMS, D. L. ..... p 4064 N92-32311
p 4065 N92-32497
ADAMS, M. L. ..... p 4057 N92-32743
ADDIS, R. P. ..... p 4013 N92-32460
ADVANI, S. ..... p 3934 N92-32845
AFTOSMIS, MICHAEL ..... p 4008 N92-32632
AGASSI, D. Y. ..... p 4084 N92-32938
AGGARWAL, S. ..... p 3988 N92-32635
AGRAWAL, GOPAL ..... p 4042 N92-32656
AHLBRANDT, T. S. ..... p 4034 N92-32333
AHMAD, I. ..... p 4082 N92-32542
AHRENS, T. J. ..... p 4014 N92-32620
AKCHURIN, N. ..... p 4064 N92-32311
p 4065 N92-32497
ALBRECHT, A. ..... p 4087 N92-32496
ALESI, A. L. ..... p 3947 N92-32515
ALEXANDER, D. ..... p 3976 N92-33243
ALEXANDER, K. B. ..... p 4084 N92-32919
ALGER, L. S. ..... p 4052 N92-33100
p 4052 N92-33101
ALHAMANY, ABDELILAH ..... p 4083 N92-32892
ALHASSID, Y. ..... p 4067 N92-32921
ALICI, GUERSEL ..... p 4018 N92-32757
ALKULA, RIITTA ..... p 4090 N92-32843
ALLEN, M. R. ..... p 3950 N92-32578
ALLEN, ROLAND E. ..... p 4084 N92-32940
ALLISON, MICHAEL ..... p 4095 N92-32363
ALTEROVITZ, S. A. ..... p 3984 N92-32975
ALTEROVITZ, SAMUEL A. ..... p 3984 N92-32976
p 3984 N92-32977
p 3984 N92-32978
p 3985 N92-32984
AMINPOUR, MOHAMMAD A. ..... p 4023 N92-33104
ANDERSON, DANA Z. ..... p 3953 N92-32674
ANDERSON, P. G. ..... p 3995 N92-32253
ANDERSON, W. ..... p 3998 N92-32264
ANDREW, PHILIP L. ..... p 3967 N92-32794
ANDRIANANTOANDRO, A. ..... p 4009 N92-32687
ANG, J. A. ..... p 4018 N92-32701
ANGULO, EARL D. ..... p 4038 N92-33032
ANKARA, A. ..... p 3959 N92-33052
ANQUEZ, L. ..... p 3957 N92-33043
ANTAKI, G. A. ..... p 3988 N92-32495
ANTHONY, R. W. ..... p 4033 N92-32502
ANTOLAK, A. J. ..... p 4014 N92-32999
ANTONSEN, T. M., JR. ..... p 4078 N92-32592
ANTRAZI, SAMI S. ..... p 4019 N92-32885
AOKI, R. ..... p 3957 N92-33042
APPELBAUM, J. ..... p 3988 N92-32243
ARCHAMBEAU, CHARLES B. ..... p 4031 N92-32572
ARDISSONE, J. P. ..... p 4009 N92-32687
ARIE, E. ..... p 4099 N92-32389
ARMANTE, R. ..... p 3943 N92-32728
AROCHO, A. ..... p 3949 N92-32530
ARON, PAUL R. ..... p 3985 N92-32980
ASCOLI, E. P. ..... p 4000 N92-32273
ASHBY, DALE L. ..... p 3929 N92-32422
ASKINS, JO ANNE ..... p 3976 N92-33242
ASSADI, S. ..... p 4080 N92-33154
ATKINS, JOHN ..... p 4091 N92-33178
AUBORN, JOHN ERIC ..... p 3936 N92-32440
p 3936 N92-32441
p 3936 N92-32443
AUGUST, ROBERT A., JR. ..... p 4073 N92-33167
AVERY, JOHN G. ..... p 3948 N92-32522
p 3950 N92-32578
AVERY, S. ..... p 3950 N92-32578
AVIS, ELIZABETH L. ..... p 4041 N92-33205
AVVA, RAM ..... p 4004 N92-32296

B

BABIKYAN, C. A. ..... p 4052 N92-33100
p 4052 N92-33101
BACA, THOMAS ..... p 4029 N92-32731
BACHE, GEORGE ..... p 3945 N92-32262
p 4002 N92-32290
BACK, D. ..... p 3967 N92-32721
BACK, D. D. ..... p 3968 N92-32896
BADOZ, J. ..... p 4099 N92-32390
p 4102 N92-32409
BAECHLER, M. C. ..... p 4030 N92-33156
BAER, F. ..... p 4028 N92-32619
BAER, T. ..... p 4068 N92-33083
BAHIR, GAD ..... p 3985 N92-32979
BAILEY, BILL ..... p 4091 N92-33178
BAILEY, J. E. ..... p 4080 N92-32992
BAINES, KEVIN H. ..... p 4097 N92-32377
BAKER, DONALD A. ..... p 4015 N92-33016
BAKER, DONALD J. ..... p 3950 N92-32575
p 3959 N92-33054
BANILOWER, HOWARD ..... p 3932 N92-33005
BANKOFF, S. G. ..... p 4013 N92-33124
BARBARO-GALTIERI, A. ..... p 4064 N92-32312
BARBER, FRANK J. ..... p 3941 N92-32456
BARBERIS, D. ..... p 3931 N92-32800
BARGER, RAYMOND L. ..... p 3929 N92-32480
BARINA, FRANK J. ..... p 3941 N92-32456
BARKER, A. R. ..... p 4069 N92-33187
BARKLOW, T. ..... p 4069 N92-32337
BARNARD, J. J. ..... p 4070 N92-32413
p 4071 N92-32904
BARNETT, T. P. ..... p 4032 N92-32331
BARNHART, CRAIG M. ..... p 3979 N92-32570
BARON, W. G. ..... p 3947 N92-32518
BARONAVSKI, A. P. ..... p 4082 N92-32512
BARRY, C. ..... p 3979 N92-32573
BARRY, W. ..... p 4069 N92-32318
BARSON, S. L. ..... p 4000 N92-32273
p 4001 N92-32283
BARTSCH, R. R. ..... p 3992 N92-33068
BASILI, VICTOR R. ..... p 4044 N92-32870
p 4045 N92-32879
BASILIO, C. I. ..... p 3977 N92-32467
BASS, S. D. ..... p 4068 N92-33137
BASSMAN, MITCHELL ..... p 4041 N92-32451
BATES, LARRY ..... p 3946 N92-32459
BAUER, MIREILLE ..... p 4019 N92-32801
BAUER, SIEGFRIED J. ..... p 4099 N92-32384
BAULD, N. R., JR. ..... p 4023 N92-33139
BAYLOG, J. G. ..... p 4059 N92-32989
BAYRAMLI, ERDAL ..... p 3961 N92-32508
BEARDEN, I. G. ..... p 4082 N92-32542
BEAUCHAMP, GARY M. ..... p 4040 N92-32851
BECK, JON ..... p 4091 N92-33096
p 4091 N92-33178
BECKER, T. G. ..... p 4050 N92-32568
BECKMAN, W. A. ..... p 4027 N92-33072
BEDDINI, ROBERT A. ..... p 4000 N92-32276
BEHRENS, R. S. ..... p 3948 N92-32519
BEHRINGER, K. ..... p 4079 N92-32822
BELAK, J. ..... p 3966 N92-32646
BELLINGER, N. C. ..... p 3957 N92-33040
BENCH, G. ..... p 4014 N92-33000
BENCH, G. S. ..... p 4014 N92-32999
BENCHABANE, M. ..... p 3976 N92-33243
BENHENNI, KARIM ..... p 4060 N92-32839
BENTLEY, C. L. ..... p 4006 N92-32468
BERBAUM, K. S. ..... p 4036 N92-32434
BERG, RICHARD L. ..... p 3940 N92-32903
BERGEAULT, ERIC ..... p 3980 N92-32739
BERGER, P. ..... p 3965 N92-33126
BERGEVIN, ROBERT ..... p 4048 N92-33212
BERGGREN, L. ..... p 4025 N92-32608
BERGQUIST, JAMES C. ..... p 4016 N92-33060
BERKOWITZ, M. ..... p 4064 N92-32418
BERKOWITZ, MAX L. ..... p 4066 N92-32682
BERTENYI, E. ..... p 3981 N92-32789
BESNARD, D. ..... p 4013 N92-33159
BESSON, J. ..... p 3943 N92-32728
BEVER, GLENN A. ..... p 3938 N92-32866
BEZARD, BRUNO ..... p 4099 N92-32389
BHASIN, KUL B. ..... p 3985 N92-32980
p 3985 N92-32981
p 3985 N92-32982
p 3985 N92-32983
BHATIA, NARAIN M. ..... p 3952 N92-32584
BHATTACHARYA, P. K. ..... p 3984 N92-32977
BI, HUA ..... p 4051 N92-32795
BIBRING, J. P. ..... p 4097 N92-32377
BIEG, K. W. ..... p 4080 N92-32992
BIGGERS, S. B. ..... p 3948 N92-32523
BIHARI, T. E. ..... p 4053 N92-32748
BILLINGS, DANA F. ..... p 4005 N92-32304
BILLINGSLEY, J. B. ..... p 3980 N92-32696
BIONDO, A. C. ..... p 4082 N92-32561
BIRCHLEY, P. N. W. ..... p 4100 N92-32391
p 4015 N92-32392
p 4102 N92-32410
BIRCKELBAW, LOURDES G. ..... p 3935 N92-32887
BISSCHOP, J. J. ..... p 4057 N92-32796
BJORAKER, G. ..... p 4099 N92-32389
BLACHER, R. ..... p 4060 N92-32716
BLACKMOND, D. G. ..... p 3966 N92-33246
BLADOS, WALTER R. ..... p 4091 N92-33237
BLAIN, LAURENT ..... p 4040 N92-32766
BLAKE, J. B. ..... p 4031 N92-32902
BLANCHARD, ROBERT C. ..... p 3944 N92-33112
BLELLY, PIERRE LOUIS ..... p 4031 N92-32889
BLUM, E. ..... p 4071 N92-32912
BLUMBERG, L. N. ..... p 4073 N92-33179
BLUMENTHAL, ROB ..... p 3945 N92-32262
BODEK, A. ..... p 4061 N92-32430
BOECKING, KLAUS F. ..... p 3937 N92-32447
BOERSTOEL, J. W. ..... p 3930 N92-32730
BOGAN, W. BRAD ..... p 3986 N92-33152
BOHON, HERMAN L. ..... p 3946 N92-32513
p 3950 N92-32574
BOLDI, D. ..... p 3950 N92-32576
BOLING, M. A. ..... p 4081 N92-32346
BOLLINGER, JOHN J. ..... p 4016 N92-33060
BOMING, O. ..... p 3973 N92-33059
BOND, GREGORY WILLIAM ..... p 4049 N92-33215
BONETTI, R. R. ..... p 3985 N92-32982
BOOKHOLT, H. ..... p 3957 N92-33042
BOON, JAAP J. ..... p 4098 N92-32379
BOOTH, T. E. ..... p 4059 N92-32481
BORCHERS, INGO U. ..... p 4062 N92-32951
p 4062 N92-32956
BORUCKI, WILLIAM J. ..... p 4098 N92-32380
BOSCH, CHRISTOPHER ..... p 4046 N92-32882
BOSCHMAN, JOHANNES ..... p 3992 N92-33145
BOWMAN, DANIEL R. ..... p 4021 N92-32621
BOYARSKI, A. ..... p 4065 N92-32426
BOYD, J. E. ..... p 3955 N92-32846
BRADBURY, E. M. ..... p 4036 N92-33181
BRADLEY, J. ..... p 3990 N92-32810
BRADLEY, SUZANNE ..... p 3934 N92-33098
BRADY, MICHAEL ..... p 4051 N92-32759
BRAY, I. ..... p 4065 N92-32499
BREIVIK, N. L. ..... p 3946 N92-32491
BRENNAN, J. J. ..... p 3953 N92-32676
BRENNAN, M. ..... p 3939 N92-32778
BRIAND, LIONEL C. ..... p 4044 N92-32875
BRIDGES, J. F. ..... p 4069 N92-32314

BRIGGS, D. p 4065 N92-32426
BRILLET, J. p 4096 N92-32366
p 4100 N92-32396
p 4102 N92-32408
BROCHER, E. p 4009 N92-32687
BROOKS, A. L. p 4071 N92-32904
BROWER, W. A. p 4032 N92-32431
BROWN, C. M. p 4050 N92-32568
BROWN, NICK p 4068 N92-33133
BROWN, R. H. p 4097 N92-32377
BROWN, S. A. p 4043 N92-32741
BROWNE, LINDSEY p 3929 N92-32422
BRUECK, S. R. p 4016 N92-32622
BRUNET, GILBERT p 4034 N92-33225
BRUNO, JOSEPH p 3947 N92-32514
BRYAN, KURT p 4059 N92-33006
BRYANT, R. M. p 4050 N92-32412
BRYANT, TIMOTHY D. p 4015 N92-33016
BRYNESTAD, MARK A. p 3940 N92-32988
BUCCI, A. p 3958 N92-33044
BUCHANAN, M. V. p 3964 N92-32925
BUCKINGHAM, A. C. p 4010 N92-32824
BUDAI, J. D. p 4082 N92-32636
p 4083 N92-32653
p 4085 N92-33023
BUELOW, PHILIP E. O. p 4001 N92-32284
BUIST, JAKOB p 4012 N92-33066
BUMPAS, S. E. p 4022 N92-32706
BUNDY, R. p 4070 N92-32567
BUNK, WOLFGANG p 3968 N92-32894
BURATTI, B. J. p 4097 N92-32377
BURCHAM, FRANK W., JR. p 3940 N92-32864
BURCHAT, P. R. p 4065 N92-32426
BURKE, L. A. p 3960 N92-32330
BURKE, M. G. p 3969 N92-33158
BURNETTE, D. p 3945 N92-32248
BURNS, W. K. p 4074 N92-32634
BURTON, D. E. p 4012 N92-33082
BUTLER, B. P. p 4052 N92-33100
p 4052 N92-33101

C

CABANE, M. p 4098 N92-32379
p 4100 N92-32393
CABO, A. J. p 4059 N92-33058
CABUK, HAYRI p 4000 N92-32274
CAI, R. p 3972 N92-32667
CAIRNS, E. J. p 3993 N92-33183
CALDIERA, GIANLUIGI p 4044 N92-32870
CALLAHAN, P. J. p 4028 N92-32543
CAMPBELL, E. M. p 4079 N92-32733
CAMPBELL, GORDON C. p 3961 N92-32553
CAMPBELL, R. B. p 4080 N92-32995
CAMPISI, I. E. p 3970 N92-32317
CAMY-PEYRET, C. p 3943 N92-32728
CANAVAN, G. H. p 3943 N92-32934
CANT, S. p 4045 N92-32877
CARLSON, A. L. p 4080 N92-32992
CARPENTER, D. A. p 3966 N92-32614
CARPENTER, M. P. p 4082 N92-32542
CARPENTER, S. H. p 4022 N92-32911
CARRINGTON, WILLIAM A. p 3973 N92-33170
CARTER, D. H. p 4040 N92-32910
CARUSI, A. p 4097 N92-32377
CASPERS, WIM p 4057 N92-32756
CASSATT, GARY G. p 3948 N92-32522
CATTON, IVAN p 4007 N92-32560
CAVIN, O. B. p 3968 N92-32991
CAZALBOU, J. B. p 4009 N92-32765
CELESTE, J. p 3946 N92-32327
CERULLO, L. J. p 4016 N92-32540
CHALLENOR, PETER G. p 4100 N92-32394
CHAMBRETTE, PIERRE p 4018 N92-32737
CHAMIS, C. C. p 3946 N92-32466
p 3949 N92-32531
CHAN, C. K. p 3961 N92-32475
CHAN, D. C. p 4001 N92-32283
CHAN, DANIEL C. p 3960 N92-32275
p 4001 N92-32285
p 4003 N92-32293
p 4003 N92-32295
CHANANI, G. R. p 3950 N92-32576
CHANDRA, TUSHAR DEEPAK p 4020 N92-32436
CHANG, J. W. p 4081 N92-32420
CHANG, LIANG p 4002 N92-32288
CHANGNON, S. A. p 4034 N92-33173
CHANTELAU, KLAUS p 4058 N92-32840
CHAO, TIEN-HSIN p 4041 N92-33057
CHAPDELAINE, E. R. p 3938 N92-33105
CHAPPELL, DAVID P. p 3949 N92-32526
CHASMAN, D. p 3945 N92-32248
CHASSAING, P. p 4009 N92-32765
CHASSEFIERE, E. p 4096 N92-32367
p 4098 N92-32379
p 4100 N92-32393
CHAWNER, JOHN R. p 4005 N92-32301
CHEESMAN, M. R. p 4082 N92-32561
CHEN, BAIO p 4042 N92-32656
CHEN, C. P. p 3997 N92-32258
p 3966 N92-32297
CHEN, CHUNG-WEN p 4021 N92-32657
CHEN, J. p 3939 N92-32778
CHEN, JENN-SHING p 3993 N92-33183
CHEN, LI CHE TED p 3955 N92-32829
CHEN, NAN p 4081 N92-32346
CHEN, P. p 4069 N92-32337
CHEN, SHU-CHENG p 4007 N92-32472
CHEN, WEI-CHUNG p 4003 N92-32293
CHEN, Y. S. p 3995 N92-32253
p 3997 N92-32260
p 4002 N92-32287
CHENG, GARY C. p 3997 N92-32260
p 4002 N92-32287
CHENG, LI-JEN p 4076 N92-33022
CHENG, R. K. p 3964 N92-32996
CHEW, MENG-SANG p 4019 N92-33031
CHOI, SANG-KEUN p 4002 N92-32289
CHOLEWA, M. p 4014 N92-33000
CHOREY, C. M. p 3985 N92-32982
CHOW, ALAN S. p 4005 N92-32303
CHRISEY, D. B. p 4082 N92-32512
CHRISTEN, D. K. p 4082 N92-32636
p 4083 N92-32653
CHU, T. L. p 4024 N92-32510
CHU, WILLIAM P. p 4031 N92-33097
CHUANG, J. C. p 4028 N92-32543
CHURCH, VICTOR E. p 4041 N92-32451
CHWALOWSKI, PAWEL p 3995 N92-32249
CLARK, ROBERT L. p 4063 N92-32959
CLARKE, B. p 3990 N92-32810
CLASPY, P. C. p 3985 N92-32981
CLAY, J. P. p 4071 N92-32904
CLAYTON, CURTIS D. p 4006 N92-32306
CLEMENT, PHILIPPE p 4057 N92-32756
CLEVE, RICHARD ERWIN ALEXANDER p 4049 N92-33230
CLOSE, F. E. p 4068 N92-33133
CLOUGH, S. A. p 4031 N92-33153
CLOUTIER, GUY M. p 4039 N92-33056
COATES, KEITH p 3945 N92-32280
COCHRAN, H. D. p 3965 N92-33185
COCHRAN, R. C. p 3958 N92-33047
COCHRAN, ROLAND C. p 3960 N92-33174
COFFEY, H. T. p 4017 N92-32615
COFFIELD, F. E. p 4071 N92-32904
COHEN, DOROTHEA p 3935 N92-33149
COHEN, M. L. p 4081 N92-32320
COHEN, N. p 3960 N92-32464
COLBAUGH, RICHARD D. p 4054 N92-33019
COLE, K. C. p 4019 N92-33077
COLLMAN, J. P. p 3990 N92-32827
COLLOREC, LUC p 4009 N92-32770
CONCILIO, A. p 4063 N92-32962
CONLEY, JOSEPH L. p 4042 N92-32507
CONRATH, BARNEY J. p 4095 N92-32360
CONSTANTIN, ROBERT HALIM p 4052 N92-33216
CONSTANTINIDES, E. D. p 4058 N92-32888
CONWAY, JOHN T. p 3931 N92-32811
CONWAY, TERRY L. p 4037 N92-32942
COOK, DONALD p 3946 N92-32459
COOLBAUGH, M. T. p 4066 N92-32556
COOPER, AUGUSTUS p 4045 N92-32878
COOPER, P. W. p 3975 N92-33003
COORAY, M. FRANCIS R. p 3986 N92-33191
COPENHAVER, MICHAEL M. p 4038 N92-32990
COPPIETERS, DIRK p 4060 N92-33055
CORADINI, ANGIOLETTA p 4093 N92-32350
p 4097 N92-32377
CORNELISON, JONI W. p 4005 N92-32304
COTTER, GLADYS A. p 4091 N92-33237
COUNSELMAN, CHARLES C., III p 3978 N92-32458
COURTIN, REGIS p 4094 N92-32356
p 4095 N92-32358
p 4095 N92-32361
COUSTENIS, ATHENA p 4094 N92-32355
p 4096 N92-32367
p 4099 N92-32389
p 4101 N92-32401
COUTANT, R. W. p 4028 N92-32543
COX, CHARLES p 4044 N92-32876
CRAMER, S. G. p 3950 N92-32576
CRASTO, A. S. p 3956 N92-33035
CRAVENS, THOMAS E. p 4099 N92-32386
CRAWFORD, K. p 4070 N92-32567
CREMER, JAMES F. p 4042 N92-32546
CRESPI, V. H. p 4081 N92-32320
CRITCHLEY, FRANK p 4058 N92-32799
CROSBY, RICHARD C. p 3961 N92-32553
CRUTCHIK, M. p 3988 N92-32243
CULIOLI, J. C. p 4018 N92-32694
CULLEN, D. E. p 4041 N92-32416
CULLINANE, THOMAS P. p 4042 N92-32627
CUMALAT, J. P. p 4069 N92-33187
CUMMINS, PATRICK F. p 4035 N92-33198
CUOMO, FRANK W. p 4076 N92-33017
CURLISS, D. B. p 3958 N92-33049
CURRAN, H. J. p 3961 N92-32544
CURTIN, L. S. p 3990 N92-32827
CURTIS, P. T. p 3957 N92-33038
p 3957 N92-33042
CUTMORE, TIM R. H. p 4054 N92-32854

D

DADKHAH, MAHYAR S. p 4023 N92-32936
DAHM, WERNER J. A. p 4007 N92-32598
DAKHOUL, Y. p 4002 N92-32286
DAKHOUL, YOUSSEF p 3999 N92-32271
DALLAQUA, RENATO SERGIO p 4014 N92-32601
DALY, P. J. p 4082 N92-32542
DANG-NHU, M. p 4099 N92-32389
p 4100 N92-32395
p 4101 N92-32400
DANIEL, R. W. p 4018 N92-32757
DANIELL, P. M. p 4015 N92-32392
p 4102 N92-32410
DANIELS, W. A. p 3998 N92-32265
DANNEVIK, W. P. p 4010 N92-32824
DARIAN, ARMEN p 4001 N92-32285
p 4003 N92-32295
DAS, A. p 4061 N92-32430
DAS, ANINDYA p 4053 N92-33224
DAVARI, SADEGH p 4042 N92-32656
DAVID, S. A. p 4020 N92-33085
DAVIS, B. H. p 3975 N92-33123
DAVIS, CHRISTOPHER C. p 4035 N92-32345
DAVIS, H. A. p 3992 N92-33068
DAVIS, J. BRADLEY p 3941 N92-32454
DAVIS, S. H. p 4013 N92-33124
DEADRICK, F. J. p 4071 N92-32904
DEALWIS, S. P. p 4069 N92-33187
DEATON, JERRY W. p 3950 N92-32577
DEBURE, KELLY R. p 4041 N92-33205
DECROIX, M. E. p 4000 N92-32273
DEGRAND, T. A. p 4069 N92-33187
DEJONG, F. J. p 3966 N92-32307
DEJONG, FREDERIK J. p 4002 N92-32289
DEJONG, H. p 4043 N92-32832
DEJONG, S. p 4043 N92-32832
DELEEUW, J. H. p 3934 N92-32845
DELEON, ROBERT L. p 3961 N92-32509
DELESALLE, DENIS p 4051 N92-32715
DELIL, A. A. M. p 4008 N92-32675
p 4010 N92-32786
DELLA-DORA, J. p 4058 N92-32838
DELUCIA, R. A. p 3938 N92-33105
DEMAZIERE, M. p 3943 N92-32728
DEME, N. p 4101 N92-32401
DEMUREN, A. O. p 4047 N92-33131
DENBOEF, ARIE JEFFREY p 4077 N92-33146
DENBY, B. p 4070 N92-32506
DENEXTER, PETRUS p 3954 N92-32677
DEO, RAVI B. p 3952 N92-32584
DEPABLO, J. J. p 3965 N92-33185
DERENZO, S. E. p 4082 N92-32493
DEVAN, J. H. p 3968 N92-32991
DEVANATHAN, R. p 4086 N92-33221
DEVANSSAY, E. p 4096 N92-32368
p 4100 N92-32397
DEWETTE, PAULA S. p 4042 N92-32627
DEXTER, H. BENSON p 3959 N92-33054
DIB, N. I. p 3983 N92-32971
DILL, HAROLD D. p 3951 N92-32580
DILL, RICHARD A. p 3994 N92-32247
p 4005 N92-32305
DILLARD, RICHARD B. p 3941 N92-32456
DILLON, W. P. p 4034 N92-32333
DINGEMANS, T. p 3972 N92-32667
DJEBLOUN, H. p 4101 N92-32400
DO, LEEJO p 4096 N92-32368
p 4100 N92-32397
DOBIE, D. p 3946 N92-32327
DOBRIJEVIC, M. p 4100 N92-32396
DODD, ROBERT S. p 3932 N92-32941
DOLOVICH, ALLAN T. p 4023 N92-33200
DONALDSON, GEORGE J. p 3990 N92-32812
DONES, L. p 4094 N92-32351
DONNELLAN, T. M. p 3958 N92-33047
DOUDA, BERNARD E. p 4013 N92-32343
DOUGHERTY, N. S. p 3996 N92-32255
DOVERSTAAL, M. p 4067 N92-32764
DOWNEY, ALAN N. p 3983 N92-32966
p 3983 N92-32968
DRAKE, J. F. p 4078 N92-32592
DRELL, S. D. p 4069 N92-33148

DRIESSEN, STEPHANUS GERARDUS ARNOLDUS J. p 4060 N92-32709
DRIGERT, M. W. p 4082 N92-32542
DRUET, L. p 3976 N92-33243
DUCHANE, D. V. p 4025 N92-32695
DUCHARME, A. R. p 4028 N92-32558
DUCKWORTH, D. C. p 3964 N92-32925
DUDLEY, MICHAEL R. p 3929 N92-32422
DUGAN, G. p 4073 N92-33134
DULIKRAVICH, GEORGE S. p 4004 N92-32298
DUNPHY, M. P. p 3961 N92-32544
DUPONT, L. p 3955 N92-32813
DURAN, R. S. p 3971 N92-32550
DWYER, HARRY A. p 3944 N92-32246
DYLLA, H. F. p 4070 N92-32567
DYTELL, RITA S. p 4037 N92-32942

E

EASTLAND, ANTHONY H. p 4003 N92-32293
EATOCK, BRIAN C. p 3982 N92-32818
EBERLY, WAYNE p 4059 N92-33231
EDDY, DOUGLAS R. p 4036 N92-32492
EICHMANN, DAVID p 4090 N92-32654
p 4091 N92-33096
p 4091 N92-33178
EICK, STEPHEN G. p 4044 N92-32873
ELALDI, F. p 3954 N92-32791
ELBAUM, NICK C. p 3961 N92-32553
ELDREDGE, DONALD p 3932 N92-32941
ELIASSON, PETER p 4057 N92-32729
ELLINGSON, W. A. p 3971 N92-32640
ELLIOTT, S. J. p 4062 N92-32957
ELSENAAR, A. p 3930 N92-32732
EMBORG, URBAN p 4062 N92-32956
ENCRENAZ, T. p 4099 N92-32389
ENG, ANTHONY T. p 3974 N92-33177
ENGELMANN, B. E. p 4020 N92-32328
ENGELS, E., JR. p 4066 N92-32702
EOM, C. B. p 4083 N92-32653
EPHREMIDES, ANTHONY p 3979 N92-32570
EPSTEIN, M. p 4016 N92-32540
ERBER, T. p 4021 N92-32681
ERBES, GERHARD p 4009 N92-32727
ERDMAN, W. W. p 4025 N92-32549
EREMIN, V. p 4064 N92-32316
ERHART, JOHN J. p 3995 N92-32252
ERICKSON, K. L. p 3974 N92-32637
ERKELENS, L. J. J. p 3933 N92-32830
ERZBERGER, HEINZ p 3933 N92-33080
p 3933 N92-33194
ESTEROWITZ, LEON p 4017 N92-33165
EUCKER, BRAD A. p 3937 N92-32446
EUCKER, SHELLY S. p 3937 N92-32446
EVANS, C. R. p 4070 N92-32647
EVANS, R. p 4077 N92-32533
EVENSON, W. E. p 3970 N92-32471
EVEQUOZ, CLAUDE p 4053 N92-33235
EVERETT, LOUIS J. p 3942 N92-32477

F

FABRIS, M. p 4101 N92-32398
FAIRALL, C. W. p 4033 N92-32714
FAKLIS, DEAN p 4076 N92-33074
FALCO, B. p 4013 N92-33140
p 4017 N92-33180
FALCO, C. M. p 3988 N92-32659
FALCONER, J. L. p 3960 N92-32332
FAMINI, G. R. p 3960 N92-32330
FAN, S. p 3999 N92-32270
FARKAS, Z. D. p 4071 N92-32751
FARLEY, GARY L. p 3959 N92-33075
FARMER, R. C. p 3995 N92-32253
FARR, R. p 3945 N92-32248
FARRELLY, F. A. p 4101 N92-32404
FEDERICO, C. p 4093 N92-32350
FEENSTRA, R. p 4083 N92-32653
FEIK, R. A. p 3935 N92-32326
FELTER, T. E. p 4068 N92-33001
FENTON, B. C. p 3938 N92-33105
FERBEL, T. p 4061 N92-32430
FERGUSON, DONALD W. p 4039 N92-32790
FERKINHOFF, D. J. p 4059 N92-32989
FERNANDES, D. N. p 4103 N92-32488
FERNANDEZ, I. p 3958 N92-33046
FERNANDO, M. C. p 3987 N92-33206
FERRANDO, WILLIAM A. p 3973 N92-33157
FERRARI, JOSE A. p 3982 N92-32820
FERREIRA, JOSE LEONARDO p 4079 N92-32662
FERRIS, J. P. p 4096 N92-32371
FEY, ROBERTUS HENRICUS BARBARA p 4056 N92-32707
FIFER, ROBERT A. p 3974 N92-32664
FILUK, A. B. p 4080 N92-32992
FINELLI, GEORGE B. p 4045 N92-32880
FINGER, K. E. p 3970 N92-32317
FINK, J. p 4081 N92-32470
p 4086 N92-33136
FINN, J. M. p 4078 N92-32592
FISCHBACH, E. p 4073 N92-33182
FISCHER, J. E. p 3970 N92-32429
FISCHER, S. K. p 3978 N92-32927
FISCHLER, M. p 4040 N92-32642
FISHER, R. J. p 4032 N92-32427
FISHER, R. K. p 4078 N92-32623
FLANAGAN, DAVID T. p 3965 N92-33029
FLASAR, F. M. p 4095 N92-32360
FLEENOR, M. C. p 3966 N92-32614
FLEMING, D. L. p 3969 N92-33132
FLYTZANI-STEPHANOPOULOS, M. p 4030 N92-33125
FOLEY, R. p 4077 N92-32533
FOLIOT, VINCENT p 4031 N92-32889
FOLKES, M. J. p 3959 N92-33052
FONTANARI, JEAN p 4031 N92-32889
FORAL, M. J. p 3975 N92-33141
FORBES, KEITH R. p 3946 N92-32339
FORD, W. T. p 4069 N92-33187
FOSTER, STEPHEN P. p 3938 N92-33102
FRANKLIN, J. A. p 3939 N92-32788
FREE, GEORGE M. p 3991 N92-33061
FRENCH, J. B. p 4069 N92-33186
FRERE, C. p 4096 N92-32368
FRICKER, DARREN p 4007 N92-32560
FRIEBELE, E. J. p 4074 N92-32613
FRIEDMAN, A. p 4071 N92-32912
FRIEDRICH, H. E. p 3977 N92-32690
FRIEDRICH, H.-E. p 3977 N92-32742
FRIEND, S. A. p 4052 N92-33100
p 4052 N92-33101
FRYE, ROBERT J. p 3991 N92-32867
FUKUYAMA, ATSUSHI p 3982 N92-32905
FULCHIGNONI, MARCELLO p 4098 N92-32380
FULLER, CHRIS R. p 4063 N92-32959
FULLER, JAMES M. p 3936 N92-32443
FUSARO, ROBERT L. p 3972 N92-32863

G

GAITONDE, DATTA p 4008 N92-32632
GALANT, DAVID p 4052 N92-32886
GALEJS, R. J. p 3980 N92-32680
GAN, L. p 4099 N92-32386
GANSKA, R. J. p 4052 N92-33100
p 4052 N92-33101
GAONKAR, GOPAL H. p 3940 N92-33107
GARCIA, R. p 4002 N92-32286
p 4003 N92-32291
GARCIADEVICUNA, JOSE LUIS p 3989 N92-32777
GARDNER, J. A. p 3970 N92-32471
GARRETT, JOSEPH L. p 3996 N92-32254
GARVEY, JAMES F. p 3961 N92-32509
p 4066 N92-32556
GARZON, SHERRY B. p 3946 N92-32513
p 3950 N92-32574
GAUDERT, P. C. p 3959 N92-33051
p 3959 N92-33078
GAUTIER, DANIEL p 4094 N92-32354
p 4095 N92-32361
p 4096 N92-32366
p 4102 N92-32408
GAVIN, J. E. p 4033 N92-32720
GEAKE, J. E. p 4101 N92-32399
GEBALLE, T. H. p 4083 N92-32653
GERBER, ALEXANDER p 4086 N92-33190
GERETY, M. p 4027 N92-32415
GIBBONS, RANDALL E. p 3965 N92-33029
GIBBS, W. S. p 4040 N92-32910
GIBELING, H. J. p 3966 N92-32307
GIBELING, HOWARD J. p 3999 N92-32269
GILBERT, C. p 3985 N92-32981
GINLEY, D. S. p 4084 N92-32920
GIRARD, R. p 4022 N92-32774
p 3954 N92-32775
p 3957 N92-33041
GIRIDHARAN, M. G. p 3996 N92-32257
GLASS, KRISTIN L. p 4054 N92-33019
GOERANSSON, PETER p 4062 N92-32956
GOERING, J. C. p 3948 N92-32519
GOLDIN, DANIEL S. p 3941 N92-33007
GOLDTHORPE, S. p 3939 N92-32778
GOMAA, HASSAN p 4046 N92-32882
GOMBOSI, TAMAS I. p 4098 N92-32383
GONG, K. F. p 4059 N92-32989
GOODALL, COLIN p 3932 N92-33005
GORETTA, K. C. p 4081 N92-32346
p 4082 N92-32561
GOULD, R. W. p 3957 N92-33040
GOUTOULLI, L. p 4100 N92-32396
GOVINDAN, T. R. p 4002 N92-32289
GOVINDARAJU, MADHAV R. p 3956 N92-32906
GOYAL, A. p 4084 N92-32919
GRAMANN, RICHARD A. p 4046 N92-32917
GRANER, G. p 4099 N92-32389
GRARD, REJEAN J. L. p 4096 N92-32365
GRASSOTTI, C. p 4034 N92-32859
GRAY, GARY W. p 4037 N92-32816
GRAY, HENRY F. p 3992 N92-33169
GRAY, ROGER L. p 3940 N92-33161
GREEN, INGE S. p 4062 N92-32952
GREEN, M. A. p 4025 N92-32565
GREEN, S. F. p 4100 N92-32394
p 4102 N92-32410
GREEN, SCOTT E. p 4044 N92-32871
GREEN, STUART p 3956 N92-33036
GREEN, WILLIAM J. p 3974 N92-33177
GREENLY, J. B. p 3992 N92-33068
GREENWALD, D. A. p 4003 N92-32291
GREGOIRE, D. J. p 3980 N92-32719
GREGOIRE, GERARD p 4056 N92-32684
GRELLA, RAY p 3953 N92-32629
GRENIER, L. A. p 4033 N92-32545
GRIFFIN, LISA W. p 3998 N92-32267
GRIFFIN, O. H., JR. p 3946 N92-32491
GRIFFIN, O. HAYDEN, JR. p 3949 N92-32528
GRIFFITH, CAITLIN p 4101 N92-32401
GRIFFITH, CAITLIN A. p 4097 N92-32374
GRIFFITH, L. V. p 4071 N92-32904
GROENEBOOM, P. p 4059 N92-33058
GROSS, K. p 3996 N92-32257
GROSSMAN, J. W. p 4025 N92-32549
GU, JUNHUA p 3962 N92-32563
GUBSER, D. U. p 3988 N92-32659
GUERDAL, Z. p 3946 N92-32491
GUILLEMIN, J. C. p 4096 N92-32371
GUINJOAN, FRANCISCO p 3990 N92-32793
GUNDY-BURLET, KAREN L. p 3938 N92-32452
GUNZELMAN, MARK J. p 4033 N92-32534
GURALNICK, S. A. p 4021 N92-32681
GUZDAR, P. N. p 4078 N92-32592
GYGI, K. F. p 4030 N92-33156

H

HACK, THEODOR p 3968 N92-32895
HACKSTEIN, H. JOSEF p 4062 N92-32951
HADID, A. H. p 3998 N92-32266
HAERDLE, WOLFGANG p 4060 N92-32718
HAFTKA, RAPHAEL T. p 3952 N92-32586
HAGEN, C. R. p 4061 N92-32430
HAGLUND, R. F. p 4085 N92-33127
HAH, C. p 3999 N92-32268
p 4003 N92-32291
HALL, D. T. p 4094 N92-32357
HALL, EARL T. p 4015 N92-33016
HALL, GREGORY E. p 4032 N92-33197
HALL, M. G. p 3967 N92-32699
HALL, PETER p 4060 N92-32718
HALL, WILLIAM J. p 4036 N92-32344
HALMSTAD, J. T. p 4033 N92-32545
HAMELUCK, DONALD p 4038 N92-32817
HAMLEY, JOHN A. p 3944 N92-33064
HAMMARSTRAND, ULLA p 4033 N92-32758
HAMMERTON, P. W. p 3930 N92-32648
HANEWALD, W. G. p 4081 N92-32346
HANSMA, P. K. p 4066 N92-32548
HANSON, F. E. p 4015 N92-32329
HARLOW, F. H. p 4013 N92-33159
HARPER, R. E. p 4052 N92-33100
p 4052 N92-33101
HARRIS, WILLIAM p 3936 N92-32440
HART-SMITH, L. J. p 3952 N92-32588
HARTFORD, E. H. p 4083 N92-32653
HARTMAN, K. O. p 3945 N92-33245
HARVEY, A. R. p 4071 N92-32904
HASKELL, WILLIAM E., III p 3947 N92-32515
HASSAM, A. B. p 4078 N92-32592
HASTI, D. E. p 4026 N92-32946
HAUGLAND, E. J. p 3984 N92-32975
HAUGLAND, EDWARD J. p 3984 N92-32976
HAVENS, STEPHEN J. p 3973 N92-33008
p 3973 N92-33015
HAY, J. p 3939 N92-32778
HAYES, F. C. p 3977 N92-32723
HAYHURST, KELLY J. p 4045 N92-32880
HAYNES, H. D. p 4019 N92-32890
HE, J. L. p 4017 N92-32615
HEAMAN, J. p 3998 N92-32263
HEATH, J. B. R. p 3957 N92-33039
HECKMAN, J. p 4070 N92-32567
HEEGER, ALAN J. p 3971 N92-32665
HEFFNER, MICHAEL p 3932 N92-33063
HEGEDUS, CHARLES R. p 3974 N92-33177

HEGGARTY, KEVEN ..... p 4075 N92-32805
HEIKKINEN, D. W. ..... p 4014 N92-32999
p 4068 N92-33001
HEIMBUERGER, ANNELI ..... p 4090 N92-32843
HEIMERDINGER, M. W. ..... p 3950 N92-32576
HEINEN, VERNON O. ..... p 3985 N92-32980
p 3985 N92-32983
HELLMAN, E. S. ..... p 4083 N92-32653
HENDERSON-SELLERS, B. ..... p 4045 N92-32877
HENDRICKSON, P. L. ..... p 4030 N92-33156
HERGENROTHER, PAUL M. ..... p 3973 N92-33008
p 3973 N92-33015
HERMAN, R. G. ..... p 3960 N92-32334
p 3975 N92-33108
HERON, K. H. ..... p 4062 N92-32954
HERR, K. C. ..... p 4074 N92-32672
HERSE, MICHEL ..... p 4031 N92-32889
HESS, B. V. ..... p 4068 N92-33001
HESS, RICHARD F. ..... p 3939 N92-32778
HICKEY, M. ..... p 3979 N92-32573
HIEL, CLEMENT C. ..... p 3949 N92-32526
HIGGINBOTHAM, SCOTT A. ..... p 3941 N92-32454
HILL, D. N. ..... p 4080 N92-32995
HILL, J. C. ..... p 4067 N92-32922
HILLYER, T. ..... p 4077 N92-32533
HIRSCH, KURT ..... p 3990 N92-32823
HIRST, DONALD J. ..... p 3974 N92-33177
HIRT, GERHARD ..... p 3978 N92-32893
HO, HENJEN ..... p 3959 N92-33075
HO, WILSON ..... p 3989 N92-32669
HO, Y. L. ..... p 4078 N92-32599
HOADLEY, SHERWOOD T. ..... p 3934 N92-32536
HOEIJMAKERS, H. W. M. ..... p 3930 N92-32673
p 3930 N92-32732
HOFFMAN, F. O. ..... p 4028 N92-32616
HOFFMAN, KNUT ..... p 4063 N92-32960
HOFFMAN, R. N. ..... p 4034 N92-32859
HOFFMEYER, J. A. ..... p 3979 N92-32555
HOGAN, AUSTIN W. ..... p 3931 N92-32900
HOGELAND, S. ..... p 4015 N92-32335
HOLLANDER, M. G. ..... p 4070 N92-32647
HOLLANDSWORTH, C. E. ..... p 3989 N92-32700
HOLLIS, A. J. ..... p 4101 N92-32403
HOLLOWAY, D. L. ..... p 3971 N92-32640
HOLM, ELIAS ..... p 4009 N92-32727
HOLT, J. ..... p 3945 N92-32248
HOLT, J. B. ..... p 3996 N92-32255
HOLTKAMP, D. ..... p 3943 N92-32934
HOLZ, D. ..... p 4088 N92-33069
HONG, K. C. ..... p 4030 N92-32933
HOOMAN, HANS JUERGEN ..... p 4063 N92-32961
HOOVER, RICHARD B. ..... p 4092 N92-33012
HOPSON, PURNELL, JR. ..... p 4076 N92-33017
HOROSCHENKOFF, ALEXANDER
p 3954 N92-32740
HORTON, R. ..... p 4042 N92-32617
HORWITZ, J. S. ..... p 4082 N92-32512
HOURDIN, F. ..... p 4095 N92-32361
HOUSER, R. M. ..... p 4025 N92-32549
HOWALD, A. W. ..... p 4078 N92-32623
HSU, IN-SHEK ..... p 3991 N92-33011
HSU, W. W. ..... p 4003 N92-32294
HU, M. ..... p 3983 N92-32966
HUAN, JIAN-CHUN ..... p 4000 N92-32274
HUANG, S. W. ..... p 4081 N92-32470
HUBBARD, ARTHUR T. ..... p 3962 N92-32591
HUBBARD, HARVEY H. ..... p 4063 N92-33160
HUDSON, DAVID H. ..... p 3986 N92-33171
HUESTIS, DAVID C. ..... p 4027 N92-33138
HUFFINGTON, NORRIS J., JR. ..... p 4023 N92-32918
HUFFLEN, JEAN-MICHEL ..... p 4051 N92-32771
HUGHES, P. Y. ..... p 4032 N92-32431
HUMMEL, J. R. ..... p 4029 N92-32860
HUMMER, C. R. ..... p 3989 N92-32700
HUNT, J. T. ..... p 4079 N92-32733
HUNTEN, DONALD M. ..... p 4094 N92-32353
HUNTEN, KEITH ..... p 3953 N92-32629
HUSH, D. R. ..... p 4041 N92-32414
HUSSIEN, BASSAM ..... p 3933 N92-32424
HWA, R. C. ..... p 4066 N92-32600
HWANG, D. Q. ..... p 4077 N92-32533
HWANG, L.-T. ..... p 3984 N92-32974
HYER, M. W. ..... p 3948 N92-32521

I

IACHELLO, F. ..... p 4067 N92-32921
IANNONE, M. ..... p 3959 N92-33053
IBRAHEEM, S. O. ..... p 4047 N92-33131
IDRISSIAZAMI, HAFIDA ..... p 4066 N92-32735
IGUCHI, STEVE K. ..... p 3929 N92-32422
IP, WING-H. ..... p 4098 N92-32382
IRICK, S. C. ..... p 4073 N92-32321
ISAACS, R. G. ..... p 4034 N92-32859
ISHIKAWA, T. ..... p 4078 N92-32552
ISRAEL, GUY ..... p 4098 N92-32379
p 4099 N92-32390
p 4100 N92-32393
ISSA, R. I. ..... p 3998 N92-32266
ITANO, WAYNE M. ..... p 4016 N92-33060
ITOH, K. ..... p 4079 N92-32745
ITOH, KIMITAKA ..... p 3982 N92-32905
ITOH, S. ..... p 4079 N92-32745
ITOH, SANAE ..... p 3982 N92-32905
IVANOV, A. ..... p 4064 N92-32316
IZYGON, MICHEL ..... p 4043 N92-32865

J

JACK, J. W. ..... p 3936 N92-32439
JAMES, IAN N. ..... p 4095 N92-32362
JANKOWSKI, M. A. ..... p 3948 N92-32525
JANSSEN, MICHAEL MARIA JOHANNES FRANCISCUS
p 4067 N92-32753
JANSSENS, R. V. F. ..... p 4082 N92-32542
JARBOE, T. R. ..... p 4078 N92-32595
JARMASZ, MARK R. ..... p 3993 N92-33193
JAYANTI, PRASAD ..... p 4020 N92-32436
JEFFERY, D. ROSS ..... p 4045 N92-32877
JEGLEY, DAWN C. ..... p 3951 N92-32582
JEHLE, ROBERT E. ..... p 3986 N92-33171
JENSEN, J. O. ..... p 3960 N92-32330
JENUS, JOSEPH, JR. ..... p 3976 N92-33241
JEROME, RICHARD ..... p 3987 N92-33207
JIMENEZ, R. D. ..... p 4028 N92-32558
JIN, KANG-REN ..... p 4005 N92-32303
JIN, S. ..... p 3988 N92-32659
JOHNSON, A. M. ..... p 3970 N92-32317
JOHNSON, B. V. ..... p 3998 N92-32265
JOHNSON, BRET D. ..... p 3929 N92-32691
JOHNSON, ERIC R. ..... p 3952 N92-32586
JOHNSON, MACDONALD ..... p 4029 N92-32650
JOHNSON, N. R. ..... p 4067 N92-32928
JOHNSON, S. L. ..... p 3996 N92-32255
JONES, J. R. ..... p 4029 N92-32860
JONES, RAY N. ..... p 3991 N92-33061
JONES, STEPHEN P. ..... p 3937 N92-32449
JONES, T. ..... p 3967 N92-32721
JORDAN, K. ..... p 4070 N92-32567
JOST, JIM ..... p 4046 N92-32883
JOW, H. N. ..... p 4072 N92-32994
JUANG, JER-NAN ..... p 4021 N92-32657
p 4019 N92-33031
JUDD, JON ..... p 3953 N92-32629
JUSZKO, BARBARA-ANN ..... p 3981 N92-32749
JUVE, DANIEL ..... p 4009 N92-32770

K

KAHANER, D. K. ..... p 4052 N92-32926
KAISER, D. P. ..... p 4032 N92-32431
KALAY, G. ..... p 3959 N92-33052
KALDEICH, BRIGITTE ..... p 4093 N92-32348
KAN, HAN PIN ..... p 3949 N92-32527
p 3951 N92-32579
p 3952 N92-32584
KANE, DAVID M. ..... p 3948 N92-32525
KANEKO, H. ..... p 4070 N92-32746
KANG, Y. W. ..... p 4069 N92-32314
KANNEN, G. ..... p 4029 N92-32841
KANT, TARUN ..... p 4022 N92-32783
KAO, Y. H. ..... p 4081 N92-32470
p 4086 N92-33136
KAPTEIN, DICK ..... p 4063 N92-32963
KARABEKOV, I. P. ..... p 4069 N92-32319
KARL, T. R. ..... p 4032 N92-32431
KARZANOV, ALEXANDER V. ..... p 4056 N92-32710
KASPAREK, W. ..... p 4071 N92-32808
KASZA, K. E. ..... p 4080 N92-33168
KATEHI, P. B. ..... p 3983 N92-32971
KATNIK, GREGORY N. ..... p 3941 N92-32454
KATZ, D. L. ..... p 4015 N92-32329
KATZ, JOSEPH ..... p 3929 N92-32422
KAUFMAN, D. Y. ..... p 4062 N92-32561
KAUFMAN, IRVING ..... p 3992 N92-33169
KAUTZ, EDWARD F. ..... p 3949 N92-32527
p 3951 N92-32579
KAZOVSKY, L. G. ..... p 3951 N92-32580
p 3979 N92-32573
p 4074 N92-32668
KAZOVSKY, LEONID ..... p 4050 N92-32628
KEEBLE, L. J. ..... p 4069 N92-33164
KEEN, ARTHUR A. ..... p 4042 N92-32658
KEIL, LANNY C. ..... p 4037 N92-32539
KEIL, WERNER H. ..... p 4088 N92-33199
KEISER, J. R. ..... p 3966 N92-32432
KELDER, ERIK MARIA ..... p 3973 N92-33065
KELLER, C. N. ..... p 4099 N92-32386
KELLER, JAMES M. ..... p 4047 N92-33093
KELLOGG, GARY ..... p 3935 N92-33149
KELLY, P. M. ..... p 4041 N92-32414
KELLY, T. J. ..... p 4028 N92-32543
KEMPEL, LEO C. ..... p 3979 N92-32559
KENNEDY, J. B. ..... p 3962 N92-32594
KENNEDY, R. S. ..... p 4036 N92-32434
KERBER, MARTIN W. ..... p 3966 N92-32626
KERCHNER, H. R. ..... p 4082 N92-32636
KERR, STEPHEN STEWART ..... p 4080 N92-33223
KERSCHBERG, LARRY ..... p 4046 N92-32882
KERSCHEN, E. J. ..... p 3930 N92-32648
KESTIN, J. ..... p 4087 N92-32566
KESTLER, MAUREEN A. ..... p 3940 N92-32903
KEVORKIAN, J. ..... p 4016 N92-32596
KHARE, BISHUN N. ..... p 4096 N92-32369
KHEYFETS, A. ..... p 4088 N92-33069
KHLIFI, M. ..... p 4096 N92-32368
p 4101 N92-32400
KHOO, T. L. ..... p 4082 N92-32542
KHOUNSARY, A. M. ..... p 4072 N92-33130
KIERAS, DAVID E. ..... p 4038 N92-32569
KIGGANS, J. O., JR. ..... p 3956 N92-32945
KIM, DONGMOON ..... p 3945 N92-32262
KIM, KWANG-JE ..... p 4017 N92-33155
KIM, R. Y. ..... p 3956 N92-33035
KIM, Y. M. ..... p 3997 N92-32258
p 3966 N92-32297
KIRBIE, H. C. ..... p 4071 N92-32904
p 4072 N92-33122
KIRIS, CETIN ..... p 4002 N92-32288
p 4012 N92-33113
KIRSCH, JAMES C. ..... p 3979 N92-32633
KITTEL, P. ..... p 4007 N92-32474
KLABUNDE, C. E. ..... p 4082 N92-32636
KLANG, ERIC C. ..... p 3953 N92-32589
KLEIMOLA, M. ..... p 3973 N92-33059
KLEIN, GARY A. ..... p 4039 N92-32433
KLEINLE, MARK ..... p 3988 N92-32964
KLIER, K. ..... p 3960 N92-32334
p 3975 N92-33108
KLIFA, CATHERINE ..... p 4043 N92-32804
KLIMAS, P. ..... p 4026 N92-32923
KLINTSOV, V. N. ..... p 4065 N92-32500
KLOEPPEL, P. K. ..... p 4069 N92-32318
KNACKE, R. F. ..... p 4097 N92-32376
KNAPPENBERGER, WILLIAM B. ..... p 4042 N92-32627
KNIGHT, NORMAN F., JR. ..... p 3949 N92-32528
p 4023 N92-33104
KNIGHT, W. D. ..... p 3969 N92-33116
KNUDTSON, J. T. ..... p 4074 N92-32672
KOBAYASHI, A. S. ..... p 4023 N92-32936
KOCH, URSULA ..... p 3968 N92-32894
p 3968 N92-32895
KOEKOEK, ROELOF ..... p 4058 N92-32836
KOFMAN, WLODEK ..... p 4031 N92-32889
KOLEV, N. I. ..... p 4011 N92-32857
p 4011 N92-32858
KOLTUN, D. S. ..... p 4069 N92-33186
KOMOROWSKI, J. P. ..... p 3957 N92-33039
KOMOROWSKI, JERZY P. ..... p 3955 N92-32813
KOONTZ, STEVEN L. ..... p 3965 N92-33009
KOREVAAR, ERIC ..... p 4016 N92-33089
KORN, PAULA ..... p 4039 N92-33099
KOSHAEVSKII, V. N. ..... p 3962 N92-32557
KOSTIUK, L. W. ..... p 3964 N92-32996
KOSTOPOULOS, V. ..... p 3959 N92-33050
KOUL, A. S. ..... p 4023 N92-33076
KOZANECKI, W. ..... p 4069 N92-32337
KOZUH-SCHNEEBERGER, JOSEF
p 4071 N92-32763
KRAFT, MICHAEL J. ..... p 3951 N92-32583
KRAMER, MARTINA ELIJDA ..... p 4058 N92-32798
KRAMER, S. L. ..... p 4015 N92-32511
KRANER, H. W. ..... p 4064 N92-32316
KRASKO, GENRICH L. ..... p 4084 N92-32939
KRASNY, ROBERT ..... p 4007 N92-32598
KRAUSZ, A. S. ..... p 4023 N92-33076
KRAUTER, G. ..... p 3946 N92-32327
KRAVETZ, J. ..... p 3939 N92-32778
KREMPL, E. ..... p 4021 N92-32698
KRESIN, V. V. ..... p 3969 N92-33116
KRINSKY, S. ..... p 4071 N92-32912
KRISHNAN, ANANTHA ..... p 3995 N92-32251
p 3996 N92-32257
KRISHNAN, P. N. ..... p 3960 N92-32330
KRISHNAPPA, G. ..... p 4062 N92-32953
KROEBER, I. ..... p 3957 N92-33042
KROEGER, D. M. ..... p 4084 N92-32919
KROGER, H. ..... p 3988 N92-32659
KROL, A. ..... p 4081 N92-32470
p 4086 N92-33136
KROLL, N. M. ..... p 4071 N92-32751
KROLL, NORBERT ..... p 4008 N92-32632
KU, W. H. ..... p 4075 N92-32935
KUHANEN, TARU ..... p 4090 N92-32843
KUIP, C. A. C. ..... p 4057 N92-32796

KUKLA, G. J. p 4033 N92-32720
KUMAR, P. R. p 4089 N92-32644
KUMRIC, H. p 4071 N92-32808
KUNATH, R. R. p 3983 N92-32968
KUNG, P. J. p 4085 N92-33026
KUNKEL, K. E. p 4034 N92-33173
KUNZ, R. p 3999 N92-32270
KUNZ, RICHARD K. p 3952 N92-32585
KUPPERMAN, D. S. p 3953 N92-32638
KUSNEZOV, D. p 4067 N92-32921
KUSTOM, R. L. p 4069 N92-32314
KUZAY, T. p 4072 N92-33130
KWAK, DOCHAN p 4002 N92-32288
p 4012 N92-33113
KWAK, SE-HUNG p 4053 N92-32748
KWON, O. p 3999 N92-32268
p 4003 N92-32291
KWONG, MAN KAM p 4047 N92-33118

L

LADANY, I. p 4077 N92-33239
LAGACE, PAUL A. p 3951 N92-32583
LAKSHMINARAYANA, B. p 3999 N92-32270
LALA, J. H. p 4052 N92-33100
p 4052 N92-33101
LALLI, VINCENT R. p 3941 N92-32456
LAM, N. Q. p 4086 N92-33221
LAN, G. L. p 3983 N92-32966
LANAGAN, M. T. p 4081 N92-32346
p 4082 N92-32561
LANG, M. A. p 4061 N92-32950
LANGEVIN, Y. p 4097 N92-32377
LANIER, R. G. p 3964 N92-32929
LANOU, R. E. p 4103 N92-33119
LARA, L. M. p 4096 N92-32367
LARMAN, KEVIN T. p 3944 N92-33112
LARRABEE, J. F. p 3980 N92-32696
LARSEN, E. W. p 4057 N92-32743
LARSEN, PETER N. p 4062 N92-32956
LASO, M. p 3965 N92-33185
LATTIMER, J. M. p 4093 N92-32993
LAU, EDMOND Y. p 4102 N92-32405
LAURITSEN, T. p 4082 N92-32542
LAVIA, A. p 3958 N92-33046
LAVINE, T. L. p 4071 N92-32751
LAVRICH, P. L. p 3962 N92-32594
LAWRENCE, R. J. p 3943 N92-32704
LEACH, B. W. p 3934 N92-32849
p 3938 N92-32850
LEBLANC, T. J. p 4050 N92-32568
LEBRETON, JEAN-PIERRE p 4099 N92-32388
p 4102 N92-32409
LECCE, LEONARDO V. p 4063 N92-32962
LECLERC, YVAN G. p 4048 N92-33204
LECOINTE, JEAN-PHILIPPE p 3972 N92-32762
LEE, GORDON p 4021 N92-32657
LEE, H. H. p 3948 N92-32521
LEE, H.-J. p 3946 N92-32466
LEE, J. J. p 3996 N92-32257
LEE, JIM P. p 3978 N92-32535
LEE, RICHARD Q. p 3983 N92-32967
p 3983 N92-32968
p 3983 N92-32969
p 3983 N92-32970
LEE, S. p 3954 N92-32791
p 3959 N92-33051
LEE, W. Y. p 4084 N92-32920
LEE, Y. p 3930 N92-32494
LEEDS, JEFFREY L. p 3935 N92-32612
LEFEBVRE, D. p 3957 N92-33039
LEFTWICH, P. W. p 4033 N92-32502
LEGGE, G. J. F. p 4014 N92-33000
LEHNER, PAUL E. p 4088 N92-32551
LEITH, C. E. p 4010 N92-32824
LELLOUCH, EMMANUEL p 4101 N92-32401
p 4102 N92-32406
LEMAY, SCOTT P. p 3930 N92-32651
LENNON, W. J. p 4050 N92-32412
LEONARD, DESIREE M. p 4041 N92-33205
LESIEUR, M. p 3931 N92-32769
LESNE, P. M. p 3954 N92-32792
LESSARD, P. p 3976 N92-33243
LESTER, H. C. p 4063 N92-32958
LEVAN, P. p 4095 N92-32361
LEWIS, R. G. p 4028 N92-32543
LEWIS, TIM p 3937 N92-32446
LI, SHENG S. p 4083 N92-32747
LI, XINING p 4048 N92-33214
LI, ZHENG p 4064 N92-32316
LIANG, PAK-YAN p 3996 N92-32256
p 3945 N92-32259
LIANG, Y. p 4082 N92-32542
LIBESKIND, MARK p 3947 N92-32514
p 3948 N92-32519
LICHTENBERG, A. J. p 3982 N92-32905
LIKHODED, A. A. p 4065 N92-32498
LILIENTAL-WEBER, Z. p 4083 N92-32693
LIN, S. J. p 4001 N92-32283
p 4003 N92-32294
LINDHOLM, JULIE M. p 4046 N92-32907
LINDSAY, HOWARD A. p 3947 N92-32517
LING, J. p 3971 N92-32640
LINK, RICHARD E. p 4022 N92-32717
LINNARTZ, JOHAN PAUL MARIE GERARD p 3982 N92-32837
LIPPENS, C. p 3943 N92-32728
LIST, F. A. p 4084 N92-32919
LISZKA, LUDWIG p 4061 N92-32842
LIU, B. L. p 3996 N92-32255
LIU, C. T. p 3968 N92-32855
LIU, DIANTONG p 4051 N92-32821
LIU, HUA-KUANG p 4076 N92-33028
LIU, TSUEN-HSI p 4076 N92-33022
LOADER, CLIVE R. p 4044 N92-32873
LOEVE, W. p 4043 N92-32833
p 4011 N92-32835
LOH, HAI-TIEN p 3995 N92-32249
LONG, M. p 3965 N92-33121
LONG, M. DAVID p 4044 N92-32873
LONGTIN, D. R. p 4029 N92-32860
LONGUET-HIGGINS, MICHAEL S. p 4061 N92-32901
LOOMANS, M. E. p 4082 N92-32561
LOOMIS, WILLIAM R. p 3972 N92-32863
LOPEZ-KRAHE, JAIME p 4058 N92-32803
LOPEZ-MORENO, J. J. p 4096 N92-32367
LORCH, D. R. p 4061 N92-32950
LORENTS, DONALD C. p 4027 N92-33138
LORENZ, RALPH p 4101 N92-32402
LORENZ, RALPH D. p 4096 N92-32364
LOUIS, D. p 4022 N92-32774
p 3954 N92-32775
LOUIS, J.-F. p 4034 N92-32859
LOVRANICH, ERNST p 4071 N92-32763
LOWDERMILK, W. H. p 4079 N92-32733
LOWNDES, D. H. p 4082 N92-32636
p 4083 N92-32653
p 4085 N92-33023
LOWRY, JOHN C. p 4038 N92-32990
LOWRY, ROBERT W. p 3944 N92-33162
LUDWIG, GERSON OTTO p 4014 N92-32601
LUDWIGSEN, J. S. p 3944 N92-33166
LUKE, GARY D. p 3944 N92-32246
LUM, HENRY, JR. p 4040 N92-32809
LUM, K. K. p 4040 N92-32851
LUNINE, JONATHAN I. p 4093 N92-32349
p 4095 N92-32358
p 4098 N92-32381
LUO, J. p 3999 N92-32270
LUO, WEI p 4075 N92-32806
LUONG, V. p 4004 N92-32299
LUTTON, EVELYNE p 4058 N92-32803
LY, UY-LOI p 4046 N92-33091
LYKKE, K. R. p 4016 N92-33114
LYON, RICHARD E. p 3970 N92-32341

M

MABON, J. C. p 3966 N92-32614
MACCABEE, BRUCE p 4076 N92-33095
MACDOUGALL, J. E. p 4066 N92-32548
MACKALL, DALE p 3935 N92-33149
MACKENZIE, C. W. p 4022 N92-32848
MACPHERSON, J. I. p 3938 N92-32850
MADANI, RAFAI-MOURAD p 4057 N92-32713
MADDEN, ROLAND A. p 4028 N92-32554
MADER, L. R. p 3936 N92-32438
MADSEN, O. S. p 4007 N92-32630
MAGNI, G. p 4093 N92-32350
MAGRUDER, R. H. p 4085 N92-33127
MAHAN, K. A. p 3989 N92-32700
MAHANTHAPPA, K. T. p 4069 N92-33187
MAHJOUB, A. R. p 4056 N92-32711
MAHJOUBI, HEDI p 3963 N92-32722
MAHLER, M. A. p 3949 N92-32527
MAILLARD, J.-P. p 4101 N92-32401
MAINE, TRINDEL p 3940 N92-32864
MAITRE, HENRI p 4058 N92-32803
MALEC, HENRY A. p 3941 N92-32456
MALEY, M. P. p 4085 N92-33026
MANGOLD, SUSAN J. p 3932 N92-32941
MANLEY, JAMES E. p 4052 N92-32937
MANNING, JEROME E. p 4062 N92-32955
MANSKE, ROBERT A. p 3937 N92-32450
MARCUS, R. K. p 3964 N92-32925
MARHEFKA, R. J. p 4058 N92-32888
MARHIC, M. E. p 4016 N92-32540
MARINHO, ERALDO PEREIRA p 4093 N92-32604
MARIS, H. J. p 4103 N92-33119
MARIS, J. H. p 4020 N92-32564
MARKS, N. p 3957 N92-33042
MARMAR, E. S. p 4078 N92-32623
MARON, Y. p 4080 N92-32992
MARSEILLE, T. J. p 4030 N92-32986
MARSH, B. D. p 4050 N92-32568
MARSHALL, J. p 4070 N92-32567
MARTELL, ARTHUR E. p 3972 N92-32913
MARTIN, JAMES A. p 3943 N92-33013
MARTIN, VINCENT p 4062 N92-32956
MARTIN, W. R. p 4057 N92-32743
MARTZAKLIS, K. S. p 3983 N92-32968
MARZARI, F. p 4101 N92-32398
MASCIOLI, A. p 3990 N92-32847
MASKELL, SUZANNE Y. p 3982 N92-32818
MASMOUDI, R. p 3957 N92-33039
MASON, A. C. p 3976 N92-33244
MASON, E. H. p 4032 N92-32431
MASON, R. J. p 3992 N92-33068
MASOTTO, T. K. p 4052 N92-33100
p 4052 N92-33101
MATHAN, LUC p 3981 N92-32807
MATIJASEVIC, V. C. p 4083 N92-32653
MATSON, DENNIS L. p 4097 N92-32377
p 4099 N92-32387
MATTHEWS, CHRISTINE G. p 4041 N92-33205
MATYJASZEWSKI, KRZYSZTOF p 3971 N92-32547
MAY, D. N. p 4061 N92-32950
MAY, NOAL D. p 4061 N92-32697
MAY, WILHELM p 4028 N92-32554
MAYER, RICHARD J. p 4042 N92-32627
p 4042 N92-32658
MAZIASZ, P. J. p 4020 N92-33085
MAZURE, MARIE-LAURENCE p 4057 N92-32761
MCCALLUM, J. C. p 4085 N92-33127
MCCARTHY, I. E. p 4064 N92-32340
p 4065 N92-32501
p 4087 N92-32649
MCCAULEY, HOWARD p 3936 N92-32441
p 3936 N92-32442
MCCAULEY, S. W. p 4082 N92-32512
MCCHESNEY, J. M. p 4078 N92-32623
MCCLEARY, SUSAN L. p 4023 N92-33104
MCCONNAUGHEY, H. V. p 4001 N92-32279
MCCREDIE, BRADLEY D. p 3984 N92-32974
MCCRIGHT, R. D. p 3969 N92-33132
MCDEVITT, J. T. p 3990 N92-32827
MCDONNELL, J. A. M. p 4102 N92-32410
MCGARRY, FRANK p 4044 N92-32872
MCGHEE, R. B. p 4053 N92-32748
MCGRAW, SANDRA M. p 3934 N92-32536
MCGUIGAN, M. p 4064 N92-32313
MCHENRY, M. E. p 4085 N92-33026
MCKAMEY, C. G. p 4020 N92-33085
MCKAY, CHRISTOPHER P. p 4095 N92-32358
p 4095 N92-32361
p 4097 N92-32372
MCLARNON, F. R. p 3993 N92-33183
MCLAUGHLIN, MICHAEL P. p 3933 N92-32537
MCMASTER, LEONARD R. p 4031 N92-33097
MCPHEE, JOHN JOSEPH p 4024 N92-33228
MEARS, OTHO L. p 3944 N92-33162
MEDLEY, S. p 4078 N92-32623
MEIJER, J. J. p 3939 N92-32750
MELISSINOS, A. C. p 4061 N92-32430
MENA, RAFAEL A. p 3984 N92-32976
p 3984 N92-32978
MENDOZA, JOHN p 4007 N92-32560
MENEGAT, A. p 4071 N92-32751
MENICUCCI, D. p 4026 N92-32923
MERCURIO, U. p 3958 N92-33044
MERKELO, HENRI p 3984 N92-32974
MERKLE, B. p 4081 N92-32465
MERKLE, C. L. p 3998 N92-32264
p 4001 N92-32282
MERKLE, CHARLES L. p 4001 N92-32284
MERRILL, CLAUDE I. p 3976 N92-33242
MESHII, M. p 4086 N92-33221
METZLER, S. p 3985 N92-32981
MEYER, A. J. p 4052 N92-33100
p 4052 N92-33101
MEYER, T. J. p 3971 N92-32631
MEYERS, ROGER M. p 3944 N92-33064
MICHAELS, ROBERT L. p 4076 N92-33074
MICKELSON, M. p 4034 N92-32859
MILES, R. p 4101 N92-32403
MILL, C. S. p 4100 N92-32391
p 4101 N92-32399
MILL, THEODORE p 4027 N92-33138
MILLAR, J. p 3935 N92-32326
MILLER, D. J. p 4081 N92-32346
MILLER, JEFFRY J. p 3992 N92-33175
MILLER, M. K. p 3969 N92-33158
MILLER, MARTIN S. p 3974 N92-32664
MILLER, W. A. p 4088 N92-33069
MILLS, HARLAN D. p 4045 N92-32881
MINER, KEVIN R. p 3948 N92-32524

MING, Z. H. ..... p 4081 N92-32470
p 4086 N92-33136
MIRANDA, FELIX A. ..... p 3985 N92-32983
MITAL, S. K. ..... p 3946 N92-32466
MOATS, CHRISTINA D. ..... p 3944 N92-33112
MODAHL, R. J. ..... p 3977 N92-32723
MODI, VIJAY ..... p 4000 N92-32274
MOELLER, R. P. ..... p 4074 N92-32634
MOHAMED, AHMED S. ..... p 4054 N92-33203
MOHEB, HAMID ..... p 3987 N92-33192
MOHN, DAVID G. ..... p 4039 N92-33079
MOLIAN, ARUL ..... p 3956 N92-32906
MOLIAN, P. ..... p 3956 N92-32906
MOLL, A. J. ..... p 4085 N92-33117
MOLTON, P. ..... p 3931 N92-32800
MONFORD, LEO G., JR. ..... p 4019 N92-33018
MONFORTON, GERALD G. ..... p 4053 N92-33217
MONK, JAN C. ..... p 3945 N92-32281
MONTES, ANTONIO ..... p 4014 N92-32601
MOONEY, JACK L. ..... p 4027 N92-33138
MOORE, GARY ..... p 4103 N92-32338
MOORE, JOAN G. ..... p 4003 N92-32292
MOORE, JOHN ..... p 4003 N92-32292
MOORE, THOMAS C., SR. ..... p 3978 N92-33020
MOORE, WILLIAM E. ..... p 3937 N92-32450
MOROSIN, B. ..... p 4084 N92-32920
MOROZ, WALTER J. ..... p 3990 N92-32812
MORRIS, G. MICHAEL ..... p 4076 N92-33074
MORRIS, TIMOTHY B. ..... p 3969 N92-33081
MORRISH, ARTHUR A. ..... p 3973 N92-33170
MORSE, D. H. ..... p 4014 N92-32999
p 4068 N92-33001
MORTON, D. P. ..... p 4052 N92-33100
p 4052 N92-33101
MORTON, JOHN ..... p 3950 N92-32532
p 3959 N92-33075
MOSER, M. ..... p 3998 N92-32264
MOSES, W. W. ..... p 4082 N92-32493
MOSKOW, HARRY J. ..... p 3988 N92-32964
MOTOJIMA, O. ..... p 4070 N92-32746
MOTOYAMA, STEPHEN M. ..... p 3947 N92-32517
MOU, Y. ..... p 3967 N92-32699
MUEHE, C. E. ..... p 3980 N92-32680
MUELLER, CHRISTIAN ..... p 4098 N92-32379
MUELLER, G. A. ..... p 4071 N92-32808
MULLER, C. ..... p 3943 N92-32728
MURRAY, ALVIN L. ..... p 3945 N92-32272
MURRAY, J. R. ..... p 4079 N92-32733
MURRAY, R. W. ..... p 3990 N92-32827
MURTHY, P. L. N. ..... p 3946 N92-32466
p 3949 N92-32531
MURTY, A. N. ..... p 3960 N92-32347
MYLES, K. M. ..... p 3988 N92-32639

N

NAESLUND, ERIK ..... p 4029 N92-32785
NAGIB, HASSAN M. ..... p 4008 N92-32671
NAHOUM, R. ..... p 4099 N92-32390
NAIR, PREMCHAND SUKUMARAN
p 4049 N92-33227
NALLAPPA, BHASHYAM ..... p 4088 N92-32551
NANTISTA, C. ..... p 4071 N92-32751
NARANG, SUBHASH ..... p 4027 N92-33138
NARAYANAN, T. SRINIVASAN ..... p 4049 N92-33232
NARDONE, S. C. ..... p 4059 N92-32989
NASH, A. S. ..... p 4082 N92-32561
NATESAN, K. ..... p 3974 N92-33247
NATISHAN, PAUL M. ..... p 3973 N92-33170
NAUENBERG, U. ..... p 4069 N92-33187
NAUTA, BRAM ..... p 3986 N92-33143
NAYAR, N. ..... p 4088 N92-33109
NAYLOR, B. ..... p 4042 N92-32617
NEAL, DONALD M. ..... p 3951 N92-32581
NEHRKORN, T. ..... p 4034 N92-32859
NEIL, V. K. ..... p 4071 N92-32904
NELSON, B. A. ..... p 4078 N92-32595
NELSON, P. A. ..... p 4062 N92-32957
NELSON, R. M. ..... p 4097 N92-32377
NELSON, RICHARD C. ..... p 4038 N92-32660
NEMETH, MICHAEL P. ..... p 3952 N92-32587
NESTHUS, THOMAS E. ..... p 4036 N92-32492
NEUBAUER, F. M. ..... p 4099 N92-32385
NEUMAN, FRANK ..... p 3933 N92-33194
NEVELS, R. D. ..... p 4055 N92-32670
NEWTON, M. A. ..... p 4071 N92-32904
p 4072 N92-33122
NG, DAVID TUNG HIM ..... p 4054 N92-33218
NG, E. G. ..... p 4055 N92-32428
p 4052 N92-32926
NGO, KIM CHI T. ..... p 3991 N92-33021
NGUYEN, CHARLES C. ..... p 4019 N92-32885
NGUYEN, HUNG T. ..... p 4056 N92-32685
NIBLETT, D. H. ..... p 4102 N92-32410
NICHOLAS, O. P. ..... p 3939 N92-32788
NICHOLS, R. ..... p 4070 N92-32567
NICKS, ORAN ..... p 3932 N92-33063
NIELSEN, C. ..... p 4065 N92-32473
NIEMANN, HASSO B. ..... p 4098 N92-32379
NIEUWENHUIS, LAMBERTUS JOHANNES MARIA
p 4047 N92-33142
NIROV, KH. S. ..... p 4055 N92-32602
NISTLER, NOEL F. ..... p 3938 N92-32435
NIX, WILLIAM D. ..... p 3946 N92-32339
NOBLE, R. D. ..... p 3960 N92-32332
NOEL, D. PETER ..... p 3993 N92-33208
NOLL, K. S. ..... p 4097 N92-32376
NORLIN, KENNETH ..... p 3935 N92-33149
NORONHA, C. ..... p 3979 N92-32573
NORTON, D. ..... p 4082 N92-32636
NORTON, D. P. ..... p 4083 N92-32653
p 4085 N92-33023
NOVAK, BRUCE M. ..... p 3955 N92-32828
NUECKER, N. ..... p 4081 N92-32470
p 4086 N92-33136

O

OCONNOR, MICHAEL ..... p 4088 N92-32551
ODONNELL, R. G. ..... p 3970 N92-32489
OETTING, J. D. ..... p 3947 N92-32518
OHAIR, MARK A. ..... p 3937 N92-32446
OHBA, MITSURU ..... p 4045 N92-32879
OKAMOTO, P. R. ..... p 4086 N92-33221
OKUBO, S. ..... p 4061 N92-32430
OLONA, G. T. ..... p 4068 N92-33001
OLSEN, GREGORY H. ..... p 4076 N92-33004
OLSEN, S. ..... p 4061 N92-32430
OPLINGER, DON W. ..... p 3947 N92-32516
ORTON, GLENN ..... p 4095 N92-32359
OSGOOD, R. M., JR. ..... p 4082 N92-32641
OSLAC, MICHAEL J. ..... p 3988 N92-32964
OSULLIVAN, S. ..... p 4070 N92-32567
OWEN, TOBIAS ..... p 4097 N92-32374
OWEN, VICKI L. ..... p 3953 N92-32589

P

PACHECO, J. E. ..... p 4027 N92-33150
PAILLARD, JACQUES ..... p 4062 N92-32956
PAILLOUS, P. ..... p 4096 N92-32368
p 4100 N92-32397
p 4101 N92-32400
PAIPETIS, S. A. ..... p 3959 N92-33050
PAJERSKI, ROSE ..... p 4044 N92-32871
PAL, S. ..... p 3998 N92-32264
PALMER, RICHARD S. ..... p 4042 N92-32546
PALMER, T. S. ..... p 4057 N92-32743
PAMULAPATI, J. ..... p 3984 N92-32977
PANKOV, A. A. ..... p 4065 N92-32498
PAO, C. K. ..... p 3983 N92-32966
PAONESSA, A. ..... p 4063 N92-32962
PAPAGEORGIU, ELENA ..... p 4068 N92-33135
PAPAVERGOS, PANAYIOTIS G. ..... p 4011 N92-32856
PAPINEAU, N. ..... p 3943 N92-32728
PARISOT, J. P. ..... p 4096 N92-32366
p 4100 N92-32396
p 4102 N92-32408
PARKER, D. H. ..... p 4016 N92-33114
PARKER, D. J. ..... p 4015 N92-32392
PARKER, M. J. ..... p 4013 N92-32460
PARKS, P. B. ..... p 4078 N92-32623
PARSONS, G. R. ..... p 3947 N92-32515
PATIL, H. S. ..... p 4022 N92-32783
PATTERSON, MICHAEL J. ..... p 3944 N92-33064
PATTERSON, W. L. ..... p 4035 N92-32688
PAUL, ALORA K. ..... p 4091 N92-33088
PAUL, GREG ..... p 3953 N92-32629
PAUL, N. L. ..... p 4029 N92-32860
PAUL, P. C. ..... p 3949 N92-32527
PAYAN, ERIC ..... p 4051 N92-32768
PEARSON, RICHARD J. ..... p 4008 N92-32683
PECK, S. R. ..... p 3990 N92-32827
PEIFER, WILLIAM R. ..... p 3961 N92-32509
PELLIN, M. J. ..... p 4016 N92-33114
PENNYCOOK, S. J. ..... p 4085 N92-33023
PERAKATH, BENJAMIN ..... p 4042 N92-32627
PERERA, L. ..... p 4066 N92-32682
PERERA, R. C. C. ..... p 4067 N92-32997
PERERA, U. ..... p 4066 N92-32702
PESCE-RODRIGUEZ, ROSE A. ..... p 3974 N92-32664
PETERS, T. J. ..... p 3982 N92-32891
PETERSEN, E. L. ..... p 4027 N92-33072
PETRIE, T. W. ..... p 4080 N92-32995
PEYTON, B. W. ..... p 4055 N92-32428
PHAM, TUAN D. ..... p 4056 N92-32685
PHELPS, R. B. ..... p 3963 N92-32666
PHILIPS, JOHN ..... p 4041 N92-32451
PIASCIK, ROBERT S. ..... p 4021 N92-32423
PIN, F. G. ..... p 4018 N92-32694
PINNINGTON, R. J. ..... p 4062 N92-32957
PITZ, W. J. ..... p 3961 N92-32544
PLATT, C. M. R. ..... p 4015 N92-33188
PLOT-LOCATELLI, SYLVIE ..... p 3931 N92-32773
PLYUSHCHAJ, M. S. ..... p 4087 N92-32603
POCHEC, PRZEMYSLAW ..... p 4077 N92-33202
POCHKOWSKI, J. M. ..... p 3964 N92-32925
POEPPEL, R. B. ..... p 4082 N92-32561
POGANY, A. ..... p 4085 N92-33127
POGGIOLINI, P. ..... p 3979 N92-32573
p 4050 N92-32628
POIRIER, P. ..... p 4015 N92-32329
POLITES, MICHAEL E. ..... p 4015 N92-33010
POLLACK, J. B. ..... p 4095 N92-32358
POLLINGER, J. P. ..... p 3971 N92-32640
PONCHAK, GEORGE E. ..... p 3983 N92-32971
POND, JEFFREY M. ..... p 3992 N92-33169
PONTAU, A. E. ..... p 4014 N92-32999
p 4068 N92-33001
POON, C. ..... p 3955 N92-32852
p 3957 N92-33040
POORMAN, RICHARD M. ..... p 3991 N92-33030
POPPE, GERT PIERRE MARIA ..... p 4074 N92-32703
PORTER, ADAM A. ..... p 4044 N92-32875
POSENAU, MARY-ANNE ..... p 4041 N92-33205
POTHEN, A. ..... p 4046 N92-33071
POWELL, ROBERT L. ..... p 3961 N92-32508
PRAGER, S. C. ..... p 4078 N92-32599
p 4080 N92-33154
PRAKASH, J. ..... p 3988 N92-32639
PRASAD, C. B. ..... p 3948 N92-32523
PREBLE, J. ..... p 4070 N92-32567
PRENGLE, H. W., JR. ..... p 4026 N92-32908
PRETTEREBNER, J. ..... p 4071 N92-32808
PRICE, G. R. ..... p 4037 N92-32916
PRIGOGINE, I. ..... p 4087 N92-32593
PRIMDAHL, K. ..... p 4069 N92-32314
PROCTOR, I. D. ..... p 4068 N92-33001
PROGAR, DONALD J. ..... p 3973 N92-33014
PROMISLOW, J. H. ..... p 3972 N92-32667
PRUEGER, GEORGE H. ..... p 4003 N92-32293
PRZEKWAS, A. J. ..... p 3996 N92-32257
PUGLIESI, V. ..... p 4009 N92-32687

Q

QUADRACCI, RICHARD ..... p 4000 N92-32274
QUANDT, EARL ..... p 4008 N92-32652
QUIGNON, J. ..... p 3936 N92-32444
p 3937 N92-32445
QUIRICO, ERIC ..... p 4102 N92-32406
QUOC, HOAN XUAN ..... p 3963 N92-32724

R

RAATSCHEN, W. ..... p 3977 N92-32825
RACCA, ROBERTO GIACOMO G. ..... p 4013 N92-33226
RADDER, J. A. ..... p 3988 N92-32495
RAGAY, FREDERIK WILLEM ..... p 3992 N92-33144
RAGHARAN, BHARATHI ..... p 4052 N92-32886
RAGHEB, H. A. ..... p 3981 N92-32787
RAIZENNE, M. D. ..... p 3957 N92-33040
RAJEEV, S. G. ..... p 4061 N92-32430
RAKULJIC, GEORGE A. ..... p 4013 N92-32323
RAMACHANDRAN, N. ..... p 3998 N92-32263
RAMAMOORTHY, P. A. ..... p 4053 N92-32625
RAMANATHAN, V. ..... p 4032 N92-32331
RANCOITA, P. G. ..... p 4064 N92-32316
RANDELL, G. P. ..... p 4089 N92-32342
RANFONE, STEFANO ..... p 4068 N92-33135
RANKIN, P. ..... p 4069 N92-33187
RANSICK, M. ..... p 3967 N92-32721
RANSOM, JONATHAN B. ..... p 3949 N92-32528
p 4023 N92-33104
RAO, D. V. ..... p 4072 N92-32994
RAO, M. ..... p 3966 N92-32432
RAPOFF, ANDREW J. ..... p 3951 N92-32580
RAPPOLD, VIRGINIA A. ..... p 4038 N92-32990
RASERA, R. L. ..... p 3970 N92-32471
RASPOTNIK, WILLIAM B. ..... p 3935 N92-32612
RATCLIFF, MARK ..... p 4004 N92-32296
RATCLIFF, P. R. ..... p 4100 N92-32391
p 4102 N92-32410
RATNAVELU, K. ..... p 4065 N92-32501
RATTAGGI, M. ..... p 4064 N92-32316
RAUENZAHN, R. M. ..... p 4013 N92-33159
RAUH, RAINER ..... p 3967 N92-32819
p 3968 N92-32697
RAULIN, FRANCOIS ..... p 4096 N92-32368
p 4098 N92-32379
p 4099 N92-32390
p 4100 N92-32395
p 4100 N92-32397
p 4101 N92-32400

RAWLIN, VINCENT K. ..... p 3944 N92-33064
RAZUMOV, A. V. ..... p 4055 N92-32602
REA, K. ..... p 4027 N92-32415
REDDY, N. N. ..... p 4061 N92-32949
REDEY, L. ..... p 3988 N92-32639
REDONDO, E. ..... p 3958 N92-33046
REESE, T. M. ..... p 4074 N92-32672
REID, L. D. ..... p 3934 N92-32845
REISTER, D. B. ..... p 4018 N92-32694
REJ, D. J. ..... p 3992 N92-33068
RENARD, J. ..... p 3954 N92-32792
RENGER, KLAUS ..... p 4062 N92-32951
RENK, T. J. ..... p 4080 N92-32992
RENLUND, A. M. ..... p 3974 N92-32637
RESKE, EDWARD J. ..... p 4005 N92-32304
RESTORFF, J. B. ..... p 4084 N92-32938
RIBNER, H. S. ..... p 3938 N92-33102
RICE, JANE K. ..... p 4082 N92-32512
RICH, JOSEPH P. ..... p 4045 N92-32878
RICHARD, M. A. ..... p 3985 N92-32981
RICHMOND, MIKE ..... p 4034 N92-33163
RIDDER, JEFFREY P. ..... p 4000 N92-32276
RIFKIN, STAN ..... p 4044 N92-32876
ROBB, J. ..... p 4070 N92-32567
ROBBINS, WILLIAM E. ..... p 4076 N92-33017
ROBERDS, W. J. ..... p 4028 N92-32558
ROBERTS, M. L. ..... p 4068 N92-33001
RODMAN, J. A. ..... p 4090 N92-32930
RODMAN, JOHN A. ..... p 4090 N92-32985
RODRIGO, R. ..... p 4096 N92-32367
RODRIGUEZ, A. T. ..... p 3958 N92-33046
ROEHL, JAMES S. ..... p 4026 N92-32943
ROELOFS, HAROLD HENDRIKUS BERNARDUS ..... p 4018 N92-32692
ROGERS, J. H. ..... p 4077 N92-32533
ROGERS, STUART ..... p 4012 N92-33113
ROLISON, DEBRA ..... p 3963 N92-32755
ROSENFELD, DAVID ..... p 3985 N92-32979
ROSENZWEIG, EDWIN L. ..... p 3960 N92-33174
ROSS, SHELDON M. ..... p 4020 N92-33151
ROSSMANITH, R. ..... p 4069 N92-32318
..... p 4069 N92-32319
ROTE, D. M. ..... p 4017 N92-32615
ROTH, CARL ..... p 4055 N92-33219
ROTH, G. ..... p 4081 N92-32470
..... p 4086 N92-33136
ROTUNDI, A. ..... p 4101 N92-32404
ROUCHON, JEAN ..... p 3958 N92-33048
ROWLAND, MICHAEL W. ..... p 4031 N92-33097
ROY, C. ..... p 3955 N92-32813
..... p 3957 N92-33039
ROY, LANGIS ..... p 3993 N92-33211
RUEB, KURT DIETER ..... p 4048 N92-33210
RUESKAMP, K. ..... p 3937 N92-32448
RUF, JOSEPH H. ..... p 3997 N92-32260
..... p 3997 N92-32261
RUGGLES, A. E. ..... p 4006 N92-32468
RUTH, R. D. ..... p 4071 N92-32751
RYAN, H. ..... p 3998 N92-32264
RYAN, J. ..... p 4057 N92-32772
RYMER, W. Z. ..... p 4016 N92-32540

S

SABLE, CLAUDE ..... p 4098 N92-32379
SABNIS, J. S. ..... p 3966 N92-32307
SABNIS, JAYANT S. ..... p 3999 N92-32269
..... p 4002 N92-32289
SADOVSKIJ, S. A. ..... p 4087 N92-32309
SAETHER, ERIK ..... p 3949 N92-32529
SAFF, C. R. ..... p 3949 N92-32527
SAGAN, CARL ..... p 4096 N92-32369
..... p 4096 N92-32370
SAGDEEV, R. Z. ..... p 4078 N92-32592
SAHAI, V. ..... p 4006 N92-32322
SAHM, P. R. ..... p 3967 N92-32619
SAIGAL, A. ..... p 3953 N92-32638
SAINT, A. ..... p 4014 N92-33000
SAK, STEVE ..... p 4088 N92-32551
SALERNO, L. J. ..... p 4007 N92-32474
SALONEN, P. ..... p 3973 N92-33059
SAMOJLENKO, V. D. ..... p 4064 N92-32310
SAMUELSON, ROBERT E. ..... p 4097 N92-32373
..... p 4098 N92-32378
SANGER, KENNETH B. ..... p 3949 N92-32527
..... p 3951 N92-32580
SANTORO, R. J. ..... p 3998 N92-32264
SANTORU, J. ..... p 3980 N92-32719
SANUKI, H. ..... p 4079 N92-32745
SAROFIM, A. F. ..... p 4030 N92-33125
SAWDY, D. ..... p 3950 N92-32578
SAWKO, PAUL M. ..... p 3970 N92-32476
SCATTERGOOD, THOMAS W. ..... p 4102 N92-32405
SCHACHAM, S. E. ..... p 3984 N92-32974
..... p 3984 N92-32975
..... p 3984 N92-32976
SCHERRER, P. H. ..... p 4103 N92-32488
SCHIESSER, W. ..... p 4060 N92-32998
SCHIESSER, W. E. ..... p 4052 N92-32926
SCHIFLETT, SAMUEL G. ..... p 4036 N92-32492
SCHILLING, LAWRENCE ..... p 3935 N92-33149
SCHMITT, BERNARD ..... p 4101 N92-32401
..... p 4102 N92-32406
SCHNACK, D. D ..... p 4078 N92-32599
SCHNETZER, G. H. ..... p 4032 N92-32427
SCHOEMIG, EWALD ..... p 4046 N92-33091
SCHOLLE, ELIZABETH ANN ..... p 4077 N92-32417
SCHRAML, STEPHEN J. ..... p 4008 N92-32683
SCHRANNER, RUDOLF ..... p 3937 N92-32448
SCHROEDER, MICHAEL A. ..... p 3974 N92-32664
SCHUELLER, P. G. ..... p 4071 N92-32808
SCHULLER, I. K. ..... p 4081 N92-32462
SCHUMACHER, R. W. ..... p 3980 N92-32719
SCHWARZ, R. B. ..... p 3969 N92-33120
SCHWENKER, R. ..... p 3970 N92-32471
SCIME, E. E. ..... p 4078 N92-32624
SCOTT, M. L. ..... p 4050 N92-32568
SCOTT, R. F. ..... p 3954 N92-32791
..... p 3959 N92-33051
SEBAG, SAMUEL ..... p 4009 N92-32725
SEEMAN, J. T. ..... p 4072 N92-33070
SEIDEL, G. M. ..... p 4103 N92-33119
SEKULA-MOISE, P. A. ..... p 3984 N92-32977
SELLBERG, B. ..... p 4027 N92-33072
SENGUPTA, S. ..... p 4081 N92-32346
SERAJI, HOMAYOUN ..... p 4054 N92-33019
SETTLES, G. S. ..... p 3930 N92-32494
SEVERS, WALTER B. ..... p 4037 N92-32539
SEYED-SOLORFOROUGH, MIR-MASOOD ..... p 4088 N92-32551
SFERRINO, V. J. ..... p 3989 N92-32678
SHAFAI, L. ..... p 3981 N92-32787
SHALKHAUSER, K. A. ..... p 3983 N92-32968
SHANG, H. M. ..... p 3997 N92-32258
SHANKLE, D. L. ..... p 4030 N92-32986
SHANNON, ROBERT V., JR. ..... p 3945 N92-32272
SHARMA, S. ..... p 4073 N92-32419
SHARP, W. M. ..... p 4070 N92-32413
SHASHKOV, MIKHAIL Y. ..... p 4009 N92-32767
SHAW, DAVID T. ..... p 3988 N92-32659
SHAW, H. A. ..... p 4102 N92-32410
SHAY, H. D. ..... p 4072 N92-33122
SHEA, DENNIS J. ..... p 4028 N92-32554
SHEALY, R. T. ..... p 4034 N92-33173
SHEARES, V. V. ..... p 3972 N92-32667
SHEEHAN, MICHAEL J. ..... p 3986 N92-32987
SHEEN, JOHN ..... p 3935 N92-33149
SHELLMAN, C. H. ..... p 4035 N92-33220
SHEMANSKY, D. E. ..... p 4094 N92-32357
SHEPARD, P. F. ..... p 4066 N92-32702
SHEPHERD, KEVIN P. ..... p 4063 N92-33160
SHERMAN, B. ..... p 3939 N92-32778
SHERMER, THOMAS C. ..... p 4049 N92-33229
SHEVENELL, L. ..... p 4028 N92-32616
SHI, D. ..... p 4081 N92-32346
SHIH, T. H. ..... p 4011 N92-32868
SHLICHTA, P. J. ..... p 4082 N92-32493
SHOEMAKER, M. ..... p 3999 N92-32268
SHU, CHI-WANG ..... p 4012 N92-33110
SHU, D. ..... p 4072 N92-33130
SHUART, M. J. ..... p 3948 N92-32523
SHYY, WEI ..... p 4000 N92-32277
SIDIKMAN, K. L. ..... p 4080 N92-33154
SIEG, R. M. ..... p 3984 N92-32977
SIGELLE, MARC ..... p 4058 N92-32802
SIGETY, P. ..... p 3957 N92-33042
SIL, AJIT K. ..... p 3983 N92-32969
SILCOX, R. J. ..... p 4063 N92-32958
SIMAR, LEOPOLD ..... p 4060 N92-32718
SIMMIE, J. M. ..... p 3961 N92-32544
SIMONICH, J. C. ..... p 3962 N92-32594
SIMONS, RAINEE N. ..... p 3983 N92-32967
..... p 3983 N92-32968
..... p 3983 N92-32969
..... p 3983 N92-32970
..... p 3983 N92-32972
..... p 3984 N92-32973
SIMPSON, M. A. ..... p 4061 N92-32950
SINDIR, M. M. ..... p 4001 N92-32283
SINDIR, MUNIR ..... p 4001 N92-32285
SINDIR, MUNIR M. ..... p 3998 N92-32266
..... p 4000 N92-32273
..... p 3960 N92-32275
SINGH, GURBAX ..... p 3974 N92-32664
SIRCAR, JAYANTA K. ..... p 4024 N92-32590
SIVERS, E. A. ..... p 3971 N92-32640
SJOEGREN, M. ..... p 3977 N92-32825
SLATTERY, P. ..... p 4061 N92-32430
SMIT, HERMAN JANNES ..... p 4056 N92-32679
SMITH, A. ..... p 3998 N92-32263
SMITH, EDWYN D. ..... p 3984 N92-32978
SMITH, G. C. ..... p 4086 N92-33136
SMITH, J. ..... p 3940 N92-32734
SMITH, J. G. ..... p 4069 N92-33187
SMITH, JAMES E. ..... p 4092 N92-32478
SMITH, KENT F. ..... p 3947 N92-32517
SMITH, M. G. ..... p 4036 N92-32434
SMITH, PAUL ..... p 3971 N92-32665
SMITH, PHILIP N. ..... p 3933 N92-32424
SMITH, W. H. ..... p 3966 N92-32614
SMITH, WENDY SARAH ..... p 3987 N92-33213
SMITHER, C. L. ..... p 4014 N92-32620
SMITHERS, G. A. ..... p 4036 N92-33103
SMOOKE, M. ..... p 3965 N92-33121
SNIPES, J. A. ..... p 4078 N92-32623
SNYDER, P. G. ..... p 3984 N92-32977
SOEDER, JAMES F. ..... p 3991 N92-32867
SOHN, LYDIA L. ..... p 4084 N92-32898
SOIZE, C. ..... p 4010 N92-32776
SOKOLOSKI, MARTIN M. ..... p 3985 N92-32980
SOLLO, ANTONIO ..... p 4062 N92-32956
SOLOVJOV, ANDREY V. ..... p 4009 N92-32767
SOMA, NEI YOSHIHIRO ..... p 4055 N92-32661
SONG, HER-KING ..... p 4027 N92-33138
SONI, BHARAT K. ..... p 4004 N92-32300
..... p 4005 N92-32302
SONI, T. ..... p 4075 N92-32935
SOO, Y. L. ..... p 4081 N92-32470
SOTIN, C. ..... p 4097 N92-32377
SOVEY, JAMES S. ..... p 3944 N92-32463
..... p 3944 N92-33064
SPEARS, K. G. ..... p 4016 N92-32540
SPEKREIJSE, S. P. ..... p 3930 N92-32730
SPENCER, A. J. M. ..... p 3957 N92-33037
SPIVAK, A. L. ..... p 4007 N92-32474
SRIDHAR, BANAVAR ..... p 3933 N92-32424
SRINIVASAN, S. R. ..... p 3969 N92-33120
SROKOSZ, MERIC A. ..... p 4100 N92-32394
ST.CLAIR, TERRY L. ..... p 3973 N92-33014
STACY, KATHRYN ..... p 4041 N92-33205
STAGER, PAUL ..... p 4038 N92-32817
STAMMES, PIET ..... p 4097 N92-32375
..... p 4102 N92-32407
STAN, M. A. ..... p 3985 N92-32984
STARNES, JAMES H., JR. ..... p 3946 N92-32513
..... p 3950 N92-32574
STEEN, GREGORY ..... p 3932 N92-33063
STEFANOVSKAYA, N. V. ..... p 3962 N92-32557
STEFANOVSKII, V. M. ..... p 3962 N92-32557
STEGER, FERDINAND ..... p 4071 N92-32763
STEINBRENNER, JOHN P. ..... p 4005 N92-32301
STELBOVICS, A. T. ..... p 4065 N92-32499
STEPHENS, DAVID G. ..... p 4061 N92-32948
STERNBERGH, D. D. ..... p 3946 N92-32339
STEUART, S. ..... p 3935 N92-32326
STEVENSON, DAVID J. ..... p 4094 N92-32352
STEVENSON, L. E. ..... p 3934 N92-32308
STEVENSON, T. J. ..... p 4102 N92-32410
STEYER, JEAN-PHILIPPE ..... p 4036 N92-32844
STOLLER, R. E. ..... p 3969 N92-33115
STOLOVITCH, L. ..... p 4058 N92-32838
STOMPEL, S. ..... p 3972 N92-32667
STONE, BRADLEY M. ..... p 4102 N92-32405
STONE, JAMES R. ..... p 3944 N92-32463
STONEMAN, ROBERT C. ..... p 4017 N92-33165
STORM, E. ..... p 4079 N92-32733
STOWE, MIKE ..... p 3953 N92-32629
STOWERS, I. F. ..... p 3966 N92-32646
STREIT, SYLVIA ..... p 4071 N92-32763
STRICKLAND, PETER C. ..... p 3987 N92-33209
STRONG, K. ..... p 4101 N92-32401
STROUD, P. ..... p 4016 N92-32736
..... p 4075 N92-32738
STRUBLE, G. L. ..... p 3964 N92-32929
STRY, JAMES ..... p 4066 N92-32556
STUCKY, G. D. ..... p 4066 N92-32548
STUFFLEBEAM, J. H. ..... p 3963 N92-32645
STURGEON, WAYNE R. ..... p 4039 N92-32790
SU, YINGZHONG ..... p 4085 N92-33111
SUBUDHI, M. ..... p 3988 N92-32635
SUGUMARAN, VIJAYAN ..... p 4046 N92-32882
SUMICH, MARK ..... p 3949 N92-32526
SUMMERS, L. K. ..... p 3970 N92-32317
SUTER, U. W. ..... p 3965 N92-33185
SUTTER, GUY ..... p 4018 N92-32726
SVENSSON, T. ..... p 4025 N92-32605
SZEWCZYK, ALBIN A. ..... p 4006 N92-32324
SZOT, HENRY J. ..... p 3937 N92-32449

T

TAIEB, CHARLEY ..... p 4031 N92-32889
TAKADA, YOSHIHIRO ..... p 4044 N92-32874
TALAGRAND, O. ..... p 4095 N92-32361
TAN, ING HWIE ..... p 4079 N92-32944
TANG, C. L. ..... p 4075 N92-32915
TANG, YUAN YAN ..... p 4048 N92-33201

TANIGUCHI, Y. ..... p 4070 N92-32746
TANVEER, S. ..... p 4010 N92-32784
TARANENKO, Y. N. ..... p 4074 N92-32668
TARBELL, T. D. ..... p 4103 N92-32488
TASHMASEBI, F. ..... p 4054 N92-33184
TAUB, SUSAN R. ..... p 3983 N92-32972
p 3984 N92-32973
TAUC, J. ..... p 4020 N92-32564
TAVAKOLI, IRAJ ..... p 4046 N92-32882
TAYLOR, SHARON A. ..... p 3961 N92-32553
TENNANKORE, K. N. ..... p 3961 N92-32475
TERRY, J. L. ..... p 4078 N92-32623
TESSLER, ALEXANDER ..... p 3949 N92-32529
THAKUR, SIDDHARTH ..... p 4000 N92-32277
THANING, LENNART ..... p 4029 N92-32785
THART, W. G. J. ..... p 3957 N92-33042
THIBOUTOT, S. ..... p 3976 N92-33243
THIEBERGER, P. ..... p 4070 N92-32411
THIONNET, A. ..... p 3954 N92-32792
THOMAS, D. K. ..... p 4085 N92-33127
THOMAS, D. R. ..... p 4062 N92-32957
THOMAS, J. C. ..... p 4077 N92-32533
THOMPSON, DANNIELLA M. ..... p 3949 N92-32528
THOMPSON, J. ..... p 3958 N92-33047
THOMPSON, J. A. ..... p 4066 N92-32702
THOMPSON, MARGARET C. ..... p 4044 N92-32874
THOMPSON, W. REID ..... p 4096 N92-32369
p 4096 N92-32370
THOMSON, J. O. ..... p 4082 N92-32636
THORDSEN, MARVIN L. ..... p 4039 N92-32433
THOREAU, D. ..... p 3936 N92-32444
THORN, C. B. ..... p 4064 N92-32313
THORNELOE, S. A. ..... p 4028 N92-32609
THUILLIER, GERARD ..... p 4031 N92-32889
THURMAN, A. G. ..... p 4030 N92-32986
TIEGS, T. N. ..... p 3956 N92-32945
TIPTON, P. ..... p 4061 N92-32430
TISONE, G. C. ..... p 4080 N92-32992
TITLE, A. M. ..... p 4103 N92-32488
TOBIN, M. T. ..... p 4079 N92-32733
TODD, J. R. ..... p 3939 N92-32778
TONCICH, S. S. ..... p 3985 N92-32982
TOON, OWEN B. ..... p 4097 N92-32372
TORII, KOJI ..... p 4044 N92-32874
TOUBLANC, D. ..... p 4096 N92-32366
p 4100 N92-32396
p 4102 N92-32408
TOUEG, SAM ..... p 4020 N92-32436
TRABOCCO, R. E. ..... p 3958 N92-33047
TRAN, HUY KIM ..... p 3970 N92-32476
TRAN, KEN ..... p 4003 N92-32295
TRAXLER, BOB ..... p 4091 N92-32505
TRENHOLME, J. B. ..... p 4079 N92-32733
TRENT, LINDA K. ..... p 4037 N92-32942
TRIBBIA, J. J. ..... p 4028 N92-32619
TRIEBER, STEVEN P. ..... p 4052 N92-32937
TRIPP, T. M. ..... p 4094 N92-32357
TROTT, W. M. ..... p 3974 N92-32637
TRUONG, TRIEU-KIE ..... p 3991 N92-33011
TRYGGVASON, GRETAR ..... p 4007 N92-32598
TRYSTRAM, DENIS ..... p 4051 N92-32715
TSAI, H. C. ..... p 3949 N92-32530
TSAI, LUNG-WEN ..... p 4054 N92-33184
TSAI, MING-YI ..... p 3959 N92-33075
TSANGARIS, PARRY ..... p 3988 N92-32964
TUCKER, KEVIN ..... p 3995 N92-32250
p 3995 N92-32251
TURLIK, I. ..... p 3984 N92-32974
TUROS, EDWARD ..... p 4066 N92-32556

U

UHERKA, K. L. ..... p 3992 N92-33128
UKLEJEWSKI, R. ..... p 4037 N92-32663
ULAMEC, STEPHAN ..... p 4102 N92-32409
UNDERWOOD, D. G. ..... p 4064 N92-32311
p 4065 N92-32497
URBAN, GERHARD ..... p 4050 N92-32689
URBANICH, ERNST ..... p 4071 N92-32763

V

VAISMAN, I. ..... p 4064 N92-32418
VALK, ERIC C. ..... p 3994 N92-33234
VANCUTSEM, BERNARD ..... p 4058 N92-32799
VANDERWIEL, SCOTT ..... p 4044 N92-32873
VANGEL, MARK G. ..... p 3951 N92-32581
VANZANI, V. ..... p 4101 N92-32398
VAUGHN, DAVID ..... p 4005 N92-32302
VAUTEY, P. ..... p 3957 N92-33043
VEATCH, MARK S. ..... p 3984 N92-32974
VENET, GERARD ..... p 4062 N92-32956
VENKATESWARAN, S. ..... p 4001 N92-32282
p 4001 N92-32284
VENTURA, SUSANNA ..... p 4027 N92-33138
VENTURINI, E. L. ..... p 4084 N92-32920
VERBITSKAYA, E. ..... p 4064 N92-32316
VERCHEVAL, J. ..... p 3943 N92-32728
VILLENEUVE, S. ..... p 3976 N92-33243
VISSERS, D. R. ..... p 3988 N92-32639
VITAGILANO, P. L. ..... p 3930 N92-32730
VITT, J. E. ..... p 3962 N92-32562
VITTA, SATISH ..... p 3985 N92-32984
VOGLER, L. E. ..... p 3979 N92-32555
VOGT, KONRAD ..... p 4062 N92-32951
VOLAKIS, JOHN L. ..... p 3979 N92-32559
VONBOEHM, HANS-DIETER ..... p 3937 N92-32448
VONOFENHEIM, BILL ..... p 4041 N92-33205
VOORHIES, COERTE V. ..... p 4031 N92-32655
VOTO, C. ..... p 3959 N92-33053
VOTTA, LAWRENCE G. ..... p 4044 N92-32873
VREEBURG, J. P. B. ..... p 4011 N92-32831
p 3943 N92-32834

W

WACHTEL, J. ..... p 4015 N92-32511
WAGNER, D. ..... p 4071 N92-32808
WALBURG, T. ..... p 3967 N92-32721
WALDEMARK, KARINA ..... p 4061 N92-32842
WALIGORA, SHARON R. ..... p 4044 N92-32872
WALTON, O. R. ..... p 4012 N92-32947
WAN, YONGBING ..... p 3993 N92-33195
WANG, A. ..... p 4025 N92-32565
WANG, FANGFU ..... p 4024 N92-33233
WANG, HAN ..... p 4051 N92-32759
WANG, MORGAN ..... p 4020 N92-32425
WANG, RUIPING ..... p 3970 N92-32471
WANG, T. S. ..... p 3997 N92-32258
p 4004 N92-32299
WANG, Z. ..... p 4081 N92-32346
p 4017 N92-32615
p 4072 N92-33130
WANG, Z. L. ..... p 4084 N92-32919
WARK, CANDACE E. ..... p 4008 N92-32671
WARMACK, R. J. ..... p 4085 N92-33023
WARNAKA, GLENN E. ..... p 3988 N92-32964
WARNER, JOSEPH D. ..... p 3985 N92-32984
WARSHAW, GABRIEL D. ..... p 4055 N92-33236
WARWICK, T. ..... p 4073 N92-32419
WATERMAN, ELLY H. ..... p 4062 N92-32956
WATT, D. M. ..... p 4089 N92-32469
WEAVER, M. J. ..... p 3964 N92-32826
WEBER, M. E. ..... p 3980 N92-32686
WEBSTER, HENRY A. ..... p 4013 N92-32343
WEEKS, JACK L. ..... p 3991 N92-33030
WEGDAM, ALFONSUS MARIA FRANSISCUS
p 4074 N92-32705
WEIJNITZ, P. ..... p 4067 N92-32764
WEINAN, E. ..... p 4012 N92-33110
WEISENHORN, A. L. ..... p 4066 N92-32548
WEISS, J. M. ..... p 4001 N92-32282
WELLER, R. R. ..... p 3964 N92-32925
WELLS, M. S. ..... p 4042 N92-32658
WENHAM, S. R. ..... p 4025 N92-32565
WENTWORTH, W. E. ..... p 4026 N92-32908
p 4026 N92-32909
WENZEK, DIDIER ..... p 4051 N92-32715
WERKMEISTER, D. ..... p 3967 N92-32721
WESTBROOK, C. K. ..... p 3961 N92-32544
WESTFALL, WALLACE D. ..... p 3986 N92-33172
WHEELER, J. A. ..... p 4088 N92-33069
WHEELER, PHILIP C. ..... p 3948 N92-32520
WHIRLEY, R. G. ..... p 4020 N92-32328
WHITE, C. W. ..... p 4085 N92-33127
WHITE, J. M. ..... p 4041 N92-32414
WHITE, JEFFERY L. ..... p 3961 N92-32553
WHITE, VANDA R. ..... p 3941 N92-33002
WHITEHEAD, ROBIN S. ..... p 3948 N92-32525
p 3951 N92-32579
WHITESIDES, HAROLD R. ..... p 3994 N92-32247
p 4005 N92-32305
WHITMORE, JEFFREY N. ..... p 4036 N92-32492
WHITNEY, J. M. ..... p 3956 N92-33035
WHITNEY, JAMES M. ..... p 3956 N92-33034
WIDDERSHOVEN, FRANCISCUS PETRUS
p 4083 N92-32760
WIE, BONG ..... p 3942 N92-32244
WIELAND, TODD M. ..... p 3950 N92-32532
WIESELTHIER, JEFFREY E. ..... p 3979 N92-32570
WIFALL, J. R. ..... p 3934 N92-32308
WIGGENRAAD, J. F. M. ..... p 4023 N92-33139
WIKRAMANAYAKE, PALITHA N. ..... p 4007 N92-32630
WILLIAMS, A. E. ..... p 3985 N92-32982
WILLIAMS, C. ..... p 4041 N92-32451
WILLIAMS, R. ..... p 4002 N92-32286
WILLIAMS, R. W. ..... p 3994 N92-32245
p 4000 N92-32278
p 4002 N92-32287
WILLIAMS, ROBERT ..... p 4004 N92-32296
WILLIAMS, T. ..... p 3939 N92-32778
WILLIAMSON, D. L. ..... p 4028 N92-32619
WILSON, P. B. ..... p 4071 N92-32751
WIMBERGER-FRIEDL, REINHOLD
p 3972 N92-32752
WINELAND, DAVID J. ..... p 4016 N92-33060
WING, N. L. ..... p 3935 N92-32326
WINKLER, P.-J. ..... p 3977 N92-32742
WINKLER, PETER-JUERGEN ..... p 3977 N92-32690
p 3967 N92-32819
p 3978 N92-32893
p 3968 N92-32894
p 3968 N92-32897
WINTER, KATHRYN P. ..... p 4037 N92-32504
WITTMANN, ERWIN ..... p 3954 N92-32740
WOHN, F. K. ..... p 4067 N92-32922
WOLF, J. S. ..... p 3968 N92-32991
WOLF, STEVE ..... p 4039 N92-32433
WOLF, THOMAS ..... p 3940 N92-32864
WONG, KAM L. ..... p 3941 N92-32456
WONG, YAN CHUN ..... p 3942 N92-32538
WOO, ALEX C. ..... p 3979 N92-32559
WOODWARD, HERBERT P. ..... p 4046 N92-32884
WOOLLAM, J. A. ..... p 3984 N92-32977
WORKMAN, GARY L. ..... p 4020 N92-32425
WRIGHT, GEOFFREY A. ..... p 3958 N92-33045
WRIGHT, M. J. ..... p 4100 N92-32391
p 4102 N92-32410
WU, C. S. ..... p 3983 N92-32966
WU, C. T. ..... p 4081 N92-32346
p 4082 N92-32561
WU, X. J. ..... p 4023 N92-33076
WU, YIYAN ..... p 4047 N92-33189
WUDL, FRED ..... p 3971 N92-32665
WURZ, P. ..... p 4016 N92-33114

Y

YABE, T. ..... p 4078 N92-32552
YAGLA, JON J. ..... p 3944 N92-33162
YAHIL, A. ..... p 4093 N92-32993
YAMAZAKI, K. ..... p 4070 N92-32746
YANASSE, HORACIO HIDEKI ..... p 4055 N92-32661
YANG, LI-FARN ..... p 4019 N92-33031
YANG, SHAOCHEN ..... p 4004 N92-32300
YANG, Z. ..... p 4011 N92-32868
YAO, H. D. ..... p 3984 N92-32977
YARBROUGH, W. A. ..... p 3971 N92-32490
YEH, H. C. ..... p 3971 N92-32640
YELLOWHORSE, L. ..... p 4027 N92-33150
YOON, ROE-HOAN ..... p 3977 N92-32467
YORK, A. R., II ..... p 3944 N92-33166
YOUNG, PAUL G. ..... p 3984 N92-32978
YOUNT, LARRY J. ..... p 3939 N92-32778
YU, C. LONG ..... p 3979 N92-32559
YU, KIN MAN ..... p 4083 N92-32693
YU, S. S. ..... p 4070 N92-32413
p 4072 N92-33122
YU, TZU-YI ..... p 4005 N92-32302
YUDIN, G. L. ..... p 4065 N92-32500
YUSHCHENKO, O. P. ..... p 4065 N92-32498

Z

ZABIN, SERENA M. ..... p 3982 N92-32899
ZACHARIA, T. ..... p 4020 N92-33085
ZAHNLE, KEVIN ..... p 4094 N92-32351
ZARNECKI, JOHN C. ..... p 4100 N92-32391
p 4015 N92-32392
p 4100 N92-32394
p 4102 N92-32410
ZEIDLER, J. R. ..... p 4075 N92-32935
ZEITLIN, ANDREW D. ..... p 3933 N92-32537
ZEMACH, C. ..... p 4013 N92-33159
ZHANG, F. ..... p 4025 N92-32565
ZHANG, X. ..... p 4015 N92-32511
ZHAO, J. ..... p 4025 N92-32565
ZHAO, WEI ..... p 4042 N92-32656
ZHENG, X. ..... p 4085 N92-33023
ZHOU, H.-C. ..... p 3971 N92-32550
ZHOU, L. ..... p 3963 N92-32607
ZHOU, Y. ..... p 4065 N92-32501
ZIEBARTH, J. P. ..... p 3997 N92-32258
p 3966 N92-32297
ZITA, E. J. ..... p 4078 N92-32599
ZUCKERWAR, ALLAN J. ..... p 4015 N92-33016
p 4076 N92-33017
p 3991 N92-33021
ZUHR, R. A. ..... p 4085 N92-33127
ZWEBEN, S. J. ..... p 4078 N92-32623

Typical Corporate Source Index Listing

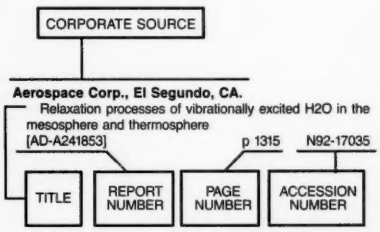

Listings in this index are arranged alphabetically by corporate source. The title of the document provides the user with a brief description of the subject matter. The report number helps to indicate the type of document cited (e.g., NASA report, translation, NASA contractor report). The accession number denotes the number by which the citation is identified. The page number helps you locate the citation in the abstract section. The titles are arranged under each corporate source in ascending accession number order.

A

ACCUWAVE CORP., SANTA MONICA, CA.
Holographic crosstalk and signal-to-noise ratio in orthogonal data storage
[AD-A250146] p 4013 N92-32323

ADVISORY GROUP FOR AEROSPACE RESEARCH AND DEVELOPMENT, NEUILLY-SUR-SEINE (FRANCE).
Integrated Target Acquisition and Fire Control Systems
[AGARD-CP-500] p 3935 N92-32437
The Utilization of Advanced Composites in Military Aircraft
[AGARD-R-785] p 3956 N92-33033
Insensitive Munitions
[AGARD-CP-511] p 3975 N92-33240

AEROJET-GENERAL CORP., IUKA, MS.
Effect of including variable gas properties and entrained particles in the flow analysis of the ASRM nozzle p 4006 N92-32306

AEROJET-GENERAL CORP., SACRAMENTO, CA.
Current status of the development of an ignition transient model for solid rocket motors p 3944 N92-32246
STME hydrogen mixer study p 3945 N92-32262

AEROJET SOLID PROPULSION CO., SACRAMENTO, CA.
Impeller tandem blade study with grid embedding for local grid refinement p 4002 N92-32290

AERONAUTICAL RESEARCH INST. OF SWEDEN, STOCKHOLM.
Improved dissipation models for central difference schemes
[FFA-TN-1991-41] p 4057 N92-32729

AERONAUTICAL RESEARCH LABS., MELBOURNE (AUSTRALIA).
Briefing notes on a manned aircraft research and support simulation facility
[AD-A250373] p 3935 N92-32326

AEROSPACE CORP., EL SEGUNDO, CA.
A molecule-specific filter modulator
[AD-A250760] p 4074 N92-32672
Phase-only synthesis for multiple-beam phased arrays with element failures
[AD-A252250] p 3982 N92-32891
The energetic radiation environment in a highly elliptical (Molniya) orbit
[AD-A252394] p 4031 N92-32902

AEROSPACE CORP., LOS ANGELES, CA.
A shock tube study of the reactions of the hydroxyl radical with combustion species
[DE92-012573] p 3960 N92-32464

AEROTHERM CORP., HUNTSVILLE, AL.
Development of the KIVA-2 CFD code for rocket propulsion applications p 3945 N92-32272

AIR FORCE ARMAMENT LAB., EGLIN AFB, FL.
The United States Air Force explosives hazards reduction program p 3976 N92-33241

AIR FORCE INST. OF TECH., WRIGHT-PATTERSON AFB, OH.
A learning enhanced flight control system for high performance aircraft
[AD-A252520] p 3938 N92-32435
An in vitro corrosion study of two implant materials using electrochemical impedance spectroscopy and potentiodynamic polarization
[AD-A252575] p 3966 N92-32626
China's aerospace industry: Technology, funding, and modernization
[AD-A252618] p 3929 N92-32691

AIR FORCE SYSTEMS COMMAND, WRIGHT-PATTERSON AFB, OH.
Heating fixture and instrumentation design for elevated temperature tests of a composite repair technique
[WL-TM-90-326-FIBE] p 3946 N92-32459

ALABAMA UNIV., HUNTSVILLE.
Combustion instability analysis for liquid propellant rocket engines p 3966 N92-32297
Study of eddy current probes
[NASA-CR-190814] p 4020 N92-32425

ALBERTA UNIV., EDMONTON.
A hybrid numerical/knowledge based system for locomotion control of a multi-legged articulated robot
[ISBN-0-315-52925-3] p 4054 N92-33203
Techniques of microwave noise measurement on cooled transistors
[ISBN-0-315-65025-7] p 3994 N92-33234

ALENIA, FOGGIA (ITALY).
CFRP stiffened panels under compression p 3958 N92-33044
Environmental resistance of amorphous bonded thermoplastic joints p 3959 N92-33053

ALENIA AERONAUTICA, NAPLES (ITALY).
Active vibrations and noise control for turboprop application research program activities p 4063 N92-32962

ALLEN CORP. OF AMERICA, ALEXANDRIA, VA.
Feasibility study for predicting human reliability growth through training and practice
[AD-A252371] p 4038 N92-32990

AMERICAN ASTRONAUTICAL SOCIETY, SAN DIEGO, CA.
Humans and machines in space: The payoff
[ISBN-0-87703-343-9] p 4039 N92-33099

AMES LAB., IA.
Formation of high temperature superconductors from the solidified melt
[DE92-012584] p 4081 N92-32465
Design and construction of a sample preparation chamber for atomic beam scattering
[DE92-014509] p 4065 N92-32473
Electrocatalysis of anodic, oxygen-transfer reactions at noble metal electrodes
[DE92-016308] p 3962 N92-32562
Studies of n-butane conversion over silica-supported platinum, platinum-silver and platinum-copper catalysts
[DE92-016309] p 3962 N92-32563
Quantum wave modeling on highly parallel distributed memory machines
[DE92-014507] p 4088 N92-33109
Use of a Fourier deconvolution method in particle size determination and use of molecular mechanics in crystal structure determinations
[DE92-014510] p 4085 N92-33111

AMOCO OIL CO., NAPERVILLE, IL.
Direct conversion of light hydrocarbon gases to liquid fuel
[DE92-015592] p 3975 N92-33141

ANDRULIS RESEARCH CORP., SALT LAKE CITY, UT.
Development of methodology and technology for identifying and quantifying emission products from open burning and open detonation thermal treatment methods. BangBox test series. Volume 3: Quality assurance and quality control
[AD-A251099] p 4029 N92-32650

APPLIED ACOUSTIC RESEARCH, STATE COLLEGE, PA.
A lightweight loudspeaker for aircraft communications and active noise control p 3988 N92-32964

ARGONNE NATIONAL LAB., IDAHO FALLS, ID.
Development of high-performance Na/NiCl2 cell
[DE92-015270] p 3988 N92-32639

ARGONNE NATIONAL LAB., IL.
High power testing of the prototype accelerating cavity (352 MHz) for the Advanced Photon Source (APS)
[DE92-016697] p 4069 N92-32314
Processing and properties of silver-clad Tl-Ba-Ca-Cu-O wires and tapes
[DE92-015266] p 4081 N92-32346
Higher superdeformed band members in Hg-190: Evidence for a band interaction?
[DE92-016778] p 4082 N92-32542
Sintering of bulk high-(Tc) superconductors: Bi-Sr-Ca-Cu-O
[DE92-016189] p 4082 N92-32561
Publications on maglev technologies
[DE92-013296] p 4017 N92-32615
Thermal strains in titanium aluminide and nickel aluminide composites
[DE92-015181] p 3953 N92-32638
Nondestructive evaluation development for process control
[DE92-015272] p 3971 N92-32640
Chemical Technology Division
[DE92-014059] p 3964 N92-32931
Proceedings of the fourth users meeting for the advanced photon source
[DE92-014061] p 4072 N92-32932
Molecular surface analysis by laser ionization of desorbed molecules
[DE92-016320] p 4016 N92-33114
Sweeping algorithms for five-point stencils and banded matrices
[DE92-017309] p 4047 N92-33118
Superconductivity: Past, present, and future
[DE92-014862] p 3992 N92-33128
Thermal and structural analysis of high precision beamline position monitors for synchrotron x ray beams
[DE92-014863] p 4072 N92-33130
ANL ITER high-heat-flux blanket-module heat transfer experiments
[DE92-017749] p 4080 N92-33168
Dynamics of radiation-induced amorphization in intermetallic compounds
[DE92-016774] p 4086 N92-33221
Coatings for improved corrosion resistance
[DE92-016779] p 3974 N92-33247

ARIZONA UNIV., TUCSON.
Some issues associated with the formation of the Saturnian system p 4093 N92-32349
The thermal structure of the atmosphere of Titan p 4094 N92-32353
A reanalysis of Voyager UVS observations of Titan p 4094 N92-32357
Plausible surface models for Titan p 4098 N92-32381
Leading-edge receptivity for blunt-nose bodies
[NASA-CR-190563] p 3930 N92-32648

ARMY ARMAMENT RESEARCH, DEVELOPMENT AND ENGINEERING CENTER, WATERVLIET, NY.
Braided composite bore evacuator chambers for tank cannons p 3948 N92-32520

Investigation into the fabrication of a composite top attack recoilless rifle p 3948 N92-32524

ARMY AVIATION SYSTEMS COMMAND, HAMPTON, VA.

Evaluation of composite components on the Bell 206L and Sikorsky S-76 helicopters p 3950 N92-32575

ARMY CHEMICAL RESEARCH AND DEVELOPMENT CENTER, ABERDEEN PROVING GROUND, MD.

Condensed-phase processes during solid propellant combustion. Part 2: Chemical and microscopic examination of conductively quenched samples of RDX, XM39, JA2, M30, and HMX-binder compositions
[AD-A250799] p 3974 N92-32664

A reexamination of the plastic flow criterion for copper
[AD-A252370] p 4023 N92-32918

ARMY COLD REGIONS RESEARCH AND ENGINEERING LAB., HANOVER, NH.

Effects of the abrasiveness of test and training site soils on parachute life
[AD-A252389] p 3931 N92-32900

Performance of insulated pavements at Newton Fields, Jackman, Maine
[CRREL-92-9] p 3940 N92-32903

ARMY LAB. COMMAND, WATERTOWN, MA.

Site competition of impurities and grain boundary stability in iron
[AD-A252411] p 4084 N92-32939

ARMY MATERIALS TECHNOLOGY LAB., WATERTOWN, MA.

Composite structural armor for combat vehicle applications p 3947 N92-32515

Applications of composites to armaments p 3947 N92-32516

Efficient finite element modeling of laminated composite plates based on higher-order theory p 3949 N92-32529

Statistically based material properties: A military handbook-17 perspective p 3951 N92-32581

ARMY MISSILE COMMAND, REDSTONE ARSENAL, AL.

Optical modulation characteristics and applications of liquid crystal televisions
[AD-A252466] p 3979 N92-32633

ATMOSPHERIC AND ENVIRONMENTAL RESEARCH, INC., CAMBRIDGE, MA.

A simple Doppler wind lidar sensor: Simulated measurements and impacts in a global assimilation and forecast system
[PL-TR-91-2253] p 4034 N92-32859

A research program on radiative transfer model development in support of the ARM program
[DE92-014495] p 4031 N92-33153

ATOMIC ENERGY OF CANADA LTD., PINAWA (MANITOBA).

A state of the art report on flame acceleration and transition to detonation in hydrogen/air/diluent mixtures
[DE92-626850] p 3961 N92-32475

B

BALLISTIC RESEARCH LABS., ABERDEEN PROVING GROUND, MD.

Characterization of flow distribution in axisymmetric shock tubes
[AD-A251095] p 4008 N92-32683

A test circuit for capacitor bank grounding sticks
[AD-A251121] p 3989 N92-32700

BATTELLE COLUMBUS LABS., OH.

Phase distributions of airborne polycyclic aromatic hydrocarbons in two US cities
[PB92-164979] p 4028 N92-32543

A review and discussion of flight management system incidents reported to the aviation safety reporting system
[AD-A252438] p 3932 N92-32941

BATTELLE MEMORIAL INST., RESEARCH TRIANGLE PARK, NC.

Rotational barriers in model compounds of poly (vinyl chloride): 2-chlorobutane and 1,3,5,7,9,11-hexachlorododecane
[AD-A250855] p 3960 N92-32330

BELL TELEPHONE LABS., INC., MURRAY HILL, NJ.

Investigating the application of capture-recapture techniques to requirement and design reviews p 4044 N92-32873

BENDIX CORP., SOUTHFIELD, MI.

Superheavyweight missions SI versus DI: Ascent flight design options and recommendations
[NASA-CR-183208] p 3942 N92-32610

BOEING MILITARY AIRPLANE DEVELOPMENT, WICHITA, KS.

Development of thermoplastic components for structural validation p 3948 N92-32522

Survivability characteristics of composite compression structure p 3950 N92-32578

BOMBARDIER, INC., MONTREAL (QUEBEC).

Further development of the CANAERO computer code to include propulsor modelling
[DREA-CR-90-425] p 3931 N92-32811

BORDEAUX 2 UNIV. (FRANCE).

Modeling of the diurnal variations of the atmosphere of Titan p 4096 N92-32366

Properties and distribution of the aerosols in the atmosphere of Titan p 4100 N92-32396

Study of transmitted light through the atmosphere of Titan p 4102 N92-32408

BRITISH AEROSPACE AIRCRAFT GROUP, WARTON (ENGLAND).

Aspects of compression in aerospace composites: Future requirements p 3956 N92-33036

An overview of concerns relating to fluid effects on composites p 3958 N92-33045

BRITISH ASTRONOMICAL ASSOCIATION, WEST BARNHAM (ENGLAND).

On the Titan/28 Sagittarii occultation of 1989 July 3 p 4101 N92-32403

BRITISH COLUMBIA UNIV., VANCOUVER.

A quasi-geostrophic circulation model of the northeast Pacific Ocean
[ISBN-0-315-55106-2] p 4035 N92-33198

Pertubative finite temperature field theory in Minkowski space
[ISBN-0-315-55158-5] p 4088 N92-33199

BRITISH PETROLEUM CO. LTD., LONDON (ENGLAND).

Spray nozzle for fire control
[CA-PATENT-APPL-SN-2-011-94] p 4011 N92-32856

BROOKHAVEN NATIONAL LAB., UPTON, NY.

Investigation of the oxygen-vacancy (A-center) defect complex profile in neutron irradiated high resistivity silicon junction particle detectors
[DE92-016952] p 4064 N92-32316

Booster Applications Facility report, phase 2
[DE92-013395] p 4070 N92-32411

Local environment around the oxygen atoms in Y-Ba-Cu-O studied X ray Absorption Fine Structure (XAFS) spectroscopy
[DE92-014165] p 4081 N92-32470

Optics of beam transport in the NSLS UV-FEL
[DE92-014166] p 4015 N92-32511

Life testing of a low voltage air circuit breaker
[DE92-014173] p 3988 N92-32635

Polarized wiggler for NSLS x ray ring design considerations
[DE92-012212] p 4071 N92-32912

Studies of Y-Ba-Cu-O single crystals by x ray absorption spectroscopy
[DE92-014687] p 4086 N92-33136

Kinematics of Compton backscattering x ray source for angiography
[DE92-014016] p 4073 N92-33179

BROWN UNIV., PROVIDENCE, RI.

Surfaces and thin films studied by picosecond ultrasonics
[DE92-016313] p 4020 N92-32564

Two studies of nonlinear processes in irreversible thermodynamics
[DE92-016855] p 4087 N92-32566

Research and development of a helium-4 based solar neutrino detector
[DE92-017390] p 4103 N92-33119

C

CALGARY UNIV. (ALBERTA).

CSP: A distributed logic programming language for discrete event simulation
[ISBN-0-315-54272-1] p 4048 N92-33214

CALIFORNIA INST. OF TECH., PASADENA.

Interior of Titan p 4094 N92-32352

Stress-relief displacements induced by drilling: Applications to holographic measurements of in situ stress
[DE92-013711] p 4014 N92-32620

CALIFORNIA UNIV., BERKELEY.

Solid fuel flame spread and mass burning in turbulent flow
[PB92-181049] p 3963 N92-32607

Ultra-low density organic-inorganic composite materials possessing thermally insulating and acoustic damping properties
[AD-A251182] p 3955 N92-32828

Stochastic models in reliability
[AD-A250934] p 4020 N92-33151

CALIFORNIA UNIV., BERKELEY. LAWRENCE BERKELEY LAB.

Heavy flavor physics at hadron colliders
[DE92-014482] p 4064 N92-32312

The influence of anharmonic phonons on the isotope effect in high-(Tc) oxides
[DE92-017083] p 4081 N92-32320

Determining surface profile from sequential interference patterns from a long trace profiler
[DE92-017117] p 4073 N92-32321

Thermal effects and mirror surface figure requirements for a diagnostic beamline at the advanced light source
[DE92-014483] p 4073 N92-32419

Low-frequency nuclear quadrupole resonance with a dc SQUID
[DE92-014506] p 4081 N92-32420

Scintillation properties of lead sulfate
[DE92-010301] p 4082 N92-32493

AC microcalorimetry of adsorbates on evaporated metal films: Orientational ordering of H2 multilayers
[DE92-008317] p 3963 N92-32666

Investigation on the lattice site location of the excess arsenic atoms in GaAs layers grown by low temperature molecular beam epitaxy
[DE92-008253] p 4083 N92-32693

Premixed turbulent combustion to opposed streams
[DE92-016996] p 3964 N92-32996

Photon excitation for satellite free x ray spectroscopy: Instrumentation challenges
[DE92-016999] p 4067 N92-32997

Implantation of carbon in GaAs
[DE92-016921] p 4085 N92-33117

Estimates of SASE power in the short wavelength region
[DE92-014504] p 4017 N92-33155

Development of advanced secondary zinc cells for power-source applications
[DE92-016358] p 3993 N92-33183

CALIFORNIA UNIV., DAVIS.

Current status of the development of an ignition transient model for solid rocket motors p 3944 N92-32246

Experimental investigation of the axial impregnation of oriented fiber bundles by capillary forces
[AD-A250758] p 3961 N92-32508

Injection of compact toroids for tokamak fueling and current drive
[DE92-010031] p 4077 N92-32533

Neutron scatter studies of chromatin structures related to functions
[DE92-014032] p 4036 N92-33181

CALIFORNIA UNIV., LA JOLLA.

Acoustical emission from bubbles
[AD-A252390] p 4061 N92-32901

CALIFORNIA UNIV., LOS ANGELES.

A computational fluid dynamics analysis of the hypersonic flights of Pegasus
[NASA-CR-186023] p 4007 N92-32560

CALIFORNIA UNIV., SAN DIEGO, LA JOLLA.

ARM Tropical Pacific Experiment (ATPEX): Role of cloud, water vapor and convection feedbacks in the coupled ocean/atmosphere system
[DE92-013772] p 4032 N92-32331

Preparation and characterization of superlattices
[DE92-012572] p 4081 N92-32462

CALIFORNIA UNIV., SANTA BARBARA.

Surface reconstruction and templating for zeolite thin film synthesis observed by atomic force microscopy
[AD-A251140] p 4066 N92-32548

Program for research in conducting polymers
[AD-A250965] p 3971 N92-32665

CAMBRIDGE COLLABORATIVE, INC., MA.

Use of SEA to predict structure-borne noise in aircraft p 4062 N92-32955

CANADAIR LTD., MONTREAL (QUEBEC).

Naval target classification and designation with the CL-227 Sea Sentinel p 3937 N92-32449

CANADIAN ASTRONAUTICS LTD., OTTAWA (ONTARIO).

Continuation of the development of a millimeter wave wideband tunable waveguide voltage controlled oscillator
[CAL-504-88P120] p 3990 N92-32847

CARLETON UNIV., OTTAWA (ONTARIO).

Multi-stage hybrid coding of digital images
[ISBN-0-315-58989-2] p 4047 N92-33189

A digital implementation of a radar coherent-on-receive system
[ISBN-0-315-59028-9] p 3987 N92-33206

Performance analysis of space-based radar tracking techniques
[ISBN-0-315-60464-6] p 3987 N92-33207

The architecture development and design considerations of a high-speed, single chip, CMOS convolutional decoder based on a modification of the Viterbi algorithm
[ISBN-0-315-60456-5] p 3993 N92-33208

Techniques for the synthesis of wideband, series-fed arrays of microstrip patch radiators
[ISBN-0-315-58991-4] p 3987 N92-33209

A low-current amplifier for mobile radio and monolithic microwave integrated circuit design techniques in the UHF and L bands
[ISBN-0-315-59034-3] p 3993 N92-33211

An evaluation of knowledge-based diagnostic techniques for debugging concurrent software
[ISBN-0-315-51189-3] p 4049 N92-33215
Analytic performance of software pipelines with rendezvous and communication tasks
[ISBN-0-315-54414-7] p 4052 N92-33216
A fast task allocator for multiprocessing systems
[ISBN-0-315-54380-9] p 4053 N92-33217
Learning systems, adaptive data structures, and random environments
[ISBN-0-315-51158-3] p 4054 N92-33218
A study of artificial intelligence planning: A framework for a planning development system
[ISBN-0-315-54378-7] p 4055 N92-33219
Investigations of adaptive control for a direct drive robotic manipulator
[ISBN-0-315-59030-0] p 4055 N92-33236

CARNEGIE-MELLON UNIV., PITTSBURGH, PA.
Towards well-defined polysilanes and polyphosphazenes
[AD-A251098] p 3971 N92-32547
Generic consequences of fundamental studies of beta phase decomposition modes in titanium and related alloy systems
[AD-A250789] p 3967 N92-32699

CATHOLIC UNIV. OF AMERICA, WASHINGTON, DC.
Autonomous berthing/unberthing of a Work Attachment Mechanism/Work Attachment Fixture (WAM/WAF)
[NASA-CR-190647] p 4019 N92-32885

CENTER FOR MATHEMATICS AND COMPUTER SCIENCE, AMSTERDAM (NETHERLANDS).
Limit theorems for functionals of convex hulls
[CWI-BS-R9115] p 4059 N92-33058

CENTRE D'ESSAIS AERONAUTIQUE TOULOUSE (FRANCE).
Evaluation of the effects of the environment on the behavior of the primary structures of composite material aircraft in service: Historic and current situation
p 3958 N92-33048

CENTRE D'ETUDE SPATIALE DES RAYONNEMENTS, TOULOUSE (FRANCE).
Polar upper atmosphere characterization and supersonic ion escape (polar wind)
[GDR-0917] p 4031 N92-32889

CENTRE NATIONAL DE LA RECHERCHE SCIENTIFIQUE, GRENOBLE (FRANCE).
Near infrared spectra of potential solids at the surface of Titan p 4102 N92-32406

CENTRE NATIONAL DE LA RECHERCHE SCIENTIFIQUE, ORSAY (FRANCE).
HCP and HCN, molecules of planetary interest
p 4100 N92-32395

CHALMERS UNIV. OF TECHNOLOGY, GOETEBORG (SWEDEN).
Environmental consequences of new energy technology. Solar heating, heat stores, and heat pumps
[PB92-180843] p 4025 N92-32605
Energy take-out from a wave energy device. A theoretical study of the hydrodynamics of a two-body problem consisting of a buoy and a submerged plate
[PB92-178821] p 4025 N92-32608

CHILWORTH RESEARCH CENTRE, SOUTHAMPTON (ENGLAND).
Waves on Titan p 4100 N92-32394

CINCINNATI UNIV., OH.
Electrocatalyst surfaces
[PB92-190420] p 3962 N92-32591
Intelligent signal processing for active control
[AD-A252232] p 4053 N92-32625

CLEMSON UNIV., SC.
Real-time processing of radar return on a parallel computer
[NASA-CR-4456] p 3932 N92-32606

COLOGNE UNIV. (GERMANY, F.R.).
Titan's magnetospheric interaction
p 4099 N92-32385

COLORADO UNIV., BOULDER.
Methane conversion to methanol
[DE92-014349] p 3960 N92-32332
Wave propagation in laterally varying media: A model expansion method
[AD-A247553] p 4031 N92-32572
Elementary particle physics and high energy phenomena
[DE92-016844] p 4069 N92-33187

COLUMBIA UNIV., NEW YORK, NY.
Optimum design of ninety degree bends
p 4000 N92-32274
Photogenerated carrier-induced reactions on UHV semiconductor surfaces
[DE92-015355] p 4082 N92-32641

COMMERCE DEPT., WASHINGTON, DC.
Information resources management plan of the Federal Government
[PB92-147198] p 4089 N92-32643

COMMITTEE ON APPROPRIATIONS (U.S. HOUSE).
Departments of Veterans Affairs and Housing and Urban Development, and independent agencies appropriations for 1993, part 6
[GAO-55-636-PT-6] p 4091 N92-32505

COMMITTEE ON SCIENCE, SPACE AND TECHNOLOGY (U.S. HOUSE).
NASA authorization, 1993, volume 1
[GPO-55-260-VOL-1] p 4092 N92-33147

COMMONWEALTH SCIENTIFIC AND INDUSTRIAL RESEARCH ORGANIZATION, MORDIALOC (AUSTRALIA).
A precise narrow-beam filter infrared radiometer and its use with lidar in the ARM Program
[DE92-016872] p 4015 N92-33188

COMMUNICATIONS RESEARCH CENTRE, OTTAWA (ONTARIO).
A 19.2 GHz cooled HEMT low noise amplifier
[CTN-92-60354] p 3990 N92-32810

CONCORDIA UNIV., MONTREAL (QUEBEC).
Pattern recognition based on entropy analysis and shape transformations
[ISBN-0-315-56074-6] p 4048 N92-33201
Primal access recognition of visual objects
[ISBN-0-315-63509-6] p 4048 N92-33212
Diagnosability and diagnosis of sparsely interconnected multiprocessor systems
[ISBN-0-315-56107-6] p 4053 N92-33224
Optimization of logic queries in knowledge base systems
[ISBN-0-315-51346-2] p 4049 N92-33227
Concurrency control scheme for design object bases
[ISBN-0-315-56113-0] p 4049 N92-33232

CONGRESS OF THE UNITED STATES, WASHINGTON, DC.
The 1991 Federal Aviation Administration plan for research, engineering and development
p 4103 N92-32453

CONSTRUCCIONES AERONAUTICAS S.A., MADRID (SPAIN).
Effects of fuel on Hercules AS-4/8552 composite material p 3958 N92-33046

CORNELL UNIV., ITHACA, NY.
Titan's organic chemistry: Results of simulation experiments p 4096 N92-32369
Organic chemistry on Titan: Surface interactions
p 4096 N92-32370
Fault-tolerant wait-free shared objects
[NASA-CR-190679] p 4020 N92-32436
SIMLAB: Automatically creating physical systems simulators
[AD-A250970] p 4042 N92-32546
High translational energy induced reaction in semiconductors
[AD-A250980] p 3989 N92-32669
Beta-barium borate optical parametric oscillator
[AD-A251177] p 4075 N92-32915
Mass resolved resonance ionization spectroscopy of combustion radicals
[DE92-016833] p 3965 N92-33222

D

DASSAULT-BREGUET AVIATION, SAINT CLOUD (FRANCE).
Innovative constituents requirements to improve composites compressive strength p 3957 N92-33043

DAVID TAYLOR RESEARCH CENTER, BETHESDA, MD.
The application of unsteady potential flow vortex loop/dipole theory to the work and acoustics of low-speed turbomachinery
[AD-A251160] p 4008 N92-32652
Mixed model fatigue crack growth behavior in a high strength steel
[AD-A250667] p 4022 N92-32717

DAYTON UNIV., OH.
Investigation of a relationship between uniaxial and biaxial chemical stress crazing of cast acrylic
[AD-A250852] p 4021 N92-32621
Issues in compression loading of composite structures
p 3956 N92-33034

DAYTON UNIV. RESEARCH INST., OH.
Temporal and spatial factors affecting the perception of computer-generated imagery
[AD-A249242] p 4046 N92-32907
A new test method to determine the compressive strength of fiber-reinforced composites
p 3956 N92-33035

DEFENCE AND CIVIL INST. OF ENVIRONMENTAL MEDICINE, DOWNSVIEW (ONTARIO).
Thermal assessment of Mustang Industries, Inc. neoprene quick-don anti-exposure immersion suits and storage evaluation for the CP140 Aurora aircraft
[DCIEM-90-23] p 4039 N92-32790
DCIEM/Central Medical Board Aircrew ECG program: Recommendations for restructuring
[DCIEM-90-47] p 4037 N92-32816
Instrument scanning and subjective workload with the peripheral vision horizon display
[CTN-92-60359] p 4038 N92-32817
Shape recognition by computer in simulated aerial images
[DCIEM-91-05] p 4054 N92-32854
An evaluation of the performance characteristics of a two-man molecular sieve oxygen generating system
[DCIEM-91-20] p 4039 N92-33079

DEFENCE RESEARCH ESTABLISHMENT, OTTAWA (ONTARIO).
Interception of LPI radar signals
[AD-A246315] p 3978 N92-32535
Coverage studies for spaced-based radar
[DREO-90-18] p 3982 N92-32818

DEFENCE RESEARCH ESTABLISHMENT PACIFIC, VICTORIA (BRITISH COLUMBIA).
Detection of honeycomb damage using hexagonal grid discontinuities
[DREP-88-9] p 3955 N92-32846

DEFENCE RESEARCH ESTABLISHMENT VALCARTIER (QUEBEC).
Development of a minimum smoke propellant based on glycidyl azide polymer and ammonium nitrate
p 3976 N92-33243

DENVER UNIV., CO.
Investigation of fracture toughness and fracture mechanisms using acoustic emission measurements
[DE92-011907] p 4022 N92-32911

DEPARTMENT OF AGRICULTURE, BELTSVILLE, MD.
Permuted keyword bank in CRIS. Terms for indexing and retrieving research projects in the current research information system
[PB92-179456] p 4090 N92-32712

DEPARTMENT OF DEFENSE, WASHINGTON, DC.
The DOD science and technology strategy
[AD-A253691] p 4104 N92-33027
DoD key technologies plan
[AD-A253692] p 4105 N92-33238

DEPARTMENT OF ENERGY/CONTRACTORS MICROGRAPHICS AND INFORMATION MANAGEMENT ASSOCIATION, WASHINGTON, DC.
Second interim report of the Interagency Commission on Alternative Motor Fuels
[DE92-013169] p 3974 N92-32483

DEPARTMENT OF NATIONAL DEFENCE, OTTAWA (ONTARIO).
Lithium sulphur dioxide battery failure following high frequency vibration
[CRAD-1-90] p 3990 N92-32812

DEPARTMENT OF THE NAVY, WASHINGTON, DC.
Depolarized light source for fiber optic sensors
[AD-D015289] p 4074 N92-32634
Electrified microheterogeneous catalysis
[AD-D015270] p 3963 N92-32755
Hot water storage tank for solar collectors
[AD-D015301] p 4026 N92-32943
Radiation selective system for target range and imaging readout
[AD-D015285] p 4076 N92-33095
Silver coated superconducting ceramic powder
[AD-D015294] p 3973 N92-33157
Method of guiding an in-flight vehicle toward a target
[AD-D015308] p 3940 N92-33161
Device and process for attachment of parts to rocket motors
[AD-D015309] p 3944 N92-33162
Resonantly pumped, erbium-doped, 2.8 micron solid state laser with high slope efficiency
[AD-D015310] p 4017 N92-33165
High efficiency fast neutron threshold deflector
[AD-D015311] p 4073 N92-33167
Ultra-low-loss strip-type transmission lines, formed of bonded substrate layers
[AD-D015312] p 3992 N92-33169
Method of growing diamond film on substrates
[AD-D015313] p 3973 N92-33170
Impulse transmitter and quantum detection radar system
[AD-D015323] p 3986 N92-33171
Transmitter location system for frequencies below HF
[AD-D015325] p 3986 N92-33172
Apparatus for preparing thermoplastic composites
[AD-D015326] p 3960 N92-33174
Adaptive filter technique for suppression of wideband or offset narrowband radio frequency interference
[AD-D015329] p 3992 N92-33175
Corrosion-resistant alkyd coatings
[AD-D015330] p 3974 N92-33177

DEUTSCHE INSURANCE GERMANY (F.R.).
Pilot noise exposure during a Boeing 747-400 round trip: Judgement of noise and analysis in respect to hearing impairment of pilots p 4063 N92-32961

DEUTSCHE LUFTHANSA A.G., FRANKFURT AM MAIN (GERMANY, F.R.).
Pilots noise exposure during a Boeing 747-400 round trip: Ambient noise and acoustic-head recording and analysis of data p 4063 N92-32960
DIRECTION GENERALE DE L'AVIATION CIVILE, PARIS (FRANCE).
Influence of an intense acoustic field on boundary layer separation
[ETN-92-92081] p 4009 N92-32687
DORNIER LUFTFAHRT G.M.B.H., FRIEDRICHSHAFEN (GERMANY, F.R.).
The Dornier 328 Acoustic Test Cell (ATC) for interior noise tests and selected test results
[AIAA PAPER 92-2164] p 4062 N92-32951
Advanced Study for Active Noise Control in Aircraft (ASANCA)
[AIAA PAPER 92-2092] p 4062 N92-32956
DOUGLAS AIRCRAFT CO., INC., LONG BEACH, CA.
Fly-by-light technology development plan
[NASA-CR-181954] p 3939 N92-32778
MD-80 aft cabin noise control: A case history p 4061 N92-32950
DOUGLAS AIRCRAFT CO., INC., SAINT LOUIS, MO.
A new approach to fibrous composite laminate strength prediction p 3952 N92-32588
DRAPER (CHARLES STARK) LAB., INC., CAMBRIDGE, MA.
Advanced information processing system: The Army fault tolerant architecture conceptual study. Volume 1: Army fault tolerant architecture overview
[NASA-CR-189632-VOL-1] p 4052 N92-33100
Advanced information processing system: The Army fault tolerant architecture conceptual study. Volume 2: Army fault tolerant architecture design and analysis
[NASA-CR-189632-VOL-2] p 4052 N92-33101
An implementation of a fault-tolerant, multidirectional, digital interpolation beamformer
[AD-A252494] p 3986 N92-33152

E

ECOLE CENTRALE DE LYON (FRANCE).
The polychromatic pyrometer in diesel combustion
[ECL-91-42] p 3963 N92-32722
Local and temporal study of the combustion and heat transfer in a direct injection diesel engine
[ECL-91-43] p 3963 N92-32724
Model of Reynolds stress on nonorthogonal grid structures: Application to a staggered tube bundle
[ETN-92-91959] p 4009 N92-32725
Contribution to the theoretical and experimental analysis of camshaft engine operation
[ETN-92-91961] p 4018 N92-32726
Dynamic systems stability with dry friction: Application to brake disc squealing
[ECL-91-48] p 4018 N92-32737
Implanted aluminum: Tribological behavior and mechanical properties of the superficial layers
[ECL-91-28] p 4019 N92-32801
ECOLE NATIONALE D'INGENIEURS DE CONSTRUCTIONS AERONAUTIQUES, TOULOUSE (FRANCE).
Massively separated flow modeling. Experimental study of the fine structure of boundary layers. Study of the influence of external turbulence level
[ETN-92-92088] p 4009 N92-32765
ECOLE NATIONALE SUPERIEURE DES TELECOMMUNICATIONS, PARIS (FRANCE).
Study and development of a six port network analyzer in the 1-18 GHz frequency range
[TELECOM-91-E-005] p 3980 N92-32739
Continuous and discrete problems in image processing
[TELECOM-91-D-007] p 4058 N92-32802
Contribution to the determination of vanishing points using Hough transform
[TELECOM-91-D-008] p 4058 N92-32803
Three dimensional object reconstruction using a very limited number of projections. Application to industrial radiography
[TELECOM-91-E-008] p 4043 N92-32804
Opto-electronic system for a formal neural network
[TELECOM-91-E-013] p 4075 N92-32805
Uses of stereovision surface models
[TELECOM-91-E-016] p 4075 N92-32806
Enhancements to speech recognition on voice response systems
[TELECOM-91-E-018] p 3981 N92-32807
ECOLE SUPERIEURE DE PHYSIQUE ET DE CHIMIE INDUSTRIELLES, PARIS (FRANCE).
Experimental determination of the refractive index of liquefied gas mixtures: Applications to hypothesized Titan oceans p 4099 N92-32390
ENGINEERING RESEARCH AND CONSULTING, INC., TULLAHOMA, TN.
SRMAFTE facility checkout model flow field analysis p 3994 N92-32247
An analysis of the flow field in the region of the ASRM field joints p 4005 N92-32305
ENVIRONMENTAL PROTECTION AGENCY, RESEARCH TRIANGLE PARK, NC.
US EPA's global climate change program: Landfill emissions and mitigation research
[PB92-180215] p 4028 N92-32609
ENVIRONMENTAL PROTECTION AGENCY, WASHINGTON, DC.
EPCRA Section 313 Roadmaps Database: User's manual, version 2.2
[PB92-169523] p 4030 N92-33062
Guide to selected national environmental statistics in the US Government
[PB92-201144] p 4030 N92-33087
EPITAXX, INC., PRINCETON, NJ.
A simple high-performance avalanche photodiode for long-wavelength optical communications, phase 1
[PB92-188259] p 4076 N92-33004
ESDU INTERNATIONAL LTD., LONDON (ENGLAND).
Aerodynamic centre of wing-body combinations
[ESDU-92024] p 3929 N92-32479
Reducing torque fluctuation in linkage drive shafts
[ESDU-92016] p 4017 N92-32482
Thermal conductivity of liquid aliphatic hydrocarbons. Part 1: Alkanes
[ESDU-92011-PT-1] p 3945 N92-32484
Thermal conductivity of gaseous halogenated hydrocarbons: Ethyienes and benzenes
[ESDU-92010] p 3945 N92-32485
Orthobaric densities and molar volumes of liquids: Halogenated ethanes
[ESDU-92009] p 3945 N92-32486
Contribution of tailplane-mounted twin fins to sideforce, yawing moment, and rolling moment derivatives due to sideslip
[ESDU-92007] p 3939 N92-32487
Guide to the effect of shot peening on fatigue strength
[ESDU-92015] p 3967 N92-32779
A background to the handling qualities of aircraft
[ESDU-92006] p 3939 N92-32780
Forced convection heat transfer in straight tubes. Part 1: Fully developed turbulent flow
[ESDU-92003-PT-1] p 4010 N92-32781
Lift and rolling moment due to spoilers on wings with trailing-edge flaps deflected at subsonic speeds
[ESDU-92002-SUPPL] p 3931 N92-32782
ESSEX CORP., ORLANDO, FL.
Correlating visual scene elements with simulator sickness incidence: Hardware and software development
[AD-A252235] p 4036 N92-32434
EUROPEAN SPACE AGENCY, PARIS (FRANCE).
Symposium on Titan
[ESA-SP-338] p 4093 N92-32348
EUROPEAN SPACE AGENCY. EUROPEAN SPACE RESEARCH AND TECHNOLOGY CENTER, ESTEC, NOORDWIJK (NETHERLANDS).
Gravitational tide in the atmosphere of Titan p 4096 N92-32364
The significance of meteoric ionisation for the propagation of lightning spherics in the atmosphere of Titan p 4096 N92-32365
The detectability of Titan's surface in the near-infrared p 4097 N92-32375
The Huygens probe p 4099 N92-32388
Huygens probe: The surface mission p 4101 N92-32402
On the interpretation of Titan's intensity and polarization phase curve p 4102 N92-32407

F

FEDERAL AVIATION ADMINISTRATION, ATLANTIC CITY, NJ.
Bird ingestion into large turbofan engines
[DOT/FAA/CT-91/17] p 3932 N92-33005
FEDERAL AVIATION ADMINISTRATION, WASHINGTON, DC.
The 1991 Federal Aviation Administration plan for research, engineering and development p 4103 N92-32453
Exposures from headset interference tones
[AD-A247175] p 4061 N92-32697
Federal aviation regulations. Part 91: General operating and flight rules
[PB92-197334] p 3929 N92-33176
FEDERAL INFORMATION EXCHANGE, INC., GAITHERSBURG, MD.
A minority research and education information service: Design, develop, pilot test, and implement on-line access for historically black colleges and universities and government agencies
[DE92-013572] p 4090 N92-32930
FEDIX on-line information service: Design, develop, test, and implement, an on-line research and education information service
[DE92-013582] p 4090 N92-32985
FERMI NATIONAL ACCELERATOR LAB., BATAVIA, IL.
Two perspectives on a decohering spin
[DE92-013021] p 4087 N92-32496
Tutorial on neural network applications in high energy physics: A 1992 perspective
[DE92-016003] p 4070 N92-32506
Balance in machine architecture: Bandwidth on board and offboard, integer/control speed and flops versus memory
[DE92-016006] p 4040 N92-32642
A study of four jet events and search for double parton scattering at square root s = 1.8 TeV
[DE92-016351] p 4069 N92-33164
FLINDERS UNIV., ADELAIDE (AUSTRALIA).
Electron-atom scattering
[DE92-625005] p 4064 N92-32340
Simplified model of electron scattering on atomic hydrogen
[DE92-625007] p 4065 N92-32499
Range of validity of distorted wave Born and impulse approximations for (e,2e)
[DE92-624821] p 4087 N92-32649
FLINDERS UNIV., BEDFORD PARK (AUSTRALIA).
Coupled-channels-optical calculation of electron-helium scattering
[DE92-625009] p 4065 N92-32501
FLORIDA ATLANTIC UNIV., BOCA RATON.
Computational aspects of helicopter trim analysis and damping levels from Floquet theory
[NASA-CR-190736] p 3940 N92-33107
FLORIDA INST. OF TECH., MELBOURNE.
A Markov model of software usage p 4045 N92-32881
FLORIDA UNIV., GAINESVILLE.
Treating convection in sequential solvers p 4000 N92-32277
Quark-antiquark Regge trajectories in large N(sub c) QCD
[DE92-016462] p 4064 N92-32313
The effect of surface pressure on the Langmuir-Blodgett polymerization of 2-pentadecyl aniline
[AD-A251141] p 3971 N92-32550
Development of ultra-low noise, high sensitivity planar metal grating coupled AlGaAs/GaAs multiquantum well IR detectors for focal plane array staring IR sensor systems
[AD-A250368] p 4083 N92-32747
FOKKER B.V., SCHIPOL-OOST (NETHERLANDS).
Active synchrophasing of propeller unbalance p 4063 N92-32963

G

GEC FERRANTI, EDINBURGH (SCOTLAND).
Multisensor airborne target acquisition systems and their integration p 3936 N92-32439
GENERAL ACCOUNTING OFFICE, WASHINGTON, DC.
NASA procurement: Improving oversight of construction projects at the Langley Research Center. Report to the Honorable John W. Warner, US Senate
[GAO/NSIAD-92-230] p 4088 N92-32618
Air traffic control: FAA's advanced automation system contract
[GAO/IMTEC-91-25] p 3934 N92-32861
GENERAL ATOMIC CO., SAN DIEGO, CA.
Alpha particle diagnostics using impurity pellet injection
[DE92-013796] p 4078 N92-32623
GENERAL SERVICES ADMINISTRATION, WASHINGTON, DC.
Information resources management plan of the Federal Government
[PB92-147198] p 4089 N92-32643
GEOLOGICAL SURVEY, RESTON, VA.
Hydrate detection
[DE92-014350] p 4034 N92-32333
GEORGE MASON UNIV., FAIRFAX, VA.
Cognitive biases and time stress in team decision making
[AD-A251153] p 4088 N92-32551
A prototype software engineering environment for domain modeling and reuse p 4046 N92-32882

GEORGIA INST. OF TECH., ATLANTA.
Signal processing in impulsive electromagnetic interference
[AD-A252385] p 3982 N92-32899
GOSUDARSTVENNYI KOMITET PO ISPOLZOVANIYU ATOMNOI ENERGII, OBNINSK (USSR).
Scaling in the processes of ion-atom excitation
[DE92-625008] p 4065 N92-32500
GOSUDARSTVENNYI KOMITET PO ISPOLZOVANIYU ATOMNOI ENERGII, SERPUKHOV (USSR).
On the choice of minimization functional in the partial wave analysis
[DE92-624689] p 4087 N92-32309
Observation of (pi)(-)p yields (omega)(eta)n reaction at 38 GeV/c momentum
[DE92-624690] p 4064 N92-32310
Comparison of spin asymmetries and invariant cross sections in production of (pi)(sup 0) mesons by polarized antiprotons and protons with 200 GeV energy
[DE92-624691] p 4064 N92-32311
First results of measurements of A(sub LL) two-spin asymmetry in inclusive production of (pi)(sup 0) mesons by polarized protons and antiprotons with 200 GeV energy
[DE92-624692] p 4065 N92-32497
Possible effects of additional vector bosons in e(sup +)e(sup -)(yields)f(bar-f) at the TRISTAN energies
[DE92-624727] p 4065 N92-32498
Equivalence between Lagrangian and Hamiltonian BRST formalisms
[DE92-624556] p 4055 N92-32602
Fractional spin: Majorana-Dirac field
[DE92-624558] p 4087 N92-32603
GRAMBLING STATE UNIV., LA.
NQR-NMR studies of higher alcohol synthesis Cu-Co catalysts
[DE92-016614] p 3960 N92-32347
GRANADA UNIV. (SPAIN).
Neutral composition of Titan's atmosphere. A theoretical model p 4096 N92-32367
GRAZ UNIV. (AUSTRIA).
Atmospheric escape from Titan p 4099 N92-32384
Dielectric constant measurements in simulated Titan ocean liquids p 4102 N92-32409
GRENOBLE-1 UNIV. (FRANCE).
Bandwidth selection for the intensity of point processes: Application to hazard rate models for censored data
[IMAG-RR-859-I/M] p 4056 N92-32684
Bootstrapping the change-point of a hazard rate
[IMAG-RR-861-M] p 4056 N92-32685
Minimum cost multiflows in undirected networks
[IMAG-RR-849-M] p 4056 N92-32710
A min-max relation for K3-covers in graphs noncontractible to K5/e
[IMAG-RR-850-I] p 4056 N92-32711
Characterization of Laborde-Mulder graphs and the halfcube
[IMAG-RR-857-I] p 4057 N92-32713
Optimal communication schemes on an SIMD distributed-memory hypercube
[IMAG-RR-848-M] p 4051 N92-32715
A new form for the central limit theorem
[IMAG-RR-852-M] p 4060 N92-32716
On the inconsistency of bootstrap distribution estimators
[IMAG-RR-856-M] p 4060 N92-32718
Geometric continuity and Frenet continuity of parametric curves
[IMAG-RR-846-M] p 4057 N92-32761
Dissimilarities, dendograms, prefillers, and multiapplications of levels
[IMAG-RR-842-M] p 4058 N92-32799
Poincare normal form (system of ordinary differential equations): An algorithmic point of view
[IMAG-RR-839-M] p 4058 N92-32838
Approximations and designs for estimating regression coefficients of independent stochastic processes
[IMAG-RR-840-M] p 4060 N92-32839
GRUMMAN AEROSPACE CORP., BETHPAGE, NY.
Design, evaluation and experimental effort toward development of a high strain composite wing for Navy aircraft p 3947 N92-32514

H

HARVARD UNIV., CAMBRIDGE, MA.
PET studies of components of high-level vision
[AD-A250873] p 4036 N92-32344
Geometrical effects in two-dimensional arrays of Josephson junctions
[AD-A252209] p 4084 N92-32898
HAWAII UNIV., MANOA.
UHM/HNEI EV test and evaluation program
[DE92-011631] p 3989 N92-32754
HELSINKI UNIV. OF TECHNOLOGY, ESPOO (FINLAND).
Influence of oil lubricant additives on tribological behavior of engineering ceramics
[PB92-180710] p 3973 N92-33059
HERCULES, INC., ROCKET CENTER, WV.
Hazards reduction for tactical missiles p 3945 N92-33245
HEWLETT-PACKARD CO., PALO ALTO, CA.
The successful introduction of software reuse across an entity p 4046 N92-32883
HUGHES RESEARCH LABS., MALIBU, CA.
Electromagnetic-wave propagation in unmagnetized plasmas
[AD-A250710] p 3980 N92-32719
HUMAN ENGINEERING LABS., ABERDEEN PROVING GROUND, MD.
Modeling the ear's response to intense impulses and the development of improved damage risk criteria
[AD-A252365] p 4037 N92-32916

I

IBM JAPAN.
A study of large scale software testing p 4045 N92-32879
ILLINOIS INST. OF TECH., CHICAGO.
Interactive control in turbulent shear layers
[AD-A250711] p 4008 N92-32671
Fatigue, hysteresis, and acoustic emission, parts 1 and 2
[AD-A251073] p 4021 N92-32681
ILLINOIS STATE WATER SURVEY, CHAMPAIGN.
Applications of statistical methods to the study of climate and flooding fluctuations in the central US
[PB92-205137] p 4034 N92-33173
ILLINOIS UNIV., URBANA.
Adaptive information processing and global optimization
[AD-A248450] p 4089 N92-32644
ILLINOIS UNIV., URBANA-CHAMPAIGN.
Large eddy simulation of compressible turbulent channel flows p 4000 N92-32276
INDIAN INST. OF TECH., BOMBAY.
Buckling of fibre reinforced composite and sandwich laminates with higher-order shear deformation theories
[IIT-B/CE/RR/92/2] p 4022 N92-32783
INSTITUT D'AERONOMIE SPATIALE DE BELGIQUE, BRUSSELS.
Grill spectrometry on the Space Shuttle during the Atlas 1 mission
[AERONAUTICA-ACTA-A-364-199] p 3943 N92-32728
INSTITUT DE MECANIQUE DE GRENOBLE (FRANCE).
Numerical simulation of turbulence at the back of the airplane
[ETN-92-91664] p 3931 N92-32769
INSTITUT NATIONAL DES SCIENCES APPLIQUEES, LYON (FRANCE).
Contribution to the study of the effect of the heterogeneous distribution of dislocations on the cyclic plasticity of single crystal aluminum
[ISAL-91-0099] p 4083 N92-32892
INSTITUT NATIONAL DES SCIENCES APPLIQUEES DE LYON, VILLEURBANNE (FRANCE).
Synthesis, morphology and properties of polyester-urethane in solution in styrene: Application to composites development
[ISAL-92-0007] p 3972 N92-32762
Contribution to robot-task adaptation, introduction and use of robot anisotropy and task object for the design of the workstation
[ISAL-91-0095] p 4039 N92-33056
INSTITUT NATIONAL POLYTECHNIQUE, GRENOBLE (FRANCE).
Study of a cellular programmable architecture: Functional definition and programming method
[ETN-92-91663] p 4051 N92-32768
Functions and genericity in a parallel programming language
[ETN-92-91667] p 4051 N92-32771
INSTITUTE FOR AEROSPACE RESEARCH, OTTAWA (ONTARIO).
Processing and environmental effects on mechanical properties of composite repairs
[NRC-LTR-ST-1826] p 3954 N92-32791
A description of the analytical methodology and reporting procedures used in the analysis and preparation of calibration reports for force measuring instruments
[NRC-LTR-ST-1817] p 4022 N92-32848
A Kalman filter integrated navigation design for the IAR Twin Otter Atmospheric Research Aircraft
[NRC-32148] p 3934 N92-32849
Tensile fracture of notched composite laminates
[NRC-32147] p 3955 N92-32852
Influence of edge effect on compression-tension fatigue of toughened graphite/epoxy laminates p 3957 N92-33039
Damage progression under compressive loading in composite laminates containing an open hole p 3957 N92-33040
Fracture surface characteristics of compressive failures in carbon fibre reinforced epoxy laminate subjected to hot/wet conditioning p 3959 N92-33051
A transgranular fatigue crack growth model based on restricted slip reversibility
[NRC-LTR-ST-1831] p 4023 N92-33076
Publications by Structures and Materials Laboratory on composite materials (January 1983 - June 1991)
[NRC-LTR-ST-1833] p 3959 N92-33078
INSTITUTE FOR COMPUTER APPLICATIONS IN SCIENCE AND ENGINEERING, HAMPTON, VA.
Singularities in the classical Rayleigh-Taylor flow: Formation and subsequent motion
[NASA-CR-189690] p 4010 N92-32784
A boundary integral method for an inverse problem in thermal imaging
[NASA-CR-189693] p 4059 N92-33006
A numerical resolution study of high order essentially non-oscillatory schemes applied to incompressible flow
[NASA-CR-189692] p 4012 N92-33110
INSTITUTO DE PESQUISAS ESPACIAIS, SAO JOSE DOS CAMPOS (BRAZIL).
Design and construction of a magnetic sector mass spectrometer
[INPE-5405-RPQ/659] p 4014 N92-32601
Implementation of a tree-code for numerical simulations of stellar systems
[INPE-5370-TDI/469] p 4093 N92-32604
Finding solutions to value independent knapsack problems
[INPE-5390-TAE/011] p 4055 N92-32661
Plasma diffusion through multidipole magnetic fields
[INPE-5384-PRE/1750] p 4079 N92-32662
INTERNATIONAL BUSINESS MACHINES CORP., POUGHKEEPSIE, NY.
A study of large scale software testing p 4045 N92-32879
IOWA STATE UNIV. OF SCIENCE AND TECHNOLOGY, AMES.
Relativistic heavy ion physics
[DE92-015025] p 4067 N92-32922

J

JAPAN SOLAR ENERGY SOCIETY, TOKYO.
The 1991 Japan Solar Energy Society. Japan Wind Energy Association Joint Conference
[DE92-530733] p 4027 N92-33090
JET PROPULSION LAB., CALIFORNIA INST. OF TECH., PASADENA.
Ground-based observations of Titan's thermal spectrum p 4095 N92-32359
Cassini: A mission to Saturn and Titan p 4099 N92-32387
VLSI architecture for a Reed-Solomon decoder
[NASA-CASE-NPO-17897-1-CU] p 3991 N92-33011
Obstacle avoidance for redundant robots using configuration control
[NASA-CASE-NPO-17852-1-CU] p 4054 N92-33019
Real-time edge-enhanced optical correlator
[NASA-CASE-NPO-18379-1-CU] p 4076 N92-33022
Real time pre-detection dynamic range compression
[NASA-CASE-NPO-18098-1-CU] p 4076 N92-33028
Auto and hetero-associative memory using a 2-D optical logic gate
[NASA-CASE-NPO-17997-1-CU] p 4041 N92-33057
JOINT INST. FOR LAB. ASTROPHYSICS, BOULDER, CO.
Applications of the photorefractive effect and damage induced effects in fibers
[AD-A250767] p 3953 N92-32674
JOINT PUBLICATIONS RESEARCH SERVICE, ARLINGTON, VA.
JPRS report: Science and technology. Central Eurasia: Materials science
[JPRS-UMS-92-011] p 3969 N92-33129
JUSZKO SCIENTIFIC SERVICES, VICTORIA (BRITISH COLUMBIA).
Parameterization of directional spectra, part 2. Volume 2: User's manual for the programs RMODEL, FITHM, and FITDM
[DREA-CR-89-445-PT-2-VOL-2] p 3981 N92-32749

K

KANSAS UNIV., LAWRENCE.
The ionosphere of Titan and its interaction with Saturnian magnetospheric electrons p 4099 N92-32386

KAUPPA-JA TEOLLISUUSMINISTERIO, HELSINKI (FINLAND).
NEMO: Advanced energy systems and technologies
[DE92-540920] p 4027 N92-33072
KENT UNIV., CANTERBURY (ENGLAND).
Laboratory determination of the refractive indices of liquid methane and ethane at temperatures appropriate to the surface of Titan p 4100 N92-32391
Laboratory determination of the thermal conductivity of liquid methane and ethane p 4015 N92-32392
A surface science package for the Huygens Titan probe p 4102 N92-32410
KENTUCKY UNIV., LEXINGTON.
Clean gasoline reforming with superacid catalysts
[DE92-013833] p 3975 N92-33123
KERNFORSCHUNGSZENTRUM G.M.B.H., KARLSRUHE (GERMANY, F.R.).
Study on lifetime specific, laser-induced ultrafast fluorescence detection in the time and frequency domain for in-situ environmental analysis of organic pollutants
[KFK-4975] p 4029 N92-32841
A three-field model of transient 3D multiphase, three-component flow for the computer code 4 A3. Part1: Theoretical basis: Conservation and state equations, numerics
[KFK-4948-PT-1] p 4011 N92-32857
A three-field model of transient 3D multiphase, three-component flow for the computer code 4 A3. Part 2: Models for the interfacial transport phenomena. Code validation
[KFK-4949-PT-2] p 4011 N92-32858
KLEIN ASSOCIATES, YELLOW SPRINGS, OH.
Observing team coordination within Army rotary-wing aircraft crews
[AD-A252234] p 4039 N92-32433
KNOWLEDGE BASED SYSTEMS, INC. COLLEGE STATION, TX.
Information Integration for Concurrent Engineering (IICE) IDEF3 process description capture method report
[AD-A252633] p 4042 N92-32627
IDEF4 object-oriented design method manual
[AD-A252634] p 4042 N92-32658
KRUG LIFE SCIENCES, INC., SAN ANTONIO, TX.
Comparative effects of antihistamines on aircrew performance of simple and complex tasks under sustained operations
[AD-A248752] p 4036 N92-32492

L

LABORATOIRE D'AUTOMATIQUE ET D'ANALYSE DES SYSTEMES, TOULOUSE (FRANCE).
Study and achievement of a parallel simulator for diffusion at the atomic level: Creation and growth of dislocation loops under electronic radiation
[LAAS-92118] p 4066 N92-32735
Fault tolerance for security management in distributed systems
[LAAS-92011] p 4040 N92-32766
A discrete nonlinear model approach to study the behavior of large signal DC to DC converters
[LAAS-90028] p 3989 N92-32777
A continuous nonlinear model approach to study the behavior of large signal DC to DC converters
[LAAS-90027] p 3990 N92-32793
On physical systems qualitative approach: Real time help for fermentation process control
[LAAS-91445] p 4036 N92-32844
LAMONT-DOHERTY GEOLOGICAL OBSERVATORY, PALISADES, NY.
Recent changes of weather patterns in North America
[DE92-014342] p 4033 N92-32720
LASER SCIENCE, INC., AMES, IA.
Laser coating of composites for enhanced wear and corrosion resistance
[AD-A249231] p 3956 N92-32906
LAWRENCE LIVERMORE NATIONAL LAB., CA.
A numerical study of natural convection in a narrow annulus
[DE92-017138] p 4006 N92-32322
Quantitative non-destructive environmental characterization of advanced materials
[DE92-011462] p 3946 N92-32327
An implementation of Hill's theory of normal anisotropic plasticity for explicit shell analysis
[DE92-011468] p 4020 N92-32328
Physical basis for a pressure-dependent yield criterion for polymers
[AD-A250763] p 3970 N92-32341
A scalable, switched circuit LAN for Gb/S channels with over Tb/S total capacity
[DE92-013444] p 4050 N92-32412
Transverse beam dynamics in recirculating accelerators for heavy-ion fusion
[DE92-013448] p 4070 N92-32413
Program PLOTTAB: A code designed to plot continuous and/or discrete physical data
[DE92-013754] p 4041 N92-32416
Shock tube ignition of ethanol, isobutene and MTBE: Experiments and modeling
[DE92-008563] p 3961 N92-32544
Molecular dynamics modeling of the mechanical properties of metal surfaces at the nanometer scale
[DE92-010705] p 3966 N92-32646
Free vibration of thick isotropic and orthotropic cylindrical shells
[DE92-011653] p 4022 N92-32706
The Nova Upgrade Facility for ICF ignition and gain
[DE92-010703] p 4079 N92-32733
PANACEA User's Manual
[DE92-011289] p 4043 N92-32741
Advanced computational transport methods for curvilinear geometries
[DE92-011290] p 4057 N92-32743
Advances in compressible turbulent mixing
[DE92-014326] p 4010 N92-32824
Study of recirculating induction accelerators as drivers for heavy ion fusion
[DE92-016980] p 4071 N92-32904
Light-ion spectroscopy with exotic targets
[DE92-017258] p 3964 N92-32929
Small passive chemical detector
[DE92-014188] p 4030 N92-32933
Numerical simulation of inclined chute flows of monodisperse, inelastic, frictional spheres
[DE92-014775] p 4012 N92-32947
The LLNL Multi-User Tandem Laboratory PIXE microprobe
[DE92-017252] p 4014 N92-32999
Applications of energy loss contrast STIM
[DE92-017254] p 4014 N92-33000
Ion microtomography using ion time-of-flight
[DE92-017257] p 4068 N92-33001
Connectivity structures and differencing techniques for staggered-grid free-Lagrange hydrodynamics
[DE92-017313] p 4012 N92-33082
Collective resonances of valence electrons in free metal clusters
[DE92-014783] p 3969 N92-33116
Development of advanced modulators for recirculating heavy ion accelerators
[DE92-014795] p 4072 N92-33122
A study of the dissolution mechanism by chemical and electrochemical oxidation-reduction of actinide dioxides (UO2, NpO2, PuO2, and AmO2) in an acid aqueous medium
[DE92-014834] p 3965 N92-33126
Electrochemical polarization measurements on pitting corrosion susceptibility of nickel-rich Alloy 825
[DE92-014885] p 3969 N92-33132
LEHIGH UNIV., BETHLEHEM, PA.
Methane oxidation over dual redox catalysts
[DE92-014358] p 3960 N92-32334
High octane ethers from synthesis gas-derived alcohols
[DE92-013802] p 3975 N92-33108
LOCKHEED AERONAUTICAL SYSTEMS CO., MARIETTA, GA.
Postbuckling of stiffened composite plates under combined loading p 3952 N92-32585
Acoustic loads prediction on jet aircraft p 4061 N92-32949
LOCKHEED ENGINEERING AND SCIENCES CO., HAMPTON, VA.
Laser to single-mode-fiber coupling: A laboratory guide
[NASA-CR-4452] p 4077 N92-33239
LOGICON, INC., SAN DIEGO, CA.
Tactical state and performance assessment during air combat maneuvering
[AD-A247426] p 3935 N92-32612
LOS ALAMOS NATIONAL LAB., NM.
An adaptive algorithm for modifying hyperellipsoidal decision surfaces
[DE92-013540] p 4041 N92-32414
National environmental compliance strategy
[DE92-013639] p 4027 N92-32415
Analytic score comparison of geometry splitting and exponential transform for a simple Monte Carlo problem
[DE92-013108] p 4059 N92-32481
High intensity negative proton beams from a SNICS ion source
[DE92-011137] p 4070 N92-32647
HDR opportunities and challenges beyond the long-term flow test isco, CA, 24-26 Mar. 1992
[DE92-011234] p 4025 N92-32695
The dependence of the anisoplanatic Strehl of a compensated beam on the beacon distribution
[DE92-011272] p 4016 N92-32736
The effect of the light round-trip time on the performance of an adaptive optics turbulence compensation system
[DE92-011273] p 4075 N92-32738
Fifty years in science, thirty years in space
[LALP-92-51] p 4104 N92-32862
Automated data acquisition and analysis in the mechanical test lab
[DE92-011231] p 4040 N92-32910
Collaborative, remote, in-depth inspection and verification of satellites with neutral particle beams
[DE92-014195] p 3943 N92-32934
Synthesis, microstructure, critical current density, magnetization and relaxation of hot-pressed YBa2Cu3O(6 + delta) through partial melting post-oxygenation
[DE92-015205] p 4085 N92-33026
Plasma opening switch for long-pulse intense ion beam
[DE92-017523] p 3992 N92-33068
Physics in knots
[DE92-017530] p 4088 N92-33069
Synthesis of MoSi2-based alloys by mechanical alloying
[DE92-017528] p 3969 N92-33120
Turbulence transport equations for variable-density turbulence and their relationship to two-field models
[DE92-017292] p 4013 N92-33159

M

MANCHESTER UNIV. (ENGLAND).
The Huygens SSP Refractometer (REF)
p 4101 N92-32399
MANITOBA UNIV., WINNIPEG.
Phased array implementation using elements with scan capability
[CTN-92-60335] p 3981 N92-32787
Electromagnetic scattering by systems of arbitrarily oriented spheroids
[ISBN-0-315-63332-8] p 3986 N92-33191
Numerical analysis of scattering from certain conducting and dielectric bodies of arbitrary shape
[ISBN-0-315-63282-8] p 3987 N92-33192
A simplified synthesis of lossless two-port wave digital and analog filters
[ISBN-0-315-63272-0] p 3993 N92-33193
MARTIN MARIETTA ENERGY SYSTEMS, INC., LIVERMORE, CA.
High temperature fabricable nickel-iron aluminides
[CA-PATENT-1-276-814] p 3968 N92-32855
MARYLAND UNIV., COLLEGE PARK.
Pulse coded biologically motivated neural-type MOS circuits
[AD-A250367] p 3988 N92-32325
Measurement of the magnetic and electrical activity of individual cells in vitro
[AD-A250881] p 4035 N92-32345
Titan's mid-IR albedo: New observations from 3 to 5 microns p 4097 N92-32376
The problems of routing and scheduling in multihop radio networks. A Hopfield neural network approach
[AD-A247431] p 3979 N92-32570
Nonlinear dynamics and plasma transport
[DE92-014246] p 4078 N92-32592
Exploitation of parallelism in climate models
[DE92-012595] p 4028 N92-32619
Methodological and architectural issues in the experience factory p 4044 N92-32870
Optimized set reduction for empirically guiding software development p 4044 N92-32875
Jacobian and stiffness analysis of a novel class of six-DOF parallel minimanipulators
[DE92-016373] p 4054 N92-33184
MASSACHUSETTS INST. OF TECH., CAMBRIDGE.
Mechanisms of the oxidation of metals and alloys with emphasis on superconductors
[DE92-016840] p 3966 N92-32315
Satellite radio interferometry
[PL-TR-91-2200] p 3978 N92-32458
Impact response of graphite/epoxy fabric structures p 3951 N92-32583
Simple models for turbulent wave-current bottom boundary layer flow
[AD-A247942] p 4007 N92-32630
Direct catalytic decomposition of nitric oxide
[DE92-013847] p 4030 N92-33125
MASSACHUSETTS INST. OF TECH., LEXINGTON.
Multichip module study
[AD-A250877] p 3989 N92-32678
Beam and filter straddle losses in an ESA search radar
[AD-A250878] p 3980 N92-32680
Airport Surveillance Radar (ASR-9) wind shear processor: 1991 test at Orlando, Florida
[AD-A252246] p 3980 N92-32686
Multifrequency measurements of radar ground clutter at 42 sites. Volume 1: Principal results
[AD-A246710] p 3980 N92-32696

MASTER SYSTEMS, INC., MCLEAN, VA.
Measurement in practice p 4044 N92-32876
MATERIALS RESEARCH LABS., ASCOT VALE (AUSTRALIA).
Calculation of the energy of elastic deformation of Kevlar backing plates for ceramic armours
[AD-A250129] p 3970 N92-32489
MAX-PLANCK-INST. FUER AERONOMIE, KATLENBURG-LINDAU (GERMANY, F.R.).
Plasma interaction of Titan with the Saturnian magnetosphere: A review of critical issues
p 4098 N92-32382
MCDONNELL AIRCRAFT CO., SAINT LOUIS, MO.
Development of composite wing carrythrough bulkheads for fighter aircraft p 3948 N92-32519
Out of plane analysis for composite structures
p 3949 N92-32527
Certification of damage tolerant composite structure
p 3951 N92-32580
MCGILL UNIV., MONTREAL (QUEBEC).
The local structure of image intensity discontinuities
[ISBN-0-315-57231-0] p 4048 N92-33204
Dynamics of Rossby waves in a parabolic jet
[ISBN-0-315-57159-4] p 4034 N92-33225
Visibility properties of polygons
[ISBN-0-315-57272-8] p 4049 N92-33229
Message delay models of packet-switching networks
[ISBN-0-315-57208-6] p 4053 N92-33235
MDA ENGINEERING, INC., ARLINGTON, TX.
Enhancements to the GRIDGEN structured grid generation system for internal and external flow applications p 4005 N92-32301
MESSERSCHMITT-BOELKOW-BLOHM G.M.B.H., BREMEN (GERMANY, F.R.).
Parallel processing in space applications using transputer networks
[MBB-UO-0172-90-PUB] p 4050 N92-32689
MESSERSCHMITT-BOELKOW-BLOHM G.M.B.H., MUNICH (GERMANY, F.R.).
The German anti tank helicopter PAH 2: An example of a future sensor platform p 3937 N92-32448
Fundamental questions concerning the application of superplastic forming and superplastic forming/diffusion bonding
[MBB-Z-0402-91-PUB] p 3977 N92-32690
The use of piezoelectric sensors to detect delamination initiation in carbon fiber reinforced composites
[MBB-Z-0391-91-PUB] p 3954 N92-32740
Aluminum based particulate composites for aerospace applications produced by different processes
[MBB-Z-0408-91-PUB] p 3967 N92-32819
Superplastic forming of Ti6Al4V at lower temperature using hydrogen
[MBB-Z-0403-91-PUB] p 3978 N92-32893
Accommodation mechanisms and dispersoid-free zone s in Al 7475 after superplastic forming
[MBB-Z-0404-91-PUB] p 3968 N92-32894
New accelerated corrosion test methods
[MBB-Z-0406-91-PUB] p 3968 N92-32895
Low cost MMC made by spray deposition
[MBB-Z-0407-91-PUB] p 3968 N92-32897
MESSERSCHMITT-BOELKOW-BLOHM G.M.B.H., OTTOBRUNN (GERMANY, F.R.).
Examples of advanced near-net shape manufacturing techniques for aerospace
[MBB-Z-0399-91-PUB] p 3977 N92-32742
METRAFLU, ECULLY (FRANCE).
Pressure field developed by the random movement of the vortices near a wall
[ETN-92-91665] p 4009 N92-32770
MICHIGAN STATE UNIV., EAST LANSING.
Study of flow properties of wet solids using laser induced photochemical anemometry
[DE92-015452] p 4013 N92-33140
Study of flow properties of wet solids using laser induced photochemical anemometry
[DE92-014031] p 4017 N92-33180
MICHIGAN UNIV., ANN ARBOR.
Mass loading at Titan and comets
p 4098 N92-32383
A finite element-boundary integral method for conformal antenna arrays on a circular cylinder
[NASA-CR-190610] p 3979 N92-32559
Human learning of schemas from explanations in practical electronics
[AD-A247429] p 4038 N92-32569
A basic research model of natural gas combustion in turbulent flow, phase 2
[PB92-190362] p 4007 N92-32598
MIDDLE EAST TECHNICAL UNIV., ANKARA (TURKEY).
The effect of heat treatment on the properties of PEEK and APC-2 p 3959 N92-33052
MIDWEST BIO-LASER INST., CHICAGO, IL.
Midwest free-electron laser program
[AD-A247264] p 4016 N92-32540
MIDWEST RESEARCH INST., GOLDEN, CO.
Thin film cadmium telluride, zinc telluride, and mercury zinc telluride solar cells
[DE92-001237] p 4024 N92-32510
Solar photo-thermal catalytic reactions to produce high value chemicals
[DE91-002140] p 4026 N92-32908
Thermochemical cycles for energy storage: Thermal decomposition of ZnSO4 systems
[DE91-002144] p 4026 N92-32909
High-flux solar photon processes
[DE92-001247] p 4027 N92-33138
MISSISSIPPI UNIV. FOR WOMEN, COLUMBUS.
An efficient and robust grid optimization algorithm
p 4004 N92-32300
CAGI: Computer Aided Grid Interface. A work in progress p 4005 N92-32302
MITRE CORP., BEDFORD, MA.
Ethernet bandwidth utilization of datafull, dataless, and diskless node workstation and x-terminals
[AD-A252374] p 4052 N92-32937
MITRE CORP., MCLEAN, VA.
Safety study of TCAS 2 for logic version 6.04
[DOT/FAA/RD-92/22] p 3933 N92-32537
Simulation test and evaluation of TCAS 2 logic version 6.04
[DOT/FAA/RD-92/23] p 3934 N92-33098
MORGANTOWN TECHNOLOGY CENTER, WV.
High-temperature Solid Oxide Fuel Cell (SOFC) generator development project: Environmental assessment
[DE92-014698] p 4026 N92-32924
MOUND LAB., MIAMISBURG, OH.
Density variations and anomalies in palladium compacts
[DE92-014382] p 3967 N92-32721
Radiography to measure the longitudinal density gradients of Pd compacts
[DE92-014383] p 3968 N92-32896

N

NAGOYA UNIV. (JAPAN).
STEL p 4103 N92-32457
NATIONAAL INST. VOOR KERNFYSICA EN HOGE ENERGIEFYSICA, AMSTERDAM (NETHERLANDS).
Supersymmetry searches at electron-proton colliders
[ETN-92-92057] p 4067 N92-32753
NATIONAL ACADEMY OF SCIENCES - NATIONAL RESEARCH COUNCIL, WASHINGTON, DC.
Independent verification and validation for Space Shuttle flight software
[NASA-CR-190826] p 4047 N92-33196
NATIONAL AERONAUTICAL ESTABLISHMENT, OTTAWA (ONTARIO).
The use of Kalman filtering techniques to improve the accuracy of flight test data
[NRC-32139] p 3938 N92-32850
NATIONAL AERONAUTICS AND SPACE ADMINISTRATION, WASHINGTON, DC.
Space Station Freedom media handbook
[NASA-TM-107981] p 3942 N92-32421
Toward the next millennium: A vision for spaceship Earth
[NASA-TM-107986] p 3941 N92-33007
An international aerospace information system: A cooperative opportunity
[NASA-TM-108171] p 4091 N92-33237
NATIONAL AERONAUTICS AND SPACE ADMINISTRATION. AMES RESEARCH CENTER, MOFFETT FIELD, CA.
CFD applications in pump flows p 4002 N92-32288
Impact origin of Titan's atmosphere
p 4094 N92-32351
The atmospheric temperature structure of Titan
p 4095 N92-32358
Numerical simulation of the circulation of the atmosphere of Titan p 4095 N92-32361
Titan's organic haze p 4097 N92-32372
VIMS/Cassini mission at Titan: Scientific objectives and observational scenarios p 4097 N92-32377
Huygens/ASI plasma wave analyzer capabilities for aerosol measurement p 4098 N92-32380
Laboratory investigations of the aerosols in the stratosphere of Titan p 4102 N92-32405
Potential flow theory and operation guide for the panel code PMARC
[NASA-TM-102851] p 3929 N92-32422
Vision-based range estimation using helicopter flight data
[NASA-TM-103930] p 3933 N92-32424
Computations of unsteady multistage compressor flows in a workstation environment
[NASA-TM-103839] p 3938 N92-32452
Thermal conductance of augmented pressed metallic contacts at liquid helium temperatures
[NASA-TM-103917] p 4007 N92-32474
Thermal degradation study of silicon carbide threads developed for advanced flexible thermal protection systems
[NASA-TM-103952] p 3970 N92-32476
A curved beam test specimen for determining the interlaminar tensile strength of a laminated composite
p 3949 N92-32526
Collaborative research on V/STOL control system/cockpit display tradeoffs under the NASA/MOD joint aeronautical program
[NASA-TM-103910] p 3939 N92-32788
Advancing automation and robotics technology for the Space Station Freedom and for the US economy
[NASA-TM-103940] p 4040 N92-32809
Analysis of a benchmark suite to evaluate mixed numeric and symbolic processing
[NASA-TM-103907] p 4052 N92-32886
Ski jump takeoff performance predictions for a mixed-flow, remote-lift STOVL aircraft
[NASA-TM-103866] p 3935 N92-32887
CTAS: Computer intelligence for air traffic control in the terminal area
[NASA-TM-103959] p 3933 N92-33080
Director's discretionary fund report for FY 1991
[NASA-TM-103902] p 4105 N92-33106
Computation of incompressible viscous flows through turbopump components
[NASA-TM-103911] p 4012 N92-33113
Analysis of delay reducing and fuel saving sequencing and spacing algorithms for arrival traffic
[NASA-TM-103880] p 3933 N92-33194
NATIONAL AERONAUTICS AND SPACE ADMINISTRATION. GODDARD INST. FOR SPACE STUDIES, NEW YORK, NY.
A preliminary assessment of the Titan planetary boundary layer p 4095 N92-32363
NATIONAL AERONAUTICS AND SPACE ADMINISTRATION. GODDARD SPACE FLIGHT CENTER, GREENBELT, MD.
Tenth Workshop for Computational Fluid Dynamic Applications in Rocket Propulsion, part 2
[NASA-CP-3163-PT-2] p 3994 N92-32245
Tenth Workshop for Computational Fluid Dynamic Applications in Rocket Propulsion, part 1
[NASA-CP-3163-PT-1] p 4000 N92-32278
The meteorology of Titan p 4095 N92-32360
Infrared properties of Titan's clouds and aerosols
p 4097 N92-32373
Cassini/CIRS capabilities for aerosol, cloud, and surface measurements p 4098 N92-32378
Huygens/ACP: An instrument for aerosols chemical composition measurements p 4098 N92-32379
The synthetic infrared spectrum of Titan at high spectral resolution p 4099 N92-32389
Development of a prototype spatial information processing system for hydrologic research
[NASA-CR-190579] p 4024 N92-32590
Steady induction effects in geomagnetism. Part 1A: Steady motional induction of geomagnetic chaos
[NASA-TP-3272-PT-1A] p 4031 N92-32655
Proceedings of the Sixteenth Annual Software Engineering Workshop
[NASA-TM-107964] p 4044 N92-32869
Cleanroom process evolution in the SEL
p 4044 N92-32871
Experiments in software engineering technology: Recent studies in the SEL (1990-1991) p 4044 N92-32872
Device for removing foreign objects from anatomic organs
[NASA-CASE-GSC-13306-1] p 4038 N92-33032
NATIONAL AERONAUTICS AND SPACE ADMINISTRATION. HUGH L. DRYDEN FLIGHT RESEARCH FACILITY, EDWARDS, CA.
User's manual for AeroFcn: A FORTRAN program to compute aerodynamic parameters
[NASA-TM-104237] p 4042 N92-32507
Flight testing and simulation of an F-15 airplane using throttles for flight control
[NASA-TM-104255] p 3940 N92-32864
The development of an airborne information management system for flight test
[NASA-TM-104251] p 3938 N92-32866
Rapid development of the X-31 simulation to support flight-testing
[NASA-TM-104256] p 3935 N92-33149
NATIONAL AERONAUTICS AND SPACE ADMINISTRATION. JOHN F. KENNEDY SPACE CENTER, COCOA BEACH, FL.
Debris/ice/TPS assessment and integrated photographic analysis for Shuttle Mission STS-49
[NASA-TM-107547] p 3941 N92-32454

NATIONAL AERONAUTICS AND SPACE ADMINISTRATION. LYNDON B. JOHNSON SPACE CENTER, HOUSTON, TX.

Microporous structure with layered interstitial surface treatment, and method and apparatus for preparation thereof
[NASA-CASE-MSC-21487-1] p 3965 N92-33009

Electromagnetic attachment mechanism
[NASA-CASE-MSC-21463-1] p 4019 N92-33018

Purification system
[NASA-CASE-MSC-21584-1] p 3965 N92-33029

NATIONAL AERONAUTICS AND SPACE ADMINISTRATION. LANGLEY RESEARCH CENTER, HAMPTON, VA.

Environmental fatigue in aluminum-lithium alloys
[NASA-TM-107640] p 4021 N92-32423

A method for designing blended wing-body configurations for low wave drag
[NASA-TP-3261] p 3929 N92-32480

Eighth DOD/NASA/FAA Conference on Fibrous Composites in Structural Design, part 1
[NASA-CP-3087-PT-1] p 3946 N92-32513

A Protection And Detection Surface (PADS) for damage tolerance p 3948 N92-32523

Global/local methods research using the CSM testbed p 3949 N92-32528

The multiple-function multi-input/multi-output digital controller system for the AFW wind-tunnel model
[NASA-TM-107600] p 3934 N92-32536

Eighth DOD/NASA/FAA Conference on Fibrous Composites in Structural Design, part 2
[NASA-CP-3087-PT-2] p 3950 N92-32574

Residual strength of repaired graphite/epoxy laminates after 5 years of outdoor exposure p 3950 N92-32577

Compression behavior of graphite-epoxy and graphite-thermoplastic panels with circular holes or impact damage p 3951 N92-32582

Buckling and postbuckling behavior of square compression-loaded graphite-epoxy plates with circular cutouts p 3952 N92-32587

Frequency domain state-space system identification
[NASA-TM-107659] p 4021 N92-32657

Analysis of data from a DO-178A software development process p 4045 N92-32880

Fourth Aircraft Interior Noise Workshop
[NASA-CP-10103] p 4061 N92-32948

Active control of interior noise in a large scale cylinder using piezoelectric actuators p 4063 N92-32958

Polyimides with carbonyl and ether connecting groups between the aromatic rings
[NASA-CASE-LAR-14001-1] p 3973 N92-33008

Integrated launch and emergency vehicle system
[NASA-CASE-LAR-13780-1] p 3943 N92-33013

Polyimide molding powder, coating, adhesive, and matrix resin
[NASA-CASE-LAR-14163-1] p 3973 N92-33014

Methyl substituted polyimides containing carbonyl and ether connecting groups
[NASA-CASE-LAR-14351-1] p 3973 N92-33015

Passive fetal monitoring sensor
[NASA-CASE-LAR-14088-1-CU] p 4015 N92-33016

High temperature fiber optic microphone having a pressure-sensing reflective membrane under tensile stress
[NASA-CASE-LAR-14402-1-CU] p 4076 N92-33017

Flush mounting of thin film sensors
[NASA-CASE-LAR-14446-1] p 3978 N92-33020

Vacuum-isolation vessel and method for measurement of thermal noise in microphones
[NASA-CASE-LAR-14567-1-CU] p 3991 N92-33021

Noncircular rolling joints for vibrational reduction in slewing maneuvers
[NASA-CASE-LAR-14515-1-CU] p 4019 N92-33031

Flight service environmental effects on composite materials and structures p 3959 N92-33054

SAGE 1 data user's guide
[NASA-RP-1275] p 4031 N92-33097

Computational methods for global/local analysis
[NASA-TM-107591] p 4023 N92-33104

Improved HIRAP flight calibration technique
[NASA-TM-107656] p 3944 N92-33112

Building vibrations induced by noise from rotorcraft and propeller aircraft flyovers
[NASA-TM-104170] p 4063 N92-33160

Image processing mini manual
[NASA-TM-107680] p 4041 N92-33205

NATIONAL AERONAUTICS AND SPACE ADMINISTRATION. LEWIS RESEARCH CENTER, CLEVELAND, OH.

Solar radiation on a catenary collector
[NASA-TM-105751] p 3988 N92-32243

A critical evaluation of a three-dimensional Navier-Stokes CFD as a tool to design supersonic turbine stages p 3999 N92-32268

Three-dimensional flow fields inside a shrouded inducer at design and off-design conditions (CFD study) p 4003 N92-32291

Reliability training
[NASA-RP-1253] p 3941 N92-32456

NASA's nuclear electric propulsion technology project
[NASA-TM-105811] p 3944 N92-32463

Computational simulation of matrix micro-slip bands in SiC/Ti-15 composite
[NASA-TM-105762] p 3946 N92-32466

Breakdown of the Karman vortex street due to forced convection and flow compressibility
[NASA-TM-105853] p 4007 N92-32472

Computational simulation of structural fracture in fiber composites p 3949 N92-32531

Liquid lubricants for advanced aircraft engines
[NASA-TM-104531] p 3972 N92-32863

Overview and evolution of the LeRC PMAD DC Testbed
[NASA-TM-105842] p 3991 N92-32867

A new time scale based k-epsilon model for near wall turbulence
[NASA-TM-105768] p 4011 N92-32868

Solid State Technology Branch of NASA Lewis Research Center
[NASA-TM-105752] p 3982 N92-32965

V-band pseudomorphic HEMT MMIC phased array components for space communications p 3983 N92-32966

Planar dielectric resonator stabilized HEMT oscillator integrated with CPW/aperture coupled patch antenna p 3983 N92-32967

An optically controlled Ka-band phased array antenna p 3983 N92-32968

Ka-band dual frequency array feed for a low cost ACTS ground terminal p 3983 N92-32969

Coplanar waveguide feeds for phased array antennas p 3983 N92-32970

Analysis of shielded CPW discontinuities with air-bridges p 3983 N92-32971

A flexible CPW package for a 30 GHz MMIC amplifier p 3983 N92-32972

A 1-W, 30-GHz, CPW amplifier for ACTS small terminal uplink p 3984 N92-32973

Comparative evaluation of optical waveguides as alternative interconnections for high performance packaging p 3984 N92-32974

Intermodulation in the oscillatory magnetoresistance of a two-dimensional electron gas p 3984 N92-32975

Reduced mobility and PPC in In(.20)Ga(.80)As / Al(.23)Ga(.77)As HEMT structure p 3984 N92-32976

Study of InGaAs-based modulation doped field effect transistor structures using variable-angle spectroscopic ellipsometry p 3984 N92-32977

Microwave properties of peeled HEMT devices sapphire substrates p 3984 N92-32978

NASA space applications of high-temperature superconductors p 3985 N92-32980

Measurement techniques for cryogenic Ka-band microstrip antennas p 3985 N92-32981

Performance of a Y-Ba-Cu-O superconducting filter/GaAs low noise amplifier hybrid circuit p 3985 N92-32982

Magnetic penetration depth of YBa2Cu3O(7-delta) thin films determined by the power transmission method p 3985 N92-32983

Magnetic flux relaxation in YBa2Cu3O(7-x) thin film: Thermal or athermal p 3985 N92-32984

The evolutionary development of high specific impulse electric thruster technology
[NASA-TM-105758] p 3944 N92-33064

NATIONAL AERONAUTICS AND SPACE ADMINISTRATION. MARSHALL SPACE FLIGHT CENTER, HUNTSVILLE, AL.

A comparative study of the effects of inhibitor stub length on solid rocket motor combustion chamber pressure oscillations: RSRM at T = 80 seconds, preliminary results p 3945 N92-32248

A status of the activities of the NASA. Marshall Space Flight Center Combustion Devices Technology Team p 3995 N92-32250

CFD analysis of the STME nozzle flowfield p 3995 N92-32251

A numerical model for atomization-spray coupling in liquid rocket thrust chambers p 3996 N92-32257

Numerical modeling for dilute and dense sprays p 3997 N92-32258

CFD modeling of turbulent flows around the SSME main injector assembly using porosity formulation p 3997 N92-32260

Computational fluid dynamics analysis of SSME phase 2 and phase 2+ preburner injector element hydrogen flow paths p 3997 N92-32261

An experimental study of the fluid mechanics associated with porous walls
[AIAA PAPER 92-0769] p 3998 N92-32263

A status of the Turbine Technology Team activities p 3998 N92-32267

Technology test bed review p 4001 N92-32279

Advanced solid rocket motor project status p 3945 N92-32280

Space Transportation Main Engine p 3945 N92-32281

A status of the activities of the NASA/MSFC pump stage technology team p 4002 N92-32286

CFD analysis of pump consortium impeller p 4002 N92-32287

CFD analysis to optimize a design modification of BSMT p 4004 N92-32296

Numerical analysis of the hot-gas-side and coolant-side heat transfer in liquid rocket engine combustors p 4004 N92-32299

Using adaptive grid in modeling rocket nozzle flow p 4005 N92-32303

Complex three-dimensional internal flows in the ASRM and RSRM aft end segments p 4005 N92-32304

NASA Marshall Space Flight Center Solar Observatory report, January - June 1992
[NASA-TM-103597] p 4092 N92-32478

Rotating-unbalanced-mass devices and methods for scanning balloon-borne-experiments, free-flying spacecraft, and space shuttle/space station attached experiments
[NASA-CASE-MFS-28425-1] p 4015 N92-33010

Multispectral variable magnification glancing incidence x ray telescope
[NASA-CASE-MFS-28013-4] p 4092 N92-33012

Arc/gas electrode
[NASA-CASE-MFS-29766-1] p 3991 N92-33030

Development of static system procedures to study aquatic biofilms and their responses to disinfection and invading species
[NASA-TM-103598] p 4036 N92-33103

NATIONAL AERONAUTICS AND SPACE ADMINISTRATION. PASADENA OFFICE, CA.

VLSI architecture for a Reed-Solomon decoder
[NASA-CASE-NPO-17897-1-CU] p 3991 N92-33011

Obstacle avoidance for redundant robots using configuration control
[NASA-CASE-NPO-17852-1-CU] p 4054 N92-33019

Real-time edge-enhanced optical correlator
[NASA-CASE-NPO-18379-1-CU] p 4076 N92-33022

Real time pre-detection dynamic range compression
[NASA-CASE-NPO-18098-1-CU] p 4076 N92-33028

Auto and hetero-associative memory using a 2-D optical logic gate
[NASA-CASE-NPO-17997-1-CU] p 4041 N92-33057

NATIONAL AEROSPACE LAB., AMSTERDAM (NETHERLANDS).

Modeling and numerical simulation of vortex flow in aerodynamics
[NLR-TP-91154-U] p 3930 N92-32673

Thermal gravitational modelling and scaling of two-phase heat transport systems for space: An assessment and a comparison of predictions and experimental results
[NLR-TP-91401-U] p 4008 N92-32675

New concepts for multi-block grid generation for flow domains around complex aerodynamic configurations
[NLR-TP-91046-U] p 3930 N92-32730

An experimental study of the flow over a sharp-edged delta wing at subsonic and transonic speeds
[NLR-TP-91117-U] p 3930 N92-32732

Integration of wall interference assessment and wall adaptation
[NLR-TP-91119-U] p 3940 N92-32734

NLR investigations of flutter behaviour of fighter aircraft with external stores
[NLR-TP-91134-U] p 3939 N92-32750

Two-phase heat transport systems for space: Thermal gravitational modelling and scaling predictions versus results of experiments
[NLR-TP-91051-U] p 4010 N92-32786

Development of new flight procedures for the Microwave Landing System (MLS)
[NLR-TP-91156-U] p 3933 N92-32830

Free motion of an unsupported tank that is partially filled with liquid
[NLR-TP-91185-U] p 4011 N92-32831

Software development practice in a scientific computing environment
[NLR-TP-91193-U] p 4043 N92-32832

Life cycle oriented method for development and production of large scale industrial mathematics software
[NLR-TP-91196-U] p 4043 N92-32833

Investigations preparatory to the Wet Satellite Model Experiment
[NLR-TP-91219-U] p 3943 N92-32834

CFD efforts in the Netherlands
[NLR-TP-91250-U] p 4011 N92-32835

GARTEUR compression behaviour of advanced CFRP p 3957 N92-33042
Global/local interlaminar stress analysis of a grid-stiffened composite panel [NASA-CR-190822] p 4023 N92-33139

NATIONAL CENTER FOR ATMOSPHERIC RESEARCH, BOULDER, CO.
Annual variation of surface temperatures over the world [PB92-193259] p 4028 N92-32554

NATIONAL DEFENCE HEADQUARTERS, OTTAWA (ONTARIO).
Operational needs for an unmanned air vehicle p 3936 N92-32438

NATIONAL DEFENCE RESEARCH ESTABLISHMENT, UMEA (SWEDEN).
A simulation of radioactive fallout using the MATHEW/ADPIC model [FCA-C-40292-4.3] p 4029 N92-32785

NATIONAL HURRICANE CENTER, CORAL GABLES, FL.
Diagnostic report of the National Hurricane Center, August and September 1991, volume 4, number 2 [PB92-179407] p 4033 N92-32503

NATIONAL INST. FOR FUSION SCIENCE, NAGOYA (JAPAN).
Two- and three-dimensional simulation code for radiation-hydrodynamics in ICF [NIFS-119] p 4078 N92-32552
Fast ion loss and radial electric field in Wendelstein 7-A stellarator [DE92-782106] p 4079 N92-32745
Status of LHD control system design [NIFS-122] p 4070 N92-32746
The role of stochasticity in sawtooth oscillation [DE92-782004] p 3982 N92-32905

NATIONAL INST. OF STANDARDS AND TECHNOLOGY, BOULDER, CO.
Trapped ions and laser cooling 3 [PB92-189547] p 4016 N92-33060
Calibration service for low-loss, three-terminal capacitance standards at 100 kHz and 1 MHz [PB92-189554] p 3991 N92-33061

NATIONAL INST. OF STANDARDS AND TECHNOLOGY, GAITHERSBURG, MD.
National Voluntary Laboratory Accreditation Program 1992 Directory [PB92-201094] p 3941 N92-33002

NATIONAL OCEANIC AND ATMOSPHERIC ADMINISTRATION, BOULDER, CO.
Boundary layer processes in coastal meteorology: Prospects for remote sensing applications [PB92-177849] p 4033 N92-32714

NATIONAL OCEANIC AND ATMOSPHERIC ADMINISTRATION, WASHINGTON, DC.
Federal plan for ocean pollution research, development, and monitoring, fiscal years 1992-1996 [PB92-185164] p 4029 N92-32708

NATIONAL RESEARCH COUNCIL OF CANADA, BOUCHERVILLE (QUEBEC).
National Research Council Industrial Materials Institute: From knowledge to know-how [CTN-92-60333] p 4103 N92-32814
National Research Council Industrial Materials Institute: From knowledge to know-how [CTN-92-60334] p 4104 N92-32815
A review of recent developments in joining high-performance thermoplastic composites [CNRC-33030] p 4019 N92-33077

NATIONAL RESEARCH COUNCIL OF CANADA, OTTAWA (ONTARIO).
The design and development of a portable, DSP micro-processor based, high-accuracy data acquisition system [NRC-32146] p 4040 N92-32851
Sound power determination using the sound intensity scanning technique p 4062 N92-32953

NATIONAL SEVERE STORMS FORECAST CENTER, KANSAS CITY, MO.
Verification of severe local storms forecasts issued by the National Severe Storms Forecast Center, 1991 [PB92-186063] p 4033 N92-32502
Severe local storm warning verification: 1991 [PB92-185982] p 4033 N92-32545

NATIONAL TELECOMMUNICATIONS AND INFORMATION ADMINISTRATION, BOULDER, CO.
New approach to HF channel modeling and simulation. Part 3: Transfer function [PB92-192848] p 3979 N92-32555

NATIONAL TRANSPORTATION SAFETY BOARD, WASHINGTON, DC.
Aircraft accident report: L'Express Airlines, Inc., Flight 508, Beech C99, N7217L weather encounter and crash near Birmingham, Alabama, July 10, 1991 [PB92-910401] p 3932 N92-32455

NATIONAL WEATHER SERVICE, SALT LAKE CITY, UT.
Forecasting heavy snow events in Missoula, Montana [PB92-196104] p 4034 N92-33163

NAVAL AIR DEVELOPMENT CENTER, WARMINSTER, PA.
A new approximate fracture mechanics analysis methodology for composites with a crack or hole p 3949 N92-32530
Environmental degradation of high temperature composites p 3958 N92-33047

NAVAL AIR PROPULSION TEST CENTER, TRENTON, NJ.
Statistics on aircraft gas turbine engine rotor failures that occurred in US commercial aviation during 1988 [DOT/FAA/CT-91/28] p 3938 N92-33105

NAVAL AIR STATION, PENSACOLA, FL.
Development of the OMPAT neuropsychological/psychomotor performance evaluation and OMPAT data and timing support [AD-A250793] p 4037 N92-32504

NAVAL COMMAND, CONTROL AND OCEAN SURVEILLANCE CENTER, SAN DIEGO, CA.
Feasibility of a 486 nm Fraunhofer laser source based on a 4F(sub 3/2) yields 4I(sub 9/2) neodymium laser [AD-A250851] p 4015 N92-32329
An evaluation of an infrared/resistance temperature device for air/sea-surface temperature measurements [AD-A252279] p 4035 N92-32688
Recursive estimation techniques for detection of small objects in infrared image data [AD-A250942] p 4075 N92-32935

NAVAL HEALTH RESEARCH CENTER, SAN DIEGO, CA.
A causal analysis of interrelationships among exercise, physical fitness, and well-being in US Navy personnel [AD-A252719] p 4037 N92-32942

NAVAL OCEAN SYSTEMS CENTER, SAN DIEGO, CA.
Feasibility of measuring transverse electric noise at VLF and LF on an ice cap [AD-A252280] p 4035 N92-33220

NAVAL POSTGRADUATE SCHOOL, MONTEREY, CA.
Tropical cyclone motion due to environmental interactions represented by empirical orthogonal functions of the vorticity fields [AD-A246137] p 4033 N92-32534
Satellite anomalies and electrostatic surface discharges [AD-A246880] p 3942 N92-32538
Rational behavior model: A tri-level multiple paradigm architecture for robot vehicle control software [AD-A250370] p 4053 N92-32748
Selecting a subset of stimulus-response pairs with maximal transmitted information [AD-A252728] p 3986 N92-32987
Investigation of the flight control requirements of a half-scale ducted fan unmanned aerial vehicle [AD-A252730] p 3940 N92-32988

NAVAL RESEARCH LAB., WASHINGTON, DC.
Probing thin-film YBa2Cu3O(7-delta) superconductors by second harmonic generation using femtosecond laser pulses [AD-A252350] p 4082 N92-32512
The problems of routing and scheduling in multihop radio networks. A Hopfield neural network approach [AD-A247431] p 3979 N92-32570
Correlation of single mode fiber fabrication factors and radiation response [AD-A247301] p 4074 N92-32613

NAVAL SURFACE WARFARE CENTER, CRANE, IN.
Radiometric and spectral measurement instruments [AD-A250771] p 4013 N92-32343

NAVAL SURFACE WARFARE CENTER, DAHLGREN, VA.
Software process assessment for small software shops p 4045 N92-32878

NAVAL SURFACE WARFARE CENTER, SILVER SPRING, MD.
Pseudopotential band calculations along a high-symmetry axis. Part 1: Central potential and the (111) direction [AD-A252399] p 4084 N92-32938

NAVAL UNDERWATER SYSTEMS CENTER, NEWPORT, RI.
Feature detection for model assessment in state estimation [AD-A252755] p 4059 N92-32989

NAVAL WEAPONS CENTER, CHINA LAKE, CA.
Generic modular imaging IR signal processor p 3936 N92-32440
Image enhancement of infrared uncooled focal plane array imagery p 3936 N92-32441
Target cuing: A heterogeneous neural network approach p 3936 N92-32442
Target detection using co-occurrence matrix segmentation and its hardware implementation p 3936 N92-32443

NEBRASKA UNIV., LINCOLN.
Semiannual status report [NASA-CR-190239] p 4046 N92-33092

NEW BRUNSWICK UNIV., FREDERICTON.
Ambient light array vision in 3-D [ISBN-0-315-55748-6] p 4077 N92-33202

NEW ENERGY DEVELOPMENT ORGANIZATION, TOKYO (JAPAN).
NEDO Alcohol/Biomass Technology Subcommittee [DE92-526270] p 3975 N92-32914

NEW MEXICO UNIV., ALBUQUERQUE.
Laser material interaction [AD-A250853] p 4016 N92-32622

NEW SOUTH WALES UNIV., KENSINGTON (AUSTRALIA).
A conceptual model of cognitive complexity of elements of the programming process p 4045 N92-32877

NICHOLS RESEARCH CORP., HUNTSVILLE, AL.
A prototype backside purge control system [NASA-CR-190816] p 3969 N92-33081

NORTH CAROLINA STATE UNIV., RALEIGH.
Shear buckling of specially orthotropic plates with centrally located cutouts p 3953 N92-32589

NORTH CAROLINA UNIV., CHAPEL HILL.
Local structural order and molecular associations in water DMSO mixtures. Molecular dynamics study [AD-A250935] p 4064 N92-32418
Excited state processes in transition metal complexes: Redox splitting in soluble polymers [DE92-011808] p 3971 N92-32631
New thiophene-based materials [AD-A250977] p 3972 N92-32667
Dynamics of ion solvation in a Stockmayer fluid [AD-A251087] p 4066 N92-32682
The response of the double layer capacitance of a high temperature superconductor/fluid electrolyte interface to the onset of superconductivity [AD-A251172] p 3990 N92-32827
The energetics and dynamics of free radicals, ions, and clusters [DE92-014124] p 4068 N92-33083

NORTH DAKOTA UNIV., GRAND FORKS.
ERIP application instructions [DE92-014103] p 4089 N92-32469

NORTHROP CORP., HAWTHORNE, CA.
Structural assessment of ultralightweight composites p 3948 N92-32525
Supportability evaluation of thermoplastic and thermoset composites p 3950 N92-32576
Damage tolerance certification methodology for composite structures p 3951 N92-32579
Postbuckling behavior of curved panels under combined compression and shear loads p 3952 N92-32584

NORTHWESTERN UNIV., EVANSTON, IL.
Thinning and rupture of a thin liquid film on a heated surface [DE92-014813] p 4013 N92-33124

NOTRE DAME UNIV., IN.
Annual progress report on imposed 3-D disturbances on bluff-body near wake flows [AD-A250366] p 4006 N92-32324

NOTTINGHAM UNIV. (ENGLAND).
Three-dimensional elasticity analysis of buckling of laminated plates p 3957 N92-33037

O

OAK RIDGE ASSOCIATED UNIVERSITIES, INC., TN.
Magnetohydrodynamic stability of plasmas with radial motion [DE92-013917] p 4077 N92-32417

OAK RIDGE NATIONAL LAB., TN.
A tight and explicit representation of Q in sparse QR factorization [DE92-014814] p 4055 N92-32428
US Historical Climatology Network daily temperature and precipitation data [DE92-014920] p 4032 N92-32431
Studies of near-surface phenomena and erosion mechanisms in metallic alloys using single- and multi-particle impacts [DE92-014921] p 3966 N92-32432
Phase distribution measurements in narrow rectangular channels using image-processing techniques [DE92-014084] p 4006 N92-32468
Heat and mass exchange during condensation of a water-ammonia mixture [DE92-014524] p 3962 N92-32557
Suggestions for improvement of the methodology and use of MEPAS, the multimedia environmental pollutant assessment system [DE92-013135] p 4028 N92-32616
Anisotropic electrical resistivity of YBCO/PBCO superlattice films grown on miscut substrates [DE92-014409] p 4082 N92-32636

T (sub c)-delta relations in YBa2Cu3O(7-delta) thin films: Effects of oxygen pressure during growth
[DE92-014432] p 4083 N92-32653
Using minimax approaches to plan optimal task commutation configurations for combined mobile platform-manipulator systems
[DE91-018864] p 4018 N92-32694
Development and proof-testing of advanced absorption refrigeration cycle concepts
[DE92-014933] p 3977 N92-32723
Pump and valve research at the Oak Ridge National Laboratory
[DE92-014419] p 4019 N92-32890
Substrate reactions and flux pinning structures in melt-processed YBa2Cu3O7 deposits on Ag-Pd alloy substrates
[DE92-014404] p 4084 N92-32919
Experiments with an ordinary differential equation solver in the parallel solution of method of lines problems on a shared memory parallel computer, part 2
[DE92-017159] p 4052 N92-32926
An analytical screening of alternatives for R-502 in low-temperature refrigerating applications
[DE92-017162] p 3978 N92-32927
The shapes and collective behavior of rapidly rotating nuclei
[DE92-017192] p 4067 N92-32928
Characterization of sintered reaction-bonded silicon nitride processed by microwave heating
[DE92-014408] p 3956 N92-32945
The oxidation of Type 310S stainless steel in mixed gases at elevated temperatures
[DE92-014941] p 3968 N92-32991
Superconducting transport properties and surface microstructure for YBa2Cu3O(7-delta) based superlattices grown by pulsed laser deposition
[DE91-014224] p 4085 N92-33023
Oak Ridge Environmental Information System (OREIS). Phase 1: System definition document
[DE92-017342] p 4090 N92-33084
Weldability of Fe3Al based iron aluminide alloys
[DE92-017802] p 4020 N92-33085
Modeling the influence of irradiation temperature and displacement rate on hardening due to point defect clusters in ferritic steels
[DE92-016897] p 3969 N92-33115
Modification of the optical properties of Al2O3 by ion implantation
[DE92-013861] p 4085 N92-33127
A combined AEM/APFIM characterization of Alloy X-750
[DE92-011049] p 3969 N92-33158
Continuum configurational bias Monte-Carlo studies of alkanes and polyethylene
[DE92-016545] p 3965 N92-33185

OAK RIDGE Y-12 PLANT, TN.
Transmission electron microscope characterization of deformation and recovery in 304L stainless steel part
[DE92-013237] p 3966 N92-32614

OBSERVATOIRE DE PARIS-MEUDON (FRANCE).
The composition of the Titan atmosphere
p 4094 N92-32354
Titan's atmosphere: Latitudinal variations in temperature and composition p 4094 N92-32355
Titan's UV albedo: Observations and modeling
p 4094 N92-32356
The spectrum of Titan in the 1.06 and 1.28 micron windows p 4101 N92-32401

OESTERREICHISCHE AKADEMIE DER WISSENSCHAFTEN, VIENNA.
Atmospheric escape from Titan p 4099 N92-32384

OESTERREICHISCHES FORSCHUNGSZENTRUM SEIBERSDORF G.M.B.H., VIENNA.
Execution of measurement sequences in the framework of the inspection of near limit regions by radioiodine and aerosol emission measurements, and ground examinations on plutonium, strontium, and gamma ray radionuclides
[OEFZS-4579] p 4071 N92-32763

OFFICE NATIONAL D'ETUDES ET DE RECHERCHES AEROSPATIALES, PARIS (FRANCE).
Resolution of convection and diffusion by the boolean automata method
[ONERA-RF-22/3419-AY-122A] p 4057 N92-32772
Research on some centered implicit methods for calculating transonic flows by solving Navier-Stokes equations
[ONERA-RSF-24/1408-AY-150A] p 3931 N92-32773
Buckling and damage of a composite plate under compression
[ONERA-RT-25/3542-RY-006-R] p 4022 N92-32774
Nonlinear transient responses of stratified composite structures
[ONERA-RT-26/3542-RY-007-R] p 3954 N92-32775
Strong coupling between inviscid fluid and boundary layer of sharp leading edges: Two-dimensional stationary and turbulent cases for isolated profiles and guard vanes
[ONERA-RT-44/1621-RY-016-R] p 4010 N92-32776
Free-edge delamination of a stratified composite: Interaction with the transversal crack
[ONERA-RT-13/7256-RY-006-R] p 3954 N92-32792
Experimental study of the vortex system generated by a missile fuselage at incidence. Part 3: Three directional laser velocimetry measurements
[ONERA-RT-47/1147-AY-146A-P] p 3931 N92-32800
Propagation of a delamination in a composite panel subjected to a compression load p 3957 N92-33041

OFFICE OF MANAGEMENT AND BUDGET, WASHINGTON, DC.
Information resources management plan of the Federal Government
[PB92-147198] p 4089 N92-32643

OFFICE OF SCIENCE AND TECHNOLOGY, WASHINGTON, DC.
Science and technology: A report to the Congress
[PB92-183219] p 4104 N92-33086

OFFICE OF THE DEPUTY SECRETARY OF DEFENSE, WASHINGTON, DC.
Defense environmental restoration program annual report to Congress for fiscal year 1991
[AD-A244196] p 4029 N92-32731

OHIO STATE UNIV., COLUMBUS.
Numerical evaluation of the incomplete airy functions and their application to high frequency scattering and diffraction
[NASA-CR-190745] p 4058 N92-32888

OLD DOMINION UNIV., NORFOLK, VA.
Convergence acceleration of the Proteus computer code with multigrid methods
[NASA-CR-190607] p 4047 N92-33131

OMNIPLAN CORP., HOUSTON, TX.
Superheavyweight missions SI versus DI: Ascent flight design options and recommendations
[NASA-CR-183208] p 3942 N92-32610

OREGON UNIV., EUGENE.
PAC spectroscopy of electronic ceramics
[DE92-014328] p 3970 N92-32471
Theory of elementary particles studies in weak interaction and grand unification and studies in accelerator design
[DE92-014320] p 4066 N92-32597
Relativistic heavy ion collisions
[DE92-014415] p 4066 N92-32600

OSAKA UNIV. (JAPAN).
Better predictions even in reduced input variable numbers using neural networks in software development
p 4044 N92-32874

OXFORD UNIV. (ENGLAND).
Influence of compliance on performance of robotic drilling
[OUEL-1917/92] p 4018 N92-32757
Parallel implementation of Droid and performance evaluation
[OUEL-1926/92] p 4051 N92-32759

P

PACIFIC NORTHWEST LAB., RICHLAND, WA.
International research into chlorofluorocarbon (CFC) alternatives
[DE92-014241] p 4030 N92-32986
Potential environmental effects of energy conservation measures in northwest industries
[DE92-013993] p 4030 N92-33156

PADUA UNIV. (ITALY).
Titan's atmospheric structure from Huygen's-ASI measurements p 4101 N92-32398

PARIS-VAL DE MARNE UNIV., CRETEIL (FRANCE).
Gas chromatography and pyrolysis-GC with capillary columns: Application to the in situ analysis of Titan's atmosphere p 4100 N92-32397
Some problems about IR band integrated intensities; 3 examples for application to Titan: C6H6, HC3N, and C4H2 p 4101 N92-32400

PARIS VI UNIV. (FRANCE).
Formation and growth of photochemical aerosols in Titan's atmosphere p 4100 N92-32393

PARIS XII UNIV., CRETEIL (FRANCE).
Organic chemistry on Titan versus terrestrial prebiotic chemistry: Exobiological implications
p 4096 N92-32368

PATRAS UNIV. (GREECE).
Jet fuel absorption and dynamic mechanical analysis of carbon fibre composites p 3959 N92-33050

PENNSYLVANIA STATE UNIV., HERSHEY.
Effects of CSF hormones and ionic composition on salt/water metabolism
[NASA-CR-190693] p 4037 N92-32539

PENNSYLVANIA STATE UNIV., UNIVERSITY PARK.
Experimental studies of characteristic combustion-driven flows for CFD validation
p 3998 N92-32264
Numerical simulation of turbomachinery flows with advanced turbulence models p 3999 N92-32270
The impact of time step definition on code convergence and robustness p 4001 N92-32282
Comparison between the PISO algorithm and preconditioning methods for compressible flow
p 4001 N92-32284
Inverse design of a proper number, shapes, sizes, and locations of coolant flow passages
p 4004 N92-32298
Thermochemical and kinetic considerations in diamond growth
[AD-A247866] p 3971 N92-32490
Swept shock/boundary layer interaction experiments in support of CFD code validation
[NASA-CR-190583] p 3930 N92-32494
Sparse matrix algorithms on distributed memory multiprocessors
[DE92-017870] p 4046 N92-33071

PENNSYLVANIA UNIV., PHILADELPHIA.
Structure and dynamics in low-dimensional guest-host systems
[DE92-014841] p 3970 N92-32429

PHILIPS GLOEILAMPENFABRIEKEN N.V., EINDHOVEN (NETHERLANDS).
Orientation, stress, and density distributions in injection-moulded amorphous polymers determined by optical techniques
[ETN-92-92052] p 3972 N92-32752
Investigation of impurity related phenomena, significant for novel semiconductor technologies
[ETN-92-92048] p 4083 N92-32760

PHILLIPS LAB., EDWARDS AFB, CA.
ESD traits of bulk propellant under pressure
p 3976 N92-33242

PITTSBURGH UNIV., PA.
Experimental particle physics at the University of Pittsburgh
[DE92-014181] p 4066 N92-32702
Probe molecule studies: Active species in alcohol synthesis
[DE92-016682] p 3966 N92-33246

POLISH ACADEMY OF SCIENCES, WARSAW.
Bone as a liquid-filled diphase porous medium
p 4037 N92-32663

PRATT AND WHITNEY AIRCRAFT, WEST PALM BEACH, FL.
NLS nozzle base flow characteristics
p 3995 N92-32252
Application of computational fluid dynamics to the design of the film cooled STME subscale nozzle for the National Launch System p 3996 N92-32254

PRINCETON UNIV., NJ.
Simulations of the carbon cycle in the oceans
[DE92-016622] p 4035 N92-32336

PURDUE UNIV., WEST LAFAYETTE, IN.
Some electronic and dynamical factors in electron-transfer chemistry: Metal complexes, clusters, and surfaces
[AD-A251169] p 3964 N92-32826
Gamma scattering in condensed matter with high intensity Moessbauer radiation
[DE92-014811] p 4085 N92-33025
A Theoretical High Energy Physics Program: Task F
[DE92-014054] p 4073 N92-33182

Q

QUEENS UNIV., KINGSTON (ONTARIO).
Design and implementation of N-dimensional digital filters
[ISBN-0-315-60747-5] p 3993 N92-33195
Developments in the theory of Cantor-type variables with application to communications over fading channels
[ISBN-0-315-61378-5] p 3987 N92-33213

R

RADIATION SCIENCE, INC., BELMONT, MA.
Volume 1. Preliminary design study: AXAF x ray calibration spectrometers. Volume 2. Revised preliminary design study: AXAF x ray calibration spectrometers
[NASA-CR-184340] p 4092 N92-33094

READING UNIV. (ENGLAND).
Simple dynamical models of Titan's atmospheric circulation p 4095 N92-32362

RENNES UNIV. (FRANCE).
Photochemistry of unsaturated nitriles on Titan
p 4096 N92-32371

RENSSELAER POLYTECHNIC INST., TROY, NY.
Inelastic deformation and damage at high temperature
[DE92-012241] p 4021 N92-32698
RESEARCH AND DEVELOPMENT LABS., CULVER CITY, CA.
United States Air Force summer research program 1991. Volume 1: Program management report
[AD-A248763] p 4103 N92-32338
RESEARCH INST. FOR COMPUTING AND INFORMATION SYSTEMS, HOUSTON, TX.
Robust stabilization of the Space Station
[NASA-CR-190627] p 3942 N92-32244
Ground Systems Development Environment (GSDE) interface requirements and prototyping plan
[NASA-CR-190713] p 4041 N92-32451
Supporting multiple domains in a single reuse repository
[NASA-CR-190640] p 4090 N92-32654
Guaranteeing synchronous message deadlines with the timed token medium access control protocol
[NASA-CR-190710] p 4042 N92-32656
Advanced software development workstation: Effectiveness of constraint-checking
[NASA-CR-190712] p 4043 N92-32865
Fuzzy set methods for object recognition in space applications
[NASA-CR-190388] p 4047 N92-33093
Object links in the repository
[NASA-CR-190644] p 4091 N92-33096
Object linking in repositories
[NASA-CR-190629] p 4091 N92-33178
ROCHESTER PHOTONICS CORP., FAIRPORT, NY.
Diffractive optics technology and the NASA Geostationary Earth Observatory (GEO)
[NASA-CR-190611] p 4076 N92-33074
ROCHESTER UNIV., NY.
Theoretical and experimental studies of elementary physics
[DE92-014877] p 4061 N92-32430
The Rochester Checkers Player: Multi-model parallel programming for animate vision
[AD-A247427] p 4050 N92-32568
Theoretical nuclear physics
[DE92-016837] p 4069 N92-33186
ROCKWELL INTERNATIONAL CORP., CANOGA PARK, CA.
Direct numerical simulation of a combusting droplet with convection p 3996 N92-32256
Modeling of SSME fuel preburner ASI p 3945 N92-32259
A numerical study of two-dimensional vortex shedding from rectangular cylinders p 3998 N92-32266
A computational design system for rapid CFD analysis p 4000 N92-32273
A multi-domain method for subsonic viscous flows p 3960 N92-32275
Development of CFD code evaluation criteria and a procedure for assessing predictive capability and performance p 4001 N92-32283
Computational fluid dynamic design of rocket engine pump components p 4003 N92-32293
SSME HPOTP impeller backcavity CFD analysis p 4003 N92-32294
NLS clutching bearing cavity flow analysis p 4003 N92-32295
ROCKWELL INTERNATIONAL CORP., HUNTSVILLE, AL.
Computational fluid dynamics analysis of Space Shuttle main engine multiple plume flows at high-altitude flight conditions p 3996 N92-32255
ROCKWELL SPACE OPERATIONS CO., HOUSTON, TX.
Superheavyweight missions SI versus DI: Ascent flight design options and recommendations
[NASA-CR-183208] p 3942 N92-32610
ROME UNIV. (ITALY).
Formation of the satellites p 4093 N92-32350
Titan in a box p 4101 N92-32404
ROYAL AEROSPACE ESTABLISHMENT, FARNBOROUGH (ENGLAND).
Recent advances in statistical energy analysis p 4062 N92-32954
A review of RAE sponsored work on the compressive behaviour of composite materials p 3957 N92-33038
ROYAL INST. OF TECH., STOCKHOLM (SWEDEN).
Environmental consequences of new energy technology. Solar heating, heat stores, and heat pumps
[PB92-180843] p 4025 N92-32605
ROYAL ORDNACE PLC, KIDDERMINSTER (ENGLAND).
The design features of rocket motors relating to insensitive munition response to thermo-mechanical stimuli p 3976 N92-33244
ROYAL RADAR ESTABLISHMENT, MALVERN (ENGLAND).
Improving the translation from data flow diagrams into Z by incorporating the data dictionary
[AD-A250769] p 4089 N92-32342
RUTHERFORD APPLETON LAB., CHILTON (ENGLAND).
Scalar mesons and kaons in phi radiative decay and their implications for studies of CP violation at DA(phi)NE
[RAL-91-085] p 4068 N92-33133
Neutrino masses in the flipped SU(5) tensor product U(1) and the SU(4) tensor product O(4) GUT models
[RAL-92-012] p 4068 N92-33135
Partons and the EMC spin effect
[RAL-92-015-PREPRINT] p 4068 N92-33137

S

SAAB AIRCRAFT CO., LINKOPING (SWEDEN).
Vibro-acoustic FE analyses of the Saab 2000 aircraft p 4062 N92-32952
SANDIA NATIONAL LABS., ALBUQUERQUE, NM.
B-52G/H nuclear certification tasks performed by the Aircraft Compatibility Division at Sandia National Laboratories
[DE92-013681] p 3934 N92-32308
Laser measurements for experiments on the TROLL accelerator
[DE92-016578] p 4015 N92-32335
The 1991 rocket-triggered lightning test of the DoD Security Operations Test Site (SOTS) munitions storage bunker, Fort McClellan, Alabama
[DE92-012449] p 4032 N92-32427
Testing of the single-element stretched-membrane dish
[DE92-013680] p 4025 N92-32549
International technology transfer to support the environmental restoration needs of the DOE complex
[DE92-013663] p 4028 N92-32558
Concentrator silicon cell research
[DE92-016576] p 4025 N92-32565
Target Cueing And Tracking System (TCATS): User's guide
[DE92-015385] p 4042 N92-32617
Use of thin-film samples to study thermal decomposition chemistry of explosives
[DE92-014616] p 3974 N92-32637
Orbital debris characterization with impact flash signatures
[DE92-010666] p 4018 N92-32701
A simple approach for the design and optimization of stand-off hypervelocity particle shields
[DE92-011383] p 3943 N92-32704
NAASW modular radar research testbed study results
[DE92-011339] p 3981 N92-32744
Thickness dependence of vortex pinning in epitaxial Tl-Ca-Ba-Cu-O thin films
[DE92-015011] p 4084 N92-32920
Solar thermal energy: Viable energy technology for today and tomorrow
[DE92-015039] p 4026 N92-32923
The photovoltics program at Sandia National Laboratories
[DE92-014617] p 4026 N92-32946
Spectroscopic characterization of LEVIS active ion source on PBFA 2
[DE92-014954] p 4080 N92-32992
Shielding analyses for repetitive high energy pulsed power accelerators
[DE92-015004] p 4072 N92-32994
Scrape-off layer modeling of radiative divertor and high heat flux experiments on D3-D
[DE92-015007] p 4080 N92-32995
Extending estimation of C-J pressure of explosives to the very low density region
[DE92-015035] p 3975 N92-33003
Summary of engineering-scale experiments for the Solar Detoxification of Water project
[DE92-013776] p 4027 N92-33150
ROAR: A 3-D tethered rocket simulation code
[DE92-017358] p 3944 N92-33166
SCIENTIFIC RESEARCH ASSOCIATES, INC., GLASTONBURY, CT.
Navier-Stokes analysis of an oxidizer turbine blade with tip clearance p 3999 N92-32269
Computation of the flow field in a centrifugal impeller with splitter blades p 4002 N92-32289
A two-phase restricted equilibrium model for combustion of metalized solid propellants p 3966 N92-32307
SECA, INC., HUNTSVILLE, AL.
Heat transfer in rocket engine combustion chambers and nozzles p 3995 N92-32253
SHERBROOKE UNIV. (QUEBEC).
Study of the mechanical behaviour of graphite/epoxy laminates subjected to static and cyclic loading
[NRC-30833] p 3955 N92-32813
SIMULA, INC., PHOENIX, AZ.
The weight optimization of an armored crashworthy crewseat through the use of advanced composites and design p 3947 N92-32517
SMITHSONIAN ASTROPHYSICAL OBSERVATORY, CAMBRIDGE, MA.
Volume 1. Preliminary design study: AXAF x ray calibration spectrometers. Volume 2. Revised preliminary design study: AXAF x ray calibration spectrometers
[NASA-CR-184340] p 4092 N92-33094
SOFTWARE ENGINEERING TECHNOLOGY, INC., VERO BEACH, FL.
A Markov model of software usage p 4045 N92-32881
SOFTWARE PRODUCTIVITY SOLUTIONS, INC., INDIALANTIC, FL.
Automatic access experiment
[AD-A252217] p 4089 N92-32611
SOUTH CAROLINA RESEARCH AUTHORITY. CHARLESTON.
PDES application protocol suite for composites (PAS-C). Functional needs report for the PAS-C program
[AD-A247886] p 3953 N92-32629
SOUTHAMPTON UNIV. (ENGLAND).
Active control of sound transmission through stiff lightweight composite fuselage constructions p 4062 N92-32957
SOUTHEASTERN UNIV. RESEARCH ASSOCIATION, NEWPORT NEWS, VA.
Absolute measurement of beam energy by Compton scattering
[DE92-016964] p 4069 N92-32318
RF cavity vacuum interlock system
[DE92-016961] p 4070 N92-32567
SOUTHERN CALIFORNIA ASSOCIATION OF GOVERNMENTS, LOS ANGELES
Microwave absorption by lossy ceramic materials
[DE92-016963] p 3970 N92-32317
High accuracy beam energy measurement for linear and circular accelerators
[DE92-016966] p 4069 N92-32319
SPARTA, INC., LEXINGTON, MA.
STAMP, the SWOE Thermal Analysis and Measurement Program: Summary of the 1990 field tests
[LTR-91-013] p 4029 N92-32860
STANFORD LINEAR ACCELERATOR CENTER, CA.
Beamstrahlung spectra in next generation linear colliders
[DE92-010730] p 4069 N92-32337
Studies of helium based drift chamber gases for high-luminosity low energy machines
[DE92-012415] p 4065 N92-32426
A high-power SLED 2 pulse compression system
[DE92-011586] p 4071 N92-32751
Accelerator physics of the Stanford Linear Collider and SLC accelerator experiments towards the next linear collider
[DE92-017552] p 4072 N92-33070
Theoretical aspects of lepton-hadron scattering
[DE92-013765] p 4069 N92-33148
STANFORD UNIV., CA.
High temperature deformation processes and strengthening mechanisms in intermetallic particulate composites
[AD-A250220] p 3946 N92-32339
Observations of high frequency and high wavenumber solar oscillations
[AD-A250099] p 4103 N92-32488
Wavelength division multiplexed local area networks
[AD-A247613] p 3979 N92-32573
STARNET: A MultiGbit/s optical local area network with both packet and circuit switching
[AD-A247617] p 4050 N92-32628
Can the speed of light in the fiber be controlled?
[AD-A247614] p 4074 N92-32668
STATE UNIV. OF NEW YORK, BUFFALO.
New applications of ionization and fluorescence techniques for detecting and characterization of open-shell organometallics in the gas phase
[AD-A250923] p 3961 N92-32509
Novel gas phase ion molecule reactions of C60(++) with O2 and NH3
[AD-A250921] p 4066 N92-32556
Workshop on research needs and opportunities in high temperature superconductivity
[AD-A252674] p 3988 N92-32659
STATE UNIV. OF NEW YORK, STONY BROOK.
Observing the surface of Titan through near-infrared windows in its atmosphere p 4097 N92-32374
Research in nuclear astrophysics: Stellar collapse and supernovae
[DE92-014988] p 4093 N92-32993
Research in theoretical nuclear physics
[DE92-016316] p 4068 N92-33067
STOCKHOLM UNIV. (SWEDEN).
Numerical methods: Solving the advection equation in flows with sharp gradients using Bott's flux scheme
[DM-59] p 4009 N92-32727
Short range forecast of the initiation of convection
[DM-60] p 4033 N92-32758

Radiative lifetime measurements of the AA pi 1/2 state in CaH
[USIP-91-03] p 4067 N92-32764

STUTTGART UNIV. (GERMANY, F.R.).
Activities report of the Institute of Plasma Research
[ETN-92-92147] p 4079 N92-32797
Conceptual design of an electron cyclotron wave system for NET/ITER
[IPF-91-6] p 4071 N92-32808
Diagnostics and modeling of ECRH microwave discharges
[IPF-91-3] p 4079 N92-32822
Detectors for lidar type Thomson scattering diagnostics
[IPF-91-5] p 3990 N92-32823

SUPERCONDUCTING SUPER COLLIDER LAB., DALLAS, TX.
MOL calculation of the solitons of the cubic Schroedinger equation
[DE92-017245] p 4060 N92-32998
Overview of SSC accelerator requirements
[DE92-014896] p 4073 N92-33134

SVERDRUP TECHNOLOGY, INC., HUNTSVILLE, AL.
Development of a CFD code for internal flows in liquid fueled engines p 3999 N92-32271

SWEDISH COUNCIL FOR BUILDING RESEARCH, STOCKHOLM.
Environmental consequences of new energy technology. Solar heating, heat stores, and heat pumps
[PB92-180843] p 4025 N92-32605
Demand controlled ventilating systems: Sensor market survey. Energy conservation in buildings and community systems programme, annex 18, December 1991
[PB92-180892] p 3977 N92-32825

SWEDISH INST. OF SPACE PHYSICS, UMEA.
Burning oil fields as a source of infrasonic waves
[IRF-PREPRINT-119] p 4061 N92-32842

SYSTEMS MANAGEMENT AMERICAN CORP., HOUSTON, TX.
Superheavyweight missions SI versus DI: Ascent flight design options and recommendations
[NASA-CR-183208] p 3942 N92-32610

T

TECHNICAL RESEARCH CENTRE OF FINLAND, ESPOO.
Hypertext and hypermedia
[VTT-RN-1154] p 4090 N92-32843

TECHNION - ISRAEL INST. OF TECH., HAIFA.
A model for the trap-assisted tunneling mechanism in diffused n-p and implanted n(+)-p HgCdTe photodiodes p 3985 N92-32979

TECHNISCHE UNIV., BERLIN (GERMANY, F.R.).
Exploiting two-dimensional explicit parallelism on vector architectures
[ETN-92-92136] p 4051 N92-32795
On 5-dimensional Kaluza-Klein theory
[ETN-92-92130] p 3982 N92-32820
Methods of fine-grain optimization for parallel computer architectures
[ETN-92-92144] p 4051 N92-32821
Schroedinger operators with singular potentials in the semiclassical limit
[ETN-92-92145] p 4058 N92-32840

TECHNISCHE UNIV., DELFT (NETHERLANDS).
Point interactions in L(sup p)
[REPT-91-97] p 4057 N92-32756
Generalizations of the classical Laguerre polynomials and some q-analogues
[ISBN-90-9003765-9] p 4058 N92-32836
Effects of fading and interference in narrowband land-mobile networks
[ISBN-90-9004491-4] p 3982 N92-32837
An intelligent gaming environment
[ISBN-90-6275-635-2] p 4060 N92-33055
Kinetics and characterization of CVD-grown BP
[ETN-92-92024] p 3973 N92-33065

TECHNISCHE UNIV., EINDHOVEN (NETHERLANDS).
Steady state behavior of reduced dynamic systems with local nonlinearities
[ISBN-90-9004680-1] p 4056 N92-32707
Statistical selection: Multiple comparison approach
[ETN-92-92051] p 4060 N92-32709

TECHNISCHE UNIV., MUNICH (GERMANY, F.R.).
Numerical simulation of two-dimensional flows by the free-Lagrangian method
[TUM-M9105] p 4009 N92-32767

TEL-AVIV UNIV. (ISRAEL).
Electric and magnetic properties of random superconductors
[ITN-92-85165] p 4086 N92-33190

TELESAT CANADA, OTTAWA (ONTARIO).
The MSAT spacecraft of Telesat Mobile, Inc.
[CTN-92-60346] p 3981 N92-32789

TEXAS A&M UNIV., COLLEGE STATION.
Visionless TRAC
[NASA-CR-190732] p 3942 N92-32477
Morphology, 31P spin diffusion, and phase transitions in a representative semicrystalline polyphosphazene by solid-state NMR
[AD-A250883] p 3961 N92-32553
Application of gauge theories to enhance numerical solutions to mixed potential integral equations
[AD-A248451] p 4055 N92-32670
Macrocyclic polycation complexes for secondary anion binding, molecular recognition, and catalysis
[AD-A251069] p 3972 N92-32913
Annual report, 1 November 1990 - 31 October 1991
[AD-A252431] p 4084 N92-32940
Further wind tunnel investigation of the SM701 airfoil with aileron and turbulators
[NASA-CR-190702] p 3932 N92-33063

TEXAS UNIV., AUSTIN.
The behavior of matter under non-equilibrium conditions: Fundamental aspects and applications
[DE92-014247] p 4087 N92-32593
ABF algorithms implemented at ARL:UT, FDS system engineering and acoustics
[AD-A252368] p 4046 N92-32917

THERMO ELECTRON TECHNOLOGIES CORP., SAN DIEGO, CA.
Transverse diode pumping of solid-state lasers
[AD-A252213] p 4016 N92-33089

THIOKOL CORP., BRIGHAM CITY, UT.
Overview of the relevant CFD work at Thiokol Corporation p 3995 N92-32249

THOMSON-CSF, BAGNEUX (FRANCE).
Automatic detection, pursuit, and classification in infrared imagery p 3937 N92-32445

THOMSON-CSF, CESSON-SEVIGNE (FRANCE).
Methods of opto-electronic fusion of infrared and visible images p 3936 N92-32444

TORONTO UNIV. (ONTARIO).
Hydrogen permeation through bilayer metallic membrranes
[UTIAS-TN-342] p 3967 N92-32794
A unique method of determining the elastic and engineering constants of unidirectional fibre-reinforced composite plates using ultrasound
[UTIAS-TN-274] p 3955 N92-32829
An evaluation of decelerating IFR approaches utilizing a helicopter flight simulator
[CTN-92-60348] p 3934 N92-32845
University of Toronto Institute for Aerospace Studies
[CTN-92-60375] p 4104 N92-32853
Ideal efficiency of propellers based on Theodorsen's theory: A review and computer study, with extended plus simplified charts
[UTIAS-TN-271] p 3938 N92-33102
Methodologies for designing block ciphers and cryptographic protocols
[ISBN-0-315-50983-X] p 4049 N92-33230
Computations for algebras and group representations
[ISBN-0-315-54684-0] p 4059 N92-33231

TRANE CO., LACROSSE, WI.
Development and proof-testing of advanced absorption refrigeration cycle concepts
[DE92-014933] p 3977 N92-32723

TRW, INC., CLEVELAND, OH.
Developing better software: A five year history of software engineering advancement p 4046 N92-32884

TRW SYSTEMS AND ENERGY, REDONDO BEACH, CA.
MHD Integrated Topping Cycle Project
[DE92-013904] p 4080 N92-33024

U

UNISYS CORP., DETROIT, MI.
Superheavyweight missions SI versus DI: Ascent flight design options and recommendations
[NASA-CR-183208] p 3942 N92-32610

UNITED TECHNOLOGIES RESEARCH CENTER, EAST HARTFORD, CT.
Turbine disk cavity aerodynamics and heat transfer p 3998 N92-32265
Axial vortices in gaseous-fired burner flow fields
[PB92-190370] p 3962 N92-32594
CARS diagnostics for solid propellant combustion investigations
[AD-A248660] p 3963 N92-32645
Interfacial studies of refractory glass-ceramic matrix/advanced SiC fiber reinforced composites
[AD-A250784] p 3953 N92-32676

UNIVERSITEIT TWENTE, ENSCHEDE (NETHERLANDS).
Synthesis, microstructure, and mechanical properties of zirconia-alumina composites
[ISBN-90-9004656-9] p 3954 N92-32677
Consistency and robustness of knowledge graphs
[ISBN-90-9003729-2] p 4056 N92-32679
Tolerance optimization of servomechanisms
[ISBN-90-9004476-0] p 4018 N92-32692
Local aspects of the optical reflection problem: The discrete dipole approach
[ISBN-90-9004118-4] p 4074 N92-32703
Topographical measuring based on the shadow and projection Moire method
[ISBN-90-9004146-X] p 4074 N92-32705
Hierarchical sets in mathematical programming modeling languages
[MEMO-990] p 4057 N92-32796
Aspects of solving non-linear boundary value problems numerically
[ETN-92-92049] p 4058 N92-32798
On the origin and acoustical behaviour of cloud cavitation
[ISBN-90-9004317-9] p 4012 N92-33066
Fault tolerance through program transformation
[ISBN-90-72125-29-0] p 4047 N92-33142
Analog CMOS filters for very-high frequencies
[ISBN-90-9004420-5] p 3986 N92-33143
High-energy ion implantation for bipolar transistor fabrication
[ISBN-90-9003883-3] p 3992 N92-33144
On the resistive transition of composite superconductors
[ISBN-90-9003899-X] p 3992 N92-33145
Scanning force microscopy using optical interferometry
[ISBN-90-9003887-6] p 4077 N92-33146

UNIVERSITY OF SOUTHERN CALIFORNIA, LOS ANGELES.
A comparison of artificial compressibility and fractional step methods for incompressible flow computations p 4001 N92-32285

UNIVERSITY OF WESTERN ONTARIO, LONDON.
Characteristics of large aspect angle VHF radar echoes in the presence and absence of optical aurora
[ISBN-0-315-59091-2] p 4032 N92-33197

V

VICTORIA UNIV. (BRITISH COLUMBIA).
Time-resolved holography for the study of shock waves
[ISBN-0-315-62369-1] p 4013 N92-33226

VIRGINIA POLYTECHNIC INST. AND STATE UNIV., BLACKSBURG.
Effects of curvature and rotation on turbulence in the NASA low-speed centrifugal compressor impeller p 4003 N92-32292
Development of the chemical and electrochemical coal cleaning process
[DE92-013353] p 3977 N92-32467
Compression of thick laminated composite beams with initial impact-like damage
[NASA-CR-190573] p 3946 N92-32491
The use of curvilinear fiber format to improve buckling resistance of plates with central circular holes p 3948 N92-32521
Scaling of fiber composite structures p 3950 N92-32532
Initial postbuckling response of an unsymmetrically laminated rectangular plate p 3952 N92-32586
Sound transmission reduction with intelligent panel systems p 4063 N92-32959
A comparison of three popular test methods for determining the shear modulus of composite materials
[NASA-CR-190659] p 3959 N92-33075

W

WASHINGTON UNIV., SAINT LOUIS, MO.
Analysis of LDEF experiment AO187-2: Chemically and isotopic measurements of micrometeoroids by secondary ion mass spectrometry
[NASA-CR-190697] p 4093 N92-32541

WASHINGTON UNIV., SEATTLE.
Bacterial responses to extreme temperatures and pressures and to heavy organic loading
[AD-A247456] p 4035 N92-32571
Formation and sustainment of a very low aspect ratio tokamak using coaxial helicity injection: Helicity Injected Torus (HIT) experiment
[DE92-014311] p 4078 N92-32595
Nonlinear resonance
[DE92-014313] p 4016 N92-32596
An experimental study on the two-parameter crack tip field
[AD-A251173] p 4023 N92-32936

Mixed H(2)/H(sub infinity): Control with output feedback compensators using parameter optimization
[NASA-CR-190070] p 4046 N92-33091

WATERLOO UNIV. (ONTARIO).
Some new perspectives in photoelasticity and curved-ray tomography
[ISBN-0-315-57756-8] p 4023 N92-33200
Hypothesis refinement for 3-D scene interpretation
[ISBN-0-315-57864-5] p 4048 N92-33210
Classical dynamics of systems with time-varying inertial properties with application to multi-rigid-body systems
[ISBN-0-315-57834-3] p 4024 N92-33228
Integrating expert vision systems and spatial database by unifying knowledge representation schemes.Development in remote sensing image analysis expert systems and geographical information systems
[ISBN-0-315-49130-2] p 4024 N92-33233

WESTINGHOUSE SAVANNAH RIVER CO., AIKEN, SC.
Wind tunnel test of Teledyne Geotech model 1564B cup anemometer
[DE92-009590] p 4013 N92-32460
System response to relay chatter
[DE92-013076] p 3988 N92-32495
RF-GD/FTMS: An FTMS system with a lensless external ion source for high resolution elemental mass spectrometry
[DE92-015343] p 3964 N92-32925

WHITE HOUSE MILITARY OFFICE, FALLS CHURCH, VA.
Toward advanced human reliability programs. Structural development considerations and options for extreme risk environments
[AD-A250786] p 4038 N92-32660

WISCONSIN UNIV., MADISON.
MHD computation of feedback of resistive-shell instabilities in the reversed field pinch
[DE92-014325] p 4078 N92-32599
Ion heating and MHD dynamo fluctuations in the reversed field pinch
[DE92-013902] p 4078 N92-32624
Edge gradient and safety factor effects on electrostatic turbulent transport in tokamaks
[DE92-014323] p 4079 N92-32944
Measurement of nonlinear mode coupling of tearing fluctuations
[DE92-013901] p 4080 N92-33154

WOODS HOLE OCEANOGRAPHIC INST., MA.
Abstracts of manuscripts submitted in 1991 for publication
[PB92-204627] p 4091 N92-33088

WORLD METEOROLOGICAL ORGANIZATION, GENEVA (SWITZERLAND).
Climate System Monitoring (CSM) Monthly Bulletin, issue no. 1 p 4034 N92-33073

WRIGHT LAB., WRIGHT-PATTERSON AFB, OH.
Infrared Targeting System (IRTS) demonstration
p 3937 N92-32446
An integrated multiple-sensor fire control system for air-to-air combat p 3937 N92-32450
MANTECH project book
[AD-A245283] p 3977 N92-32461
An examination of several high resolution schemes applied to complex problems in high speed flows
[AD-A250814] p 4008 N92-32632
Vortex flow visualization using colored and fluorescent dyes on flat plate delta wing with leading edge extension
[AD-A251139] p 3930 N92-32651
Fluid effects: Thermoset and thermoplastic matrix composites p 3958 N92-33049

WRIGHT RESEARCH DEVELOPMENT CENTER, WRIGHT-PATTERSON AFB, OH.
Design, analysis, and testing of a reusable wingbox for ballistic evaluation of composite structures
p 3947 N92-32518

Y

YALE UNIV., NEW HAVEN, CT.
Nuclear theory
[DE92-015012] p 4067 N92-32921
Computational and experimental study of laminar flames
[DE92-017978] p 3965 N92-33121

YORK UNIV. (ONTARIO).
Theory and numerical simulation of some wide-angle wide-bandpass plasma particle analyzers
[ISBN-0-315-58015-1] p 4080 N92-33223

Z

ZEISS (CARL), OBERKOCHEN (GERMANY, F.R.).
Airborne experimental FLIR program
p 3937 N92-32447

Typical Contract Number Index Listing

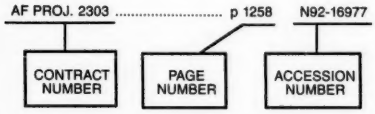

Listings in this index are arranged alphanumerically by contract number. Under each contract number the accession numbers denoting documents that have been produced as a result of research done under that contract are arranged in ascending order. The page number helps to locate the citation in the abstract section. The accession number denotes the number by which the citation is identified.

AERO/RD-134/100/10/88-89/518 p 4022 N92-32783
AF PROJ. 1123 ..... p 4046 N92-32907
AF PROJ. 2307 ..... p 4008 N92-32632
AF PROJ. 2309 ..... p 3978 N92-32458
AF PROJ. 6670 ..... p 4034 N92-32859
AF-AFOSR-0019-91 ..... p 4020 N92-33151
AF-AFOSR-0090-90 ..... p 4012 N92-33110
AF-AFOSR-0136-91 ..... p 4021 N92-32681
AF-AFOSR-0171-90 ..... p 4008 N92-32671
AF-AFOSR-0198-90 ..... p 3953 N92-32674
AF-AFOSR-0201-89 ..... p 3946 N92-32339
AF-AFOSR-0335-88 ..... p 3989 N92-32669
AF-AFOSR-0336-91 ..... p 3998 N92-32264
AF-AFOSR-0337-89 ..... p 4016 N92-32622
AF-AFOSR-0550-89 ..... p 3967 N92-32699
CICYT-ESP88-0566 ..... p 4096 N92-32367
CICYT-ESP88-0567 ..... p 4096 N92-32367
CNPQ-201237/88.1 ..... p 4055 N92-32661
DA PROJ. 1C1-62622-A-553 ..... p 3960 N92-32330
DA PROJ. 1L1-61102-AH-43 ..... p 3974 N92-32664
p 3989 N92-32700
p 4023 N92-32918
DA PROJ. 1L1-61102-B-74-A ..... p 4037 N92-32916
DA PROJ. 1L1-62618-AH-80 ..... p 3961 N92-32508
DA PROJ. 2Q1-62785-A-791 ..... p 4039 N92-32433
DA PROJ. 3M1-61102-BS-15 ..... p 4035 N92-32345
DA PROJ. 3M2-63002-D-995 ..... p 4037 N92-32504
DAAD09-87-D-0008 ..... p 4029 N92-32650
DAAL03-86-D-0001 ..... p 3960 N92-32330
DAAL03-87-C-0005 ..... p 3963 N92-32645
DAAL03-88-K-0046 ..... p 4089 N92-32644
DAAL03-91-C-0040 ..... p 3956 N92-32906
DAAL03-91-C-0050 ..... p 4013 N92-32323
DAAL03-91-G-0123 ..... p 4012 N92-33110
DAMD17-90-Z-0052 ..... p 4035 N92-32345
DE-AC02-76CH-00016 ..... p 4064 N92-32316
p 4070 N92-32411
p 4081 N92-32470
p 4015 N92-32511
p 3988 N92-32635
p 4071 N92-32912
p 4086 N92-33136
p 4073 N92-33179
DE-AC02-76CH-03000 ..... p 4064 N92-32312
p 4087 N92-32496
p 4070 N92-32506
p 4040 N92-32642
p 4069 N92-33164
DE-AC02-76CH-03073 ..... p 4078 N92-32623
DE-AC02-76ER-01428 ..... p 4073 N92-33182
DE-AC02-83CH-10093 ..... p 4024 N92-32510
p 4026 N92-32908
p 4026 N92-32909
p 4027 N92-33138
DE-AC03-76SF-00098 ..... p 4064 N92-32312
p 4081 N92-32320
p 4073 N92-32321
p 4073 N92-32419
p 4081 N92-32420
p 4082 N92-32493
p 3963 N92-32666
DE-AC03-76SF-00515 ..... p 4083 N92-32693
p 3964 N92-32996
p 4067 N92-32997
p 4085 N92-33117
p 4017 N92-33155
p 3993 N92-33183
p 4069 N92-32337
p 4065 N92-32426
p 4071 N92-32751
p 4072 N92-33070
p 4069 N92-33148
DE-AC03-89ER-53277 ..... p 4078 N92-32623
DE-AC04-76DP-00789 ..... p 3934 N92-32308
p 4015 N92-32335
p 4032 N92-32427
p 4025 N92-32549
p 4028 N92-32558
p 4025 N92-32565
p 3974 N92-32637
p 4018 N92-32701
p 3943 N92-32704
p 3981 N92-32744
p 4084 N92-32920
p 4026 N92-32923
p 4026 N92-32946
p 4080 N92-32992
p 4072 N92-32994
p 4080 N92-32995
p 4014 N92-32999
p 3975 N92-33003
p 4027 N92-33150
p 3944 N92-33166
DE-AC04-88DP-43495 ..... p 3967 N92-32721
p 3968 N92-32896
DE-AC05-76OR-00033 ..... p 4077 N92-32417
DE-AC05-84ER-40150 ..... p 3970 N92-32317
p 4069 N92-32318
p 4069 N92-32319
p 4070 N92-32567
DE-AC05-84OR-21400 ..... p 4055 N92-32428
p 4032 N92-32431
p 3966 N92-32432
p 4006 N92-32468
p 3962 N92-32557
p 4028 N92-32616
p 4082 N92-32636
p 4083 N92-32653
p 4018 N92-32694
p 3977 N92-32723
p 4019 N92-32890
p 4084 N92-32919
p 4052 N92-32926
p 3978 N92-32927
p 4067 N92-32928
p 3956 N92-32945
p 3968 N92-32991
p 4085 N92-33023
p 4090 N92-33084
p 4020 N92-33085
p 3969 N92-33115
p 4085 N92-33127
p 3969 N92-33158
p 3965 N92-33185
DE-AC05-84OS-21400 ..... p 3966 N92-32614
DE-AC06-76RL-01830 ..... p 4030 N92-32986
p 4030 N92-33156
DE-AC09-89SR-18035 ..... p 4013 N92-32460
p 3988 N92-32495
p 3964 N92-32925
DE-AC22-87PC-79892 ..... p 3977 N92-32467
DE-AC22-87PC-90274 ..... p 4080 N92-33024
DE-AC22-88PC-88948 ..... p 4013 N92-33140
p 4017 N92-33180
DE-AC22-89PC-89866 ..... p 3975 N92-33141
DE-AC22-90PC-90044 ..... p 3975 N92-33108
DE-AC22-90PC-90049 ..... p 3975 N92-33123
DE-AC35-89ER-40486 ..... p 4052 N92-32926
p 4060 N92-32998
p 4073 N92-33134
DE-AI21-83MC-20422 ..... p 4034 N92-32333
DE-AM03-76SF-00010 ..... p 4065 N92-32426
DE-AS03-89ER-40527 ..... p 4071 N92-32751
DE-FC07-79NV-10031 ..... p 3989 N92-32754
DE-FG02-85ER-45179 ..... p 3966 N92-32315
DE-FG02-85ER-45182 ..... p 4022 N92-32911
DE-FG02-85ER-45199 ..... p 4085 N92-33025
DE-FG02-85ER-53198 ..... p 4078 N92-32624
p 4079 N92-32944
p 4080 N92-33154
DE-FG02-85ER-53212 ..... p 4078 N92-32599
DE-FG02-85ER-60372 ..... p 4033 N92-32720
DE-FG02-86ER-13508 ..... p 3965 N92-33222
DE-FG02-86ER-13566 ..... p 4021 N92-32698
DE-FG02-86ER-13641 ..... p 4013 N92-33124
DE-FG02-86ER-45254 ..... p 3970 N92-32429
DE-FG02-86ER-45267 ..... p 4020 N92-32564
DE-FG02-87ER-13687 ..... p 4087 N92-32566
DE-FG02-87ER-40317 ..... p 4093 N92-32993
DE-FG02-88ER-13966 ..... p 3965 N92-33121
DE-FG02-88ER-40388 ..... p 4068 N92-33067
DE-FG02-88ER-40425 ..... p 4069 N92-33186
DE-FG02-88ER-40452 ..... p 4103 N92-33119
DE-FG02-90CE-15991 ..... p 4089 N92-32469
DE-FG02-90ER-14104 ..... p 4082 N92-32641
DE-FG02-90ER-54084 ..... p 4078 N92-32623
DE-FG02-90ER-61052 ..... p 4035 N92-32336
DE-FG02-90ER-61064 ..... p 4031 N92-33153
DE-FG02-91ER-25095 ..... p 4046 N92-33071
DE-FG02-91ER-40608 ..... p 4067 N92-32921
DE-FG02-91ER-40646 ..... p 4066 N92-32702
DE-FG02-91ER-40672 ..... p 4069 N92-33187
DE-FG02-91ER-40685 ..... p 4061 N92-32430
DE-FG02-92ER-40692 ..... p 4067 N92-32922
DE-FG02-92ER-61373 ..... p 4015 N92-33188
DE-FG03-85ER-13422 ..... p 4014 N92-32620
DE-FG03-87ER-13812 ..... p 3960 N92-32464
DE-FG03-87ER-45332 ..... p 4081 N92-32462
DE-FG03-88ER-60673 ..... p 4036 N92-33181
DE-FG03-90ER-54102 ..... p 4077 N92-32533
DE-FG03-91ER-61198 ..... p 4032 N92-32331
DE-FG05-86ER-13633 ..... p 3971 N92-32631
DE-FG05-86ER-40272 ..... p 4064 N92-32313
DE-FG05-88ER-13897 ..... p 4087 N92-32593
DE-FG05-88ER-13950 ..... p 4068 N92-33083
DE-FG05-88ER-13977 ..... p 4054 N92-33184
DE-FG05-89ER-53301 ..... p 4078 N92-32592
DE-FG05-89ER-75527 ..... p 4090 N92-32985
DE-FG05-90ER-75602 ..... p 4090 N92-32930
DE-FG05-91ER-61219 ..... p 4028 N92-32619
DE-FG06-85ER-40224 ..... p 4066 N92-32597
DE-FG06-85ER-45191 ..... p 3970 N92-32471
DE-FG06-86ER-25019 ..... p 4016 N92-32596
DE-FG06-90ER-54095 ..... p 4078 N92-32595
DE-FG06-91ER-40637 ..... p 4066 N92-32600
DE-FG21-89MC-26039 ..... p 3960 N92-32334
DE-FG21-90MC-27115 ..... p 3960 N92-32332
DE-FG22-89PC-89762 ..... p 3960 N92-32347
DE-FG22-90PC-90305 ..... p 3966 N92-33246
DE-FG22-91PC-91293 ..... p 4030 N92-33125
DOD/FA7INA-AP ..... p 3938 N92-33105
DREA-W7707-8-1140-01-SC ..... p 3931 N92-32811
DREA-W7707-9-0214-01-OCS ..... p 3981 N92-32749
DREO-055SS-W7714-8-5684 ..... p 3981 N92-32787
DRET-89-168 ..... p 4009 N92-32687
DRET-89-174 ..... p 4031 N92-32889
DRET-89-204 ..... p 3931 N92-32769
DRET-89-34-001 ..... p 4057 N92-32772
p 3931 N92-32773
p 4022 N92-32774
p 3954 N92-32775
p 4010 N92-32776
p 3954 N92-32792
p 3931 N92-32800
DRET-90-1177A ..... p 4009 N92-32770
DSS-W7714-8-5705-01-ST ..... p 3990 N92-32847
DTFA01-89-C-00001 ..... p 3933 N92-32537
p 3934 N92-33098
DTFA01-89-Z-02030 ..... p 3980 N92-32686
DTFA01-89-Z-02050 ..... p 3940 N92-32903
EEC-AERO-0028-C ..... p 4062 N92-32956
EPA-68-D0-0007 ..... p 4028 N92-32543
FE220788NRC21 ..... p 3957 N92-33039
p 3957 N92-33040
FU-D-NET-419/90-4 ..... p 4071 N92-32808
F04611-86-C-0096 ..... p 3966 N92-32307
F04701-88-C-0089 ..... p 4074 N92-32672

	p 3982	N92-32891
	p 4031	N92-32902
F19628-86-K-0009	p 3978	N92-32458
F19628-88-C-0038	p 4029	N92-32860
F19628-88-K-0033	p 4031	N92-32572
F19628-89-C-0137	p 4034	N92-32859
F19628-90-C-0002	p 3989	N92-32678
	p 3980	N92-32680
	p 3980	N92-32696
F30602-89-C-0003	p 4089	N92-32611
F33615-83-C-3228	p 3950	N92-32578
F33615-84-C-3220	p 3952	N92-32584
F33615-84-C-3404	p 4021	N92-32621
F33615-86-C-0012	p 3935	N92-32612
F33615-88-C-5447	p 3948	N92-32525
F33615-89-C-0603	p 4036	N92-32492
F33615-89-C-5628	p 3953	N92-32676
F33615-90-C-0012	p 4042	N92-32627
	p 4042	N92-32658
F33615-91-C-5713	p 3953	N92-32629
F49620-89-C-0063	p 3980	N92-32719
F49620-90-C-0076	p 4103	N92-32338
F49620-92-J-0009	p 3946	N92-32339
GRI-5086-260-1404	p 3962	N92-32591
GRI-5087-234-1492	p 3962	N92-32594
GRI-5088-260-1692	p 4007	N92-32598
ISU-80-3717	p 4102	N92-32406
ISU-91-3720	p 4102	N92-32406
MDA903-87-C-0523	p 4039	N92-32433
NAE-31946-7-0005/01-SS	p 3955	N92-32813
NAGW-1039	p 4093	N92-32349
	p 4098	N92-32381
NAGW-1366	p 4098	N92-32383
NAGW-1588	p 4099	N92-32386
NAGW-185	p 4094	N92-32352
NAGW-2022	p 3988	N92-32243
NAGW-2162	p 4098	N92-32383
NAGW-2194	p 4097	N92-32376
NAGW-649	p 4094	N92-32357
NAG1-1053	p 3959	N92-33075
NAG1-1135	p 3930	N92-32648
NAG1-1145	p 4012	N92-33110
NAG1-1174	p 4093	N92-32541
NAG1-1260	p 3932	N92-33063
NAG1-168	p 3952	N92-32586
NAG1-343	p 3946	N92-32491
	p 3950	N92-32532
NAG1-537	p 3952	N92-32586
NAG1-665	p 3948	N92-32521
NAG1-917	p 3953	N92-32589
NAG2-592	p 3930	N92-32494
NAG2-593	p 4020	N92-32436
NAG2-629	p 4046	N92-33091
NAG2-727	p 3940	N92-33107
NAG3-1329	p 4047	N92-33131
NAG3-440751	p 3985	N92-32984
NAG5-1415	p 4019	N92-32885
NAG5-1466	p 4024	N92-32590
NAG5-1612	p 4046	N92-33092
NAG9-549	p 3942	N92-32477
NANB7D737	p 3963	N92-32607
NASA ORDER C-99066-6	p 4011	N92-32868
NASA ORDER H-13026-D	p 4076	N92-33074
NASW-4003	p 4047	N92-33196
NAS1-15949	p 3952	N92-32585
NAS1-17925	p 4023	N92-33139
NAS1-18028	p 3939	N92-32778
NAS1-18565	p 4052	N92-33100
	p 4052	N92-33101
NAS1-18605	p 4010	N92-32784
	p 4059	N92-33006
	p 4012	N92-33110
NAS1-19000	p 4077	N92-33239
NAS1-19480	p 4059	N92-33006
	p 4012	N92-33110
NAS3-25088	p 3983	N92-32966
NAS8-36123	p 4092	N92-33094
NAS8-36955	p 4020	N92-32425
NAS8-37462	p 3998	N92-32265
NAS8-38862	p 3998	N92-32264
NAS8-38865	p 3999	N92-32269
NAS8-38871	p 3997	N92-32260
NAS8-39203	p 3969	N92-33081
NAS9-18000	p 3942	N92-32610
NCA2-543	p 3979	N92-32559
NCC2-127	p 4037	N92-32539
NCC2-374	p 4007	N92-32560
NCC9-16	p 3942	N92-32244
	p 4041	N92-32451
	p 4090	N92-32654
	p 4042	N92-32656
	p 4043	N92-32865
	p 4047	N92-33093
	p 4091	N92-33096
	p 4091	N92-33178
NGR-33-015-141	p 4097	N92-32374

NGT-50363	p 4000	N92-32276
NGT-50414	p 3932	N92-32606
NGT-50472	p 4099	N92-32386
NIVR-01604-N	p 3930	N92-32730
NIVR-2404-N	p 4008	N92-32675
	p 4010	N92-32786
NR PROJ. MR0-095	p 4037	N92-32942
NR PROJ. RR0-1308	p 4082	N92-32512
NR PROJ. RR0-1310	p 4082	N92-32512
NR PROJ. RR0-3308	p 4035	N92-33220
NSF ATM-89-96116	p 4099	N92-32386
NSF ATM-90-22249	p 4103	N92-32488
NSF CCR-89-01780	p 4020	N92-32436
NSF CCR-90-05633	p 4050	N92-32568
NSF CCR-91-02231	p 4020	N92-32436
NSF CDA-88-22724	p 4050	N92-32568
NSF DMS-91-00383	p 4012	N92-33110
NSF DMS-91-07608	p 4010	N92-32784
NSF ECS-86-57951	p 3983	N92-32971
NSF ECS-88-18975	p 4077	N92-32417
NSF IRI-89-03582	p 4050	N92-32568
NSF IRI-89-20771	p 4050	N92-32568
NSF ISI-86-60941	p 4076	N92-33004
NSG-1492	p 4058	N92-32888
N00014-82-K-0193	p 4050	N92-32568
N00014-87-C-2412	p 4016	N92-33089
N00014-88-K-0133	p 4038	N92-32569
N00014-88-K-0451	p 3972	N92-32913
N00014-88-K-0483	p 3961	N92-32509
	p 4066	N92-32556
N00014-89-J-1023	p 4084	N92-32898
N00014-89-J-1024	p 4103	N92-32488
N00014-89-J-1048	p 4035	N92-32571
N00014-89-J-1169	p 4064	N92-32418
	p 4066	N92-32682
N00014-89-J-1276	p 4023	N92-32936
N00014-89-J-1633	p 4053	N92-32625
N00014-90-C-0028	p 4016	N92-32540
N00014-90-C-2200	p 4075	N92-32915
N00014-90-J-1114	p 3988	N92-32325
N00014-90-J-1159	p 4066	N92-32548
N00014-90-J-1186	p 3971	N92-32547
N00014-90-J-1230	p 3990	N92-32827
N00014-90-J-1334	p 4055	N92-32670
N00014-90-J-1680	p 4088	N92-32551
N00014-90-J-4083	p 4006	N92-32324
N00014-91-J-1126	p 4084	N92-32940
N00014-91-J-1235	p 3971	N92-32665
N00014-91-J-1243	p 4036	N92-32344
N00014-91-J-1334	p 3982	N92-32899
N00014-91-J-1409	p 3964	N92-32826
N00014-91-J-1475	p 3961	N92-32553
N00014-91-J-1582	p 4061	N92-32901
N00014-91-J-1655	p 3971	N92-32550
N00014-91-J-1772	p 3955	N92-32828
N00014-91-J-1857	p 3979	N92-32573
	p 4050	N92-32628
	p 4074	N92-32668
N00014-91-J-1976	p 4083	N92-32747
N00014-91-J-4036	p 3988	N92-32659
N00014-92-J-1125	p 3971	N92-32490
N00014-92-J-1374	p 3972	N92-32667
N00019-85-C-0090	p 3951	N92-32583
N00019-91-C-0149	p 4036	N92-32434
N00039-91-C-0082	p 4046	N92-32917
N62269-87-C-0226	p 3949	N92-32527
N62269-87-C-0227	p 3951	N92-32580
N62269-87-C-0259	p 3951	N92-32579
RICIS PROJ. MS-03	p 3942	N92-32244
RICIS PROJ. SE-34	p 4041	N92-32451
RICIS PROJ. SE-42	p 4047	N92-33093
RICIS PROJ. SE-43	p 4090	N92-32654
	p 4091	N92-33096
	p 4091	N92-33178
RICIS PROJ. SR-02	p 4043	N92-32865
RTOP 307-51-50	p 4105	N92-33106
RTOP 474-42-10	p 3991	N92-32867
RTOP 476-14-01	p 4040	N92-32809
RTOP 505-59-00	p 4012	N92-33113
RTOP 505-59-30	p 3935	N92-32887
RTOP 505-59-40	p 4007	N92-32560
RTOP 505-59-53-01	p 3929	N92-32480
RTOP 505-60-00	p 3938	N92-32452
RTOP 505-61-71	p 3929	N92-32422
RTOP 505-62-21	p 4011	N92-32868
RTOP 505-62-52	p 4007	N92-32472
RTOP 505-63-01-09	p 3946	N92-32513
	p 3950	N92-32574
RTOP 505-63-5A	p 3972	N92-32863
RTOP 505-63-5B	p 3946	N92-32466
RTOP 505-63-50-15	p 3934	N92-32536
RTOP 505-63-53-01	p 4023	N92-33104
RTOP 505-64-12-02	p 3932	N92-32606
RTOP 505-64-13	p 3933	N92-33080
	p 3933	N92-33194
RTOP 505-64-30	p 3935	N92-33149

RTOP 505-64-36	p 3933	N92-32424
RTOP 505-64-52-53	p 4052	N92-33100
	p 4052	N92-33101
RTOP 505-68-50	p 3938	N92-32866
RTOP 505-90-52-01	p 4010	N92-32784
	p 4059	N92-33006
	p 4012	N92-33110
RTOP 505-90-53-02	p 4041	N92-33205
RTOP 506-41-11	p 3988	N92-32243
RTOP 506-42-31	p 3944	N92-33064
RTOP 506-43-31	p 3970	N92-32476
RTOP 506-46-21-05	p 3939	N92-32778
RTOP 506-48-11-04	p 3944	N92-33112
RTOP 506-59-31	p 4052	N92-32886
RTOP 506-72-1B	p 3982	N92-32965
RTOP 533-02-36	p 4042	N92-32507
	p 3940	N92-32864
RTOP 533-02-37	p 3939	N92-32788
RTOP 535-03-11-03	p 4061	N92-32948
	p 4063	N92-33160
RTOP 538-02-10-01	p 4021	N92-32423
RTOP 572-10-00	p 3941	N92-32456
RTOP 590-14-61-01	p 4021	N92-32657
RTOP 590-31-41	p 4007	N92-32474
RTOP 590-32-31	p 4077	N92-33239
RTOP 593-72-41	p 3944	N92-32463
RTOP 665-45-30-21	p 4031	N92-33097
SERC-GR/H00581	p 4101	N92-32399
SERC/GR/F/68942	p 4055	N92-32661
S01-15526	p 4092	N92-33094
TEES PROJ. 30540-AE	p 3932	N92-33063
TTN77-1038	p 4012	N92-33066
USGS-14-08-0001-G1731	p 4034	N92-33173
W-31-109-ENG-38	p 4069	N92-32314
	p 4081	N92-32346
	p 4082	N92-32542
	p 4082	N92-32561
	p 4017	N92-32615
	p 3953	N92-32638
	p 3988	N92-32639
	p 3971	N92-32640
	p 3964	N92-32931
	p 4072	N92-32932
	p 4016	N92-33114
	p 4047	N92-33118
	p 3992	N92-33128
	p 4072	N92-33130
	p 4080	N92-33168
	p 4086	N92-33221
	p 3974	N92-33247
W-7405-ENG-36	p 4041	N92-32414
	p 4027	N92-32415
	p 4059	N92-32481
	p 4070	N92-32647
	p 4025	N92-32695
	p 4016	N92-32736
	p 4075	N92-32738
	p 4104	N92-32862
	p 4040	N92-32910
	p 3943	N92-32934
	p 4085	N92-33026
	p 3992	N92-33068
	p 4088	N92-33069
	p 3969	N92-33120
	p 4013	N92-33159
W-7405-ENG-48	p 4006	N92-32322
	p 3946	N92-32327
	p 4020	N92-32328
	p 3970	N92-32341
	p 4050	N92-32412
	p 4070	N92-32413
	p 4041	N92-32416
	p 3961	N92-32544
	p 3966	N92-32646
	p 4022	N92-32706
	p 4079	N92-32733
	p 4043	N92-32741
	p 4057	N92-32743
	p 4010	N92-32824
	p 4071	N92-32904
	p 3964	N92-32929
	p 4030	N92-32933
	p 4012	N92-32947
	p 4014	N92-32999
	p 4014	N92-33000
	p 4068	N92-33001
	p 4012	N92-33082
	p 3969	N92-33116
	p 4072	N92-33122
	p 3985	N92-33126
	p 3969	N92-33132
W-7405-ENG-82	p 4081	N92-32465
	p 4065	N92-32473
	p 3962	N92-32562
	p 3962	N92-32563
	p 4088	N92-33109

	p 4085	N92-33111
W2207-7-AF69/01-SS	p 3934	N92-32845
W7711-7-7004/01-SE	p 4038	N92-32817

Typical Report Number Index Listing

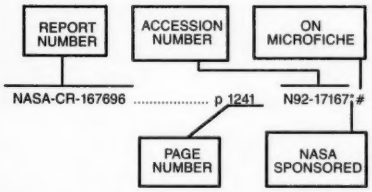

Listings in this index are arranged alphanumerically by report number. The accession number denotes the number by which the citation is identified. The page number helps to locate the citation in the abstract section. An asterisk (*) indicates that the item is a NASA report. A pound sign (#) indicates that the item is available on microfiche.

A-90244 ..... p 3929 N92-32422 * #
A-91074 ..... p 3938 N92-32452 * #
A-91156 ..... p 3935 N92-32887 * #
A-91203 ..... p 3933 N92-33194 * #
A-91218 ..... p 4105 N92-33106 * #
A-92023 ..... p 4052 N92-32886 * #
A-92039 ..... p 3939 N92-32788 * #
A-92041 ..... p 4012 N92-33113 * #
A-92055 ..... p 4007 N92-32474 * #
A-92085 ..... p 3933 N92-32424 * #
A-92110 ..... p 4040 N92-32809 * #
A-92146 ..... p 3970 N92-32476 * #
A-92156 ..... p 3933 N92-33080 * #

AD-A244196 ..... p 4029 N92-32731 #
AD-A245283 ..... p 3977 N92-32461 #
AD-A246137 ..... p 4033 N92-32534 #
AD-A246315 ..... p 3978 N92-32535 #
AD-A246710 ..... p 3980 N92-32696 #
AD-A246880 ..... p 3942 N92-32538 #
AD-A247175 ..... p 4061 N92-32697 #
AD-A247264 ..... p 4016 N92-32540 #
AD-A247301 ..... p 4074 N92-32613 #
AD-A247426 ..... p 3935 N92-32612 #
AD-A247427 ..... p 4050 N92-32568 #
AD-A247429 ..... p 4038 N92-32569 #
AD-A247431 ..... p 3979 N92-32570 #
AD-A247456 ..... p 4035 N92-32571 #
AD-A247553 ..... p 4031 N92-32572 #
AD-A247613 ..... p 3979 N92-32573 #
AD-A247614 ..... p 4074 N92-32668 #
AD-A247617 ..... p 4050 N92-32628 #
AD-A247866 ..... p 3971 N92-32490 #
AD-A247886 ..... p 3953 N92-32629 #
AD-A247942 ..... p 4007 N92-32630 #
AD-A248450 ..... p 4089 N92-32644 #
AD-A248451 ..... p 4055 N92-32670 #
AD-A248660 ..... p 3963 N92-32645 #
AD-A248752 ..... p 4036 N92-32492 #
AD-A248763 ..... p 4103 N92-32338 #
AD-A249231 ..... p 3956 N92-32906 #
AD-A249242 ..... p 4046 N92-32907 #
AD-A250099 ..... p 4103 N92-32488 #
AD-A250129 ..... p 3970 N92-32489 #
AD-A250146 ..... p 4013 N92-32323 #
AD-A250220 ..... p 3946 N92-32339 #
AD-A250366 ..... p 4006 N92-32324 #
AD-A250367 ..... p 3988 N92-32325 #
AD-A250368 ..... p 4083 N92-32747 #
AD-A250370 ..... p 4053 N92-32748 #
AD-A250373 ..... p 3935 N92-32326 #
AD-A250667 ..... p 4022 N92-32717 #
AD-A250710 ..... p 3980 N92-32719 #
AD-A250711 ..... p 4008 N92-32671 #
AD-A250758 ..... p 3961 N92-32508 #
AD-A250760 ..... p 4074 N92-32672 #
AD-A250763 ..... p 3970 N92-32341 #
AD-A250767 ..... p 3953 N92-32674 #
AD-A250769 ..... p 4089 N92-32342 #
AD-A250771 ..... p 4013 N92-32343 #
AD-A250784 ..... p 3953 N92-32676 #
AD-A250786 ..... p 4038 N92-32660 #
AD-A250789 ..... p 3967 N92-32699 #
AD-A250793 ..... p 4037 N92-32504 #
AD-A250799 ..... p 3974 N92-32664 #
AD-A250814 ..... p 4008 N92-32632 #
AD-A250851 ..... p 4015 N92-32329 #
AD-A250852 ..... p 4021 N92-32621 #
AD-A250853 ..... p 4016 N92-32622 #
AD-A250855 ..... p 3960 N92-32330 #
AD-A250873 ..... p 4036 N92-32344 #
AD-A250877 ..... p 3989 N92-32678 #
AD-A250878 ..... p 3980 N92-32680 #
AD-A250881 ..... p 4035 N92-32345 #
AD-A250883 ..... p 3961 N92-32553 #
AD-A250921 ..... p 4066 N92-32556 #
AD-A250923 ..... p 3961 N92-32509 #
AD-A250934 ..... p 4020 N92-33151 #
AD-A250935 ..... p 4064 N92-32418 #
AD-A250942 ..... p 4075 N92-32935 #
AD-A250965 ..... p 3971 N92-32665 #
AD-A250970 ..... p 4042 N92-32546 #
AD-A250977 ..... p 3972 N92-32667 #
AD-A250980 ..... p 3989 N92-32669 #
AD-A251069 ..... p 3972 N92-32913 #
AD-A251073 ..... p 4021 N92-32681 #
AD-A251087 ..... p 4066 N92-32682 #
AD-A251095 ..... p 4008 N92-32683 #
AD-A251098 ..... p 3971 N92-32547 #
AD-A251099 ..... p 4029 N92-32650 #
AD-A251121 ..... p 3989 N92-32700 #
AD-A251139 ..... p 3930 N92-32651 #
AD-A251140 ..... p 4066 N92-32548 #
AD-A251141 ..... p 3971 N92-32550 #
AD-A251153 ..... p 4088 N92-32551 #
AD-A251160 ..... p 4008 N92-32652 #
AD-A251169 ..... p 3964 N92-32826 #
AD-A251172 ..... p 3990 N92-32827 #
AD-A251173 ..... p 4023 N92-32936 #
AD-A251177 ..... p 4075 N92-32915 #
AD-A251182 ..... p 3955 N92-32828 #
AD-A252209 ..... p 4084 N92-32898 #
AD-A252213 ..... p 4016 N92-33089 #
AD-A252217 ..... p 4089 N92-32611 #
AD-A252232 ..... p 4053 N92-32625 #
AD-A252234 ..... p 4039 N92-32433 #
AD-A252235 ..... p 4036 N92-32434 #
AD-A252246 ..... p 3980 N92-32686 #
AD-A252250 ..... p 3982 N92-32891 #
AD-A252279 ..... p 4035 N92-32688 #
AD-A252280 ..... p 4035 N92-33220 #
AD-A252350 ..... p 4082 N92-32512 #
AD-A252365 ..... p 4037 N92-32916 #
AD-A252368 ..... p 4046 N92-32917 #
AD-A252370 ..... p 4023 N92-32918 #
AD-A252371 ..... p 4038 N92-32990 #
AD-A252374 ..... p 4052 N92-32937 #
AD-A252385 ..... p 3982 N92-32899 #
AD-A252389 ..... p 3931 N92-32900 #
AD-A252390 ..... p 4061 N92-32901 #
AD-A252394 ..... p 4031 N92-32902 #
AD-A252399 ..... p 4084 N92-32938 #
AD-A252411 ..... p 4084 N92-32939 #
AD-A252431 ..... p 4084 N92-32940 #
AD-A252438 ..... p 3932 N92-32941 #
AD-A252466 ..... p 3979 N92-32633 #
AD-A252494 ..... p 3986 N92-33152 #
AD-A252520 ..... p 3938 N92-32435 #
AD-A252575 ..... p 3966 N92-32626 #
AD-A252618 ..... p 3929 N92-32691 #
AD-A252633 ..... p 4042 N92-32627 #
AD-A252634 ..... p 4042 N92-32658 #
AD-A252674 ..... p 3988 N92-32659 #
AD-A252719 ..... p 4037 N92-32942 #
AD-A252728 ..... p 3986 N92-32987 #
AD-A252730 ..... p 3940 N92-32988 #
AD-A252755 ..... p 4059 N92-32989 #
AD-A253691 ..... p 4104 N92-33027 #
AD-A253692 ..... p 4105 N92-33238 #

AD-D015270 ..... p 3963 N92-32755 #
AD-D015285 ..... p 4076 N92-33095 #
AD-D015289 ..... p 4074 N92-32634 #
AD-D015294 ..... p 3973 N92-33157
AD-D015301 ..... p 4026 N92-32943 #
AD-D015308 ..... p 3940 N92-33161
AD-D015309 ..... p 3944 N92-33162
AD-D015310 ..... p 4017 N92-33165
AD-D015311 ..... p 4073 N92-33167
AD-D015312 ..... p 3992 N92-33169
AD-D015313 ..... p 3973 N92-33170
AD-D015323 ..... p 3986 N92-33171
AD-D015325 ..... p 3986 N92-33172
AD-D015326 ..... p 3960 N92-33174
AD-D015329 ..... p 3992 N92-33175
AD-D015330 ..... p 3974 N92-33177

AD-E200882 ..... p 4031 N92-32572 #
AD-E951843 ..... p 3979 N92-32633 #

AECL-10459 ..... p 3961 N92-32475 #

AERONAUTICA-ACTA-A-364-1992 p 3943 N92-32728

AFIT/CI/CIA-92-023 ..... p 3966 N92-32626 #
AFIT/CI/CIA-92-028 ..... p 3929 N92-32691 #
AFIT/CI/CIA-92-039 ..... p 3938 N92-32435 #

AFOSR-92-0167TR-VOL-1 ..... p 4103 N92-32338 #
AFOSR-92-0294TR ..... p 3980 N92-32719 #
AFOSR-92-0313TR ..... p 3953 N92-32674 #
AFOSR-92-0356TR ..... p 3946 N92-32339 #
AFOSR-92-0367TR ..... p 4016 N92-32622 #
AFOSR-92-0374TR ..... p 4008 N92-32671 #
AFOSR-92-0386TR ..... p 3967 N92-32699 #
AFOSR-92-0428TR ..... p 4020 N92-33151 #
AFOSR-92-0445TR ..... p 3989 N92-32669 #
AFOSR-92-0453TR-PT-1-2 ..... p 4021 N92-32681 #
AFOSR-92-1 ..... p 3946 N92-32339 #

AGARD-CP-500 ..... p 3935 N92-32437 #
AGARD-CP-511 ..... p 3975 N92-33240 #

AGARD-R-785 ..... p 3956 N92-33033 #

AIAA PAPER 92-0769 ..... p 3998 N92-32263 * #
AIAA PAPER 92-1465 ..... p 3943 N92-32704 #
AIAA PAPER 92-2092 ..... p 4062 N92-32956 * #
AIAA PAPER 92-2164 ..... p 4062 N92-32951 * #
AIAA PAPER 92-4109 ..... p 3940 N92-32864 * #
AIAA PAPER 92-4113 ..... p 3938 N92-32866 * #
AIAA PAPER 92-4176 ..... p 3935 N92-33149 * #

AL-TP-1992-0001 ..... p 3935 N92-32612 #

AL-TR-1991-0104 ..... p 4036 N92-32492 #
AL-TR-1991-0140 ..... p 4046 N92-32907 #
AL-TR-1992-0056 ..... p 4042 N92-32658 #
AL-TR-1992-0057 ..... p 4042 N92-32627 #

AMSMI/TR-RD-WS-92-6 ..... p 3979 N92-32633 #

ANL-92/15 ..... p 3964 N92-32931 #

ANL/APS-CP-4 ..... p 4072 N92-32932 #

ANL/CP-74239 ..... p 4082 N92-32561 #
ANL/CP-74658 ..... p 4072 N92-33130 #
ANL/CP-74829 ..... p 4081 N92-32346 #
ANL/CP-75691 ..... p 4082 N92-32542 #
ANL/CP-75762 ..... p 3953 N92-32638 #
ANL/CP-75802 ..... p 3992 N92-33128 #
ANL/CP-75863 ..... p 4069 N92-32314 #
ANL/CP-75875 ..... p 3988 N92-32639 #
ANL/CP-75942 ..... p 4016 N92-33114 #
ANL/CP-76077 ..... p 3971 N92-32640 #
ANL/CP-76309 ..... p 3974 N92-33247 #
ANL/CP-76482 ..... p 4086 N92-33221 #

ANL/ESD/TM-29 ..... p 4017 N92-32615 #

ANL/FPP/TM-262 ..... p 4080 N92-33168 #

ANL/MCS-TM-165 ..... p 4047 N92-33118 #

ARI-RN-92-39 ..... p 4038 N92-32990 #
ARI-RN-92-40 ..... p 4039 N92-32433 #

ARL-GD-029 ..... p 3935 N92-32326 #

ARL-TR-92-7 ..... p 4046 N92-32917 #

ARO-24413.6-CH ..... p 3963 N92-32645 #
ARO-29044.1-MS-SBI ..... p 3956 N92-32906 #
ARO-29211.1-PHS ..... p 4013 N92-32323 #

ATC-189 ..... p 3980 N92-32686 #

B-242745 ..... p 3934 N92-32861 #
B-248821 ..... p 4088 N92-32618 #

BNL-NUREG-47471 ..... p 3988 N92-32635 #

BNL-47235 ..... p 4081 N92-32470 #
BNL-47236 ..... p 4086 N92-33136 #
BNL-47317 ..... p 4071 N92-32912 #
BNL-47376 ..... p 4015 N92-32511 #
BNL-47503 ..... p 4073 N92-33179 #
BNL-47550 ..... p 4064 N92-32316 #
BNL-52291-PHASE-2 ..... p 4070 N92-32411 #

BRL-CR-689 ..... p 3970 N92-32341 #
BRL-CR-690 ..... p 3961 N92-32508 #

BRL-MR-3980 ..... p 3989 N92-32700 #

BRL-TR-3337 ..... p 3974 N92-32664 #
BRL-TR-3353 ..... p 4008 N92-32683 #
BRL-TR-3368 ..... p 4023 N92-32918 #

B91-0099 ..... p 3991 N92-33061 #

C-238 ..... p 3973 N92-33059 #

CA-PATENT-APPL-SN-2-011-945 p 4011 N92-32856

CA-PATENT-1-276-814 ..... p 3968 N92-32855

CAL-504-88P120 ..... p 3990 N92-32847 #

CCMS-92-16 ..... p 3946 N92-32491 * #

CEBAF-PR-92-005 ..... p 4069 N92-32319 #
CEBAF-PR-92-008 ..... p 4069 N92-32318 #
CEBAF-PR-92-012 ..... p 4070 N92-32567 #
CEBAF-PR-92-015 ..... p 3970 N92-32317 #

CERC/CR/DRP-91-1 ..... p 4007 N92-32630 #

CMOTT-92-07 ..... p 4011 N92-32868 * #

CNRC-33030 ..... p 4019 N92-33077 #

COLO-HEP-287 ..... p 4069 N92-33187 #

CONF-8810234 ..... p 4010 N92-32824 #
CONF-9001172-1 ..... p 4040 N92-32642 #
CONF-9103235-1 ..... p 4018 N92-32701 #
CONF-910399-7 ..... p 3946 N92-32327 #
CONF-9104192-11 ..... p 4085 N92-33023 #
CONF-9105180 ..... p 4072 N92-32932 #
CONF-9106289-6 ..... p 4064 N92-32312 #
CONF-9107217 ..... p 4064 N92-32340 #
CONF-910730-31 ..... p 4073 N92-32321 #
CONF-9108127-4 ..... p 4012 N92-32947 #
CONF-910836-5 ..... p 4069 N92-33148 #
CONF-9109102-6 ..... p 4081 N92-32470 #
CONF-9109102-7 ..... p 4086 N92-33136 #
CONF-9109328-2 ..... p 4069 N92-32337 #
CONF-9109364-1 ..... p 4020 N92-32328 #
CONF-9109371-1 ..... p 4087 N92-32496 #
CONF-9109393 ..... p 4027 N92-33090 #
CONF-910945-12 ..... p 3969 N92-33132 #
CONF-9110146-16 ..... p 4073 N92-32419 #
CONF-9110146-22 ..... p 4067 N92-32997 #
CONF-9110258-5 ..... p 4070 N92-32647 #
CONF-9110397-1 ..... p 4088 N92-33069 #
CONF-911050-11 ..... p 3971 N92-32640 #
CONF-911106-89 ..... p 4082 N92-32493 #
CONF-911131-2 ..... p 4079 N92-32733 #
CONF-911202-60 ..... p 4083 N92-32693 #
CONF-920141-8 ..... p 4081 N92-32320 #
CONF-920172-7 ..... p 4070 N92-32506 #
CONF-9202111-1 ..... p 4017 N92-33155 #
CONF-920219-1 ..... p 4065 N92-32426 #
CONF-920240-5 ..... p 4084 N92-32919 #
CONF-920311-14 ..... p 4080 N92-32995 #
CONF-9203140-2 ..... p 3964 N92-32996 #
CONF-920315-13 ..... p 4071 N92-32751 #
CONF-920315-34 ..... p 4070 N92-32413 #
CONF-920315-37 ..... p 4015 N92-32511 #
CONF-920315-39 ..... p 4072 N92-33122 #
CONF-920315-40 ..... p 4069 N92-32314 #
CONF-9203154-3 ..... p 4069 N92-33164 #
CONF-9203162-2 ..... p 4067 N92-32928 #
CONF-920331-47 ..... p 4073 N92-33134 #
CONF-920362-31 ..... p 4078 N92-32623 #
CONF-920367-8 ..... p 4050 N92-32412 #
CONF-920373-4 ..... p 3943 N92-32704 #
CONF-920375-15 ..... p 3988 N92-32635 #
CONF-920378-1 ..... p 4025 N92-32695 #
CONF-920402-12 ..... p 3956 N92-32945 #
CONF-920402-13 ..... p 4082 N92-32636 #
CONF-920402-19 ..... p 4084 N92-32920 #
CONF-920402-26 ..... p 4085 N92-33026 #
CONF-920402-30 ..... p 4081 N92-32346 #
CONF-920402-7 ..... p 4085 N92-33127 #
CONF-920402-9 ..... p 4083 N92-32653 #
CONF-920432-13 ..... p 3992 N92-33128 #
CONF-920439-5 ..... p 3966 N92-32646 #
CONF-9205115-1 ..... p 4026 N92-32946 #
CONF-9205123-12 ..... p 4020 N92-33085 #
CONF-9205139-1 ..... p 4040 N92-32910 #
CONF-920515-26 ..... p 3992 N92-33068 #
CONF-920515-2 ..... p 4080 N92-32992 #
CONF-9205196-1 ..... p 3964 N92-32925 #
CONF-9205213-1 ..... p 3974 N92-33247 #
CONF-920540-2 ..... p 4018 N92-32694 #
CONF-920548-1 ..... p 4082 N92-32542 #
CONF-920574-9 ..... p 4016 N92-33114 #
CONF-920584-10 ..... p 3960 N92-32334 #
CONF-920584-7 ..... p 3960 N92-32332 #
CONF-920584-8 ..... p 4034 N92-32333 #
CONF-920604-3 ..... p 3953 N92-32638 #
CONF-920606-19 ..... p 4072 N92-32994 #
CONF-9206102-5 ..... p 4041 N92-32414 #
CONF-9206112-2 ..... p 3978 N92-32927 #
CONF-9206174-1 ..... p 3969 N92-33116 #
CONF-9206185-4 ..... p 4060 N92-32998 #
CONF-9206185-6-PT-2 ..... p 4052 N92-32926 #
CONF-9206185-7 ..... p 4012 N92-33082 #
CONF-9206195-2 ..... p 4082 N92-32561 #
CONF-9206195-3 ..... p 3969 N92-33120 #
CONF-9206201-2 ..... p 4014 N92-32999 #
CONF-9206201-3 ..... p 4068 N92-33001 #
CONF-9206201-4 ..... p 4014 N92-33000 #
CONF-9206202-1 ..... p 4086 N92-33221 #
CONF-920631-21 ..... p 3988 N92-32495 #
CONF-920631-36 ..... p 4072 N92-33130 #
CONF-920658-2 ..... p 4026 N92-32923 #
CONF-920669-6 ..... p 3988 N92-32639 #
CONF-920673-6 ..... p 3969 N92-33115 #
CONF-920707-19 ..... p 3961 N92-32544 #
CONF-9207105-1 ..... p 3965 N92-33185 #
CONF-920716-5 ..... p 4064 N92-32316 #
CONF-920732-2 ..... p 4019 N92-32890 #
CONF-920796-2 ..... p 3974 N92-32637 #
CONF-920796-3 ..... p 3975 N92-33003 #
CONF-920819-7 ..... p 3969 N92-33158 #
CONF-920851-6 ..... p 4028 N92-32558 #
CONF-9209143-2 ..... p 4054 N92-33184 #

CRAD-1-90 ..... p 3990 N92-32812 #

CRDEC-CR-144 ..... p 3960 N92-32330 #

CRREL-SR-92-11 ..... p 3931 N92-32900 #

CRREL-92-9 ..... p 3940 N92-32903 #

CSC/TR-90/6155 ..... p 4041 N92-32451 * #

CSCC-A-9 ..... p 4041 N92-33205 * #

CSDL-T-1131 ..... p 3986 N92-33152 #

CTN-92-60328 ..... p 3981 N92-32749 #
CTN-92-60333 ..... p 4103 N92-32814 #
CTN-92-60334 ..... p 4104 N92-32815 #
CTN-92-60335 ..... p 3981 N92-32787 #
CTN-92-60346 ..... p 3981 N92-32789 #
CTN-92-60348 ..... p 3934 N92-32845 #
CTN-92-60350 ..... p 3955 N92-32846 #
CTN-92-60351 ..... p 4039 N92-32790 #
CTN-92-60353 ..... p 4037 N92-32816 #
CTN-92-60354 ..... p 3990 N92-32810 #
CTN-92-60355 ..... p 3990 N92-32847 #
CTN-92-60357 ..... p 3931 N92-32811 #
CTN-92-60359 ..... p 4038 N92-32817 #
CTN-92-60360 ..... p 3982 N92-32818 #
CTN-92-60361 ..... p 3990 N92-32812 #
CTN-92-60367 ..... p 3955 N92-32813 #
CTN-92-60368 ..... p 4022 N92-32848 #
CTN-92-60369 ..... p 3934 N92-32849 #
CTN-92-60370 ..... p 3954 N92-32791 #
CTN-92-60371 ..... p 3938 N92-32850 #
CTN-92-60372 ..... p 4040 N92-32851 #
CTN-92-60373 ..... p 3955 N92-32852 #
CTN-92-60375 ..... p 4104 N92-32853 #
CTN-92-60376 ..... p 3967 N92-32794 #
CTN-92-60377 ..... p 3955 N92-32829 #
CTN-92-60378 ..... p 3938 N92-33102 #
CTN-92-60379 ..... p 4023 N92-33076 #
CTN-92-60380 ..... p 4019 N92-33077 #
CTN-92-60381 ..... p 3959 N92-33078 #
CTN-92-60386 ..... p 4039 N92-33079 #
CTN-92-60387 ..... p 4054 N92-32854 #
CTN-92-60389 ..... p 3968 N92-32855
CTN-92-60391 ..... p 4011 N92-32856
CTN-92-60516 ..... p 4080 N92-33223
CTN-92-60517 ..... p 4034 N92-33225
CTN-92-60519 ..... p 4032 N92-33197
CTN-92-60520 ..... p 4035 N92-33198
CTN-92-60521 ..... p 4013 N92-33226
CTN-92-60522 ..... p 4088 N92-33199
CTN-92-60523 ..... p 4023 N92-33200
CTN-92-60524 ..... p 4024 N92-33228
CTN-92-60525 ..... p 4048 N92-33201
CTN-92-60526 ..... p 4077 N92-33202
CTN-92-60527 ..... p 4048 N92-33210
CTN-92-60528 ..... p 4054 N92-33203
CTN-92-60529 ..... p 4048 N92-33214
CTN-92-60530 ..... p 4049 N92-33215
CTN-92-60531 ..... p 4052 N92-33216
CTN-92-60532 ..... p 4053 N92-33217
CTN-92-60533 ..... p 4054 N92-33218
CTN-92-60534 ..... p 4055 N92-33219
CTN-92-60535 ..... p 4053 N92-33224
CTN-92-60536 ..... p 4049 N92-33227
CTN-92-60537 ..... p 4049 N92-33232
CTN-92-60538 ..... p 4053 N92-33235
CTN-92-60539 ..... p 4048 N92-33204
CTN-92-60540 ..... p 4049 N92-33229
CTN-92-60541 ..... p 4049 N92-33230
CTN-92-60542 ..... p 4059 N92-33231
CTN-92-60543 ..... p 4024 N92-33233
CTN-92-60544 ..... p 3994 N92-33234
CTN-92-60545 ..... p 3987 N92-33206
CTN-92-60546 ..... p 3987 N92-33207
CTN-92-60547 ..... p 3993 N92-33208
CTN-92-60548 ..... p 3987 N92-33209
CTN-92-60549 ..... p 4055 N92-33236
CTN-92-60550 ..... p 4047 N92-33189
CTN-92-60551 ..... p 3986 N92-33191
CTN-92-60552 ..... p 3987 N92-33192
CTN-92-60553 ..... p 3993 N92-33193
CTN-92-60554 ..... p 3993 N92-33195
CTN-92-60555 ..... p 3993 N92-33211
CTN-92-60556 ..... p 4048 N92-33212
CTN-92-60567 ..... p 3987 N92-33213

CU-TR-14 ..... p 3932 N92-32606 * #

CWI-BS-R9115 ..... p 4059 N92-33058 #

DCIEM-90-23 ..... p 4039 N92-32790 #
DCIEM-90-47 ..... p 4037 N92-32816 #
DCIEM-91-05 ..... p 4054 N92-32854 #
DCIEM-91-20 ..... p 4039 N92-33079 #

DE91-002140 ..... p 4026 N92-32908 #
DE91-002144 ..... p 4026 N92-32909 #
DE91-014224 ..... p 4085 N92-33023 #
DE91-018864 ..... p 4018 N92-32694 #
DE92-001237 ..... p 4024 N92-32510 #
DE92-001247 ..... p 4027 N92-33138 #
DE92-008253 ..... p 4083 N92-32693 #
DE92-008317 ..... p 3963 N92-32666 #
DE92-008563 ..... p 3961 N92-32544 #
DE92-009590 ..... p 4013 N92-32460 #
DE92-010031 ..... p 4077 N92-32533 #
DE92-010301 ..... p 4082 N92-32493 #
DE92-010666 ..... p 4018 N92-32701 #
DE92-010703 ..... p 4079 N92-32733 #
DE92-010705 ..... p 3966 N92-32646 #
DE92-010730 ..... p 4069 N92-32337 #
DE92-011049 ..... p 3969 N92-33158 #
DE92-011137 ..... p 4070 N92-32647 #
DE92-011231 ..... p 4040 N92-32910 #
DE92-011234 ..... p 4025 N92-32695 #
DE92-011272 ..... p 4016 N92-32736 #
DE92-011273 ..... p 4075 N92-32738 #
DE92-011289 ..... p 4043 N92-32741 #
DE92-011290 ..... p 4057 N92-32743 #
DE92-011339 ..... p 3981 N92-32744 #
DE92-011383 ..... p 3943 N92-32704 #
DE92-011462 ..... p 3946 N92-32327 #
DE92-011468 ..... p 4020 N92-32328 #
DE92-011586 ..... p 4071 N92-32751 #

DE92-011631 ..... p 3989 N92-32754 #
DE92-011653 ..... p 4022 N92-32706 #
DE92-011808 ..... p 3971 N92-32631 #
DE92-011907 ..... p 4022 N92-32911 #
DE92-012212 ..... p 4071 N92-32912 #
DE92-012241 ..... p 4021 N92-32698 #
DE92-012415 ..... p 4065 N92-32426 #
DE92-012449 ..... p 4032 N92-32427 #
DE92-012572 ..... p 4081 N92-32462 #
DE92-012573 ..... p 3960 N92-32464 #
DE92-012584 ..... p 4081 N92-32465 #
DE92-012595 ..... p 4028 N92-32619 #
DE92-013021 ..... p 4087 N92-32496 #
DE92-013076 ..... p 3988 N92-32495 #
DE92-013108 ..... p 4059 N92-32481 #
DE92-013135 ..... p 4028 N92-32616 #
DE92-013169 ..... p 3974 N92-32483 #
DE92-013237 ..... p 3966 N92-32614 #
DE92-013296 ..... p 4017 N92-32615 #
DE92-013353 ..... p 3977 N92-32467 #
DE92-013395 ..... p 4070 N92-32411 #
DE92-013444 ..... p 4050 N92-32412 #
DE92-013448 ..... p 4070 N92-32413 #
DE92-013540 ..... p 4041 N92-32414 #
DE92-013572 ..... p 4090 N92-32930 #
DE92-013582 ..... p 4090 N92-32985 #
DE92-013639 ..... p 4027 N92-32415 #
DE92-013663 ..... p 4028 N92-32558 #
DE92-013680 ..... p 4025 N92-32549 #
DE92-013681 ..... p 3934 N92-32308 #
DE92-013711 ..... p 4014 N92-32620 #
DE92-013754 ..... p 4041 N92-32416 #
DE92-013765 ..... p 4069 N92-33148 #
DE92-013772 ..... p 4032 N92-32331 #
DE92-013776 ..... p 4027 N92-33150 #
DE92-013796 ..... p 4078 N92-32623 #
DE92-013802 ..... p 3975 N92-33108 #
DE92-013833 ..... p 3975 N92-33123 #
DE92-013847 ..... p 4030 N92-33125 #
DE92-013861 ..... p 4085 N92-33127 #
DE92-013901 ..... p 4080 N92-33154 #
DE92-013902 ..... p 4078 N92-32624 #
DE92-013904 ..... p 4080 N92-33024 #
DE92-013917 ..... p 4077 N92-32417 #
DE92-013993 ..... p 4030 N92-33156 #
DE92-014016 ..... p 4073 N92-33179 #
DE92-014031 ..... p 4017 N92-33180 #
DE92-014032 ..... p 4036 N92-33181 #
DE92-014054 ..... p 4073 N92-33182 #
DE92-014059 ..... p 3964 N92-32931 #
DE92-014061 ..... p 4072 N92-32932 #
DE92-014084 ..... p 4006 N92-32468 #
DE92-014103 ..... p 4089 N92-32469 #
DE92-014124 ..... p 4068 N92-33083 #
DE92-014165 ..... p 4081 N92-32470 #
DE92-014166 ..... p 4015 N92-32511 #
DE92-014173 ..... p 3988 N92-32635 #
DE92-014181 ..... p 4066 N92-32702 #
DE92-014188 ..... p 4030 N92-32933 #
DE92-014195 ..... p 3943 N92-32934 #
DE92-014241 ..... p 4030 N92-32986 #
DE92-014246 ..... p 4078 N92-32592 #
DE92-014247 ..... p 4087 N92-32593 #
DE92-014311 ..... p 4078 N92-32595 #
DE92-014313 ..... p 4016 N92-32596 #
DE92-014320 ..... p 4066 N92-32597 #
DE92-014323 ..... p 4079 N92-32944 #
DE92-014325 ..... p 4078 N92-32599 #
DE92-014326 ..... p 4010 N92-32824 #
DE92-014328 ..... p 3970 N92-32471 #
DE92-014342 ..... p 4033 N92-32720 #
DE92-014349 ..... p 3960 N92-32332 #
DE92-014350 ..... p 4034 N92-32333 #
DE92-014358 ..... p 3960 N92-32334 #
DE92-014382 ..... p 3967 N92-32721 #
DE92-014383 ..... p 3968 N92-32896 #
DE92-014404 ..... p 4084 N92-32919 #
DE92-014408 ..... p 3956 N92-32945 #
DE92-014409 ..... p 4082 N92-32636 #
DE92-014415 ..... p 4066 N92-32600 #
DE92-014419 ..... p 4019 N92-32890 #
DE92-014432 ..... p 4083 N92-32653 #
DE92-014482 ..... p 4064 N92-32312 #
DE92-014483 ..... p 4073 N92-32419 #
DE92-014495 ..... p 4031 N92-33153 #
DE92-014504 ..... p 4017 N92-33155 #
DE92-014506 ..... p 4081 N92-32420 #
DE92-014507 ..... p 4088 N92-33109 #
DE92-014509 ..... p 4065 N92-32473 #
DE92-014510 ..... p 4085 N92-33111 #
DE92-014524 ..... p 3962 N92-32557 #
DE92-014616 ..... p 3974 N92-32637 #
DE92-014617 ..... p 4026 N92-32946 #
DE92-014687 ..... p 4086 N92-33136 #
DE92-014698 ..... p 4026 N92-32924 #
DE92-014775 ..... p 4012 N92-32947 #
DE92-014783 ..... p 3969 N92-33116 #
DE92-014795 ..... p 4072 N92-33122 #
DE92-014811 ..... p 4085 N92-33025 #
DE92-014813 ..... p 4013 N92-33124 #
DE92-014814 ..... p 4055 N92-32428 #
DE92-014834 ..... p 3965 N92-33126 #
DE92-014841 ..... p 3970 N92-32429 #
DE92-014862 ..... p 3992 N92-33128 #
DE92-014863 ..... p 4072 N92-33130 #
DE92-014877 ..... p 4061 N92-32430 #
DE92-014885 ..... p 3969 N92-33132 #
DE92-014896 ..... p 4073 N92-33134 #
DE92-014920 ..... p 4032 N92-32431 #
DE92-014921 ..... p 3966 N92-32432 #
DE92-014933 ..... p 3977 N92-32723 #
DE92-014941 ..... p 3968 N92-32991 #
DE92-014954 ..... p 4080 N92-32992 #
DE92-014988 ..... p 4093 N92-32993 #
DE92-015004 ..... p 4072 N92-32994 #
DE92-015007 ..... p 4080 N92-32995 #
DE92-015011 ..... p 4084 N92-32920 #
DE92-015012 ..... p 4067 N92-32921 #
DE92-015025 ..... p 4067 N92-32922 #
DE92-015035 ..... p 3975 N92-33003 #
DE92-015039 ..... p 4026 N92-32923 #
DE92-015181 ..... p 3953 N92-32638 #
DE92-015205 ..... p 4085 N92-33026 #
DE92-015266 ..... p 4081 N92-32346 #
DE92-015270 ..... p 3988 N92-32639 #
DE92-015272 ..... p 3971 N92-32640 #
DE92-015343 ..... p 3964 N92-32925 #
DE92-015355 ..... p 4082 N92-32641 #
DE92-015385 ..... p 4042 N92-32617 #
DE92-015452 ..... p 4013 N92-33140 #
DE92-015592 ..... p 3975 N92-33141 #
DE92-016003 ..... p 4070 N92-32506 #
DE92-016006 ..... p 4040 N92-32642 #
DE92-016189 ..... p 4082 N92-32561 #
DE92-016308 ..... p 3962 N92-32562 #
DE92-016309 ..... p 3962 N92-32563 #
DE92-016313 ..... p 4020 N92-32564 #
DE92-016316 ..... p 4068 N92-33067 #
DE92-016320 ..... p 4016 N92-33114 #
DE92-016351 ..... p 4069 N92-33164 #
DE92-016358 ..... p 3993 N92-33183 #
DE92-016373 ..... p 4054 N92-33184 #
DE92-016462 ..... p 4064 N92-32313 #
DE92-016545 ..... p 3965 N92-33185 #
DE92-016576 ..... p 4025 N92-32565 #
DE92-016578 ..... p 4015 N92-32335 #
DE92-016614 ..... p 3960 N92-32347 #
DE92-016622 ..... p 4035 N92-32336 #
DE92-016682 ..... p 3966 N92-33246 #
DE92-016697 ..... p 4069 N92-32314 #
DE92-016774 ..... p 4086 N92-33221 #
DE92-016778 ..... p 4082 N92-32542 #
DE92-016779 ..... p 3974 N92-33247 #
DE92-016833 ..... p 3965 N92-33222 #
DE92-016837 ..... p 4069 N92-33186 #
DE92-016840 ..... p 3966 N92-32315 #
DE92-016844 ..... p 4069 N92-33187 #
DE92-016855 ..... p 4087 N92-32566 #
DE92-016872 ..... p 4015 N92-33188 #
DE92-016897 ..... p 3969 N92-33115 #
DE92-016921 ..... p 4085 N92-33117 #
DE92-016952 ..... p 4064 N92-32316 #
DE92-016961 ..... p 4070 N92-32567 #
DE92-016963 ..... p 3970 N92-32317 #
DE92-016964 ..... p 4069 N92-32318 #
DE92-016966 ..... p 4069 N92-32319 #
DE92-016980 ..... p 4071 N92-32904 #
DE92-016996 ..... p 3964 N92-32996 #
DE92-016999 ..... p 4067 N92-32997 #
DE92-017083 ..... p 4081 N92-32320 #
DE92-017117 ..... p 4073 N92-32321 #
DE92-017138 ..... p 4006 N92-32322 #
DE92-017159 ..... p 4052 N92-32926 #
DE92-017162 ..... p 3978 N92-32927 #
DE92-017192 ..... p 4067 N92-32928 #
DE92-017245 ..... p 4060 N92-32998 #
DE92-017252 ..... p 4014 N92-32999 #
DE92-017254 ..... p 4014 N92-33000 #
DE92-017257 ..... p 4068 N92-33001 #
DE92-017258 ..... p 3964 N92-32929 #
DE92-017292 ..... p 4013 N92-33159 #
DE92-017309 ..... p 4047 N92-33118 #
DE92-017313 ..... p 4012 N92-33082 #
DE92-017342 ..... p 4090 N92-33084 #
DE92-017358 ..... p 3944 N92-33166 #
DE92-017390 ..... p 4103 N92-33119 #
DE92-017523 ..... p 3992 N92-33068 #
DE92-017528 ..... p 3969 N92-33120 #
DE92-017530 ..... p 4088 N92-33069 #
DE92-017552 ..... p 4072 N92-33070 #
DE92-017749 ..... p 4080 N92-33168 #
DE92-017802 ..... p 4020 N92-33085 #
DE92-017870 ..... p 4046 N92-33071 #
DE92-017978 ..... p 3965 N92-33121 #
DE92-526270 ..... p 3975 N92-32914 #
DE92-530733 ..... p 4027 N92-33090 #
DE92-540920 ..... p 4027 N92-33072 #
DE92-624556 ..... p 4055 N92-32602 #
DE92-624558 ..... p 4087 N92-32603 #
DE92-624689 ..... p 4087 N92-32309 #
DE92-624690 ..... p 4064 N92-32310 #
DE92-624691 ..... p 4064 N92-32311 #
DE92-624692 ..... p 4065 N92-32497 #
DE92-624727 ..... p 4065 N92-32498 #
DE92-624821 ..... p 4087 N92-32649 #
DE92-625005 ..... p 4064 N92-32340 #
DE92-625007 ..... p 4065 N92-32499 #
DE92-625008 ..... p 4065 N92-32500 #
DE92-625009 ..... p 4065 N92-32501 #
DE92-626850 ..... p 3961 N92-32475 #
DE92-782004 ..... p 3982 N92-32905 #
DE92-782106 ..... p 4079 N92-32745 #

DM-59 ..... p 4009 N92-32727 #
DM-60 ..... p 4033 N92-32758 #

DODA-AR-006-839 ..... p 3970 N92-32489 #
DODA-AR-007-052 ..... p 3935 N92-32326 #

DOE/CE-15991/5 ..... p 4089 N92-32469 #
DOE/CE-92013169 ..... p 3974 N92-32483 #

DOE/EA-0510 ..... p 4026 N92-32924 #

DOE/ER-01428/T10 ..... p 4073 N92-33182 #
DOE/ER-13422/T1 ..... p 4014 N92-32620 #
DOE/ER-13508/4 ..... p 3965 N92-33222 #
DOE/ER-13566/5 ..... p 4021 N92-32698 #
DOE/ER-13633/11 ..... p 3971 N92-32631 #
DOE/ER-13641/3 ..... p 4013 N92-33124 #
DOE/ER-13687/12 ..... p 4087 N92-32566 #
DOE/ER-13812/T1 ..... p 3960 N92-32464 #
DOE/ER-13897/13 ..... p 4087 N92-32593 #
DOE/ER-13950/T1 ..... p 4068 N92-33083 #
DOE/ER-13966/3 ..... p 3965 N92-33121 #
DOE/ER-14104/3 ..... p 4082 N92-32641 #
DOE/ER-25019/25 ..... p 4016 N92-32596 #
DOE/ER-25095/1 ..... p 4046 N92-33071 #
DOE/ER-40150/186 ..... p 4070 N92-32567 #
DOE/ER-40150/190 ..... p 3970 N92-32317 #
DOE/ER-40150/191 ..... p 4069 N92-32318 #
DOE/ER-40150/193 ..... p 4069 N92-32319 #
DOE/ER-40224/214 ..... p 4066 N92-32597 #
DOE/ER-40272/160 ..... p 4064 N92-32313 #
DOE/ER-40317/T2 ..... p 4093 N92-32993 #
DOE/ER-40388/90 ..... p 4068 N92-33067 #
DOE/ER-40425/256 ..... p 4069 N92-33186 #
DOE/ER-40452/7 ..... p 4103 N92-33119 #
DOE/ER-40608/1 ..... p 4067 N92-32921 #
DOE/ER-40637/1 ..... p 4066 N92-32600 #
DOE/ER-40646/2 ..... p 4066 N92-32702 #
DOE/ER-40672/1 ..... p 4069 N92-33187 #
DOE/ER-40685/712 ..... p 4061 N92-32430 #
DOE/ER-40692/1 ..... p 4067 N92-32922 #
DOE/ER-45179/9 ..... p 3966 N92-32315 #
DOE/ER-45182/6 ..... p 4022 N92-32911 #
DOE/ER-45191/19 ..... p 3970 N92-32471 #
DOE/ER-45199/2 ..... p 4085 N92-33025 #
DOE/ER-45254/7 ..... p 3970 N92-32429 #
DOE/ER-45267/6 ..... p 4020 N92-32564 #
DOE/ER-45332/T1 ..... p 4081 N92-32462 #
DOE/ER-53198/190 ..... p 4080 N92-33154 #
DOE/ER-53198/193 ..... p 4079 N92-32944 #
DOE/ER-53198/194 ..... p 4078 N92-32624 #
DOE/ER-53212/195 ..... p 4078 N92-32599 #
DOE/ER-53301/4 ..... p 4078 N92-32592 #
DOE/ER-54095/2 ..... p 4078 N92-32595 #
DOE/ER-54102/T1 ..... p 4077 N92-32533 #
DOE/ER-60372/7 ..... p 4033 N92-32720 #
DOE/ER-60673/T4 ..... p 4036 N92-33181 #
DOE/ER-61052/2 ..... p 4035 N92-32336 #
DOE/ER-61064/2 ..... p 4031 N92-33153 #
DOE/ER-61198/T1 ..... p 4032 N92-32331 #
DOE/ER-61219/1 ..... p 4028 N92-32619 #
DOE/ER-61373/1 ..... p 4015 N92-33188 #
DOE/ER-75527/4 ..... p 4090 N92-32985 #
DOE/ER-75602/4 ..... p 4090 N92-32930 #

DOE/MC-20422/92/C0030 ..... p 4034 N92-32333 #
DOE/MC-26039/92/C0031 ..... p 3960 N92-32334 #
DOE/MC-27115/92/C0035 ..... p 3960 N92-32332 #

DOE/NV-10031/T1 ..... p 3989 N92-32754 #

DOE/OR-00033/T479 ..... p 4077 N92-32417 #

DOE/PC-79892/T19 ..... p 3977 N92-32467 #
DOE/PC-88948/T14 ..... p 4013 N92-33140 #

DOE/PC-88948/T2 ..... p 4017 N92-33180 #
DOE/PC-89762/T14 ..... p 3960 N92-32347 #
DOE/PC-89866/T5 ..... p 3975 N92-33141 #
DOE/PC-90044/T1 ..... p 3975 N92-33108 #
DOE/PC-90049/T4 ..... p 3975 N92-33123 #
DOE/PC-90274/T14 ..... p 4080 N92-33024 #
DOE/PC-90305/T7 ..... p 3966 N92-33246 #
DOE/PC-91293/1 ..... p 4030 N92-33125 #

DOT-VNTSC-FAA-92-2 ..... p 3932 N92-32941 #

DOT/FAA/AM-92/4 ..... p 4061 N92-32697 #

DOT/FAA/CT-91/17 ..... p 3932 N92-33005 #
DOT/FAA/CT-91/28 ..... p 3938 N92-33105 #

DOT/FAA/NR-92/7 ..... p 3980 N92-32686 #

DOT/FAA/RD-92/20 ..... p 3932 N92-32606 * #
DOT/FAA/RD-92/22 ..... p 3933 N92-32537 #
DOT/FAA/RD-92/23 ..... p 3934 N92-33098 #
DOT/FAA/RD-92/2 ..... p 3932 N92-32941 #
DOT/FAA/RD-92/8 ..... p 3940 N92-32903 #

DREA-CR-89-445-PT-2-VOL-2 ..... p 3981 N92-32749 #
DREA-CR-90-425 ..... p 3931 N92-32811 #

DREO-90-18 ..... p 3982 N92-32818 #
DREO-91-23 ..... p 3978 N92-32535 #

DREP-89-9 ..... p 3955 N92-32846 #

DRIC-BR-309398 ..... p 4089 N92-32342 #

DTRC-PAS-91/55 ..... p 4008 N92-32652 #

DTRC-SME-91/74 ..... p 4022 N92-32717 #

D18:1991 ..... p 4025 N92-32605 #

E-5456 ..... p 3941 N92-32456 * #
E-6407 ..... p 3972 N92-32863 * #
E-7156 ..... p 3988 N92-32243 * #
E-7160 ..... p 3982 N92-32965 * #
E-7170 ..... p 3944 N92-33064 * #
E-7179 ..... p 3946 N92-32466 * #
E-7194 ..... p 4011 N92-32868 * #
E-7212 ..... p 4007 N92-32472 * #
E-7242 ..... p 3944 N92-32463 * #
E-7285 ..... p 3991 N92-32867 * #

ECL-91-28 ..... p 4019 N92-32801 #
ECL-91-42 ..... p 3963 N92-32722 #
ECL-91-43 ..... p 3963 N92-32724 #
ECL-91-48 ..... p 4018 N92-32737 #

EPA/DF/DK-92/040A ..... p 4030 N92-33062 #

EPA/230/R-92/003 ..... p 4030 N92-33087 #
EPA/600/A-92/102 ..... p 4028 N92-32609 #

ES/ER/TM-34-PHASE-1 ..... p 4090 N92-33084 #

ESA-SP-338 ..... p 4093 N92-32348 #

ESD-TR-91-061-VOL-1 ..... p 3980 N92-32696 #
ESD-TR-91-238 ..... p 3989 N92-32678 #
ESD-TR-91-245 ..... p 3980 N92-32680 #
ESD-TR-92-051 ..... p 4052 N92-32937 #

ESDU-AERO-C.01.01.02 ..... p 3939 N92-32487

ESDU-67016 ..... p 4010 N92-32781
ESDU-68007 ..... p 4010 N92-32781
ESDU-75003 ..... p 3945 N92-32484
ESDU-90030 ..... p 3931 N92-32782
ESDU-92002-SUPPL ..... p 3931 N92-32782
ESDU-92003-PT-1 ..... p 4010 N92-32781
ESDU-92006 ..... p 3939 N92-32780
ESDU-92007 ..... p 3939 N92-32487
ESDU-92009 ..... p 3945 N92-32486
ESDU-92010 ..... p 3945 N92-32485
ESDU-92011-PT-1 ..... p 3945 N92-32484
ESDU-92015 ..... p 3967 N92-32779
ESDU-92016 ..... p 4017 N92-32482
ESDU-92024 ..... p 3929 N92-32479

ESM-32 ..... p 4064 N92-32340 #
ESM-36 ..... p 4087 N92-32649 #
ESM-37 ..... p 4065 N92-32499 #

ETDE/JP-MF-92526270 ..... p 3975 N92-32914 #

ETN-92-91338 ..... p 4071 N92-32763 #
ETN-92-91509 ..... p 4067 N92-32764 #
ETN-92-91641 ..... p 4059 N92-33058 #
ETN-92-91663 ..... p 4051 N92-32768 #
ETN-92-91664 ..... p 3931 N92-32769 #
ETN-92-91665 ..... p 4009 N92-32770 #
ETN-92-91667 ..... p 4051 N92-32771 #
ETN-92-91670 ..... p 4057 N92-32772 #
ETN-92-91671 ..... p 3931 N92-32773 #
ETN-92-91672 ..... p 3954 N92-32792 #
ETN-92-91673 ..... p 4022 N92-32774 #
ETN-92-91674 ..... p 3954 N92-32775 #
ETN-92-91675 ..... p 4010 N92-32776 #
ETN-92-91676 ..... p 3989 N92-32777 #
ETN-92-91677 ..... p 3990 N92-32793 #
ETN-92-91678 ..... p 4036 N92-32844 #
ETN-92-91747 ..... p 4057 N92-32796 #
ETN-92-91847 ..... p 4057 N92-32756 #
ETN-92-91957 ..... p 3963 N92-32722 #
ETN-92-91958 ..... p 3963 N92-32724 #
ETN-92-91959 ..... p 4009 N92-32725 #
ETN-92-91961 ..... p 4018 N92-32726 #
ETN-92-91975 ..... p 4093 N92-32348 #
ETN-92-91976 ..... p 4009 N92-32727 #
ETN-92-91977 ..... p 4033 N92-32758 #
ETN-92-91978 ..... p 4029 N92-32785 #
ETN-92-91979 ..... p 3943 N92-32728
ETN-92-91980 ..... p 4057 N92-32729 #
ETN-92-91981 ..... p 4068 N92-33133 #
ETN-92-91982 ..... p 4068 N92-33135 #
ETN-92-91983 ..... p 4068 N92-33137 #
ETN-92-91994 ..... p 3930 N92-32730 #
ETN-92-91995 ..... p 4010 N92-32786 #
ETN-92-91996 ..... p 4023 N92-33139 * #
ETN-92-91997 ..... p 3930 N92-32732 #
ETN-92-91998 ..... p 3940 N92-32734 #
ETN-92-91999 ..... p 3939 N92-32750 #
ETN-92-92000 ..... p 3930 N92-32673 #
ETN-92-92001 ..... p 3933 N92-32830 #
ETN-92-92002 ..... p 4011 N92-32831 #
ETN-92-92003 ..... p 4043 N92-32832 #
ETN-92-92004 ..... p 4043 N92-32833 #
ETN-92-92005 ..... p 3943 N92-32834 #
ETN-92-92006 ..... p 4011 N92-32835 #
ETN-92-92008 ..... p 4008 N92-32675 #
ETN-92-92022 ..... p 4058 N92-32836 #
ETN-92-92023 ..... p 3982 N92-32837 #
ETN-92-92024 ..... p 3973 N92-33065 #
ETN-92-92035 ..... p 4060 N92-33055 #
ETN-92-92036 ..... p 4047 N92-33142 #
ETN-92-92037 ..... p 3986 N92-33143 #
ETN-92-92038 ..... p 3992 N92-33144 #
ETN-92-92039 ..... p 3992 N92-33145 #
ETN-92-92040 ..... p 4077 N92-33146 #
ETN-92-92041 ..... p 4012 N92-33066 #
ETN-92-92042 ..... p 4074 N92-32703 #
ETN-92-92043 ..... p 4074 N92-32705 #
ETN-92-92044 ..... p 3954 N92-32677 #
ETN-92-92046 ..... p 4056 N92-32679 #
ETN-92-92047 ..... p 4018 N92-32692 #
ETN-92-92048 ..... p 4083 N92-32760 #
ETN-92-92049 ..... p 4058 N92-32798 #
ETN-92-92050 ..... p 4056 N92-32707 #
ETN-92-92051 ..... p 4060 N92-32709 #
ETN-92-92052 ..... p 3972 N92-32752 #
ETN-92-92057 ..... p 4067 N92-32753 #
ETN-92-92065 ..... p 4018 N92-32757 #
ETN-92-92066 ..... p 4051 N92-32759 #
ETN-92-92067 ..... p 4056 N92-32710 #
ETN-92-92068 ..... p 4056 N92-32711 #
ETN-92-92070 ..... p 4057 N92-32713 #
ETN-92-92071 ..... p 4058 N92-32838 #
ETN-92-92072 ..... p 4060 N92-32839 #
ETN-92-92074 ..... p 4058 N92-32799 #
ETN-92-92075 ..... p 4057 N92-32761 #
ETN-92-92076 ..... p 4051 N92-32715 #
ETN-92-92077 ..... p 4060 N92-32716 #
ETN-92-92078 ..... p 4060 N92-32718 #
ETN-92-92079 ..... p 4056 N92-32684 #
ETN-92-92080 ..... p 4056 N92-32685 #
ETN-92-92081 ..... p 4009 N92-32687 #
ETN-92-92082 ..... p 3931 N92-32800 #
ETN-92-92083 ..... p 4031 N92-32889 #
ETN-92-92084 ..... p 4083 N92-32892 #
ETN-92-92085 ..... p 3972 N92-32762 #
ETN-92-92086 ..... p 4039 N92-33056 #
ETN-92-92088 ..... p 4009 N92-32765 #
ETN-92-92089 ..... p 4040 N92-32766 #
ETN-92-92090 ..... p 4066 N92-32735 #
ETN-92-92091 ..... p 4019 N92-32801 #
ETN-92-92092 ..... p 4018 N92-32737 #
ETN-92-92093 ..... p 4058 N92-32802 #
ETN-92-92094 ..... p 4058 N92-32803 #
ETN-92-92095 ..... p 3980 N92-32739 #
ETN-92-92096 ..... p 4043 N92-32804 #
ETN-92-92097 ..... p 4075 N92-32805 #
ETN-92-92098 ..... p 4075 N92-32806 #
ETN-92-92099 ..... p 3981 N92-32807 #
ETN-92-92102 ..... p 4009 N92-32767 #
ETN-92-92111 ..... p 4050 N92-32689 #
ETN-92-92117 ..... p 3954 N92-32740 #
ETN-92-92118 ..... p 3977 N92-32742 #
ETN-92-92119 ..... p 3977 N92-32690 #
ETN-92-92120 ..... p 3978 N92-32893 #
ETN-92-92121 ..... p 3968 N92-32894 #
ETN-92-92123 ..... p 3968 N92-32895 #
ETN-92-92124 ..... p 3968 N92-32897 #
ETN-92-92125 ..... p 3967 N92-32819 #
ETN-92-92130 ..... p 3982 N92-32820 #
ETN-92-92136 ..... p 4051 N92-32795 #
ETN-92-92144 ..... p 4051 N92-32821 #
ETN-92-92145 ..... p 4058 N92-32840 #
ETN-92-92147 ..... p 4079 N92-32797 #
ETN-92-92150 ..... p 4071 N92-32808 #
ETN-92-92153 ..... p 4079 N92-32822 #
ETN-92-92155 ..... p 3990 N92-32823 #
ETN-92-92156 ..... p 4011 N92-32857 #
ETN-92-92157 ..... p 4011 N92-32858 #
ETN-92-92159 ..... p 4029 N92-32841 #
ETN-92-92160 ..... p 4061 N92-32842 #
ETN-92-92161 ..... p 4090 N92-32843 #

FEI-2189 ..... p 4065 N92-32500 #

FFA-TN-1991-41 ..... p 4057 N92-32729 #

FIAS-R-215 ..... p 4065 N92-32501 #

FNAL/C-92/121-E ..... p 4070 N92-32506 #
FNAL/C-92/125 ..... p 4040 N92-32642 #
FNAL/C-92/161-E ..... p 4069 N92-33164 #
FNAL/C-92/41-A ..... p 4087 N92-32496 #
FNAL/C-92/45-E ..... p 4064 N92-32312 #

FOA-C-40292-4.3 ..... p 4029 N92-32785 #

GA-A-20870 ..... p 4078 N92-32623 #

GAO-55-636-PT-6 ..... p 4091 N92-32505 #

GAO/IMTEC-91-25 ..... p 3934 N92-32861 #

GAO/NSIAD-92-230 ..... p 4088 N92-32618 #

GDR-0917 ..... p 4031 N92-32889 #

GMU/C3I-220-R ..... p 4088 N92-32551 #

GPO-55-260-VOL-1 ..... p 4092 N92-33147 #

GRI-91/0391-PHASE-2 ..... p 4007 N92-32598 #
GRI-92/0084 ..... p 3962 N92-32594 #
GRI-92/0137 ..... p 3962 N92-32591 #

H-1675 ..... p 4042 N92-32507 * #
H-1826 ..... p 3940 N92-32864 * #
H-1835 ..... p 4007 N92-32560 * #
H-1839 ..... p 3938 N92-32866 * #
H-1857 ..... p 3935 N92-33149 * #

HAC-REF-G8200 ..... p 3980 N92-32719 #

HEL-TN-5-92 ..... p 4037 N92-32916 #

IAR-AN-71 ..... p 3955 N92-32852 #
IAR-AN-72 ..... p 3934 N92-32849 #

ICASE-92-37 ..... p 4010 N92-32784 * #
ICASE-92-38 ..... p 4059 N92-33006 * #
ICASE-92-39 ..... p 4012 N92-33110 * #

ICOMP-92-11 ..... p 4011 N92-32868 * #

IFVE-OEF-91-15 ..... p 4087 N92-32309 #
IFVE-OEF-91-37 ..... p 4064 N92-32310 #
IFVE-OEF-91-51 ..... p 4064 N92-32311 #
IFVE-OEF-91-52 ..... p 4065 N92-32497 #

IHEP-OEF-91-15 ..... p 4087 N92-32309 #

IHEP-OTF-91-116 ..... p 4065 N92-32498 #
IHEP-OTF-91-67 ..... p 4055 N92-32602 #
IHEP-OTF-91-90 ..... p 4087 N92-32603 #

IIT-B/CE/RR/92/2 ..... p 4022 N92-32783 #

IMAG-RR-839-M ..... p 4058 N92-32838 #
IMAG-RR-840-M ..... p 4060 N92-32839 #
IMAG-RR-842-M ..... p 4058 N92-32799 #
IMAG-RR-846-M ..... p 4057 N92-32761 #
IMAG-RR-848-M ..... p 4051 N92-32715 #
IMAG-RR-849-M ..... p 4056 N92-32710 #
IMAG-RR-850-I ..... p 4056 N92-32711 #
IMAG-RR-852-M ..... p 4060 N92-32716 #
IMAG-RR-856-M ..... p 4060 N92-32718 #

IMAG-RR-857-I ..... p 4057 N92-32713 #
IMAG-RR-859-I/M ..... p 4056 N92-32684 #
IMAG-RR-861-M ..... p 4056 N92-32685 #

IMI-91RT-31200-1155-G ..... p 4019 N92-33077 #

INPE-5370-TDI/469 ..... p 4093 N92-32604 #
INPE-5384-PRE/1750 ..... p 4079 N92-32662 #
INPE-5390-TAE/011 ..... p 4055 N92-32661 #
INPE-5405-RPQ/659 ..... p 4014 N92-32601 #

INT-PATENT-CLASS-A61B-5/02 . p 4015 N92-33016 *
INT-PATENT-CLASS-A61M-1/00 p 4038 N92-33032 *

INT-PATENT-CLASS-B05B-1/00 . p 4011 N92-32856
INT-PATENT-CLASS-B23K-9/24 . p 3991 N92-33030 *
INT-PATENT-CLASS-B29C-65/48 p 3978 N92-33020 *
INT-PATENT-CLASS-B64G-1/40 . p 3943 N92-33013 *
INT-PATENT-CLASS-B64G-1/66 . p 4015 N92-33010 *

INT-PATENT-CLASS-C22C-19/00 p 3968 N92-32855
INT-PATENT-CLASS-C22C-19/03 p 3968 N92-32855

INT-PATENT-CLASS-F16H-21/16 p 4019 N92-33031 *
INT-PATENT-CLASS-F16H-49/00 p 4019 N92-33031 *

INT-PATENT-CLASS-G01K-7/30 . p 3991 N92-33021 *
INT-PATENT-CLASS-G02B-27/42 p 4076 N92-33022 *
INT-PATENT-CLASS-G03B-1/16 . p 4076 N92-33022 *
INT-PATENT-CLASS-G05B-19/42 p 4054 N92-33019 *
INT-PATENT-CLASS-G06F-11/10 p 3991 N92-33011 *
INT-PATENT-CLASS-G21K-7/00 . p 4092 N92-33012 * #

INT-PATENT-CLASS-H01J-3/14 .. p 4076 N92-33028 *
INT-PATENT-CLASS-H01J-40/14 p 4076 N92-33017 *

IPF-91-3 ..... p 4079 N92-32822 #
IPF-91-5 ..... p 3990 N92-32823 #
IPF-91-6 ..... p 4071 N92-32808 #

IRF-PREPRINT-119 ..... p 4061 N92-32842 #

IS-T-1569 ..... p 3962 N92-32562 #
IS-T-1570 ..... p 4081 N92-32465 #
IS-T-1578 ..... p 4065 N92-32473 #
IS-T-1591 ..... p 4085 N92-33111 #
IS-T-1594 ..... p 3962 N92-32563 #
IS-T-1599 ..... p 4088 N92-33109 #

ISAL-91-0095 ..... p 4039 N92-33056 #
ISAL-91-0099 ..... p 4083 N92-32892 #
ISAL-92-0007 ..... p 3972 N92-32762 #

ISBN-0-16-036004-8 ..... p 4089 N92-32643 #
ISBN-0-16-038597-0 ..... p 4091 N92-32505 #
ISBN-0-16-038832-5 ..... p 4092 N92-33147 #
ISBN-0-315-49130-2 ..... p 4024 N92-33233
ISBN-0-315-50983-X ..... p 4049 N92-33230
ISBN-0-315-51158-3 ..... p 4054 N92-33218
ISBN-0-315-51189-3 ..... p 4049 N92-33215
ISBN-0-315-51346-2 ..... p 4049 N92-33227
ISBN-0-315-52925-3 ..... p 4054 N92-33203
ISBN-0-315-54272-1 ..... p 4048 N92-33214
ISBN-0-315-54378-7 ..... p 4055 N92-33219
ISBN-0-315-54380-9 ..... p 4053 N92-33217
ISBN-0-315-54414-7 ..... p 4052 N92-33216
ISBN-0-315-54684-0 ..... p 4059 N92-33231
ISBN-0-315-55106-2 ..... p 4035 N92-33198
ISBN-0-315-55158-5 ..... p 4088 N92-33199
ISBN-0-315-55748-6 ..... p 4077 N92-33202
ISBN-0-315-56074-6 ..... p 4048 N92-33201
ISBN-0-315-56107-6 ..... p 4053 N92-33224
ISBN-0-315-56113-0 ..... p 4049 N92-33232
ISBN-0-315-57159-4 ..... p 4034 N92-33225
ISBN-0-315-57208-6 ..... p 4053 N92-33235
ISBN-0-315-57231-0 ..... p 4048 N92-33204
ISBN-0-315-57272-8 ..... p 4049 N92-33229
ISBN-0-315-57756-8 ..... p 4023 N92-33200
ISBN-0-315-57834-3 ..... p 4024 N92-33228
ISBN-0-315-57864-5 ..... p 4048 N92-33210
ISBN-0-315-58015-1 ..... p 4080 N92-33223
ISBN-0-315-58989-2 ..... p 4047 N92-33189
ISBN-0-315-58991-4 ..... p 3987 N92-33209
ISBN-0-315-59028-9 ..... p 3987 N92-33206
ISBN-0-315-59030-0 ..... p 4055 N92-33236
ISBN-0-315-59034-3 ..... p 3993 N92-33211
ISBN-0-315-59091-2 ..... p 4032 N92-33197
ISBN-0-315-60456-5 ..... p 3993 N92-33208
ISBN-0-315-60464-6 ..... p 3987 N92-33207
ISBN-0-315-60747-5 ..... p 3993 N92-33195
ISBN-0-315-61378-5 ..... p 3987 N92-33213
ISBN-0-315-62369-1 ..... p 4013 N92-33226
ISBN-0-315-63272-0 ..... p 3993 N92-33193
ISBN-0-315-63282-8 ..... p 3987 N92-33192
ISBN-0-315-63332-8 ..... p 3986 N92-33191
ISBN-0-315-63509-6 ..... p 4048 N92-33212
ISBN-0-315-65025-7 ..... p 3994 N92-33234
ISBN-0-85679-807-X ..... p 3931 N92-32782
ISBN-0-85679-808-8 ..... p 4010 N92-32781
ISBN-0-85679-811-8 ..... p 3939 N92-32780
ISBN-0-85679-812-6 ..... p 3939 N92-32487
ISBN-0-85679-814-2 ..... p 3945 N92-32486
ISBN-0-85679-815-0 ..... p 3945 N92-32485
ISBN-0-85679-816-9 ..... p 3945 N92-32484
ISBN-0-85679-820-7 ..... p 4017 N92-32482
ISBN-0-85679-823-1 ..... p 3967 N92-32779
ISBN-0-85679-829-0 ..... p 3929 N92-32479
ISBN-0-87703-343-9 ..... p 4039 N92-33099
ISBN-90-6275-635-2 ..... p 4060 N92-33055 #
ISBN-90-72125-29-0 ..... p 4047 N92-33142 #
ISBN-90-9003729-2 ..... p 4056 N92-32679 #
ISBN-90-9003765-9 ..... p 4058 N92-32836 #
ISBN-90-9003883-3 ..... p 3992 N92-33144 #
ISBN-90-9003887-6 ..... p 4077 N92-33146 #
ISBN-90-9003899-X ..... p 3992 N92-33145 #
ISBN-90-9004118-4 ..... p 4074 N92-32703 #
ISBN-90-9004146-X ..... p 4074 N92-32705 #
ISBN-90-9004317-9 ..... p 4012 N92-33066 #
ISBN-90-9004420-5 ..... p 3986 N92-33143 #
ISBN-90-9004476-0 ..... p 4018 N92-32692 #
ISBN-90-9004491-4 ..... p 3982 N92-32837 #
ISBN-90-9004656-9 ..... p 3954 N92-32677 #
ISBN-90-9004680-1 ..... p 4056 N92-32707 #
ISBN-91-540-5369-2 ..... p 4025 N92-32605 #
ISBN-91-540-5417-6 ..... p 3977 N92-32825 #
ISBN-92-835-0658-8 ..... p 3935 N92-32437 #
ISBN-92-835-0666-9 ..... p 3956 N92-33033 #
ISBN-92-835-0679-0 ..... p 3975 N92-33240 #
ISBN-92-9092-194-3 ..... p 4093 N92-32348 #
ISBN-951-22-0900-4 ..... p 3973 N92-33059 #
ISBN-951-47-4472-1 ..... p 4027 N92-33072 #
ISBN-9651-38-3803-X ..... p 4090 N92-32843 #

ITN-92-85165 ..... p 4086 N92-33190

JPRS-UMS-92-011 ..... p 3969 N92-33129 #

KBSI-IICE-90-STR-01-0592-01 ..... p 4042 N92-32658 #
KBSI-IICE-90-STR-01-0592-02 ..... p 4042 N92-32627 #

KFK-4948-PT-1 ..... p 4011 N92-32857 #
KFK-4949-PT-2 ..... p 4011 N92-32858 #
KFK-4975 ..... p 4029 N92-32841 #

KTM/E-B-105 ..... p 4027 N92-33072 #

L-16832-PT-1 ..... p 3946 N92-32513 * #
L-16832-PT-2 ..... p 3950 N92-32574 * #
L-16879 ..... p 4031 N92-33097 * #
L-17095 ..... p 3929 N92-32480 * #

LA-UR-92-1261 ..... p 4041 N92-32414 #
LA-UR-92-1495 ..... p 4085 N92-33026 #
LA-UR-92-1853 ..... p 4088 N92-33069 #
LA-UR-92-1870 ..... p 3969 N92-33120 #
LA-UR-92-1915 ..... p 3992 N92-33068 #
LA-UR-92-479 ..... p 4016 N92-32736 #
LA-UR-92-693 ..... p 4075 N92-32738 #
LA-UR-92-905 ..... p 4070 N92-32647 #
LA-UR-92-958 ..... p 4040 N92-32910 #
LA-UR-92-978 ..... p 4025 N92-32695 #

LA-11804-MS ..... p 3943 N92-32934 #
LA-12258 ..... p 4059 N92-32481 #
LA-12260-MS ..... p 4027 N92-32415 #
LA-12303-MS ..... p 4013 N92-33159 #

LAAS-90027 ..... p 3990 N92-32793 #
LAAS-90028 ..... p 3989 N92-32777 #
LAAS-91445 ..... p 4036 N92-32844 #
LAAS-92011 ..... p 4040 N92-32766 #
LAAS-92118 ..... p 4066 N92-32735 #

LALP-92-51 ..... p 4104 N92-32862 #

LBL-30464 ..... p 4073 N92-32321 #
LBL-30990 ..... p 4083 N92-32693 #
LBL-31124 ..... p 4081 N92-32420 #
LBL-31456 ..... p 4082 N92-32493 #
LBL-31532 ..... p 4073 N92-32419 #
LBL-31576 ..... p 3963 N92-32666 #
LBL-31741 ..... p 4067 N92-32997 #
LBL-31865 ..... p 4081 N92-32320 #
LBL-31886 ..... p 4064 N92-32312 #
LBL-31931 ..... p 3993 N92-33183 #
LBL-31969 ..... p 4017 N92-33155 #
LBL-32020 ..... p 3964 N92-32996 #
LBL-32253 ..... p 4085 N92-33117 #

LTR-91-013 ..... p 4029 N92-32860 #

M-276-REV-1 ..... p 4043 N92-32741 #
M-693-PT-1 ..... p 4000 N92-32278 * #
M-693-PT-2 ..... p 3994 N92-32245 * #

MBB-UO-0172-90-PUB ..... p 4050 N92-32689 #

MBB-Z-0391-91-PUB ..... p 3954 N92-32740 #
MBB-Z-0399-91-PUB ..... p 3977 N92-32742 #
MBB-Z-0402-91-PUB ..... p 3977 N92-32690 #
MBB-Z-0403-91-PUB ..... p 3978 N92-32893 #
MBB-Z-0404-91-PUB ..... p 3968 N92-32894 #
MBB-Z-0406-91-PUB ..... p 3968 N92-32895 #
MBB-Z-0407-91-PUB ..... p 3968 N92-32897 #
MBB-Z-0408-91-PUB ..... p 3967 N92-32819 #

MEMO-990 ..... p 4057 N92-32796 #

MHD-ITC-91-039 ..... p 4080 N92-33024 #

MLM-3746 ..... p 3967 N92-32721 #
MLM-3747 ..... p 3968 N92-32896 #

MRAD-TD-2271 ..... p 4035 N92-32688 #

MRL-TN-596 ..... p 3970 N92-32489 #

MTL-TR-92-38 ..... p 4084 N92-32939 #

MTR-11282 ..... p 4052 N92-32937 #

NAE-CR-2 ..... p 3955 N92-32813 #

NAS 1.15:102851 ..... p 3929 N92-32422 * #
NAS 1.15:103597 ..... p 4092 N92-32478 * #
NAS 1.15:103598 ..... p 4036 N92-33103 * #
NAS 1.15:103839 ..... p 3938 N92-32452 * #
NAS 1.15:103866 ..... p 3935 N92-32887 * #
NAS 1.15:103880 ..... p 3933 N92-33194 * #
NAS 1.15:103902 ..... p 4105 N92-33106 * #
NAS 1.15:103907 ..... p 4052 N92-32886 * #
NAS 1.15:103910 ..... p 3939 N92-32788 * #
NAS 1.15:103911 ..... p 4012 N92-33113 * #
NAS 1.15:103917 ..... p 4007 N92-32474 * #
NAS 1.15:103930 ..... p 3933 N92-32424 * #
NAS 1.15:103940 ..... p 4040 N92-32809 * #
NAS 1.15:103952 ..... p 3970 N92-32476 * #
NAS 1.15:103959 ..... p 3933 N92-33080 * #
NAS 1.15:104170 ..... p 4063 N92-33160 * #
NAS 1.15:104237 ..... p 4042 N92-32507 * #
NAS 1.15:104251 ..... p 3938 N92-32866 * #
NAS 1.15:104255 ..... p 3940 N92-32864 * #
NAS 1.15:104256 ..... p 3935 N92-33149 * #
NAS 1.15:104531 ..... p 3972 N92-32863 * #
NAS 1.15:105751 ..... p 3988 N92-32243 * #
NAS 1.15:105752 ..... p 3982 N92-32965 * #
NAS 1.15:105758 ..... p 3944 N92-33064 * #
NAS 1.15:105762 ..... p 3946 N92-32466 * #
NAS 1.15:105768 ..... p 4011 N92-32868 * #
NAS 1.15:105811 ..... p 3944 N92-32463 * #
NAS 1.15:105842 ..... p 3991 N92-32867 * #
NAS 1.15:105853 ..... p 4007 N92-32472 * #
NAS 1.15:107547 ..... p 3941 N92-32454 * #
NAS 1.15:107591 ..... p 4023 N92-33104 * #
NAS 1.15:107600 ..... p 3934 N92-32536 * #
NAS 1.15:107640 ..... p 4021 N92-32423 * #
NAS 1.15:107656 ..... p 3944 N92-33112 * #
NAS 1.15:107659 ..... p 4021 N92-32657 * #
NAS 1.15:107680 ..... p 4041 N92-33205 * #
NAS 1.15:107964 ..... p 4044 N92-32869 * #
NAS 1.15:107981 ..... p 3942 N92-32421 * #
NAS 1.15:107986 ..... p 3941 N92-33007 * #
NAS 1.15:108171 ..... p 4091 N92-33237 * #
NAS 1.26:181954 ..... p 3939 N92-32778 * #
NAS 1.26:183208 ..... p 3942 N92-32610 * #
NAS 1.26:184340 ..... p 4092 N92-33094 * #
NAS 1.26:186023 ..... p 4007 N92-32560 * #
NAS 1.26:189632-VOL-1 ..... p 4052 N92-33100 * #
NAS 1.26:189632-VOL-2 ..... p 4052 N92-33101 * #
NAS 1.26:189690 ..... p 4010 N92-32784 * #
NAS 1.26:189692 ..... p 4012 N92-33110 * #
NAS 1.26:189693 ..... p 4059 N92-33006 * #
NAS 1.26:190070 ..... p 4046 N92-33091 * #
NAS 1.26:190239 ..... p 4046 N92-33092 * #
NAS 1.26:190388 ..... p 4047 N92-33093 * #
NAS 1.26:190563 ..... p 3930 N92-32648 * #
NAS 1.26:190573 ..... p 3946 N92-32491 * #
NAS 1.26:190579 ..... p 4024 N92-32590 * #
NAS 1.26:190583 ..... p 3930 N92-32494 * #
NAS 1.26:190607 ..... p 4047 N92-33131 * #
NAS 1.26:190610 ..... p 3979 N92-32559 * #
NAS 1.26:190611 ..... p 4076 N92-33074 * #
NAS 1.26:190627 ..... p 3942 N92-32244 * #
NAS 1.26:190629 ..... p 4091 N92-33178 * #
NAS 1.26:190640 ..... p 4090 N92-32654 * #
NAS 1.26:190644 ..... p 4091 N92-33096 * #
NAS 1.26:190647 ..... p 4019 N92-32885 * #
NAS 1.26:190659 ..... p 3959 N92-33075 * #

NAS 1.26:190679 ..... p 4020 N92-32436 * #
NAS 1.26:190693 ..... p 4037 N92-32539 * #
NAS 1.26:190697 ..... p 4093 N92-32541 * #
NAS 1.26:190702 ..... p 3932 N92-33063 * #
NAS 1.26:190710 ..... p 4042 N92-32656 * #
NAS 1.26:190712 ..... p 4043 N92-32865 * #
NAS 1.26:190713 ..... p 4041 N92-32451 * #
NAS 1.26:190732 ..... p 3942 N92-32477 * #
NAS 1.26:190736 ..... p 3940 N92-33107 * #
NAS 1.26:190745 ..... p 4058 N92-32888 * #
NAS 1.26:190814 ..... p 4020 N92-32425 * #
NAS 1.26:190816 ..... p 3969 N92-33081 * #
NAS 1.26:190822 ..... p 4023 N92-33139 * #
NAS 1.26:190826 ..... p 4047 N92-33196 * #
NAS 1.26:4452 ..... p 4077 N92-33239 * #
NAS 1.26:4456 ..... p 3932 N92-32606 * #
NAS 1.55:10103 ..... p 4061 N92-32948 * #
NAS 1.55:3087-PT-1 ..... p 3946 N92-32513 * #
NAS 1.55:3087-PT-2 ..... p 3950 N92-32574 * #
NAS 1.55:3163-PT-1 ..... p 4000 N92-32278 * #
NAS 1.55:3163-PT-2 ..... p 3994 N92-32245 * #
NAS 1.60:3261 ..... p 3929 N92-32480 * #
NAS 1.60:3272-PT-1A ..... p 4031 N92-32655 * #
NAS 1.61:1253 ..... p 3941 N92-32456 * #
NAS 1.61:1275 ..... p 4031 N92-33097 * #

NASA-CASE-GSC-13306-1 ..... p 4038 N92-33032 *

NASA-CASE-LAR-13780-1 ..... p 3943 N92-33013 *
NASA-CASE-LAR-14001-1 ..... p 3973 N92-33008 *
NASA-CASE-LAR-14088-1-CU ..... p 4015 N92-33016 *
NASA-CASE-LAR-14163-1 ..... p 3973 N92-33014 *
NASA-CASE-LAR-14351-1 ..... p 3973 N92-33015 *
NASA-CASE-LAR-14402-1-CU ..... p 4076 N92-33017 *
NASA-CASE-LAR-14446-1 ..... p 3978 N92-33020 *
NASA-CASE-LAR-14515-1-CU ..... p 4019 N92-33031 *
NASA-CASE-LAR-14567-1-CU ..... p 3991 N92-33021 *

NASA-CASE-MFS-28013-4 ..... p 4092 N92-33012 * #
NASA-CASE-MFS-28425-1 ..... p 4015 N92-33010 *
NASA-CASE-MFS-29766-1 ..... p 3991 N92-33030 *

NASA-CASE-MSC-21463-1 ..... p 4019 N92-33018 *
NASA-CASE-MSC-21487-1 ..... p 3965 N92-33009 *
NASA-CASE-MSC-21584-1 ..... p 3965 N92-33029 *

NASA-CASE-NPO-17852-1-CU ..... p 4054 N92-33019 *
NASA-CASE-NPO-17897-1-CU ..... p 3991 N92-33011 *
NASA-CASE-NPO-17997-1-CU ..... p 4041 N92-33057 *
NASA-CASE-NPO-18098-1-CU ..... p 4076 N92-33028 *
NASA-CASE-NPO-18379-1-CU ..... p 4076 N92-33022 *

NASA-CP-10103 ..... p 4061 N92-32948 * #
NASA-CP-3087-PT-1 ..... p 3946 N92-32513 * #
NASA-CP-3087-PT-2 ..... p 3950 N92-32574 * #
NASA-CP-3163-PT-1 ..... p 4000 N92-32278 * #
NASA-CP-3163-PT-2 ..... p 3994 N92-32245 * #

NASA-CR-181954 ..... p 3939 N92-32778 * #
NASA-CR-183208 ..... p 3942 N92-32610 * #
NASA-CR-184340 ..... p 4092 N92-33094 * #
NASA-CR-186023 ..... p 4007 N92-32560 * #
NASA-CR-189632-VOL-1 ..... p 4052 N92-33100 * #
NASA-CR-189632-VOL-2 ..... p 4052 N92-33101 * #
NASA-CR-189690 ..... p 4010 N92-32784 * #
NASA-CR-189692 ..... p 4012 N92-33110 * #
NASA-CR-189693 ..... p 4059 N92-33006 * #
NASA-CR-190070 ..... p 4046 N92-33091 * #
NASA-CR-190239 ..... p 4046 N92-33092 * #
NASA-CR-190388 ..... p 4047 N92-33093 * #
NASA-CR-190563 ..... p 3930 N92-32648 * #
NASA-CR-190573 ..... p 3946 N92-32491 * #
NASA-CR-190579 ..... p 4024 N92-32590 * #
NASA-CR-190583 ..... p 3930 N92-32494 * #
NASA-CR-190607 ..... p 4047 N92-33131 * #
NASA-CR-190610 ..... p 3979 N92-32559 * #
NASA-CR-190611 ..... p 4076 N92-33074 * #
NASA-CR-190627 ..... p 3942 N92-32244 * #
NASA-CR-190629 ..... p 4091 N92-33178 * #
NASA-CR-190640 ..... p 4090 N92-32654 * #
NASA-CR-190644 ..... p 4091 N92-33096 * #
NASA-CR-190647 ..... p 4019 N92-32885 * #
NASA-CR-190659 ..... p 3959 N92-33075 * #
NASA-CR-190679 ..... p 4020 N92-32436 * #
NASA-CR-190693 ..... p 4037 N92-32539 * #
NASA-CR-190697 ..... p 4093 N92-32541 * #
NASA-CR-190702 ..... p 3932 N92-33063 * #
NASA-CR-190710 ..... p 4042 N92-32656 * #
NASA-CR-190712 ..... p 4043 N92-32865 * #
NASA-CR-190713 ..... p 4041 N92-32451 * #
NASA-CR-190732 ..... p 3942 N92-32477 * #
NASA-CR-190736 ..... p 3940 N92-33107 * #
NASA-CR-190745 ..... p 4058 N92-32888 * #
NASA-CR-190814 ..... p 4020 N92-32425 * #
NASA-CR-190816 ..... p 3969 N92-33081 * #
NASA-CR-190822 ..... p 4023 N92-33139 * #

NASA-CR-190826 ..... p 4047 N92-33196 * #
NASA-CR-4452 ..... p 4077 N92-33239 * #
NASA-CR-4456 ..... p 3932 N92-32606 * #

NASA-RP-1253 ..... p 3941 N92-32456 * #
NASA-RP-1275 ..... p 4031 N92-33097 * #

NASA-TM-102851 ..... p 3929 N92-32422 * #
NASA-TM-103597 ..... p 4092 N92-32478 * #
NASA-TM-103598 ..... p 4036 N92-33103 * #
NASA-TM-103839 ..... p 3938 N92-32452 * #
NASA-TM-103866 ..... p 3935 N92-32887 * #
NASA-TM-103880 ..... p 3933 N92-33194 * #
NASA-TM-103902 ..... p 4105 N92-33106 * #
NASA-TM-103907 ..... p 4052 N92-32886 * #
NASA-TM-103910 ..... p 3939 N92-32788 * #
NASA-TM-103911 ..... p 4012 N92-33113 * #
NASA-TM-103917 ..... p 4007 N92-32474 * #
NASA-TM-103930 ..... p 3933 N92-32424 * #
NASA-TM-103940 ..... p 4040 N92-32809 * #
NASA-TM-103952 ..... p 3970 N92-32476 * #
NASA-TM-103959 ..... p 3933 N92-33080 * #
NASA-TM-104170 ..... p 4063 N92-33160 * #
NASA-TM-104237 ..... p 4042 N92-32507 * #
NASA-TM-104251 ..... p 3938 N92-32866 * #
NASA-TM-104255 ..... p 3940 N92-32864 * #
NASA-TM-104256 ..... p 3935 N92-33149 * #
NASA-TM-104531 ..... p 3972 N92-32863 * #
NASA-TM-105751 ..... p 3988 N92-32243 * #
NASA-TM-105752 ..... p 3982 N92-32965 * #
NASA-TM-105758 ..... p 3944 N92-33064 * #
NASA-TM-105762 ..... p 3946 N92-32466 * #
NASA-TM-105768 ..... p 4011 N92-32868 * #
NASA-TM-105811 ..... p 3944 N92-32463 * #
NASA-TM-105842 ..... p 3991 N92-32867 * #
NASA-TM-105853 ..... p 4007 N92-32472 * #
NASA-TM-107547 ..... p 3941 N92-32454 * #
NASA-TM-107591 ..... p 4023 N92-33104 * #
NASA-TM-107600 ..... p 3934 N92-32536 * #
NASA-TM-107640 ..... p 4021 N92-32423 * #
NASA-TM-107656 ..... p 3944 N92-33112 * #
NASA-TM-107659 ..... p 4021 N92-32657 * #
NASA-TM-107680 ..... p 4041 N92-33205 * #
NASA-TM-107964 ..... p 4044 N92-32869 * #
NASA-TM-107981 ..... p 3942 N92-32421 * #
NASA-TM-107986 ..... p 3941 N92-33007 * #
NASA-TM-108171 ..... p 4091 N92-33237 * #

NASA-TP-3261 ..... p 3929 N92-32480 * #
NASA-TP-3272-PT-1A ..... p 4031 N92-32655 * #

NAVSWC-TR-91-324 ..... p 4084 N92-32938 #

NAVY-CASE-72926 ..... p 4074 N92-32634 #
NAVY-CASE-73545 ..... p 3963 N92-32755 #
NAVY-CASE-73767 ..... p 4026 N92-32943 #

NCAR/TN-372+STR ..... p 4028 N92-32554 #

NCS-TIB-91-11 ..... p 4074 N92-32613 #

NDP-042 ..... p 4032 N92-32431 #

NHRC-91-27 ..... p 4037 N92-32942 #

NIFS-103 ..... p 3982 N92-32905 #
NIFS-117 ..... p 4079 N92-32745 #
NIFS-119 ..... p 4078 N92-32552 #
NIFS-122 ..... p 4070 N92-32746 #

NIST/GCR-92/602 ..... p 3963 N92-32607 #

NIST/SP-810-ED-1992 ..... p 3941 N92-33002 #

NIST/TN-1348 ..... p 3991 N92-33061 #
NIST/TN-1353 ..... p 4016 N92-33060 #

NLR-TP-91046-U ..... p 3930 N92-32730 #
NLR-TP-91051-U ..... p 4010 N92-32786 #
NLR-TP-91052-U ..... p 4023 N92-33139 * #
NLR-TP-91117-U ..... p 3930 N92-32732 #
NLR-TP-91119-U ..... p 3940 N92-32734 #
NLR-TP-91134-U ..... p 3939 N92-32750 #
NLR-TP-91154-U ..... p 3930 N92-32673 #
NLR-TP-91156-U ..... p 3933 N92-32830 #
NLR-TP-91185-U ..... p 4011 N92-32831 #
NLR-TP-91193-U ..... p 4043 N92-32832 #
NLR-TP-91196-U ..... p 4043 N92-32833 #
NLR-TP-91219-U ..... p 3943 N92-32834 #
NLR-TP-91250-U ..... p 4011 N92-32835 #
NLR-TP-91401-U ..... p 4008 N92-32675 #

NOAA-TM-ERL-WPL-220 ..... p 4033 N92-32714 #

NOAA-TM-NWS-NSSFC-33 ..... p 4033 N92-32545 #
NOAA-TM-NWS-NSSFC-34 ..... p 4033 N92-32502 #

NOAA-TM-NWS-WR-217 ..... p 4034 N92-33163 #

NOSC/TR-1492 ..... p 4035 N92-33220 #

NPSCS-92-003 ..... p 4053 N92-32748 #

NRAD-TR-1480 ..... p 4015 N92-32329 #

NRC-LTR-ST-1817 ..... p 4022 N92-32848 #
NRC-LTR-ST-1826 ..... p 3954 N92-32791 #
NRC-LTR-ST-1831 ..... p 4023 N92-33076 #
NRC-LTR-ST-1833 ..... p 3959 N92-33078 #

NRC-30833 ..... p 3955 N92-32813 #
NRC-32139 ..... p 3938 N92-32850 #
NRC-32146 ..... p 4040 N92-32851 #
NRC-32147 ..... p 3955 N92-32852 #
NRC-32148 ..... p 3934 N92-32849 #

NREL/TP-253-4275 ..... p 4026 N92-32908 #
NREL/TP-253-4279 ..... p 4026 N92-32909 #
NREL/TP-253-4471 ..... p 4027 N92-33138 #
NREL/TP-413-4791 ..... p 4024 N92-32510 #

NRL-TR-1 ..... p 4082 N92-32512 #

NRL/FR/5521-91-9366 ..... p 3979 N92-32570 #

NRL/MR/6505-92-6939 ..... p 4074 N92-32613 #

NSF/ISI-87031-PHASE-1 ..... p 4076 N92-33004 #

NSWCCR/RDTN-92/0003 ..... p 4013 N92-32343 #

NTIA-92-284 ..... p 3979 N92-32555 #

NTSB/AAR-92/01 ..... p 3932 N92-32455 #

NUSC-TR-7064 ..... p 4059 N92-32989 #

OEFZS-4579 ..... p 4071 N92-32763 #

ONERA-RF-22/3419-AY-122A ..... p 4057 N92-32772 #

ONERA-RSF-24/1408-AY-150A .. p 3931 N92-32773 #

ONERA-RT-13/7256-RY-006-R ... p 3954 N92-32792 #
ONERA-RT-25/3542-RY-006-R ... p 4022 N92-32774 #
ONERA-RT-26/3542-RY-007-R ... p 3954 N92-32775 #
ONERA-RT-44/1621-RY-016-R ... p 4010 N92-32776 #
ONERA-RT-47/1147-AY-146A-PT-3p 3931 N92-32800 #

ORNL/CDIAC-50 ..... p 4032 N92-32431 #

ORNL/ER-47 ..... p 4028 N92-32616 #

ORNL/SUB-86-17498/1 ..... p 3977 N92-32723 #

ORNL/TM-11887 ..... p 3968 N92-32991 #
ORNL/TM-11946 ..... p 3966 N92-32432 #
ORNL/TM-12011 ..... p 4006 N92-32468 #
ORNL/TM-12059 ..... p 4055 N92-32428 #

ORNL/TR-91/33 ..... p 3962 N92-32557 #

OSU-725311-1 ..... p 4058 N92-32888 * #

OUEL-1917/92 ..... p 4018 N92-32757 #
OUEL-1926/92 ..... p 4051 N92-32759 #

PASC002-01-00 ..... p 3953 N92-32629 #

PB92-147198 ..... p 4089 N92-32643 #
PB92-164979 ..... p 4028 N92-32543 #
PB92-169523 ..... p 4030 N92-33062 #
PB92-177849 ..... p 4033 N92-32714 #
PB92-178821 ..... p 4025 N92-32608 #
PB92-179407 ..... p 4033 N92-32503 #
PB92-179456 ..... p 4090 N92-32712 #
PB92-180215 ..... p 4028 N92-32609 #
PB92-180710 ..... p 3973 N92-33059 #
PB92-180843 ..... p 4025 N92-32605 #
PB92-180892 ..... p 3977 N92-32825 #
PB92-181049 ..... p 3963 N92-32607 #
PB92-183219 ..... p 4104 N92-33086 #
PB92-185164 ..... p 4029 N92-32708 #
PB92-185982 ..... p 4033 N92-32545 #
PB92-186063 ..... p 4033 N92-32502 #
PB92-188259 ..... p 4076 N92-33004 #
PB92-189547 ..... p 4016 N92-33060 #
PB92-189554 ..... p 3991 N92-33061 #
PB92-190362 ..... p 4007 N92-32598 #
PB92-190370 ..... p 3962 N92-32594 #
PB92-190420 ..... p 3962 N92-32591 #
PB92-192848 ..... p 3979 N92-32555 #
PB92-193259 ..... p 4028 N92-32554 #

PB92-196104 ..... p 4034 N92-33163 #
PB92-197334 ..... p 3929 N92-33176 #
PB92-201094 ..... p 3941 N92-33002 #
PB92-201144 ..... p 4030 N92-33087 #
PB92-204627 ..... p 4091 N92-33088 #
PB92-205137 ..... p 4034 N92-33173 #
PB92-910401 ..... p 3932 N92-32455 #

PL-TR-91-2113 ..... p 4031 N92-32572 #
PL-TR-91-2200 ..... p 3978 N92-32458 #
PL-TR-91-2242 ..... p 4029 N92-32860 #
PL-TR-91-2253 ..... p 4034 N92-32859 #

PNL-8015 ..... p 4030 N92-33156 #
PNL-8086 ..... p 4030 N92-32986 #

RAL-91-085 ..... p 4068 N92-33133 #
RAL-92-012 ..... p 4068 N92-33135 #
RAL-92-015-PREPRINT ..... p 4068 N92-33137 #

REPT-91-97 ..... p 4057 N92-32756 #
REPT-92B00100 ..... p 4031 N92-32655 * #

RL-TR-91-406 ..... p 4089 N92-32611 #

RPC-TR-1276-102-G-AR ..... p 4076 N92-33074 * #

RS-30 ..... p 4092 N92-33094 * #

RSRE-92004 ..... p 4089 N92-32342 #

SAND-90-1439 ..... p 3944 N92-33166 #
SAND-91-1704C ..... p 4018 N92-32701 #
SAND-91-2203 ..... p 4025 N92-32549 #
SAND-91-2343 ..... p 4032 N92-32427 #
SAND-91-2495-VOL-1 ..... p 3981 N92-32744 #
SAND-91-2506C ..... p 4080 N92-32995 #
SAND-91-2664 ..... p 3934 N92-32308 #
SAND-91-2789C ..... p 4026 N92-32923 #
SAND-91-7016 ..... p 4025 N92-32565 #
SAND-92-0081C ..... p 3974 N92-32637 #
SAND-92-0128C ..... p 4084 N92-32920 #
SAND-92-0385 ..... p 4027 N92-33150 #
SAND-92-0397 ..... p 4042 N92-32617 #
SAND-92-0662C ..... p 3943 N92-32704 #
SAND-92-0680C ..... p 4026 N92-32946 #
SAND-92-0770C ..... p 4072 N92-32994 #
SAND-92-0959C ..... p 4028 N92-32558 #
SAND-92-1130C ..... p 3975 N92-33003 #
SAND-92-1230C ..... p 4080 N92-32992 #
SAND-92-7065 ..... p 4015 N92-32335 #

SAO-AXAF-FR-92-004 ..... p 4092 N92-33094 * #

SEL-91-006 ..... p 4044 N92-32869 * #

SER-A-23 ..... p 4025 N92-32608 #

SLAC-PUB-5718 ..... p 4069 N92-32337 #
SLAC-PUB-5720 ..... p 4069 N92-33148 #
SLAC-PUB-5748 ..... p 4072 N92-33070 #
SLAC-PUB-5782 ..... p 4071 N92-32751 #

SSCL-PREPRINT-105 ..... p 4060 N92-32998 #
SSCL-PREPRINT-84 ..... p 4073 N92-33134 #

SSD-TR-92-05 ..... p 4074 N92-32672 #
SSD-TR-92-07 ..... p 4031 N92-32902 #
SSD-TR-92-09 ..... p 3982 N92-32891 #

STSOC-RT-001283 ..... p 3942 N92-32610 * #

SU-SLAC-PUB-5745 ..... p 4065 N92-32426 #

TELECOM-91-D-007 ..... p 4058 N92-32802 #
TELECOM-91-D-008 ..... p 4058 N92-32803 #
TELECOM-91-E-005 ..... p 3980 N92-32739 #
TELECOM-91-E-008 ..... p 4043 N92-32804 #
TELECOM-91-E-013 ..... p 4075 N92-32805 #
TELECOM-91-E-016 ..... p 4075 N92-32806 #
TELECOM-91-E-018 ..... p 3981 N92-32807 #

TR-0091(6940-05)-2 ..... p 4031 N92-32902 #
TR-0091(6940-09)-2 ..... p 4074 N92-32672 #
TR-128 ..... p 3964 N92-32826 #
TR-1 ..... p 3971 N92-32490 #
TR-24 ..... p 4066 N92-32548 #
TR-29 ..... p 3971 N92-32547 #
TR-2 ..... p 3972 N92-32667 #
TR-31 ..... p 4066 N92-32556 #
TR-32 ..... p 3961 N92-32509 #
TR-33 ..... p 4084 N92-32898 #
TR-4 ..... p 3971 N92-32550 #
TR-53 ..... p 3990 N92-32827 #
TR-7 ..... p 4066 N92-32682 #
TR-91-1246 ..... p 4042 N92-32546 #

TR-91/ONR-34 ..... p 4038 N92-32569 #
TR-92(2930)-3 ..... p 3982 N92-32891 #
TR-9 ..... p 4064 N92-32418 #

TR92-1298 ..... p 4020 N92-32436 * #

TTC-2459-R ..... p 4016 N92-33089 #

TUM-M9105 ..... p 4009 N92-32767 #

UCRL-CR-109223 ..... p 4057 N92-32743 #

UCRL-ID-109125 ..... p 4006 N92-32322 #
UCRL-ID-110176 ..... p 4030 N92-32933 #
UCRL-ID-110240 ..... p 4041 N92-32416 #

UCRL-JC-105233 ..... p 3946 N92-32327 #
UCRL-JC-107065 ..... p 3969 N92-33132 #
UCRL-JC-107386 ..... p 4079 N92-32733 #
UCRL-JC-107883 ..... p 4020 N92-32328 #
UCRL-JC-108341 ..... p 4012 N92-32947 #
UCRL-JC-108512 ..... p 4070 N92-32413 #
UCRL-JC-108513 ..... p 4072 N92-33122 #
UCRL-JC-109024 ..... p 3966 N92-32646 #
UCRL-JC-109055 ..... p 3961 N92-32544 #
UCRL-JC-109601 ..... p 4050 N92-32412 #
UCRL-JC-109750 ..... p 4014 N92-32999 #
UCRL-JC-110177 ..... p 3969 N92-33116 #
UCRL-JC-110489 ..... p 3964 N92-32929 #
UCRL-JC-110555 ..... p 4012 N92-33082 #
UCRL-JC-110753 ..... p 4014 N92-33000 #
UCRL-JC-110792 ..... p 4068 N92-33001 #

UCRL-LR-108095 ..... p 4071 N92-32904 #
UCRL-LR-109428 ..... p 4022 N92-32706 #

UCRL-TT-108428 ..... p 3965 N92-33126 #

UDR-TR-90-127 ..... p 4021 N92-32621 #

UFIFT-HEP-92-12 ..... p 4064 N92-32313 #

UMICH-TR-945 ..... p 3989 N92-32678 #
UMICH-TR-947 ..... p 3980 N92-32680 #

UMICH-027723-6-F ..... p 3979 N92-32559 * #

US-PATENT-APPL-SN-249443 ..... p 3986 N92-33172
US-PATENT-APPL-SN-429739 ..... p 3965 N92-33009 *
US-PATENT-APPL-SN-433812 ..... p 3973 N92-33008 *
US-PATENT-APPL-SN-444253 ..... p 3992 N92-33169
US-PATENT-APPL-SN-480449 ..... p 3991 N92-33011 *
US-PATENT-APPL-SN-481013 ..... p 4041 N92-33057 *
US-PATENT-APPL-SN-516585 ..... p 3973 N92-33170
US-PATENT-APPL-SN-527462 ..... p 4015 N92-33010 *
US-PATENT-APPL-SN-545008 ..... p 4092 N92-33012 * #
US-PATENT-APPL-SN-552670 ..... p 4015 N92-33016 *
US-PATENT-APPL-SN-560717 ..... p 3973 N92-33014 *
US-PATENT-APPL-SN-560959 ..... p 4073 N92-33167
US-PATENT-APPL-SN-561750 ..... p 3973 N92-33157
US-PATENT-APPL-SN-575737 ..... p 3943 N92-33013 *
US-PATENT-APPL-SN-586369 ..... p 4076 N92-33017 *
US-PATENT-APPL-SN-589571 ..... p 3973 N92-33015 *
US-PATENT-APPL-SN-615668 ..... p 4054 N92-33019 *
US-PATENT-APPL-SN-620671 ..... p 3940 N92-33161
US-PATENT-APPL-SN-627670 ..... p 3974 N92-33177
US-PATENT-APPL-SN-631582 ..... p 3992 N92-33175
US-PATENT-APPL-SN-633746 ..... p 4076 N92-33028 *
US-PATENT-APPL-SN-636531 ..... p 4019 N92-33018 *
US-PATENT-APPL-SN-638600 ..... p 3965 N92-33029 *
US-PATENT-APPL-SN-662678 ..... p 3960 N92-33174
US-PATENT-APPL-SN-664010 ..... p 3944 N92-33162
US-PATENT-APPL-SN-674828 ..... p 4038 N92-33032 *
US-PATENT-APPL-SN-677182 ..... p 3991 N92-33030 *
US-PATENT-APPL-SN-678551 ..... p 4019 N92-33031 *
US-PATENT-APPL-SN-687602 ..... p 3986 N92-33171
US-PATENT-APPL-SN-699288 ..... p 3978 N92-33020 *
US-PATENT-APPL-SN-705048 ..... p 4017 N92-33165
US-PATENT-APPL-SN-765979 ..... p 4092 N92-33012 * #
US-PATENT-APPL-SN-773376 ..... p 3991 N92-33021 *
US-PATENT-APPL-SN-797569 ..... p 4076 N92-33022 *
US-PATENT-APPL-SN-806384 ..... p 4074 N92-32634 #
US-PATENT-APPL-SN-822812 ..... p 3963 N92-32755 #
US-PATENT-APPL-SN-841699 ..... p 4026 N92-32943 #
US-PATENT-APPL-SN-878597 ..... p 4076 N92-33095 #

US-PATENT-APPL-156-241 ..... p 3978 N92-33020 *
US-PATENT-APPL-156-285 ..... p 3978 N92-33020 *
US-PATENT-APPL-156-293 ..... p 3978 N92-33020 *
US-PATENT-APPL-264-272.15 ..... p 3978 N92-33020 *
US-PATENT-APPL-29-856 ..... p 3978 N92-33020 *

US-PATENT-CLASS-128-715 ..... p 4015 N92-33016 *
US-PATENT-CLASS-128-775 ..... p 4015 N92-33016 *
US-PATENT-CLASS-148-402 ..... p 4038 N92-33032 *
US-PATENT-CLASS-210-198.2 .... p 3965 N92-33009 *
US-PATENT-CLASS-210-209 ..... p 3965 N92-33029 *
US-PATENT-CLASS-210-266 ..... p 3965 N92-33029 *
US-PATENT-CLASS-210-269 ..... p 3965 N92-33029 *
US-PATENT-CLASS-210-287 ..... p 3965 N92-33029 *
US-PATENT-CLASS-210-502.1 .... p 3965 N92-33009 *
US-PATENT-CLASS-210-635 ..... p 3965 N92-33009 *
US-PATENT-CLASS-210-670 ..... p 3965 N92-33029 *
US-PATENT-CLASS-210-748 ..... p 3965 N92-33029 *
US-PATENT-CLASS-210-758 ..... p 3965 N92-33029 *
US-PATENT-CLASS-219-72 ..... p 3991 N92-33030 *
US-PATENT-CLASS-219-75 ..... p 3991 N92-33030 *
US-PATENT-CLASS-244-158R .... p 4015 N92-33010 *
US-PATENT-CLASS-244-158R .... p 3943 N92-33013 *
US-PATENT-CLASS-244-160 ..... p 3943 N92-33013 *
US-PATENT-CLASS-244-161 ..... p 4019 N92-33018 *
US-PATENT-CLASS-244-172 ..... p 3943 N92-33013 *
US-PATENT-CLASS-244-315 ..... p 3940 N92-33161
US-PATENT-CLASS-244-324 ..... p 3944 N92-33162
US-PATENT-CLASS-250-216 ..... p 4076 N92-33026 *
US-PATENT-CLASS-250-227.21 .. p 4076 N92-33017 *
US-PATENT-CLASS-250-231.19 .. p 4076 N92-33017 *
US-PATENT-CLASS-294-65.5 ..... p 4019 N92-33018 *
US-PATENT-CLASS-294-86.2 ..... p 4019 N92-33018 *
US-PATENT-CLASS-294-86.4 ..... p 4019 N92-33018 *
US-PATENT-CLASS-294-907 ..... p 4019 N92-33018 *
US-PATENT-CLASS-318-567 ..... p 4054 N92-33019 *
US-PATENT-CLASS-318-568.11 .. p 4054 N92-33019 *
US-PATENT-CLASS-318-568.19 .. p 4054 N92-33019 *
US-PATENT-CLASS-329-318 ..... p 3992 N92-33175
US-PATENT-CLASS-333-238 ..... p 3992 N92-33169
US-PATENT-CLASS-342-21 ..... p 3986 N92-33171
US-PATENT-CLASS-342-465 ..... p 3986 N92-33172
US-PATENT-CLASS-343-766 ..... p 4015 N92-33010 *
US-PATENT-CLASS-358-12 ..... p 4076 N92-33017 *
US-PATENT-CLASS-359-107 ..... p 4041 N92-33057 *
US-PATENT-CLASS-359-108 ..... p 4041 N92-33057 *
US-PATENT-CLASS-359-241 ..... p 4076 N92-33028 *
US-PATENT-CLASS-359-559 ..... p 4076 N92-33022 *
US-PATENT-CLASS-359-559 ..... p 4041 N92-33057 *
US-PATENT-CLASS-359-561 ..... p 4076 N92-33022 *
US-PATENT-CLASS-359-561 ..... p 4041 N92-33057 *
US-PATENT-CLASS-359-7 ..... p 4076 N92-33022 *
US-PATENT-CLASS-364-191 ..... p 4054 N92-33019 *
US-PATENT-CLASS-365-49 ..... p 4041 N92-33057 *
US-PATENT-CLASS-371-37.1 ..... p 3991 N92-33011 *
US-PATENT-CLASS-374-175 ..... p 3991 N92-33021 *
US-PATENT-CLASS-376-154 ..... p 4073 N92-33167
US-PATENT-CLASS-378-210 ..... p 4092 N92-33012 * #
US-PATENT-CLASS-378-43 ..... p 4092 N92-33012 * #
US-PATENT-CLASS-382-31 ..... p 4041 N92-33057 *
US-PATENT-CLASS-382-32 ..... p 4041 N92-33057 *
US-PATENT-CLASS-395-90 ..... p 4054 N92-33019 *
US-PATENT-CLASS-414-737 ..... p 4019 N92-33018 *
US-PATENT-CLASS-423-446 ..... p 3973 N92-33170
US-PATENT-CLASS-425-50A ..... p 3960 N92-33174
US-PATENT-CLASS-428-315.5 .... p 3965 N92-33009 *
US-PATENT-CLASS-428-315.7 .... p 3965 N92-33009 *
US-PATENT-CLASS-428-404 ..... p 3965 N92-33009 *
US-PATENT-CLASS-505-1 ..... p 3973 N92-33157
US-PATENT-CLASS-524-396 ..... p 3974 N92-33177
US-PATENT-CLASS-528-125 ..... p 3973 N92-33008 *
US-PATENT-CLASS-528-125 ..... p 3973 N92-33014 *
US-PATENT-CLASS-528-125 ..... p 3973 N92-33015 *
US-PATENT-CLASS-528-126 ..... p 3973 N92-33014 *
US-PATENT-CLASS-528-128 ..... p 3973 N92-33008 *
US-PATENT-CLASS-528-128 ..... p 3973 N92-33014 *
US-PATENT-CLASS-528-128 ..... p 3973 N92-33015 *
US-PATENT-CLASS-528-172 ..... p 3973 N92-33008 *
US-PATENT-CLASS-528-172 ..... p 3973 N92-33015 *
US-PATENT-CLASS-528-173 ..... p 3973 N92-33014 *
US-PATENT-CLASS-528-179 ..... p 3973 N92-33014 *
US-PATENT-CLASS-528-182 ..... p 3973 N92-33014 *
US-PATENT-CLASS-528-185 ..... p 3973 N92-33008 *
US-PATENT-CLASS-528-185 ..... p 3973 N92-33015 *
US-PATENT-CLASS-528-188 ..... p 3973 N92-33014 *
US-PATENT-CLASS-528-229 ..... p 3973 N92-33008 *
US-PATENT-CLASS-528-352 ..... p 3973 N92-33008 *
US-PATENT-CLASS-528-352 ..... p 3973 N92-33015 *
US-PATENT-CLASS-528-353 ..... p 3973 N92-33008 *
US-PATENT-CLASS-528-353 ..... p 3973 N92-33015 *
US-PATENT-CLASS-530-413 ..... p 3965 N92-33009 *
US-PATENT-CLASS-564-315 ..... p 3973 N92-33015 *
US-PATENT-CLASS-606-106 ..... p 4038 N92-33032 *
US-PATENT-CLASS-606-127 ..... p 4038 N92-33032 *
US-PATENT-CLASS-606-78 ..... p 4038 N92-33032 *
US-PATENT-CLASS-73-1H ..... p 3991 N92-33021 *
US-PATENT-CLASS-73-571 ..... p 3991 N92-33021 *
US-PATENT-CLASS-73-705 ..... p 4076 N92-33017 *
US-PATENT-CLASS-74-25 ..... p 4019 N92-33031 *
US-PATENT-CLASS-74-437 ..... p 4019 N92-33031 *
US-PATENT-CLASS-74-61 ..... p 4015 N92-33010 *
US-PATENT-CLASS-74-87 ..... p 4015 N92-33010 *
US-PATENT-CLASS-901-40 ..... p 4019 N92-33018 *
US-PATENT-CLASS-901-47 ..... p 4054 N92-33019 *

US-PATENT-5,073,784 ..... p 3986 N92-33172

US-PATENT-5,075,094 ..... p 3973 N92-33170
US-PATENT-5,075,655 ..... p 3992 N92-33169
US-PATENT-5,078,951 ..... p 4073 N92-33167
US-PATENT-5,082,200 ..... p 3940 N92-33161
US-PATENT-5,082,826 ..... p 3973 N92-33157
US-PATENT-5,086,432 ..... p 4017 N92-33165
US-PATENT-5,089,551 ..... p 3974 N92-33177
US-PATENT-5,095,312 ..... p 3986 N92-33171
US-PATENT-5,097,221 ..... p 3992 N92-33175
US-PATENT-5,106,034 ..... p 3944 N92-33162
US-PATENT-5,116,216 ..... p 3960 N92-33174
US-PATENT-5,129,600 ..... p 4015 N92-33010 *
US-PATENT-5,130,530 ..... p 4076 N92-33028 *
US-PATENT-5,130,990 ..... p 3991 N92-33011 *
US-PATENT-5,131,055 ..... p 4041 N92-33057 *
US-PATENT-5,133,721 ..... p 4038 N92-33032 *
US-PATENT-5,140,992 ..... p 4015 N92-33016 *
US-PATENT-5,141,636 ..... p 3965 N92-33029 *
US-PATENT-5,141,806 ..... p 3965 N92-33009 *
US-PATENT-5,143,327 ..... p 3943 N92-33013 *
US-PATENT-5,145,227 ..... p 4019 N92-33018 *
US-PATENT-5,145,937 ..... p 3973 N92-33008 *
US-PATENT-5,145,942 ..... p 3973 N92-33015 *
US-PATENT-5,146,083 ..... p 4076 N92-33017 *
US-PATENT-5,146,482 ..... p 4092 N92-33012 * #
US-PATENT-5,146,780 ..... p 3991 N92-33021 *
US-PATENT-5,146,803 ..... p 4019 N92-33031 *
US-PATENT-5,147,966 ..... p 3973 N92-33014 *
US-PATENT-5,149,387 ..... p 3978 N92-33020 *
US-PATENT-5,149,932 ..... p 3991 N92-33030 *
US-PATENT-5,150,026 ..... p 4054 N92-33019 *
US-PATENT-5,150,228 ..... p 4076 N92-33022 *

USDA-CRIS-PKB-91-05 ..... p 4090 N92-32712 #

USGS/G-1731 ..... p 4034 N92-33173 #

USIP-91-03 ..... p 4067 N92-32764 #

UTIAS-TN-271 ..... p 3938 N92-33102 #
UTIAS-TN-274 ..... p 3955 N92-32829 #
UTIAS-TN-342 ..... p 3967 N92-32794 #

UTRC/R92-918246-4 ..... p 3953 N92-32676 #
UTRC/R92-957787-F ..... p 3963 N92-32645 #
UTRC/R92-957912-23 ..... p 3962 N92-32594 #

UWA/DME/TR-92/69 ..... p 4023 N92-32936 #

UWAERP-35 ..... p 4078 N92-32595 #

VPI-E-92-15 ..... p 3946 N92-32491 * #

VTT-RN-1154 ..... p 4090 N92-32843 #

WHOI-92-19 ..... p 4091 N92-33088 #

WL-TM-90-326-FIBE ..... p 3946 N92-32459 #
WL-TM-92-323 ..... p 3930 N92-32651 #

WL-TR-91-3076 ..... p 4021 N92-32621 #
WL-TR-91-3089 ..... p 4008 N92-32632 #
WL-TR-92-8017 ..... p 3953 N92-32629 #

WSRC-MS-91-521 ..... p 3964 N92-32925 #
WSRC-MS-92-124 ..... p 3988 N92-32495 #

WSRC-RP-91-415 ..... p 4013 N92-32460 #

Y/DW-1125 ..... p 3966 N92-32614 #

Typical Accession Number Index Listing

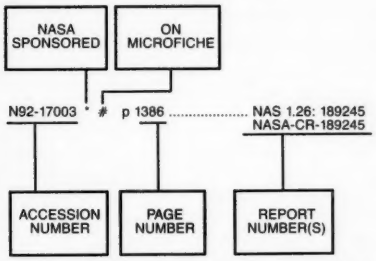

Listings in this index are arranged alphanumerically by accession number. The page number helps to locate the citation in the abstract section. An asterisk (*) indicates that the item is a NASA report. A pound sign (#) indicates that the item is available on microfiche.

N92-32243* # p 3988 ..... E-7156
N92-32243* # p 3988 ..... NAS 1.15:105751
NASA-TM-105751
N92-32244* # p 3942 ..... NAS 1.26:190627
NASA-CR-190627
N92-32245* # p 3994 ..... M-693-PT-2
NAS 1.55:3163-PT-2
NASA-CP-3163-PT-2
N92-32246* # p 3944 ..... NO REPORT NUMBER
N92-32247* # p 3994 ..... NO REPORT NUMBER
N92-32248* # p 3945 ..... NO REPORT NUMBER
N92-32249* # p 3995 ..... NO REPORT NUMBER
N92-32250* # p 3995 ..... NO REPORT NUMBER
N92-32251* # p 3995 ..... NO REPORT NUMBER
N92-32252* # p 3995 ..... NO REPORT NUMBER
N92-32253* # p 3995 ..... NO REPORT NUMBER
N92-32254* # p 3996 ..... NO REPORT NUMBER
N92-32255* # p 3996 ..... NO REPORT NUMBER
N92-32256* # p 3996 ..... NO REPORT NUMBER
N92-32257* # p 3996 ..... NO REPORT NUMBER
N92-32258* # p 3997 ..... NO REPORT NUMBER
N92-32259* # p 3945 ..... NO REPORT NUMBER
N92-32260* # p 3997 ..... NO REPORT NUMBER
N92-32261* # p 3997 ..... NO REPORT NUMBER
N92-32262* # p 3945 ..... NO REPORT NUMBER
N92-32263* # p 3998 ..... AIAA PAPER 92-0769
N92-32264* # p 3998 ..... NO REPORT NUMBER
N92-32265* # p 3998 ..... NO REPORT NUMBER
N92-32266* # p 3998 ..... NO REPORT NUMBER
N92-32267* # p 3998 ..... NO REPORT NUMBER
N92-32268* # p 3999 ..... NO REPORT NUMBER
N92-32269* # p 3999 ..... NO REPORT NUMBER
N92-32270* # p 3999 ..... NO REPORT NUMBER
N92-32271* # p 3999 ..... NO REPORT NUMBER
N92-32272* # p 3945 ..... NO REPORT NUMBER
N92-32273* # p 4000 ..... NO REPORT NUMBER
N92-32274* # p 4000 ..... NO REPORT NUMBER
N92-32275* # p 3960 ..... NO REPORT NUMBER
N92-32276* # p 4000 ..... NO REPORT NUMBER
N92-32277* # p 4000 ..... NO REPORT NUMBER
N92-32278* # p 4000 ..... M-693-PT-1
NAS 1.55:3163-PT-1
NASA-CP-3163-PT-1
N92-32279* # p 4001 ..... NO REPORT NUMBER
N92-32280* # p 3945 ..... NO REPORT NUMBER
N92-32281* # p 3945 ..... NO REPORT NUMBER
N92-32282* # p 4001 ..... NO REPORT NUMBER
N92-32283* # p 4001 ..... NO REPORT NUMBER
N92-32284* # p 4001 ..... NO REPORT NUMBER
N92-32285* # p 4001 ..... NO REPORT NUMBER
N92-32286* # p 4002 ..... NO REPORT NUMBER
N92-32287* # p 4002 ..... NO REPORT NUMBER
N92-32288* # p 4002 ..... NO REPORT NUMBER
N92-32289* # p 4002 ..... NO REPORT NUMBER
N92-32290* # p 4002 ..... NO REPORT NUMBER
N92-32291* # p 4003 ..... NO REPORT NUMBER
N92-32292* # p 4003 ..... NO REPORT NUMBER
N92-32293* # p 4003 ..... NO REPORT NUMBER
N92-32294* # p 4003 ..... NO REPORT NUMBER
N92-32295* # p 4003 ..... NO REPORT NUMBER
N92-32296* # p 4004 ..... NO REPORT NUMBER
N92-32297* # p 3966 ..... NO REPORT NUMBER
N92-32298* # p 4004 ..... NO REPORT NUMBER
N92-32299* # p 4004 ..... NO REPORT NUMBER
N92-32300* # p 4004 ..... NO REPORT NUMBER
N92-32301* # p 4005 ..... NO REPORT NUMBER
N92-32302* # p 4005 ..... NO REPORT NUMBER
N92-32303* # p 4005 ..... NO REPORT NUMBER
N92-32304* # p 4005 ..... NO REPORT NUMBER
N92-32305* # p 4005 ..... NO REPORT NUMBER
N92-32306* # p 4006 ..... NO REPORT NUMBER
N92-32307* # p 3966 ..... NO REPORT NUMBER
N92-32308 # p 3934 ..... DE92-013681
SAND-91-2664
N92-32309 # p 4087 ..... DE92-624689
IFVE-OEF-91-15
IHEP-OEF-91-15
N92-32310 # p 4064 ..... DE92-624690
IFVE-OEF-91-37
N92-32311 # p 4064 ..... DE92-624691
IFVE-OEF-91-51
N92-32312 # p 4064 ..... CONF-9106289-6
DE92-014482
FNAL/C-92/45-E
LBL-31886
N92-32313 # p 4064 ..... DE92-016462
DOE/ER-40272/160
UFIFT-HEP-92-12
N92-32314 # p 4069 ..... ANL/CP-75863
CONF-920315-40
DE92-016697
N92-32315 # p 3966 ..... DE92-016840
DOE/ER-45179/9
N92-32316 # p 4064 ..... BNL-47550
CONF-920716-5
DE92-016952
N92-32317 # p 3970 ..... CEBAF-PR-92-015
DE92-016963
DOE/ER-40150/190
N92-32318 # p 4069 ..... CEBAF-PR-92-008
DE92-016964
DOE/ER-40150/191
N92-32319 # p 4069 ..... CEBAF-PR-92-005
DE92-016966
DOE/ER-40150/193
N92-32320 # p 4081 ..... CONF-920141-8
DE92-017083
LBL-31865
N92-32321 # p 4073 ..... CONF-910730-31
DE92-017117
LBL-30464
N92-32322 # p 4006 ..... DE92-017138
UCRL-ID-109125
N92-32323 # p 4013 ..... AD-A250146
ARO-29211.1-PHS
N92-32324 # p 4006 ..... AD-A250366
N92-32325 # p 3988 ..... AD-A250367
N92-32326 # p 3935 ..... AD-A250373
ARL-GD-029
DODA-AR-007-052
N92-32327 # p 3946 ..... CONF-910399-7
DE92-011462
UCRL-JC-105233
N92-32328 # p 4020 ..... CONF-9109364-1
DE92-011468
UCRL-JC-107883
N92-32329 # p 4015 ..... AD-A250851
NRAD-TR-1480
N92-32330 # p 3960 ..... AD-A250855
CRDEC-CR-144
N92-32331 # p 4032 ..... DE92-013772
DOE/ER-61198/T1
N92-32332 # p 3960 ..... CONF-920584-7
DE92-014349
DOE/MC-27115/92/C0035
N92-32333 # p 4034 ..... CONF-920584-8
DE92-014350
DOE/MC-20422/92/C0030
N92-32334 # p 3960 ..... CONF-920584-10
DE92-014358
DOE/MC-26039/92/C0031
N92-32335 # p 4015 ..... DE92-016578
SAND-92-7065
N92-32336 # p 4035 ..... DE92-016622
DOE/ER-61052/2
N92-32337 # p 4069 ..... CONF-9109328-2
DE92-010730
SLAC-PUB-5718
N92-32338 # p 4103 ..... AD-A248763
AFOSR-92-0167TR-VOL-1
N92-32339 # p 3946 ..... AD-A250220
AFOSR-92-0356TR
AFOSR-92-1
N92-32340 # p 4064 ..... CONF-9107217
DE92-625005
ESM-32
N92-32341 # p 3970 ..... AD-A250763
BRL-CR-689
N92-32342 # p 4089 ..... AD-A250769
DRIC-BR-309398
RSRE-92004
N92-32343 # p 4013 ..... AD-A250771
NSWCCR/RDTN-92/0003
N92-32344 # p 4036 ..... AD-A250873
N92-32345 # p 4035 ..... AD-A250881
N92-32346 # p 4081 ..... ANL/CP-74829
CONF-920402-30
DE92-015266
N92-32347 # p 3960 ..... DE92-016614
DOE/PC-89762/T14
N92-32348 # p 4093 ..... ESA-SP-338
ETN-92-91975
ISBN-92-9092-194-3
N92-32349* # p 4093 ..... NO REPORT NUMBER
N92-32350 # p 4093 ..... NO REPORT NUMBER
N92-32351* # p 4094 ..... NO REPORT NUMBER
N92-32352* # p 4094 ..... NO REPORT NUMBER
N92-32353 # p 4094 ..... NO REPORT NUMBER
N92-32354 # p 4094 ..... NO REPORT NUMBER
N92-32355 # p 4094 ..... NO REPORT NUMBER
N92-32356 # p 4094 ..... NO REPORT NUMBER
N92-32357* # p 4094 ..... NO REPORT NUMBER
N92-32358* # p 4095 ..... NO REPORT NUMBER
N92-32359* # p 4095 ..... NO REPORT NUMBER
N92-32360* # p 4095 ..... NO REPORT NUMBER
N92-32361* # p 4095 ..... NO REPORT NUMBER
N92-32362 # p 4095 ..... NO REPORT NUMBER
N92-32363* # p 4095 ..... NO REPORT NUMBER
N92-32364 # p 4096 ..... NO REPORT NUMBER
N92-32365 # p 4096 ..... NO REPORT NUMBER
N92-32366 # p 4096 ..... NO REPORT NUMBER
N92-32367 # p 4096 ..... NO REPORT NUMBER
N92-32368 # p 4096 ..... NO REPORT NUMBER
N92-32369* # p 4096 ..... NO REPORT NUMBER
N92-32370* # p 4096 ..... NO REPORT NUMBER
N92-32371 # p 4096 ..... NO REPORT NUMBER
N92-32372* # p 4097 ..... NO REPORT NUMBER
N92-32373* # p 4097 ..... NO REPORT NUMBER
N92-32374* # p 4097 ..... NO REPORT NUMBER
N92-32375 # p 4097 ..... NO REPORT NUMBER
N92-32376* # p 4097 ..... NO REPORT NUMBER
N92-32377* # p 4097 ..... NO REPORT NUMBER
N92-32378* # p 4098 ..... NO REPORT NUMBER
N92-32379* # p 4098 ..... NO REPORT NUMBER
N92-32380* # p 4098 ..... NO REPORT NUMBER
N92-32381* # p 4098 ..... NO REPORT NUMBER
N92-32382 # p 4098 ..... NO REPORT NUMBER
N92-32383* # p 4098 ..... NO REPORT NUMBER
N92-32384 # p 4099 ..... NO REPORT NUMBER
N92-32385 # p 4099 ..... NO REPORT NUMBER
N92-32386* # p 4099 ..... NO REPORT NUMBER
N92-32387* # p 4099 ..... NO REPORT NUMBER
N92-32388 # p 4099 ..... NO REPORT NUMBER
N92-32389* # p 4099 ..... NO REPORT NUMBER
N92-32390 # p 4099 ..... NO REPORT NUMBER
N92-32391 # p 4100 ..... NO REPORT NUMBER
N92-32392 # p 4015 ..... NO REPORT NUMBER
N92-32393 # p 4100 ..... NO REPORT NUMBER
N92-32394 # p 4100 ..... NO REPORT NUMBER
N92-32395 # p 4100 ..... NO REPORT NUMBER
N92-32396 # p 4100 ..... NO REPORT NUMBER

N92-32397 # p 4100 ..... NO REPORT NUMBER
N92-32398 # p 4101 ..... NO REPORT NUMBER
N92-32399 # p 4101 ..... NO REPORT NUMBER
N92-32400 # p 4101 ..... NO REPORT NUMBER
N92-32401 # p 4101 ..... NO REPORT NUMBER
N92-32402 # p 4101 ..... NO REPORT NUMBER
N92-32403 # p 4101 ..... NO REPORT NUMBER
N92-32404 # p 4101 ..... NO REPORT NUMBER
N92-32405* # p 4102 ..... NO REPORT NUMBER
N92-32406 # p 4102 ..... NO REPORT NUMBER
N92-32407 # p 4102 ..... NO REPORT NUMBER
N92-32408 # p 4102 ..... NO REPORT NUMBER
N92-32409 # p 4102 ..... NO REPORT NUMBER
N92-32410 # p 4102 ..... NO REPORT NUMBER
N92-32411 # p 4070 ..... BNL-52291-PHASE-2
DE92-013395
N92-32412 # p 4050 ..... CONF-920367-8
DE92-013444
UCRL-JC-109601
N92-32413 # p 4070 ..... CONF-920315-34
DE92-013448
UCRL-JC-108512
N92-32414 # p 4041 ..... CONF-9206102-5
DE92-013540
LA-UR-92-1261
N92-32415 # p 4027 ..... DE92-013639
LA-12260-MS
N92-32416 # p 4041 ..... DE92-013754
UCRL-ID-110240
N92-32417 # p 4077 ..... DE92-013917
DOE/OR-00033/T479
N92-32418 # p 4064 ..... AD-A250935
TR-9
N92-32419 # p 4073 ..... CONF-9110146-16
DE92-014483
LBL-31532
N92-32420 # p 4081 ..... DE92-014506
LBL-31124
N92-32421* # p 3942 ..... NAS 1.15:107981
NASA-TM-107981
N92-32422* # p 3929 ..... A-90244
NAS 1.15:102851
NASA-TM-102851
N92-32423* # p 4021 ..... NAS 1.15:107640
NASA-TM-107640
N92-32424* # p 3933 ..... A-92085
NAS 1.15:103930
NASA-TM-103930
N92-32425* # p 4020 ..... NAS 1.26:190814
NASA-CR-190814
N92-32426 # p 4065 ..... CONF-920219-1
DE92-012415
SU-SLAC-PUB-5745
N92-32427 # p 4032 ..... DE92-012449
SAND-91-2343
N92-32428 # p 4055 ..... DE92-014814
ORNL/TM-12059
N92-32429 # p 3970 ..... DE92-014841
DOE/ER-45254/7
N92-32430 # p 4061 ..... DE92-014877
DOE/ER-40685/712
N92-32431 # p 4032 ..... DE92-014920
NDP-042
ORNL/CDIAC-50
N92-32432 # p 3966 ..... DE92-014921
ORNL/TM-11946
N92-32433 # p 4039 ..... AD-A252234
ARI-RN-92-40
N92-32434 # p 4036 ..... AD-A252235
N92-32435 # p 3938 ..... AD-A252520
AFIT/CI/CIA-92-039
N92-32436* # p 4020 ..... NAS 1.26:190679
NASA-CR-190679
TR92-1298
N92-32437 # p 3935 ..... AGARD-CP-500
ISBN-92-835-0658-8
N92-32438 # p 3936 ..... NO REPORT NUMBER
N92-32439 # p 3936 ..... NO REPORT NUMBER
N92-32440 # p 3936 ..... NO REPORT NUMBER
N92-32441 # p 3936 ..... NO REPORT NUMBER
N92-32442 # p 3936 ..... NO REPORT NUMBER
N92-32443 # p 3936 ..... NO REPORT NUMBER
N92-32444 # p 3936 ..... NO REPORT NUMBER
N92-32445 # p 3937 ..... NO REPORT NUMBER
N92-32446 # p 3937 ..... NO REPORT NUMBER
N92-32447 # p 3937 ..... NO REPORT NUMBER
N92-32448 # p 3937 ..... NO REPORT NUMBER
N92-32449 # p 3937 ..... NO REPORT NUMBER
N92-32450 # p 3937 ..... NO REPORT NUMBER
N92-32451* # p 4041 ..... CSC/TR-90/6155
NAS 1.26:190713
NASA-CR-190713
N92-32452* # p 3938 ..... A-91074
NAS 1.15:103839
NASA-TM-103839
N92-32453 # p 4103 ..... NO REPORT NUMBER
N92-32454* # p 3941 ..... NAS 1.15:107547
NASA-TM-107547
N92-32455 # p 3932 ..... NTSB/AAR-92/01
PB92-910401
N92-32456* # p 3941 ..... E-5456
NAS 1.61:1253
NASA-RP-1253
N92-32457 # p 4103 ..... NO REPORT NUMBER
N92-32458 # p 3978 ..... PL-TR-91-2200
N92-32459 # p 3946 ..... WL-TM-90-326-FIBE
N92-32460 # p 4013 ..... DE92-009590
WSRC-RP-91-415
N92-32461 # p 3977 ..... AD-A245283
N92-32462 # p 4081 ..... DE92-012572
DOE/ER-45332/T1
N92-32463* # p 3944 ..... E-7242
NAS 1.15:105811
NASA-TM-105811
N92-32464 # p 3960 ..... DE92-012573
DOE/ER-13812/T1
N92-32465 # p 4081 ..... DE92-012584
IS-T-1570
N92-32466* # p 3946 ..... E-7179
NAS 1.15:105762
NASA-TM-105762
N92-32467 # p 3977 ..... DE92-013353
DOE/PC-79892/T19
N92-32468 # p 4006 ..... DE92-014084
ORNL/TM-12011
N92-32469 # p 4089 ..... DE92-014103
DOE/CE-15991/5
N92-32470 # p 4081 ..... BNL-47235
CONF-9109102-6
DE92-014165
N92-32471 # p 3970 ..... DE92-014328
DOE/ER-45191/19
N92-32472* # p 4007 ..... E-7212
NAS 1.15:105853
NASA-TM-105853
N92-32473 # p 4065 ..... DE92-014509
IS-T-1578
N92-32474* # p 4007 ..... A-92055
NAS 1.15:103917
NASA-TM-103917
N92-32475 # p 3961 ..... AECL-10459
DE92-626850
N92-32476* # p 3970 ..... A-92146
NAS 1.15:103952
NASA-TM-103952
N92-32477* # p 3942 ..... NAS 1.26:190732
NASA-CR-190732
N92-32478* # p 4092 ..... NAS 1.15:103597
NASA-TM-103597
N92-32479 p 3929 ..... ESDU-92024
ISBN-0-85679-829-0
N92-32480* # p 3929 ..... L-17095
NAS 1.60:3261
NASA-TP-3261
N92-32481 # p 4059 ..... DE92-013108
LA-12258
N92-32482 p 4017 ..... ESDU-92016
ISBN-0-85679-820-7
N92-32483 # p 3974 ..... DE92-013169
DOE/CE-92013169
N92-32484 p 3945 ..... ESDU-75003
ESDU-92011-PT-1
ISBN-0-85679-816-9
N92-32485 p 3945 ..... ESDU-92010
ISBN-0-85679-815-0
N92-32486 p 3945 ..... ESDU-92009
ISBN-0-85679-814-2
N92-32487 p 3939 ..... ESDU-AERO-C.01.01.02
ESDU-92007
ISBN-0-85679-812-6
N92-32488 # p 4103 ..... AD-A250099
N92-32489 # p 3970 ..... AD-A250129
DODA-AR-006-839
MRL-TN-596
N92-32490 # p 3971 ..... AD-A247866
TR-1
N92-32491* # p 3946 ..... CCMS-92-16
NAS 1.26:190573
NASA-CR-190573
VPI-E-92-15
N92-32492 # p 4036 ..... AD-A248752
AL-TR-1991-0104
N92-32493 # p 4082 ..... CONF-911106-89
DE92-010301
LBL-31456
N92-32494* # p 3930 ..... NAS 1.26:190583
NASA-CR-190583
N92-32495 # p 3988 ..... CONF-920631-21
DE92-013076
WSRC-MS-92-124
N92-32496 # p 4087 ..... CONF-9109371-1
DE92-013021
FNAL/C-92/41-A
N92-32497 # p 4065 ..... DE92-624692
IFVE-OEF-91-52
N92-32498 # p 4065 ..... DE92-624727
IHEP-OTF-91-116
N92-32499 # p 4065 ..... DE92-625007
ESM-37
N92-32500 # p 4065 ..... DE92-625008
FEI-2189
N92-32501 # p 4065 ..... DE92-625009
FIAS-R-215
N92-32502 # p 4033 ..... NOAA-TM-NWS-NSSFC-34
PB92-186063
N92-32503 # p 4033 ..... PB92-179407
N92-32504 # p 4037 ..... AD-A250793
N92-32505 # p 4091 ..... GAO-55-636-PT-6
ISBN-0-16-038597-0
N92-32506 # p 4070 ..... CONF-920172-7
DE92-016003
FNAL/C-92/121-E
N92-32507* # p 4042 ..... H-1675
NAS 1.15:104237
NASA-TM-104237
N92-32508 # p 3961 ..... AD-A250758
BRL-CR-690
N92-32509 # p 3961 ..... AD-A250923
TR-32
N92-32510 # p 4024 ..... DE92-001237
NREL/TP-413-4791
N92-32511 # p 4015 ..... BNL-47376
CONF-920315-37
DE92-014166
N92-32512 # p 4082 ..... AD-A252350
NRL-TR-1
N92-32513* # p 3946 ..... L-16832-PT-1
NAS 1.55:3087-PT-1
NASA-CP-3087-PT-1
N92-32514* # p 3947 ..... NO REPORT NUMBER
N92-32515* # p 3947 ..... NO REPORT NUMBER
N92-32516* # p 3947 ..... NO REPORT NUMBER
N92-32517* # p 3947 ..... NO REPORT NUMBER
N92-32518* # p 3947 ..... NO REPORT NUMBER
N92-32519* # p 3948 ..... NO REPORT NUMBER
N92-32520* # p 3948 ..... NO REPORT NUMBER
N92-32521* # p 3948 ..... NO REPORT NUMBER
N92-32522* # p 3948 ..... NO REPORT NUMBER
N92-32523* # p 3948 ..... NO REPORT NUMBER
N92-32524* # p 3948 ..... NO REPORT NUMBER
N92-32525* # p 3948 ..... NO REPORT NUMBER
N92-32526* # p 3949 ..... NO REPORT NUMBER
N92-32527* # p 3949 ..... NO REPORT NUMBER
N92-32528* # p 3949 ..... NO REPORT NUMBER
N92-32529* # p 3949 ..... NO REPORT NUMBER
N92-32530* # p 3949 ..... NO REPORT NUMBER
N92-32531* # p 3949 ..... NO REPORT NUMBER
N92-32532* # p 3950 ..... NO REPORT NUMBER
N92-32533 # p 4077 ..... DE92-010031
DOE/ER-54102/T1
N92-32534 # p 4033 ..... AD-A246137
N92-32535 # p 3978 ..... AD-A246315
DREO-91-23
N92-32536* # p 3934 ..... NAS 1.15:107600
NASA-TM-107600
N92-32537 # p 3933 ..... DOT/FAA/RD-92/22
N92-32538 # p 3942 ..... AD-A246880
N92-32539* # p 4037 ..... NAS 1.26:190693
NASA-CR-190693
N92-32540 # p 4016 ..... AD-A247264
N92-32541* # p 4093 ..... NAS 1.26:190697
NASA-CR-190697
N92-32542 # p 4082 ..... ANL/CP-75691
CONF-920548-1
DE92-016778
N92-32543 # p 4028 ..... PB92-164979
N92-32544 # p 3961 ..... CONF-920707-19
DE92-008563
UCRL-JC-109055
N92-32545 # p 4033 ..... NOAA-TM-NWS-NSSFC-33
PB92-185982
N92-32546 # p 4042 ..... AD-A250970
TR-91-1246
N92-32547 # p 3971 ..... AD-A251098
TR-29
N92-32548 # p 4066 ..... AD-A251140
TR-24
N92-32549 # p 4025 ..... DE92-013680
SAND-91-2203
N92-32550 # p 3971 ..... AD-A251141
TR-4
N92-32551 # p 4088 ..... AD-A251153
GMU/C3I-220-R
N92-32552 # p 4078 ..... NIFS-119
N92-32553 # p 3961 ..... AD-A250883
N92-32554 # p 4028 ..... NCAR/TN-372+STR
PB92-193259
N92-32555 # p 3979 ..... NTIA-92-284

PB92-192848
N92-32556 # p 4066 ..... AD-A250921
TR-31
N92-32557 # p 3962 ..... DE92-014524
ORNL/TR-91/33
N92-32558 # p 4028 ..... CONF-920851-6
DE92-013663
SAND-92-0959C
N92-32559* # p 3979 ..... NAS 1.26:190610
NASA-CR-190610
UMICH-027723-6-F
N92-32560* # p 4007 ..... H-1835
NAS 1.26:186023
NASA-CR-186023
N92-32561 # p 4082 ..... ANL/CP-74239
CONF-9206195-2
DE92-016189
N92-32562 # p 3962 ..... DE92-016308
IS-T-1569
N92-32563 # p 3962 ..... DE92-016309
IS-T-1594
N92-32564 # p 4020 ..... DE92-016313
DOE/ER-45267/6
N92-32565 # p 4025 ..... DE92-016576
SAND-91-7016
N92-32566 # p 4087 ..... DE92-016855
DOE/ER-13687/12
N92-32567 # p 4070 ..... CEBAF-PR-92-012
DE92-016961
DOE/ER-40150/186
N92-32568 # p 4050 ..... AD-A247427
N92-32569 # p 4038 ..... AD-A247429
TR-91/ONR-34
N92-32570 # p 3979 ..... AD-A247431
NRL/FR/5521-91-9366
N92-32571 # p 4035 ..... AD-A247456
N92-32572 # p 4031 ..... AD-A247553
AD-E200882
PL-TR-91-2113
N92-32573 # p 3979 ..... AD-A247613
N92-32574* # p 3950 ..... L-16832-PT-2
NAS 1.55:3087-PT-2
NASA-CP-3087-PT-2
N92-32575* # p 3950 ..... NO REPORT NUMBER
N92-32576* # p 3950 ..... NO REPORT NUMBER
N92-32577* # p 3950 ..... NO REPORT NUMBER
N92-32578* # p 3950 ..... NO REPORT NUMBER
N92-32579* # p 3951 ..... NO REPORT NUMBER
N92-32580* # p 3951 ..... NO REPORT NUMBER
N92-32581* # p 3951 ..... NO REPORT NUMBER
N92-32582* # p 3951 ..... NO REPORT NUMBER
N92-32583* # p 3951 ..... NO REPORT NUMBER
N92-32584* # p 3952 ..... NO REPORT NUMBER
N92-32585* # p 3952 ..... NO REPORT NUMBER
N92-32586* # p 3952 ..... NO REPORT NUMBER
N92-32587* # p 3952 ..... NO REPORT NUMBER
N92-32588* # p 3952 ..... NO REPORT NUMBER
N92-32589* # p 3953 ..... NO REPORT NUMBER
N92-32590* # p 4024 ..... NAS 1.26:190579
NASA-CR-190579
N92-32591 # p 3962 ..... GRI-92/0137
PB92-190420
N92-32592 # p 4078 ..... DE92-014246
DOE/ER-53301/4
N92-32593 # p 4087 ..... DE92-014247
DOE/ER-13897/13
N92-32594 # p 3962 ..... GRI-92/0084
PB92-190370
UTRC/R92-957912-23
N92-32595 # p 4078 ..... DE92-014311
DOE/ER-54095/2
UWAERP-35
N92-32596 # p 4016 ..... DE92-014313
DOE/ER-25019/25
N92-32597 # p 4066 ..... DE92-014320
DOE/ER-40224/214
N92-32598 # p 4007 ..... GRI-91/0391-PHASE-2
PB92-190362
N92-32599 # p 4078 ..... DE92-014325
DOE/ER-53212/195
N92-32600 # p 4066 ..... DE92-014415
DOE/ER-40637/1
N92-32601 # p 4014 ..... INPE-5405-RPQ/659
N92-32602 # p 4055 ..... DE92-624556
IHEP-OTF-91-67
N92-32603 # p 4087 ..... DE92-624558
IHEP-OTF-91-90
N92-32604 # p 4093 ..... INPE-5370-TDI/469
N92-32605 # p 4025 ..... D18:1991
ISBN-91-540-5369-2
PB92-180843
N92-32606* # p 3932 ..... CU-TR-14
DOT/FAA/RD-92/20
NAS 1.26:4456
NASA-CR-4456
N92-32607 # p 3963 ..... NIST/GCR-92/602
PB92-181049
N92-32608 # p 4025 ..... PB92-178821
SER-A-23
N92-32609 # p 4028 ..... EPA/600/A-92/102
PB92-180215
N92-32610* # p 3942 ..... NAS 1.26:183208
NASA-CR-183208
STSOC-RT-001283
N92-32611 # p 4089 ..... AD-A252217
RL-TR-91-406
N92-32612 # p 3935 ..... AD-A247426
AL-TP-1992-0001
N92-32613 # p 4074 ..... AD-A247301
NCS-TIB-91-11
NRL/MR/6505-92-6939
N92-32614 # p 3966 ..... DE92-013237
Y/DW-1125
N92-32615 # p 4017 ..... ANL/ESD/TM-29
DE92-013296
N92-32616 # p 4028 ..... DE92-013135
ORNL/ER-47
N92-32617 # p 4042 ..... DE92-015385
SAND-92-0397
N92-32618 # p 4088 ..... B-248821
GAO/NSIAD-92-230
N92-32619 # p 4028 ..... DE92-012595
DOE/ER-61219/1
N92-32620 # p 4014 ..... DE92-013711
DOE/ER-13422/T1
N92-32621 # p 4021 ..... AD-A250852
UDR-TR-90-127
WL-TR-91-3076
N92-32622 # p 4016 ..... AD-A250853
AFOSR-92-0367TR
N92-32623 # p 4078 ..... CONF-920362-31
DE92-013796
GA-A-20870
N92-32624 # p 4078 ..... DE92-013902
DOE/ER-53198/194
N92-32625 # p 4053 ..... AD-A252232
N92-32626 # p 3966 ..... AD-A252575
AFIT/CI/CIA-92-023
N92-32627 # p 4042 ..... AD-A252633
AL-TR-1992-0057
KBSI-IICE-90-STR-01-0592-02
N92-32628 # p 4050 ..... AD-A247617
N92-32629 # p 3953 ..... AD-A247886
PASC002-01-00
WL-TR-92-8017
N92-32630 # p 4007 ..... AD-A247942
CERC/CR/DRP-91-1
N92-32631 # p 3971 ..... DE92-011808
DOE/ER-13633/11
N92-32632 # p 4008 ..... AD-A250814
WL-TR-91-3089
N92-32633 # p 3979 ..... AD-A252466
AD-E951843
AMSMI/TR-RD-WS-92-6
N92-32634 # p 4074 ..... AD-D015289
NAVY-CASE-72926
US-PATENT-APPL-SN-806384
N92-32635 # p 3988 ..... BNL-NUREG-47471
CONF-920375-15
DE92-014173
N92-32636 # p 4082 ..... CONF-920402-13
DE92-014409
N92-32637 # p 3974 ..... CONF-920796-2
DE92-014616
SAND-92-0081C
N92-32638 # p 3953 ..... ANL/CP-75762
CONF-920604-3
DE92-015181
N92-32639 # p 3988 ..... ANL/CP-75875
CONF-920669-6
DE92-015270
N92-32640 # p 3971 ..... ANL/CP-76077
CONF-911050-11
DE92-015272
N92-32641 # p 4082 ..... DE92-015355
DOE/ER-14104/3
N92-32642 # p 4040 ..... CONF-9001172-1
DE92-016006
FNAL/C-92/125
N92-32643 # p 4089 ..... ISBN-0-16-036004-8
PB92-147198
N92-32644 # p 4089 ..... AD-A248450
N92-32645 # p 3963 ..... AD-A248660
ARO-24413.6-CH
UTRC/R92-957787-F
N92-32646 # p 3966 ..... CONF-920439-5
DE92-010705
UCRL-JC-109024
N92-32647 # p 4070 ..... CONF-9110258-5
DE92-011137
LA-UR-92-905
N92-32648* # p 3930 ..... NAS 1.26:190563
NASA-CR-190563
N92-32649 # p 4087 ..... DE92-624821
ESM-36
N92-32650 # p 4029 ..... AD-A251099
N92-32651 # p 3930 ..... AD-A251139
WL-TM-92-323
N92-32652 # p 4008 ..... AD-A251160
DTRC-PAS-91/55
N92-32653 # p 4083 ..... CONF-920402-9
DE92-014432
N92-32654* # p 4090 ..... NAS 1.26:190640
NASA-CR-190640
N92-32655* # p 4031 ..... NAS 1.60:3272-PT-1A
NASA-TP-3272-PT-1A
REPT-92B00100
N92-32656* # p 4042 ..... NAS 1.26:190710
NASA-CR-190710
N92-32657* # p 4021 ..... NAS 1.15:107659
NASA-TM-107659
N92-32658 # p 4042 ..... AD-A252634
AL-TR-1992-0056
KBSI-IICE-90-STR-01-0592-01
N92-32659 # p 3988 ..... AD-A252674
N92-32660 # p 4038 ..... AD-A250786
N92-32661 # p 4055 ..... INPE-5390-TAE/011
N92-32662 # p 4079 ..... INPE-5384-PRE/1750
N92-32663 # p 4037 ..... NO REPORT NUMBER
N92-32664 # p 3974 ..... AD-A250799
BRL-TR-3337
N92-32665 # p 3971 ..... AD-A250965
N92-32666 # p 3963 ..... DE92-008317
LBL-31576
N92-32667 # p 3972 ..... AD-A250977
TR-2
N92-32668 # p 4074 ..... AD-A247614
N92-32669 # p 3989 ..... AD-A250980
AFOSR-92-0445TR
N92-32670 # p 4055 ..... AD-A248451
N92-32671 # p 4008 ..... AD-A250711
AFOSR-92-0374TR
N92-32672 # p 4074 ..... AD-A250760
SSD-TR-92-05
TR-0091(6940-09)-2
N92-32673 # p 3930 ..... ETN-92-92000
NLR-TP-91154-U
N92-32674 # p 3953 ..... AD-A250767
AFOSR-92-0313TR
N92-32675 # p 4008 ..... ETN-92-92008
NLR-TP-91401-U
N92-32676 # p 3953 ..... AD-A250784
UTRC/R92-918246-4
N92-32677 # p 3954 ..... ETN-92-92044
ISBN-90-9004656-9
N92-32678 # p 3989 ..... AD-A250877
ESD-TR-91-238
UMICH-TR-945
N92-32679 # p 4056 ..... ETN-92-92046
ISBN-90-9003729-2
N92-32680 # p 3980 ..... AD-A250878
ESD-TR-91-245
UMICH-TR-947
N92-32681 # p 4021 ..... AD-A251073
AFOSR-92-0453TR-PT-1-2
N92-32682 # p 4066 ..... AD-A251087
TR-7
N92-32683 # p 4008 ..... AD-A251095
BRL-TR-3353
N92-32684 # p 4056 ..... ETN-92-92079
IMAG-RR-859-I/M
N92-32685 # p 4056 ..... ETN-92-92080
IMAG-RR-861-M
N92-32686 # p 3980 ..... AD-A252246
ATC-189
DOT/FAA/NR-92/7
N92-32687 # p 4009 ..... ETN-92-92081
N92-32688 # p 4035 ..... AD-A252279
MRAD-TD-2271
N92-32689 # p 4050 ..... ETN-92-92111
MBB-UO-0172-90-PUB
N92-32690 # p 3977 ..... ETN-92-92119
MBB-Z-0402-91-PUB
N92-32691 # p 3929 ..... AD-A252618
AFIT/CI/CIA-92-028
N92-32692 # p 4018 ..... ETN-92-92047
ISBN-90-9004476-0
N92-32693 # p 4083 ..... CONF-911202-60
DE92-008253
LBL-30990
N92-32694 # p 4018 ..... CONF-920540-2
DE91-018864
N92-32695 # p 4025 ..... CONF-920378-1
DE92-011234
LA-UR-92-978
N92-32696 # p 3980 ..... AD-A246710
ESD-TR-91-061-VOL-1
N92-32697 # p 4061 ..... AD-A247175

DOT/FAA/AM-92/4
N92-32698 # p 4021 CE92-012241
DOE/ER-13566/5
N92-32699 # p 3967 AD-A250789
AFOSR-92-0386TR
N92-32700 # p 3989 AD-A251121
BRL-MR-3980
N92-32701 # p 4018 CONF-9103235-1
DE92-010666
SAND-91-1704C
N92-32702 # p 4066 DE92-014181
DOE/ER-40646/2
N92-32703 # p 4074 ETN-92-92042
ISBN-90-9004118-4
N92-32704 # p 3943 AIAA PAPER 92-1465
CONF-920373-4
DE92-011383
SAND-92-0662C
N92-32705 # p 4074 ETN-92-92043
ISBN-90-9004146-X
N92-32706 # p 4022 DE92-011653
UCRL-LR-109428
N92-32707 # p 4056 ETN-92-92050
ISBN-90-9004680-1
N92-32708 # p 4029 PB92-185164
N92-32709 # p 4060 ETN-92-92051
N92-32710 # p 4056 ETN-92-92067
IMAG-RR-849-M
N92-32711 # p 4056 ETN-92-92068
IMAG-RR-850-I
N92-32712 # p 4090 PB92-179456
USDA-CRIS-PKB-91-05
N92-32713 # p 4057 ETN-92-92070
IMAG-RR-857-I
N92-32714 # p 4033 NOAA-TM-ERL-WPL-220
PB92-177849
N92-32715 # p 4051 ETN-92-92076
IMAG-RR-848-M
N92-32716 # p 4060 ETN-92-92077
IMAG-RR-852-M
N92-32717 # p 4022 AD-A250667
DTRC-SME-91/74
N92-32718 # p 4060 ETN-92-92078
IMAG-RR-856-M
N92-32719 # p 3980 AD-A250710
AFOSR-92-0294TR
HAC-REF-G8200
N92-32720 # p 4033 DE92-014342
DOE/ER-60372/7
N92-32721 # p 3967 DE92-014382
MLM-3746
N92-32722 # p 3963 ECL-91-42
ETN-92-91957
N92-32723 # p 3977 DE92-014933
ORNL/SUB-86-17498/1
N92-32724 # p 3963 ECL-91-43
ETN-92-91958
N92-32725 # p 4009 ETN-92-91959
N92-32726 # p 4018 ETN-92-91961
N92-32727 # p 4009 DM-59
ETN-92-91976
N92-32728 p 3943 AERONAUTICA-ACTA-A-364-1992
ETN-92-91979
N92-32729 # p 4057 ETN-92-91980
FFA-TN-1991-41
N92-32730 # p 3930 ETN-92-91994
NLR-TP-91046-U
N92-32731 # p 4029 AD-A244196
N92-32732 # p 3930 ETN-92-91997
NLR-TP-91117-U
N92-32733 # p 4079 CONF-911131-2
DE92-010703
UCRL-JC-107386
N92-32734 # p 3940 ETN-92-91998
NLR-TP-91119-U
N92-32735 # p 4066 ETN-92-92090
LAAS-92118
N92-32736 # p 4016 DE92-011272
LA-UR-92-479
N92-32737 # p 4018 ECL-91-48
ETN-92-92092
N92-32738 # p 4075 DE92-011273
LA-UR-92-693
N92-32739 # p 3980 ETN-92-92095
TELECOM-91-E-005
N92-32740 # p 3954 ETN-92-92117
MBB-Z-0391-91-PUB
N92-32741 # p 4043 DE92-011289
M-276-REV-1
N92-32742 # p 3977 ETN-92-92118
MBB-Z-0399-91-PUB
N92-32743 # p 4057 DE92-011290
UCRL-CR-109223
N92-32744 # p 3981 DE92-011339
SAND-91-2495-VOL-1
N92-32745 # p 4079 DE92-782106
NIFS-117
N92-32746 # p 4070 NIFS-122
N92-32747 # p 4083 AD-A250368
N92-32748 # p 4053 AD-A250370
NPSCS-92-003
N92-32749 # p 3981 CTN-92-60328
DREA-CR-89-445-PT-2-VOL-2
N92-32750 # p 3939 ETN-92-91999
NLR-TP-91134-U
N92-32751 # p 4071 CONF-920315-13
DE92-011586
SLAC-PUB-5782
N92-32752 # p 3972 ETN-92-92052
N92-32753 # p 4067 ETN-92-92057
N92-32754 # p 3989 DE92-011631
DOE/NV-10031/T1
N92-32755 # p 3963 AD-D015270
NAVY-CASE-73545
US-PATENT-APPL-SN-822812
N92-32756 # p 4057 ETN-92-91847
REPT-91-97
N92-32757 # p 4018 ETN-92-92065
OUEL-1917/92
N92-32758 # p 4033 DM-60
ETN-92-91977
N92-32759 # p 4051 ETN-92-92066
OUEL-1926/92
N92-32760 # p 4083 ETN-92-92048
N92-32761 # p 4057 ETN-92-92075
IMAG-RR-846-M
N92-32762 # p 3972 ETN-92-92085
ISAL-92-0007
N92-32763 # p 4071 ETN-92-91338
OEFZS-4579
N92-32764 # p 4067 ETN-92-91509
USIP-91-03
N92-32765 # p 4009 ETN-92-92088
N92-32766 # p 4040 ETN-92-92089
LAAS-92011
N92-32767 # p 4009 ETN-92-92102
TUM-M9105
N92-32768 # p 4051 ETN-92-91663
N92-32769 # p 3931 ETN-92-91664
N92-32770 # p 4009 ETN-92-91665
N92-32771 # p 4051 ETN-92-91667
N92-32772 # p 4057 ETN-92-91670
ONERA-RF-22/3419-AY-122A
N92-32773 # p 3931 ETN-92-91671
ONERA-RSF-24/1408-AY-150A
N92-32774 # p 4022 ETN-92-91673
ONERA-RT-25/3542-RY-006-R
N92-32775 # p 3954 ETN-92-91674
ONERA-RT-26/3542-RY-007-R
N92-32776 # p 4010 ETN-92-91675
ONERA-RT-44/1621-RY-016-R
N92-32777 # p 3989 ETN-92-91676
LAAS-90028
N92-32778* # p 3939 NAS 1.26:181954
NASA-CR-181954
N92-32779 p 3967 ESDU-92015
ISBN-0-85679-823-1
N92-32780 p 3939 ESDU-92006
ISBN-0-85679-811-8
N92-32781 p 4010 ESDU-67016
ESDU-68007
ESDU-92003-PT-1
ISBN-0-85679-808-8
N92-32782 p 3931 ESDU-90030
ESDU-92002-SUPPL
ISBN-0-85679-807-X
N92-32783 # p 4022 IIT-B/CE/RR/92/2
N92-32784* # p 4010 ICASE-92-37
NAS 1.26:189690
NASA-CR-189690
N92-32785 # p 4029 ETN-92-91978
FOA-C-40292-4.3
N92-32786 # p 4010 ETN-92-91995
NLR-TP-91051-U
N92-32787 # p 3981 CTN-92-60335
N92-32788* # p 3939 A-92039
NAS 1.15:103910
NASA-TM-103910
N92-32789 # p 3981 CTN-92-60346
N92-32790 # p 4039 CTN-92-60351
DCIEM-90-23
N92-32791 # p 3954 CTN-92-60370
NRC-LTR-ST-1826
N92-32792 # p 3954 ETN-92-91672
ONERA-RT-13/7256-RY-006-R
N92-32793 # p 3990 ETN-92-91677
LAAS-90027
N92-32794 # p 3967 CTN-92-60376
UTIAS-TN-342
N92-32795 # p 4051 ETN-92-92136
N92-32796 # p 4057 ETN-92-91747
MEMO-990
N92-32797 # p 4079 ETN-92-92147
N92-32798 # p 4058 ETN-92-92049
N92-32799 # p 4058 ETN-92-92074
IMAG-RR-842-M
N92-32800 # p 3931 ETN-92-92082
ONERA-RT-47/1147-AY-146A-PT-3
N92-32801 # p 4019 ECL-91-28
ETN-92-92091
N92-32802 # p 4058 ETN-92-92093
TELECOM-91-D-007
N92-32803 # p 4058 ETN-92-92094
TELECOM-91-D-008
N92-32804 # p 4043 ETN-92-92096
TELECOM-91-E-008
N92-32805 # p 4075 ETN-92-92097
TELECOM-91-E-013
N92-32806 # p 4075 ETN-92-92098
TELECOM-91-E-016
N92-32807 # p 3981 ETN-92-92099
TELECOM-91-E-018
N92-32808 # p 4071 ETN-92-92150
IPF-91-6
N92-32809* # p 4040 A-92110
NAS 1.15:103940
NASA-TM-103940
N92-32810 # p 3990 CTN-92-60354
N92-32811 # p 3931 CTN-92-60357
DREA-CR-90-425
N92-32812 # p 3990 CRAD-1-90
CTN-92-60361
N92-32813 # p 3955 CTN-92-60367
NAE-CR-2
NRC-30833
N92-32814 # p 4103 CTN-92-60333
N92-32815 # p 4104 CTN-92-60334
N92-32816 # p 4037 CTN-92-60353
DCIEM-90-47
N92-32817 # p 4038 CTN-92-60359
N92-32818 # p 3982 CTN-92-60360
DREO-90-18
N92-32819 # p 3967 ETN-92-92125
MBB-Z-0408-91-PUB
N92-32820 # p 3982 ETN-92-92130
N92-32821 # p 4051 ETN-92-92144
N92-32822 # p 4079 ETN-92-92153
IPF-91-3
N92-32823 # p 3990 ETN-92-92155
IPF-91-5
N92-32824 # p 4010 CONF-8810234
DE92-014326
N92-32825 # p 3977 ISBN-91-540-5417-6
PB92-180892
N92-32826 # p 3964 AD-A251169
TR-128
N92-32827 # p 3990 AD-A251172
TR-53
N92-32828 # p 3955 AD-A251182
N92-32829 # p 3955 CTN-92-60377
UTIAS-TN-274
N92-32830 # p 3933 ETN-92-92001
NLR-TP-91156-U
N92-32831 # p 4011 ETN-92-92002
NLR-TP-91185-U
N92-32832 # p 4043 ETN-92-92003
NLR-TP-91193-U
N92-32833 # p 4043 ETN-92-92004
NLR-TP-91196-U
N92-32834 # p 3943 ETN-92-92005
NLR-TP-91219-U
N92-32835 # p 4011 ETN-92-92006
NLR-TP-91250-U
N92-32836 # p 4058 ETN-92-92022
ISBN-90-9003765-9
N92-32837 # p 3982 ETN-92-92023
ISBN-90-9004491-4
N92-32838 # p 4058 ETN-92-92071
IMAG-RR-839-M
N92-32839 # p 4060 ETN-92-92072
IMAG-RR-840-M
N92-32840 # p 4058 ETN-92-92145
N92-32841 # p 4029 ETN-92-92159
KFK-4975
N92-32842 # p 4061 ETN-92-92160
IRF-PREPRINT-119
N92-32843 # p 4090 ETN-92-92161
ISBN-9651-38-3803-X
VTT-RN-1154
N92-32844 # p 4036 ETN-92-91678
LAAS-91445
N92-32845 # p 3934 CTN-92-60348
N92-32846 # p 3955 CTN-92-60350
DREP-89-9
N92-32847 # p 3990 CAL-504-88P120
CTN-92-60355
N92-32848 # p 4022 CTN-92-60368

NRC-LTR-ST-1817
N92-32849 # p 3934 CTN-92-60369
IAR-AN-72
NRC-32148
N92-32850 # p 3938 CTN-92-60371
NRC-32139
N92-32851 # p 4040 CTN-92-60372
NRC-32146
N92-32852 # p 3955 CTN-92-60373
IAR-AN-71
NRC-32147
N92-32853 # p 4104 CTN-92-60375
N92-32854 # p 4054 CTN-92-60387
DCIEM-91-05
N92-32855 p 3968 CA-PATENT-1-276-814
CTN-92-60389
INT-PATENT-CLASS-C22C-19/00
INT-PATENT-CLASS-C22C-19/03
N92-32856 p 4011 CA-PATENT-APPL-SN-2-011-945
CTN-92-60391
INT-PATENT-CLASS-B05B-1/00
N92-32857 # p 4011 ETN-92-92156
KFK-4948-PT-1
N92-32858 # p 4011 ETN-92-92157
KFK-4949-PT-2
N92-32859 # p 4034 PL-TR-91-2253
N92-32860 # p 4029 LTR-91-013
PL-TR-91-2242
N92-32861 # p 3934 B-242745
GAO/IMTEC-91-25
N92-32862 # p 4104 LALP-92-51
N92-32863* # p 3972 E-6407
NAS 1.15:104531
NASA-TM-104531
N92-32864* # p 3940 AIAA PAPER 92-4109
H-1826
NAS 1.15:104255
NASA-TM-104255
N92-32865* # p 4043 NAS 1.26:190712
NASA-CR-190712
N92-32866* # p 3938 AIAA PAPER 92-4113
H-1839
NAS 1.15:104251
NASA-TM-104251
N92-32867* # p 3991 E-7285
NAS 1.15:105842
NASA-TM-105842
N92-32868* # p 4011 CMOTT-92-07
E-7194
ICOMP-92-11
NAS 1.15:105768
NASA-TM-105768
N92-32869* # p 4044 NAS 1.15:107964
NASA-TM-107964
SEL-91-006
N92-32870* # p 4044 NO REPORT NUMBER
N92-32871* # p 4044 NO REPORT NUMBER
N92-32872* # p 4044 NO REPORT NUMBER
N92-32873* # p 4044 NO REPORT NUMBER
N92-32874* # p 4044 NO REPORT NUMBER
N92-32875* # p 4044 NO REPORT NUMBER
N92-32876* # p 4044 NO REPORT NUMBER
N92-32877* # p 4045 NO REPORT NUMBER
N92-32878* # p 4045 NO REPORT NUMBER
N92-32879* # p 4045 NO REPORT NUMBER
N92-32880* # p 4045 NO REPORT NUMBER
N92-32881* # p 4045 NO REPORT NUMBER
N92-32882* # p 4046 NO REPORT NUMBER
N92-32883* # p 4046 NO REPORT NUMBER
N92-32884* # p 4046 NO REPORT NUMBER
N92-32885* # p 4019 NAS 1.26:190647
NASA-CR-190647
N92-32886* # p 4052 A-92023
NAS 1.15:103907
NASA-TM-103907
N92-32887* # p 3935 A-91156
NAS 1.15:103866
NASA-TM-103866
N92-32888* # p 4058 NAS 1.26:190745
NASA-CR-190745
OSU-725311-1
N92-32889 # p 4031 ETN-92-92083
GDR-0917
N92-32890 # p 4019 CONF-920732-2
DE92-014419
N92-32891 # p 3982 AD-A252250
SSD-TR-92-09
TR-92(2930)-3
N92-32892 # p 4083 ETN-92-92084
ISAL-91-0099
N92-32893 # p 3978 ETN-92-92120
MBB-Z-0403-91-PUB
N92-32894 # p 3968 ETN-92-92121
MBB-Z-0404-91-PUB
N92-32895 # p 3968 ETN-92-92123
MBB-Z-0406-91-PUB
N92-32896 # p 3968 DE92-014383
MLM-3747
N92-32897 # p 3968 ETN-92-92124
MBB-Z-0407-91-PUB
N92-32898 # p 4084 AD-A252209
TR-33
N92-32899 # p 3982 AD-A252385
N92-32900 # p 3931 AD-A252389
CRREL-SR-92-11
N92-32901 # p 4061 AD-A252390
N92-32902 # p 4031 AD-A252394
SSD-TR-92-07
TR-0091(6940-05)-2
N92-32903 # p 3940 CRREL-92-9
DOT/FAA/RD-92/8
N92-32904 # p 4071 DE92-016980
UCRL-LR-108095
N92-32905 # p 3982 DE92-782004
NIFS-103
N92-32906 # p 3956 AD-A249231
ARO-29044.1-MS-SBI
N92-32907 # p 4046 AD-A249242
AL-TR-1991-0140
N92-32908 # p 4026 DE91-002140
NREL/TP-253-4275
N92-32909 # p 4026 DE91-002144
NREL/TP-253-4279
N92-32910 # p 4040 CONF-9205139-1
DE92-011231
LA-UR-92-958
N92-32911 # p 4022 DE92-011907
DOE/ER-45182/6
N92-32912 # p 4071 BNL-47317
DE92-012212
N92-32913 # p 3972 AD-A251069
N92-32914 # p 3975 DE92-526270
ETDE/JP-MF-92526270
N92-32915 # p 4075 AD-A251177
N92-32916 # p 4037 AD-A252365
HEL-TN-5-92
N92-32917 # p 4046 AD-A252368
ARL-TR-92-7
N92-32918 # p 4023 AD-A252370
BRL-TR-3368
N92-32919 # p 4084 CONF-920240-5
DE92-014404
N92-32920 # p 4084 CONF-920402-19
DE92-015011
SAND-92-0128C
N92-32921 # p 4067 DE92-015012
DOE/ER-40608/1
N92-32922 # p 4067 DE92-015025
DOE/ER-40692/1
N92-32923 # p 4026 CONF-920658-2
DE92-015039
SAND-91-2789C
N92-32924 # p 4026 DE92-014698
DOE/EA-0510
N92-32925 # p 3964 CONF-9205196-1
DE92-015343
WSRC-MS-91-521
N92-32926 # p 4052 CONF-9206185-6-PT-2
DE92-017159
N92-32927 # p 3978 CONF-9206112-2
DE92-017162
N92-32928 # p 4067 CONF-9203162-2
DE92-017192
N92-32929 # p 3964 DE92-017258
UCRL-JC-110489
N92-32930 # p 4090 DE92-013572
DOE/ER-75602/4
N92-32931 # p 3964 ANL-92/15
DE92-014059
N92-32932 # p 4072 ANL/APS-CP-4
CONF-9105180
DE92-014061
N92-32933 # p 4030 DE92-014188
UCRL-ID-110176
N92-32934 # p 3943 DE92-014195
LA-11804-MS
N92-32935 # p 4075 AD-A250942
N92-32936 # p 4023 AD-A251173
UWA/DME/TR-92/69
N92-32937 # p 4052 AD-A252374
ESD-TR-92-051
MTR-11282
N92-32938 # p 4084 AD-A252399
NAVSWC-TR-91-324
N92-32939 # p 4084 AD-A252411
MTL-TR-92-38
N92-32940 # p 4084 AD-A252431
N92-32941 # p 3932 AD-A252438
DOT-VNTSC-FAA-92-2
DOT/FAA/RD-92/2
N92-32942 # p 4037 AD-A252719
NHRC-91-27
N92-32943 # p 4026 AD-D015301
NAVY-CASE-73767
US-PATENT-APPL-SN-841699
N92-32944 # p 4079 DE92-014323
DOE/ER-53198/193
N92-32945 # p 3956 CONF-920402-12
DE92-014408
N92-32946 # p 4026 CONF-9205115-1
DE92-014617
SAND-92-0680C
N92-32947 # p 4012 CONF-9108127-4
DE92-014775
UCRL-JC-108341
N92-32948* # p 4061 NAS 1.55:10103
NASA-CP-10103
N92-32949* # p 4061 NO REPORT NUMBER
N92-32950* # p 4061 NO REPORT NUMBER
N92-32951* # p 4062 AIAA PAPER 92-2164
N92-32952* # p 4062 NO REPORT NUMBER
N92-32953* # p 4062 NO REPORT NUMBER
N92-32954* # p 4062 NO REPORT NUMBER
N92-32955* # p 4062 NO REPORT NUMBER
N92-32956* # p 4062 AIAA PAPER 92-2092
N92-32957* # p 4062 NO REPORT NUMBER
N92-32958* # p 4063 NO REPORT NUMBER
N92-32959* # p 4063 NO REPORT NUMBER
N92-32960* # p 4063 NO REPORT NUMBER
N92-32961* # p 4063 NO REPORT NUMBER
N92-32962* # p 4063 NO REPORT NUMBER
N92-32963* # p 4063 NO REPORT NUMBER
N92-32964* # p 3988 NO REPORT NUMBER
N92-32965* # p 3982 E-7160
NAS 1.15:105752
NASA-TM-105752
N92-32966* # p 3983 NO REPORT NUMBER
N92-32967* # p 3983 NO REPORT NUMBER
N92-32968* # p 3983 NO REPORT NUMBER
N92-32969* # p 3983 NO REPORT NUMBER
N92-32970* # p 3983 NO REPORT NUMBER
N92-32971* # p 3983 NO REPORT NUMBER
N92-32972* # p 3983 NO REPORT NUMBER
N92-32973* # p 3984 NO REPORT NUMBER
N92-32974* # p 3984 NO REPORT NUMBER
N92-32975* # p 3984 NO REPORT NUMBER
N92-32976* # p 3984 NO REPORT NUMBER
N92-32977* # p 3984 NO REPORT NUMBER
N92-32978* # p 3984 NO REPORT NUMBER
N92-32979* # p 3985 NO REPORT NUMBER
N92-32980* # p 3985 NO REPORT NUMBER
N92-32981* # p 3985 NO REPORT NUMBER
N92-32982* # p 3985 NO REPORT NUMBER
N92-32983* # p 3985 NO REPORT NUMBER
N92-32984* # p 3985 NO REPORT NUMBER
N92-32985 # p 4090 DE92-013582
DOE/ER-75527/4
N92-32986 # p 4030 DE92-014241
PNL-8086
N92-32987 # p 3986 AD-A252728
N92-32988 # p 3940 AD-A252730
N92-32989 # p 4059 AD-A252755
NUSC-TR-7064
N92-32990 # p 4038 AD-A252371
ARI-RN-92-39
N92-32991 # p 3968 DE92-014941
ORNL/TM-11887
N92-32992 # p 4080 CONF-920515-2
DE92-014954
SAND-92-1230C
N92-32993 # p 4093 DE92-014988
DOE/ER-40317/T2
N92-32994 # p 4072 CONF-920606-19
DE92-015004
SAND-92-0770C
N92-32995 # p 4080 CONF-920311-14
DE92-015007
SAND-91-2506C
N92-32996 # p 3964 CONF-9203140-2
DE92-016996
LBL-32020
N92-32997 # p 4067 CONF-9110146-22
DE92-016999
LBL-31741
N92-32998 # p 4060 CONF-9206185-4
DE92-017245
SSCL-PREPRINT-105
N92-32999 # p 4014 CONF-9206201-2
DE92-017252
UCRL-JC-109750
N92-33000 # p 4014 CONF-9206201-4
DE92-017254
UCRL-JC-110753
N92-33001 # p 4068 CONF-9206201-3
DE92-017257
UCRL-JC-110792
N92-33002 # p 3941 NIST/SP-810-ED-1992
PB92-201094

N92-33003 # p 3975 ..... CONF-920796-3
DE92-015035
SAND-92-1130C
N92-33004 # p 4076 ..... NSF/ISI-87031-PHASE-1
PB92-188259
N92-33005 # p 3932 ..... DOT/FAA/CT-91/17
N92-33006* # p 4059 ..... ICASE-92-38
NAS 1.26:189693
NASA-CR-189693
N92-33007* # p 3941 ..... NAS 1.15:107986
NASA-TM-107986
N92-33008* p 3973 ..... NASA-CASE-LAR-14001-1
US-PATENT-APPL-SN-433812
US-PATENT-CLASS-528-125
US-PATENT-CLASS-528-128
US-PATENT-CLASS-528-172
US-PATENT-CLASS-528-185
US-PATENT-CLASS-528-229
US-PATENT-CLASS-528-352
US-PATENT-CLASS-528-353
US-PATENT-5,145,937
N92-33009* p 3965 ..... NASA-CASE-MSC-21487-1
US-PATENT-APPL-SN-429739
US-PATENT-CLASS-210-198.2
US-PATENT-CLASS-210-502.1
US-PATENT-CLASS-210-635
US-PATENT-CLASS-428-315.5
US-PATENT-CLASS-428-315.7
US-PATENT-CLASS-428-404
US-PATENT-CLASS-530-413
US-PATENT-5,141,806
N92-33010* p 4015 INT-PATENT-CLASS-B64G-1/66
NASA-CASE-MFS-28425-1
US-PATENT-APPL-SN-527462
US-PATENT-CLASS-244-158R
US-PATENT-CLASS-343-766
US-PATENT-CLASS-74-61
US-PATENT-CLASS-74-87
US-PATENT-5,129,600
N92-33011* p 3991
..... INT-PATENT-CLASS-G06F-11/10
NASA-CASE-NPO-17897-1-CU
US-PATENT-APPL-SN-480449
US-PATENT-CLASS-371-37.1
US-PATENT-5,130,990
N92-33012* # p 4092 INT-PATENT-CLASS-G21K-7/00
NASA-CASE-MFS-28013-4
US-PATENT-APPL-SN-545008
US-PATENT-APPL-SN-765979
US-PATENT-CLASS-378-210
US-PATENT-CLASS-378-43
US-PATENT-5,146,482
N92-33013* p 3943 INT-PATENT-CLASS-B64G-1/40
NASA-CASE-LAR-13780-1
US-PATENT-APPL-SN-575737
US-PATENT-CLASS-244-158R
US-PATENT-CLASS-244-160
US-PATENT-CLASS-244-172
US-PATENT-5,143,327
N92-33014* p 3973 ..... NASA-CASE-LAR-14163-1
US-PATENT-APPL-SN-560717
US-PATENT-CLASS-528-125
US-PATENT-CLASS-528-126
US-PATENT-CLASS-528-128
US-PATENT-CLASS-528-173
US-PATENT-CLASS-528-179
US-PATENT-CLASS-528-182
US-PATENT-CLASS-528-188
US-PATENT-5,147,966
N92-33015* p 3973 ..... NASA-CASE-LAR-14351-1
US-PATENT-APPL-SN-589571
US-PATENT-CLASS-528-125
US-PATENT-CLASS-528-128
US-PATENT-CLASS-528-172
US-PATENT-CLASS-528-185
US-PATENT-CLASS-528-352
US-PATENT-CLASS-528-353
US-PATENT-CLASS-564-315
US-PATENT-5,145,942
N92-33016* p 4015 INT-PATENT-CLASS-A61B-5/02
NASA-CASE-LAR-14088-1-CU
US-PATENT-APPL-SN-552670
US-PATENT-CLASS-128-715
US-PATENT-CLASS-128-775
US-PATENT-5,140,992
N92-33017* p 4076 INT-PATENT-CLASS-H01J-40/14
NASA-CASE-LAR-14402-1-CU
US-PATENT-APPL-SN-586369
US-PATENT-CLASS-250-227.21
US-PATENT-CLASS-250-231.19
US-PATENT-CLASS-358-12
US-PATENT-CLASS-73-705
US-PATENT-5,146,083
N92-33018* p 4019 ..... NASA-CASE-MSC-21463-1
US-PATENT-APPL-SN-636531
US-PATENT-CLASS-244-161
US-PATENT-CLASS-294-65.5
US-PATENT-CLASS-294-66.2
US-PATENT-CLASS-294-86.4
US-PATENT-CLASS-294-907
US-PATENT-CLASS-414-737
US-PATENT-CLASS-901-40
US-PATENT-5,145,227
N92-33019* p 4054
..... INT-PATENT-CLASS-G05B-19/42
NASA-CASE-NPO-17852-1-CU
US-PATENT-APPL-SN-615668
US-PATENT-CLASS-318-567
US-PATENT-CLASS-318-568.11
US-PATENT-CLASS-318-568.19
US-PATENT-CLASS-364-191
US-PATENT-CLASS-395-90
US-PATENT-CLASS-901-47
US-PATENT-5,150,026
N92-33020* p 3978
..... INT-PATENT-CLASS-B29C-65/48
NASA-CASE-LAR-14446-1
US-PATENT-APPL-SN-699288
US-PATENT-APPL-156-241
US-PATENT-APPL-156-285
US-PATENT-APPL-156-293
US-PATENT-APPL-264-272.15
US-PATENT-APPL-29-856
US-PATENT-5,149,387
N92-33021* p 3991 INT-PATENT-CLASS-G01K-7/30
NASA-CASE-LAR-14567-1-CU
US-PATENT-APPL-SN-773376
US-PATENT-CLASS-374-175
US-PATENT-CLASS-73-1H
US-PATENT-CLASS-73-571
US-PATENT-5,146,780
N92-33022* p 4076
..... INT-PATENT-CLASS-G02B-27/42
INT-PATENT-CLASS-G03B-1/16
NASA-CASE-NPO-18379-1-CU
US-PATENT-APPL-SN-797569
US-PATENT-CLASS-359-559
US-PATENT-CLASS-359-561
US-PATENT-CLASS-359-7
US-PATENT-5,150,228
N92-33023 # p 4085 ..... CONF-9104192-11
DE91-014224
N92-33024 # p 4080 ..... DE92-013904
DOE/PC-90274/T14
MHD-ITC-91-039
N92-33025 # p 4085 ..... DE92-014811
DOE/ER-45199/2
N92-33026 # p 4085 ..... CONF-920402-26
DE92-015205
LA-UR-92-1495
N92-33027 # p 4104 ..... AD-A253691
N92-33028* p 4076 INT-PATENT-CLASS-H01J-3/14
NASA-CASE-NPO-18098-1-CU
US-PATENT-APPL-SN-633746
US-PATENT-CLASS-250-216
US-PATENT-CLASS-359-241
US-PATENT-5,130,530
N92-33029* p 3965 ..... NASA-CASE-MSC-21584-1
US-PATENT-APPL-SN-638600
US-PATENT-CLASS-210-209
US-PATENT-CLASS-210-266
US-PATENT-CLASS-210-269
US-PATENT-CLASS-210-287
US-PATENT-CLASS-210-670
US-PATENT-CLASS-210-748
US-PATENT-CLASS-210-758
US-PATENT-5,141,636
N92-33030* p 3991 INT-PATENT-CLASS-B23K-9/24
NASA-CASE-MFS-29766-1
US-PATENT-APPL-SN-677182
US-PATENT-CLASS-219-72
US-PATENT-CLASS-219-75
US-PATENT-5,149,932
N92-33031* p 4019 INT-PATENT-CLASS-F16H-21/16
INT-PATENT-CLASS-F16H-49/00
NASA-CASE-LAR-14515-1-CU
US-PATENT-APPL-SN-678551
US-PATENT-CLASS-74-25
US-PATENT-CLASS-74-437
US-PATENT-5,146,803
N92-33032* p 4038 INT-PATENT-CLASS-A61M-1/00
NASA-CASE-GSC-13306-1
US-PATENT-APPL-SN-674828
US-PATENT-CLASS-148-402
US-PATENT-CLASS-606-106
US-PATENT-CLASS-606-127
US-PATENT-CLASS-606-78
US-PATENT-5,133,721
N92-33033 # p 3956 ..... AGARD-R-785
ISBN-92-835-0666-9
N92-33034 # p 3956 ..... NO REPORT NUMBER
N92-33035 # p 3956 ..... NO REPORT NUMBER
N92-33036 # p 3956 ..... NO REPORT NUMBER
N92-33037 # p 3957 ..... NO REPORT NUMBER
N92-33038 # p 3957 ..... NO REPORT NUMBER
N92-33039 # p 3957 ..... NO REPORT NUMBER
N92-33040 # p 3957 ..... NO REPORT NUMBER
N92-33041 # p 3957 ..... NO REPORT NUMBER
N92-33042 # p 3957 ..... NO REPORT NUMBER
N92-33043 # p 3957 ..... NO REPORT NUMBER
N92-33044 # p 3958 ..... NO REPORT NUMBER
N92-33045 # p 3958 ..... NO REPORT NUMBER
N92-33046 # p 3958 ..... NO REPORT NUMBER
N92-33047 # p 3958 ..... NO REPORT NUMBER
N92-33048 # p 3958 ..... NO REPORT NUMBER
N92-33049 # p 3958 ..... NO REPORT NUMBER
N92-33050 # p 3959 ..... NO REPORT NUMBER
N92-33051 # p 3959 ..... NO REPORT NUMBER
N92-33052 # p 3959 ..... NO REPORT NUMBER
N92-33053 # p 3959 ..... NO REPORT NUMBER
N92-33054* # p 3959 ..... NO REPORT NUMBER
N92-33055 # p 4060 ..... ETN-92-92035
ISBN-90-6275-635-2
N92-33056 # p 4039 ..... ETN-92-92086
ISAL-91-0095
N92-33057* p 4041 ... NASA-CASE-NPO-17997-1-CU
US-PATENT-APPL-SN-481013
US-PATENT-CLASS-359-107
US-PATENT-CLASS-359-108
US-PATENT-CLASS-359-559
US-PATENT-CLASS-359-561
US-PATENT-CLASS-365-49
US-PATENT-CLASS-382-31
US-PATENT-CLASS-382-32
US-PATENT-5,131,055
N92-33058 # p 4059 ..... CWI-BS-R9115
ETN-92-91641
N92-33059 # p 3973 ..... C-238
ISBN-951-22-0900-4
PB92-180710
N92-33060 # p 4016 ..... NIST/TN-1353
PB92-189547
N92-33061 # p 3991 ..... B91-0099
NIST/TN-1348
PB92-189554
N92-33062 # p 4030 ..... EPA/DF/DK-92/040A
PB92-169523
N92-33063* # p 3932 ..... NAS 1.26:190702
NASA-CR-190702
N92-33064* # p 3944 ..... E-7170
NAS 1.15:105758
NASA-TM-105758
N92-33065 # p 3973 ..... ETN-92-92024
N92-33066 # p 4012 ..... ETN-92-92041
ISBN-90-9004317-9
N92-33067 # p 4068 ..... DE92-016316
DOE/ER-40388/90
N92-33068 # p 3992 ..... CONF-920515-26
DE92-017523
LA-UR-92-1915
N92-33069 # p 4088 ..... CONF-9110397-1
DE92-017530
LA-UR-92-1853
N92-33070 # p 4072 ..... DE92-017552
SLAC-PUB-5748
N92-33071 # p 4046 ..... DE92-017870
DOE/ER-25095/1
N92-33072 # p 4027 ..... DE92-540920
ISBN-951-47-4472-1
KTM/E-B-105
N92-33073 # p 4034 ..... NO REPORT NUMBER
N92-33074* # p 4076 ..... NAS 1.26:190611
NASA-CR-190611
RPC-TR-1276-102-G-AR
N92-33075* # p 3959 ..... NAS 1.26:190659
NASA-CR-190659
N92-33076 # p 4023 ..... CTN-92-60379
NRC-LTR-ST-1831
N92-33077 # p 4019 ..... CNRC-33030
CTN-92-60380
IMI-91RT-31200-1155-G
N92-33078 # p 3959 ..... CTN-92-60381
NRC-LTR-ST-1833
N92-33079 # p 4039 ..... CTN-92-60386
DCIEM-91-20
N92-33080* # p 3933 ..... A-92156
NAS 1.15:103959
NASA-TM-103959
N92-33081* # p 3969 ..... NAS 1.26:190816
NASA-CR-190816
N92-33082 # p 4012 ..... CONF-9206185-7
DE92-017313
UCRL-JC-110555
N92-33083 # p 4068 ..... DE92-014124
DOE/ER-13950/T1
N92-33084 # p 4090 ..... DE92-017342
ES/ER/TM-34-PHASE-1
N92-33085 # p 4020 ..... CONF-9205123-12

DE92-017802
N92-33086 # p 4104 ... PB92-183219
N92-33087 # p 4030 ... EPA/230/R-92/003
PB92-201144
N92-33088 # p 4091 ... PB92-204627
WHOI-92-19
N92-33089 # p 4016 ... AD-A252213
TTC-2459-R
N92-33090 # p 4027 ... CONF-9109393
DE92-530733
N92-33091* # p 4046 ... NAS 1.26:190070
NASA-CR-190070
N92-33092* # p 4046 ... NAS 1.26:190239
NASA-CR-190239
N92-33093* # p 4047 ... NAS 1.26:190388
NASA-CR-190388
N92-33094* # p 4092 ... NAS 1.26:184340
NASA-CR-184340
RS-30
SAO-AXAF-FR-92-004
N92-33095 # p 4076 ... AD-D015285
US-PATENT-APPL-SN-878597
N92-33096* # p 4091 ... NAS 1.26:190644
NASA-CR-190644
N92-33097* # p 4031 ... L-16879
NAS 1.61:1275
NASA-RP-1275
N92-33098 # p 3934 ... DOT/FAA/RD-92/23
N92-33099 p 4039 ... ISBN-0-87703-343-9
N92-33100* # p 4052 ... NAS 1.26:189632-VOL-1
NASA-CR-189632-VOL-1
N92-33101* # p 4052 ... NAS 1.26:189632-VOL-2
NASA-CR-189632-VOL-2
N92-33102 # p 3938 ... CTN-92-60378
UTIAS-TN-271
N92-33103* # p 4036 ... NAS 1.15:103598
NASA-TM-103598
N92-33104* # p 4023 ... NAS 1.15:107591
NASA-TM-107591
N92-33105 # p 3938 ... DOT/FAA/CT-91/28
N92-33106* # p 4105 ... A-91218
NAS 1.15:103902
NASA-TM-103902
N92-33107* # p 3940 ... NAS 1.26:190736
NASA-CR-190736
N92-33108 # p 3975 ... DE92-013802
DOE/PC-90044/T1
N92-33109 # p 4088 ... DE92-014507
IS-T-1599
N92-33110* # p 4012 ... ICASE-92-39
NAS 1.26:189692
NASA-CR-189692
N92-33111 # p 4085 ... DE92-014510
IS-T-1591
N92-33112* # p 3944 ... NAS 1.15:107656
NASA-TM-107656
N92-33113* # p 4012 ... A-92041
NAS 1.15:103911
NASA-TM-103911
N92-33114 # p 4016 ... ANL/CP-75942
CONF-920574-9
DE92-016320
N92-33115 # p 3969 ... CONF-920673-6
DE92-016897
N92-33116 # p 3969 ... CONF-9206174-1
DE92-014783
UCRL-JC-110177
N92-33117 # p 4085 ... DE92-016921
LBL-32253
N92-33118 # p 4047 ... ANL/MCS-TM-165
DE92-017309
N92-33119 # p 4103 ... DE92-017390
DOE/ER-40452/7
N92-33120 # p 3969 ... CONF-9206195-3
DE92-017528
LA-UR-92-1870
N92-33121 # p 3965 ... DE92-017978
DOE/ER-13966/3
N92-33122 # p 4072 ... CONF-920315-39
DE92-014795
UCRL-JC-108513
N92-33123 # p 3975 ... DE92-013833
DOE/PC-90049/T4
N92-33124 # p 4013 ... DE92-014813
DOE/ER-13641/3
N92-33125 # p 4030 ... DE92-013847
DOE/PC-91293/1
N92-33126 # p 3965 ... DE92-014834
UCRL-TT-108428
N92-33127 # p 4085 ... CONF-920402-7
DE92-013861
N92-33128 # p 3992 ... ANL/CP-75802
CONF-920432-13
DE92-014862
N92-33129 # p 3969 ... JPRS-UMS-92-011
N92-33130 # p 4072 ... ANL/CP-74658
CONF-920631-36
DE92-014863
N92-33131* # p 4047 ... NAS 1.26:190607
NASA-CR-190607
N92-33132 # p 3969 ... CONF-910945-12
DE92-014885
UCRL-JC-107065
N92-33133 # p 4068 ... ETN-92-91981
RAL-91-085
N92-33134 # p 4073 ... CONF-920331-47
DE92-014896
SSCL-PREPRINT-84
N92-33135 # p 4068 ... ETN-92-91982
RAL-92-012
N92-33136 # p 4086 ... BNL-47236
CONF-9109102-7
DE92-014687
N92-33137 # p 4068 ... ETN-92-91983
RAL-92-015-PREPRINT
N92-33138 # p 4027 ... DE92-001247
NREL/TP-253-4471
N92-33139* # p 4023 ... ETN-92-91996
NAS 1.26:190822
NASA-CR-190822
NLR-TP-91052-U
N92-33140 # p 4013 ... DE92-015452
DOE/PC-88948/T14
N92-33141 # p 3975 ... DE92-015592
DOE/PC-89866/T5
N92-33142 # p 4047 ... ETN-92-92036
ISBN-90-72125-29-0
N92-33143 # p 3986 ... ETN-92-92037
ISBN-90-9004420-5
N92-33144 # p 3992 ... ETN-92-92038
ISBN-90-9003883-3
N92-33145 # p 3992 ... ETN-92-92039
ISBN-90-9003899-X
N92-33146 # p 4077 ... ETN-92-92040
ISBN-90-9003887-6
N92-33147 # p 4092 ... GPO-55-260-VOL-1
ISBN-0-16-038832-5
N92-33148 # p 4069 ... CONF-910836-5
DE92-013765
SLAC-PUB-5720
N92-33149* # p 3935 ... AIAA PAPER 92-4176
H-1857
NAS 1.15:104256
NASA-TM-104256
N92-33150 # p 4027 ... DE92-013776
SAND-92-0385
N92-33151 # p 4020 ... AD-A250934
AFOSR-92-0428TR
N92-33152 # p 3986 ... AD-A252494
CSDL-T-1131
N92-33153 # p 4031 ... DE92-014495
DOE/ER-61064/2
N92-33154 # p 4080 ... DE92-013901
DOE/ER-53198/190
N92-33155 # p 4017 ... CONF-9202111-1
DE92-014504
LBL-31969
N92-33156 # p 4030 ... DE92-013993
PNL-8015
N92-33157 p 3973 ... AD-D015294
US-PATENT-APPL-SN-561750
US-PATENT-CLASS-505-1
US-PATENT-5,082,826
N92-33158 # p 3969 ... CONF-920819-7
DE92-011049
N92-33159 # p 4013 ... DE92-017292
LA-12303-MS
N92-33160* # p 4063 ... NAS 1.15:104170
NASA-TM-104170
N92-33161 p 3940 ... AD-D015308
US-PATENT-APPL-SN-620671
US-PATENT-CLASS-244-315
US-PATENT-5,082,200
N92-33162 p 3944 ... AD-D015309
US-PATENT-APPL-SN-664010
US-PATENT-CLASS-244-324
US-PATENT-5,106,034
N92-33163 # p 4034 ... NOAA-TM-NWS-WR-217
PB92-196104
N92-33164 # p 4069 ... CONF-9203154-3
DE92-016351
FNAL/C-92/161-E
N92-33165 p 4017 ... AD-D015310
US-PATENT-APPL-SN-705048
US-PATENT-5,086,432
N92-33166 # p 3944 ... DE92-017358
SAND-90-1439
N92-33167 p 4073 ... AD-D015311
US-PATENT-APPL-SN-560959
US-PATENT-CLASS-376-154
US-PATENT-5,078,951
N92-33168 # p 4080 ... ANL/FPP/TM-262
DE92-017749
N92-33169 p 3992 ... AD-D015312
US-PATENT-APPL-SN-444253
US-PATENT-CLASS-333-238
US-PATENT-5,075,655
N92-33170 p 3973 ... AD-D015313
US-PATENT-APPL-SN-516585
US-PATENT-CLASS-423-446
US-PATENT-5,075,094
N92-33171 p 3986 ... AD-D015323
US-PATENT-APPL-SN-687602
US-PATENT-CLASS-342-21
US-PATENT-5,095,312
N92-33172 p 3986 ... AD-D015325
US-PATENT-APPL-SN-249443
US-PATENT-CLASS-342-465
US-PATENT-5,073,784
N92-33173 # p 4034 ... PB92-205137
USGS/G-1731
N92-33174 p 3960 ... AD-D015326
US-PATENT-APPL-SN-662678
US-PATENT-CLASS-425-50A
US-PATENT-5,116,216
N92-33175 p 3992 ... AD-D015329
US-PATENT-APPL-SN-631582
US-PATENT-CLASS-329-318
US-PATENT-5,097,221
N92-33176 # p 3929 ... PB92-197334
N92-33177 p 3974 ... AD-D015330
US-PATENT-APPL-SN-627670
US-PATENT-CLASS-524-396
US-PATENT-5,089,551
N92-33178* # p 4091 ... NAS 1.26:190629
NASA-CR-190629
N92-33179 # p 4073 ... BNL-47503
DE92-014016
N92-33180 # p 4017 ... DE92-014031
DOE/PC-88948/T2
N92-33181 # p 4036 ... DE92-014032
DOE/ER-60673/T4
N92-33182 # p 4073 ... DE92-014054
DOE/ER-01428/T10
N92-33183 # p 3993 ... DE92-016358
LBL-31931
N92-33184 # p 4054 ... CONF-9209143-2
DE92-016373
N92-33185 # p 3965 ... CONF-9207105-1
DE92-016545
N92-33186 # p 4069 ... DE92-016837
DOE/ER-40425/256
N92-33187 # p 4069 ... COLO-HEP-287
DE92-016844
DOE/ER-40672/1
N92-33188 # p 4015 ... DE92-016872
DOE/ER-61373/1
N92-33189 p 4047 ... CTN-92-60550
ISBN-0-315-58989-2
N92-33190 p 4086 ... ITN-92-85165
N92-33191 p 3986 ... CTN-92-60551
ISBN-0-315-63332-8
N92-33192 p 3987 ... CTN-92-60552
ISBN-0-315-63282-8
N92-33193 p 3993 ... CTN-92-60553
ISBN-0-315-63272-0
N92-33194* # p 3933 ... A-91203
NAS 1.15:103880
NASA-TM-103880
N92-33195 p 3993 ... CTN-92-60554
ISBN-0-315-60747-5
N92-33196* # p 4047 ... NAS 1.26:190826
NASA-CR-190826
N92-33197 p 4032 ... CTN-92-60519
ISBN-0-315-59091-2
N92-33198 p 4035 ... CTN-92-60520
ISBN-0-315-55106-2
N92-33199 p 4088 ... CTN-92-60522
ISBN-0-315-55158-5
N92-33200 p 4023 ... CTN-92-60523
ISBN-0-315-57756-8
N92-33201 p 4048 ... CTN-92-60525
ISBN-0-315-56074-6
N92-33202 p 4077 ... CTN-92-60526
ISBN-0-315-55748-6
N92-33203 p 4054 ... CTN-92-60528
ISBN-0-315-52925-3
N92-33204 p 4048 ... CTN-92-60539
ISBN-0-315-57231-0
N92-33205* # p 4041 ... CSCC-A-9
NAS 1.15:107680
NASA-TM-107680
N92-33206 p 3987 ... CTN-92-60545
ISBN-0-315-59028-9
N92-33207 p 3987 ... CTN-92-60546
ISBN-0-315-60464-6
N92-33208 p 3993 ... CTN-92-60547
ISBN-0-315-60456-5

N92-33209 p 3987 ..... CTN-92-60548
ISBN-0-315-58991-4
N92-33210 p 4048 ..... CTN-92-60527
ISBN-0-315-57864-5
N92-33211 p 3993 ..... CTN-92-60555
ISBN-0-315-59034-3
N92-33212 p 4048 ..... CTN-92-60556
ISBN-0-315-63509-6
N92-33213 p 3987 ..... CTN-92-60567
ISBN-0-315-61378-5
N92-33214 p 4048 ..... CTN-92-60529
ISBN-0-315-54272-1
N92-33215 p 4049 ..... CTN-92-60530
ISBN-0-315-51189-3
N92-33216 p 4052 ..... CTN-92-60531
ISBN-0-315-54414-7
N92-33217 p 4053 ..... CTN-92-60532
ISBN-0-315-54380-9
N92-33218 p 4054 ..... CTN-92-60533
ISBN-0-315-51158-3
N92-33219 p 4055 ..... CTN-92-60534
ISBN-0-315-54378-7
N92-33220 # p 4035 ..... AD-A252280
NOSC/TR-1492
N92-33221 # p 4086 ..... ANL/CP-76482
CONF-9206202-1
DE92-016774
N92-33222 # p 3965 ..... DE92-016833
DOE/ER-13508/4
N92-33223 p 4080 ..... CTN-92-60516
ISBN-0-315-58015-1
N92-33224 p 4053 ..... CTN-92-60535
ISBN-0-315-56107-6
N92-33225 p 4034 ..... CTN-92-60517
ISBN-0-315-57159-4
N92-33226 p 4013 ..... CTN-92-60521
ISBN-0-315-62369-1
N92-33227 p 4049 ..... CTN-92-60536
ISBN-0-315-51346-2
N92-33228 p 4024 ..... CTN-92-60524
ISBN-0-315-57834-3
N92-33229 p 4049 ..... CTN-92-60540
ISBN-0-315-57272-8
N92-33230 p 4049 ..... CTN-92-60541
ISBN-0-315-50983-X
N92-33231 p 4059 ..... CTN-92-60542
ISBN-0-315-54684-0
N92-33232 p 4049 ..... CTN-92-60537
ISBN-0-315-56113-0
N92-33233 p 4024 ..... CTN-92-60543
ISBN-0-315-49130-2
N92-33234 p 3994 ..... CTN-92-60544
ISBN-0-315-65025-7
N92-33235 p 4053 ..... CTN-92-60538
ISBN-0-315-57208-6
N92-33236 p 4055 ..... CTN-92-60549
ISBN-0-315-59030-0
N92-33237* # p 4091 ..... NAS 1.15:108171
NASA-TM-108171
N92-33238 # p 4105 ..... AD-A253692
N92-33239* # p 4077 ..... NAS 1.26:4452
NASA-CR-4452
N92-33240 # p 3975 ..... AGARD-CP-511
ISBN-92-835-0679-0
N92-33241 # p 3976 ..... NO REPORT NUMBER
N92-33242 # p 3976 ..... NO REPORT NUMBER
N92-33243 # p 3976 ..... NO REPORT NUMBER
N92-33244 # p 3976 ..... NO REPORT NUMBER
N92-33245 # p 3945 ..... NO REPORT NUMBER
N92-33246 # p 3966 ..... DE92-016682
DOE/PC-90305/T7
N92-33247 # p 3974 ..... ANL/CP-76309
CONF-9205213-1
DE92-016779

Appendix

NASA SCIENTIFIC AND TECHNICAL INFORMATION PROGRAM PRODUCTS AND SERVICES

The NASA Scientific and Technical Information (STI) Program provides for the collection and announcement of aerospace-related reports and literature obtained worldwide through agreements and exchanges. The result of the collection is the comprehensive NASA STI Database that covers aeronautics, space, and supporting disciplines.

The STI Database, documents generated or obtained by NASA, and products and services derived from or supporting the database are made available to the NASA research community and to the public. Descriptions and sources of these items are presented in the following pages.

Scientific and Technical Aerospace Reports (*STAR*) is an abstract journal, listing citations with abstracts for aerospace-related reports obtained from worldwide sources. *STAR* is issued on the 8th and 23rd of each month and announces current documents that have been entered into the NASA STI Database during the previous two weeks. The reports are of the following types:

- NASA, NASA contractor, and NASA grantee reports;
- Reports issued by other U.S. Government agencies, domestic and foreign institutions, universities, and private firms;
- Translations in report form;
- NASA-owned patents and patent applications;
- Other U.S. Government agency and foreign patents and patent applications;
- Domestic and foreign dissertations and theses.

Journal, book, and conference literature, journal translations, and certain foreign dissertations having the same subject scope as *STAR* are announced in a companion journal, *International Aerospace Abstracts* (*IAA*). *IAA* is issued on the 1st and 15th of each month and is available from the American Institute of Aeronautics and Astronautics, Technical Information Service, 555 West 57th Street, 12th Floor, New York, NY 10019.

ELIGIBILITY AND REGISTRATION FOR NASA STI PRODUCTS AND SERVICES

Organizations of the type listed below that have registered with NASA can receive products and services.

- NASA offices and installations, contractors, subcontractors, grantees, and consultants;
- Other U.S. Government agencies and their contractors;
- Libraries in the United States that have arrangements with NASA to maintain collections of NASA documents for public reference;
- Other organizations in the United States having a need for NASA documents in work related to aeronautics and space research;
- Organizations abroad that have established reciprocal documents exchange arrangements with NASA.

The central service points — central points of document acquisition and control within qualified organizations — or individuals are eligible to register for NASA STI products and services. Domestic organizations or individuals may be eligible to receive various classes of NASA publications and services and should address their requests for registration or further information to:

NASA Center for AeroSpace Information
ATTN: Registration Services
P.O. Box 8757
Baltimore, MD 21240-0757
301-621-0390

Organizations abroad should direct requests to:

National Aeronautics and Space Administration
Scientific and Technical Information Program (JTT)
International STI Program
Washington, DC 20546-0001
USA
703-271-5640

SUBJECT SCOPE

The subject scope of *STAR* and *IAA* includes all aspects of aeronautics and space research and development, supporting basic and applied research, and applications. Aerospace aspects of Earth resources, energy development, conservation, oceanography, environmental protection, urban transportation, and other topics of high national priority are also covered.

HOW TO USE *STAR* SUBJECT CATEGORIES

Abstracts in *STAR* are categorized by 10 major subject divisions that are divided further into 76 specific subject categories. The subject divisions and categories are listed in the Table of Contents together with a note for each that defines its scope and provides any cross-references. For example:

16 SPACE TRANSPORTATION
Includes passenger and cargo space transportation, e.g., shuttle operations; and space rescue techniques. For related information see also *03 Air Transportation and Safety* and *18 Spacecraft Design, Testing and Performance.* For space suits see *54 Man/System Technology and Life Support.*

CROSS-REFERENCES

Individual *STAR* abstracts are not ordinarily cross-referenced, except for certain conference reports or book translations that have had separate abstracts written for their component papers or chapters. Citations and abstracts of the components follow immediately after those of the parent document. When the subject content of a component differs sufficiently from the general content of the parent, a cross-reference citation also is printed at the end of the category to which it normally would have been assigned if it were independent.

DOCUMENTS ON MICROFICHE

Documents available on microfiche are designated by a pound sign (#) following the accession number.

LIMITED REPRODUCIBILITY

A note of limited reproducibility appears in the citation, if there are factors affecting the reproducibility of more than 20% of the document. These factors include faint or broken type, color photographs, black and white photographs, foldouts, dot matrix print, or some other factor that limits the reproducibility of the document. This notation also appears on the microfiche header.

COLOR COPIES

An increasing number of NASA scientific and technical reports are being produced with color graphs, charts, illustrations, and photographs. An indication that a document has color pages follows the source and pricing (SAP) information in the *STAR* citation.

Registered users of the NASA Scientific and Technical Information Program will receive ordered documents with color at no additional cost, as long as stock copies of the document are available. Otherwise, an additional fee of $2.00 per color page will be charged. The NASA Center for AeroSpace Information staff will contact registered users to determine individual user's needs.

NASA PATENTS AND PATENT APPLICATIONS

Patents and patent applications owned by NASA are announced in *STAR* under appropriate subject categories and are referenced in the *STAR* indexes. In the Report/Accession Number Index, patents are indexed by the NASA Case Number, and the U.S. Patent Class. Patent applications are indexed by the NASA Case Number and the U.S. Patent Application Serial Number.

Printed copies of patents (which are not microfiched) are available for purchase from the U.S. Patent and Trademark Office.

When ordering patents, the U.S. Patent Number should be used, and payment must be remitted in advance, by money order or check payable to the Commissioner of Patents and Trademarks. Prepaid purchase coupons for ordering are also available from the U.S. Patent and Trademark Office.

NASA patent application specifications are sold in both paper copy and microfiche by the NASA Center for AeroSpace Information (CASI). The N accession number should be used in ordering either paper copy or microfiche from CASI.

The patents and patent applications announced in *STAR* are owned by NASA and are available for royalty-free licensing. Requests for licensing terms and further information should be addressed to:

National Aeronautics and Space Administration
Associate General Counsel for Intellectual Property
Code GP
Washington, DC 20546-0001

SOURCES FOR DOCUMENTS

One or more sources from which a document announced in *STAR* is available to the public is given in each citation. The most commonly indicated sources and their acronyms or abbreviations are listed below, and their addresses are listed on page A-6. If the publication is available from a source other than those listed, the publisher and address will be displayed on the availability line or in combination with the corporate source line.

Avail: CASI. Sold by the NASA Center for AeroSpace Information. Prices for hard copy (HC) and microfiche (MF) are indicated by a price code following the letters HC or MF in the *STAR* citation. Current values for the price codes are given in the tables on page A-7.

NOTE ON ORDERING DOCUMENTS: When ordering publications from CASI, use the N accession number or other report number. It is also advisable to cite the title and other bibliographic identification.

Avail: SOD (or GPO). Sold by the Superintendent of Documents, U.S. Government Printing Office, in hard copy.

Avail: BLL (formerly NLL): British Library Lending Division, Boston Spa, Wetherby, Yorkshire, England. Photocopies available from this organization at the price shown. (If none is given, address inquiry to the BLL.)

Avail: DOE Depository Libraries. Organizations in U.S. cities and abroad that maintain collections of Department of Energy reports, usually in microfiche form, are listed in *Energy Research Abstracts*. Services available from the DOE and its depositories are described in a booklet, *DOE Technical Information Center - Its Functions and Services* (TID-4660), which may be obtained without charge from the DOE Technical Information Center.

Avail: ESDU. Pricing information on specific data, computer programs, and details on Engineering Sciences Data Unit (ESDU) topic categories can be obtained from ESDU International Ltd. Requesters in North America should use the Virginia address while all other requesters should use the London address, both of which are on page A-6.

Avail: Fachinformationszentrum, Karlsruhe. Gesellschaft für wissenschaftlich-technische Information mbH 7514 Eggenstein-Leopoldshafen 2, Germany.

Avail: HMSO. Publications of Her Majesty's Stationery Office are sold in the U.S. by Pendragon House, Inc. (PHI), Redwood City, CA. The U.S. price (including a service and mailing charge) is given, or a conversion table may be obtained from PHI.

Avail: Issuing Activity, or Corporate Author, or no indication of availability. Inquiries as to the availability of these documents should be addressed to the organization shown in the citation as the corporate author of the document.

Avail: NASA Public Document Rooms. Documents so indicated may be examined at or purchased from the National Aeronautics and Space Administration (JBD-4), Public Documents Room (Room 1H23), Washington, DC 20546-0001, or public document rooms located at NASA installations, and the NASA Pasadena Office at the Jet Propulsion Laboratory.

Avail: NTIS. Sold by the National Technical Information Service. Initially distributed microfiche under the NTIS SRIM (Selected Research in Microfiche) are available. For information concerning this service, consult the NTIS Subscription Section, Springfield, VA 22161.

Avail: Univ. Microfilms. Documents so indicated are dissertations selected from *Dissertation Abstracts* and are sold by University Microfilms as xerographic copy (HC) and microfilm. All requests should cite the author and the Order Number as they appear in the citation.

Avail: US Patent and Trademark Office. Sold by Commissioner of Patents and Trademarks, U.S. Patent and Trademark Office, at the standard price of $1.50 each, postage free. (See discussion of NASA patents and patent applications below.)

Avail: (US Sales Only). These foreign documents are available to users within the United States from the National Technical Information Service (NTIS). They are available to users outside the United States through the International Nuclear Information Service (INIS) representative in their country, or by applying directly to the issuing organization.

Avail: USGS. Originals of many reports from the U.S. Geological Survey, which may contain color illustrations, or otherwise may not have the quality of illustrations preserved in the microfiche or facsimile reproduction, may be examined by the public at the libraries of the USGS field offices whose addresses are listed on page A-6. The libraries may be queried concerning the availability of specific documents and the possible utilization of local copying services, such as color reproduction.

FEDERAL DEPOSITORY LIBRARIES: To provide the general public with greater access to U.S. Government publications, Congress established the Federal Depository Library Program under the Government Printing Office (GPO), with 53 regional depositories responsible for permanent retention of material, inter-library loan, and reference services. (These libraries are not sales outlets.) At least one copy of nearly every NASA and NASA-sponsored publication, either in printed or microfiche format, is received and retained by the 53 regional depositories. A list of the regional GPO libraries, appears on page A-8. A local library can contact a regional depository library to help locate specific reports, or direct contact may be made by an individual.

PUBLIC COLLECTION OF NASA DOCUMENTS

An extensive collection of NASA and NASA-sponsored publications is maintianed by the British Library Lending Divison, Boston Spa, Wetherby, Yorkshire, England, for public access. The British Library Lending Division also has available many of the non-NASA publications cited in *STAR*.

European requesters may purchase facsimile copy or microfiche of NASA and NASA-sponsored documents, those identified by both the symbols # and * from ESA—Information Retrieval Service, European Space Agency, 8-10 rue Mario-Nikis, 75738 Paris CEDEX 15, France.

SUBMITTING DOCUMENTS

All users of this abstract service are urged to forward reports to be considered for announcement in *STAR*. This will aid NASA in its efforts to provide the fullest possible coverage of all scientific and technical publications that might support aeronautics and space research and development. If you have prepared relevant reports (other than those you will transmit to NASA, DOD, or DOE through the usual contract- or grant-reporting channels), please send them for consideration to the NASA Center for AeroSpace Information, P.O. Box 8757, Baltimore, MD 21240-0757.

Reprints of journal articles, book chapters, and conference papers are also welcome. These will be considered for announcement in *STAR*'s companion journal, *IAA*.

You may specify a particular source to be included in a report announcement if you wish; otherwise the report will be placed on a public sale at the NASA Center for AeroSpace Information. Copyrighted publications will be announced but not distributed or sold.

PURCHASE OF *STAR*

STAR is publicly available on annual subscription from the NASA Center for AeroSpace Information (CASI) at $114.00.

STAR is available to registered users on annual subscription from the NASA Center for AeroSpace Information, ATTN: Registration Services, P.O. Box 8757, Baltimore, MD 21240-0757.

Microfiche of the abstract sections of *STAR* are available, on annual subscription, from CASI. Annual subscription rates are $216.00 North America; $432.00 foreign.

ADDRESSES OF ORGANIZATIONS

American Institute of Aeronautics and Astronautics
Technical Information Service
555 West 57th Street, 12th Floor
New York, New York 10019

British Library Lending Division,
Boston Spa, Wetherby, Yorkshire,
England

Commissioner of Patents and Trademarks
U.S. Patent and Trademark Office
Washington, DC 20231

Department of Energy
Technical Information Center
P.O. Box 62
Oak Ridge, Tennessee 37830

European Space Agency-Information Retrieval Service
ESRIN
Via Galileo Galilei
00044 Frascati (Rome) Italy

Engineering Sciences Data Unit International
P.O. Box 1633
Manassas, Virginia 22110

Engineering Sciences Data Unit International, Ltd.
251-259 Regent Street
London, W1R 7AD, England

Fachinformationszentrum Karlsruhe
Gesellschaft für wissenschaftlich-technische
Information mbH
7514 Eggenstein-Leopoldshafen 2, Germany

Her Majesty's Stationery Office
P.O. Box 569, S.E. 1
London, England

NASA Center for AeroSpace Information
P.O. Box 8757
Baltimore, Maryland 21240-0757

National Aeronautics and Space Administration
Scientific and Technical Information Program (JTT)
Washington, DC 20546-0001

National Technical Information Service
5285 Port Royal Road
Springfield, Virginia 22161

Pendragon House, Inc.
899 Broadway Avenue
Redwood City, California 94063

Superintendent of Documents
U.S. Government Printing Office
Washington, DC 20402

University Microfilms
A Xerox Company
300 North Zeeb Road
Ann Arbor, Michigan 48106

University Microfilms, Ltd.
Tylers Green
London, England

U.S. Geological Survey Library National Center
MS 950
12201 Sunrise Valley Drive
Reston, Virginia 22092

U.S. Geological Survey Library
2255 North Gemini Drive
Flagstaff, Arizona 86001

U.S. Geological Survey
345 Middlefield Road
Menlo Park, California 94025

U.S. Geological Survey Library
Box 25046
Denver Federal Center, MS914
Denver, Colorado 80225

CASI PRICE TABLES

(Effective October 1, 1991)

STANDARD PRICE DOCUMENTS

PRICE CODE	NORTH AMERICAN PRICE	FOREIGN PRICE
A01	$ 9.00	$ 18.00
A02	12.50	25.00
A03	17.00	34.00
A04-A05	19.00	38.00
A06-A09	26.00	52.00
A10-A13	35.00	70.00
A14-A17	43.00	86.00
A18-A21	50.00	100.00
A22-A25	59.00	118.00
A99	69.00	138.00

MICROFICHE

PRICE CODE	NORTH AMERICAN PRICE	FOREIGN PRICE
A01	$ 9.00	$ 18.00
A02	12.50	25.00
A03	17.00	34.00
A04	19.00	38.00
A06	26.00	52.00
A10	35.00	70.00

IMPORTANT NOTICE

CASI Shipping and Handling Charges
U.S. — ADD $3.00 per TOTAL ORDER
Canada and Mexico — ADD $3.50 per TOTAL ORDER
All Other Countries — ADD $7.50 per TOTAL ORDER
Does NOT apply to orders
requesting CASI RUSH HANDLING.
Contact CASI for charge.

FEDERAL REGIONAL DEPOSITORY LIBRARIES

ALABAMA

AUBURN UNIV. AT MONTGOMERY LIBRARY
Documents Dept.
7300 University Drive
Montgomery, AL 36117-3596
(205) 244-3650 FAX: (205) 244-0678

UNIV. OF ALABAMA
Amelia Gayle Gorgas Library
Govt. Documents
Box 870266
Tuscaloosa, AL 35487-0266
(205) 348-6046 FAX: (205) 348-8833

ARIZONA

DEPT. OF LIBRARY, ARCHIVES, AND PUBLIC RECORDS
Federal Documents
Third Floor State Capitol
1700 West Washington
Phoenix, AZ 85007
(602) 542-4121 FAX: (602) 542-4400; 542-4500

ARKANSAS

ARKANSAS STATE LIBRARY
State Library Services
One Capitol Mall
Little Rock, AR 72201
(501) 682-2869

CALIFORNIA

CALIFORNIA STATE LIBRARY
Govt. Publications Section
914 Capitol Mall - P.O. Box 942837
Sacramento, CA 94237-0001
(916) 322-4572 FAX: (916) 324-8120

COLORADO

UNIV. OF COLORADO - BOULDER
Norlin Library
Govt. Publications
Campus Box 184
Boulder, CO 80309-0184
(303) 492-8834 FAX: (303) 492-2185

DENVER PUBLIC LIBRARY
Govt. Publications Dept. BS/GPD
1357 Broadway
Denver, CO 80203
(303) 571-2135

CONNECTICUT

CONNECTICUT STATE LIBRARY
231 Capitol Avenue
Hartford, CT 06106
(203) 566-4971 FAX: (203) 566-3322

FLORIDA

UNIV. OF FLORIDA LIBRARIES
Documents Dept.
Library West
Gainesville, FL 32611-2048
(904) 392-0366 FAX: (904) 392-7251

GEORGIA

UNIV. OF GEORGIA LIBRARIES
Govt. Documents Dept.
Jackson Street
Athens, GA 30602
(404) 542-8949 FAX: (404) 542-6522

HAWAII

UNIV. OF HAWAII
Hamilton Library
Govt. Documents Collection
2550 The Mall
Honolulu, HI 96822
(808) 948-8230 FAX: (808) 956-5968

IDAHO

UNIV. OF IDAHO LIBRARY
Documents Section
Moscow, ID 83843
(208) 885-6344 FAX: (208) 885-6817

ILLINOIS

ILLINOIS STATE LIBRARY
Reference Dept.
300 South Second
Springfield, IL 62701-1796
(217) 782-7596 FAX: (217) 524-0041

INDIANA

INDIANA STATE LIBRARY
Serials/Documents Section
140 North Senate Avenue
Indianapolis, IN 46204
(317) 232-3678 FAX: (317) 232-3728

IOWA

UNIV. OF IOWA LIBRARIES
Govt. Publications Dept.
Washington & Madison Streets
Iowa City, IA 52242
(319) 335-5926 FAX: (319) 335-5830

KANSAS

UNIV. OF KANSAS
Govt. Documents & Map Library
6001 Malatt Hall
Lawrence, KS 66045-2800
(913) 864-4660 FAX: (913) 864-5380

KENTUCKY

UNIV. OF KENTUCKY LIBRARIES
Govt. Publications/Maps Dept.
Lexington, KY 40506-0039
(606) 257-3139 FAX: (606) 257-1563; 257-8379

LOUISIANA

LOUISIANA STATE UNIV.
Middleton Library
Govt. Documents Dept.
Baton Rouge, LA 70803
(504) 388-2570 FAX: (504) 388-6992

LOUISIANA TECHNICAL UNIV.
Prescott Memorial Library
Govt. Documents Dept.
305 Wisteria Street
Ruston, LA 71270-9985
(318) 257-4962 FAX: (318) 257-2447

MAINE

TRI-STATE DOCUMENTS DEPOSITORY
Raymond H. Fogler Library
Govt. Documents & Microforms Dept.
Univ. of Maine
Orono, ME 04469
(207) 581-1680

MARYLAND

UNIV. OF MARYLAND
Hornbake Library
Govt. Documents/Maps Unit
College Park, MD 20742
(301) 454-3034 FAX: (301) 454-4985

MASSACHUSETTS

BOSTON PUBLIC LIBRARY
Govt. Documents Dept.
666 Boylston Street
Boston, MA 02117
(617) 536-5400 ext. 226
FAX: (617) 267-8273; 267-8248

MICHIGAN

DETROIT PUBLIC LIBRARY
5201 Woodward Avenue
Detroit, MI 48202-4093
(313) 833-1440; 833-1409
FAX: (313) 833-5039

LIBRARY OF MICHIGAN
Govt. Documents Unit
P.O. Box 30007
Lansing, MI 48909
(517) 373-0640 FAX: (517) 373-3381

MINNESOTA

UNIV. OF MINNESOTA
Wilson Library
Govt. Publications Library
309 19th Avenue South
Minneapolis, MN 55455
(612) 624-5073 FAX: (612) 626-9353

MISSISSIPPI

UNIV. OF MISSISSIPPI
J.D. Williams Library
Federal Documents Dept.
106 Old Gym Bldg.
University, MS 38677
(601) 232-5857 FAX: (601) 232-5453

MISSOURI

UNIV. OF MISSOURI - COLUMBIA
Ellis Library
Govt. Documents
Columbia, MO 65201
(314) 882-6733 FAX: (314) 882-8044

MONTANA

UNIV. OF MONTANA
Maureen & Mike Mansfiel Library
Documents Div.
Missoula, MT 59812-1195
(406) 243-6700 FAX: (406) 243-2060

NEBRASKA

UNIV. OF NEBRASKA - LINCOLN
D.L. Love Memorial Library
Documents Dept.
Lincoln, NE 68588
(402) 472-2562

NEVADA

UNIV. OF NEVADA
Reno Library
Govt. Publications Dept.
Reno, NV 89557
(702) 784-6579 FAX: (702) 784-1751

NEW JERSEY

NEWARK PUBLIC LIBRARY
U.S. Documents Div.
5 Washington Street - P.O. Box 630
Newark, NJ 07101-0630
(201) 733-7812 FAX: (201) 733-5648

NEW MEXICO

UNIV. OF NEW MEXICO
General Library
Govt. Publications Dept.
Albuquerque, NM 87131-1466
(505) 277-5441 FAX: (505) 277-6019

NEW MEXICO STATE LIBRARY
325 Don Gaspar Avenue
Santa Fe, NM 87503
(505) 827-3826 FAX: (505) 827-3820

NEW YORK

NEW YORK STATE LIBRARY
Documents/Gift & Exchange Section
Federal Depository Program
Cultural Education Center
Albany, NY 12230
(518) 474-5563 FAX: (518) 474-5786

NORTH CAROLINA

UNIV. OF NORTH CAROLINA - CHAPEL HILL
CB#3912, Davis Library
BA/SS Dept.—Documents
Chapel Hill, NC 27599
(919) 962-1151 FAX: (919) 962-0484

NORTH DAKOTA

NORTH DAKOTA STATE UNIV. LIBRARY
Documents Office
Fargo, ND 58105
(701) 237-8886 FAX: (701) 237-7138
In cooperation with Univ. of North Dakota, Chester Fritz Library
Grand Forks

OHIO

STATE LIBRARY OF OHIO
Documents Dept.
65 South Front Street
Columbus, OH 43266
(614) 644-7051 FAX: (614) 752-9178

OKLAHOMA

OKLAHOMA DEPT. OF LIBRARIES
U.S. Govt. Information Div.
200 NE 18th Street
Oklahoma City, OK 73105-3298
(405) 521-2502, ext. 252, 253
FAX: (405) 525-7804

OKLAHOMA STATE UNIV.
Edmon Low Library
Documents Dept.
Stillwater, OK 74078
(405) 744-6546 FAX: (405) 744-5183

OREGON

PORTLAND STATE UNIV.
Millar Library
934 SW Harrison - P.O. Box 1151
Portland, OR 97207
(503) 725-3673 FAX: (503) 725-4527

PENNSYLVANIA

STATE LIBRARY OF PENN.
Govt. Publications Section
Walnut St. & Commonwealth Ave. - P.O. Box 1601
Harrisburg, PA 17105
(717) 787-3752

SOUTH CAROLINA

CLEMSON UNIV.
Cooper Library
Public Documents Unit
Clemson, SC 29634-3001
(803) 656-5174 FAX: (803) 656-3025
In cooperation with Univ. of South Carolina, Thomas Cooper Library, Columbia

TENNESSEE

MEMPHIS STATE UNIV. LIBRARIES
Govt. Documents
Memphis, TN 38152
(901) 678-2586 FAX: (901) 678-2511

TEXAS

TEXAS STATE LIBRARY
United States Documents
P.O. Box 12927 - 1201 Brazos
Austin, TX 78711
(512) 463-5455 FAX: (512) 463-5436

TEXAS TECH. UNIV. LIBRARY
Documents Dept.
Lubbock, TX 79409
(806) 742-2268 FAX: (806) 742-1920

UTAH

UTAH STATE UNIV.
Merrill Library & Learning Resources Center, UMC-3000
Documents Dept.
Logan, UT 84322-3000
(801) 750-2684 FAX: (801) 750-2677

VIRGINIA

UNIV. OF VIRGINIA
Alderman Library
Govt. Documents
Charlottesville, VA 22903-2498
(804) 924-3133 FAX: (804) 924-4337

WASHINGTON

WASHINGTON STATE LIBRARY
Document Section
MS AJ-11
Olympia, WA 98504-0111
(206) 753-4027 FAX: (206) 753-3546

WEST VIRGINIA

WEST VIRGINIA UNIV. LIBRARY
Govt. Documents Section
P.O. Box 6069
Morgantown, WV 26506
(304) 293-3640

WISCONSIN

ST. HIST. SOC. OF WISCONSIN LIBRARY
Govt. Publications Section
816 State Street
Madison, WI 53706
(608) 262-2781 FAX: (608) 262-4711
In cooperation with Univ. of Wisconsin-Madison, Memorial Library

MILWAUKEE PUBLIC LIBRARY
Documents Div.
814 West Wisconsin Avenue
Milwaukee, WI 53233
(414) 278-2167 FAX: (414) 278-2137

*U.S. G.P.O.:342-599:60023

National Aercnautics and
Space Administration
Code JTT
Washington, D.C.
20546-0001

Official Business
Penalty for Private Use, $300

SPECIAL FOURTH-CLASS RATE
POSTAGE & FEES PAID
NASA
PERMIT No. G27

NASA

POSTMASTER: If Undeliverable (Section 158
Postal Manual) Do Not Return